



IMCET 2022

Türkiye 27. Uluslararası Madencilik Kongresi ve Sergisi
27th International Mining Congress and Exhibition of Turkey
22-25 Mart, March 2022, Antalya

Proceedings of the 27th International Mining Congress and Exhibition of Turkey



TMMOB
Maden Mühendisleri Odası

Antalya

www.imcet.org.tr



UCTEA
Chamber of Mining Engineers

ISBN: 978-605-01-1494-2

Published by
Baskı

TMMOB Maden Mühendisleri Odası
Kültür Mh. Yüksel Cd. No: 40 Çankaya/Ankara

March/Mart 2022
Ph/Tel: +90 312 425 10 80
Fax/Faks: +90 312 417 52 90

www.maden.org.tr
maden@maden.org.tr

IMCET 2022

**Proceedings of the 27th International Mining Congress
and Exhibition of Turkey**
*Türkiye 27. Uluslararası Madencilik Kongresi ve Sergisi
Bildiriler Kitabı*

Editors

Editörler

Dr. Okay Altun
Dr. Deniz Aydın
Dr. Namık Atakan Aydoğan
Dr. Ahmet Deniz Baş
Dr. Hakan Dünder
Dr. Ece Kundak
Dr. Mehtap Gülsün Kılıç
Dr. Emre Yılmazkaya



UCTEA Chamber of Mining Engineers
TMMOB Maden Mühendisleri Odası

Executive Committee of the Congress

Kongre Yürütme Kurulu

Chair Başkan	Yusuf AYDIN
Deputy Co-Chairs Başkan Yardımcıları	Dr. Okay ALTUN Dr. Mehtap GÜLSÜN KILIÇ Dr. Nejat TAMZOK Dr. Bülent TOKA
Secretary Yazman	Nadir AVŞAROĞLU Gülcan KOÇ
Treasurer Sayman	Veyis SIR
Members Üyeler	M. Erşat AKYAZILI Selim ALTUN Dr. Deniz AYDIN Dr. Namık Atakan AYDOĞAN Dr. Ahmet Deniz BAŞ Dr. Hakan DÜNDAR Necmi ERGİN Niyazi KARADENİZ Ümit KILIÇ Pelin KERTMEN Dr. Ece KUNDAK Fatih ÖZKAN Selçuk SARIDOĞAN Muharrem TORALIOĞLU İmge TÜMÜKLÜ Dr. Emre YILMAZKAYA

Board Members of UCTEA Chamber of Mining Engineers

Maden Mühendisleri Odası Yönetim Kurulu

President <i>Başkan</i>	Ayhan YÜKSEL
Vice president <i>II. Başkan</i>	Veyis SIR
Secretary <i>Yazman</i>	M. Erşat AKYAZILI
Treasurer <i>Sayman</i>	Mehmet ZAMAN
Members <i>Üyeler</i>	Hakan Baran KIRMAÇ Cem LAFÇI Gözde SALAR

FOREWORD

These Congress proceedings contain the papers which were submitted to 27th International Mining Congress and Exhibition of Turkey (IMCET 2022) held in Antalya, Turkey between March 22-25, 2022.

IMCET 2022 has been organized to gather the people from the academic world and the business world, in order to further explore and share ways to discuss topics in their respective research areas. The Congress was initiated in 1969 and has become one of the most prestigious congresses in Turkey. IMCET congresses have been a major driving force in the promotion of scientific and technical knowledge in areas such as mine planning, drilling and blasting, rock mechanics, comminution, mineral beneficiation, sustainability of the mining operations and their social impacts. The contributions of all the participants help to make the conference as outstanding as it has been.

These Proceedings are believed to furnish the scientists of the world with an excellent reference book to stimulate further study and research in all these areas. IMCET 2022 received over 150 abstracts from 20 different countries. Papers submitted to the congress went through a peer-review process for publication in these Congress proceedings. We would like to express our gratitude and appreciation for all of the reviewers who helped us maintain the high quality of manuscripts.

We would also like to take this opportunity to thank authors who submitted their papers to the Congress, sponsors and exhibitors for their support and members of the Organizing Committee working for the success of the Congress.



Ayhan YÜKSEL
Chamber of Mining Engineers
President



Yusuf AYDIN
IMCET 2022
Chairman

2013-2020 YILLARI ARASI TÜRKİYE MADENCİLİK SEKTÖRÜNDE MEYDANA GELEN İŞ KAZALARININ NİCELİKSEL ANALİZİ <i>QUANTITATIVE ANALYSIS OF OCCUPATIONAL ACCIDENTS IN THE TURKISH MINING SECTOR BETWEEN 2013-2020</i> E.G. Uçkaç, S. Önder	1
A COMPUTATIONAL ALGORITHM TO PERFORM PROBABILISTIC SAMPLING FOR MINERAL ASSAY DETERMINATION M. Camalan	13
A COMPUTER APPLICATION MODULE EVALUATING ROCK MASS QUALITY RATING H.O. Dönmez , H. Tunçdemir	22
A HYBRID SEMI-QUANTITATIVE APPROACH FOR MINE CLOSURE RISK MANAGEMENT IN ANGURAN MINE, IRAN N. Samadinia, M. Osanloo, S. Amirshenava	31
A REVIEW OF THE NITRATE POLLUTION AND GROUNDWATER PROBLEMS DUE TO MINE BLASTS G.G.U. Aksoy, C. Okay Aksoy, M. Akpınar	43
A STUDY OF EFFECTIVE PARAMETERS IN UNDERGROUND MINING METHOD SELECTION USING Z-NUMBERS THEORY Zeinab Jahanbani, Majid Ataee-pour, Ali Mortazavi	51
AGGLO COLUMN FLOTATION OF TURKISH LIGNITE SLIME AND ŞIRNAK ASPHALTITE BY MICRO SELECTIVE COAGULATION IN MODIFIED COLUMN FLOTATION SEPARATOR Y. I. Tosun, F. Çiçek	62
ALTIN İÇERİKLİ GALEN MİNERALİNİN YÜZEY KİMYASI VE FLOTASYON ÖZELLİKLERİNİN ARAŞTIRILMASI <i>INVESTIGATION OF THE SURFACE CHEMISTRY AND FLOTATION PROPERTIES OF THE GOLD-BEARING GALENA MINERAL</i> G. Erçelik, M. Terzi, I. Kursun Unver, O. özdemir	73
APPLICATION OF NANO BUBBLES IN COLUMN FLOTATION: BENEFICIATION OF IRON AND PHOSPHATE SLIMES F. Nakhaei, M. B. Fathi, Z. Pourkarimi, F. Taghavi	84
APPLICATION OF RESPONSE SURFACE METHODOLOGY IN OPTIMIZING LEACHING PARAMETERS FOR NICKEL RECOVERY FROM SPENT CATALYST A. M. Beygian, M.Rezaei, E. K. Alamdari	91
AŞİDİK DRENAJ AÇISINDAN MADEN ATIKLARI YÖNETMELİĞİ ÜZERİNE BİR İNCELEME <i>AN INVESTIGATION ON THE MINING WASTE REGULATION IN TERMS OF ACIDIC DRAINAGE</i> M. Karadeniz	103
BİR AÇIK OCAK KROM SAHASININ BİRİM MALİYETİNİN UZUN KISA-VADELİ BELLEK (LSTM) YÖNTEMİ İLE TAHMİN EDİLMESİ <i>PREDICTION OF UNIT COST OF AN OPEN-PIT CHROME MINE USING LONG SHORT-TERM MEMORY (LSTM) METHOD</i> A.C. Özdemir	116
BİR TAŞ OCAĞINDA YAPILAN PATLATMALARIN DARICA-2 HES YAPISINA OLAN ÇEVRESEL ETKİLERİNİN ELEKTRONİK ATEŞLEME SİSTEMİ İLE EN AZA İNDİRİLMESİ: ÖRNEK UYGULAMA <i>MINIMIZING THE ENVIRONMENTAL EFFECTS OF EXPLOSIONS IN A QUARRY ON THE DARICA-2 HES STRUCTURE BY ELECTRONIC IGNITION SYSTEM: A CASE STUDY</i> G.G.U. Aksoy, C.O. Aksoy, H. E. Yaman, A. İlhan	127
CHARACTERIZATION OF PHOSPHATE DUST FROM DJBEL-ONK, NORTHERN ALGERIA M.I Zohir, B. Assia, B. Said, C. Abdessalam	139
COMMUNITION VS. LIBERATION: A COMPARATIVE ANALYSIS OF THEORIES AND PRACTICES ON COMMUNITION FROM INVESTMENT POINT OF VIEW, A CASE STUDY FROM URUGUAY I.Tarjan, D. Segovia, H. Ferrizo	145
CONCEPTUAL INVESTIGATION ON PNEUMATIC AND MECHANICAL FLOTATION REACTOR CELLS FROM DESIGNING AND METALLURGICAL PERSPECTIVES A. Hassanzadeh, M. Safari, D.H. Hoang, M.K. Güner, T. Sambrook, P.B. Kowalczuk	152
COPPER RAFFINATE REUSE FOR INITIAL LEACHING, A BOX-BEHNKEN DESIGN H. Movahhedi, A.M. Beygian, E.K. Alamdari	163
CUMHURİYETİMİZİN 100. YILINDA ENERJİ HAMMADDELERİ ÜRETİMİMİZİN SPSS MODELLEMESİ İLE TAHMİNİ <i>PREDICTION OF OUR ENERGY RAW MATERIALS PRODUCTION IN THE 100TH ANNIVERSARY OF OUR REPUBLIC WITH SPSS MODELING</i> A. K. Özdoğan, Y. Kınaş	169
ÇOK OCAK İÇEREN AÇIK İŞLETMELERDE GÜVENLİK FAKTÖRÜ DEĞİŞİMİNİN İNCELENMESİ <i>INVESTIGATION OF THE SAFETY FACTOR CHANGE IN OPEN PIT WITH MULTI-QUARRY</i> C.O. Aksoy, G.G.U. Aksoy, H. E. Yaman	177

DATA-BASED DECISION-MAKING IN UNDERGROUND DRILLING OPERATIONS A. Yıldız, M. Erkayaoğlu	186
DENİZLİ AVDAN VE NARLI KÖMÜR SAHALARI KAYNAK MODELİ <i>DENİZLİ AVDAN AND NARLI COAL MINE SITES RESOURCE MODEL</i> C.A. Öztürk, M. Lashgari, Y. Türkmen	196
DETERMINATION OF FACTORS AFFECTING METHANE EMISSION USING THE FAULT TREE ANALYSIS METHOD <i>METAN EMİSYONUNA ETKİ EDEN FAKTÖRLERİN HATA AĞACI ANALİZİ YÖNTEMİ İLE BELİRLENMESİ</i> N. Kursunoglu	206
DETERMINATION OF STRENGTH PARAMETERS FOR SPECIMENS PREPARED BY 3D PRINTED DISCONTINUITY PLANES A. Kirmacı, Asst.Prof.Dr. M. Erkayaoğlu, Asst.Prof.Dr. A.G. Yardımcı	213
DETERMINATION OF THE DEGREE OF RELEASE OF MINERAL PARTICLES BY IMAGE ANALYSIS SOFTWARE T. D. Figueiredo, A. M. Braga, R. J. A. Fidelis, D. G. Magalhães, P. H. L. Silva, C. A. Pereira	226
“DIGITAL REVOLUTION 4.0” IN THE RAW MATERIALS AND MINING INDUSTRY <i>MADENCİLİK VE HAMMADDELER SEKTÖRÜNDE DİJİTAL DEVRİM 4.0</i> H.A. Kahraman, C. Klötzer, M. Katapotis	233
DÜŞÜK TENÖRLÜ LATERİTİK NİKEL CEVHERİNDEN YIĞIN LIÇI İLE NİKEL KAZANIMININ ARAŞTIRILMASI <i>INVESTIGATION OF NICKEL RECOVERY FROM LOW-GRADE LATERITIC NICKEL ORE BY USING THE HEAP LEACHING</i> A.F. Değirmenci, Ö.Canieren, O.Yılmaz, C.Karagüzel	246
ECO-EFFICIENCY IN DRY COMMUNITION PRACTICES USING VERTICAL ROLLER MILL (VRM) - TECHNICAL AND ECONOMICAL ASPECTS H.R. Manouchehri	256
EFEMÇUKURU ALTIN MADENİ ATIK DEPOLAMA TESİSİNİN EKİM 2020 EGE DENİZİ DEPREMİNDEKİ DURAYLILIK PERFORMANSI <i>STABILITY PERFORMANCE OF EFEMÇUKURU GOLD MINE WASTE STORAGE FACILITY IN OCTOBER 2020 AEGEAN SEA EARTHQUAKE</i> G. Uzunçelebi, S. Ennis, E. R. Castro, Y. S. İnci, H. Ürkmez	267
EFEMÇUKURU ALTIN MADENİ'NDE FİLTRELENMİŞ ATIK DEPOLAMA YÖNTEMİ UYGULAMASI <i>APPLICATION OF FILTERED TAILINGS STORAGE METHOD AT EFEMÇUKURU GOLD MINE</i> Y.S. İnci, P. Kimball, G. Uzunçelebi, H. Ürkmez, M.A. Erol	277
EFFECT OF HEMATITE MORPHOLOGY ON FLOTATION EFFICIENCY T. D. Figueiredo, D. S. Moreira, F. São José, G. H. G. Rodrigues, C. A. Pereira	291
EFFECTS OF TEMPERATURE AND CONFINING PRESSURE ON ENERGY EVOLUTION CHARACTERISTICS AND ROCK BURST MECHANISM IN BRITTLE ROCKS S. Akdag, M. Karakus, G. D. Nguyen, A. Taheri	298
ELEKTRON TRANSFER YÖNTEMİNDE FARKLI İYONLARIN KÖMÜRDEN ORGANİK KÜLKÜRT UZAKLAŞTIRILMAYA ETKİSİ <i>EFFECT OF DIFFERENT IONS IN ELECTRON TRANSFER METHOD ON REMOVAL OF ORGANIC SULFUR FROM COAL</i> U. Demir, A. Aydın	305
EMPLOYING THE MINERALOGICAL DATA FOR SELECTING THE BEST BENEFICIATION METHOD FOR A REFRACTORY GOLD ORE S. Gökdemir, B. Töngür, B. Aksarı, A. Harzanak	314
ENERGY OPTIMIZATION OF A GRINDING CIRCUIT AT A COPPER MINE <i>BİR BAKIR MADENİNDE ÖĞÜTME DEVRESİNİN ENERJİ OPTİMİZASYONU</i> T. Sert, O. Altun, N.A. Toprak, D. Altun, Ö. Darılmaz	324
ENVIRONMENTAL IMPACT ASSESSMENT FOOTPRINT IN OPEN-PIT COPPER MINING M. Heydari, M. Osanloo, A. Başçetin	335
EVALUATION OF THE EXTRACTION OF VALUABLE MINERALS IN THE BEACH BLACK SAND IN THE COAST OF URUGUAY: SMALL SCALE MINING, ENVIRONMENT AND SOCIAL ISSUES I.Tarjan, H. Ferrizo, F. Perez, Y. Castillo	345
EXTRACTION DESIGN OF HIGHWALL MINING IN INDIA TO RECOVER LOCKED-UP COAL USING EMPIRICAL AND NUMERICAL SIMULATIONS P. Pal Roy	355
FARKLI TÜR ÇİMENTOLARIN ÖĞÜTME DAVRANIŞLARININ İNCE TANE BOYUTUNDA ARAŞTIRILMASI <i>INVESTIGATION OF THE GRINDING BEHAVIOR OF DIFFERENT TYPES OF CEMENT IN FINE SIEVE SIZE</i> Y. Umucu, V. Deniz, Y. H. Gürsoy, H. S. Gökçen, S. Oluklulu	367

GAZ KROMATOĞRAFI (HEADSPACE GC-FID) KULLANILARAK FENOL BAZLI DOLGU MALZEMELERİNİN İÇERİĞİNDEKİ FORMALDEHİT MİKTARLARININ TESPİT EDİLMESİ <i>DETERMINATION OF FORMALDEHYDE CONTENTS IN PHENOL BASED FILLING MATERIALS USING GAS CHROMATOGRAPH (HEADSPACE GC-FID)</i>	374
M. Bilen, C. Tuz, A. Rasskazova, R. Kızılgedik, İ. Torođlu, S. Yılmaz, A. Çakır, E. Kaymakçı	
GÖRÜNTÜ İŞLEME TEKNİKLERİ İLE TENÖR KONTROLÜ; DEMİR EXPORT DİVRİĞİ DEMİR MADENİ <i>GRADE CONTROL WITH IMAGE PROCESSING; A CASE STUDY, DEMİR EXPORT DİVRİĞİ IRON ORE MINE</i>	385
H.Çınar, B.Aksarı, P. Tekin, A.Yıldız	
HASANDAĞ VOLKANİKLERİNİN TEK EKSENLİ BASINÇ DAYANIM DEĞERLERİ İLE NOKTA YÜK İNDEKS DEĞERLERİ ARASINDAKİ İLİŞKİNİN İNCELENMESİ <i>INVESTIGATION OF THE RELATIONSHIP BETWEEN UNIAXIAL COMPRESSIVE STRENGTH VALUES AND POINT LOAD INDEX VALUES OF HASANDAĞ VOLCANICS</i>	394
M.A. Demirçin, H. Tunçdemir	
HIG MILL PERFORMANCE AT COPPER FLOTATION CIRCUIT REGRIND APPLICATION <i>BAKIR FLOTASYON DEVRESİ REGRIND UYGULAMASINDA HIG DEĞİRMEN PERFORMANSI</i>	409
O. Altun, Ö. Darılmaz, A. Hür, C.E. Karahan, Z. Göller, T. Sert, D. Altun, N.A. Toprak	
IMPACT OF REGIONAL FAULTS ON COAL AND GAS OUTBURST; A CASE STUDY IN TABAS PARVADEH COAL MINE <i>S. Karimpour, J. K. Hamidi, J. Karami, A. Hosseini</i>	417
INDUSTRIAL USE OF BACTERIAL IRON OXIDATION IN-SITU RECOVERY OF URANIUM <i>B. Shiderin, A. Altynbek, Y. Bektay, G. Turysbekova, M. Erzhan, A. Kalmukambetov, M. Bektayev, A. Duisenbay</i>	425
INTEGRATION OF RENEWABLE ENERGY IN THE PRODUCTION SCHEDULING PROBLEM USING GRAVITATIONAL SEARCH ALGORITHM <i>K. Tolouei, E. Moosavi</i>	436
INVESTIGATION OF ENRICHMENT OPPORTUNITIES OF ESKİŞEHİR BEYLİKAHİR REGION BARITE AND FLUORITE WITH PHYSICAL METHODS <i>ESKİŞEHİR BEYLİKAHİR BÖLGESİ BARİT VE FLORİT'İN FİZİKSEL YÖNTEMLER İLE ZENGİNLEŞTİRME OLANAKLARININ ARAŞTIRILMASI</i>	442
E. Baştürkcü, C. Şavran, A. E.Yüce, H. Topal	
INVESTIGATION OF FRACTURE AND MECHANICAL PROPERTIES OF SEMI-CIRCULAR BENDING SHOTCRETE SPECIMENS USING 3D PRINTED MOLDS <i>C. Karataş Batan, M. Erkayaođlu</i>	450
JEOSENTETİK MALZEMELERİN ÇEVREYE VE TOPLUMA SAĞLADIĞI KATKILAR <i>THE CONTRIBUTION OF GEOSYNTHETIC MATERIALS TO THE ENVIRONMENT AND SOCIETY</i>	458
C. Ozan	
KANADA MADENCİLİK DERNEĞİ- SÜRDÜRÜLEBİLİR MADENCİLİK- ATIK YÖNETİM PROTOKOLÜ VE TÜRKİYE'DEKİ UYGULAMASI <i>MINING ASSOCIATION OF CANADA- TOWARDS SUSTAINABLE MINING TAILINGS MANAGEMENT PROTOCOL AND APPLICATION IN TURKEY</i>	467
H. Ürkmez, C. Dumaresq, B. Chalmers, Y.S. İnci, G. Uzuncelebi, S. Ennis, E.R. Castro	
KARDEMİR A.Ş. KİREÇ FABRİKALARINDAKİ YANMIŞ KİREÇ TAŞI ELEME SİSTEMİNDE KULLANILAN ELEK PANELLERİNİN İYİLEŞTİRİLMESİ <i>IMPROVEMENT OF SIEVE PANELS USED IN BURNT LIMESTONE SCREENING SYSTEM AT KARDEMİR A.Ş. LIME PLANTS</i>	480
E. Nakaş, C. Cantürk, F. Esin, O. Acur, M. Sevim	
KARDEMİR A.Ş'DE YERLİ VE İTHAL TOZ CEVHERLER İLE HAZIRLANAN HARMANLARDA ÜRÜN SİNER KALİTESİNİN DEĞERLENDİRİLMESİ <i>EVALUATION OF PRODUCT SINTER QUALITY IN BLENDS PREPARED WITH DOMESTIC AND IMPORTED FINE ORES AT KARDEMİR A.Ş.</i>	491
T. Timur, C. Cantürk, F. Esin, O. Acur, M. Sevim	
KİMYASAL DOLGU MALZEMELERİNİN KARAKTERİSTİKLERİ VE KÖMÜRÜN KENDİLİĞİNDEN YANMASI ÜZERİNE ETKİSİNİN İNCELENMESİ <i>INVESTIGATION OF THE CHARACTERISTICS OF CHEMICAL FILLING MATERIALS AND THE EFFECT ON SPONTANEOUS COMBUSTION OF COAL</i>	501
C. Tuz, M. Bilen, E. Kaymakçı, İ. Torođlu, Ö. Yılmaz, S. Yılmaz	

KOK BATARYALARI SULU SÖNDÜRME SİSTEMİ PARAMETRELERİNİN OPTİMİZE EDİLEREK SU TÜKETİMİNİN AZALTILMASI <i>REDUCING WATER CONSUMPTION BY OPTIMIZING COKE OVEN BATTERIES WET QUENCHING PARAMETERS</i>	515
H. Zümrüt, Ö. Ece, S.C Güner	
KOK BATARYALARINDA SÖNDÜRME PROSESİNİN OPTİMİZASYONU VE ÜRETİLEN KOKUN YÜKSEK FIRINLARDA ENERJİ VERİMLİLİĞİNE ETKİSİNİN İNCELENMESİ <i>OPTIMIZATION OF THE QUENCHING PROCESS IN COKE BATTERIES AND INVESTIGATION OF THE EFFECT OF PRODUCED COKE ON ENERGY EFFICIENCY IN BLAST FURNACES</i>	521
H. Kalay, Z. Özer	
KONYA İLGIN KÖMÜR SAHASI KAYNAK MODELİ <i>KONYA İLGIN COAL MINE SITE RESOURCE MODEL</i>	530
C.A. Öztürk, E. Nasuf, G. Eken, H. Ketizmen , R. Bozkurt	
KÖMÜR FLOTASYONUNDA JAMESON FLOTASYON HÜCRESİ KİNETİĞİNİN MODELLENMESİ <i>MODELING OF JAMESON FLOTATION CELL'S KINETICS IN COAL FLOTATION</i>	541
S. Karaca, O. Şahbaz, A. Uçar	
KSANTAT ZİNCİR YAPISININ GALEN FLOTASYONUNA ETKİSİ <i>EFFECT OF CHAIN STRUCTURE OF XANTHATE ON GALENA FLOTATION</i>	549
S. Özün, G. Ergen	
LIFE CYCLE ASSESSMENT IN DEEP OPEN-PIT COPPER MINES	558
M. Heydari, M. Osanloo, A. Başçetin	
LONG TERM PRODUCTION SCHEDULING OPTIMIZATION IN AN UNDERGROUND PB/ZN MINE	574
M. Shenavar, M. Ataee-pour, M. Rahmanpour	
MALİYET YAKLAŞIMI İLE ERKEN EVRE KÖMÜR SAHALARININ DEĞERLEMESİ <i>VALUATION OF EARLY-STAGE COAL FIELDS BY COST APPROACH</i>	584
M. Aktan, A.E. Tercan	
MEVZUAT DEĞİŞİKLİĞİ İLE BİRLİKTE YÜKSEK BASINÇLI HAVA PATLATMALI KAZI TEKNOLOJİSİNİN ZONGULDAK HAVZASI DİK KÖMÜR DAMARLARINDA YENİDEN UYGULANABİLMESİ <i>RE-APPLICATION OF HIGH PRESSURE AIR BLAST EXCAVATION TECHNOLOGY IN VERTICAL COAL SEAMS OF THE ZONGULDAK BASIN WITH THE LEGISLATIVE CHANGE</i>	596
C. Yamudi	
MICRO GRINDING IN VERTICAL MILL OF ŞIRNAK ASPHALTITE SLIME, FLY ASH/ CHAR/ SOOT BY MICROWAVE RADIATION	606
Y.I. Tosun, F. Çiçek	
MİNİMUM EĞRİLİK ALGORİTMASI İLE YÖNLÜ SONDAJ VE KOMPOZİTLEME BİLGİSAYAR PROGRAMI <i>DRILLHOLE DATABASE APPLLET: MINIMUM CURVATURE ALGORITHM AND DOWNHOLE COMPOSITE</i>	615
G. Ertunç, A. İmer	
MODELLING OF COPPER ELECTROREFINING IN IONIC DIFFUSION CONTROL CONDITION BY COMSOL MULTIPHYSICS	626
M.D. Inalou, A.M. Beygian, E.K. Alamdari	
MODELLING OF ROCK COMMINUTION USING STATISTICAL AND SOFT COMPUTING ANALYSES – A CASE STUDY ON A LABORATORY-SCALE JAW CRUSHER	637
E. Köken	
NADİR TOPRAK ELEMENTLERİNİN KAZANIMI İÇİN POTANSİYEL BİR KAYNAK: KÖMÜR YIKAMA TESİSİ ATIKLARI <i>A POTENTIAL SOURCE FOR RECOVERY OF RARE EARTH ELEMENTS: COAL WASHERY WASTE</i>	647
N.İ. Dinç, F. Burat	
NARROW, TABULAR STOPE 3D SCANNING IN DEEP-LEVEL GOLD MINES USING AN IPAD PRO LIDAR	658
C. Birch, A. Olivier	
NEW AND ECOLOGICAL METHOD FOR THE PRODUCTION OF CR2O3 FROM CHROMITE ORE <i>YENİ VE EKOLOJİK YÖNTEMLE KROMİT CEVHERİNDEN Cr2O3 ÜRETİMİ</i>	670
H. Şahan, H. Xu	
NEW ERA OF AUTOMATION IN LEAK DETECTION INDUSTRY	682
T. Gregor	
NÜMERİK MODELLEME İLE KAYA TASARIMINDA DEFORMASYON MODÜLÜNÜN ÖNEMİ <i>THE IMPORTANCE OF DEFORMATION MODULUS ON DESIGN OF ROCKS WITH NUMERICAL MODELING</i>	687
C.O. Aksoy, G.G. Uyar Aksoy, H.E. Yaman	

PARAMETRIC STUDY OF HIGH-LEVEL NUCLEAR WASTE STORAGE IN UNDERGROUND HARD ROCK CAVERNS T.E. Altıntaş, A.A.A. Abduljabar, A.G. Yardımcı	708
PATLATMA KAYNAKLI TİTREŞİMLERİN 3 BOYUTLU NÜMERİK MODELLEME İLE TAHMİN EDİLMESİ <i>PREDICTION OF BLAST INDUCED VIBRATION WITH 3D DYNAMIC NUMERICAL MODELING</i> C.O. Aksoy, G.G.U. Aksoy, H. E. Yaman	718
POST-MINING LAND-USE PLANNING: AN INTEGRATION OF MINED LAND SUITABILITY ASSESSMENT AND SWOT ANALYSIS IN CHADORMALU IRON ORE MINE OF IRAN S. Amirshenava, M. Osanloo	726
POTAŞ CEVHERİNİN AMİN TİPİ TOPLAYICI İLE FLOTASYONUNDA ŞLAM UZAKLAŞTIRMASININ ETKİSİ <i>EFFECT OF SLIME REMOVAL IN THE FLOTATION OF POTASH ORE WITH AMINE TYPE COLLECTOR</i> A. Hamrayev, M. Terzi, C. Gungoren, I. Kursun Unver, O. Ozdemir	742
POTENTIAL DIFFERENCE BETWEEN PRE-PASSIVE AND NON-PASSIVE ANODES IN COPPER ELECTROWINNING PROCESS IN THE PRESENCE OF IRON IONS H. L. Shahsavari, A. M. Beygjan, E. K. Alamdari	749
PREDICTIVE MAINTENANCE: A VIABLE MAINTENANCE OPTION FOR MACHINES/EQUIPMENT/PLANTS IN MINING AND MINERAL PROCESSING O. Dayo-Olupona, B. Genc, S. Bada, T. Celik	759
PREMATURE MINE CLOSURE, RISK ASSESSMENT AND POST-MINING LAND-USE OF GALALI OPEN-PIT IRON MINE OF IRAN <i>M. Zangeneh, M. Osanloo, S. Amirshenava</i>	766
PROPOSITION OF A NEW SCALED DISTANCE EQUATION IN OPEN PIT BLASTING <i>AÇIK OCAK PATLATMALARINDA YENİ BİR ÖLÇEKLİ MESAFE DENKLEMİ ÖNERME</i> A. Tosun, S. Ercins, V.O. Tenorio	780
PULSE TIME RATIO OPTIMIZATION IN A PRC COPPER ELECTROWINNING SYSTEM <i>H. Zerafat, A. M. Beygjan, E. K. Alamdari</i>	785
REMOVAL OF ORGANIC MATTER FROM BLACK PHOSPHATES BY CALCINATIONS; CASE OFF DJEBEL ONK PHOSPHATE; ALGERIA <i>D. Nettour, S. Grairia , S. Bensehamdi, M. Chettibi</i>	793
RİSK ESASLI MADEN ATIK YÖNETİMİ <i>RISK BASED TAILINGS MANAGEMENT</i> H. Ürkmez, Y.S. İnci , S. Ennis, E.R. Castro, G. Uzunçelebi	803
RMQR SİSTEMİNİN HONAZ TÜNELİ İÇİN UYGULANABİLİRLİĞİNİN DEĞERLENDİRİLMESİ <i>EVALUATION OF THE APPLICABILITY OF THE RMQR SYSTEM FOR HONAZ TUNNEL</i> E. Karakaplan, D. Alkaya, H. Başarır	814
SCALE INHIBITION IN HIGH SOLIDS SLURRY – FINANCIAL AND PRODUCTION IMPACT IN A GOLD MINE OPERATION K. Bakeev, O. Toprak, V. Lugo-Gonzalez, F. Espinosa, F. Ramirez, L. Danks, A. Zhang, E. Martinez, W. Vargas	825
SİNER TEŞİSİNDE SO ₂ EMİSYON AZALTICI ÜRE UYGULAMASI <i>SO₂ EMISSION REDUCTION UREA APPLICATION IN SINTER PLANT</i> B.E. Kesemen, V. Kızılay, S. Balaban	835
STATE OF THE ART BULK DOZING IN MINING <i>MADENCİLİKTE DOZERLE YIĞIN ÖTELEME İŞİNDEKİ EN SON TEKNOLOJİLER</i> M. Doktan, Y.S. İnci	842
SURFACE CHEMISTRY OF THE LOCKED PARTICLES FOR SULPHIDE MINERALS <i>SÜLFÜRLÜ MİNERALLERDE BAĞLI TANELERİN YÜZEY KİMYASI</i> D. İzerdem	855
ŞLAM KÖMÜRDEN ORGANİK REAKTİFLERLE SÜPER TEMİZ KÖMÜR ÜRETİMİ <i>SUPER CLEAN COAL PRODUCTION WITH ORGANIC REAGENTS FROM SLIME COAL</i> A. Akin, H. Hacifazlıoğlu	864
TEMEL SÜRTÜNME AÇISI TESTİNDE DENEY ÖRNEĞİ ŞEKLİNİN ETKİSİ <i>EFFECT OF EXPERIMENT SAMPLE SHAPE ON BASIC FRICTION ANGLE TEST</i> M. Özdemir, S. Beyhan, A. Özgür	873
THE ARCHAEOLOGICAL USE OF MINING AND ROCK MECHANICS KNOWLEDGE G.G.U. Aksoy, C.O. Aksoy	881

THE DETERMINATION OF SYNERGIC EFFECTS OF DIFFERENT TYPES OF FROTHERS IN FLOTATION G. Güven, B. Tunç, Ş.B. Aydın, G. Bulut	888
THE EFFECT OF FINE GRINDING ON CYANIDE LEACHING OF GOLD MINE TAILINGS B. Bıyıklı, S. Sevgül, H. Dünder	895
THE EFFECT OF STATIC ELECTRIC ON SETTLING BEHAVIOUR OF AN INDUSTRIAL BLAST FURNACE WASTE WATER E. Gülcan	904
THE IMPACT OF MAIN HAUL ROAD IN SELECTION OF WASTE DUMP IN OPEN-PIT MINES REGARDING ENVIRONMENTAL CONSIDERATION A. Hajarian, M. Osanloo	913
TUNÇBİLEK ŞLAM GÖLETİNDEN KAZANILAN KÖMÜRÜN BİRİKETLENMESİNDE BASINÇ DAYANIMI TAHMİNİ <i>PREDICTION OF COMPRESSIVE STRENGTH IN BRIQUETTING COAL RECOVERED FROM TUNÇBİLEK SLIME POND</i> S. Karaca, O. Şahbaz, A. Uçar	926
TÜRKİYE YERALTI KÖMÜR MADENLERİNDE DELME PATLATMA PROBLEMLERİ VE ÇÖZÜM ÖNERİLERİ <i>DRILLING BLASTING PROBLEMS AT THE UNDERGROUND COAL MINES IN TURKEY AND SUGGESTIONS FOR ITS SOLUTION</i> M. Erdil	935
TÜRKİYE'DE PÜLPTE KARBON ALTIN İŞLEME YÖNTEMİNİN SU AYAK İZİ DEĞERLENDİRMESİ <i>WATER FOOTPRINT ASSESSMENT OF CARBON IN PULP GOLD PROCESSING IN TURKEY</i> E. Güney, N. Demirel	940
ULTRASONİK ÖN İŞLEMİN FLOTASYON YÖNTEMİ İLE KÖMÜRDEN KÜL VE KÜKÜRT UZAKLAŞTIRMAYA ETKİSİNİN ARAŞTIRILMASI <i>INVESTIGATION OF THE EFFECT OF ULTRASONIC PRETREATMENT ON COAL DEMINERALIZATION AND DESULFURIZATION BY FROTH FLOTATION METHOD</i> U. Demir, A. Aydın	947
UTILISATION OF BY-PRODUCTS AND ALTERNATIVE CONSTRUCTION MATERIALS IN MINE CONSTRUCTION <i>M. Koivulahti, H. Jyrävä, P. Potila, A. Virtanen, A. Nissinen</i>	959
ÜNYE (ORDU) BÖLGESİNE AİT KALSİYUM TİP BENTONİTİN UV-VIS ABSORPSİYON SPEKTROSKOPİSİ İLE KARAKTERİZASYONU <i>CHARACTERIZATION OF CALCIUM TYPE BENTONITE FROM ÜNYE (ORDU) REGION BY UV-VIS ABSORPTION SPECTROSCOPY</i> Y. Erdoğan, O.E. Kök	972
YAŞ ÖĞÜTME VE MEKANİK DAĞITMANIN KIZILDAM HALLOYSİT CEVHERİNİN SİNERLEME ÖZELLİKLERİNE ETKİSİ <i>EFFECT OF WET GRINDING AND MECHANICAL DISPERSION ON THE SINTERING PROPERTIES OF KIZILDAM HALLOYSITE ORE</i> E. Durgut, M. Terzi, I. Kursun Unver, M. Cinar, O. Ozdemir	979
YERALTI İŞLETME OPTİMİZASYONU VE İŞLEVSEL PLANLAMA <i>A TUTORIAL on STOPE OPTIMISATION and OPERATIONAL SCHEDULING</i> A. Eşiyok, B. Kahraman	986
YERALTI KÖMÜR İŞLETMELERİNE YAPILAN DESTEK ÖDEMELERİ VE ÖNEMİ <i>SUPPORT PAYMENTS AND IMPORTANCE OF UNDERGROUND COAL BUSINESS</i> B. Kocaman, C. Doğruöz, R. Kocaman, C. Acar	996
YERALTI KÖMÜR MADENCİLİĞİNDE HALAT SAPLAMA OPERASYONUNUN MEKANİZE DELGİ VE ENJEKSİYON SİSTEMLERİ İLE GELİŞTİRİLMESİ: YATAĞAN ÖRNEK ÇALIŞMASI <i>DEVELOPMENT OF CABLE BOLT OPERATION IN UNDERGROUND COAL MINING WITH MECHANIZED DRILLING AND INJECTION SYSTEMS: YATAGAN CASE STUDY</i> A. Erel, C. Tuz	1008
YERALTI KÖMÜR MADENLERİNDE KULLANILAN FENOL BAZLI DOLGU MALZEMELERİNİN KANSEROJEN FORMALDEHİD İÇERİĞİ ve İSG AÇISINDAN DEĞERLENDİRİLMESİ <i>EVALUATION OF PHENOL BASED FILLING MATERIALS IN TERMS OF CARCINOGENIC FORMALDEHYD CONTENT AND OHS (OCCUPATIONAL HEALTH AND SAFETY)</i> S. Yılmaz, M. Bilen, E. Kaymakçı, C. Tuz, E. Bahadır, İ. Toroğlu, H. Hacifazlıoğlu, M. Şahin, Ö. Yılmaz	1017
ZİNCİRLİ KOLLU KESİCİ MAKİNALARDA TEKNOLOJİK GELİŞMELER VE KESME TAKIMINDA KIRILMA NEDENLERİ <i>TECHNOLOGICAL DEVELOPMENTS ON CHAIN SAW MACHINES AND REASONS OF BROKEN CHAIN SAW PARTS</i> S. Kulaksız	1025
BAKIR CEVHERİ İÇİN FARKLI PARÇACIK BOYUTU GRUPLARINA AİT KIRILMA PARAMETRELERİNİN TEK DARBELİ KIRILMA İLE BELİRLENMESİ <i>DETERMINATION OF BREAKAGE PARAMETERS FOR SEVERAL SIZE CLASSES OF COPPER ORE BY SINGLE IMPACT BREAKAGE TEST</i> İ.C. Duman, B. Ozlu, M. İtik	1036

**2013-2020 YILLARI ARASI TÜRKİYE MADENCİLİK SEKTÖRÜNDE MEYDANA GELEN İŞ
KAZALARININ NİCELİKSEL ANALİZİ**
*QUANTITATIVE ANALYSIS OF OCCUPATIONAL ACCIDENTS IN THE TURKISH MINING SECTOR
BETWEEN 2013-2020*

E.G. Uçkaç^{1*}, S. Önder¹

¹ *Eskişehir Osmangazi Üniversitesi, Maden Mühendisliği Bölümü*
(*Sorumlu yazar: eguckac@gmail.com)

ÖZET

Madencilik sektörü tüm sektörlerle kıyasla iş kazasının en çok yaşandığı sektörlerin başında gelmektedir. İş kazalarının önlenmesi için kazalara neden olan faktörlerin analiz edilmesi gerekir. Bu çalışmada, SGK tarafından kayıt altında tutulan 2013-2020 yılları arasında meydana gelmiş olan madencilik sektörüne ait 103.815 adet iş kazası niceliksel olarak incelenmiştir. Analizde kazaya sebep olan olay, yaralanma nedeni, yaralanma türü, yaralanan uzuv, yürütülen faaliyet, yaş, eğitim düzeyi, kaza saati, meslek gibi parametrelerin kazanın oluşumu üzerindeki etkileri incelenmiştir. Sonuç olarak; iş kazalarının çoğunlukla yeraltı işletmelerinde ve kömür-linyit çıkarılmasında olduğu, üretimde çalışan ve eğitim düzeyi düşük olan çalışanların iş kazası eğilimlerinin yüksek olduğu bulunmuştur. El makinaları ile çalışmalarda, 25-34 yaş aralığında, işe başlangıcın 2. ve 3. saatinde, operatör ve montaj gurubunda, malzeme taşıma sırasında, el ve kollarından yaralanmalarının yüksek olduğu da tespit edilmiştir.

Anahtar Sözcükler: İş kazası, kaza analizi, madencilik

ABSTRACT

Mining sector is one of the sectors where occupational accidents are experienced the most compared to all sectors. In order to prevent occupational accidents, the factors causing the accidents should be analyzed. In this study, 103,815 occupational accidents in the mining sector, which occurred between 2013 and 2020, which were recorded by the SGK, were quantitatively examined. In the analysis, the effects of parameters such as the event that caused the accident, the cause of the injury, the type of injury, part of body, the activity carried out, age, education level, time of the accident, and occupation on the occurrence of the accident were examined. As a result; It has been found that occupational accidents are mostly in underground mines and coal-lignite extraction, and workers with low education level and working in production have a high tendency to work accident. It has also been determined that injuries from the hands and arms are high in the 25-34 age range, at the 2nd and 3rd hours of the start of work, in the operator and assembly group, during material handling, while working with hand machines.

Keywords: Occupational accidents, accident analysis, mining

GİRİŞ

Madencilik sektörü, maddi ve manevi büyük kayıpların olduğu iş kazalarının gerçekleştiği çok tehlikeli çalışma kollarından birisidir. İş kazaları sebebiyle meydana gelen yaralanmalar, uzuv kayıpları ve ölümler konunun sosyal boyutunu, iş gücü ve iş günü kaybı, tıbbi müdahaleler ve tazminatlar, maddi kayıplar (makine, teçhizat, bina vb.), üretim ve verimin düşmesi ise ekonomik boyutunu ortaya

koymaktadır (Yıldırım, 2009).

Özellikle iş sağlığı ve güvenliği ile ilgili yasal düzenlemelerin temel amacının iş kazalarını önlemek olduğu dikkate alınacak olursa, bu bağlamda ve yasal düzenlemeler kapsamında alınan tüm önlemlere rağmen iş kazaları meydana gelmeye devam etmektedir. İş kazalarını önleyebilmek için kazaya sebep olan nedenlerin bilinmesi gerekir. Bu durumda iş kazası analizlerinin önemi ortaya çıkmaktadır. Bu yüzden kaza kayıtları doğru bir şekilde tutulmalı, devamlı güncellenmeli, kaza sebepleri doğru bir şekilde belirlenmeli ve alınacak tedbirlerin kararlaştırılması gereklidir (Önder vd., 2015).

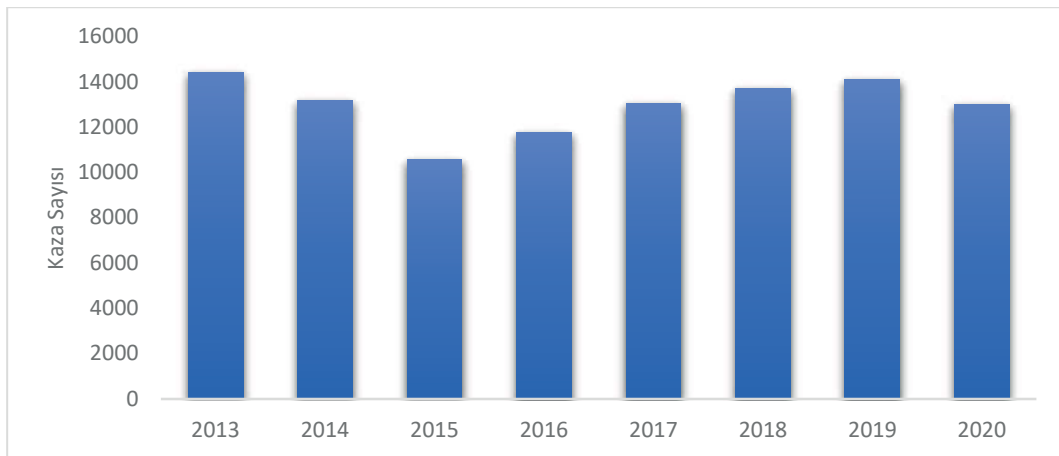
Bilim vd. (2018), yaptıkları çalışmada SGK'nın 2012-2016 yıllarına ait istatistiklerini değerlendirdiklerinde, iş kazaları ve meslek hastalıkları oranlarında düşüş gözlenmektedir. Ancak bu düşüşün yeterli olmadığı belirtilmiştir. Kılıç vd. (2018), yaptıkları çalışmada ülkemizdeki kömür madenlerinde 2010-2017 yılları arasındaki yaşanan ölümlü iş kazalarını incelemişlerdir. Kömür üretiminde kullanılan yöntemlerin çeşitliliğinden kaynaklı, iş sağlığı ve güvenliği önlemlerinin yetersiz olduğunu belirlemişlerdir. Şensöğüt vd. (2019), yaptıkları çalışmada Garp Linyitleri İşletmesine ait 2015-2017 yılları arasındaki iş kazası verilerini üretim ile birlikte değerlendirmişlerdir. İş kazaları oranlarının yıllar içinde arttığı görülmekte olup kaza nedenlerinin çoğunlukla bireysel hatalardan kaynaklanmakta olduğu tespit edilmiştir. Oral (2021), yaptığı çalışmada SGK'nın 2013-2019 yılları arasındaki madencilikteki iş kazaları istatistikleri analiz edilmiş, iş kazasına uğramayan çalışanların, her 10000 'lik iş saatinde iş kazasına uğrama olasılığı %0,17 olarak tespit edilmiştir.

Bu çalışmada, 2013-2020 yılları arasına ait madencilik sektöründe meydana gelen tüm iş kazalarının analizi gerçekleştirilmiştir. Çalışmada, Sosyal Güvenlik Kurumu (SGK) tarafından elektronik ortamda tutulan İş Kazası Bildirim Formlarına ait iş kazası verileri kullanılmıştır (SGK, 2021). Veriler SGK ile yapılan yazışmalar sonucunda izinle alınmıştır.

İŞ KAZALARININ ANALİZİ

Bu çalışmada ülkemizde 2013 – 2020 yılları arasında tüm madencilik faaliyet sınıflamalarında meydana gelmiş olan iş kazaları ayrıntılı bir şekilde analiz edilmiştir. SGK tarafından iş kazası bildirim formları 2013 yılından itibaren Avrupa Birliği Standartlarına uygun olarak ESAW sınıflandırmasına göre tutulmaya başlanmıştır (ESAW, 2013). Bu nedenle verileri daha sağlıklı ele alabilmek adına 2013 yılı ve sonrası bildirim formları değerlendirilmiştir.

Türkiye’de 2013 – 2020 yılları arasında madencilik sektörüne ait toplam 103.815 adet iş kazaları verisi bulunmaktadır. Meydana gelen bu iş kazalarının yıllara göre dağılımları Şekil 1’de verilmiştir.



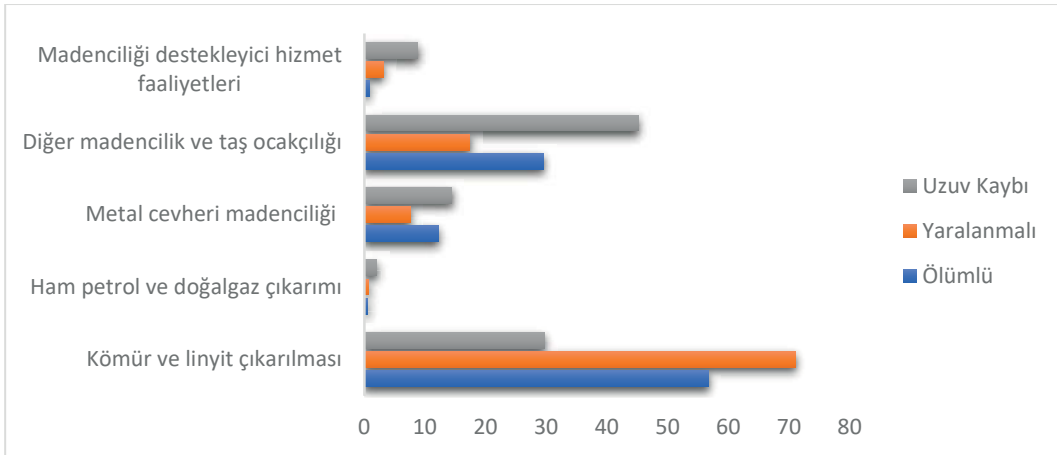
Şekil 1. Türkiye’de madencilik sektöründe meydana gelen iş kazalarının yıllara göre dağılımı

Şekil 1 incelendiğinde, iş kazalarının sayısında önce bir azalma, 2015 yılından sonra bir artış gözlenmektedir. 2015 yılındaki azalmanın, 13 Mayıs 2014’ de meydana gelen Soma kazası sonrasında işletmelerde iş sağlığı ve güvenliği ile ilgili tedbirleri ve önlemlerinin etkinliğinin arttırılmış olması sonucuna ulaşılabilir. Ayrıca 2020 yılında pandemiden kaynaklı olabilecek, bir önceki yıla göre bir miktar azalma olduğu görülmektedir. Şekil 2’de iş kazası geçiren çalışanların faaliyet gruplarına dağılımları verilmiştir.



Şekil 2. 2013-2020 yılları arasında iş kazası geçiren çalışanların faaliyet gruplarına göre dağılımı

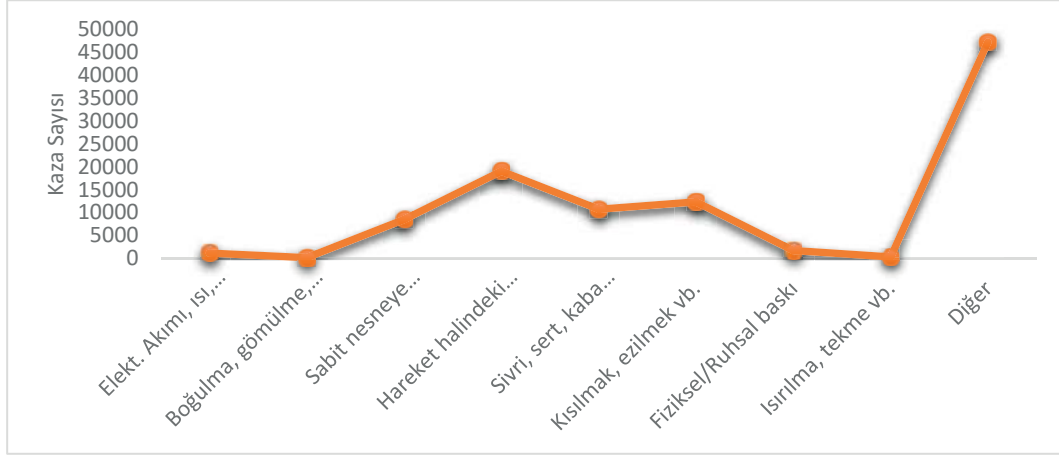
Şekil 2’deki 2013-2020 yılları arasında faaliyet gruplarına göre bakıldığında; kömür ve linyit çıkarılması faaliyet grubunda meydana gelen kazalar, madencilik sektöründeki toplam iş kazalarının %68,87’ sini oluşturmaktadır. Bu durum diğer madencilik gruplarına göre kömür ve linyit grubu madencilik sektöründe çalışan sayılarının fazla olmasından da kaynaklanmaktadır. Şekil 3’te meydana gelen ölümlü, yaralanmalı ve uzuv kayıplı iş kazalarının faaliyet gruplarına göre dağılımı gösterilmektedir.



Şekil 3. 2013-2020 yılları arasında meydana gelen ölümlü, yaralanmalı ve uzuv kayıplı iş kazalarının faaliyet gruplarına göre dağılımı

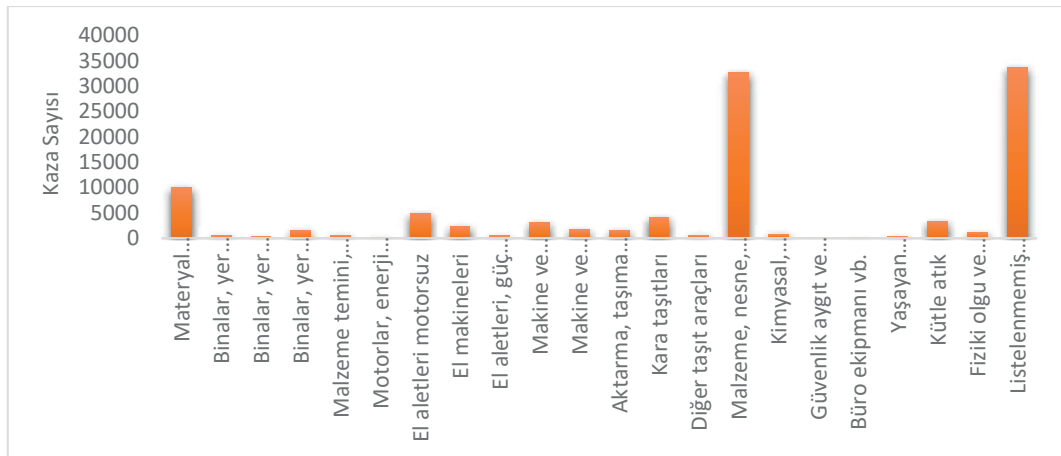
Şekil 3 incelendiğinde, 2013-2020 yılları arasındaki meydana gelen ölümlü iş kazalarının %56,76’sı kömür ve linyit çıkarılması, %29,57 diğer madencilik ve taş ocakçılığı ve %12,23’ünde metal cevheri madenciliği faaliyet grubunda meydana geldiği görülmektedir. Kömür ve linyit çıkarılması faaliyet grubundaki sayısının fazla olması, 2014 yılında Soma’da meydana gelen 301 çalışanın ölümü ile sonuçlanan kazadan kaynaklanmaktadır. Bu kazanın gerçekleşmemiş olması durumunda diğer

madencilik ve taş ocakçılığı faaliyet grubundaki ölümlü iş kazası sayısının daha fazla olacağı da gözlenmektedir. Şekil 3'te 2013-2020 yılları arasında meydana gelen uzuv kayıplı kazalardan %45,12'sinin diğer madencilik ve taş ocakçılığı faaliyet grubunda olması dikkat çekmektedir. %29,74'ü kömür ve linyit çıkarılması ve %14,35'i metal cevheri madenciliği faaliyet gruplarında meydana gelmiştir. Şekil 3'te 2013-2020 yılları arasında meydana gelen yaralanmalı iş kazalarına bakıldığında; toplam yaralanmalı iş kazalarının %71,13'ünün kömür ve linyit çıkarılması faaliyet grubundan olduğu görülmektedir. %17,39'unun diğer madencilik ve taş ocakçılığı ve %7,57'sinin de metal cevheri madenciliği faaliyet gruplarında meydana gelmiştir. Şekil 4'te 2013-2020 yılları arasında meydana gelen iş kazalarının yaralanmaya neden olan olaylara göre dağılımları verilmiştir.



Şekil 4. 2013-2020 yılları arasında meydana gelen iş kazalarının yaralanmaya neden olan olaylara göre dağılımları

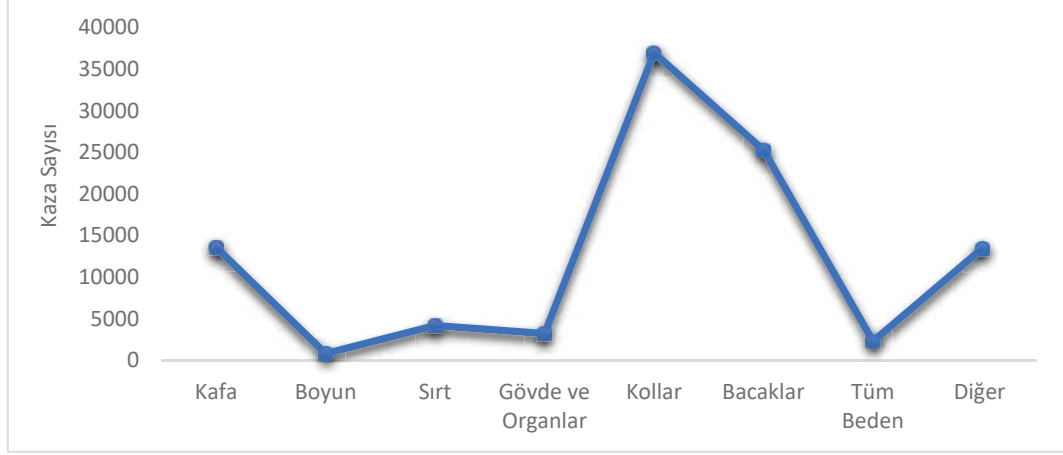
SGK tarafından iş kazalarında yaralanmaya neden olan olaylar 9 farklı grupta sınıflandırılmaktadır. Grafik incelendiğinde diğer yani “bu sınıflandırmada listelenmemiş yaralanmaya sebep olan hareket (olay)” sınıfındaki kazaların %45,52 oranında olduğu görülmektedir. Ayrıca %18,38'inin “hareket halindeki bir nesnenin çarpması, çarpışması”, %11,88'inin “kısılmak, ezilmek vb.” ve %10,34'ünün “sivri, uçlu, sert veya kaba bir materyal araç ile temas” yaralanmaya neden olan olayların diğerlerine göre daha fazla olduğu gözlenmektedir. 2013-2020 yılları arasında meydana gelen iş kazalarında yaralanmaya sebep olan araç/gereçlerin dağılımları Şekil 5'te verilmiştir.



Şekil 5. Yaralanmaya neden olan araç/gereçlerin dağılımları

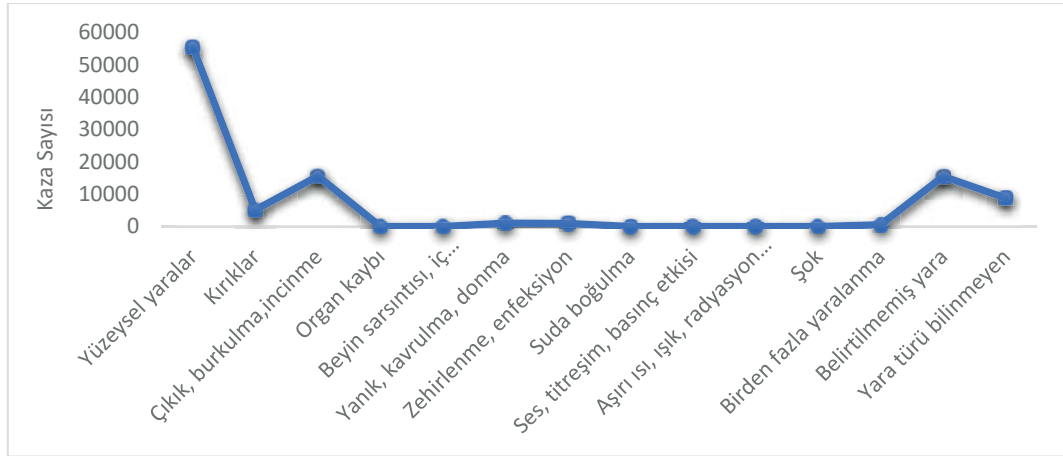
SGK tarafından iş kazalarında yaralanmaya neden olan araç/gereçler 22 farklı grupta

sınıflandırılmaktadır. Şekil 5 incelendiğinde, meydana gelen en fazla iş kazalarının %32,45'inin "listelenmemiş başka araçlardan", %31,50'sinin de "malzeme, nesne, ürün, makine aksamı, enkaz, tozdan" kaynaklandığı görülmektedir. Şekil 6'da 2013-2020 yılları arasında meydana gelen iş kazaları sonucunda yaralanan bölgenin vücuttaki yerlerinin dağılımları verilmiştir.



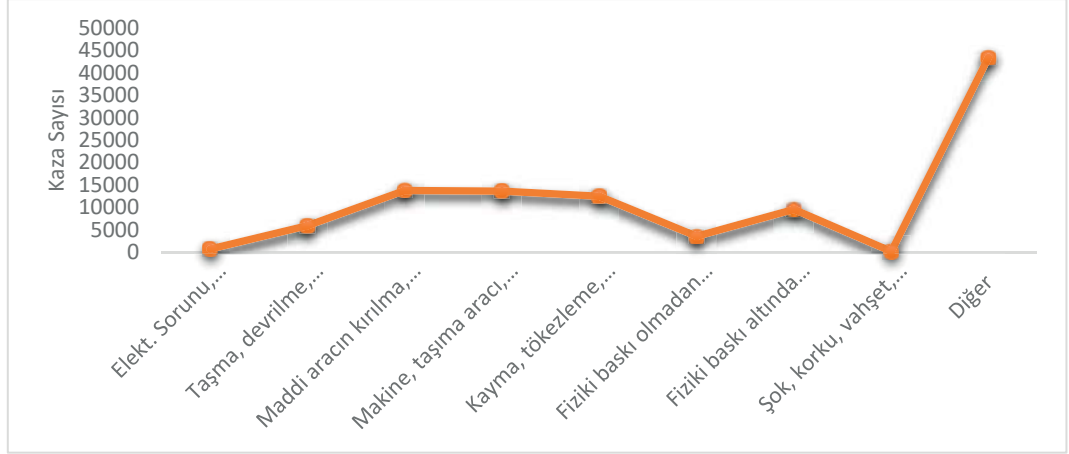
Şekil 6. Yaralanın vücuttaki yerinin dağılımları

En fazla yaralanan vücut bölgelerinin, diğer vücut bölgelerine göre %35,6 oranında kollarda ve %24,3 oranında bacaklarda olduğu gözlenmektedir. Şekil 7, 2013-2020 yılları arasındaki iş kazaları sonucunda oluşan yaralanmaların türünün dağılımlarını göstermektedir.



Şekil 7. Yaralanın türünün dağılımları

İş kazası sonucunda meydana gelen yaralanın türü 14 farklı grupta ele alınmaktadır. İş kazası geçiren çalışanlarda oluşan en fazla yaralanma türünün %53,35' inin yüzeysel yaralanmalar olduğu görülmektedir. 2013-2020 yılları arasında meydana gelen iş kazalarına sebep olan olayların dağılımı Şekil 8'de verilmiştir.



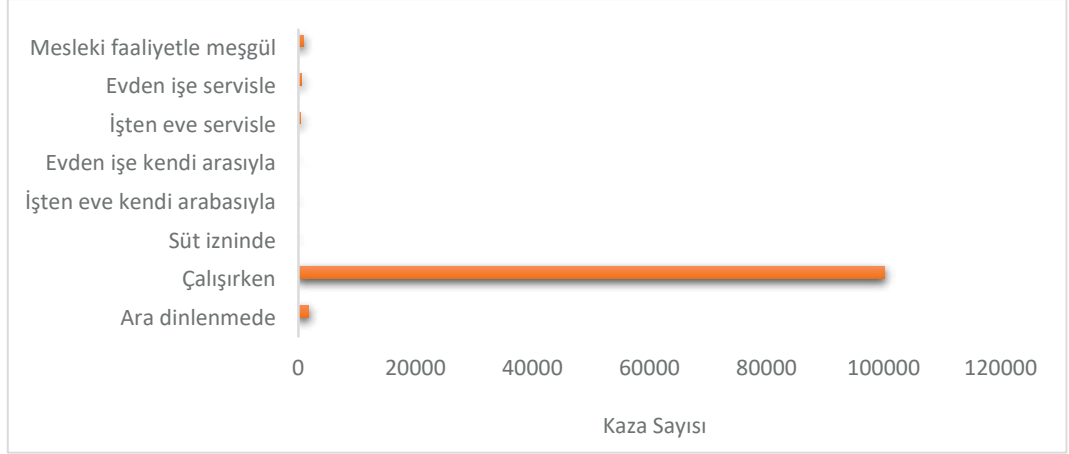
Şekil 8. Kazaya sebep olan olayların dağılımı

SGK iş kazası bildirim formunda kazaya sebep olan olayları 9 farklı grupta kayıt altına almaktadır. Şekil 8’deki grafik incelendiğinde, “diğer” yani “bu sınıflandırmada listelenmemiş başka sapma” grubunda bulunan kazalar diğer gruplara göre %41,91 oranında daha fazladır. Bunun nedeninin form doldurulurken yanlış veya dikkatsizce doldurulduğu düşünülebilir. Bunun dışında, kazaya sebep olan olaylar arasında fazla sayıda kaza bulunan gruplardan; %13,30’ u “maddi aracın kırılma, patlama, ayrılma, kayma, düşme, çökmesi”, %13,19’ u “bir makinenin, taşıma aracının veya işleme ekipmanının, elle kullanılan alet, nesne, hayvanın denetimden çıkması (tam veya kısmi)” ve %12’ si “kayma veya tökezleme, düşme, kişilerin düşmesi” dir. 2013-2020 yılları arasında meydana gelen iş kazalarının çalışılan ortama göre dağılımları Şekil 9’da gösterilmiştir.



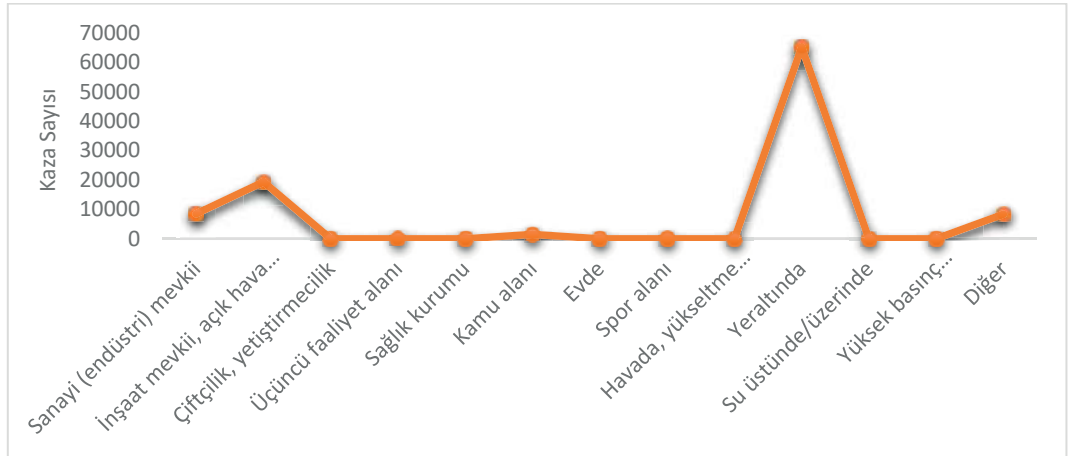
Şekil 9. Çalışılan ortama göre dağılım

İncelendiğinde, madencilik sektöründe meydana gelen toplam iş kazalarının %56,23’ü çalışanın sürekli olarak çalıştığı sabit işyerinde, %29,75’i diğer çalışılan ortamda, %10,59’u geçici işyerinde (görevlendirme, iş seyahati vb.) ve %3,42’si belirtilmemiş ortamda meydana geldiği görülmektedir. Şekil 10’da iş kazalarının gerçekleştiği ortama göre dağılım verilmiştir.



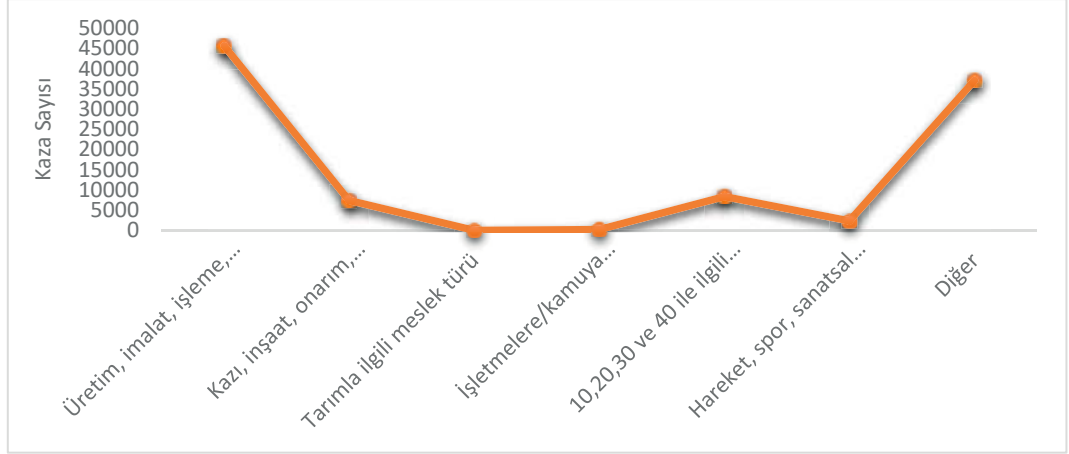
Şekil 10. 2013-2020 yılları arasında meydana gelen iş kazalarının gerçekleştiği ortama göre dağılımları

SGK iş kazası verilerinin kaydını tutarken, iş kazalarının gerçekleştiği yeri “işyeri” ve “işyeri dışında” olarak ayırmaktadır. Ara dinlenme ve çalışırken olan kazaları işyerinde, bunların dışında kalanları ise işyeri dışında olarak kabul etmektedir. Şekil 10 incelendiğinde; çalışırken ve ara dinlenmede olan kazalar sırasıyla, toplam kazaların %96,40’ını ve %1,72’sini oluşturduğu görülmektedir. Burada, “evden işe kendi arabasıyla” ve “işten eve kendi arabasıyla” grupları altında bulunan kazaların, 5510 sayılı kanunun 13. maddesine göre iş kazası kapsamına girmemesinden dolayı kayıtlarının tutulması gerekmemektedir (SSGSK, 2006). İşveren tarafından sağlanan bir taşıt ile yapılması durumunda iş kazası olarak kaydı tutulabilir. 2013-2020 yılları arasında meydana gelen iş kazalarının Şekil 11’de kazanın gerçekleştiği yer/bölüme ait dağılımları yer almaktadır.



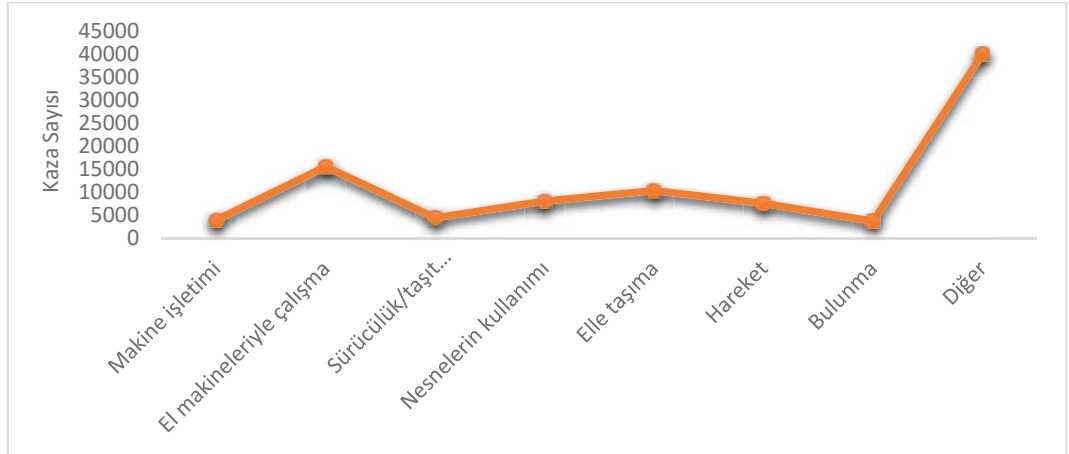
Şekil 11. 2013-2020 yılları arasında meydana gelen iş kazalarının gerçekleştiği yer/bölüm göre dağılımları

İş kazalarının gerçekleştiği yer/bölüm, SGK tarafından 13 ayrı grup altında ele alınmaktadır. Bakıldığında, toplam kazaların %62,80’inin yeraltında ve %18,61’inin açık hava madeni grubunda meydana geldiği görülmektedir. Ayrıca “evde” yani işyeri dışında meydana gelen ve iş kazası kapsamına girmeyen kazaların kayıtlarının tutulması gerekmemektedir. Şekil 12’de 2013-2020 yılları arasında meydana gelen iş kazalarında kazazedenin kaza anında yürütmekte olduğu genel faaliyete göre dağılımları verilmiştir.



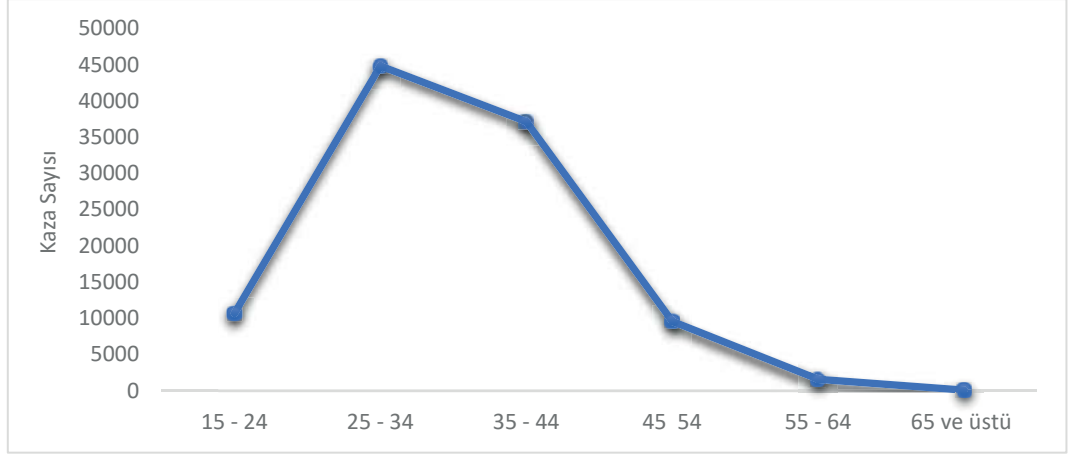
Şekil 12. Kazazedenin yürütmekte olduğu genel faaliyete göre dağılım

Yürütülmekte olan bu genel faaliyetler 7 grup altında değerlendirilmektedir. En fazla iş kazasının meydana geldiği üretim, imalat, işleme, depolama faaliyetlerinde gerçekleşen kazaların, toplam iş kazalarına göre %43,9 oranında olduğu görülmektedir. “Diğer” faaliyetler esnasında meydana gelen kazalar ise %35,80 oranındadır. Bu oranın fazla olmasından dolayı neler olduğunun ayrıntılı olarak bakılması gerekebilir. 2013-2020 yılları arasında gerçekleşen iş kazalarında, kazadan az önceki zamanda kazazedenin yürüttüğü özel faaliyetlerin dağılımları Şekil 13’te verilmektedir.



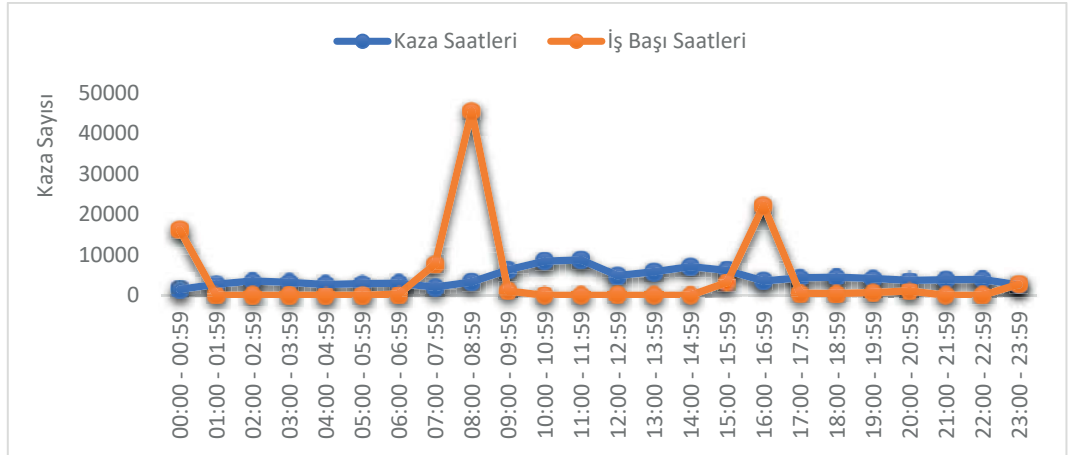
Şekil 13. Kazazedenin yürütmekte olduğu özel faaliyete göre dağılım

Bu yürütülen özel faaliyetler 8 grupta ele alınmaktadır. Şekil 13 incelendiğinde, en fazla kazanın %38,65 oranla diğer (sınıflandırmada listelenmemiş başka kaza anında kazazedenin yaptığı faaliyet) grubunda olduğu gözlenmektedir. Bunun dışında toplam kazaların, %15’i el makineleriyle çalışma, %10’u elle taşıma, %7,82’si nesnelerin kullanımı, %7,35’i hareket, %4,37’si sürücülük/taşıtlarında bulunma, %3,84’ü makine işletimi ve %3,63’ü bulunma faaliyetlerinde olduğu görülmektedir. Diğer grubunda bulunan kazaların sayısının çok daha fazla olmasından dolayı bu grup içerisinde yer alan özel faaliyetler incelenmelidir. Şekil 14, madencilik sektöründe 2013-2020 yılları arasında iş kazası geçiren çalışanların yaşlarına göre dağılımlarını göstermektedir.



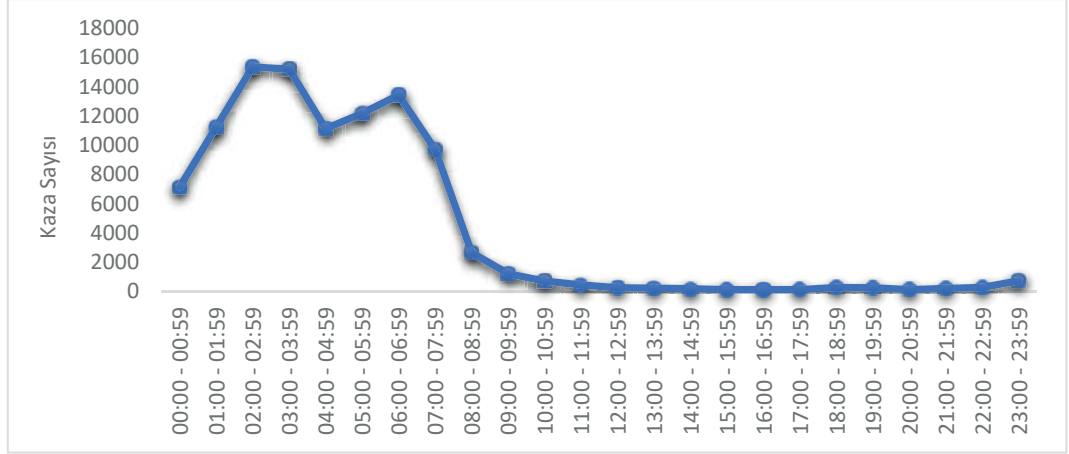
Şekil 14. Çalışanların yaşlarına göre dağılım

2013-2020 yılları arasında en fazla iş kazası geçiren çalışanların %43,15'inin 25-34 yaş aralığında ve %35,75'inin 35-44 yaş aralığında olduğu görülmektedir. 2013-2020 yılları arasında meydana gelen iş kazalarının, kazaların oluş saatlerine göre dağılımları Şekil 15'te görülmektedir.



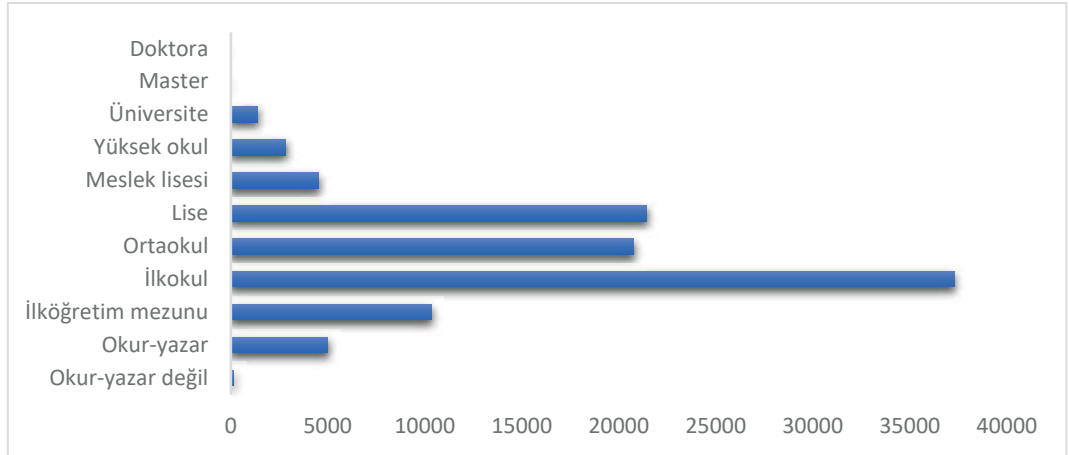
Şekil 15. İş kazalarının meydana geldiği saatler ve kaza günü iş başı saatlerinin dağılımları

Saat dilimleri ESAW Standartlarına ve SGK istatistiklerine bakılarak gruplandırılmıştır. Yukarıdaki şekilde en fazla kazanın gerçekleştiği saat dilimlerine bakıldığında, toplam iş kazalarına göre 10:00-10:59 ile 11:00-11:59 saatleri aralığında meydana gelen iş kazalarının sırası ile %8,15 ile %8,46 oranında olduğu görülmektedir. Bunun sebebi öğlen yemeği molasına yaklaştıkça çalışanların acıkmalarından kaynaklanabilecek dalgınlıklardan olduğu düşünülebilir. Şekil 17'de 2013-2020 yılları arasında gerçekleşen iş kazalarının, kazanın olduğu gün iş başı saatlerine göre dağılımları verilmiştir. Bakıldığında, %43,93'ünün 08:00-08:59 arası saatlerde, %21,45'inin 16:00-16:59 arası saatlerde ve %15,67'sinin ise 00:00-00:59 arası saatlerde iş başı yaptığı görülmektedir. Madencilik sektöründe, genellikle ikili veya üçlü vardiya sistemleri şeklinde çalışma yapılmaktadır. İlk vardiya 08:00-16:00, ikinci vardiya 16:00-24:00 ve varsa eğer üçüncü vardiya 24:00-08:00 saatleri arasında olabilir. Bu sebeple, yüzdelerin fazla olduğu saat dilimleri, bu vardiya başlangıç saatlerine denk gelmektedir. Şekil 16'da 2013-2020 yılları arasında iş kazası geçirmiş olan çalışanların, kaza günü iş başı saatleri ile kazanın meydana geldiği saat arasındaki farkların dağılımları gösterilmektedir.



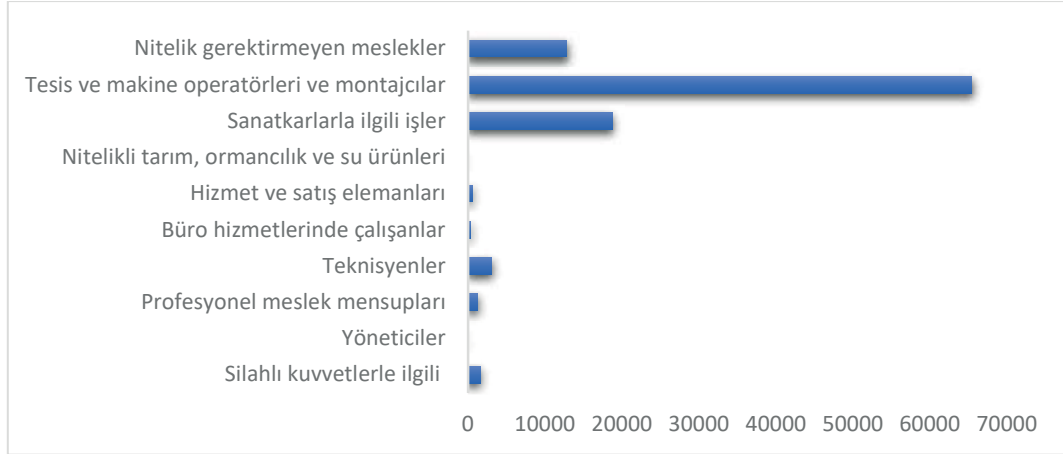
Şekil 16. İş başı saati ile kaza saati arasındaki farkın dağılımları

Meydana gelen kazalarda, en fazla %14,80'inin işe başladıktan ikinci saat diliminde (02:00-02:59) ve %14,65'inin üçüncü saat diliminde (03:00-03:59) gerçekleştiği görülmektedir. 2013-2020 yılları arasında iş kazası geçiren çalışanların öğrenim durumlarına göre dağılım Şekil 17'de verilmiştir.



Şekil 17. Çalışanların öğrenim durumlarına göre dağılım

İş kazası geçiren çalışanlar arasından %35,9'u ilköğretim mezunu, %20,6'sı lise ve %20'si de ortaokul mezunu olduğu görülmektedir. Eğitim seviyesinin artması ile kaza geçiren çalışan sayısının azaldığı gözlenmektedir. Ancak madencilik sektöründe toplam çalışan sayısının öğrenim durumu göz önüne alındığında, yüksek öğrenim mezunu çalışan sayısının da az olabileceği düşünülmelidir. Şekil 18, 2013-2020 yılları arasında iş kazası geçirmiş olan çalışanların meslek gruplarına göre dağılımlarını vermektedir.



Şekil 18. Çalışanların meslek gruplarına göre dağılımları

Çalışanların mesleklerine göre yapılan incelemeler, genel bir sınıflandırma olarak ele alınmıştır. Şekil 18'e göre en fazla iş kazası geçirmiş çalışanların, %63'ünün tesis ve makine operatörleri ve montajcılar grubundan olduğu görülmektedir. Bunun sebebi ise madenci, kazmacı, iş makinesi operatörü, kamyon şoförü, mermer ocakçısı ve yeraltı maden işletmesi hazırlık elemanı gibi mesleklerin bu grup altında bulunmasıdır.

SONUÇ VE TARTIŞMA

Madencilikte ortam şartlarının sürekli olarak değişmesinden dolayı iş kazalarının meydana gelmesinin önüne geçilememektedir. Ortam şartları dışındaki iş kazalarının asıl sebeplerinin neler olduğunun tespit edilmesi durumunda kazalar önlenabilir veya azaltılabilir. Bunun içinde geçmiş kaza kayıtlarından faydalanılmalıdır. Bu çalışmada, işverenlerin SGK'ya bildirmek zorunda oldukları iş kazası bildirim formları kullanılmıştır. SGK, 2013 yılından itibaren iş kazası bildirim formlarını elektronik ortamda ve ESAW'a uygun şekilde kayıt altına almaktadır. Bu nedenle 2013 yılından 2020 yılı da dahil olmak üzere tüm madencilik faaliyet sınıflamasına giren iş kazası verileri kullanılmıştır.

Madencilik sektörlerine ait 103.815 adet iş kazası verileri incelendiğinde, kazaların %68,87'si kömür ve linyit çıkarılması faaliyet sınıfında meydana gelmiştir. Meydana gelen iş kazalarından yaralanmalı, ölümlü ve uzuv kayıplı olarak sonuçlanmış olanlar vardır. Ölümlü iş kazalarının %56,76'sı kömür ve linyit çıkarılması, uzuv kayıplı iş kazalarının %45,12'si diğer madencilik ve taş ocakçılığı ve yaralanmalı iş kazalarının %71,13'ü kömür ve linyit çıkarılması faaliyet sınıfındadır. İş kazalarının %18,38'i hareket halindeki bir nesnenin çarpması, çarpışması sonucunda yaralanmaya neden olmuştur. İş kazalarının %31,50'si malzeme, nesne, ürün, makine aksamı, enkaz, tozdan kaynaklanan yaralanmaya neden olan araç/gereçlerdendir. İş kazalarının %35,6'sı kollardan ve %24,3'ü bacaklardan yaralanma ile sonuçlanmaktadır. İş kazaları sonucunda %53,35 oranında yüzeysel yaralanmalar meydana gelmiştir. İş kazalarında kazaya sebep olan olaylara bakıldığında %13,30'u maddi aracın kırılması, patlaması, ayrılması, kayması, düşmesi, çökmesinden, %13,19'u bir makinenin taşıma aracının, işleme ekipmanı, elle kullanılan alet, nesne, hayvan gibi denetimden çıkması sonucunda meydana gelmiştir. İş kazalarının %96,40'ı çalışırken meydana gelmiştir. İş kazalarından %56,23'ü çalışanın sürekli olarak çalıştığı sabit işyerinde kaza geçirmiştir. İş kazalarının %62,80'i yeraltında ve %18,61'i açık ocak madenlerinde gerçekleşmiştir. İş kazası esnasında kaza geçirmiş çalışanların %43,9'u üretim, imalat, işleme, depolama gibi genel faaliyetleri yürütmektedir. İş kazası meydana gelmeden az önceki zamanda kaza geçirmiş çalışanların %15'i el makineleriyle ve %10'u elle taşıma özel faaliyetlerini yürütmektedir. İş kazası geçiren çalışanların %43,15'i 25 – 34 ve %35,75'i 35 – 44 yaş aralığında yer almaktadır. İş kazalarının %8,15'i 10:00 – 10:59 ve %8,46'sı 11:00 – 11:59 saat aralıklarında meydana gelmiştir. İş kazası geçirenlerin %43,93'ü 08:00 – 08:59, %21,45'i 16:00 – 16:59 ve %15,67'si 00:00 – 00:59 saat aralığında iş başı

yapmıştır. Meydana gelen kazalar iş başı yaptıktan ikinci veya üçüncü saat diliminde gerçekleştiği görülmektedir. İş kazası geçiren çalışanların %35,9'u ilkökul, %20,6'sı lise ve %20'si de ortaokul mezunu olduğu görülmektedir. İş kazası geçirmiş çalışanların %63'ünün tesis ve makine operatörleri ve montajcılar grubundan olduğu görülmektedir.

Sonuç olarak iş kazalarının sebepleri, yaralanmanın büyüklüğü, türü ve nasıl olduğu gibi etkenlerin incelenmesi, iş kazalarının tekrarlanmaması veya önlenmesi açısından önemlidir. Madencilik sektöründe iş kazası geçiren çalışanların çoğunun öğrenim durumlarının yüksek olmaması ve en fazla kazanın da üretim vb. faaliyetlerde gerçekleşmiş olmasından dolayı, çalışanların yapacakları işe uygun öncelikle etkin bir mesleki eğitim ve işyerinde davranış değişikliğini hedefleyen iş sağlığı ve güvenliği eğitimlerinden geçmeleri oldukça önemlidir. Çalışanlarda iş güvenliği kültürünün oluşması ile ilerleyen yıllarda iş kazalarında belirgin azalmalar kaydedilecektir.

KAYNAKLAR

Bilim, N., DüNDAR, S. ve Bilim, A. (2018). Ülkemizdeki Maden Sektöründe Meydana Gelen İş Kazası ve Meslek Hastalıklarının Analizi. *BEÜ Fen Bilimleri Dergisi* 7 (2), 423-432.

ESAW. (2013). European Statistics on Accidents at Work – Summary Methodology. Publications Office of the European Union, Luxembourg.

Kılıç, A. M., Kahraman, E. ve Kılıç, Ö., (2018). Türkiye Kömür Madenciliğinde Ölümlü İş Kazalarının Değerlendirilmesi. M. E. Bilir, M. Geniş, H. Duru, U. Sakız & K. Kel (Eds.), Türkiye 21. Uluslararası Kömür Kongresi Bildiriler Kitabı (s. 449-458).

Oral, T. (2021). 2012-2019 Yılları Arasında Maden Sektöründe Yaşanan İş Kazalarının Analizi ve ÇKKV Yöntemlerinin Katkısı. *Bilim, Teknoloji ve Mühendislik Araştırmaları Dergisi* 2(2): 101-109.

Önder, M., Önder S., Mutlu, M. ve Adıgüzel, E. (2015). Yerüstü Kömür Madenlerindeki Gün Kayıplı İş Kazalarının Loglineer Model ve Uyum Analizi ile İncelenmesi. Ö. Kılıç, A. M. Kılıç, M. Altınar & M. Yılmaz (Eds.), Maden İşletmelerinde İşçi Sağlığı ve İş Güvenliği Sempozyumu (s. 163-180).

Sosyal Güvenlik Kurumu Veri Yönetimi Daire Başkanlığı. (2021). Madencilik Sektörüne ait Veriler, Ankara

Sosyal Sigortalar ve Genel Sağlık Sigortası Kanunu, (2006). <https://www.mevzuat.gov.tr/mevzuat?MevzuatNo=5510&MevzuatTur=1&MevzuatTertip=5>

Şensöğüt, C., Ören Ö. ve Kasap Y. (2019). Garp Linyitleri İşletmesinde Son Yıllarda Meydana Gelen İş Kazalarının Analizi. *M C B Ü Soma Meslek Yüksekokulu Teknik Bilimler Dergisi* 28 (I), 13-19.

Yıldırım, H. (2009). Kapalı Devre Suni Solunum Sağlayan Cihazlar. A. M. Kılıç & Ö. Kılıç (Eds.), Maden İşletmelerinde İş Sağlığı ve Güvenliği Sempozyumu Bildiriler Kitabı (s. 273-280).

A COMPUTATIONAL ALGORITHM TO PERFORM PROBABILISTIC SAMPLING FOR MINERAL ASSAY DETERMINATION

M. Camalan

Ankara, Turkey
(camalanmahmut@gmail.com)

ABSTRACT

Mineral assay or grade of a population of particles are measured from the subsets or samples. However, sampling is prone to several sources of errors, which are impossible to determine exactly through physical surveys. A computational algorithm is presented to simulate probabilistic sampling surveys on a particle population. The use of the algorithm can lead to a true comparison between a population and its samples as the particle properties (particle size, mass, mineral grade) are known in both. The algorithm was tested on the populations with binary mineral mixtures. Although the simulated variances in sample grades are related to the fundamental sampling errors, the effect of particle size distribution on these errors may not be foreseen in Gy's equation. Some sampling methods may be susceptible to severe errors that are not related to probabilistic sampling. Also, the simulation results provide some insights for the probabilistic sampling surveys.

Keywords: Mineral, grade, probabilistic sampling, variance, simulation

INTRODUCTION

Mineral assay or grade can be broadly defined as the mass content (%) of a target mineral in a population of ore particles. The correct determination of the mineral grade is necessary not only for the mineral process design but also for the periodic monitoring of the process. The mineral grade is determined from the subsets of the particle population, which are called samples. They are collected by following sophisticated sampling protocols that aim to decrease the differences between the population and sample grade to an acceptable degree. The associated differences appear because of (i) the sampling errors by the composition heterogeneity of the population that even distribute both spatially and temporally, as well as (ii) the errors at sample preparation and analysis. These errors had been conceptually defined by Gy (1976), and later revised by the same author (Gy, 1979, 1992). Even it is impossible to avoid the fundamental sampling errors (FSE) unless (i) the samples are identical to the population or (ii) there is no composition heterogeneity (Gy, 1992; Pitard, 2019). Therefore, it is necessary to evaluate how sampling protocols and the associated errors affect the sample quality. The true evaluation, however, requires the comparison between the mineral grades of a population and its samples, which is always impossible as the former cannot be known.

This study proposes a computational algorithm that can simulate sampling surveys on any dataset of particle population containing particle properties such as particle size, shape factor, mineral composition, etc. The algorithm collects the samples by selecting and extracting the particle data from the population dataset. The particle selection in the proposed algorithm is probabilistic (equiprobable), i.e., each particle has the same probability to be selected into the sample. The algorithm can be used to simulate sampling surveys on the population. As the particle properties are known in a population and its simulated samples, they can be exactly compared without performing physical sampling surveys and rigorous statistical treatments.

The algorithm was used to simulate samples from the populations of binary mineral mixtures. Then, the mineral grades of the simulated samples were evaluated with the mineral grade of their population. As the particle selection in sampling simulations was probabilistic, the differences between a population and its simulated samples should be related to FSE, which is the error of equiprobable sampling (Gy, 1992). However, the simulated samples may not reflect the errors due to (i) spatial/temporal heterogeneity of the population and (ii) sample preparation/analysis.

METHODOLOGY

Generation of the Particle Population

The population of the ore particles consisted of binary mixtures of pyrite (density = 5 g/cm³) and chalcopyrite (4.2 g/cm³) minerals. The mass of the generated populations was set at 25-100 kg. The mass-weighted size distributions of the particle populations were generated by using the GGS (Eq.1) or RRB (Eq.2) distributions:

$$F_{mass}(x) = \left(\frac{x}{k}\right)^n \quad (1)$$

$$F_{mass}(x) = 1 - \exp\left(-\left(\frac{x}{k}\right)^n\right) \quad (2)$$

where $F_{mass}(x)$ is the mass percent passing below the screen size of x , k and n are the size and distribution moduli, respectively. The k values for GGS and RRB were set at 25.4 and 9.53 mm, respectively. The n value of either distribution varied between 0.5 and 4. The populations generated from any GGS and RRB distribution are described as the GGS and RRB population, respectively, throughout the text.

The discrete size distributions of the populations were calculated from F_{mass} :

$$f_{mass}(i) = F_{mass}(x_i) - F_{mass}(x_{i+1}) \quad (3)$$

where $f_{mass}(i)$ is the mass percentage of the size interval i , $F_{mass}(x_i)$ and $F_{mass}(x_{i+1})$ are the mass percentages passing below the upper (x_i) and lower (x_{i+1}) screens of the size interval i , respectively. The ratio between the upper and lower screens of each size class, except the finest size fraction (pan), was nearly equal to $\sqrt{2}$. The upper and lower screens of the sink size fraction were set at 1.18 and 0 mm, respectively. The $f_{mass}(i)$ in Eq.3 was multiplied with the population mass to determine the total mass of particles in the size class i . Then, random particles were generated in the size class i :

$$x_{(i)} = (x_i - x_{i+1}) * U(0,1) * +x_{i+1} \quad (4)$$

Where $x_{(i)}$ is the diameter of a random particle in the size class i , and $U(0,1)$ is a pseudorandom real number uniformly distributed in an open interval between 0 and 1. The pseudorandom number was generated by using MATLAB's built-in RAND function based on the Mersenne-Twister algorithm (Matsumoto and Nishimura, 1998). The random particle generation was performed for each size class as long as the total mass of the generated particles was smaller than the mass of the respective size class:

$$\sum_{j(i)} [x_{j(i)}^3 * (\rho_{py} * (100 - g_{j(i)}) + \rho_c * g_{j(i)}) / 100] < f_{mass}(i) \quad (5)$$

where $x_{j(i)}$ and $g_{j(i)}$ are the diameter and chalcopyrite grade of the j^{th} random particle in the size class i , respectively, while ρ_{py} and ρ_c are the pyrite and chalcopyrite densities, respectively. No

shape factor was used to calculate particle volumes assuming that random particle generation imposed a wide distribution of the particle shape.

The chalcopyrite was distributed to the population particles, based on the rule that the chalcopyrite grades of particles followed the normal distribution. To distribute the chalcopyrite in a population, normal random grades were assigned to all particles by using MATLAB's built-in NORMRND function with a mean grade of 6 % and a standard deviation (σ) of 2. The σ was calculated from the smallest of the differences from the mean grade to grade limits (0 %, 100 %), which was further set at 3σ . The calculated σ ensured that the normal random grade could mostly fall between the grade limits due to the three-sigma rule (Pukelsheim, 1994). Nevertheless, when the random grade was lower than 0 % or higher than 100 %, the respective grade was set to the nearest grade limit.

Simulation of the Sampling Algorithm

The diameters, masses, and mineral grades of the particles in a particle population (Section 2.1) were stored in a matrix where each row included the corresponding data of a single particle. Then, a sampling survey was performed on the population matrix by selecting the data of population particles one-by-one. Each particle selection was performed by using MATLAB's built-in RANDI function based on the Mersenne-Twister algorithm (Matsumoto and Nishimura, 1998): The function generated a random integer index from the row indices of the population matrix. The particle data at the index was carried from the population to the sample matrix. Then, the same data in the population matrix was changed to zero. This ensured that when a particle was carried from the population to the sample, it could be only re-added to the sample as a dummy particle. Instead, the carried particle could have been removed from the population matrix, yet this process would reduce the computational speed severely. After the simulation had ended, the data of dummy particles were removed from the sample matrix by using logical operators and indexing.

The selection and carriage of the population particles to a sample were repeated as long as the total sample mass was smaller than the threshold sample mass (% mass of the population). Then, the sample grade was calculated from the sample matrix:

$$\text{Sample Grade (\%)} = 100 * \frac{\sum_k [x_k^3 * (\rho_c * g_k)]}{\sum_k [x_k^3 * (\rho_{py} * (100 - g_k) + \rho_c * g_k)]} \quad (6)$$

where x_k and g_k are the diameter and chalcopyrite grade (%) of the k^{th} particle in the sample, respectively. The variance in the chalcopyrite grades of the simulated samples was calculated with respect to the population grade:

$$\text{Sample Variance} = \frac{\sum_s^N (g_s - g_{pop})^2}{N} \quad (7)$$

where g_s is the chalcopyrite grade (%) of the s^{th} sample, g_{pop} is the chalcopyrite grade (%) of the population, N is the number of simulated samples. The sample variances were calculated by simulating and evaluating 100 samples from the populations. Also, some additional simulations were conducted to test whether changing the number of samples affected the calculated sample statistics. Figure 1, for example, showed the sample variances, which are estimated after simulating up to 10,000 samples from a GGS population ($n=2$, $k=25.4$ mm). The figure suggests that the sample variances are similar, regardless of the number of samples evaluated. Therefore, changing the number of probabilistic samples does not affect the calculated sample variance.

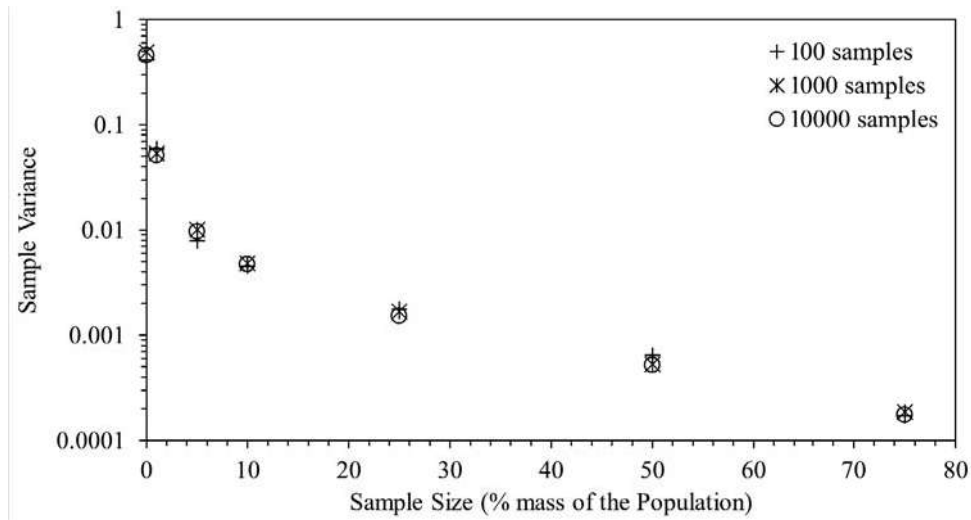


Figure 1. The simulated sample variances from a GGS population ($n=2, k=25.4$ mm), which are estimated from 100-10000 samples. The samples are taken from the population at unequal masses. The population mass = 100 kg.

RESULTS AND DISCUSSION

Figure 2 shows the mean, maximum and minimum grades of the samples, which are simulated from the GGS or the RRB populations with varying n . The figure suggests that the mean grades of samples are quite similar, but they are not numerically equal to their respective population grade. The result is consistent with Gy's postulation that the mean of the FSE, which is the error of equiprobable sampling, cannot be zero (Gy, 1992). Meanwhile, the distance between the maximum and minimum sample grades varies as a function of the population's size distribution: If the samples are simulated from the GGS populations with increasing n , the distance seems to expand (Figure 2a), suggesting higher variation in sample grades. If the samples are simulated from the RRB populations with increasing n , the difference will funnel (Figure 2b), showing smaller variation in the sample grades. Figure 3 also shows the sample variances, which are estimated after simulating samples from the RRB or the GGS populations with varying n . The figure suggests that the samples from the RRB populations, unlike the ones from the GGS populations, yield smaller sample variance as the n of the population increases. Gy's equation adopts the particle size range as a variable affecting the FSE variance (σ_{FSE}^2):

$$\sigma_{FSE}^2 = \left(\frac{1}{m_s} - \frac{1}{M}\right) * c * L * f * r * d^3 \tag{8}$$

where m_s is sample mass, M is the lot or population mass being sampled, d is the nominal size (95 % passing screen size) of the coarsest particle in the lot, c, L, f, r are the composition, liberation, shape, and size range factors, respectively. It is postulated that the r term in Eq.5 decreases as the ratio between d and the nominal size of the finest particle, i.e., 5 % passing screen size, increases (Gy, 1979; Wills and Finch, 2016). In other words, Eq.8 imposes that the narrower spread of particle sizes, equivalently higher n , should yield higher r and thus higher σ_{FSE}^2 . However, wider GGS populations should yield higher sample variances, as discussed early, and demonstrated in Figure 3. Therefore, the sample variances can also depend on the nature of the particle size distribution, which may not be foreseen in Gy's equation.

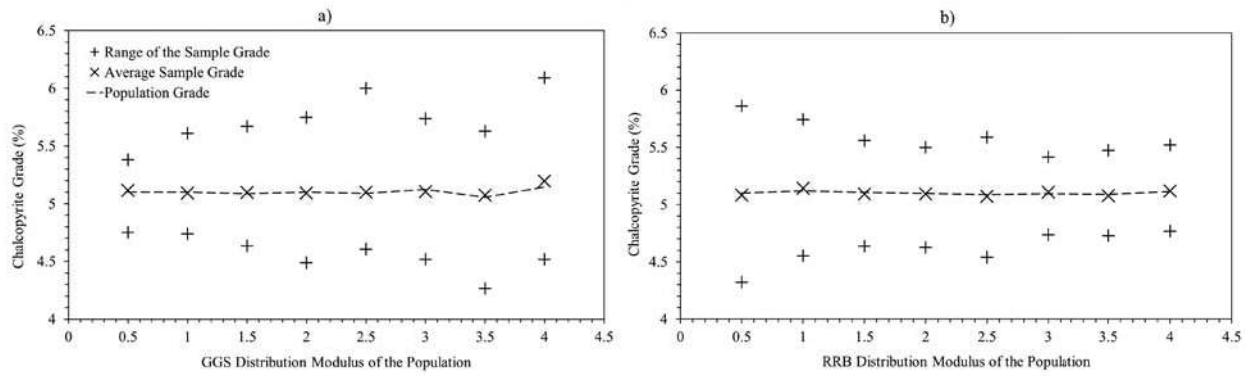


Figure 2. The mean, maximum, and minimum chalcopyrite grades of the samples, simulated from the GGS (a) or the RRB populations (b) with varying n . Population mass = 100 kg, sample size = 1 % mass of the population, number of samples = 100.

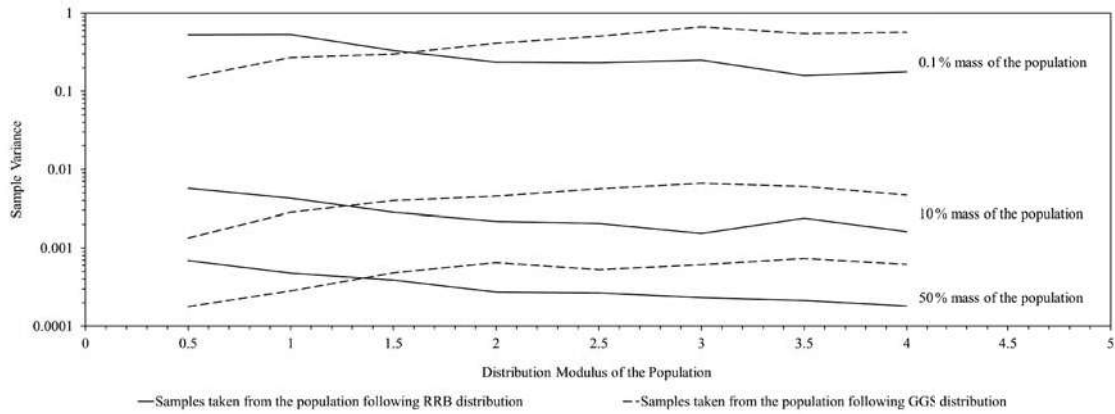


Figure 3. The sample variances that are estimated after simulating samples from the RRB or the GGS populations with varying n . The samples are taken from the populations at unequal masses. Population mass = 100 kg, number of samples = 100.

Figure 4 demonstrates the sample variances that are estimated after simulating samples of unequal masses from the GGS populations with varying n . The figure shows that taking larger samples from the GGS populations should decrease the sample variance as larger samples approach the population. Also, the sample variance can be adequately estimated by using a power function (dashed lines in Figure 4) of sample mass with an exponent of -1.16. This function is comparable with the inverse proportionality between σ_{FSE}^2 and m_s in Gy's Equation (Eq.8). Meanwhile, Figure 4 points out a rapid escalation of the sample variance when the sample size is reduced under 10-15 % mass of the population. Sampling surveys on a binary sand mixture suggested that equal-sized samples by rotary riffing yield lower sample error than the halved mixture by chute riffing or the quartered mixture by coning-quartering (Allen, 2003). These results contradict the fact that larger samples must yield less variance after probabilistic sampling, as observed in Figure 4. Therefore, the author suspects the presence of severe sampling errors on the above methods, which should not be related to probabilistic sampling.

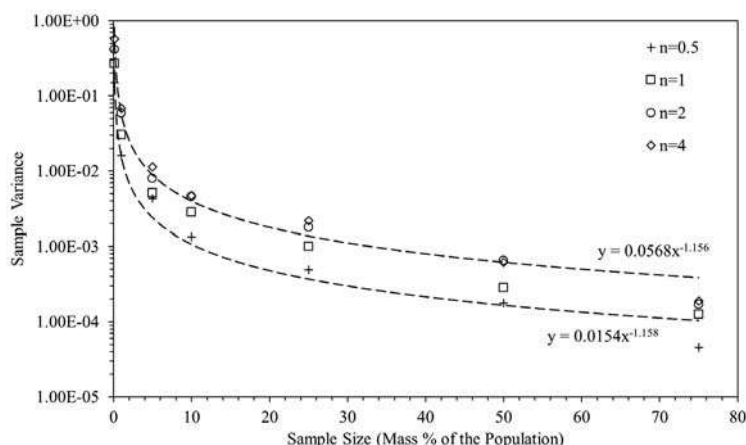


Figure 4. The sample variances that are estimated after simulating samples from the GGS populations with varying n . The samples are taken from the populations at unequal masses. Population mass = 100 kg, number of samples = 100. y = sample variance, x = sample size.

As sample variance propagates very fast under a threshold sample size (Figure 5), taking samples smaller than this threshold mass can cause large variances in the sample grades. Then, instead of collecting such samples directly, it may be beneficial to collect them after successive sampling from relatively larger samples. Figure 5, for example, shows the simulated sample variances after successive halving or quartering of the GGS populations with varying n . The results show that quartering produces smaller sample variance only if the population's n is 1.5. However, the successive halving from other populations can produce a smaller or equal variance, as compared to quartering. These results strongly suggest that successive sampling is superior to direct sampling. However, successive sampling can still suffer from the sampling errors: To demonstrate this fact, samples were simulated from the GGS populations of different masses, simply done at a constant ratio between the sample and population mass, i.e., m_s/M . Figure 6 suggests that taking samples from smaller population masses can yield larger sample variances, which will even escalate if the GGS populations have narrower particle size distribution. Such escalation can be well described by a power function (dashed lines in Figure 6) of the population mass, having a negative exponent between -0.9 and -1.2. Gy's equation (Eq. 8) imposes that the σ_{FSE}^2 should be inversely proportional to M at a fixed m_s/M . Therefore, as the mass being sampled reduces at successive sampling, the reduced mass should become more susceptible to sampling errors.

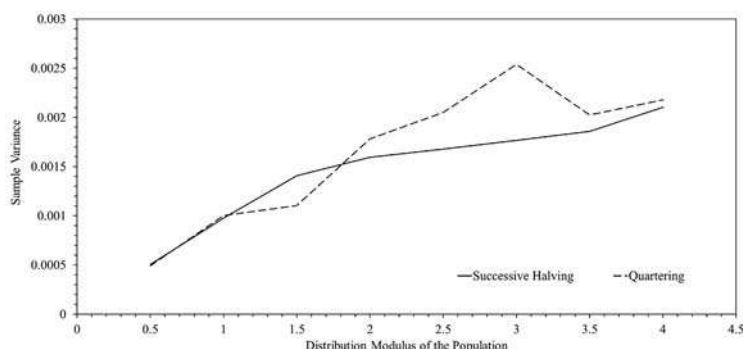


Figure 5. The simulated sample variances after successive halving or single quartering of the GGS populations with varying n . Population mass = 100 kg, sample size = 25 % of the population mass, the number of samples = 100.

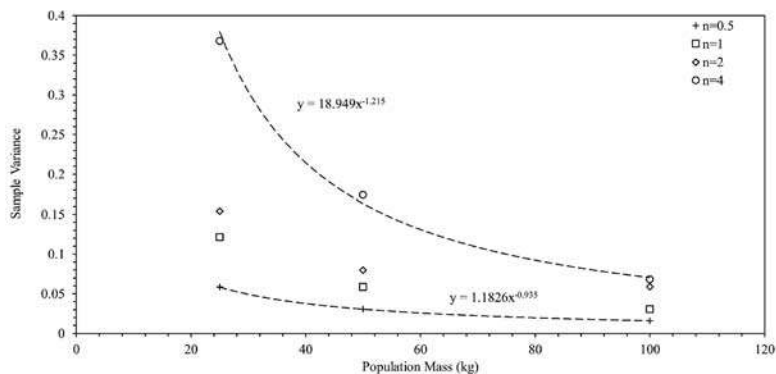


Figure 6. The sample variances that are estimated after simulating samples from the GGS populations with varying n . The populations are generated from unequal masses. Sample size = 1 % of the population mass, number of samples = 100. y = sample variance, x = population mass.

The sampling simulations were conducted on the populations in which chalcopyrite grade was normally distributed in all population particles (Section 2.1). In reality, however, the minerals may be accumulated to specific size fractions in the population, which may bring additional heterogeneity. To assess the impact of this heterogeneity, samples were simulated from a GGS population where chalcopyrite was normally distributed in the finest size fraction. Then, these samples were compared with the ones after chalcopyrite was normally distributed to all population particles. Figure 7 shows that if chalcopyrite is accumulated to the finest size fraction of the population, the sample variances will be 10 to 100 times higher, as compared to the respective variances after chalcopyrite is distributed to all population particles. Therefore, probabilistic sampling becomes inadequate if the target mineral is accumulated to a specific size fraction in the population.

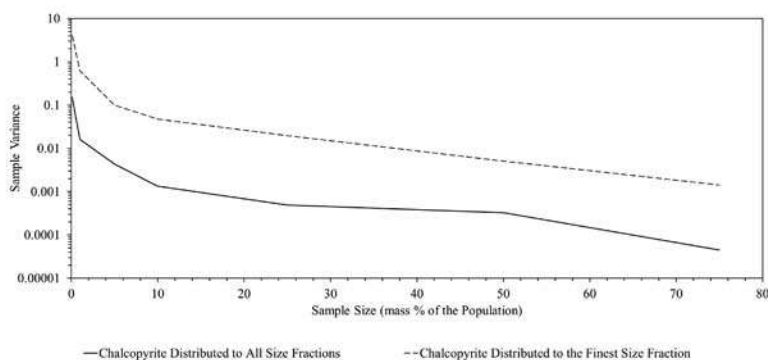


Figure 7. The sample variances that are estimated after simulating samples from the GGS population ($n=0.5$, $k=25.4$ mm, chalcopyrite grade = 5.1 %). The samples are taken from the population at unequal masses. Chalcopyrite is either distributed to all size fractions or the finest size fraction in the population. The population mass = 100 kg, the number of samples = 100.

Most of the sampling simulations were conducted on the populations in which the chalcopyrite grade of each particle was randomly generated from a normal distribution with a mean grade (Section 2.1). Also, additional simulations were conducted to assess the effect of the population’s mineral grade on sample variance. For this purpose, samples were simulated from the GGS populations ($n=0.5$, $k=25.4$ mm) where the chalcopyrite grade of each particle was randomly generated from a normal distribution with varying mean grades. Then the sample variances were plotted as a function of the population grade. As shown in Figure 8, the sample variance yields a bell-shaped curve where the maximum variance is at 45-50 % population grade. It is postulated that the composition variance or σ_{FSE}^2 is

proportional to the product of the grades of the binary compositions (Wills and Finch, 2016): This proportionality causes σ_{FSE}^2 to become maximum at 50 % mineral composition, yet σ_{FSE}^2 will decay to zero as the composition approaches either to 0 or 100 %. Therefore, the bell-shaped curve of sample variance (Figure 8) is consistent with the above postulation, indicating that the probabilistic sampling errors are related to the composition variance. However, as demonstrated in Figure 9, the coefficient of sample variation ($100 * \sqrt{\text{Sample Variance}/g_{pop}}$) cannot reduce as the population grade reduces from 50 % to zero. Then, the sample variance should be high with respect to g_{pop} as the latter approaches to 0 %. Gy (1992) also pointed out that it would be dangerous to accept negligible FSE if the target content in a lot is concentrated below the ppb (part per billion) range. However, the algorithm could not estimate the sample variance when g_{pop} reduced below ppb level, which could be due to the number format used at the computation. Therefore, the algorithm cannot be used to assess if it is safe to accept negligible sample variances at such trace concentrations.

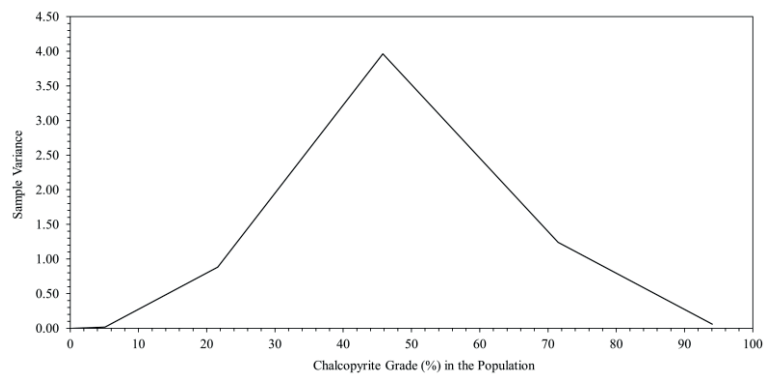


Figure 8. The sample variances from the GGS populations ($n=0.5, k=25.4$ mm) with varying chalcopyrite grades. The population mass = 100 kg, sample size = 1 % mass of the population, the number of samples = 100.

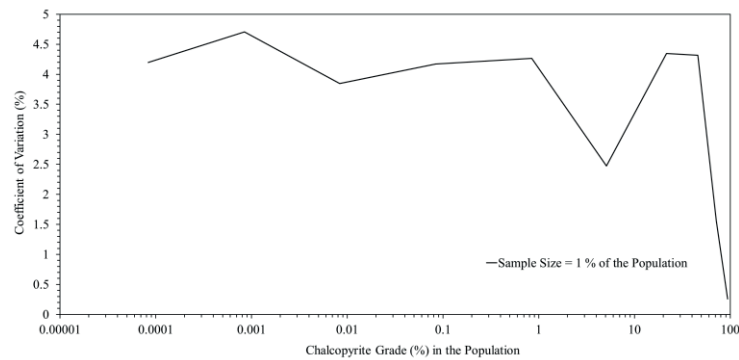


Figure 9. The coefficient of variation in sample grades that are taken from the GGS populations ($n=0.5, k=25.4$ mm) with varying chalcopyrite grades. The population mass = 100 kg, sample size = 1 % mass of the population, the number of samples = 100.

CONCLUSION

A computational algorithm is presented to simulate probabilistic sampling surveys on the datasets of different particle populations. The algorithm can truly assess the impact of probabilistic sampling surveys on estimating the mineral grade of particle populations. The outcomes of this study are as follows:

The variances in simulated sample grades show that the probabilistic sampling errors are related to the composition heterogeneity. However, these variances also depend on the nature of the population's particle size distribution, which may not be foreseen in Gy's equation. Also, as the mineral grade of the population approaches to 0 %, the sample variance should be very high with respect to the population. Some sampling methods may be susceptible to severe errors, which are not related to probabilistic sampling.

The results also provide some insights on probabilistic sampling surveys: Although successive sampling is susceptible to sampling errors, it may be beneficial to collect small samples by successive sampling from relatively larger samples. Probabilistic sampling surveys are inadequate if the mineral of interest is accumulated to a size fraction of the population. The number of samples taken by probabilistic sampling surveys should not affect the sample variance.

REFERENCES

- Allen, T. (2003). *Powder Sampling and Particle Size Determination*. Amsterdam: Elsevier. <https://doi.org/10.1016/B978-0-444-51564-3.X5000-1>
- Gy, P. M. (1976). The sampling of particulate materials — A general theory. *International Journal of Mineral Processing*, 3(4), 289–312. [https://doi.org/10.1016/0301-7516\(76\)90020-X](https://doi.org/10.1016/0301-7516(76)90020-X)
- Gy, P. M. (1979). *Sampling of Particulate Materials Theory and Practice*. Amsterdam: Elsevier.
- Gy, P. M. (1992). *Sampling of Heterogeneous and Dynamic Material Systems: Theories of Heterogeneity, Sampling and Homogenizing*. Amsterdam: Elsevier.
- Matsumoto, M., and Nishimura, T. (1998). Mersenne Twister: A 623-Dimensionally Equidistributed Uniform Pseudo-Random Number Generator. *ACM Transactions on Modeling and Computer Simulation*, 8(1), 3–30. <https://doi.org/10.1145/272991.272995>
- Pitard, F. F. (2019). *Theory of Sampling and Sampling Practice* (Third Edit). Boca Raton: CRC Press.
- Pukelsheim, F. (1994). The Three Sigma Rule. *The American Statistician*, 48(2), 88–91.
- Wills, B. A., and Finch, J. A. (2016). *Wills' Mineral Processing Technology*. Amsterdam: Elsevier.

A COMPUTER APPLICATION MODULE EVALUATING ROCK MASS QUALITY RATING

H.O. Dönmez^{1, *}, H. Tunçdemir¹

¹ *Istanbul Technical University, Mining Engineering Department*
 (*Corresponding author: donmezhu@itu.edu.tr)

ABSTRACT

The Rock Mass Quality Rating (RMQR) classification system has become one of the attractive rock classification systems today, due to its up-to-date and user-friendly nature. When the system was proposed in 2014, correlations were also provided for finding out the equivalents of the rock quality score obtained from the RMQR system in other frequently used rock classification systems like RMR and Q. This option has contributed the system easier to use for researchers and engineers. The RMQR system classifies the rock environment according to 6 basic parameters. The ranges given for these parameters and based on the scoring are the issues that should be carefully considered in determining the rock class. In this study, the ranges used to calculate the RMQR system and the relations that digitize them have been converted into MATLAB functions. Based on these converted functions, a Windows-based computer application module has been coded that basically calculates the RMQR, determines the class of the rock and gives its equivalents in the RMR and Q systems. This module, called "RMQRCalc", is an open source software by using the MATLAB graphical user interface, and is considered as a basic module that is a part of rock classification library to be made in this regard.

Keywords: Rock mass quality rating, computer application module, RMQRCalc.

INTRODUCTION

Rock Mass Quality Rating System (RMQR)

For those who will work in the rock environment, it is important to estimate the mechanical properties of the rock environment such as strength and deformation with the least cost and in the most accurate way. This is because the rock classification systems are developed that describe the characteristics of the rock environment from various parameters. One of the newly developed rock classification systems is the Rock Mass Quality Rating System (RMQR) aimed at estimating the geomechanical properties of rock masses. The RMQR System has been developed to better define the physical state of rock masses, bearing in mind the important parameters used in quantitative contemporary rock mass classification systems and avoiding parameter duplication. The system is based on input parameters such as weathering degree, the number of discontinuity sets, discontinuity range, discontinuity condition, groundwater infiltration, and water absorption conditions. The RMQR values ranging from 0 to 100 are determined from the scores assigned to them (Aydan et al., 2014). The system also defines the relationships by some practical equations that calculate the RMQR value from other commonly used rock classification systems or vice versa.

PROBLEM DEFINITION

Rock classification systems are the useful methods that the practitioners perform in the earth science engineering during the feasibility planning phase. Although many rock classification systems have been proposed until now, a few of them have been widely accepted and are actively used. Based on this phenomenon, it is essential creating an electronic library in which the most used rock

classification systems is brought and processed together. For this library, in the current study, initially, a simple computer application module, RMQRCalc, which evaluates RMQR based on Aydan (2014) is coded by the MATLAB graphical user interface. In Figure 1, the complete parameters and their relevant formulations, rock mass class information, and the code interface are given altogether.

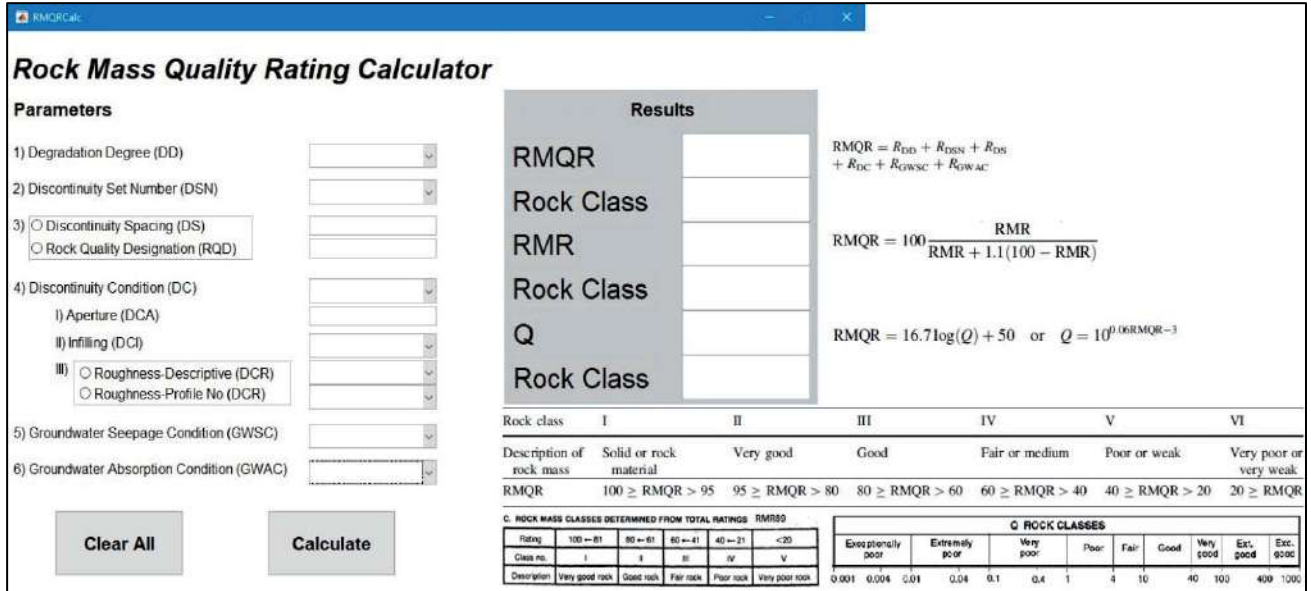


Figure 1. The code interface and parameters in the RMQR calculation based on Aydan (2014)

In RMQR, similar to other rock classification systems, the properties of most parameters are directly selected and rated. While calculating the rock quality in RMQR calculation, 6 parameters in Figure 1 and their corresponding rating values in Figure 2, 3, 4, 5, 6, 7, 8, 9, and 10 are used. These parameters are respectively degradation degree (DD) and R_{DD} , discontinuity set number (DSN) and R_{DSN} , discontinuity spacing (DS) or rock quality designation (RQD) and R_{DS} , discontinuity condition (DC) and R_{DC} , groundwater seepage condition (GWSC) and R_{GWSC} , and Groundwater absorption condition (GWAC) and R_{GWAC} .

1) Degradation Degree (DD)	<div style="border: 1px solid black; padding: 5px;"> <input type="button" value="v"/> <ul style="list-style-type: none"> Fresh Stained Slight degradation Moderate degradation Heavy degradation Decomposed </div>					
2) Discontinuity Set Number (DSN)						
3) <input type="radio"/> Discontinuity Spacing (DS) <input type="radio"/> Rock Quality Designation (RQD)						
4) Discontinuity Condition (DC)						
Degradation degree (DD)	Fresh	Stained	Slight degradation	Moderate degradation	Heavy degradation	Decomposed
Rating (R_{DD})	15	12	9	6	3	1-0

Figure 2. Degradation degree (DD) and rating values (R_{DD})

1) Degradation Degree (DD)

2) Discontinuity Set Number (DSN)

3) Discontinuity Spacing (DS)
 Rock Quality Designation (RQD)

4) Discontinuity Condition (DC)
 I) Aperture (DCA)
 II) Infilling (DCI)

None (solid or massive)
 One set plus random
 Two sets plus random
 Three sets plus random
 Four sets plus random
 Crushed or shattered

Discontinuity set number (DSN)	None (solid or massive)	One set plus random	Two sets plus random	Three sets plus random	Four sets plus random	Crushed or shattered
Rating (R_{DSN})	20	16	12	8	4	1-0

Figure 3. Discontinuity set number (DSN) and R_{DSN}

1) Degradation Degree (DD)

2) Discontinuity Set Number (DSN)

3) Discontinuity Spacing (DS)
 Rock Quality Designation (RQD)

4) Discontinuity Condition (DC)
 I) Aperture (DCA)
 II) Infilling (DCI)

Discontinuity spacing (DS) or RQD	None or DS ≥ 24 m	24 > DS ≥ 6 m	6 m > DS ≥ 1.2 m	1.2 m > DS ≥ 0.3 m	0.3 m > DS ≥ 0.07 m	0.07 m > DS
	100			100 > RQD ≥ 75	75 > RQD ≥ 35	35 > RQD
Rating (R_{DS})	20	16	12	8	4	1-0

Figure 4. Discontinuity spacing (DS) or rock quality designation (RQD) and R_{DS}

1) Degradation Degree (DD)

2) Discontinuity Set Number (DSN)

3) Discontinuity Spacing (DS)
 Rock Quality Designation (RQD)

4) Discontinuity Condition (DC)

I) Aperture (DCA)

II) Infilling (DCI)

III) Roughness-Descriptive (DCR)
 Roughness-Profile No (DCR)

None

Healed or intermittent

Other (Please fill the I, II, and III.)

Discontinuity condition (DC)	None	Healed or intermittent	Rough	Relatively smooth and tight	Slickensided with thin infill or separation (t < 5 mm)	Thick fill or separation (t > 10 mm)
Rating (R_{DC})	30	26	22	15	7	1

Figure 5. Discontinuity condition (DC) and R_{DC}

4) Discontinuity Condition (DC)

I) Aperture (DCA)

II) Infilling (DCI)

III) Roughness-Descriptive (DCR)
 Roughness-Profile No (DCR)

5) Groundwater Seepage Condition (GWSC)

6) Groundwater Absorption Condition (GWAC)

Clear All

Calculate

Aperture or separation	None or very tight, <0.1 mm	0.1–0.25 m m	0.25–0.5 mm	0.5–2.5 mm	2.5–10 mm	>10 mm
Rating (R_{DCA})	6	5	4	3	2	1

Figure 6. Aperture or separation (DCA) and R_{DCA}

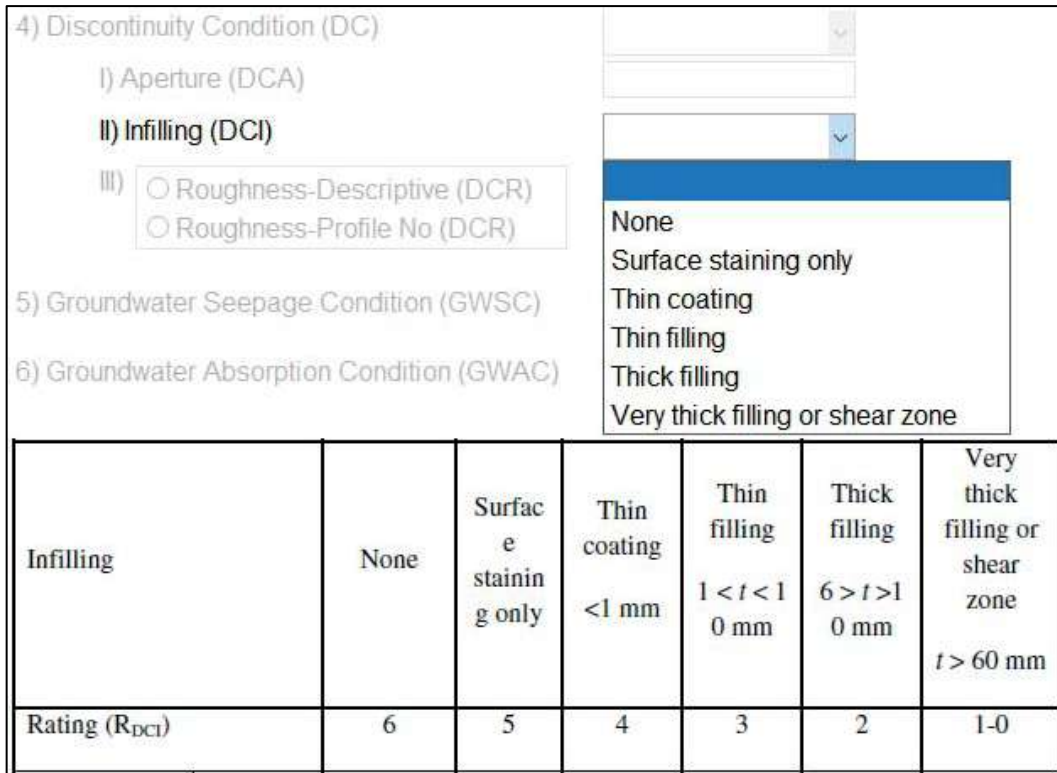


Figure 7. Infilling (DCI) and R_{DCI}

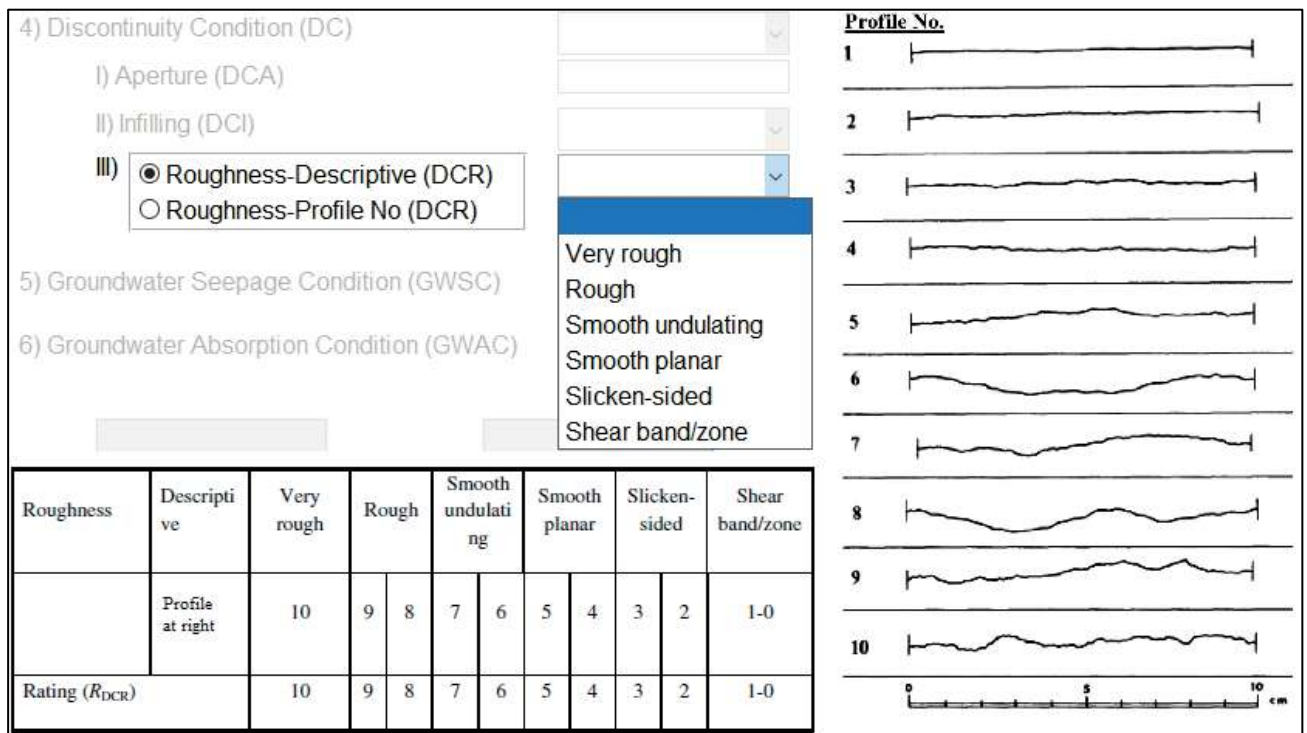


Figure 8. Roughness (DCR) and R_{DCR}



Figure 9. Groundwater seepage condition (GWSC) and R_{GWSC}

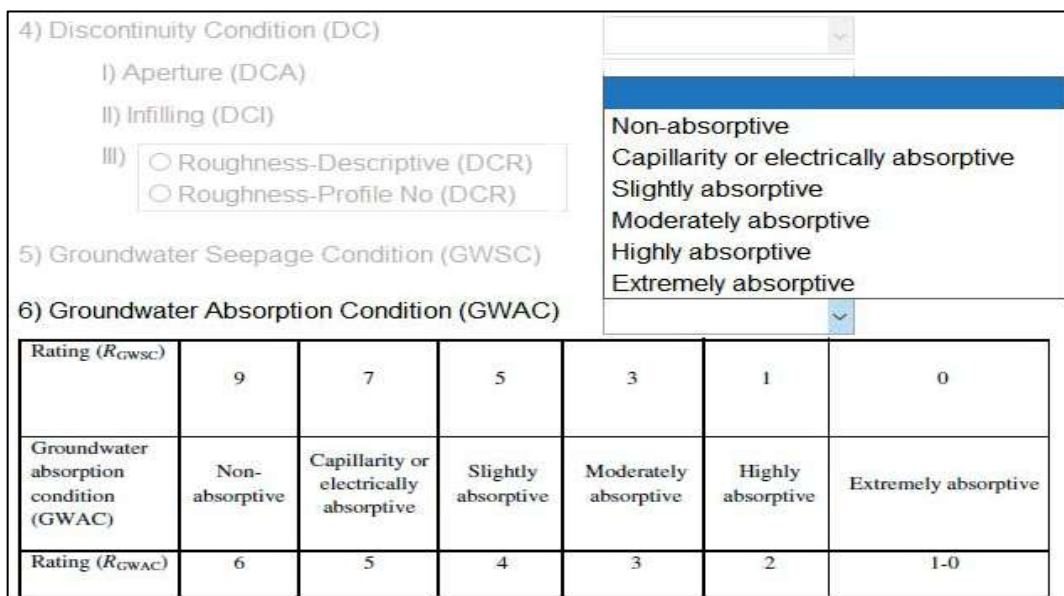


Figure 10. Groundwater absorption condition (GWAC) and R_{GWAC}

The discontinuity condition excluding the classes named by “None” and “Healed or intermittent” is calculated the appropriate parameters in RMQR are represented by some of the functions in the same publication. it is possible to obtain precise results in terms of 2 criteria (DS, DCA) in the system. Among these criteria, the equation proposed by the system for RDS and the equation derived within the scope of this study will be used for RDCA. Except for these two parameters, all parameters are kept constant, and it is shown in Table 1 that the rock class differs for the extreme values of each parameter. But it is not possible to detect this using only the RMQR chart.

Table 1. An example of the problem in calculating RMQR.

Parameter	Values		Ratings		RMQR Calc Ratings	
	Case 1	Case 2	Case 1	Case 2	Case 1	Case 2
1. Degradation degree (DD)	Moderate degradation	Moderate degradation	6	6	6	6
2. Discontinuity set number (DSN)	Three sets plus random	Three sets plus random	8	8	8	8
3. Discontinuity spacing (DS)	1.1	0.3	8	8	9.46	5.83
4. Discontinuity condition (DC)						
a) Aperture or separation	0.26	0.49	4	4	4.73	4.11
b) Infilling	Thin coating <1 mm	Thin coating <1 mm	4	4	4	4
c) Roughness	Smooth undulating	Smooth undulating	6	6	6	6
5. Groundwater seepage condition (GWSC)	Dripping	Dripping	3	3	3	3
6. Groundwater absorption condition (GWAC)	Moderately absorptive	Moderately absorptive	3	3	3	3
RMQR			42	42	44.19	39.94
Rock Class			Fair or medium	Fair or medium	Fair or medium	Poor or weak

METHODOLOGY

The aim of this study is to turn the RMQR system, which is a module of the electronic rock classification library to be created, into a computer program. Thus, the system will become more useful and capable of more precise classification.

In the RMQR system, scores for degradation degree (DD), discontinuity set number (DSN), infilling (DCI), roughness (DCR), groundwater seepage condition (GWSC) and groundwater absorption condition (GWAC) parameters consist of direct selections. In this section, users are directly selected without making any changes. However, it is possible to score more precisely by using the equations for Discontinuity spacing (DS), RQD and Aperture (DCA). Here, the equations given in the publication (Aydan et al., 2014) were used for DS and RQD, and the equation derived in this publication for DCA (Figure 11).

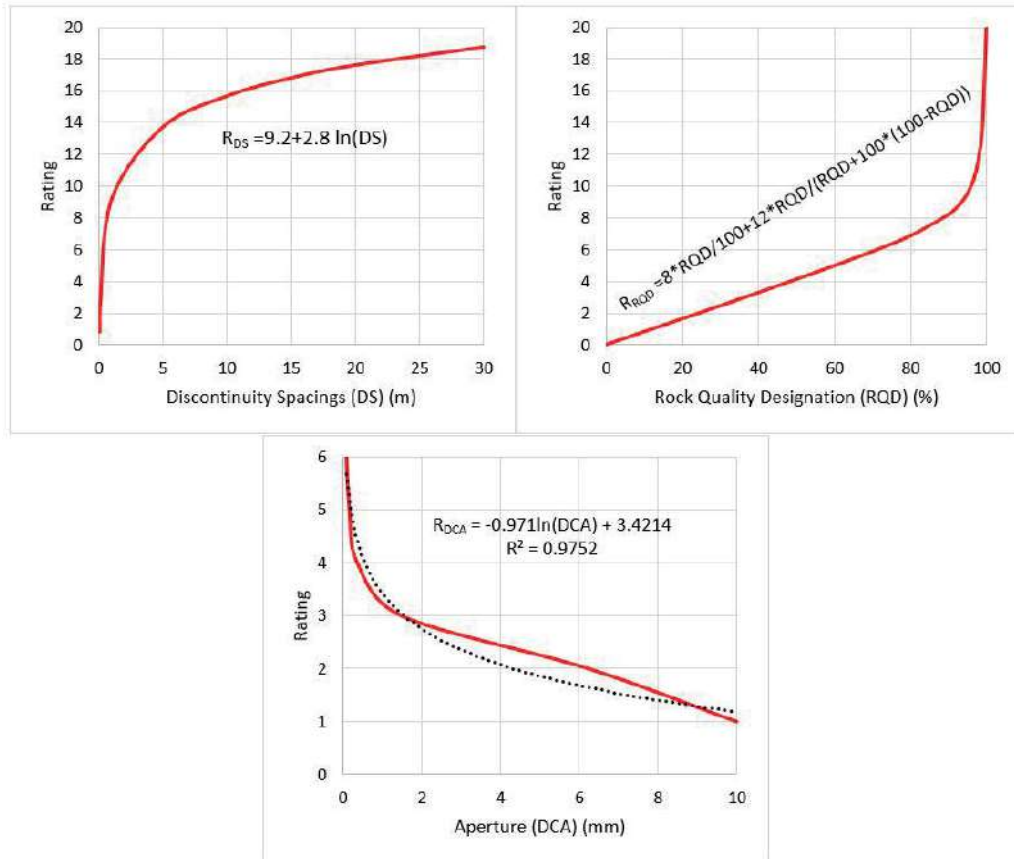


Figure 11. Curves of equations used in RMQRCalc

THE COMPUTER APPLICATION RMQRCalc

A Windows-based computer application named 'RMQRCalc' has been developed to obtain an accurate classification and an easy-to-calculate RMQR. The RMQRCalc application was designed using the MATLAB graphical user interface (GUI). The RMQRCalc obtains scores for each parameter from the values typed or selected by a user, thanks to the functions derived, and calculates the RMQR for the sum of these scores. Based on the RMQR value it has obtained, it gives its equivalents in the RMR (Bieniawski, 1989) and Q (Barton et al., 1974) systems. It determines the rock classes of each system. Screenshot of the application is given in Figure 12.

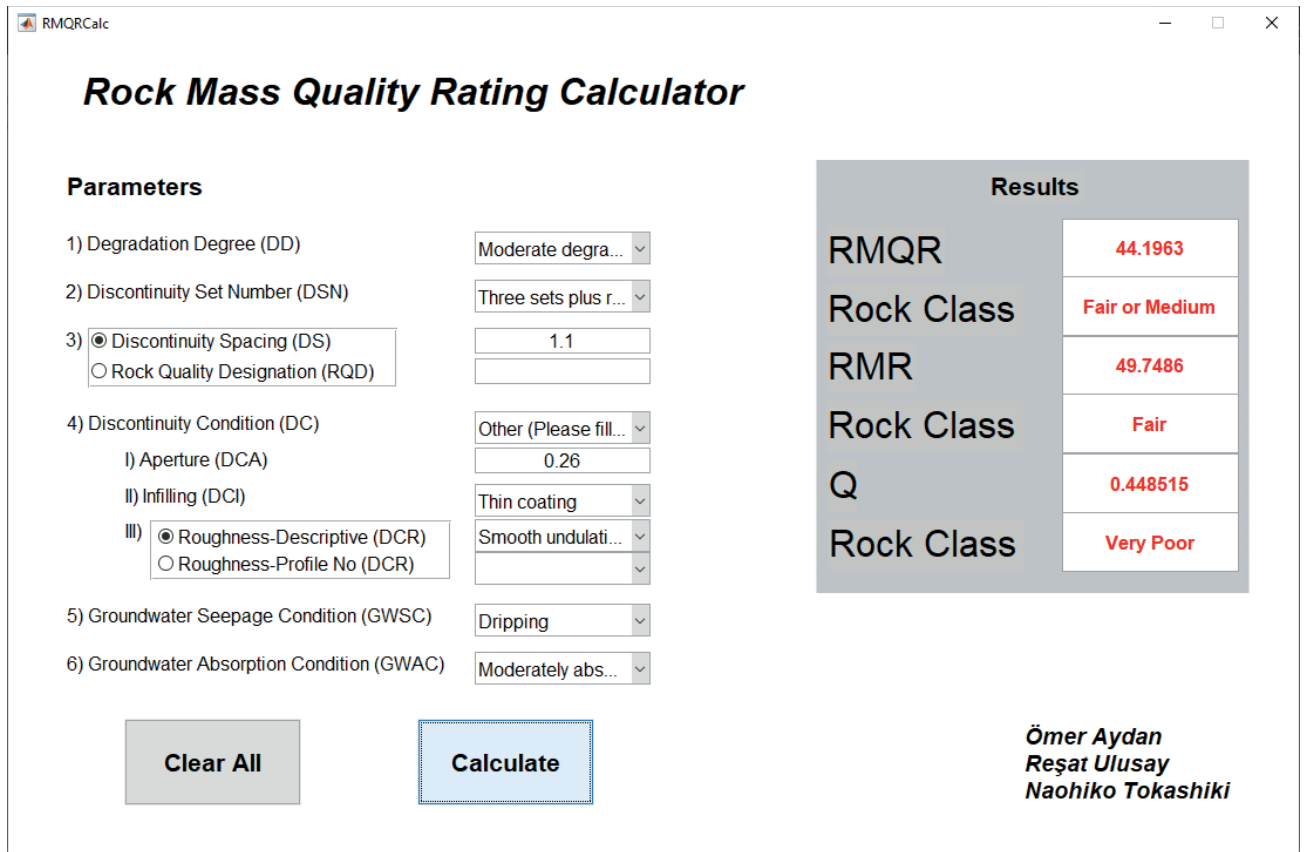


Figure 12. Screenshots from the RMQRCalc application

The program can be accessed free of charge from the link shared under this notice. The published version is 1.0 and the program will be updated with the studies and feedbacks, and access will be provided from the link.

RESULTS

The RMQR system proposed by Aydan et al. in 2014 was coded in the MATLAB graphical user interface and turned into a windows-based computer application. With the equations suggested by Aydan et al. and the equation suggested in this publication, the system has been made more precise classification. It is planned that this study will be a module of the electronic rock classification library. The program is shared with the link in this study, open to the access of all participants.

REFERENCES

- Aydan, Ö., Ulusay, R., and Tokashiki, N. (2014). A New Rock Mass Quality Rating System: Rock Mass Quality Rating (RMQR) and Its Application to the Estimation of Geomechanical Characteristics of Rock Masses. *Rock Mechanics and Rock Engineering*, 47, 1255–1276.
- Bieniawski, Z.T., 1989. Engineering rock mass classifications: a complete manual for engineers and geologists in mining, civil, and petroleum engineering. John Wiley & Sons.
- Barton, N., Lien, R., & Lunde, J. (1974). Engineering classification of rock masses for the design of tunnelsupport (NGI Publication No. 106, p. 48). Oslo: Norwegian Geotechnical Institute.
- RMQRCalc Link: <https://kovan.itu.edu.tr/index.php/s/dy8DBMOLi9XCNM5>

A HYBRID SEMI-QUANTITATIVE APPROACH FOR MINE CLOSURE RISK MANAGEMENT IN ANGURAN MINE, IRAN

N. Samadinia¹, M. Osanloo^{1,*}, S. Amirshenava¹

¹*Amirkabir University of Technology, Department of Mining Engineering*
 (*Corresponding author: morteza.osanloo@gmail.com)

ABSTRACT

Mining is temporary land use, and the mine life ends with the exhaustion of mineable reserve or other factors that lead mine to unplanned closure. Premature mine closure is associated with various risks. Deviation from achieving sustainable development (SD) goals is the main consequence of premature mine closure risks. The present study aimed to implement the risk management of premature mine closure and mine closure impacts. In this regard, the comprehensive approach was proposed to identify the causes that led mine to close prematurely. In addition, the impacts of mine closure risks were assessed, and the risk treatment stage was investigated to prevent or diminish the detected risks in each stage. Mine reclamation is a risk treatment option that requires the selection of suitable Post-Mining Land Use (PMLU). The suitable PMLU option is chosen based on the identified and assessed risks. To this end, a two-dimensional (2D) risk model and Multi-Criteria Decision Making (MCDM) methods were developed. The Anguran mine was selected as a case study; the results showed that the final product price reduction is the most critical reason that threatened the lead and zinc of Anguran mine to early closure. To treat this risk, by analyzing the correlation between the prices of different metals and availability factors, iron investment simultaneously was proposed to the mining company due to its adverse correlation with the price of zinc and lead. Besides, among the mine closure risks, the highest risk level is related to economic risks. To appropriate response against the recognized impacts of mine closure risks, the recreation center was recommended as the suitable PMLU.

Keywords: Premature mine closure, sustainable development, risk management, mine reclamation, multi-criteria decision making

INTRODUCTION

Mining activities promote economic growth and improve the region's social conditions, but premature mine closure will create many challenges for the area (Laurence, 2006). It is noteworthy that a significant proportion of mines are closed prematurely due to environmental, economic, and social factors (Laurence, 2006; Minaei Mobtaker and Osanloo, 2015). Premature mine closure has environmental, safety, health, social, financial, and technical risks. These occurrences can pose several challenges to achieving the region's sustainable development (SD) goals (Laurence, 2001; Kung et al., 2020). In countries with rich resources but poor government management, mine closure risks are more severe (Cui et al., 2020). Therefore, it is vital to forecast the factors that cause the mine to close prematurely and implement the risk management approach. The risk management process is a comprehensive strategy for investigating and assessing identified risks and managing high-level risks that can make an unsustainable situation (ISO 31000, 2009).

The risk management process includes three stages: risk identification, risk assessment, and risk treatment. Various researchers have considered the risk management process in the mine closure plan. (Mansouri et al., 2014; Mercer and Biggs, 2013; Sanders et al., 2019; Tones et al., 2021). However, these

cases have not developed a comprehensive approach to implement all risk management stages in mine closure. After risk identification, the most appropriate method should be considered for the risk assessment process. Numerous methods exist for assessing the risks; nevertheless, the 2D risk model is the most common method for mine closure (Gheisari et al., 2014; Laurence 2001; Kadir et al., 2017). In 2018, Amirshenava and Osanloo developed the 3D risk matrix considering the time factor in the risk management process. Implementing the mine reclamation plan and choosing the Post-Mining Land Use (PMLU) are the best procedures for the risk treatment stage. Mine reclamation can make the conditions of the mined lands safe and stable and decrease or eliminate the adverse impacts of mining activities on the site. Thus, mine reclamation based on the identified and assessed risks can be deemed a practical effort to improve the situations for Sustainable Development (SD) of the region (Amirshenava and Osanloo, 2021; Laurence, 2011; Sloss, 2013;). Reclamation planning begins from the exploration level and is completed at the end of the mine life cycle (Lappi, 2020; Osanloo, 2017). Figure 1 shows the mine life cycle and each stage's importance based on the time and the labor force required (ICMM, 2012b).

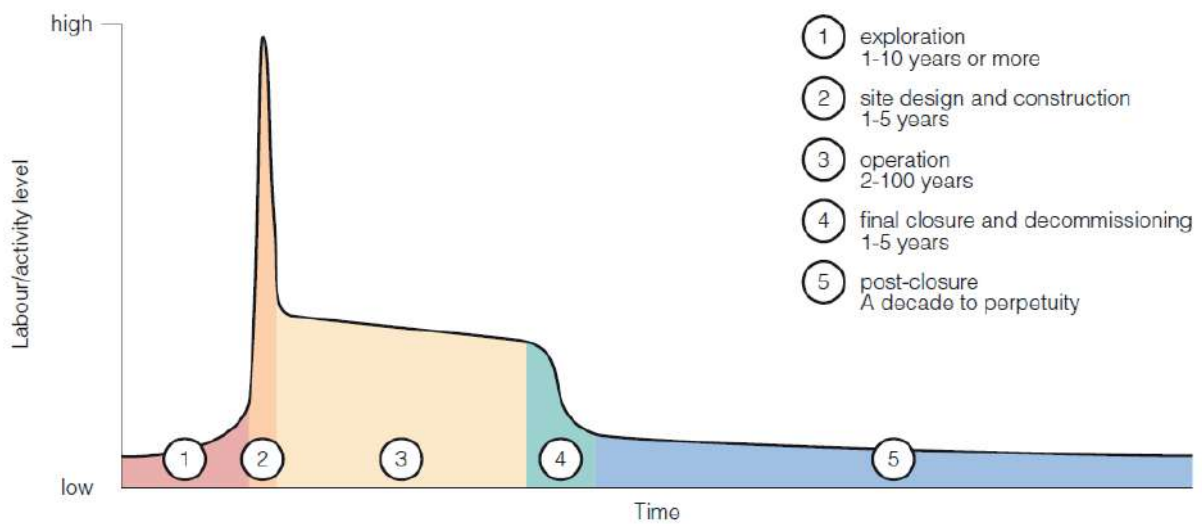


Figure 1. Mine project life cycle (ICMM, 2012b)

In choosing PMLU, the opinions of all stakeholders should be considered. Stakeholders can include local people, environmental experts, economic teams, and law authorities (Galvin, 2017; Hajkazemiha et al., 2021; Mborah et al., 2016). A reclamation plan is crucial in the mine life cycle because it covers the risks of premature mine closure and balances the consequences of mining operations in the region. According to the regions' situation, several PMLU can be selected for mined lands.

A noteworthy point in the present study is implementing the comprehensive approach for the risk management of mine closure. In this regard, as the first step, the risks that led mine to close earlier have been recognized. In the next step, the probable consequences of the mine closure were assessed. For these aims, risk levels are classified using the 2D risk assessment matrix. The most suitable PMLU has been investigated based on the determined high-level risks. To this end, the Multi-Criteria Decision Making (MCDM) method was considered the best way to figure out the most proper PMLU. Finally, the proposed comprehensive approach is verified in Iran's lead and zinc mine.

METHODOLOGY

This study seeks to provide a solution to reduce or avoid the risks of mine closure. As shown in Figure 2, a comprehensive risk management approach was developed in three stages.

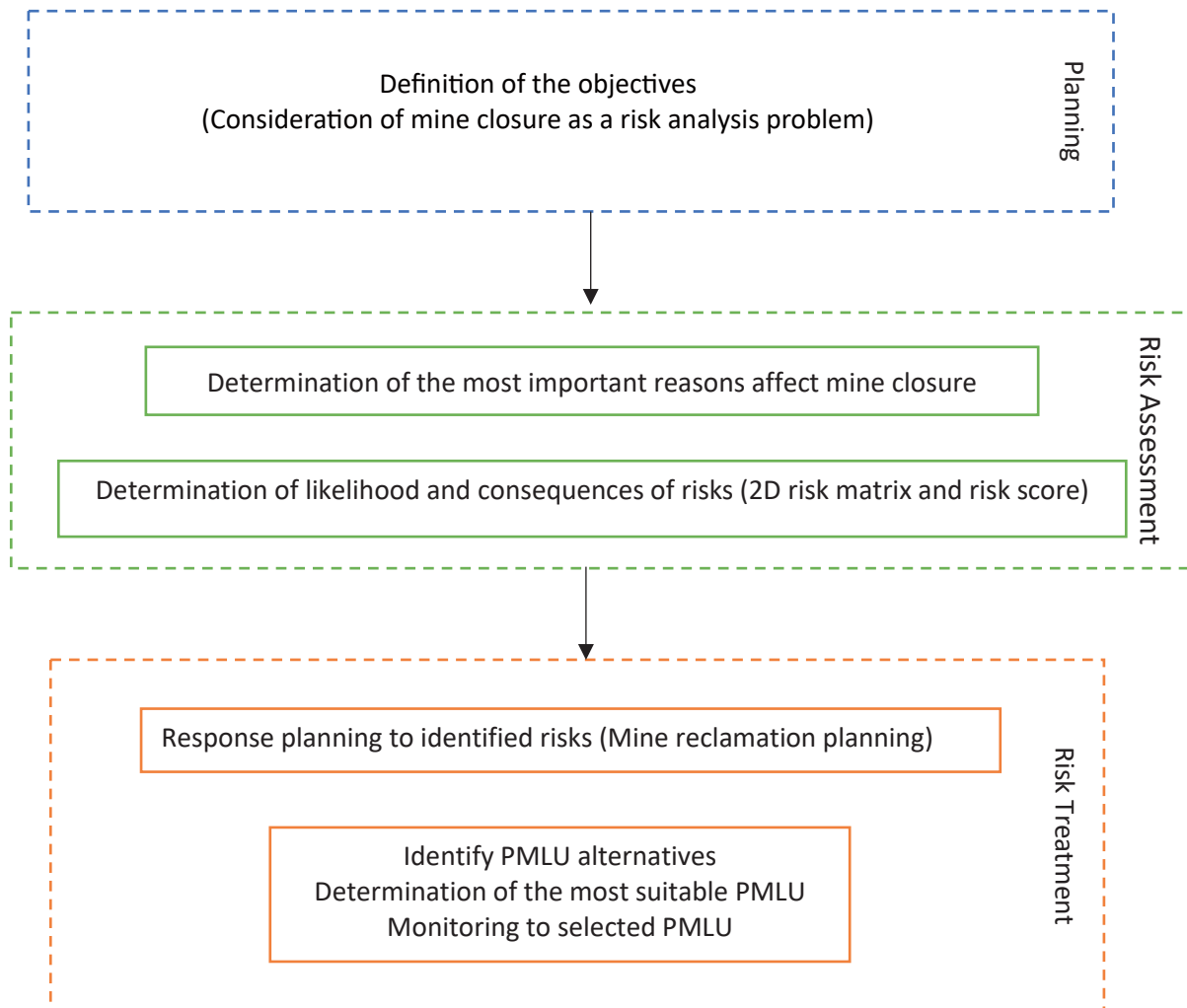


Figure 2. The framework of the mine closure risk management

Planning

The first step in the risk analysis process is problem definition and information gathering. The problem is defined as diminishing or avoiding the impacts of premature mine closure. In this regard, the Anguran mine was selected as a case study. Anguran is located 445 km northwest of Tehran in Zanjan province (Figure 3). The climate condition in this mine is cold and semi-arid. The average annual precipitation in this site is 347 mm (IMPASCO, 2021).

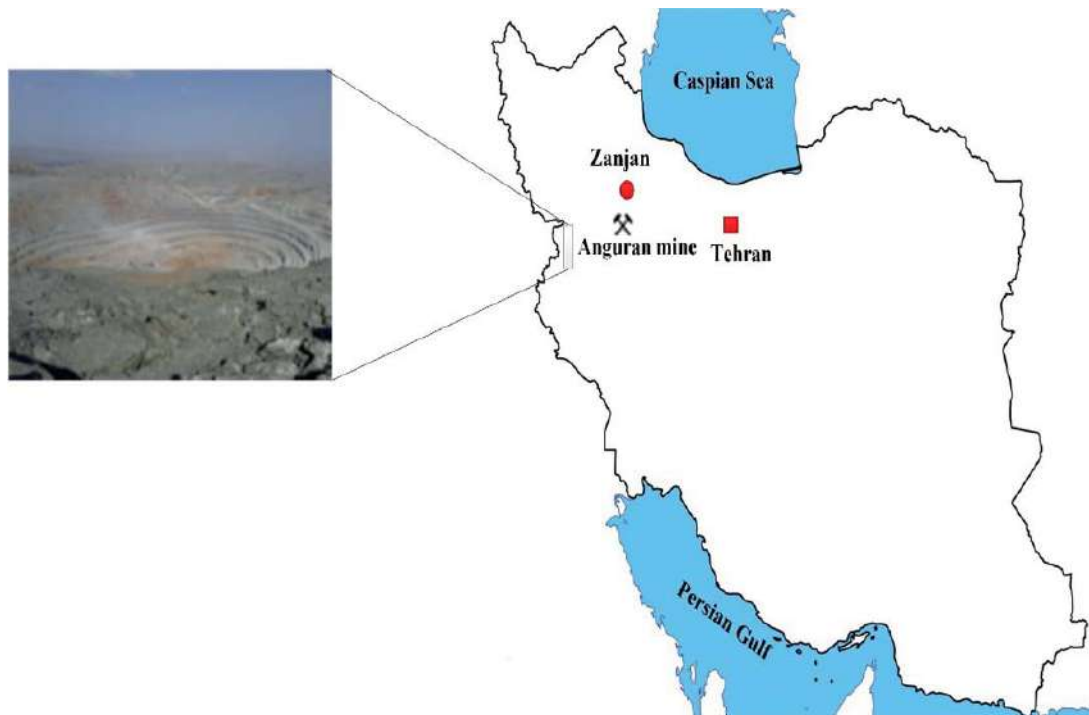


Figure 3. The Anguran mine in 445 Km of Tehran- Capital of Iran

Risk Assessment

At this risk management stage, the causes of premature mine closure risks are first identified. The probable consequences of this risk are then discussed. Semi-quantitative methods have been developed for achieving the results in this study. Qualitative methods are not accurate enough, and quantitative methods have complex calculations; Therefore, semi-quantitative methods are often used for risk analysis (Cui et al., 2020). The two-dimensional risk matrix is the basis of the research. In this risk matrix, one dimension represents the likelihood of the risk occurrence, and the other represents the risk intensity. Each matrix array converts qualitative expressions such as high, medium, and low into quantitative parameters (Amirshenava and Osanloo, 2019). Tables 1 and 2 illustrate the related causes and the possible consequences of premature mine closure.

Table 1. Causes of premature mine closure

Code	Causes of premature mine closure
R1	Increasing operating costs
R2	Reducing the price of the final product of the mine
R3	End of open-pit mining
R4	Loss of the final product sales market
R5	Overestimating of grade and tonnage
R6	Facing faults, joints, and complex geological conditions
R7	collapses of the mine pit wall
R8	Failure of tailing dam
R9	AMD generation
R10	Contamination of surface and groundwater
R11	Contamination of soil with toxic elements




R12	Excessive equipment depreciation
R13	Defect or lack of mining equipment
R14	Changing government policies under pressure from lawmakers
R15	Existence of disputes and conflicts in the ownership of the mine site
R16	The local people are against mining

A team of 10 experts was determined to answer the related questionnaires. These experts consist of engineers and managers of Anguran mine in different fields. First, after predicting the risk factors associated with premature mine closure, experts were asked about the likelihood and intensity of each risk factor occurrence. The classification of score range was formed between one and five, and the closer the score is to five, the higher the probability of occurrence and the severity of each risk factor. The Risk Score (RS) is obtained by multiplying the likelihood and intensity of risk factor occurrence. 2D risk matrix can be formed with the RS. After calculating the RS, risk levels can be categorized into three levels. Table 3 shows the relationship between the RS and risk levels.

Table 2. Consequences of premature mine closure

Code	Mine closure Risks
C1	Decreasing economic growth in the region
C2	Unexploded blast hole
C3	Decreasing skills in the region
C4	Falling into the pit
C5	Pit slop failure
C6	Unemployment
C7	Inability to pay employees' salaries
C8	Dust
C9	Changing people's lifestyles
C10	Water pollution
C11	Soil pollution
C12	AMD generation
C13	Increasing crime and violence in the region
C14	Failure to complete the reclamation plan
C15	Inability to repay debts and loans
C16	Inability to pay taxes to the government

Table 3. The relationship between the RS and risk levels

Risk Score (RS)	Risk Level	Color code
RS < 4	Low	
4 ≤ RS ≤ 14	Moderate	
RS > 14	High	

Risk Treatment

After the risk planning and risk assessment, an appropriate response should be considered to the identified risks. Risk response or treatment can be carried out to avoid, reduce, optimize, and transfer risks (Amirshenava and Osanloo, 2021). The best solution to risk treatment is mine reclamation. After reducing the site's pollution, mined land is prepared for PMLU implementation in the reclamation plan (Maqsoud et al., 2021). According to the mine's identified risks and general conditions, PMLU alternatives are shown in Table 4.

Table 4. Classification of PMLU alternatives

ID	PMLU	Description
P1	Agriculture	Arable land to produce the crop and earn money
P2	Forestry	Production commercial lumbers and creating a beautiful landscape
P3	Lake or Pool	Aquaculture, fishing pond, boating
P4	Construction	Construction of residential, educational, and industrial complexes
P5	Wildlife habitat	Natural parks
P6	Recreation center	Sports field, sailing, hunting, park, museum or exhibition
P7	Solar power station	Establishment of a solar power plant at the mine site

Finding the best alternatives for PMLU, related criteria were determined. Experts give a score between 1 and 10 for each option considering different criteria. A low score indicates minor positive importance, and a high score represents a high positive significance. Nevertheless, this definition is reversed in the case of capital and operating costs due to their negative nature. Table 5 illustrates the decision-making criteria for choosing the suitable PMLU.

Table 5. Decision-making criteria in PMLU selection

code	criteria
M1	Capital cost
M2	Operating and monitoring cost
M3	Increasing the income of local communities
M4	Creating job opportunities
M5	Flexibility with the local lifestyle
M6	Exposure to sunlight
M7	Precipitation
M8	Access to water resources
M9	Impact on desertification
M10	Land slope
M11	Soil quality
M12	Access

TOPSIS method is the most proper for solving this problem (Hwang and Yoon, 1981). The average and standard deviation of experts' scores to each factor are decision-making criteria. Based on the defined criteria, the most suitable PMLU can be selected.

RESULTS

Determining the Causes of Premature Mine Closure

The average and standard deviation of the experts' scores to each risk factor are shown in Table 6. Also, the risk factors are arranged by calculating the similarity index in Figure 4. According to the results, the final product's price reduction (R2) has been obtained as the most crucial reason for the early closure of the Anguran mine. The decline of minerals prices is inevitable because it is affected by many uncertainty parameters that are not easy to forecast. However, historical analysis of prices helps obtain future metals price trends, which can inform mining managers and engineers about the future conditions to take proper action.

Table 6. Result of risk causes analysis

Code	Causes of premature mine closure	Average	Standard deviation
R1	Increasing operating costs	1	0
R2	Reducing the price of the final product of the mine	2	0
R3	End of open-pit mining	2.875	0.330719
R4	Loss of the final product sales market	2.75	0.433013
R5	Overestimating of grade and tonnage	2	0
R6	Facing faults, joints, and complex geological conditions	3	0.866025
R7	collapses of the mine pit wall	2.125	0.927025
R8	Failure of tailing dam	1.875	0.330719
R9	AMD generation	2.75	0.433013
R10	Contamination of surface and groundwater	2.75	0.968246
R11	Contamination of soil with toxic elements	2.625	1.111024
R12	Excessive equipment depreciation	2.5	0.707107
R13	Defect or lack of mining equipment	2.25	0.433013
R14	Changing government policies under pressure from lawmakers	2.75	1.391941
R15	Existence of disputes and conflicts in the ownership of the mine site	1.875	0.599479
R16	The local people are against mining	1.5	0.5

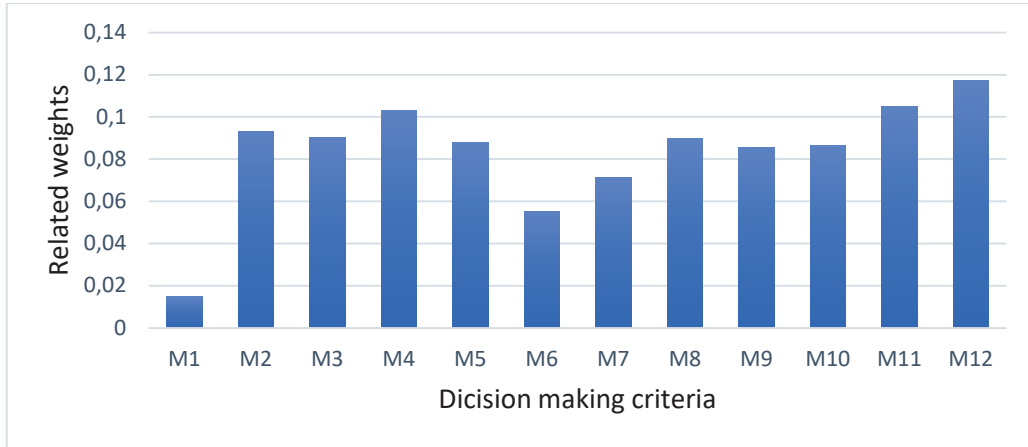


Figure 4. Comparison ranking of risk factors

Risk Matrix of Premature Mine Closure

According to Table 3, risk levels are divided into low, medium, and high-risk categories. Table 7 represents the result of the risk assessment. In addition, the 2D risk matrix is obtained by considering the likelihood in one dimension and the intensity of occurrence values in the other dimension. Figure 5 illustrates the 2D risk matrix.

Table 7. Results of risk assessment

Code	Likelihood	Consequences	RS	Color code
C1	3.25	3.5	11.375	Yellow
C2	2.5	2.25	5.625	Yellow
C3	2.75	3	8.25	Yellow
C4	3.25	3.25	10.5625	Yellow
C5	2.125	2	4.25	Yellow
C6	4	4.75	19	Red
C7	4.25	4.25	18.0625	Red
C8	1.625	1.625	2.640625	Green
C9	1.125	1.125	1.265625	Green
C10	2.25	2.25	5.0625	Yellow
C11	3	3.25	9.75	Yellow
C12	2.875	2.875	8.265625	Yellow
C13	1	1	1	Green
C14	2	1	2	Green

C15	2.25	2.125	4.78125	
C16	2.625	2.625	6.890625	

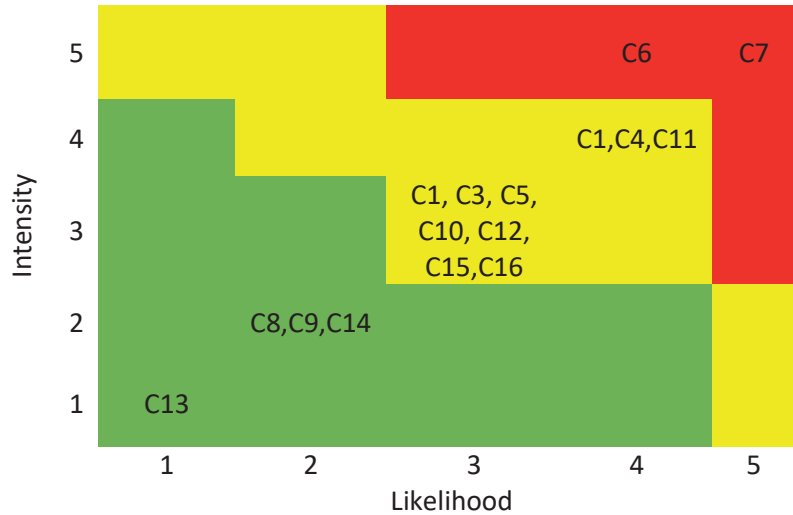


Figure 5. 2D risk matrix

Based on the results in Figure 5, many identified risks (63%) belong to the medium risk level (RS between 4 and 14). Unemployment and the inability to pay staff salaries (C6, C7) are at the highest risk of premature mine closure (RS is more than 14). Thus, making the necessary efforts to control these threats should be a priority for the mining company.

Determining of PMLU

Based on the MCDM method, a comparison between appropriate alternatives for PMLU has been developed. In Figure 6, the results of the TOPSIS method for selecting the suitable PMLU have been shown.

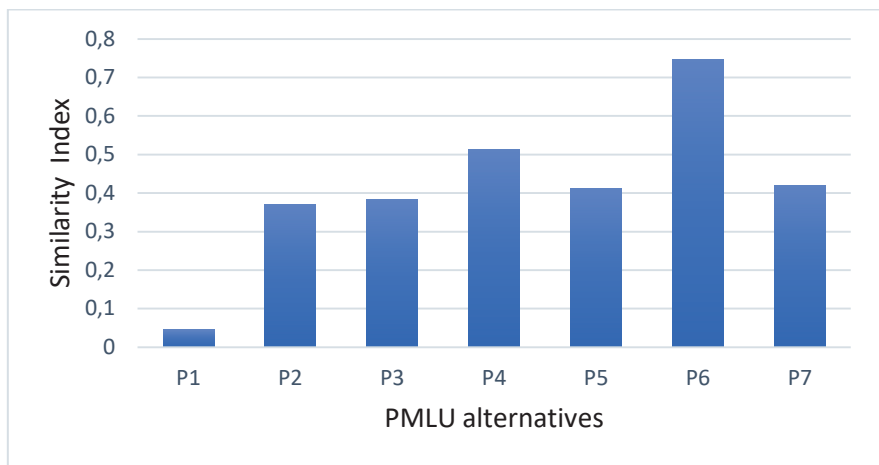


Figure 6. Results of PMLU ranking by the TOPSIS

According to Figure 6, recreation centers (P6) were obtained as the most suitable PMLU for the Anguran mine. Recreation centers can include sports complexes, boating, parks, museums, or exhibitions. Recreation centers can generate a sustainable income in the region. Therefore, by choosing this PMLU, the main risks due to the mine closure (C6, C7) are reduced or prevented.

DISCUSSION

Premature mine closure poses many risks to the mining area. These risks can be a threat to achieving the goals of SD. Therefore, in modern mining, mine closure risk management plays a vital role in maintaining mining activities in line with the principles of SD. The study evaluated premature mine closure by developing the 2D risk model and MCDM techniques. Compared to other similar studies, this research is preferred because it considers all stages of the risk management in the mine closure problem. In the planning stage, the problem was defined, and information was collected. In the risk assessment stage, recognizing possible risks that led mine to close earlier has been carried out. Finally, the most suitable PMLU was selected by MCDM analysis to treat the detected threats. For reducing the harmful impacts of mining activities, the implementation of reclamation projects has a significant role. Different reclamation methods are applied for different mines according to mineral type, mining methods, ecosystem, climate conditions, and legal requirements.

The results indicated that the final product's price reduction was known as the most crucial reason for premature mine closure. The best solution for avoiding the detected risk factor is investing in other minerals industries. In this regard, historical data of lead and zinc prices were collected and compared with other mineral prices (LME, 2021). Based on the correlation between lead and zinc prices with other minerals, correlation coefficients have been illustrated in Table 8.

Table 8. Correlation coefficients of mineral prices (January 2010 to October 2021)

	Zn	Pb	U	Pa	Al	Sn	Ag	Pt	Ni	Au	Cu	Fe
Zn	1.00	0.82	-0.49	0.44	0.79	0.37	-0.04	-0.38	-0.01	0.16	0.24	0.02
Pb	0.82	1.00	0.17	-0.13	0.69	0.64	-0.01	0.20	0.49	0.07	0.54	-0.13

Based on the results, zinc has a strong positive correlation with lead. In other words, price fluctuations are similar between zinc and lead roughly. It can be seen in Table 8 that several minerals have a negative correlation with zinc and lead. For selecting the most appropriate investment option for a mining company, in addition to the correlation coefficients, the availability factor is important too. Considering the general condition of the mining region and the possibility of investment are significant to achieve an accurate solution.

According to the results, iron investment was simultaneously proposed to the mining company due to its adverse correlation and availability factor around the mining region. Therefore, the iron market can be a reliable investment option when lead and zinc prices decline.

For risk treatment, first, the high-level risks were identified. It was observed that economic risk factors significantly impact premature mine closure consequences. By investigating seven alternatives of PMLU and twelve decision criteria, recreation centers were selected as the most suitable PMLU. Recreation centers improve the individual and social conditions in the region and play a significant role in reducing social conflicts. Suitable employment, job opportunities, local income is created by choosing

this PMLU. Thereby, this PMLU can cover the mine closure identified risks. The distance of mines from crowded cities and centers, reclamation costs, problems of polluting elements, and low probability of return on investment are among the limiting factors for choosing recreation centers as a PMLU. However, due to the lack of recreational centers in the Anguran region, selecting this option seems rational. Since the MCDM methods are compatible in this case study; Selecting these methods was the correct and most appropriate option for achieving the results.

CONCLUSION

The current study focuses on implementing the comprehensive risk management approach for premature mine closure risks. In this regard, three stages of the risk analysis were considered to manage the risks. First, identifying risks that could influence early mine closure occurrence was studied. The 2D risk matrix and MCDM techniques were developed for the risk assessment stage. Verifying this approach in the Anguran lead and zinc mine in Iran, the determination of the most critical possible reasons for the premature mine closure was on the agenda. The metal price reduction was the main risk factor that led the mine to close prematurely. By investigating the correlation of metals prices with each other and availability factors, iron investment was proposed to reduce or prevent the occurrence of this risk factor. Then, unemployment and the inability to pay staff salaries were the main consequences of premature mine closure. Also, the 2D risk matrix's results show that economic risks had significant impacts on the mining company. The seven PMLU alternatives were ranked by the TOPSIS method compared to the twelve criteria for the risk treatment stage. Finally, recreation centers were introduced as the most suitable PMLU. Different mining companies can implement the presented comprehensive approach in this study to manage the risks that threaten the SD goals in the region.

REFERENCES

- Amirshenava, S., Osanloo, M., (2018). Mine closure risk management: An integration of 3D risk model and MCDM techniques. *Journal of Cleaner Production*, 184, 389-401. doi.org/10.1016/j.jclepro.2018.01.186
- Amirshenava, S., Osanloo, M., (2019). A hybrid semi-quantitative approach for impact assessment of mining activities on sustainable development indexes. *Journal of Cleaner Production*, 218, 823-834. https://doi.org/10.1016/j.jclepro.2019.02.026
- Amirshenava, S., Osanloo, M. (2021). Mined land suitability assessment: a semi-quantitative approach based on a new classification of post-mining land uses. *International Journal of Mining, Reclamation and Environment*, 35(10), 743-763. https://doi.org/10.1080/17480930.2021.1949864
- Cui, C., Wang, B., Zhao, Y., Zhang, Y., and Xue, L., (2020). Risk management for mine closure: A cloud model and hybrid semi-quantitative decision method. *International Journal of Minerals, Metallurgy and Materials*, 27, 1021-1035. doi.org/10.1007/s12613-020-2002-7
- Galvin, J., (2017). Critical role of risk management in ground engineering and opportunities for improvement, *International Journal of Mining Science. Technology*, 27,725-731. https://doi.org/10.1016/j.ijmst.2017.07.005
- Gheisari, N., Osanloo, M., Esfahanipour, A., and Mansouri, M. (2014). Closure Risk Assessment in Atashkooch Stone Quarry Using Risk Matrix. In *Mine Planning and Equipment Selection* (pp. 791-802). Springer, Cham.
- Hajkazemiha, N., Shariat, M., Monavari, M., and Ataei, M. (2021). Evaluation of Mine Reclamation Criteria using Delphi-Fuzzy Approach. *Journal of Mining and Environment*, 12(2), 367-384. http://dx.doi.org/10.22044/jme.2020.9674.1880
- Hwang, C. L., Yoon, K. (1981). Methods for multiple attribute decision making. In *Multiple attribute decision making* (pp. 58-191). Springer, Berlin, Heidelberg. doi.org/10.1007/978-3-642-48318-9
- ICMM (2012b), Mining's contribution to sustainable development - an overview. International Council on Mining and Metals, London, UK. Available at: www.icmm.com/library

- IMPASCO, Iran Minerals Production and Supply Company, <http://www.impasco.gov.ir/> (accessed 10.09.21).
- ISO 31000, (2009). Risk Management - Principles and Guidelines. International Organization for Standardization.
- Kodir, A., Hartono, D. M., Haeruman, H., and Mansur, I. (2017). Integrated post mining landscape for sustainable land use: A case study in South Sumatera, Indonesia. *Sustainable Environment Research*, 27(4), 203-213.
- Kung, A., Everingham, J., and Vivoda, V., (2020). Social aspects of mine closure: Governance & Regulation. Brisbane: Center for Social Responsibility in Mining. The University of Queensland.
- Lappi, P., (2020). A model of optimal extraction and site reclamation. *Resource and Energy Economics*, 59. <https://doi.org/10.1016/J.RESENEECO.2019.101126>
- Laurence, D., (2001). Classification of risk factors associated with mine closure. *Mineral Resources Engineering*, 10(03), 315–331. doi.org/10.1142/s0950609801000683
- Laurence, D., (2006). Optimization of the mine closure process. *Journal of Cleaner Production*, 14, 285-298. doi.org/10.1016/j.jclepro.2004.04.011
- Laurence, D., (2011). Establishing a sustainable mining operation: an overview. *Journal of Cleaner Production*, 19, 278-284. doi.org/10.1016/j.jclepro.2010.08.019
- LME, London Metal Exchange, www.lme.com (accessed 10.11.21).
- Mansouri, M., Osanloo, M., and Gheisari, N. (2014). Establishing a sustainable model to reduce the risk of mine closure. In *Mine Planning and Equipment Selection* (pp. 1427-1436). Springer, Cham.
- Maqsoud, A., Diaby, S., and Mbonimpa, M. (2021). Evaluation of mine site reclamation performance using physical models: Case of Ity mine (Ivory coast). *Journal of African Earth Sciences*, 176, 104110.
- Mborah, C., Bansah, K., and Boateng, K., (2016). Evaluating alternate Post-Mining land uses: A review. *Canadian Center of science and education*, 5, 14-22. [10.5539/ep.v5n1p14](https://doi.org/10.5539/ep.v5n1p14)
- Mercer, K. G., and Biggs, B. (2013, September). Managing organisational risk for mine closure. In *Proceedings of the Eighth International Seminar on Mine Closure* (pp. 523-535). Australian Centre for Geomechanics.
- Minaei Mobtaker, M., Osanloo, M., (2015). Chaos in iron ore price prediction. In: *The Southern African Institute of Mining and Metallurgy MPES 2015 – Smart Innovation in Mining at: Sandton Convention Centre, Johannesburg, South Africa*.
- Osanloo, M., (2017). Mine Reclamation, third ed. Amirkabir University of Technology Publication, ISBN 964-463-090-4, p. 222 [in Persian].
- Sanders, J., McLeod, H., Small, A., and Strachotta, C. (2019). Mine closure residual risk management: identifying and managing credible failure modes for tailings and mine waste. In *Proceedings of the 13th International Conference on Mine Closure* (pp. 535-552). Australian Centre for Geomechanics.
- Sloss, L., (2013). Coal Mine Site Reclamation. IEA Clean Coal Centre. ISBN 978-92-9029-536-5, p. 70. doi.org/10.13140/RG.2.2.23405.13288
- Tones, A., Howe, L., and du Plooy, J. (2021). Knowledge makes the work go round: Knowledge management in mine closure planning. In *Mine Closure 2021: Proceedings of the 14th International Conference on Mine Closure*. QMC Group.
- Vrklijan, D., Brisevak, Z., (2016). Innovative waste management and mine closure. Minerals policy guidance for Europe.

A REVIEW OF THE NITRATE POLLUTION AND GROUNDWATER PROBLEMS DUE TO MINE BLASTS

G.G.U. Aksoy^{1,*}, C. Okay Aksoy², M. Akpınar¹

¹Hacettepe University, Ankara, Turkey

(*Corresponding author: gulsevaksoy@hacettepe.edu.tr)

²Dokuz Eylul University, İzmir, Turkey

ABSTRACT

Underground water resources have an important place in the life of living things. The pollution and decrease of these resources cause significant problems for humanity. It is possible that blasting operations at mine sites contaminate groundwater and damage groundwater resources. One of the most important reasons for this situation is the nitrate resources found in high rates in explosives used during blasting operations. Nitrate released from explosives pollutes groundwater, making groundwater harmful to health. For this reason, nitrate pollution should be monitored and prevented as much as possible during the operations carried out at the mine sites. There are lots of nitrate sources other than explosives, these sources are used in many ways. Since the variety of nitrate sources makes it difficult to determine the cause of nitrate contamination, methods have been developed to detect it. In addition, monitoring the increase in nitrate pollution in a region is an important step to prevent this pollution. Another step to prevent nitrate pollution from mining activities is the correct use of nitrate resources in the mine site and the correct nitrate removal of these resources.

Keywords: Mining, blasting operations, groundwater, nitrate pollution

INTRODUCTION

Blasting operations performed during mining processes have huge and devastating effects on its surrounding. These operations are common for most of the mining activities. Therefore, each of these activities has adverse impacts on the environment, the health of its workers and also communities near to the mining fields. These effects can be listed mainly as follows: probability of subsidence in the mine area, groundwater pollution, sound pollution as well as air pollution at the time of drilling and blasting, and lowering of groundwater table due to excessive pumping of subsurface water. (Nowsher, 2013) In order to reduce these effects and find solutions to them, we must first be able to identify them and find their reasons. As Nowsher said, the environmental deterioration caused by mining occurs mainly as a result of inappropriate and wasteful working practices and rehabilitation measures (Nowsher, 2013).

In this article, we will review studies about the effects of blasting operations on groundwater and treatment techniques of these effects. Groundwater is one of the most valuable water sources for all living things, and affecting these sources in a bad way may result in disastrous impacts on the life of these creatures. As mentioned at the beginning, one of the effects of blasting operations on groundwater is lowering of groundwater table. Underground mining can change not only groundwater table but also groundwater flow paths and the geochemical environment (Nowsher, 2013). These changes need to be investigated carefully to diminish their effects on quality of groundwater. Mining may increase the permeability of rock units, create fresh rock surfaces, and allow water flow between previously disconnected units or between surface and groundwater. This may disturb natural geochemical systems causing dissolution/precipitation reactions and result in disturbances to groundwater quality (Nowsher, 2013). We can see the effects of these processes on the quality of

groundwater by looking at the values in Table 1 through the example of Madhyapara Granite Mine (Bangladesh).

Table 1. Water test result of sample (MGMCL-GHS-W-01) of MGM and test was conducted by BRTC, BUET (Nowsher, 2013)

SL No.	Water Quality Parameter	Unit	Concentration Present in Sample: MGMCL-GHS-W-01	Bangladesh Standard for Drinking Water (ECR, 97)	WHO Guideline Value, 2004
01	pH	-	9.54	6.5-8.5	6.5-8.5
02	Color	Pt-Co	242	15	15
03	Turbidity	NTU	115	10	10
04	Total Alkalinity (as CaCO ₃)	mg/liter
05	Chloride (Cl ⁻)	mg/liter	46	150-600	250
06	Iron (Fe)	mg/liter	...	0.3-1.0	0.3
07	Nitrate- Nitrogen (NO ₃ -N)	mg/liter	4.8	10	50
08	Fluoride (F)	mg/liter	...	1	1.5
09	Total Dissolved Solids (TDS)	mg/liter	362	1000	1000
10	Fecal Coliform (FC)	CFU/100 ml	Nil	0	0
11	Total Coliform (TC)	CFU/100 ml	15	0	0
12	Total Hardness (as CaCO ₃)	mg/liter	18	200-500	500
13	Electrical Conductivity (EC) at 25	µS/cm	510
14	Nitrite- Nitrogen (NO ₂ -N)	mg/liter	0.013	<1	3
15	Silica (SiO ₂), Colloidal silica	mg/liter	59.9
16	Sulphate (SO ₄)	mg/liter	45.4	400	250
17	Total Suspended Solids (TSS)	mg/liter	27	10	...
18	Hydrogen Sulphide (H ₂ S)/Odor	mg/liter	0.03	Odorless	...
19	Mercury (Hg)	mg/liter	0.002	0.001	0.001

Besides all the other effects of blasting operations, groundwater pollution related to nitrate is one of the most crucial effects. In the article, nitrate pollution is the key point of our discussion. In the following parts, we will review studies about nitrate sources, discussing how to identify nitrate sources (if it is related to blasting materials or not), making some recommendations to manage and monitor nitrate impacts, and finally suggesting treatment methods.

NITRATE

Nitrate is an anion containing nitrogen which is the main element composing the atmosphere. Chemical formula of the Nitrate is NO_3^- , and it is a component of ammonium nitrate, which is approximately 90 percent of commonly used explosives by weight (Pelham et al, 2015).

Harmful Effects of Nitrate

Nitrate is a harmful compound for water resources and also human bodies; therefore it shouldn't contaminate groundwater. Effects of nitrate on water resources may be listed as follows, eutrophication and changing oxygen concentration. In a human body, nitrate can be converted into ammonia which is a base and also very harmful for human bodies. This reaction may lead to composing N-nitroso compounds which are carcinogen for humans and also animals (Ardıç, 2013).

Sources of Nitrate

With the increasing population of humans, pollution of groundwater is scaling up and one of the reasons for this pollution is Nitrate. In addition to explosives used in mining activities, fertilizers, automobiles, animal manures and nitrogen oxides emissions from coals are also sources of nitrate pollution. With these sources, nitrate, which mixes with soil and surface waters, dissolves in groundwater after a while. As nitrate dissolves in groundwaters, pollution that will affect a wide environment may occur and adversely affect the lives of living things.

When we begin to examine nitrate pollution caused by explosives, we can observe that nitrate dissolves in the soil and then groundwater in many different ways. Degnan listed some of these ways as follows: leaching of nitrate from unexploded nitrate bearing explosive compounds such as NH_4NO_3 , oxidation (nitrification) of reduced N components of explosives such as NH_4NO_3 , TNT, RDX, etc. and injection of soluble NO_3^- or NO_x gases into the subsurface by blasting (Degnan et al, 2016).

Besides these processes, we can list nitrate sources in an open pit as follows (Bosman, 2009),

1. Bedrock Disturbance through Blasting, and Rock Dumps
2. Pitwater
3. Pollution Control Dam
4. Metallurgical Process Plant
5. Tailings Dam
6. Exposure Pathways

HOW TO IDENTIFY NITRATE SOURCES

The variety of nitrate sources makes it difficult to detect nitrate pollution from explosion processes. According to Patel, the largest source of nitrate in the soil is fertilizers (Patel, 2016) , and various techniques are used to separate the nitrate effect of explosives from other nitrate sources. One of the main reasons for making this distinction is to reduce the pollution that mines will create around them by observing and detecting nitrate pollution.

One of the primary ways to determine the nitrate source is to examine the ratios of nitrogen and oxygen isotopes. In order to examine these ratios, water wells should be opened near the mining area and groundwater samples can be taken from them. The nitrate pollution caused by explosives can be determined by taking these samples before and after blasting and comparing them and then analyzing these samples.

When the ratio of nitrogen and oxygen isotopes was examined, it was observed that these ratios differ between the nitrate used in explosives and other nitrate sources. Blasting related nitrate peaks were characterized by low $\delta^{15}\text{N}$ and high $\delta^{18}\text{O}$ which is indicative of synthetic nitrate used in explosives (Pelham et al, 2015).

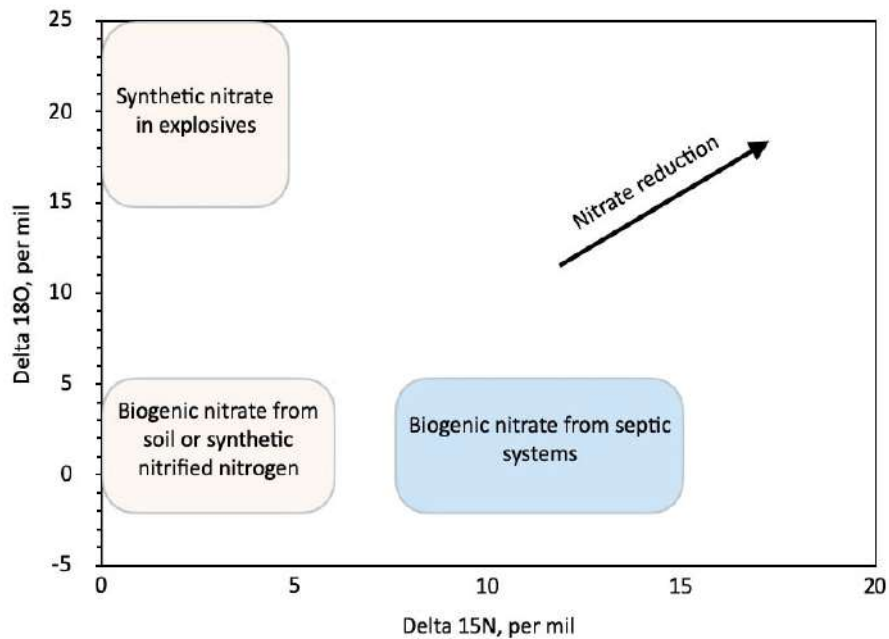


Figure 1. Graphs showing relation between $\delta^{15}\text{N}$ and $\delta^{18}\text{O}$ nitrate (Pelham et al, 2015)

As Pelham (2015), Degnan studied whether it is possible to find the source of nitrate in groundwater using N and O isotopes after a year. It is stated that the source of nitrate can be determined in this way, however nitrate should not be modified by the biological activities since the ratio of N and O isotopes is changed by denitrification. As mentioned before, in Degnan in 2016, they took samples from 12 wells and also 2 springs while constructing a highway in Windham, New Hampshire. By analysing elements, ions, dissolved gases and ratios of H, N and O isotopes with these samples, they concluded that the source of nitrate was synthetic. This reason is shown by low $\delta^{15}\text{N}$ and high $\delta^{18}\text{O}$ since these ratios differentiate at nitrate sourced by biogenic soil (which is constructed by nitrification) (Degnan et al, 2016).

Another interesting result which was stated by Degnan is that after eliminating effects of nitrification and computing initial grades of nitrates, it is possible to determine the source of nitrate by looking isotope graphs since these graphs show us clearly the source which can be by three types: synthetic nitrate based on blasting, biogenic nitrate based on nitrification and biogenic nitrate based on septic systems (Degnan et al, 2016).

Stable isotope analysis in R environment (SIAR) is another method used in order to determine the source of nitrate. This method is used by Kazakis in 2020 with samples from groundwater at different locations after statistical analysis. The results of this study which used SIAR (a bayesian isotope mixing model) also seems promising (Kazakis et al, 2020).

RECOMMENDATIONS FOR NITRATE IMPACT MANAGEMENT AND MONITORING

Considering the negative effects of nitrate on the health of living things, some arrangements should be made in the mine fields in order to reduce these effects. By examining these regulations under two different titles as management and monitoring, we can review some suggestions for these topics.

Management Measures

The nitrate pollution that will occur can be reduced by installing some equipment at the right points in the mine site. Bosman talked about some of these equipment and the ways of using them as follows:

Implementation of appropriate stormwater management around the excavation to prevent the ingress of run-off into the excavation. This will reduce the volume of pitwater that are contaminated with nitrate, which would reduce the costs associated with the management of this water (Bosman, 2009).

Implementation of appropriate stormwater management around rock dumps through the establishment of a clean and dirty water system, which would reduce the volume of run-off contaminated with nitrate from the rock dumps (Bosman, 2009).

Implementation of appropriate containment measures for all impoundments used to store contaminated water, such as pollution control dams, return water dams and tailings dams, such as clay and plastic linings (Bosman, 2009).

In addition to these ways, we can examine the methods offered by Kemen as "Best Management Practices" under five headings.

Loading Practices

These practices should be done in the first phase before the blasting. Kemen listed these practices as follows (Kemen, 2010);

1. Drilling logs shall be maintained by the driller and communicated directly to the blaster.
2. Explosive products shall be managed on-site.
3. Spillage around the borehole shall either be placed in the borehole or cleaned up and returned to an appropriate vehicle.
4. Loaded explosives shall be detonated as soon as possible and shall not be left in the blast holes overnight.
5. Loading equipment shall be cleaned in an area where wastewater can be properly contained and handled in a manner that prevents release of contaminants to the environment.
6. Explosives shall be loaded to maintain good continuity in the column load to promote complete detonation.
- 7.

Explosive Selection

As Kemen stated, while selecting explosives, site conditions should be considered, especially water conditions (Kemen, 2010).

Prevention of Misfires

As Kemen stated, it is important to implement practices in order to prevent misfires (Kemen, 2010).

Muck Pile Management

As Kemen stated, muck piles should be removed from the blasting area as soon as possible and it should be prevented from contaminating groundwater (Kemen, 2010).

Spill Prevention Measures and Spill Mitigation

The fuel storage and fuel handling requirements should be paid attention. The training should be received describing what to do in the event of a spill of regulated substances (Kemen, 2010).

Monitoring Measures

We can detect the pollution caused by explosives by observing various values at various points around the mine site. Thanks to these observations, the source of the pollution that will occur later can be determined and studies can be started to reduce that pollution.

As Bosman stated, using groundwater pollution detection monitoring programs around mines, we can examine the following items: pH, electrical conductivity, sulphates, chlorides, cyanide, selected heavy metals, nitrates, ammonia, total coliforms or E. Coli, and phosphate (Bosman, 2009).

However, while making these observations, it is necessary to consider other conditions that may occur in the environment while evaluating the analyzed data. If these conditions are ignored, the results of the observations may be misinterpreted. To give an example of these inaccuracies from Bosman, in the investigation referred to above, a conclusion was made that “since no nitrate was found in samples taken from the tailings effluent, the tailings dam cannot be a source of nitrate in the community groundwater” . (Bosman, 2009) As stated, the absence of nitrate in tailings effluent does not indicate that the tailings dam is not a nitrate source. Because, as Bosman points out, in the reducing environment at the tailings dam, nitrogen is present as the ammonia species, and not as the nitrate species (Bosman, 2009).

In another study, pollutants occurred during the blasting operations at Sungun copper mine have been monitored and dissipation of these pollutants has been observed. It seems that most of these pollutants occurred because of blasting operations, have been dropped back to the mining sites and continued to mix into the atmosphere with the mining activities (Abdollahisharif et al, 2016).

An-Fo

In addition to the recommendations, it is important to know the best practices while using ANFO.

What is ANFO?

ANFO is one of the most used explosives in blasting operations during mining activities. Because of this, ANFO is one of the main nitrate resources in mining fields, which makes ANFO the biggest source of nitrate which dissolves in groundwater because of blasting operations.

4th Reduce “blow-back” if loading ANFO pneumatically.

5th Loading equipment should be cleaned in the proper area and the product shouldn't be stored on site.

Factors contributing to the non-ideal detonation behavior of ANFO (Brochu, 2010)

1st Soil preparation

2nd Dissolution

3rd Oil wicking

4th Type of ANFO

5th Physical characteristics of AN particles

6th Storage and handling controls

7th Blast considerations

8th Loading controls

DISCUSSION

Blasting operations during mining activities cause serious environmental impacts which include groundwater pollution. These operations contaminate groundwater with nitrate. Identification of blasting operations impacts is difficult because of other nitrate sources such as fertilizers and decomposing vegetation. In order to identify source of nitrate, isotope ratios of nitrogen and oxygen in nitrate can be used. In addition to the identification process, some best practices should be followed in mining sites. Also, nitrogen removal techniques are needed to be used in order to prevent nitrate pollution.

REFERENCES

- Abdollahisharif, J., Bakhtavar, E., & Nourizadeh, H. (2016). Monitoring and assessment of pollutants resulting from bench-blasting operations. *Journal of Mining and Environment*, 7(1), 109-118.
- Ardıç, C. (2013). İçme suyundaki nitrat konsantrasyonunun insan sağlığı üzerine oluşturduğu risklerin belirlenmesi (Master's thesis, Fen Bilimleri Enstitüsü).
- Bosman, C. (2009). *The Hidden Dragon: Nitrate Pollution from Open-pit Mines—A case study from the Limpopo Province, South Africa*. Carin Bosman Sustainable Solutions, Pretoria, Gauteng, Republic of South Africa.
- Brochu, S. (2010). *Assessment of ANFO on the environment*. Defence Research And Development Canada Valcartier (Quebec).
- Degnan, J. R., Bohlke, J. K., Pelham, K., Langlais, D. M., & Walsh, G. J. (2016). Identification of groundwater nitrate contamination from explosives used in road construction: isotopic, chemical, and hydrologic evidence. *Environmental science & technology*, 50(2), 593-603.
- Jermakka, J., Wendling, L., Sohlberg, E., Heinonen, H., Merta, E., Laine-Ylijoki, J., ... & Mroueh, U. M. (2015). Nitrogen compounds at mines and quarries: Sources, behaviour and removal from mine and quarry waters-Literature study.
- Jermakka, J., Merta, E., Mroueh, U. M., Arkkola, H., Eskonniemi, S., Wendling, L., ... & Puhakka, J. (2015). Solutions for control of nitrogen discharges at mines and quarries: Miniman project final report.
- Kazakis, Nerantzis, et al. "Origin, implications and management strategies for nitrate pollution in surface and ground waters of Anthemountas basin based on a $\delta^{15}\text{N-NO}_3^-$ and $\delta^{18}\text{O-NO}_3^-$ isotope approach." *Science of The Total Environment* 724 (2020): 138211.
- Kernen, B. (2010). Rock blasting and water quality measures that can be taken to protect water quality and mitigate impacts. *New Hampshire Department of Environmental Services*, 1-3.
- Nowsher, M. N., Ratul-Al-Istiaq, H. M., Mahid, T. R., Biswas, B., Huda, S. A., Ahmed, M. T., & Hossain, H. Z. (2013). Environmental Impact Assessment of Madhyapara Granite Mine, Northwest Bangladesh. In *International Conference on Mechanical, Industrial and Materials Engineering (ICMIME2013)*, RUET, Rajshahi, Bangladesh, Paper Id: RT-12.

- Patel, R. K. (2016). Nitrates-its generation and impact on environment from mines: a review. In National conference on sustainable mining practice (pp. 2-3).
- Pelham, K., Lane, D., Smerenkanicz, J. R., & Miller, W. (2009). A proactive approach to limit potential impacts from blasting to drinking water supply wells, Windham, New Hampshire. In 60th Highway Geology Symposium (p. 16).
- Pelham, K., & Langlais, D. M. (2015). Sources of Nitrate in Groundwater Near Roadway Rock Blasting Sites. In 66th Highway Geology Symposium Highway Geology Symposium.
- Revey, G. F. (1996). Practical methods to control explosives losses and reduce ammonia and nitrate levels in mine water. *Mining Engineering*, 48(7), 61-64.

A STUDY OF EFFECTIVE PARAMETERS IN UNDERGROUND MINING METHOD SELECTION USING Z-NUMBERS THEORY

Zeinab Jahanbani¹, Majid Ataee-pour^{2,*}, Ali Mortazavi³

¹Ph. D Candidate of Mining Engineering, Amirkabir University of Technology, Dept. of Mining Engineering

^{2,*}Associate Professor, Amirkabir University of Technology, Dept. of Mining Engineering,

(*Corresponding author: map60@aut.ac.ir)

³Professor, Amirkabir University of Technology, Dept. of Mining Engineering,

ABSTRACT

The process of selecting an underground mining method is a critical decision-making issue with multiple criteria and depends on many important parameters such as geotechnical and geological features, technical, operational, environmental and economic parameters, political, social, and geographical factors. These factors face uncertainty, and existing uncertainties must be taken into account in the decision-making process of selecting the appropriate underground mining method. Fuzzy parameters are generally estimated through expert knowledge, but the degree of confidence in the opinion of different experts is different and the uncertainty and difference in the reliability of their opinion cannot be ignored. In this regard, Z-numbers Theory has been proposed. Each Z-number is represented by a pair of fuzzy numbers such that the first component indicates the fuzzy importance of each parameter and the second component is the reliability of the prediction of the first component. In this study, after classifying the effective factors in the selection of underground mining methods, the Z-numbers theory was used to rank and determine their importance. The results showed that in the main group of criteria technical factors and among the sub-criteria geological conditions, geometry conditions of the deposit, income per ton of ore, geomechanical conditions, and costs are the most important parameters, respectively.

Keywords: Influencing factors, underground mining method selection, uncertainty, fuzzy numbers, Z-numbers theory

INTRODUCTION

The selection of appropriate underground mining method to extract minerals from a deposit is one of the first and most important decisions in mining engineering activities from the perspective of safety, productivity, and economic issues. Different parts of an ore deposit normally vary widely in their geological, physical, chemical, and structural aspects. Depending on the dip, depth, size, and shape of the deposit, as well as the strength of the ore and host rock, several technically feasible methods may be adopted for a particular ore deposit. However, safety, financial, economic, and environmental parameters are of the most important and due attention should be paid to these parameters to select the safest and most profitable method. Therefore, selecting the most suitable method for an ore deposit, is a critical and challenging task owing to its compliance with a set of criteria (Gupta and Kumar, 2013).

To study the important and effective parameters in choosing the appropriate method for mining, many studies have been done for a long time. The first model or guide for the mining method selection is the method introduced by Peele in 1941 (Samimi Namin, 2009). Subsequently, different

researchers have used different factors in their studies in order to decide on the mining method selection. Table 1 summarizes some of these studies.

Table 1. Criteria considered for selecting the appropriate mining method in various studies

Author	year	Criteria considered in the study
Boshkov and Wright	1973	Thickness, Shape, Dip, Strength of ore, HW, FW
Morrison	1976	Ore thickness, Strain energy accumulation
Laubscher	1981	RQD, Spacing of fractures, Joint’s conditions, Underground water (hydrologic conditions)
Nicholas	1981-1992	Thickness, Shape, Dip, Overburden thickness, Grade distribution, RSS, RQD, Natural fractures and discontinuities shear strength of the ore zone, HW, FW
Hartman	1987	Depth, Strength of ore, HW, FW, Geometry conditions (Thickness, Shape, Dip)
Pakalnis et al.	1995	Thickness, Shape, Dip, Depth, Grade distribution, RMR and RSS of ore, HW, FW
Meech et al.	2002	Thickness, Shape, Dip, Depth, Grade distribution, RMR and RSS of ore, HW, FW
Alpay & Yavuz	2007	Spatial characteristics of the deposit, Geologic and hydrologic conditions, Geotechnical (soil and rock mechanics) properties, Economic considerations, Technological factors, Environmental concerns
Azadeh et al.	2010	Geometry conditions, Geomechanical conditions, Geographical conditions, Production, Mining operations, Mining aspects, Capital costs, Operating costs, Reclamation/rehabilitation costs, Income per ton of ore, Equipment worth and its usages
Gupta & Kumar	2013	Intrinsic factors, Extrinsic factors
Balusa & Singam	2017	Deposit thickness, RMR of hanging wall, Deposit dip, Deposit shape, RMR of ore, Ore grade, Ore uniformity, Recovery, Production, RMR of footwall, Technology, Depth, Dilution
FU et al.	2018	Economic benefit (Economic efficiency), Technical feasibility (physical parameters), Management complexity (the complexity of production management), Security status (safety of mining production), Environmental benefit (damage to the environment of mining methods)
Balusa & Gorai	2019	Dip, Shape, Thickness, Depth, Grade distribution, RMR of ore, RMR of hanging wall, RMR of foot wall, Productivity, Recovery, Dilution, RSS of ore, RSS of hanging wall, RSS of foot wall, Flexibility, Safety
Bajić et al.	2020	Technical, Production, Economic

A number of these influencing criteria in the selection of underground mining methods face uncertainty and they are difficult to quantify (Gupta and Kumar, 2013). Fuzzy theories can, to some extent, fully address this uncertainty in computations. Fuzzy parameters are generally estimated through expert knowledge, but the degree of confidence in the opinion of different experts is different and the uncertainty and difference in the reliability of their opinion cannot be ignored. In this regard,

Zadeh (2011) proposed a concept called Z-numbers. Z-numbers try to do calculations based on numbers that are not completely reliable. Accordingly, each Z-number is expressed based on a pair of fuzzy numbers (\tilde{A}, \tilde{R}) . The first component (\tilde{A}) is a constraint on the actual value of the given variable. The second component (\tilde{R}) also shows the reliability of the first component. Of course, the concept of Z-numbers was not the first attempt to show uncertainty in fuzzy numbers, but the theory of fuzzy sets of the second type, in which the degree of membership of a fuzzy set is itself fuzzy, was expressed before the theory of Z-numbers. However, this theory, unlike the theory of Z-numbers, is not able to show the degree of reliability in most sentences (Kang et al., 2012a, 2012b; Zadeh, 2011).

After Zadeh introduced the theory of Z-numbers in 2011, this theory was quickly used in various sciences such as economics, business, planning and the decision-making process (Kang et al., 2012a, 2012b). In the mining industry, due to its nature, the existence of uncertainty and variability in the influencing parameters in selection of underground mining methods play important and effective roles in the design and sustainability of underground mines (Heidarzadeh et al., 2020). Uncertainty and unreliability in these factors can be expressed as $Z = (\tilde{A}, \tilde{R})$ numbers. For example, the "deposit depth" parameter follows the fuzzy number \tilde{A} ; While the reliability of this prediction by the expert can be indicated by another fuzzy number such as \tilde{R} . In the present study, due to the nature of mining and the existence of uncertainty in the factors influencing the selection of underground mining method (such as geological, operational, and geotechnical parameters, etc.), the Z-numbers theory has been used to study and classify these factors.

Z-NUMBERS

A Z-number consists of a pair of fuzzy numbers in the form of $Z = (\tilde{A}, \tilde{R})$; So that the first component (\tilde{A}) , a restriction on the values, is a real-valued uncertain variable X and the second component (\tilde{R}) is a measure of the reliability for the first component. The numbers \tilde{A} and \tilde{R} also represent two fuzzy numbers defined by Equation (1) (Azadeh et al., 2013; Kang et al., 2012a, 2012b).

$$A = \{ \langle x, \mu_A(x) \rangle | x \in X \} \tag{1}$$

Where: A : a fuzzy set on a universe X , $\mu_A: X \rightarrow [0,1]$: membership function of A and $\mu_A(x)$: membership value that describes the degree of belongingness of $x \in X$ in A .

In a graphical representation, a Z-number can be represented as Figure 1. In this example, \tilde{A} is a trapezoidal fuzzy number and \tilde{R} is a triangular fuzzy number (Azadeh et al., 2013; Kang et al., 2012a, 2012b).

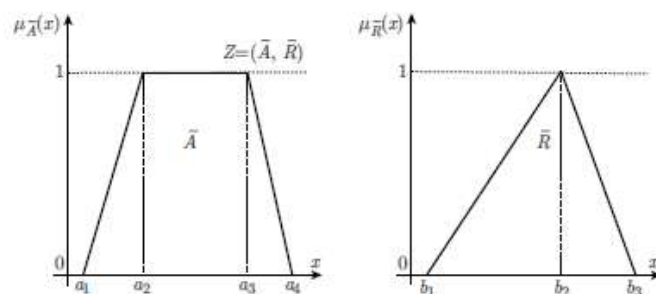


Figure 1. An example of a Z-number (Kang et al., 2012a)

Fuzzy Expectation of a Fuzzy Set

If A is a fuzzy set in which $\mu_A: X \rightarrow [0,1]$ is a membership function of A, the fuzzy Expectation of a fuzzy set is defined by Equation (2) (Kang et al., 2012a).

$$E_A(x) = \int_X x\mu_A(x) dx \tag{2}$$

This concept is different from the meaning of the Expectation of probability space.

Converting Z-numbers to classical fuzzy numbers

Direct calculations using Z-numbers are difficult and long calculations and have limited conditions (Zadeh, 2011). Therefore, to use these numbers, they are first converted to classical fuzzy numbers and then calculations are performed by fuzzy numbers. This process simplifies the calculations (Azadeh et al., 2013; Kang et al., 2012a).

Assume $Z = (\tilde{A}, \tilde{R})$ is a Z-number and the fuzzy numbers \tilde{A} and \tilde{R} are defined as

$\tilde{A} = \{(x, u_{\tilde{A}}(x)) | x \in [0,1]\}$ and $\tilde{R} = \{(x, u_{\tilde{R}}(x)) | x \in X\}$, in which $u_{\tilde{A}}(x)$ is a trapezoidal membership function and $u_{\tilde{R}}(x)$ is a triangular membership function. In this case, the following steps are performed to convert Z-number to a classical fuzzy number:

- 1) First, the second component of Z-number (reliability value) is converted to a crisp number (Equation 3).

$$\alpha = \frac{\int x\mu_{\tilde{R}}(x)dx}{\int \mu_{\tilde{R}}(x)dx} \tag{3}$$

- 2) The weight of the second component (reliability value) is combined with the first component (restriction). The weighted Z-number can be denoted as $\tilde{Z}^\alpha = \{(x, \mu_{\tilde{A}^\alpha}(x)) | \mu_{\tilde{A}^\alpha}(x) = \alpha\mu_{\tilde{A}}(x), x \in [0,1]\}$ (Equation 4 and 5).

$$E_{\tilde{A}^\alpha}(x) = \alpha E_{\tilde{A}}(x), \quad x \in X \tag{4}$$

$$s. t. \quad \mu_{\tilde{A}^\alpha}(x) = \alpha\mu_{\tilde{A}}(x), \quad x \in X \tag{5}$$

- 3) Now the irregular fuzzy number (weighted restriction) becomes the regular fuzzy numbers (Equation 6 and 7). The obtained fuzzy set can be denoted as $\tilde{Z}' = \{(x, \mu_{\tilde{Z}'}(x)) | \mu_{\tilde{Z}'}(x) = \mu_{\tilde{A}}\left(\frac{x}{\sqrt{\alpha}}\right), x \in [0,1]\}$, and it is expressed through Equation (8) that (\tilde{Z}') has the same fuzzy expectation with \tilde{Z}^α .

$$E_{\tilde{Z}'}(x) = \alpha E_{\tilde{A}}(x), \quad x \in \sqrt{\alpha}X \tag{6}$$

$$s. t. \quad \mu_{\tilde{Z}'}(x) = \mu_{\tilde{A}}\left(\frac{x}{\sqrt{\alpha}}\right), \quad x \in \sqrt{\alpha}X \tag{7}$$

Equation (8) can be deduced from equations 4 and 6.

$$E_{\tilde{Z}'}(x) = E_{\tilde{A}^\alpha}(x) \tag{8}$$

By studying the equations in this section and converting a Z-number to a classical fuzzy number, it is sufficient to first determine the value of α through Equation (3) and after taking the square root of it, multiply in each parameter of the first component of Z-number, i.e. \tilde{A} .

INVESTIGATION AND CLASSIFICATION OF EFFECTIVE FACTORS IN THE SELECTION OF UNDERGROUND MINING METHODS

Mining method selection is one of the most important stages of mine design. Every deposit has its unique features. Numerous studies indicate that the underground mining method selection depends on the large number of factors. These factors can be classified into the following groups, i.e.: (Bogdanovic et al., 2012; Karimnia & Bagloo, 2015).

- Physical and mechanical characteristics of deposit such as local geological conditions, the strengths of the hanging and footwall, ore thickness, general shape of the deposit, slope, depth below the surface, overburden thickness, grade distribution, and quality. The main geological conditions include shear strength of the intact rock, natural fractures, shear strength of the in continuities, the orientation, length, spacing and locality of the geological structures, in situ stresses and hydrological conditions.
- Technical factors such as annual productivity, applied equipment, environmental considerations, mine recovery, flexibility of methods, machinery and mining rate
- Economic factors, such as: capital cost, operating cost, mineable ore tons, orebody grades and mineral value, and
- Exploitation factors such as annual exploitation, equipment, efficiency and environmental aspects.

In the present study, with the aim of classifying the effective parameters in the selection of underground mining methods, the available resources in this field were studied and the effective factors were investigated. Each of these studies has presented its classification to select the best mining method. In this article, by reviewing various research, a comprehensive classification of important factors in the selection of underground mining methods was performed. As shown in Table 2, the given criteria are divided into 4 main categories of technical, ambient, economic and operational/ mining factors and also 13 sub-criteria (Alpay and Yavuz, 2007, Alpay and Yavuz, 2009; Ataei et al., 2008; Ataei et al., 2013; Azadeh et al., 2010; Bajić et al., 2020; Balusa & Gorai, 2019a, 2019b; Balusa & Singam, 2017; BOGDANOVIC et al., 2012; Dehghani et al., 2017; FU et al., 2018; Gupta & Kumar, 2013; Iphar & Alpay, 2018; Karadogan et al., 2008; Karimnia & Bagloo, 2015; MIKAEIL et al., 2009; Popović et al., 2019; Yavuz, 2015; Yazdani-Chamzini et al., 2012 Zare Naghadehi et al., 2009).

Table 2. Classification of effective factors in the selection of underground mining methods in the present study

No.	Criteria	No.	Sub-criteria
1	Technical Factors	1	Geometry Conditions of the Deposit
		2	Geomechanical Condition
		3	Geological Conditions
2	Ambient Factors	4	Geographical Conditions
		5	Static and Dynamic Loading
3	Mining & Operational Factors	6	Technological Factors
		7	Productivity Factors
		8	Environmental Concerns
		9	the complexity of production management
		10	Safety of production
4	Economic Factor	11	Costs
		12	Income
		13	Initial Investment Rate of Returns

MATERIAL AND METHODS

In this study, using the Z-numbers theory, the factors influencing the selection of underground mining methods were classified. The steps of conducting the research are presented as bellow.

Selection of Experts and Determining the Weighting Factors of Them

When sufficient information does not exist, experts’ opinions are used. In this study, 10 experts were selected to determine the weighting. It should be realized that these experts do not have the same weighting score. For this reason, in order to determine weighting scores of experts, title, experience, education time and age criteria were used. The weighting factor of each expert was obtained by dividing the sum of scores obtained from him/her divided by the total scores obtained by all experts participating in the study (Lavasani et al., 2015; Lavasani et al., 2015; Renjith et al., 2010).

Steps Used to Apply Z-Numbers

Quantification of experts' predictions about each parameter (\tilde{A})

Linguistic terms have been used for quantifying expert’s opinions or determining their opinion’s weighting regarding each parameter. Five applied linguistic terms include very low, low, medium, high, very high which in short is VL, L, M, H, and VH. To fuzzy this section, trapezoidal fuzzy number has been used. Figure 2 represents the fuzzy domain of applied linguistic terms in this study (Chen & Hwang, 1992; Lavasani et al., 2015; Lavasani et al., 2015; Renjith et al., 2010).

Quantification of the reliability of the first component (\tilde{R})

In this paper, to quantify the reliability of the first component for each parameter, the language variables Very Low (VL), Low (L), Medium (M), High (H) and Very High (VH) have been used. To fuzzy this section, a triangular fuzzy number has been used, which Figure 3 shows the fuzzy range of linguistic variables used in this research (Kang et al., 2012b).

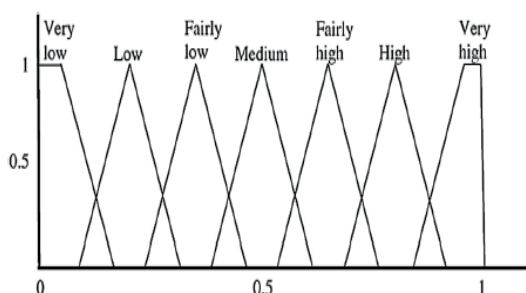


Figure 2. Linguistic terms used by experts (Mottahedi & Ataei, 2019; Renjith et al., 2010)

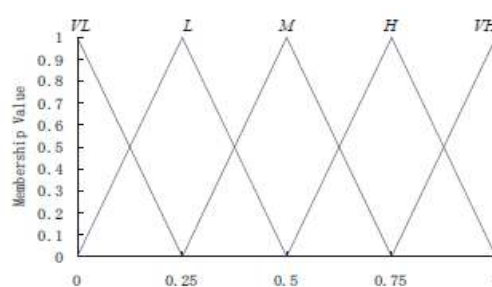


Figure 3. Linguistic variables used to quantify \tilde{R} (Kang et al., 2012b)

Table 3 shows a part of the survey forms submitted. In this questionnaire, experts, based on their knowledge and experience in selecting the appropriate underground mining method, estimated the importance of each parameter (\tilde{A}) in the left part of that parameter. And in the right part, they considered the reliability of their predictions about each factor (\tilde{R}).

Table 3. A part of the survey forms used in this study

Influencing factors in underground mining method selection										
The importance of each criterion					Criteria	The reliability of experts' predictions about each criterion				
VL	L	M	H	VH		VL	L	M	H	VH
Technical Factors										
Ambient Factors										
Mining & Operational Factors										
Economic Factor										

Converting Z-Numbers to Classical Fuzzy Numbers

In this section, according to the contents of concepts section, a Z-number was converted to a classical fuzzy number (Azadeh et al., 2013; Kang et al., 2012a).

- 1) Determining α in each parameter using fuzzy number \tilde{R} : The value of α for the second component of Z-number is determined using the equation 3.
- 2) Multiplying $\sqrt{\alpha}$ in each parameter of the first component of Z-number (\tilde{A}): As mentioned, to convert Z-numbers to classical fuzzy numbers, the $\sqrt{\alpha}$ obtained from the previous step must be multiplied in each parameter of the first component of Z-number, i.e., \tilde{A} .

Aggregating Expert’s Opinions

For aggregating experts’ opinions, the weighting factor of each expert is multiplied in his/her linguistic terms score (fuzzy number). This has been done according to equation (9) and based on a study by Clemen and Wrinkler (1999) and Renjith et al. (2010).

$$M_i = \sum_{j=1}^n W_j A_{ij} \quad (i = 1,2,3, \dots, m) \tag{9}$$

Where: A_{ij} : Linguistic terms in relation to each parameter i by expert j , w_j : Experts’ weighting factor j , m : the number of parameters and n : the fuzzy number of aggregating expert’s opinions in relation to each parameter i .

Defuzzification And Converting Each Parameter to A Crisp Number

Defuzzification of fuzzy numbers is an important procedure for decision-making in fuzzy environment. In this study, center of area (centroid) defuzzification technique has been selected. This technique has been developed by Sugeno in 1985. This is the most used technique and is accurate. Defuzzification of trapezoidal fuzzy number $\tilde{A} = (a_1, a_2, a_3, a_4)$ is obtained using Equation 10 (Lavasani et al., 2015; Lavasani et al., 2015).

$$X^* = \frac{1}{3} \frac{(a_4 + a_3)^2 - a_4 a_3 - (a_1 + a_2)^2 + a_1 a_2}{(a_4 + a_3 - a_2 - a_1)} \tag{10}$$

Ranking of Influencing Parameters in Underground Mining Method Selection

In this section, after calculating the final weight of each parameter using Equation (10), the importance of each factor was determined and ranked based on the obtained weights. According to the results of calculations and quantify the uncertainty of parameters using Z-number theory, in the main group of criteria technical factors with a weight of 0.745, are the most important parameters. Economic factors (0.685), mining/operational factors (0.639) and ambient factors (0.594) are also in the next categories, respectively (Table 4 and Figure 4).

Among the sub-criteria influencing the selection of underground mining method, geological conditions (0.730), geometry conditions (0.717) and income per ton of ore (0.715) are the most important factors. After these parameters, geomechanical conditions, costs and initial investment rate of returns are the most important parameters, respectively (Table 5 and Figure 5).

Table 4. Final weight of criteria and their rank

Criteria	Final Weight	Ranking of Criteria
Technical Factors	0.745	1
Ambient Factors	0.594	4
Mining & Operational Factors	0.639	3
Economic Factor	0.685	2

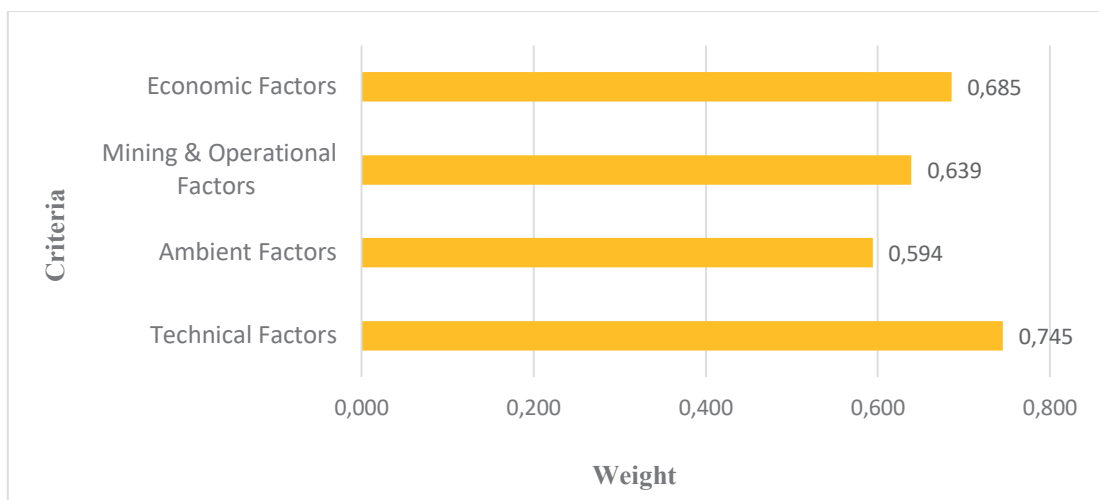


Figure 4. Final weight of criteria and their rank

Table 5. Final weight of sub-criteria and their rank

Criteria	Sub-criteria	Final Weights	Ranking of sub-criteria
Technical Factors	Geometry Conditions of the Deposit	0.717	2
	Geomechanical Condition	0.677	4
	Geological Conditions	0.730	1
Ambient Factors	Geographical Conditions	0.485	11
	Static and Dynamic Loading	0.517	9
Mining &	Technological Factors	0.493	10

Operational Factors	Productivity Factors	0.574	7
	Environmental Concerns	0.391	13
	The complexity of production management	0.466	12
	Safety of production	0.526	8
Economic Factor	Costs	0.631	5
	Income	0.715	3
	Initial Investment Rate of Returns	0.601	6

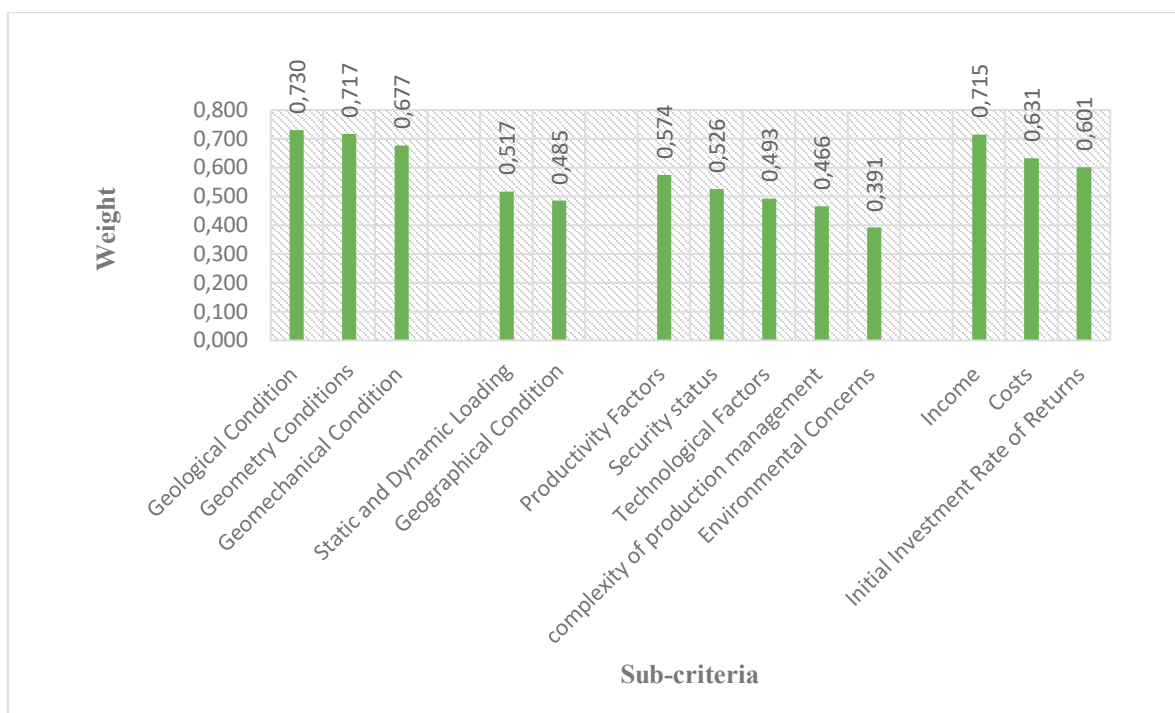


Figure 5. Final weight of sub-criteria and their rank

CONCLUSION

Selecting the best underground mining method among many alternatives is a multicriteria decision-making problem. The important factors for mining method selection include geological and mineralogical factors, geometrical features of deposit, safety, environmental parameters, economic variables, geographic characteristics, and local considerations. A number of these influencing criteria face uncertainty and they are difficult to quantify. The existing uncertainties must be considered in the decision-making process of selecting the appropriate underground mining method. Fuzzy parameters are generally estimated through expert knowledge, but the degree of confidence in the opinion of different experts is different and the uncertainty and difference in the reliability of their opinion cannot be ignored. In this regard, Z-numbers Theory has been proposed. Each Z-number is represented by a pair of fuzzy numbers such that the first component indicates the fuzzy importance of each parameter, and the second component is the reliability of the prediction of the first component. In this study, after classifying the effective factors in the selection of underground mining methods, the Z-numbers approach was used to rank and determine their importance. The results showed that in the main group of criteria technical factors and among the sub-criteria geological conditions, geometry conditions of the deposit, income per ton of ore, geomechanical conditions, and costs are the most important parameters, respectively.

REFERENCES

- Alpay, S., Yavuz, M. (2007). A Decision Support System for Underground Mining Method Selection. *International Conference on Industrial, Engineering and Other Applications of Applied Intelligent Systems*, 4570, 334-343.
- Alpay, S., Yavuz, M. (2009). Underground mining method selection by decision-making tools. *Tunnelling and Underground Space Technology*, 24, 137-184.
- Ataei, M., Jamshidi, M., Sereshki, F., Jalali, S. M. E. (2008). Mining method selection by AHP approach. *The Journal of the Southern African Institute of Mining and Metallurgy*, 108, 741-749.
- Ataei, M., Shahsavany, H., Mikaeil, R. (2013). Monte Carlo Analytic Hierarchy Process (MAHP) approach to selection of optimum mining method. *International Journal of Mining Science and Technology*, 23, 573–578.
- Azadeh, A., Osanloo, M., Ataei, M. (2010). A new approach to mining method selection based on modifying the Nicholas technique. *Applied Soft Computing*, 10, 1040-1061.
- Azadeh, A., Saberi, M., Zandi Atashbar, N., Chang, E., Pazhoheshfar, P. (2013). Z-AHP: A Z-number Extension of Fuzzy Analytical Hierarchy Process. *7th IEEE International Conference on Digital Ecosystems and Technologies (DEST)*, 141-147.
- Bajić, S., Bajić, D., Glušcević, B., Vakanjac, V. R. (2020). Application of Fuzzy Analytic Hierarchy Process to Underground Mining Method Selection. *Symmetry*, 12, 192.
- Balusa, B. C., Gorai, A. K. (2019). Sensitivity analysis of fuzzy-analytic hierarchical process (FAHP) decision-making model in selection of underground metal mining method. *Journal of Sustainable Mining*, 18, 8–17.
- Balusa, B. C., Gorai, A. K. (2019). A Comparative Study of Various Multi-criteria Decision-Making Models in Underground Mining Method Selection. *Journal of The Institution of Engineers (India): Series D*, 100, 105–121.
- Balusa, B. C., Singam, J. (2017). Underground Mining Method Selection Using WPM and PROMETHEE. *Journal of The Institution of Engineers (India): Series D*, 99, 165–171.
- Bogdanovic, D., Nikolic, D., Ilic, I. (2012). Mining method selection by integrated AHP and PROMETHEE method. *Annals of the Brazilian Academy of Sciences*, 84, 219-233.
- Chen, S. J., Hwang, C. L. (1992). *Fuzzy Multiple Attribute Decision Making*, 1st Ed. Springer-Verlag Berlin. Heidelberg, Germany, ISBN: 3-540-54998-6.
- Clemen, R. T., Winkler, R. L. (1999). Combining probability distributions from experts in risk analysis. *Risk analysis*, 19, 187-203.
- Dehghani, H., Siami, A., Haghi, P. (2017). A new model for mining method selection based on grey and TODIM methods. *Journal of Mining & Environment*, 8, 49-60.
- Fu, Z., Wu, X., Liao, H., Herrera, F. (2018). Underground Mining Method Selection with the Hesitant Fuzzy Linguistic Gained and Lost Dominance Score Method. *IEEE Access*, 6, 66442-66458.
- Gupta, S., Kumar, U. (2013). An analytical hierarchy process (AHP)-guided decision model for underground mining method selection. *International Journal of Mining, Reclamation and Environment*, 26, 324-336.
- Heidarzadeh, Sh., Saeidi, A., Rouleau, A. (2020). Use of Probabilistic Numerical Modeling to Evaluate the Effect of Geomechanical Parameter Variability on the Probability of Open Stope Failure: A Case Study of the Niobec Mine, Quebec (Canada). *Rock Mechanics and Rock Engineering*, 53, 1411-1431.
- Iphar, M., Alpay, S. (2018). A mobile application based on multi-criteria decision-making methods for underground mining method selection. *International Journal of Mining, Reclamation and Environment*, 33, 480-504.
- Kang, B., Wei, D., Li, Y., Deng, Y. (2012). A Method of Converting Z-number to Classical Fuzzy Number. *Journal of Information & Computational Science*, 9, 703-709.

- Kang, B., Wei, D., Li, Y., Deng, Y. (2012). Decision Making Using Z-numbers under Uncertain Environment. *Journal of Information & Computational Science*, 8, 2807-2814.
- Karadogan, A., Kahriman, A, Ozer, U. (2008). Application of fuzzy set theory in the selection of underground mining method. *The Journal of the Southern African Institute of Mining and Metallurgy*, 108, 73-79.
- Karimnia, H., Bagloo, H. (2015). Optimum mining method selection using fuzzy analytical hierarchy process–Qapiliq salt mine, Iran. *International Journal of Mining Science and Technology*, 25, 225-230.
- Lavasani, M. R., Wang, J., Yang, Z., Finlay, J. (2011). Application of Fuzzy Fault Tree Analysis on Oil and Gas Offshore Pipelines. *International Journal of Marine Science and Engineering*, 1, 29-42.
- Lavasani, S. M., Zendgani, A., Celik, M. (2015). An extension to Fuzzy Fault Tree Analysis (FFTA) application in petrochemical process industry. *Process Safety and Environment Protection*, 93, 75-88.
- Mikaeil, R., Zare Naghadehi, M., Ataei, M., Khalokakaie, R. (2009). A Decision Support System Using Fuzzy Analytical Hierarchy Process (AHP) and TOPSIS Approaches for Selection of the Optimum Underground Mining Method. *Mining Sciences*, 54, 349-368.
- Mottahedi, A., Ataei, M. (2019). Fuzzy fault tree analysis for coal burst occurrence probability in underground coal mining. *Tunnelling and Underground Space Technology*, 83, 165–174.
- Popović, G., Đorđević, B., Milanović, D. (2019). Multiple Criteria Approach in the Mining Method Selection. *Industrija*, 47, 47-62.
- Renjith, V. R., Madhu, G., Lakshmana Gomathi Nayagam, V., Bhasi, A. B. (2010). Two-dimensional fuzzy fault tree analysis for chlorine release from a chloralkali industry using expert elicitation. *Journal of Hazardous Materials*, 183, 103-110.
- Samimi Namin, F., Shahriar, K., Bascetin, A., Ghodsypour, S. H. (2009). Practical applications from decision-making techniques for selection of suitable mining method in Iran. *Gospodarka Surowcami Mineralnymi*, 25, 57-77.
- Yavuz, M. (2015). The application of the analytic hierarchy process (AHP) and Yager’s method in underground mining method selection problem. *International Journal of Mining, Reclamation and Environment*, 29, 453-475.
- Yazdani-Chamzini, A., Haji Yakchali, S., Zavadskas, E. K. (2012). Using an integrated mcdm model for mining method selection in presence of uncertainty. *Economic Research*, 25, 869-904.
- Zadeh, L. A. (2011). A Note on Z-numbers. *Information Sciences*, 181, 2923-2932.
- Zare Naghadehi, M., Mikaeil, R., Ataei, M. (2009). The application of fuzzy analytic hierarchy process (FAHP) approach to selection of optimum underground mining method for Jajarm Bauxite Mine, Iran. *Expert Systems with Applications*, 36, 8218–8226.

AGGLO COLUMN FLOTATION OF TURKISH LIGNITE SLIME AND ŞIRNAK ASPHALTITE BY MICRO SELECTIVE COAGULATION IN MODIFIED COLUMN FLOTATION SEPARATOR

Y. I. Tosun^{1,*}, F. Çiçek²

^{*1}*Şirnak University, Engineering Faculty, Mining Engineering Department, Şirnak*
(*Sorumlu yazar: yildirimismailtosun@gmail.com)

²*Azerbaijan National Science Academy, Radiation Institute, Baku*

ABSTRACT

The asphaltite reserves and current coal mining in Şirnak, were 83% of total Turkey's asphaltite reserves. This type of asphaltite should be washed with a washing plant to operate in areas where sulfur content and ash content of asphaltite were removed. Tunçbilek, Bolu Mengen and Kütahya Gediz lignite were tested in selective agglomeration by asphaltite together. The ash and sulfur contents in coal washing provided great issue due to hard washability of Şirnak asphaltite. This evaluation gave great benefits in terms of reduced costs as well as transport and environmental protection. The coal slime recovery ranged from a 20-120 mg/l fuel oil solution through with mechanical agitation of fuel oil micro coagulation followed by modified centrifuge baffle was researched. Micrographs and particle size measurements indicated that coagulates were the fine agglomerate of fuel oil micro coagulation and slime, with size ranging from 70 to 100 µm. Micro column flotation proved much as other mechanical techniques such as inclined lamella plates in column and coagulation effect was managed in agitation conditioner by fuel oil. Modified column flotation cell used to recover coagulates on the lamella bafflers temporarily. The fuel oil and surfactant adsorption was evaluated through control measurements. The influence of collector fuel oil concentration, pH and bubble size on slimes recovery was investigated. In the absence of collector, a combustible recovery of 45% was achieved, while in the presence of 20 mg/L of fuel oil it was increased to 80%, at pH 8. The slime recovery also increased with fuel oil micro coagulation increase to 30gr/l slurry and bubble size decrease, reaching 50-150 micron coagulates and bubble size around 60 µm.

Keywords: Modified flotation column, column baffling, fuel oil coagulate, selective agglomeration, slime aggro-flotation, lignite slime, aggro-flotation, slime

INTRODUCTION

In coal recovery the selective agglomeration and coagulation of solid coal slimes were tested as self coagulation with fuel oil micro coagulation and asphaltite coagulation was effective and inclined lamella baffle or flow rate and collector dosages were needed in slime coagulation and aggro-settling rates was managed at the attrition speed of 500-600 rev/min at higher speeds the agglomerated particles deteriorated and combustible yields decreased to 76% at waste management and coal recovery. The plant-based settling can be operated as mobile or integrated depending on solid content and dewatering slime and wastes evaluation methods in Şirnak. For this reason selective coagulation waste was critical on the quality of which it will be used in the oil agglomerated settling or flotation. The collection of coal slime from tailings pool and bio-waste pyrolysis was affecting the cost of waste management and recovery of coal. The application of the waste separation method was also affected the amount of solid waste to be recovered or the amount of compost to be produced. In Şirnak province, approximately 120 thousand tons of annual solid waste

and 60 thousands as coal slime at dry weight have been formed. This project has been studied in a mobile incineration plant project considering similar wastes in neighboring countries Siirt and Hakkari. In this way, it will be beneficial to recycle wastes, energy gain as well as environmental effect which can be done consciously waste classification from garbage and bio waste stream in the regions. The slime aggro-flotation and coal recovery units that integrated were also linked to the mobile system in the study and an economically sustainable economical solid waste management and combustion system in the integrated plant designed. The designed mobile coagulation and slime aggro-flotation unit ensured that the problems such as water and soil pollution and environmental waste loss, including energy production, were minimized. If the integrated mobile system is economically sustainable, it is aimed that the operating cost was low and the management was slightly economical and portable in conformity with Şırnak City Province, and an issue in Southeastern Anatolian region due to the fact of less poverty and scarcity of water resources in hard geographical conditions.

Coal Slime and Waste

The almost 211TWh total electricity in 2011, Turkey were produced primarily from imported natural gas and domestic coal [TKI, 2013]. The total amount of asphaltite resource in reserves and production in Şırnak City are over 82 million tons of available asphaltite reserve and 400 thousand tons per year, respectively [TKI 2009]. The most effective and cost-effective technologies are needed for clean coal products in today's modern technologies [EIA,2015]. Turkish coal industry needs washing technologies and high performances at lower cost with various types of local coals.

Evaluation of natural resources, in parallel with the energy needs of our country will provide economic benefits by reducing fuel imports. Basically, energy production is made from imported natural gas and has a 46% share of health. After the energy production from coal imported natural gas is located in the second row and is provided by burning coal in thermal power plants with a share of 26% (TKI, 2013). Depending on the future energy demand, the ratio is expected to increase. A total of 83 million Zones per annum of lignite and coal in boilers and industrial furnaces production was evaluated as the need for heating and energy. The quality of coal ash minerals comprised micronized size particles (Ketkar et al., 2010,). In this study, the opening of the quarry closed in Şırnak region and the high-calorie but ash and sulfur content can be produced by washing it is considered to be the economic contribution of higher asphaltites. Şırnak asphaltites the washability studies made by developing potential flowsheets were compared accordingly wash washing plant investment and operating costs. The result of the feasibility study has identified suitable premises.

Asphaltites of Southeastern Anatolia is located in the Şırnak and Hakkari 's provinces in Turkey 120 million tons of proven reserves of Şırnak and Hakkari possible asphaltite of 0.2-1% moisture, 37-65% ash, sulfur burning 6,3-7.5% total sulfur 5.5-5.7%, 60-65% volatile matter and 2800-5600 kcal / kg has a lower temperature. Şırnak asphaltites beds are distributed or block-shaped space rock in the vein location [TTK 2009]. Avgamasya and production is done in Karatepe veins approximately 15 years. Avgamasya and Karatepe veins 15-25 and 10-20 m thick clumps form. Also Hakkari, Uludere district was spread around 1-20 m thick layer of scattered asphaltite seam and as bed layers and as veins. As well as limestone bed rock, shale, marl clay, marl and argillaceous limestone is located. Şırnak asphaltite coal is soft with shale ash and macro sized calcite, micronized minerals as pyrite and pyrrhotite inclusions are widely distributed in coal and asphaltite shale.

Washing with the Selective Agglomeration of Slime

Slime settling for washing the fine size coal (Jameson, 2001) is a method most commonly used. Some studies of coal particle size and density of mineral distribution in coal slime settling (Warner, 1985) determined that significant side kinetic and may affect efficiency. Studies particle

size increases, as can be shown that the yield decreases rapidly (Schubert, 2008). Generally yield falls in the slime settling of coarse coal, but slime settling rate is very low. Particle size is too big, not sticking on the bubbles. In contrast, a high efficiency in the fine coal slime settling and slime settling kinetics also increase (Gupta et al., 2001). In contrast, slime settling rate depends strongly on the grain size medium size coal particles. In addition, the bubble clusters formed around the coarse coal particles was determined to be effective in the coal particles floated by slime settling. Slime settling in size, the solid ratio of reagent dosage and reactive species stated that effective slime settling success (Wills and Napier-Munn, 2006, Klimpel and Hansen, 1987, Rules 1991).

Besides, the grain size on the slime settling of coal ash and mineral substances with a coupling degree of covering of the mineral ash has been determined to be in effect (Laskowski 2001, Erol et al., 2003). Washing the slime settling proper size range was found to be -500 microns. Bigger size and mechanical mixing of fine particles of coal has created different hydrodynamic effect (Jameson, 2001).

Şirnak asphaltites about coal reserves with the washability of the petrographic studies with standard slime settling pyrite and clay depending on the structure of asphaltite moved, it has been identified as hard coal washability.

Washing the Coal with Selective Agglomeration of Slime and Column Flotation

Column slime flotation of fine coal is determined could very well yield can be floated in the microbubbles (Yianatos et al., 1988). Microbubble washing water in the form of shower foam zones consisting of may be possible to obtain cleaner product coal with the addition. (Hadler et al., 2012 and Jameson, 2001) washable particularly difficult and shale and shale is a method used successfully in coal at high rates. Particle size and type of coal as the slime aggro-flotation column can easily affect efficiency. However, operating parameters, especially the foam height of the column unit, the wash water is added, and the bias ratio is flammable operating parameters affect efficiency (Finch and Dobby, 1990, Yoon, 1993, Yoon, 2000).

It was formed on an inclined foam zone to increase the effectiveness of the foam so that gravity was stated to reduce drift foam. These essential principles laid cyclonic column slime aggro-flotation cell (S-FCMC) provided a foam zone comprising inclined channels (FCMC) it proved to be effective in coal washing and widely China (Rubio, 1996) was used. The foam product has a third zone of the foam sediment are removed (Valderrama et al., 2011).

Industrial development currently demands a growing consumption of solid fuel resources in the country with the concern of environment in order to supply energy needs. This wide utilization of coals and lignite leads to a considerable amount of washing based wastes being discharged into tailings ponds, demanding previous treatment to avoid pollution. Additionally, waste waters or sewage sludge can be treated by washing and sludge let to the soil, providing humus carbon source and fertilizers. The environmental pollution of streams near coal fields still cause the eutrophication issue, a phenomenon characterized by algae overpopulation and the rapid growth of aquatic plants, which impair the penetration of light in the water, thus reducing photosynthesis reactions and, consequently, the amount of dissolved oxygen in the water, suffocating aquatic animals and converting the water body into an open sewer (EIA 2012). Thus, the development of carbon management was critical in strategies in the environment. There has been a considered issue for quality of energy, leading to the search for new technologies to recover the coal slimes, offering opportunities for its recovering, and contributing to energy sustainability (TTK 2009). At the present time, chemical and physicochemical processes are the most used for finer size and ultrafine size near micron sized particles and particle removal from wastewaters using sufficient conditioning (Chakner

et al., 1987, Degner 1986). Aluminum and iron salts present the disadvantage of generating coagulation of sewer sludge, which cannot be reused or reclaimed (Oats et al., 2010 a b) (Xi, 1999; Xie, 2001). Thus, there was necessary to employ solid/liquid separation for recovery of fuel oil micro coagulation and carrier techniques, such as slime aggro-flotation, which is a well-established technique for minerals separation and is also commercially used for wastewater treatment (Fuerstenau 1976, Gupta et al., 1971). This technique is based on the different hydrophobic manner of the particles to be separated. Thus, hydrophobic particles can be captured by gas bubbles and float to the liquid surface. The slime aggro-flotation requires the use of surfactants to render the particle surface more hydrophobic. The efficiency of this process depends on the probability of particle-bubble collision and attachment. For small particles there is a need for small bubbles such as those produced by column slime flotation produced finer bubbles (Nunes et al.,2011, Dai et al., 2000).

MATERIALS AND METHODS

In this study, a modified type centrifuge baffle was investigated for coagulate settling. The particle breaking and screen washing effect the agglomeration of coal. The micro coagulation conditioning with fuel oil and coagulation provided in efficient column slime aggro-flotation process, as activated sludge was considered the most versatile wave effect could be forced to move at the direction of upward bubble flow instead of settling down and was so efficient at high dense liquid medium and less efficient at less density difference. While among the many oil slime settling type of chemical processes, oil slime aggro-flotation through the use of carbon coagulation by collectors were widely employed as seen from in Figure 3.

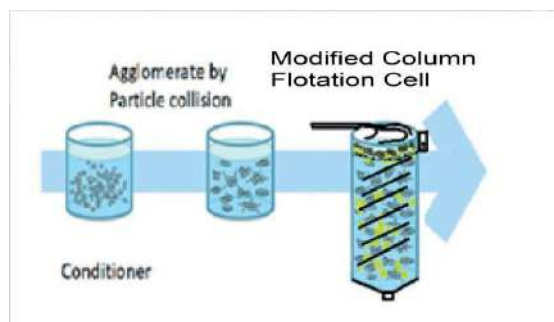


Figure 3. Schematic view of the carrier - column, slime aggro-flotation system with lamella baffle phase and air bubbling.

However, coagulates and agglomerates of carrier slime aggro-flotation by fuel oil micro coagulation fines were difficult to settle, requiring the use of bubble contact and lamella aggro-flotation separation

The particle size of the slime and the average bubble diameter were determined with a Malvern Instruments Mastersizer 2000SM capable of analyzing particles with diameters between 0.1-2000 μm . The average coagulates diameter was determined with the help of a specially designed acrylic cylindrical cell with a volume of 1 L, to fit in a Malvern Instruments Mastersizer 2000SM device. The influence of pH and current density on oil droplet diameter in a 0.1 mol/L HCl and NaCl solution was evaluated.

Column slime aggro-flotation tests were carried out in a 3L volume 110 mm diameter glass cell, with a 5 mm mesh stainless lamella at 45° as shown in Figure 3. Fuel oil was used as collector conditioning and managed following separation in the lamella settling of the modified column cell.

The influence of fuel oil concentration, pH, sodium chloride concentration and flow rate on the coal yield, combustible recovery and on the carrier slime aggro-flotation and coagulation of the pH was evaluated. The coagulant sludge used in the feed of column slime aggro-flotation tests used 20 mg/L of fuel oil and 25-120 g/L fuel oil micro coagulation at 10 % solid weight rate and 0.1 mol/L NaCl as electrolyte with 0,1 mol/l HCl or NaOH as pH regulators. All reagents used were obtained from MERCK and were analytical grade.

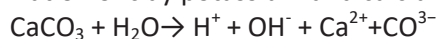
For each test, a coal column slime aggro-flotation feed with a certain solid liquid ratio of 10% was fed into the column slime aggro-flotation cell. After 20 minutes the lamella baffle collection of the slime and lamella baffle with coagulation was determined by the micrometric method (Nikon Instruments).

RESULTS AND DISCUSSION

Coal Slime Characterization

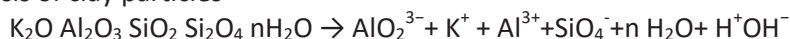
The X-ray diffractogram of the coal clay and shale obtained from coal site selectively containing smectite and chlorite is presented in Figure 4. It can be observed that the coal slime was of a mixture of smectite clay with calcium carbonate and chlorite, which is a rate of 3,4/1,2/0,4 weight. However, the coagulation with fuel oil of clay stone particles was ion changing reactions in the sludge but chloride waters were effective in fuel oil micro coagulation site activation with coal particles instead of clay fines. Coagulation kinetics is not favored by slime and other species, such as calcium carbonate particles in the slime. It is proposed a two-step mechanism for the coagulation of coal slime was fuel oil micro coagulation activation and collector cover conditioning which is lately shown in the Figure 1 and 2.

Ionization of clay potassium and calcium carbonate



(6)

Hydrolysis of clay particles



(7)

Where that iron and alkali cations was resulting in the cation exchange of Ca and Fe cations, it was found that hydrogen medium activation, hydrolysis of ions may activate clay particles for coagulation to fuel oil micro coagulation of asphaltite and carrier coagulant.

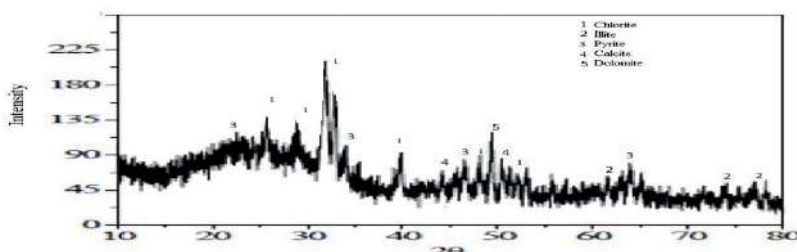


Figure 4. X-ray test result of Coal waste clay and shale

The coagulate size distribution is showed in Figure 5. Test results received by the particle size analyzer was the cumulative fractions that followed the result accumulated below a given fraction size. The frequency curve defined in the Figure 5 as the curve with peaks obtained by

Gaussian cumulative distribution. It was observed that 7% of fines in the sample have diameters below 15 µm, 70% of slimes in the coal sample had diameters below 35 µm .The average particle size of the sample was 45 micron regarded as slime but fuel oil micro coagulation was 100 micron average size and 90% of slimes in the sample have diameters below 78 µm, a size small enough to justify the use of column slime aggro-flotation to recover the coal carrier fuel oil micro coagulation agglomerates. Hence, this column centrifuge aggro-flotation method produced high aggro-flotation rates than those produced in the conventional slime settling process or even in centrifuge slime settling.

The chemical properties of Şırnak asphaltite marl and clay are given in Table 1. The proximate analysis of Şırnak asphaltite is given in Table 2.

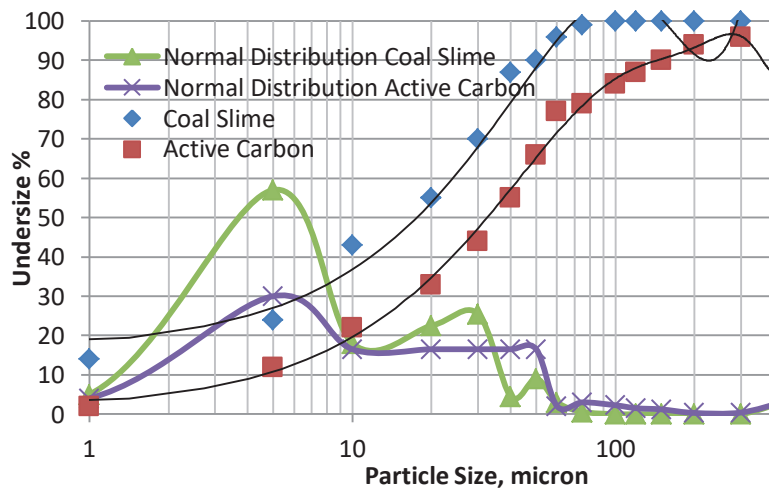


Figure 5. The size distribution and normal size distribution of Slime active carbon coagulates obtained from at pH 7,7 in Selective Coagulation

Table 1. The composition of Ash matter; Ash clay and Ash Marly shale of Şırnak Asphaltite in Selective Coagulation

%Component	ŞırnakMarl	ŞırnakŞhale
SiO ₂	24.14	48.53
Al ₂ O ₃	12.61	24.61
Fe ₂ O ₃	7.34	7.59
CaO	29.18	9.48
MgO	4.68	3.28
K ₂ O	3.32	2.51
Na ₂ O	1.11	0.35
loss	21.43	3.09
SO ₃	0.2	0.32

Table 2. The proximate analysis of Şırnak Asphaltite Slime Selective Coagulation

Coal	C%	H%	Ash%	S%	Moisture,%	Heat Value,kcal/kg
ŞırnakAsphltite Slime	17	4,5	42,1	6,6	0,5	3540

Effect Of Fuel Oil on The Coal Slime Recovery

The effect of kerosene concentration on the coal recovery by column slime flotation and on the carrier of the fuel oil micro coagulation particles is presented in Figure 4. It was observed that, in the absence of fuel oil micro coagulation, a coal recovery of 45% was achieved. The coagulated slime are randomly dissolved ions may activate shale species, hydrophilic and having average diameter around 3-5 μm depressed coal particles.

According to this research, coagulated particles caused higher entrainment and the slime agglomeration mechanism did not show any separation between hydrophobic and hydrophilic shale particles. This phenomenon improved higher effect on separation by ultrasonic wave forces when the particles enter the act of the wave direction to the lamella baffle column in much effect of finer clay particles occupying the spaces between the agglomerates and let remain in liquid phase. Some of the larger particles are drained back into the pulp, but the sink is carried upwards and is ultimately recovered in the concentrate. The finer the particle (<10 μm), was affected the more to remain suspended in the inter-bubble water and to be recovered by entrainment rather than by true slime agglomeration, a process that occurs only with hydrophobic particles (Figure 6).

In the presence of fuel oil micro coagulation, it was seen that a higher coal recovery was in the range of 68-74 % at less concentration of fuel oil (20-30 mg/ L) and a decrease of combustible recovery for concentrations above 50 mg/L.

It was shown the fuel oil adsorption on the fuel oil micro coagulation was sufficient even porous structure. According to the lamella baffle concentration was seen on fuel oil micro coagulation due to yields received by collectorless slime floating. The surface cations (Ca^{2+} or Fe^{+3}), forming apolar micelles and rendering the surface contact with shale. This kind of chemical interaction is a specific adsorption, and therefore of difficult desorption, which activated shale by sticking lamella baffle surfactant micelles and the increase of combustible recovery in the lamella baffle but ash content and yield with a recovery of 76% in the presence of 30 mg L^{-1} of fuel oil.

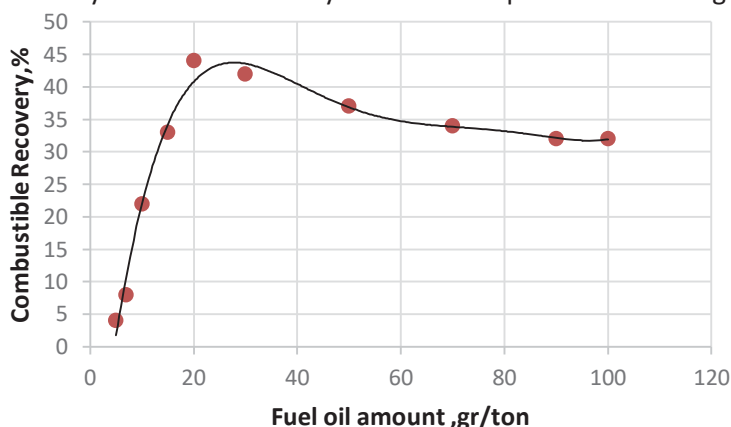


Figure 6. The coal yield of coagulate as a function of the fuel oil concentration added a 0.1mol/L HCl solution at pH 7,7 in Selective Coagulation.

Effect of pH on Coal Yield in Selective Coagulation

The effect of pH on the coal recovery and on the zeta potential of fuel oil micro coagulation and coal surfaces with fuel oil as collector is illustrated in Figure 7. It can be observed that, without fuel oil collector addition, the combustible recovery was not high at neutral pH, increased from 23% to 42% when the pH is increased from 4 to 9. Acidic pH improved the activation over coal surfaces with cleaning with the pH increase, which can contribute to the increasing clay activation by ion exchange with resulting entrainment.

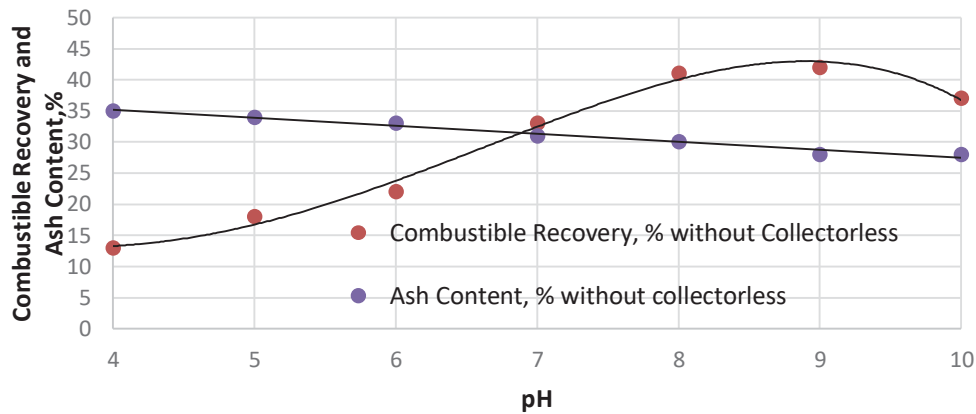


Figure 7. The asphaltite recovery in the inclined lamella column slime aggro-flotation, as change at pH changed by HCl in the presence of 50 mg/L fuel oil.

Project Design of Coal Washing Plant

The cleaning of washable hard coal needed the pre-cleaning, which was widely used heavy medium coal washing in large drums. At the fine coal in size (18-1mm) that cleaning was considered as heavy media cyclone unit (Anonymous a, b, c, 2015). Şırnak asphaltites the washing of these units Larcodems or fine coal washing unit that uses Humphrey spirals in mind it would be useful wash plant designs are made for efficiency cannot be achieved. According to the above washing test results it was analyzed in terms of investment and operating costs of the following two different designs. Implementing both A and B model design used the slime aggro-flotation column with coal slime aggro-flotation plant design also includes units shown in Figure 8. The B design that uses only coal slime aggro-flotation unit is shown in Figure 8.

Design Facility mainly heavy media cyclones, Humphrey spirals, pneumatic slime aggro-flotation unit Wemco column includes a slime aggro-flotation unit. The recently developed high-performance column slime aggro-flotation units in the slime coal washing, used with success. The conventional gravity techniques were beneficial of asphaltite washing as given plant flow diagram as shown below for the B design as shown in Figure 8.

As noted above Şırnak asphaltites 1.7 g/cm^3 can be obtained as an average of 5.25% washed clean coal ash. Şırnak asphaltites density of coal shale minerals 2.5 and has about 8% pores. That showed a washing coal density difference between $0.4\text{-}0.5 \text{ g/cm}^3$ which defines a close difference. That created many middlings by product in gravity separation at coarser size washing over 1 mm and nut size.

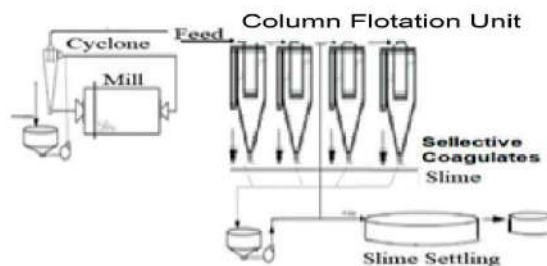


Figure 8. The proposed plant design for asphaltite cleaning with the column slime aggro-flotation.

CONCLUSIONS

The results demonstrated that coal recovery with fuel oil micro coagulation and column slime aggro-flotation can be used to recover asphaltite slime from the sludge. Slime particle sizes ranging from 30 to 76µm were obtained with 50 mg/L of fuel oil addition and 20 min conditioning was sufficient for column slime aggro-flotation. A recovery of 76% of fine slime and fuel oil micro coagulation agglomerates was managed in the control collectorless column slime aggro-flotation; however, the collector addition increased the recovery over 80% combustible matters. The addition of fuel oil micro coagulation for carrier slime aggro-flotation improved coal recovery and decreased collector reagent need at an amount one third. The combustible recovery reached a recovery of 43% without collector addition at pH 7,7 and 79 % at 120 mg/L fuel oil addition.

The test results showed that ultrasound slime aggro-flotation was an effective alternative treatment for sludge type pulps and effectively increased by decreasing pulp density in the slurry with low solid concentrations.

Due to the high ash content of Şırnak asphaltites and show that conventional slime aggro-flotation can be as low as column slime aggro-flotation The yield was also higher at certain fuel conditioning time of 20 minutes, but it was determined that the centrifuge aggro-flotation did not disturbed coagulates and not reduced combustible yield below to 56% which was sufficient, and well as clean coal product contained less sulfur. The ash content in the aggro-flotation washing plant was removed from the 42 % to 26% as waste material at high weight rate 62 %. Thus, 38% of the combustible sulfur could be disposed off.

Clean asphaltite with 25.2% ash could be produced in washing process, if carried out, and would have the 4.3% combustible sulfur, and a 6700 kcal/kg, lower heat value could be beneficial for both heating and for industrial boilers using washed clean fuel.

This washing application should be mandatory. Especially the company off-product quality, excavated shale rocks of the same color will be involved in the production by mixing will be reduced. Also washing process because there is very little difference between the density of the shale and coal will be more difficult.

The plant capacity to reduce costs researchers widely used in coal washing "modified column slime aggro-flotation" (Anonymous a, b, c, 2015). The majority needed to seek the optimal method to wash hardly washable Şırnak and Hakkari asphaltites.

Şırnak asphaltites may be washable with our technological conditions over difficult macro-economic factors that restrict the installation of washing facilities, fuel imports, environmental threats, such as economic sanctions will need to be examined.

REFERENCES

- Akdemir, Ü., and I. Sönmez. (2003). Investigation Of Coal And Ash Recovery And Entrainment In Flotation. *Fuel Processing Technology* 82(1): 1–9
- Anonymous a, (2015), *MultotecŞirket* web sayfası, <http://www.multotec.com/category/industry/coal>
- Anonymous b, (2015), *MBE Şirket* web sayfası, <http://www.mbe-cmt.com/en/products/pneufлот%2%AE/pneufлот%2%AE>
- Anonymous c, (2015), *CWP Şirket* web sayfası, <http://cwp.com.tr/en/products.aspx?id=30>

- Aplan F.F., (1977), Use of the Flotation Proess Desulphurization of Coal, *Coal Desulfurization: Wheelock T.D. (ed), ACS Symposium Series, Washington*
- Ata, S., and Jameson G. J. (2005), The formation of bubble clusters in flotation cells, *International Journal of Mineral Processing 76: 123 – 139*
- Ata, S. (2012). Phenomena in the froth phase of flotation—A review. *International Journal of Mineral Processing 102: 1–12.*
- Chander S, Sharma VN. (1976), Fine Particles Processing, P. Somasundran; 525-543
- Chander S., Mohal B. R., and Aplan F. F. (1987), Wetting Behavior of Coal in the Presence of Some Nonionic Surfactants, *Colloids & Surfaces* , Vol. 26 , pp. 205 – 213.
- Dai, Z., Fornasiero, D. and Ralston, J., (2000), Particle-Bubble Collision Models - A Review, *Advances in Colloid and Interface Science, 85*, No. 2-3, 231-256.
- Degner V.R., (1986), Flotation Machine Size Selection, *COALPREP86 Conference papers*, p319-349
- Despotovic, R, (1976),;Radiometric Characterization Of Precipitation Process, Fine Particles Processing ,P. Somasundran, 481-491
- Erol, M., C. Colduroglu, and Z. Aktas. (2003). The Effect Of Reagents And Reagent Mixtures On Froth Flotation Of Coal Fines. *International Journal of Mineral Processing 71(1): 131–145.*
- Falutsu, M., and G. S. Dobby. (1992). Froth performance in commercial sized flotation columns. *Minerals Engineering 5(10): 1207–1223*
- Fuerstenau M.C., (1976), *Flotation*, AIME, New York
- Gupta, A. K., P. K. Banerjee, A. Mishra, and P. Satish. (2007). Effect Of Alcohol And Polyglycol Ether Frothers On Foam Stability, Bubble Size And Coal Flotation. *Fine Coal Processing*, eds. S. K. Mishra and R. R. Klimpel, 78–109. Park Ridge, NJ: Noyes Publications.
- Hadler, K., M. Greyling, N. Plint, and J. J. Cilliers. (2012). The Effect Of Froth Depth On Air Recovery And Flotation Performance. *Minerals Engineering 36: 248–253.*
- Hogg R,(1976), Characterization Of Mineral Surfaces, Fine Particles Processing,P. Somasundran: 482-524 IEA, 2012, World Energy Outlook
- Jameson , G. J. (2001) . The Flotation Of Coarse And Ultrafine Particles. *International Journal of Mineral Processing 72 : 12 – 15*
- Ketkar, D. R., Mallikarjunan, R. and Venkatachalam, S., (1991), Electroflotation Of Quartz Fines. *International Journal of Mineral Processing, 31*, No. 1-2, 127-138
- Klimpel , R. R. , and R. D. Hansen . (1987). *Fine Coal Processing* . New York : Noyes Publications
- Klimpel, R. R., and R. D. Hansen. (1987). Chemistry of fine coal flotation. *Fine Coal Processing 78–109*
- Matis, K. A. (Ed.), (1995), *Flotation Science and Engineering*. Marcel Dekker, New York
- Miettinen, T., Ralston, J. and Fornasiero, D., The limits of fine particle flotation, *Minerals Engineering, 23*, No. 5, 420-437 (2010).
- Nunes, A. P. L., Peres, A. E. C., Araujo, A. C. and Valadão, G. E. S., (2011), Electrokinetic Properties Of Wavellite And Its Floatability With Cationic And Anionic Surfactants, *Journal of Colloid and Interface Science, 361*, 632-638
- Oats, W. J., O. Ozdemir, and A. V. Nguyen. (2010). Effect Of Mechanical And Chemical Clay Removals By Hydrocyclone And Dispersants On Coal Flotation. *Minerals Engineering 23(5): 413–419.*
- Rubio, J. (1996). Modified Column Flotation Of Mineral Particles. *International Journal of Mineral Processing 48(3): 183–196*
- Rubio, J. (1996). Modified Column Flotation Of Mineral Particles. *International Journal of Mineral Processing 48(3): 183–196*
- Schubert, H. (2008). On The Optimization Of Hydrodynamics In Fine Particle Flotation. *Minerals Engineering 21(12): 930–936*
- Schubert, H. (2008). On The Optimization Of Hydrodynamics In Fine Particle Flotation. *Minerals Engineering 21(12): 930–936.*
- TKI, (2009), The Turkish Ministry of Energy, Energy, Dept., Lignite Coal Report

- TTK, (2009), The Turkish Ministry of Energy, Energy, Dept., Hard Coal Report
- Valderrama, L., M. Santander, M. Paiva, and J. Rubio. (2011). Modified-Three-Product Column (3PC) Flotation Of Copper-Gold Particles In A Rougher Feed And Tailings. *Minerals Engineering* 24(13): 1397–1401
- Warren, L. J. (1985). Determination Of The Contributions Of True Flotation And Entrainment In Batch Flotation Tests. *International Journal of Mineral Processing* 14(1): 33–44
- Wills , B. A. , and Napier-Munn T. J., (2006) . *Wills' Mineral Processing Technology* . Boston : Butterworth-Heinemann
- Xie , G. Y. , and Ou Z. S.. (1999) . Research on coal washing desulfurization . Journal of China University of Mining & Technology 28 (5): 502 – 505
- Xie , G. Y. , and Ou Z. S.. (1999) . The study and practice of cyclonic microbial flotation column of ash and pyritic sulfur rejection from coals . Mining Science and Technology 5 : 511 – 514.
- Xie , G. Y. (2001) . *Mineral Processing* . Xu Zhou, China University of Mining and Technology Press
- Yianatos, J. B., J. A. Finch, and A. R. Laplante. 1988. Selectivity in column flotation froths. *International Journal of Mineral Processing* 23(3): 279–292.
- Yoon, R. H. (1993). Microbubble flotation. *Minerals Engineering* 6(6): 619–630.
- Yoon, R. H. (2000). The role of hydrodynamic and surface forces in bubble–particle interaction. *International Journal of Mineral Processing* 58(1): 129–143.

ALTIN İÇERİKLİ GALEN MİNERALİNİN YÜZEY KİMYASI VE FLOTASYON ÖZELLİKLERİNİN ARAŞTIRILMASI
INVESTIGATION OF THE SURFACE CHEMISTRY AND FLOTATION PROPERTIES OF THE GOLD-BEARING
GALENA MINERAL

G. Erçelik¹, M. Terzi¹, I. Kursun Unver^{1,*}, O. Özdemir¹

¹ *İstanbul Üniversitesi-Cerrahpaşa, Mühendislik Fakültesi, Maden Mühendisliği Bölümü*
(*Sorumlu yazar: ilginkur@iuc.edu.tr)

ÖZET

Bu çalışmada, İzmir ili sınırları içerisinde, Menderes bölgesinden temin edilen altın içerikli sülfürlü cevherden elde edilen saf galen minerali üzerinde yüzey kimyası incelemeleri ve flotasyon deneyleri yürütülmüştür. Bu kapsamda zeta potansiyel, kabarcık-tane yapışma süresi ölçümleri ve mikro-flotasyon deneyleri gerçekleştirilmiştir. pH'ya bağlı yapılan zeta potansiyel ölçümlerinde pH 5-11 arasındaki değerlerde galen minerali negatif yüzey yüküne sahip olduğu belirlenmiş, sıfır yük noktasının (SYN) ise pH<3 değerinde olduğu düşünülmüştür. Farklı toplayıcı türleri olan SIBX, Aero MX-505 ve Aero S-8045 ile yapılan kabarcık-tane yapışma süresi ölçümlerinde, MX-505 ile tüm dozaj ve temas sürelerinde yapışma verimi %100 olarak gerçekleşmiştir. Bu sonuç, MX-505 varlığında galen taneleri ve hava kabarcığı arasında çok kuvvetli bir etkileşim olduğunu ortaya koymuştur. Mikro-flotasyon deneylerinde ise en yüksek verim yine MX-505 varlığında sağlanmıştır. MX-505'in tüm dozajlarında, %85 üzerinde flotasyon verimi elde edilmiştir. Bununla beraber SIBX dozaj miktarındaki artışla birlikte flotasyon verimi artmış ve $2,39 \times 10^{-8}$ mol/L değerinde en yüksek verim değerine ulaşılmıştır. S-8045'in tekil kullanımında ise düşük verimler elde edilmiştir.

Anahtar Sözcükler: Galen, altın, yüzey kimyası, zeta potansiyel, kabarcık-tane yapışma süresi, mikro-flotasyon

ABSTRACT

In this study, surface chemistry studies were performed on the pure galena mineral obtained from gold-containing sulfide ore of Menderes region, İzmir. In this context, the zeta potential, bubble-particle attachment time, and micro-flotation experiments were carried out. In the case of zeta potential experiments as a function of pH, the galena mineral showed a negative charge at pH 5 and 11, and no zero point of charge (ZPC) was determined, and it was thought that ZPC of galena was around at pH<3. The bubble-particle attachment experiments carried out in the presence of SIBX, Aero MX-505, and Aero S-8045 collectors indicated that the attachment efficiency was 100% in the presence of MX-505 at all dosage and contact times. This result revealed that there was a very strong interaction between the galena and the air bubble in the presence of MX-505. When the results obtained in the micro-flotation experiments were evaluated, the highest efficiency was obtained with MX-505. At all dosages of MX-505, a flotation efficiency of over 85% was obtained. Besides, with the increase in the dosage of SIBX, the flotation recovery increased and the highest recovery was obtained at 2.39×10^{-8} mol/L. On the other hand, S-8045 collector showed lower efficiency in its single-use.

Keywords: Galena, gold, surface chemistry, zeta potential, bubble-particle attachment time, micro-flotation

GİRİŞ

Metalik cevherlerin prospeksiyonu, madenciligi ve zenginleştirilmesi, kapsamlı ve emek gerektiren yoğun prosesler sonucunda gerçekleştirilmektedir. Zenginleştirilecek olan cevherin mineralojisi ve metalürjik özellikleri, üretim yöntemini ve uygulanacak zenginleştirme prosesini belirlemektedir.

Genel olarak, serbest haldeki nabit altın, tane boyutu çok küçük olmadığı sürece gravite yöntemleriyle zenginleştirilmektedir. Bununla birlikte altın birçok cevherde son derece ince boyutlarda ve genellikle katı çözelti kapanımları şeklinde bulunabilmektedir. Altın, pirit ve arsenopirit gibi bazı sülfidler içerisinde yüksek oranlarda bulunabilmektedir (Yalcin ve Kelebek, 2011). Bu minerallere ek olarak, Dünya genelindeki çeşitli sülfürlü rezervlerde altının galen ile ilişkili cevherleşmelerine de sıklıkla rastlanılmaktadır (Elliot, 1992; Ahmad vd., 2018; Khan vd., 2018). Bu tür rezervler, ince boyutlu altın tanelerinin cevher taşıyıcı mineral içerisinde kapanım halinde bulunması nedeniyle refrakter altın cevherleri olarak adlandırılırlar (Valenzuela vd., 2013). Refrakter bir cevherden altın kazanımında, siyanürleme işleminden önce altın içeren sülfid minerallerinin ve ultra ince boyutlu altın parçacıklarını konsantre edilmesi amacıyla köpük flotasyonu yöntemi kullanılabilir (Cilek ve Tuzci, 2021).

Endüstriyel ölçekli zenginleştirme yöntemlerinden biri olan köpük flotasyonunda, optimum verim ve tenör değerini yakalayabilmek için cevherin mineralojisini ve yüzey kimyasını iyi bilmek gerekmektedir. Her ne kadar literatürde galen minerali üzerine çok fazla çalışma olduğu düşünülse de, mineralin yatak özelliklerine ve oluşum şekillerine bağlı olarak, mineraller farklı özellik ve davranışlar gösterebilmektedir. Bu yüzden her bölgeye özgü farklı cevherler üzerinde detaylı test çalışmaları yapılması gerektiği düşünülmektedir. Flotasyon işleminin verimi önemli ölçüde hava kabarcıklarının hidrofobik mineral tanelerini toplama davranışına bağlıdır. Genelde ise bir mineralin flotasyon özelliği temas açısı ölçümleri ile saptanmaktadır. Bununla beraber birçok çalışmada göstermiştir ki bu yöntem her zaman bir mineralin flotasyon özelliğini tahmin edememektedir (Ye ve Miller, 1988; Yoon ve Yordan 1991).

Bir mineralin yüzebilirliğini tahmin etmede diğer bir yöntem ise bir tanenin bir hava kabarcığına yapışması için gerekli olan sürenin tespit edildiği kabarcık-tane yapışma süresi tayini ölçümleri olup bir mineralin flotasyon davranışını belirlemede temas açısına nazaran daha doğru bir yaklaşım vermektedir (Ye ve Miller, 1988; Gu vd., 2003; Su vd., 2006; Ozdemir vd. 2009; Albijanic vd., 2010). Ayrıca bir pülp içinde hemen her mineralin yüzey yükünü sıfır yapan bir pH değeri vardır. Buna Sıfır Yük Noktası (SYN) denilmektedir. Zeta potansiyel ölçümleriyle elde edilen tanelerin elektrokinetik özellikleri flotasyonla ayırma işlemini anlamada önemli bilgiler içerir (Nguyen, 1994).

Bu çalışmada İzmir ili sınırları içerisinde, Menderes bölgesinden temin edilen sülfürlü altın cevherden elde edilen saf galen minerali üzerinde, zeta potansiyeli ve kabarcık-tane yapışma süresi ölçümleri ve mikro-flotasyon deneyleri gerçekleştirilmiştir. Bu kapsamda SIBX, Aero MX-505 ve Aero S-8045 toplayıcıların altın içerikli saf galen mineralinin mikro-flotasyon kazanma verimi üzerine etkileri, dozaja bağlı olarak incelenmiştir.

MALZEME VE YÖNTEM

Malzeme

Deneylerde kullanılan altın içerikli galen cevheri; İzmir ili sınırları içerisinde, Menderes bölgesinden temin edilmiş olup, bölgede faaliyet gösteren özel bir firmanın tesis beslemesinden temsili

olarak alınmıştır. Deneylere esas numunelerin kimyasal bileşimi hakkında bilgi edinilmesi amacıyla kimyasal analize tabi tutulmuştur. Kimyasal analiz sonuçları Çizelge 1’de gösterilmiştir.

Çizelge 1. Cevherin kimyasal analiz sonuçları

Element	(%)	Element	(ppm)
S	3,23	Au	10,30
Al	1,65	Ag	15,50
Ca	3,93	Cu	661,50
Fe	5,52	Ni	68,50
K	0,96	As	1105,00
Mg	0,43	Ba	147,50
Na	0,07	Co	31,25
Ti	0,08	Cr	58,00
Mn	8,49	P	102,50
Pb	0,49	W	227,50
Zn	0,48	Mo	10,75
Si	25,82	Sr	18,60
Hafif Element	48,58		

Kimyasal analiz sonuçları değerlendirildiğinde; cevher içerisinde tespit edilen en yüksek yüzdeye sahip elementler; %48,58 oranında hafif elementler (O₂ vb.), %25,82 oranında silisyum elementidir. Bu elementler dışında %8,49 mangan, %5,52 demir, %3,93 kalsiyum, %3,23 sülfür, %1,65 alüminyum, %0,96 potasyum, %0,49 kurşun, %0,48 çinko, %0,43 magnezyum, 10,3 ppm altın, 15,5 ppm gümüş, 661 ppm bakır, 1105 ppm arsenik, 227,5 ppm volfram ve 10,75 molibden elementleri tespit edilmiştir.

Mineralojik Analiz

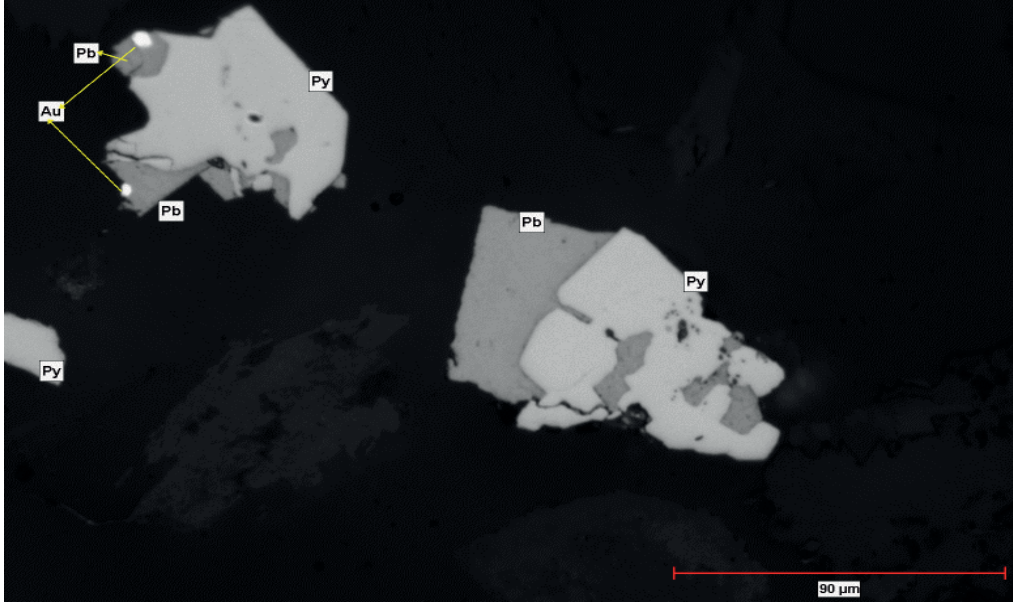
Deneylere esas numunelerin mineralojik özellikleri hakkında bilgi edinilmesi amacıyla her bir fraksiyonun parlak kesitleri üzerinde Nikon LV 250 optik mikroskop ve Clemex optik yazılımı kullanılarak bir dizi incelemeler yürütülmüştür. Optik mikroskop görüntüleri Şekil 1-3’te gösterilmiştir.



Şekil 1. + 0,106 mm fraksiyonun 50× mercekle altında görüntüsü



Şekil 2. + 0,090 mm fraksiyonun 50× mercekte altında görüntüsü



Şekil 3. + 0,038 mm fraksiyonun 50× mercekte altında görüntüsü

Cevherin mineralojik bileşiminin belirlenmesi amacıyla X-Işını Kırınımı (XRD) analizi, kimyasal analiz ve mikroskop analizi gerçekleştirilmiştir. Cevher kabaca, sülfid mineralleri ile ilişkili kuvars damarları, cevherli ve hornblend kontak metamorfik kayalar oluşmaktadır. Cevherleşme ile ilişkili alterasyon fazı ana olarak; rodonit, rodokrozit, aksinit ve kuvars, yan kayada ise gang mineralleri olarak klorit, serizit, illit ve kaolinit mineralleri ihtiva ettiği tespit edilmiştir. Pirit, sfalerit, galen, kalkopirit ana mineralleridir.

Altın taneleri çok küçük boyutlarda (1-20 µm) pirit, sfalerit, galen, kalkopirit mineralleri içerisinde dağılım şeklinde bulunduğu tespit edilmiştir. Zaman zaman pirit, sfalerit ve galen minerallerinin ortak bulunduğu gözlemlenmiştir.

Numune Hazırlama

Bu kapsamda öncelikle kapalı devre olarak gerçekleştirilen kırma-eleme işlemleri sonucunda malzemenin tamamı -2 mm tane boyutuna indirilmiştir ve kuru eleme yöntemi ile üç farklı fraksiyonel boyuta (-2+1 mm, -1+0,5 mm ve -0,5 mm) sınıflandırılmıştır. Elde edilen -2+1 mm ve -0,5 mm boyutlu fraksiyonlar ise Wilfley sallantılı masa ile gravite ayırımına tabi tutulmuş ve deney sırasında konsantre bandı manuel olarak en üst noktadan kesilerek ağır mineral konsantreleri elde edilmiştir. Elde edilen konsantreler ivedi olarak 50°C’de etüvde kurutulmuş ve paketlenmiştir. Sallantılı masadan elde edilen -2+1 mm boyutlu konsantre, saf galen tanelerinin triyaj (el ile ayıklama) yöntemi ile seçilmesi ile daha ileri derecede saflaştırılmıştır. -0,5 mm boyutlu konsantrenin ise çok yüksek oranda galen içeriğine sahip olduğu gözlenmiş ve bu nedenle daha ileri bir saflaştırma işlemine tabi tutulmamıştır. El ile seçilen saf galen taneleri Şekil 4’te gösterilmiştir.



Şekil 4. Galen numunesi

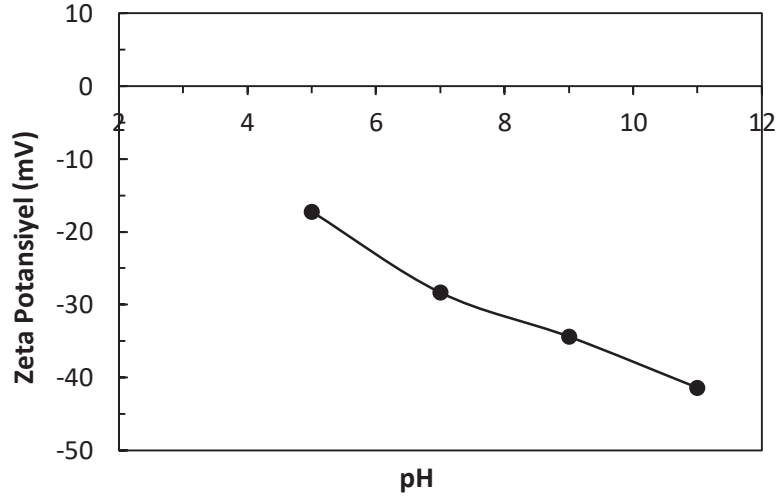
Seçilen numuneler, yüzey kimyası çalışmaları için uygun tane fraksiyonuna ufulanması amacıyla el havanı ve Restch RM 200 agat öğütücü kullanılarak kademeli olarak öğütülmüştür. Öğütülen numuneler üzerinde kuru eleme işlemi uygulanarak -63+38 µm ve -38 µm tane boyutunda numuneler elde edilmiştir.

Zeta potansiyeli ölçümlerine uygun boyutta numune hazırlamak amacıyla ise kuru elemenden elde edilen -38 µm fraksiyonundaki galen ve pirit taneleri, havanlı öğütücüde 20 dk süre ile öğütülerek daha da ince ($d_{80} = 10 \mu\text{m}$) boyuta getirilmiştir.

YÖNTEM

Zeta Potansiyel Ölçümleri

Zeta potansiyel ölçümleri Brookhaven Zetaplus Zetametre ile elektroforetik yöntem kullanılarak yürütülmüştür. Bu kapsamda -38 µm boyutlu 0,3 gr galen numunesi ve 30 mL saf su (TDS<10 / pH ≈ 7) ile %1 katı oranında süspansiyon hazırlanmış ve yeterli miktarda süspansiyon 4 mL hacimli ölçüm hücresine transfer edilmiştir. Doğal pH’da gerçekleştirilen ölçümlerin ardından süspansiyona 0,1 M HCl ya da 0,1 M NaOH çözeltisi eklenmesi ile pH ayarlaması yapılmış ve farklı pH’larda (5, 7, 9, 11) ölçümler alınmıştır. Her bir pH değeri için 10 ölçüm alınmıştır. Galen mineralinin pH’ya bağlı zeta potansiyel ölçüm sonuçları Şekil 5’te gösterilmiştir.



Şekil 5. Galen numunesinin zeta potansiyel-pH profili

Zeta potansiyel deneyleri kapsamında pH 5, 7, 9 ve 11 noktalarında ölçümler alınmıştır. $pH \leq 4$ değerinden sonra cihazın elektrot akım değerinin artması ile sağlıklı sonuçlara ulaşamadığı için pH 4 ve altındaki değerlerde ölçüm alınmamıştır. Zeta potansiyeli ölçümlerinde galen mineralinin sıfır yük noktası (SYN) tespit edilememiştir. Literatürdeki diğer bazı çalışmalarda da bazı galen mineralinin SYN'ının bulunamadığı veya $pH < 3$ değerinde olabileceği ortaya konulmuştur (Marek, 2009).

Mikro-Flotasyon Deneyleri

Mikro-flotasyon deneyleri tesis koşullarının simüle edilmesi amacıyla, $-68+38 \mu m$ tane boyutunda galen numunesi ve saf su kullanılarak gerçekleştirilmiştir. Flotasyon deneylerinde 55 mL hacimli mikro-flotasyon hücresi kullanılmıştır ve katı oranı %1 olarak seçilmiştir. Kollektör ve köpürtücü olarak ise sırasıyla Sodyum İzoButil Ksantat (SIBX), Aero S-8045 promotor, Aerofloat MX-505 Promotor ve Frother Ore Prep F-549 kullanılmıştır. Kullanılan mikro-flotasyon hücresi Partridge and Smith hücre tasarımına sahiptir. Mikro flotasyon deney düzeneği ve SIBX kimyasalı ile örnek bir mikro-flotasyon testi Şekil 6'da, deney parametreleri ve koşulları ise Çizelge 2'de gösterilmiştir.



Şekil 6. Mikro-flotasyon deney düzeneği ve örnek bir deney

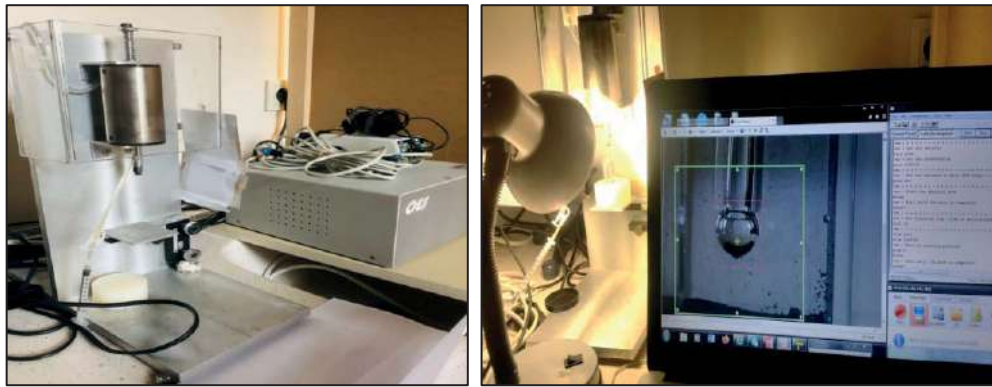
Çizelge 3. Mikro-flotasyon test parametreleri ve koşulları

Parametre	Koşul
Hücre Hacmi	55 mL
Su	Saf Su (TDS<10 / pH ≈ 7)
Saf Numune Miktarı	0,55 gr
Tane Boyutu	-63+38 µm
Katı Oranı	%1
Kondüsyonlama Karıştırıcı Hızı	500 dev/dk
Gaz (N2) Debisi	15 mL/dk
pH	Doğal pH (8,0-9,0)
Kollektör Türü	SIBX (Quimidroga), S-8045 (Solvay), MX-505 (Solvay)
Kollektör Kondüsyonlama Süresi	5 dk
Köpürtücü Türü	Frother Ore Prep F-549 (Solvay)
Flotasyon Süresi	1 dk

55 mL hacimde ve %1 katı oranındaki galen süspansiyonu bir manyetik karıştırıcı yardımıyla (500 dev/dk) kondüsyonlanmıştır. Kondüsyonlama süresi toplayıcı için 8 dk ve ardından köpürtücü için 2 dk süresince yapılmıştır. Kondüsyonlama işlemi bittikten sonra mikro-flotasyon hücresine aktarılan süspansiyon, 15 mL/dk azot gazı ile 1 dk boyunca mikro-flotasyona tabii tutulmuştur. Yüzen ve batan kısım bir filtre kâğıdı yardımıyla susuzlandırıldıktan sonra etüvde 105°C'de kurutulmuştur. Kurutulan flotasyon ürünleri tartılarak flotasyon verimi gravimetrik olarak hesap edilmiştir.

Kabarcık-Tane Yapışma Verimi Ölçümleri

Kabarcık-tane yapışma süresi tayini için Glembotsky tasarım konsepti kullanılmış olup, ölçümler Bratton Mühendisliğin kabarcık-tane süre tayin cihazı ile gerçekleştirilmiştir. Mineral tane yatağı ve hava kabarcığı kullanılarak yapışma sürelerinin belirlendiği bu test günümüzde yaygın olarak kullanılmaktadır (Glembotsky, 1953; Ozdemir vd., 2009; Albijanic vd., 2011; Albijanic vd., 2014). Kabarcık-tane yapışma süresi ölçümlerinde -63+38 µm tane boyutundaki saf galen numuneleri kullanılmıştır. Deneyde kullanılan cihaz Şekil 7'de gösterilmiştir.



Şekil 7. Kabarcık-Tane Yapışma Süresi Tayin Cihazı – Bratton Mühendislik A.B.D.

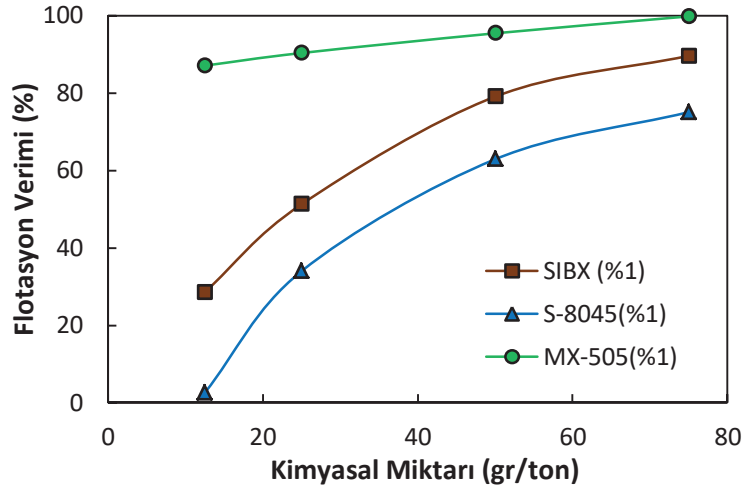
Hassas tartı yardımıyla 0,50 g galen numunesi tartılmış ve 50 mL saf su içerisine eklenmiş böylece %1 katı oranında süspansiyon hazırlanmıştır. Hazırlanan süspansiyona istenilen dozajda toplayıcı eklenmiş ve 10 dk'lık kondüsyonlama süreci sonrasında bir damlalık yardımıyla, hücredeki yatak kalınlığı ≈1 mm olacak şekilde 4 mL'lik ölçüm hücresine transfer edilmiştir. Kabarcık-tane yapışma süresi ölçümlerinde 1 ms, 10 ms, 100 ms ve 1000 ms temas süreleri kullanılmıştır. Her bir süre için hücrede oluşturulan yatak yüzeyinin 10 farklı noktasından ölçüm alınmıştır.

BULGULAR

Mikro-Flotasyon Deneyleri

SIBX ile pH'ya bağı (5, 7, doğal, 9 ve 11) olarak yapılan mikro-flotasyon deneyleri sonucunda elde edilen flotasyon verimleri sırasıyla %65,82; %70,73; %83,45; %79,82 ve %45,82 olmuştur. En yüksek verim, doğal pH değerinde, %83,45 olarak elde edilmiştir. Buna göre optimum pH değeri doğal pH (8,7) olarak belirlenmiştir. Akabinde farklı toplayıcıların ve bu toplayıcıların dozajlarının etkisini görebilmek amacıyla köpürtücü dozajı ve pH değeri (doğal pH) sabit tutularak bir dizi mikro-flotasyon deneyi yapılmıştır.

Köpürtücü dozajı ve pH değeri sabit tutularak yürütülen deneylerde farklı toplayıcı dozajlarında SIBX toplayıcı için en yüksek flotasyon verimi $2,39 \times 10^{-8}$ mol/L dozajında %89,64, S-8045 toplayıcı için $1,71 \times 10^{-8}$ dozajında %75,09, MX-505 toplayıcı için ise $1,79 \times 10^{-9}$ mol/L dozajında %99,82 olarak tespit edilmiştir. Mikro-flotasyon deney sonuçları Şekil 8'de gösterilmiştir.

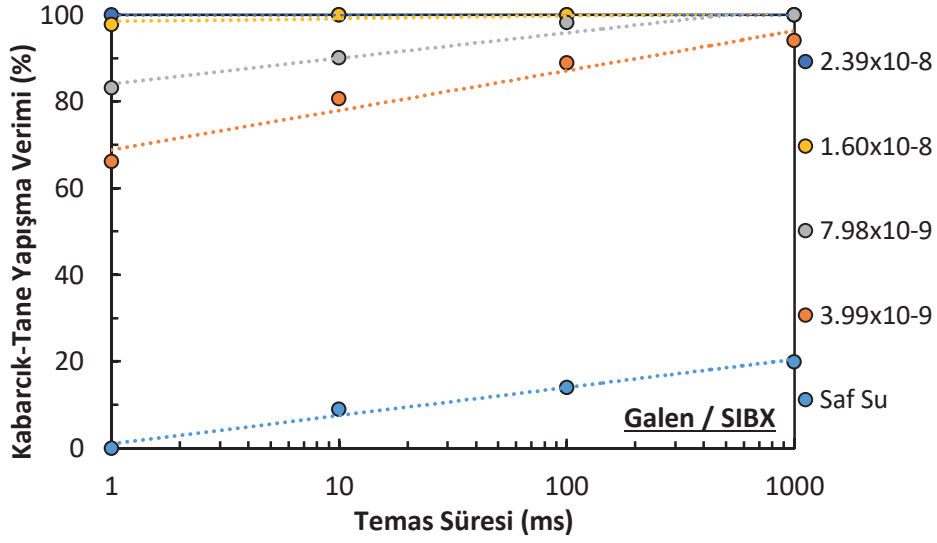


Şekil 8. Farklı toplayıcı dozajlarında mikro-flotasyon deney sonuçları

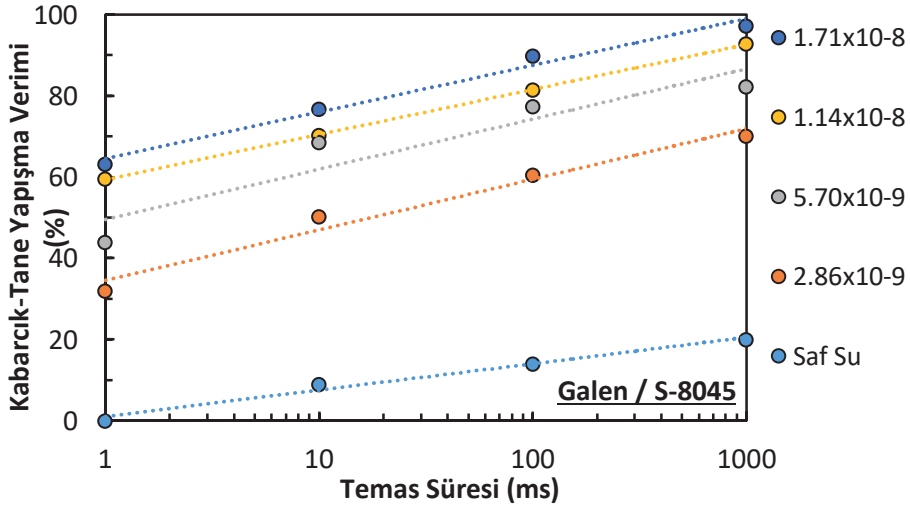
Mikro-flotasyon deneylerinde en yüksek verim MX-505 kimyasalında sağlanmıştır. MX-505'in tüm dozajlarında, %85 üzerinde flotasyon verimi elde edilmiştir. Bununla beraber SIBX kimyasalı dozaj miktarındaki artışla birlikte flotasyon verimi artış göstermiş ve $2,39 \times 10^{-8}$ mol/L değerinde en yüksek verim değerine ulaşılmıştır. S-8045 toplayıcısı ise tekil kullanımında diğer toplayıcılara oranla düşük verimler elde edilmiştir. S-8045 flotasyonda yardımcı toplayıcı olarak görev yapmaktadır ve elde edilen flotasyon sonuçlarına göre tekil kullanımında diğer iki toplayıcı kadar etkin olmadığı gözlemlenmiştir.

Kabarcık-Tane Yapışma Verimi Ölçümleri

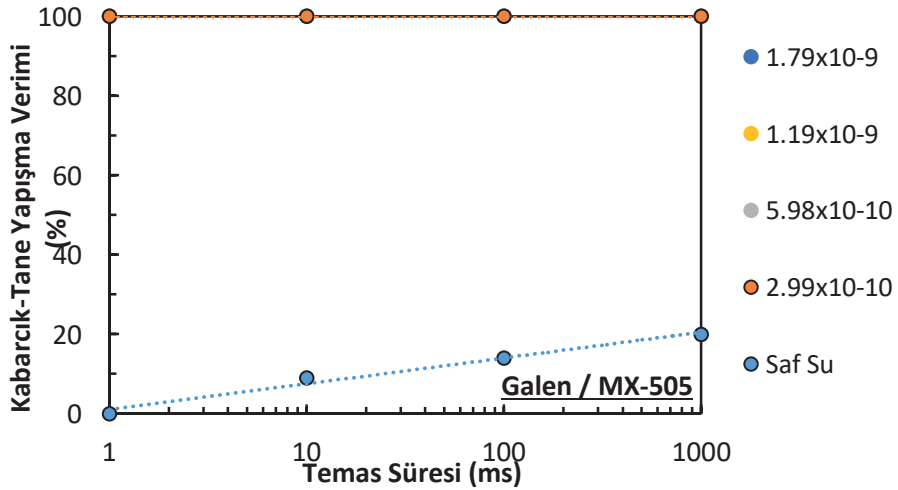
Mikro-flotasyon deneyleri ile aynı toplayıcı dozajlarında, SIBX, S-8045 ve MX-505 toplayıcıları kullanılarak gerçekleştirilen kabarcık-tane yapışma süresi ölçüm sonuçları sırasıyla Şekil 9, Şekil 10 ve Şekil 11'de verilmiştir.



Şekil 9. SIBX varlığında kabarcık-tane yapışma süresi tayini ölçüm sonuçları



Şekil 10. S-8045 varlığında kabarcık-tane yapışma süresi tayini ölçüm sonuçları



Şekil 11. MX-505 varlığında kabarcık-tane yapışma süresi tayini ölçüm sonuçları

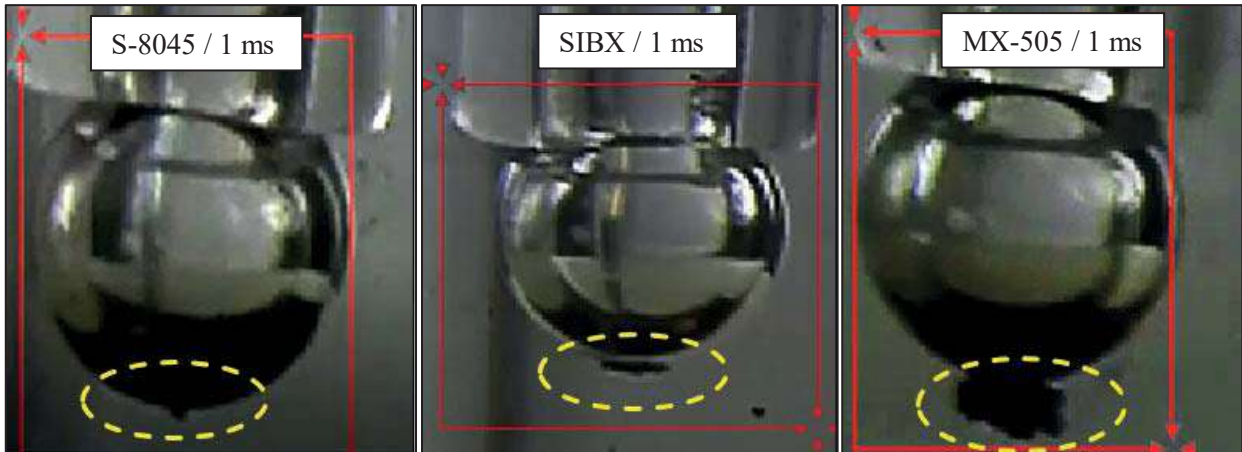
Ölçüm sonuçlarına göre, galen tanelerinin kollektörsüz ortamda en yüksek temas süresinde bile hava kabarcığına %20 ihtimalle yapışmaktadır. Bir başka deyişle kabarcık-tane yapışma süresi ölçüm sonuçları galenin saf su içerisinde hidrofил davranış gösterdiğini teyit etmiştir. Farklı toplayıcıların farklı dozajlarında yapılan ölçümlerin sonuçlarında ise tüm dozajlarda galen taneleri ile hava kabarcığı arasında bir etkileşim olduğu ortaya konulmuştur.

Genel olarak en zayıf etkileşim S-8045 ile gözlenmiş olup, bu toplayıcının $2,86 \times 10^{-9}$ mol/L ve $5,70 \times 10^{-9}$ mol/L dozajlarında düşük temas sürelerinde yapışma verimi %50'nin altında kalmıştır. $1,14 \times 10^{-8}$ mol/L ve $1,71 \times 10^{-8}$ mol/L dozajlarında, tüm temas sürelerinde yapışma verimi %50'nin üzerinde gerçekleşmiş olup, bu noktadaki kabarcık-tane yapışma süresinin (yapışma verimi > %50) 1 ms'nin altında olduğu söylenebilmektedir.

SIBX ile de S-8045'e benzer sonuçlar elde edilmiş olmakla birlikte, bu toplayıcının varlığında tüm dozaj ve temas sürelerinde yapışma verimi %50'nin üzerinde gerçekleşmiştir. Özellikle $1,60 \times 10^{-8}$ mol/L ve $2,39 \times 10^{-8}$ mol/L dozajlarında 1 ms temas süresinde bile yapışma verimi %95-100 aralığında olmuştur. Yapışma verimindeki bu artış, SIBX varlığında galen taneleri ve hava kabarcığı arasında S-8045'e göre daha kuvvetli bir etkileşim olduğunu ortaya koymaktadır. Sonuç olarak tüm dozaj ve temas süreleri için kabarcık-tane yapışma süresinin yine 1 ms'nin altında olduğu söylenebilmektedir.

MX-505 ile ise tüm dozaj ve temas sürelerinde yapışma verimi %100 olarak gerçekleşmiştir. Bu sonuç, MX-505 varlığında galen taneleri ve hava kabarcığı arasında çok kuvvetli bir etkileşim olduğunu ortaya koymaktadır.

Kabarcık-tane yapışma süresi ölçümlerinde 25 gr/ton dozaj miktarında yani $2,86 \times 10^{-9}$ mol/L S-8045, $3,99 \times 10^{-9}$ mol/L SIBX ve $2,99 \times 10^{-10}$ mol/L MX-505 kimyasal dozajında çekilen görüntüler Şekil 12'de gösterilmiştir.



Şekil 13. Kabarcık-tane yapışma süresi tayini görseli

TARTIŞMA VE SONUÇ

Bu çalışmada, İzmir ili sınırları içerisinde, Menderes bölgesinden temin edilen numune; epidermal yatak özelliği göstermekte olup, cevher kuvars-rodonit içerisinde saçınım şeklinde oluştuğu tespit edilmiştir. Altın pirit ve galen mineralleri içinde ihtiva ettiği gözlemlenmiştir. Zeta potansiyel, mikro-flotasyon deneyleri ve kabarcık-tane yapışma verimi ölçümleri kullanılarak yürütülen bu çalışmada, altın içerikli galen mineralinin ksantat ve farklı iki türde ditiofosfat toplayıcıları ile flotasyonunun başarı ile yapılabileceği ortaya konmuştur. Galen mineralinin sıfır yük noktası (SYN) değeri

tespit edilememiş olup, zeta potansiyel profili incelendiğinde $SYN < 3$ olabileceği düşünülmektedir. Kabarcık-tane yapışma süresi açısından 1 ms sürede en etkin sonuca MX-505 kimyasalı kullanılarak ulaşılmıştır. Alkol içerikli ditiofosfat tipi bir toplayıcı olan MX-505'in galen flotasyonunda özellikle etkin olduğu tespit edilmiştir. Üç toplayıcı türü içerisinde galen flotasyon verimi açısından en iyi sonuçlara MX-505 ile ulaşılmıştır.

KAYNAKLAR

- Ahmad, L., Khan, S.D., Tahir Shah, M., & Jehan, N. (2018). Gold Mineralization In Bubin Area, Gilgit-Baltistan, Northern Areas, Pakistan. *Arabian Journal of Geosciences*, 11(2), 1-12.
- Albijanic, B., Amini, E., Wightman, E., Ozdemir, O., Nguyen, Bradshaw, D.J., (2011). A relationship between the bubble–particle attachment time and the mineralogy of a copper–sulphide ore. *Minerals Engineering*, 24, 1335–1339.
- Albijanic, B., Ozdemir, O., Hampton, M.A., Nguyen, P.T., Nguyen, A.V., Bradshaw, D. (2014). Fundamental aspects of bubble–particle attachment mechanism in flotation separation. *Minerals Engineering*, 65, 187–195.
- Albijanic, B., Ozdemir, O., Nguyen, A.V. ve Bradshaw, D. (2010). “A review of induction and attachment times of wetting thin films between air bubbles and particles and its relevance in the separation of particles by flotation”, *Adv Colloid Interface Sci*, 159(1), 1-21.
- Cilek, E.C., & Tuzci, G. (2021). Flotation behavior of native gold and gold-bearing sulfide minerals in a polymetallic gold ore. *Particulate Science and Technology*, 1-9.
- Elliott, R.G. (1992). The geology and geochemistry of the Omai goldfield, Guyana (Doctoral dissertation, Oxford Brookes University).
- Glembokij, V.A. (1953). The time of attachment of air bubbles to mineral particles in flotation and its measurement, *Izv. Akad. Nauk SSSR (OTN)*, No. 11: 1524-1531.
- Gu, G., Z. Xu, vd. (2003). Effects of physical environment on induction time of air-bitumen attachment, *Int. J. Miner. Process.*, 69(1-4): 235-250.
- Khan, S.D., Okyay, Ü., Ahmad, L., & Shah, M.T. (2018). Characterization of gold mineralization in northern Pakistan using imaging spectroscopy. *Photogrammetric Engineering & Remote Sensing*, 84(7), 425-434.
- Kosmulski, M. (2009). *Surface charging and points of zero charge* (Vol. 145). CRC press, 756-759
- Nguyen, A.V. (1994). The collision between fine particles and single air bubbles in flotation, *J. Colloid Interface Sci.*, 162(1): 123-128.
- Ozdemir, O., Karaguzel, C., Nguyen, A.V., Celik, M.S. ve Miller, J.D. (2009). Contact angle and bubble attachment studies in the flotation of trona and other soluble carbonate salts, *Miner Eng*, 22(2), 168-175.
- Su, L., Z. Xu, vd. (2006). Role of oily bubbles in enhancing bitumen flotation, *Minerals Engineering* 19(6-8): 641-650.
- Valenzuela, A., Valenzuela, J.L., & Parga, J.R. (2013). Effect of pretreatment of sulfide refractory concentrate with sodium hypochlorite, followed by extraction of gold by pressure cyanidation on gold removal. *Advances in Chemical Engineering and Science*, 3, 171-177
- Yalcin, E., & Kelebek, S. (2011). Flotation kinetics of a pyritic gold ore. *International Journal of Mineral Processing*, 98(1-2), 48-54.
- Ye, Y. ve J.D. Miller (1988). Bubble/particle contact time in the analysis of coal flotation, *Coal Prep.* (Gordon & Breach), 5(3-4): 147-166.
- Yoon, R.H. ve Jordan, J.L. (1991). Induction time measurements for the quartz-amine flotation system, *Journal of Colloid and Interface Science*, 141(2): 374-383.

APPLICATION OF NANO BUBBLES IN COLUMN FLOTATION: BENEFICIATION OF IRON AND PHOSPHATE SLIMES

F. Nakhaei^{1,*}, M.B. Fathi², Z. Pourkarimi³, F. Taghavi⁴

¹North West University, School of Chemical and Minerals Engineering
(*Corresponding Author: 36598704@nwu.ac.za)

²Urmia University, Engineering Faculty, Mining Department

³Department of Mineral Processing and Applied Research, Iran Mineral Processing Research Center

⁴University of Tehran, College of Engineering, School of Mining Engineering

ABSTRACT

Fine particle flotation has been one of the main problems in many mineral processing plants. Beneficiation of iron ore and phosphate slimes is important from economic and environmental aspects. This study aimed at the purification of fine particles of iron and phosphate ores by a pilot scale flotation column (10.2 cm diameter and 400 cm height) in which Nano bubbles (NBs) were produced using a specially designed venturi hydrodynamic cavitation tube.

The iron slime sample (d_{80} equal to $45\mu\text{m}$) was obtained from Gole-Gohar iron ore mine, one of the biggest iron concentrate producers in Iran, containing 67.5% Fe and 0.95% S. Phosphate particles with d_{80} finer than $30\mu\text{m}$ contained 15.9% P_2O_5 . This study addressed the processing of fine tailings (slimes) from phosphate and iron ore concentrators via flotation, despite the traditional view that ultrafine particles do not float. To reach this aim, an especial laboratory column flotation cell was manufactured and several comparative flotation tests were performed in presence and absence of NBs. Various parameters such as reagents dosage, air flowrate, froth depth, and NBs ratio to the cell volume were studied and optimum amounts were obtained. Results showed, flotation in presence of NBs obtained the significant increase in the phosphate recovery more than 23% versus conventional flotation cell. Also, the sulfur content of iron concentrate could be reduced from 0.95% to 0.26% with iron recovery above 88% in presence of NBs.

Keywords: Iron ore, slime, phosphate, desulfurization, column flotation, nano bubbles

INTRODUCTION

In general, fine and ultrafine particles, profitable products nowadays, are disposed to the tailing dams. So, fine particles processing is important in terms of ecological and economic benefits. Flotation using nanobubbles (NBs) ($<1\mu\text{m}$ diameters) is one of the effective techniques in the recovery of fine mineral particles (Azevedo et al., 2016; Etchepare et al., 2017; Oliveira et al., 2018). In conventional processing methods such as flotation for particles less than $40\mu\text{m}$, because of the poor attachment (low probability of bubble-particle capture), the separation efficiency decreases and fall sharply for the ultrafine particles ($<15\mu\text{m}$). The results from previous studies depicted that because of NBs' large surface area, high concentration, long stability and high hydrophobic affinity, they adsorb rapidly at surfaces, and also by capillary impacts they can aggregate fine minerals, perform as nuclei for conventional bubbles, and float those aggregates (Theodorakis., 2019 ;Vaziri Hassas et al., 2018; Vaziri Hassas and Miller, 2019). So, large bubbles did not play a significant role in the process, instead the fine ones effectively adsorb the fine particles. The results of previous works showed that the purification of fine particles using NBs can improve the flotation selectivity index by more than 25% (Fan et al., 2010). Several techniques such as solvent exchange, temperature change, pressure reduction, ultrasonic method, and hydrodynamic

cavitation technique are introduced to generate nanobubbles (Hampton and Nguyen, 2010; Cho et al., 2005). Since the work of adhesion between a particle and water is always smaller than the work of cohesion of water, nanobubbles are selectively nucleated at the surface of hydrophobic particles. On the other hand, increasing solid surface hydrophobicity measured by the contact angle will lead to decrease the work of adhesion (Sobhy and Tao, 2013). On the other hand, generated nanobubbles on a particle surface also can play as a secondary collector that increase the probability of adhesion and therefore this phenomenon can reduce the need of surfactants/chemical reagents.

In this research, the capability of a column flotation assisted by hydrodynamic cavitation-generated NBs in processing of two different fine particles (phosphate and iron ores) was investigated and the results were compared with a conventional bubble generator type.

MATERIALS AND METHODS

Sampling

Flotation tests were performed on phosphate fine particles from Esfordi phosphate processing plant, located in Yazd province of Iran, and iron ore fines from Gole-Gohar iron complex located in Kerman province south of Iran.

In the Esfordi phosphate plant the main problem is that in the desliming process (the overflow of the second hydrocyclone) more than 30% of plant capacity is delivered to the tailing dam as particles with d_{80} smaller than 30 μm . These materials are similar to the feed (16% P_2O_5 content), and due to the fineness and reduction of recovery, these particles are removed from the flotation circuit. The flotation is fed from the second hydrocyclone underflow which is the final product of the grinding circuit. So, the sample of phosphate fine particles was obtained from the overflow stream of desliming hydrocyclone.

The iron sample with a relative high-grade iron was obtained from the complex waste damp which is fed by the rejected material from the main processing plant.

The analyses of sample particle-size distribution were measured by wet sieve and cyclosizer analysis for the iron ore and Laser Practice Size Analyzer (LPSA) Malvern 2000 MS, UK, for the phosphate ore. The results indicated that about 80% of the iron and phosphate samples have a particle size less than 42 μm and 29.13 μm respectively. Chemical analyses of representative samples were done to identify the amount of available compositions. The results depicted that the phosphate sample contained 15.95% P_2O_5 and 32.01% Fe_{Total} while for the iron sample about 42.2% and 1.98% were Fe and Sulphur. Based on the XRD analyses and the optical mineralogy study, the main components in the phosphate sample were apatite, hematite, quartz, calcite, talc and chlorite while for the iron sample, the gangue minerals were dickite, talk calcite, quartz, and pyrite and the main minerals were hematite, magnetite, and goethite.

Experimental Conditions and Procedures

A flotation column made of Plexiglas with a 4cm diameter and 2 m height was featured with a cavitation tube to generate NBs and a porous sparger to generate microbubbles (conventional-sized bubbles), respectively, as shown in Fig. 1.

The column was fitted with a mixing tank for the preparation and conditioning of slurry feed. The appropriate amount of reagents (collector, frother, pH regulator, and depressant) were added to the tank. The pulp feed is introduced to the upper part of the column via a peristaltic pump. Air and recirculating tailings were passed through the cavitation tube, designed for generating Nano bubbles, before being injected into the lower portion. The bottom of the flotation column was specially designed with two outlets. One of them was concentrate (for iron sample)/ tailing (for phosphate sample) stream and the other one was recycled stream that pumped through the cavitation tube for further recovery. Major process parameters such as collector dosage, gas and feed flowrates were examined individually to investigate their effects on flotation performance in the presence of nanobubbles.

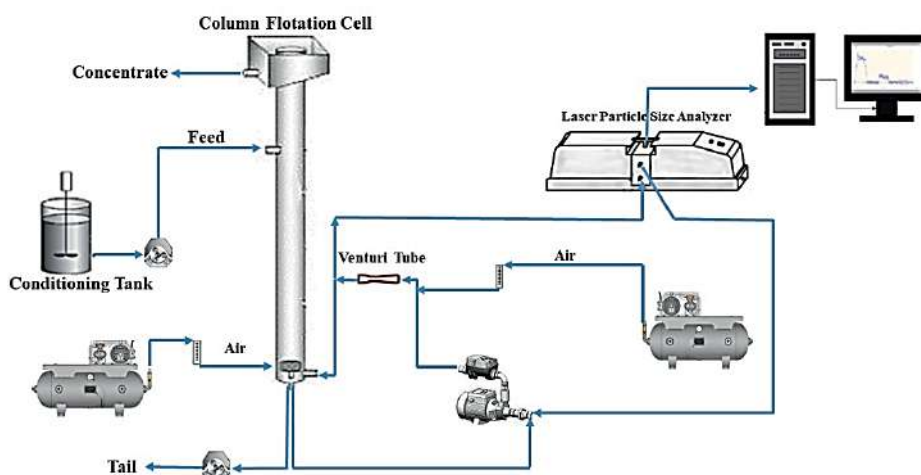


Figure 1. A schematic diagram of the applied flotation apparatus

The feed slurry was conditioned for 5 minutes with collector and frother prior to each test. All flotation tests were performed under the previous work optimum conditions that are presented in Table 1 and 2 (Nakhaei and Pourkarimi, 2020; Taghavi et al., 2022).

Table 1. Optimum conditions used in Phosphate column flotation

Parameters	Value
Froth depth (cm)	30
Gas flow rate (l/min-cm/s)	0.8
Flo-Y-S collector dosage (g/t)	400
Starch dosage (g/t)	500
Feed slurry flow rate (l/min-cm/s)	0.93
Wash water flow rate (l/min-cm/s)	0.13
Feed slurry solids concentration (%)	10

Table 2. Optimum conditions used in reverse column flotation of iron ores

Parameters	Value
Froth depth (cm)	20
Gas flow rate (l/min-cm/s)	0.9
Potassium Amyl Xanthate (PAX) dosage (g/t)	200
MIBC frother concentration (g/t)	100
Feed slurry flow rate (l/min-cm/s)	0.8
Feed slurry solids concentration (%)	9
Nanobubble aeration rate (l/min-cm/s)	0.15

Using venturi tubes the generation of nanobubbles was done based on the cavitation phenomenon. A Malvern mastersizer 2000 LPSA was employed for measuring the size distribution and volume of the bubbles. Before sending the solution into the venturi tubes the frother was added into the tank and mixed in appropriate time. Then the compressed air before entering the pump was added to the solution. In order to measure the bubble size, the solution containing nanobubbles was transferred to the laser particle size analyzer through pump propulsion.

RESULTS AND DISCUSSION

Bubble Size Distribution

In order to generate NBs, a venturi tube with the specified geometry, entrance diameters of 2.2 mm were used. Fig.2 shows the size characterization of bubbles generated by the optimally designed cavitation venturi tube. There are two major distribution peaks observed on the population frequency curve. As seen from the results, the average size (d_{50}) of generated nanobubbles by the cavitation tube is approximately 230 nm and for the micro size bubbles is about 100 μm . It is noteworthy that the measurement of the bubble size distribution (BSD) generated by the porous sparger, image sets with a high-speed digital camera coupled to an image analysis software (Image J) and a data acquisition system were applied. To determine the microbubble size, $D_b(0.5)$ term at which 50% by volume of the bubbles are smaller was used as instrument output. The results showed that the diameter of the bubbles produced was in the range of 800 to 2500 μm with d_{50} 1800 μm .

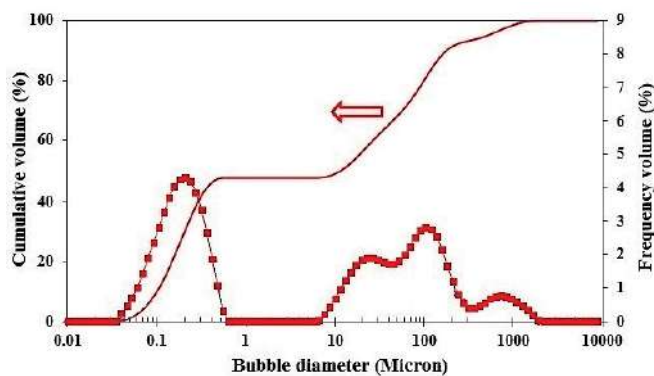


Figure 2. Bubble size distribution generated by the cavitation venturi tube (Nanobubble aeration rate = 0.11 l/min)

Column Experiments on Phosphate Minerals

The results obtained from the column tests in the presence and absence of Nano bubbles have been compared in the same conditions (Table 3). As results indicate, there are big differences in some important metallurgical performances among the flotation tests in studied settings. As the trends show in the presence of Nano bubbles, the P_2O_5 recovery has a drastic increase of 8.5% compared to the conventional conditions. On the other hand, comparison between S.E figures shows a step of 5% in increasing the values.

Table 3. Column flotation comparative results for phosphate fine particles in the presence and absence of NBs

Condition	P_2O_5 (%)	Recovery (%)	Enrichment Ratio(c/f)	S.E
NBs absence	31.66	32.74	1.99	25.60
NBs presence	30.44	41.26	1.91	30.94

Usually, the improvements of flotation S.E in presence of NBs can be attributed to the selectivity of bubbles for hydrophobic particles. In order for particles to have a successful collection with air bubbles, particles behavior in three sub-processes, including collision, adhesion, and finally detachment

occurring in flotation should go on the desired path. So, a higher collection in flotation generally leads to an improved separation efficiency (Fan et al., 2019).

In the slurry, because of NBs small ascending velocity, they will rise slowly in the slurry and have many chances to collide with and attach to fine phosphate particles (Etchepare et al., 2017, Calgaroto et al., 2015). The bubbles number density or concentration in the slurry is an important factor in flotation. Increasing the bubble number density will promote the particles collision rates and with a higher bubble number density a more efficient flotation process can take place. In contrast, the conventional-sized bubbles generated by a normal sparger due to their sizes and low collision probability cannot collect fine particles effectively. Therefore, by utilizing NBs and a such mechanism the efficiency of fine particles flotation can be effectively improved.

After clarifying the effect of NBs on the process, different flow rates in the range of 0-0.9 L/min (0-1.19 cm/s), was also investigate to determine the optimum value (Table 4).

Table 4. Effect of NBs flowrate on the column flotation performance of Phosphate ores

NBs flowrate (Cm/S)	Recovery (%)	Grade (%)
0	32.74	31.70
0.60	35.12	31.39
0.73	38.25	30.52
0.90	41.26	30.43
1.19	34.97	27.61

The results indicate that the flotation performances can be affected by NBs flow rate. As it clearly shows the ideal in the recovery can be achieved with NBs flow rate of 0.93 cm/s. As described before, in this condition the hydrophobic particles are aggregate by NBs. This aggregation can create a capillary bridging that provides more collision and connection probability. The examination on current flotation test results proves that the applied NBs are selectively attached to the surface of apatite fine particles and then the hydrophobicity of particle surfaces is improved. This phenomenon will increase the floatability rate by increasing the contact angle of particle-bubble and connectivity forces.

Column Experiments on Iron Minerals

In a specific designed laboratory-scale flotation column the effects of nanobubbles on desulfurization of iron ore was evaluated. Keeping the introduced optimum conditions, the flotation behavior of pyrite in presence of NBs was investigated. In this condition, the aeration rate of nanobubbles was adjusted to column flotation cell equal to 0.11 l/min (0.15 cm/s). The obtained results for pyrite flotation depicted that using the cavitation system noticeably results in higher flotation recovery compared in absence of NBs (Table 5). As seen from the results, variations show that in tests with optimum operational conditions, the Sulphur recovery toward the absence of nanobubbles was increased by 20% and reached around 82%. Based on the literatures, by using NBs the wettability and floatability of particles are changed through the selective adsorption of nanobubbles on the surfaces of ultra-fine pyrite and consequently improving the flotation performance and also separation efficiency are taken place.

Table 5. Column flotation comparative results for desulfurization of iron ore concentrate and sulfur recovery in the presence and absence of NBs

Condition	S grade (%)	S recovery (%)
NBs absence	1.2	61
NBs presence	0.22	81.6

The results of an optimum test were observed that in presence of nanobubbles the final concentrate with the grade of 67.7% Fe and 0.22% S can be obtained.

CONCLUSIONS

A feasibility study was carried out to evaluate the effects of nanobubbles (NBs) presence in flotation on purification of two types of fine ores (Phosphate and Iron minerals). The results for phosphate minerals showed that using NBs can significantly enhance the process efficiency with favourable grade and recovery. In the presence of NBs, the recovery of fine phosphate particles increased by 8.5%, compared to the absence of NBs. Also, in the presence of NBs a significant increase in the process separation efficiency (S.E) by 5% was observed. The results revealed that applying NBs in column flotation tests of iron ores the desulfurization efficiency of iron ore concentrate can enhance significantly. In the presence of Nano bubbles, in concentrate part (reverse flotation) the recovery of sulphur minerals increased by 20%, while the sulphur content of iron concentrate (column tailing part) reduced from 1.2% to 0.22%.

REFERENCES

- A. Azevedo, R. Etchepare, S. Calgaroto, and J. Rubio, (2016), Aqueous dispersions of nanobubbles: generation, properties and features, *Int. J. Miner. Eng.*, *94*, p. 29.
- A. Sobhy, D. Tao, (2013), High-Efficiency Nanobubble coal flotation, *International Journal of Coal Preparation and Utilization*, *33*:242–256.
- B. Vaziri Hassas, J. Jin, L.X. Dang, X. Wang, and J.D. Miller, (2018), Attachment, Coalescence, and Spreading of Carbon Dioxide Nanobubbles at Pyrite Surfaces, *Int. J. Langmuir*, *34*, (No. 47, p. 14317.
- B. Vaziri Hassas, J.D. Miller, (2019) The effect of carbon dioxide and nitrogen on pyrite surface properties and flotation response, *Int. J. Minerals Engineering*, *144*.
- F. Nakhaei, Z. pourkarimi, (2020), "Desulphurization of Iron Ore Slime by Column Flotation with Nano-Micro Bubbles", XXX International Mineral Processing Congress in Cape Town, South Africa, 18 - 22 October.
- F. Taghavi, M. Noaparast, Z. Pourkarimi, F. Nakhaei, (2022), Comparison of mechanical and column flotation performances on recovery of phosphate slimes in presence of nano-microbubbles, *J. Cent. South Univ.* *29*: 102—115
- H. Oliveira, A. Azevedo, and J. Rubio, (2018), Nanobubbles generation in a high-rate hydrodynamic cavitation tube, *Int. J. Miner. Eng.*, *116*, p. 32.
- M. A. Hampton, A. V. Nguyen. (2010). Nanobubbles and the nanobubble bridging capillary force. *Advances in Colloid and Interface Science* *154*(1–2): 30–55.
- M. Fan, D. Tao, and Y. Tao, (2019), Effects of nanobubbles in column flotation of Chinese sub-bituminous coal, *Int. J. Coal Preparation and Utilization*.
- M. Fan, D. Tao, R. Honaker, and Zh. Luo, (2010), Nanobubble generation and its applications in froth flotation (part III): specially designed laboratory scale column flotation of phosphate, *Int. J. Mining Science and Technology (China)*, *20*, No. 3, p. 317.
- P.E. Theodorakis, Z. Che, Surface nanobubbles (2019) Theory, simulation, and experiment: a review, *Int. J. Advances in Colloid and Interface Science*.

- R. Etchepare, H. Oliveira, M. Nicknig, A. Azevedo, and J. Rubio, (2017), Nanobubbles: generation using a multiphase pump, properties and features in flotation, *Int. J. Miner. Eng*, *112*, p. 19.
- S. Calgaroto, A. Azevedo, and J. Rubio, (2015) Flotation of quartz particles assisted by nanobubbles, *Int. J. Mineral Processing*, *137*, p. 64.
- S. H. Cho, J. Y. Kim, J. H. Chun, and D. J. Kim. (2005). Ultrasonic formation of nanobubbles and their zeta-potentials in aqueous electrolyte and surfactant solutions, *colloids and surfaces A. Physicochemical Engineering Aspects* *269*: 28–34.

APPLICATION OF RESPONSE SURFACE METHODOLOGY IN OPTIMIZING LEACHING PARAMETERS FOR NICKEL RECOVERY FROM SPENT CATALYST

A.M. Beygian¹, M.Rezaei¹, E. K. Alamdari^{1,*}

¹ *Department of Materials and Metallurgical Engineering, Amirkabir University of Technology*
 (*Corresponding Author: alamdari@aut.ac.ir)

ABSTRACT

Reuse and recovery of nickel from different types of waste is of great environmental and economic importance. The purpose of this study was to recover nickel from steam reforming catalyst by optimizing the operating parameters using response surface methodology (RSM). To this aim, nickel oxide was converted into nickel sulfate using sulfuric acid through leaching process. The influence of three numerical independent variables, i.e., time (3-12 h), sulfuric acid concentration (1-4 molar) and liquid-to-solid ratio (3-12 mL/g), and one categorical independent variable, i.e., particle size (coarse, fine, powder) were evaluated. In order to correlate the independent variables for maximum nickel recovery, a two-factor interaction (2FI) model was suggested using central composite design (CCD) method. The results indicate that under optimum parameters of 6 h time, liquid-to-solid ratio of 9 mL/g and acid concentration of 3 M for coarse particles, maximum recovery of 94% can be attained. The characterization of nickel was examined by atomic absorption spectroscopy for confirmation of nickel recovery. The most effective parameter based on F value analysis was determined to be the liquid-to-solid ratio. Application of lower acid concentration and the fact that there is no need to crush the spent catalyst residues, decrease costs of process significantly.

Keywords: Reforming catalyst, sulfuric acid, leaching, nickel recovery, response surface methodology

INTRODUCTION

Nickel can be considered as a highly applicable metal source since it is used in various industries such as manufacture of steel and its alloys (Bassioni et al., 2015), catalyst and battery industries (Zeifert and Salmones, 2008; Goula et al., 2015; Tarabay and Karami, 2015), nickel-based alloys (Valitov, 2016), coating industries (López et al., 2012), ceramic industries (Yahia and Adel, 2014) and paint-and-varnish (Kvasnikov and Romanova, 2015). There is also a considerable demand for this metal worldwide (Apostolikas et al., 2009; Nieto et al., 2013). After stainless steel, the major use of nickel happens in manufacture of catalysts (Coulter et al., 1994). Being high-tech and expensive, these catalysts lose their catalytic properties after a specific lifetime period and become waste (Mortensen and Gardini, 2014). On the other hand, nickel is reported to have harmful properties (Duda-Chodak and Blaszczyk, 2008; Das and Reddy, 2018) and accumulation of this metal over time can have devastating effects on the environment. This is why the recovery of nickel in any way possible can prevent both additional costs and environmental damages. Several authors reported that nickel was recovered by various methods like using chelating ion exchange resin (Padh et al., 2019), ultra-sonication-assisted leaching (Oza et al., 2011), chelating agents like EDTA (Vuyyuru et al., 2010), electro-less plating and magnetic separation (Taninouchi et al., 2017).

One of the general methods used for recovery of nickel is leaching process (Wang, 2000). In this process, nickel salt is extracted from an oxide compound using an acidic medium and then joins the acid-

dependent salt composition (Kolosnitsyn et al., 2006; Nazemi and Rashchi, 2012). Nickel salts extracted in this way can be reused in industrial applications such as plating and coating, or the elemental nickel itself can be recovered through the electrowinning process. Various parameters are effective in leaching process such as time, acid concentration, particle size, temperature, liquid-to-solid ratio, etc. (Alex et al., 1993; Ghanem et al., 2008). Invascano and Roman (1975) dissolved ammonia plant's catalysts in 80% sulfuric acid solution for 50 minutes at 70 °C and reached to 99% nickel recovery in the form of nickel sulfate; this was done when catalyst particle size was about 0.09 millimeter. Loboiko et al. (1983) found that recovery of nickel in a solution of nitric acid with a purity of 60-70% at 120 °C for 2-3 h would be significant. With catalyst leaching by hydrochloric acid, Chandhary et al. (1993) found that recovery of nickel from a low-grade nickel catalyst would be up to 17.7%. Vicol et al. (1986) tried to extract a used catalyst with aqueous solution containing 15-23% ammonia at a temperature of 60 to 90 °C and in a pH range of 7.5 to 9 for retrieving nickel. Al-Mansi and Abdel Monem (2002) recycled nickel in the form of sulfate salt by direct crystallization in a concentration of 50% sulfuric acid, a solid to liquid ratio of 1:12, and a particle size smaller than 500 microns. A nickel recovery of 99% was obtained after about 5 h leaching at 800 rpm and 100 °C.

Recently, various statistical experimental design procedures have been used in different sectors for optimization of process parameters (Arshadi et al., 2016). Optimizing a system of several variables in the convectional mode requires many experiments which is time consuming and costly. Furthermore, such methods do not provide combined effect of variables and need more data for determining optimum level (Kumar et al., 2018). RSM can be a thorough approach to study a process and to figure out the best correlation among the parameters of a process, additionally This is done via developed models based on the statistical methods to configure the relation between the inputs and outputs of any process and optimizing the effect of these parameters to attain the desirable response (Mohamad Said and Mohamed Amin, 2015). To develop a model based on the statistical methods, it is necessary first to recognize the parameters that exhibit significant influence in the process. Then, experimental procedure should be designed in a way that it takes into account all the process parameters at several levels. This is followed by analyzing the experimental results using the analysis of variance (ANOVA) technique to determine which parameters show the strongest interactions and/or exhibit significant influences on the outputs of process. Based on the process response as a statistical model, the process is optimized using the variables range predicted by model. For example, Haghshenas et al. (2012) optimized physicochemical parameters in order to undertake bioleaching of sphalerite by *Acidithiobacillus ferrooxidans* using shaking bioreactors using RSM methodology.

To the best of our knowledge, there is no report on using RSM method to optimize operating parameters of leaching process to recover nickel from spent catalysts. This paper examines the combined effects of time, concentration, liquid-to-solid ratio and particle size on the leaching process. An experimental procedure was designed using central composite design (CCD) in conjunction with RSM method to optimize the leaching recovery response of nickel catalyst. Three models were presented for predicting the recovery percentages of the three different nickel catalyst particle sizes.

EXPERIMENTAL PROCEDURE

The catalyst in this study is the Rhine Catalyst, known as the steam reformer catalyst, which is used in the petrochemical industry to accelerate the production of hydrogen from methane, which is why it is also called a reformer catalyst. The overall composition of this catalyst is mainly alumina and nickel oxide, which can be called a rich source. The method for nickel extraction is generally leaching (acidification). The reaction of nickel oxide with sulfuric acid is a heterogeneous reaction. In the systems of such a reaction, the

general relationship of the rate is complicated due to the cross between physical and chemical processes. The main reaction is as follows, Where NiO is the limiting reactant.

By the means of atomic absorption spectroscopy (AAS), while dissolving 0.5 grams of this spent catalyst in an aqua containing 15 cm³ HF, 2 cm³ H₂SO₄ and 2cm³ HCl, the result and therefore the composition of this solid sample is shown in table (1) Commercial grade 98% sulfuric acid was selected as the solvent for the metal oxides to produce sulfate. Distilled water was used to dilute this acid. As one of three numeric factors, acid concentrations of 1, 2, 3, and 4 molars as well as 2.5 M as the mean, were selected. This range of data was to show that the other studies used very high acid concentrations which may cause problems in deacidification and subsequent processes.

Table 1. Composition of the spent catalyst sample obtained from AAS

Substance	Co	Ni	Zn	Mg	Ca	Al	Fe	Oil	Humidity	O,C,S
Amount (wt.%)		10.43		0.18	0.02	25.36	0.058	N.D.	N.D.	Balance
(ppm)	76		57							

As the only categorical variable, the catalyst particle size was determined after two stages of crushing and mill grinding followed by a thorough screen breakdown. The resulting mixture was divided into three groups. The powder sample with a mean grain size of 1.2 mm, the fine sample with a mean grain size of 4 mm and finally the coarse sample which is the catalyst in its uncrushed form. To provide the required temperature for the leaching process, a simple resistive heater with a pre-heated aluminum bath as a heat transfer media was used. Contrary to other studies, the temperature of 85±3 ° C was taken as one of the constant parameters of the process. Another constant parameter, turbulence, was considered with the agitator rotation speed parameter. The reason for this, as in the case of temperature, is that it is difficult to generate turbulence in large processes. However, turbulence in this study was achieved by using a mechanical stirrer with a heavier base against vibration, and electric motor, with a polymer coated stirrer. The agitator rotational speed according to the standards of this machine was selected a constant value of 400±10 rpm.

The second numeric variable of the leach, was considered to be the ratio of liquid to solid. The L/S fraction in ml/g, with the values of 3, 6, 9, 12 and 7.5 as the mean value, were selected. According to this value and the amount of solution that was 500 milliliters, the solid catalyst content was weighed by an electronic scale of 0.01-gram accuracy and washed with distilled water in a plastic acid-resistant container. Further, the amount of water required was calculated and then measured using a graduated cylinder. Then under suitable ventilation conditions (due to the rapid release of SO₂ and H₂S) acid was slowly added to the solution. Finally, the last parameter for the leach was considered to be time, and its values were set for 3, 6, 9, 12 and 7.5 as mean. It must be noted that the alpha value for corresponding axial point for the variable parameters is set to be 3 so that axial points are in logical comparison to center points and leaching parameter ranges, as shown in table (2) The Design Expert software used in this study, offered 51 leaching experiments, Taking into account the number of replicates and central and axial points. After the completion of the leach process, a diluted solution was prepared as a final sample for atomic absorption spectroscopy to obtain the recovered nickel content.

Table 2. The variable values of leaching parameters for central composite RSM modeling

Variable Parameter	Coded Values				
	-alpha (-3)	-1	0	+1	+alpha (+3)
A: L/S (ml.g ⁻¹)	1	2	2.5	3	4
B: Time (hour)	3	6	7.5	9	12
C: Acid Concentration (molarity)	3	6	7.5	9	12
D: Particle size (categorical)		Powder	Fine	Coarse	

RESULTS AND DISCUSSION

The results of the 51 leaching experiments after analysis via AAS, are presented in table (3). Leverage is the potential for a design point to influence the fit of the model coefficients, based on its position in the design space. Leverages near 1 should be avoided. As seen in table (3) all leverages are below 1 and the center points have the lowest of them all, it can be deduced that the model that will be fit to this data is more significant near the central points. The ratio of maximum to minimum of the responses is 2.53. A ratio greater than 10 usually indicates that a transformation is required. For ratios less than 3, transformations have little effect. No transformation was done to the response results.

As presented in table (4), sum of squares is the sum of the squared deviations from the mean for each model. The SS for the Mean is calculated first, followed by Linear model, Quadratic model, Special Cubic, Cubic, Residuals and Total. The degrees of freedom for the mean will be 1. The df for the linear, quadratic, special cubic and cubic models is the number of additional terms added to the model. The residual will contain any remaining degrees of freedom. For each source, the mean square is the sum of squares divided by the degrees of freedom. This is used to calculate the F-value for the models. The F-value is used to test the significance of adding new model terms to those terms already in the model. For instance, the significance of the linear terms is tested after removing the effect of the average and the blocks. Then, the significance of the quadratic terms is tested after removing the average, block and linear effects and so on. The P-value is the probability associated with adding these additional terms to the model. And to summarize this all, table (4) suggests a 2FI (2 factor interaction) model to be used to provide a model for the resulted responses, as the main focus is on maximizing R-Squared and to avoid lack of fits.

After further analysis of variance as shown in Table (5), The Model F-value of 12.06 implies the model is significant. There is only a 0.01% chance that a "Model F-Value" this large could occur due to noise. P-values less than 0.0500 indicate model terms are significant. In this case A, B, C, D and AB are significant model terms. Values greater than 0.1000 indicate the model terms are not significant. If there are many insignificant model terms, model reduction may improve model, not needed in this case. The "Lack of Fit F-value" of 1.94 implies the Lack of Fit is not significant. "Adeq Precision" measures the signal to noise ratio. A ratio greater than 4 is desirable. The model ratio of 15.808 indicates an adequate signal. Both the facts that the model F-value is significant and The "Lack of Fit F-value" is not, proves that this model can be used to navigate the design space. Finally, software presented 3 model equations, one for each of the categorical particle sizes in term of actual factors used.

Eq. (1) for Powder samples:

$$R\%_{Ni} = 287.29141 - 35.08166 \times \frac{L}{S} - 75.48491 \times C - 7.69325 \times t + 12.05388 \times \frac{L}{S} \times C + 1.19337 \times \frac{L}{S} \times t - 0.29291 \times C \times t \quad (1)$$

Eq. (2) for Fine samples:

$$R\%_{Ni} = 267.30083 - 34.17316 \times \frac{L}{S} - 77.04768 \times C - 6.47129 \times t + 12.05388 \times \frac{L}{S} \times C + 1.19337 \times \frac{L}{S} \times t - 0.29291 \times C \times t \quad (2)$$

Eq. (3) for Coarse samples:

$$R\%_{Ni} = 265.52177 - 32.51455 \times \frac{L}{S} - 80.23930 \times C - 4.70234 \times t + 12.05388 \times \frac{L}{S} \times C + 1.19337 \times \frac{L}{S} \times t - 0.29291 \times C \times t \quad (3)$$

Table 3. Central Composite design arrangement and response results

Standard Experiment Number	Variable Parameters			Response		Leverage	Point Type
	A:L/S (ml.g ⁻¹)	B: Acid Concentration (molar)	C: Time (hour)	D: Particle Size (nominal)	Ni Recovery (%)		
1	9	3	6	Powder	85.48	0.265	Fact
2	9	3	6	Powder	92.58	0.265	Fact
3	9	2	9	Powder	64.35	0.265	Fact
4	9	2	9	Powder	57.49	0.265	Fact
5	6	3	9	Powder	66.80	0.265	Fact
6	6	3	9	Powder	57.54	0.265	Fact
7	6	2	6	Powder	76.66	0.265	Fact
8	6	2	6	Powder	67.16	0.265	Fact
9	3	2.5	7.5	Powder	43.01	0.600	Axial
10	12	2.5	7.5	Powder	85.06	0.600	Axial
11	7.5	1	7.5	Powder	39.68	0.600	Axial
12	7.5	4	7.5	Powder	75.41	0.600	Axial
13	7.5	2.5	3	Powder	59.34	0.600	Axial
14	7.5	2.5	12	Powder	67.29	0.600	Axial
15	7.5	2.5	7.5	Powder	57.64	0.094	Center
16	7.5	2.5	7.5	Powder	49.72	0.094	Center
17	7.5	2.5	7.5	Powder	66.81	0.094	Center
18	9	3	6	Fine	64.95	0.265	Fact
19	9	3	6	Fine	72.71	0.265	Fact
20	9	2	9	Fine	55.84	0.265	Fact
21	9	2	9	Fine	48.67	0.265	Fact
22	6	3	9	Fine	35.70	0.265	Fact
23	6	3	9	Fine	46.32	0.265	Fact
24	6	2	6	Fine	44.95	0.265	Fact
25	6	2	6	Fine	57.00	0.265	Fact
26	3	2.5	7.5	Fine	36.53	0.600	Axial
27	12	2.5	7.5	Fine	81.57	0.600	Axial
28	7.5	1	7.5	Fine	40.86	0.600	Axial
29	7.5	4	7.5	Fine	77.65	0.600	Axial
30	7.5	2.5	3	Fine	53.69	0.600	Axial
31	7.5	2.5	12	Fine	69.98	0.600	Axial
32	7.5	2.5	7.5	Fine	57.34	0.094	Center
33	7.5	2.5	7.5	Fine	62.15	0.094	Center
34	7.5	2.5	7.5	Fine	71.49	0.094	Center
35	9	3	6	Coarse	86.79	0.265	Fact
36	9	3	6	Coarse	94.48	0.265	Fact
37	9	2	9	Coarse	78.94	0.265	Fact
38	9	2	9	Coarse	86.45	0.265	Fact
39	6	3	9	Coarse	64.70	0.265	Fact
40	6	3	9	Coarse	56.61	0.265	Fact
41	6	2	6	Coarse	66.43	0.265	Fact
42	6	2	6	Coarse	57.75	0.265	Fact
43	3	2.5	7.5	Coarse	39.95	0.600	Axial
44	12	2.5	7.5	Coarse	92.23	0.600	Axial
45	7.5	1	7.5	Coarse	55.42	0.600	Axial
46	7.5	4	7.5	Coarse	78.46	0.600	Axial
47	7.5	2.5	3	Coarse	58.24	0.600	Axial
48	7.5	2.5	12	Coarse	86.09	0.600	Axial
49	7.5	2.5	7.5	Coarse	88.14	0.094	Center
50	7.5	2.5	7.5	Coarse	80.49	0.094	Center
51	7.5	2.5	7.5	Coarse	77.36	0.094	Center

Table 4. Sequential Model Sum of Squares

Source	Sum of Squares	Degree of Freedom	Mean Square	F-Value	p-value	
Mean vs Total	218532.54	1	218532.54			
Linear vs Mean	8488.25	5	1697.65	17.94	< 0.0001	
2FI vs Linear	2017.81	9	224.19	3.6	0.0028	Suggested
Quadratic vs 2FI	204.18	3	68.06	1.10	0.3616	
Cubic vs Quadratic	471.10	13	36.24	0.46	0.9211	Aliased
Residual	1564.23	20	78.21			
Total	231278.11	51	4533.57			

Table 5. Analysis of variance (ANOVA) for response surface

Source	Sum of Squares	Degree of Freedom	Mean Square	F- Value	p-value	
Model	10505.97	14	750.43	12.06	< 0.0001	significant
A-L/S	3237.38	1	3237.38	52.04	< 0.0001	
B-C	1521.63	1	1521.63	24.46	< 0.0001	
C-t	452.14	1	452.14	7.27	0.0106	
D-Size	2162.07	2	1080.04	17.38	< 0.0001	
AB	1357.96	1	1357.96	21.83	<0.0001	
AC	119.79	1	119.79	1.93	0.1738	
AD	198.25	2	99.12	1.59	0.2172	
BC	0.80	1	0.80	0.013	0.9102	
BD	76.34	2	38.17	0.61	0.5470	
CD	264.57	2	132.29	2.13	0.1340	
Residual	2239.52	36	62.21			
Lack of Fit	1478.64	18	82.15	1.94	0.0841	Not significant
Pure Error	760.88	18	42.27			
Total	12745.48	50				
R ²	82.43					
Adeq Precision	15.808					

Table 6. Proposed practical research values for Optimum leaching process

A: L/S (ml.g ⁻¹)	B: C (mol. L ⁻¹)	C: t (hour)	D: Size	Actual Recovery (%)	Predicted Recovery (%)
9	3	7.5	Coarse	94.36	96.32

After several repeated runs, verification was done in order to report the optimum conditions of leaching process, shown in Table (6). The value presented as the actual recovery is the average of mentioned runs. Due to F-values of 52.04 and 24.46 respectively for L/S and acid concentration, significance of the model is affected greatly by these parameters. Also, between the interaction factors in the model, AB which is the product of L/S and C, shows the highest F-value and hence the highest significance. According

to the results of this experiment in Fig. 1(a), it can be stated that from acid concentration of about 2.5 M above and simultaneously at L/S values more than about 8.5, the recovery is significant, with a concentration of 2.75 molar acid Upward and L/S of about 8.75 upwards, recovery percentages cross the 90% limit, which is desirable.

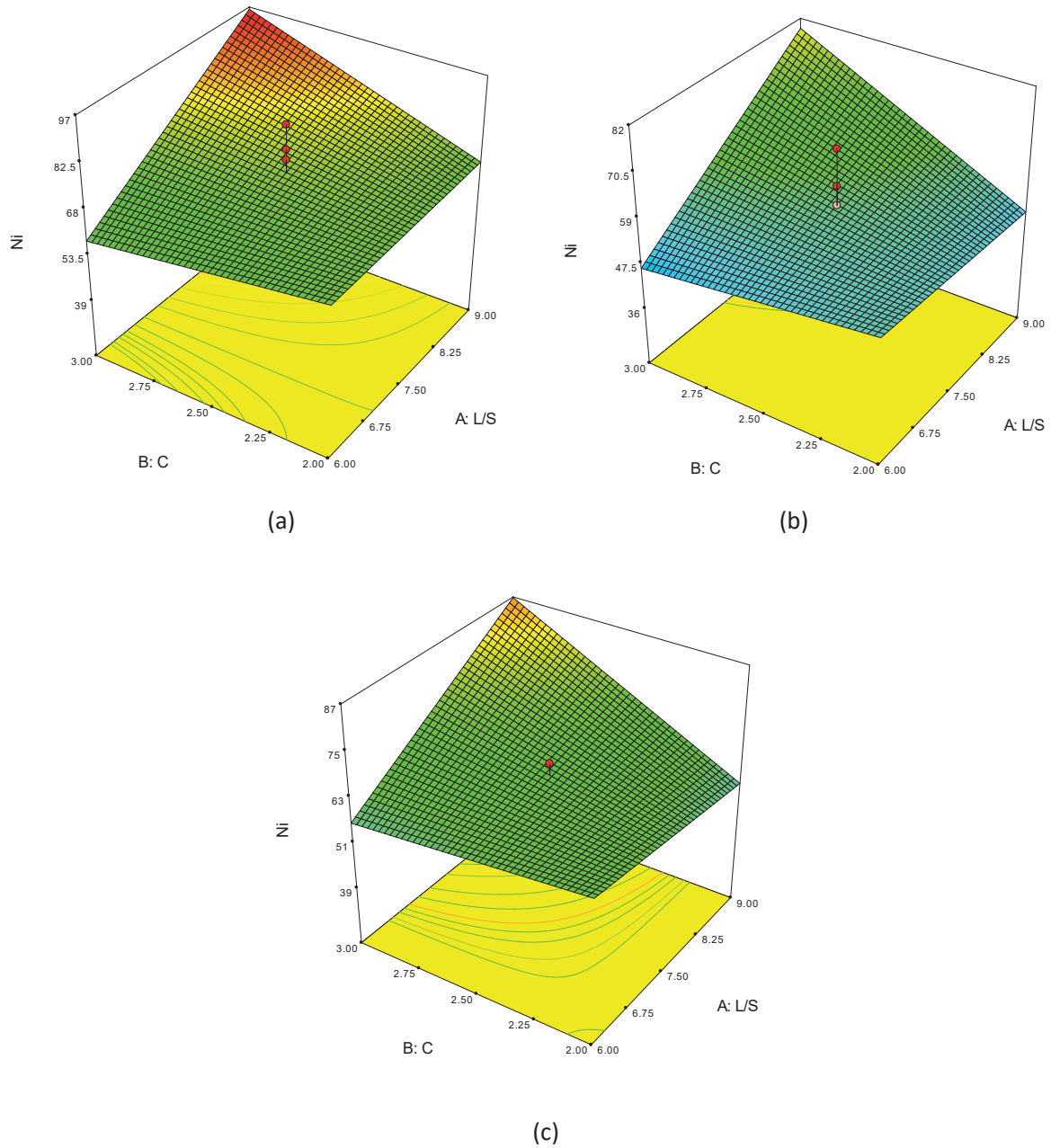


Figure 1. Surface plots of Ni recovery with respect to L/S and C for (a)Coarse, (b)Fine and (c)Powder samples at 7.5 h.

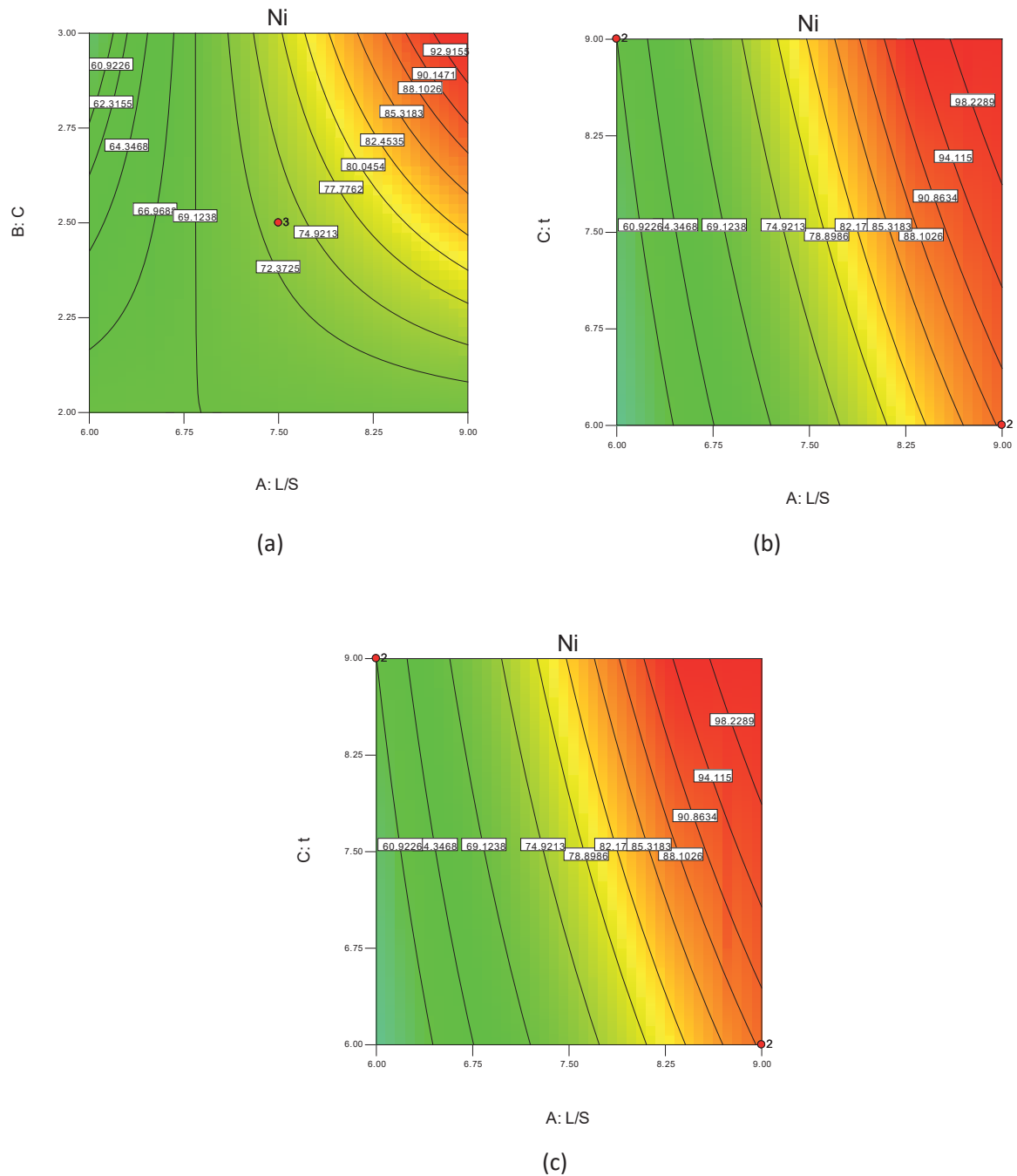


Figure 2. Contour plots of Ni recovery for coarse sample with respect to (a) L/S and C (at t=7.5), (b) L/S and t (at C=3) and (c) C and t (at L/S=9).

According to the contours drawn in Fig. 2(a), it can be seen that these two factors can be changed in opposite directions, which means that for higher recovery by adding to the L/S value, lower acid

concentration can reach the same results, and also by increasing the amount of acid concentration, it is also possible to produce the leach with the same results with lower L/S. Increasing recovery by increasing concentrations of acid and L/S values is predictable, because with increasing acid concentration, there are more sulfate ions to remove nickel from its oxide compound, which ultimately increases the reaction efficiency; by increasing L/S, the amount of solution to react with a constant amount of solid is increased, and fresh acid is added to the reaction surface to further increase efficiency. According to Fig. 2(b), longer than

7.5 hour processes may show better recovery results, but further filtration and purification, turned out to be challenging because of more impurity dissolution. And of course longer times mean more amount of energy for mixer and later follow up on batch production. By extrapolating the plots of Fig. 2. It is obvious in leaching that using acid concentrations of 4 molar and higher and L/S of 12 will prove recovery to be possible at shorter times, yet further diacidification and lower nickel content concentration (which then must be concentrated again to be used for electrowinning) prove that such high parameters are not suitable for overall production process. Fig. 1(b), shows that in the case of fine specimens with a particle size of about 4 millimeters, given that in this size, fracture and crushing was in a way that there are particles that have been pulled and look pointy (this can be due to the particular synthesis or a particular crystalline structure of catalysts), which can be said to be sharp and heterogeneous particles, lead to a lower level for presence in the reaction. And also a slight disruption of mixing. Therefore, according to the results, the range of significant recoveries has become smaller, as at acid concentrations above 3 mol/L and L/S values higher than 9, recovery can be done up to about 80%. And according to the results for these particles, at concentrations of less than 2.5 M, recovery can not be advanced forward. In these samples, to achieve recovery above 95%, the concentration of more than 4 M and L/S of more than about 12 are essential; however, energy and cost should be used for grinding.

For powder samples with a size of about 1 millimeter, as illustrated in Fig. 1(c), which have more uniform particles with a spherical shape, the results are more in common with the results of Coarse catalysts; however, the limits of significant recovery are larger in the non-crushed sample. In this sample, a recovery of about 87% can be achieved at concentrations higher than 3 mol/L and L/S values higher than 9. This range is larger than the Fine specimen range; although the cost and energy to produce these samples are double the Fine samples.

CONCLUSION

In general, increasing the amount of recovery by adding to the values of leaching parameters such as time, acid concentration and liquid to solid fraction is obvious and natural. But the point is that in some experiments under certain conditions, this natural process is not followed.

Coarse Samples

In these samples, from 7.5 hours' time up, under the same conditions, no significant change is observed in the recovery. For example, in the same conditions with an increase of time from 7.5 to 9, recovery only increased by about 3%.

The liquid to solid fraction at a constant period of time, has a significant effect on the recovery efficiency; for example, increasing this ratio from 6 to 9 restores recovery from 58% to over 96%.

In general, optimum recovery conditions for these samples can be considered as follows: the time from 6 to 7.5 hours, the concentration of acid is about 3 M and the fraction of the liquid to solid is about 9,

to recover about 96% of Ni content. it is to be noted that the parameter of the fraction of liquid to solid can be described as the most influential parameter in these samples.

Fine Samples

In these samples, recovery is generally not high; process times of 7.5 hours and longer, not only lack a positive effect, but also result in less recovery.

The effect of the liquid-to-solid fraction is very much affected by the concentration of acid in a way that it can be deduced that the recovery rate is related to the product of these two quantities.

Generally, the optimum recovery for these samples, at 7.5 h, the concentration of 3 molar acid and the liquid to solid fraction of 9, reached about 79%.

Powder Samples

In these samples, an optimal recovery time of about 9 hours can be reported. In this crushed samples, increasing time leads to more reaction of alumina. Less time is not enough to react the total amount of nickel.

In general, the simultaneous effect of the concentration of acid and the liquid to solid fraction can be expressed as a Product. The concentration of acid is better to stay in the middle and the ratio of liquid to solid should not be less than 9.

In these conditions, the optimal recovery for these samples at 9 hours' time, the acid concentration of 3 molars and the liquid to solid fraction of 9, reached about 90%.

Consequently, a non-crushed sample can be considered as the most suitable one for recovery of this nickel catalyst. This might be due to the fact that nickel is mostly accumulated on the surface on these spent catalysts. The unnecessary of grinding the specimen itself, reduces the cost of the process dramatically. The results suggest that high recovery can be attained without the use of extremely high acid concentrations, high temperatures and high liquid-to-solid ratios.

REFERENCES

- Alex, Pamela, T.K. Mukherjee, and M. Sundaresan, (1993). "Leaching behaviour of nickel in aqueous chlorine solutions and its application in the recovery of nickel from a spent catalyst." *Hydrometallurgy* 34: 239-253.
- Al-Mansi, N.M., and N.M. Abdel Monem. (2002). "Recovery of nickel oxide from spent catalyst." *Waste Management* 22: 85-90.
- Apostolikas, A, E Frogoudakis, and J Bakallbashi. (2009). "Nickel, World Production and Demand." *3rd Balkan Mining Congress, BALKANMINE*. Izmir-TURKEY.
- Arshadi. M, S.M. Mousavi, and P Rasoulnia. (2016). "Enhancement of simultaneous gold and copper recovery from discarded mobile phone PCBs using *Bacillus megaterium*: RSM based optimization of effective factors and evaluation of their interactions." *Waste Management*.
- Bassioni, Ghada, A. Korin, and A. El-Din Salama. (2015). "Stainless Steel as a Source of Potential Hazard due to Metal Leaching into Beverages." *International Journal of Electrochemical Science* 10: 3792 - 3802.

- Chandhary, AJ; Donaldson, JD, and SC: Grimes, SM Boddington. (1993). "Heavy metal in the environment. Part II: a hydrochloric acid leaching process process for the recovery of nickel value from a spent catalyst." 34-137.
- Coulter, Kent, Xueping Xu, and D. Wayne Goodman. (1994). "Structural and Catalytic Properties of Model Supported Nickel Catalysts." *Phys. Chem* 98: 1245-1249.
- Das, Kusal K., and R. Chandramouli Reddy. (2018). "Primary concept of nickel toxicity – an overview." *Journal of basic and clinical physiology and pharmacology*.
- Dehghani, Kamran, Atiye Nekahi, and Mohammad Ali Mohammad Mirzaie. (2010). "Optimizing the bake hardening behavior of Al7075 using response surface methodology." *Materials and Design* 31: 1768-1775.
- Duda-Chodak, Aleksandra and U. Blaszczyk. (2008). "The Impact Of Nickel On Human Health." *Hournal of Elementol* 13: 685-696.
- Ghanem, R, H Farag, Y Eltaweel, and Mona E Ossman. (2008). "Recovery of nickel from spent catalyst by single- and multi-stage leaching process." *International Journal of Environment and Waste Management* 2: 540-551.
- Goula, Maria A, Nikolaos D. Charisiou, Kiriakos N. Papageridis, and Andreas Delimitis. (2015). "Nickel On Alumina Catalysts For The Production Of Hydrogen Rich Mixtures Via The Biogas Dry Reforming Reaction: Influence of the synthesis method." *International Journal Of Hydrogen Energy* 40: 9183-9200.
- Haghshenas, Davoud, Babak Bonakdarpour, Eskandar Keshavarz Alamdari, and Bahram Nasernejad. (2012). "Optimization Of Physicochemical Parameters For Bioleaching Of Sphalerite by Acidithiobacillus Ferrooxidans Using Shaking Bioreactors." *Hydrometallurgy* 111: 22-28.
- Ivascanu, St, and O Roman. (1975). "Nickel Recovery From Spent Catalysts." *Bullnst Politeh Iasi Sect 2*: 21-47.
- Kolosnitsyn, V. S., S. P. Kosternova, and O. A. Yapryntseva. (2006). "Recovery of Nickel with Sulfuric Acid Solutions from Spent Catalysts for Steam Conversion of Methane." *Russian Journal of Applied Chemistry* 79: 539-543.
- Kumar, Anil, Harvinder Singh Saini, and Sudhir Kumar. (2018). "Enhancement Of Gold And Silver Recovery From Discarded Computer Printed Circuit Boards by Pseudomonas Balearica SAE1 Using Response Surface Methodology (RSM)." *Biotech* 3: 8-19.
- Kvasnikov, M. Yu., and O. A. Romanova. (2015). "Electrodeposited Paint-and-Varnish Nickel–Polymer Coatings." *Russian Journal of Applied Chemistry* 88: 1870-1876.
- Loboiko, Aya, VI Atroshchenko, G Grin, VV Kutovoi, and NP Fedorova. (1983). "Recovering Nickel From Spent Catalyst." *Otkrytiya, Izobret, PromObraztsy, Tovarnye Zanki* 14-33.
- López, JR, G Stremmsdoerfer, G Trejo, R Ortega, JJ Pérez, and Y Meas. (2012). "Corrosion Resistance of Nickel Coatings Obtained by Electrodeposition in a Sulfamate Bath in the Presence of Samarium (III)." *International Journal of Electrochemical Science* 7: 12244-12253.
- Mohamad Said, Khairul Anwar, and Mohamed Afizal Mohamed Amin. (2015). "Overview on the Response Surface Methodology (RSM) in Extraction Processes." *Journal of Applied Science & Process Engineering* 2: 8-16.
- Mortensen, Peter M., and Diego Gardini. (2014). "Stability And Resistance Of Nickel Catalysts For Hydrodeoxygenation." *Catalysis Science & Technology* 4: 3672-3686.
- Nazemi, M., and F. Rashchi. (2012). "Recovery Of Nickel From Spent NiO/Al₂O₃ Catalyst Through Sulfuric Acid Leaching, Precipitation And Solvent Extraction." *Waste Management & Research* 30: 492-497.
- Nieto, A, V Montaruli, and M Cardu. (2013). "The Strategic Importance Of Nickel: Scenarios And Perspectives Aimed At Global Supply." *Transactions Of The Society For Mining, Metallurgy, And Exploration* 332: 510-518.
- Oza, Rachit, Nikhil Shah, and Sanjay Patel. (2011). "Recovery Of Nickel From Spent Catalysts Using Ultrasonication-Assisted Leaching." *Journal of Chemical Technology & Biotechnology* 86: 1276-1281.

ASİDİK DRENAJ AÇISINDAN MADEN ATIKLARI YÖNETMELİĞİ ÜZERİNE BİR İNCELEME
AN INVESTIGATION ON THE MINING WASTE REGULATION IN TERMS OF ACIDIC DRAINAGE

M. Karadeniz *

(*Sorumlu yazar: mhmtkaradeniz@gmail.com)

ÖZET

“Maden Atıkları Yönetmeliği”, sülfürlü madenlerde karşılaşılan asit maden drenajı (AMD) sorununa ilişkin maddeleri yönünden incelendiğinde görülmektedir ki, yönetmelik hem kavram ve hem de yöntem bakımından yanlış yönlendirebilecek bazı ifadeler içermektedir. Özellikle, yöntemler hakkındaki ifadeler çok daha önemlidir, zira sahayı temsil eden örneklerin belirlenen asit potansiyeli, gerçek değerinin altında bulunursa, alınacak önlemlerin yetersizliğine yol açması söz konusudur. Tersine, gerçek potansiyelin üzerinde bulunursa da fazladan yatırım maliyetine sebep olması olasıdır. Çünkü asit üretme potansiyelinin (AÜP) kestiriminde ön eleme amacıyla kullanılan statik testler, esas itibarıyla, kimi ön kabullere dayanarak geliştirilmiştir ve bu kabuller, incelenen sahanın mineralojik özellikleriyle uyumsuz olduğunda, gerçeğe aykırı sonuçlar elde edilebilmektedir. Buradan hareketle, bu çalışmada, AMD kestiriminde kullanılan statik test yöntemlerinin, uygulandıkları maden sahasının mineralojik özelliklerine göre, karşılaşılabilecek zaafı ve üstünlükleri irdelenmiş, yönetmeliği iyileştirmek adına kimi öneriler yapılmıştır.

Anahtar Sözcükler: Yönetmelik, asit maden drenajı, statik testler, aba

ABSTRACT

When the “Mining Wastes Regulation” is examined in terms of its articles related to the acid mine drainage problem encountered in sulfide mines, it is seen that the regulation contains some statements that may mislead with regards to both concept and method. Especially, the statements about the methods are much more important because if the determined acid potential of the samples representative of the field is found below the actual value, it may lead to the inadequacy of the measures to be taken. Conversely, if it is above the actual potential, it is likely to cause additional investment costs. Because the static tests used for pre-screening in predicting the acid production potential (APP) were mainly developed based on some preliminary assumptions and when these assumptions are inconsistent with the mineralogical properties of the investigated field, unrealistic results can be obtained. From this point of view, in this study, the weaknesses and advantages of the static test methods used in the prediction of acid mine drainage, according to the mineralogical characteristics of the mine field where they are applied, were gone through and some suggestions were made in order to improve the regulation.

Keywords: Regulation, acid mine drainage, static tests, aba

GİRİŞ

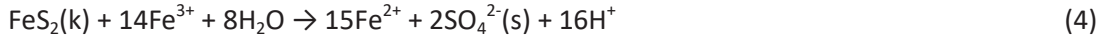
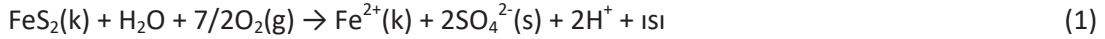
“Maden Atıkları Yönetmeliği” ve onu tamamlayan mahiyetteki iki metin, “Yönetmeliğin Ekleri” ve “Maden Atıkları Yönetmeliğinin Uygulanmasına İlişkin Açıklamalar” incelendiğinde, AMD’nin (bir yerde ‘asit kaya drenajı’ olarak ifade edilmiş), sülfür (S^{2-}) içeren atıklarda oluşabileceği değerlendirilmesinin yapıldığı anlaşılmaktadır. Bu yargı, Ek- 3 ve Ek- 4’te açık biçimde ifade edilmektedir. Ek- 4’te, “İnert Maden Atıklarının Belirlenmesi” başlığı altında, izlenecek yol için bir algoritma verilmişse de atıkların asit üretme potansiyellerinin belirlenmesinde uygulanacak yöntemler için bilgilendirme,

“Maden Atıkları Yönetmeliğinin Uygulanmasına İlişkin Açıklamalar” metninin, “Maden Atıklarının Karakterizasyonu ve Maden Atığı Bertaraf Tesislerinin Sınıflandırılması ile İlgili Açıklamalar” kısmında yapılmaktadır. Madde 3, aynen şöyle kaleme alınmıştır: “Maden atıklarının karakterizasyonunda öncelikle sülfür-sülfür (ASTM E1915, EPA 600, CEN-EN 14582) miktarına bağlı olarak asit üretme potansiyeli belirlenir. Atığın sülfür-sülfür (S^{-2}) miktarı %0,1’in üzerinde ise statik test yapılır (pr en 15875, ABA, SOBEK, Modifiye SOBEK). Bu testin sonucuna göre NP/AP<1 ise asit üreten tehlikeli maden atığı olarak sınıflandırılır ve atık karakterizasyonu sonlandırılır. NP/AP>3 ise asit üretmeyen maden atığı olarak tanımlanır.”

Yönetmelik ve tamamlayıcı metinler, AMD yönünden bazı eksiklikler ve çelişkili hükümler barındırmaktadır. Kavram, algoritma ve statik test yöntemleri hakkındaki değerlendirme ve yorumlama, “Yönetmeliğin AMD Yönünden Değerlendirilmesi” bölümünde ele alınacaktır. Ancak bunun için öncelikle statik test yöntemlerini, genel hatlarıyla ele almak gerekir.

AMD KAVRAMI

Sülfürlü maden sahalarında, metal sülfürler, nemli koşullarda havayla temas ettiklerinde oksitlenirler. Ardından, bir dizi kimyasal tepkime (1, 2, 3 ve 4) meydana gelir ve açığa çıkan H^+ , ortamdaki suların asitliğini yükseltir. Süreci tetikleyen mineraller demir sülfürlerdir. Genellikle, düşen pH ile birlikte, bakteriler (thiobacillus gibi) sürece dâhil olup, katalizör etkisi yaparak, tepkimelerin hızını arttırırken, tepkimeler biyo- kimyasal nitelik de kazanır.



Oluşan asidik drenaj (AMD), potansiyel zehirli maddeleri (metaller, iyonlar, askıda katılar gibi) kimyasal, fiziksel ve biyo-kimyasal süreçle bünyesine alır. Önlem alınmadığında, kirlenmiş drenaj, karıştığı sulardaki canlıları doğrudan, ilişkideki eko-sistemi ve sonuçta insanları dolaylı biçimde etkiler. Sürekliliği, yaygınlığı, hareketliliği ve sorunu gidermenin yüksek maliyeti (Karadeniz, 2011), AMD oluşma potansiyelinin, madencilik faaliyetlerinin başlamasından önce saptanmasını elzem kılar.

Maden sahalarının asit üretebilirliğinin kestiriminde, öteden beri, çeşitli yöntemler kullanılmaktadır. Bunlar; jeokimyasal statik ve jeokimyasal dinamik (kinetik) testler, jeokimyasal ve jeostatistiksel modellemeler, özütlenme (leaching) testleri olarak sayılabilir. Saha ve laboratuvarında elde edilen verilerin, benzer başka sahalara ait verilerle karşılaştırılması ve yorumlanması da yapılabilecekler arasındadır. Belirsizlikler içermelerine karşın, jeokimyasal statik yöntemlere, basitlikleri, çabuk sonuç vermeleri, yönlendirici ve düşük maliyetli olmalarından dolayı sıklıkla başvurulmaktadır. Statik yöntemler arasında en yaygın kullanılanı, ABA (Acid- Base Accounting) testleridir. Ancak kömür madeni artıkları için önerilen standart ABA’dan başlayarak, zaman içinde, farklı ABA testleri tasarlanmıştır. Esasen, numunedeki sülfürün, kimyasal analizle bulunup hesaplama yoluyla AÜP’nin ve test ile de oluşacak asidi nötrleştirme potansiyelinin (NP- özellikle Avustralya literatüründe asit nötrleştirme kapasitesi- ANC olarak ifade edilir) ölçüldüğü testlerdir. Bunlar, B. C. Araştırma Başlangıç testi (BCAB- British Columbia Research Initial test), Alkali Üretim Potansiyeli: Sülfür Oranı testi, modifiye ABA ve NP (pH6) testidir. Ayrıca, farklı coğrafik, jeolojik ve mineralojik şartlarda, 1970’lerden itibaren devam eden araştırmalarda, adı geçen yöntemler üzerinde, geniş bir literatürü kapsayan çok sayıda değişiklik önerileri sunulmuştur.

ABA'dan ayrı olarak, temel ilkeleri farklı olan diğer bazı testler de kullanılmaktadır. Numunenin saf veya deiyonize suyla karıştırılıp doğrudan pH'nın ölçülerek asit oluşumu olup olmadığını tayine yönelik Çamur pH'ı (Sobek et al., 1978; Page et al., 1982; Price, 1997), en basit testtir. ABA testlerinin bir alt kümesi olarak nitelenen Net Asit Üretme (NAP- Net Acid Production) (Coastech Research Inc., 1989) ve Net Asit Oluşturma (NAG- Net Acid Generation) (Sobek et al., 1978; Miller et al., 1990; O'shay et al., 1990; Stewart, 2006) testleri, hidrojen peroksidin (H_2O_2) demir sülfür minerallerini hızlı oksitlemesine dayanır. ANC'ye alternatif olarak geliştirilen, Asit Tamponlama Karakteristiği Eğrisi (ABCC- Acid Buffering Characteristics Curve) (Miller ve Jeffery, 1995), numunenin yavaş titrasyonunu ve bu esnada pH değerlerinin sürekli izlenmesini içeren bir testtir.

Geliştirilen birçok yönteme ve kimi zaafalarına karşın, dünya genelinde ABA yöntemleri daha fazla kabul görmektedir.

JEOKİMYASAL STATİK TESTLER

ABA Testleri

ABA Kavramının Ortaya Çıkışı ve Gelişimi

Yerkabuğunun bileşiminin tahmin edilmesine dönük çalışmalar göstermiştir ki, yerkabuğunda, reaktif hâlde bulunan katyonik elementlerin (Ca, Mg, K ve Na gibi) oranı, anyonik veya asit üreten elementlere (S, Cl, F ve P gibi) kıyasla, daha yüksektir. Fe, Al, Si ve O dâhil, bol bulunan diğer elementlerin çözünürlükleri zayıf veya tepkime eğilimleri görece düşüktür. Asitlik veya alkalinite üzerindeki etkileri de ikincil derecededir. Bundan dolayı, kayaç içindeki baskın elementin, o kayacın gelecekte asit üretip üretmeyeceğini tayin edeceği düşünülmüştür (Skousen et al., 1996). AMD kavramının temeli bu düşüncedir.

Başlangıçta, maden artık yığınları için sınıflama yapılmış, kayaç ve asitlik dercesine dayalı üç tür malzeme tanımlanmıştır (Skousen et al., 1996: Smith ve Tyner, 1945'den). Bu sınıflandırma, yığındaki $CaCO_3$ 'ün yüzdesini pozitif, SO_4 'ün yüzdesini negatif altsimge sayılarla ifade ederek, bir adım ileri götürülmüştür (Knabe, 1964). Sonrasında, Knabe (1973), tüm asitlere, asit üreten minerallere (sülfidler) ve katyonların değişim kapasitesine karşı, tüm bazların toplamını dengeleyen ve "baz- asit dengesi" adını verdiği bir yöntem kullanmıştır. Kayaç rengi, sertliği, çizgi rengi, pürüzlülüğü, seyreltik HCl'de tepkimesi gibi parametrelerle her bir katmanın tanımlanmasını; pH, toplam veya piritik sülfür ve NP ölçümüyle, katmanların toksisitesinin belirlenmesini de içeren, ayrıntılı bir ABA açıklaması, ilk kez 1973'de yapılmıştır (Grube et al., 1973). Ardından ABA, Smith et al. (1974) tarafından geliştirilmiş ve kömür örtü malzemelerinin sınıflandırılmasına yönelik kullanışlı bir yöntem olarak sunulmuştur. Nihayet 1978'de, ABA yöntemi üzerinde bazı değişiklikler yapılarak (standart ABA), saha ve laboratuvar araştırmaları için işlem süreçleri yayımlanmıştır (Sobek et al., 1978).

Standart ABA

Kömür sahaları için geliştirilen, ama sonraki yıllarla beraber, metal madenlerine de uygulanan standart ABA'da, AÜP, basit bir eşitlikle (Eşitlik 5) bulunur.

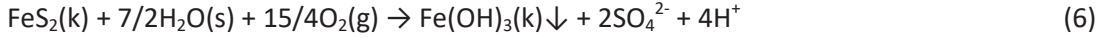
$$AÜP = \%S * 31,25 \text{ t } CaCO_3 \text{ eşdeğeri} / 1.000 \text{ t} \quad (5)$$

Bu eşitlik, arkasında mineralojiyi, tepkime süreçlerini ve yerel koşulları içeren, bir dizi kabulü barındırır (Morin ve Hutt, 1997):

1. Numunedeki tüm sülfür, sülfid (S_2^{2-}) hâindedir ve kaynağı pirittir.
2. Tüm sülfür oksitlenir ve sülfata (SO_4^{2-}) dönüşür.

3. Oksitleyiciler, sadece su ve oksijendir (O₂).
4. Pirit oksitlendiğinde, demir (Fe²⁺) de Fe³⁺'e yükseltgenir.
5. Tüm demir, Fe(OH)₃ hâlinde çökelir.

Kabullerin dayanağı da ortama H⁺ sağlayan ve açığa çıkan H⁺'i tüketen iki kimyasal tepkimedir.



İşte, hesaplamada, üstteki eşitlikten de görülebileceği üzere, Σ sülfür dikkate alınır. Öte yandan, (6) ve (7) numaralı tepkimeler uyarınca; 2 mol CaCO₃(200 g), 1 mol FeS₂'nin (64 g) üreteceği asidi nötrleştirecektir. Özetle; %1 sülfür içeren 1.000 t kayayı nötrleştirmek için, 31,25 t CaCO₃ gerekecektir. Bu dayanaktan hareketle, Σ kükürt yüzdesi 31,25 ile çarpılarak AÜP elde edilir.

NP'nin kaynağı karbonatlar, özellikle de CaCO₃ ve MgCO₃'tür. NP'yi belirlemek için, hacmi ve derişimi fışirdama testi (fizz rating) ile (Sobek et al., 1978) saptanan HCl asit, -250 µm tane boyutundaki numuneye eklenip, tepkime duruncaya kadar kaynatıldıktan sonra, soğutulan çözelti, son pH 7 olacak şekilde NaOH ile geriye titre edilip, test tamamlandığında, tüketilen NaOH ve HCl miktarlarından, numunenin NP'i hesaplanır.

Modifiye ABA

Coastech Research Inc. (1989) tarafından geliştirilip, ayrıntılarını Lawrence'ın (1990) verdiği modifiye ABA'da, sülfatların (jips, barit gibi) asit üretmediği, o nedenle, AÜP hesabında dikkate alınmamaları gerektiği vurgulanmıştır. Sadece sülfitlerin ve ayrıca, test öncesinde numunede, sülfitlerin oksitlenmesiyle oluşmuş sülfat varlığı söz konusuysa, bunların, kolayca hidrolize olabilen oksitlenme ürünü olmaları dolayısıyla, AMD'ye katkıları olacağından, değerlendirmeye alınmaları gerektiği belirtilmiştir. NP'nin fazla tahmin edilme olasılığını azaltmak için; a) tane boyutu %80 -75 µm'ye indirilen numunenin, düşük sıcaklıkta (25- 35 °C) ve 24 saat süreyle HCl ile muamele edilmesi, b)- asidin kademeli ilâvesiyle, süreç tamamlandığında, çözelti pH'ının 1,5- 2,0 aralığında tutulması önerilmiştir. Geriye titrasyonda, son pH, 7,0 yerine, duraylılığı (stabilite) daha iyi olan pH 8,3 kullanılmıştır. pH 8,3, asitlik titrasyonlarında alışlageldik nokta olup, karbonik asidin, en baskın zayıf asit olduğu doğal sulardaki karbonat/bikarbonat için stokiyometrik denklik noktasına karşılık gelmektedir (Lawrence, 1990; Lawrence ve Wang, 1996).

Sonrasında, standart ABA yönteminde, NP değerinin, kullanılan asit miktarına bağlı olduğuna, daha yüksek fışirdama derecesinin, yüksek NP sonucunu doğuracağına, bu testin sübjektifliğine işaret edilerek, numunenin fışirdama testinde vereceği tepkiye göre, asit şiddeti ve miktarında değişiklik yapılmıştır. Fazladan NP tahminini engellemek için, asidin kademeli eklenmesi, asitleme işlemi sonunda pH'ın 2,0- 2,5 arasında tutulması önerilmiştir (Wang, 1998; Lawrence ve Wang, 1997).

British Columbia Araştırma Başlangıç Testi (BCAB)

Duncan ve Bruynesteyn (1979) tarafından geliştirilen yöntem, AÜP hesaplamasında standart ABA ile bire bir aynı olmasına karşın, NP tayininde, standart ABA'dan ayrışır. Kullanılan asit, terminoloji ve nicelik birimleri farklıdır. Fışirdama testi, ısı işlem ve bir bazla geriye titrasyon yoktur. Öğütülüp, %70 - 44 µm boyutuna indirilen numune saf su eklenip karıştırılır. Sonrasında çözelti, pH, 3,5'te sabitleninceye kadar H₂SO₄ ile titre edilir. pH'ın 3,5 seçilme nedeni, bu değer, oksitleyici biyolojik etkinlik sınırını temsil ettiği düşüncesidir. Tüketilen asit miktarından NP hesaplanır.

NP (pH6) testi

Genel olarak uygulanan su niteliği standardının pH 6,0 olduğu gerekçesiyle, BCAB testi işlem sürecinde, son pH, 6,0 olarak değiştirilmiştir ki, bu iki test arasındaki tek farktır (Lapakko, 1994). NP (pH6) testinin, asit etkinliğinin, asidik ortamdan ziyade, pH 6,0 civarında olduğu, bunun da testi diğerlerinden kayda değer ölçüde ayırdığı ifade edilmektedir (White et al., 1999).

AÜP'nin kestiriminde, Lapakko'nun (1994) önerisinden farklı olarak, maden artığının depolandığı tane boyutunda değişiklik yapmaksızın kimyasal analiz yapılması ve sülfürün, asitte çözünür sülfür üzerinden belirlenmesi gerektiği savunulmuştur (Karadeniz, 2011). NP belirlenirken, H₂SO₄ asit ilâvelerinin ardından çözeltinin karıştırılması, çözeltinin pH'ı 6,0'da sabitlendiğinde, beherin 70°C sıcaklıktaki su banyosuna alınıp, gaz çıkışı ya da kabarcıklanma sona erene kadar bekletilmesi, bu aşama sonrasında pH yükselme eğilimi gösterirse, pH sabitleninceye değin, asit ilâvesinin sürmesi önerilmiştir. Ayrıca, NP testlerine sokulan numunelerin tane boyutunun depolama boyutu ile aynı olması gerektiği savunulmuştur (Karadeniz, 2011).

Modifiye NP (pH6) testi

Maden atığı numunesi, eser miktarda Ca ve/veya Mg karbonat içeriyorsa ya da içerdiği karbonatlar, ağırlıklı olarak siderit (FeCO₃), ankerit [Ca(Fe,Mg,Mn)(CO₃)₂] gibi demir karbonat ise, NP (pH6) yöntemi için bir değişiklik gerekir. Çünkü BCAB ve NP (pH6) yöntemlerindeki titrasyon uygulandığında, titrantın ilâve ilk damlasıyla, son pH'nın aşılması söz konusudur. Sorunu gidermek için; katı numune, 6 ilâ 8 adet beherlere alınıp deiyonize su eklenir. Birinci beher H₂SO₄ ilâvesi yapılmazken, diğerlerinin her birine, sırasıyla, artan hacimde ilâve yapılır. Tüm beherler, karıştırıcı yardımıyla çalkalanır. Belli aralıklarla çalkalamaya ara verilip, çözeltilerin pH'ları ölçülür. Ölçülen pH değerleri H⁺ konsantrasyonuna çevrilir. Her bir numune için, pH 6'yı temsil eden H⁺ konsantrasyonu ve ona karşılık gelen asit hacmi, ara kestirimle (enterpolasyon) bulunur. pH 6'da kestirilen asit hacmi, CaCO₃ eşdeğeri NP'ye çevrilir. Bu, "etkin" NP'dir (White et al., 1999).

Avrupa Birliği- EN 15875 Test Standardı

EN 15875, Avrupa Birliği'nde standart olarak kabul edilen bir ABA yöntemidir. Avrupa Standardizasyon Komitesi, hem AÜP, hem de NP'nin belirlenmesinde, kimi değişiklikler yapmıştır (Technical Committee, 2011). AÜP hesaplanırken, toplam sülfüre veya sülfid sülfürüne dayanılabileceği; burada, numunenin mineralojik yapısının belirleyici olduğu ifade edilmiştir.

Esas itibarıyla modifiye ABA ile uyumlu EN 15875'de, NP'nin belirlendiği, işlem süreciyle ilgili olarak; testte, numune tane boyutu (%95 -125 µm) ile birlikte, asit hacim ve şiddetinin tayini gibi birincil, ortam sıcaklığının 20±5 °C olması, demineralize su kullanılması gibi ikincil değişikliklere gidilmiştir. Asitlemede kullanılacak asidin hacmini tayin için de fışrdama testi yerine, numunenin karbonat içeriği esas alınmıştır (Technical Committee CEN/TC 292, 2011).

Alkali Üretme Potansiyeli: Sülfür Oranı Testi

Yöntem, Caruccio et al. (1981) tarafından, kömür atıklarının AÜP'ni ölçmek için geliştirilmiş, Coastech Research Inc. (1989) tarafından da modifiye edilmiştir. Numunenin AÜP'i, standart ABA'da olduğu gibi, toplam sülfür dikkate alınarak belirlenir. Alkali üretme potansiyeli, numunenin -23 µm boyutuna öğütülmesinden sonra, oda sıcaklığında HCl asit ile muamele edilip belirli süre beklendikten sonra, son pH 5,0 olacak şekilde geriye titre edilerek saptanır.

ABA Haricindeki Testler

Çamur pH'ı

Ne zaman ve kim tarafından geliştirildiği tartışma konusu olan bir yöntemdir (Karadeniz, 2011). Bir numunenin hazır asitliğini- alkaliliğini tayin etmekte kullanılan, görece hızlı, basit bir testtir. Yalnızca, çözünür tuzlar ve tepkime eğilimi yüksek mineraller sürece etkiyebilir. Numune, genellikle -1 mm tane boyutuna indirildikten sonra, damıtık su ile işleme sokulur. Belirli bir süre beklenip, çamurun pH'ı ve iletkenliği ölçülür.

Net Asit Üretme (Net Acid Generation- NAG veya NAP)

NAG testi, numunedeki demir süflürlerin güçlü bir oksitleyici olan H_2O_2 vasıtasıyla hızla oksitlenmesine dayanan bir yöntemdir (Lawrence et al., 1988). Süflürler oksitlenince, ortam asitleşir, asidik ortam da nötrleştirici mineralleri çözer. Böylelikle, numunenin asit üretme ve nötrleştirme potansiyeli doğrudan ölçülebilir. Bu yöntemde, süflür tayinine gerek duyulmaz. Öğütölüp -75 μm boyutuna indirilen numune, H_2O_2 ile muamele edilir ve tepkimeler bittiğinden emin olunduktan sonra belirli bir süre (gece boyu) beklenir. Ardından, pH'ı ölçölüp kaydedilen çözelti, son pH önce 4,5 sonra 7,0 olacak şekilde NaOH ile titre edilir (Stewart et al., 2006). Tüketilen NaOH hacmi ve molaritesinden, net asit üretme potansiyeli hesaplanır.

NAG testi için, oksitlemenin yetersiz olabileceği durumlar göz önüne alınarak, ardışık NAG (Sequential NAG) testi önerilmiştir. Test, tek bir H_2O_2 ilâvesi şeklinde değil, NAG pH $\geq 4,5$ 'e ulaşınca kadar tekrarlanır. Hesaplama, her tekrarda kullanılan NaOH hacmi toplanarak, hesap yapılır.

Statik Test Sonuçlarının Değerlendirilmesi- Yorumlanması

AÜP ve NP bulununca, geriye, iki değer arasındaki oranın ya da farkın hesaplanacağı, bir aritmetik işlem yapılması kalmış gibi görünür. Ancak, kömür ya da süflürlü maden sahalarında, AMD kestirimi için sayısız çalışma yapılmış, genel yorumlara ulaşmaya çalışılmıştır. Sonuçta, maden yataklarının ve buldukları coğrafyanın, çoğunlukla, kendine özgü olması nedeniyle, yorumlamaların da buna göre ve karşılaştırmalı yapılmasının daha doğru olacağı görölmüştür. Bununla beraber, önerilen bazı kıstaslar Çizelge 1'de verilmiştir.

Bu kıstaslar arasında, Brodie et al. (1991) tarafından önerilen, en yaygın kabul görendir. Burada, NP/AÜP<1 ise, numune asit üretir; 1<NP/AÜP<3 ise, numune belirsizlik aralığındadır ve kinetik testlerin yapılması gerekir ve nihayet, NP/AÜP>3 ise de numune asit üretmez şeklinde değerlendirilir.

Statik Testlerde Hata Kaynakları

Aynı sahaya ait numunelerin AÜP ve NP'i farklı statik testlerle bulunması doğrultusunda yapılan çalışmalar, çoğu zaman, birbirlerini doğrulamayan, tutarsız sonuçlara ulaşıldığını göstermektedir. Kuşkusuz ilk akla gelen sebep, sahadan alınan numunelerin temsiliyeti ya da doğru bölünmemiş olma olasılığıdır. Yine, laboratuvarlarda testleri yürüten kişiye bağlı hatalarla karşılaşılması da olağandır. Bu aşamalarda bir hata yapılmamışsa bile, yine de farklı sonuçlar bulunabilmektedir. Yöntemlerin işlem süreçleri, en başında yapılan kimi kabullere dayalı olduğundan ve kabuller her sahada geçerli olamadığından, durum, doğal olarak sonuçlara yansımaktadır.

AÜP: Başta standart ABA olmak üzere, bir kısım ABA yönteminde, numunedeki süflürün tamamının çözüneceği kabul edilir. Ancak barit ($BaSO_4$), jips ($CaSO_4 \cdot 2H_2O$), anhidrit ($CaSO_4$), epsomit ($MgSO_4 \cdot 7H_2O$) gibi sülfat mineralleri asit üretmez. Numune bu mineralleri içeriyorsa, bulunacak AÜP değeri gerçeğin üzerinde olacaktır. Modifiye ABA gibi, testten önce, süflitlerin oksitlenmesiyle oluşmuş

sülfatlar dışındaki sülfatların asit üretmediğini kabul ederken, brokantit (Cu₄SO₄(OH)₆), alunit (KAl₃(SO₄)₂(OH)₆), jarosit [KFe₃(SO₄)₂(OH)₆] ve melanterit (FeSO₄·7H₂O) gibi sülfatlar, çözüldüklerinde asit üretirler. Dolayısıyla, teste tâbi tutulan numunedeki çözünebilir sülfatlar hesaba katılmaksızın bulunacak AÜP, gerçek değerinde olacaktır.

Ayrıca, organik S, kimyasal tepkimeye girmeye eğilimli değildir. O nedenle, organik S ya asit oluşumuna etki etmez veya etkisi ihmal edilebilecek denli düşüktür.

Çizelge 1. ABH testi yapılan numuneler için, net nötrleştirme potansiyeli (NNP) (% CaCO₃) veya NP/AÜP bazında AÜP'nin yorumlanması (White et al., 1999)

ABH	Asit	Belirsiz	Asit Değil
<u>NNP veya (NP-AÜP)</u>			
Appalachian Kömür-Madeni ¹ Kıstası	< -5	k/b	k/b
B. C. Metal-Madeni Kıstası ²	≤ 0	k/b	k/b
Ferguson, Morin, 1991	k/b	-20<NNP<+20	k/b
Day, 1989	<+10	k/b	k/b
<u>NP/AÜP</u>			
Brodie et al., 1991	< 1	1<NP/AÜP<3	> 3
Morin and Hutt, 1994	< 1	1<NP/AÜP<1,3 – 4,0	> 1.3 – 4,0

¹Sobek et al., 1978

²Ferguson and Morin, 1991

* k/b kaynakta belirtilmemiş

NP: ABA testlerinde, işlem süreçlerine ilişkin değişiklik önerileri, büyük ölçüde, NP üzerine yoğunlaşmıştır. Üstelik S oranı, analizlere dayalı iken, NP değeri laboratuvarında test yapılarak belirlenir. Bu yüzden, yöntemler arasındaki asıl farklılık, NP değerinin tespitinde ortaya çıkar (Şekil 1 ve Çizelge 2).

NP'nin hesapla bulunmasına ilişkin öneriler de yapılmıştır. Maden atığında sadece kalsiyum ve magnezyum karbonatın, pH seviyesini 6,0 civarında tamponlayacağı varsayılarak, numunenin mineralojisine bağlı "MinNP" kullanılmış, bunun için aşağıdaki eşitlik (Eşitlik 8) verilmiştir (Lapakko, 1992).

$$\text{MinNP} = 10 * (\% \text{CaCO}_3) + 11,9 * (\% \text{MgCO}_3) \text{ kg / t CaCO}_3 \quad (8)$$

Hızlı çözünen kalsiyum bazlı karbonat minerallerinin, asitliğini hızla nötrleştireceği ve tüm karbonun karbonatlardan geldiği kabulüyle, karbonat NP (KaNP) hesaplanabileceği ifade edilmiştir (Morin ve Hutt, 1997). Bunun için verilen eşitlik (Eşitlik 9);

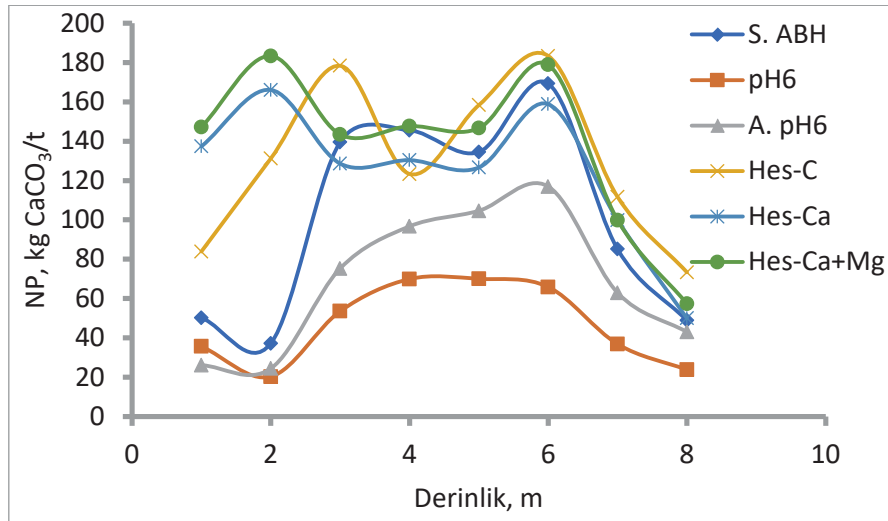
$$\text{KaNP} = 83,3 * (\% \text{C}) \text{ kg / t CaCO}_3 \text{ veya } \text{KaNP} = 22,7 * (\% \text{CO}_2) \text{ kg / t CaCO}_3 \quad (9)$$

Paktunç (1999) da asit üreten ve tüketen bileşenler arasındaki dengenin belirlenmesinde, örneklerin mineralojik bileşimine dayalı, ayrıca diğer sülfidlerin ve birden fazla nötrleştirici mineral türünün varlığının dikkate alındığı yeni bir yaklaşım önermiştir (Eşitlik 10).

$$YNP = \sum_{x=1}^k \frac{W_a \times X_i \times 10}{n_{M,i} \times W_i} \tag{10}$$

Burada; YNP: yığın nötrleştirme potansiyeli, kg H₂SO₄/t, k: nötrleştirici minerallerin sayısı, W_a: H₂SO₄'ün moleküler ağırlığı, (g/mol), X_i: i mineralinin miktarı, % ağırlık, n_{M,i}: stokiyometrik faktör, (1 mol H₂SO₄'ü tüketmek için gereken nötrleştirici mineralin mol değeri) ve W_i: nötrleştirici i mineralinin g/mol olarak moleküler ağırlığıdır.

NP, kimyasal ve mineralojik analiz sonuçlarına dayalı hesaplama ile belirlenmesi, AÜP hesabında olduğu gibi, minerallerin tümünden çözüneceği kabulüne dayanır.



Şekil 1. Balıkesir- Balya maden sahası büyük yığın sondaj numunelerinin NP değerlerinin farklı yöntemlere göre, derinlikle değişimi (Karadeniz, 2011)

Çizelge 2. Hidrotermal kuvars- karbonat içeren altın artıklarının farklı yöntemlerle belirlenen NP değerlerinin mukayesesi- çizelge kısaltılmıştır (White et al., 1999)

Numune	NP, kg/t CaCO ₃		
	Standart ABA	Modifiye ABA	CaCO ₃ + MgCO ₃
1 (T1)	230	200	207
2 (T3)	195	130	163
3 (T5)	98	92	65
4 (T7)	270	220	229
5 (T9)	18	16	14

NP testlerinde ise, kimyasal çözündürme, fiili bir durumdur. Yönteme bağlı olarak, çeşitli işlem basamaklarından oluşur, dolayısıyla fazla sayıda, hataya açık değişken (protocol variables) mevcuttur. Bunlar, maden artığının tane boyutu, kullanılan asit, asidin miktarı ve derişimi, ortam sıcaklığı, asitle muamele süresi ve eğer çözeltiliye, geri-titrasyon uygulanacaksa, son pH'tır.

Tane boyutu: ABA yöntemlerine göz atıldığında, test yapılırken numunelerin tane boyutunun - 250 µm ile -23 µm arasında değiştiği görülür. Tesadüfen denk gelmiyorsa, test uygulama boyutu, maden artığının depolama boyutundan farklıdır. Malzemenin tane boyutu küçüldükçe yüzey alanı artarak, kimyasal tepkimelerin hızına etki eder. Diğer yandan, artığın depolandığı tane boyutunun altına öğütülerek test edilmesi hâlinde, yığın içinde kimyasal tepkimeye girme olasılığı hiç olmayabilecekken (örneğin, çözünmeyen bir silis tanesinin içinde hapis konumu), öğütme sayesinde yeni yüzeyler açılacağından, tepkimeye de girmesi mümkün kılınmış olur. Doğru tane boyutu, o yüzden, artığın depolandığı boyuttur.

Asit türü: NP belirlenirken, karbonatları çözdüğü için, çoğunlukla, HCl asit kullanılır. BCAB ve NP(pH6) gibi az sayıda testte ise H₂SO₄ asit tercih edilir. Öte yandan, minerallerin, farklı asitler içindeki tepkime kinetikleri ve tepkime ürünleri aynı değildir. Maden sahalarında, asidik drenaj geliştiğinde, demir sülfürlerin çözünmesiyle H₂SO₄ asit oluşur. Örneğin, hidratlanmış üç değerlikli demir oksitin farklı asitlerde çözünme hızının sırasıyla HF > HCl > H₂SO₄ > HClO₄ olduğu, bu sıralamanın, anyonlarla Fe⁺³ iyonları arasında oluşturulan karmaşıkların azalan kararlılık sırasına uyduğu belirtilmektedir (Burkin, 1965). Pirotinin ise, H₂SO₄'e kıyasla HCl'de daha fazla çözünür olduğuna işaret edilmektedir (White et al., 1999). O nedenle, esasen testlerde H₂SO₄ asit kullanılması doğrusudur.

Asit miktarı ve derişimi: Numune, asit ile muamele edildiğinde, kullanılan asidin miktarı ve derişimi, ortam pH'ını doğrudan etkilediğinden, minerallerin çözünme hızlarına da etkisi olur. Gerekenden fazla derişimde ve miktarda asit kullanıldığında, NP değeri olması gerekenin üzerinde ya da yetersiz derişimde ve miktarda asit eklenirse de NP değeri olması gerekenden düşük bulunabilir.

Sıcaklık: Arrhenius denkleminde bilinir ki, ortam sıcaklığının artmasıyla, tepkime hızları, genelde artar. ABA testlerinde, farklı sıcaklık uygulamaları vardır. Bunun da farklı sonuçlar doğuracağı açıktır. Ayrıca, (1) numaralı tepkimeden görüleceği üzere, tepkime ekzotermiktir ve ısı açığa çıkmaktadır. Lefebvre et al. (2001), piritin oksitlenme sürecinde her mol için 1.409 kJ ısı açığa çıktığı ve bu ısının, atık kaya yığınlarında sıcaklığı 70°C'a kadar çıkardığı belirtilmiştir. Bu bakımdan, testlerin bu sıcaklığa uygun ortamda gerçekleştirilmesi gerekir.

Süre: NP belirlenirken, asitle muamele süresi genellikle sabittir, ama yöntemden yönteme değişkenlik gösterir. Oysa numunelerin mineralojik bileşim ve yapıları, tepkime süresini doğrudan etkiler. Her numuneye aynı şekilde uygulanan süre, bazıları için yeterli olabilirken, başkaları için yetersiz kalabilir. Bu durumda, belirlenen NP değeri, gerçek değerinin altında bulunabilir.

Nötrleştirme tepkimelerinde başlıca mineraller, şüphesiz karbonatlardır ve karbonat mineralleri, çoğunlukla, hızlı çözünürler. NP değerini göz ardı edilemeyecek oranda etkileyebilen silikatlar arasında görece hızlı çözünebilirler varsa bile, genelde yavaş çözünürler. O nedenle, süre uygulamalarında da maden yatağının mineralojik özelliklerinin göz önünde bulundurulması, hataların azaltılması bakımından önem taşır.

Geriye- titrasyon: BCAB ve NP (pH6) testlerinde geriye- titrasyon uygulanmaz. Standart ABA, modifiye ABA ve EN 15875 yöntemlerinde, nötrleştiricilerin parçalanmasını takiben, kalan asit miktarını saptamak amacıyla geriye- titrasyon uygulanır. Bu uygulamada son pH, standart ABA'da 7,0, diğerlerinde ise, 8,3'tür. pH 7,0, nötr ortam olarak değerlendirilmesine karşın, bu çözeltilerde, hâlâ bir miktar asitlik vardır. Geriye- titrasyonda son pH 7,0'da ölçülen NP değeri, pH 8,3'e göre, 20 ilâ 30 kg/t CaCO₃ daha yüksektir (White et al., 1999).

YÖNETMELİĞİN AMD YÖNÜNDEN DEĞERLENDİRİLMESİ

“Maden Atıkları Yönetmeliği” ile beraber, onu tamamlayan diğer iki metin, asidik drenaj kavramları bakımından irdelendiğinde, “asit maden drenajı” ve “asit kaya drenajı” ifadelerinin aynı anlamda kullanıldığı anlaşılmaktadır. Esasen doğrudur, zira literatürde, bu ikisinin birbirleri yerine kullanıldığı bilinmektedir. Diğer taraftan, madencilik faaliyetleri dışında da asidik drenaja rastlanabilmektedir.

Demir sülfür içeren cevher oluşumları, yeryüzüne yakın seviyelerde yatakladıklarında, yüzeyleri atmosfere açıksa, oksijen ve nem etkisiyle, tamamen doğal oksitlenme tepkimeleri gelişir. Bu aşamayı çözünme, ardından da ikincil minerallerin meydana gelmesi ve çökelmeleri izler. Demir şapka (gossan) oluşur (Downing ve Mills, 2000). Yüzey suları, demir şapka ile temas ettiğinde asidik drenajlar gelişir.

Derin kazılar gerektiren büyük mühendislik yapılarının inşaa faaliyetlerinde, demir sülfürlerin bulunduğu bir formasyonun yüzeyi açılırsa, yüzey akıntıları, asidik drenaja neden olabilmektedir (örnek, Halifax, Nova Scotia Airport- Kanada) (Skousen, 1996). Bu iki olgunun madencilik faaliyeti ile ilgisi olmadığından, asit maden değil, asit kaya drenajı olarak adlandırılması daha doğru olacaktır.

İkinci nokta, “Maden Atıkları Yönetmeliğinin Uygulanmasına İlişkin Açıklamalar” metninin Ç Maddesi’nin 2. Bendi’nde, “Okistli- karbonatlı cevherler dışında kalan sülfürlü cevherlerin (bakır, kurşun ve çinko madenleri ile bunları ihtiva eden pirit, pirotin, sfalerit, galen vb. ile kompleks cevherlerin) zenginleştirilmesinden kaynaklanan atıklar...” ifadesinin, kömür yataklarını kapsamadığı, hatta üç metinden hiçbirinde, “kömür ya da linyit” sözcüklerinin geçmediği görülmektedir. Oysa, geliştirilen ilk test yöntemi olan standart ABA’da çalışılan malzeme, ABD’de, Appalachia Bölgesi kömür sahalarından (coal overburden and minesoils) temin edilmiştir (Sobek et al., 1978)

Üçüncüsü, “ABA” terimi ile ilgilidir. Yine, Ç Maddesi’nin 3. Bendi’nde, “... Atığın sülfid-sülfür (S^{-2}) miktarı %0,1’in üzerinde ise statik test yapılır (pr en 15875, ABA, SOBEK, Modifiye SOBEK) ...” cümlesine yer verilmiştir. Bu cümle, birden fazla yanlış içermektedir. Parantez içinde verilen statik yöntemlerin tümü (‘pr en 15875’, kesin standarda dönüştürülerek ‘EN 15875’ olmuştur), ABA yöntemleridir. Standart ABA, literatürde ‘Sobek’ ve ‘EPA 600 ABA’ adlarıyla da anılır.

Bu cümlenin, algoritma bakımından da yanlışı vardır, çünkü başta standart ABA olmak üzere, birkaç ABA yönteminde, AÜP hesaplamasında, sadece S^{-2} değil, numunedeki (maden artığındaki) tüm sülfür, yani SO_4 da dikkate alınır. Dolayısıyla, cümle kendi içinde çelişki barındırır.

SONUÇ

AMD kestiriminde, 40 yılı aşkın bir süredir kullanılagelen statik testler, ABA ya da diğerleri, bazı kabuller üzerine kuruludur. Ancak AMD denilen olgu, oluşum ve gelişim bakımlarından, sadece maden yatağının kendi koşullarına değil, aynı zamanda, bulunduğu yerin coğrafi şartlarına, dolayısıyla, birçok paraparametreye bağlıdır (Karadeniz, 2008). Kabuller, sahaya özgü koşullarla uyuşmadığında ki, sıklıkla uyuşmaz, uygulanan yöntem yanıltıcı sonuçlar verebilir. O nedenle, yöntem tercihinde, başta maden yatağının mineralojik yapısı olmak üzere, yerel özelliklerin dikkate alınması zorunludur. Yanlış yöntem, AÜP ve NP’nin, gerçek değerlerinin üzerinde veya altında bir değer bulunmasına, bu da, alınacak tedbirlerin yetersizliğine ya da aşırı önlem dolayısıyla, gereğinden yüksek maliyete yol açabilir.

Yönetmelikte, maden artıklarının içerdiği sülfür olarak, sadece sülfidik sülfürün hesaba katılması, bazen doğru sonuç verse de bu, her zaman için geçerli olmaz.

Yönetmeliğin, birden fazla yöntemin uygulanabilmesine olanak sağlaması doğru bir yaklaşımdır, ama eksiktir. NAG gibi, diğer yöntemlerin de hâlihazırda yer verilenlere eklenmesi yerinde olur. Örneğin,

NAG yöntemi Avustralya’da kullanılmaktadır. Doğrusu, saha karakterizasyonunun başarılı yapılması ve sonrasında, yöntemin seçilmesi, gerekirse, birbirlerini doğrulamak üzere, birden fazla yöntemin uygulanmasıdır.

KAYNAKLAR

Brodie, M. J., Broughton, L. M., Robertson, A. (1991). A Conceptual Rock Classification System For Waste Management And A Laboratory Method For ARD Prediction From Rock Piles, In Proc. Second International Conference on the Abatement of Acidic Drainage. (pp. 119-135). Vol. 3., Montreal, Quebec, September 16-18, MEND Program (ed.), Quebec Mining Association, Ottawa.

Burkin, A.R. (1965). Hidrometalurjik süreçlerin kimyası, Utine, T. (Çev. 1988), TMMOB Maden Mühendisleri Odası Yayını, Net Ofset, Ankara.

Caruccio, F. T., Geidel, G., Pelletier, M. (1981). Occurrence And Prediction of Acid Drainages. *J. Energy Div. Amer. Soc. Civil Engineers*, 107, No. EYI, May.

Coastech Research Inc. (1989). Investigation Of Prediction Techniques for Acid Mine Drainage. MEND Project Report 1.16.1a, MEND, Ottawa, Ontario.

Day, S. J. (1989). Comments after presentation of: A Practical Approach To Testing For Acid Mine Drainage In The Mine Planning And Approval Process. Presented at the Thirteenth Annual British Columbia Mine Reclamation Symposium. (pp. 7-9). June 7-8. Vernon, British Columbia.

Downing, B. W. (2014). Acid–base accounting test procedures. Acid mine drainage, rock drainage, and acid sulfate soils: causes, assessment, prediction, prevention, and remediation, Editor(s): James A. Jacobs, Jay H. Lehr, Stephen M. Testa. 229-252.

Duncan, D. W. and Bruynesteyn, A. (1979). “Determination Of Acid Production Potential of Waste Materials, *Met. Soc. AIME*, paper A79-29, 10 p.

Ferguson, K. D. and Morin, K. A. (1991). The Prediction of Acid Rock Drainage - Lessons from the Data Base. In Proceedings of the Second International Conference on the Abatement of Acidic Drainage. (pp. 83-106). September 16-18. Montreal, Canada.

Grube, W. E., Smith, R. M., Singh, R. N., Sobek, A. A. (1973). “Characterization Of Coal Overburden Materials And Minesoiles In Advance Of Surface Mining”, In: Research and Applied Technology Symposium on Mined Land Reclamation. (pp. 134- 151). NCA/BCR, Pittsburg, PA.

Karadeniz, M. (2011). Balıkesir-Balya Kurşun-Çinko Madeni Flotasyon Artıklarının Asit Maden Drenajı Oluşum Potansiyelinin Derinlikle Değişiminin Araştırılması. Hacettepe Üniversitesi Fen Bilimleri Enstitüsü, Doktora Tezi, Ankara.

Knabe W. (1964). “A Visiting Scientist's Observations And Recommendations Concerning Strip-Mine Reclamation In Ohio”, *The Ohio Journal of Science*, 64(2), March, 132- 157.

Knabe, W. (1973). Development And Application of the ‘Domsdorf Ameliorative Treatment` on Toxic Spoil Banks Of Lignite Opencast Mines in Germany”, In: Jutnik, R. J. and Davis, G. (Eds.), Ecology and reclamation of devastated land. Vol: 2, Gordon and Breach Publishers, Inc., New York, NY. 273- 294.

Lapakko, K. A. (1992). Characterization And Static Testing Of Ten Gold Mine Tailings. In American Society for Surface Mining and Reclamation Meeting. (pp. 370- 384). Duluth- Minnesota.

Lapakko, K. A. (1994). Evaluation of Neutralization Potential Determinations for Metal Mine Waste and a Proposed Alternative. Proc. International Land Reclamation and Mine Drainage Conference, (pp. 129-137). Pittsburgh, USBM SP 06A-94.

Lawrence, R. W. and Wang, Y. (1997). Determination of Neutralization Potential in the Prediction of Acid Rock Drainage. Proceedings of Fourth International Conference on Acid Rock Drainage, (pp. 451-464). Volume I. Vancouver B. C. Canada.

Lawrence, R. W., and Wang, Y. (1996). Determination of Neutralization Potential for Acid Rock Drainage Prediction. Canadian Mend Report (89 p). Project, 1.16.3, for Hudson Bay Mining and Smelting and for Environment Canada.

Lawrence, R.W. (1990). Prediction of the Behavior of Mining and Processing Wastes in the Environment. In pro. Western Regional Symposium on Mining and Mineral Processing Wastes. (pp. 115-121). Doyle, F., (ed.), Soc. for Mining, Metallurgy and Exploration, Inc., Littleton, CO.

Lawrence, R.W., Jaffe, S. and Broughton, L.M. (1988). In-House Development of the Net Acid Production Test Method, Coastech Research.

Lefebvre, R., Hockley, D., Smolensky, J., Gélinas, P. (2001). "Multiphase transfer processes in waste rock piles producing acid mine drainage: 1: Conceptual Model And System Characterization, *Journal Of Contaminant Hydrology*, 52.1-4 137-164.

Maden Atıkları Yönetmeliği ve Ekleri, 15.07.2015 tarih ve 29717 sayılı resmî gazete (16.07.2016 tarih 29772 sayılı resmî gazete ile değişik).

Maden Atıkları Yönetmeliğinin Uygulanmasına İlişkin Açıklamalar, <https://webdosya.csb.gov.tr/db/cygm/duyurular/may-ac-klama201805-20180601164229.pdf>, Erişim tarihi- 25.01.2022.

Miller, S. and Jeffery, J. (1995). Advances in the Prediction of Acid Generating Mine Waste Materials. In: Proceedings of the Second Australian Acid Mine Drainage Workshop. (pp. 33-43). Charters Towers, Queensland, 28-31 March. eds. N. J. Grundon and L. C. Bell, Australian Centre for Minesite Rehabilitation Research, Brisbane.

Miller, S. D., Jeffery, J. J., and Murray, G. S. C. (1990). Identification And Management Of Acid Generating Mine Wastes - Procedures and practices in Southeast Asia and the Pacific Regions", In: Acid mine drainage designing for closure, J. W. Gadsby, J. A. Malick, S.J. Day (eds.) BiTech Publishers Ltd., Vancouver, B.C. 1-11.

Morin, K. A. and Hutt, N. M. (1994). Observed Preferential Depletion Of Neutralization Potential Over Sulfide Minerals İn Kinetic Tests: Site Specific Criteria For Safe NP/AP Ratios. In Proceedings of the International Land Reclamation and Mine Drainage Conference on the Abatement of Acidic Drainage. (pp. 148-156). April 24-29. Pittsburgh, PA.

Morin, K. A., and Hutt, N. M. (1997). Environmental Geochemistry Of Minesite Drainage: Practical Theory And Case Studies, MDAG Publishing, Vancouver, Canada.

O'Shay, T. A., Hossner, L. R., Dixon, J. B., (1990). "A Modified Hydrogen Peroxide Oxidation Method For Determination Of Potential Acidity İn Pyritic Overburden", *Journal of Environmental Quality*, 19, 778-782.

Page, A.L., Miller, R. H. and Keeney, D. R. (1982), Methods of Soil Analysis: Part 2 - Chemical and Microbiological Properties, 2nd Edn., American Society of Agronomy Inc., Soil Science Society of America Inc. 199-209.

Paktunç, A. D. (1999). Characterization Of Mine Wastes For Prediction Of Acid Mine Drainage. In: Azcue JM (ed) Environmental impacts of mining activities, Springer-Verlag, Berlin Heidelberg New York. 19- 40.

Price, W. A. (1997). DRAFT. Guidelines And Recommended Methods For The Prediction Of Metal Leaching And Acid Rock Drainage At Minesites İn British Columbia. (170 p). British Columbia Ministry of Employment and Investment, Energy and Minerals Division, Smithers, BC.

Skousen, J. G., Smith, R., Sencindiver, J. (1996). The Development Of The Acid-Base Account, Acid Mine Drainage Control And Treatment (Compiled by J. G. Skousen and P. F. Ziemkiewicz), W.V.Univ., and N.M.L.R.C. 15-20.

Smith, R. M., Grube, Jr., W. E., Arkle, T., J., Sobek, A. A. (1974). Mine Spoil Potentials For Soil And Water Quality, (320 p). Environmental Protection Technology Series (EPA- 670/2- 74- 070).

Sobek, A. A., Schuller, W. A., Freeman, J. R. and Smith, R. M. (1978). Field And Laboratory Methods Applicable To Overburdens And Minesoils. (203 p). EPA-600/2-78-054. U.S. Environmental Protection Agency, Cincinnati, OH.

Stewart, W. A., Miller, S. D., Smart, R. (2006). Advances in Acid Rock Drainage (Ard) Characterisation of Mine Wastes. Paper Presented at the 7 th International Conference on Acid Rock Drainage (ICARD).

(pp. 2098 – 2119). March 26-30. St Louis MO. R.I. Barnhisel (ed.) Published by the American Society of Mining and Reclamation (ASMR), 3134 Montavesta Road, Lexington, KY 40502.

Technical Committee CEN/TC 292, 2011; “BS EN 15875- Characterization Of Waste -Static Test For Determination Of Acid Potential And Neutralization Potential Of Sulfidic Waste.

Wang, Y. (1998). Evaluation Of Np Determination By Static Tests for ARD Prediction (Doctoral Dissertation, University Of British Columbia).

White, W. W. III., Lapakko, K. A. and Cox, R. L. (1999). Static-Test Methods Most Commonly Used To Predict Acid-Mine Drainage: Practical Guidelines For Use And Interpretation”, In: Reviews in economic geology, V. 6A, The environmental geochemistry of mineral deposits, Part A: Processes, techniques, and health issues, Plumlee, G. S. and Logsdon, M. J. (eds.), Society of Economic Geologists, Inc., Littleton, CO. 325-338.

BİR AÇIK OCAK KROM SAHASININ BİRİM MALİYETİNİN UZUN KISA-VADELİ BELLEK (LSTM) YÖNTEMİ İLE TAHMİN EDİLMESİ

PREDICTION OF UNIT COST OF AN OPEN-PIT CHROME MINE USING LONG SHORT-TERM MEMORY (LSTM) METHOD

A.C. Özdemir

*Çukurova Üniversitesi, Mühendislik Fakültesi, Maden Mühendisliği Bölümü
(*Sorumlu yazar: acozdemir@cu.edu.tr)*

ÖZET

Maden varlığı tespit edilen bir sahanın ilk olarak ekonomik yönden değerlendirilmesi gerekmektedir. Bu aşamada, toplam üretim maliyetinin toplam üretim miktarına oranı olarak bilinen birim maliyetin hesaplanması önem kazanmaktadır. Bu değer, maden sahasında üretim yapılmasının ekonomik olup olmadığına bir göstergesidir. Bu nedenle, ekonomik ve sürdürülebilir madencilik için bu parametrenin hassas bir şekilde hesaplanması ve takip edilmesi gerekmektedir. Ancak, günümüz şartlarında birim maliyetin çok fazla değişkenlik göstermesi madencilik sektörünü olumsuz etkileyen bir belirsizlik ortamı oluşturmaktadır. Bu çalışmada, birim maliyetin belirsizlik probleminin çözümünde bir derin öğrenme yöntemi olan Uzun Kısa-Vadeli Bellek (LSTM) yönteminin kullanılabilirliği araştırılmıştır. Bu yöntemin performansını değerlendirmek için örnek bir açık ocak krom madenine ait birim maliyet tahmini gerçekleştirilmiştir. Eğitim parametreleri değiştirilerek 9 farklı LSTM modeli geliştirilmiş ve bu modellerin başarısı korelasyon katsayısı (R), ortalama mutlak yüzde hata (MAPE) ve kök ortalama kare hata (RMSE) performans değerlendirme kriterleri kullanılarak ölçülmüştür. Geliştirilen modeller arasında en iyi model ile elde edilen sonuçlar (R=0.72, RMSE=2.47 ve MAPE=4.37) LSTM yönteminin başarılı bir performans gösterdiğini kanıtlamıştır. Böylece, LSTM yönteminin birim maliyetin tahmin edilmesinde kullanılabilir olduğu ve ekonomik belirsizlik probleminde bir çözüm olabileceği belirlenmiştir.

Anahtar Sözcükler: Açık ocak, krom cevheri, birim maliyet, tahmin, uzun kısa-vadeli bellek (LSTM)

ABSTRACT

An area where mineral assets are detected must first be evaluated economically. At this stage, it is important to calculate the unit cost, known as the ratio of the total production cost to the total production amount. This value is an indicator of whether it is economical to produce at the mining site. Therefore, this parameter needs to be calculated and followed precisely for economical and sustainable mining. However, the high variability of unit costs in today's conditions creates an environment of uncertainty that negatively affects the mining industry. In this study, the usability of the Long Short-Term Memory (LSTM) method, which is a deep learning method, was investigated in solving the unit cost uncertainty problem. To evaluate the performance of this method, a unit cost estimation of a sample open pit chrome mine was made. By changing the training parameters, 9 different LSTM models were developed and the success of these models was measured using the correlation coefficient (R), mean absolute percent error (MAPE) and root mean square error (RMSE) performance evaluation criteria. Among the developed models, the results obtained with the best model (R=0.72, RMSE=2.47 and MAPE=4.37) proved that the LSTM method showed a successful performance. Thus, it has been determined that the LSTM method can be used in predicting the unit cost and can be a solution to the economic uncertainty problem.

Keywords: Open-pit mine, chromite ore, unit cost, prediction, long short-term memory (LSTM)

GİRİŞ

Günümüzde sürdürülebilirlik, kaynak verimliliği ve sera gazları emisyonu gibi kavramlar birçok sektörde olduğu gibi madencilik sektöründe de yaygınlaşmaktadır. Madencilik faaliyetlerinin başarılı bir şekilde yürütülebilmesi için bu kavramların iyi yorumlanması ve çalışmalara entegre edilmesi gerekmektedir. Gelişmiş ülkelerin birçoğu bu kavramların önemini benimsemiş ve Dünya genelinde insanların yaşam standartları dahil bir çok etken parametre gözden geçirilmektedir (Papetti vd., 2019). 2021 yılında yayınlanan Avrupa Yeşil Mutabakatı ve buna paralel olarak Türkiye Cumhuriyeti Ticaret Bakanlığı tarafından yayınlanan Yeşil Mutabakat Eylem Planı 2021’de Ülkelerin temiz ve döngüsel bir ekonomi politikası yürütmeleri vurgulanmıştır (European Commission, 2021; Türkiye Cumhuriyeti Ticaret Bakanlığı, 2021). Buradan da anlaşılacağı gibi herhangi bir faaliyet alanında özellikle sürdürülebilirliğin ve kaynak verimliliğinin sağlanması için ekonomik üretim modelinin geliştirilmesi zorunludur. Ülkelerin gelişimi, kalkınması ve rekabetçi olabilmesi sahip oldukları ekonomik güçle doğru orantılıdır.

Madencilik sektöründe üretime devam edilmesi veya üretimin durdurulması gibi hayati kararların alınmasında en önemli kriter o günün ekonomik koşullarıdır (Shafiee vd., 2009). Sürdürülebilir ve yüksek kaynak verimliliğine sahip bir madencilik için maliyetlerin, cevher fiyatlarının ve gelir-gider bilgilerinin eksiksiz bir şekilde kayıt altına alınması gerekmektedir. Delme-patlatma, yükleme, nakliye, akaryakıt, işçilik, bakım-onarım, yedek parça, elektrik, iş sağlığı ve güvenliği, eğitim, çevre vb. gider kalemleri üzerinde en çok durulan maliyetler arasında bulunmaktadır. Hesaplamalarda kolaylık sağlanması açısından genel olarak bu maliyetler; kazı (madencilik), konsantre (proses) ve genel-idari yönetim maliyeti olmak üzere 3 grupta değerlendirilebilir. Bir maden sahasının birim maliyet değeri bu maliyetlerin toplamının toplam üretim miktarına oranı olarak kabul edilir ve \$/ton veya TL/ton cinsinden ifade edilir (Curry vd., 2014; Ahmadi ve Bazzazi, 2019; Khan ve Asad, 2019). Birim maliyet, madencilik faaliyetleri başlamadan önce hesaplanmalı ve üretim devam ederken belirli periyotlarda güncellenmelidir (Shafiee ve Topal, 2012). Burada gözlemlenecek herhangi beklenmedik veya sıra dışı bir değişimin (artış veya azalış) nedenleri mutlaka araştırılmalıdır.

Bir maden firmasının içinde bulunduğu zamanı ve geleceğini önemli derecede etkileyen birim maliyet değerinin tahmin edilmesinde ciddi belirsizlikler gözlenmektedir. 2019 yılında başlayan ve halen devam eden pandemi süreci madencilik sektöründe birim maliyetin belirlenmesini olumsuz yönde etkilemiştir. Ayrıca, pandeminin de etkisiyle son zamanlarda yaşanan ekonomik dalgalanmalar da bu belirsizlik sorunu göz ardı edilemeyecek şekilde ortaya çıkarmıştır. Birim maliyet değeri düzenli zaman aralıklarında hesaplandığından ve takip edildiğinden dolayı bir zaman serisi olarak düşünülmüştür. Özel bir yinelemeli sinir ağ türü olan uzun kısa-vadeli bellek (LSTM) yönteminin zaman serisi problemlerinin çözümünde yaygın olarak kullanıldığı bilinmektedir (Arslan ve Sekertekin, 2019). Son zamanlarda, birçok bilim alanında LSTM yöntemi ile çok değişkenli sınıflandırma ve tahmin problemleri üzerine başarılı çalışmalar gerçekleştirilmiştir (Zhang vd., 2019; Yildirim vd., 2019; Xiao vd., 2018; Zhang vd., 2018; Qin, 2019; Han vd., 2019; Tong vd., 2019; Li ve Cao, 2018). Bu nedenle, zaman serisi tahmininde yaygınlığı sürekli artan LSTM yönteminin birim maliyet tahmininde kullanılması önerilmiştir.

Bu çalışmanın amacı, LSTM yönteminin madencilik sektöründe birim maliyet değerinin tahmin edilmesinde kullanılabilirliğinin araştırılmasıdır. Bu kapsamda, LSTM yöntemi ile örnek bir açık ocak krom sahasının birim maliyet değerinin tahmini gerçekleştirilmiştir. Model eğitim parametreleri değiştirilerek 9 farklı LSTM modeli geliştirilmiş ve bu modeller performans değerlendirme kriterlerine göre karşılaştırılmıştır. Sonuç olarak, birim maliyet tahmin performansı en iyi olan LSTM modeli belirlenmiştir.

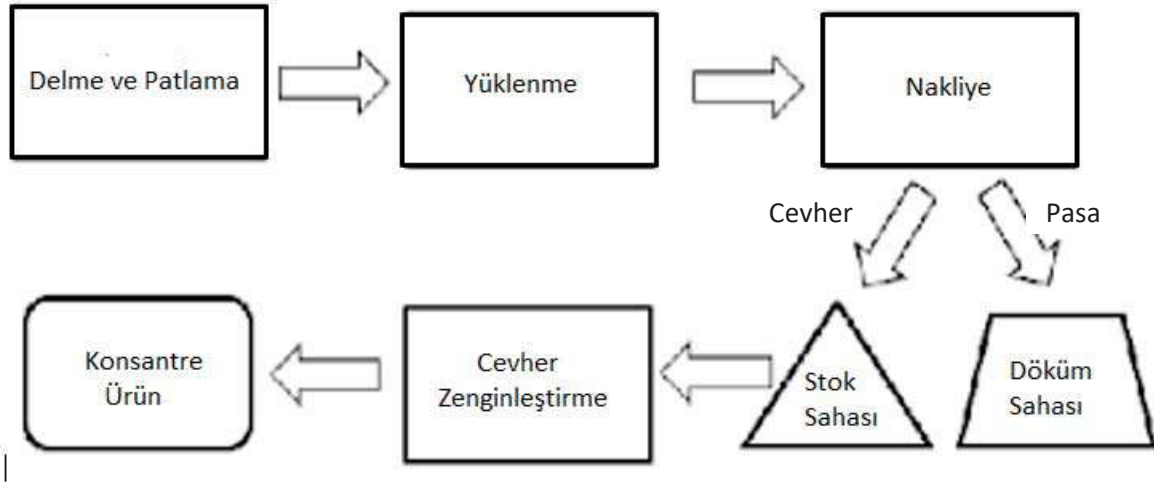
Bildirinin geri kalan kısmı şu şekilde tasarlanmıştır: çalışma sahası ve veri seti hakkında bilgilerin verildiği materyal bölümü, LSTM yönteminin açıklandığı ve performans değerlendirme kriterlerinden bahsedilen yöntem bölümü, geliştirilen modellerin örnek saha üzerinde uygulanması sonucu elde edilen çıktılar verildiği sonuçlar ve tartışma bölümü ve son olarak çalışmanın genel olarak yorumlandığı yorum bölümü yer almaktadır.

MATERYAL

Çalışma Sahası

Çalışma sahası olarak Marmara bölgesinde bulunan orta ölçekli bir açık ocak krom madeni seçilmiştir. Maden sahasında kazı ve nakliye faaliyetleri ekskavatör + kamyon sistemi ile yürütülmektedir. Sahanın ekskavatör kazısı için uygun olmayan kısımlarında delme-patlama yöntemi uygulanarak kazılacak malzemenin gevşetilmesi sağlanmaktadır. Daha sonra ekskavatör yardımı ile kamyonlara yüklenen malzeme pasa ise döküm sahasına, cevher ise stok sahasına gönderilmektedir. Stok sahasında biriktirilen malzeme cevher zenginleştirme tesisine beslenmektedir ve proses sonucunda konsantre ürün elde edilmektedir. Çalışma sahasında uygulanan iş akım şeması Şekil 1’de görülmektedir.

Krom cevherinin ortalama tenörü %10-12 cevher zenginleştirme tesisinden elde edilen konsantre ürünün tenör değeri ise %46-48 arasında değişiklik göstermektedir. Makine parkı göz önünde bulundurulduğunda aylık kazı kapasitesi ortalama 120 000 – 150 000 m³ arasında değişmektedir. Cevher zenginleştirme tesisi ise aylık ortalama 15 000 – 20 000 ton besleme kapasitesi ile çalışmaktadır.



Şekil 1. Çalışma sahasında uygulanan iş akım şeması

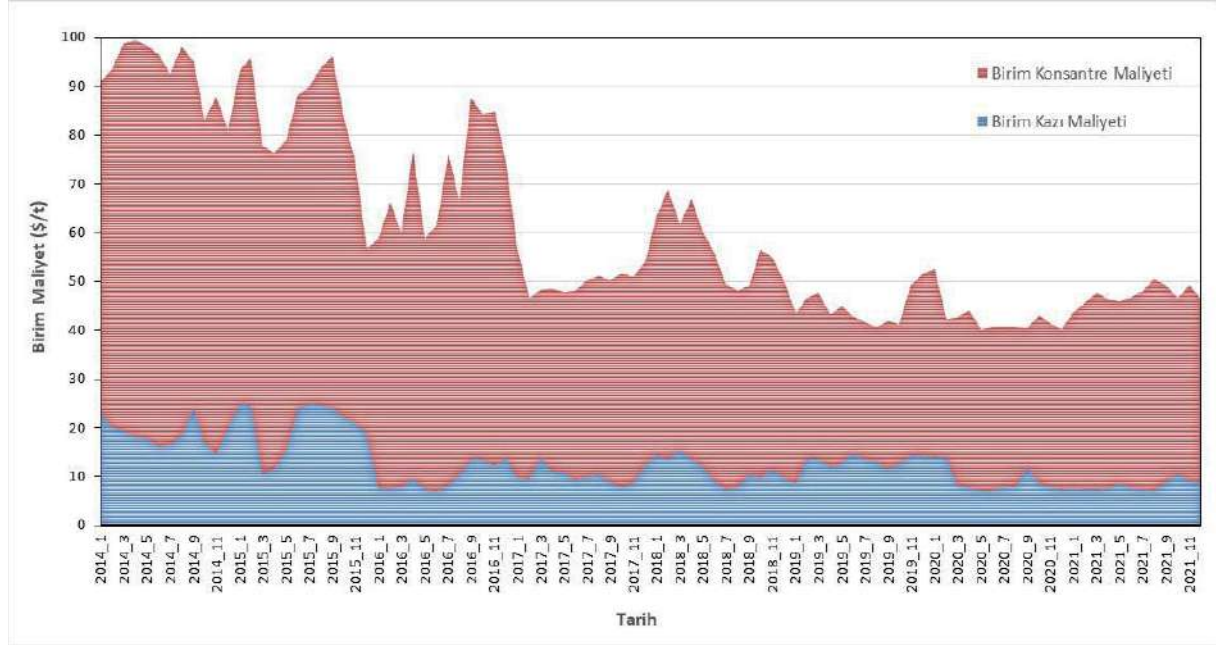
Veri Seti

Çalışmada, 2014 Ocak-2021 Aralık dönemi arasında aylık kazı maliyeti, konsantre maliyeti, kazı miktarı ve konsantre miktarı bilgilerinin yer aldığı toplam 96 adet örnekten oluşan veri seti kullanılmıştır. Birim kazı maliyeti ve birim konsantre maliyeti sırasıyla Eşitlik 1 ve 2 kullanılarak hesaplanmıştır.

$$\text{Birim Kazı Maliyeti } (\$/t) = \frac{\text{Toplam Kazı Maliyet}}{\text{Toplam Kazı Miktarı}} \quad (1)$$

$$\text{Birim Konsantre Maliyeti } (\$/t) = \frac{\text{Toplam Konsantre Maliyeti}}{\text{Toplam Konsantre Miktarı}} \quad (2)$$

Birim maliyet değeri, birim kazı maliyeti ve birim konsantre maliyeti değerlerinin toplamı olarak belirlenmiştir. Birim maliyet hesaplanırken evrensellik sağlanması için para birimi olarak Dolar seçilmiştir. Para birimi dönüşümlerinde Türkiye Cumhuriyeti Merkez Bankasının aylık ortalama Dolar kuru değerleri esas alınmıştır (TCMB, 2022). Aylık birim kazı maliyeti ve birim konsantre maliyeti değerlerinin değişimi Şekil 2’de görülmektedir.



Şekil 2. Aylık birim kazı ve birim konsantre maliyet değerlerinin değişimi

Veri seti üzerinde tanımlayıcı istatistiksel analiz uygulanmış olup elde edilen sonuçlar Çizelge 1’de verilmiştir. Veri seti, geliştirilen modellerin eğitim ve test aşamalarında kullanılması için %80’ i eğitim (77 veri) geri kalan %20’si (19 veri) test olmak üzere 2 gruba ayrılmıştır. Tüm çalışmalar bu veri seti üzerinden gerçekleştirilmiştir.

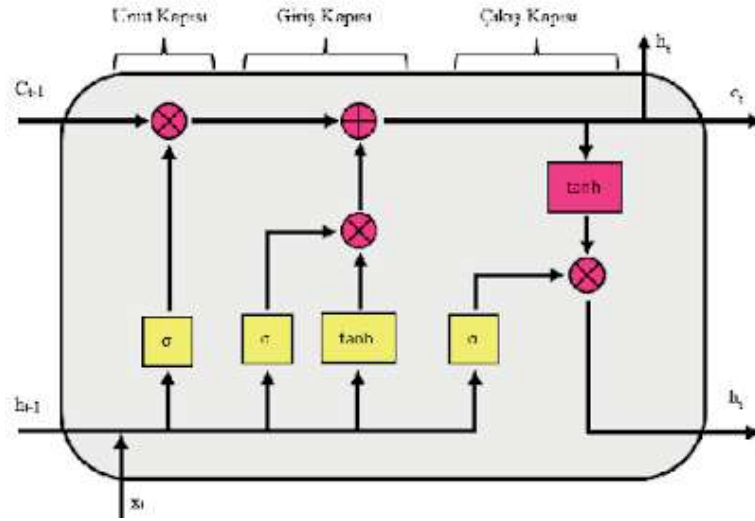
Çizelge 1. Tanımlayıcı özet istatistik değerleri

	Birim Kazı Maliyeti (\$/t)	Birim Konsantre Maliyeti (\$/t)	Birim Maliyet (\$/t)
Ortalama	12.63	48.54	61.18
Ortanca	11.48	41.79	51.59
Standart Sapma	5.12	15.74	19.19
Varyans	26.21	247.66	368.21
Basıklık	0.15	-0.97	-0.94
Çarpıklık	1.01	0.61	0.74
Aralık	17.92	53.82	59.18
En Büyük	7.02	27.38	40.10
En Küçük	24.94	81.20	99.29

YÖNTEM

Uzun Kısa-Vadeli Bellek (LSTM)

LSTM ilk olarak 1997 yılında Hochreiter ve Schmidhuber tarafından ortaya çıkarılmıştır. Bu yöntem tekrarlayan sinir ağlarının özel bir türü olup zaman serilerinin tahmini için kullanılabilir (Hochreiter ve Schmidhuber, 1997). LSTM yöntemi standart ileri beslemeli sinir ağlarından farklı olarak geri besleme bağlantılarına sahiptir (Siegelmann and Sontag, 1992). Geleneksel sinir ağlarının yetersiz kaldığı özellikle uzun vadeli bağımlılıkların öğrenilmesi konusunda ön plana çıkmaktadır. LSTM, çeşitli denetimli dizi öğrenme başarısı ve hafıza geçişli mimarisi sayesinde zaman serisi problemlerinde oldukça avantajlı bir yöntemdir (Ahmadi vd., 2019). LSTM ağını bir birine bağlı tekrarlayan LSTM birimleri oluşturur (Şekil 3).



Şekil 3. Her LSTM biriminin temel mimarisi

$x = (x_1, x_2, x_3, \dots, x_t)$ dizi verisi giriş katmanı olsun, gizli (çıkış) katmanı tahmin etmek için sırasıyla $h = (h_1, h_2, h_3, \dots, h_t)$ ve hücre katmanı $c = (c_1, c_2, c_3, \dots, c_t)$ kullanılır. x dizisinin ilk değeri (x_1) ilk LSTM birimine uygulandığında gizli katmanın ilk değeri (h_1) ve güncellenmiş hücre katmanının ilk değeri (c_1) elde edilir.

t zamanında, LSTM birimi (c_{t-1}, h_{t-1}) ile beslenmesi durumunda sonuç olarak h_t ve güncellenmiş hücre katmanı c_t çıktılarına ulaşılır. t zamanında gizli katman hücre katmanı (c_t) ile şu şekilde ifade edilebilir;

$$h_t = o_t \odot \tanh \tanh c_t \quad (3)$$

burada \odot Hadamard çarpımını (vektörlerin eleman bazında çarpımı) ve o_t ise çıkış kapısını gösterir. LSTM ağı, kapılar gibi yapılar yardımıyla hücre durumuna bilgi ekleyerek veya çıkararak yönetilir. Önceki adımlardan bilgileri içeren hücre durumu, t zaman adımı için aşağıdaki gibi verilebilir (Hochreiter ve Schmidhuber, 1997; Mathworks, 2021):

$$c_t = f_t \odot c_{t-1} + i_t \odot g_t \quad (4)$$

Eşitlik 4’te yer alan değişkenlerden giriş kapısı (i_t) Eşitlik 5’te, unut kapısı (f_t) Eşitlik 6’da, katman girişi (g_t) Eşitlik 7’de ve çıkış kapısı (o_t) Eşitlik 8’de verilmiştir (Hochreiter ve Schmidhuber, 1997; Mathworks, 2021).

$$i_t = \sigma(W_i x_t + R_i h_{t-1} + b_i) \tag{5}$$

$$f_t = \sigma(W_f x_t + R_f h_{t-1} + b_f) \tag{6}$$

$$g_t = \tanh \tanh (W_g x_t + R_g h_{t-1} + b_g) \tag{7}$$

$$o_t = \sigma(W_o x_t + R_o h_{t-1} + b_o) \tag{8}$$

burada σ sigmoid fonksiyonudur ve $\sigma(x) = (1 + e^{-x})^{-1}$ olarak ifade edilir. W girdi ağırlıklarını, R tekrarlayan ağırlıkları ve b bias değerini temsil etmektedir (Eşitlik 9).

$$W = [W_i \ W_f \ W_g \ W_o \], R = [R_i \ R_f \ R_g \ R_o \], b = [b_i \ b_f \ b_g \ b_o \] \tag{9}$$

Performans Değerlendirme Kriterleri

Geliştirilen modellerin tahmin doğruluğunu belirlemek için literatürde yaygın olarak kullanılan performans değerlendirme kriterlerinden; korelasyon katsayısı (R), ortalama mutlak yüzde hata (MAPE) ve kök ortalama kare hata (RMSE) kullanılmıştır.

R bilinmeyen değerlerin bilinen değerlere göre ne kadar iyi tahmin edildiğinin istatistiksel bir ölçüsüdür. R değeri 0-1 arasında değer alır ve 1 değerine yaklaştıkça tahminin doğruluğu artar (Jamei vd., 2021). MAPE regresyon ve zaman serileri modellerinde tahminlerin doğruluğunu ölçmek için en sık kullanılan kriterlerden birisidir. Bu değer %10’dan küçük ise çok iyi tahmin; 11-20 arasında ise iyi tahmin ve 20-50 arasında ise kabul edilebilir tahmin olarak yorumlanmaktadır (Lewis, 1982). Ayrıca, hatanın büyüklüğünü ölçen RSME kriteri de makine öğrenmesi yöntemlerinde yaygın olarak kullanılmaktadır. RMSE değerinin 0’a yakın olması tahminin doğruluğu göstermektedir (Gilan vd. 2012). R, MAPE ve RMSE değerleri sırasıyla Eşitlik 10-12’de verilen formüller ile hesaplanır:

$$R = \frac{\sum_{i=1}^n (y_{pi} - \underline{y}_p)(y_{mi} - \underline{y}_m)}{\sqrt{\sum_{i=1}^n (y_{pi} - \underline{y}_p)^2 \cdot \sum_{i=1}^n (y_{mi} - \underline{y}_m)^2}} \tag{10}$$

$$MAPE = \frac{100}{n} \sum_{i=1}^n \left| \frac{y_{mi} - y_{pi}}{y_{mi}} \right| \tag{11}$$

$$RMSE = \sqrt{\frac{1}{n} \sum_{i=1}^n (y_{mi} - y_{pi})^2} \tag{12}$$

burada y_{mi} ve y_{pi} sırasıyla i . örneğin gerçek ve tahmini değerlerini, \underline{y}_m ve \underline{y}_p sırasıyla gerçek ve tahmin değerlerin ortalamasını ve n ise örnek sayısını temsil etmektedir.

SONUÇLAR VE TARTIŞMA

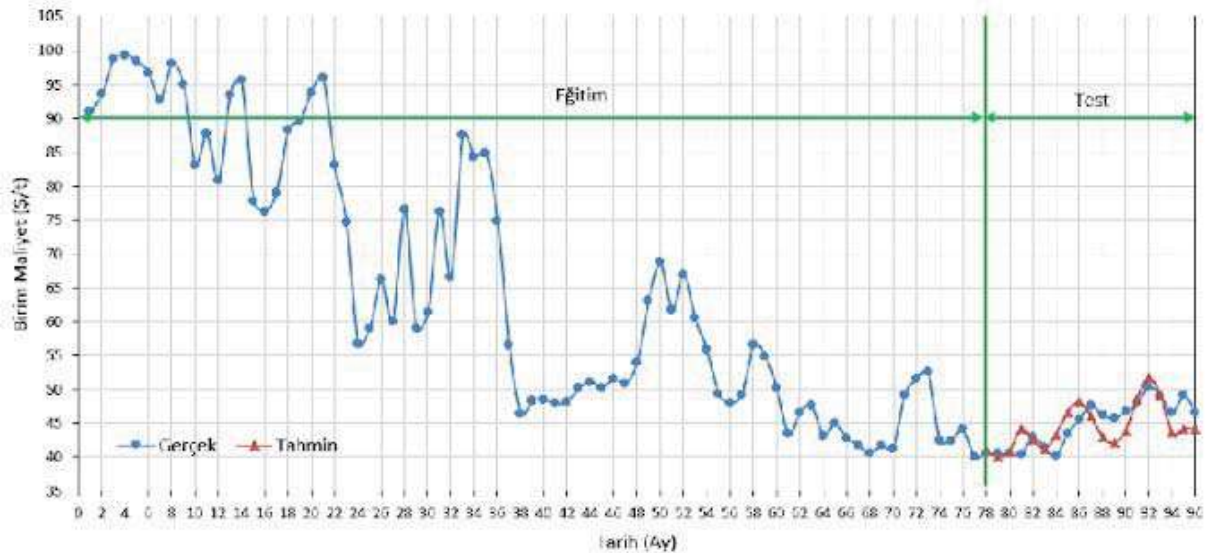
Model parametrelerinden gizli katman sayısı 425-475, eğitim sayısı ise 125-175 değeri arasında 25 birim kadar değiştirilerek toplam 9 farklı LSTM modeli geliştirilmiştir. Eğitim aşamasında, stokastik amaç fonksiyonlarının gradyan tabanlı optimizasyonu için uyarlamalı moment tahmini (Adam) optimize edici algoritması kullanılmıştır. Bu algoritmanın seçilmesinde uygulanmasının basit, hesaplama açısından verimli, çok az bellek gereksinimine sahip ve büyük ölçekli (veri ve/veya parametre açısından)

problemler için oldukça uygun olması gibi avantajları dikkate alınmıştır (Kingma ve Ba, 2014). Geliştirilen modellerin parametre bilgileri ve elde edilen performans kriterleri Çizelge 2’de verilmiştir.

Çizelge 2. Geliştirilen modeller ve elde edilen performans kriterleri

Model	Model Parametreleri		Performans Kriterleri		
	Gizli Katman Sayısı	Eğitim Sayısı	RMSE	MAPE	R
1	425	125	5.22	9.04	0.34
2	425	150	5.07	10.21	0.80
3	425	175	4.60	8.37	0.66
4	450	125	4.01	7.26	0.36
5	450	150	2.85	5.56	0.66
6	450	175	2.47	4.37	0.72
7	475	125	4.01	7.75	-0.03
8	475	150	5.34	9.25	-0.12
9	475	175	5.26	8.76	0.20

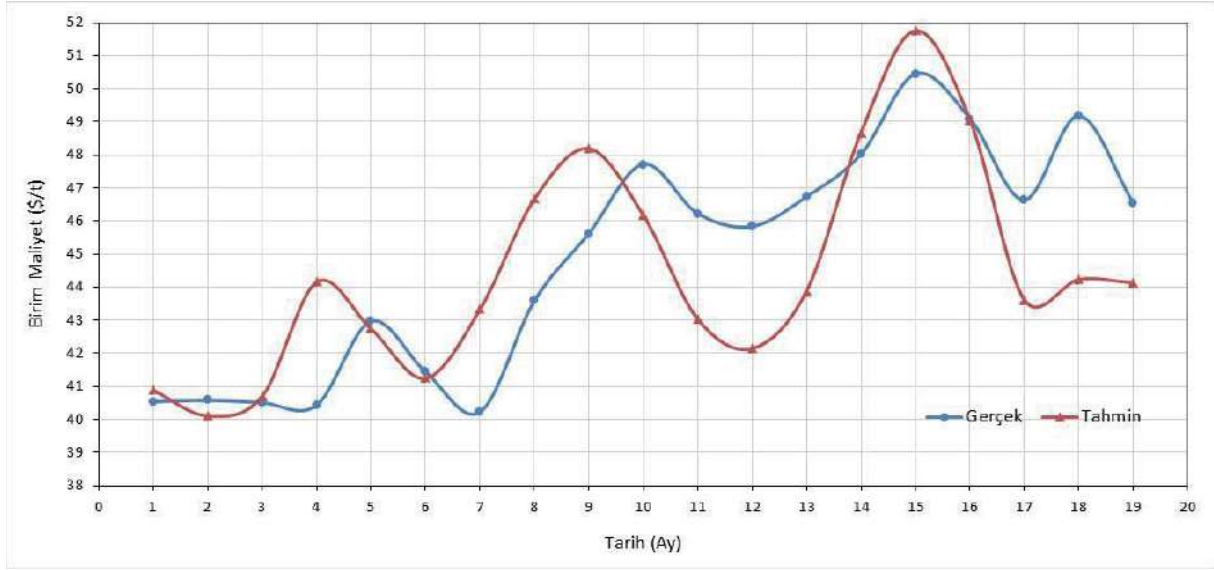
Elde edilen sonuçlar değerlendirildiğinde en düşük RMSE (2.47) ve MAPE (4.37) değerlerine 6 numaralı LSTM modelinin sahip olduğu görülmektedir. Bu modeli RMSE ve MAPE kriterlerine göre sırasıyla 5, 4 ve 7 numaralı modeller takip etmektedir. R değerleri incelendiğinde en yüksek değer 0.80 ile 2 numaralı modele ait olduğu ve bu modelden sonra 0.72 değeri ile 6 numaralı modelin geldiği anlaşılmaktadır. Sonuç olarak, birim maliyet değerinin tahmin edilmesinde 450 gizli katman ve 175 eğitimi sayısına sahip 6 numaralı modelinin en başarılı LSTM modeli olduğu tespit edilmiştir.



Şekil 4. Gerçek ve tahmin birim maliyet değerlerinin değişimi

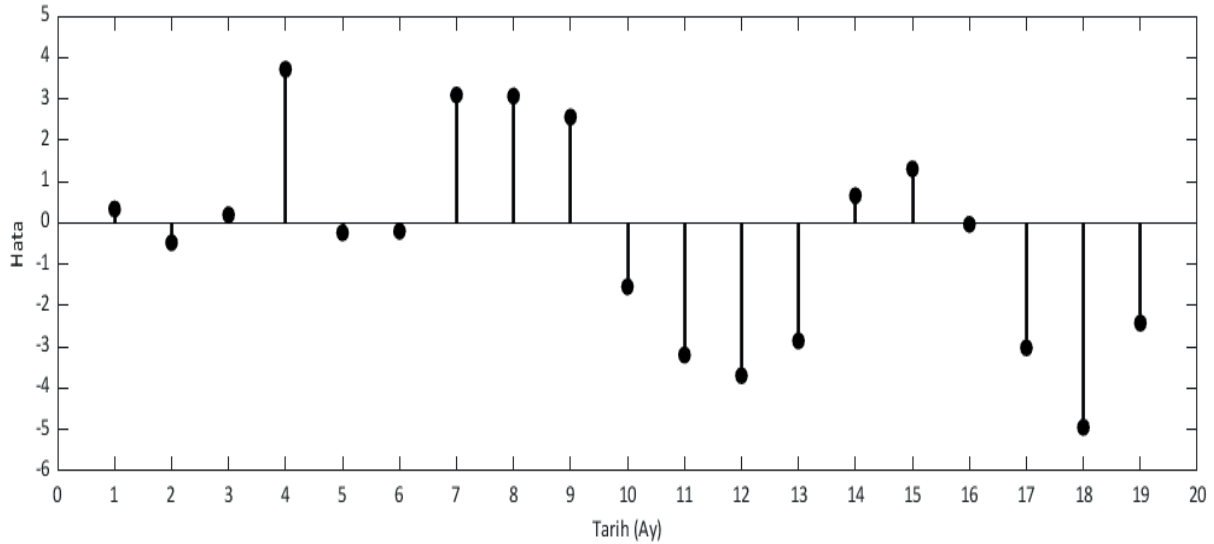
LSTM modelinin tahmin performansının daha iyi anlaşılabilmesi için grafikler çizdirilmiştir. Şekil 4’te gerçek ve tahmin edilmiş birim maliyet değerlerinin değişimi görülmektedir. Test verisi üzerindeki değişimin daha iyi anlaşılabilmesi için Şekil 5’te yakınlaştırılmış görüntüsü sunulmuştur. Eğitim verilerinin

dağılımı incelendiğinde birim maliyet değerinin son aylarda bir miktar yükseliş göstermesine rağmen genel olarak bir düşüş eğiliminde olduğu fark edilmektedir. Test veri seti için elde edilen tahmin değerleri ile gerçek değerlerin benzer bir eğilim gösterdiği anlaşılmaktadır.



Şekil 5. Test veri seti için gerçek ve tahmin birim maliyet değerlerinin değişimi

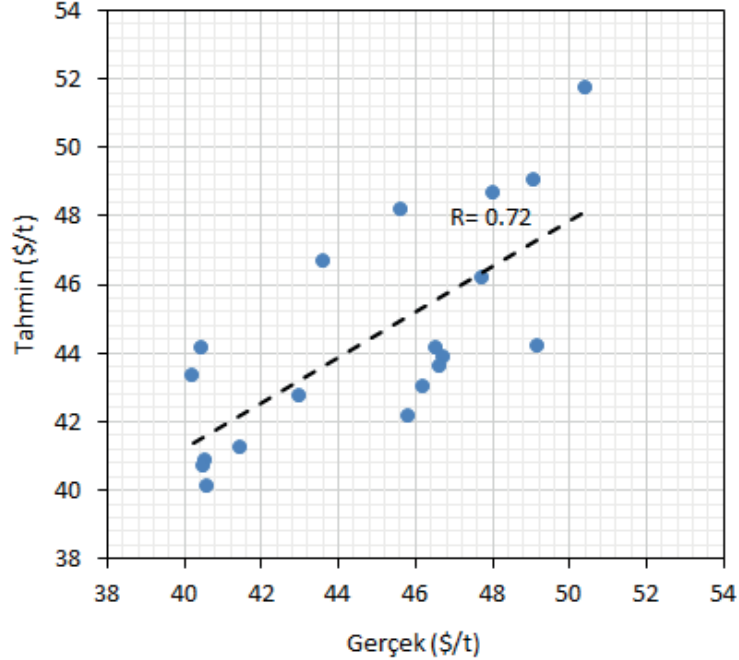
Şekil 6’da ise tahmin değerlerinin gerçek değerlerden farkını gösteren hata grafiği verilmiştir. Hata grafiğinde verilerin bir kısmının 0 çizgisine oldukça yakın yer aldığı, geri kalanların ise kabul edilebilir uzaklıkta dağıldığı görülmektedir. Bu durum LSTM modelinin tahmin doğruluğunu desteklemektedir.



Şekil 6. Tahminin hata grafiği

Şekil 5 ve 6 beraber incelendiğinde 4. (2020-9. ay), 12. (2021-5. ay) ve 18. (2021-11.ay) aylarda gerçek ile tahmin değerleri arasındaki farkın nispeten daha fazla olduğu görülmektedir. Belirtilen tarihlerde TL-Dolar kurunda büyük hareketliliklerin olduğu gözlemlenmiştir. Bu durumun hata değerini arttırdığı ve tahmin performansını olumsuz yönde etkilediği anlaşılmaktadır.

Gerçek ve tahmin edilmiş birim maliyet değerlerinin arasındaki ilişkiyi gösteren korelasyon grafiği Şekil 7’de görülmektedir. Burada, R değerinin %70’in üzerinde olması geliştirilen LSTM modelinin güvenilir bir tahmin sonucu üretmiş olduğunu işaret etmektedir. Aynı zamanda tahminin doğruluğu belirtir ve %72 doğruluk ile tahmin yapıldığı şeklinde ifade edilebilir.



Şekil 7. Gerçek ve tahmin birim maliyet değerlerinin korelasyon grafiği

Ayrıca, gelişen bilgisayar teknolojileri ve modelleme yöntemleri sayesinde tahmin işlemlerinin oldukça kısa sürelerde tamamlandığı bilinmektedir. Bu süre kullanılan veri setinin büyüklüğüne ve bilgisayarın teknik özelliklerine göre değişmektedir. Bu çalışmada, Intel (R) Core (TM) i9-9900K CPU @ 3.60 GHz işlemci, 64 GB RAM ve Windows 64-bit işletim sistemine sahip bir bilgisayar kullanılmıştır. Geliştirilen her bir modelin sonuç üretmesi yaklaşık 2-3 dakika gibi çok kısa bir süre içerisinde gerçekleşmiştir.

YORUM

Bu çalışmada, bir açık ocak krom sahasının birim maliyet değerlerinin tahmini LSTM yöntemi kullanılarak gerçekleştirilmiştir. Model parametreleri üzerinde değişiklikler yapılarak 9 farklı LSTM modeli geliştirilmiş olup tahmin performansları karşılaştırılmıştır. Geliştirilen modellerin değerlendirilmesi sonucu RMSE= 2.47, MAPE= 4.37 ve R= 0.72 değerlerine sahip 6 numaralı modelin (450 gizli katman ve 175 eğitim sayısı ile) en başarılı LSTM modeli olduğu belirlenmiştir. Sonuç olarak, LSTM yönteminin birim maliyet değerinin tahminindeki başarısı bir açık ocak krom madenine uygulanarak kanıtlanmıştır. Ayrıca, LSTM yöntemi benzer zaman serisi verilerinin tahmininde kullanıcılara iş gücü/zaman tasarrufu sağlayacak ve hızlı sonuç üretebilme yeteneği sayesinde kısa sürede birçok alternatif modelin karşılaştırılması imkânı sunacaktır. Gelecek çalışmalarda, birim maliyet değerini etkileyen parametrelerin de veri setine dahil edildiği LSTM modelleri geliştirilerek bu parametrelerin tahmin performansına etkileri araştırılacaktır.

TEŞEKKÜR

Bu çalışma, Çukurova Üniversitesi Bilimsel Araştırma Fonu (Proje No: FBA-2019-11998) tarafından desteklenmiştir.

KAYNAKLAR

- Ahmadi, M. R., Bazzazi, A.A. (2019). Cutoff grades optimization in open pit mines using meta-heuristic algorithms. *Resources Policy*, 60, 72–82. <https://doi.org/10.1016/j.resourpol.2018.12.001>
- Ahmadi, N., Constandinou, T., Bouganis, C. (2019). Decoding Hand Kinematics from Local Field Potentials Using Long Short-Term Memory (LSTM) Network. 9th International IEEE EMBS Conference on Neural Engineering (NER 2019), 1-5s.
- Arslan, N., Sekertekin, A. (2019). Application of Long Short-Term Memory neural network model for the reconstruction of MODIS Land Surface Temperature images. *Journal of Atmospheric and Solar–Terrestrial Physics*, 194, 105100. <https://doi.org/10.1016/j.jastp.2019.105100>
- Curry, J.A., Ismay, M.J.L., ve Jameson, G.J. (2014). Mine operating costs and the potential impacts of energy and grinding. *Minerals Engineering*, 56, 70–80 <https://doi.org/10.1016/j.mineng.2013.10.020>.
- European Commission, (2021). A European Green Deal, https://ec.europa.eu/info/strategy/priorities-2019-2024/european-green-deal_en (erişim tarihi: 02.11.2021)
- Gilan, S.S., Jovein, H.B., Ramezaniyanpour, A.A. (2012). Hybrid support vector regression–particle swarm optimization for prediction of compressive strength and RCPT of concretes containing metakaolin. *Construction and Building Materials*, 34, 321–329, <https://doi.org/10.1016/j.conbuildmat.2012.02.038>.
- Han, S., Qiao, Y.H., Yan, J., Liu, Y.Q., Li, L., ve Wang, Z. (2019). Mid-to-long term wind and photovoltaic power generation prediction based on copula function and long short term memory network. *Applied Energy*, 239, 181-191. <https://doi.org/10.1016/j.apenergy.2019.01.193>.
- Hochreiter, S., Schmidhuber, J. (1997). Long short-term memory. *Neural Comput.* 9, 1735–1780. <https://doi.org/10.1162/neco.1997.9.8.1735>.
- Jamei, M., Ahmadianfar, I., Olumegbon, I.A., Karbasi, M., Asadi, A. (2021). On the assessment of specific heat capacity of nanofluids for solar energy applications: Application of Gaussian process regression (GPR) approach. *Journal of Energy Storage*, 33, 102067. <https://doi.org/10.1016/j.est.2020.102067>.
- Khan, A., Asad, M.W.A. (2019). A method for optimal cut-off grade policy in open pit mining operations under uncertain supply. *Resources Policy*, 60, 178–184. <https://doi.org/10.1016/j.resourpol.2018.12.003>
- Kingma, D.P., Ba, J. (2014). Adam: A method for stochastic optimization. arXiv:1412.6980.
- Lewis, C.D. (1982). *Industrial and Business Forecasting Methods: a Practical Guide to Exponential Smoothing and Curve Fitting*, London; Boston: Butterworth Scientific, 143 s.
- Li, Y., ve Cao, H. (2018). Prediction for tourism flow based on LSTM Neural Network. *Procedia Computer Science*, 129, 277-283. <https://doi.org/10.1016/j.procs.2018.03.076>.
- Mathworks, (2021). Long Short-Term Memory Networks [WWW Document]. <https://www.mathworks.com/help/deeplearning/ug/long-short-term-memory-networks.html> (erişim tarihi: 06.12.21).
- Papettia, A., Menghia, R., Domizioa, G.D., Germania, M., ve Marconi, M. (2019). Resources value mapping: A method to assess the resource efficiency of manufacturing systems. *Applied Energy*, 249, 326-342. <https://doi.org/10.1016/j.apenergy.2019.04.158>
- Qin, Y., Li, K., Liang, Z., Lee, B., Zhang, F., Gu, Y., Zhang, L., Wu, F., ve Rodriguez, D. (2019). Hybrid forecasting model based on long short term memory network and deep learning neural network for wind signal. *Applied Energy*, 236, 262-272. <https://doi.org/10.1016/j.apenergy.2018.11.063>.
- Shafiee, S., Nehring, M., ve Topal, E. (2009). Estimating average total cost (ATC) of open pit coal mines in Australia, Proc. Australian Mining Technology Conf., Brisbane, Qld, Australia, October, CRC Mining, 134–145.
- Shafiee, S., ve Topal, E. (2012). New approach for estimating total mining costs in surface coal mines, *Mining Technology*, 121(3), 109-116, <https://doi.org/10.1179/1743286312Y.0000000011>

- Siegelmann, H.T., Sontag, E.D. (1992). On the computational power of neural nets. In: Proceedings of the Fifth Annual Workshop on Computational Learning Theory - COLT '92. ACM Press, New York, New York, USA, pp. 440–449. <https://doi.org/10.1145/130385.130432>.
- TCMB, (2022). Döviz kurları. https://evds2.tcmb.gov.tr/index.php?/evds/serieMarket/#collapse_2 (erişim tarihi: 03.01.2022)
- Tong, W., Li, L., Zhou, X., Hamilton, A., ve Zhang, K. (2019). Deep learning PM_{2.5} concentrations with bidirectional LSTM RNN. *Air Quality, Atmosphere & Health*, 12(4), 411-423. <https://doi.org/10.1007/s11869-018-0647-4>.
- Türkiye Cumhuriyeti Ticaret Bakanlığı, (2021). Yeşil Mutabakat Eylem Planı 2021. <https://ticaret.gov.tr/data/60f1200013b876eb28421b23/MUTABAKAT%20YE%C5%9E%C4%B0L.pdf> (erişim tarihi: 02.11.2021)
- Xiao, L., Wang, G., Zuo, Y. (2018). Research on Patent Text Classification Based on Word2Vec and LSTM. 11th International Symposium on Computational Intelligence and Design (ISCID), Hangzhou, China, 71-74.
- Yildirim, Ö., Baloğlu, U.B., Tan, R., Ciaccio, E., Acharya, R. (2019). A new approach for arrhythmia classification using deep coded features and LSTM networks. *Computer Methods and Programs in Biomedicine*, 176, 121-133.
- Zhang, D., Chen, Y., ve Meng, J. (2018). Synthetic well logs generation via Recurrent Neural Networks. *Petroleum Exploration and Development*, 45(4), 598-607. <https://doi.org/10.11698/PED.2018.04.06>.
- Zhang, J., Zhu, Y., Zhang, X., Ye, M., ve Yang, J. (2018). Developing a Long Short-Term Memory (LSTM) based model for predicting water table depth in agricultural areas. *Journal of Hydrology*, 561, 918-929. <https://doi.org/10.1016/j.jhydrol.2018.04.065>.
- Zhang, T., Song, S., Li, S., Ma, L., Pan, S., Han, L. (2019). Research on Gas Concentration Prediction Models Based on LSTM Multidimensional Time Series. *Energies*, 12(1), 161, doi.org/10.3390/en12010161.

**BİR TAŞ OCAĞINDA YAPILAN PATLATMALARIN DARICA-2 HES YAPISINA OLAN ÇEVRESEL ETKİLERİNİN
ELEKTRONİK ATEŞLEME SİSTEMİ İLE EN AZA İNDİRİLMESİ: ÖRNEK UYGULAMA**
*MINIMIZING THE ENVIRONMENTAL EFFECTS OF EXPLOSIONS IN A QUARRY ON THE DARICA-2 HES
STRUCTURE BY ELECTRONIC IGNITION SYSTEM: A CASE STUDY*

G.G.U. Aksoy^{1,*}, C.O. Aksoy², H. E. Yaman³, A. İlhan⁴

¹ *Hacettepe Üniversitesi, Maden Mühendisliği Bölümü
(*Sorumlu yazar: gulsevaksoy@hacettepe.edu.tr)*

² *Dokuz Eylül Üniversitesi Maden Mühendisliği Bölümü*

³ *Dokuz Eylül Üniversitesi Torbalı Meslek Yüksek Okulu*

⁴ *Soner Temel İnşaat ve San. Tic. A.Ş.*

ÖZET

Bu çalışmanın amacı, kapasite artışına gidecek olan bir taş ocağında yapılacak patlatma çalışmalarının olası titreşim, hava şoku, taş savrulması risklerinin çevreye ve özellikle Darıca-2 HES proje alanına olan etkilerini incelemek ve buraya herhangi bir olumsuz etki yaratmayacak kontrollü patlatma tasarımlarını belirleyerek uygulamalı olarak sonuçlarını değerlendirmektir. Projeye konu olan faaliyet sahasını ve Darıca-2 HES lokasyonu ve projeye konu olan sahaya yakınlığını görebilmek için 10.07.2021 tarihinde yerinde gözlem, inceleme ve değerlendirmeler yapılmış; iki farklı ateşleme sistemi ile iki adet patlatma gerçekleştirilerek patlatma kaynaklı sismik ölçümler (titreşim, dalga boyu, frekans), hava şoku ölçümleri yapılmıştır. Ayrıca jeoteknik amaçlı hat etüdü gerçekleştirilmiştir. Tüm saha ölçümleri ve deneyimlerin harmanlanması ile Darıca-2 HES yapısı ve çevresine hasar vermeyecek kontrollü patlatma tasarımı yapılmış ve başarıyla uygulanmıştır.

Anahtar Sözcükler: Patlatma, titreşim, HES, hava şoku, taş savrulması, elektronik ateşleme sistemi

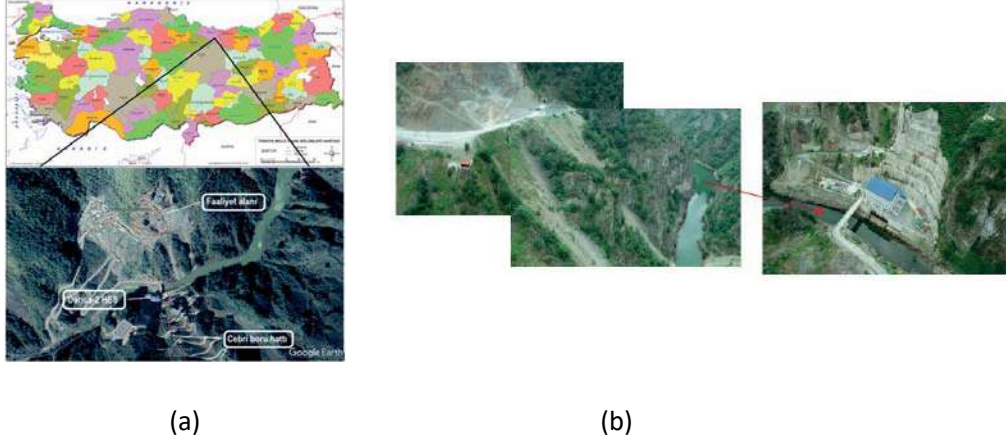
ABSTRACT

The aim of this study is to examine the effects of possible vibration, air shock, fly rock risks on the environment and especially on the Darıca-2 HES project area of the blasting works to be carried out in a quarry that will go to capacity increase and to determine the controlled blasting designs that will not cause any negative impact there. On-site observations, examinations and evaluations were made by us on 10.07.2021 in order to see the activity area that is the subject of the project and the Darıca-2 HES location and its proximity to the site that is the subject of the project; Two detonations were carried out with two different ignition systems, and seismic measurements (vibration, wavelength, frequency) and air shock measurements were made. In addition, a geotechnical study was carried out. With the blending of all field measurements and experiences, a controlled blasting design that will not damage the Darıca-2 HES structure and its surroundings has been made and successfully implemented.

Keywords: Blasting, vibration, HES, air shock, fly rock, electronic initiation system

GİRİŞ

Ordu ili, Mesudiye İlçesi, Darıca Mahallesi'ndeki bir taş ocağı sınırları içerisinde "Patlatmalı Taş (Bazalt) Ocağı Kapasite Artışı" planlanan sahaya ait yer bulduru haritası Şekil 1-a'da; Taş ocağının HES'e göre konumu, aradaki yol, vadi ve derenin lokasyonu ise Şekil 1-b'de verilmiştir.



Şekil 1.a) Ordu İli, Mesudiye İlçesi ruhsat sahası sınırları içerisinde faaliyet alanı, Darıca-2 HES ve Cebri boru hattının lokasyonları b) Taş ocağı, vadi, dere, Darıca-2 HES lokasyonunu gösteren drone fotoğrafı

10.07.2021 tarihinde Ordu ili, Mesudiye ilçesi Darıca mahallesi'nde bulunan Taş (Bazalt) Ocağında, "I-Blast" patlatma yazılımı yardımı ile kontrollü patlatma tasarımı yapılmış olup; yapılan tasarımın uygulandığı grup patlatması gerçekleştirilmiştir. Bu patlatmada, HES yapısı ve çevresinin hassasiyeti nedeniyle elektronik ateşleme yapılarak bu sistemin üstünlüğü ve güvenliğinden faydalanılmıştır.

Bu bildiriye, bu sahadaki gibi etrafında kritik ve önemli yapılar olan sahalarda elektronik ateşleme sisteminin sağladığı güvenlik, hassasiyet ve duyarlılık parametrelerinin getirdiği başarılı ve kontrollü patlatma uygulamasından bahsedilmiştir.

ELEKTRONİK ATEŞLEME SİSTEMİ İLE YAPILAN UYGULAMA

Elektronik patlatıcılar bir piroteknik bileşimin yanma hızına dayanan geleneksel piroteknik patlatıcılardan daha doğru zamanlama sağlar. Elektronik patlatıcının zamanlama doğruluğu yeteneği; patlayıcı enerjisinin daha verimli uygulanmasını, parça boyutu homojenliğini, hafriyat verimliliğinde artışı, hafriyat işlemlerinde maliyet tasarrufu, patlatmanın halk tarafından daha iyi kabul görmesini, patlamanın neden olduğu titreşimlerin ve hava şokunun kontrolünü, çevre stabilitesine katkısı sağlamaktadır (Cardu vd. 2013, Cardu vd. 2015). Proje konusu patlatmaların Darıca-2 HES yapısına herhangi bir titreşim, taş savrulması, hava şoku gibi olumsuzluklar yaratmaması için tasarladığımız kontrollü patlatmada belirlediğimiz gecikmelerin zamanlama doğruluğunu tam olarak sağlayabildiği için bu uygulamada elektronik kapsüller tercih edilmiştir. Bu sebeple de hem daha güvenli hem de 0 ile 15.000 milisaniye arasında 1'er ms'lik artışlarla gecikme ataması sağlamakta olan detEX elektronik kapsüller bu uygulamada kullanılmıştır. Elektronik kapsül sisteminin ortaya koyduğu esnek gecikme atama imkânı sayesinde sahada gerçekleştirilen patlatmada delik gecikmelerinin ortaya çıkarttıkları mükerrerliğin en aza indirilmesi amaçlanmıştır.

Bu uygulama sırasında alınmış koordinatlardan anlaşıldığı üzere, Darıca-2 HES ile elektronik grup patlatma sahası arasındaki mesafe 340 metredir (Şekil 2-a). Cebri boru hattı ile elektronik grup patlatma sahası arasındaki mesafe 400 m olarak belirlenmiştir (Şekil 2-b).



Şekil 2. a) Elektronik grup patlatma ve Darıca-2 HES arasındaki mesafe, b) Elektronik grup patlatma ve Cebri boru hattı arasındaki mesafe 10.07.2021

Ocakta yapılan elektronik ateşleme sistemi uygulamalarındaki patlatma tasarımı Çizelge 1’de verilmiştir (Patlatma Tasarımları ve Patlatma Kaynaklı Çevresel Etkiler Kılavuzu, 2018).

Çizelge 1. 10.07.2021 Ocakta yapılan elektronik ateşleme sistemi uygulamalarındaki patlatma tasarımı

Patern Kodu	Elektronik Ateşleme Grubu	
	Patlatma Kotu	536
Patlatma Tarihi	10.07.2021	
Delik Sayısı	73 adet	
Geometri	2,6m	x 3.30m
Dip Delgi	1 m	
Delik Çapı	89 mm	
Ort. Delik Metraji	10.5 m	
Patlayıcı Miktarı (kg)	2336kg toplam; 32kg/delik ortalama	
Yemleme Dinamiti (kg)	73 kg ; 1 kg/delik Emulsiyon bazlı kartuş dinamit	
Patlatma Saati	6:30:00 PM	
Yüzey Bağlantıları	Elektronik gecikmeler, bkz. Şekil 5	
Patern Koordinatları	X	37 T 403692.41
	Y	4508628.64
	Z	522m
Patern Litolojisi	BAZALT	

Şekil 3, patlatma deliklerinin hazırlanışını göstermektedir. Bu uygulamada KIRLIOĞLU Patlayıcı Firması tarafından üretilen, ilk yerli marka elektronik kapsüller ve ateşleme sistemi, detEX kullanılmıştır (Şekil 11).

Elektronik kapsül gecikmeleri, KIRLIOĞLU Firmasının lisanslı yazılımına sahip olduğu I-blast programı ile tarafımızca belirlenerek logger'a yüklenmiş ve sahada kapsüllere tanımlanmıştır.

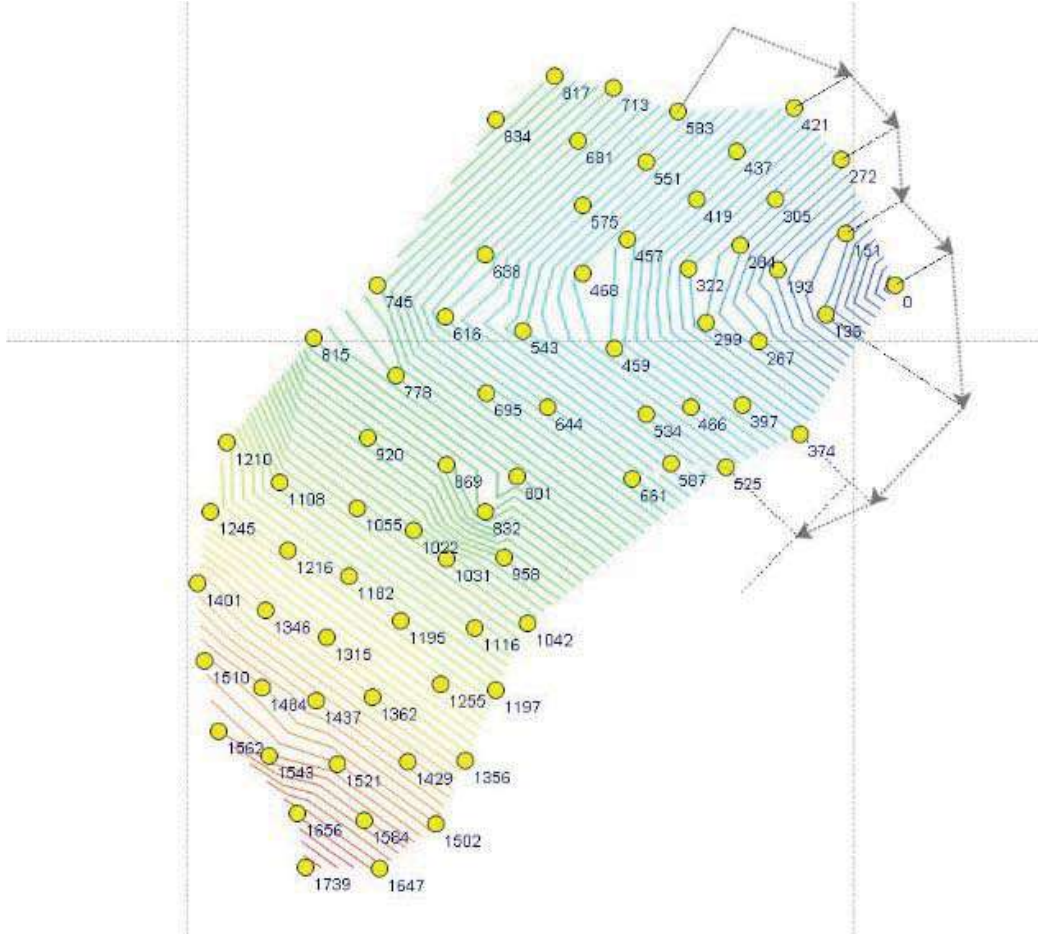


Şekil 3. Patlatma deliklerinin hazırlanışı



Şekil 4. Elektronik kapsüllerin saha uygulamasından bir görüntü

Şekil 5, deliklerin ateşleme sırası ve uygulanan elektronik gecikmeleri göstermektedir.



Şekil 5. Deliklere uygulanan elektronik kapsül gecikmeleri

Şekil 6’da ise sismografların ve mikrofonların yerleştirilmesini göstermektedir.



Şekil 6. Sismografların yerleşimi

Çizelge 2, elektronik ateşleme ile yapılan grup patlatmadan oluşan sismik dalgaların, sismograflarda ölçülen 3 bileşenli (T: transversal-yanal, V: Vertical-düsey, L: Longitudinal-boyuna, PVS: peak vectorel sum, vektörel toplam) parçacık hız ve frekans değerlerini göstermektedir.

Çizelge 2. Elektronik ateşlemeli grup patlatmasından oluşan sismik dalgaların, sismograflarda ölçülen parçacık hız ve frekans değerleri

Sismograf	Patlatma	Ölçüm Mesafe, m	T mm/s	V mm/s	L mm/s	PVS mm/s	Hakim Frekans Hz	Hava Şoku Pa	Hava Şoku dB
12269	Elektronik	86	18,16	22,48	17,65	27,76	20	25,00	121,9
14465	Elektronik	270	1,524	1,270	1,778	1,943	32,88	4,750	107,5
13638	Elektronik	365	-	-	-	-	-		
12270	Elektronik	447	0,127	1,397	0,254	1,408	24,00	0,750	91,48
micro	Elektronik	490	0,284	0,300	0,260	0,371	18,00	3,010	103,5

Bu patlatmada kullanılan toplam patlayıcı ve kapsül miktarları: 2263 kg Anfo, 73 kg kapsüle duyarlı patlayıcı (her bir adedi 1 kg) olmak üzere toplamda 2336 kg patlayıcı; 73 adet elektronik kapsüldür. Elektronik kapsüllerle yapılan patlatmanın drone görüntüsü Şekil 7’de verilmiştir. Drone videosundan anlaşıldığı üzere elektronik ateşleme sistemi ile gerçekleştirilen patlatmada hiç taş savrulması olmadığı gibi, titreşimler de planladığı gibi kontrollü patlatmaya yakışır düzeyde izin verilen limit değerlerin çok altında ölçülmüştür (Çizelge 2). Çizelge 2’deki elektronik kapsüllerle yapılan patlatmanın sismograflarda ölçülen yanal bileşen titreşim hızı değerleri ve hava şoku değerleri Şekil 8’de Google Earth de sismografların üzerine yazılarak gösterilmiş; böylece HES’e etkilerinin daha iyi anlaşılması sağlanmıştır.

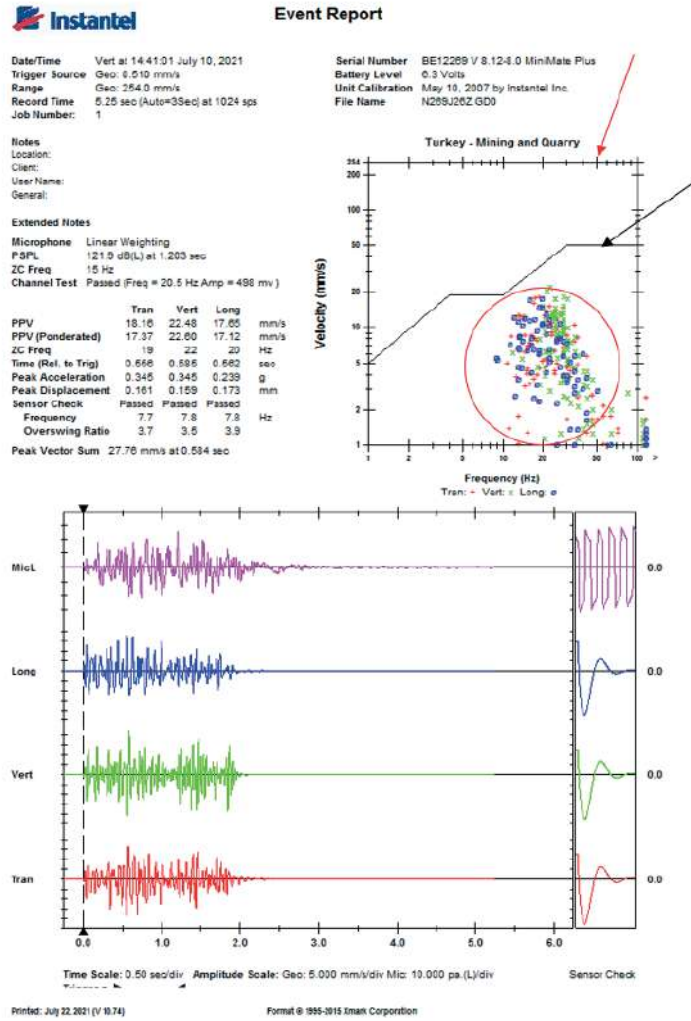


Şekil 7. Elektronik ateşleme ile gerçekleştirilen patlatma görüntüsü



Şekil 8. Sismograflardan ölçülen titreşim ve hava şoku değerlerinin Google Earth üzerinde gösterimi

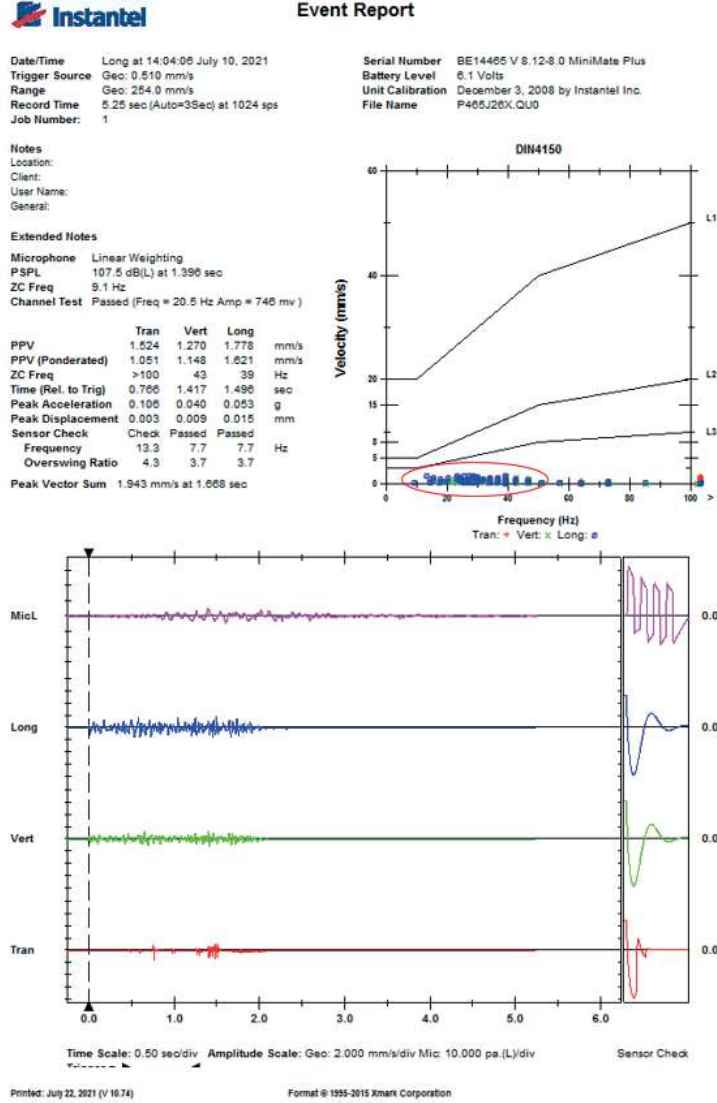
Her ne kadar Çizelge 2’de patlatma kaynaklı sismik dalgaların ölçüm noktasındaki titreşim hız değerleri 3 bileşende verilse de (yanal, düşey ve boyuna), Şekil 8’de sadece yanal bileşen değerleri harita üzerinde gösterilmiştir. Çünkü patlatma kaynaklı titreşimlerden yapılara ve şevlere en çok hasar veren yanal bileşenlerdir. Şekil 8’deki sismografların patlatmaya göre konumlarına ve mesafelerine dikkat edilirse, patlatmaya 86 m mesafede yol kenarına yerleştirilen sismografta 18.16 mm/s titreşim hızı ölçülmüştür. Bu sismograftan alınan sismik ve hava şoku değerlerini gösteren Şekil 9’da kırmızı ok ile gösterilen Türkiye titreşim limitleri grafiğine bakılırsa, hakim frekanslar 20 Hz civarında olduğu için 3 bileşendeki tüm titreşim hız değerlerinin (kırmızı elips ile gösterildi) hasar çizgisinin (siyah ok) altında olduğu görülebilir. Şekil 9’da verilen bir olay raporudur (event-report). Her sismograf ölçümü sonrasında bu olay raporu yazılımdan oluşturulur. Rapordan görüleceği üzere yanal (Tran), düşey (Vert), boyuna (Long) bileşende ve vektörel toplamda (PVS) titreşim hız değerleri bulunduğu gibi, sismografa eklenen mikrofona ölçülen hava şoku değeri (micL) ve üç bileşende sismik dalga formları da raporda yer almaktadır. Patlatmaya en yakın mesafede, yol kenarına yerleştirilen sismograftan alınan 3 bileşenli dalga formları incelendiğinde, kontrollü patlatma için planlandığı gibi 2,5 saniyede sönümlenen dalga biçimleri yaratılmıştır.



Şekil 9. Sismograf 12269'a ait olay raporu

Patlatma grubuna 270 m mesafedeki sismograf 14465'te ölçülen titreşim hızı yanal bileşende 1.524 mm/s dir ki bu değer Türk standartlarına göre olduğu gibi, en muhafazakar ve korumacı Alman standartlarına göre bile tarihi eserlere dahi hasar vermeyecek izin verilen değer olan 5 mm/s'nin altındadır (Şekil 10). Frekans açısından incelendiğinde ise, elektronik kapsülle yapılan ateşlemede, literatürde de denildiği gibi (Cardu, 2013; IME 2017; Kara vd. 2014; Mishra vd. 2017) daha yüksek frekanslı dalgalar oluşmuştur. Yüksek frekanslı dalgalar çabuk soğrulma özelliği taşıdıkları için titreşime neden olarak zarar verme özelliklerini yitirmektedirler. Bu açıdan, şevlerin duraylılığına tehdit oluşturmadan soğrulma yöneliminde olmaları istenilen bir özelliktir. Yapılar açısından değerlendirildiğinde de yüksek frekanslı dalgalar her zaman düşük frekanslı dalgalara tercih edilirler. Çünkü düşük frekanslı dalgalar yapıların doğal frekansı ile uyumlandıkları takdirde yapıları rezonansa sokarak daha büyük titreşime ve dolayısıyla hasara sebebiyet verirler. Şekil 10, sismograf 14465'e ait olay raporunu göstermektedir. Titreşim hızları bu raporda Alman DIN4150 standartına göre grafiklenmiştir. Kırmızı elips ile gösterilen üç bileşendeki titreşim hızları görüldüğü üzere tarihi yapılara dahi hasar vermeyecek limitlerin altındadır. Sismik dalgalar, vadi tabanına doğru sönümlenme eğiliminde olduğu için sismik dalgaların patlatmaya 270 m uzaklıkta sönümlenmesi bilimsel olarak şaşırtıcı değildir. S dalgalarının sudan geçemediği bilindiği için, elektronik kapsül gecikmelerini

sismik dalgaların derenin genişliğini geçemeyecek dalga boyu üretecek şekilde belirlememiz neticesinde derenin diğer tarafında bulunan HES yapılarına yakın mesafedeki sismograf 13638 hiç titreşim hızı ölçmemiş; sismograf 12270 ve cebri boru yanındaki sismograf micromate ise sırasıyla 0.127 mm/s ve 0.284 mm/s titreşim hızı kaydetmiştir. Bu son iki değer aslında titreşim hız eşik değeri olan 0.5mm/s'nin altındadır yani jeofonun sismik kayıt alma eşik değerinin bile altındadır. Normalde mikrofon aparatı takılı olmasaydı ölçüm almayacak olan bu iki sismograf, Mikrofon takılı olduğu için hava şokundan tetiklenerek açılmış ve kayıt almıştır. Şekil 19, 20 ve 21 sırasıyla sismograf 13338, 12270 ve micromate'in lokasyonlarını göstermektedir.



Şekil 10. Sismograf 14465'in olay rapor

JEOTEKNİK DEĞERLENDİRME

Taş ocağında farklı kaya kütlesi özelliği gösteren farklı lokasyonlarda 4 adet hat etüdü yapılmıştır. Şekil 11, bu hat etüdlerinden birine ait görseli vermektedir.



Şekil 11. Taş ocağında yapılan hat etüdü çalışmalarından bir görünüm

İncelenen bölgedeki kayaç malzemesi olan bazaltın sahada alınan numuneleri üzerinde yapılan kaya mekaniği deneyleri sonucunda ortalama porozitesi % 1.8, ortalama ağırlıkça su emme miktarı % 0.14, tek eksenli basınç dayanımı 40-80 MPa, poisson oranı 0.27, elastisite modülü 57 Gpa olarak belirlenmiş olup inceleme bölgesinde yapılan hat etüdüleri neticesinde elde edilen kaya parametreleri toplu olarak Çizelge 3'te verilmiştir.

Çizelge 3. Hat etüdüleri neticesinde elde edilen kaya parametreleri

Hat Etüdü No	Deformasyon Modülü (MPa)	Kohezyon (kPa)	İçsel Sürtünme Açısı (°)
1	1995,26	1130	19,39
2	1778,28	1061	18,39
3	1258,93	867	15,55
4	1122,02	806	14,64

SONUÇLAR

1. Patlatmaların çevresel etkilerinin değerlendirilmesinde kaya mekaniği deneylerine ihtiyaç duyulmamakla birlikte sahadan alınan numuneler üzerinde kaya mekaniği deneyleri yapılmış, jeoteknik hat etüdüleri yapılmış ve jeomekanik açıdan saha değerlendirilmiştir. Buna göre, iyi planlandığı takdirde sahadaki kaya kütesinin patlatmaların çevresel etkilerini (titreşim, hava şoku ve taş savrulması) kontrol edebilmeye izin verdiği belirlenmiştir.
2. İyi bir patlatma planlanması halinde, karayolu tüneline 120 m koruma mesafesi uygulanması şart değildir. Kaldı ki tarafımızca yapılan patlatmaya en yakın 86 m mesafedeki yolda herhangi bir olumsuz etki yaratacak titreşim, hava şoku, taş savrulması etkileri ölçülmemiştir. Karayolu tüneline ölçüm alınmamıştır (yol, HES, cebri boru hattında sismik dalga yayılım mekanizmasını anlamak için). Ancak yola çok yakın olan tünel girişinde de, literatüre göre izin verilen 200 mm/s limit değer düşünülürse, yolda ölçülen 18.6 mm/s titreşimin herhangi bir zarar vermeyeceği düşünülmektedir.
3. Hava şoku değerleri izin verilen 140 dB'in çok altında ölçülmüş olduğu gibi herhangi bir taş savrulması olmamıştır.
4. Ocak sınırları içerisinde olan yola, doğru patlatma tasarımı ile 30 m mesafeye kadar patlatma yapılabilir. Çok gerekli olması durumunda burada alınabilecek önlem patlatma sırasında yolun kapatılması ve patlatma örtüsü kullanılmasıdır.
5. Çok eski yıllarda ve hangi saha ve kayada üretildiği bilinmeyen, kullanılan parametrelerin belirtilmediği formüllerle titreşim, hava şoku, taş fırlaması vb. etkilerin belirlenmesi bilimsel gerçeklikle bağdaşmamaktadır.
6. Bilinenin aksine, 1 tek delik patlatılarak alınan sismik sinyallerin modellenmesi ile çevreye zarar vermeyecek 400-500 delikli grup patlatmaları planlanabilir. Bu bilimsel gerçekle ilgili uluslararası patentler, uluslararası yayınlar tarafımızca yapıldığı gibi literatürde de bolca bulunmaktadır. Burada önemli olan delik sayısı değil doğru patlatma tasarımı yapılması ve bu tasarımın doğru patlatma elemanları ile gerçekleştirilmesidir.
7. Yapılan çalışmada olduğu gibi doğru patlatma tasarımı yapıldığında ve bu tasarımın sahada hassasiyetle uygulanması halinde sahada yapılacak patlatmaların çevre yapılarına, yol, baraj tünel vb. hasar vermeyeceği; çevresel kirlenmeyi tetiklemeyeceği, yeraltı suyu akış rejimine dikkate değer etkisi olmayacağı düşünülmektedir. Çünkü bu yapılan çalışma ölçülebilir ve denetlenebilir sonuçlar içermektedir; herhangi bir formülden ya da yaklaşımdan üretilmemiştir, tamamen sahanın kendi parametrelerini içermektedir.
8. 85 delikli patlatmanın etkilerini görmek için 85 delikli patlatma yapmaya gerek yoktur. Tek delik patlatması ile de sismik dalga yayılım mekanizması öğrenilir ve 85 delikli, çevreye zarar vermeyecek kontrollü patlatmalar tasarlanabilir. 10.07.2021 tarihinde sahada 73 delikli elektronik ateşleme ile yapılan kontrollü patlatmanın titreşim, hava şoku değerlerinin, yol, HES yakını, cebri boru yakınında eser miktarda ölçülmesinden dolayı bilimsel olarak söylenebilir ki, 85 delikli grup patlatmaları, verilen paterne ve patlayıcı ve patlatma elemanlarına uyulması durumunda Darıca-2 HES yapısına, cebri borulara, tünel girişlerine herhangi bir çevresel olumsuz etki yaratmayacaktır.

TEŞEKKÜR

Bu çalışmada kendilerine ait yerli üretim Elektronik ateşleme sisteminin kullanılmasına imkan tanıyan Kıriloğlu Patlayıcı Firmasına ve sahada patlatma operasyonunda yer alan firma mühendisi E. Taylan Edis'e teşekkür ederiz.

KAYNAKLAR

- Cardu M., (2013), "A Review Of The Benefits Of Electronic Capsüls", RemRevistaEscola de Mines.
- Cardu M, Mucci A., Uyar GG., (2015), "Investigating The Effects Of Benchgeometry And Delaytimes On The Blastinducedvibrations İn An Open-Pitquarry", GEAM, Vol. 144. 45-56.
- DIN 4150-3. Structural vibration-effects of vibration on structures. <http://webstore.ansi.org/>; 1999.
- IME, (2017), "EBIS Guideline, Electronic Blast Initiation System".
- Kara S., Adamson W.R., Reis W.J., Trowse I R., (2014), "The Latest Generation Of The Electronic System Enhancedsafety And Productivity". *Proceda Engineering, Vol. 83*, 432- 440.
- Mishra A.K., Nigem Y.K., Singh D.R. (2017), "Controlled Blasting in a Limestone Mine Using Electronic Detonators", Journal of Geological Society of India.
- Patlatma Tasarımları ve Patlatma Kaynaklı Çevresel Etkiler Kılavuzu, (2018), <http://ced.csb.gov.tr/kilavuz-rehber-form-i-320>

CHARACTERIZATION OF PHOSPHATE DUST FROM DJBEL-ONK, NORTHERN ALGERIA

M.I Zohir ^{1,*}, B. Assia ¹, B. Said ¹, C. Abdessalam ¹

¹*Badji-Mokhtar University Annaba, Laboratory of Mineral Processing and Environment "LAVAMINE"*
(*Corresponding Author: mektizohir@yahoo.fr)

ABSTRACT

Dusts are solid particles mainly due to industrial activity and especially mining activity. Their size is therefore reduced and placed on a microscopic or even nanoscopic scale. In the literature, different terms are often used indiscriminately to define this type of pollution among them: aerosols are formed of solid or liquid particles of size less than 100 micrometres. "Black smoke" are carbon particles with a diameter of less than 05 µm up to about 0.1 µm. In Algeria, the SOMIPHOS plant in Djebel El Onk is specialized in the exploitation and treatment of phosphates, dust emissions are quite high at the level of the quarry and the treatment plant, because of the use blasting and the preparation of phosphate by the dry mechanical method. The main aim of this work is to characterize the dust emitted due to the exploitation and processing of phosphate ores. The results obtained show that the dust level exceeds the international standard (1g/m²/day), the size and size distribution of the particles is determined by the laser particle size, the FRX and the DRX are used to determine the chemical composition and mineralogical. The level of heavy metals in dust was evaluated by the analysis of Atomic Absorption Spectrometry.

Keywords: Phosphate dust, PM, airborne pollution, Algeria, Djbel –Onk plant, environment

INTRODUCTION

The Djebel El Onk SOMIPHOS plant; specializes in the exploitation and processing of phosphates, it is located in the south-east of Algeria, 100 km from the Wilaya of Tébessa and 20 km from the Algerian-Tunisian border (Fig. 01). It is implanted within in the framework of treating and producing a phosphate rich in P₂O₅, intended for various industries; such as the ASMIDAL plant located in the wilaya of Annaba either by rail or by road transport. The total production is in the order of a few million tonnes which is exported as raw material to several countries around the world (BEZZI N. 2005).

Due to the quality of the phosphate mining, is currently focused on Kef Essenoun. In this place ; there are two different colors of phosphate which are dark color (gray) and light color (beige).

The Djebel El Onk area consists of two parts: an open pit mine and the phosphate processing plant (Nouioua et al. 2016).

Like other human activities, the mining industry corresponding to the Djebel Onk mining complex; today poses very acute environmental problems, such as the emissions of very fine and sometimes-toxic dust, because it contains metals trace elements, which can cause pollution of air, soil and water and they can create many regional or global problems for living beings and for humans in the event of respiration.



Figure 1. Location of Djbel-Onk complex

MATERIAL AND METHODS

The phosphate dust sample are obtained during collection at several points on the site, such as the waistline, the mechanical preparation workshop; the edges of the transport paths, the processing plant and finally the loading wagons and trucks silos. To achieve the objective of this work; several tests have been carried out. Beginning with the chemical composition by the FRX, the mineralogical composition carried out by XRD, the particle size distribution carried out by the laser particle size distribution, finally the shape of the particles is analyzed by the SEM imaging.

Chemical Composition

To determine the origin of the PM collected, we carried out chemical analysis of the samples by the XRF; all the samples are mixed; homogenized and analyzed. The result of the chemical composition of the dust collected, are compared with that given by the laboratory of the Djebel Onk phosphate complex (Table 1).

Table 1. Chemical composition of PM phosphate samples

Elements	P ₂ O ₅	CO ₂	SO ₃	CaO	MgO	Fe ₂ O ₃	Al ₂ O ₃	Na ₂ O	K ₂ O	SiO ₂	F	Cl (ppm)
PM of phosphate	29.31	6.93	2.80	50.8	1.67	0.32	0.33	1.27	0.071	2.16	3.56	553
Djebel-Onk phosphate	30.22	6.86	3.00	52.3	0.83	0.12	0.50	1.35	0.078	3.21	4.02	449

The comparison of the values of the composition of PM of phosphate; shows a correlation with the chemical composition of Djebel Onk phosphate. These results clearly prove that the PM collected in the installations is generated by the process of unloading, storage and unloading of phosphate.

Mineralogical Composition

X-ray diffractometer (XRD) analysis of the different particle size fractions of phosphate dust has identified the following main mineralogical phases (Figure2.):

1-) Phosphate elements of the apatitic class such as: Carbonate apatite $Ca_{10}(PO_4)_6$, Carbonate hydroxyapatite $Ca_{10}(PO_4)_3(CO_3)_3(OH)_2$, Fluorapatite $(Ca_5(PO_4)_3F)$, Carbonate fluorapatite $Ca_{10}(PO_4)_5CO_3F_{1.5}(OH)_{0.5}$, hydroxyapatite $Ca_5(PO_4)_3(OH)$ and Phosphate hydrate (NETTOUR D. 2018).

2-) Elements of gangue: Are represented mainly by carbonate and siliceous minerals such as dolomite $CaMg(CO_3)_2$, silicas in the form of Calcite $CaCO_3$, quartz SiO_2 and gypsum $CaSO_4$.

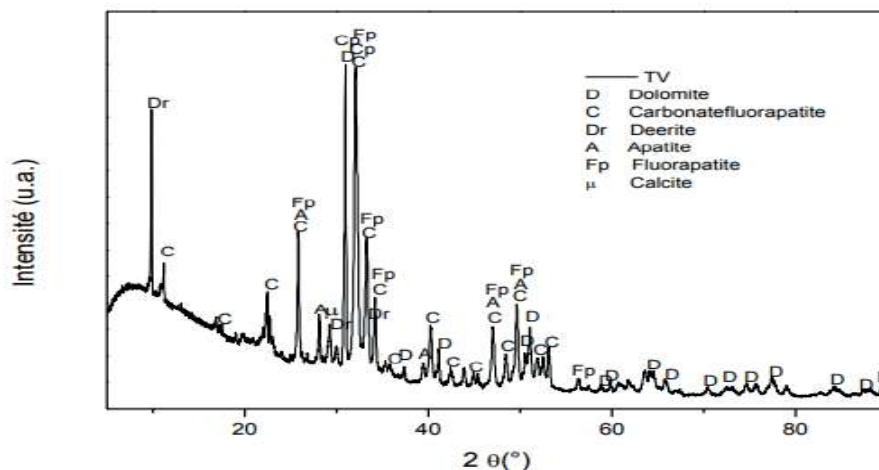


Figure 2. DRX du minerai de la poussière de phosphate

Determination of Particle Size Distributions

The particle size distribution of the phosphate dust sample; is obtained from the analysis by laser diffraction (Fig. 3). The result of the analysis showed that, more than 90% of the particles with a smaller diameter at 118μm; 50% of the particles with a diameter less than 13.3μm, and 10% of the particles have a diameter of less than 5.5μm.

These results favour deep pulmonary deposition. PM10 (particles with an aerodynamic diameter of less than 10 μm) are of major concern today, as they are small enough to penetrate deep into the lungs. Particle size can behave on the human body as follows:

Chest dust: mass fraction of inhaled particles entering the larynx (<30 μm);

Alveolar dust: mass fraction of inhaled particles, penetrating the non-ciliated airways (<15 μm).

These fractions are included in the ISO 7708 standard and in the Afnor X 43-100 standard.

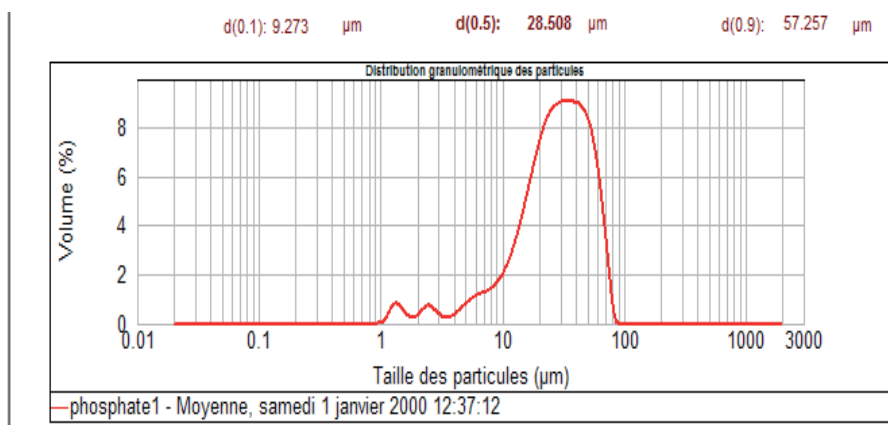


Figure.3. PM particle size by laser diffraction

Phosphate PM Morphology

The shape of PM in general can promote flight and decrease the sedimentation rate of a particle: a flat particle behaves like a leaf during its fall and will therefore settle more slowly than a spherical particle (Imen Bel Hadj 2013). The fall speed is a function of the aerodynamic diameter. PM of phosphate captured at the port of Annaba; have different morphology and irregular shape (Fig. 4).

The angular shape of the particle surface; is mainly due to the mechanical preparation of phosphates at the Djebel Onk plant, unlike natural particles where the surface is smooth and the grains are spherical in shape. For particles of irregular shape, relative movement becomes difficult due to the presence of more points of contact between them. If they are elongated and hook-shaped particles, it will be more complicated because they tend to form bridges by interlocking particles.

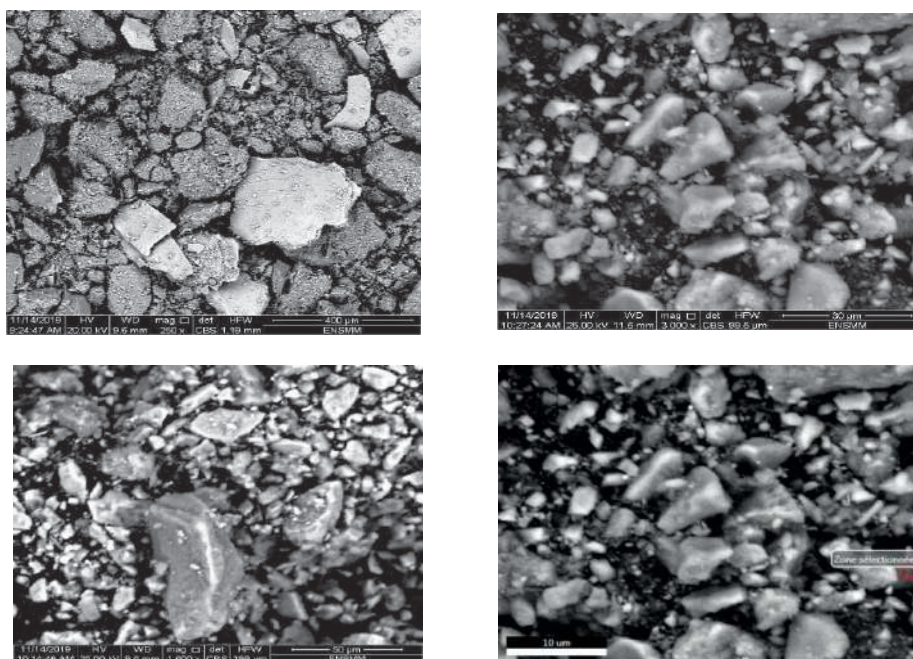


Figure 4. Phosphate dust morphology, by X-ray microanalysis coupled with a scanning electron microscope (SEM / EDX)

Heavy Metals Content in Phosphate Dust

From a purely scientific and technical point of view, heavy metals can be defined as: any metal with a density greater than 5 g/cm³. Any metal with a high atomic number, generally higher than that of Sodium (Z = 11), presenting a danger to the environment and to humans. Any metal that can be toxic to biological systems. In environmental sciences, the heavy metals associated with the concepts of pollution and toxicity are generally: arsenic (As), cadmium (Cd), chromium (Cr), copper (Cu), mercury (Hg), manganese (Mn), nickel (Ni), lead (Pb), tin (Sn), and zinc (Zn). In our study, the composition of heavy metals and some trace metallic elements was determined by, atomic absorption spectrometry (Table 4).

Table 2. Daily and surface concentration of metals detected ($\mu\text{g}/\text{m}^2/\text{d}$), German standardization.

Element	Cd	Zn	Pb	Cu	Cr	Ni	Mn	Hg	Co	Sb
Limit $\mu\text{g}/\text{m}^2/\text{d}$	2	400	100	100	250	15	15	1	15	100
S1	8.3	113.2	15.8	23.4	122.2	13.5	11.3	3.2	2.2	12.4

The results of the metal concentrations measured for the eight stations; presents different values, those, which are higher than the German limit values, and those that are lower. We observe that the guide values for the metals of Cadmium (Cd) and mercury (Hg); have been exceeded. The limit value of Cd is $2 \mu\text{g}/\text{m}^2/\text{d}$, on the other hand the recorded values varied between 8.7 and $1.2 \mu\text{g}/\text{m}^2/\text{d}$.

The limit value of Hg according to the German standard, is $1 \mu\text{g}/\text{m}^2/\text{d}$, but the results of the latter's analyzes vary between 3.2 and $0.3 \mu\text{g}/\text{m}^2/\text{d}$ in the eight measuring stations. The values of Zn, Pb, Cu, Cr, Ni, Mn, Co and Sb are below the limit of quantification. The points most exposed to fallout from the site have the highest levels of heavy metals.

Recommendation

Usually to control dust emissions, several methods can be applied. For phosphate dust, the method is special, because the product must not be touched by humidity, otherwise it will be contaminated, and therefore it is strictly forbidden to spray the dust with water especially at the unloading points of trucks and wagons. The most effective methods for reducing phosphate dust are:

1. Complete cover of the product conveyor belts
2. Unloading of trucks and wagons in well closed and airtight sheds, to prevent dust from escaping outside the installation
3. Spray the road with water Complete cover of the product conveyor belts
4. Unloading of trucks and wagons in well closed and airtight sheds, to prevent dust from escaping outside the installation.
5. Spray the road with water to prevent dust from flying away during the passage of trucks.

CONCLUSIONS

Certainly, the effects and consequences of these emissions on man and the environment are disastrous. It is probable that in the future an in-depth study will be carried out on the effects of these emissions on man, the environment, fauna and flora.

Based on the results obtained in this study, the following conclusions can be listed:

1. The chemical composition of the PM determined by the XRF, shows a correlation between the chemical composition of the PM samples from the samples and the chemical composition of the phosphate from the Djebel-Onk plant.
2. The particle size distribution of PM, determined by laser diffraction, show that more than 90% of particles with a diameter less than $118\mu\text{m}$, 50% of particles with a diameter less than $13.3\mu\text{m}$ and 10% of particles have a diameter less than $5.5 \mu\text{m}$. These results promote deep lung deposition upon inhalation of PM by humans.
3. PM of phosphate captured; have morphology and irregular shape of different size. The angular shape of the particle surface; is mainly due to the mechanical preparation of phosphates at the Djebel Onk phosphate plant, unlike natural particles where the surface is smooth and the grains are spherical in shape.
4. The values of Zn, Pb, Cu, Cr, Ni, Mn, Co and Sb are below the limit of quantification. The points most exposed to fallout from the site have the highest levels of heavy metals.

REFERENCES

- Ben Hamla, F., Ameziane, N., & Morakchi, K. (2015). Etude physico-chimique et minéralogique d'un matériau naturel.
- Benselhoub, A., Kanlı, A. I. (2020). Environmental Impacts of Air Pollution on Human Health in Annaba Region (Northeast of Algeria). In *Toxic Chemical and Biological Agents* (pp. 209-216). Springer, Dordrecht.
- Benselhoub, A., Kharytonov, M., Bouabdallah, S., Bounouala, M., Idres, A., & Boukelloul, M. L. (2015). Bioecological assessment of soil pollution with heavy metals in Annaba (Algeria). *Studia Universitatis "Vasile Goldis" Arad. Seria Stiintele Vietii (Life Sciences Series)*, 25(1), 17.
- Benselhoub, A., Kharytonov, M., Bounouala, M., Chaabia, R., & Badjoudj, S. (2015). Estimation of soil's sorption capacity to heavy metals in Algerian megacities: case of Algiers and Annaba. *INMATEH-Agricultural Engineering*, 46(2).
- Bezzi, N., Aifa, T., Hamoudi, S., & Merabet, D. (2012). Trace elements of Kef Es Sennoun natural Phosphate (Djebel Onk, Algeria) and how they affect the various Mineralurgic modes of treatment. *Procedia Engineering*, 42, 1915-1927.
- Chiazze, L., Watkins, D.K. et Fryar, C., 1992: «A case-control study of malignant and non-malignant respiratory disease among employees of a fibreglass manufacturing facility», *ibid.*, vol. 49, pp. 326-331.
- Giannadaki, D., Pozzer, A. et Lelieveld, J. (2014). Modélisation des effets mondiaux de la poussière du désert en suspension dans l'air sur la qualité de l'air et la mortalité prématurée. *Chimie et physique atmosphériques*, 14 (2), 957-968.
- Henni-Chebra, K., A. Bougara, and A. Halla (2009). "IMPACT DES RETOMBEES DE POUSSIERES CAUSEES PAR L'INDUSTRIE CIMENTIERE SUR L'ENVIRONNEMENT."
- Khadidja Henni-Chebra, Abdelkader Bougara, El-Hadj Kadri (2011). Détermination du niveau d'empoussièrement engendrée par la fabrication du ciment. XXIXe Rencontres Universitaires de Génie Civil. Tlemcen, 29 au 31 Mai 2011.
- Kharytonov, M., Benselhoub, A., Klimkina, I., Bouhedja, A., Idres, A., & Aissi, A. (2016). Air pollution mapping in the Wilaya of Annaba (NE of Algeria). *Mining Science*, 23.
- Merlen, R. (2015). La biosurveillance: outil de surveillance de l'impact sur l'environnement des émissions atmosphériques industrielles et d'évaluation des risques sanitaires. 2268-3798.
- Nordberg G, Jin T, Bernard A, Fierens S, Buchet JP, Ye T. (2002). « Low bone density and renal dysfunction following environmental cadmium exposure in China » *Ambio*. 31(6):478–481.
- Orlowski C, Piotrowski JK, Subdys JK, Gross A. (1998). « Urinary cadmium as indicator of renal cadmium in humans: an autopsy study » *Hum Exp Toxicol*;17 (6):302–306.
- Romdhane, S. B. (2017). Effets du climat et de la pollution de l'air sur la santé respiratoire à Tunis (Doctoral dissertation, Université Sorbonne Paris Cité ; Université des lettres, arts et sciences sociales-Tunis I. Faculté des sciences humaines et sociales).
- Roy, D., & Singh, G. (2014). Source apportionment of particulate matter (PM10) in an integrated coal mining complex of Jharia coalfield, Eastern India: A review. *International Journal of Engineering Research and Applications*, 4(4), 97-113.

COMMUNITION VS. LIBERATION: A COMPARATIVE ANALYSIS OF THEORIES AND PRACTICES ON COMMUNITION FROM INVESTMENT POINT OF VIEW, A CASE STUDY FROM URUGUAY

I.Tarjan^{1,*}, D. Segovia¹, H. Ferrizo¹

¹ *Universidad de la Republica, Uruguay, Centro Universitario Region del Este*
(*Corresponding author: ivan.tarjan@cure.edu.uy)

ABSTRACT

Long been the discussion on different comminution techniques to achieve desired granulometry for ores and rocks for their application and/or metallurgical use with emphasis on energy saving, environmental issues and efficiency. Energy plays an important role knowing that the comminution requires the biggest part of energy supply in the processing industry, the economy (amortization) have often been left out or paid little attention when decision is made. Comminution machines use different phenomenon. From the energy side it is necessary to define working indices to establish the capacity of the machine. Sometimes, liberation is not a need, while others look for the highest liberation possible. However, much depends on the buyer's requirements of the material run out of the plant. If the "product" should be transported for further processing than the grain size will depend on logistics, price, etc. more than professional goals. The two approaches lead to some antagonistic questions and economic considerations. In general, the lower the grain size the higher the liberation, superfine is not economic to transport. Also, the higher the concentration grade the higher the price, but the grade depends on the granulometry. This paper aims to summarize recent innovations with suggestions on prioritizing operations through the case study in a magnetite ore deposit in the North-East part of Uruguay.

Keywords: Crushing, grinding, liberation, circuit improvement, energy efficiency, economy

INTRODUCTION

In the recent years a very promising iron-ore resource was found in the North-East part of Uruguay. Exploration and prospection were done in a very accurate and professional manner and probed a rich magnetite deposit, so the elaboration of a business plan and the procedure for the environmental and extraction permissions acquisition was started.

During that time the processing plant design establishment arose different issues regarding the beneficiation of the material such as concentration grade and grain size. It turned out that there are several problems to satisfy both of needs on the most economical way of separation, especially when the product price is highly volatile.

THE OBJECTIVE

According to the "buyer's specification" the product should satisfy several conditions, however, from our point of view there are two that has specific interests. Namely: the grain size cannot exceed 125 microns more than 7% (this is the condition of transportability) whereas the concentrate should reach 62% minimum (quality condition).

It worth to mention that the quality is denominated in percentage of Fe content that can lead to some misunderstanding (however it is a technical issue), simply because of the composition of hematite

itself. If we want 62% Fe content the product should be more than 100% pure hematite, clearly impossible. Therefore, the quality is meant in hematite (FeFe2O3) content. In general, the mineral is composed of magnetite (25-30%), quartz and clinopyroxenes.

The ore in general is considered to have a natural granulometry small, within 45-250 microns with exception of those collectibles that can reach of 2 cm crystals. Therefore, from the beneficiation point of view, it is very important to liberate the particles as much as possible, meanwhile the raw magnetic separation needs only an exposure of it. This is to say it is sufficient to make part of the surface of the particle free to be able to interact in the magnetic field. Consequently, during the crushing process it is possible to save considerable energy to put into it sacrificing the quality as the particles will contain big amount of additional materials and minerals that are gangue and dilute the concentration.

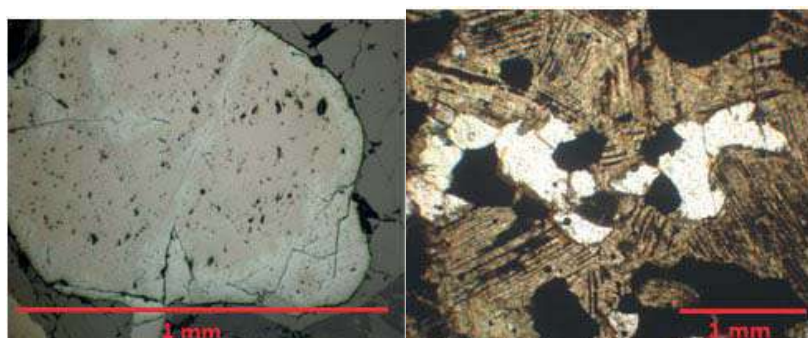


Figure 1: Show big crystals of magnetite at the size of 1-3 mm that is very favorable to all the beneficiation process.

On the other hand, with total liberation we have to consider a product size of around 75-100 microns at least, which is the common practice when the briquetting plant is located right next to the beneficiation plant. It might be an option to install a compacting machine to aggregate the powder to improve air quality and handling issues. The actual case does not require grinding to this size theoretically as the petrography shows big crystals.

However, tests made on samples do not support this idea. At the grain size range of 1-10 mm the maximum concentration reached was 41,56%, meanwhile in the range of 180 microns 63% was obtained with magnetic dry separation in our laboratory. (It is supposed that a wet separation in the lower grain size would result even better outcome, but for different reasons this method is not considered to be viable.)

Table 1. Test results at 1-10 mm grain size

Mineral separation process	Fe2O3 percentage	Productivity percentage	Mass recovery percentage
Raw ore - Feeding material (crushed to the size of -2 mm)	27.30	100	100
Result material – Concentrate material	41.56	56.78	86.42
Tailing	8.58	43.22	13.58

Table 2. Test results at a 180-micron grain size

Mineral separation process	Fe2O3 percentage	Productivity percentage	Mass recovery percentage
Raw ore - Feeding material (crushed to the size of -2 mm)	33.61	100	100
Result material – Concentrate material	62.73	50.09	95.03
Tailing	4.38	39.3	4.09

This clearly shows that there must be an inefficient liberation during the comminution process, breakage post probably occurs within the homogeneous grain within the particle instead of through the boundaries of a heterogeneous particle. (Michaud, 2016)

It is well known that higher the quality higher the price can achieve, so it is worthwhile to look into the crushing and grinding procedures as places of expenditures in a short and a long term (capital expenditure vs. energy consumption and maintenance costs) in regards of the benefits on product price, so ROI.

THEORIES AND PRACTICES OF COMMINUTION FROM THE EFFICIENCY POINT OF VIEW

There were several attempts to establish a solid theoretical background on comminution both crushing and grinding. None of them works perfectly, so we have to assume that this does not exist.

The main reason is the complexity of the process especially of grinding. The variables are numerous, there effect on the processes varies as well. Explaining grinding makes it even worth when the grinding medium is added into the consideration and has to be modelled the system entirely.

As there is no applicable solid based theory of comminution processes most of the working principles were deduced from experimental results, empirical way, most recently with the aid of statistical methods and nowadays utilizing Artificial Intelligence. Nevertheless, all of them is based on the historical results looking for different levels of approval and relationship among the “traditional” models.

Considering the three basic laws of comminution as by Rittinger, Kick and Bond all of them is widely appreciated and used in the practice, mainly for the crushing and grinding machine design and production.

Models were made in several manners that describe, measure and conclude results of different factors of fractions. For example, test and experiments of single particle breakage, particle bed formation on surfaces both on the medium and the linings and how these affect the outcome of the process and the energy consumption. An excellent summary of all of them can be found here. (Michaud, 2016)

There are promising experiments on adding extra energy before the comminution process by ultrasound handling that shows significant energy savings. (Gholami et al., 2020).

It seems like the energy density of the particle is most important factor!

In general, the energy input discussed in all theoretical scenes are supposed to use for the comminution, very little considered as waste. However, it is a very important part of recent investigations and attempts on improvements to get a better-quality product at a lower energy input with lower carbon emission.

The waste of energy is result of heat, electromechanical resistance and noise, etc. The heat mainly comes from two sources: the inner source is the release of the elastic energy accumulated in the particle at the moment of breaking apart, the outer one is the friction within the particles and/or within particles and grinding medium (these partly might contribute to the grinding process) and/or within the grinding medium only (that purely is waste if the process does not result better quality at higher temperatures). An overall 1% of energy input causes breakage (Borg et al. 2020).

Important work was done on the investigation to improve the efficiency of the comminution by experiments, using different machinery like HPGR as a highly effective solution, eliminating wet processes to improve resource savings and usage, a priori feed preparation, improving on environmental issues and sustainability (Jankovic et al., 2016; Baawuah et al.,2020; Komar Kawatra 2006; Weerasekara et al., 2013)

Something New

Because of the above one can get to a conclusion that something is missing, and process should be looked at in another way.

If all of the comminution techniques attempt to augment the energy density of the particle and it is approved working well but could not get to the level sufficiently high, it would be worth to investigate.

Conventional comminution uses compression – slow or impact – sheer forces. In primary crushing the slow compression is applied mainly (jaw crusher, roll crushers), secondary crushing applies sheering and impact, while grinding is a very complex and sophisticated way to level up the energy density. Simplifying a bit radically, the energy input comes from transfer of kinetic energy into potential energy in the case of impact crushers and cylindrical mills like ball mill or rod mill. Augmenting the energy density inside the particle a priori to crushing and grinding makes these latter more efficient and the liberation is even better. This suggests that achieving its critical level when a particle falls apart should be possible by one single step and it can happen at a considerably good liberation factor, too. As a matter of fact, there is nothing new in it, the first mention looks back around 55 years (Wiegl et al., 1967).

The potential energy is given by – simplified – the particle/grinding medium particle mass. It can be measured and/or calculated from the uniaxial, tri-axial compression tests, a drop ball test or other experiments. It cannot be found literature to test equally high force or tension resulted by the transfer of the kinetic energy that can provide the mass of the particle itself. Instead, it seems like the energy accumulation without relaxation time generates resonances that differs regarding the material composition and/or physical properties, suffering reflections and deformation on the particle contact surfaces resulting great tensions than final disintegration (Borg et al., 2020). Even further, how it can be continuously increased to maintain the comminution ratio high when a particle loses mass during the process.

The idea can be to apply the force necessary to break a particle at the force given from a uniaxial compression test and calculate the energy required. Equaling it to a kinetic energy that is a result of the mass of a particle and its velocity and find a way to achieve this in a crusher or mill and test whether it works. Other tests can be carried out with lower velocity but repeated high energy impacts as it is suggested from a “pulsing” compression test, so saving energy on this way might also be possible. (Borg et al., 2016)

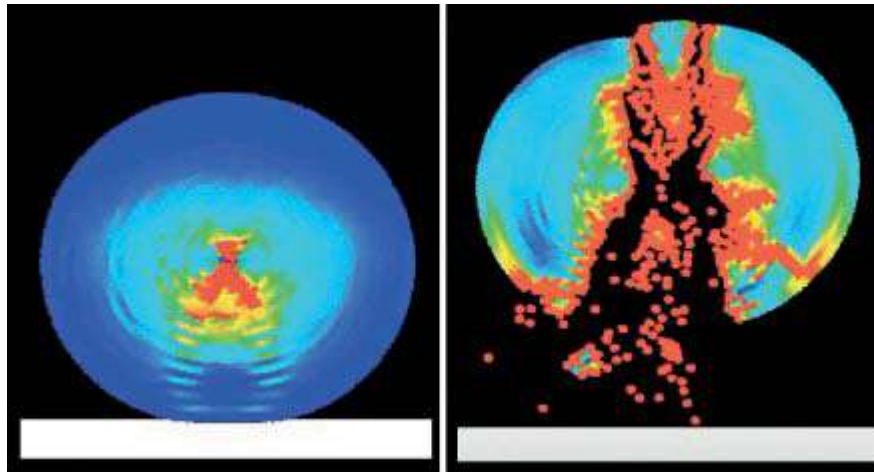


Figure 2. Numerical modelling illustration (by courtesy of Paul Cleary CSIRO) of a high velocity impact of a round particle to a solid tool at the moment of contact (left) and later disintegration (right)

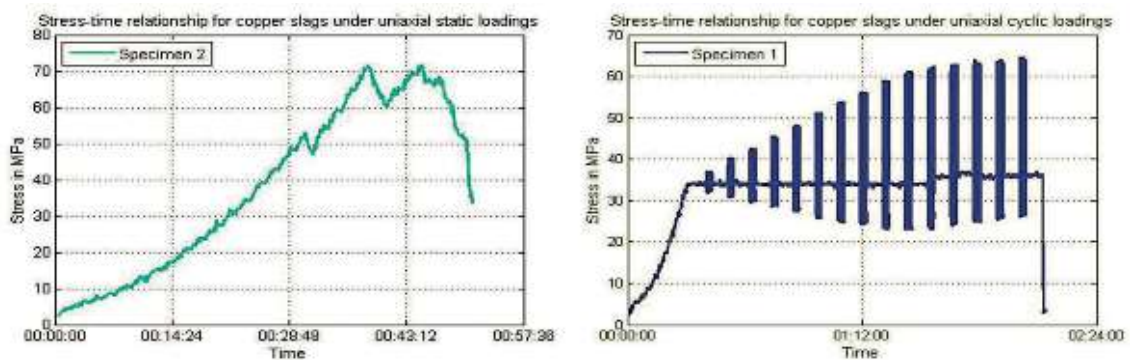


Figure 3. Results of uniaxial dynamic load test (right) and pulsated loads in several steps (left) (Borg et al.,2016)

Furthermore, in case the outcome is promising, increase the efficiency by repeat these events after constructing a model (numerical modelling, or other computational technique).

Given the above data and/or model the theoretical energy consumption can be calculated as well.

Exactly this is what happened with one of the German machine producers to be able to provide a versatile product for a versatile production.

The equipment is tested, run as pilot project in several mining sites and the efficiency is surprisingly good. The product can be graded by grain size and the liberation factor can reach to almost 100%. (Borg et al., 2020)

THE ECONOMY

Considering the above-mentioned issues and want to plan a crushing and grinding plant the capital investment comes into the discussion.

A general beneficiation plant starts with the crushing than the grinding circuit, then come all the processes to produce products running out of the plant. The energy consumption takes the highest part of the plant, as well as the capital expenditure (machine prices and installation, construction work takes considerable percentage from the entire investment.

Planning such a plant there are basic engineering practices and assumptions like i) the fines produced in every step of crushing/grinding should be taken out, ii) the reduction ratio should be established according to the minimal loss possible (fines), iii) energy consumption in efficiency/effectivity should be considered as priority. From the point of view energy efficiency, the first consideration is vital. The fine in the system causes most of the loss in the conversion of the energy input into effective energy to breakage.

It has to be noted, however, that in some special cases fines are a must in order to make the comminution more effective, such cases are when there must “build” a layer of material on the grinding elements (Michaud, 2016 (1)).

Aiming to improve the Return of Investment there are two ways as general: Lowering the capital expenditure and/or augmenting the incomes meanwhile saving on running costs (energy and maintenance). Might there be an equilibrium!

In our specific case the planned beneficiation plant consists of:

Option 1.	Option 2.
Jaw crusher	Jaw crusher
Cone crusher	Cone crusher
Multi-cylinder cone crusher	Multi cylinder crone crusher
Ball mill	Vertical mill
Magnetic separation	Magnetic separation

The planned CAPEX on these layouts is estimated to:

2.000.000 USD	5.600.000 USD
Considering replacing the secondary crushing and the grinding circuit to one of the machines described it would augment the CAPEX to 6.000.000 USD	

Calculating the running costs on this equipment would result:

Energy savings: 1.700 kWh in case of option 1, and 1.600 kWh in case of option 2.

The price premium for higher quality products can be considered as between 10% and 60% of standard price.

Maintenance costs should be considered as constant based on the initial expenditure, therefore the higher investment should be covered by the energy saving and the income growth.

The planned capacity is 100 t/h concentrate product in a normal yearly workload (that is 200 days, 8 hours/shift, 2 shifts/day)

Calculating with 0,40 USD/kWh energy price the savings result as 2.176.000 USD (option 1), and 2.048.000 USD (option 2), and 300.000 tons/year at a 100 USD/t price an average 15% premium should result 4.500.000 USD/year extra income. Totaling of 6.048.000 USD/year minimum result considering only the use of a different machine for size reduction, that is in the first year the investment (if it were to be considered as a change or improvement) would pay it back.

Resulting the ROI that is considerable to favor of changing the technology even in the case of short term and small-scale extraction projects.

CONCLUSIONS AND FURTHER INVESTIGATION

Improvements on comminution techniques and machinery is constantly on the steak, little has been achieved, however, as breakthrough.

Common practices help making the crushing and grinding circuits more effective like taking the fines out of the system, changing equipment to more efficient and adding and combining different phenomenon. Digital modelling helps a lot as well.

Nevertheless, for lack of well-founded theoretical bases most of this work lays on experiments and practices. It seems that investigating other types of physical characteristics of mineral particles regarding their behaviors given by homogeneity or heterogeneity, resonance frequency and its energy level, critical breakage conditions would lead us toward a more appropriate manner of comminution. Investigation must be done to measure and define these parameters and conditions as a general and – as already has been introduced – in pilot and industrial plants.

Being appropriate means sustainable, environmentally friendly, better resource management practices including energy, water, chemical usage, that finally results in better economy.

REFERENCES

- Baawuah, E., Kelsey, C., Addai-Mensah, J., Skinner, W. (2020): Economic and Socio-Environmental Benefits of Dry Beneficiation of Magnetite Ores (*Journal of Minerals, MDPI, 2020, 10, 955*)
- Borg G., Scharfe, F., Kamradt, A., (2016): High velocity comminution of massive sulphide ores by VeRo Liberator technology for more energy efficient size reduction and particle liberation. (*World Mining - Surface and Underground, 68, pp. 45-52*)
- Borg, G., Scharfe, F., Lempp, C., Kamradt, A., (2020): Overcoming breakage-inefficiency by high velocity impact comminution-the VeRo Liberator technology (*World of Mining-Surface and Underground-June 2020 pp 147-156*)
- Gholami, H. et al. (2020): The effect of microwave's location in a comminution circuit on improving grindability of porphyry copper deposit. (*Energy sources, part A: Recovery, utilization and environmental effects, <https://doi.org/10.1080/15567036.2020.1753859>*)
- Jankovic, A., Ozer, C., Valery, W., Duffy, K., (2016): Evaluation of HPGR and VRM for dry comminution of mineral ores (*Journal of Mining and Metallurgy, 52 A (1) (2016) pp. 11-25*)
- Komar Kawatra, S. (2006): Advances in Comminution (*Society for Mining, Metallurgy and Exploration Inc. 2006, ISBN-13: 978-0-87335-246-8, ISBN-10: 0-87335-246-7*)
- Michaud, D. (2016): <https://www.911metallurgist.com/blog/comminution>
- Weerasekara, N.S., Powell, M.S., Cleary, P.W., Tavares, L.M., Evertsson, M., Morrison, R.D., (2013): The contribution of DEM to the science of comminution (*Powder Technology 248 (2013) pp. 3-24*)
- Wieg, R.L., Li, K. (1967): A random model for mineral liberation by size reduction. - (*Transact. Soc. Mining Engineers, 238: pp. 179-189*)

CONCEPTUAL INVESTIGATION ON PNEUMATIC AND MECHANICAL FLOTATION REACTOR CELLS FROM DESIGNING AND METALLURGICAL PERSPECTIVES

A. Hassanzadeh^{1,*}, M. Safari², D.H. Hoang¹, M.K. Güner³, T. Sambrook¹, P.B. Kowalczyk²

¹ *Maelgwyn Mineral Services Ltd.*

(*Corresponding author: ahassanzadeh@maelgwyn.com)

² *Mintek, Minerals Processing Division*

³ *Norwegian University of Science and Technology, Department of Geoscience and Petroleum*

⁴ *Helmholtz-Institute Freiberg for Resource Technology, Department of Processing*

ABSTRACT

Re-designing pneumatic flotation cells and their industrial applications have drawn mineral processors' attention over the last three decades. However, their principal privileges over the conventional mechanical and column cells have not been yet well disclosed and clearly identified in the literature. To this end, the present paper comparatively investigates the key advantages of Imhoflot™, Jameson™, and Reflux™ flotation cells over the conventionally used mechanical and column cells from different aspects. The impact of slurry means retention time, gas hold-up, bubble size distribution, and energy dissipation rate on recovery improvement of ultra-fine particles (<20 µm) were studied for all cell types. The diagnostic results showed that Reflux™, Jameson, and Imhoflot™ functionally operate similarly based on providing intensive turbulence in the downcomer and fast kinetics rate of flotation in the separation unit. Formation of sub-micron and micron-sized bubbles, effective hydrodynamic characteristics, and low capital and operating costs were found as their major advantages over the conventionally used cells on improving the recoverability of ultra-fine particles. These cells provide greater gas-hold-up values (40-60%) over the mechanical (5-20%) and column cells (5-25%) with substantially lower power inputs. It was indicated that extremely low mean slurry retention time (i.e., 1-4 min) led to a potential enhancement on their throughputs. However, the effectiveness of these cells on selective separation and improving the grade remains uncertain in the literature.

Keywords: Pneumatic flotation cell, energy dissipation rate, gas hold-up, mean particle retention time, fine particles

INTRODUCTION

Froth flotation is a physiochemically-based technique widely applied to treat thousands of million tonnes of raw materials annually. Through the years, it has been scientifically and technically proven that conventionally used mechanical flotation cells are significantly inefficient for recovering ultra-fine (<20 µm) and coarse (>200 µm) particles, time and energy-consuming (Gaudin et al., 1931; Trahar and Waren, 1976).

As known, fine and ultrafine particles cannot be easily floated using mechanical and column flotation cells (Hassanzadeh et al., 2019). One part of this poor flotation tendency lies in particle properties, including massive surface area, rapid surface oxidation, low particle inertial force, and limited particle-bubble collision probability (Gontijo et al., 2007; Safari et al., 2017; Safari et al., 2020a). The other part relates to the cell drawbacks including the inability to produce small bubbles, short retention time for such fine particles, poor and inefficient turbulence. To overcome these obstacles, one group of researchers enlarged particle size using flocculation-flotation processes (Yin et al., 2011; Li et al., 2021), another group applied micro/nano-bubble assisted flotation (Fan et al., 2012; Chipakwe et al.,

2021), while some intensified cell turbulence (Schubert, 2008; Safari et al., 2014; Testa et al., 2017; Hoseinian et al., 2019). The last group of scientists changed the cell hydrodynamics and invented reactor-separator flotation cells creating remarkable gas hold-up, small bubble sizes, and intensive turbulences (Imhof, 2006; Jameson, 2010; Cole et al., 2020). For instance, the specific advantages of Jameson cell include short residence time, small cell size, high throughput, and high concentrate production rates. It operates with no compressed air input (self-aeration system and vacuum generated in downcomer), and the vacuum developed within the downcomer produces interactions.

Since the mine cut-off grades dropped and ore mineralogy became extremely complex, the challenge of poor floatability of ultrafine and coarse particle ranges has become a serious concern for the mining and mineral processing sector. To this end, mining companies have endeavored to adapt pneumatic flotation cells into the existing circuits by replacing the column cells mainly in the cleaning and re-cleaning stages to reduce the risk (Atkinson et al., 1993). After many successful case studies for a wide variety of ore types, pioneer mining companies recently seek new technologies for effective and selective separations of ultrafine and coarse particles. For instance, Metso: Outotec Inc. presently utilizes Concorde™ and Nova™ Cells to recover ultrafine and coarse particles, respectively. Glencore Technology applies Jameson cell mainly for ultrafine particles coupled with Isamills and also for a broad spectrum of particle ranges. FLSmidth Inc. examines Reflux™ Flotation Cell (RFC) design for initial installation in a re-cleaning stage of copper ore for upgrading recovery of a wide range of particles (Dickinson et al., 2019). Eriez testes Hydrofloat™ cell and Stack flotation reactor for improving recovery of fine and ultrafine particles and coarse ones, respectively. Maelgwyn Mineral Services Ltd focuses on the Imhoflot flotation reactor using three various designs including G (gyratory), V (vertical), and H (hybrid)-cells favourable for recovering ultrafine, coarse, and wide particle ranges, respectively. Allmineral produces Allflot™ for improving the recovery of ultrafine particles. Among these technologies, Imhoflot™ flotation reactor is the oldest and widely applied for coal, base metals, and potash industries, whereas Jameson cell has more than 500 installations across the world (mainly for the coal industry) and can be considered as the most applied one. The RFC can be considered the latest technology, first tested in fine size coal flotation (Galvin et al., 2014; Galvin and Dickinson, 2014; Dickinson et al., 2015, Jiang et al., 2016). This was followed by ion flotation (Dickinson et al., 2016; Ireland et al., 2019; Baynham et al., 2020), coarse coal flotation (Sutherland et al., 2020) and pilot-scale copper flotation (Dickinson et al., 2019). Figure 1 demonstrates these advanced technologies and the corresponding suitable particle range for each one. It is worth mentioning that such graphical description (recovery vs. particle size) can be also used for flotation rate constant versus particle size qualitatively.

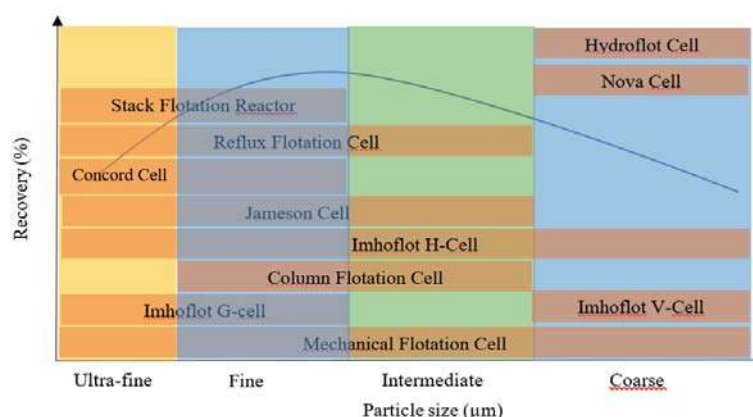


Figure 1. A schematic overview of conventionally and newly applied flotation cells

Imhoflot™, Jameson™ and Reflux™ are considered more complicated than the older flotation technologies i.e., mechanically agitated and column cells. It should not be forgotten that in the 1930s the Denver flotation cell was considered revolutionary and only in the 1950s using mechanical cells

became a norm. A similar story for column flotations appears from the early 1960s, however, it was only around the 1980s that a huge interest and demand started. Although pneumatic flotation machines e.g., Imhoflot™, and Jameson cell were invented in the 1980s, their application in mining industries compared to mechanical cells has still been limited for some reasons. Detailed information regarding each cell and a historical overview is given elsewhere (Moore, 2021; Mondal et al., 2021; Hassanzadeh et al., 2021a). The present work identifies some of the key characteristics of such cells and compares them with the conventional ones.

Five flotation cell types are considered in this research study: two conventional cells as mechanically agitated and column cells and three pneumatic flotation vessels i.e., Imhoflot™, Jameson Cell, and Reflux™ flotation cells. Five fundamental operating properties consist of energy dissipation rate (a.k.a turbulence kinetic energy), slurry mean residence time, gas hold-up, and bubble size distribution were conceptually and comparatively studied in detail. Since there is little information regarding the pneumatic flotation cells, the present work aims at fulfilling this gap in the literature. A conceptual description of such cells was proposed, and the crucial influential factors were analyzed in comparison with the conventionally used mechanical and column flotation cells. We believe this paper is one of the first attempts in compiling recent developments in flotation cell technologies and opens several avenues for their developments.

MATERIALS AND METHODS

Residence Time Distribution (RTD) Measurement

A laboratory Imhoflot™ V-20 flotation reactor was subjected to the RTD measurement using NaCl as a tracer. An approximate 30-50 L of water was localized in the conditioning tank before feeding the cell. Circulating water through the tank and the cell was stabilized by monitoring the feed and tailing pump speeds/flow rates to reach a steady-state condition. Noteworthy, the cell was operated in an open-circuit mode (without re-circulation) in the absence of any reagents. Afterward, a pre-prepared 30 mL of highly concentrated NaCl was injected into the aerator while feeding a water flow rate of 5 L/min and aeration rate of 3 L/min. A series of time-wised samples were taken from the tailing stream and their conductivity and pH were measured afterward. The obtained data were analyzed through an in-house developed software using N-Mixer and Welller models as described elsewhere (Hassanzadeh, 2017).

Bubble Size Measurement (BSD)

A modified McGill bubble viewer was used for measuring the bubble size distribution on a pilot-scale Imhoflot™ H-16 cell. To this end, while the cell was operated by processing water, a bubble sampling tube was positioned at a specific location within the separator tank after ensuring the cell works in a steady-state condition. The measurements were performed in the absence of any frother because of having residual chemical reagents in the recirculating water. Sampled bubbles were monitored and filmed on the viewing chamber and later analyzed with the image processing toolbox of the Matlab software. The size of approximately 2000-3000 bubbles was measured and statistically analyzed. More detailed information regarding the setup can be found elsewhere (Hoang et al., 2019).

Impact Of Key Parameters

Mean Residence Time (MRT)

Slurry retention time determines the number of flotation cells and stages in a circuit required to reach a desirable grade-recovery curve. This term is typically measured by radioactive, pH, and conductivity tracers to monitor slurry/liquid discharge in open- and closed-circuits. Measuring MRT for

the mechanical and column cells in pilot and industrial scales has been broadly reported in the literature. The typical mean residence time for a mechanical cell circuit is ca. 4-20 min at the rougher stage, depending on the mineral type and the number of cells in a bank, and up to 30 min for scavengers, while for the flotation column is in the range of 18-23 min, depending on the column design (Metso, 2006). Yianatos et al. (2017) measured and modelled the residence time distribution (RTD) of industrial cells from seven flotation plants. The results showed that the RTD ranged from 9 to 41 min. The large and small tanks in series (LSTS) and two parallel perfect mixers models could reasonably represent the experimental data compared to the axial dispersion and perfect mixer (PM) models. Kennedy (2008) stated that a column cell typically requires approximately twice the residence time of a 4-cell bank of conventional cells and three times the residence time of a batch laboratory flotation cell.

It is clear that the conventional cells need long retention times to achieve an acceptable selective separation for fine and ultrafine particles. However, pneumatic-type cells show fast flotation kinetics rates due to short residence time. This is a highly critical factor for fine particles due to being oxidized through time rendering physicochemical reactions on the particle surfaces and reducing their hydrophobicities/floatabilities (Pokrajcic et al., 2020). Short residence time allows high throughput and the replacement of few cell numbers instead of several conventional cells. For instance, Harbort et al. (1997) reported the reduction in MRT of a mechanical rougher-scavenger (17.9 min) and cleaner-scavenger (30 min) circuits down to 7.5 min and 2.5 min using Jameson cells with identical flotation performances. Table 1 presents several industrial examples of Jameson flotation cell for various operating circuits reducing the number of mechanically used flotation cells (Moore, 2021). Figure 2 exhibits the liquid residence time measurement results performed on a laboratory IFR operated in a continuous mode illustrating MRT of 2.6 min. Detailed information regarding the experimental procedure and modeling will be presented in the extended version of this paper.

In the case of the RFC, one of the studies showed that residence time in the downcomer shorter than 1 s could be achieved (Jiang et al., 2019). It was considered a reasonable assumption for three reasons: i) particle collection was achieved mainly in the high shear zone within the downcomer, ii) the RFC was operated without a conventional froth zone, which was associated with particle detachment, and iii) very short cell residence times of <60 s were reported typically (Jiang et al., 2014; Dickinson et al., 2015; Jiang et al., 2019). The liquid residence time in the system ranged between 16–26 s, and the cell residence time was ranged between 23-48 sec. The cell residence time provided was calculated based on the volume of the RFC (~16 L) and all volumetric inlet flows (Cole et al., 2021). Given the system isoperated under flooding conditions, the active cell volume is the entire cell, and the cell residence time equals the cell volume divided by the volumetric feed flow, giving a cell residence time of 25.2 s (Dickinson et al., 2015)

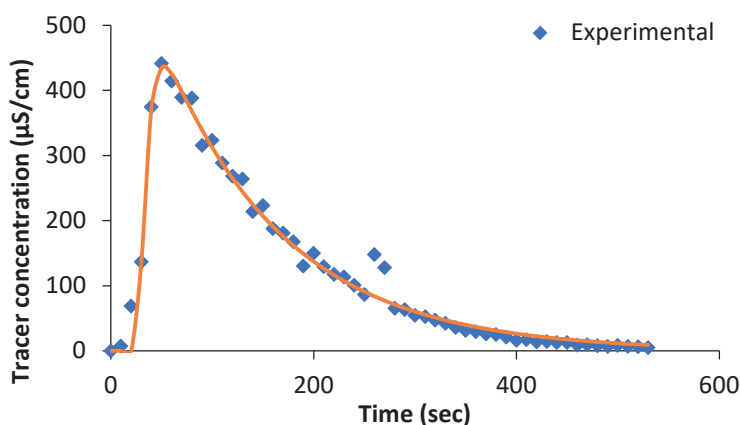


Figure 2. Presentation of RTD data experimentally measured and modeled (via the Weller model) for a V-20 (IFR cell) at feed and air flowrates of 5 L/min and 3 L/min

Table 1. Industrial installations of JFC for reducing the number of mechanical flotation cells (MFC) (Moore, 2021)

Concentration plant	Number of cells	Replacement
Hudbay’s New Britannia	4	11 MFC
Philex Cu-Au mine	10	50 MFC
Ozernoye zinc mine	19	63 MFC

Bubble Size Distribution (BSD)

Bubble size distribution plays a crucial role in the particle-bubble interaction of flotation processes and significantly impacts the flotation rate and recovery of fine and ultrafine particles. As broadly reported, fine and ultrafine particles require small bubbles (micro and sub-micron-sized bubbles) to be recovered efficiently (Hassanzadeh et al., 2016; Farrokhpay et al., 2021). Figure 3 presents an approximative visualization of bubble ranges typically observed in the given cells. These ranges can vary slightly depending on the operating conditions, frother type and dosages, slurry temperature, particle properties, and mono and multivalent ions in the cell (Vazirizadeh et al., 2016; Safari et al., 2019). As seen, conventional flotation cells (i.e., MFC and column flotation cell (CFC)) cannot produce bubble diameters smaller than 0.5 mm due to their natural bubble generation mechanisms. Recently, Zahab Nazouri et al. (2021) stated that there is no unique and promising model to be used for predicting the bubble size in a column flotation cell based on the sparger orifice size and other hydrodynamic factors. Further, the Tate equation was found inapplicable for the column cells, which was in line with the results of formerly reported studies (Cho and Laskowski, 2002; Hernandez-Aguilar et al., 2006).

In contrast with MFC and CFC, reactor-separator-type cells, where the particle-bubble collision and attachment occur in a downcomer, generate a massive number of bubbles with a diameter of 0.1-0.7 mm. For example, Figure 4 demonstrates the BSD of a laboratory V-cell (one type of IFR) manifesting a 0.1-0.4 mm domain for the generated bubbles. The cavitation mechanism created by the Venturi tube and specific nuzzle designs generates such micro-bubbles. Almost the same concept is valid for JFC supplying an enormous number of small bubbles with a diameter of 0.2-0.7 mm (Harbort et al., 2002). It is worth noting that most of the methods utilized for measuring the BSD have been performed in a 2-phase (liquid-gas) system and ex-situ, while an accurate technique applicable in dynamic, in-line, and at a 3-phase (liquid-solid-gas) environment is substantially required. Broadly applied approach for measuring BSD is the photographic and optical techniques, while more detailed information regarding different approaches is given elsewhere (Khoshdast et al., 2022). Generally, there is limited practical data in the literature concerning the bubble size distributions performed in such cells, and further experimental data is required.

In the case of the Reflux flotation cell, at the highest feed-to-gas flux ratio of 9.1, the bubble diameters were remarkably small, approaching a mean value of 0.37 mm at a feed flux of 15.4 cm/s. These micro-bubbles were observed to be only a small portion of the overall population of bubbles. Hence, the reported diameters were a conservative overestimate of the mean bubble diameters, and the actual mean diameters were found slightly smaller. The bubble surface flux increased to an extraordinary 600 s^{-1} , based on a mean bubble diameter of 0.55 mm, while the underflow liquid flux was 9.5 cm/s and bubble surface flux between $178 - 600 \text{ s}^{-1}$ (Jing et al., 2014). The bubble size at the end of the downcomer for an ion flotation process, and the top size of the bubbles for the lower two jo/jg ratios were declared around 0.74 mm (Baynham et al., 2020).

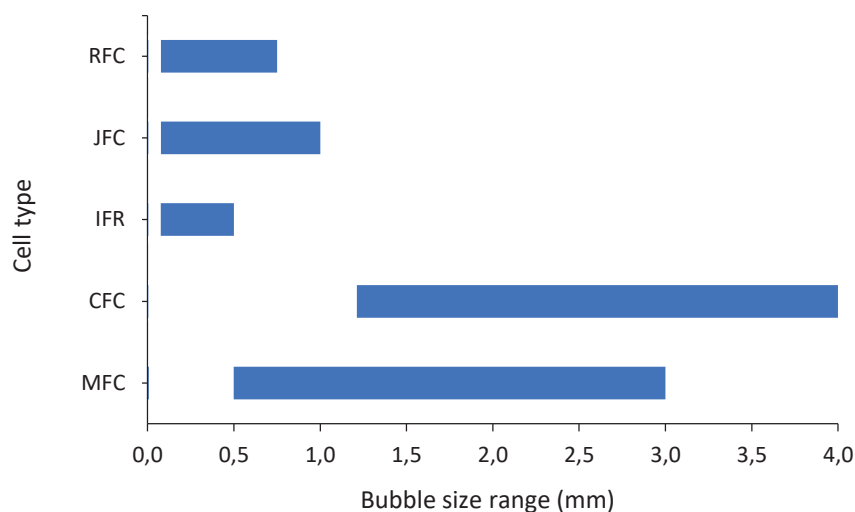


Figure 3. A demonstrative graph of the bubble size range for five types of flotation cells

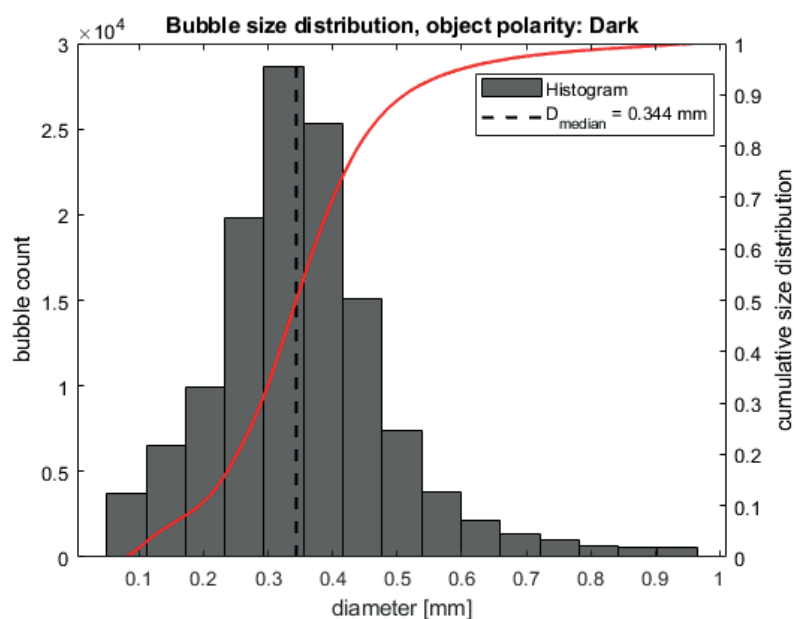


Figure 4. A typical bubble size distribution generated using Imhoflot™ H-16 cell (one type of IFR) by a modified McGill bubble size viewer (in a feldspar flotation plant, using process water without adding reagents (airflow rate=15 m³/h, feed rate=66 m³/h, feed pressure 2.02 bar)

Gas Hold-Up and Energy Dissipation Rate

Gas hold-up ($\epsilon_g, \%$), the volume fraction of the mixture occupied by gas at any point in a flotation cell, is a critical hydrodynamic parameter in all flotation cells. This parameter is dependent on the magnitude of the gas flow rate, size and number of bubbles, frother type, and dosage (Miskovic, 2011). It has been commonly calculated by a drift-flux technique i.e., measuring the pressure difference between two tapping points and changing the measurement points through the flotation cell height to obtain the ϵ_g profile (Diaz-Penafiel and Dobby, 1994). This value for the mechanical and column cells is limited to 5-20% and 5-25%, respectively while exceeding these ranges leads to an undesirable turbulent and non-bobbly flow regime.

It has been widely reported that fine and ultrafine particles require intensive turbulence to reach desirable particle-bubble collision efficiency, which is predominantly controlled by the hydrodynamic properties of the cell (Schubert 2008; Kouachi et al., 2017). The typical energy input used in industrial mechanical cells (a.k.a. tank cells) ranges from 0.6-3 kW/m³ (Deglon et al., 2000; Safari et al. 2016), although energy levels of up to 12 kW/m³ are reported for fine particle applications. By enlarging the flotation cell volume, most of the energy is consumed for suspending the slurry than maximizing the particle-bubble interactions (Hoang et al., 2019). For example, it was shown that cells with a volume of higher than 300 m³ reduce the specific energy input of 0.5-0.7 kW/m³, which is 1 kW/m³ for smaller cells. Mechanical cells have an inherently inhomogeneous distribution of energy input through the cell, with high energy input found near the impeller and much lower levels in the bulk of the cell (Koh and Schwarz, 2003). The fact that the processes of particle suspension, bubble break-up, and energy generation are all interdependent makes it difficult or impossible to optimize the conditions for flotation (Schubert, 2008). Despite these weaknesses, the robustness of the design has meant that mechanical cells overwhelmingly dominate in industrial applications, despite competition from several other cell technologies. There is little quantitative information regarding the energy consumption of reactor-separator flotation cells. Nevertheless, the energy level is significantly low due to having no moving parts (agitators) and more minor scales (in the order of ca. 5) compared to the mechanical and column flotation cells.

CONCLUSIONS

The present work demonstrates the role of four key parameters of flotation cells (i.e., slurry retention time, bubble size distribution, energy dissipation rate, and gas hold-up) in the floatability of minerals by categorizing them into two classes i.e., conventional (mechanical and column) and reactor-separator (ImhoflotTM, Jameson, and RefluxTM) flotation cells. The comparative outcomes are summarized in Table 2. The results showed that JFC, IFR, and RFC are principally operated similarly with slight differences. Their key advantages over the mechanical and column cells were fast flotation kinetics, low residence time, high gas hold-up, intensive turbulence in the downcomer, small bubble sizes, low capital and operating costs, small scales, and low maintenance.

Table 2. Summarized data for all studied cells considering their key parameters

Cell type	MFC	CFC	RFC	IFR	JFC
Cell residence time (MRT, min)	4-20	9-41	1-4	1-4	1-5
Superficial gas velocity (Jg, cm/sec)	0.7-2.7	2.3-4.8	1-5	0.1-0.7*	0.5-4
Gas hold-up (ϵ_g , %)	5-20	5-25	45-70	30-70	40-60
Bubble surface area flux (S_b , s ⁻¹)	50.7 (5.7-178.2)	UN**	100-200	10-90	55
Aeration pressure (psi)	3-17	22-94	90	0	0
Carrying capacity (g/min/cm ²)	1	1.27	UN	UN	2.77
First installation	1930s	1960s	2020s	1980s	1980s
BSD (mm)	0.7-3.0	1.5-3.0	0.3-0.7	0.1-0.3	0.3-0.7
Wash water	Yes (re)-cleaner	Yes	Yes	No	Yes
Energy input (kW/m ³)	1-5	UN	UN	0.5-1.5	1-2
Moving parts	Yes	No	No	No	No
Common application	Rougher-Scavenger	Cleaner	Cleaner	Cleaner	Cleaner
Throughput	High	Mid	Mid	High	High
Footprint	High	Mid	Small	Small	Small
Froth depth	Low	High	Mid	Mid	Mid

Mixing intensity	Mid	Low	High	High	High
Scale-up factor	Yes	Yes	No	No	No
Largest size (m ³)	680	110	0.1	66	40
Installed power (kW)	515	110	UN	UN	215***

* In the separator part of the cell, and the value is ca. 10-70 cm/s within the downcomer.

** UN: unknown

*** Power consumption by pumps

ACKNOWLEDGMENT

This study was performed and financially supported by The European Union’s Horizon 2020 research and innovation program under grant number of 958307 (HARARE project). Authors M.K. Güner and P.B. Kowalczyk thank all partners (EIT RawMaterials, FLSmidth, KGHM, Solvay and IVL) of the project RFC-Upscaling: New Reflux Flotation Cell Technology Upscaling for Ore Flotation for our ongoing collaboration.

REFERENCES

- Atkinson, B.W., Griffin, P.T., Jameson G.J., Espinosa-Gomez, R. (1993). Jameson cell Test work on copper streams in the copper concentrator of Mount Isa mines Limited, XVIII International Mineral Processing Congress, AusIMM, 23-28 May.
- Baynham, S., Ireland, P., and Galvin, K.P. (2020). Enhancing ion flotation through decoupling the overflow gas and liquid fluxes, *Minerals*, *10*(12), 1–17. <https://doi.org/10.3390/min10121134>
- Chipakwe, V., R. Jolsterå, and Chelgani, S.C. (2021). Nanobubble-assisted flotation of apatite tailings: Insights on beneficiation options, *ACS Omega*, *6*, 13888-13894. DOI: 10.1021/acsomega.1c01551
- Cole M.J., Dickinson J.E., Galvin K.P. (2020). Recovery and cleaning of fine hydrophobic particles using the Reflux™ Flotation Cell, *Separation and Purification Technology* *240*, 116641. Doi: 10.1016/j.seppur.2020.116641.
- Cole, M. J., Galvin, K.P., and Dickinson, J.E. (2021). Maximizing recovery, grade and throughput in a single stage Reflux Flotation Cell, *Minerals Engineering*, *163*, 106761. <https://doi.org/10.1016/j.mineng.2020.106761>
- de F. Gontijo, C., Fornasiero, D., Ralston, J. (2007). The limits of fine and coarse particle flotation, *The Canadian Journal of Chemical Engineering*, *85*, 739-747. <https://doi.org/10.1002/cjce.5450850519>
- Deglon, D.A., Egya-Mensah, D., Franzidis, J.P. (2000). Review of hydrodynamics and gas dispersion in flotation cells on South African platinum concentrators, *Minerals Engineering*, *13*(3), 235-244. [https://doi.org/10.1016/S0892-6875\(00\)00003-0](https://doi.org/10.1016/S0892-6875(00)00003-0)
- Diaz-Penafiel, P. and Dobby, G.S. (1994). Kinetic studies in flotation columns: Bubble size effect, *Minerals Engineering*, *7*(4), 465-478. [https://doi.org/10.1016/0892-6875\(94\)90159-7](https://doi.org/10.1016/0892-6875(94)90159-7)
- Dickinson, J., Dabrowski, B., Lelinski, D., Christodoulou, L., Galvin, K. (2019). Pilot trial of a new high rate flotation machine, Procemin Geomet, Santiago, Chile.
- Dickinson, J.E., and Galvin, K.P. (2014). Fluidized bed desliming in fine particle flotation—part I. *Chemical Engineering Science*, *108*, 283-298. <https://doi.org/10.1016/j.ces.2013.11.006>
- Dickinson, J.E., Jiang, K., and Galvin, K.P. (2015). Fast flotation of coal at low pulp density using the Reflux Flotation Cell, *Chemical Engineering Research and Design*, *101*, 74–81. <https://doi.org/10.1016/j.cherd.2015.04.006>
- Dickinson, J.E., Neville, F., Ireland, P.M., and Galvin, K.P. (2016). Uncoupling the inherent bubble-liquid hydrodynamics of conventional Ion flotation using reflux flotation. *Chemeca 2016: Chemical Engineering-Regeneration, Recovery and Reinvention*, 100.
- Fan, M., Zhao, Y., and Tao, D. (2012). Fundamental studies of nanobubble generation and applications in flotation. *Separation Technologies for Minerals, Coal and Earth Resources*, 459-469.

- Farrokhpay, S., Filippov, L., Fornasiero, D. (2021). Flotation of Fine Particles: A Review, *Mineral Processing and Extractive Metallurgy Review*, 42(7), 473-483. <https://doi.org/10.1080/08827508.2020.1793140>
- Galvin, K.P., and Dickinson, J.E. (2014). Fluidized bed desliming in fine particle flotation–part II: flotation of a model feed, *Chemical Engineering Science*, 108, 299-309. <https://doi.org/10.1016/j.ces.2013.11.027>
- Galvin, K.P., Harvey, N.G., and Dickinson, J.E. (2014). Fluidized bed desliming in fine particle flotation–Part III flotation of difficult to clean coal, *Minerals Engineering*, 66, 94-101. <https://doi.org/10.1016/j.mineng.2014.02.008>
- Gaudin, A.M., Groh, J.O. and Henderson, H.B. (1931). Effect of particle size on flotation, AIME Technical Publications, pp. 414, 3-23.
- Harbort, G.J., Manlapig, E.V., Debono, S.K. (2002). Particle collection within the Jameson cell downcomer, *Mineral Processing and Extractive Metallurgy*, 111(1), 1-10. <https://doi.org/10.1179/mpm.2002.111.1.1>
- Hassanzadeh, A. (2017). Measurement and modeling of residence time distribution of overflow ball mill in continuous closed circuit, *Geosystem Engineering*, 20(5), 251-260. <https://doi.org/10.1080/12269328.2016.1275824>
- Hassanzadeh, A., Azizi, A., Kouachi, S., Karimi, M., Celik, M.S. (2019). Estimation of flotation rate constant and particle-bubble interactions considering key hydrodynamic parameters and their interrelations, *Minerals Engineering*, 141, 105836. <https://doi.org/10.1016/j.mineng.2019.105836>
- Hassanzadeh, A., Safari, M., Hoang, D.H. (2021). Fine, coarse and fine-coarse particle flotation in mineral processing with a particular focus on the technological assessments, In *Proceedings of the 2nd International Conference on Mineral Science*, Online, 1–15 March 2021. <https://doi.org/10.3390/iecms2021-09383>
- Hassanzadeh, A., Vaziri Hassas, B., Kouachi, S., Brabcova, Z., Çelik, M.S. (2016). Effect of bubble size and velocity on collision efficiency in chalcopyrite flotation, *Colloids and Surfaces A: Physicochemical and Engineering Aspects*, 498, 258-267. <https://doi.org/10.1016/j.colsurfa.2016.03.035>
- Hernandez-Aguilar, J.R., Cunningham, R., and Finch, J.A. (2006). A test of the Tate equation to predict bubble size at an orifice in the presence of frother, *International Journal of Mineral Processing*, 79(2), 89–97. <https://doi.org/10.1016/j.minpro.2005.12.003>
- Hoang, D.H., Hassanzadeh, A., Peuker, U.A., Rudolph, M. (2019). Impact of flotation hydrodynamics on the optimization of fine-grained carbonaceous sedimentary apatite ore beneficiation, *Powder Technology*, 345, 223-233. <https://doi.org/10.1016/j.powtec.2019.01.014>
- Hoseinian, F.S., Rezai, B., Kowsari, E., Safari, M. (2019). Effect of impeller speed on the Ni(II) ion flotation, *Geosystem Engineering* 22(3), 161-168. <https://doi.org/10.1080/12269328.2018.1520651>
- Imhof, R. US Patent No. 7,108,136 B2, Pneumatic Flotation Separation Device, application filed 19. March 2001; published 19. Sept. 2006.
- Ireland, P. M., Neville, F., Dickinson, J.E., and Galvin, K.P. (2019). Enhancing extraction in ion flotation using the boycott effect, *Chemical Engineering and Processing-Process Intensification*, 145, 107678. <https://doi.org/10.1016/j.cep.2019.107678>
- Jameson, G.J., New directions in flotation machine design (2010). *Minerals Engineering*, 23, 11–13, 835-841. <https://doi.org/10.1016/j.mineng.2010.04.001>
- Jiang, K., Dickinson, J.E., and Galvin, K.P. (2019). The kinetics of fast flotation using the Reflux Flotation Cell, *Chemical Engineering Science*, 196, 463–477. <https://doi.org/10.1016/j.ces.2018.11.012>
- Jing, K., Dickinson, J. E., and Galvin, K.P. (2014). Maximizing bubble segregation at high liquid fluxes. *Advanced Powder Technology*, 25(4), 1205-1211. <https://doi.org/10.1016/j.appt.2014.06.003>
- Kennedy, D.L. (2008). Redesign of industrial column flotation circuits based on a simple residence time distribution model, MSC Thesis, Mining and Minerals Engineering, Virginia Polytechnic Institute and State University, U.S.A.
- Khoshdast, H., Hassanzadeh, A., Kowalcuk, P.B., Farrokhpay, S. (2022). Characterization techniques of flotation frothers - A review, *Mineral Processing and Extractive Metallurgy Review*, In press.

- Koh, P.T.L., Schwarz, M.P. (2003). CFD modelling of bubble–particle collision rates and efficiencies in a flotation cell, *Minerals Engineering*, 16, 1055–1059. <https://doi.org/10.1016/j.mineng.2003.05.005>
- Kouachi, S., Vaziri Hassas, B., Hassanzadeh, A., Çelik, M.S., Bouhenguel, M. (2017). Effect of negative inertial forces on bubble-particle collision via implementation of Schulze collision efficiency in general flotation rate constant equation, *Colloids and Surfaces A: Physicochemical and Engineering Aspects*, 517, 20, 72-83. <https://doi.org/10.1016/j.colsurfa.2017.01.002>
- Li, M., Xiang, Y., Chen, T., Gao, X., Liu, Q. (2021). Separation of ultra-fine hematite and quartz particles using asynchronous flocculation flotation, *Minerals Engineering*, 164, 106817. <https://doi.org/10.1016/j.mineng.2021.106817>
- Metso (2006). Basics in Minerals Processing, Section 4 – Separations. Separations. Metso Minerals.
- Miskovic, S. (2011). An investigation of the gas dispersion properties of mechanical flotation cells: an in-situ approach, PhD Thesis, Mining and Minerals Engineering, Virginia Polytechnic Institute and State University, U.S.A.
- Mondal, S., Acharjee, A., Mandal, U., Saha, B. (2021). Froth flotation process and its application, *Vietnam Journal of Chemistry*, 2021, 59(4), 417-425. DOI: 10.1002/vjch.202100010
- Moore, P., Flotation factors, (2021). *International Mining Magazine*, 36.
- Pokrajcic, Z., Harbort, G.J., Lawson, V., Reemeyer, L. (2020). Benefits of high intensity flotation at the head of base metal flotation circuits, *Jameson Cell-2020 compendium of Technical Papers*, 378-387.
- Safari, M., Deglon, D. (2020). Evaluation of an attachment–detachment kinetic model for flotation. *Minerals* 10(11), pp. 1–12. <https://doi.org/10.3390/min10110978>
- Safari, M., Harris, M., Deglon, D. (2014). The effect of energy input on the flotation kinetics of galena in an oscillating grid flotation cell. In: *Proceedings of XXVII International Mineral Processing Congress*, Santiago.
- Safari, M., Harris, M., Deglon, D. (2017). The effect of energy input on the flotation of a platinum ore in a pilot-scale oscillating grid flotation cell, *Minerals Engineering* 110, 69-74. <https://doi.org/10.1016/j.mineng.2017.04.012>
- Safari, M., Harris, M., Deglon, D., Leal Filho, L., Testa, F. (2016). The effect of energy input on flotation kinetics. *International Journal of Mineral Processing*, 156, 108-115. <https://doi.org/10.1016/j.minpro.2016.05.008>
- Safari, M., Hoseinian, F.S., Deglon, D., Leal Filho, L.S., Souza Pinto, T.C. (2020b). Investigation of the reverse flotation of iron ore in three different flotation cells: Mechanical, oscillating grid and pneumatic, *Minerals Engineering*, 150, 106283. <https://doi.org/10.1016/j.mineng.2020.106283>
- Schubert, H.J. (2008). On the optimization of hydrodynamics in fine particle flotation. *Minerals Engineering*, 21 (12–14), 930–936. <https://doi.org/10.1016/j.mineng.2008.02.012>
- Sutherland, J.L., Dickinson, J.E., and Galvin, K.P. (2020). Flotation of coarse coal particles in the Reflux™ Flotation Cell, *Minerals Engineering*, 149, 106224. <https://doi.org/10.1016/j.mineng.2020.106224>
- Testa, F., Safari, M., Deglon, D., Filho, L.L. (2017). Influence of agitation intensity on flotation rate of apatite particles, *REM - International Engineering Journal R. Esc. Minas*, 70(4), 491-495. <https://doi.org/10.1590/0370-44672017700010>
- Trahar, W.J., Warren, L.J. (1976). The flotability of very fine particles—a review. *Int. J. Miner. Process.* 3(2), 103–131. [https://doi.org/10.1016/0301-7516\(76\)90029-6](https://doi.org/10.1016/0301-7516(76)90029-6)
- Vazirizadeh, A., Bouchard, J., Chen, Y. (2016). Effect of particles on bubble size distribution and gas hold-up in column flotation, *International Journal of Mineral Processing*, 157, 163-173. <https://doi.org/10.1016/j.minpro.2016.10.005>
- Yianatos, J., Vinnett, L., Panire, I., Alvarez-Silva, M., Díaz, F. (2017). Residence time distribution measurements and modelling in industrial flotation columns, *Minerals Engineering*, 110, 139-144. <https://doi.org/10.1016/j.mineng.2017.04.018>
- Yin, W., Yang, X., Zhou, D., Li, Y., Lü, Z. (2011). Shear hydrophobic flocculation and flotation of ultrafine Anshan hematite using sodium oleate. *Transactions of Nonferrous Metals Society of China*, 21(3), 652-664. [https://doi.org/10.1016/S1003-6326\(11\)60762-0](https://doi.org/10.1016/S1003-6326(11)60762-0)
- Zahab Nazouri, A., Shojaei, V., Khoshdast, H., Hassanzadeh, A. (2021). Hybrid CFD-experimental investigation into the effect of sparger orifice size on the metallurgical response of coal in a pilot-

scale flotation column, International Journal of Coal Preparation and Utilization,
<https://doi.org/10.1080/19392699.2021.1960318>

COPPER RAFFINATE REUSE FOR INITIAL LEACHING, A BOX-BEHNKEN DESIGN

H. Movahhedi¹, A.M. Beygian¹, E.K. Alamdari^{1,*}

¹Amirkabir University of Technology, Dept. of Materials Science and Engineering
 (*Corresponding author: alamdari@aut.ac.ir)

ABSTRACT

The raffinate in hydrometallurgical processes contains remarkable amounts of acid and metal ions of the target element, the release of which causes the loss of resources and environmental problems. This study proposes a method to reuse the raffinate in the extraction process cycle as a leaching agent for the copper leaching process with considerable concentrations of iron ions. Due to cementation in the process cycle and the subsequent presence of iron ions in the raffinate solution, the parameters of acid concentration, iron concentration, and liquid/solid ratio that are expected to affect leaching recovery were considered to increase copper concentration in re-leaching. The effects of leaching parameters were investigated and optimized using the Box-Behnken of response surface methodology (RSM). The concentration of copper was determined by Atomic Absorption Spectrophotometer (AAS). In addition, the comparative features of samples before and after the leaching process were analyzed using X-ray diffraction (XRD). A maximum copper concentration of 6.17 (gr/L) can be obtained under the initial acidity of 326 (gr/kg of ore), 14 (gr/L) of iron concentration, and 4 (cc/gr) of liquid/solid ratio at a leaching time of 1 hour.

Keywords: Copper leaching, raffinate, response surface methodology

INTRODUCTION

Copper is a precious and widely used element in various industries because of its high ductility, thermal and electrical conductivity (Wang, Zhang, et al. 2018). Nowadays, hydrometallurgical processes are used in copper extraction due to their high efficiency and advantages (Panda, Akcil et al. 2015). A raffinate is produced in a hydrometallurgical process which contains ions of the target element, heavy metals, and high concentrations of acid. Therefore, raffinate is an essential solution and needs to be reused (Das and Krishna 1996). Hydrometallurgical extraction processes consist of three steps: leaching, solvent extraction, and electrowinning. The leaching process is crucial and can be affected by various factors.

Generally, there are four types of leaching: heap leaching, in-situ leaching, tank leaching, and vat leaching, each of which has its advantages and disadvantages and is used under different conditions. Hip leaching requires less capital and consumes less energy than other methods (Saldaña, Toro et al. 2019). In situ leaching has the advantage of reducing drilling costs, and the resulting environmental pollution is reduced. This method is economically viable and highly effective for low-grade mines and reserves (Sinclair and Thompson 2015). In all leaching processes, the quality of the final product can be vitiated by the possible impurities entering the solution phase. The presence of iron in the electrowinning solution has destructive effects such as decreased efficiency, increased energy consumption, and altered cathodic copper morphology (Izadi, Mohebbi et al. 2017). As mentioned, solvent extraction is one of the main stages

of hydrometallurgical processes, and its purpose is to purify and increase the purity and concentration of the target element from the leaching solution (Rotuska and Chmielewski 2008).

After the extraction process is completed, the copper-free solution, if obtained from electrolysis, has a high concentration of iron (III) and, if obtained from cementation, has a higher concentration of iron but less iron (III). In this study, due to the presence of different amounts of iron with different capacities (generally resulting from cementation), experimental design with different levels of iron (II) and sulfuric acid concentrations, as well as liquid/solid ratio, was performed to optimize and increase the final copper concentration in order to eliminate solvent extraction and utilize direct electrolysis which will be discussed in future papers.

EXPERIMENTAL

Soil containing copper oxide (according to the results of XRD analysis, which will be discussed later) prepared from a copper mine was used as a raw material in leaching experiments. First, crushing and milling processes were performed on the soil. About 75% of the soil was in the particle size range of 140-320 microns. Then ICP MS analysis was performed to determine the amount of copper element. According to this analysis, the soil contains 3.9 percent of copper. XRD analysis was also performed to determine the phase of essential compounds, and the results are shown in Figure 1. Also, XRF analysis was performed to determine the values of other vital compounds in the soil, and the results are listed in Table 1.

Table 1. Soil compounds values based on XRF analysis report

Compound	SiO2	CaO	Al2O3	MnO
wt%	32	19	5.7	6.5
Compound	MgO	Fe2O3	K2O	SO3
wt%	1.65	5.6	1.24	1.4

Leaching tests were performed on a 1-liter spherical glass reactor, the temperature of which was controlled by a water bath at 85°C, and equipped with a backflow cooler (glass condenser) to prevent solution evaporation. A mechanical stirrer was also used to mix the solutions at a constant stirring speed of 300 rpm during leaching. Laboratory raffinates were produced and used to optimize the copper concentration after the leaching. In each experiment, a solution with a volume of 750 cc and the required amount of sulfuric acid used as a leaching agent and soil according to the amount of liquid/solid ratio and Iron (II) sulfate heptahydrate to prepare the required amount of iron in the solution. At the end of each experiment, the vacuum filtration method was used to prepare the sample for analysis. The amount of copper in the samples was determined by AAS.

The Box-Behnken design module in the response surface methodology (RSM) was adopted using "Design-Expert" software to optimize the leaching process and the final copper concentration of the samples and analyze the interaction between the parameters. The three factors of acid and iron concentration and liquid/solid ratio were selected as variables, each with three different levels, all of which are listed in Table 2.

RESULTS AND DISCUSSION

According to the fit summary data obtained from "Design-Expert," shown in Table 3. , the linear model is a suitable model for statistical analysis and discussion of data.

Table 3. Fit summary

Source	Sequential p-value	Lack of Fit p-value	Adjusted R ²	Predicted R ²	
Linear	< 0.0001	0.4804	0.8917	0.8416	Suggested
2F	0.5121	0.4307	0.8869	0.7447	
Quadratic	0.1202	0.7460	0.9262	0.8369	
Cubic	0.7460		0.9021		Aliased

Table 2. lists the copper concentration values after 1 hour of leaching in each of the 17 operating surface compositions created by the RSM principles in the range of 2.798 to 7.237 (gr/L). The ANOVA results are presented in Table 2. Low p values for regression (P <0.001) and non-fit of the model were not significant (P> 0.05), indicating the suitability of the model. The final equation in terms of actual factors was proposed as follows:

Table 2. Experimental design and obtained results

RUN	Leaching Variables			Response
	Acid concentration (gr/kg of ore)	Fe concentration (gr/L)	liquid/solid ratio	Cu concentration (gr/L)
1	250	5	6	3.796
2	300	5	4	6.288
3	250	15	4	5.096
4	300	15	6	4.47
5	300	15	6	4.64
6	250	25	6	3.352
7	300	25	8	2.798
8	350	15	4	7.237
9	300	15	6	4.031
10	300	5	8	3.498
11	250	15	8	2.908
12	350	25	6	4.529
13	300	25	4	5.073
14	350	5	6	5.158
15	300	15	6	3.878
16	350	15	8	3.975
17	300	15	6	4.65

Table 2. ANOVA table

Source	Sum of Squares	Degree of Freedom	Mean Square	F-Value	P-Value
--------	----------------	-------------------	-------------	---------	---------

Model	19.07	3	6.36	44.89	<0.0001	Significant
A- Acid concentration	4.13	1	4.13	29.16	0.0001	
B- Fe concentration	1.12	1	1.12	7.88	0.0148	
C- Liquid/solid ratio	13.82	1	13.82	97.63	<0.0001	
Residual	1.84	13	0.1416			
<u>Lack of Fit</u>	<u>1.33</u>	<u>9</u>	<u>0.1476</u>	<u>1.15</u>	<u>0.4804</u>	<u>Not significant</u>
Pure Error	0.5117	4	0.1279			

$$Y = 4.62707 + 0.014367 X_1 - 0.03735 X_2 - 0.657188 X_3 \tag{1}$$

Where Y is the response value of copper concentration, X₁, X₂, and X₃ represent the initial acidity, iron concentration, and liquid/solid ratio, respectively. The coefficient of determination R² for Equation (1) was 0.91, demonstrating the predicted copper concentration is in high accordance with the experiment results.

The composition of copper soil in optimal conditions before and after leaching was detected by the XRD and shown in Figure 1. As can be seen from it, the diffraction peak of tenorite (CuO), cuprite (Cu₂O), and copper (I) iron (III) oxide in the samples after leaching were distinctly weakened, indicating a large proportion of copper components was removed through reacting with the raffinate.

In addition to the above tables and statistical data, the 3D surface figure, the software's output, is attached in Figure 2.

CONCLUSIONS

In the present study, Box-Behnken, a module of RSM was used to discuss the interaction between factors in the process of recovering copper from copper soil using a 1-liter agitator reactor with the following results:

1. According to the developed statistical model, increasing the sulfuric acid and decreasing the initial iron concentration and liquid/solid ratio leads to an increase in the final concentration of copper.
2. According to the equation obtained from the model and the coefficients of the variables, the effect of liquid/solid ratio reduction on increasing the final copper concentration is more significant than other variables. Also, the sulfuric acid variable has a more significant effect than the initial iron concentration.

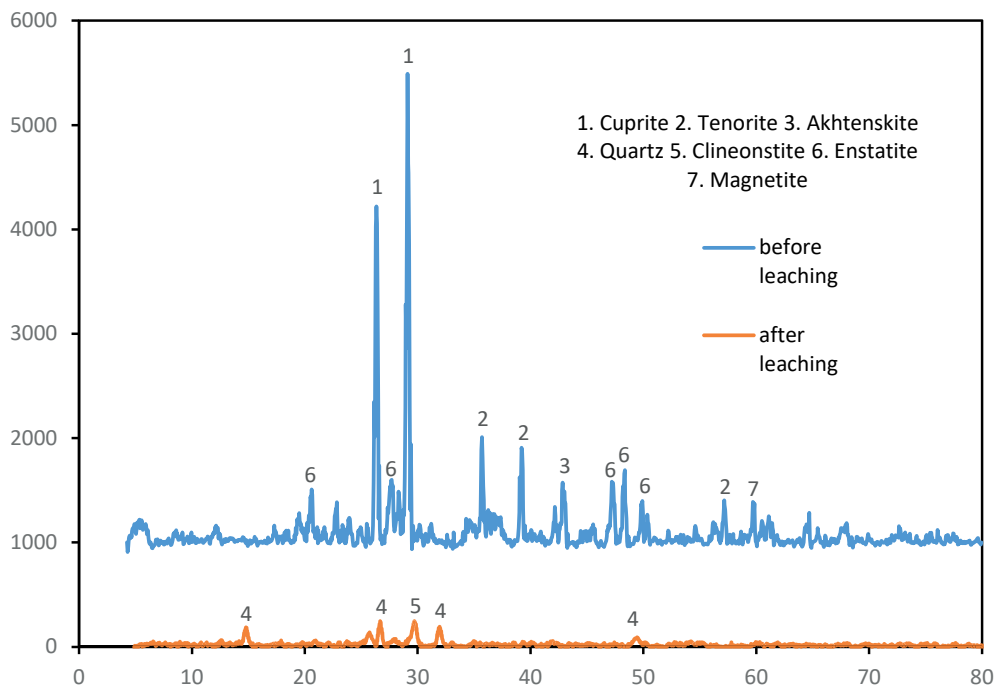


Figure 1. XRD diagram of samples before and after leaching

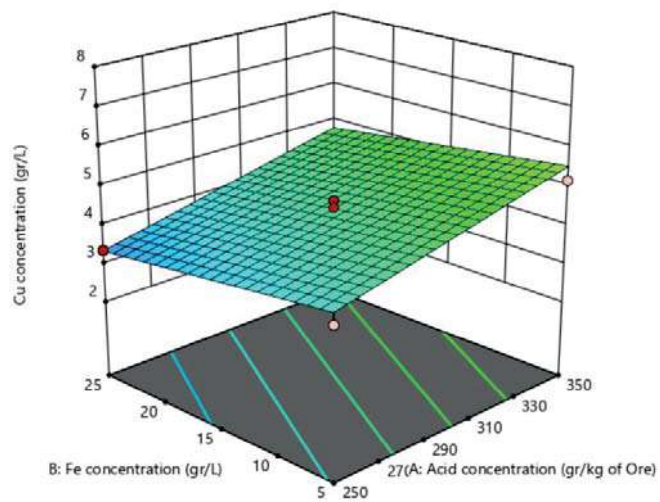


Figure 2. 3D Surface

-The effect of sulfuric acid concentration on copper recovery is more significant at low iron concentrations. Also, in a high liquid/solid ratio, the effect of acid concentration is more significant than in a low liquid/solid ratio.

-The maximum final concentration of copper that can be achieved after 60 minutes of leaching copper soil in a 1-liter reactor at a speed of 300 rpm is 7.237 (gr/L) in the following conditions: sulfuric acid: 326 (gr/kg of ore) and initial iron concentration: 14 (gr/L) and liquid/solid ratio: 4 (cc/gr).

REFERENCES

- Das, S. and P. G. Krishna (1996). "Effect of Fe (III) during copper electrowinning at higher current density." *International journal of mineral processing* 46,(1-2), 91-105.
- Izadi, A., A. Mohebbi, M. Amiri and N. Izadi (2017). "Removal of iron ions from industrial copper raffinate and electrowinning electrolyte solutions by chemical precipitation and ion exchange." *Minerals Engineering* 113, 23-35.
- Panda, S., A. Akcil, N. Pradhan and H. Deveci (2015). "Current scenario of chalcopyrite bioleaching: a review on the recent advances to its heap-leach technology." *Bioresource technology* 196: 694-706.
- Rotuska, K. and T. Chmielewski (2008). "Growing role of solvent extraction in copper ores processing." *Physicochemical Problems of Mineral Processing* 42, 29-36.
- Saldaña, M., N. Toro, J. Castillo, P. Hernández and A. Navarra (2019). "Optimization of the heap leaching process through changes in modes of operation and discrete event simulation." *Minerals* 9(7), 421.
- Sinclair, L. and J. Thompson (2015). "In situ leaching of copper: Challenges and future prospects." *Hydrometallurgy* 157, 306-324.
- Wang, Y., Z. Zhang, S. Kuang, G. Wu, Y. Li, Y. Li and W. Liao (2018). "Selective extraction and recovery of copper from chloride solution using Cextrant 230." *Hydrometallurgy* 181, 16-20.

CUMHURİYETİMİZİN 100. YILINDA ENERJİ HAMMADDELERİ ÜRETİMİMİZİN SPSS MODELLEMESİ İLE TAHMİNİ

PREDICTION OF OUR ENERGY RAW MATERIALS PRODUCTION IN THE 100TH ANNIVERSARY OF OUR REPUBLIC WITH SPSS MODELING

A. K. Özdoğan^{1*}, Y. Kınaş²

^{1,2}Mevlana Bulvarı No:76, Beştepe/ANKARA
(*Sorumlu Yazar: akozdogan@gmail.com)

ÖZET

SPSS, İngilizce açılımı Statistical Package for the Social Sciences (Sosyal Bilimler İçin İstatistik Programı) olan ve Sosyal Bilimlerin yanında Fen Bilimleri vb. alanlarda, tahmin yapmak amacıyla da sıklıkla kullanılan bir bilgisayar programıdır. Program tüm yazılımlarda çalışabilmekte ve Microsoft Excel programı gibi basit ve anlaşılabilir bir görünüme sahiptir. Cumhuriyetimizin 100. Yılında Enerji Hammaddeleri Üretimimizin SPSS Modellemesi ile tahmini yapılarak geleceğe ışık tutması amacıyla toplam enerji hammaddeleri üretimi hakkında öngöründe bulunulmuştur. 2015 yılı sonrasında yaşanmış olan ölümlü kaza sayıları da değerlendirilecek olup, üretim tahmini ve yaşanabilecek ölümlü iş kazaları hakkında farkındalık oluşturmak adına değerlendirme yapılacaktır. Bu amaçla yıllara göre üretim değerleri SPSS programı ile analiz edilmiş olup değerlendirmeler yapılmıştır.

Anahtar kelimeler: Kömür, Linyit, SPSS, İSG

ABSTRACT

SPSS, which stands for Statistical Package for the Social Sciences (Statistics Program for Social Sciences) in English, and Social Sciences as well as Science and so on. It is a computer program that is frequently used in fields for making predictions. The program can work in all software and has a simple and understandable appearance like the Microsoft Excel program. In the 100th Anniversary of our Republic, our Energy Raw Materials Production was estimated with SPSS Modeling and a prediction was made about the total energy raw materials production in order to shed light on the future. The number of fatal accidents experienced after 2015 will also be evaluated, and an evaluation will be made to raise awareness about production forecasts and possible fatal occupational accidents. For this purpose, the production values according to the years were analyzed with the SPSS program and evaluations were made.

Keywords: Coal, Lignite, SPSS, OHS

GİRİŞ

Madenler hayatın her alanında kullanılmaktadır. Örneğin yaşadığımız evlerden, ulaşım için kullandığımız araçlara kadar madenlerin kullanılmadığı alan bulunmamaktadır. Türkiye dünyadaki toplam maden üretiminde 22. ve üretilen maden çeşitliliği açısından ise 8. sırada yer almaktadır.

Milyonlarca yıl önce oluşmuş bitkilerin zamanla fosile dönüşmesi ile hâkim elementi karbon olan kayaç türüne kömür denilmektedir. Kömüre dair ilk bilgiler eski Çin kaynaklarında yer almakta ve kömürü kullanan ilk toplumun Çinliler olduğu düşünülmektedir. Sömürgeleşme Döneminin sonu ve Sanayileşme Döneminin başı olan 18. Yüzyılın ikinci yarısından hemen önce insanoğlunun buhar makinesinin keşfi ile

kömür kullanımı artmıştır. Sanayileşme ile birlikte endüstri devriminin insanlığa yön vermesine sebep olmuştur. Günümüze geldiğimizde kömürün dünyada toplam görünür rezerv miktarı bir trilyon tonun üzerine çıkmıştır. Türkiye'nin toplam rezervi ise bu miktarın yaklaşık %2,1'i civarındadır. İşletilebilir rezervimiz önemli oranda linyit olup, dünya linyit üretim sıralamasında toplam üretim bakımından 1. Olan Almanya'nın ardından 2. sırada yer almaktadır. (WMD,2021) Bu bağlamda gelecek yıllardaki üretim miktarlarının tahmin edilmesi sektör paydaşlarına fikir vereceğinden önem arz etmektedir.

İşletme Ruhsat Sayıları ve Toplam Üretim Miktarlarının Genel Değerlendirmesi

Madenlerin aranması ve işletilmesi ile ilgili günümüzde yürürlükte olan 3213 sayılı Maden Kanunu gereği ruhsatlandırma süreçleri Enerji ve Tabii Kaynaklar Bakanlığı'na bağlı kuruluş olan Maden ve Petrol İşleri Genel Müdürlüğü'nce yürütülmektedir.

Maden ve Petrol İşleri Genel Müdürlüğü tarafından 31.03.2021 tarihinde yayınlanan istatistikler incelendiğinde; 3213 sayılı Maden Kanunu 2. Maddesinde alt grup olarak tanımlanmış olan arama ve işletme ruhsatlarının tamamının toplamının 14.863 olduğu, 31.03.2021 tarihi itibarıyla işletme izni olup faaliyetlerin sürdürüldüğü 7.457 ruhsat bulunmaktadır (MAPEG,2021).

Maden Kanunu 2. Maddesinde sayılan maden grupları içerisinde; "Turba, Linyit, Taşkömürü, Antrasit, Asfaltit, Bitümlü Şist, Bitümlü Şeyl, Kokolit ve Sapropel (Petrol Kanunu hükümleri mahfuz kalmak kaydıyla)" IV. Grup madenlerin (b) bendinde yer alır. Bu bent kapsamında işletme izni düzenlenmiş işletme ruhsat sayılarının toplamının 476 olup, bunların 326 tanesi linyit işletme izni düzenlenmiş işletme ruhsat sahasıdır (MAPEG,2021).

Türkiye'nin toplam kömür rezervi son yıllarda yapılan çalışmalar ile 20 milyar tonun üzerine çıkarılmış olup, rezervlerin geliştirilmesine yönelik arama faaliyetleri devam etmektedir. Üretimin yapıldığı bölgelerin genel değerlendirmesinde ise; taşkömürü üretiminde Zonguldak-Bartın bölgesi, asfaltit üretiminde Şırnak-Hakkâri bölgesi ve linyit üretiminde ise Afşin-Elbistan, Soma- Kınık, Gediz-Tavşanlı, Kale-Yatağan, Malkara- Uzunköprü, Merzifon- Osmaniye, Çan-Balya, Çayırhan-Koyunağlı, Ermenek, Tufanbeyli, Orhaneli, Mengen ve Ilgın bölgeleri önemli üretim noktaları olarak öne çıkmaktadır.

Maden ve Petrol İşleri Genel Müdürlüğü tarafından 31.03.2021 tarihinde yayınlanan üretim istatistikleri incelendiğinde; Türkiye'nin son yıllardaki (2011-2020) yıllık enerji hammaddeleri üretiminde, özellikle 2018 yılında diğer yıllara oranla daha fazla üretim yapıldığı ve yıllık ortalama üretimin 82,4 milyon bandında olduğu görülmektedir. Asfaltit özelinde üretimlerin son dört yılı incelendiğinde ise her geçen yıl üretimin arttığı görülmektedir. Taşkömürü özelinde ise üretimin son yıllarda genel olarak azalma eğiliminde olduğu gözlenmiştir. Özel sektörün linyit üretiminin ise toplam linyit üretimi içinde yaklaşık %47 ve toplam enerji hammaddeleri üretimi içinde ise %44 seviyesinde olduğu görülmektedir.

SGK tarafından yayınlanan madencilik sektöründe iş kazası sonucu hayatını kaybeden çalışan sayıları incelendiğinde; 2015 yılında 26 çalışan, 2016 yılında 11 çalışan, 2017 yılında 31 çalışan, 2018 yılında 11 çalışan, 2019 yılında 13 çalışan ve 2020 yılında 21 çalışan kömür üretim faaliyetleri sırasında hayatını kaybetmiştir (SGK,2021).

Toplam üretim miktarları esas alınarak geleceğe yönelik üretim miktarı tahmininde bulunmak enerji hammaddeleri konusunda faaliyet gösteren kamu ve özel sektör paydaşlarına fikir verecek olup, yaşanan iş kazaları sonucu hayatını kaybeden çalışanlar üzerinden değerlendirme yaparak üretim faaliyetlerinde proaktif yaklaşım için farkındalık oluşturacaktır.

YÖNTEM

Türkiye'deki linyit ve taşkömürüne ait üretim değerlerinin (bin ton) zamana göre değişimini göstermek ve ileriye dönük tahminlerde bulunabilmek amacıyla zaman serileri analiz tekniği kullanılmıştır.

Zaman Serileri Analizi

Zaman serisi analizi belirli bir zaman dilimi içerisinde gerçekleşen olayların analiz edilmesi ve ileriye yönelik bir tahminde bulunabilmek amacıyla yapılmaktadır. Zaman serileri, gözlem değerlerinin zaman içerisindeki dağılımına göre kesikli ve sürekli zaman serileri olarak ikiye ayrılmaktadır. Gözlem değerleri belirli bir zaman dilimi içerisinde sürekli elde ediliyorsa bu zaman serilerine sürekli zaman serileri denilmektedir. Kesikli zaman serilerinde ise gözlem değerleri belirli zaman aralıklarıyla elde edilmektedir.

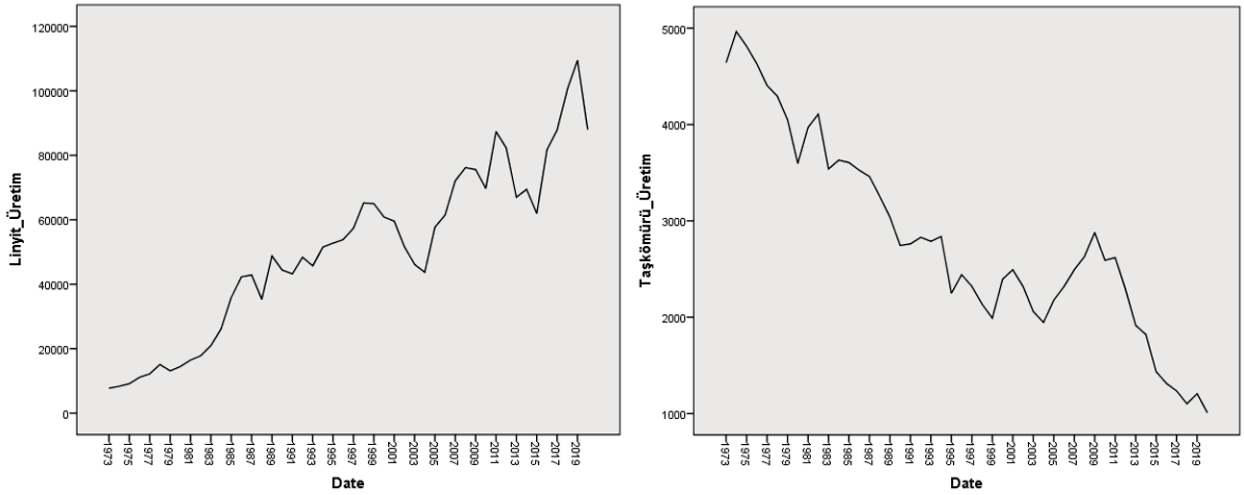
Zaman serileri; kesikli, doğrusal ve stokastik süreç içeriyorsa Box-Jenkins modeli olarak adlandırılır. Genel doğrusal ve durağan Box-Jenkins modelleri AR, MA ve ARMA'dır. Otoregresif (AR-AutoRegressive) modeller Yule, Hareketli Ortalama (MA-MovingAverage) modeli Slutsky, AR ve MA modellerinin karışımı olan Otoregresif Hareketli Ortalama (ARMA-AutoRegressive Moving Average) modelleri ise Wold tarafından geliştirilmiştir (Ergül, 2018).

Box-Jenkins modellerinde az parametre ile zaman serisine en iyi uyan doğrusal modelin elde edilmesi amaçlanmaktadır (Hamzaçebi ve Kutay, 2004). İlk aşama modelin belirlenmesi ikinci aşama ise modelin BIC (Bayesian Bilgi Kriteri) değerine göre değerlendirmektir. En küçük BIC değerine sahip model istenen geçici model olarak belirlenir. Bu aşamalardan sonra parametrelerin ve modelin anlamlılığı test edilir. Modelin genel anlamlılığı ise Ljung-Box Q test istatistiği ile değerlendirilir. Elde edilen anlamlı model yardımıyla da ileriye yönelik tahmin yapılır (Akgül, 2003; Kadılar, 2005).

Bulgular

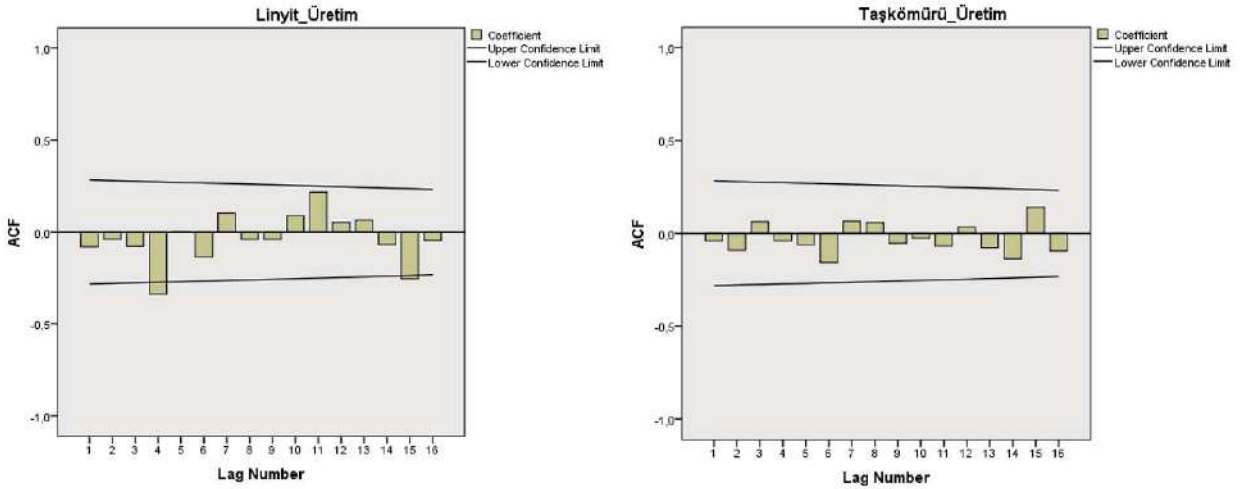
1973-2020 yılları arasında Türkiye'deki linyit ve taşkömürüne ait üretim değerleri (bin ton), TKİ (Türkiye Kömür İşletmeleri) ve MAPEG (Maden ve Petrol İşleri Genel Müdürlüğü) internet sayfalarından alınmıştır. Bu çalışmada linyit ve taşkömürüne ait üretim değerleri (bin ton) için zaman serileri analizi yapılarak ileriye yönelik tahmin yapılmıştır. İstatistiksel analizler için SPSS 22.0 versiyonu kullanılmıştır.

Zaman serileri analizinde kullanılan Box- Jenkins yönteminde tahmin yapılırken kullanılacak modelin belirlenebilmesi için ilk olarak zaman serisi grafiği, otokorelasyon fonksiyonu grafiği (ACF) ve kısmi otokorelasyon fonksiyonu grafikleri elde edilmiştir. Linyit ve taşkömürüne ait üretim değerleri (bin ton) grafiği Şekil 1'de verilmiştir.

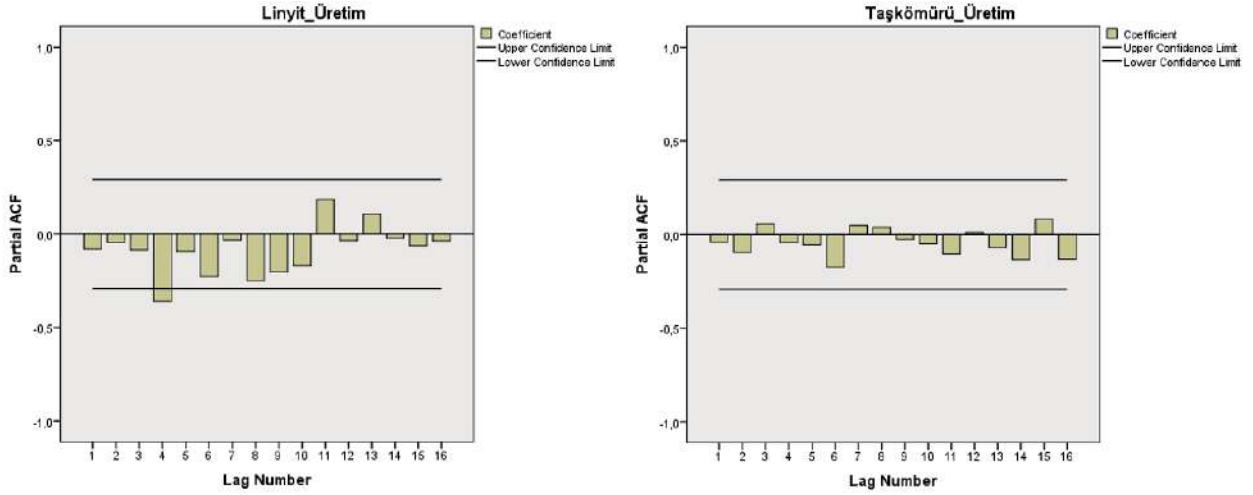


Şekil 1. Üretim değerleri (ton) grafikleri

Şekil 1’de yer alan grafik incelendiğinde grafiklerin dalgalı olduğu görülmektedir. Linyit üretim grafiği artan yönde taşkömürü üretim grafiği ise azalan yönde bir eğilim göstermiştir. Buna göre seriler durağan çıkmamıştır. Zaman serileri analizinde Box-Jenkins yönteminin kullanılabilmesi için serinin durağan olması gerekmektedir. Verilerin durağan olabilmesi için ise fark alınarak ACF ve PACF testleri yapılmıştır. Zaman serisine ait ACF ve PACF grafikleri Şekil 2 ve Şekil 3’te gösterilmiştir.



Şekil 2. Üretim değerleri (bin ton) ACF grafikleri



Şekil 3. Üretim değerleri (bin ton) PACF grafikleri

Şekil 2 ve Şekil 3'e göre seri durağan hale gelmiştir. Böylelikle linyit ve taşkömürü üretim değerleri (bin ton)'nin ileriye yönelik tahmin edilebilmesi için farklı ARIMA modelleri test edilmiş ve sonuçlar Çizelge 1'de yer almıştır. Çizelge 1'e göre BIC değerleri birbirine yakın çıkmıştır. Dolayısıyla bu çalışmada geçici model ARIMA (1,0,0) olarak belirlenmiştir.

Çizelge 1. Linyit ve taşkömürü üretim değerleri (bin ton) için farklı ARIMA modelleri ve BIC değerleri

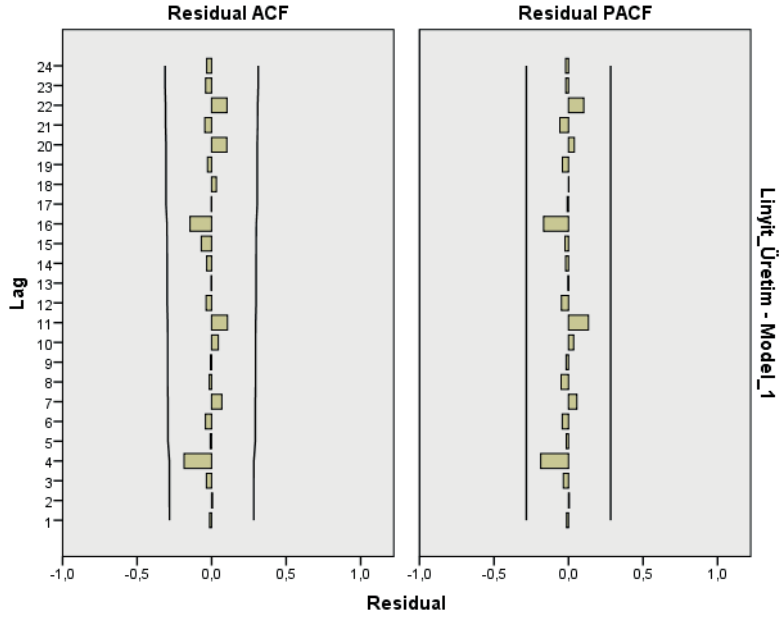
Arıma Modelleri	BIC Değerleri (Linyit)	BIC Değerleri (Taşkömürü)
ARIMA (1,0,0)	18,551	11,937
ARIMA (1,0,1)	18,655	12,055
ARIMA (1,1,1)	17,997	11,103
ARIMA (0,0,1)	19,868	13,097
ARIMA (1,1,0)	18,074	11,046
ARIMA (0,1,1)	19,568	11,286

Söz konusu modelin parametre tahminlerinin anlamlılığı test edilmiştir. Bulunan değerler Çizelge 2'de gösterilmiştir.

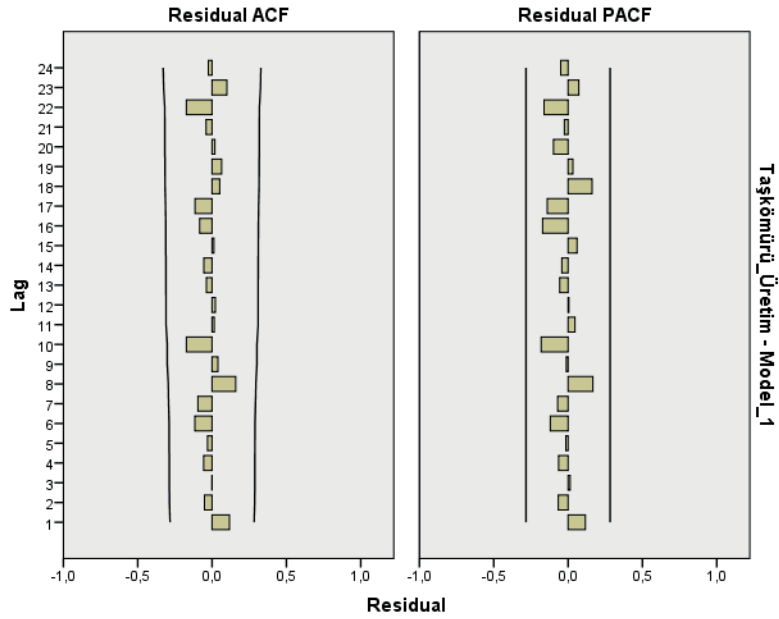
Çizelge 2. Linyit ve taşkömürü üretim değerleri (bin ton) için ARIMA (1,0,0) parametre tahmin değerleri

Parametre	Linyit		Taşkömürü	
	Sabit	AR	Sabit	AR
Tahmin Değeri	48.480,98	0,971	2.818,24	0,988
se	29.456,67	0,038	2.279,86	0,029
t	0,646	25,393	1,236	34,655
p	0,107	0,001	0,223	0,001

Çizelge 2'ye göre hesaplanan olasılık değeri $\alpha=0,05$ anlamlılık düzeyinden küçük olduğu için ARIMA(1,0,0) modelinin parametre tahminleri anlamlı çıkmıştır.



Şekil 4. Linyit ve Taşkömürü üretim değerleri (bin ton) için ARIMA(1,0,0) hata terimleri ACF grafiği



Şekil 5. Linyit ve Taşkömürü üretim değerleri (bin ton) için ARIMA(1,0,0) hata terimleri PACF grafiği

Geçici modelin uygunluğu, Ljung-Box testi ile test edilmiştir. Sonuçlar Çizelge 3’te gösterilmiştir.

Çizelge 3. Ljung-Box testi sonuçları

	Linyit	Taşkömürü
İstatistik Değeri	5,370	7,956
df	17	17
p	0,997	0,967

Ljung-Box testi sonucuna göre hesaplanan olasılık değerleri $\alpha=0,05$ anlamlılık düzeyinden büyük olduğu için geçici model uygun bulunmuştur. Buna göre ARIMA (1,0,0) modeli kullanılarak 2021, 2022 ve 2023 yılları için tahminler yapılmış ve Çizelge 4’te gösterilmiştir.

Çizelge 4. Linyit ve taşkömürü üretim değerlerinin ARIMA(1,0,0) modeli ile tahmin değerleri

Yıl	Linyit Üretimi Tahmin Değeri (milyon ton)	Taşkömürü Üretimi Tahmin Değeri (milyon ton)
2021	110.228.000	1.050.000
2022	95.620.000	987.000
2023	102.047.000	1.102.000

SONUÇ VE ÖNERİLER

Enerji hammaddelerinin sanayi devriminde payı göz önünde bulundurulduğunda insanlığın gelişimi için geçmişte olduğu gibi günümüzde de önemi açıkça anlaşılabilmektedir. Türkiye’nin yıllık ortalama enerji hammaddeleri üretimi 82 milyon ton’un üzerinde olup son yıllarda Türkiye’de üretim miktarlarının arttığı göze çarpmaktadır.

Linyit üretim miktarlarının ARIMA ile tahmin değerleri 2021 yılında 110,22 milyon ton, 2022 yılında 95,62 milyon ton ve Cumhuriyetin 100. yılında 102,04 milyon ton olacağı tahmin edilmiştir.

Taşkömürü üretim miktarlarının ise ARIMA ile tahmin değerleri 2021 yılında 1,05 milyon ton, 2022 yılında 0,98 milyon ton ve Cumhuriyetin 100. yılında 1,1 milyon ton olacağı tahmin edilmiştir.

Toplam enerji hammaddeleri üretiminin ARIMA ile tahmin değerleri 2021 yılında 111,27 milyon ton, 2022 yılında 96,6 milyon ton ve Cumhuriyetin 100. yılında 103,14 milyon ton olacağı tahmin edilmiştir.

Son yıllarda yaşanmış olan ölümle sonuçlanmış iş kazalarının enerji hammaddeleri üretimi bakımından değerlendirilmesinde ölümlü iş kazası ortalamasının 4,6 milyon ton üretim başına 1 adet olduğu hesap edilmiştir. Üretimin 103 milyonun üzerinde olacağı tahmini göz önünde tutularak, üretimde proaktif yaklaşım ile işletmelerin geçmiş dönemde yaşanmış kazalarının oluş şekillerine göre değerlendirme yaparak tahmini üretim değerleri üzerinden oluşabilecek iş kazalarının önlenmesine ilişkin tahmin yürütmesi ve önlem alması olumlu katkı sağlayacaktır.

Bu çalışmada zaman serileri analizi yöntemi kullanılarak enerji hammaddeleri üretim miktarına ilişkin bir tahmin yapılmıştır. Dolayısıyla bu çalışmanın enerji hammaddeleri üretimine ilişkin verilerin zaman serileri analizi yöntemi ile analiz edilmesi ve buna bağlı olarak ileriye yönelik tahmin yapılması bakımından ilk çalışma olduğu söylenebilir. Çalışmada kullanılan veriler farklı madenler için araştırılarak söz konusu madenlerin geleceği hakkında geniş kapsamlı tahminlerde bulunulabilir.

KAYNAKLAR

- Akgül, İ., (2003). Zaman Serileri Analizi ve ARI-MA Modelleri. Der Yayınları, İstanbul.
 Ergül, B., (2018). Türkiye’deki İş Kazalarının Zaman Serisi Analiz Teknikleri ve Yapay Sinir Ağları Tekniği ile İncelenmesi, *Karaelmeas İş Sağlığı ve Güvenliği Dergisi*, 2(2): 63-74.

Hamzaçebi, C. ve Kutay, F., (2004). Yapay Sinir Ağları ile Türkiye elektrik Enerjisi Üretimini 2010 Yılına Kadar Tahmini. Gazi Üniversitesi Mühendislik Mimarlık Fakültesi Dergisi, 19(3).

Kadılar, C., (2005). SPSS Uygulamalı Zaman Serileri Analizine Giriş. Bizim Büro Basımevi, Ankara.

Reichl, C., Schatz, M., (2021). World Mining Data (Iron and Ferro-Alloy Metals Non-Ferrous Metals Precious Metals Industrial Minerals Mineral Fuels), Volume:36, Vienna. <https://www.world-mining-data.info/wmd/downloads/PDF/WMD2021.pdf> (erişim tarihi:07.12.2021)

Maden Tetkik ve Arama Genel Müdürlüğü (MTA), (2020). Kömür Arama Araştırmaları, <https://www.mta.gov.tr/v3.0/arastirmalar/komur-arama-arastirmalari> (erişim tarihi: 08.12.2021)

Maden ve Petrol İşleri Genel Müdürlüğü (MAPEG), (2021). Maden Üretim Değerleri, https://www.mapeg.gov.tr/maden_istatistik.aspx (erişim tarihi: 08.12.2021)

Maden ve Petrol İşleri Genel Müdürlüğü (MAPEG), 2021. Mayıs 2021 Tüm Ruhsat Listesi (yayınlanmamış).

Türkiye Kömür İşletmeleri Kurumu (TKİ), (2020). Türkiye Kömür Üretim -Tüketim İstatistikleri, <https://www.tki.gov.tr/istatistikler> (erişim tarihi: 08.12.2021)

Türkiye Kömür İşletmeleri Kurumu (TKİ), (2020). Dünya ve Türkiye Kömür Kaynak ve Rezerv Durumu, <https://www.tki.gov.tr/istatistikler> (erişim tarihi: 08.12.2021)

ÇOK OCAK İÇEREN AÇIK İŞLETMELERDE GÜVENLİK FAKTÖRÜ DEĞİŞİMİNİN İNCELENMESİ INVESTIGATION OF THE SAFETY FACTOR CHANGE IN OPEN PIT WITH MULTI-QUARRY

C.O. Aksoy^{1,*}, G.G.U. Aksoy², H. E. Yaman³

¹ Dokuz Eylül Üniversitesi Maden Mühendisliği Bölümü
(*Sorumlu yazar: okay.aksoy@deu.edu.tr)

² Hacettepe Üniversitesi, Maden Mühendisliği Bölümü

³ Dokuz Eylül Üniversitesi Torbalı Meslek Yüksek Okulu

ÖZET

Madencilikte her gün birçok şey değişiyor ve gelişiyor. Gelişmekte olan madencilik sektöründe, küçük madencilik alanları artık ihtiyaçları karşılayamamaktadır. Özellikle metal madenlerinde yapılan küçük ölçekli madencilik operasyonları, ekonomik çalışabilirliklerini her geçen gün kaybetmektedir. Bu nedenle günümüzde çok büyük ölçekte işletilen birçok maden sahası bulunmaktadır. Bu bildiride, birden fazla açık ocak içeren bir maden işletmesinde araştırmalar yapılmıştır. Araştırmalar, her bir açık ocağın tek başına güvenlik faktörleri ile bütün açık ocakların birlikte analiz edilmesiyle ortaya çıkan bütünleşik güvenlik faktörünün karşılaştırılması üzerine yapılmıştır. Sonuçlar incelendiğinde, bütüncül güvenlik faktörünün daha düşük olduğu görülmüştür.

Anahtar Sözcükler: Açık maden işletmesi, nümerik modelleme, şev stabilitesi, güvenlik faktörü

ABSTRACT

Many things change and develop everyday in mining. In the developing mining industry, small mining areas can no longer meet the needs. Small-scale mining operations, especially in metal mines, lose their economic operability day by day. For this reason, there are many mining sites operated on a very large scale today. In this paper, researches were conducted in a mining operation that includes more than one open pit. Research has been done on the comparison of the safety factors of each open pit alone and the integrated safety factor that is obtained by analyzing all open pits together. When the results were examined, it was seen that the overall safety factor was lower.

Keywords: Open-pit mine, numerical analysis, slope stability, Safety Factor

GİRİŞ

Açık ocak işletmelerinde şev stabilitesi ocak güvenliği için çok önemlidir. İşletme yaparken ekonomik açıdan şevleri mümkün olduğu kadar yüksek açıda tutmak, ancak güvenli sınırdan çok önemlidir. Bu sayede dekapaj oranı azalacak ve maden ekonomik olarak işletilebilecektir. Ama güvenlik önce gelmektedir. Bu nedenle, ocak genel şev açısı genellikle düşüktür. Ayrıca, yeraltı suyu, kaya türü, süreksizlikler vb. parametreler şev stabilitesini önemli ölçüde etkiler. Şekil 1'de şev stabilitesini etkileyen faktörler verilmiştir (Atkinson, 1977).



Şekil 1. Şev stabilitesini etkileyen faktörler (Atkinson, 1977)

Kaya Kütle Parametrelerinin Belirlenmesi

Kaya mühendisliğinde nihai tasarımın gerçekleştirilmesi uzun ve pahalı bir süreç gerektirir. Çalışmaların başlangıcında kaya parametrelerinin ve özelliklerinin belirlenmesi çok kritiktir. Bu amaçla bazı araştırmalar tarafından geliştirilen kaya kütle sınıflandırma sistemleri Çizelge 1'de verilmiştir (Palmström, 1995, Edelbro, 2006, Palmström ve Stille, 2007, Aksoy, 2012). Kaya kütlelerinin deformasyon modülünün yerinde testlerinin, hem ekipmandan, hem test sahasının hazırlanmasından hem de test sırasında patlatma hasarından kaynaklanan ölçüm hatalarına tabi olduğu genel olarak bilinmektedir (Palmstrom ve Singh, 2001). Bu nedenle, kaya kütlelerinin iyi saha karakterizasyonları ve uygun bir dolaylı yöntemin kullanılması birçok durumda pahalı yerinde ölçümlerden daha iyi sonuçlar verebilir (Palmstrom ve Singh, 2001). Mevcut deneysel veriler kullanılarak, farklı mekanik özellikler arasındaki bazı ampirik doğrudan ilişkiler ve çeşitli araştırmacılar tarafından önerilen bazı kaya kütle sınıflandırma parametreleri Çizelge 2'de listelenmiştir (Aydan ve diğerleri, 2014).

İnceleme alanında, mika şist, kuvars, feldspat, kalker, andezit olmak üzere 5 kaya türü hakimdir. Gerçekleştirilen analizlerde kullanılan verilerin bir kısmı tarafımıza maden sahası tarafından verilmiş olup, bir kısmı tarafımızca maden sahasından alınan sondaj numuneleri üzerinde yapılan laboratuvar analizleri ile belirlenmiştir.

Çizelge 1. Bazı kaya sınıflandırma sistemleri (Palmström, 1995, Edelbro, 2006, Palmström ve Stille, 2007, Aksoy, 2012)

İsim	Form ve Tip*	Ana Uygulamalar ve Açıklamalar	Yazar ve İlk Versiyonu
Terzaghi kaya yükü sınıflama sistemi	Tanımlayıcı ve davranışsal form	Çelik tahkimatlı tüneller (modern tünel açma için uygun değildir)	Terzaghi (1946)
	İşlevsel tür		
Lauffer'in desteksiz durma süresi sınıflaması	Tanımlayıcı form ve Genel tür	Tünel tasarımında girdi için (muhafazakar)	Lauffer (1958)
Yeni Avustralya Tünel Açma Yöntemi (NATM)	Tanımlayıcı ve davranışsal form Tünel açma konsepti	Dayanımsız zeminlerde kazı ve tasarım için (sıkışma zemini koşullarında kullanılır)	Rabcewicz (1964, 1965)
Kaya mekaniği	Tanımlayıcı form	Kaya mekaniğine girdi için	Patching ve Coates (1968)
Zemin ve kayaların birleşik sınıflaması	Genel tür Tanımlayıcı form	Parçacıklara ve bloklara dayalı iletişim için	Deere vd. (1969)
Kaya Kalitesi Belirteci (RQD)	Genel tür Nümerik form	Karot loglamasına bağlı olarak diğer sınıflama sistemlerinde kullanılır.	Deere and Deere (1988) Deere vd. (1967)
Boyut dayanım sınıflaması	Genel tür Nümerik form	Esas olarak madencilikte kullanılan kaya dayanımı ve blok çapına göre	Franklin (1975)
Kaya Yapısı Değeri (RSR)	Fonksiyonel tür Nümerik form	Tünellerde (çelik) tahkimat tasarımı için (çelik donatılı püskürtme beton ile kullanışlı değildir)	Wickham vd. (1972)
	Fonksiyonel tür		
Jeomekanik Sınıflama Sistemi (RMR)	Nümerik form	Tünellerin, madenlerin ve temellerin tasarımı için	Bieniawski (1973)
Q Sınıflama Sistemi	Fonksiyonel tür Nümerik form	Yeraltı kazılarında tahkimat tasarımı için (tünel, geniş yeraltı açıklıkları)	Barton vd. (1974)
Madencilik RMR (MRMR)	Nümerik form	Madencilikte kaya tahkimatı	Laubscher (1975)

Tipolojik sınıflama	Fonksiyonel tür Tanımlayıcı form	İletişimde kullanım için	Laubscher (1977) Matula ve Holzer (1978)
Birleştirilmiş kaya sınıflama sistemi	Genel tür Tanımlayıcı form	İletişimde kullanım için	Williamson (1980)
Temel jeoteknik sınıflama (BGD)	Genel tür Tanımlayıcı form	Genel uygulamalar için	ISRM (1981)
Şev Kütle Puanlaması (SMR)	Nümerik form Fonksiyonel tür	Şevler için tahmini duraylılık problemleri ve destek teknikleri	Romana (1985)
Jeolojik Dayanım İndeksi (GSI)	Nümerik form Fonksiyonel tür	Mühendislik uygulamalarına girdi olarak kaya kütlelerinin dayanımını gösterir	Hoek (1994)
Rock Mass Index (RMI)	Nümerik form Fonksiyonel tür	Kaya mühendisliği, genel karakterizasyon, tahkimat dizaynı	Palmström (1995)

*

Tanımlayıcı biçim: sisteme giriş, esas olarak açıklamalara dayalıdır;
 Nümerik biçim: girdi parametrelerine karakterlerine göre nümerik değerler verilir;
 Davranışsal form: girdi, bir tüneldeki kaya kütlesi davranışına dayalıdır;
 Genel tip: sistem, genel bir karakterizasyon işlevi görecektir şekilde tasarlanmıştır;
 Fonksiyonel tip: sistem özel bir uygulama için yapılandırılmıştır (örneğin, kaya desteği için).

Çizelge 2. Kaya kütlesi sınıflandırması ile kaya kütlesinin özellikleri arasındaki doğrudan ilişkiler (Aydan vd., 2014).

Property	Empirical relation	Proposed by
Deformation modulus, E_m	$E_m = 2RMR - 100$ (GPa) (for $RMR > 50$)	Bieniawski (1978)
	$E_m = 10^{(RMR-10)/40}$ (GPa)	Serafim and Pereira (1983)
	$E_m = e^{(4.407+0.081 \cdot RMR)}$ (GPa)	Jašarević and Kovačević (1996)
	$E_m = 0.0097RMR^{3.54}$ (MPa)	Aydan et al. (1997)
	$E_m = 25 \log Q$ (GPa)	Grimstad and Barton (1993)
	$E_m = (1 - \frac{D}{2}) \sqrt{\frac{GSI}{100}} 10^{((GSI-10)/40)}$ (GPa) (for $\sigma_{ci} < 100$ MPa)	Hoek et al. (2002)
	$E_m = 100 \frac{(1-0.5D)}{1+e^{(0.75+20D-0.5D)/11}}$ (GPa)	Hoek and Diederichs (2006)
	$E_m = 0.135 [E_i 1 + \frac{1}{WD} \cdot \frac{RQD}{100}]^{1.1811}$ (GPa)	Kayabasi et al. (2003)
	$E_m = 5.6RMI^{0.3}$ (GPa) (for $RMI > 0.1$)	Palmström (1996)
	$E_m = 0.1(RMR/10)^3$	Mitri et al. (1994)
	$E_m = 7(\pm 3) \sqrt{10^{(RMR-44)/21}}$ (GPa)	Diederichs and Kaiser (1999)
	$E_m = 10Q^{1/3}$ (GPa)	Barton (1995)
	$E_m = 10(\frac{Q}{100})^{1/3}$ (GPa)	Barton (2002)
	$E_m = 10^{((GSI-10)/40)} \sqrt{\frac{GSI}{100}}$ (GPa)	Hoek and Brown (1997)
	$E_m = 0.0876RMR$ (GPa) (for $RMR > 50$)	Galera et al. (2005)
$E_m = 0.0876RMR + 1.056(RMR - 50) + 0.015(RMR - 50)^2$ (GPa) (for $RMR \leq 50$)	Galera et al. (2005)	
Uniaxial compressive strength, σ_{cm} (MPa)	$\sigma_{cm} = 0.0016RMR^{2.5}$	Aydan et al. (1997)
	$\sigma_{cm} = 5\gamma(\frac{Q}{100})^{1/3}$	Barton(2002)
Friction angle, ϕ_m (°)	$\phi_m = 20 + 0.5RMR$	Aydan and Kawamoto (2001)
	$\phi_m = 20\sigma_{cm}^{0.25}$	Aydan et al. (1993)
	$\phi_m = \tan^{-1}(\frac{J_c}{J_r} \times \frac{J_a}{J_w})$	Barton (2002)
Cohesion, c_m (MPa)	$c_m = \frac{\sigma_{cm} (1 - \sin \phi_m)}{2 \cos \phi_m}$	Aydan and Kawamoto (2001)
	$c_m = (\frac{RQD}{J_c} \times \frac{1}{SRF} \times \frac{\sigma_{ci}}{100})$	Barton (2002)
Poisson's ratio, ν_m	$\nu_m = 0.25(1 + e^{-\sigma_{cm}/4})$	Aydan et al. (1993)
	$\nu_m = 0.5 - 0.2 \frac{RMR}{RMR+0.2(100-RMR)}$	Tokashiki and Aydan (2010)

E_m Kaya Kütlesi Deformasyon Modülü, E_i Sağlam Kaya Young Modülü, RMR Kaya Kütlesi Oranı, Q Kaya Kütle Kalitesi, GSI Jeolojik Dayanım İndeksi, D Bozulma Faktörü, σ_{ci} Sağlam Kayanın Tek Eksenli Basınç dayanımı, σ_{cm} Kaya Kütlesinin Tek Eksenli Basınç Dayanımı, RQD Kaya Kalitesi Göstergesi, RMI Kaya Kütle İndeksi, WD Ayrışma Derecesi, m Kaya Kütlesinin Sürtünme Açısı, c_m Kaya Kütlesinin Kohezyonu, ν_m Kaya Kütlesi Poisson'un Oranı, J_n Eklem Seti Sayısı, J_r Eklem Pürüzlülük Derecesi, J_w Eklem Suyu Derecesi, J_a Eklem Alterasyon Derecesi, SRF Gerilme Azaltma Faktörü, d Kaya Yoğunluğu (t/m^3)

Nümerik modelde kullanılan kaya parametreleri Tablo 2'deki formüllerden yararlanılarak belirlenmiş ve Çizelge 3'te verilmiştir.

Çizelge 3. Nümerik modelde kullanılan kaya parametreleri

Kaya Türleri	d (kN/m ³)	σ_c (MPa)	ϕ (°)	ν	c (kPa)	E_m (MPa)
MİKA ŞİST	22,80	10,67	16,71	0,25	273	405,96
FELDSPAT	22,75	20,87	22,75	0,20	414	525,87
ANDEZİT	23,61	18,53	22,62	0,22	667	553.20
KALKER	22,30	7,04	24,34	0,27	234	524.90
KUVARS	23,84	7,49	24,08	0,25	264	480.92

Nümerik Modelleme Analizi

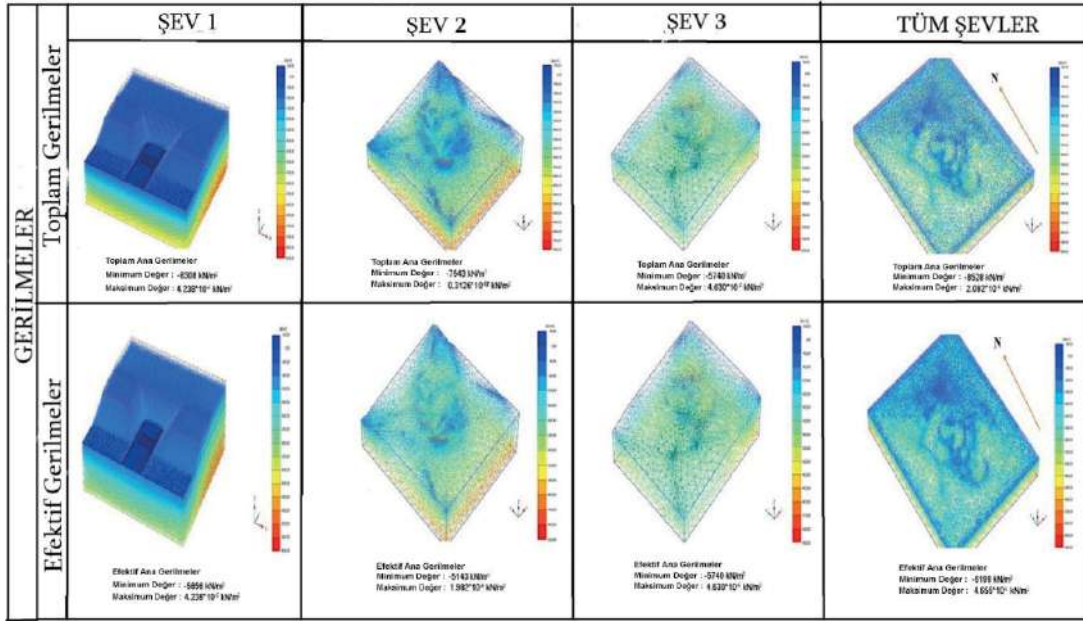
Bu çalışmada birbirine yakın konumlanmış üç farklı açık ocağın ayrı ayrı nümerik modelleme analizi yapılmıştır. Ayrıca, tüm bu üç açık ocağı kapsayan bir nümerik modelleme analizi yapılmış ve

	1. AÇIK OCAK
	2. AÇIK OCAK
	3. AÇIK OCAK
	BÜTÜN AÇIK OCAKLAR

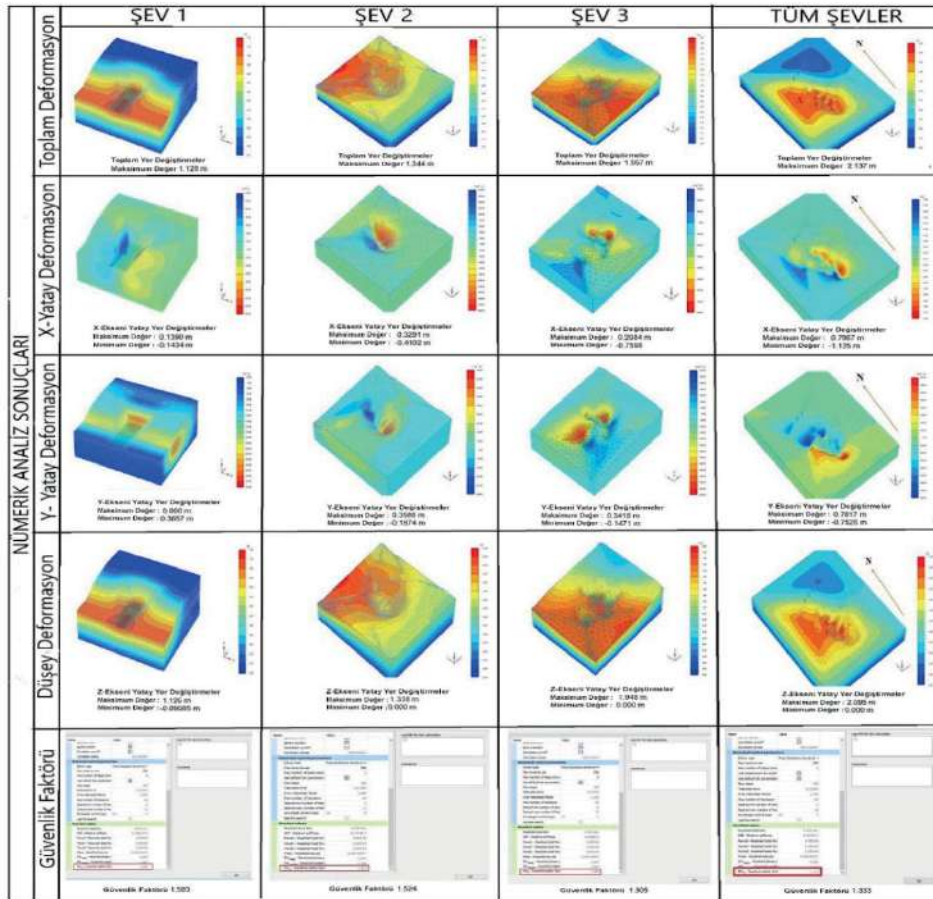
Şekil 2. Şevlerin durumu

1. Açık Ocak mikaşist, 2. Açık Ocak volkanik kaya, metamorfik kaya ve intruzif kaya, 3. Açık Ocak ise QFP ve mikaşistlerden oluşmaktadır. Şev stabilitesi analizlerinde kullanılan nümerik modelleme yazılımı “Sonlu Elemanlar Metodu” ile çalışmakta olup, 3B çözümlene yapılmıştır. Sonlu Elemanlar Yöntemi, matematiksel olarak geliştirilen ilk yöntem olduğu için diğer yöntemlerden çok daha iyi performans göstermektedir. Nümerik modelleme analizlerinde Mohr-Coulomb Yenilme Kriterleri kullanılmıştır.

Analizler genel olarak 3 aşamada gerçekleştirilmiştir, Birinci aşama, başlangıç aşaması olup, gravite yüklemesi ile başlangıç koşullarının oluşturulduğu aşamadır. İkinci aşama tüm kazı aşamalarının (her bir açık ocağı basamak sayısına göre alt aşamalar içermektedir) yapıldığı aşama ve , üçüncü aşama ise c-Phi yöntemi ile güvenlik faktörünün belirlendiği aşamadır. Açık Ocak 1 (Şev 1), Açık Ocak 2 (Şev 2), Açık Ocak 3 (Şev 3) ve Tüm Açık Ocaklar (Tüm Şevler) için nümerik modelleme sonuçları Şekil 3 ve Şekil 4'te verilmiştir.



Şekil 3. Tüm nümerik model analizinin sonuçları (toplam ve efektif gerilmeler)



Şekil 4. Tüm nümerik modelleme analizlerinin sonuçları (deformasyonlar ve güvenlik faktörü)

NÜMERİK MODELLEME ANALİZLERİNİN SONUÇLARININ DEĞERLENDİRMESİ

Açık Ocak 1 için tüm kazılar tamamlandıktan sonra modelde meydana gelen toplam deformasyonların 1.128 m olduğu görülmektedir. Modelin yatay x-ekseninde 0.1434 m maksimum deformasyon meydana gelmiştir. Modelin yatay y-ekseninde 0.3657 m maksimum deformasyon meydana gelmiştir. Modelin düşey z-ekseninde maksimum 1.126 m deformasyon meydana gelmiştir. Model minimum $4.238 \cdot 10^{-6}$ kN/m² ve maksimum 5856 kN/m² ana efektif gerilmelere sahiptir. Model minimum $4.238 \cdot 10^{-6}$ kN/m² ve maksimum 8308 kN/m² ana toplam gerilmelere sahiptir. Tüm kazı aşamaları tamamlandıktan sonra c-Phi indirgeme yöntemi ile güvenlik faktörü belirlenmiştir. Modelin nihai versiyonu itibariyle oluşan güvenlik katsayısı ise 1.593 olarak belirlenmiştir.

Açık Ocak 2 için tüm kazılar tamamlandıktan sonra modelde meydana gelen toplam deformasyonların 1.344 m olduğu görülmektedir. Modelin yatay x-ekseninde maksimum 0,4102 m yatay y-ekseninde maksimum 0.3588 m, düşey y-ekseninde maksimum 1.338 m deformasyon meydana gelmiştir. Modelde maksimum 5143 kN/m² efektif gerilmelere ve maksimum 7543 kN/m² toplam gerilme olduğu tahmin edilmiştir. Tüm kazı aşamaları tamamlandıktan sonra c-Phi indirgeme yöntemi ile güvenlik faktörü belirlenmiştir. Modelin nihai versiyonu itibariyle oluşan güvenlik katsayısı ise 1.524 olarak belirlenmiştir.

Açık Ocak 3 için tüm kazılar tamamlandıktan sonra modelde meydana gelen toplam deformasyonların 1.957 m olduğu görülmektedir. Yatay x-ekseninde meydana gelen maksimum deformasyon miktarının 1.125 m olduğu görülmüştür. Modelin yatay y-ekseninde maksimum 0.7817 m, düşey y-ekseninde maksimum 2.095 m deformasyon meydana geldiği tahmin edilmektedir. Model sonuçlarına göre maksimum efektif gerilmenin 5740 kN/m² maksimum toplam gerilmenin ise 5740 kN/m² olacağı değerlendirilmiştir. Bu açık ocak için tüm kazı aşamaları tamamlandıktan sonra c-Phi indirgeme yöntemi ile güvenlik faktörü hesaplaması sonrasında, güvenlik faktörünün 1.305 olduğu belirlenmiştir.

Birbirine çok yakın olan 3 açık ocağı birbiri ile etkileşiminin incelendiği modelde meydana gelen toplam deformasyonların 2.137 m olduğu görülmektedir. Modelin yatay x-ekseninde meydana gelen deformasyonlar maksimum 1.125 m, yatay y-ekseninde 0.782 m maksimum, düşey y-ekseninde 2.095 m maksimum deformasyon olduğu görülmüştür. c-Phi indirgeme yöntemi ile yapılan hesaplamada güvenlik faktörünün 1.333 olarak belirlenmiştir.

Üç açık ocağın incelendiği modele baktığımızda, Açık Ocak 1'deki toplam deformasyonun diğer ocakların etkileşimi ile yaklaşık 1.45 m'ye yükseldiği görülmektedir. Yatay deformasyonların x-ekseni ve y-eksenindeki maksimum değerlerinin sırasıyla yaklaşık 0,25 m ve 0,50 m'ye yükseldiği, z-eksenindeki düşey deformasyon değerlerinin yaklaşık 1.8 m'ye yükseldiği gözlemlenmiştir. Maksimum toplam ve efektif gerilmelerin yaklaşık 6100 kN/m² ve 8500 kN/m²'ye yükseldiği görülmektedir.

Açık Ocak 2'deki toplam deformasyonun diğer ocakların etkileşimi ile yaklaşık 2 m'ye yükseldiği görülmektedir. Yatay deformasyonların x-ekseni ve y-eksenindeki minimum değerlerinin sırasıyla yaklaşık 1.125 m ve 0.78 m'ye yükseldiği, z-eksenindeki düşey deformasyon değerlerinin yaklaşık 2.095 m'ye yükseldiği gözlemlenmiştir. Maksimum toplam ve efektif gerilmelerin yaklaşık 5800 kN/m² ve 7800 kN/m²'ye yükseldiği görülmektedir.

Son olarak, üç açık ocağın etkileşiminin incelendiği nümerik modele baktığımızda, Açık Ocak 3'deki toplam deformasyonun diğer ocaklardaki deformasyon etkilerinden etkilendiği ve 2.1 m'ye yükseldiği görülmektedir. Yatay deformasyonların x-ekseni ve y-eksenindeki minimum değerlerinin sırasıyla yaklaşık 1 m ve 0.8 m'ye yükseldiği, z-eksenindeki düşey deformasyon değerlerinin yaklaşık 2.095 m'ye yükseldiği gözlemlenmiştir. Maksimum toplam ve efektif gerilmelerin yaklaşık 6000 kN/m² ve 8000 kN/m²'ye yükseldiği görülmektedir.

SONUÇ

Görüldüğü gibi birbirinden bağımsız olarak yapılan analizler ile tüm şevlerin bir arada ele alındığı analizler arasında farklılıklar bulunmaktadır. Tüm şevler birlikte değerlendirildiğinde, toplam efektif gerilmelerin ve yatay-düşey deformasyonların her şev için bağımsız analizlerden daha yüksek olduğu görülmektedir. Bu durum özellikle güvenlik faktörünün düşük olduğu şevler için daha güvenli bir bölgede kalma gerekliliğini ortaya koymaktadır.

Tüm şevlerin analizinde, emniyet faktörü aşaması analiz edildiğinde, Şev-1 bölgesinde olası yenilme olasılığının olduğu sonucuna varılmaktadır. Bu durumda analize göre güvenlik faktörü 1.333 olarak hesaplanmıştır.

KAYNAKLAR

- Aksoy C. O., Geniş M., Uyar Aldaş GG., Özacar V., Özer S.C., Yılmaz Ö., “A comparative study of the determination of rock mass deformation modulus by using different empirical approaches”, *Engineering Geology*, 131-132, 19-28
- Atkinson, T., 1977. “Surface Mining. De ingénieur”, jrg 89, nr 28/29.
- Aydan Ö., Ulusay A., Tokashiki N., 2014. “A New Rock Mass Quality Rating System: Rock Mass Quality Rating (RMQR) and Its Application to the Estimation of Geomechanical Characteristics of Rock Masses”, *Rock Mech. Rock Eng.*, 47, 1255-1276
- Edelbro, C., Sjoberg, J., Nordlund, E., 2006. A quantitative comparison of strength criteria for hard rock masses. *Tunnell. Undergr. Space Technol.* 22, 57–68.
- Palmström, A., 1995. RMI-a Rock Mass Characterization System For Rock Engineering Purposes. Ph.D. thesis. Univ. of Oslo, (www.rockmass.net).
- Palmstrom, A., Stille, H., 2007. Ground behaviour and rock engineering tools for underground excavations. *Tunnell. Undergr. Space Technol.* 22, 363–376.

DATA-BASED DECISION-MAKING IN UNDERGROUND DRILLING OPERATIONS

A. Yıldız^{1,*}, M. Erkayaoğlu¹

¹ *Middle East Technical University, Department of Mining Engineering*
(*Corresponding author: artun.yildiz@metu.edu.tr)

ABSTRACT

Natural resources are an essential part of sustainable development, and as shallow resources become depleted, the mining industry shifts intensively to underground mining. Equipment-intensive mining activities such as drilling can generate important data, particularly when consumables are examined, as they directly relate to the total production cost. The purpose of this study is to develop a data-driven approach for underground drilling activities in order to evaluate drilling efficiency using consumables. During a 1-month period, 35, 35, 30 percent of the total number of holes drilled and 35, 34, 31 percent of the total drilling were completed at night, day, and evening shifts, respectively. The distribution of failure codes in total for the night, day, and evening shifts occurred as 36, 24, and 19, respectively. The failure code 2, denoted by the bit breakout characteristic, was the most frequent failure code, with 21 pieces. The study's main purpose is to collect operational data to create a dashboard and generate online reports with consumable performance (service life and rate of penetration) outcomes. These reports can be used as supporting elements in mine management decision-making and as tools to improve the drilling efficiency of operations teams.

Keywords: Drilling, business intelligence, data analysis

INTRODUCTION

Drilling activities have downstream impacts that might cause ore dilution, the stability of underground openings, and the creation of undesired blocks in underground mining. This study aims to collect operational data for business intelligence purposes such as dashboards and online reports for rock tool performance. However, the proposed structure may also be applied for other phases of operations utilizing operational data. The developed dashboard utilizes data from an underground gold mine with a corporate data infrastructure. The increasing demand for higher production rates requires investment in mining technology. Another major factor leading operations to focus on equipment efficiency is low-grade orebodies. The potential improvements achieved through this study could generate high added value for downstream mining processes due to data utilization. Actionable processes and data visualizations can be driving forces for using data in all stages of management. Mining operations with comparably lower technology infrastructure rely on manually collected data, and it is known that the potential advantage of data is proportional to the quality and content. Data utilization and analysis have become conventional for various industries, and most modern mining operations generate vast amounts of data. The proposed data-driven dashboard and online reports provide insight into the rock tools used by different operators daily.

LITERATURE REVIEW

Increases in productivity in an equipment-intensive industry like mining may significantly influence the production capacity of raw materials. Drilling operations may be regarded as early stages of underground mining production similar to blasting, loading and hauling, development, support, and others. Various researchers utilized data analysis applications to identify mining equipment-related inefficiencies. Most of the studies are concentrated on measurement while drilling (MWD) and wear mechanisms of rock drill components. According to Teale (1965), mechanical specific energy is expressed as the proportion of work required to drill one cubic content of the rock. Kosolapov (2020) derived an equation for mechanical specific energy (MSE), a key indicator of drilling efficiency, and defined a relationship between MSE and the strength index of Protodyakonov. The association between specific explosive energy and mechanical specific energy (MSE) allows the measurement of MSE during blasthole drilling and the computation of specific explosive energy and rock strength index in the case of rotary, hydraulic, and electric drill rigs. Regotunov and Sukhov (2016) presented the results after examining the rock mass strength during roller-bit drilling. Their approach for calculating the strength properties of the local rock mass, which will be blasted, is described in detail in their paper. For determining the strength and technical features of the rocks, one of the most critical metrics was their power consumption (specific energy). Brown and Barr (1978) studied drilling parameters with a perspective of the geomechanical characteristics of rock material. It was concluded that only continuous drilling data might provide reliable mechanical information. Using rotary percussive drilling, all characteristics were divided into dependent and independent groups, as seen in Figure 1 (Isheyskiy and Sanchidrián, 2020). The rock mass properties identified were found to be independent of drill rig capacity or drilling style.

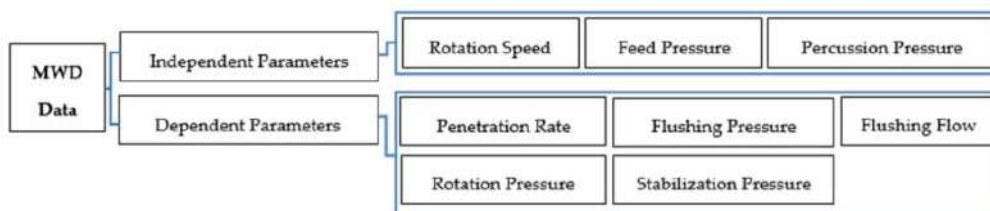


Figure 1. Brown and Barr's classification of dependent and independent measurement while drilling (MWD) features (1978)

According to Brown et al. (1984), geological variables, compressive strength, and MSE might be used to approximate mechanical and physical attributes of rocks. The rock mass's cavities and closed and open fractures were also identified using this method. Leighton (1982) identified the optimum drilling and blasting criteria for contour blasting in an open-pit copper mine. This work (Isheyskiy and Sanchidrián, 2020) was among the first to demonstrate how drilling and blasting activities may be improved by using drilling variables to calculate the rock quality index (RQI). Only two drilling metrics, thrust and penetration rate, composed the RQI and were subjected only to one kind of drilling technique. To circumvent the limitations of rock quality indicators, Lopez (1995) developed a characterization index for rocks contingent on drilling diameter, thrust, bit rotation speed, and penetration rate. It was observed that rock characterization index (I_p) was linked to rock strength since penetration rate was mainly related to geomechanical properties, so that powder factor was studied for varying I_p index values. Blastability index (BI) contingent on rock mass description (RMD) was proposed by Lilly (1986). Block structure (joint plane spacing (JPS) and joint plane orientation (JPO)) and the uniaxial compression strength of rocks (hardness), as well as specific gravity (specific gravity influence (SGI)) of rocks, were shown to be the most critical factors in blasting efficiency, according to this research. Using the given parameters, an equation for calculating BI was introduced (Isheyskiy and Sanchidrián, 2020).

$$BI = 0.5 \times (RMD + JPS + JPO + SGI + HD) \quad (1)$$

The blastability of rock masses was also investigated by Yin and Liu (2001) using drill log data. According to Isheyskiy and Sanchidrián (2020), a novel RQI equation with two invariants has been developed, differing from previous formulations. A study by Scoble et al. (1987 and 1989) examined how drilling parameters are linked with geophysical logging. Even if it was established that the stated link was insufficient, this mainly was owing to the challenges in assessing data provided by rigs. Like Brown and Barr (1978), it was revealed that rotary drilling characteristics might be divided into two categories: driller-controlled independent variables like the speed of rotation or weight of bit and rock-dependent variables. When Schunnesson (1990) looked at different types of rocks, he found that a single criterion could be used to determine the quality of the rocks being drilled. For example, penetration rate could be used. Thus, several drilling parameters and their interactions were considered necessary (Isheyskiy and Sanchidrián, 2020). Schunnesson (1996) used revolutions per minute, torque, and penetration rate to study MWD-based rock quality concerning structural faults. The severity of rock fractures was linked to changes in rotation pressure and penetration rate. Severe fractures had been found to signify that the penetration rate and RPM were going down while the torque increased, like a jammed or stuck drill bit would. Schunnesson (1997) suggested a step-by-step normalization approach for separating interdependent drilling parameters. Only data directly dependent on differences in rock features remained after normalization, which might be used to define rock indices more correctly. It was decided to use principal component analysis (PCA) to minimize the number of measurements, such as torque and normalized penetration rate, as well as their respective variances. To eliminate depth-dependent fluctuations in the normalized parameters, Ghosh et al. (2017) utilized an expanded PCA approach that incorporated more measured and computed variables than the prior PCA approach. The authors defined five classes based on their shapes and interconnections, and the model was validated utilizing real data collected on-site. Another common research topic studied is the wear mechanisms of rock drill components.

Cement carbide rock drill inserts were tested under dry, wet, and abrasive conditions (Angseryd, From, Wallin, Jacobson, & Norgren, 2013). Difficult control circumstances and inhomogeneity resulted in poor test results. A wet and dry environment, SiO₂ and Al₂O₃ particle sizes, and load were investigated in three test series. Despite the absence of percussive impact, the top hammer inserts' surface degradation process was identical. The hardness of the insert had a considerable effect on wear. It increased the wear rate while decreasing sample hardness, and the field behavior under wet situations reflected the lab test results. A temperature gradient may also induce tensile stresses in carbide because of the cooling impact of water. Similarly, the effect of temperature was investigated via a series of experiments with findings compared across a range of conditions. As a result, contrary to common belief, the temperature had no effect on the process of wearing. It had a significant effect on the adhered rock particles. Otherwise, the areas that did not have any rock particles looked the same as the wet areas, which shows that temperature does not affect how long it takes to wear down (Angseryd et al.,2013). When working with comparably hard Al₂O₃ and comparatively soft SiO₂ minerals, the size, and shape of the particles in the wear mechanism may be challenged. The increasing wear effect of Al₂O₃ and decreasing effect of SiO₂ was the final result of evaluating the influence of various materials on wear. However, the lower impact of SiO₂ was unknown. Furthermore, internally generated particles were sufficient to simulate SiO₂ conditions, while Al₂O₃ did not affect the wear process. The relationship between load and wear was found to be non-existent. Pressure between the rock and the insert can cause it to break apart when it is strong enough to do so. Overall, the WC (tungsten carbide) grains break or split, which is a common side effect of the wear mechanism (Angseryd et al.,2013).

X-ray diffraction (XRD) and energy-dispersive X-ray spectroscopy (EDX) were utilized to analyze the chemical interactions between the rock and the bit, as well as the effects of the ion beam

scanning electron microscope (FIB-SEM) on these interactions (Jones, Norgren, Kritikos, Mingard, and Gee, 2017). Tribochemical calculations were also examined the impact of rock quartz content on wear. Although quartz has a harder structure than the cobalt binder phase, prior studies showed that SiO₂ presence does not considerably fracture WC crystallites, representing the predominant part of the composite. The CO combines with quartz to generate CO₂, contributing to bit wear.

The chemical wear mechanism was defined as a blend of abrasion and oxidation with the assistance of water vapor in another research study (Jones et al., 2017). A rock substance embedded in the surface was monitored by Beste and Jacobsson (2009). The aim was to learn more about how quartz affects rock wear by magnifying locations where the oxide layer developed with varying elements proportions and thickness. The carbide and binder wear damage diagnosis was based on the surface oxide layer characteristics. It was explored in two situations with distinct thickness and silica/calcium-rich features, intergranular or transgranular. Jones et al. (2017) noted that the results are consistent with the findings of Beste et al. (2001, 2006, 2008) and Basse-Larssen (1985), that is, the absence of a binder phase in the outermost surface layers of the inserts. There were gaps at the boundary between the surface material and the binder phase because cobalt and carbide were split apart. There is a risk that cobalt might be released via these routes. Jones et al. (2017) stated that findings supported cobalt on the hard metal surface beneath the oxide layer (Jones et al., 2017). The conclusions of Montgomery (1968) conflicts with this study's findings; despite the assertion that the gauge and front button wear mechanisms were distinct, they were the same.

ANALYSIS OF DATA

This research's basic concept is to implement a data-driven strategy in the mining industry. The data is the basis of this notion and requires an investment in technology to generate, collect, and analyze it. This stage also includes the management standpoint, which acknowledges the critical role of data utilization in the decision-making process. Databases allow continuous improvement to give information on operational outcomes. An underground mine provided the information from the corporate database.

As represented in Figure 2, the proposed framework describes the system that enables immediate insight for managers' decision-making processes by generating online reports through the obtained rock tools-related data. It is possible to achieve data integration by merging the data gathered at different operating stages of the drill jumbos, which are the primary data source for rock tools, with manually produced safety reports and drilling failure reports. It is possible to develop different data visualizations in the form of customized reports generated from the database established with other information from the mine, such as asset information, operational cost, and production plans.

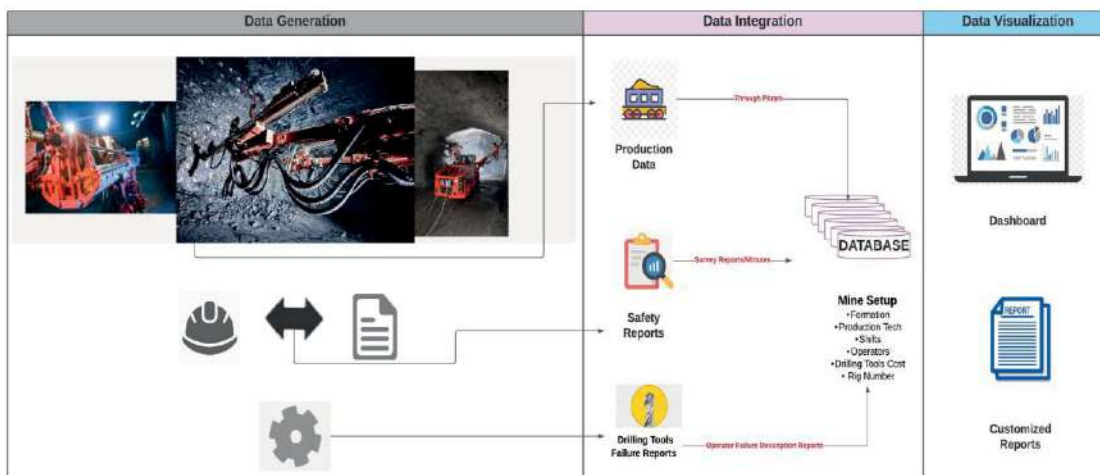


Figure 2. Framework for data visualization

Databases provide a structured environment for integration and can be considered as the essential information source for analytical tasks. Dashboards, customizable reports, and scorecards are some of the commonly used business intelligence applications that may be used to assist managers, supervisors, engineers, and operators on site. Data sources must be characterized in detail before data integration to understand the available potential. The existing data sources used in this study cover operator information, equipment data, failure codes, and type of drilling activity, as summarized in Table 1.

Table 1. Available data sources

Operators			
Operator-1	Operator-2	Operator-3	Operator-4
Operator-5	Operator-6	Operator-7	Operator-8
Operator-9	Operator-10	Operator-11	Operator-12
Operator-13	Operator-14	Operator-15	Operator-16
Equipments			
Equipment-1	Equipment-2	Equipment-3	Equipment-4
Types of Drilling			
4.2m Face	2.4m Split Set	Special Drilling	Reamed Hole
Rebar		Contour Holes	
Error Types			
Failure Code-1	Failure Code-2	Failure Code-3	Failure Code-4
Failure Code-5	Failure Code-6	Failure Code-7	Failure Code-8
Failure Code-9		Failure Code-10	
Failure Code-11			

Different dashboards were developed from the existing datasets and examined in detail. Numerous aspects of the underground drilling operation, such as drilling materials used, different kinds of drilling activities carried out in various shifts, failure codes associated with bits, and overall drilling performance, are shown in Figure 3. The visualization of the one-month duration for operational data provided an overview of the critical performance indicators of the drilling operation, which might be useful both for planning future operations and analyzing the current situation.



Figure 3. Overview of dashboard

Failure codes vary due to the changes in the lithological formation, operator experience, and the state of the rock bit being used. There are 11 error codes defined, and the distribution of recorded failure events throughout various shifts is shown in Figure 4. A comparison between the frequency of occurrences of the different failure codes revealed that failure code 2 defined for bit breakout is recorded 14 times during the night shift, which generates a noteworthy circumstance related to the night shift and the error code associated with it.

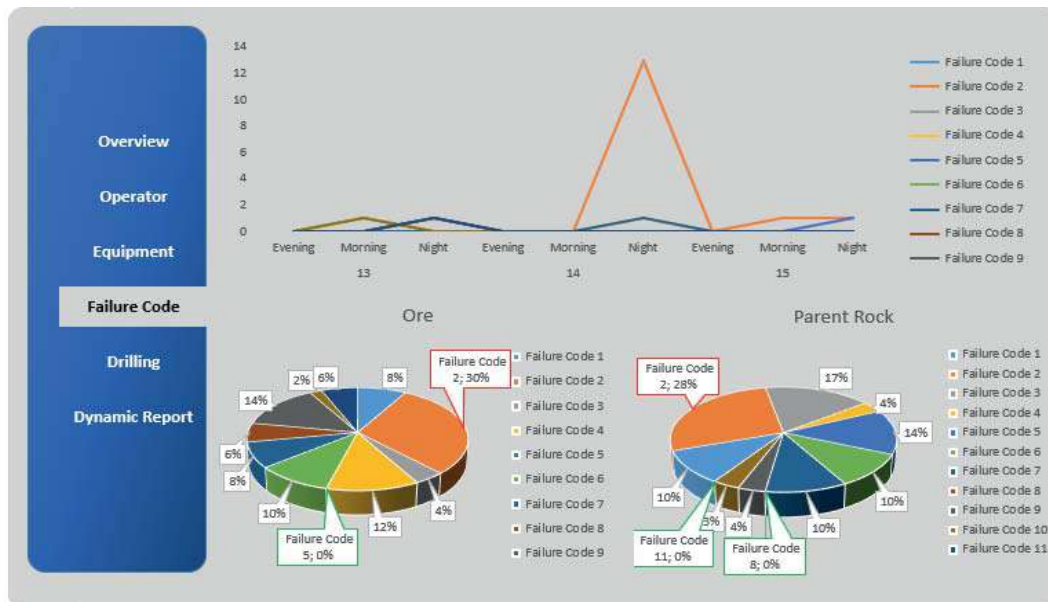


Figure 4. Distribution of failure codes based on material type

Figure 4 depicts the frequency of failure codes in relation to the kind of material being drilled. Similar to the overall frequency, failure code 2 was the most often encountered event for both material types. In contrast to failure code 5, which was the least often recorded code for ore material, failure codes 8 and 11 were the least frequently encountered codes for the material type defined as parent rock. Even though this circumstance necessitates the evaluation of other factors, it

might be a preventative measure to consider alterations in material type or equipment-related technical difficulties. Once this information is shared with the related technical staff, a maintenance event could be planned prior to an extended production loss due to this failure.

The distribution of drilling operations performed during shifts is visualized in Figure 5, together with the operators' information. The entire quantity of drilling (58,001 m) was proportioned for the evening, morning, and night shifts, and the percentage values were determined to be 35, 34, and 31, respectively. This situation demonstrates a specific operational condition of this mine as opposed to the notion that typically night shifts have comparably better performance. Production activities are more frequently interrupted in the day and evening shifts, as well as the fact that there are more factors to distract the employees supports this assumption.

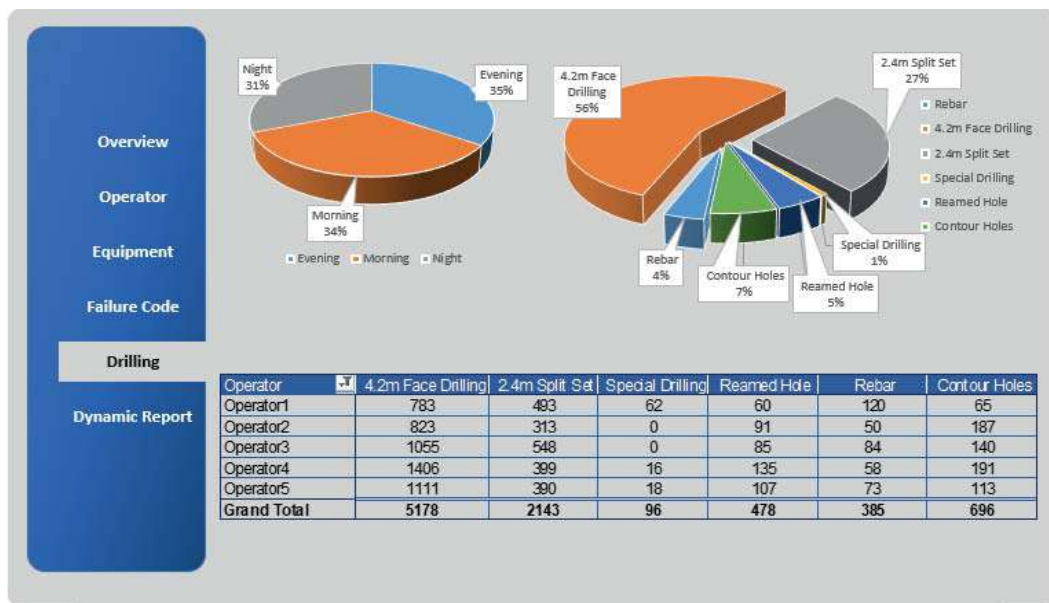


Figure 5. Analysis of drill type based on shifts and operators

The data visualization for the relevant month reveals that it is necessary to investigate this case in more detail. At this point, the evaluation of shift drilling performances based on the drill types performed and the relevant operator information serves as a more representative analysis aiming to improve drilling performances per shift. The distribution of failure codes recorded for the different bits used on the jumbo drills and the distribution of different types of drilling activities performed with different equipment are shown in Figure 6.

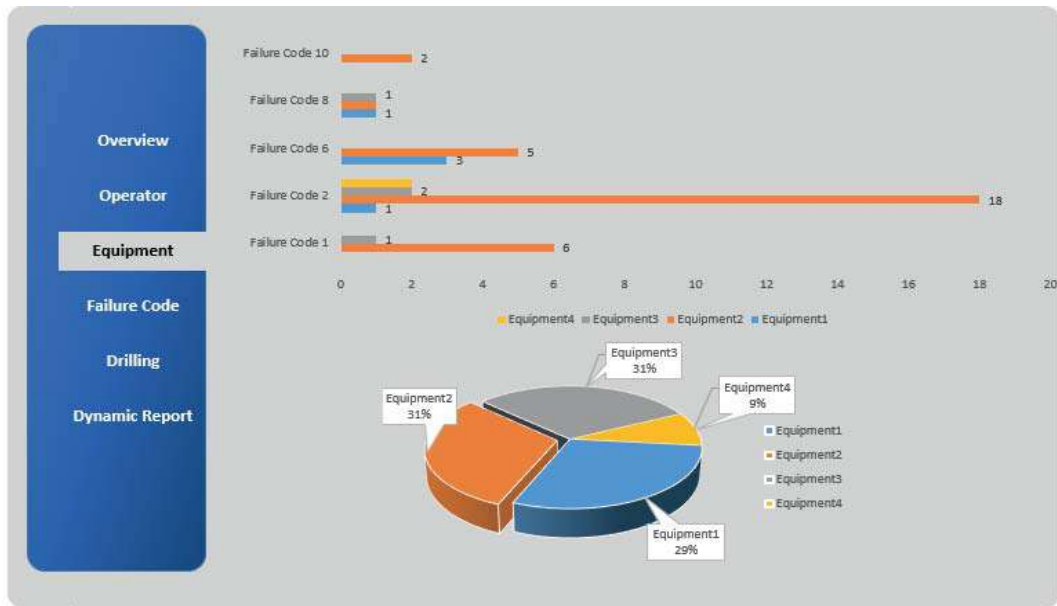


Figure 6. Type of drilling activities and failure codes based on equipment

Equipment-2 had a statistically significant increase in failure codes 2, 1, and 6 compared to other failure codes. Other operational factors that may contribute to the increased frequency of these failure codes should be explored in addition to the operator, the type of material being drilled, and the condition of the drill bit. Figure 7 depicts the monthly drilling target and achieved total drilling quantities for the operators and the monthly drilling targets together with failure code frequencies.



Figure 7. Operator evaluation based on targeted-actual total drilling-failure code

A dynamic report developed for the type of drilling, as seen in Figure 8, is an example of reporting that could be provided explicitly for operators, equipment, material type, and shifts over a period of time. The corporate data infrastructure available on site can be utilized to integrate extensive data. It will not only allow for comparison purposes and multi-dimensional analysis in case management perspective becomes accustomed to utilize data.

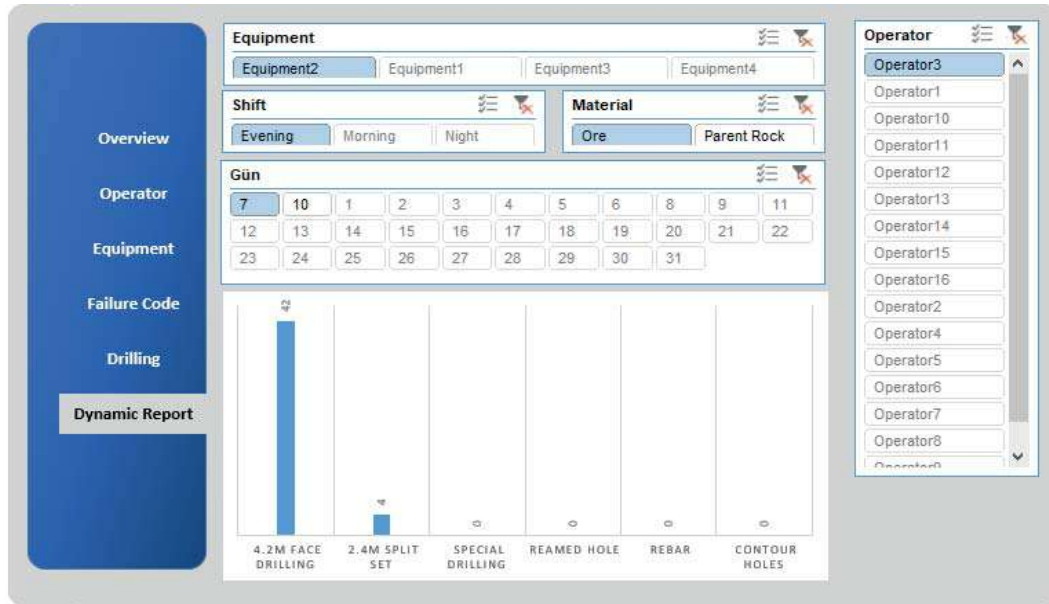


Figure 8. Operator-drill type dynamic report over a one-month period

In today's world, where the effective use of natural resources is becoming more vital, the active use of data will not only serve this goal but will also contribute positively to the corporate visibility of organizations by increasing their prominence in the field. The data that has been appropriately collected and integrated into a data warehouse can be considered the primary way of assessing performance that might be used to create a scorecard. Similarly, data usage will make it easier for the relevant operational units and managers to arrange training activities for operators, who play a critical role in the overall efficiency of the operation.

CONCLUSION AND RECOMMENDATIONS

Operational problems related to drilling operations in underground mining are evaluated by a data-based decision-making process. The main objective of the proposed processes could be to minimize the cost of drilling operations and improve productivity through the use of data. This study proves that investment in available technology to develop a data infrastructure is possible for corporate mining companies. In order to benefit from the existing data, technical expertise is required, and modern mines need the skills for data analysis and strategy development. Data analysis and data integration provide the infrastructure to build the management perspective that utilizes analytics and reporting for decision-making. Performance evaluation based on predefined targets allows for the quick assessment of operational issues and root-cause investigation using data. The widespread use of data for mining activities will become even more crucial for the efficient production of limited natural resources in the near future.

REFERENCES

Angseryd, J., From, A., Wallin, J., Jacobson, S., & Norgren, S. (2013). On a wear test for rock drill inserts. *Wear*, 301(1–2), 109–115.

Brown, E.T., Barr, M.V., (1978). Instrumented Drilling as an Aid to Site Investigations. In Proceedings of the 3rd International Congress of the International Association of Engineering Geology, Madrid, Spain, 4–8 September 1978; pp. 21–28.

Brown, E.T., Carter, P., Robertson, W., (1984). Experience with a Prototype Instrumented Drilling Rig. *Geodrilling* 1984, 24, 10–14.

- Ghosh, R., Schunnesson, H., Gustafson., (2017). A. Monitoring of Drill System Behavior for Water-Powered In-The-Hole (ITH) Drilling. *Minerals* 2017, 7, 121.
- J. Larsen-Basse, Binder extrusion in sliding wear of WC-Co alloys, *Wear* 105 (1985) 247–256.
- Jones, H. G., Norgren, S. M., Kritikos, M., Mingard, K. P., & Gee, M. G. (2017). Examination of wear damage to rock-mining hardmetal drill bits. *International Journal of Refractory Metals and Hard Materials*, 66, 1–10.
- Kosolapov, A.I., (2020). Modern Methods and Tools for Determining Drillability and Blastability of Rocks. *Iop Conf. Ser. Earth Environ. Sci.*, 459, 022097.
- Leighton, J.C. Development of a Correlation between Rotary Drill Performance and Controlled Blasting Powder Factors. Master's Thesis, University of British Columbia, Vancouver, BC, Canada, 1982.
- Lilly, P., (1986). An Empirical Method of Assessing Rock mass blastability. In Proceedings of the Large Open Pit Mining Conference, Newman, Australia, 27–29 October 1986; pp. 89–92.
- Lopez, C.; Lopez, E.; Javier, F., (1995) Drilling and Blasting of Rocks; CRC Press: Boca Raton, FL, USA, p. 408.
- Navarro, J., Sanchidrian, J. A., Segarra, P., Castedo, R., Paredes, C., & Lopez, L. M. (2018). On the mutual relations of drill monitoring variables and the drill control system in tunneling operations. *Tunnelling and Underground Space Technology*, 72, 294–304.
- R.S. Montgomery, (1968). The mechanism of percussive wear on tungsten carbide composites, *Wear* 12, 309–329.
- Regotunov, A.S.; Sukhov, R.I., (2016) The Results of Studies of Strength Properties of Local Arrays in the Drilling Process using software and hardware complex. *Subsoil Use Probl.* 2016, 4, 121–129.
- Schunnesson, H., (1990). Drill process monitoring in percussive drilling: A multivariate approach to data analysis. Licentiate Thesis, University of Technology, Luleå, Sweden.
- Schunnesson, H., (1996). RQD Predictions Based on Drill Performance Parameters. *Tunn. Undergr. Space Technol.*, 11, 345–351
- Schunnesson, H., (1997). Drill Process Monitoring in Percussive Drilling for Location of Structural Features, Lithological Boundaries and Rock Properties, and for Drill Productivity Evaluation. Ph.D. Thesis, Luleå University of Technology, Luleå, Sweden.
- Schunnesson, H., (1998). Rock Characterization using Percussive Drilling. *Int. J. Rock Mech. Min. Sci.*, 35, 711–725.
- Scoble, M.J.; Peck, J.A., (1987). Technique for ground characterization using automated production drill monitoring. *Int. J. Surf. Min. Reclam. Environ.* 1, 41–54.
- Scoble, M.J.; Peck, J.; Hendricks, C., (1989). Correlation between rotary drill performance parameters and borehole geophysical logging. *Min. Sci. Technol.*, 8, 301–312.
- Teale, R., (1965). The Concept of Specific Energy in Rock Drilling. *Int. J. Rock Mech. Min. Sci. Geomech. Abstr.* 2, 57–73.
- U. Beste, T. Hartzell, H. Engqvist, N. Axén, (2001). Surface damage on cemented carbide rock-drill buttons, *Wear* 249,324–329.
- U. Beste, E. Coronel, S. Jacobson, (2006). Wear induced material modifications of cemented carbide rock drill buttons, *Int. J. Refract. Met. Hard Mater.* 24, 168–176.
- U. Beste, S. Jacobson, (2008). A new view of the deterioration and wear of WC/Co cemented carbide rock drill buttons, *Wear* 264 (11–12),1129–1141.
- U. Beste, S. Jacobson, S. Hogmark, (2008). Rock penetration into cemented carbide drill buttons during rock drilling, *Wear* 264 (11–12) ,1142–1151.

DENİZLİ AVDAN VE NARLI KÖMÜR SAHALARI KAYNAK MODELİ
DENİZLİ AVDAN AND NARLI COAL MINE SITES RESOURCE MODEL

C.A. Öztürk^{1,*}, M. Lashgari¹, Y. Türkmen¹

¹ *İstanbul Teknik Üniversitesi, Maden Mühendisliği Bölümü*
(*Sorumlu yazar: atilla.ozturk@itu.edu.tr)

ÖZET

Denizli ili Tavas ilçesinde bulunan Avdan ve Narlı kömür sahaları bölgede tesis edilebilecek termik santrale hizmet edebileceği gibi aynı zamanda, Ege bölgesinde bulunan diğer termik santraller için de hammadde deposu olarak kullanılabilir özelliklerdedir. Kömür sahası Yenidere ve Sekköy olarak isimlendirilen iki farklı kömür zonunu içerir. Kömür zonları kömür damarları ve aralarına yerleşmiş bulunan ara kesmelerden oluşmaktadır. Oluşum Yenidere ve Sekköy kömürleri için benzerlik göstermemektedir. Sahada yapılan kaynak modelleme çalışmasında, bölgede yapılmış olan sondaj verilerini kullanarak kömür zonlarının katı modelleri ve daha sonra blok modelleri üretilmiştir. Kriging tekniğinin çalıştırılmasıyla bloklara değer atanmış ve böylece kaynağın miktar ve kalite modellemesi elde edilmiştir. Çalışmanın amacı, iki farklı ruhsat ile sınırlandırılan Avdan ve Narlı kömür sahalarının kaynak modelinin elde edilmesinin yanında, ruhsatların birleştirilmesi durumunda oluşacak yeni koşulun olası etkilerinin araştırılmasıdır.

Anahtar Sözcükler: Enerji, kaynak modelleme, kömür, ruhsat birleştirme.

ABSTRACT

Avdan and Narlı coal mine sites located in Denizli City Tavas Province is going to serve as raw material source for thermal power plant that will be constructed close to the mine site or existing Aegean region's thermal power plants. The coal mine sites consist of two different coal zones that are Yenidere and Sekkoy coal zones. Coal zones are the sum of coal seams and interburden among them. The formation are similar both for Yenidere and Sekkoy coal zones. Solid models of the coal zones were firstly determined based on the drill log database and then block models were executed. Hence, estimation of coal quality could be proceed after running kriging to determine coal resource and quality modelling. The purpose of the study is to model these two coal mine sites to understand the overall resource potential as well as the effect of merging adjacent mining area licenses sites for the optimized use of coal mine sits for energy production.

Keywords: Energy, resource modelling, coal, license merging.

GİRİŞ

Yerli kömürden enerji üretimi ülkemiz enerji politikaları açısından son yıllarda gittikçe önemi artan önemli hedeflerden biridir. Bu durum özellikle ülke ekonomisi ve gelişmişliği açısından kilit öneme sahip olan enerji üretiminin yerli kaynaklardan sağlanması ve dışa bağımlılığın azaltılması açısından son derece önemlidir. Denizli ili Tavas ilçesinde bulunan kömür sahası, bölgede tesis edilecek olan termik santrale hizmet vermeyi hedeflemenin yanında, kaynağın büyüklüğüne bağlı olarak Ege bölgesinde bulunan termik santral için de kullanılabilir bir hammadde deposuna dönüşecektir.

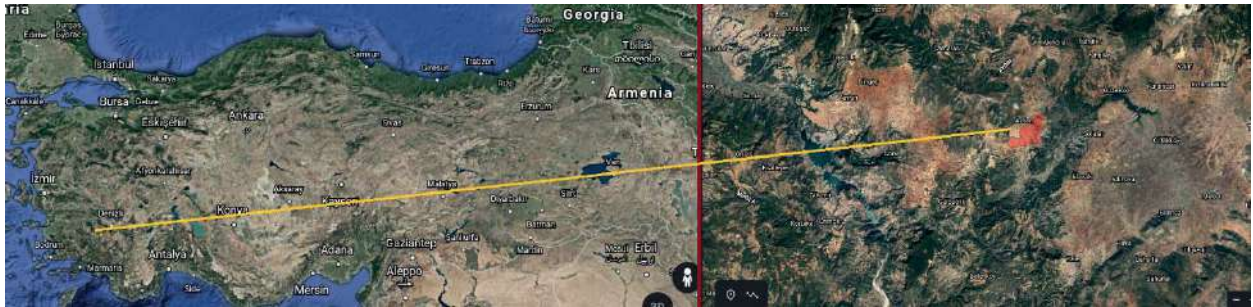
Bölgede kömür yapısı Sekköy ve Yenidere olarak isimlendirilen iki farklı kömür zonundan oluşmaktadır. Her iki kömür zonunda da kömür damarları ve damarların arasına yerleşmiş ara kesmeler bulunmaktadır. Kömürün mostra vermesi ve 200 m derinlere kadar ulaşmasından dolayı üretimin açık işletme faaliyetleri ile gerçekleştirilmesi planlanmaktadır. Bu durumda kömür üretim faaliyetleri sırasında dekapaj kazı miktarının yanında ara kesme miktarının da tayinine ihtiyaç duyulmaktadır. Ayrıca, kömür damarlarının sahada yapılacak madencilik faaliyetleri sırasında kısa dönem faaliyetlerine uygun olarak modellenmesi ve ara kesmelerin seleftik madencilik esaslarına göre alınmasında yarar vardır. Bu sayede kömürün üretim kaynaklı kirlenmesinin en aza indirilmesi ve termik santrale beslenecek kömürün ideal olarak temini sağlanmış olacaktır.

Kömür sahaları Avdan ve Narlı olarak isimlendirilen birbirine komşu iki farklı ruhsat ile sınırlandırılmaktadır. Kaynağın modellenmesi amacıyla oluşturulan sondaj veri tabanında Avdan sahasının kullanılabilir 103 adet sondaj verisi kullanılmıştır. Narlı bölgesindeyse modelleme 18 sondaj verisiyle gerçekleştirilmiştir. Avdan sahasındaki sondajlardan 98'i kömür damarlarını keserken, Narlı bölgesindeki tüm sondajlarda kömür kesilmiştir. Sekköy ve Yenidere kömür zonlarına ait katı modeller oluşturulduktan sonra kaynak modelleme çalışmaları yapılmıştır. Yenidere kömür zonu kendi içerisinde 3 farklı yapıdan oluşmaktadır. Ancak katı modellerde Yenidere-2 ve Yenidere-3 kömür zonları da ortaya çıkartılmıştır. Sondaj verisinin yetersiz olmasından dolayı bu kömür zonlarına ait modellerin devamı Narlı bölgesinde takip edilememiştir. Bu iki kömür zonu açık işletme faaliyetleriyle yeryüzüne çıkartılmayacak derinlikte olması ve yeterli kaynak miktarına sahip bulunmamasından dolayı kaynak olarak değerlendirilmemiştir. Bildiriye konu olan çalışmaların temel amacı, kömür sahasındaki linyitin kömür zonları özelinde kaynak ve kalite değerlendirilmesinin yapılarak, kömür sahalarının termik santralleri besleme potansiyelinin ortaya çıkartılmasıdır.

BÖLGENİN TANITIMI VE KISA JEOLJİSİ

Kömür sahası, Denizli ili Tavas İlçesi Avdan – Narlı ve Adamharmanı köyü hudutları içerisinde yer almaktadır. Açık işletme faaliyetleri ile linyit üretiminin gerçekleştirileceği saha, Tavas ilçesinin batısında Kale ilçesinin kuzeyinde Avdan Köyü civarında bulunmaktadır. Tavas'a 37 km, Kale'ye 22 km. uzaklıktadır. Sahaya asfalt yolla ulaşılmaktadır. Kömür sahasının yer buldu haritası Şekil 1'de verilmiştir.

Ruhsat sahası değişik morfolojik özelliklere sahiptir. Derin vadilerle ayrılmış platolar üzerinde yer alan ruhsatlar olabildiği gibi tatlı meyilli ruhsat sahaları da bulunmaktadır. Bölgede İç Ege Bölgesi'nin iklimi görülmekte olup yazları serin ve kurak, kışları ılık ve yağışlıdır.



Şekil 1. Kömür sahası lokasyonu

Sahanın temelini paleozoyik- mesozoyik yaşlı kuvarsit, mermer, şist, kireçtaşı, radyolarit ve ofiyolitik kayalar oluşturur. Temel kayaların üzerinde uyumsuzlukla gelen tersiyer yaşlı kayalar yer almaktadır. Akçay Grubu (Karadere, Mortuma, Yenidere, Kale ve bununla geçişli Künar Formasyonu) ve Muğla Grubu (Turgut, Sekköy, Yatağan ve Milet Formasyonu) olarak adlandırılan iki gruptan oluşmaktadır.

Çalışma sahası ve civarı Yenidere, Sekköy ve Yatağan formasyonları ile temsil edilmektedir. Yenidere formasyonu (Ty), oligosen yaşlı Mortuma formasyonu üzerine açısız diskordansla gelir. Kalınlığı 250- 1450 m'dir. Formasyon; Esenkaya (Tye), Ortaköy (Tyo) ve Karakaya (Tyk) Üyesi olmak üzere üçe ayrılmıştır. Esenkaya üyesi; iri çakıltaşı, çamurtaşı, kumtaşı ve siltaşlarından oluşur. 25- 550 m arasında kalınlığa sahiptir. Ortaköy üyesi; kumtaşı, siltaşı, kiltası ve çakıltaşından oluşmaktadır. Üyenin orta kesimlerinde kalınlıkları 2.90 m'ye kadar ulaşan linyit damarları içeren linyit horizonu bulunmaktadır. Üyenin kalınlığı 125- 600 m arasında değişmektedir. Karakaya üyesi; kiltası ve siltaşından oluşan üyenin kalınlığı 70- 100 m arasındadır. Yenidere Formasyonu örgülü, menderesli ırmak, kıyı ovası, lagün, delta, alüvyon ve kumsal ortamlarda çökelmişlerdir. Yaşı alt miyosendir.

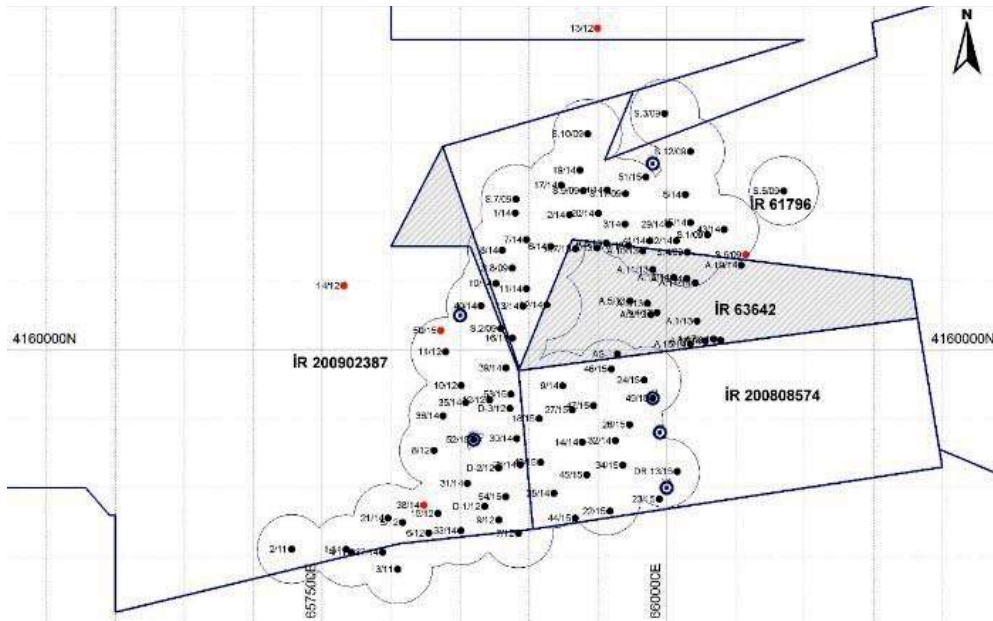
Sekköy formasyonu (Tms), Avdan civarında Yenidere formasyonu üzerine uyumsuz olarak gelir. Kalınlık 50- 150 m arasındadır. Sarımsı beyaz renkli killi- mikritik- kırıntılı kireçtaşı, gri renkli siltaşı, tuf ve tufitten oluşmaktadır. Formasyonun tabanında; kalınlıkları 0,05 – 2,20 m arasında değişen linyit damarları içeren bir zon bulunmaktadır. Sekköy Formasyonu bataklık ve göl ortamında çökelmiştir.

Yatağan formasyonu (Tmy), Sekköy üzerine uyumlu olarak gelir. Çakıltaşı, çamurtaşı, kumtaşı, tuf ve tufitten oluşmaktadır. Kalınlığı 250 m.'ye ulaşmaktadır. Alüvyon yelpazesi çökel ortamında çökelmiştir.

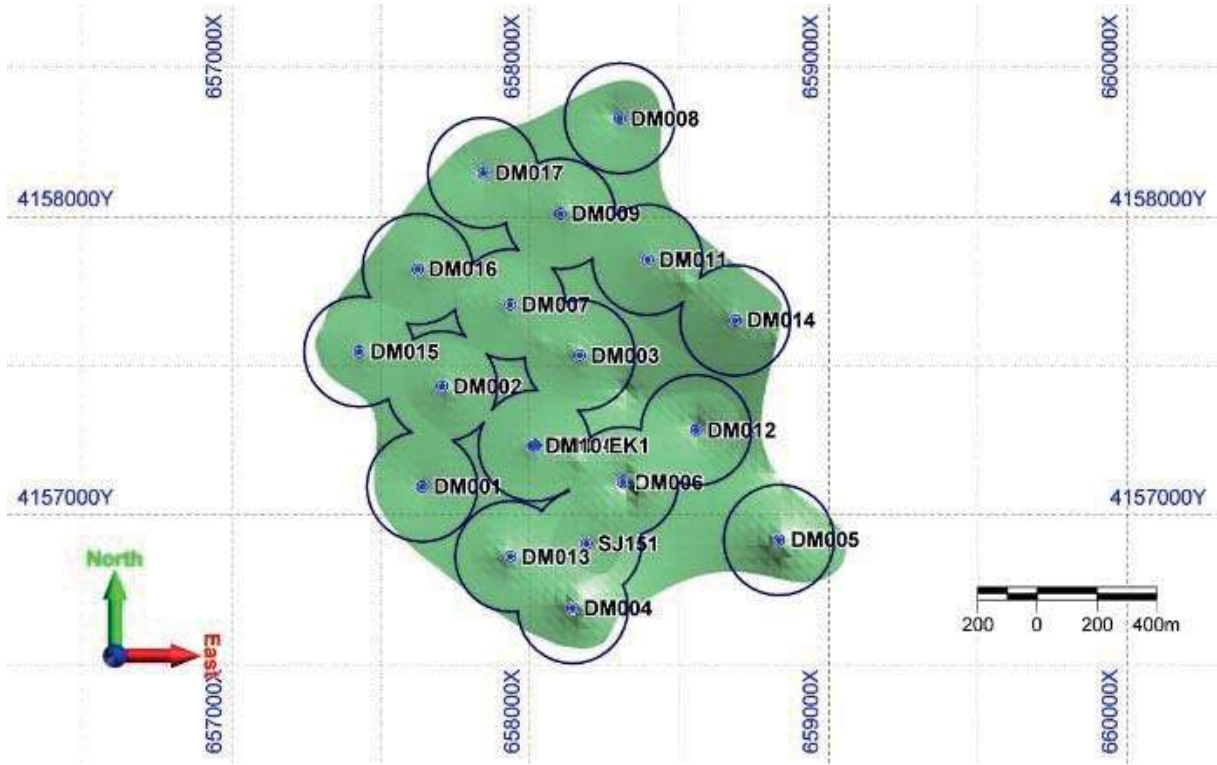
Milet formasyonu (Tmm): Yatağan formasyonunun üzerine uyumlu şekilde gelir. Çalışma sahası civarında düz ve yüksek platolar oluşturmaktadır. Beyaz renkli kireçtaşı ve sarımsı bej renkli killi kireçtaşlarından oluşan birimin kalınlığı 100 – 120 m civarındadır. Göl ortamında çökelen formasyonun yaşı pliyosendir (Akgün ve Sözbilir, 2001; Alççek, 2010; Hakyemez, 1989; Sözbilir vd., 2000; Sözbilir, 2002).

AVDAN VE NARLI KÖMÜR SAHALARI KAYNAK MODELİ

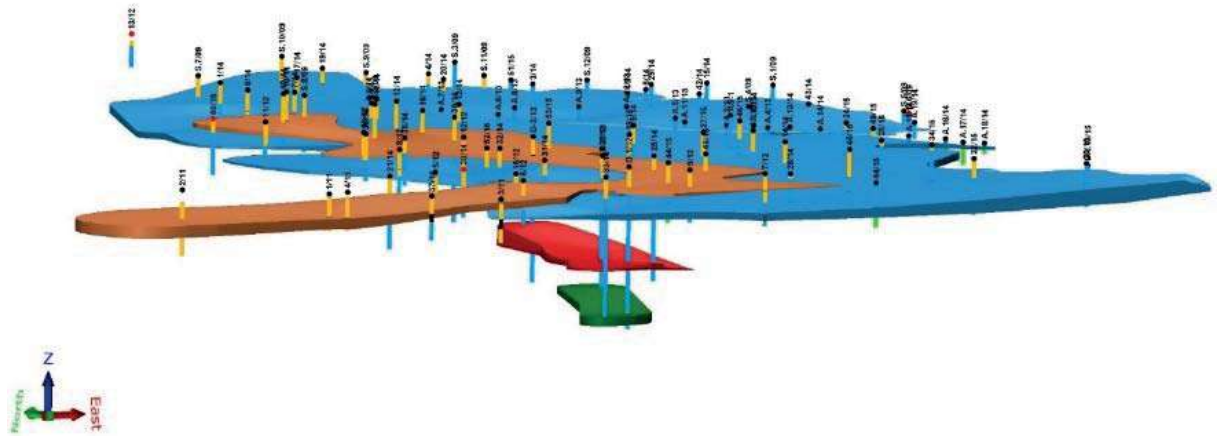
Çalışma sahasında modellemede kullanılan sondajlara ait plan görünüm Şekil 2 ve Şekil 3'te verilmiştir. Sekköy ve Yenidere kömür zonlarının katı modelleri çıkartılmıştır. Yapılan çalışmadan üretilen katı modellerin izometrik görünümleri Şekil 4 ve Şekil 5'te görülmektedir.



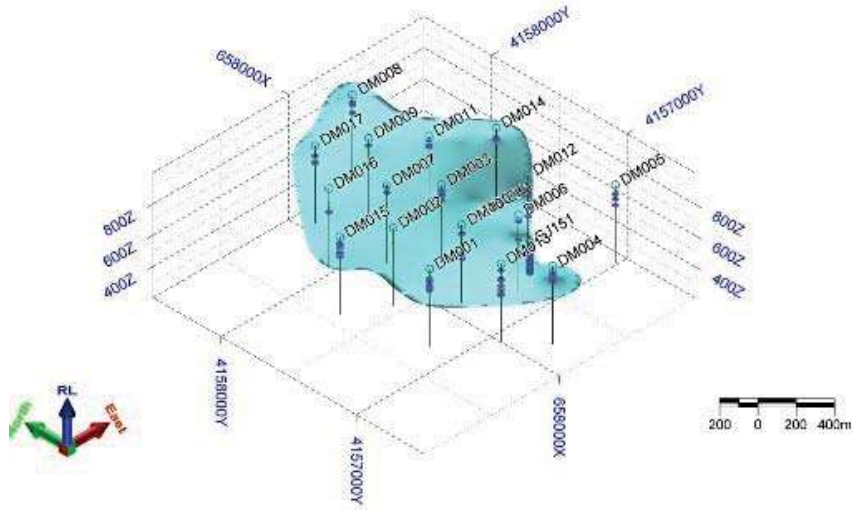
Şekil 2. Avdan sondaj lokasyonlarının plan görünümü



Şekil 3. Narlı sondaj lokasyonlarının plan görünümü



Şekil 4. Avdan kömür zonlarının katı modeli (Lashgari vd., 2016)



Şekil 5. Narlı kömür zonlarının katı modeli

İstatistiksel Değerlendirmeler

Kömürün kalitesinin tespit edilmesi amacıyla yaptırılan test çalışmaları sonucunda, kömürün alt ısıl değeri, toplam kükürt, nem, kül, uçucu madde ve yoğunluk değerleri tespit edilmiş ve elde edilen sonuçlara ait istatistiksel değerlendirme Çizelge 1’de ve Çizelge 2’de kömür sahaları için ayrı ayrı verilmiştir.

İki komşu saha için yapılan testlerden elde edilen kalite değişkenlerine ait basit istatistiksel çıkarımlar sahadaki kömürün kalitesinin benzerliğine işaret etmektedir. Avdan sahasındaki ortalama alt ısıl değerin 1703 kcal/kg olarak tayin edilirken bu değer Narlı sahasında 1779 kcal/kg olarak belirlenmiştir. Ortalama değerlerin bu derece birbirine yakın olması, birbirine komşu bu iki sahadaki kömürün aynı kömür zonu olduğunu desteklemektedir.

Çizelge 1. Avdan sahası kömür kalite değerlerine ait istatistiksel değerlendirmeler

Tanımlama	Alt Isıl Değeri (kcal/kg)	Toplam Kükürt (%)	Nem (%)	Kül (%)	Uçucu Madde (%)	Yoğunluk (gr/cm ³)
Ortalama	1703	2.61	41.57	25.47	24.34	1.48
Std. Sapma	410	1.18	5.50	9.56	5.15	0.11
Veri Sayısı	219	214	219	219	219	131

Çizelge 2. Narlı sahası kömür kalite değerlerine ait istatistiksel değerlendirmeler

Tanımlama	Alt Isıl Değeri (kcal/kg)	Toplam Kükürt (%)	Nem (%)	Kül (%)	Uçucu Madde (%)	Yoğunluk (gr/cm ³)
Ortalama	1779	2.24	40.09	27.25	24.75	1.42
Std. Sapma	586	1.18	7.12	11.21	5.97	0.14
Veri Sayısı	307	307	307	307	307	307

Kaynak ve Kalite Modellemesi

Avdan kömür sahasına ait ön değerlendirme sonucunda, Sekköy formasyonunda bir, Yenidere formasyonunun da ise üç farklı linyit yapısı tespit edilmiştir. Sahadaki linyit oluşum olarak delta yapısı olmasından dolayı, kömür damarlarının korelasyonundan ziyade kömür zonu olarak modellenmeleri

tercih edilmiştir. Katı modellerden de görüleceği üzere kömür zonları Sekköy, Yenidere-1, Yenidere-2 ve Yenidere-3 olarak isimlendirilmiştir. Sekköy ve Yenidere-1 olarak isimlendirilen kömür zonlarındaki linyitin açık işletmecilik faaliyetleri üretilmesi mümkündür. Yenidere-2 ve Yenidere-3 kömür zonları ise yeter ve gerek veriye sahip olmadığı için bu kömür zonlarının yeni bir dizi sondaj ile sınırlarının ve büyüklüğünün tespit edilmesine ihtiyaç vardır. Yenidere-3 kömür zonunda iki sondajda kömür kesilmiş ve kesilen kömürün kalınlığı 5.5 m'dir. Diğer sondajlarda bu derinliğe ulaşılmadığı için, Yenidere-3 kömür zonunun kaynak miktarıyla ilgili güvenilir bir bilgiye sahip olunamamaktadır. Bu iki kömür zonunu hedefleyecek bir dizi sondaj çalışmasıyla havzadaki kaynağın miktarının artması mümkün gözükmemektedir.

Narlı kömür sahasında ise daha önce gerçekleştirilen çalışmadan da faydalanarak (MCS, 2015) bölgedeki kömür damarları 8 sektöre ayrılmıştır. Bu sektörler kendi içerisinde toplam 53 alt damara ayrılmıştır. Yapılan çalışmada kullanılan 19 sondajın verisinden yola çıkarak çalışma tekrar edilmiştir.

Sahadaki kömür kaynağının miktar ve kalite dağılımlarının araştırılması için jeostatistiksel yöntemlerden faydalanılmıştır. Bu sayede, özellikle kömür kalitesinin denetlendiği değişkenlerin bölgesel olarak büyüklüklerinin en aza hata ile kestirimlerinin yapıldığı matematiksel modeller kullanılmıştır (İsaak ve Srivastava, 1989; Öztürk, 2001). Linyit zonları, jeolojik formasyonlar ve linyit kalitesinin belirlenmesinde en uygun modelleme ve interpolasyon yönteminin kullanılabilmesi için araştırmalar yapılmıştır. Modelleme çalışmalarında klasik kesit yönteminin hata payının yüksek olmasından dolayı sahadaki linyit damarları için grid model kullanılmasına karar verilmiştir. Jeolojik katmanlar ve linyit zonu damarlarının tavan ve taban yüzeyleri grid yöntemi kullanılarak modellenmiştir. Grid yönteminin kullanılması sırasında jeostatistiksel olarak çalışmalar yapılmış ve yüzeylerin kot farklılıkları tahmin edilmeye çalışılmıştır. Yapılan çalışmalar sonucu variogram model olarak doğrusal variogram modeli ile çalışmaya karar verilmiştir. Bu sayede elde edilen tavan ve taban yüzeyleri sayesinde hem jeolojik formasyonlar hem de linyit zonları 3B katı modele çevrilmiştir.

Avdan sahasında katı model çalışmasından sonra blok modelleme yapılmıştır. En düşük boyutu 40 cm, en büyük boyutu 4 m olan yaklaşık 3,2 milyon bloktan oluşan blok model sayesinde sahadaki kömürün kalitesi bölgesel olarak modellenmiştir. Narlı sahasında ise en düşük boyutu 25 cm en büyük boyutu 10 m olan toplam 7,04 milyon bloktan oluşan bir blok model oluşturulmuştur.

Alt Isıl Değer Dağılım Modelleri

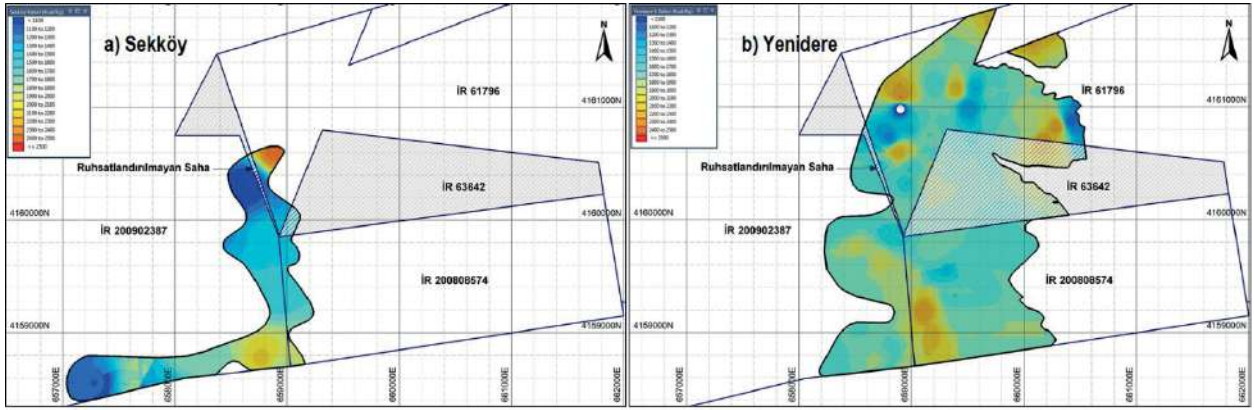
Çalışma sahasındaki linyitin alt ısıl değerinin, kömür zonları özelinde dağılım haritaları modellenmiş ve elde edilen sonuçlar Şekil 6'da Avdan sahası için, Şekil 7'de ise Narlı sahası için verilmiştir.

Yapılan analiz sonuçlarına göre, Yeniköy kömür zonu alt ısıl değeri açısından Sekköy kömürlerine nazaran bir miktar daha zengindir. Sahanın kuzey ve güneyinde 2000 kcal/kg ve daha yüksek alt ısıl değere sahip olunurken sahanın geri kalan kısmında ise alt ısıl değeri 1500 ile 2000 kcal/kg olarak değişmektedir. Sekköy kömürlerinde ise bu oluşum tam ters olarak görülmekte sahanın ortasında daha zengin sahanın kuzey ve güneyinde ise alt ısıl değer yönünden daha fakir bölgeler yer almaktadır.

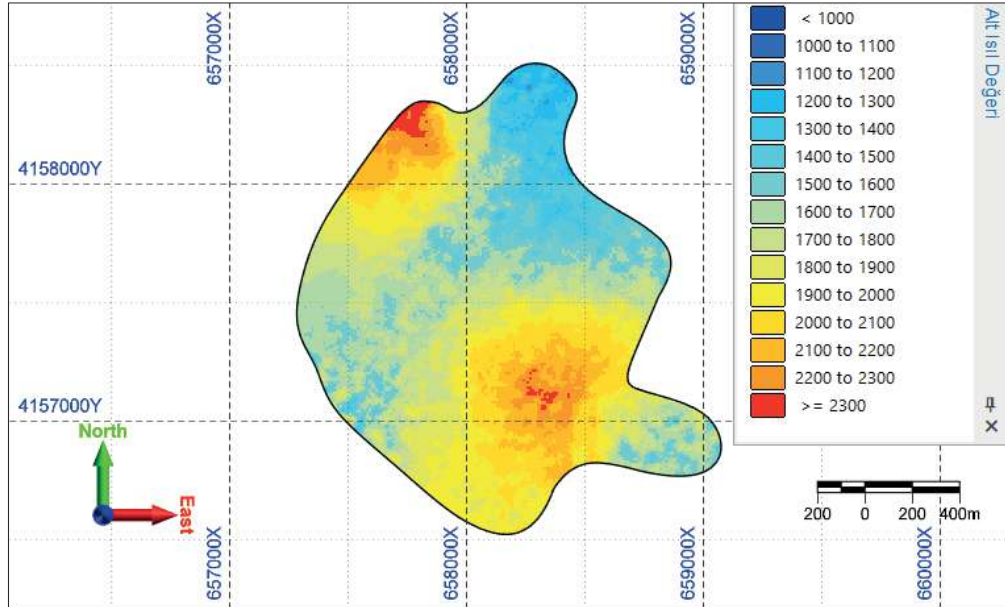
Narlı bölgesinde ise sahanın güney doğu ve kuzey batı bölgelerinde kömürün ortalama alt ısıl değeri 1800 kcal/kg ile 2300 kcal/kg değerleri arasındayken, sahanın geri kalan kısmında 1000 kcal/kg ile 1500 kcal/kg arasında değişmektedir.

Sahada kaliteyi denetleyen nem, kül, kükürt ve uçucu madde değişkenleri için de benzer dağılım haritaları elde edilerek, her bir bloğun kalite değeri tayin edilmiştir.

Bu bölümde sadece alt ısıl değerinin dağılım haritaları verilerek, diğer kalite parametrelerine ait haritaların verilmesi yerine blok modellerden elde edilen değerlerin verilmesi yoluna gidilmiştir.



Şekil 6. Avdan bölgesi kömür zonlarının alt ısı değer dağılım haritaları a) Sekk y b) Yenidere



Şekil 7. Narlı bölgesi kömür zonlarının alt ısı değer dağılım haritaları

Kaynak Kalite ve Miktar Sonuçları

Avdan bölgesinde yapılan modellemeler sonucunda, kaynağın Sekk y, Yenidere-1, Yenidere-2 ve Yenidere-3 olarak isimlendirilen d rt farklı kömür zonundan oluştuđu ve bu zonlardaki linyit kaynağının miktar ve kalite değerlerine ait bilgiler elde edilmiştir. Çizelge 3'te yapılan çalışmalardan elde edilen sonuçlar verilmiştir. Yenidere-3 kömürü sadece iki sondaj ile temsil edilmesinden dolayı hesaplarda gösterilmemektedir. Yenidere-2 kömürü ise açık işletme faaliyetleriyle üretilebilir gözükmemektedir. Benzer çalışma Narlı bölgesi için de tekrar edilmiş ve elde edilen sonuçlar Çizelge 4'de verilmiştir. Narlı bölgesinde 7 farklı kömür zonu ile yapılan modellemenin çıktılarını ayrı ayrı göstermek mümkün olmadığı için blok modelin görünümü verilmiş ve Çizelge 4'de her bir kömür zonunun ve toplamda da ağırlıklı ortalamaların elde edildiđi sahanın geneline ait sonuçlar verilmiştir.

Çizelge 3. Avdan sahası kaynak değerlendirme sonucunda elde edilen miktar ve kalite değerleri

Kömür Zonu	Kaynak (Ton)	Yoğunluk (gr/cm ³)	Kalori (Kcal/kg)	Nem (%)	Kül (%)	Uçucu Madde (%)	Kükürt (%)
Sekköy	4 978 236	1.54	1465	39.6	28.3	26.5	2.70
Yenidere - 1	25 494 492	1.48	1768	42.5	24.0	23.6	2.34
Yenidere - 2	1 181 852	1.71	1225	30.8	43.8	18.5	4.02
Genel Toplam	31 654 580	1.50	1700	41.6	25.4	23.8	2.46

AVDAN VE NARLI KÖMÜR SAHALARININ BİRLEŞTİRİLMESİ

Kaynak modelleri hazırlanırken, kömürün devamlı olduğu sahalarda, kömür sınırları ruhsat sınırları olarak alınmakta ve kaynak miktarı ona göre hazırlanmaktadır. Ruhsat sınırları kömür sınırlarına göre tayin edilmediğinden, bu durumda sahadaki kaynağın gerçek miktarının önünde bir engel teşkil etmektedir.

Bunun yanında, birbirine komşu iki ruhsat ile sınırlandırılan kömür sahalalarında, özellikle açık işletme faaliyetleri ile üretim yapılırken, işletmeler birbirlerinin dekapajını yapmak zorunda kalmamak adına kömürü topuk olarak bırakmakta bu da sahadaki kömürün zayı olmasına sebebiyet vermektedir. Şekil 6’da Avdan ve Narlı kömürlerinin ayrı iki açık ocak ile üretilmesi durumunda ortaya çıkacak muhtemel geometri verilmiştir.

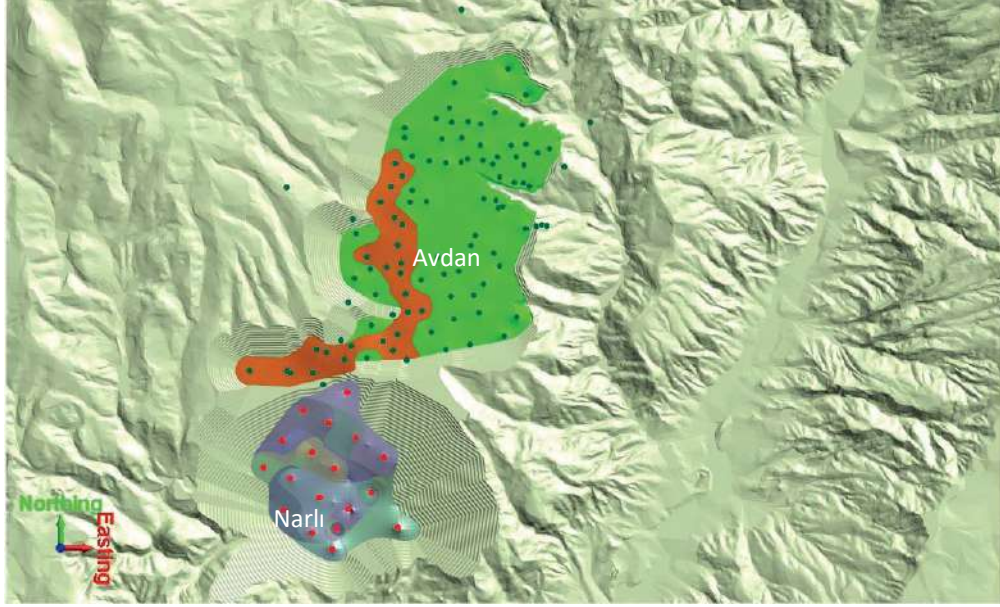
Çizelge 4. Narlı sahası kaynak değerlendirme sonucunda elde edilen miktar ve kalite değerleri

Kömür zonu	Kaynak (Ton)	Birim Hacim Ağırlığı (ton/m ³)	Alt Isıl Değeri (kcal/kg))	Kükürt (%)	Nem (%)	Uçucu Madde (%)	Kül (%)
A	45,596	1.30	1979	2.97	49.48	27.09	17.58
B	839,991	1.29	1939	2.84	49.77	29.48	17.86
C	1,011,775	1.35	1933	1.97	43.82	28.28	21.48
D	999,161	1.37	1820	1.98	42.39	22.86	25.58
E	6,965,540	1.38	1883	2.02	41.77	25.89	25.13
F	13,594,886	1.38	1958	2.22	41.23	26.37	23.95
G	16,155,695	1.41	1936	2.61	38.6	24.99	27.42
Toplam	39,612,644	1.39	1931	2.35	40.54	25.75	25.41

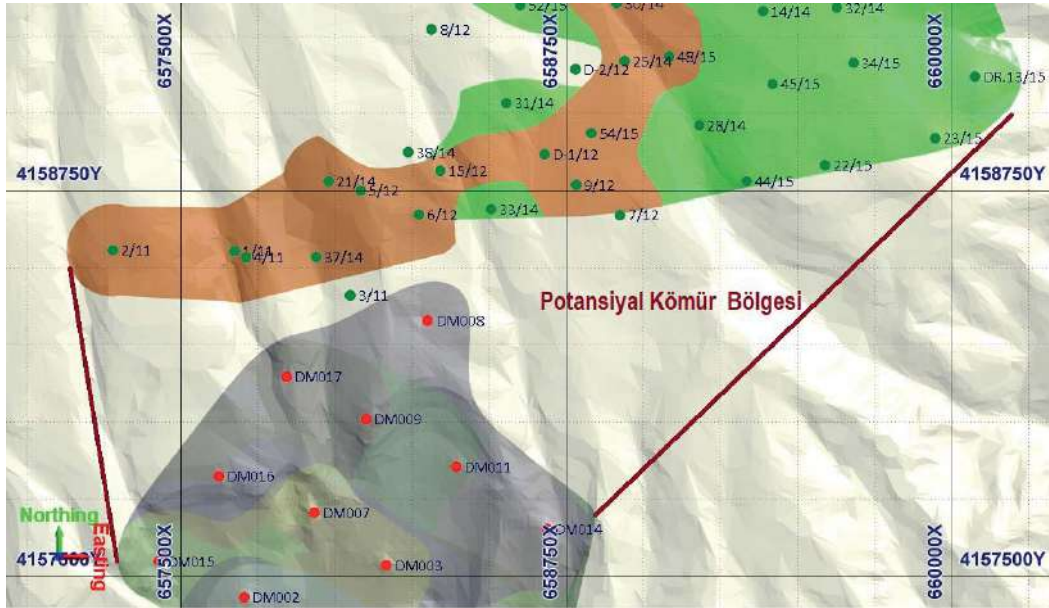
İki ocak arasında kalan bölgenin Avdan bölgesinde başlayan ve Narlı bölgesinde devam eden kömür ile dolu olma ihtimali çok yüksektir. Bu durumda, Şekil 7’de verildiği üzere, sahada yapılacak bir seri arama faaliyetiyle birlikte sahadaki kömür kaynağının artırılması mümkün olacaktır. Kömürün yüzeydeki izinden yapılan basit bir kestirimle aşağıda gösterilen bölgede 2,5 milyon ton ile 5 milyon ton arasında kömür olma ihtimali öne çıkmaktadır.

Ruhsatların birleştirilmesi kaynağın artmasını sağladığını, üretim optimizasyonu için çok daha büyük bir alanda çok farklı opsiyonlara imkân sağlamaktadır. Bunun yanında, iç döküme çok daha hızlı geçilmesine ve bağlı olarak çok daha fazla malzemenin iç dökümde depolanmasını sağlamaktadır. Bu da çevresel etkinin en aza indirilmesi anlamına gelmektedir. Ruhsat birleştirilmesi, aynı miktarda dekapaj ile

çok daha fazla kömür üretimi sağlayacağı için, madenin ekonomikliğini artıracığı gibi, komşu ruhsatların topuk bırakma mecburiyetinden kaynaklanan kömür kaybına da engel olacaktır.



Şekil 8. Avdan ve Narlı kömürleri muhtemel açık ocak sınırları.



Şekil 9. İki işletme arasında kalan ve muhtemel kömür bulunan bölge.

SONUÇLAR

Bu çalışmada, Avdan ve Narlı kömür sahasındaki linyitin kaynak modellemesi için yapılan çalışmalardan elde edilen sonuçlar paylaşılmıştır. Kaynağın tespitine yönelik sondaj veri tabanı inceleme çalışmalarından sonra, Avdan ve Narlı bölgelerindeki kömür zonlarının katı ve blok modelleri üretilerek, kömür kaynağının miktar ve kalite değerleri elde edilmiştir. Elde edilen sonuçlara göre, Şekil 8’de sınırları verilen Avdan sahasında 31,6 milyon ton kaynağın ortalama alt ısıl değeri 1700 kcal/kg olarak belirlenirken, Narlı bölgesindeki kaynağın ortalama alt ısıl değeri 1936 kcal/kg olan 39,6 milyon ton kömürden oluştuğu tespit edilmiştir. Avdan bölgesinde kömür modelinde kullanılan sondaj sayısının sahayı temsil etme yeteneği yeterli olduğundan kaynak görünür olarak sınıflandırılırken, Narlı

bölgesindeki sınırlı sondaj sayısından dolayı kaynak muhtemel olarak sınıflandırılmaktadır. Birbirine komşu iki ruhsat sahasının tek bir üretim projesiyle değerlendirilmesi durumunda kaynak modeli tüm kömürleri kapsayacak şekilde revize edileceğinden kaynak miktarının artması sağlanacaktır. Böylece, aynı dekapaj miktarıyla çok daha fazla kömür üretimi olacağından; üretim maliyetlerinin düşmesi, iç döküme hızlı geçilebilmesi sonucunda döküm maliyetlerinin azalmasının, dökümün çevreye olan etkilerinin en düşük seviyede tutulması ve bağlı olarak kaynağın enerji üretimde çok daha verimli bir şekilde kullanılması mümkün hale gelecektir. Bölgede üretilecek olan kömürün, 450 MWe kapasiteli bir termik santrale beslenmesiyle ilgili bir örneğin değerlendirilmesi durumunda, santralin yaklaşık 20 yıllık kömür ihtiyacının karşılanacağı ve bunun için yıllık 3,7 milyon tonluk bir üretim hedefine ihtiyaç duyulacağı sonuçları ortaya çıkmaktadır. İki ruhsatın birleştirilmesi durumunda ise, yukarıda sayılan avantajlardan dolayı, üretim kayıplarının azalması ve ruhsatlar arasındaki kömürün de üretilmesi sonucunda, termik santralin çok daha uzun yıllar bölgeden çıkartılacak kömürle beslenebileceği anlaşılmaktadır. Bu araştırma özelinde elde edilen sonuçların tüm komşu ruhsat sahaları için de geçerli olabileceği düşünülecek olursa, ruhsat birleştirilmesi sonucunda, ülke kaynaklarının çok daha verimli kullanılacak ve ülkemiz yeraltı zenginliklerinin israf edilmesinin önüne geçilecektir.

TEŞEKKÜR

Bildiri konusu faaliyetler, Avdan Madencilik Enerji San. ve Tic. A.Ş. ve As Madencilik AŞ'ye ait Avdan ve Narlı kömür sahalarında yapılan proje faaliyetlerinin birer değerlendirilmesi olup, yazarlar, ruhsat sahibi işletmelere vermiş oldukları destek ve izinden dolayı teşekkür ederler.

KAYNAKLAR

- Akgün, F., Sözbilir, H. (2001). A palynostratigraphic approach to the SW Anatolian molasse basin: Kale-Tavas molasse and Denizli molasse. *Geodinamica Acta*, 14, 71-93
- Alçıçek, H. (2010). Stratigraphic correlation of the Neogene basins in southwestern Anatolia: Regional palaeogeographical, palaeoclimatic and tectonic implications. *Palaeogeography, Palaeoclimatology, Palaeoecology*, 291, 297-318.
- Hakyemez, H.Y. (1989). Kale-Kurbalık (GB Denizli) bölgesindeki Senozoyik yaşlı çökel kayaların jeolojisi ve stratigrafisi. *Maden Tetkik ve Arama Dergisi*, 109, 9-21.
- Isaaks, E. H. ve Srivastava, R. M. (1989). An introduction to applied geostatistics. Oxford University Press, New York.
- Lashgari, M. vd. (2016). Modelling a multi layer coal mine deposit a case study of Avdan lignite site in Denizli Turkey. Thirty - Third Annual Pittsburgh Coal Conference.
- MCS (2015). Independent technical report to JORC (2012) Guidelines Narli coal project for As Madencilik. Proje no:30148, Teknik Rapor.
- Öztürk, C.A. (2001). Maden yataklarının değerlendirilmesinde PCSV ve kriging tekniklerinin karşılaştırılması. Yüksek Lisans Tezi, İTÜ Fen Bilimleri Enstitüsü.
- Sözbilir, H. (2002). Revised stratigraphy and facies analysis of the Palaeocene-Eocene supra-allochthonous sediments and their tectonic significance (Denizli, SW Turkey). *Turkish Journal of Earth Sciences*, 11, 127.
- Sözbilir, H., Özer, S., Sarı, B. (2000). Stratigraphy and tectonics of the late Palaeocene-Eocene supra-allochthon basin formed on the Lycian nappes, Denizli province-SW Turkey. International Earth Sciences Colloquium on the Aegean Region (pp 32). Abstracts.

DETERMINATION OF FACTORS AFFECTING METHANE EMISSION USING THE FAULT TREE ANALYSIS METHOD

METAN EMİSYONUNA ETKİ EDEN FAKTÖRLERİN HATA AĞACI ANALİZİ YÖNTEMİ İLE BELİRLENMESİ

N. Kursunoglu ^{1,*}

¹Batman University, Department of Petroleum and Natural Gas Engineering
(*Corresponding author: nilufer.kursunoglu@batman.edu.tr)

ABSTRACT

The coalification process produces coal mine methane (CMM). When organic material decomposes, it creates methane gas, as well as nitrogen, carbon dioxide, and other gases. Due to the explosive nature of CMM, it is considered a hazard for underground coal mining. During mining operations, a significant amount of adsorbed methane from the coal structure is released into the mine air, posing a threat to worker safety and reducing production efficiency. Despite the use of many measures to mitigate methane leaks, methane remains a major hazard in underground coal mines. Thus, it is critical to understand the components that contribute to methane emissions to guarantee a safe work environment and effective gas control planning. The fault tree analysis (FTA) method was used in this study to determine the parameters responsible for methane emissions in coal mines. The FTA, which is a flexible and systematic approach to risk assessment that enables the identification and classification of hazards, was used to determine the effective emission factors of the study.

Keywords: Methane, emission, mine, coal, risk, fault tree analyses

ÖZET

Metan gazı kömürleşme sürecinde meydana gelir. Kömürün oluşma sürecinde, ayrışan organik materyaller metan gazının yanı sıra nitrojen, karbondioksit ve farklı gazlar üretir. Metan gazı patlayıcı özelliği nedeniyle yer altı kömür madenciliği için bir risk teşkil etmektedir. Madencilik faaliyetleri sırasında, kömür yapısındaki büyük miktarda adsorbe edilmiş metan gazı ocak havasına yayılır, bu durum iş güvenliğini tehdit eder ve üretim verimliliğini düşürür. Metan emisyonunu kontrol etmek için çeşitli yöntemler uygulanmasına rağmen, yeraltı kömür madenleri için tehdit olmaya devam etmektedir. Bu nedenle, metan emisyonunu etkileyen faktörlerin belirlenmesi, güvenli bir çalışma ortamı ve gaz kontrol planlaması sağlamak için gereklidir. Bu çalışmada, kömür madenlerinde metan emisyonuna neden olan parametreleri belirlemek amacıyla hata ağacı analizi (FTA) yöntemi kullanılmıştır. Tehlikelerin tanımlanmasına ve sınıflandırılmasına olanak tanıyan, esnek ve sistematik bir risk değerlendirme yaklaşımı olan FTA, çalışmada etkili emisyon faktörlerinin belirlenmesi için kullanılmıştır.

Anahtar Sözcükler: Metan, emisyon, maden, kömür, risk, hata ağacı analizi

INTRODUCTION

Methane is one of the most dangerous gases found in underground coal mines. It has no color, no odor, and is lighter than air. Methane that has accumulated in the roof is extremely dangerous. Because it is explosive and also results in suffocation as it depletes the oxygen content of the air. Outside of certain limits, methane is flammable. The intensity with which methane burns is dependent on the amount of oxygen and methane in the air. Between 5.5% and 15%, it is explosive. Explosions of

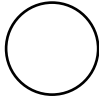
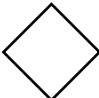



gas are highly hazardous for workers and mines. As a result, precautions against gas explosions in mines should be taken. These measures are intended to reduce the amount of methane in the air and to prevent explosions. Methane is a product of the gradual transformation of plant wastes accumulated during the carboniferous period. Numerous environmental factors convert these plant wastes first to peat, then to lignite, and finally to bituminous coal, whose rank increases over time. Several gases are formed at varying rates and time intervals during this process. Various gases escaped in various ways and mixed with the air or leaked between the layers. Others remained trapped within the organic matrix. A part of the free gas permeates into the pores and cracks of the coal and the adjacent layers. However, coal absorbs and adsorbs the majority of methane. The adsorbed gas is compressed onto the porous coal or stone surface. The absorbed gas is contained within the coal. During coal mining, methane gas is partially released into the atmosphere. This occurs in three distinct ways: (1) Gases are continuously emitted from extremely small pores in coal or stone, (2) Gas emissions from visible cracks and holes frequently persist for an extended period, (3) A sudden, massive gas eruption accompanied by large amounts of coal and stones. Methane emissions increase proportionally to the mine's depth. Because the methane accumulated in the depths was unable to permeate the earth.

Underground coal mining is subject to several natural hazards, the most dangerous of which is methane. It is caused by methane leakage during the hard coal extraction process. When this gas reaches a specific concentration, it turns flammable and explosive. Explosions or ignitions of methane in an underground mine heading pose a significant risk, one that has been observed to be increasing in recent years. This is due to the exploitation of methane-bearing coal beds, the depth of mining operations, and the high concentration of extraction. Fault tree analysis is one of the most effective methods for incident analysis. Accident investigations are deductive, and fault tree analysis is frequently used to determine the underlying causes of accidents. Fault tree analysis is conducted to identify the factors that contributed to the unfavorable top event. It is easier to see the relationships between the causes and to identify the root causes when the tree is constructed (McPherson, 1993; Rajput and Thakur, 2016). The purpose of this study was to investigate the root causes of methane emissions that may occur in underground coal mines using the fault tree analysis method. The study concluded by determining the probabilities of the parameters affecting methane emission.

Fault Tree Analyses

The purpose of fault tree analysis is to systematically identify the primary faults that contribute to the undesirable situation. Fault tree analysis (FTA) is a technique used for both qualitative and quantitative risk assessment. At first, qualitative analysis is used. Qualitative analysis is used to determine the top event and, as a result, the root causes by identifying the events and circumstances that prompted it. Probability theory and Boolean equations are the foundations of quantitative analysis. FTA consists primarily of two gates: And-Gate and Or-Gate. The development of these two doors essentially resulted in the development of the other doors. If all And-Gate-related events fail, the output event occurs, which is a higher-level fault tree event. According to Boolean algebra, it is represented by "+," and the probabilities of the events connected by this gate are summed. The term "Or-Gate" refers to the output event that occurs when at least one of the output events occurs. According to Boolean algebra, it is represented by "•," and the probability of the output events is determined by multiplying their probabilities (Stamatelatos and Caraballo, 2002). Table 1 contains the symbols and definitions for these gates. The FTA consists of eight main steps (Figure 1).

Table 1. Events and gates used in Fault Tree Analysis (Whitesitt, 1995).

Symbol	Description
 Basic event	Means an event that does not require further development or progress
 Undeveloped event	Signifies an unfinished event. This indicates that the event was unable to be developed due to a lack of data or for any other reason.
 Intermediate event	Connects one or more antecedent events between logic gates.
 AND-gate	To output events occur, all events connected by the And-Gate should occur.
 OR-gate	The input event is caused by the occurrence of at least one of the output events.

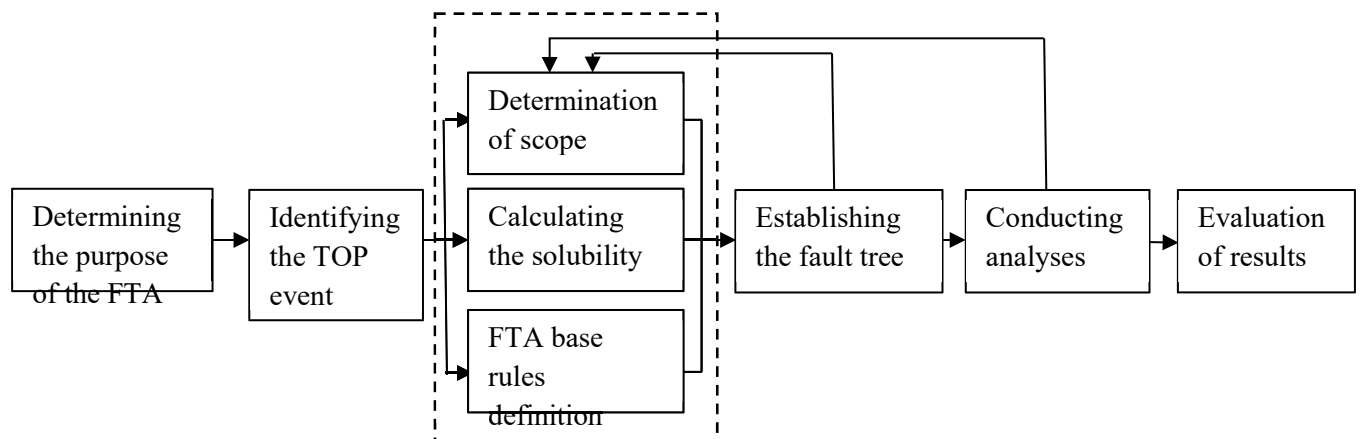


Figure 1. Fault Tree Analysis flowchart (Stamatelatos and Caraballo, 2002).

Application Of Fault Tree Analysis

The world's underground mining industry has resulted in many disasters involving methane ignition and explosions. It should be emphasized that underground coal exploitation is inevitably linked to the methane hazard and always will be. This is because methane was formed concurrently with the formation of coal beds. As a result, exploitation of these beds will naturally result in the release of this gas, which is referred to as coal-mine methane or coal-bed methane in this case. Additionally, it should be emphasized that methane, in addition to posing a safety risk in coal mines, is one of the most harmful greenhouse gases and poses a significant risk to the natural environment (Tutak and Brodny, 2019).

While the number of injuries and fatalities caused by methane emissions has decreased over time, there are still several safety concerns. As a result, a comprehensive risk assessment is a necessary component of determining the sources of methane emissions and preventing the occurrence of hazards to improve the mine environment's safety. Risk assessment is a process that enables the analysis of risk in terms of outcomes and possibilities before determining how potential risk may affect objectives and determining whether additional intervention is necessary. After hazard identification, various methods are required to comprehend the hazards' nature and mechanism of action, as well as the consequences of notable hazards. Numerous risk analysis methodologies are available. Risk assessment can be conducted qualitatively, quantitatively, or hybrid. Qualitative assessment approaches contain “what-if” analyses, checklists, task analyses, safety audits, sequentially timed event plotting (STEP) technique, and hazard and operability (HAZOP). Quantitative risk assessment approaches contain the proportional risk-assessment technique (PRAT), failure mode and effects analysis (FMEA), Fine Kinney, decision matrix risk-assessment (DMRA), and weighted risk analysis (WRA). Hybrid risk assessment approaches contain human error analysis techniques (HEAT), fault tree analysis (FTA), event tree analysis (ETA), and risk-based maintenance (RBM) (Animah and Shafiee, 2020). To analyze the events that result in methane emissions and determine their consequences in this study, the fault tree analysis method was chosen. FTA analysis was carried out using the DPL 9 Fault Tree software. The top event was determined as 'coal methane emission' as the first step of the FTA. After defining the top event, three major factors influencing the occurrence of these accidents were identified. These factors were determined as “coal properties”, “geological conditions”, and “mining parameters” (Figure 2). These factors were interconnected with the OR-gate.

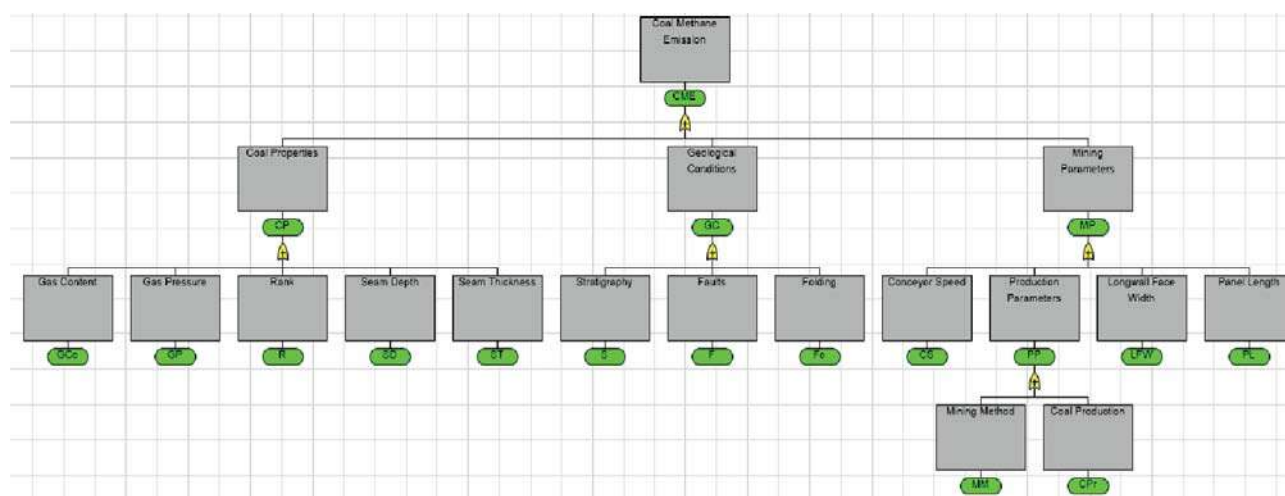


Figure 2. Fault tree of the study

The possible causes of coal properties were determined as “gas content”, “gas pressure”, “rank”, “seam depth”, and “seam thickness”. These branches could have an impact on the coal

properties. Thus, the OR-gate was used to connect them to “coal properties” (Figure 3). “Geological conditions” can be influenced by “stratigraphy”, “faults”, or “folding”. For this reason, these four parameters were connected with the OR-gate to “geological conditions” (Figure 4). “Mining parameters” can be impacted by one of four distinct basic events: “conveyor speed”, “production parameters”, “longwall face width”, or “panel length”. “Production parameters” can be affected by “mining method” or “coal production” (Figure 5).

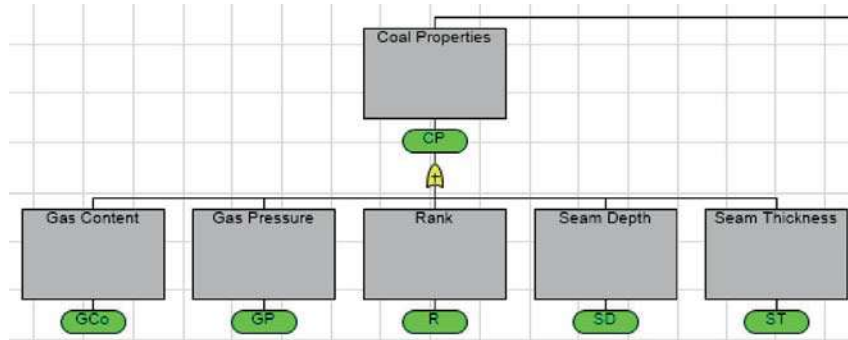


Figure 3. Fault tree of coal properties

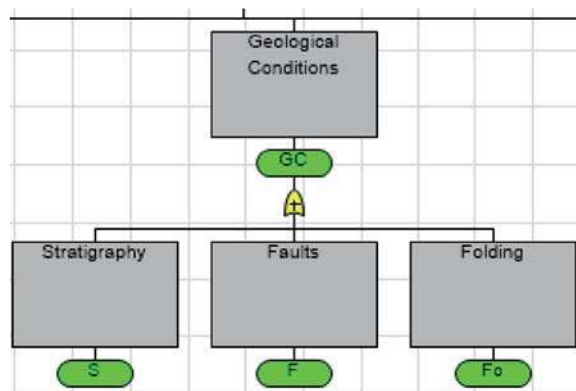


Figure 4. Fault tree of geological conditions

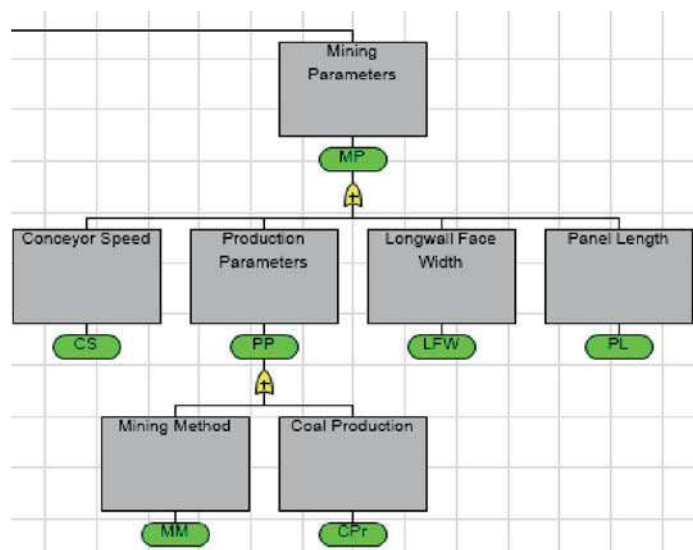


Figure 5. Fault tree of mining parameters

RESULTS

To determine the prominent emission factors, the probabilities of the basic events were assigned using the scale in Table 2. The probability of gates calculated by the software is given in Table 3. Figure 6 depicts the results graphically. The major events that resulted in methane emission were identified, including gas content, seam depth, and seam thickness.

Table 2. Probability scale (Iverson et al., 2001)

Qualitative values	Quantitative values
Certain	1
Very high	10^{-1}
High	10^{-2}
Moderate	10^{-3}
Low	10^{-4}
Very low	10^{-5}
Extremely low	10^{-6}
Practically zero	10^{-7}

Table 3. Probabilities of the basic events and gates

Gate	Basic Event	Probability
<i>Coal Methane Emission</i>		0.126691
<i>Coal Properties</i>		0.119673
	Gas content	0.100
	Gas pressure	0.001
	Rank	0.001
	Seam depth	0.010
	Seam thickness	0.010
<i>Geological Conditions</i>		0.002997
	Stratigraphy	0.001
	Faults	0.001
	Folding	0.001
<i>Mining Parameters</i>		0.004990
	Conveyor speed	0.001
	Longwall face width	0.001
	Panel length	0.001
<i>Production Parameters</i>		0.001999
	Mining method	0.001
	Coal production	0.010

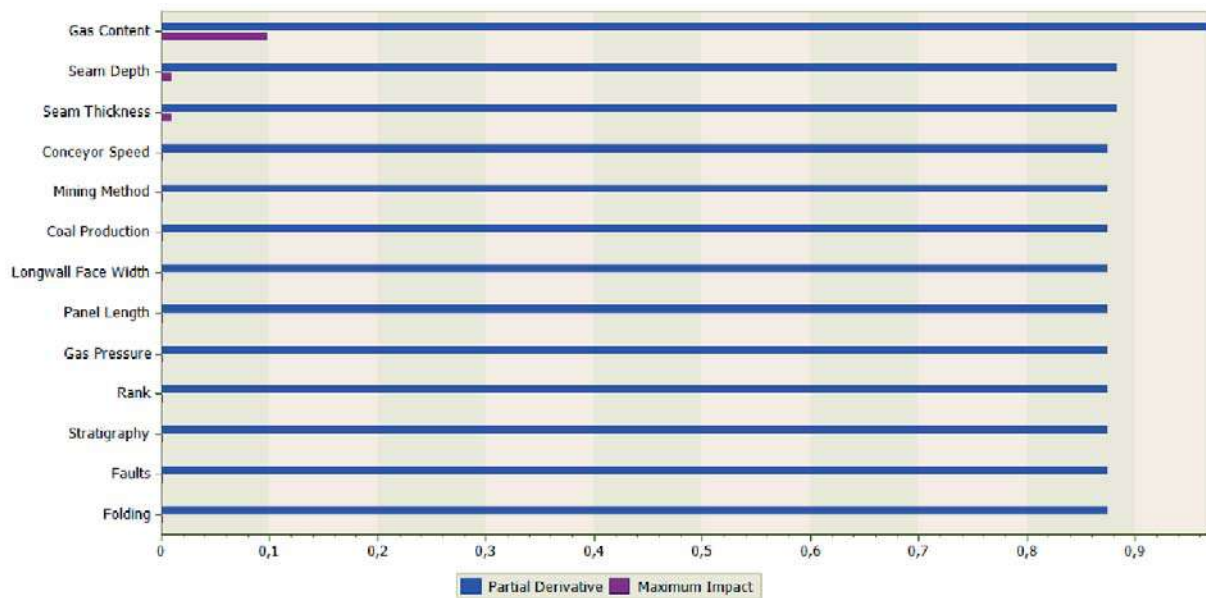


Figure 6. Graphical representation of the results

CONCLUSIONS

Several factors influence methane emissions from coal mines, including coal characteristics, geological conditions, and mining parameters. The potential methane emission causes could have a substantial effect on the incidence of emissions during mining. It is vital to identify these elements so that efficient preventive actions may be implemented, and mine ventilation air can be planned. Thus, the fault tree analysis method was chosen for analyzing the factors affecting the emission formation within the scope of the study. The fault tree analysis allows for the most effective measures to be taken to mitigate the effects of an error or failure. The prioritizing of contributors (intermediate faults and events) to unwanted occurrences is one of the most essential features of the fault tree analyses. 13 significant basic events were identified in this study. The most efficient criteria for methane emission were determined to be gas content, seam depth, and seam thickness using fault tree analyses. The probability of methane emission as a result of basic events was calculated to be 12.66%. This study enables the identification of possible causes of accidents in underground mines and the quantification of their impacts.

REFERENCES

- Animah, I., Shafiee, M. (2020). Application of risk analysis in the liquefied natural gas (LNG) sector: An overview. *Journal of Loss Prevention in the Process Industries*. 63, 103980.
- Iverson, S., Kerkering, J.C., Coleman, P. (2001). Using fault tree analysis to focus mine safety research. 108th Annual Exhibit and Meeting, Society for Mining, Metallurgy, and Exploration, Denver, CO.
- McPherson, M. J. (1993). *Subsurface Ventilation Environmental and Engineering*. Chapman & Hall.
- Rajput, S., Thakur, N. K. (2016). *Geological controls for gas hydrates and unconventional* (1st ed.) Elsevier.
- Stamatelatos, M., Caraballo, J. (2002). *Fault tree handbook with aerospace applications*. Washington, DC: NASA.
- Tutak, M., Brodny, J. (2019). Forecasting methane emissions from hard coal mines including the methane drainage process. *Energies*. 12, 3840.
- Whitesitt, J. E. (1995). *Boolean algebra and its applications* (1st ed.). Mineola, New York: Courier Dover Publications.

DETERMINATION OF STRENGTH PARAMETERS FOR SPECIMENS PREPARED BY 3D PRINTED DISCONTINUITY PLANES

A. Kirmaci^{1,*}, Asst.Prof.Dr. M. Erkayaoğlu¹, Asst.Prof.Dr. A.G. Yardımcı¹

¹ *Middle East Technical University, Mining Engineering Department*

**Corresponding Author: Email: kirmaci@metu.edu.tr*

ABSTRACT

Mining activities in sustainable and safely operated underground mines depend on the design of openings using rock strength-related parameters representing site conditions as much as possible. Rock specimens must be collected and prepared for experiments to obtain intact rock properties. In particular, it is almost impossible to represent field conditions in experimental environments completely. A well-known example of this challenge is the representation of discontinuities on site. At this point, using current technologies could improve the level of representation of specimens where 3D printers could be used to manufacture existing discontinuity planes that reduce the strength of intact rock material. In this context, a 3D printed discontinuity plane is used to prepare concrete mortar specimens. Static deformability experiments of these samples were completed to determine the strength parameters. As a result, the uniaxial compressive strength value of concrete samples without discontinuity planes was obtained in addition to the samples with rough, wavy, and smooth discontinuity planes. Finally, the results were compared with stress concentration factors obtained from the numerical models.

Keywords: 3D printer, 3D printed discontinuity, concrete, numerical modeling

INTRODUCTION

Mining activities have a significant role in the sustainable development of countries. Turkey is located in a geographical region wealthy in terms of underground and surface resources. The continuously increasing demand for energy and raw materials has reinstated the critical role of mining activities. Rock mechanics experiments are of great importance in the realization of these activities. The accuracy of the rock mechanics test results and the design criteria defined according to these results ensure the continuity and reliability of mining, especially in underground operations.

In some cases, the collection and preparation of rock samples used during rock mechanics experiments can cause technical difficulties. In recent years, samples printed with 3D printers have been used worldwide by various researchers as an alternative to the samples collected and prepared in a laboratory environment. Thus, it is aimed to reduce the effort of sample preparation for the experiments and to reflect the conditions on-site more accurately by including weakness planes and different filling materials. For example, collecting core samples containing a representative discontinuity requires an expert opinion. It is expected that rock-like samples prepared by 3D printing will result in a better representation of discontinuities within the scope of the study.

As a result of the preliminary literature research in this field, 3D printer technology has been used in different areas of rock mechanics-related research (Jaber et al., 2020; Jiang et al., 2016; Ju et al., 2017; Zhou, Zhu and Xie, 2020; Wu et al., 2020). Some researchers printed rock-like samples with 3D printers, whereas others printed discontinuity planes to be placed within rock samples to carry experiments. Different researchers investigated the load displacement response for various purposes (B.

Tarasov and Potvin 2013; Verma, et al., 2021). In this study, concrete samples were prepared by using 3D-printed molds. Afterward, the individual parts of the samples were joined with plaster, which has a comparably lower strength than the laboratory samples. Static deformability tests were performed to compare mechanical properties of the different roughness profiles of discontinuities. It is foreseen that this study will contribute to rock mechanics literature and the implementation of 3D printing technology for laboratory testing of rocks.

The collection of rock samples during field studies can be considered one of the first stages of sample preparation for laboratory experiments. At this point, 3D printers might provide convenience to researchers that use complex specimen geometries for fracture mechanics or profiles that represent discontinuities. One of the research questions is whether a 3D printed sample can be used instead of a rock sample. Based on the work of Hucka and Das (1974), it has been shown that each rock type has a unique index of brittleness. This index is calculated using the formula shown below.

$$\text{Brittleness Index} = \frac{\sigma_c + \sigma_t}{\sigma_c - \sigma_t} \quad (1)$$

The symbols σ_c and σ_t used in the formula represent the uniaxial compressive strength value and the direct tensile strength value, respectively. The brittleness index value differs according to the rock types. While this value generally varies between 5-25 in actual rock samples, this value varies between 3.5-4 in 3D printed samples (Vrkljan, 2009). At this point, the material used in printing samples with 3D printers is creating a variance of mechanical properties. As a result of the comparison of values, it is seen that 3D printed samples might be used as artificial copies of rock samples for specific conditions.

Since the desired model can be printed easily and quickly with 3D printers, Song et al. (2018) designed four different tunnel models. The results were compared with tunneling case studies, artificial models, and numerical simulation models. PLA (polylactic acid) and powder-based materials are commonly used in 3D printers. A conventional tunnel model, single fault tunnel, double fault tunnel, and a tunnel model with rock bolt and tunnel lining were designed. Compression tests were completed with all four models, and some similarities were found in the deformation curves and failure characteristics. Likewise, these results showed similarities with the numerical simulation models developed. It has been determined that rock bolts and tunnel linings significantly reduce damage in the tunnel and increase the carrying capacity of the tunnel. The experiments were also monitored with digital image correlation systems, which captured displacement, crack initiation, and propagation.

Monitoring the failure behavior of rock samples during laboratory experiments, such as crack formation and propagation during uniaxial compressive strength testing or indirect tensile strength testing, with current technologies such as digital image correlation, high-speed cameras, thermal cameras, and acoustic emission provides researchers crucial information. Sharafisafa et al. (2019) conducted indirect tensile strength tests using disk-shaped samples taken from a 3D printer. The effect of the filling material on the failure behavior of the rock samples was investigated by opening cracks at different angles on the samples they prepared and filling the cracks in some samples with a material of different properties. Likewise, the differences between the samples with cracks not filled and samples filled with material were examined. In such analyses, it is essential to determine the exact moment of crack formation and the crack propagation behavior. The researchers were able to achieve detailed results by using a digital image correlation system. As a result of their experiments, it was determined that the samples with filling material were able to resist against higher load than the samples without filling, and shear cracks caused by shear displacement vectors during failure were observed.

Zhu et al. (2018) scanned the rock samples taken from a mine site using an X-ray computed tomography device and structurally copied them with the help of a 3D printer. Static deformability and indirect tensile strength tests were performed on the printed and actual samples recorded with a high-

speed camera. As a result, it has been observed that the uniaxial compressive strength values are very close to each other, but there is a significant difference in the unit deformation values. The reason for this is shown as the difference in the modulus of elasticity. On the other hand, crack initiation and propagation in disc samples used in direct tensile strength tests were determined with the help of the high-speed camera. As a result of the experiment, it was observed that tensile strength values were very close to each other for both samples.

Zhou and Zhu (2018) obtained five different types of samples using ceramic, gypsum, polymethyl methacrylate, SR20 (acrylic copolymer), and resin, respectively, from the materials used in 3D printers and performed static deformability experiments with them. The purpose of conducting these experiments was to determine the material that might be closest to a brittle rock. As a result of the experiments, it has been seen that the most suitable material for the brittle rock type is the resin according to the material's behavior and the maximum applied load. However, it has been mentioned that there is a problem with the brittleness properties of the resin samples. Therefore, there is still potential improvement using the testing methods such as thermal treatment or adding artificial macro and micro cracks.

Fereshtenejad and Song (2016) examined different materials in powder-based 3D printers in their study. It was observed that the materials used showed relatively lower strength values and ductile behavior. Therefore, improvement methods have been studied to enhance these properties. These methods were defined as printing direction, printing layer thickness, the saturation level of binder, uniaxial compressive strength test of samples heated to different temperatures, and examination of stress-strain deformation graphs.

By considering the printing direction, the highest strength value was observed in the samples printed with 0°, while the lowest strength value was found in the samples at 25°. Different printing layer thicknesses were tried, and it was seen that the layer thickness was not an important parameter that could affect the sample strength. Likewise, different amounts of binder saturation level were applied, and it was observed that the uniaxial compressive strength value increased by these varying amounts as an increase in the saturation level. In addition, the temperature of the materials was increased to 70°C, 100°C, 120°C, 150°C, and 170°C, respectively. The results in their initial state were compared with the samples whose temperature was increased. As a result, the value that increases the uniaxial compressive strength value the most and seems to be the ideal temperature has been found as 150 °C.

Ban et al. (2020) scanned five concrete samples with different surfaces with 3D morphology scanner systems and completed direct shear tests on 20 samples in total by taking four different samples from each sample with the help of a 3D printer. Four different normal loads, 0.5 MPa, 1 MPa, 1.5 MPa, and 2 MPa, were applied to each surface, and shear values were obtained. As a result of the experiments, a new peak shear strength model was created.

As a result of the reviewed literature, it has been seen that the introduction of 3D printer systems into rock mechanics research in the mining industry might provide advantages during sample preparation. The convenience of preparing specimens, using a pre-designed type of material, cracks, fillings, and other structures that can be added within the samples are some of the main benefits of using 3D printers.

EXPERIMENTAL STUDY

Rock mechanics related research has been improving by integrating new technologies recently. It is possible to represent features such as discontinuities and micro-cracks in rock samples by using 3D printing technology. In this way, the effect of these conditions on the mechanical properties of the rock material can be investigated.

This study aims to examine the mechanical properties of concrete samples containing discontinuity planes by using 3D printer technology prepared for static deformability tests. The following aims will be achieved as a result of the experiments:

- Concrete samples prepared into 3D-printed molds containing different discontinuity planes were joined, and their mechanical properties were determined.
- The plaster material used to join the concrete samples was varied to represent the infilling of the printed discontinuity.
- Test results of the 3D printed concrete samples with discontinuities were compared with intact concrete samples.

The methodology of this study covers the laboratory experiments on the 3D printed concrete samples. MTS 815 test system, which provides displacement-controlled loading, was used during the experiments. The experimental setup can be seen in Figure 1.



Figure 1: MTS 815 test system and an experiment which conducted static deformability test

The 3D printer used to produce the molds is a Zortrax M300 with a single printing head, as seen in Figure 2. The maximum dimensions that can be printed are limited to 300x300x300 mm and were considered sufficient for the samples prepared for the experiments. The molds were initially designed with the help of a CAD software and then exported as STL files, as seen in Figure 2. The printer uses ABS-type filament to print the molding material due to its comparably higher strength properties. According to the technical data of the filament, the tensile strength and maximum bending stress are 30.5 MPa and 46.3 MPa, respectively.



Figure 2: Zortrax M300 Plus printer and an example of 3D printed model

Three different 3D printed molds were designed to include varying discontinuity profiles. The three types of molds have a 45° inclination plane, and for each mold sample, the roughness plane was printed as smooth, rough, and wavy, as shown in Figure 3, respectively.

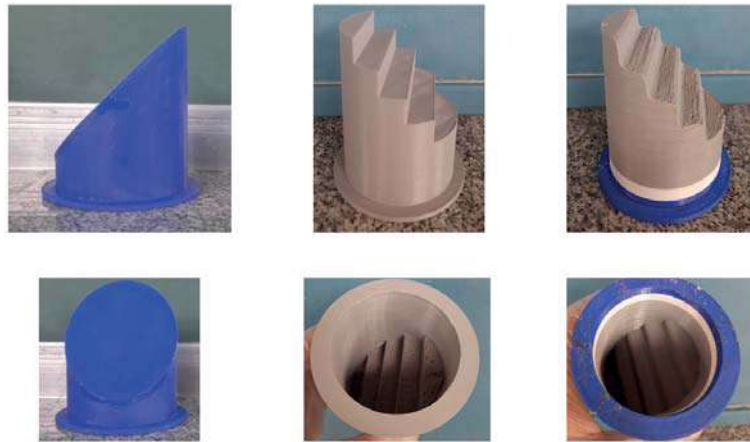


Figure 3: Different roughness planes prepared with the help of 3D printing technology

Concrete samples prepared for the laboratory tests have a mix design of cement, aggregates, and water ratio of 1:4:0.75. The prepared concrete mixture was poured into the 3D printer molds and cured for a total of seven days. Concrete samples extracted from the molds can be seen in Figure 4.



Figure 4: The concrete samples prepared with the help of 3D printed molds

Finally, the samples prepared using the 3D printed molds were joined with plaster material. The purpose of using plaster as filling material that was cured for 1 day to ensure that the discontinuity plane is represented by a material with lower strength than the rock sample. In Figure 5, the samples with smooth, rough, and wavy discontinuity planes joined with the help of plaster are seen.



Figure 5: Concrete samples with smooth, rough, and wavy discontinuity planes joined with plaster, respectively

Static deformability tests were completed on three concrete samples and four plaster samples that do not have any discontinuity planes. In this way, the mechanical properties of the concrete and plaster materials were obtained. For the concrete samples, the mix design of cement, sand, and water was kept the same. In Figure 6, the before test and after test photographs of the concrete samples can be seen.



Figure 6: Before test and after test images of concrete samples

Four different ratios were used as plaster sample designs, and the most suitable ratio was used to join the samples. In sample A1, 80% plaster and 20% aggregates, for the A2 sample, 50% plaster and 50% aggregates were used. In A3 and A4 samples, cement was substituted for aggregate, and 80% plaster, 20% cement, 50% plaster, and 50% cement ratios were used. In Figure 7, before test and after test images of 4 different plaster samples can be seen.



Figure 7: Before test and after test images of plaster samples

RESULTS AND DISCUSSION

In this section, the static deformability test results of concrete and plaster samples will be discussed. First, three concrete samples prepared with the same cement, aggregate, and water ratio were tested. Before test and after test images of concrete samples are presented in Figure 6. The experiment results for concrete samples are summarized in Table 1.

Table 1. Static Deformability Test Results for Concrete Samples with no discontinuity (Core material)

Specimen	Dia. (mm)	Length (mm)	UCS (MPa)	E (GPa)
B1	72.2	154.8	5.2	3.2
B2	72.6	152.4	2.6	7.4
B3	72.4	152.2	5.5	3.0
Average			4.4	4.5

According to the results of the experiments, an average uniaxial compressive strength value of 4.4 MPa was observed for the concrete samples, while the elastic modulus was calculated as 4.5 GPa.

After the concrete samples, static deformability tests were performed on four different plaster samples. Plaster-sand and plaster-cement ratios are mentioned in the “Experimental Study” section Table 2 shows the mechanical parameters obtained as a result of the experiments. Since plaster samples represent infilling material for the discontinuity, it was expected to have lower strength than concrete samples. Accordingly, as a result of the experiments, it was seen that the strength value of the A1 sample was lower than required, and the A4 sample was higher than required. Therefore, it was considered to use A2 (50% plaster and 50% aggregates) or A3 (80% plaster and 20% cement) samples during the experiments as the most suitable material for joining the samples. As a result, plaster samples with uniaxial compressive strength of 2.3 MPa were used to assemble the samples prepared with the 3D molds.

Table 2: Static Deformability Test Results for Plaster Samples with no discontinuity (Filling material)

Specimen	Dia. (mm)	Length (mm)	UCS (MPa)	E (GPa)
A1	71.1	154.9	1.2	1.4
A2	71.9	155.3	2.3	3.2
A3	71.9	154.9	2.9	4.6
A4*	72.1	152.2	13.1	5.2
Average			2.2	3.1
* outlier				

After the mechanical parameters of the concrete samples and the appropriate plaster ratio to be used to combine the samples were found, the samples taken from the 3D printers were combined, and static deformability tests were carried out. Firstly, static deformability tests of concrete samples with a 45-degree inclination and smooth discontinuity plane were carried out. Two concrete specimens with a smooth discontinuity plane were tested. In Figure 8, the before test and after test images of these experiments can be seen.

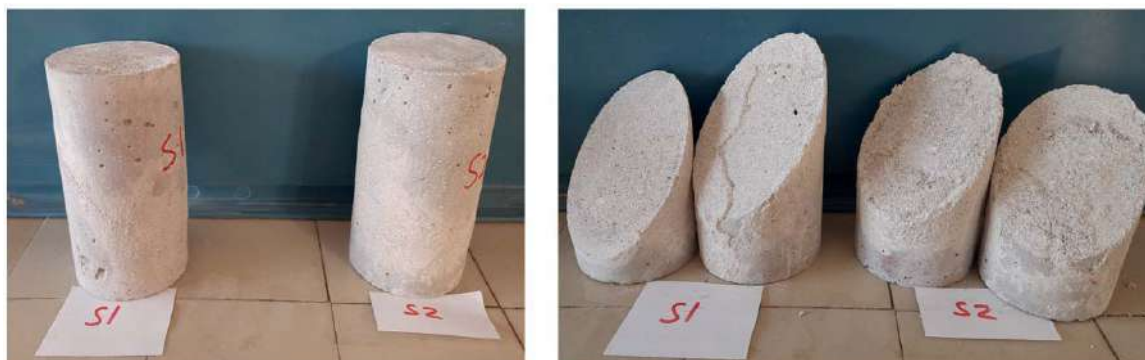


Figure 8: Before test and after test images of concrete samples with smooth discontinuity planes

As shown in Figure 8, the sample failed from the discontinuity plane, which has a lower strength value. Table 3 shows the mechanical parameters obtained as a result of these experiments.

Table 3: Static Deformability Test Results for Concrete Samples with smooth discontinuity planes

Specimen	Dia. (mm)	Length (mm)	UCS (MPa)	E (GPa)
S1	72.7	140.4	1.7	6.7
S2	72.1	145.9	3.7	3.7
Average			2.7	5.2

By considering Table 3, the average UCS value for specimens with smooth discontinuity planes is 2.7 MPa, while elastic modulus is 5.2 GPa.

Similarly, static deformability tests of concrete samples with a 45-degree inclination and rough discontinuity plane were carried out. Two concrete specimens with a rough discontinuity plane were tested. In Figure 9, the before test and after test images of these experiments can be seen.



Figure 9: Before test and after test images of concrete samples with rough discontinuity planes

As shown in Figure 9, the failure surfaces representing lower strength regions filled with plaster materials were observed. Unlike the smooth plane samples, failures occurred at the top, where the thinnest layer is located. This was explained as the stress concentration regions created by the sharp transitions of the geometry during the static deformability test. Table 4 shows the mechanical parameters obtained as a result of these experiments.

Table 4: Static Deformability Test Results for Concrete Samples with rough discontinuity planes

Specimen	Dia. (mm)	Length (mm)	UCS (MPa)	E (GPa)
R1	63.3	132.7	3.9	2.3
R2	63.1	132.1	6.5	1.7
Average			5.2	2.0

By considering Table 4, the average UCS value for specimens with rough discontinuity planes is 5.2 MPa, while elastic modulus is 2.0 GPa.

Finally, static deformability tests were carried out of concrete samples with a 45-degree inclination and wavy discontinuity plane. Two concrete specimens with a wavy discontinuity plane were tested. In Figure 10, the before test and after test images of these experiments can be seen.



Figure 10: Before test and after test images of concrete samples with wavy discontinuity planes

As shown in Figure 10, the failure properties of the wavy discontinuity planes on the concrete samples are similar to the rough discontinuity plane samples. Similarly, failure occurred in the weak plaster layer within the samples with the wavy plane, and similar stress concentration points were observed at the top of the specimen. Table 5 shows the mechanical parameters obtained as a result of these experiments.

Table 5: Static Deformability Test Results for Concrete Samples with wavy discontinuity planes

Specimen	Dia. (mm)	Length (mm)	UCS (MPa)	E (GPa)
W1	63.1	131.1	4.9	0.8
W2	63.3	131.9	4.9	2.5
Average			4.9	1.7

By considering Table 5, the average UCS value for specimens with wavy discontinuity planes is 4.9 MPa, while elastic modulus is 1.7 GPa.

Numerical modeling of each concrete sample with a different roughness plane was performed in FLAC 8.0, a time marching code based on 2D plane-strain assumption. For the input parameters of concrete and plaster, the results of the laboratory experiments were used. After generating the 2D

model, a uniaxial loading condition was defined by applying velocity from the top and bottom ends of the model. Stress analyses were carried out using an elastic material model. Interpretations considering stress concentration around discontinuity planes for the pre-failure region are presented. First, a concrete sample with a smooth discontinuity plane was modeled, as shown in Figure 11.

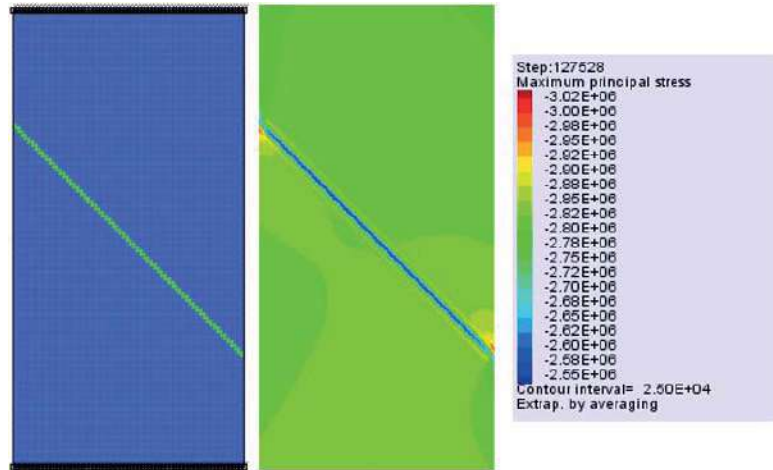


Figure 11: Numerical model and maximum principal stress for the concrete sample with smooth discontinuity plane

The numerical assessment of maximum principal stress determined from FLAC 8.0 model at 0.54 mm displacement is obtained as 3.0 MPa and it is consistent with the laboratory experiments. As shown in Figure 11, stresses observed around the plaster fill material represent a comparably lower strength than concrete. The stress distribution behavior on the numerical model is also consistent with the laboratory experiment results.

The concrete samples with a rough discontinuity plane were modeled, and the stress distribution behavior was similarly found to be conforming with the laboratory test results. Accordingly, maximum stress on the model at 0.35 mm displacement is obtained as 4.7 MPa, which is close to the laboratory testing results. Inferences related to the stress accumulation regions are also supported, as seen in Figure 12. The interpreted results indicate the stress concentration regions being closer to the sharp transition regions and lower at the thinnest layer.

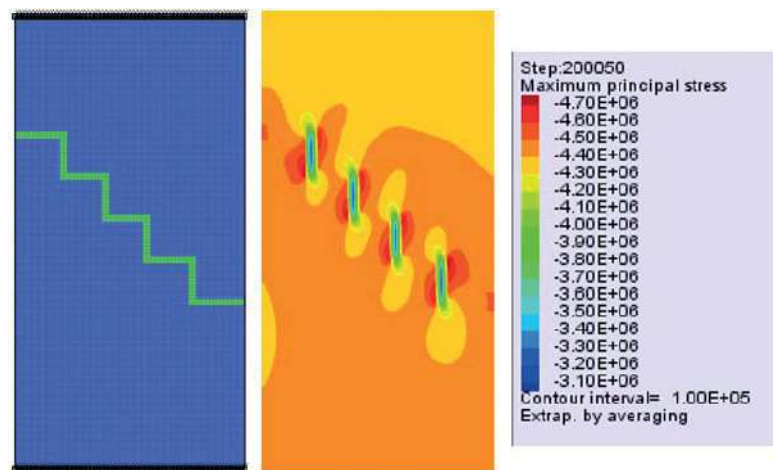


Figure 12: Numerical model and maximum principal stress for the concrete sample with smooth discontinuity plane

Finally, the 2D model of the concrete samples with a wavy profile for the discontinuity plane was modeled. According to the numerical model results, it was seen that the stress distribution behavior is similar to the rough discontinuity planes and the results are also consistent with the laboratory test results. Consequently, the stress value obtained as 3.9 MPa at a displacement of 0.54 mm, is also close to the laboratory test results. Figure 13 shows the stress distribution behavior and the maximum stress value of the concrete sample with a wavy discontinuity plane.

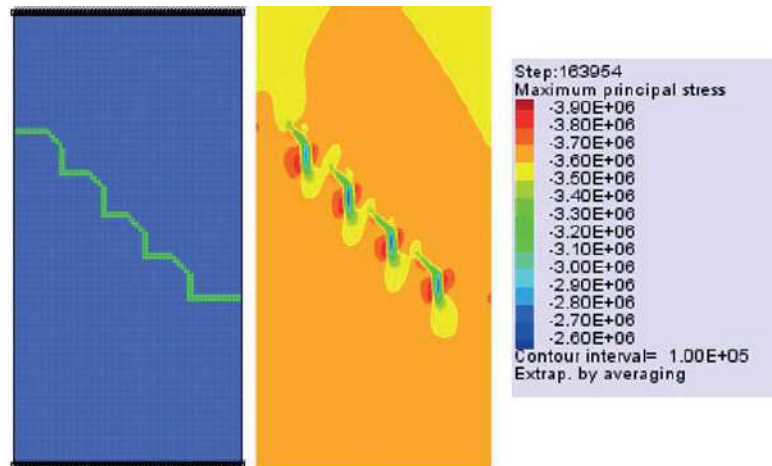


Figure 13: Numerical model and maximum principal stress for the concrete sample with wavy discontinuity plane

Stress concentration on the sample geometry was investigated by defining critical points on the models. The stress concentration values were calculated by the ratio of the stress value and the maximum stress obtained from the test results of the intact specimen. The points used for stress concentration analysis for intact specimens and specimens with different roughness planes can be seen in Figure 14.

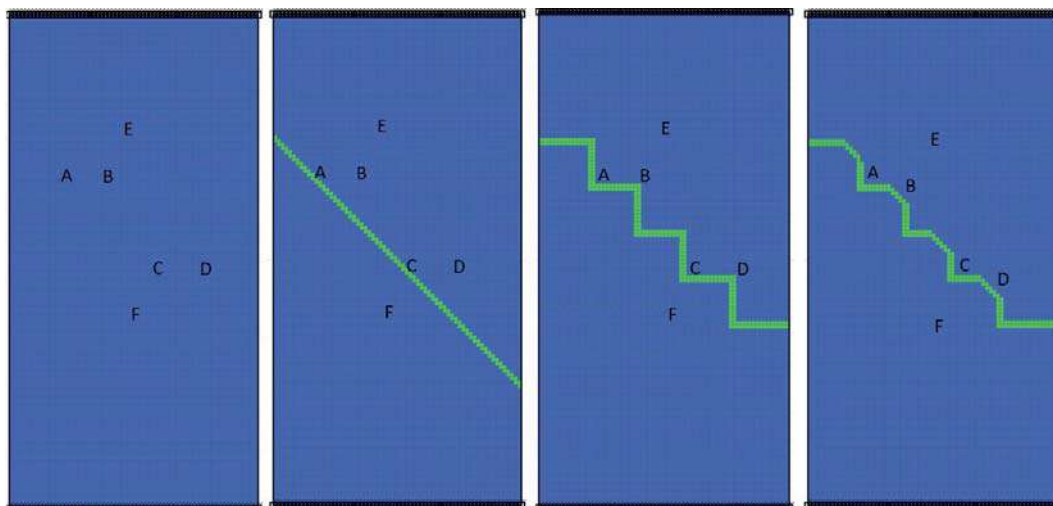


Figure 14: History points for intact specimen, smooth, rough, and wavy discontinuity planes

According to the results obtained from FLAC 8.0, the stress values were higher at the bottom part of the specimens and comparably lower at the top part. For the rough and wavy discontinuity planes, points A and C are defined to represent the region closest to the thinnest layer. In contrast, points B and D indicate the thinnest layer. As summarized in Table 6, the stress concentration values are

higher, almost more than 50%, at the close regions of the sharp transitions than the regions where the actual sharp transitions occur. These values support the inference made for the laboratory experiments results related to stress concentration regions. Stress concentration is obtained at much lower levels than the lower strength region for the smooth discontinuity plane.

Table 6: Stress Concentration Factor values for history points on the specimens

Specimen Type	Stress Concentration Factor					
	A	B	C	D	E	F
No Plane						
Smooth Plane	0.6	0.6	0.6	0.6	0.6	0.6
Rough Plane	0.9	1.1	0.9	1.1	1.0	1.0
Wavy Plane	0.8	0.9	0.8	0.9	0.8	0.8

CONCLUSION

This study covers the tests performed to obtain the mechanical properties of concrete samples with different roughness planes. First, static deformability tests were performed on concrete samples without any discontinuity plane. As a result, a uniaxial compressive strength value of 4.4 MPa, and elastic modulus of 4.5 GPa were obtained. For plaster samples representing the infilling of the discontinuity plane between the concrete specimens, it has been determined that the most suitable ratio was the mixture of 50% plaster and 50% aggregates. This mixture has a uniaxial compressive strength value of 2.3 MPa. These values are considered suitable as it was estimated that the plaster layer representing the discontinuity plane should have a lower strength value than the concrete sample itself. In the test results performed on the samples with different roughness surfaces, it was observed that the uniaxial compressive strength values in the samples with rough and wavy discontinuity planes were very close to each other. Also, these samples provided higher load values originating from the stress accumulation regions on the sharp edges. On the contrary, it was observed that the samples with smooth surface planes slipped directly from the weak plaster layer. The numerical model of the concrete samples with the different roughness discontinuity planes was also examined with the help of the 2D numerical modeling software, FLAC 8.0. Accordingly, the results are very close to the interpreted results of the 2D numerical model. It also supported the inferences from the laboratory tests about the stress concentration regions. The interpreted results indicate the stress concentration is higher at regions closer to the sharp transition and lower at the thinnest layer at the maximum displacement amount. As a result of the analysis, it was seen that the use of 3D printers for manufacturing molds could reduce the time and effort related to sample preparation. Therefore, further experimental studies will be performed with different roughness planes, infilling types, and infilling thicknesses.

REFERENCES

Ban, L., Qi, C., Chen, H., Yan, F., & Ji, C. (2020). A new criterion for peak shear strength of rock joints with a 3D roughness parameter. *Rock Mechanics and Rock Engineering*, 53(4), 1755-1775.

Fereshtenejad, S., & Song, J. J. (2016). Fundamental study on the applicability of powder-based 3D printer for physical modeling in rock mechanics. *Rock Mechanics and Rock Engineering*, 49(6), 2065-2074.

Hucka, V., & Das, B. (1974, October). Brittleness determination of rocks by different methods. In *International Journal of Rock Mechanics and Mining Sciences & Geomechanics Abstracts* (Vol. 11, No. 10, pp. 389-392). Pergamon.

- Jaber, J., Marianne, C., Deck, O., Mohamed, M., Godard, O., & Samuel, K. (2020). Investigation of the mechanical behavior of 3D printed polyamide-12 joints for reduced scale models of rock mass. *Rock Mechanics and Rock Engineering*, 53(6), 2687-2705.
- Jiang, C., Zhao, G. F., Zhu, J., Zhao, Y. X., & Shen, L. (2016). Investigation of dynamic crack coalescence using a gypsum-like 3D printing material. *Rock mechanics and rock engineering*, 49(10), 3983-3998.
- Ju, Y., Wang, L., Xie, H., Ma, G., Zheng, Z., & Mao, L. (2017). Visualization and transparentization of the structure and stress field of aggregated geomaterials through 3D printing and photoelastic techniques. *Rock Mechanics and Rock Engineering*, 50(6), 1383-1407.
- Sharafisafa, M., Shen, L., Zheng, Y., & Xiao, J. (2019). The effect of flaw filling material on the compressive behaviour of 3D printed rock-like discs. *International Journal of Rock Mechanics and Mining Sciences*, 117, 105-117.
- Song, L., Jiang, Q., Shi, Y. E., Feng, X. T., Li, Y., Su, F., & Liu, C. (2018). Feasibility investigation of 3D printing technology for geotechnical physical models: study of tunnels. *Rock Mechanics and Rock Engineering*, 51(8), 2617-2637.
- Tarasov, B., & Potvin, Y. (2013). Universal criteria for rock brittleness estimation under triaxial compression. *International Journal of Rock Mechanics and Mining Sciences*, 59, 57-69.
- Verma, R. K., Nguyen, G. D., Karakus, M., & Taheri, A. (2021). Capturing snapback in indirect tensile testing using AUSBIT-Adelaide University Snap-Back Indirect Tensile test. *International Journal of Rock Mechanics and Mining Sciences*, 147, 104897.
- Vrkljan, I. (Ed.). (2009). *Rock engineering in difficult ground conditions-soft rocks and karst*. CRC Press.
- Wu, Z., Zhang, B., Weng, L., Liu, Q., & Wong, L. N. Y. (2020). A new way to replicate the highly stressed soft rock: 3D printing exploration. *Rock Mechanics and Rock Engineering*, 53(1), 467-476.
- Zhou, T., & Zhu, J. B. (2018). Identification of a suitable 3D printing material for mimicking brittle and hard rocks and its brittleness enhancements. *Rock Mechanics and Rock Engineering*, 51(3), 765-777.
- Zhou, T., Zhu, J., & Xie, H. (2020). Mechanical and volumetric fracturing behaviour of three-dimensional printing rock-like samples under dynamic loading.
- Zhu, J. B., Zhou, T., Liao, Z. Y., Sun, L., Li, X. B., & Chen, R. (2018). Replication of internal defects and investigation of mechanical and fracture behaviour of rock using 3D printing and 3D numerical methods in combination with X-ray computerized tomography. *International Journal of Rock Mechanics and Mining Sciences*, 106, 198-212.

DETERMINATION OF THE DEGREE OF RELEASE OF MINERAL PARTICLES BY IMAGE ANALYSIS SOFTWARE

T. D. Figueiredo^{1,*}, A. M. Braga², R. J. A. Fidelis², D. G. Magalhães², P. H. L. Silva¹, C. A. Pereira¹

¹*Federal University of Ouro Preto (UFOP), Dept of Mining Engineering*

*(*Corresponding author: thiagoduarte1926@hotmail.com)*

²*Federal Center of Technological Education of Minas Gerais (CEFET/MG)*

ABSTRACT

The degree of release of the mineral particles is of great importance in ore treatment operations. The incorrect interpretation of this parameter directly affects the efficiency of the mineral processing stages, and may even render projects unviable. Currently, the most usual method of determining the degree of release is the so-called Gaudin method, whose representativeness of the results depends heavily on the good practice and interpretation of the operator. This work aims to implement an image analysis software to determine the degree of freedom of minerals, reducing human participation in the process and giving greater certainty to the results. For this, the degree of release of iron ore samples from the municipality of Guanhães/MG was determined using the Gaudin method and the software developed for this study. The respective results were compared, proving the effectiveness of the computational program, concluding that, release-rate analyzes could be performed through computation, with greater speed, accuracy and accuracy.

Keywords: Release degree, computational analysis, iron ore

INTRODUCTION

Mineral concentration operations have as main objective the separation of the element of interest, called mineral-ore from gangue minerals, in order to obtain products to be used industrially. For such separation to occur, physical or physicochemical differences must exist between mineral species, and, also, that the minerals of interest are physically disaggregated to those that have no economic interest (Ferreira, 2013).

In certain mineral deposits, the ore is naturally released, eliminating stages of fragmentation. However, in most situations, the minerals of interest are consolidated, requiring comminution steps to increase the degree of mineral release. According to Delbem (2010), the release of mineral particles is proportional to fragmentation, that is, the more fragmented the ore, the greater its degree of release. However, due to the high operational cost and the unsatisfactory performance of ultrafine particles in concentration operations, mineral fragmentation should be limited to what is necessary for operational viability.

According to Rodrigues (2016), among the variety of methods of determining the degree of release, the most used in the mineral sector is the so-called Gaudin method (1939). This method defines as a degree of freedom the percentage of a given mineral species that occurs as a free particle in relation to the total particles of a sample, and can be used for different minerals, requiring only that the mineral to be analyzed present visual difference for the other minerals. One of the main disadvantages of gaudin's method is the high dependence of the operator, since a result with greater precision needs to good practice and interpretation of it.

Taking into account this dependence of the operator, the use of computational analysis of images is increasingly justified in the study of mineral release (Ferreira, 2013). Some techniques are already widespread, such as electron microscopy and optical image analysis, both with important limitations, whether referring to representativeness or reproducibility of results (Donskoi et al., 2014).

Delbem et al. (2015) proposes a digital analysis system capable of characterizing and determining the degree of release of different types of mineral samples semi-automatically, seeking to increase the accuracy of the procedure by reducing human influence on the results. Based on studies and methodologies such as those already mentioned, this article proposes the creation of an image analysis program that, together with mathematical software, allows obtaining quantitative results in real time, about the degree of release of ores.

MATERIALS AND METHODS

For the study, two samples of iron ore were used, made available by a mining company located in the municipality of Guanhães- MG. The first (Am1) comes from the mining front in the northern region of the mine and the second (Am2) comes from the homogenization pile.

The samples were homogenized using the canvas homogenization technique and quartered in jones type quarter. After preparation, they were submitted to the stages of washing and granulometric separation by sieving. Subsequently, the degree of release of the particles in different size ranges was determined, using the conventional method defined by Gaudin and the computational method by the aid of a software. Figure 1 summarizes the methodology used in this work, showing the procedures of this stage.

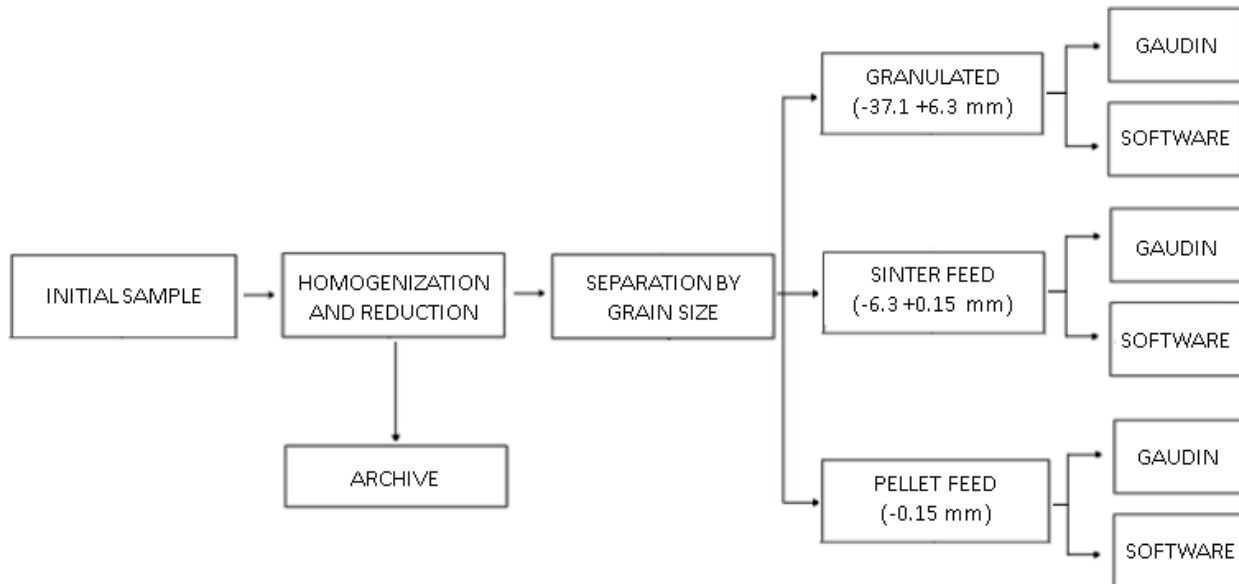


Figure 1. Methodology flowchart

Separation by Size by Sieving

This step was performed in order to separate the material into three granulometric ranges corresponding to the products of iron ore, pellet feed (<0.150 mm), sinter feed (0.150 mm to 6.3 mm) and granulated (6.3 mm to 37.1 mm). The process was performed in wet and with the use of a CDC suspended sieve, model PV-08. Figure 2 represents the three granulometric bands sampled.

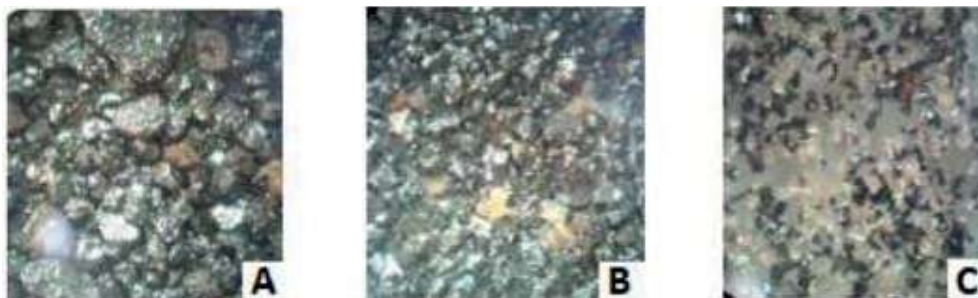


Figure 2. Granulated ore (A)- sinter feed (B) - pellet feed (C)

Determination of the Degree of Release by the Conventional Method (Gaudin)

The degree of release of the analyzed samples was determined using the Gaudin method. This method consists of counting the mineral grains of a sample in a given particle size range, evaluating the release of each particle and classifying them according to the proportion of the mineral of interest in the grain. Each particle presents a release index proportional to the percentage of the grain occupied by the mineral of interest, in the case analyzed, hematite.

For this study, 800 particles were analyzed, one by one, with the aid of a stereoscopic microscope, for each of the granulometric ranges resulting from the sieving, as shown in Figure 3. According to their respective degree of release, the particles were classified in the following ranges: (0-25%], (25%-50%], (50-75%], (75-100%).



Figure 3. Release analysis by conventional method

Particles defined in the intervals (0-25%] and (75-100%) were considered free, while the remaining particles were defined mixed particles. Thus, Eq. 1 could be applied from the formulation proposed by Gaudin (1939), providing the degree of freedom of the samples:

$$Df = \frac{\sum P_f}{\sum P_f + \sum P_m} \tag{1}$$

Being:

- Df = Degree of freedom.

- P_f = Number of free particles.
- $P_m P_m$ = Number of mixed particles.

Determination of the Degree of Release by Computational Method

The determination of the degree of particle release by the computational method was performed by means of photographs captured by a high resolution camera and analysis through self-authoring software. The developed software's function is to determine the particle release index through a color differentiation algorithm.

Figure 4 exemplifies the functioning of the computational release degree analysis program, which consists of capturing the images of particles (A), followed by binarization of them for grayscale (B). Thus, through the differentiation of shades (C), the program is able to delimit the boundaries of the particles and consequently the area of the particles by the Watershed method (D).

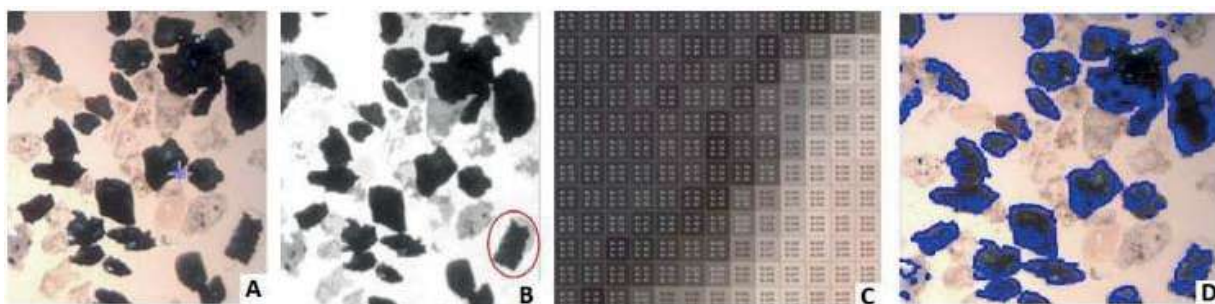


Figure 4. Principle of the software operation with a sinter feed sample.

Considering as mineral-ore darker regions and gangue the transparent or lighter areas of the grains, the software performs by identifying and counting pixels the measurement of the release of particles. The analysis performed by the program can be summarized, therefore in 5 basic steps, as described in the diagram in Figure 5.

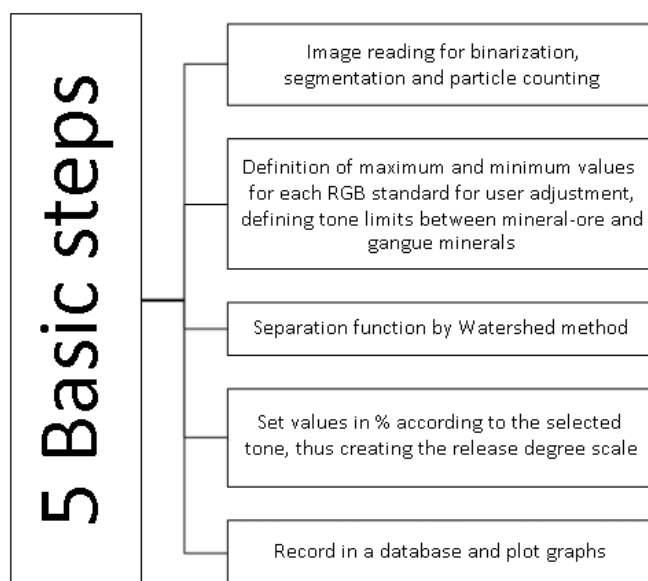


Figure 5. Basic steps to check image quality.

RESULTS AND DISCUSSION

Analysis by Conventional Method

The analysis of the degree of release of iron ore samples was initially done by the conventional method (Gaudin), with the aid of optical microscopy. The two samples (Am1 and Am2) were visually analyzed by the operator, who performed the count separately for each size fraction and, with subsequent application of Eq.1, obtained the results presented in Figure 6.

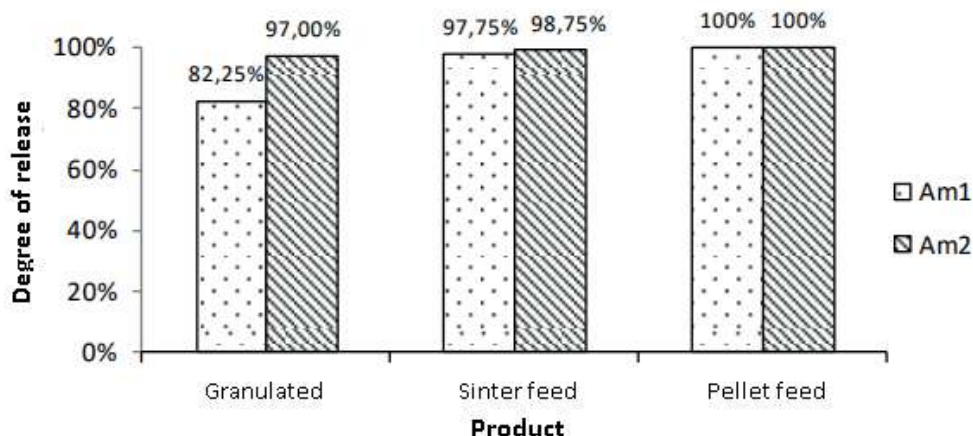


Figure 6. Degree of release of Am1 and Am2 samples by conventional method.

It is possible to observe a high release of particles from both samples, with values above 80% even in granulometry in the granulated product range. It is observed that the particles that are considered free cover a fairly extensive range of 0-25% and 75-100% and thus, a large amount of mineral grains is considered released.

Determination of the Degree of Release by Computational Method

The degree of release of am1 and am2 samples determined by the computational method could be analyzed and compared graphically. Thus, Figure 7 presents the results related to the analyses performed by software.

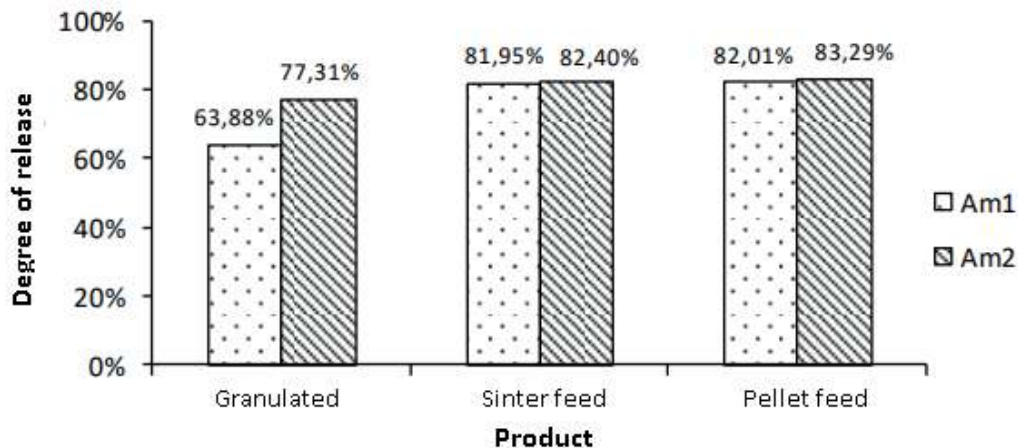


Figure 7. Degree of release of Am1 and Am2 samples by computational method.

It is possible to note that the results obtained by the computational method present a trend similar to those observed by the conventional method (Gaudin). The software demonstrated a higher degree of release referring to the particles of the Am2 sample, as well as the conventional method.

It is noticed that in granulometry in the pellet feed product range, the behavior of the samples was similar, presenting values close to particle release. This characteristic is mainly due to the fact that, as mentioned by Rodrigues and Brandão (2017), the greater the comminution of a mineral, the greater its release.

Comparison of Results by Means of Software and Conventional Method (Gaudin)

After obtaining the results of the degree of release of the samples by conventional (Gaudin) and computational methods, it was possible to compare the performance of both, determining their main peculiarities. The release of particles, when determined by the conventional method (Gaudin), presents values up to 36% higher than those obtained through the software. In addition, it is perceived that for finer granulometry, the results obtained by both methods present closer values.

This is mainly due to the fact that smaller particles have a higher degree of release and, therefore, greater ease in optical microscopy analysis. The analysis of the degree of release through the software presents values lower than those observed by the conventional method (Gaudin). Thus, it is perceived that the software provides more conservative results for the degree of particle release, thus avoiding overestimations of the data.

With this, it can be said that the software reduces the possibilities of operational problems due to errors in the definition of the degree of release of particles. Moreover, due to the fact that the computer program uses fully computerized analyses, its reliability is higher, since there is a pattern of calculation of degree of release, abandoning dependence on personal interpretations and reducing uncertainties.

CONCLUSIONS

Conventional methods of analysis of release degrees are closely related to operator expertise, which reduces the reliability and accuracy of results. With this the creation and deployment of software for this process is of great value, because it allows more accurate and faster results.

The software used has great potential for large-scale application, whether in industry or for the academic sector. Its results presented in comparison to the Gaudin method are satisfactory and promising, increasing the efficiency of mineral analysis processes.

The computational method avoids overestimations of the degree of release of the mineral, since it presents lower values and more accurately than conventional methods, because its standard of measurements is steady and uses high-tech for analysis. Thus, computational measurements of mineral release generate more stable results, so that subsequent operations of ore treatment and operational parameters defined from the degree of release of particles will not present major distortions.

ACKNOWLEDGEMENT

The authors thank CAPES, CNPq, CEFET-MG and UFOP for the support and trust deposited during the performance of this work.

REFERENCES

- Delbem I. (2010). Processamento e análise digital de imagens aplicados aos estudos de liberação mineral, Msc. Thesis, Federal University of Minas Gerais, Belo Horizonte, M.G., 99 pp .
- Delbem I.D., Galéry R. Brandão, P.R.G., Peres, A.E.C. (2015). Semi-automated iron ore characterisation based on optical microscope analysis: Quartz/resin classification. *Minerals Engineering* , 8, 90-96.
- Donskoi E., Manuel J., Austin P., Poliakov A., Peterson M., Hapugoda S. (2014). Comparative study of iron ore characterization using a scanning electron microscope and optical image analysis. *Applied Earth Science*, 122, 217-229.
- Ferreira, R.F. (2013). Estudo de liberação das fases minerais em minérios de ferro. Msc. Thesis, School of mines of Federal University of Ouro Preto, Ouro Preto, M.G., 211 pp.
- Gaudin, A.M. (1939). Principles of mineral dressing. (1st. ed., Vol. 1). London, McGraw-Hill.
- Rodrigues R.S. (2016). Grau de Liberação de Diferentes Tipos de Minério de Ferro das Minas de Alegria (Mariana -MG) e sua influência nas etapas de cominuição e concentração. Msc. Thesis, Engineering School of Federal University of Minas Gerais, Belo Horizonte, M.G. ,275 pp.
- Rodrigues, R.S. and Brandão, P.R.G. (2017). Influência da Liberação Mineral nas Etapas de Moagem e Flotação do Minério de Ferro. *Tecnologia em Metalurgia, Materiais e Mineração*, 14, 279–287.

"DIGITAL REVOLUTION 4.0" IN THE RAW MATERIALS AND MINING INDUSTRY
MADENCİLİK VE HAMMADDELER SEKTÖRÜNDE DİJİTAL DEVRİM 4.0

H.A. Kahraman ^{1,*}, C. Klötzer ¹, M. Katapotis ¹

¹ DMT GmbH & Co.

(* Corresponding Author: hakan.arden@dm-group.com)

ABSTRACT

The concept of 'Industrial Revolution 4.0', which was first introduced in Germany and has rapidly spread to other developed countries, describes the ongoing automation of traditional production and industrial applications using modern digital technology. In this new era of Industrial Revolution 4.0, the mining industry too has inevitably started to focus on technology and digitalisation. As there are many challenges ahead in this transformation process, DMT's approach to this new era is to offer innovative and holistic Industry 4.0 solutions developed through a fastidious strategy which is expected in assisting to shape the autonomous mining vision of the future. DMT's approach to this digital transformation is to go through initially a "Digital Due Diligence Process" to assess the existing business, identify digital potentials and operating opportunities and define a digitalisation roadmap. DMT's recommendation is that this process is accompanied by independent engineering and technology advice coming from an experienced partner in process design who will establish a "Digital Transformation Office" how these identified points can deliver the expected quality, efficiency, and improvements in health and safety in line with the environmental sustainability. This approach includes three fundamental components:

"Operations" which cover the services used to provide companies with comprehensive guidance and support, systematic approaches to continually expand the offering of digital products and services covering the entire lifecycle of raw material extraction such as Reconnaissance, Exploration, Planning and Project Evaluation, Construction, Optimisation of Mining Operations, Environmental Aspects, Mine Closure and Site Remediation;

"People" which covers a corresponding digital transformation program for all employees of mining companies;

"Processes" which covers process optimisation for its Clients' operations.

This paper describes how a holistic approach can be implemented in this new digital era from the Consultant point of view.

Keywords: Digital revolution 4.0, mining, geology, artificial intelligence, internet of things, sensors

ÖZET

İlk olarak Almanya'da ortaya atılan ve diğer gelişmiş ülkelere de hızla yayılan "Endüstriyel Devrim 4.0" kavramı, geleneksel üretim ve endüstriyel uygulamaların modern dijital teknoloji kullanılarak süregelen otomasyonunu anlatır. Bu yeni Endüstri Devrimi 4.0 çağında, madencilik sektörü de kaçınılmaz olarak teknoloji ve dijitalleşmeye odaklanmaya başlamıştır. Bu dönüşüm sürecinde önümüze çıkacak bir yığın zorluk olduğundan, DMT'nin bu yeni döneme yaklaşımı, geleceğin otonom madencilik vizyonunu şekillendirmeye yardımcı olması amacıyla titiz bir strateji ile geliştirdiği yenilikçi ve bütünsel Endüstri 4.0 çözümleri sunmaktır. DMT'nin dijital dönüşüme

yaklaşımı, var olan işin ayrıntılı olarak değerlendirilmesi, dijital potansiyelleri ve işletme fırsatlarının belirlenmesi ve bir dijitalleşme yol haritası belirlemek için başlangıçta bir "Dijital Durum Durum Saptama Süreci"nden geçilmesidir. DMT'nin tavsiyesi, bu sürece, süreç tasarımı deneyimli bir bağımsız mühendislik ve teknoloji ortağının/danışmanın eşlik etmesi; ve bir "Dijital Dönüşüm Ofisi"nin kurularak kalite, randıman, iş sağlığı ve güvenliği ile ilgili beklentilerin çevresel sürdürülebilirlikle uyumlu tesliminin gerçekleşmesidir. Bu yaklaşım şunları içerir:

”Operasyonlar: Madencilik operasyonlarının optimizasyonu gibi hammadde çıkarmanın tüm yaşam döngüsünü kapsayan dijital ürün ve hizmetlerin sunumunu sürekli olarak genişletmek için sistematik yaklaşımlar, şirketlere kapsamlı rehberlik ve destek sağlamak için kullanılan hizmetler, keşif, arama, planlama ve proje değerlendirme, inşaat, çevresel unsurlar, maden kapatma ve saha iyileştirme;

“İnsanlar”: Madencilik şirketlerinin tüm çalışanları için ilgili bir dijital dönüşüm programı;

“İşlemler”: Müşteriler için süreç optimizasyonu.

Bu makale bu yeni dijital çağda bütünsel bir yaklaşımın nasıl uygulanabileceğini, Danışmanın bakışıyla yansıtmaktadır.

Anahtar Sözcükler: Dijital devrim 4.0, madencilik, jeoloji, yapay zeka, IOT, sensörler

INDUSTRIAL REVOLUTIONS

As we all are witnessing the latest period of societal transformation in human history through a revolution in industrial development currently, the previous industrial revolutions had also been the product of a similar magnitude of changes that resulted in a major structural transformation in the fabric of the societies.

The “First Industrial Revolution” is generally regarded as the transition period between 1760 and 1820 that involved a number of steam/ water-powered machine inventions that enabled and transformed limited quantity of hand production into massive production in textile manufacturing, iron industry, agriculture, and mining. This period was an inevitable culmination of the advancement made in science and technology in the late 18th Century and the beginning of the 19th Century.

The “Second Industrial Revolution”, also commonly known as the “Technological Revolution”, is the period between 1871 and 1914 that resulted in the installation of the extensive network of railways, telegraph, and electricity. A faster transfer of people and produced goods between the distant points was achieved through journeys made in railways whilst the telegrams allowed a rapid exchange of ideas and communication beyond the national boundaries at the time. Increased use of electrification also allowed factories to develop the modern production lines that resulted in a period of great economic growth at the expense of a surge in unemployment as many factory workers were replaced by machines.

The “Third Industrial Revolution”, also known as the “Digital Revolution”, started in the 1960s following the devastation of World War 2 and reached its culmination in the latter part of the 20th century. This was the period, which was catalysed by the development of semiconductors, mainframe computing (the 1960s), personal computing (1970s and 1980s), and the use of the internet (1990s). This was also the era where complex computation has started to emerge by the use of supercomputers that has enabled less human intervention in large computational process.

The concept of the “Fourth Industrial Revolution” (or “Industrial Revolution 4.0”), which was first introduced in Germany (Schwab, 2013) and has spread rapidly to other developed countries (Schwab, 2016), describes the ongoing automation of traditional production and industrial

applications using modern smart technology which was introduced in the later part of the Third Industrial Revolution. In this new system, a new production platform has been prepared by integrating large-scale machine-to-machine communication, internet of objects, rapidly increasing automation, advanced communication network, and self-monitoring and smart machines that can analyse and diagnose problems without the need for human intervention.

The common denominators observed in the previous industrial revolutions are that the fabric of the society and scale of the economics have significantly changed resulting in a new order of business and corresponding legal and administrative adjustments and changes.

The Fourth Industrial Revolution has already identified a number of structural transformation and paradigm shifts in the societies that are expected in the coming years (Schwab, 2016). These particularly include amongst many others:

The Internet of and for Things;
 Automated vehicles;
 Artificial Intelligence (AI) and Decision-Making;
 Robotics and Services;
 Cryptocurrencies and the Blockchain;
 The Sharing Economy (the use of a physical good/asset, or share service or provide a service by sharing);
 3D Printing in Manufacturing, Human health and Consumer Products; and
 Designer beings (humans/living things) and
 Neurotechnologies (first human with fully artificial memory implanted in the brain).

FOURTH INDUSTRIAL REVOLUTION AND MINING

As more of the “things” start to communicate and interact with each other in a more smart and artificial way in this Fourth Industrial Revolution particularly in the developed countries, it is inevitable that the mining segment will also benefit from this latest transformation in these economies.

Especially in countries with mining industries where wages are high, resource savings and economic extraction of raw materials can only be achieved with more automation and digitalisation.

As Schwab (2016) prophetically concluded, the winners will be those who are able to participate fully in innovation-driven ecosystems by providing new ideas, business models, products and services, rather than those who can offer only low-skilled labour or ordinary capital.

Considering the competitive nature of the business, especially the large international mining companies have already started to adjust themselves by digitising their mining operations across the value chain in line with the future generation of mines. This obviously requires a remodelling of the business for growth and sustainability while using digital technology and innovation as a catalytic enabler within an existing legacy environment that behave like individual isolated units along the route from mine to processing to transport.

The examples of this new approach have already started to populate the mines. The introduction of remotely controllable equipment and autonomous machines such as trains, trucks, drilling machines, as well as sensor driven equipment monitoring have already proven that they can significantly reduce the use of personnel in mining operations and thus the risks to human life.

In addition, the increasingly complex geological conditions encountered in the mines confront companies with the obligation to preserve and, where possible, increase the quality and quantity of raw materials by using efficient methods and equipment as well as prioritising the areas where these challenges can be met by using digital technologies.

Despite many gadgets and devices being a customary part of our daily life for many years, their widespread use in mining has just started. This includes, among other things that are taken for granted in daily life, the establishment of the “internet network” with relevant safety standards in underground mining operations. The implementation of the sensor technology currently standard in automobiles has just been started being implemented after adapting the specific requirements of mining and the associated nuisance effects of dust, mechanical stress, extreme temperatures, water or explosive gases (Clausen and others, 2020). The sensors have particularly become the driving force in efficiency and safety improvements in many mines where the digitalisation is playing a crucial role.

As Virtual Reality (VR) / Augmented Reality (AR) are commonly used in gaming industries, they also make their way into the mining industry to train and upskill the workforce used in high-risk tasks and problem solving the key operational challenges. The competency development can be reinforced better when experiential learning, gamification (adding game mechanics into nongame environments) and just-in-time reinforcement using digitally enhanced environments are used (Pagnini, 2019).

Drones are now commonly used in every aspect of the economy from delivery of goods to remote survey to entertainment. Mine industry has also started to use the drone technology both for inventory management, slope failure management of waste dumps, site surveying, traffic management, and maintenance.

It is also possible that the advancement in 3D printing may enable spare parts to be produced without sacrificing the downtime and production levels in the remote corners of the planet in near future (Pagnini, 2019).

As the satellite technology now allows shipment tracking to be monitored anywhere in the world, opportunity to create better performance in route optimisation and fleet dispatching as well as production level adjustments at the pit level that can result in an optimised integration approach from pit to port (Pagnini, 2019).

Especially in small to medium sized projects/operations in mining, it is difficult to decide where to lay the digital emphasis on and how to prioritise digitalisation and resolve many challenges which can include high capital investments in automated operations and equipment, personnel commitments, IT security, data security and protection, data processing and analysis, information quality and granularity, communication standards, legal hurdles and frameworks, concerns on quality, health, safety and environment (QHSE) and many more. The real challenge is where and how to connect the “silos” and transfer them into a digital hub.

Barnewold and Lottermoser (2021) demonstrated that 107 different digital technologies are currently pursued in mining whilst an analysis from 158 active surface and underground mines showed that the actual implementation of digital technologies is slow in general, and the uptake increases with the run-of-mine production. Large-scale mining operations appear to select and apply digital technologies suitable to their needs, whereas operations with lower production rates do not implement the currently available digital technologies to the same extent. These minor producers

may require other digital transformation solutions tailored to their capabilities and needs and applicable to their scale of operations (Barnewold and Lottermoser, 2021).

Unlike the slow-take of mining companies, the organisations which provide consultancy services to the mining operations have embraced this new digital era with open arms and started providing a number of products and services to their customers.

As an example, for these digitally equipped consultancy companies, DMT's activities, which have a history of more than two centuries in mining consultancy, also focused on technology and digitalisation in this new period of Industrial Revolution 4.0.

As part of prioritising the overall business strategy in this new era, DMT has established a digital technical group which specialised in different aspects of mining by using a range of state-of-art digital techniques to solve a number of issues.

This group can advise its clients on the upcoming challenges of digital transformation based on a broad market study and in-house technical expertise. This process generally starts with a "Digital Due Diligence" of the operations and usually continues with the establishment of a "Digital Transformation Office" (Figure 1).

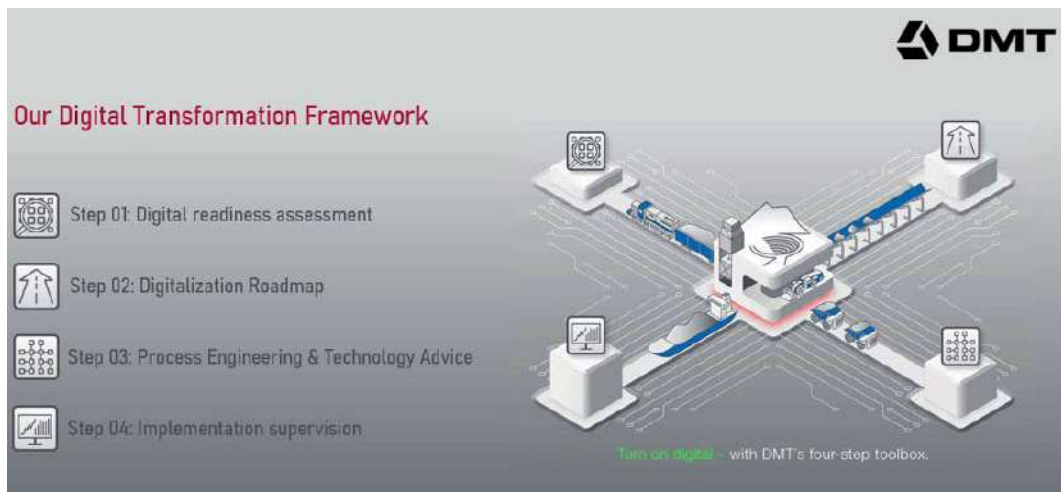


Figure 1. DMT four step toolbox approach in digital transformation for Mining 4.0

The proposed "Digital Due Diligence Process" involves assessing the existing business, identifying digital potentials and operating opportunities and defining a digitalisation roadmap and priorities (Figure 1). DMT's recommendation is that this process is accompanied by independent engineering and technology advice coming from an experienced partner in process design who will establish a "Digital Transformation Office" to deliver these identified priorities in line with the expected quality, efficiency, and improvements in health and safety and environmental sustainability (Figure 1).

As the leader of TÜV NORD GROUP's engineering division, DMT currently offers its customers innovative and holistic Industry 4.0 solutions that cover the following three main pillars (Figure 2) based on the principles of the toolbox approach explained above. These are namely Operations; People and Processes.



Figure 2. Main pillars of DMT's Mining 4.0 portfolio

OPERATIONS

In this context, the word "operations" represents the operational business that exists and DMT presents here both technologies developed in-house, and services used to provide companies with comprehensive guidance and support. Many of the in-house digital technologies in the form of advanced tools and gadgets developed by DMT are already making a significant impact for the mining operations around the world.

In addition to the development of such company-specific operational tailor-made solutions, the impact of digital transformation on the clients' employees in terms of Mining 4.0 should not be ignored. In particular, far-reaching technological changes require wide acceptance among the workforces. In addition, long-term employees, especially in the company, need to be adapted to the challenges of digitalisation. To this end, the structure and culture within the company should be further developed where DMT's corresponding transformation program for the digital world through the Digital Academy of TÜV NORD GROUP may assist all employees of its customers in great extent.

There is also a huge saving potential within mining companies, thanks to an integrated view of the technical and administrative areas. With the implementation of shared and interconnected digital systems, quality, productivity, and throughput times can be optimised from raw material extraction to product distribution. Streamlining administrative processes avoiding isolated solutions in individual areas frees up resources, which can be used to further improve operational processes. DMT has many years of experience in process optimisation, together with an extensive network of collaborators.

Core Operations

DMT is definitely at the forefront of the trend to increase productivity through digitalisation in the raw materials industry. All processes along the entire value chain are affected by this trend, with a wide range of technical solutions already available in the service portfolio. Beyond that, systematic approaches are underway to continually expand the offering of digital products and services covering the entire lifecycle of raw material extraction (Figure 3).



Figure 3. Life cycle of the mining industry

Reconnaissance Studies

Reconnaissance is often the first phase of mining projects, and the high degree of uncertainty at this stage is the main reason for intense efforts to minimise investment risks. The use of state-of-the-art digital technologies enables the acquisition and evaluation of high-quality data through optimum use of people and equipment. To support this work step efficiently, DMT has the power to effectively deploy adequately equipped drones, with the support of technology collaborators. Regarding integrating future developments in this sector, DMT is participating in a research project on the use of sensor-equipped drones within the framework of the European Union-funded "European Institute of Innovation and Technology Raw Materials (EIT Raw Materials)" program. DMT is developing a key technology module in the form of a software solution that, among other things, integrates the acquired data with standard software such as ArcGIS and AutoCAD, thereby greatly accelerating the creation of geological maps.

Exploration Studies

Technical progress under Industrial Revolution 4.0 also has a significant impact on exploration. That is, new advances in automation of data collection, evaluation, analysis, and model building can have a positive impact on the amount of time spent and money invested. An example of this is DMT CoreScan®3 (Figure 4), which enables the digitisation and evaluation of entire drill cores (360°) and their export to a corresponding drill core database. In addition to the analysis of the mine inventory and grain size distribution, a detailed structural evaluation can also be made in this way.

Other DMT solutions in the field of exploration, apart from active involvement in borehole drilling, borehole surveying and logging, include the application of seismic methods such as 2D and 3D seismic reflection, seismic refraction, seismic tomography, as well as their interpretation and modelling, in which large amounts of data are directed and evaluated. The results from these studies can best be used to create a "digital twin" of the mineral deposit, which is constantly updated in real time. At this point, by increasing the degree of automation, the dependence on personal experience in modelling can be reduced, thereby increasing the degree of objectivity. For this purpose, DMT uses modern proprietary software where workflow can be stored and recorded, thus ensuring better reproducibility of results.



Figure 4. DMT CoreScan®3

Planning and Project Evaluation

Within the scope of operational work, complementary short and medium-term plans are made sequentially and at regular intervals. In particular, the short-term plan should be updated daily to get the most out of machinery and other resources. Here, automation and digitisation offer a very high potential for cost savings. For example, the geological models can be updated immediately when excavating seams/ores or driving the developments in underground mines or creating blastholes in open pit mines using appropriate sensor technology. On the other hand, in the case of using transport systems, it can record in real time the motion paths of mining equipment as well as idle and downtime, resulting in significant reductions in cycle times. DMT also supports employers and investor credit institutions in feasibility studies and determination of resources and reserves in accordance with the international standards. In this process, the basis for further planning is laid by creating three- or four-dimensional models (Figure 5.) and creating initial databases. For visualisation purposes, the most advanced Virtual Reality (VR) facilities are used. With VR glasses, planning can literally be made "touchable", even for non-experts. With the use of proprietary software and a broad market study, DMT is able to offer its customers holistic solutions that integrate data from various sources. These solutions include deposit and machine data, as well as data from geotechnical monitoring systems.

In addition to providing advice to mining companies, DMT is also involved in the development of CERA, a standardised analytical and integrated certification system that guarantees the ecological, social and economic sustainability of the extraction, processing, trade and production of all mineral raw materials, including fossil fuels. This system ensures reliable traceability of certified raw materials using various technologies and proof-of-origin methods throughout the value chain. Digital technologies such as the Distributed Ledger or Blockchain play an important role, for example, as transaction databases to track trade and transport routes in a verifiable way.

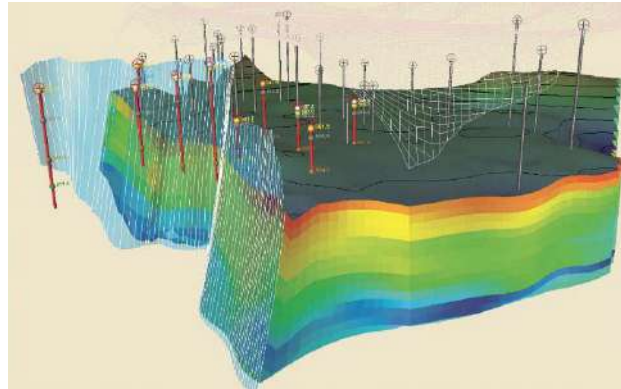


Figure 5. Utilisation of special software for the 3D visualisation of a mine

Construction

DMT's approach on this is to offer "tailor-made" engineering solutions from a single source. For example, the digitalisation used has reduced the construction times of mining-related infrastructure projects and contributed to a more efficient use of investment capital. DMT is represented at this event space by measuring instruments such as the IMAGER 5006EX (Figure 6c), the world's only high-precision, explosion-proof 3D laser scanner. The fully automatic GYROMAT can also record measurement data in real time and transmit it wirelessly (Figure 6a). With a diameter of less than 2.5 cm, the DMT SlimBoreholeScanner allows to record the number and condition of cracks in equally small boreholes and then visualise them along the entire length (Figure 6b). In contrast, geo-radar and ground radar provide high resolution searching of the ground to inspect road surfaces, power transmission lines and boreholes. Data from all devices can be combined, processed, and visualised by purpose for on-premises data platforms.



Figure 6. DMT's cutting-edge products a) GYROMAT b) SlimBoreholeScanner c) IMAGER 5006EX

Optimisation of Mining Operations

In this context, DMT provides the MineSafe® platform which was developed as an in-house machine diagnostic system specifically designed for condition monitoring of machines and plants (pumps, crushers, large belt conveyors, vehicles, etc.) in the mining and processing industry. MineSafe can also be implemented as a customer-specific, controller-integrated system providing all the essential functions and components of a modern online condition monitoring system and is now available as such on Caterpillar's automation platform. The modular design allows for a wide variety of applications and a high degree of expandability thanks to the relatively simple integration of existing control systems. DMT is currently developing "MAMMA - Maintained Mine and Machine", which aims to significantly reduce the maintenance costs of machinery and systems in mining

operations by gathering, processing and clearly visualising all relevant data. This system allows for longer maintenance intervals and increased equipment availability. In the field of ventilation, systematic studies are carried out to implement adequate and adaptable practices by using "Ventilation on Demand-VOD" systems.

Whether it is the question of automating individual work steps or adapting entire process chains, DMT has positioned itself to provide tailor-made solutions and choices and support for the Clients during implementation phase.

Environmental Aspects

In addition to high productivity, Mining 4.0's objectives include security, increased efficiency, sustainability and transparency as the public's attention on the environment has significantly grown in the recent years. Negative environmental impacts due to the collapse or failure of tailings dams or similar events occurring on the mine sites impacting the environment have become immediate headlines recently. To avoid such events, continuous monitoring measures are required in addition to drilling planning. For this purpose, the DMT SAFEGUARD network platform has been developed by placing sensors in complex geo-monitoring systems with alarm functions to record ground motions, object deformations, vibrations, or geotechnical parameters. It does not matter whether the data is recorded and archived just a few times a day or more than 1000 times per second, and whether it is also temperature, water level, vibration, or video data. All information is automatically visualised according to the requirements and is accessible at any time via a decentralised and location-independent network portals. Based on SAFEGUARD, DMT is currently developing an all-in-one solution for waste monitoring under the "EIT RawMaterials" project "STINGS" and is successfully using it in a model plant in South America. This system detects ground motions using remote sensing techniques, as well as planning and installing a sensor network for geotechnical monitoring of waste. All measurement data is stored in a central database that enables complex models to be built to assess the safety of facilities and detect and warn of hazards at an early stage.

Mine Closure and Site Remediation

The life cycle of a mine is often combined with the improvement of the mine site following the end of the mining operation. Such processes are also known as "remitting funding". In many well-developed mining countries, mine operators have to allocate the monetary resources necessary during the extraction phase to ensure the regular upgrading of the mines in relation to the ultimate mine closure. The most obvious example of this is the management of water pumps in closed mines in the Ruhr and Saar region of Germany. Optimisation, automation, and digitalisation are tools used to ensure that the amount of monetary funds allocated to costs is not exceeded. As part of its water management activities, DMT compiles three-dimensional images of ground and surface waters, allowing mine operators to perform more complex analyses and calculations with "digital twins" of the groundwater. In this way, the effects of technical interventions can be predicted in different scenarios and correct measures can be taken. The SAFEGUARD system described above can also be used for continuous monitoring of indoor mining operations. By doing this, mining-induced ground motions such as slope failures can be detected and even predicted. The system is method independent and works with any data from geotechnical, surveying, geophysics, noise and vibration fields.

In addition, DMT with its global partners have developed a new system called CLOSUREMATIC which plans the closure and rehabilitation of a mine while it is still under construction. This digital product aims to eliminate the typical problems in mine closure such as loss of continuity upon changes in management and ownership, difficulties in cost estimation and

tracking, loss of closure-related data, poor coordination in closure activity and operations that compromise the goals of closure, inadequate consultation etc. The use of CLOSUREMATIC also reduces the closure related environmental and social risks. The guidance section (one of CLOSUREMATICs unique features) helps the operator to focus the actions to sectors that they are most effective and needed in a continuous manner. This has been designed in a way that the closure related actions and useful links to a knowledge base can be managed from the beginning of the mining activity even prior to mining at planning phase. Due to the precise descriptive nature of the closure process, the CLOSUREMATIC will probably be the most accurate tool in the market to estimate the costs of closure. This information can be used in determination of the financial closure related liabilities in the permitting process and also lowering the liabilities through development of a more developed and detailed closure plan.

PEOPLE

More than half of industrial companies in Germany have embedded “digital transformation” in their business strategy to simplify operations, increase sales and improve customer satisfaction. On the other hand, 30 percent of companies identify the insufficient digital qualifications of their employees as a major problem and thus a significant barrier to implementation. In addition, more than half of the companies criticise the need for a more open corporate culture in which “failure” is discussed in their companies.

These are the points where DMT, in collaboration with TÜV NORD GROUP's Digital Academy, stepped in to make employees the key to digitalisation. The core element of the employee motivation and motivation program within the company is a certified training course to become a "Digital Specialist". After all, the latest and greatest machines are only as good as the people who run them. The more digital the products, processes and machines become, the more important the education and training of employees becomes. For this reason, employees as well as managers should be prepared for a comprehensive digital transformation. The various training programs on this subject can be individually tailored to the needs and challenges of the respective companies in terms of content and duration. Due to this meticulous work, DMT's parent company TÜV NORD was twice awarded the German Excellence Award 2020 in the "Education and Further Education" category, recognising the accuracy of the VR training of candidate experts in the fields of steam and pressure, on the one hand, and on the other hand, in the "Conversion" category. At this point, TÜV NORD and DMT can provide mining companies with tailored support solutions through courses such as using VR in the training and education of workers in both general and customer-specific mining equipment.

PROCESSES

Detailed analyses form the basis for further process optimisation. With its partners, DMT also provides consultancy services that serve to improve the performance of mining operations in terms of "Operational Excellence". The planning of equipment and materials, the control of cash flows and the management of personnel are challenging issues in terms of administrative responsibilities of mining companies. In terms of planning processes, using modern "ERP-Enterprise Resource Planning" software, accounting, shift planning, time recording, and invoicing automation are just a few examples of potential savings that can be achieved. For a company's production divisions, such systems offer advantages in material supply and storage. Through further analysis, it is also possible to timely identify materials that are required more frequently or that are particularly critical to a smooth working process. By doing this, countermeasures can be taken at the right time. As a result, there are fewer production delays, unnecessary material storage is avoided, and capacities can be lightened.

It has been pointed out before that the digital gadgets and inputs using the digital technology that have been taken for granted in our daily life for years have not yet been created or applied in mining on a large scale. In addition to the inability to provide internet signals throughout the area with relevant security standards in underground mining operations, it can be stated that even in open pit mining, communication over mobile data cannot be provided directly due to shadowing effects and dead spots. Co-synergies can be created by taking a holistic view of the existing and future necessary infrastructures. Accordingly, DMT, in collaboration with its global partners, supports and advises companies through its years of mining expertise and broad knowledge of far-reaching processes, providing one-stop solutions to help them meet the challenges of digital transformation.

CONCLUSION

In recent years, the continued digitisation of mining has brought about continuous changes in the way the raw materials industry discovers its resources, runs mining operations, processes products and ultimately delivers them to their customers. This article demonstrates DMT's Mining 4.0 concept, which is based on three pillars: "operations", "people" and "processes" and covers digital transformation holistically throughout the entire lifecycle of the raw materials industry.

Based on its long-proven ability to capture new developments and integrate them into its core competencies, DMT is passionate about the digitisation of existing products and services, but also very heavily on the development of new digital business models. DMT's aim through its stakeholders and partners inside and outside of TÜV NORD GROUP is to be at the forefront of Industrial Revolution 4.0 in the spirit of the 'Engineering-Performance' motto, to provide digitised, smart and connected solutions for the raw material sector, and thus assisting to shape the smart (autonomous) mining vision of the future. For this purpose, DMT has developed a modular four-step strategy, starting with the assessment of current processes within a company or operation (through a digital readiness assessment) and culminating in the implementation supervision of all services and solutions a customer needs for his successful digital transformation.

The mining industry like any other segments of the global economy faces new challenges in the coming years due to the introduction of many new ways and methodologies to deal with the traditional issues. The authors of this paper believe that the mining industry is in a unique position to manage the things in a completely new way as the world is rapidly moving into an era where the "artificial intelligence" and "internet of the things" will be a dominant force in decision making process. The winners will be determined by those who are able to participate fully in this innovation-driven period. One thing is definitely sure that the old and new operations will face similar challenges in implementing the ideas and innovations, but the ones who move with the time and trends will be ahead of the game. Therefore, choosing a right partner in this process is also a crucial decision in this new era.

REFERENCES

- Barnewold I. and Lottermoser B.G. (2021). Identification of digital technologies and digitalisation trends in the mining industry. *International Journal of Mining Science and Technology* Volume 30, Issue 6, November 2020, Pages 747-757.
- Clausen, E.; Nienhaus, K.; Bartnitzki, T; Baltés, R. (2020): Bergbau 4.0. In: Frenz, W. (eds.): *Handbuch Industrie 4.0: Recht, Technik, Gesellschaft*. Berlin: Springer, pp. 919-937.
- Pagnini M. (2019). Data Mining for Miners from Pit to Port: Digitalization Trends in the Mining Sector. <https://www.consultdss.com/digitalization-in-mining/>

Schwab, Klaus (2013). "Industrie 4.0: Mit dem Internet der Dinge auf dem Weg zur 4. Industrial Revolution - vdi-nachrichten.com". 4 March 2013. Archived from the original on 4 March 2013. <https://web.archive.org/web/20130304101009/http://www.vdi-nachrichten.com/artikel/Industrie-4-0-Mit-dem-Internet-der-Dinge-auf-dem-Weg-zur-4-industriellen-Revolution/52570/1>

Schwab, Klaus (2016). "The Fourth Industrial Revolution". World Economic Forum. ISBN-13: 978-1-944835-01-9. 172pp.

DÜŞÜK TENÖRLÜ LATERİTİK NİKEL CEVHERİNDEN YIĞIN LIÇI İLE NİKEL KAZANIMININ ARAŞTIRILMASI

INVESTIGATION OF NICKEL RECOVERY FROM LOW-GRADE LATERITIC NICKEL ORE BY USING THE HEAP LEACHING

A.F. Değirmenci^{1,*}, Ö.Caniren¹, O.Yılmaz¹, C.Karagüzel¹

¹Dumlupınar Üniversitesi, Maden Mühendisliği Bölümü
(* Sorumlu yazar: ffarukddegirmenci@gmail.com)

ÖZET

Önemli bir alaşım elementi olan nikel, gelişen teknoloji ile birlikte kullanımı her geçen gün artış gösteren bir elementtir. Batarya, otomotiv, savunma sanayi başta olmak üzere birçok endüstri alanında kullanılan nikel üretimi, lateritik ve sülfidik maden yataklarından ve ikincil kaynaklardan fiziksel, kimyasal ve fizikokimyasal prosesler ile yapılmaktadır. Nikel zenginleştirmede kullanılan en yaygın proses ise basınç altında yapılan liç işlemleridir (HPAL). Bu çalışma ile Gördes Nikel-Kobalt İşletmesi'nin yüksek basınç liçi öncesi sınıflandırma ile stokladığı düşük tenörlü (%0,3 Ni içerikli) ara ürün olarak nitelendirilen cevherin yığın liçi ile kazanılması amacıyla laboratuvar ortamında kolon liçi testleri gerçekleştirilmiştir. Yığın liçini simüle edecek iki farklı kolon (kare ve dairesel) ile yapılan liç testlerinde tane boyutu (-150mm, -20mm, -5mm), çözücü konsantrasyonu (-150-250gr/lit serbest asit) , liç süresi gibi çalışma parametrelerinin metal kazanma verimi üzerine etkileri araştırılmıştır. Yapılan çalışmalar sonunda düşük nikel içerikli çalışma konusu ara üründen -5mm tane boyutunda, 17 lt/ms/h besleme hızı ile verilen liç çözeltisi, 250 gr/lit serbest asitli yüksüz çözelti ile %78 verimle nikel kazanılabileceği belirlenmiştir.

Anahtar kelimeler: Yığın liçi, lateritik nikel cevheri, sülfürik asit liçi.

ABSTRACT

Nickel is an essential alloying element, which utilization is increasing day by day with the developing technology. It is used in many industrial areas, especially in the battery, automotive and defense industries. Nickel production is made from lateritic and sulphidic mineral deposits and secondary sources by physical, chemical and physicochemical processes. The most common process used in nickel beneficiation is leaching under pressure (HPAL). In this study, column leaching tests in a laboratory scale were carried out to recover the low grade (0.3% Ni content) ore by heap leaching. Two different columns (square and circular) were used to represent heap leaching. In the leaching tests, the effects of working parameters such as particle size (-150mm, -20mm, -5mm), solvent concentration (-150-250gr/lit free acid) and leaching time were investigated on metal recovery efficiency. At the end of the studies, it was observed that the nickel could be recovered from low grade ore with 78% efficiency under the optimum conditions (HL6; -5mm, 17lt/ms/h, 250 gr/lit free acid).

Keywords: Heap leach, lateritic nickel ore, sulfuric acid leaching.

GİRİŞ

Nikel, sahip olduğu fiziksel ve kimyasal özellikler sayesinde başta çelik endüstrisi olmak üzere pek çok alanda kullanılan bir metaldir. Sahip olduğu özellikler ve teknolojik gelişmeler sebebiyle nikel olan ilgi son yıllarda büyük artış göstermiş olup, mevcut veriler ışığında, nikelin 21. yüzyılda daha da fazla aranan bir metal haline geleceği beklenmektedir (Baştürkçü, 2016). Nikel-Kobalt yatakları genel olarak sülfürler, oksitler, sülfotuzlar ve arsenitler olarak sınıflandırılmaktadır. Ancak nikel ve kobalt içeriklerine göre sülfür yatakları ve laterit yatakları olarak sınıflandırılmaktadır (Çoban, 2014). Dünyadaki en büyük nikel oluşumları lateritik yataklar içerisinde bulunmaktadır. Ancak lateritik yatakların düşük tenörlü olması sebebiyle, nikel üretiminde genellikle sülfürlü yataklar tercih edilmektedir (Oxley ve Barcza, 2013). Yıllar içerisinde sülfürlü yatakların azalmasına rağmen, nikel ve nikel bileşiklerine olan talebin sürekli artışı, lateritik nikel yataklarının önemini artırmaktadır. Bunun bir sonucu olarak da lateritik nikel yataklarının ekonomik olarak değerlendirilebilirlikleri konusunda son yıllarda çok sayıda çalışma gerçekleştirilmiştir. Bu çalışmalardan bazıları aşağıda verilmiştir.

Çoban, 2014 lateritik formdaki nikel cevherini kullandığı çalışmada, atmosferik liç ve asitle muamele-kavurma-liç aşamalarından oluşan iki ayrı hidrometalurjik proses kullanmıştır. Optimum koşullarda yapılan (150g/lt asit konsantrasyonu, 80°C liç sıcaklığı ve 120 dakika liç süresi, %10 pülp yoğunluğu ve tane boyutu 0,074 mm) atmosferik liç sonucunda, lateritik cevherden nikel %69,89 verim ile kazanırken, optimum koşullarda yapılan (cevher ağırlığının 1,5 katı asit miktarı, 300°C kavurma sıcaklığı ve 60 dakika kavurma süresi, kavurma sonrası 30 dakika liç süresi ve 0,125 g/lt pülp yoğunluğunda) asitle muamele-kavurma-liç prosesi uygulanması sonucunda ise, lateritik cevherden nikel %76,8 verim ile kazanmıştır. Nasuh, 2014 çalışmada lateritik nikel cevherinin yüksek basınç altında sülfirik asit ile kazanılabilirliğini incelemiştir. Yapılan deneysel çalışmalar sonucunda optimum çözünme koşullarını 0,3 asit/cevher oranı, 240°C liç sıcaklığı ve 60 dakikalık liç süresi olarak belirlemiş ve bu koşullarda gerçekleştirdiği yüksek basınç sülfirik asit liçi deneyi sonucunda cevherde bulunan nikelin %92,8'ini kazanmıştır. Atik, 2015 yürüttüğü çalışmada, asidofilik bakteriler (*At. ferrooxidans*, *At. thiooxidans*, *L. ferrooxidans*) ve *Aspergillus niger* fungusu kullanılarak biyoliç yöntemiyle Çaldağ (Manisa, Türkiye) lateritik nikel cevherinden nikel kazanımını araştırmıştır. En yüksek nikel çözünme verimi, karışık bakteri kültürü ile %1 katı oranında %7 kükürt ve 2,22 g/l Fe^{+2} içeren ortamda yapılan biyoliç işleminde %97 olarak gerçekleşmiştir. Leonardou ve Dimaki, 1994 düşük tenörlü (<%1) lateritik nikel cevheri kullandığı çalışmada, yığın liçini temsilen kolon liçi testleri gerçekleştirmiştir. Bu testlerde, sülfirik asit konsantrasyonu, kolon uzunluğu, tane boyutu ve çözeltideki katı miktarının nikel kazanımına etkisini araştırmıştır. 80 gün devam eden liç testi sonucunda, lateritik nikel cevherinden %86 verim ile nikel kazanılmıştır.

Lateritik cevherlerden nikel pirometalurjik ve hidrometalurjik olarak elde edilebilmektedir. Pirometalurjik yöntemde cevher; kurutma, kalsinasyon, kavurma, redüksiyon, ergitme gibi yüksek sıcaklıklarda gerçekleşen proseslere tabi tutulurken, hidrometalurjik yöntem atmosferik basınç veya yüksek basınç altında asit liçi yöntemlerinden oluşmaktadır (McDonald ve Whittington, 2008; Li vd., 2009). Literatürde bulunan lateritik formdaki nikel cevherinin hidrometalurjik olarak kazanıldığı çalışmalar incelendiğinde, az da olsa atmosferik şartlarda tank içinde karıştırma esasına dayanan liç tekniği, genellikle yüksek basınç liçi tekniği ve az da olsa biyolojik kazanım tekniklerinin tercih edildiği görülmektedir. Ancak lateritik nikel gibi değerli fakat cevherleşme açısından düşük tenörlü yatakların kazanımı için daha uygun olan yığın liçi tekniği üzerine sınırlı sayıda çalışmanın literatürde bulunduğu görülmektedir.

Bu çalışmada, Manisa-Gördes'te bulunan lateritik nikel yatağından alınan cevher numunesinin yığın liçi tekniği ile çözündürülme koşullarının belirlenmesi amaçlanmıştır. Bu amaca yönelik olarak, cevher yatağından alınan temsili numunelerin ilk olarak kimyasal ve mineralojik yönden tanımlanmaları gerçekleştirilmiş, daha sonra farklı koşullarda sülfürik asit liçine tabi tutulan cevherin içerisinde bulunan esas olarak nikel (Ni), kobalt (Co), demir (Fe) ve mangan (Mn) bileşenlerinin çözünme oranları incelenmiştir. Liç deneylerinde, yığın liçini temsilen iki farklı kolon liç düzeneği kullanılmış olup, sülfürik asit konsantrasyonu, liç süresi ve tane boyutunun nikel kazanma verimine etkisi araştırılmış ve optimum şartlar belirlenmiştir.

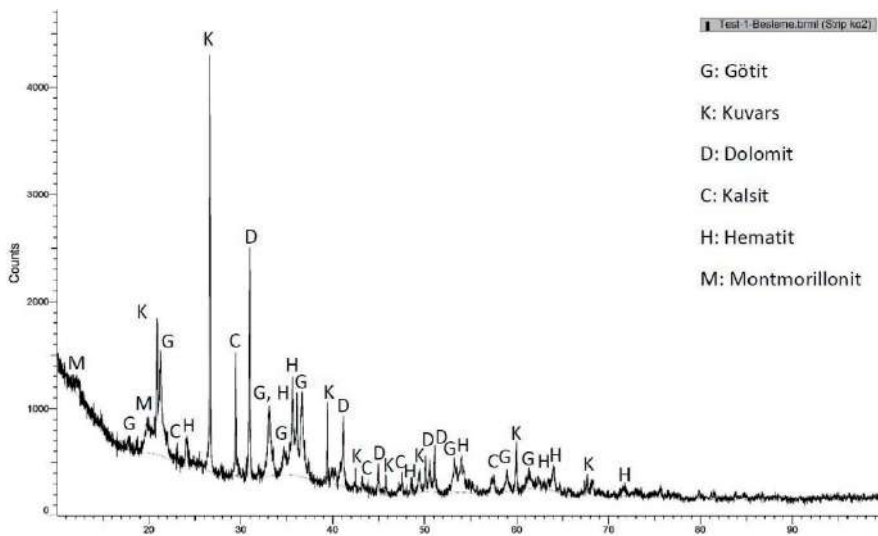
MALZEME VE YÖNTEM

Malzeme

Çalışmaya konu olan cevher numuneleri META Nikel Kobalt AŞ.'ye ait Gördes bölgesinden temin edilmiştir. Numuneler zenginleştirme tesisinde basınç liçi öncesi yapılan eleme ile elde edilen %0.3 Ni tenörlü ön zenginleştirme ürünü olup, kimyasal analizleri ve mineralojik analizleri Tablo 1'de ve Şekil 1'de verilmiştir. Söz konusu düşük tenörlü ön zenginleştirme ürününden yaklaşık 10 ton temsili numune iş makineleri yardımıyla deneysel çalışmalarda kullanılmak üzere alınmıştır. Daha sonra alınan numuneler konileme-dörtleme yöntemi uygulanarak azaltılmış olup, bir kısmı deneysel çalışmalar için ayrılırken, diğer kısmına ise mineralojik ve kimyasal analizler yapılmıştır. Deneysel çalışmalarda kullanılacak numuneler, gerekli boyut küçültme işlemlerini takiben, -150+0,75 mm, -20mm, -5mm olacak şekilde 3 farklı tane boyutuna sınıflandırılmıştır.

Çizelge 1. Düşük tenörlü lateritik nikel cevherine ait kimyasal analiz.

Al (ppm)	Ca (ppm)	Co (ppm)	Cr (ppm)	Fe (ppm)	Mg (ppm)	Mn (ppm)	Ni (ppm)	Si (ppm)
6646	118758	170	1914	91677	37409	1138	3191	201344

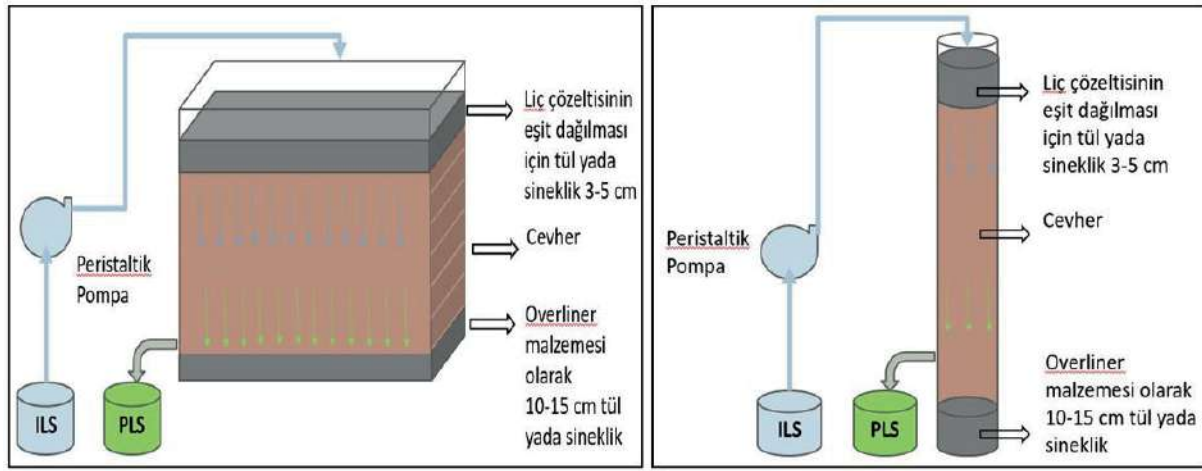


Şekil.1 Düşük tenörlü nikel cevherine ait XRD sonucu.

Şekil 1’de verilen XRD sonucu incelendiğinde; numunenin baskın olarak götit ve kuvars içerdiği gözlemlenmiştir. Bunun yanı sıra, kalsit, dolomit ve hematit mineralleri görülmüştür. Bunlara ek olarak ise, az miktarda olduğu düşünülen kil minerallerinden montmorillonite rastlanmıştır.

Yöntem

Lateritik nikel cevherinin sülfürik asit ile çözündürülmesine yönelik yapılan kolon liçi deneylerinde kullanılan düzenek Şekil 2 verilmiştir. Şekil 2’de görüldüğü gibi deney düzeneği iki farklı kolon ve sisteme boş çözücü göndermek amacıyla kullanılan peristaltik pompadan oluşmaktadır.



Şekil 2. Kolon liçi deney düzeneği.

Liçi deneylerinde, tesiste kili uzaklaştırılmış lateritik nikel cevherleri, fleksiğlas kolona (150mm çap * 2000mm yükseklik) ve kare kesitli kolona (IBC 1m*1m*1m) doldurulmuştur. Literatür verilerine göre, yığın liçi testlerinde seçilecek olan kolonun çapının, beslenecek cevherin maksimum tane boyutunun en az altı katı olacak şekilde seçilmiştir. Bu nedenle, -150+0,75 mm tane boyutlu cevhere kare kesitli kolon (IBC) ve diğer iki tane boyut grubu numuneler ise (-20mm ve -5mm) silindirik kolona doldurulmuştur. Dolum sırasında cevherin çökmesi ve mümkün olduğu kadar fazla cevher alması için hafifçe kolon duvarlarına vurularak cevherin sıkışması sağlanmıştır. Liçi deneylerinde kullanılmak üzere iki farklı konsantrasyonda sülfürik çözeltisi hazırlanmıştır (düşük asit konsantrasyonu= 150 gr/lit, yüksek asit konsantrasyonu= 250 gr/lit alınmıştır). Bu çözeltiler hazırlanırken (%95-98) saflıkta sülfürik asit (H₂SO₄) ve tesis suyu kullanılmıştır. Testlerde birim cevhere liçi çözeltisi debisi 17 lt/m²/h’dir. Belirli periyotlarla biriken yüklü çözelti (PLS) serbest asit konsantrasyonu ayarlandıktan sonra yüksüz çözelti (ILS) olarak geri döndürülmüştür. Stok çözeltisinde ve sıvı analizlerinden kademeli metal kazanma verimleri hesaplanmıştır. Cevherin nem tutma kapasitesinin yüksek olması nedeniyle çıkarılan metallerin kazanma verimleri hesaplamalarında aşağıdaki formüller kullanılmıştır.

Kazanım edilmiş metalin kütlesi;
Kolon Dahil;

$$g = V_p.C_p + V_f.C_f + (V_w).C_h \quad (1)$$

Kolon hariç;

$$g = V_p.C_p + V_f.C_f \quad (2)$$

- Vp = Artmış PLS hacmi, lt
 Cp = Artmış PLS hacmindeki metal konsantrasyonu, gr/lt
 Vf = Besleme sıvısının ILS hacmi, lt
 Cf = Beslemedeki ILS metal konsantrasyonu, gr/lt
 Vw = Kolonda bulunan son nemi, lt
 Ch = Beklemedeki ortalama sıvı konsantrasyonu, (Cp+Cf / 2)

Son metal kazanma verileri başlangıç değerlerine göre yeniden hesaplanmıştır.

Gerekli asit lt. =

$$(PLS \text{ 'den ILS 'ye aktarılan lt}) \times (ILS \text{ serbest asit} - PLS \text{ serbest asit}) \times \frac{1.05}{(1000 \times 1.84)}$$

(3)

Testler yapılırken perkolasyon (süzülme) problemi olmadıkça test devam edilmiştir. Co çözünmesini artırmak amacıyla sodyum bisülfid eklemesi yapılmıştır. Soydum bifülfid eklemesi Mn içeriğine göre ayarlanmıştır (SMBS/Mn = 1,5:1).

Liç deneyleri boyunca, kontrol altında tutulan ve nikel kazanma verimine etkisi incelenen çalışma parametreleri Tablo 2’de verilmiştir.

Çizelge 2. Kolon liçi deney parametreleri.

Test No	Tane boyutu, mm	Asit konsantrasyonu, gr/lt	Numune miktarı, kg	Kolon Tipi
T1-HL1	-150 +0,75	150	1344	Kare Kolon
T2-HL2	-150 +0,75	250	1359	
T3-HL5	-5	150	36,5	Dairesel Kolon
T4-HL6	-5	250	37,9	
T5-HL7	-20	150	37,9	
T6-HL8	-20	250	37,3	

DENEYSEL VERİLER

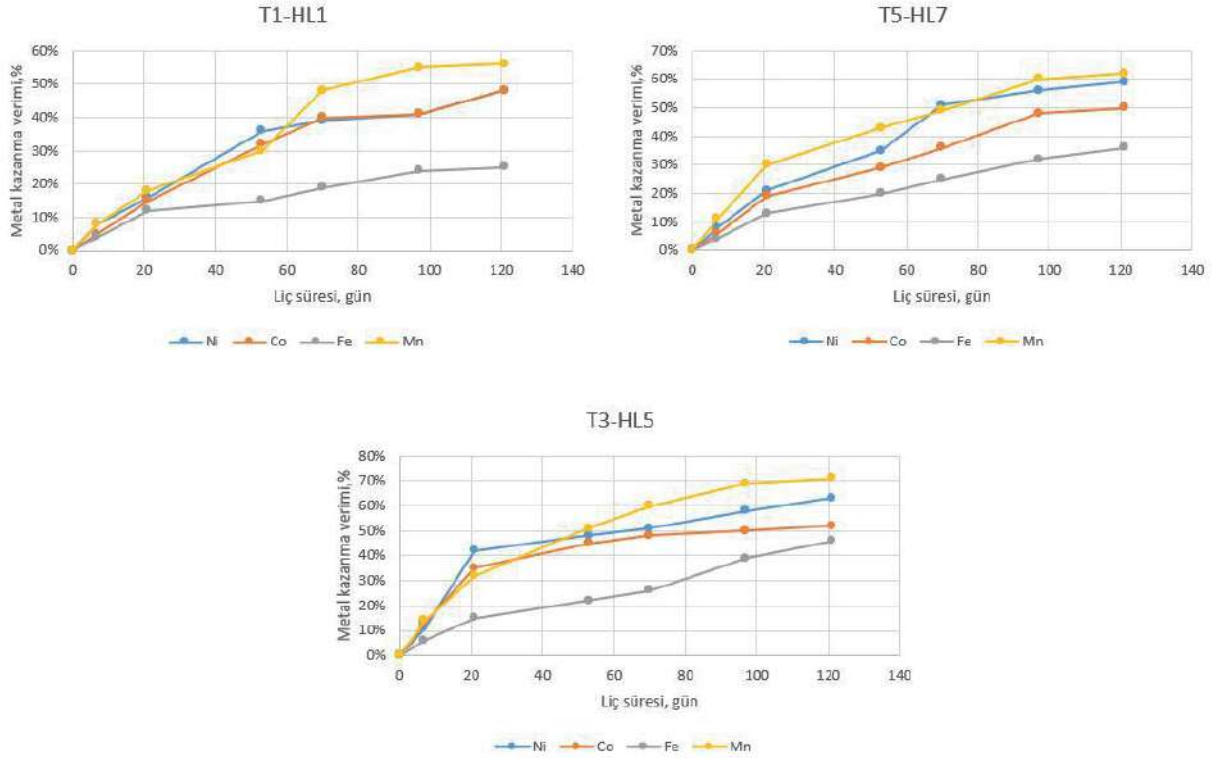
Yığın liçini simule etmek amacıyla laboratuvar ortamında oluşturulan kolon liçi testlerine 121 gün boyunca devam edilmiştir. Kolonlardan belirli aralıklarla numune alınmış ve numune sonuçlarına göre boş çözeltisinin (ILS) serbest asit konsantrasyonu aşağıdaki belirlenen değerlerde tutulmuştur. Yapılan kolon liçi testlerinin sonuçları Tablo 3’te verilmiştir.

Çizelge 3. Kolon liçi testlerinin sonuçları.

Test No	Tane Boyutu, mm	ILS H ₂ SO ₄ Miktarı, gr/lit	Asit Tüketim kg/t	Ekstraksiyon, %				Gün
				Ni	Co	Fe	Mn	
T1-HL1	-150	150	500	48	48	25	56	121
T5-HL7	-20		800	59	50	36	62	
T3-HL5	-5		1000	63	52	46	71	
T2-HL2	-150	250	600	65	55	46	62	
T6-HL8	-20		1000	75	59	52	70	
T4-HL6	-5		1200	78	59	55	77	

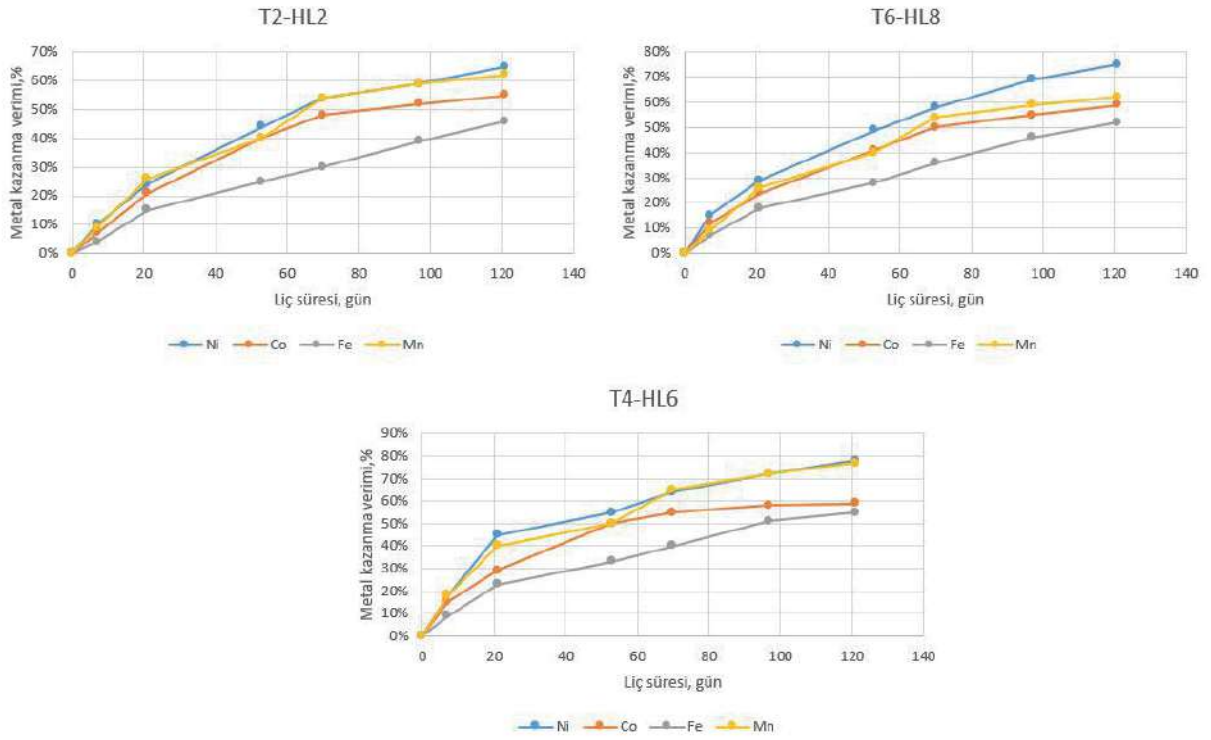
Çizelge 3’te cevher tane boyutundaki değişimin metal kazanımına etkisi incelendiğinde; ince tane boyutunda tablodaki tüm metallerin (Ni-Co-Fe Mn) liç verimlerinin yükseldiği, Co metalinin ise liç verimi diğer metallere göre daha az miktarda arttığı görülmektedir. Liç besleme çözeltisinin serbest asit derişimi arttıkça, tablodaki tüm metallerin liç verimi artmıştır. Ni metalinin ise, liç veriminin tablodaki diğer metallere göre daha fazla arttığı gözlemlenmiştir. Liç besleme çözeltisindeki serbest asit konsantrasyonunun artması ile liç verimlerinin yanında asit tüketim değeri de artmaktadır. Ni-Fe metalleri için aynı tane boyutunda liç çözeltisindeki asit konsantrasyonu artırıldığında 53-121 günlerinde liç veriminin arttığı tespit edilmiştir. Co-Mn metalleri için aynı tane boyutunda liç çözeltisindeki asit konsantrasyonu artırıldığında 97-121 günlerindeki liç veriminin yükselme eğiliminin azaldığı gözlemlenmiştir.

Gerçekleştirilen kolon liçi testlerinde Ni-Co-Fe-Mn metallerinin zamana bağlı değişen metal kazanma verimleri kullanılan asit konsantrasyonu miktarına bağlı olarak gruplandırılarak Şekil 3 ve Şekil 4’te verilmiştir.



Şekil 3. Düşük konsantrasyonlu asit çözeltisi ile yapılan kolon lıçı testlerinin gün-metal kazanma grafikleri (T1-HL1; T5-HL7; T3-HL5).

Düşük konsantrasyonlu asit çözeltisi ile yapılan lıç testlerinin sonuçları incelendiğinde; T1-HL1, T5-HL7 nolu testlerde ilk 21 günde tüm metallerin lıç verimleri birlikte hareket ederken 21-70 günleri arasında Fe metalinin lıç verimi diğer metallere göre daha az miktarda artmıştır. 70-121 günleri arasında ise tüm metallerin lıç verimlerindeki yükseliş hızı azalmıştır. T3-HL5 testinde ise Fe metalinin lıç verimi 121 gün boyunca artmıştır. Tablodaki tüm metaller için lıç süreleri incelendiğinde, tane boyutu azaldıkça lıç verimi artmaktadır. Bunun yanında, ince tane boyutlarında Ni-Fe-Mn metallerinin, Co metaline göre daha verimli kazanıldığı gözlemlenmiştir. Farklı tane boyutlarında ilk 53-70 gün içerisinde Mn metalinin lıç verimi artmış, takip eden günlerde ise lıç veriminde daha az miktarda artışlar gözlenmiştir.



Şekil 4. Yüksek konsantrasyonlu asit çözeltisi ile yapılan kolon lıç testlerinin gün- metal kazanma grafikleri (T2-HL2; T6-HL8; T4-HL6).

Yüksek konsantrasyonlu asit çözeltisi ile yapılan lıç testlerinin sonuçları incelendiğinde; 97-121 günleri arasındaki lıç verimlerinde yükselme eğilimi azalmıştır.

Tüm metaller için tane boyutunun metal kazanma verimlerine etkisi incelendiğinde tane boyutu azaldıkça lıç verimi arttığı görülmüştür. Tane boyunun metal kazanımına etkisinin Ni-Fe-Mn metalleri için Co metaline göre daha fazla olduğu gözlemlenmiştir. Buna bağlı olarak tane boyutu ve lıç süresinin ters orantılı olduğu belirlenmiştir. Sonuç olarak, benzer yığın lıç çalışmalarında görüldüğü gibi (Rashidi, 2020), ince tane boyutu ile gerçekleştirilen lıç deneyinde, iri tane boyutlarına göre maksimum lıç verimlerine daha kısa sürelerde ulaşılmıştır. Bu durum ince tanelerin çözücü ile temas edeceği yüzey alanının iri taneye göre daha büyük olması ile açıklanmaktadır.

SONUÇLAR

Bu çalışmada, Gördes nikel cevherinin düşük tenörlü elek üstü ürünün değerlendirilmesi amaçlanmıştır. Düşük tenörlü ve kilinden arındırılmış (yıkamış eleküstü) olması nedeniyle yığın liçi prosesinin uygulanabilirliği değerlendirilmiştir. Cevher hazırlama bölgesinde elek üstü olarak ayrılan düşük tenörlü cevherden temsili numune alınmıştır. Yaklaşık alınan 10 ton numuneyi dörtleme yapılarak 6 adet test numunesi elde edilmiş ve laboratuvar testleri yapılmıştır. Çalışma kapsamında; tane boyutu, sülfürik asit konsantrasyonu ve liç süresinin Ni-Co-Fe-Mn gibi elementlerin kazanımına etkileri incelenmiştir.

Elde edilen deney bulgularına göre;

Nikel metali değerli olduğu için maksimum oranda çözünmesi hedeflenmiştir. Yürütülen testler sonucunda, en yüksek liç verimi (%78) -5mm tane boyutunda ve 250gr/lt serbest asit liç çözeltisinde T3-HL5 nolu testte elde edilmiştir. Bu testteki birim asit tüketim değeri cevher tonu başına 1200kg/ton'dur.

Kobaltda nikel gibi değerli bir metaldir. Liç verimleri dikkate alındığında, aynı nikel metalinde olduğu gibi tane boyutunun azalmasına ve asit konsantrasyonunun artışına bağlı olarak, kazanma verimi de artmaktadır. Kobalt metalinin liç verimindeki artış, diğer metallere göre daha az miktarda gerçekleşmiştir. En yüksek liç verimi (%59) -5mm tane boyutunda ve 250gr/lt serbest asit liç çözeltisinde T3-HL5 testinde elde edilmiştir.

Mevcut proseste demir empürite olarak tabir edilen bir metaldir. Liç veriminin artması sonraki safsızlaştırma aşamalarında prosesin zorlaşmasına, maliyetlerinin yükselmesine ve üretim veriminin düşmesine sebep olabilmektedir. Demir metali için en düşük liç verimi (%25) -150mm tane boyutunda ve 150gr/lt serbest asit liç çözeltisinde T1-HL1 testinde elde edilmiştir. Bu testteki birim asit tüketim değeri cevher tonu başına 500kg/ton'dur.

Mangan da demir gibi empürite metalidir. Aynı demir empüritesi gibi liç veriminin artması sonraki safsızlaştırma aşamalarında prosesin zorlaşmasına, maliyetlerinin yükselmesine ve üretim veriminin düşmesine sebep olmaktadır. Mangan için en düşük liç verimi (%56) -150mm tane boyutunda ve 150gr/lt serbest asit liç çözeltisinde T1-HL1 testinde elde edilmiştir.

Testlerindeki liç verimleri dikkate alınarak 121 gün liç süresi tutulmuştur. Test süresi 121 sonrasında liç verimlerinin artışı azalmıştır.

Testler değerlendirildiğinde, değerli metaller olan nikel ve kobaltın çözünürlüğü arttıkça; empürite metallerinin çözünürlükleri ve birim asit tüketimi de artmaktadır. Bu nedenle, pH yükseltilerek empürite metallerinin ortamda azaltılması gerekmektedir. Ancak bu durumun safsızlaştırma prosesinin zorlaşmasına, üretim maliyetinin yükselmesine dolayısıyla üretim verimliliğinin düşmesine neden olacağı düşünülmektedir.

Optimum test koşullarının belirlenmesi özellikle safsızlaştırma prosesine bağlı olsa da, yığın liçini temsilen yapılan kolon liçi testleri sonucunda bazı bulgular elde edilmiştir. Elde edilen bulgulara göre, nikel kazanma verimini etkileyen en önemli iki parametre tane boyutu ve serbest asit konsantrasyonudur. Bu durum, yığın liçi tekniği ile en kısa sürede en yüksek nikel kazanma veriminin elde edilmesi için tane boyutunun minimum, ortama sağlanan asit konsantrasyonunun ise maksimum düzeyde olması gerektiğini göstermektedir.

Testlerde nikel ve kobalt çözünürlükleri göz önüne alındığında, liç verimlerinin sırasıyla %78 ve %59'a ulaştığı, bununla birlikte empürite olarak tabir ettiğimiz demir ve mangan metallerinin, mevcut HPAL prosesine göre ortamda çok daha fazla çözündüğü gözlemlenmiştir. Lateritik nikel cevherlerinin, hidrometalurjik yöntemler ile ekonomik şekilde kazanılması, birim asit tüketimi ve empürite çözünmelerine doğrudan bağlı olan bir durumdur. Elde edilen sonuçlar ve son yıllardaki nikel fiyatları dikkate alındığında, düşük tenörlü lateritik nikel cevherlerinin yığın liçi yöntemi ile kazanılmasının ekonomik olmadığını göstermektedir. Ancak ülke kaynaklarının değerlendirilmesi ve gelecek fiyatlama projeksiyonları göz önüne alındığında bu ve benzeri çalışmaların geliştirilerek devam ettirilmesi gereklilik olarak görülmektedir.

KAYNAKLAR

- Atik, S. (2015). Biyoliç Yöntemiyle Lateritik Cevherden Nikel Kazanımı. Yüksek Lisans Tezi, Süleyman Demirel Üniversitesi, Fen Bilimleri Enstitüsü, Isparta.
- Baştürkçü, H. (2016). Fiziksel ve Kimyasal Ön İşlemlerin Lateritik Nikel Cevherlerinin Atmosferik Liçine Etkisi. Doktora Tezi, İstanbul Teknik Üniversitesi, Fen Bilimleri Enstitüsü, İstanbul.
- Çoban, O. (2014). Çaldağ Lateritik Nikel Cevherlerinden Hidrometalurjik Yöntemlerle Nikel ve Kobalt Eldesi. Yüksek Lisans Tezi, İstanbul Teknik Üniversitesi, Fen Bilimleri Enstitüsü, İstanbul.
- McDonald, R.G., Whittington, B.I. (2008). Atmospheric Acid Leaching Of Nickel Laterites Review Part I. Sulphuric acid Technologies. *Hydrometallurgy*, 91, 35-55.
- Nasuh, A. (2014). Eskişehir-Karaçam Lateritik Cevherinden Basıncılı Sülfürik Asit Liçi İle Nikel Kazanımı. Doktora Tezi, Hacettepe Üniversitesi, Fen Bilimleri Enstitüsü, Ankara.
- Leonardou, A.S., Dimaki, D. (1994). Heap Leaching Of Poor Nickel Laterites By Sulphuric Acid At Ambient Temperature, International Symposium Hydrometallurgy '94, (pp. 193-208), Cambridge, England
- Li, J., Li, X., Hu, Q., Wang, Z., Zhou, Y., Zheng, J. (2009). Effect Of Pre-Roasting On Leaching Of Laterite. *Hydrometallurgy*, 99, 84-88.
- Listyarini, S. (2017). Designing Heap Leaching For Nickel Production That Environmentally And Economically Sustain, Vol.8, No:12.
- Rashidi, A. (2020). Yığın Liçi İle Altın Kazanımında Yığın Özelliklerinin İyileştirilmesi. Yüksek Lisans Tezi, Zonguldak Bülent Ecevit Üniversitesi, Fen Bilimleri Enstitüsü, Zonguldak.

ECO-EFFICIENCY IN DRY COMMINUTION PRACTICES USING VERTICAL ROLLER MILL (VRM) - TECHNICAL AND ECONOMICAL ASPECTS

H.R. Manouchehri^{1,*}

¹Northland OreTech AB,
Mining, Mineral and Metallurgical Processing and Waste Management Consulting
(Corresponding Author: hmanouchehri@yahoo.com)

ABSTRACT

Mining industry, as the cornerstone of human civilization, is directly and indirectly responsible for up to 45% of the global economy. The industry is an energy and water consumer. It is projected that about 6-7% of total world's energy is consumed by mining activities, while about 6-8 Billion m³ of water per annum is consumed through mining activities. The industry, facing different challenges, including resource efficiency, access to energy and water, reducing environmental foot-print, etc. Accordingly, inventing and developing machineries and processes that help to overcome these challenges are highly projected for sustainable in mining industry

Since considerable amount of energy is consumed in comminuting ores and the energy per ton of product increases as deeper and more competent reserves are brought into operations, as well as its environmental, economic and political aspects need to be considered seriously in design and operation of future mineral processing activities.

Moving towards "Green Economy" requires responsible attempts to understand and implement eco-efficient technologies. One identified technology, would be dry comminution practices by using Vertical Roller Mill (VRM). Herein the results from a collaborative scaleup project supported by European EIT-RawMats on technical, economic and environmental aspects of dry comminution process by VRM is presented and discussed.

Keywords: Eco-efficiency, dry comminution, vertical roller mill (vrm), energy, wear

INTRODUCTION

Mining industry has been the cornerstone of human civilization which is directly and indirectly contributes to 45% of the global economy. The industry is an energy and water consumer. It is projected that about 6-7% of total world's energy is consumed by mining activities from which almost half goes for size reduction for processing of the values from the rocks (Michaux, 2011; Morrison and Cleary, 2008; Batterham, 2007). The industry is responsible for 4-7% of the world's GHG emissions as well (McKinsey, 2020). Furthermore, mining activities consume 7-9 Billion m³ of water per annum and is partly responsible for polluting water by different processes which must be carefully understood and taking care of.

The industry faces different challenges, including resource efficiency, access to energy and water, reducing environmental foot-print, license to operate, etc. Accordingly, inventing and developing machineries and processes that help to overcome these challenges are necessities for future sustainability.

Mineral processing represents the largest consumer of energy and water and therefore mining companies are assessing mineral processing technologies and innovative approaches to improve energy and water consumption and related environmental foot print.

There is strong link between the eco-efficiency and sustainability in mining industry. The future direction for the industry is moving towards eco-efficiency. Both energy and water are critical valuables for development and must be conserved to make a balance between the environmental foot-print and economy. Minerals and metals industry contribute greatly to the global economy; however, the related environmental impact plays a critical role for future sustainability. That includes the consumption and depletion of the natural resources and producing mining wastes, emissions of GHG and pollutant to the ari, as well as water consumption and water pollutant due to releasing of different ion species and insoluble during mining and processing.

Metals and minerals production rate has been dramatically increases due to industrialization, increasing population, and technology development. Extracting of raw materials, including fuels, has dramatically increased during last 20 years, from 11.3 billion tonnes in 2000 to 17.9 billion tonnes in 2019, i.e., 58% increasing (World Mining Data, 2021).

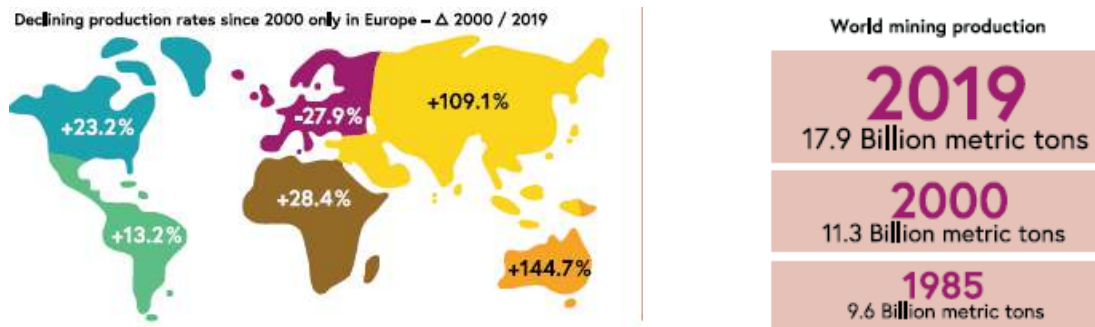


Figure 1. Mining production and declining/increasing rates of production by continents

To sustain production, mining industry requires withdrawal of freshwater. Water consumption is an important sustainability factor in particular in arid areas, such as Australia, Africa, Middle East, and South America. For example, to produce various types of metals the water consumption ranging from 2.9 m³/t for steel production to more than 250 m³/t for gold production.

Furthermore, water and energy consumption are directly related to the ore grade from which the metal is produced. An estimation indicated that as the grade (%) is decreasing the water consumption per ton of metal production is increasing (Norgate and Lovel, 2004).

$$Water\ Consumption(m^3/t) = 167.7 \times G^{-0.9039} \tag{1}$$

Water is strategic asset and has become a source of strategic advantage and a growing source of conflict. It is an expensive asset which accounts for 10% capital expenses for infrastructures. Furthermore, mining activities impact the local water system and are responsible to contribute in an integrated water management program. Furthermore, mining is potentially a source of polluting water, therefore mining and process water must be treated before it is released to the environment. The global mining industry facing challenges due to water scarcity, global warming, lack of transparent legislations in water quality control and are seen as key partner in global sustainable development. Therefore, managing water consumption and reducing/minimizing its pollution are key in sustainability.

It is also worth to mention that the global water treatment market has reached over 260 BUS\$ in 2018, from which about 4,7 BUS\$ is the share of mining industry. Therefore, considering dry efficient comminution processes offer a great opportunity in reducing water consumption and minimizing its pollution (Global Water Market, 2021).

Dry Eco-Efficient Comminution for Sustainability in Mining Industry

In 2020, the world’s energy consumption has reached $155 \cdot 10^{12}$ kWh (558 Exa-Joule) and it is supposed to reach $265 \cdot 10^{12}$ kWh by 2050 (i.e., an increasing of 1.5% per annum). Mining industry consumed about 6-7% of that energy, with the highest consumption in comminution (3-3.5%).

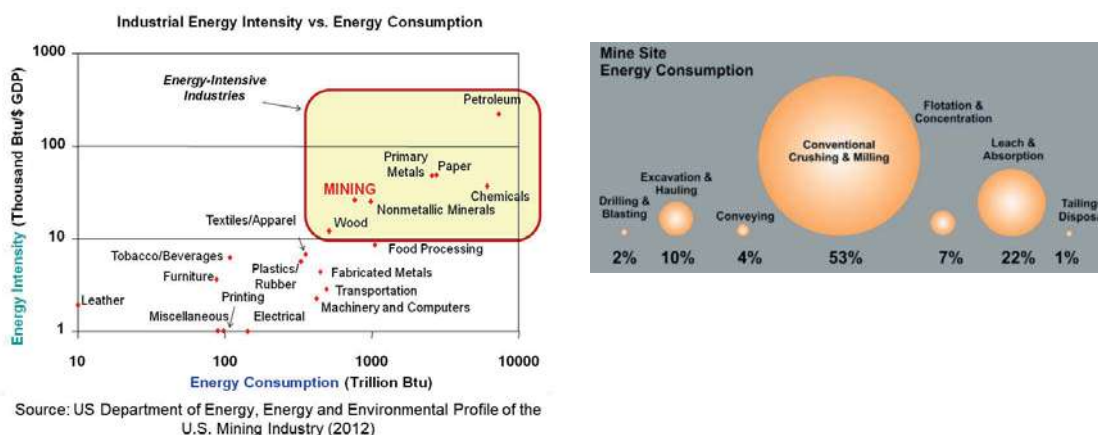


Figure 2. Industrial energy intensity (left) and distribution of mine site energy (right)

The industry is also responsible for 4-7% of the world’s GHG emissions which must be reduced significantly by considering different strategies. The goals can be achieved by reducing, reusing and recycling (3Rs), reduction in energy consumption, carbon capturing and sequestration, etc.

Furthermore, the water withdrawal and its environmental impact must be reduced. In fact, grinding of the ore in wet mode to achieve the liberation for processing not only consumes water but the process water may be polluted. Therefore, moving towards dry comminution may avoid/reduce the release of different chemical species to the mine water circuit. Additionally, during milling the grinding media are consumed to size down the ore, however, the media consumption per ton of comminuted ore is defined by the ore characteristics, i.e., its hardness and abrasiveness. As the harder and more abrasive ore is ground to a specific size the media consumption is increased. It is also well understood that the media wear or media consumption is much higher in wet grinding. That means the wear is considerably less in dry grinding. Based on the type of media used for grinding, there is an embodied energy in manufacturing the media which is estimated to be at average 5-6 MW/t. consequently, the reduction in media consumption by dry grinding results in saving energy and reducing the related GHG emission.

With the decline of water resources, increasing of energy costs, and the efforts to reduce energy consumption and minimise CO₂ emission, mining companies are increasingly mindful of the value of water, energy, as well as the potential CO₂ emission and water pollutants to be reduced. Accordingly, an eco-efficient dry comminution technology, which can reduce water consumption and its polluting while reducing energy consumption would be of prime interest. The comminution stage and downstream processes should be designed and integrated through circular economy concept in which reliable grade-engineering is combined with dry comminution to improve quality of the feed and reduce tonnage in downstream wet separation process(es) to sustainably reduce water usage.

Vertical Roller Mill (VRM)

Vertical Roller Mill (VRM) is an eco-efficient dry comminution technology that can be considered for hard rock comminution and processing. A comprehensive study has been devoted to assess the potential of implementation of the technology for hard rocks and slags from metallurgical plant through the European Innovation and Technology (EIT) program on raw materials. It is a kind of roller mill that is widely used in the cement industry. Within the VRM, the interparticle comminution takes place in a material filled gap between the rotating flat grinding table and the conical grinding rollers as shown in Fig.3.

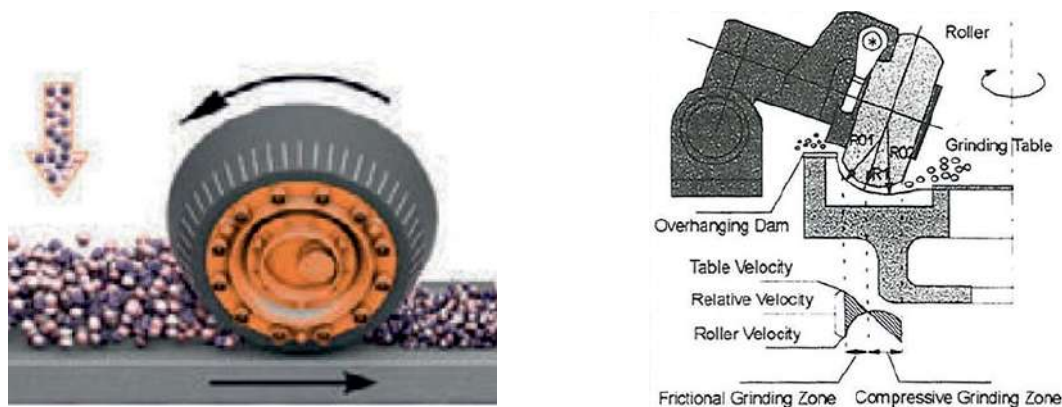


Figure 3. Interparticle comminution of the roller mill

Grinding/comminution with roller mill is done in a material filled gap between the rotating flat grinding table and the conical grinding rolls. The feed is charged to the center of the flat table and moves affected by centrifugal forces and friction towards the table's edge. Based on the mill size, the feed is nipped by conical rollers installed at the outside of the table. The grinding force is provided by rollers that are attached to the hydraulic cylinders). An efficient dynamic air classifier (air cyclone) is incorporated inside the mill to separate the ground particles (Schaefer, 2001). For optimal performance of the mill and minimizing the down-time of the mill, the rollers are equipped with wear resistant tyres made of high-Cr casting or other resistant alloys. The comminution pressure is provided by hydro-pneumatic spring system. A high pressure between 50 to 100 bar is provided to ground the ore within the gap between the rollers and the table. The low-pressure side of the hydraulic cylinder has a pressure of about 10% of the high-pressure side, therefore, the difference between high- and low-pressure sides allowing elastic movement of the roller. Within VRM comminution is done mainly by compression, however, shearing is involved as well. Furthermore, due to introducing hot air to the mill, raw materials with high moisture can be easily tolerated.

In comparison with conventional ball milling, VRM can accept larger feed size, up to 140mm. Accordingly, part of crushing might be eliminated. Furthermore, due to flexibility in adjusting grinding pressure, the fluctuations in feed properties can be easily tolerated. Overgrinding can be avoided due to possible controlling of grinding pressure and the high performance of air classifier.

MATERIALS AND METHOD

Materials

Two different raw materials/samples were received for testing, a sulfide ore from Boliden Minerals AB and a ferromanganese slag from EraMet. The samples were characterized for their comminution behaviors. Accordingly, crushing, rod milling and ball milling Bond work indexes were

determined for the materials. Furthermore, the abrasion index of the samples was defined, using standard Bond abrasion tests. The results from characteristic of the samples are shown in Table 1. The results indicates that sulfide ore can be categorized as soft to medium ore (rather low competency), however; the slag sample could be considered medium to hard ore/material (rather high competency).

Table 1. The comminution characteristics of the samples

	Crushing Work Index (Wic)	Rod Mill Work Index (Wir)	Ball Mill Work Index (Wib)	Abrasion (Ai)
Sulfide Ore	10 (kWh/t)	13 (kWh/t)	12,5 (kWh/t)	0.15 - 0.18
FeMn Slag	14 (kWh/t)	17.7 (kWh/t)	17 (kWh/t)	0.38 – 0.51

Comminution Tests

After characterization, the samples were ground to explore the potential of implementing of VRM technology for eco-efficient comminution. The comminution tests were conducted at Loesche pilot facilities in Germany. The criteria for comminution were defined on the basis of mineralogical analysis of the samples and the related processes for downstream. Accordingly, the target product sizes for comminuting were considered as $d_{80}=60-65 \mu\text{m}$ for sulfide ore and $d_{80}\approx 300 \mu\text{m}$ for the ferromanganese slag.

Comminution tests were also conducted in both wet and dry modes in ball milling in order to compare the energy consumption by different comminution technologies. Moreover, the media needed for the grinding the samples were estimated based on specific energy consumption. Accordingly, the energy needed to size down the samples to the specific target size was estimated for different comminution modes. Furthermore, the media wear for both comminution modes were calculated to estimate the related wear costs.

RESULTS AND DISCUSSIONS

Series of comminution tests were completed by using VRM and the energy needed for comminuting the samples were defined. Fig. shows the results to achieve the target sizes for the samples. For conducting grinding tests, the received samples were crushed to obtain -20 mm product. The size distribution of the crushed samples revealed that the d_{80} of crushed samples were at 16 mm and 8 mm for slag and sulfide ore respectively. The grinding tests were conducted, using VRM to achieve the target sizes. The results are depicted in Figs 4 and 5. Accordingly, the energy needed to gain the $d_{80} = 60-65 \mu\text{m}$ is at about 7 kWh/t. However, about 4.4 kWh/t was needed to grind the slag sample to a target size of to $d_{80} = 300 \mu\text{m}$.

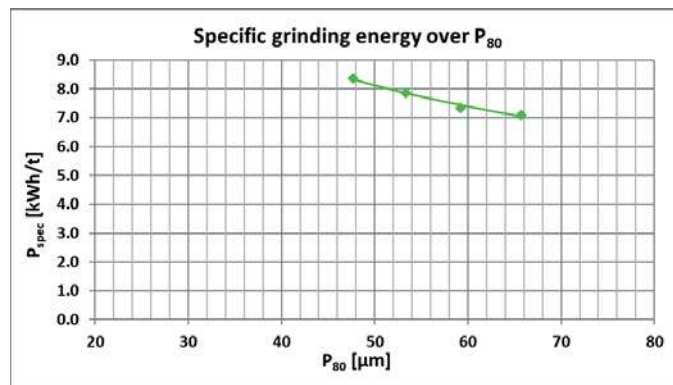


Figure 4. Energy consumption vs particle size in comminution, using VRM for sulfide ore

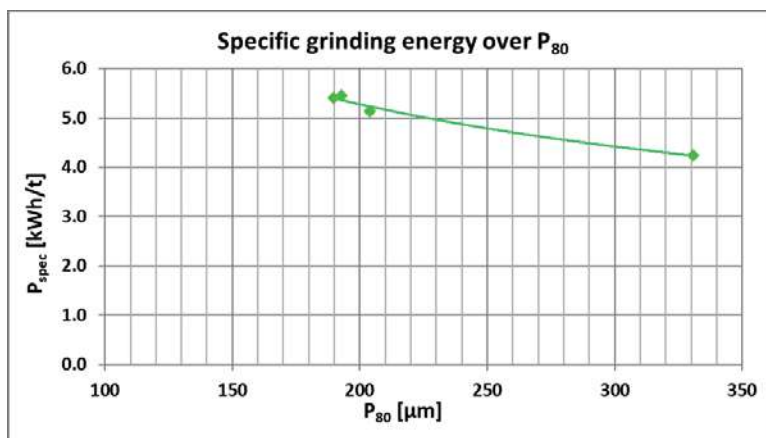


Figure 5. Energy consumption vs particle size in comminution, using VRM ferromanganese slag

Energy Estimation for Ball Milling (Based on Bond Equations)

According to the Bond theory, to comminute a material/sample to certain size, crushing followed by rod and ball millings are considered. In fact, rod milling is rather low energy consumption device, tailoring a good feed for ball mill. In theory, after crushing the feed, the rod mill accepts a feed size up to 35 mm and provide a product at d80 ~ 2mm for ball milling. However, nowadays, in practices, i.e., plant design and operation, no rod milling is considered. One reason is that high performance crushers are emerged to efficiently size down the feed to about 10 mm or even smaller and more powerful and efficient ball mill are manufactured to grind the crushed material. The energy consumption to size down the two raw materials to the target product size was estimated based on Bond equations. A rough calculation for the energy consumption are shown in Table 2.

Table 2. Estimated energy consumption for the samples in both dry and wet modes

	$E_{total} = EF_s (10 W_i ((1/VP80)-(1/VF80)))$			
	F80m(μm)	P80 (μm)	Energy (kWh/t) – Wet	Energy (kWh/t) – Dry
Sulfide ore	8000	65	14.8	19.24
FeMn Slag	16000	300	9.10	11.83

According to the results, the energy consumption for grinding the samples, using VRM, is considerably lower than the conventional tumbling milling in both wet and dry modes. However, as the classification is done within the VRM, there will be additional energy consumption to separate/classified the ground products.

Except the energy calculations based on Bond equations for dry and wet comminution of the samples, a series of laboratory ball milling tests was conducted to define the energy consumption for comminuting the samples. Accordingly, the energy consumption for comminuting the sulfide ore to the target size was defined at range of 19.73 to 21,2 kWh/t in dry comminution, while for wet comminution the energy consumption was estimated at 17.9 kWh/t. Nevertheless, the calculated energy consumption are based on the finer feed size to the laboratory ball mill based on Bond ball milling tests. The same procedures were completed for FeMn slag sample and the energy needed to comminute the material to target size were at 8.75 and 10.5 kWh/t for wet and dry mode respectively.

It must be noted that, except the direct energy needed to grind the sample to specific target size, there will be an energy consumption for classification within the VRM. The energy consumption for

classification, using air cyclone, is defined on the basis of feed specifics, including feed size, its density, the product size as well as mill size, etc. Accordingly, the energy needed for classification can normally range from 50% and 100% of the energy needed for direct size reduction. However, in some cases when the coarse product is required, the energy consumption in classification may be higher than the energy needed for direct size reduction. Further calculations were done to define the total energy needed for comminuting and classifying the samples. Accordingly, the relation between the energy needed for grinding and classification were at 100% and 130% for sulfide ore and slag sample respectively. Consequently, the total energy needed for grinding and classification of sulfide ore and ferromanganese slag were estimated at 13.8 (kWh/t) and 8.9 (kWh/t) respectively.

Wear Consideration in Comminution

Grinding media wear represents a significant cost in comminution, particularly grinding. In general, the total wear process of grinding involves a number of mechanisms including abrasive and corrosive wear. More knowledge about the wear mechanisms and the relative importance of each wear component would enable one to better select grinding media for specific applications, and could lead to the development of alloys with improved resistance to wet grinding wear.

The impact of grinding media consumption on the cost of grinding. In fact, comminution accounts for an estimated 30–50% of typical mining operating costs, and of these, liner wear and media consumption account for roughly 50% of the cost. However, in some instances, media wear can constitute up to 40–45% of the total cost of comminution. Two types of wear are common in grinding practices. i.e., abrasion and corrosive wear. However, in dry grinding, the abrasion wear plays the role that is directly related to the abrasiveness of the material to be ground and the energy needed to size down the material to the specific size. Nevertheless, in wet grinding, the corrosive wear would be predominant which is affected not only by the inherent characteristics of the ore, but by pH and Eh of the environment, type of the media used, etc. Despite the fact that the energy consumption is higher in dry grinding, the wear is higher when wet grinding is employed for sizing down any specific ore/material.

Furthermore, the filling rate and size distribution of the media play a significant role in comminution efficiency and related cost. Improper size distribution or filling level of the media charge can reduce the efficiency of grinding, causing in losing media at higher rate. Accordingly, the cost associated with grinding media is chiefly determined by two factors, i.e., the wear performance (quality) and the price of the grinding media.

Moreover, it must be noted that in comminution practices there are power consumptions related to ancillary equipment and embodied energy in media manufacturing. Steel media, e.g., rods and balls, are frequently used in tumbling to assist in ore breakage. Media consumption can cost as much as comminution power consumption (Daniel et al., 2010). Additionally, the mining, smelting, casting, and shipping of media consumes a substantial quantity of energy. Therefore, the embodied energy consumed through media wear is an important factor to be considered in evaluating eco-efficiency in comminution. Apart from the understanding of the phenomena involved in the wear of grinding media, the media consumption is typically reported as steel grams required per ore ton of treated ore. Converting the media consumption into the embodied energy consumption can help in defining more eco-efficient comminution practices. Studies have revealed that the energy consumption to produce a ton of steel an average energy of 6 MWh is required. That is without considering of recycling through life cycle assessment. The production data indicated that 2 ton of CO₂ is emitted for producing a ton of steel (Yang and Broadbent, 2017). The energy consumed by diesel trucks can be between 0.15 and 0.25 kWh/kg.km (Nylund and Erkkilä, 2005). However, the figures may change for other alloys since the metallurgy of the media and type of alloy to be used plays a role herein. For example, forged balls and low/high chrome balls require completely different manufacturing processes and feed materials (Ballantyne 2018). Accordingly, the embodied energy to manufacture both forged balls, as well as high

and low chromium balls varies from 4.8 to 6.6 kWh/kg, depending upon metallurgy type, ratio of recycled steel in the feedstock, and other parameters including transportation transport the media to site. It must be added that considerable amount of CO₂ is emitted during production of steel and other alloys, which is indirectly contribute to global warming and reducing general eco-efficiency (CO₂ emission for steel production $\sim 2t_{CO_2}/t_{steel}$).

Furthermore, steel plants are water consumers that must be taken into account in a life cycle assessment of the comminution route. Steel is produced through two alternative routes, i.e., the integrated cycle, where steel is produced from virgin raw materials, and the electric route, which produces steel by melting scrap in an electric arc furnace (EAF). The average water intake for an modern integrated steelworks is 28.6 m³ per ton of produced steel, with an average water discharge of 25.3 m³ per ton of steel. For the electric route, however, the average intake is 28.1 m³ per ton of steel, with an average discharge of 26.5 m³ per ton of steel. Accordingly, the overall water consumption per ton of steel produced is between 1.6 m³ and 3.3 m³ per ton of steel (Colla et al., 2017). Steel plants use freshwater, salty and brackish ones, however, the water consumption in practices may vary and being higher base on the plant and related technology. For example, an average fresh water consumption of 7 - 8.3 m³ per ton of steel were reported for most big steel enterprises of China in 2008, which was merely lower at range of 3 to 4.2m³ per ton of steel (Gao, et al, 2011) in developed countries.

Accordingly, by reducing the wear/media consumption in comminution practices, possibilities offer towards reduction in embodied energy in comminution as well as conserving water per ton of reduction in steel and/or different alloy consumptions.

Wear Calculations in Comminuting Tested Samples

Although, there is no common formula/equation to determine the wear, there are different equations to estimate the wear in comminution, however, in defining the wear rate must be defined in practices by running comprehensive tests. There have been attempts in estimating wear rates in both dry and wet practices that are mainly based on collecting data from tests and plant practices. In general, as the ore abrasiveness is increasing the amount of wear is increased, however, as indicated above the wear rate is increased as the energy consumption to grind the raw material is increased. Furthermore, in wet grinding the mill electrochemistry, i.e., pulp pH and Eh, dissolved oxygen, etc., are determining factors. While, the type of media used in comminution is another determining factor. Based on the type of comminution, related energy consumption to achieve the target size, and the abrasiveness of the sample the media consumption can be calculated. Herein, the wear rates for grinding sulfide ore and ferromanganese slag were estimated considering steel media. The estimations were done based on Bond’s wear equations for dry and wet grinding. Nevertheless, the wear calculations were conducted on the basis of the equation proposed by (Giblett and Seidel, 2011).

Wear in Wet grinding (Bond equation)

$$\text{Wear Rate/Ball Consumption (kg/kWh)} = 0.159 \cdot (A_i - 0.015)^{0.33}$$

$$\text{Wear Rate/Ball Consumption (kg/t)} = \text{Energy Consumption (kWh/t)} * (0.159 \cdot (A_i - 0.015)^{0.33}$$

Wear in Wet grinding (Giblett and Seidel 2011)

$$\text{Wear Rat /Ball Mill Media (kg/kWh)} = 0.0817 \cdot (A_i)^{0.498}$$

$$\text{Wear Rate /Ball Mill Media (kg/t)} = \text{Energy Consumption(kWh/t)} * 0.0817 \cdot (A_i)^{0.498}$$

Wear in Dry grinding (Bond equation)

$$\text{Wear Rate (kg/kWh)} = 0.05 \cdot (A_i)^{0.5}$$

$$\text{Wear Rate (kg/t)} = \text{Energy Consumption (kWh/t)} \cdot 0.05 \cdot (A_i)^{0.5}$$

In general, there are different factors affecting the degree of media wear in comminution practices. The media type (metallurgy), the ore/sample abrasiveness, the type of comminution device rod, ball, stirred, roller, etc.), operational parameters in grinding (speed, tonnage, filling rate) and media size are the key factors defining the media wear.

Table 3 depicted the wear rate calculations for grinding the samples based on the abrasion index, A_i , and the energy consumption to grind the samples to the target size. Herein the wear was calculated based two different abrasion indexes. The calculations indicated that the wear in wet milling is considerably higher than that of dry milling. It seems that the wear calculations, based Bond equation in wet mode are rather high, however, the calculations based on Gibelett and Seidel (2011) show considerably lower values.

Table 3. Estimating the wear in milling samples

	Energy- Wet (kWh/t)	Energy- Dry (kWh/t)	Abrasion Index (A_i)	Wear* (g/t)– Wet (Bond equation)	Wear* (g/t) – Dry (Bond equation)	Wear [§] (kg/t)- Wet (Gibelett & Seidel)
Sulf-Ore	9.1	11.83	0.15 - 0.18	747 - 783	229- 251	289 – 316
FeMn Slag	14,8	19.24	0.38 - 0.51	1687 - 1865	593 – 687	747- 865

Wear in Grinding by VRM

The wear measurement for grinding the samples with VRM were estimated after the pilot test. The wear for grinding rollers was measured as the bulk wear rate over the complete duration of the grinding test.

For slag sample the wear was defined as 186 g/t of mild steel. In fact, the wear was measured with C45 mild steel rollers and determined as bulk average wear over the set point for the target particle size. That means the grinding media consumption is a level of medium to high based on the VRM grinding experiences. On the basis of industrial processes and the installed mill, in practice the use of different types of rollers have been experienced. Accordingly, the Metal Matrix Compound (MMC) grinding elements have considerably higher abrasive resistant, resulting is much lower specific grinding media consumption. The wear rate in industrial size Loesche VRM would, using MMC alloy, be considerably lower, i.e., about 15 times lower, than that of mild steel resulting in a specific wear rate of ~ 12 g/t.

In similar way the wear was calculated for sulfide ore. The bulk wear rate over the complete duration of the grinding test was defined as 129 g/t of mild steel. The lower wear rate for sulfide ore is due to lower abrasion index for the ore. Based on experiences in industrial processes, using Metal Matrix Compound (MMC) grinding elements, the grinding wear can be considerably reduced. Accordingly, the wear is reduced by about 15 times, resulting in a specific wear rate of ~ 8 g/t when the rollers are made from a high quality MMC material.

In fact, MMC has considerably higher abrasive wear resistant which is governed by a combination of both high hardness and toughness. MMCs are made of different hard components, including CW

(Tungsten Carbide) which significantly improves wear resistance and hardness in comparison with the composition of matrix. Due to strong metallurgical bond between the matrix and reinforced region considerably higher mechanical performances are expected, resulting in dramatically reduction in wear.

CONCLUDING REMARKS

Mining is one of the most energy intensive industries which consumes 6–7% of the world’s energy. Comminution is the most energy intensive within mining processes which is responsible for almost 50% of total energy consumption in mining, from which almost 90% goes for grinding part. Accordingly, comminution processes, in particular grinding, attempts have been made to introduce grinding equipment and flowsheets to conserve energy. According to an investigation by US Department of Energy (2007), there is a potential to reduce the energy consumption in US mining industry to half by implementing the best practices scenario(s) and conducting the outcomes from research and development (R&D) activities that improve technologies. The study indicated that there are certain areas that offer tremendous opportunities in energy saving. The largest energy saving opportunities were found to be grinding and materials handling.

Moving towards “Green Economy” requires responsible attempts to implement eco-efficient technologies. One identified technology would be dry comminution practices by using Vertical Roller Mill (VRM). Within this study, an effort was made to implement VRM technology in size reduction to grind the raw material to micron sizes and evaluate its potential in reducing energy and costs in mining industry. The results indicated that the energy consumption in grinding can be considerably reduced by implementing VRM technology in comparison with conventional tumbling mills. The reduction in energy consumption is much larger when comparing VRM grinding energy with conventional milling. Considering for the sulfide ore the reduction would be more than 30% while considering the energy for classification within VRM. The reduction in energy consumption is less when comparing wet ball milling with VRM, ranging from 2.5% to 7% for comminuting slag and sulfide ore respectively. However, considering the energy needed for classification, the reduction in total energy would be higher.

Furthermore, the results from media consumption showed promising prospect in reduction in wear which is an important part of operation cost in comminution practices. Reduction in wear indirectly reduced the energy consumption as the embodied energy in manufacturing wear parts, i.e., energy needed in metallurgy and related raw materials as well as energy for the transportation, etc.

At last, but not least, moving towards energy-efficient dry comminution, could preserve the water. Water consumption is reduced and its pollutant can be avoided or minimized. Water is valuable strategic asset and has become of strategic advantages. Mining activities impact the local water system resulting in contaminating and polluting the water sources due to dissociation of different ionic species and insoluble materials. Milling operation could be a source of contaminating/polluting the water. So, dry comminution can help in reducing water consumption and its pollutants. That also reduces the costs and energy in process water treatment. However, reduction in wear/media consumption, indirectly affects the water consumption in wear materials production.

REFERENCES

- Ballantyne, G. (2018). Energy Curve Enhancement Blog:7, Including grinding media consumption in the comminution energy curves.
- Colla, V., Matino, I., Branca, T., Fornai, B., Romaniello, L., Rosito, F. (2017). Efficient Use of Water Resources in the Steel Industry. *Water* 9, 874, 1-15.
- Daniel, M., Lane, G., McLane, E. (2010). Efficient, economics, energy and emission – emerging criteria for comminution circuit decision making. In Proceedings of XXV International Mineral Processing Congress (IMPC).

- Gao, C., Wang, D., Dong, H., Cai, J., Zhu, W., Du, T., (2011). Optimization and evaluation of steel industry's water-use system. *Journal of Cleaner Production* 19, 64-69.
- McKinsey, 2020. Climate risk and decarbonization: What every mining CEO needs to know. <https://www.mckinsey.com/business-functions/sustainability/our-insights/climate-risk-and-decarbonization-what-every-mining-ceo-needs-to-know>.
- Michaux, S. (2011). Sustainability in Comminution Design: Six Caveats that will change Mining Culture and Design. SMI Lecture, <http://www.ceecthefuture.org/publications/sustainability-in-comminution-design-six-caveats-that-will-change-mining-culture-and-design/>
- Morrison, R.D., & Cleary, P.W. (2008). Towards a virtual comminution machine. *Minerals Engineering* 21, pp. 770–781.
- Nylund, N-O., Erkkilä, K. (2005). Heavy-duty truck emissions and fuel consumption simulating real-world driving in laboratory conditions, DEER Conference, Chicago, Illinois.
- Roland, C.A., (2002). Selecting of Rod Mills, Ball Mills and Regarding Mills, in *Mineral Processing Plant Design, Practice and Control, Vol 1*, pp. 710-754
- Schaefer, H.U. (2001). Loesche vertical roller mill for the comminution of ores and minerals. *Minerals Engineering*, 14(10), pp. 1155-1160.
- U.S. Department of Energy, (2007). Mining Industry Energy Bandwidth Study. 47 pp.
- World Mining Data, (2021), International Organizing Committee for the World Mining Congresses, <https://www.world-mining-data.info/wmd/downloads/PDF/WMD2021.pdf>

**EFEMÇUKURU ALTIN MADENİ ATIK DEPOLAMA TESİSİNİN EKİM 2020 EGE DENİZİ DEPREMİNDEKİ
DURAYLILIK PERFORMANSI**
*STABILITY PERFORMANCE OF EFEMÇUKURU GOLD MINE WASTE STORAGE FACILITY IN OCTOBER 2020
AEGEAN SEA EARTHQUAKE*

G. Uzunçelebi^{1,*}, S. Ennis², E. R. Castro², Y. S. İNCİ¹, H. Ürkmez¹

¹ *TÜPRAG Efemçukuru Altın Madeni, İZMİR*
(* Sorumlu yazar: gorkem.uzuncelebi@tuprag.com)
² *Stantec, CANADA*

ÖZET

30 Ekim 2020 tarihinde merkez üssü Ege Denizi olan 7.0 (USGS) büyüklüğünde bir deprem Türkiye'nin batısında bulunan İzmir ili ve çevresini etkilemiştir. Meydana gelen deprem, yüksek nüfuslu bölgeler dahil olmak üzere geniş kapsamlı bir alanı etkileyen yer sarsıntıları ile birlikte tsunami taşkınlarına, yapıların çökmesine ve 118 kişinin ölümüne neden olmuştur. Deprem merkez üssü, İzmir şehrine yaklaşık 63 km ve Efemçukuru Altın Madeni sahasına yaklaşık 50 km uzaklıkta yer almaktadır. Efemçukuru Altın Madeni'nde yeraltı madencilik faaliyetleri süresince flotasyon atıkları ve ekonomik olmayan kayaçlar olmak üzere iki tip maden atığı ortaya çıkmaktadır. Flotasyon atıklarının bir kısmı macun dolgu olarak yeraltında kullanılmakta ve bir kısmı da susuzlaştırılarak yerüstünde inşa edilmiş kuru atık depolama tesisinde depolanmaktadır. Tüm ekonomik olmayan kayaçlar ise yerüstündeki depolama tesisinde ayrı olarak depolanmaktadır. Bu makalede söz konusu depremin karakteristik özellikleri, mevcut maden atık depolama tesislerinin deprem yükleri altındaki duraylılık performansı ve ve acil durum müdahale planının devreye alınması sunulmaktadır. Belgenin ayrıntıları görsel gözlemlere ve izleme araçlarına dayalı olarak sismik tasarımın ve ilgili performansın incelemesini içermektedir. Kuru atık depolama tesisi odak alınarak saha için hazırlanan mevcut atık yönetim sistemine ve deprem öncesi ve sonrası yapılan uygulamalara değinilmektedir. Acil durumlarda ve atık depolama tesisinin deprem yükleri altında performansını arttıracak yönetim stratejileri işletmeci ve tasarımcı işbirliği ile yıllar içinde başarılı bir şekilde geliştirilmiştir. Bu yönetim stratejisine de değinilecektir.

Anahtar Kelimeler: 2020 ege denizi depremi, efemçukuru altın madeni, sismik tasarım, acil durum planı, atık yönetim sistemi, işletme, bakım ve izleme kılavuzu (İŞBİK)

ABSTRACT

On 30 October 2020 the city of Izmir was impacted by an earthquake of magnitude 7.0 (USGS) originated in the Aegean Sea. The earthquake produced wide-ranging effects including tsunami run-up, ground shaking with local zones of high intensity that led to the collapse of structures and 118 fatalities. The epicenter was located at approximately 63 km from the city of Izmir and at approximately 50 km from the Efemçukuru mine site. The Efemçukuru mine site produces mine waste that is composed of tailings and uneconomic mine rock. A portion of the tailings and all uneconomic mine rock are stored in a surface storage facility. The remaining tailings material is stored underground. This document will describe the characteristic of the earthquake and the performance of the mine waste facilities and the emergency response plan. Details of the facilities seismic design and associated performance based on monitoring instrumentation will be presented. A focus will be placed on the current tailings management system for the site and their implementation pre and post-earthquake. Management strategies for dealing with upset conditions and improving the seismic performance of the structure

have also been developed successfully over time through a close operator designer cooperation. These management strategies will also be discussed.

Keywords: 2020 aegean sea earthquake, efemçukuru mine site, seismic design, emergency response plan , tailings management system, operation maintenance and surveillance (OMS)

GİRİŞ

Ege Denizi (Samos Adası) depremi 30 Ekim 2020'de sırasıyla Yunanistan ve Türkiye'de yerel saatler ile 13:51/14:51'de meydana gelmiştir. Deprem sonucunda, her iki ülkede yüksek yoğunluklu yerleşim bölgelerini kapsayan geniş bir alanda yer sarsıntıları meydana gelmiş, bazı bölgelerde tsunami oluşumları gözlenmiş ve birçok yapının hasarlanması ve yıkılması nedeni ile 118 kişi hayatını kaybetmiştir. Depremden etkilenen bölgelerde sivilaşma, yer değiştirme ve kaya düşmeleri gibi çeşitli jeoteknik etkiler de gözlemlenmiştir.

Çalışma Alanı

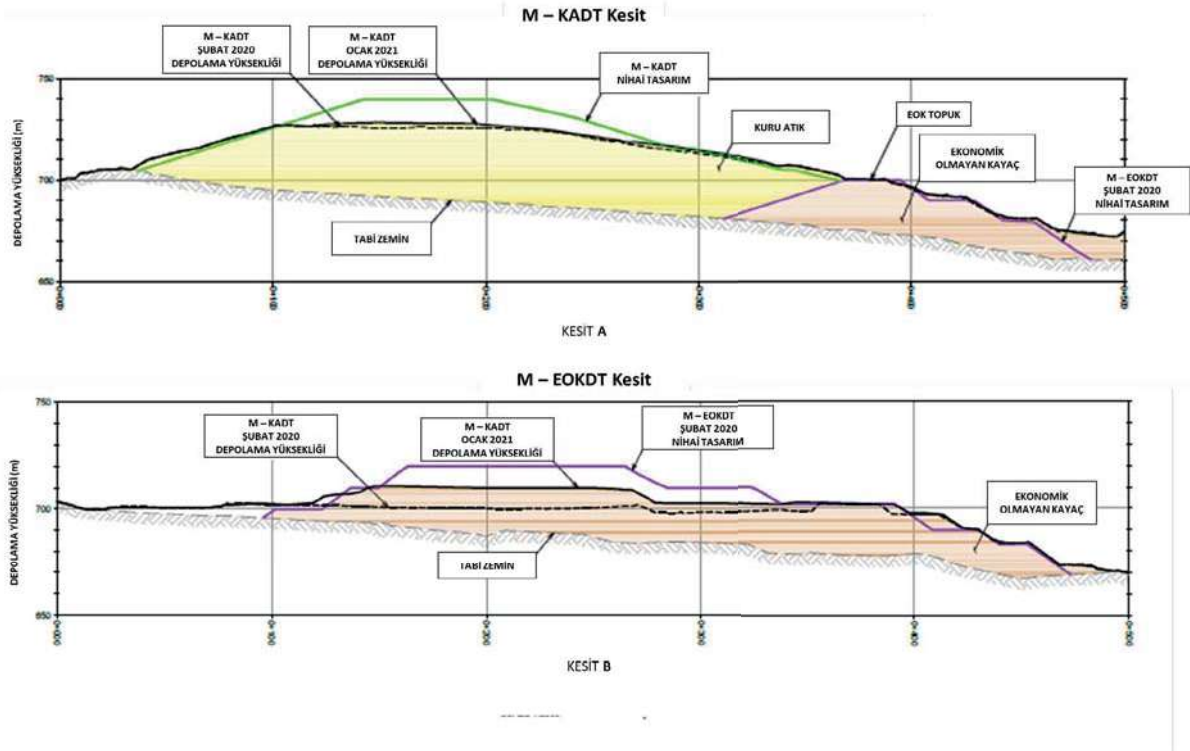
Efemçukuru Altın Madeni, Türkiye'nin batısında, İzmir İli'nin yaklaşık 45 km güneyinde bulunan bir yeraltı madenidir. Maden sahası, deniz seviyesinden 550 ila 770 metre yükseklikte, yarı kurak, dağlık bir bölgede yer almaktadır. Bölgedeki genel topografya, dik tepeler ve dar vadilerle karakterizedir. Farklı yağışlı ve kurak mevsimlere yayılmış ortalama yıllık yağış yaklaşık 740 mm'dir. Madencilik faaliyetinden süresince oluşan atıklar, flotasyon atığı ve ekonomik olmayan maden kayaçlarını (pasa) kapsamaktadır. Flotasyon atıklarının bir kısmı yeraltı madenciliğin tamamlandığı alanlarda macun dolgu olarak tahkimat amaçlı olarak yeraltında kullanılmakta, kalan malzeme ise susuzlaştırılarak yerüstü kuru atık depolama tesisinde depolanmaktadır. Yeraltından çıkarılan pasa ise yerüstünde belirlenmiş ayrı bir alanda depolanmaktadır. Yerüstünde mevcutta kullanılan maden atık depolama tesisleri; Merkez Kuru Atık Depolama Alanı (M-KADT – C-TSF), Merkez Ekonomik Olmayan Kaya Depolama Alanı (M-EOKDT – C-MRSF) ve Güney Kuru Atık Depolama Alanı (G-KADT – S-TSF) olmak üzere Şekil 1.'de gösterilmektedir. Genel depolama tasarımında pasa depolama tesislerinin yerleşimi kuru atık depolama tesislerini destekleyecek şekilde entegre edilmiştir.



Şekil 1. Efemçukuru Altın Madeni Yerüstü Maden Atıkları Depolama Tesisleri Yerleşimi (Kasım 2020)

Flotasyon Atığı (tailings) tesiste filtrelenerek susuzlaştırılan atıklardır, ekonomik olmayan maden kaya (pasa) ise yeraltı çalışmalarından çıkarılarak taşınan ve yüzeyde depolanan malzemedir. Hem kuru atık depolama alanları hem de ekonomik olmayan kaya depolama alanları su tutucu baraj yapıları gerektirmeyen ve duraylı yapılar olarak tasarlanmış ve inşa edilmiştir (Şekil 2.). Sahanın performans hedeflerini karşılaması adına kuru atıkların ve ekonomik olmayan kayaların yerleştirilmesi için saha atık yönetimi ekibi (yerüstü işleri birimi) tarafından sıkı yerleştirme ve sıkıştırma prosedürleri ve QA/QC uygulamaları ile yürütülmektedir. Efemçukuru Altın Madeni Kuru Atık Depolama Tesis’inde herhangi su birikimi yapılmamakta yada sıvılaşabilir malzeme tutulmamaktadır. Efemçukuru Altın Madeni’nde Kuru Atık Depolama Tesisi (KADT) ve Ekonomik Olmayan Depolama Tesisi (EOK) “Atık Dökümü ve Atık Depolama Tesisi Derecelendirme ve Tehlike Sınıflandırma Sistemi” (Waste Dump and Stockpile Rating and Hazard Classification System (WSRHC-Hawley and Cuning, 2017)) değerlendirmelerine dayalı olarak, “Orta Derecede (moderate) Riskli” tesisler olarak sınıflandırılmıştır (Stantec, 2019a ve 2019b).

KADT ve EOK tesisleri, geçirimsizlik sistemi sızıntı suyunun yer altı suyuna karışmasını önleyecek şekilde hazırlanan zemin üzerinde farklı jeosentetik geçirimsizlik malzemeleri kullanılarak inşa edilmiştir. Merkez ve Güney KADT sahalarında, birincil ve ikincil (çift astar) geçirimsizlik tabakaları ve aralarına yerleştirilen bir sızıntı tespit sistemi mevcuttur. Kuru Atık Depolama alanında jeosentetik kil astar (GCL) ve pürüzlü jeomembran kullanılmıştır. EOKDTY sahalarında ise jeomembran ile geçirimsizlik sistemi ile inşa edilmiştir. Depolama alanlarından kaynaklanan yüzey suyu akışı ve sızıntı suları, kanallar ve drenaj boruları sistemi vasıtasıyla çökeltme havuzunda toplanmakta ve atıksu arıtma tesisine gönderilmektedir. KADT ve EOKDT için tasarım depolama kapasiteleri sırasıyla yaklaşık 2,54 Mm³ kuru atık ve 1,51 Mm³ pasadır. 2011’den beri faaliyette olan madende, maden atık depolama tesislerinin hali hazırda nihai kotlarına ulaşan bazı kısımlarında yasal mevzuatlara uygun olarak kapatma (rehabilitate) çalışmaları yapılmıştır (Şekil 1.). M-KADT ve M-EOKDT atık yerleşim kesitleri Şekil 2.’de gösterilmiştir.



Şekil 2. Efemçukuru Altın Madeni Yerüstü Maden Atıkları Depolama Tesisleri Atık Yerleşimi (Kasım 2020)

Sismik Tektonik Hareketler

Ege Denizi bölgesinde, tarihsel olarak son 100 yılda 250 km'lik bir yarıçap içinde M6'dan daha büyük olan, orta ila büyük sismik derecede, yaklaşık 29 deprem meydana gelmiştir. Bölge etrafındaki sismotektonik ortam kompleks bir yapıya sahiptir, güneyde Afrika levhası kuzeye doğru Avrasya levhasının (Helen Yayı) altına dalar; doğuya doğru ise Anadolu levhası kuzey kenarında sağ yanal faylanma sürerek batıya doğru hareket eder. Tipik olarak, bölgedeki sismik olaylar, Helen Yayı'nın güneye doğru göçü tarafından yönlendirilen kuzey-güney uzantılarıdır. Daha yakın yıllarda bölge, 1956 yılında Yunanistan'da 20. yüzyılın en büyük sismik olayı olarak kabul edilen M 7.7 büyüklüğündeki bir depremle sarsılmıştır. (Çetin K.O.2020)

30 Ekim 2020 Ege Denizi Depremi

30 Ekim 2020'de Yunanistan'ın Samos Adası açıklarında Ege Denizi merkezli bir deprem (M 7.0) meydana gelmiştir. Deprem, Samos Adası'nın kuzeyinde, Avrasya levhasında siğ kabuk derinliğinde normal faylanmadan kaynaklanmış ve odak mekanizma çözümüne dayalı olarak, olay doğuya veya batıya doğru uzanan ve kuzey-güney yönlü uzantılı olarak gerçekleşmiştir. Büyüklük, bu fay için tahmin edilen maksimum büyüklüğü biraz aşmaktadır ve tarihsel arşivler, bu fay üzerinde son 19 yüzyılda bu büyüklükte bir olaya işaret etmemektedir (Çetin vd. 2020).

Yerel kuvvetli yer hareketi istasyonları fay kırılmasından sonraki 200 km içinde Yunanistan'da 11 ve Türkiye'de 66 adet olmak üzere deprem kaydetmeyi başarmış, ayrıca 200'den fazla ivmeölçer, kırılmadan 600 km'ye KADTr olan depremleri kaydetmiştir. Bu enstrümanlardan ikisi kırılma düzleminden yaklaşık 10 km uzaktadır ve en güçlü kayıtlar bu ölçümlerden sağlanmıştır (yaklaşık 0.23 g'lık pik yer ivmesi ve yaklaşık 22 cm/s'lik pik yer hızı).

USGS (ABD Jeoloji Araştırma Kurumu) tarafından geliştirilen çevrimiçi araçlar kullanılarak en yüksek yer ivmesi (PGA) konturları ve 1 saniyedeki (Sa-1s) spektral ivmenin konturları Şekil.3'te gösterildiği gibi oluşturulmuştur.



Şekil 3. Deprem konumu ve Pik Yer İvmelerinin konturları. Veriler USGS web sitesinden uyarlanmıştır.



Şekil 4. Deprem konumu ve 1 saniyedeki Spektral İvmenin konturları. Veriler USGS web sitesinden uyarlanmıştır.

Ekim 2020 Depremi sırasında sahada bir ivmeölçer olmamasına rağmen, bu projeksiyonlara dayanarak Efemçukuru Altın Madeni sahasındaki PGA'nın 0.1g ile 0.2g arasında olduğu ve Sa-1s'nin 0.2g'den yüksek olduğu tahmin edilmektedir.

Efemçukuru Altın Madeni'ne ait KADT ve EOKDT'nın Temel Sismik Tasarım Özellikleri

2016 yılında Stantec (eski adıyla Norwest Corp.), 7,2 büyüklüğündeki bir depreme dayalı olarak sismik değerlendirmeler için aşağıdaki tabloda (Tablo.1 ve 2) verilen KADT ve EOKDT tasarım temel kriterlerini geliştirmiştir. Çalışma alanında geçmişte kayıtlı sismik olayların potansiyel şiddeti göz önüne alındığında, tasarım kriterlerinde yer değiştirme membranlı alandaki potansiyel kayma yüzeyleri için 20

cm'den daha az ve membranlı alanı kesmeyen kayma yüzeyleri için ise 50 cm'den daha az olacak şekilde belirlenmiştir.

Çizelge 1. KADT ve EOKDT Duraylılık Tasarım Kriterleri (Güvenlik katsayısı değerleri)

Değerlendirme	Yükleme Koşulu	Tasarım Kriteri Hedefi
Statik	İnşa sırasında veya sonunda Uzun Dönem	Güvenlik Faktörü ≥ 1.3 Güvenlik Faktörü ≥ 1.5 Güvenlik Faktörü ≥ 1.0 Tolere Edilebilir Yer Değiştirme $\leq 20\text{cm}$
Sismik	Eşdeğer Sismik (Pseudo-static)	(Membranlı alanlar) Tolere Edilebilir Yer Değiştirme $\leq 50\text{cm}$ (Membranlı alanlar)
	Deprem sonrası (operasyon)	Güvenlik Faktörü ≥ 1.2

Çizelge 2. KADT ve EOKDT Sismik Tasarım Kriterleri

Döngü periyodu	PGA	Sa (02s)	Sa (1.0s)	Tasarım Dönemi
475 yılda 1	0.485	1.215	0.485	Operasyonel
2475 yılda 1	0.972	2.43	0.97	Kapama

KADT ve EOKDT yapıları, ulusal mevzuat gerekliliklerini ve Kanada Madencilik Birliği yönergelerini takip etmek için geliştirilmiş bir işletme, Bakım ve İzleme (İŞBİK -OMS) kılavuzuna sahiptir. Deprem sonrası tesislerin performansı ile ilgili yapılması gereken izleme faaliyetleri yüzey prizma istasyonları, piyezometreler ve dikey su seviyesi gözlem boruları, sızıntı akışı izleme ve kapsamlı görsel denetimler olarak belirlenmiştir. Deprem sonrası izleme faaliyetlerine aşağıdaki bölümlerde yer verilmiştir.

Deprem Sonrası Yapılan Müdahaleler ve Sahanın Performansı

Acil Durum Hazırlık ve Eylem Planı

Efemçukuru Madeni için hazırlanan Kuru Atık ve Ekonomik Olmayan Kaya Depolama Tesisleri Acil Durum Eylem Planı'nda (KADT ve EOK ADEP / Emergency Response Plan - ERP), atık depolama tesislerinde meydana gelebilecek jeoteknik duraysızlık ve tehlike durumlarında veya acil durumlarda müdahalede rehberlik edecek ve yardımcı olacak bir dizi prosedür bulunmaktadır. Acil Durum Eylem Planı dökümanının, TÜPRAG'ın İŞBİK gibi mevcut yönetim sistemlerini desteklemesi ve maden genelini kapsayan Acil Durum ve Kriz Yönetim Planı (ADKYP - Emergency and Crisis Management Plan / ECMP) ile entegre edilmesi amaçlanmıştır.

Kuru Atık ve Ekonomik Olmayan Kaya Depolama Tesisleri için hazırlanan Acil Durum Eylem Planı aşağıdakileri içerir:

1. Acil Durum Eylem Planını etkinleştirmek için prosedürler ve alınacak önlemler de dahil olmak üzere, KADT ve EOKDT'de tesislerinde duraylılık ile ilgili beklenmedik acil durumlara müdahale etmek için bir plan,
2. KADT ve EOKDT tesislerini etkileyebilecek farklı olası tehlikelere karşı alınacak önlemler,
3. Potansiyel olarak etkilenen alanlar ve altyapı ile birlikte olası hasar alanlarını gösteren uygulanabilir haritalar ve tablolar,

4. Acil duruma müdahale etmek için gerekli kaynakların listesi,
5. Görev ve sorumlulukların listesi ve ilgili personelin iletişim bilgileri,
6. Acil bir durumda genel komut zinciri ve dahili bildirim protokolü,
7. ADEP'i test etmek için prosedürler ve sıklıklar; ve
8. ADEP yönetimi ve güncellenmesi için prosedürler.

Deprem Müdahalesi Planı

Depremler Kuru Atık ve Ekonomik Olmayan Kaya Depolama Tesisi şevlerinin fiziksel duraylılığını etkileyebilir, bu nedenle Efemçukuru kuru atık ve EOK depolama tesisleri için hazırlanan tasarımlarda sismik hususlar dikkate alınmıştır. Oluşabilecek hasar depremin büyüklüğüne, kaynağından olan mesafelere ve yer hareketinin özelliklerine bağlı olabilir. Acil Durum Eylem Planı yönetimi veya olay sonrası acil inceleme gerektiren durumların özeti Çizelge 4'te verilmektedir.

Çizelge 4. ADEP Yönetimi veya Olay Sonrası Acil İnceleme Gerektiren Deprem Olaylarının Özeti

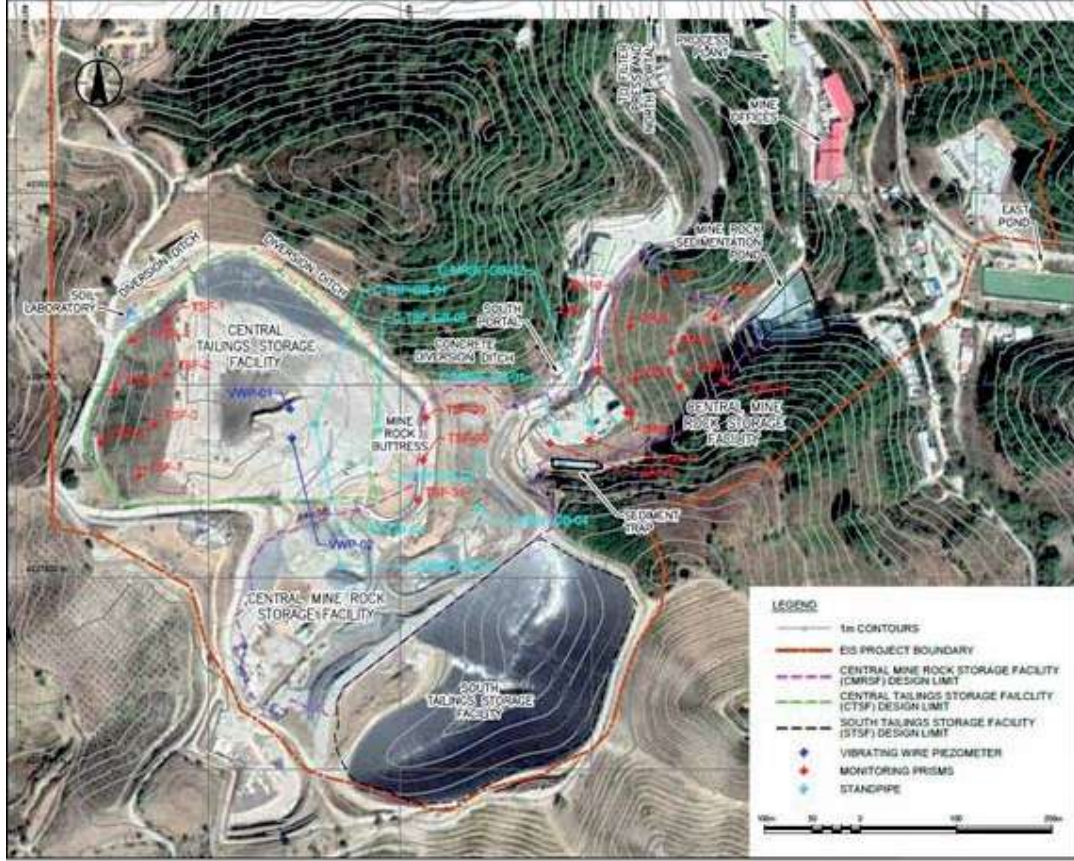
Richter Deprem Büyüklüğü	Yapıya Uzaklık (Km), ICOLD'den, 1998
> 4.0	≤ 25 km
> 5.0	≤ 50 km
> 6.0	≤ 80 km
> 7.0	≤ 125 km
> 8.0	≤ 200 km

Deprem Müdahalesi

Ekim 2020'de meydana gelen depremin hemen ardından yaşanan sismik olayın maden atık depolama tesislerine ve ek olarak yerüstü ve yeraltı altyapısı da dahil olmak üzere madendeki bir dizi yapıyı olumsuz etkileme potansiyeli nedeniyle tüm saha çapında Acil Durum ve Kriz Yönetim Planı etkinleştirilmiştir. İlgili tesislerin derhal denetlenmesi ve ardından izleme kayıtlarının kontrol edilmesi dahil olmak üzere Kuru Atık ve Ekonomik Olmayan Kaya Depolama Tesisleri Acil Durum Eylem Planında belirtilen prosedürler takip edilmiştir. Görsel incelemeler, izleme sonuçları ve sızıntı tespit sisteminin gözden geçirilmesi sonucunda KADT ve EOKDT yapıları üzerinde gözlemlenebilir hiçbir olumsuz etki tespit edilmemiştir. İzleme lokasyonları Şekil 5.'te verilmiştir.

Deprem sonrası ADEP ve İŞBİK prosedürlerine uygun olarak Tüprag Efemçukuru Altın Madeni Atık Depolama tesisleri sorumlusu ile Kayıt Mühendisi (Engineer of Record - EoR) ve ilgili firması Stantec arasında aşağıdaki iletişim zinciri gerçekleşmiştir:

1. 30 Ekim 2020'de Tüprag Efemçukuru Altın Madeni, Kayıt Mühendisi'ne deprem olayı hakkında herhangi bir görsel hasar gözlemlenmediğini ve tüm personelin güvende olduğunu bildirmiştir.
2. 3 Kasım 2020'de Tüprag Efemçukuru Altın Madeni, Kayıt Mühendisi'ne deprem sonrası verilerin işlenmesi ve incelemesi için aşağıdaki izleme noktalarının verilerini göndermiştir:
 - 2.1. Dikey Su Seviyesi Gözlem Boruları: C-TSF-GB-01, C-TSF-GB-02, C-TSF-GB-03, C-MRSF-GB-01, C-MRSF-GB-02, C-MRSF-GB-03, C-MRSF-GB-04, C-MRSF-GB-05 verileri,
 - 2.2. Sızıntı Tespit Sistemi verileri,
 - 2.3. Piyezometre okuma: VWP-01 ve VWP-02 (Merkez KADT tabanında yer alan piye-zometreler) verileri.



Şekil 5. Efemçukuru Altın Madeni Maden Atıkları Depolama Tesisleri İzleme Lokasyonları

İlk verilerin incelemesi sonucunda Kayıt Mühendisi, deprem olayının tesisler üzerinde olumsuz etkisi olduğuna dair bir bulgu olmadığını belirtmiştir. 5 Kasım 2020 tarihinde Kayıt Mühendisi, Efemçukuru’nda alınan önlemleri destekleyen, İŞBİK kılavuzunun ve Acil Durum Eylem Planı’nın ilgili prosedürlerini takip etmenin önemini vurgulayan bir rapor göndermiştir.

20 Kasım 2020 tarihinde Tüprağ Efemçukuru Altın Madeni, Kayıt Mühendisi’ne incelenmek üzere bir deprem olayı raporu ve ayrıca aşağıdakileri içeren ek saha bilgileri göndermiştir:

1. AFAD ve Boğaziçi Üniversitesi Kandilli Rasathanesi Deprem Araştırma Enstitüsü’nden 30 Ekim 2020 tarihine ait deprem teknik raporları,
2. M-KADT ve M-EOKDT deformasyon prizmaları okuma değerleri,
3. Sızıntı tespit sistemi izleme kayıtları.

İzleme bilgilerinin gözden geçirilmesi sismik olayın ölçeği hakkında daha fazla ayrıntı sağlamıştır. Prizma okuma değerleri normal aralıklar dışında herhangi bir değişim göstermemiş ve sızıntı gözlem noktalarında herhangi bir değişiklik gözlenmemiştir.

Saha Performansı

Yukarıda belirtilen önlemleri takiben, maden atıkları depolama tesisleri sorumlusu olan Tüprağ Efemçukuru Altın Madeni Yerüstü Birimi tarafından, görsel inceleme bulgularını özetleyen bir deprem raporu ve aşağıdaki Çizelge 5’te sunulan tesislerin izleme verilerinin olduğu bir ön inceleme çizelgesi hazırlamıştır.

Çizelge 5. Tüprag Efemçukuru Altın Madeni Yerüstü Birimi Deprem Sonrası İnceleme Özeti

Yapı	Kontroller	İnceleme	Sonuç
I. Kuru Atık Depolama Alanı			
a. Şevler	Çatlak, Oturma, Şişme Deformasyon	Görsel inceleme: tespit edilmedi. Deformasyon Noktaları ölçümü	Geçti Geçti
b. Membran Yüzeyleri	Hasar	Görsel inceleme: tespit edilmedi.	Geçti
c. Piezometre Ölçümleri	Piezometre Seviyesi	Piezometre ölçümleri	Geçti
d. Dikey Su Gözlem Borusu	Su Seviyesi	Aletsel Ölçüm	Geçti
e. Membran Altı Sızıntı Boruları	Sızıntı	Görsel inceleme: tespit edilmedi.	Geçti
II. EOK Depolama Alanı			Geçti
a. Şevler	Çatlaklar, Oturma	Görsel inceleme: tespit edilmedi.	Geçti
b. Membran Yüzeyleri	Hasar	Görsel inceleme: tespit edilmedi.	Geçti
c. Dikey Su Gözlem Borusu	Su Seviyesi	Aletsel Ölçüm	Geçti
III. Rehabilitasyon Alanları			Geçti
a. Şevler	Deformasyon	Deformasyon Noktaları ölçümü	Geçti
IV. Betonarme Su Yapıları			Geçti
a. KADT Ön Sediman Yakalama Havuzu	Yapısal Bozukluk	Görsel inceleme: tespit edilmedi.	Geçti
b. EOKDT Sediman Havuzu (WRSP)	Yapısal Bozukluk	Görsel inceleme: tespit edilmedi.	Geçti
c. Doğu Havuz (East Pond)	Yapısal Bozukluk	Görsel inceleme: tespit edilmedi.	Geçti
d. Kuşaklama Kanalları	Yapısal Bozukluk	Görsel inceleme: tespit edilmedi.	Geçti
e. Diğer Yönlendirme Havuzları	Yapısal Bozukluk	Görsel inceleme: tespit edilmedi.	Geçti
V. Depolama Alanları Çevreyolları			Geçti
VI. Kuzey Portal			Geçti
	Çatlak, Oturma	Görsel inceleme: tespit edilmedi.	Geçti

Sismik olayın hemen ardından özellikle takip edilen unsurlar şev duraysızlığı ve astar hasarına yol açan iç deformasyon potansiyeli ile ilgili oluşabilecek olumsuzluklardır. Görsel incelemeler, prizmalardan elde edilen deformasyon ölçümleri ve sızıntı sisteminin izlenmesi sonucunda şev duraysızlığı ve astar hasarı sorununun olmadığını görülmüştür. Merkez Kuru Atık Depolama Tesisi'nde geçirimsizlik tabakası yakınlarına yerleştirilen piyezometre verileri incelendiğinde boşluk basınçlarında sıvılaşma ile ilişkilendirilebilecek herhangi bir sıradışı artış tespit edilmemiştir. Bu durum, atık depolama tesislerinin inşaat ve işletilme sürecinde uygulanan kalite kontrol prosedürlerinin etkinliğini açıkça ortaya koymaktadır.

SONUÇ

20 Ekim Ege depremi, İzmir bölgesinde yapısal hasar ve ölümlerle sonuçlanan önemli bir bölgesel sismik olay olmuştur. Deprem önemli bir büyüklükte (M 7.0) olmasına rağmen, Efemçukuru Altın Madeni sahası için yaşanan sismik ivme için tahminler 0,2 aralığında bir PGA hesaplanmıştır. Bu, 0,485'e eşit bir PGA olarak belirlenen operasyonel tasarım kriterlerinden çok daha düşüktür. Görsel inceleme ve izleme kayıtlarının sonuçları KADT ve EOKDT yapılarının performansının sismik olaydan olumsuz şekilde etkilenmediğini göstermiştir. Sahadaki tasarım, inşaat ve izleme uygulamaları göz önüne alındığında da bu beklenen bir durumdur.

Sismik olayın büyüklüğü tasarım kriterlerinin altında olsa da maden atık yönetim ekibinin verdiği yanıt, acil durum eylem planının değerini ve atık yönetimi ekibinin prosedürleri uygulamadaki etkinliğini göstermiştir. Sorumlu personelin bildirimini, olay sonrası hızlı denetimler ve izleme ve kayıt mühendisi ile iletişim, sahanın genel Acil Durum ve Kriz Yönetim Planına uygun olarak tamamlanmıştır. Efemçukuru Altın Madeni sahasındaki deneyim, atık yönetim planının geliştirilmesinde MAC-TSM standartlarının sağladığı rehberliğin önemini ve yapılan uygulamalar sonrasında ekibin çabalarının karşılığını aldığını göstermektedir.

KAYNAKLAR

- Canadian Dam Association (CDA), (2014). Technical Bulletin: Application of Dam Safe-ty Guidelines to Mining Dams.
- Cetin, K.O., Mylonakis, G., Sextos, A., Stewart, J., (2020). Seismological and engineering effects of the M 7.0 Samos Island (Aegean Sea) Earthquake. HAAE (Greece), EEA & EF (Turkey), EERI (USA), GEER-069. Dec. 31, 2020.
- Eldorado Gold Corporation, (2017). Eldorado Gold Corporation Environmental Policy. October 2017
- Hawley, P.M. and Cunning, J., 2017. Guidelines for Mine Waste Dump and Stockpile Design. 2017
- Mining Association of Canada (MAC), (2019). Tailings Management Protocol.2019
- Norwest Corporation, (2018). Review of Efemçukuru's Gold Mine's Tailings Management System and with MAC's Tailings Management Guidelines. January22, 2018
- Norwest Corporation, (2015). Efemçukuru Mine: 2015 Central Valley Tailings Storage Facility Site Investigation and Liquefaction Assessment – Rev 0. December 18, 2015
- Norwest Corporation, (2014). 2013 CPT & Drilling Investigation – Summary and Evaluation Rev. 0. May 8, 2014
- Developing an Operation, Maintenance, and Surveillance Manual for Tailings and Water Management Facilities, Mining Association of Canada (Second Edition). February 2019.
- Stantec Consulting International Ltd., (2019a). Central TSF Classification and Risk Assessment Rev. 1. PowerPoint Presentation. December 2019
- Stantec Consulting International Ltd., (2019b). Central MRSF Risk Assessment Rev. 0. PowerPoint presentation. October 2019
- Stantec Consulting International Ltd., (2019c). Efemçukuru Central TSF 2019 Site Investigation and Instrumentation Plan – Rev. 0. December 2019
- Stantec Consulting International Ltd., (2020a). Assessment of Effectiveness of the Mine's Tailings Management System 2019 Memorandum. February 2020
- Stantec Consulting International Ltd., (2020b). July 2020 Preliminary MRSF Capacity Optimization Analysis. PPT document. July 10, 2020
- Stantec Consulting International Ltd., (2020c). October 2020 Earthquake Event-EOR Report. December 23, 2020
- Tüprag Metal Madencilik, (2014). Crisis & Emergency Management Plan. Document No EFM-5000-Pln-001T. April 2014

EFEMÇUKURU ALTIN MADENİ'NDE FİLTRELENMİŞ ATIK DEPOLAMA YÖNTEMİ UYGULAMASI APPLICATION OF FILTERED TAILINGS STORAGE METHOD AT EFEMÇUKURU GOLD MINE

Y.S. İnci ^{1,*}, P. Kimball ², G. Uzunçelebi ³, H. Ürkmez ⁴, M.A. Erol ⁵

¹ TÜPRAG Efemçukuru Altın Madeni, İZMİR
(*Sorumlu Yazar: yavuz.inci@tuprag.com)

² Stantec, CANADA

³ TÜPRAG Efemçukuru Altın Madeni, İZMİR

ÖZET

Efemçukuru Altın Madeni'nde uygulanmakta olan Filtrelenmiş Atık Depolama Yöntemi madenin atık yönetim planının bir parçasıdır. Özütleme tesisinden filtre tesisine pompalanan şlam , bu tesiste pres filtreler kullanılarak susuzlaştırılır. Ardından, susuzlaştırılan filtre keki (Filtre edilmiş atık) tabanı düşük geçirgenlikli tabakalarla kaplanarak inşa edilmiş olan bir Atık Depolama Alanı'nda depolanır. Bu yöntem, sıvılaşma riskinin azalması nedeni ile depolanan yığının fiziksel duraylılığının artması, malzemenin istiflenerek yığılabilmesi nedeni ile daha küçük depolama alanı gerektirmesi, yüksek miktarlarda su depolama ihtiyacının olmaması, depolama alanı yüzeyinde yapılacak rehabilitasyon işlerinin erkenden , kademeli olarak başlanabilmesine olanak sağlayarak çevresel getirisinin yüksek olması nedenleri ile, son yıllarda, dünya madencilğinde, giderek artan sayıdaki madende uygulanır hale gelmiştir. Bu yazıda, Filtrelenmiş Atık Depolama Yöntemi uygulamasının getirileri anlatılmakta ve sahada yapılan uygulamadan elde edilen pratik bilgiler paylaşılmaktadır.

Anahtar Sözcükler: Filtrelenmiş atık, filtrelenmiş yığın, filtrelenmiş atık yönetimi, sürdürülebilir madencilik, mevcut en iyi uygulamalar (MEU – BAP), mevcut en iyi teknikler (MET- BAT)

ABSTRACT

The Efemçukuru Gold Mine uses the filtered tailings storage method as part of its mine waste management plan. Slurry is pumped from the ore process plant to the filter plant where it is dewatered using filter presses. The dewatered filter cake (Filtered Tailings) is then stored in a tailings storage facility constructed with a low permeability base liner. This method has been increasingly applied in mining in recent years due to several benefits, including improved physical stability of stored tailings by mitigating the risk of liquefaction, reduced storage footprint due to stacking of material, not storing large volumes of water (i.e., no supernatant pond), and the environmental advantages associated with progressive reclamation. This article discusses the benefits of implementing the filtered tailings storage method and shares practical information obtained as a result of direct operational experience.

Keywords: Filtered tailings, filtered stack, filtered tailings management , sustainable mining, best available practices (BAP), best available techniques (BAT)

GİRİŞ

Efemçukuru Altın Madeni İzmir ili sınırları içindeki bir madendir. Üretim yeraltı işletmesinden yapılmakta olup günlük cevher üretimi yaklaşık 1.500 ton'dur. Cevherin zenginleştirilmesi sonucunda, su içeriği %60-70 oranında olan şlam ortaya çıkmaktadır. Bu şlam bir filtre tesisine (Şekil 1) pompalanmakta ve bu tesiste jeoteknik nem oranı %20'nin altına düşürülmektedir.



Şekil 1. Efemçukuru Madeni filtre tesisi

Madende inşaat işlerine 2008 yılında başlanmış, üretim ve de filtre tesisi 2011 yılında faaliyete başlamıştır. Filtrelenmiş atık Filtrelenmiş Atık Depolama Alanı'na Kamyonlar ile nakledilmektedir. Atık depolama alanı düşük geçirgenliğe sahip sentetik tabakalar ile kaplanmıştır.

Efemçukuru Altın Madeni'nde Filtrelenmiş Atık Depolama Yöntemi'nin Türkiye' de ilk uygulandığı madendir. Bu uygulama sırasında dikkate değer tecrübeler elde edilmiştir. Bu bildiriye, Filtrelenmiş Atık Depolama Yöntemi uygulamasının sağladığı faydalar anlatılmakta ve sahada yapılan çalışmalarda elde edilen Pratik bilgiler paylaşılmaktadır.

Filtrelenmiş Atık Depolama Yönteminin Alışlagelmiş Yöntemlere Kıyasla Sağladığı Faydalar

Bu bölümde, atığın filtre edilmesi tekniğinin bir madende uygulanmasının sağlayacağı faydalardan bahsedilmektedir. Bu faydalar geleneksel atık teknolojisi ile kıyaslanarak sunulmuştur. Geleneksel atıktan kasıt su içeriği yüksek olup pompalanabilen şlamdır. Bu yöntemde şlam, atık içindeki su ve akışkan haldeki atığı emniyetli bir şekilde tutabilecek yapıların içine pompalanarak boşaltılır. Filtrelenmiş atık nedeni ile elde edilen faydalar şu şekildedir;

1. Filtrelenmiş atığın depolanma alanı geleneksel yöntem için gerekenden küçüktür. Bu durum iki nedenden dolayı böyledir; nem içeriği düşürülmüş olan atık duraylı bir yığın oluşturabilecek şekilde depolanabilir ve de sıkıştırılabilir, ikincisi filtrelenmiş atığın depolanması için bir baraj ya da su tutucu yapıya gerek duyulmaz. Geleneksel yöntemlerin uygulanabilmesi için bir atık barajı ve tutucu yapı gerekir. Baraj ve atık seviyesinin bu yapılar içinde güvenli bir yükseklikte oluşturulması gereklidir.
2. Önerilen yöntemde işletmede su geri kazanımı yüksektir. Filtre tesisinde elde edilen su sisteme, geleneksel yöntemlerdeki buharlaşma veya kaçaklar olmaksızın, doğrudan beslenebilir. Bu durum özellikle su kaynaklarının kısıtlı olduğu coğrafyalarda önemlidir. Ayrıca pompalama ve borulama işlerinde dikkate değer oranlarda azalacaktır.
3. Oluşturulan yapının duraylılığının yüksek olması nedeni ile bu yöntem bir su tutucu baraj yapısına gereksinim duymaz. Su tutucu atık barajlarının tasarım ve inşaatı bu yönetime kıyasla daha karmaşıktır.
4. Atıkların filtrelenerek depolanması, bir atık barajının patlayarak akış yönünde bulunabilecek insan, çevre ve altyapıya zarar vermesi riskini elimine eder. Bunun nedeni atıktaki suyun filtre tesisinde alıkonulması ve böylece oluşturulan atık yığınının sıvılaşma riskinin en aza indirilmesidir. Geleneksel yöntemde, doğal olarak, yeni gelen akışkan malzeme öncekinin üstüne yerleşir ve büyük hacimlerdeki atık potansiyel olarak sıvılaşabilir durumunu koruyarak birikir.

- Atıkların filtrelenerek depolanması yöntemi kademeli rehabilitasyon işlemini destekler. Bu, yeni sistemin en önemli getirilerinden birisidir. Bu sistemde rehabilitasyon, maden ömrünün daha başlarında, depolama alanlarının son durumuna kavuşan kısımlarında erkenden başlayabilir. Bu durum çevresel faydalar, toplum gözünde olumlu sonuçlar doğurur, rehabilitasyon işinin, dolayısı ile de ilgili maliyetlerin zamana yayılması nedeni ile de şirkete mali faydalar sağlar.
- Filtre edilen malzemenin taşınması kolaydır ve çalışmada esneklik sağlar. Susuzlaştırılan malzeme kolaylıkla, loder ile yüklenebilir (Şekil 2), kamyon ya da lastik bantlı konveyörler ile taşınabilir, dozer ile serilebilir ve silindir kullanılarak, tasarım gereksinimi doğrultusunda, sıkıştırılabilir.



Şekil 2. Filtrelenmiş atığın kamyonu yüklenmesi



Şekil 3. Filtrelenmiş atık depolama alanı geçirimsizlik sistemi inşaatından bir görünüm

- Filtrelenmiş atık depolama alanı inşaatına ait yatırım ve işletme maliyetleri geleneksel yöntemle kıyasla yüksek olabilir. İki sistemin maliyet karşılaştırması projeye ve tesis yerine özgü olacaktır. Diğer yandan ise firma yetkilileri şirketin sürdürülebilirlik performansını gözetiyor olacaktır. Bu sistemde elde edilen yüksek dayanıklılık, küçük depolama alanı gereksinimi, su geri kazanımı, kademeli rehabilitasyon uygulanması ve azalan izleme gereksinimleri nedeni ile elde edilen dikkate değer getirilerin de projenin tümünün değerlendirilmesine dahil edilmesi gereklidir. Filtrelenmiş atık depolama tesisi geçirimsizlik sistemi Maden Atıkları Yönetmeliği hükümlerine uygun şekilde inşa edilir (Şekil 3).

Efemçukuru'nda Filtrelenmiş Atık Depolama Uygulaması Sırasında Elde Edilen Tecrübeler

- Efemçukuru Altın Madeni'nde filtrelenmiş atık filtre, tesisinden atık depolama alanına, belden kırma kamyonlar ile taşınmaktadır. (Şekil 4) Malzemenin serilmesi işlemi geniş paletli bir dozer kullanılarak ince dilimler halinde yapılır. Nihai sıkıştırma işlemi ise bir silindir ile yapılır. (Şekil 5). Atığın alana yerleştirilmesi alttan üste doğru yapılır. Tabana döşeli geçirimsizlik sisteminin zarar görmemesi için ilk serim kalınlığı 50 cm. olarak uygulanır. Bu kalınlık alanda kullanılacak araç cinsine göre değişebilir. Daha sonraki tabaka kalınlıkları, serilen malzemenin uygun sıkıştırma için gereken nem içeriğine bağlı olarak en fazla 30 cm. olacak şekilde uygulanır.



Şekil 4. Filtrelenmiş atığın nakli




Şekil 5. Serme ve sıkıştırma

2. Geçirimsizlik sisteminin alana inşası hava sıcaklığının daha düşük olduğu, bu tabakaların birleştirilmesi (kaynak işlemleri) ise sıcaklığın daha yüksek olduğu zamanlarda yapılmalıdır. Alanda serim yapılırken, jeosentetik tabakalarda oluşabilecek kıvrımların kırılmamasına özen gösterilmelidir.
3. Filtre tesisinden depolama alanına gelen atığın nemi ve bu malzemenin serilip sıkıştırılmasını takiben sıkışma değerleri devamlı olarak ölçülmelidir (Şekil 6). Efemçukuru Altın Madeni filtrelenmiş atık için minimum sıkışma değeri %97 Standart Proktor olarak belirlenmiştir. Yeni projelendirme çalışmaları sırasında sahaya özel atığın kendine has sıkışma değeri tespit edilmelidir.

TÜPRAG		NÜKLEER PROKTOR DENEYİ RAPORU FORMU										
Sıhhiyet No		Uygulanma Tarihi	Sıhhiyet İşletme No	Sayfa No								
EYM-1110-Prot.2 Form 10.1		18/05/18		91								
Dünya No / Location of Field		Taliye Alanı / Tailing Area		Tarih / Date : 26.08.2017								
DÜZELTİLMİŞ TAYIN		TSP Değeri / TSP Value		Taliye No / Tailing No : 4								
Taliye Alanı / Tailing Area		Taliye Alanı / Tailing Area		Taliye No / Tailing No : 4								
Test No	Derinlik / Location	Taliye / Depth (cm)	Zaman (sn) / Time (sec)	Çöküş (mm) / Depth (mm)	H_w	w_L	e_v	S_u	Form	M/Baraj	Coordination / Koordinasyon	
1		15	300	15.5	17.6	2.136	1.840	1.850	89.7		427707	427707
		15	190	15.5	16.5	2.154	1.883	1.850	88.8			
2	Taliye Alanı	15	300	15.5	16.8	2.166	1.879	1.850	89.8		427723	427723
		15	190	15.5	16.1	2.148	1.889	1.850	89.9			
3	Taliye Alanı	15	300	15.5	16.3	2.208	1.805	1.850	97.8		427721	427721
		15	190	15.5	17.3	2.190	1.842	1.850	96.6			
4		15	300	15.5	16.9	2.198	1.879	1.850	89.4		427710	427710
		15	190	15.5	16.1	2.182	1.879	1.850	89.3			

Kısa Notlar / Notes: (1) - (4) : Hava Nem / Humidity



Şekil 6. Nükleer proktor test formu örneği

İstenen sıkışmanın temini için malzemenin nem içeriğinin uygun olması önemlidir. Bu nedenle istenen nem içeriği fizibilite çalışmaları sırasında tesbit edilmeli ve işletme sırasında da devamlı takip edilmelidir. Efemçukuru Altın Madeni için optimum nem içeriği (Jeoteknik nem) % 15,5 +/- 2' dir. Filtre tesisi malzemeyi her zaman optimum değerde üretemeyebilir ya da iklim koşulları nem oranını etkileyebilir. Nem oranı yüksek, çalışılan hava koşulları uygun ise, yüksek nemli malzeme daha ince kalınlıklarda serilebilir. Hava koşuluna bağlı olarak bu malzeme kısa süre tekrar serilmek üzere geçici bir yığın oluşturularak saklanabilir. Nem yüksek ve hava koşulları da uygun değilse bu malzeme, atık depolama tesisinde daha önceden tasarlanmış bir bölgede, mevsim koşullarının uygun olduğu zamanda serilmek ve sıkıştırılmak üzere saklanmalıdır. Alanda geçici olarak depolanan atıkların daha fazla neme maruz kalmaması için gerekli önlemler alınmalıdır.

Atığın alana serilmesi ve sıkıştırılmasının ardından yapılan ölçümler istenen sonucu vermez ise bu alan dozer ile riparlenerek nemini istenilen seviyeye kadar kaybetmesi sağlanmalıdır. (Şekil 7-8)



Şekil 7. Atığın nemini azaltabimesi için dozele yapılan ripperleme işlemi.



Şekil 8. Nemini azaltmış olan alanın tekrar serilerek sıkıştırılması.

Geçici olarak biriktirilen nemli malzeme iklim koşullarının iyileşmesini takiben, gelecek sezonun hazırlığı kapsamında, vakit geçirmeksizin kalite iyileştirme çalışmaları kapsamında yeniden işlenerek depolama alanına, taşınmalı, serilmeli, gerekirse ripperlenmeli ve kuruması sağlandıktan sonra sıkıştırma işlemi yapılmalıdır. (Şekil 9)

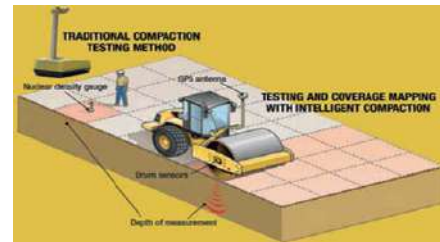


Şekil 9. Yüksek nem içeriğine sahip atık yığınının iyileştirilmesi çalışmaları

4. Nem, sıkıştırma değerlerinin tesbiti, değerlendirilmesi, takibi için, sadece Kuru Atık Depolama Alanı için hizmet vermek üzere, sahada bir laboratuvar kurulmalıdır. Ayrıca Akredite laboratuvarlarda malzemenin testleri (standart proktor, nem tayini, atterberg test, hidrometri, özgül ağırlık v.b.) düzenli olarak yaptırılmalıdır.
5. Sıkışma değerlerinin ölçümü için bir Nükleer Proktor Cihazı gerekecektir (Şekil 10). Cihazın temini, nakliyesi, saklanması, çalıştırılması için TAEK kurallarının gereklilikleri sağlanmalıdır. Sıkışma değerlerinin anlık takip edilebilmesi için silindirlere eklenen sistemler çalışma etkinliğini üst düzeye çıkarabilmektedir. Silindir operatörü bu sistem sayesinde anlık olarak, makina içindeki ekrandan, sıkıştırılmış alanları takip edebilmektedir. Ayrıca bu kayıtların dijital olarak depolanması sağlanabilmektedir. Hatta bu sistem sayesinde bilginin bilgisayarlardan anlık takibi de yapılabilmektedir. (Şekil 11)



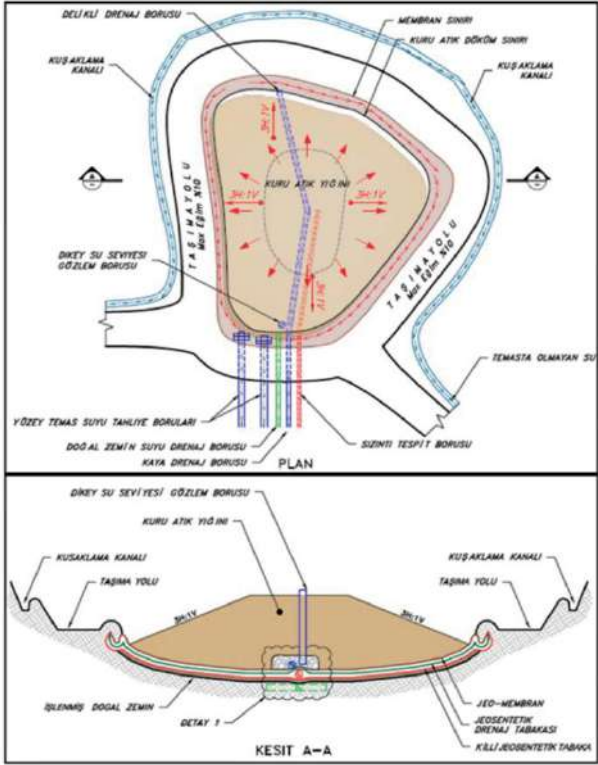
Şekil 10. Nükleer proktor cihazının kuru atık depolama alanında kullanılması



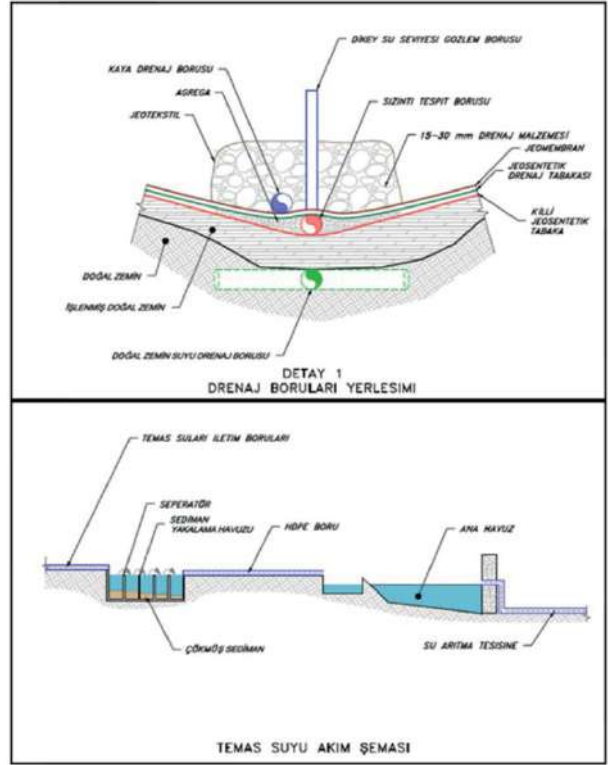
Şekil 11. Silindir kabinine yerleştirilerek zemin sıkışmasını ölçen sistem.

6. Filtre atığı nemi konusu çok boyutlu olarak ele alınmalıdır.
 - 6.1. Atık nemi filtre tesisi performansı ve iklim koşullarına bağlı olarak her zaman uygun miktarlarda olmayabilir. Bu nedenle alanda çalışan operatörler hangi malzemeyi sereceğini, hangi malzemeyi geçici stok alanında biriktireceğini iyi bilmelidir.
 - 6.2. Nem içeriği yağmur, kar yağışı, don, çığ, sıcak hava nedeni ile de etkilenecektir. Bu nedenle, filtre tesisinin ürettiği malzemenin özellikle aşırı yağıştan korunabilmesi için, filtre tesisi yakınında, atık depolama alanına gönderilmeden önce içinde 1-2 gün geçici depolama yapabileceğiniz kapalı bir alan oluşturulması faydalı olacaktır. Çığ oluşumu da alanda çalışma zorluğu yaratacaktır. Alana gelen malzemenin zamanında işlenmesi bu etkiyi azaltacaktır. Kar yağışı ya da don sonrasında da depolama alanında çalışmak zorlaşacaktır. Yağış sonrasında yüzeydeki karın ya da donan malzemenin temizlenmesi ve çalışma yüzeyinin kurumması beklenmelidir. Sonuçta, yağmur, kar, don, çığ sonrasında yüzeyler kurumadan yeni serime geçilmemelidir. Eğer nemli koşullarda yüzeylere yeni serim yapılacak olursa, altta kalan nemli malzeme yığında jeoteknik olarak zayıf tabakalar oluşturacaktır. Ayrıca nemi yüksek, kaygan yüzeylerde çalışmak iş güvenliği sorunları yaratacaktır.
 - 6.3. Nem içeriği yağışlar nedeni ile arttığı gibi aşırı sıcak iklim koşullarında, alana gelen atık serilip sıkıştırılmaz ise nem içeriği azalarak optimum nem değerinin altına düşebilir. Bu durumda malzemenin sıkıştırılması mümkün olmayacaktır. Bu nedenle alana gelen uygun neme sahip malzemenin vakit geçirmeksizin serilmesi ve sıkıştırılması gereklidir.
7. Meteoroloji istasyonları takip edilerek yağmur, kar, don, aşırı rüzgar vb. iklim olaylarının takibi yapılarak bu bilgiler ışığında çalışmalar yönlendirilmeli, bilgiler çalışanlara iletilmeli, olası aşırı iklim olaylarının etkilerine karşı önceden hazırlıklar yapılmalıdır.
8. Su Yönetimi' ne özel önem verilmelidir.

İşletme projesi hazırlanırken su bütçesi iyi irdelenmeli, ilgili kanallar ve boyutları, boru boyut ve sayıları olası su gelirini taşıyabilecek şekilde tasarlanmalıdır. Bölgeye ait tarihsel meteorolojik veriler toplanarak incelenmeli ve bu rakamlar su bütçesi hesaplarında yerini almalıdır. Su iletim hatları alanda, yığın içinde atık yığını tabanında su birikimine müsaade etmeyecek şekilde oluşturulmalıdır. (Şekil 13), (Şekil 12-13)



Şekil 12. Kuru atık depolama alanı su yönetim sistemi şematik örneği



Şekil 13. Kuru atık depolama alanı su yönetim sistemi ayrıntı şematik örneği



Şekil 14. Filtrelenmiş atık depolama alanından su boşaltımı için kullanılan borular

- Yağış sırasında atık depo yığınının yüzeyinden akacak suya karışacak sedimanı çöktürmek için bir sistem oluşturulmalıdır. Atık depolama alanından toplanan temas suyunun bir ana havuzda biriktirilmesi atıksu arıtma tesisinde arıtılması gerekmektedir. Yağış sırasında yığın yüzeyindeki aşınım nedeni ile suya bir miktar malzeme karışmaktadır. (Şekil 13) Sediman içeren bu suyun direk ana havuzun kapasitesi sedimanyükünden etkilenecektir. Bu durumun önlenmesi için bir ön sediman yakalama havuzu inşa edilerek sedimanın bu havuzda yakalanması sonrasında temas suyunun ana havuza yönlendirilmesi faydalı olacaktır. Bu ön havuz sisteminde çöktürülen sedimanın temizlenmesi işlemi bir ekskavatör ve kamyonlar kullanılarak kolayca yapılabilir. (Şekil 14) Temizlenen sedimanın kurutulması için atık depolama alanı üzerinde belirlenen bir kısımda geçici (dönemsel) kurutma havuzları hazırlanması faydalı olacaktır.



Şekil 15. Kuru atık depolama alanı yüzeyinin yağışlar sonrasındaki erozyon nedeni ile aldığı şekil



Şekil 16. Sediman yakalama havuzundan çamur temizliği yapılması

Yağış esnasında, depolama alanı yüzeyinde, yağış nedeniyle oluşabilecek bozulmaları dolayısı ile de suya karışacak sediman miktarını azaltmak için, depo yüzeyinde sentetik malzemeler kullanarak geçici kanallar oluşturmak faydalı olacaktır. (Şekil 17)



Şekil 17. Filtrelenmiş atık depolama alanında, erozyonun etkisini azaltmak üzere, oluşturulan geçirimsiz su atım kanalları

10. Alana döşenen su borularına ait bilgilerin kaydının tutulması gerekmektedir.

Çalışma alanına etkisi olan suların boru sistemleri (Şekil 18) ile toplanarak havuzlara iletilmesi gereklidir. Borulardan gelen suyun kalitesi, miktarı, sediman içeriği vb. konuların takibinin yapılması gereklidir. Bunun takibi için hangi borunun nereden su taşıdığının bilinmesi gerekir. Bu nedenle bu boruların döşenmesi sırasında gerekli kot, koordinat ölçümleri yapılarak bu bilgiler kayda geçirilmelidir.

Boruların su girişlerine, tıkanmaları önlemek için, yedekli su girişleri yerleştirmek ve bu girişlere uygun göz açıklığına sahip süzgeçler yerleştirmek yerinde olacaktır. (Şekil 19)



Şekil 18. Su borusu döşeme işleri



Şekil 19. Kesintisiz su akışına uygun hale getirilmiş boru ağı

11. Depolama alanının duraylılığının takibi için izleme sistemi oluşturulmalıdır.

Bu amaç için yığının içine piezometreler (Şekil 20), yığın boyunca su seviyesi dikey gözlem boruları (Şekil 21) yerleştirilebilir, su seviyesi kontrol kuyuları tesis edilebilir, deformasyon ölçüm noktaları (Şekil 22) oluşturulabilir. Buralardan alınacak periyodik ölçüm değerleri bir arşive kaydedilerek incelenmelidir.

TÜPRAG EFENCÜKURU		PİEZOMETRE DATA OKUMA RAPORU FORMU		291	
Doküman No EFM-1110-Prd-2-Fmr-0-T		Düzenlenme Tarihi 27/06/2013		Revizyon Tarihi ve No 08/03/2016 - Rev.01	
Sayfa No 1/1					
Name	Multi Channel VW Logger D32055	C.F	0.00025001 MPa/Pa	C.F	0.00024830 MPa/Pa
Serial Number	820396	T1	26.68.00.0	T1	26.68.00.0
Hardware Version	v1.29	T2	0.00002911 MPa/°C	T2	0.00002904 MPa/°C
Software Version	v1.09 (Aug 28 2013)	T3	15.99 °C	T3	16.80 °C
Sampling Status	LOGGING APPLIED	$P = C.F.(I1-I2) - T2(I1-T3)$			
Sampling Rate	40000				
Current Interval	1 Hours 0 Minutes 0 Seconds				
Start Time	Thu Nov 30 11:57:18 AM				
Current Time	Mon Dec 28 12:11:58 AM				
Number Of Samples	10				
Number Of Records	9886				
Current Upload Num / Error Code	1 / 200				
TIMESTAMP		RECORD BATTERY		PORT 1	
LOGSERIALTIME	ACTUAL DATE TIME TURKEY	VW 1	Therm 1	VW 2	Therm 2
Units		#	Volts	#	Volts
		#	deg.C	#	deg.C

Şekil 20. Piezometre izleme formu örneği

TÜPRAG EFENCÜKURU		MADEN ATIĞI BERTARAF TESİSLERİ SU SEVİYESİ GÖZLEM BACALARI KONTROL LİSTESİ				
Doküman No EFM-1110-Prd-2-Lst-2-T		Düzenlenme Tarihi 27/06/2013		Revizyon Tarihi ve No 30/03/2017 - Rev.03		
Sayfa No 1 / 2						
Kontrol Eden		Halil ÜRKMEZ		Tarih 13.05.2019		
				Hafta 20		
C-TSF-GB-01	N: 4237050.32 - E: 497711.30			C-TSF-GB-02	N: 4237050.06 - E: 497711.18	
	Baca Üst Kotu	721.95			Baca Üst Kotu	722.30
	Baca Alt Kotu	686.08			Baca Alt Kotu	685.89
	Baca Yüksekliği (m)	35.87			Baca Yüksekliği (m)	36.41
	Su Seviye Kotu	0			Su Seviye Kotu	0
Su Yüksekliği (m)	0	Su Yüksekliği (m)	0			
Gözlem Borusunda ölçülen su var mı?		EVET HAYIR		Gözlem Borusunda ölçülen su var mı?		
		✓		✓		

Şekil 21. Su seviyesi dikey gözlem boruları izleme formu örneği



Şekil 22. Deformasyon ölçüm noktası

12. Depolama alanına giriş-çıkış trafiğinin kesintisiz olabilmesi için, depolama alanında Zemin iyileştirilmesi yapılmalıdır.

Yağış sonrasında depolama alanı yüzeyi kayganlaşarak araç trafiğini olanaksız hale getirmektedir. Bu durumlarda araçların depolama alanına giriş, çıkış, manevra, boşaltma işlemlerinin aksamaması için alan içerisinde kullanılan yol yüzeyi geçici olarak inert kırmataş ile kaplanarak sorun çözülebilir. (Şekil 23)

13. Depolama alanı yüzeyinin her daim silindir ile sıkıştırılmış olmasının sağlanması gerekir. (Şekil 24)



Şekil 23. Kuru atık depolama alanında, kesintisiz nakil sağlamak amaçlı olarak oluşturulan sağlam zemine sahip bölge.



Şekil 24. Malzemenin serim sonrası silindir ile sıkıştırılarak kabuk oluşturulması

Filtrelenmiş atığın alanda dozerle serilmesini takiben, gecikmeksizin silindirle sıkıştırılmasının bir çok faydası vardır. Dozerin çalışması sonucunda dozer paletlerinin yüzeyde oluşturduğu parçalı yapı nedeni ile serilen malzeme nemini hızlı bir şekilde kaybedecektir. Hava yağışlı ise bu parçalanmış yüzey yapısı daha fazla suyun tutulmasını sağlayacaktır ve yığın yüzeyi çamur ile kaplı bir alana dönüşecektir. Halbuki, serimin ardından yüzeyin silindir ile sıkıştırılması yığın yüzeyinde bir kabuk oluşturarak (Şekil 25) sıcak hava koşullarında nem kaybını, yağışlı hava koşullarında su tutulmasını ve de sıcak ve rüzgarlı havalarda toz üretilmesini önleyecektir.



Şekil 25. Dozerle yapılan serimin ardından silindirin sıkıştırma işlemi yaparak alanın yüzey pürüzlülüğünü yok ederek kabuk oluşturması

14. Silindir ile yüzeyde oluşturulan kabuğun korunması gerekmektedir. Yığın yüzeyinde oluşturulan kabuğun korunabilmesi için, eğer burada bir araç trafiği var ise trafiğin aynı izi takip ederek sürdürülmesi sağlanmalıdır.
15. Çalışma alanlarından ortaya çıkabilecek toz miktarının en az seviyeye indirilmesi sağlanmalıdır. Depolama alanı ciddi bir toz kaynağı olabileceği gibi örneğin nakliye yolları da ciddi toz üretimine neden olabilir. Toz bastırma işleminin etkin kılınabilmesi için şu uygulamalar faydalı olacaktır.
 - 15.1. Depolama alanı yüzeyinde silindir ile kabuk oluşturulması ve korunması gereklidir. Yüzeylerin zaman zaman sulanması ve ardından kurumaya bırakılması bu kabuğun kalitesini artıracaktır.
 - 15.2. Depolama alanı yüzeyi ile nakliye yollarının yıkanması/sulanması için bir arazöz kullanılmalıdır. Bu arazöz üstten su püskürtme sistemi ile donatılmış olmalıdır. (Şekil 26-27)



Şekil 26. Atık nakliye yolunda toz bastırma amacı ile arazöz kullanılması



Şekil 27. Filtrelenmiş atık depolama alanının üstten püskürtme ile sulanması

15.3. Nakliye yollarının asfalt ile kaplanmış olması da toz üretimini azaltacak, tozla mücadeleyi kolaylaştıracaktır. (Şekil 28)

15.4. Nakliye yollarının temizliği için bir Zemin Temizleme Aracı çalıştırılmalıdır. (Şekil 29)



Şekil 28. Asfalt kaplamalı nakliye yolu



Şekil 29. Zemin temizleme aracı

15.5. Nakliye yolları boyunca kurulacak fiskiye sistemi de tozun bastırılmasına yardımcı olacaktır. (Şekil 30)

15.6. Asfalt yollar dışında kalan stabilize yol kısımlarında lingo-sülfat kullanımı tozla mücadelede etkin olacaktır.

15.7. Depolama alanının nihai şekline kavuşan kısımlarının rehabilite edilmesi bu kısımlarda toz üretimini sonlandıracaktır. (Şekil 31)



Şekil 30. Nakliye yoluna yerleştirilen fiskiyeler ile yapılan sulama işlemi



Şekil 31. Nihai duruma ulaşan yüzeylerde yapılan rehabilitasyon işlemi

16. Kış aylarında olabilecek kar yağışı, don gibi durumlarda kullanılmak üzere, kesintisiz nakliyenin sağlanabilmesi için, bir Kar Kürüme ve Yol Tuzlama aracının sahada bulundurulması faydalı olacaktır.(Şekil 32)



Şekil 32. Kar kürüme ve yol tuzlama aracı

17. Yapılan işlerin tümünü kapsayan bütünleşik bir yönetim sistemi oluşturulmalıdır. “Sürdürülebilir Atık Yönetimi” ne ait uluslararası ilkeler belirlenerek gerekleri yerine getirilmelidir. Firma tutarlı duruşunu, atık yönetimi konusundaki ilkelerini firmanın politika ve taahhütlerine yerleştirerek işe başlamalıdır. Şirket bu işte çalışanlara ait hiyerarşik yapıyı kurmalı, iş tanımlarını yazılı hale getirmelidir. Şirket işle ilgili ekonomik ve yasal gereksinimleri uygulayıcıya sunmalıdır.

17.1. Uygulayıcılar atık depolama alanlarındaki işleri kapsayan bir “ İşletme, Bakım, İzleme Kılavuzu” hazırlamalıdır. Bu kılavuzda depolama alanı sınıflaması, yasal gereklilikler, kılavuz kontrolü ve revizyonlar, yıllık gözden geçirme, roller ve sorumluluklar, yetkinlikler ve eğitimler, tesise ait tasarım ve işletme kriterleri, su yönetimi kriterleri, bitkisel toprak depolama işleri, saha ile ilgili toprak, erozyon, jeolojik, deprensellik, iklim vb. bilgiler, depolama alanı, filtre tesisi, çevresel koruma işleri, alanın bakımı ve performans izleme işleri, acil durum hazırlık planı hakkındaki bilgiler ayrıntılı olarak yer almalıdır.

17.2. Risk bazlı çalışma sistemi oluşturulmalıdır. Bu sisteme ulaşmak için; çalışma alanındaki tüm riskler tanımlanmalı, risk matrisi hazırlanmalı, risklerin yönetilebilmesi için gereken kritik kontroller belirlenmeli, acil durum başlatma eşik değerleri belirlenmelidir. Bunun sonucunda hazırlanacak “Acil Durum Eylem Planları” nın maden genelinde geçerli olan “Acil Durum Eylem Planı” ile uyumlu hale getirilmelidir.

18. Atık yönetim sisteminin iç ve dış denetlemeye tabi tutulması sağlanmalıdır.

19. Depolama alanı yöneticilerince her yıl için bir “Yıllık Gözden Geçirme Raporu” hazırlanmalı ve bu rapor firma yönetimine sunulmalıdır.

20. Depolama alanı dolgusu yükseldikçe, yapılan dolgunun istenen değerlere sahip olup olmadığının test edilebilmesi için, SPT (Standart Penetration Test)(Şekil 33), CPT (Conic penetration Test)(Şekil 34) çalışmalarının yapılması gereklidir.



Şekil 33. Filtrelenmiş atık depolama alanı'nda SPT çalışması



Şekil 34. Filtrelenmiş atık depolama alanı'nda SPT çalışması

21. Depolama alanı yüzeylerinde zaman zaman 3-4 metre derinliğindeki araştırma çukurlar kazılarak yapılacak olan sıkışma kontrolleri (Şekil 35) yapılan işin test edilebilmesi için iyi bir yoldur.

TÜPRAĞ - ELDORADO GOLD
EFEMÇUKURU ALTIN MADENİ / EFEMÇUKURU GOLD MINE

İSİA MÜHÜRÜ
İSİA MÜHÜRÜ

NÜKLEER PROKTOR DENEYİ / NUCLEAR PROKTOR TEST


Deney Yeri / Location of Test: Taling Alanı / Taling Area (Phase II)
Deney Malzemesi / Sample Material: Çarpıştırıcı / Compacted by Driller & Roller

Tarih / Date: 20.05.2024
Sayfa / Page: 01
Revizyon / Revision: 01

Deney No / Test No	Deney Yeri / Location of Test	Deney Malzemesi / Sample Material	Nükleer Proktor Deneyi / Nuclear Proktor Test		P _{max}	w _p	L _c	N _c	N _{max}	K _{max}	K _{min}	K _{avg}	K _{std}
			Uygulanmış / Applied	Ölçülen / Measured									
1	Taling Alanı / Taling Area (Phase II)	0.50 Lm	10	100	10.0	18.0	1.000	1.000	1.000	100.0	100.0	100.0	100.0
			10	100	10.0	18.0	1.000	1.000	1.000	100.0	100.0	100.0	100.0
2	Taling Alanı / Taling Area (Phase II)	0.50 Lm	10	100	10.0	18.0	1.000	1.000	1.000	100.0	100.0	100.0	100.0
			10	100	10.0	18.0	1.000	1.000	1.000	100.0	100.0	100.0	100.0
3	Taling Alanı / Taling Area (Phase II)	0.50 Lm	10	100	10.0	18.0	1.000	1.000	1.000	100.0	100.0	100.0	100.0
			10	100	10.0	18.0	1.000	1.000	1.000	100.0	100.0	100.0	100.0

* Aşağıdaki tabloların her bir satırında bir dizi veri bulunmaktadır.

Maden Kontrol / Quality Control: İSİA MÜHÜRÜ / İSİA MÜHÜRÜ
Talep / Request: Taling Alanı / Taling Area (Phase II)



Şekil 35. Test çukuru sıkışma izleme formu

22. Kuru atığın nakliyesi kamyonlar ile yapılacaksa kamyon damperinin polimer ile kaplanması dampere malzeme yapışmasını önleyecektir. Bu durum daha emniyetli ve düşük maliyetli çalışmanızı beraberinde getirecektir. (Şekil 36)



Şekil 36. Polimer ile kaplanmış kamyon damperi

SONUÇ

“Filtrelenmiş Atık Depolama Yöntemi” uygulaması dünya madenciliğinde, terkedilmekte olan geleneksel depolama yöntemleri yerine, uygulaması hızla artan bir yöntemdir. Bu yöntem atık depolama yöntemleri içinde “Mevcut En İyi Teknikler” (MET - BAT) ve “Mevcut En İyi Uygulamalar (MEU - BAP)” olarak kabul edilmiştir.

Efemçukuru Altın Madeni’nde yapılan uygulamalar , bu yöntemden beklenen faydaların fazlası ile elde edildiğini göstermiştir.

Önerilen yöntem ile oluşturulan atık yığınının mükemmel duraylılığa sahip olması nedeni ile atıkların yayılarak çevresel zararlar oluşturması olası değildir. Bu nedenle, maden yöneticilerinin işletme

projelerinin hazırlanması sırasında bu yöntemin uygulanabilmesi için özel gayret sarf etmeleri tavsiye olunur.

KAYNAKLAR

- Global Tailings Review (2020). Global Industry Standard on Tailings Management. <https://globaltailingsreview.org/global-industry-standard/>
- Mining Association of Canada (2019a). A Guide to the Management of Tailings Facilities *Version 3.1*. <https://mining.ca/our-focus/tailings-management/tailings-guide/>
- Mining Association of Canada (2019b). Developing an Operation, Maintenance, and Surveillance Manual for Tailings and Water Management Facilities *Second Edition*. <https://mining.ca/our-focus/tailings-management/oms-guide/>
- Norwest Corporation, (2014). 2013 CPT & Drilling Investigation – Summary and Evaluation Rev. 0. May 8, 2014
- Norwest Corporation, (2018). Review of Efemçukuru’s Gold Mine’s Tailings Management System and with MAC’s Tailings Management Guidelines. January 22, 2018
- Stantec Consulting International Ltd., (2019a). Central TSF Classification and Risk Assessment Rev. 1. PowerPoint Presentation. December 2019
- Stantec Consulting International Ltd., (2019c). Efemçukuru Central TSF 2019 Site Investigation and Instrumentation Plan – Rev. 0. December 2019
- Stantec Consulting International Ltd., (2020a). Assessment of Effectiveness of the Mine’s Tailings Management System 2019 Memorandum. February 2020
- TSM Tailings Review Task Force (2015). Report of the TSM Tailings Review Task Force. <https://mining.ca/documents/report-tsm-tailings-review-task-force/>

EFFECT OF HEMATITE MORPHOLOGY ON FLOTATION EFFICIENCY

T.D. Figueiredo ^{1*}, D.S. Moreira ², F. São José ², G.H.G. Rodrigues ¹, C.A. Pereira ¹

¹ *Federal University of Ouro Preto (UFOP), Dept of Mining Engineering*
 (*Corresponding author: thiagoduarte1926@hotmail.com)

² *Federal Center of Technological Education of Minas Gerais (CEFET/MG)*

ABSTRACT

Iron ore is the main mineral input in Brazilian production, being exploited in high quantities and from different minerals, among which stands out hematite (Fe₂O₃), mineral responsible for most of the national production of iron ore. Hematite presents different morphologies, occurring in the compact or specular form, which directly influences the efficiency of processing circuits, such as fragmentation and concentration. Knowing this, this work seeks, through microflotation tests, to evaluate the influence of morphologies of specular and compact hematite on flotation processes. The optimal operating conditions were determined by varying parameters such as pulp pH, nitrogen gas flow, reagent dosage and fragmentation mechanism. After the tests, the influence of morphology and type of hematite fragmentation for the flotation process were confirmed. The use of cationic collector allowed the mutual recovery of compact hematites and specular hematites. The ideal operating parameters were defined at: 50 cm³/min of nitrogen flow, collector dosage of 20 mg/L and pH ≥ 8, with flotation recoveries over 85% for all minerals conditions analyzed.

Keywords: Specular hematite, compact hematite, microflotation, floatability.

INTRODUCTION

Brazil is one of the largest producers of iron ore in the world, being this the main mineral input in terms of quantity and economic representativeness in the country. Currently Brazil is the third largest producer of iron ore globally, with production estimated at approximately 430 Mt, distributed in the states of Minas Gerais (with 82.9% of the national reserves), Pará (9.9%) and Mato Grosso do Sul (2.3%) (Jesus and Joaquim, 2017).

Iron ore in Brazil is found predominantly in the form of hematite (Fe₂O₃), also occurring in a smaller amount in minerals such as ilmenite (FeTiO₂), goethite (FeO(OH)) and magnetite (Fe₃O₄) (Gomes et al., 2013). Hematite, the most exploited mineral for iron production in Brazil, has varied morphologies, being found, for example, in its specular and compact form. These different morphologies for the same mineral stand out mainly in the physical and mechanical parameters, such as preferential fracture planes, mechanical resistance, shape and distribution of crystals. According to Gomes et al. (2013), compact hematite has higher mechanical strength, as well as reduced porosity and reducibility in relation to specular hematite.

For flotation to occur efficiently, several variables are taken into account, requiring to be conditioned according to optimal parameters, determined through laboratory tests. According to Aguiar (2014), in the last 40 years, the reverse cationic flotation has become one of the main methods used for hematite concentration. This process is normally performed using amine as the collector of silicate gangue minerals and starch as an iron oxide depressant.

The definition of the ideal flotation parameters of hematite therefore depends directly on its morphology. For this, one of the methods for analyzing the behavior of these minerals in processing plants is based on floatability tests, such as microflotation in Hallimond tubes. Through these tests, it is possible to compare different parameters for a flotation step and define the best operating conditions, whether for hematite recovery with specular or compact characteristics.

MATERIALS AND METHODS

The procedures performed during the present study are described in this topic. The characterization tests of the samples were carried out in CEFET-MG Campus II and UFMG material laboratories, while the remaining tests were carried out in chemistry laboratory of CEFET-MG Campus Araxá and UFOP Flotation laboratory. This work consisted of the analysis of representative samples of specular and compact hematite, both provided by Companhia Siderúrgica Nacional (CSN) – Casa de Pedra mine, with particle size above 150 µm.

Technological Characterization

For the technological characterization tests, a small portion of the hematite samples was reduced to less than 38 µm. The remaining material was sieved into size fraction of -150 + 106 µm for microflotation tests.

In order to analyze the influence of the fragmentation mechanism on ore characteristics, a fraction of specular hematite was fragmented by rod mill and another by disc mill. The same procedure was performed for the fraction of compact hematite, to compare the effects caused by different fragmentation mechanisms on the structure of ore grains and its behavior during the tests.

In technological characterization of the samples, their physical and morphological characteristics were determined and compared by Scanning Electron Microscopy (SEM). In addition, the specular and compact hematite samples were characterized by X-ray Diffraction analysis (XRD), seeking to determine the mineralogical composition of the samples, an important parameter for microflotation tests.

Microflotation

The microflotation tests were performed using the modified Hallimond tube, equipment coupled with a height extender, that reduces the hydrodynamic drag of fines particles during the process. This equipment allows to analyze the floatability of hematite using small samples of the mineral (aliquots from 1 to 2g).

To this end, a mathematical artifact is applied, capable of determining the degree of floatability of the mineral particle. Thus, the tendency of the mineral sample to be collected is represented by Eq.1.

$$Flotability (\%) = \frac{Flotated\ mass\ (g) \times 100}{Sample\ mass\ (g)} \quad (1)$$

The first floatability assay of compact and specular hematites aimed to evaluate the behavior of minerals in relation to variation of nitrogen gas flow in the system without reagents addition. For this, the pH of the solution was set at 10.5, a value that, according to Viana (2006), is in the ideal pH range for iron ore flotation.

After the system adjustment, the tests for natural floatability of specular and compact hematite were performed, increasing the flow of nitrogen injected into the system by 10 cm³/min at each assay.

The initial and final values of gas flow rate was 20 cm³/min and 110 cm³/min, respectively. Thus, it was possible to determine the optimal flow rate for flotation of each type of hematite.

The ideal flow rate was fixed and applied in the next tests, which evaluate the ideal dosage of reagents for hematite flotation. Collector reagent solutions (Amina Flotigam EDA 3) were prepared with 0.1% (w/v). The collector dosage had its minimum value defined at 0,5 mg/L, being gradually increased by 0.5 mg/L up to 2 mg/L. The dosage was then increased sequentially by 2 mg/L and the tests was performed until the final value of 12 mg/l.

Finally, with the optimal values of reagent dosage and gas flow defined, microflotation tests were performed to verify the optimal pH values of the system. By varying the pH values, it was possible to compare the optimal results found with the values suggested by the literature, and to determine whether the behavior of hematite during flotation follows the precepts already defined in previous studies. With the use of NaOH and HCl as pH modifiers, microflotation tests occurred at initial pH 2, ranging from 2 units to the maximum value of pH 12, in which the last test was performed. All tests performed in this stage were done in triplicate. Thus, the average values among the 3 results obtained are considered representative.

Zeta Potential

The tests for calculation of hematite Zeta potential, whose equipment used was Zeta Meter 4.0, were performed to determine the Point of Zero Charge (PZC) and the Isoelectric Point (PIE) of the mineral. For the tests, performed in duplicate, a solution of KNO₃ was used as indifferent electrolyte. The pH values analyzed were 2, 4, 6 8 and 10, being adjusted by pH modulators (NaOH and HCl) at a concentration of 1% (w/v).

RESULTS AND DISCUSSION

Technological Characterization of Hematite Samples

Initially, the X-ray Diffraction assays evaluated the purity of the samples, as illustrated by Fig. 1. It is possible to observe the presence of pure hematite compact samples (a), while the presence of quartz was observed with the specular hematites (b).

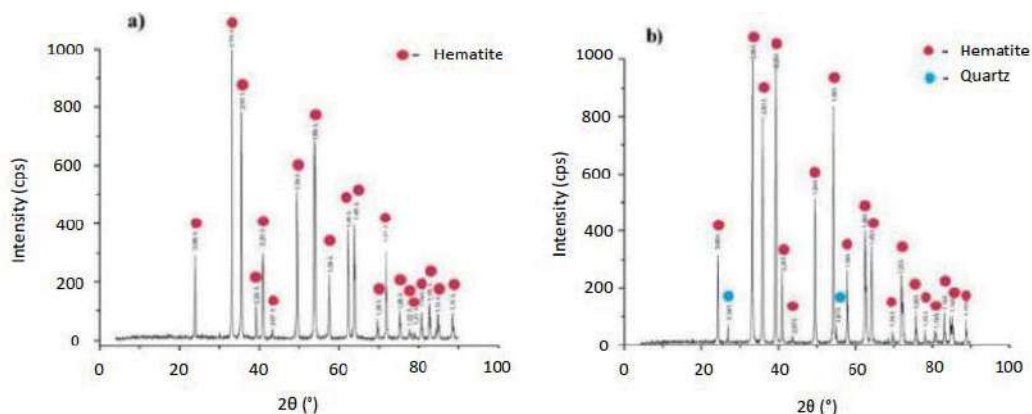


Figure 1. X-ray diffraction spectra of the hematite samples

The compact hematite samples have a high degree of purity. The specular hematite present quartz contamination promoting the reduction of the specific mass of the sample.

The analysis of the SEM results (see Fig. 2), allows us to observe that the hematites fragmented by disc mill (B and D) have greater homogeneity in relation to the samples cominuated by bar mills (A and C), presenting greater regularity in the size and shape of the grains.

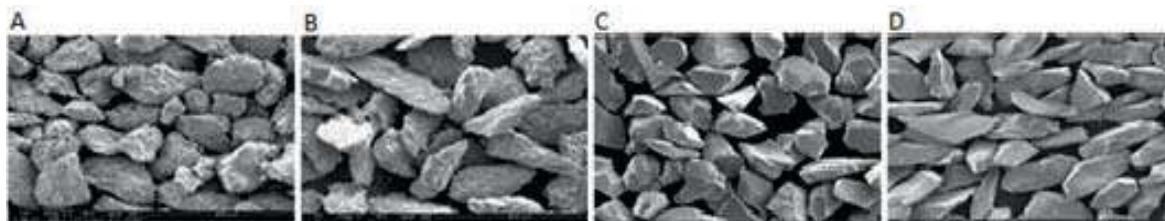


Figure 2. Specular hematite fragmented by bar mill (A) and disk mill (B). Compact hematite fragmented by bar mill (C) and disk mill (D)

There is also a difference between specular hematites (A and B) and compact hematites (C and D). The images suggest that specular hematite presents greater porosity, thus having a lower specific mass in relation to compact samples, in addition to a greater propensity to flotability.

Zeta Potential

As shown by Figure 6, the isoelectric point for compact hematite was approximately 7.2, while for specular hematite it was 6.8. It is noted that at pH above 7, the surface loads of hematites are negative, thus justifying the use of cationic collectors.

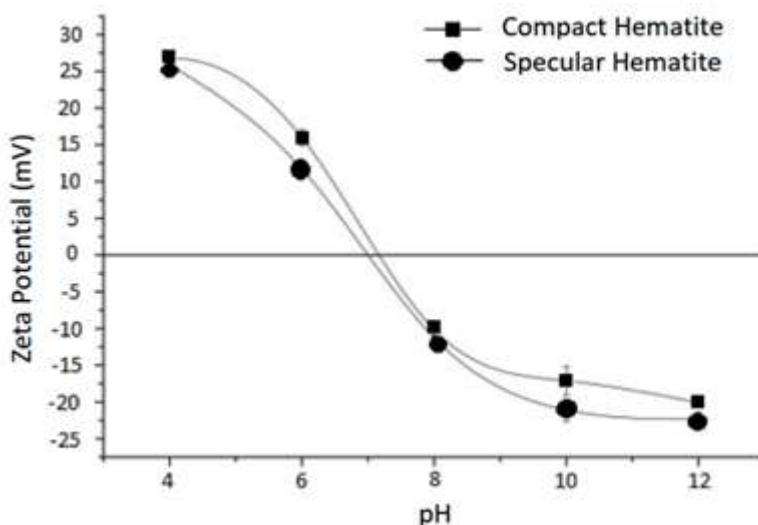


Figure 6. Zeta potential of compact and specular hematites

The zeta potential graph presents similar results to those obtained by Alexandrino (2012) and Henriques (2009). The authors performed Zeta potential tests for several iron minerals, including compact and specular hematite. As in the present article, the authors found isoelectric point values in pH range between 6 and 8.

Microflotation Tests

Flotation tests allowed the floatability of hematites in several scenarios to be evaluated. The first test sought to determine the natural floatability of hematites and optimal conditions of gas flow in the system, whose results are represented by Figure 3.

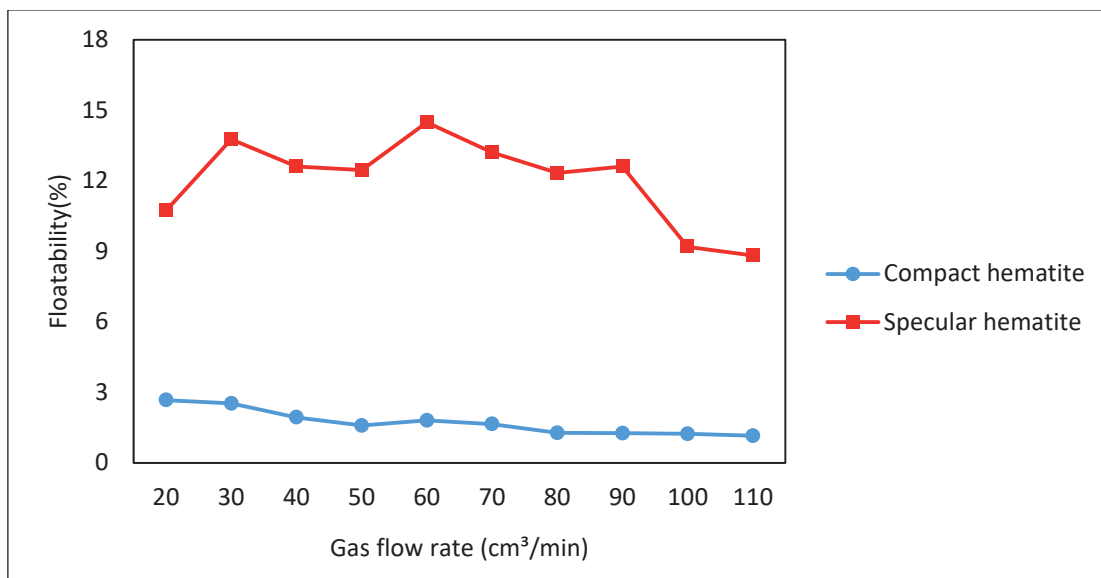


Figure 3. Natural floatability of compact and specular hematite vs gas flow ratio in pH 10.5.

It is possible to notice that compact hematite presents natural floatability up to seven times lower than specular hematite. This is due to the greater porosity of specular hematite, which decreases the specific mass of particles and increases their surface area, which facilitates their loading and increases the contact area for particle-bubble interaction.

In addition, the nitrogen flows that provided a higher floatability of hematites are in the range between 50 and 60 cm³/min, with floatability of 14.5% and 2% for specular and compact hematites, respectively. These values are supported by Baltar (2010), who defined that when gas flow is less than 50 cm³/min, an effective interaction between mineral particles and bubbles cannot be achieved, as well as high flows promote turbulence in the system and prevent adsorption from being stable. For all this, it was concluded that the optimal flow rate for the next microflotation tests was 50 m³/min.

Hematite floatability as a function of reagent dosage was performed with optimum gas flow (50 cm³/min). The results in Fig. 4 show that with the addition of collector in the system, the floatability of hematite increased significantly, reaching in some scenarios values above 80% for both specular and compact hematite.

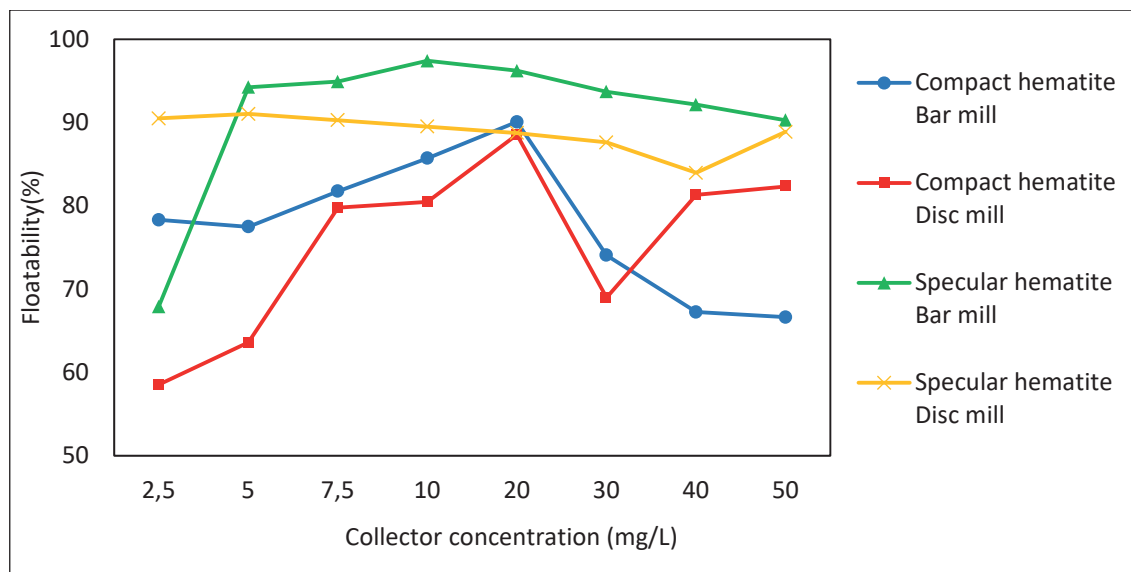


Figure 4. Effect of collector dosage on floatability of compact and specular hematite. (pH 10.5 and gas flow rate of 50cm³/min)

It is possible to observe a higher yield of specular hematites, in relation to compact hematite. The reagent dosage with the highest floatability was approximately 20 mg/L, with results between 85 and 95% of mineral recovery for all samples analyzed. However, it is seen that a small variation in this dosage value leads to a considerable drop in system yield, especially for compact hematite. Thus, the optimal rate of reagent dosage among those used in the assays was defined at 20 mg/L.

With the definition of optimum flow rate (50 cm³/min) and collector dosage (20 mg/L), the optimum pH for hematite flotation was determined. It is observed in Fig. 5 that the best results were obtained at pH 8, where the four samples analyzed present similar results, with floatability near of 90%. With the increase in pH, the floatability of hematites did not change significantly. Corroborating Viana (2010), at pH 10 the recovery values of hematite remained high.

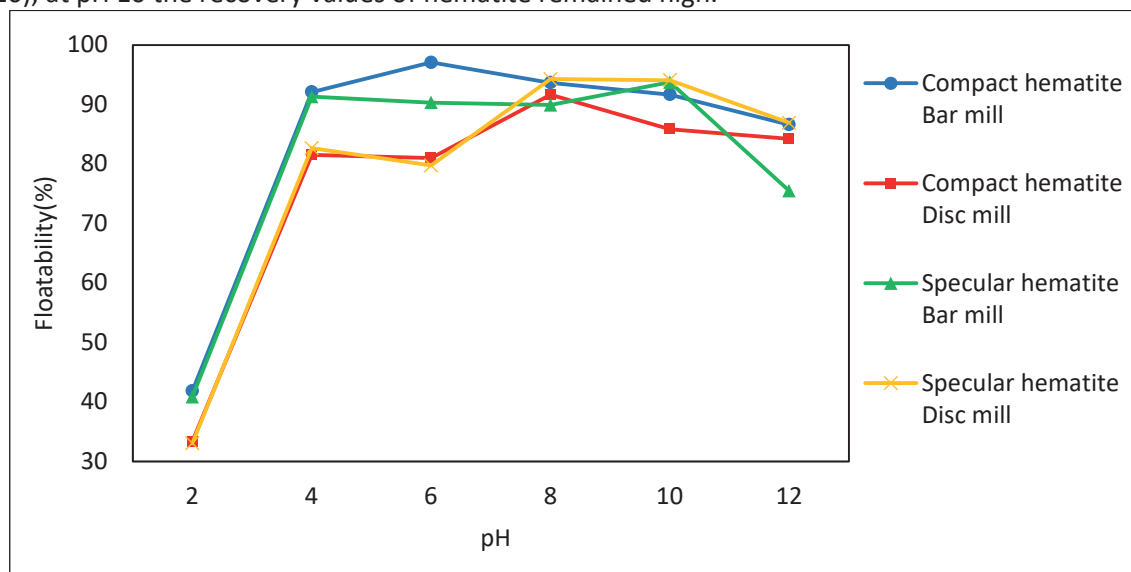


Figure 5. Effect of pulp pH on floatability of compact and specular hematite (Collector dosage of 20 mg/L and gas flow rate of 50cm³/min)

CONCLUSIONS

After analyzing the behavior of the compact and specular hematites of the Casa de Pedra Mine in flotation processes, it is perceived that the morphology of minerals has a direct and significant influence on the efficiency of their recovery. Specular hematites, because they had a lower specific mass and higher porosity in relation to compact ones, showed higher flotability.

With the addition of cationic collector, this difference was reduced, giving the mutual recovery of specular and compact hematites, with average floatability in the range of 85%. The optimal operational parameters for the cationic flotation of hematites were defined at: 50 cm³/min of Gas flow rate, collector dosage of 2 mg/L and optimum pH in range equal or above 8. Finally, after the Zeta potential assays, the PIE values for the specular and compact hematites were defined, being located at pH values 6.8 and 7.2, respectively.

THANKS

The authors thanks CNPq, Gorceix Foundation, CEFET-MG and UFOP for the support and trust deposited during the performance of this work.

REFERENCES

- Aguiar M. (2014). Clatratos na Flotação Catiônica Reversa de Minério de Ferro, Msc. Thesis, Engineering School of Federal University of Minas Gerais, Belo Horizonte, M.G., 108 pp.
- Alexandrino J. (2013). Correlação Entre Estado de Dispersão, Propriedades Eletrocinéticas e Flotabilidade de Hematita. Dsc.D. Thesis, Engineering School of Federal University of Minas Gerais, Belo Horizonte, MG, 125 pp.
- Baltar, A. (2010). Flotação no Tratamento de Minérios.(2rd. ed., Vol. 1). Recife, Editora Pernanbuco.
- Gomes, O Iglesias, J., Paciornik, S., Vieira, M., (2013). Morfometria e Classificação Automática de Hematita em Minérios de Ferro. 44th Seminário de Redução de Minério de Ferro e Matérias-Primas & 4th Simpósio Brasileiro de Minério de Ferro & 1st Simpósio Brasileiro de Aglomeração de Minério de Ferro. Belo Horizonte, Brazil.
- Henriques, A. (2012). Caracterização e Estudo das Propriedades Eletrocinéticas dos Minerais de Ferro: Hematita, Goethita e Magnetita. Msc. Thesis, Federal University of Minas Gerais, Belo Horizonte, M.G., 208 pp.
- Jesus, C. and Joaquim, L. (2017). Ferro. In DNPM, Sumário mineral 2016, (35nd ed., pp. 64 – 65). Brasília: DNPM.
- Martins, M., Lima, N., Filho, L., (2012). Depressão de minerais de ferro: influência da mineralogia, morfologia e pH de condicionamento, *Revista Escola de Minas*, 65, 393-399.
- Viana P., (2006). Flotação de Espodumênio, Microclina, Muscovita e Quartzo com Coletores Aniônicos, Catiônicos, Anfotéricos e Mistura de Coletores. Dsc.D. Thesis, Engineering School of Federal University of Minas Gerais, Belo Horizonte, MG, 202 pp.

EFFECTS OF TEMPERATURE AND CONFINING PRESSURE ON ENERGY EVOLUTION CHARACTERISTICS AND ROCK BURST MECHANISM IN BRITTLE ROCKS

S. Akdag^{1,*}, M. Karakus¹, G. D. Nguyen¹, A. Taheri¹

*University of Adelaide, School of Civil, Environmental & Mining Engineering
(*Corresponding author: selahattin.akdag@adelaide.edu.au)*

ABSTRACT

The aim of this research is to study the energy evolution characteristics of brittle rocks and understand the effects of temperature and confinement on bursting mechanism. A new method based on post-peak energy characteristics and acoustic emission response obtained from a series of uniaxial and triaxial compression tests is developed for rock burst analysis on granite samples exposed to high temperature. The axial loading is controlled using the feedback from lateral strain to obtain snap-back behaviour that is associated with energy evolution and the material response under self-sustaining failure. For each loading scenario, excess strain energies are calculated. The elastic strain energy, energy consumed by dominant cohesion weakening, and energy dissipated during mobilisation of frictional loss are quantified. The experimental results underlined that the amount of accumulated elastic strain energy increases as the confinement increases, resulting in a large potential for rock burst. It was also observed that the dominant failure pattern of granite changes from multiple longitudinal splitting to a single shear fracture and finally to multiple conjugate shear fractures as the level of temperature and confinement increases. Thermally induced damage causes less strain energy accumulation and hence the excess strain energy decreases (by ~43% compared to the room temperature conditions) with increasing temperature.

Keywords: Post-peak energy evolution, rock burst, circumferential strain control, triaxial compression test, temperature.

INTRODUCTION

As mining and civil engineering related projects such as caving mining and tunnelling operations progress to greater depths, the number of rock burst hazards has increased resulting in operational and safety challenges (Cai and Kaiser, 2018; Gao and Yang, 2021). The influence of elevated ground temperature has become remarkably significant on triggering rock burst with the increasing excavation depth (Su et al., 2017; Akdag et al., 2018). The coupling of high-stressed ground conditions and thermal damage will alter the overall mechanical behaviour of hard brittle rocks which can trigger bursting in deep engineering operations. Therefore, a deeper insight into the underlying damage mechanism of brittle rocks under high-pressure-temperature conditions is necessary to facilitate the safe construction and operation of underground excavations.

Prediction of rock burst proneness of rocks is one of the basic problems in the field of rock burst research. Various criteria and indices have been proposed to assess the rock burst proneness of rocks using, for example, strain energy storage index (W_{ET}) (Kidybiński, 1981), potential elastic strain energy (PES) (Wang and Park, 2001), peak strain energy storage index (W_{et}^p) (Gong et al., 2019), and residual elastic energy index (C_{EF}) (Gong et al., 2021). Despite the significant contributions of these studies for estimating and classifying the rock burst proneness of rock materials, limited work has focused on quantitatively investigating the influence of high-temperature-pressure on rock burst proneness. Therefore, further work is required to improve the understanding of rock burst proneness in highly-

stressed deep rock engineering applications. It has also been acknowledged that the manifestation of rock burst is related to the elastic stored strain energy and how this stored energy is released during unstable spontaneous failure (Tarasov and Potvin, 2013; Akdag et al., 2021). The intensity of rock burst is closely related to the energy storage capacity and dissipation of rocks. However, most, if not all, present evaluation methods do not consider the energy dissipation and excess strain energy (potential energy for rock burst) at the post-peak stage.

In the current paper, the authors investigated the rockburst proneness of thermally-treated granite under confinement. A series of circumferential strain-controlled uniaxial and triaxial compression tests were carried out on granite subjected to different temperatures under compression. The effects of high temperature and confinement on the mechanical characteristics, time-domain AE responses and energy evolution behaviour of granite were analysed. The rock burst proneness of the granite is discussed based on the energy evolution characteristics.

TEST METHODOLOGY

Circumferential Strain Controlled Uniaxial and Triaxial Compression Tests

For Uniaxial Compressive Strength (UCS) tests, rock samples were subjected to a monotonic axial loading by a closed-loop servo-controlled Instron 1282 hydraulic testing machine (Fig. 1a). The applied axial load was initially controlled using axial-strain feedback at a rate of 0.001 mm/mm/s until reaching approximately 70% of the expected peak force and then the control mode was switched to circumferential control, keeping lateral-strain rate constant by the circumferential extensometer (see Fig. 1b).

Circumferential strain controlled triaxial tests were conducted on the granite specimens exposed to temperatures up to 250 °C over confining pressures of 20, 40 and 60 MPa using the same Instron 1282 hydraulic testing machine. Circumferential strain control was utilised by means of a Hoek cell membrane fitted with four lateral strain gauges internally within the cell (Fig. 1c). The specimen was loaded axially with constant growth of a lateral strain of 1×10^{-6} mm/mm/s (Fig. 1d) and PCI-2 AE system was used to monitor the damage within the granite specimens during loading.

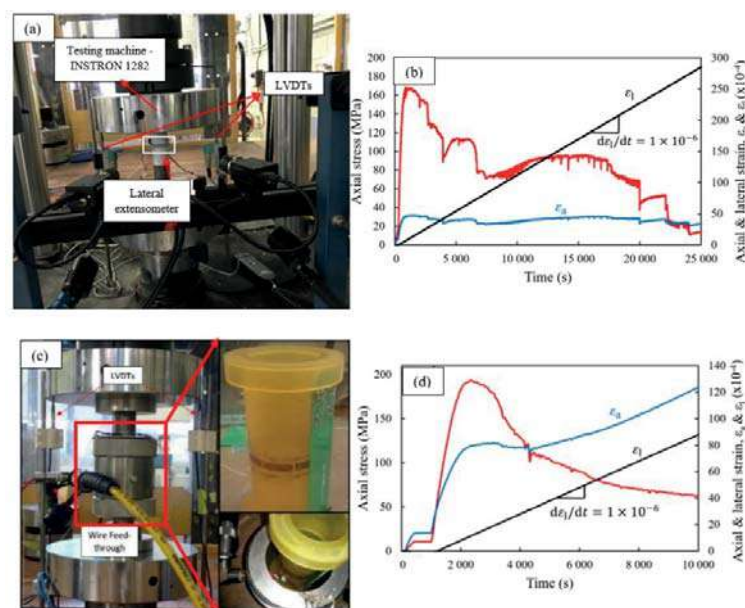


Figure 1. Testing setup and loading rates for lateral strain-controlled uniaxial (a, b) and triaxial compression tests (c, d).

TEST RESULTS

Stress-Strain Curves and Failure Modes

Fig. 2 presents the complete stress-strain curves of thermally-treated granite under different confining pressures. The failure mode of the granite changed from multiple splitting tensile fractures along the loading direction or a single shear fracture to conjugate shear failure with increasing temperature (see Fig. 2). Based on the experimental results, peak stress at 250 °C declined by ~25% when compared with the results at room temperature (25 °C) under unconfined conditions. It is the authors' interpretation that the main reason for this descending trend might have been the thermally induced micro-cracks that could cause mechanical degradation by weakening the bonding among mineral grains due to the differences in the thermal expansion properties of constituent rock minerals. This observation is consistent with the existing literature (Xu and Karakus, 2018; Yang et al., 2020), however, further investigation is needed to prove the above postulation. As confinement increased (up to 60 MPa), the peak stresses decreased by 21, 13 and 6% with increasing temperature from 25 °C to 250 °C, respectively. The confining pressure restrains the displacement and enhances the friction among grains under the condition of higher temperature.

The main failure feature of the granite was the multiple longitudinal splitting failure pattern accompanied by local shear failure when $\sigma_3 = 0$ MPa. The formation of extension cracks oriented in the direction of principal stress was the prevailing pattern of macroscopic fracturing in uniaxial compression. In moderate confining pressures, the granite specimens mainly failed by shear localisation along an inclined macroscopic shear band. Under high confinement, a conjugate shearing or ductile failure was observed in which the thermal heating could also enhance the ductility of the rock samples, as shown in Fig. 2.

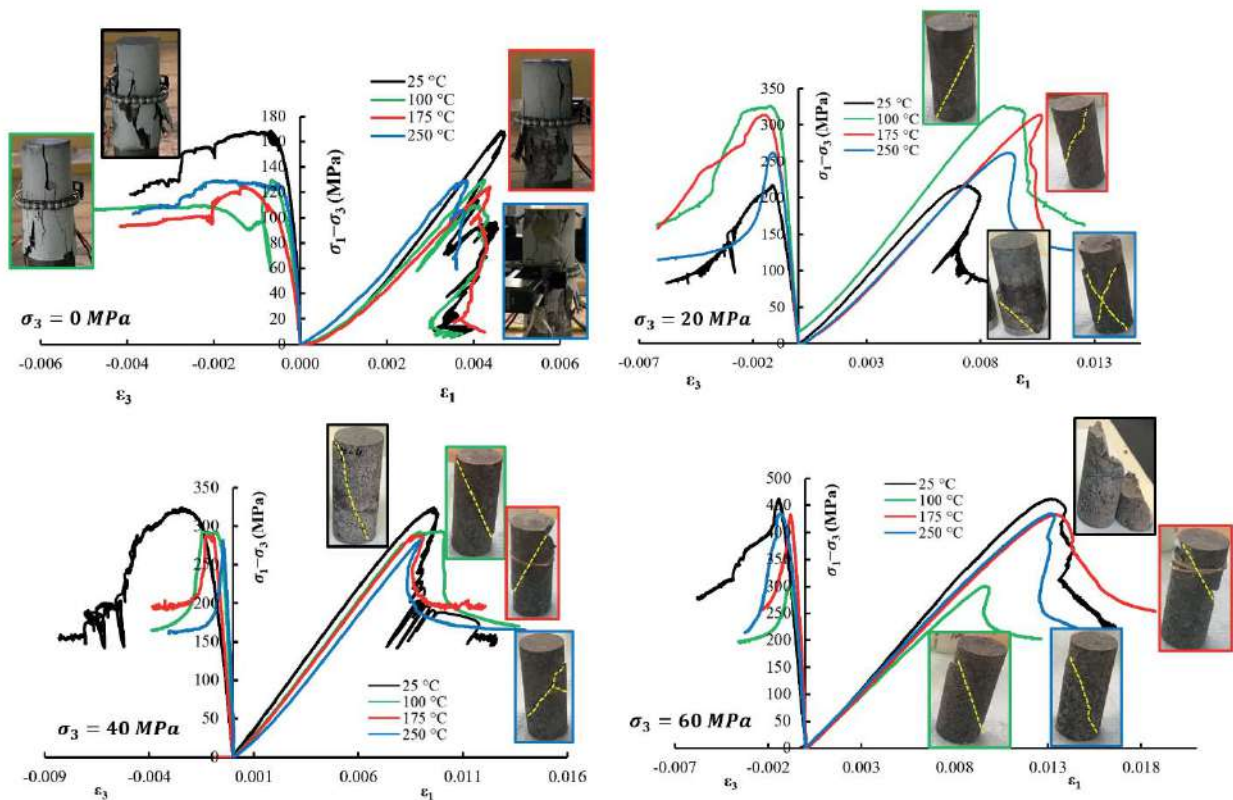


Figure 2. Complete stress-strain curves and failure modes of thermally-treated granite at various confinement

The typical AE characteristics of granite after temperature treatment under various confinement are shown in Fig.3. It can be seen that with the increase of temperature, the evolution of accumulated AE hits for granite specimens becomes slower and slower, which indicates that at higher temperatures, the granite samples undergo more ductile failure and released less elastic strain energy due to the thermally induced damage.

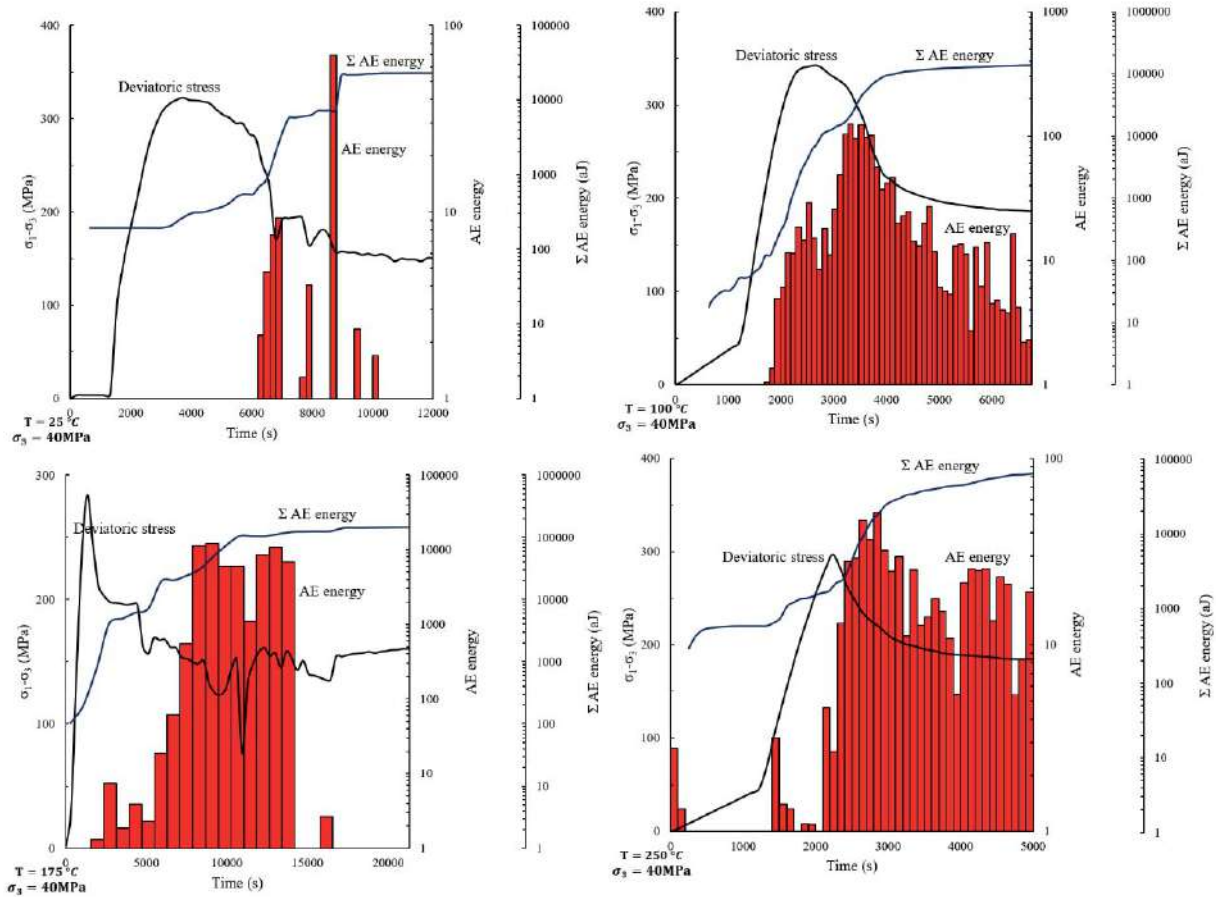


Figure 3. Evolution of AE characteristics of granite after temperature treatment ($T = 25\text{ }^{\circ}\text{C}, 100\text{ }^{\circ}\text{C}, 175\text{ }^{\circ}\text{C}$ and $250\text{ }^{\circ}\text{C}$)

Post-Peak Energy Calculation Principle

Rock burst is a type of instantaneous brittle failure of rock which mainly occurs due to the stress concentration and rapid energy release at the conditions of high geo-stress. Therefore, in compression stage, enough elastic strain energy is accumulated in the rock, ensuring that it can transfer this energy into kinetic energy at the failure. The buckling of slabs or rock ejection in the sidewalls of underground excavations is a typical manifestation of rock burst damage. It is of great importance to analyse energy evolution characteristics during rock fracturing under compression condition because of the significant function of identifying the energy source of the rock burst and revealing the rock burst’s vulnerability. In this study, recently proposed energy method (Akdag et al. 2021) is used to evaluate the post-peak energy balance of thermally-treated granite under different confining pressures. Fig. 4 and Eqs. 1-5 show the calculation method for the energies at the post-peak stage.

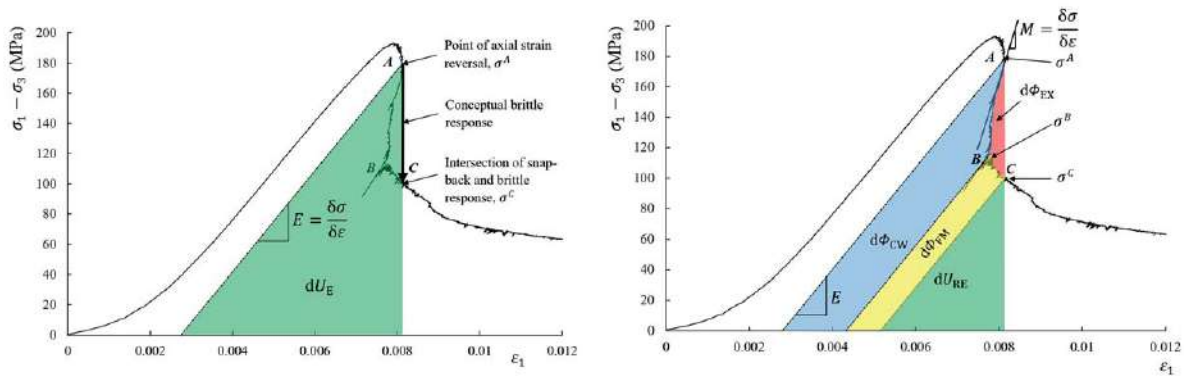


Figure 4. Energy calculation method based on the post-peak energy balance of snap-back behaviour (Akdag et al., 2021)

Here, a new energy-based rock burst proneness index Ω_{RB} is proposed:

$$\Omega_{RB} = \frac{d\Phi_{EX}}{dU_E} \quad (1)$$

where $d\Phi_{EX}$ and dU_E are the excess strain energy released during brittle failure (rock burst) and the elastic stored strain energy after Class II behaviour starts, respectively. The energy calculations are shown as follows:

$$dU_E = \frac{1}{2E} [\sigma_1^2 + 2\sigma_3^2 - 2\mu(2\sigma_1\sigma_3 + \sigma_3^2)] \quad (2)$$

$$U_1 = \int \sigma_1 d\varepsilon_1 = \sum_{i=0}^n \frac{1}{2} (\varepsilon_{1i+1} - \varepsilon_{1i}) (\sigma_{1i} + \sigma_{1i+1}) \quad (3)$$

$$U_3 = 2 \int \sigma_3 d\varepsilon_3 = \sum_{i=0}^n (\varepsilon_{3i+1} - \varepsilon_{3i}) (\sigma_{3i} + \sigma_{3i+1}) \quad (4)$$

$$d\Phi_{EX} = dU_E - d\Phi_{CW} - d\Phi_{FM} - dU_{RE} \quad (5)$$

where σ_{1i} , σ_{3i} , ε_{1i} , ε_{3i} are the axial and confining stresses and strains at a point i on stress-strain curve, respectively, Φ_{CW} is the energy consumption dominated by cohesion degradation during stable fracturing, Φ_{FM} is the energy dissipated during the mobilisation of frictional failure, U_{RE} is the residual stored elastic strain energy, σ_A is the point of axial strain reversal, σ_B is the point of brittle failure intersection, E is the elastic stiffness of the specimen and M ($M = \delta\sigma/\delta\varepsilon$) is the post-peak modulus between two incremental stress points, σ_i and σ_{i+1} which can vary significantly with the fracture development.

Rock Burst Proneness

The energy balance in the post-peak stage reflects the mechanism of excess strain energy which is related to the rock burst intensity. The rock burst proneness of pre-heated granite under confinement are shown in Fig.5. The results show that high-temperature-confinement have a significant influence on rock burst proneness. Based on the energy evolution analysis above, the larger the maximum dissipation energy density was, the more likely were the damage and plastic deformation occur in the granite which would result in severe rock burst. The dissipated energy can indirectly reflect the irreversible plastic deformation that occurs in the rock and the friction dissipation effect between internal fissure planes. The greater the confinement was, the larger the stored elastic strain energy and dissipated energy for cohesion weakening and friction mobilisation were. The confining pressure could restrain the

deformation within the granite and enhance the plastic deformation. In the field, however, confinement loss due to excavation is one of the major factors causing rock burst in the high-stress areas in deep mines. Therefore, assuming the accumulated elastic strain energy under confinement is released in the lab conditions, which can be considered as a free face or ‘excavation’ during the test, the bursting potential of the rock would be more severe at higher confining pressures.

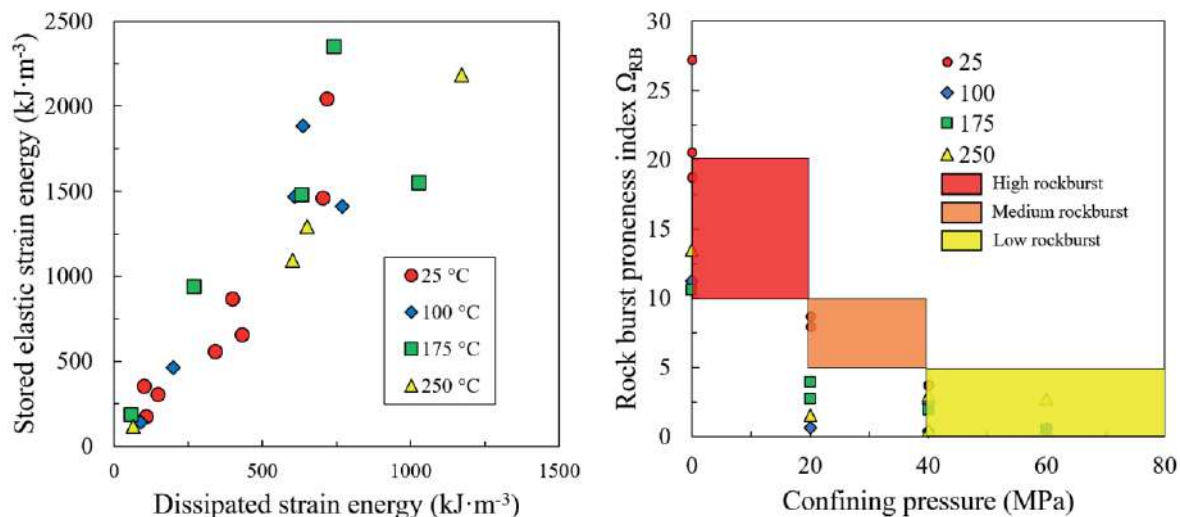


Figure 5. Rock burst proneness of thermally-treated granite under different confinement

CONCLUSION

This work proposes a simple yet effective experimental analysis for the rock burst proneness of thermally-treated granite under triaxial compression. The results show that high-temperature-confinement has a significant influence on the rock burst proneness. At the post-peak stage, higher confining pressure caused greater stored elastic strain energy and dissipated energy which would result in more severe rock burst damage in case of any confinement loss. With the increase of temperature, the strength of granite gradually weakened and the plastic failure characteristics were considerably enhanced due to the thermally-induced cracking. This approach could provide a preliminary assessment of the instability of brittle rocks in burst-prone areas to avoid potential hazards.

ACKNOWLEDGEMENTS

The authors gratefully acknowledge the financial support from the Australian Research Council and the Partner Organisation, OZ Minerals for the Linkage Project (LP150100539).

REFERENCES

- Akdag, S., Karakus, M., Nguyen, G., Taheri, A., & Bruning, T. (2021). Evaluation of the propensity of strain burst in brittle granite based on post-peak energy analysis. *Undergr Space*, 6(1), 1-11.
- Akdag, S., Karakus, M., Taheri, A., Nguyen, G., & He, M. (2018). Effects of thermal damage on strain burst mechanism for brittle rocks under true-triaxial loading conditions. *Rock Mech Rock Eng*, 51, 1657-1682.
- Cai, M., & Kaiser, P. (2018). *Rockburst support reference book, Rockburst phenomenon and support characteristics (Vol. 1)*. Sudbury: MIRARCO-Mining Innovation, Laurentian University.
- Gao, F., & Yang, L. (2021). Experimental and numerical investigation on the role of energy. *Rock Mech Rock Eng*, 54, 5057-5070.
- Gong, F., Wang, Y., Wang, Z., Pan, J., & Luo, S. (2021). A new criterion of coal burst proneness based on the residual elastic energy index. *Int J Min Sci Technol*, 31(4), 553-563.
- Gong, F., Yan, J., Li, X., & Luo, S. (2019). A peak-strength strain energy storage index for rock burst proneness of rock materials. *Int J Rock Mech Min Sci*, 117, 76-89.
- Kidybiński, A. (1981). Bursting liability indices of coal. *Int J Rock Mech Min Sci*, 18, 295-304.
- Su, G., Chen, Z., Ju, J., & Jiang, J. (2017). Influence of temperature on the strainburst characteristics of granite under true triaxial loading conditions. *Eng Geol*, 222, 38-52.
- Tarasov, B., & Potvin, Y. (2013). Universal criteria for rock brittleness estimation under triaxial compression. *Int J Rock Mech Min Sci*, 59, 57-69.
- Wang, J., & Park, H. (2001). Comprehensive prediction of rockburst based on analysis of strain energy in rocks. *Tunn Undergr Space Technol*, 16(1), 49-57.
- Xu, X., & Karakus, M. (2018). A coupled thermo-mechanical damage model for granite. *Int J Rock Mech Min Sci*, 103, 195-204.
- Yang, S., Tian, W., Elsworth, D., Wang, J., & Fan, L. (2020). An experimental study of effect of high temperature on the permeability evolution and failure response of granite under triaxial compression. *Rock Mech Rock Eng*, 53, 4403-4427.

ELEKTRON TRANSFER YÖNTEMİNDE FARKLI İYONLARIN KÖMÜRDEN ORGANİK KÜKÜRT UZAKLAŞTIRILMAYA ETKİSİ

EFFECT OF DIFFERENT IONS IN ELECTRON TRANSFER METHOD ON REMOVAL OF ORGANIC SULFUR FROM
COAL

U. Demir^{1,*}, A. Aydın¹

¹ Kütahya Dumlupınar Üniversitesi Mühendislik Fakültesi, Maden Mühendisliği Bölümü
(Sorumlu yazar: ugur.demir@dpu.edu.tr)

ÖZET

Özellikle termik santrallerde kullanılan kömürde bulunan kükürt, önemli çevresel sorunlara neden olmaktadır. Bu çalışmada yüksek oranda kükürt içeren Kütahya-Gediz yöresi kömürlerinden organik kükürdün uzaklaştırılmasında Elektron Transfer Yöntemi (ETY) uygulanmıştır. Bu yöntem ile daha çok kömür bünyesinde bulunan organik kükürt bileşikleri arasındaki C-S, S-S bağlarının zayıflatılması veya kırılması amaçlanmaktadır. Direkt organik kükürdün uzaklaştırılmasına yönelik yapılan çalışmaların sayısı oldukça sınırlı seviyede, olması bu çalışmayı öne çıkarmaktadır. İki aşamada gerçekleştirilen bu çalışmada, birinci aşamada inorganik kükürdün hemen hemen tamamı uzaklaştırılmış, ikinci aşamada inorganik kükürdü uzaklaştırılmış olan kömürden, organik kükürt ETY ile uzaklaştırılmaya çalışılmıştır. Elektron transfer reaktifi olarak çeşitli metalik iyonlarının (Zn^{+2} , Ni^{+2} , Hg^{+2}) organik kükürt uzaklaştırmaya etkileri araştırılmıştır. En yüksek oranda organik kükürdün uzaklaştırılması amacıyla farklı iyon konsantrasyonları (%0,1-5), ortam sıcaklığı (22-90 °C), reaksiyon süresi (15-240 dak) ve karıştırma hızlarında (300-1300 dev/dak) deneyler gerçekleştirilmiştir. Elde edilen sonuçlardan az da olsa organik kükürdün ETY ile uzaklaştırılabildiği (yaklaşık %3) tespit edilmiştir.

Anahtar Kelimeler: Organik kükürt, elektron transfer yöntemi, kükürt uzaklaştırma

ABSTRACT

Sulfur in coal is caused several serious environmental problems especially in coal combustion and coal-fired power plants. In this study, Electron Transfer Method (ETY) was applied for removal of organic sulfur from Kütahya-Gediz coal. With this method, it is aimed to weaken or break the C-S, S-S bonds between organic sulfur compounds in coal. The reason why this study stands out is that the number of studies on the direct removal of organic sulfur is quite limited. This study was carried out in two stage, in first stage, inorganic sulfur was completely removal and in second stage organic sulfur was attempted to be removed from inorganic sulfur free coal. Different metallic ions (Zn^{2+} , Ni^{2+} , Hg^{2+}) were used as an electron transfer reagents/chemicals for removal of organic sulfur. To determination of highest organic desulfurization rate, effect of experimental parameters such as ion concentration (%0,1-5), temperature (22-90 oC), reaction time (15-240 dak) and stirring speed (300-1300 rpm) were investigated. As a result, low level organic desulfurization rate (%3) has been obtained by electron transfer method.

Keywords: Organic Sulfur, Electron Transfer Method, Desulfurization

GİRİŞ

Bütün fiziksel ve kimyasal kükürt uzaklaştırma yöntemlerinde olduğu gibi, Elektron Transfer Yönteminde (ETY) de yapılması gereken ilk işlem, kömürün bünyesinde bulunan kükürt türlerinin

belirlenmesidir. Kömür bilindiği gibi, organik ve inorganik kükürt olmak üzere iki tür kükürt içermektedir. İnorganik kükürdün (pirit, markasit, jibs gibi yapılar) fiziksel kükürt uzaklaştırma yöntemleri ile tamamına yakını uzaklaştırılabilirken, organik kükürdün fiziksel yöntemler ile uzaklaştırılması mümkün değildir. Bu nedenle organik kükürt uzaklaştırmada kimyasal yöntemlerin uygulanma zorunluluğu ortaya çıkmaktadır (Mayers vd. 1972, Atar ve Corcoran 1977, Kawatra ve Eisele 2001, Sütçü 2004, Jorjani vd. 2004, Uzun ve Özdoğan 2006, Mi vd. 2007).

Kömürde bulunan organik kükürdün, aromatik ve alifatik olmak üzere iki grupta toplanması mümkündür. Aromatik ve alifatik kükürt bileşikleri farklı özellikler sergilemekte, bu özellik farklılığı uygulanan kükürt uzaklaştırma yöntemine bağlı olarak uzaklaştırılan kükürt miktarını doğrudan etkilemektedir. Alifatik kükürt bileşiklerinden bazıları arly-alkly, difenil sülfidler ve merkaptanlar sayılabilirken, aromatik kükürt bileşiklerinden bazıları tiofen, benzotiyofen ve dibenzotiyofenler olarak sayılabilir. Bu yapılar incelendiğinde, aromatik kükürt bileşiklerinin, alifatik kükürt bileşiklerine göre kimyasal işlemlere karşı daha yüksek direnç gösterdiği, bu nedenle, uzaklaştırılan kükürt bileşiklerinin içerisinde daha çok alifatik bileşiklerin olduğu görülmektedir. Ayrıca benzer durum kömüre uygulanan ısı işlem sırasında da karşımıza çıkmaktadır. Alifatik kükürt bileşikleri düşük sıcaklıklarda (>350 °C) bozunarak deformasyona uğrarlarken, aromatik kükürt bileşikleri daha yüksek sıcaklıklara kadar yapılarını muhafaza ederek, stabil bir durum sergilemektedirler. Aromatik ve alifatik organik kükürt bileşikleri arasındaki bağların kırılması için gerekli enerji birbirinden oldukça farklıdır. C-S bağlarının kırılması için gerekli enerjiler incelendiğinde, aromatik kükürt bileşikleri arasındaki bağı kırmak için gerekli olan enerji, alifatik kükürt bileşiklerindeki bağları kırmak için gerekli olan enerjiden daha fazladır. Bu nedenle kömür bünyesinde bulunan aromatik ve alifatik organik kükürt bileşiklerinin miktarlarının ve özelliklerinin bilinmesi kükürt uzaklaştırmada büyük önem arz etmektedir (Kawatra ve Eisele 2001, Calkins 1994, Van Aelst vd. 1997, Hamamcı vd. 1997, Borah vd. 2001).

Birçok araştırmacı tarafından son zamanlarda, kömürden organik kükürt uzaklaştırma çalışmalarında Elektron Transfer Yöntemi (EYT) uygulanmaktadır. Bu yöntem ile daha çok kömür bünyesinde bulunan organik kükürt bileşikleri arasındaki C-S, S-S bağlarının zayıflatılması veya kırılması amaçlanmaktadır. Daha sonra, dışarıdan ilave edilen metal iyonları ile bağları kırılan bu kükürtlü yapıların yeni bağlar kurmaları sağlanarak, çözünebilir kükürtlü bileşiklerin oluşturulması, böylece kükürdün kömür bünyesinden uzaklaştırılması gerçekleştirilmektedir. Elektron transfer yönteminde, transfer reaktifi olarak Cu^+ , Sn^{+2} , Ni^{+2} , Co^{+2} , Hg^{+2} , Sb^{+3} gibi iyonlar birçok araştırmacı tarafından kullanılmıştır (Prayuenyong 2002, Jagtap ve Wheelock 1995, Borah ve Baruah 1999, Borah ve Baruah 2000, Srivastava 2003, Borah 2005, Demirbaş 2006, Demir 2011, Demir ve Aydın 2016).

Yapılan kömür analizleri (kimyasal) sonucunda, kömür bünyesinde çeşitli sülfidli yapıların (FeS, PbS, ZnS vs.) varlığının tespit edilmesi, kükürdün metal iyonlarına ilgisinin olduğunu göstermektedir. Kükürt ile metal iyonları, doğal ortamda uygun şartlar oluştuğunda bağ kurmaları, elektron transfer yönteminin doğal şartlarda da oluştuğunu göstermektedir. Bu sülfidli bileşiklerin oluşması: kömür oluşumu esnasında kömürü oluşturan organik kalıntılarda bulunan kükürtlü yapılar, yeraltı sularında bulunan farklı değerliklerde ve farklı tiplerdeki eriyik haldeki metal iyonlarının (Cu^+ , Sn^{+2} , Zn^{+2} , Ni^{+2} , Co^{+2} , Sb^{+3} gibi) kömür havzasındaki kırık ve çatlaklardan geçerken, uygun şartların oluşması sonucunda, belirtilen sülfid bileşiklerinin oluşmasına neden olduğu, şeklinde açıklanmaktadır. Doğal yollar ile elektron transferinin gerçekleşmesini sağlayan birçok reaktif madde vardır. Bu maddeler çeşitli enzimler, metaloenzimler ve bazı organik maddelerdir, bunlar doğada meydana gelen elektron transferinin sorumlularıdır. Bunların yanında birçok kükürt içeren bileşikler, özellikle amino asitler (cysteine, cystine, methiamine) de elektron transferinde önemli bir rol oynamaktadır. Elektron transferinin gerçekleşmesinde, bu reaktiflerin yanı sıra ortam pH'sı, redox potansiyeli ve metal iyonlarının konsantrasyonları da önem arz etmektedir (Borah ve Baruah 2000, Demir ve Aydın 2016).

Borah ve Baruah (2000) hem tüvenan hem de civa ile muamele edilen yüksek kükürt içerikli Hindistan Meghalaya kömürlerine, farklı sıcaklıklarda yapılan oksidasyon işleminden sonra, elektron

transfer yöntemi uygulanmıştır. En yüksek oranda kükürt uzaklaştırma tüvenan kömürde naftalin varlığında %19.17, civa ile muamele edilmiş kömürde ise %17.78 olarak gerçekleştirilmiştir. Bu yöntem uygulanarak tüvenan kömürde organik kükürdün %27.38'i uzaklaştırılabilirken, civa ile muamele edilmiş kömürde bu oran %28.45 olarak tespit edilmiştir. Yazarlar Hg ile naftalinin kullanılması, kükürt uzaklaştırma işlemi üzerinde önemli bir etkisinin olmadığını ifade etmişlerdir. Borah ve diğ. (2001) başka bir çalışmalarında aynı yöre kömürünü kullanarak civanın kükürt uzaklaştırmaya olan etkilerini araştırmışlardır. Civanın hem oksitlemeyi hızlandırdığı hem de kükürt uzaklaştırmada etkili bir madde olduğu ifade edilmektedir. Kükürde yüksek afiniteye sahip olduğu belirtilen civa, C-S arasındaki bağları zayıflattığı ve kükürt uzaklaştırma verimini arttırdığı ifade edilmiştir. Borah ve Baruah (1999) ve Borah (2005) 'de yaptıkları çalışmalarında farklı metal iyonlarının (Cu^+ , Co^{2+} , Ni^{2+} , Sn^{2+} ve Sb^{3+}) organik kükürdün bünyeden uzaklaştırılmasındaki etkileri incelenmiştir. Srivastava (2003) farklı oranlarda kükürt ve kül içeren 12 Hindistan kömürlerinden, mineral madde ve kükürt uzaklaştırmak amacıyla demir sülfat ($\text{Fe}_2(\text{SO}_4)_3$) kullanmış, yaptığı bu çalışma ile oldukça ince boyut dağılımına sahip olan piritin %90'ından fazlasının uzaklaştırılabildiğini ifade etmiştir. $\text{Fe}_2(\text{SO}_4)_3$ kullanmasının nedeni olarak da piritte selektif olarak etki etmesi ve geri kazanılabilesinin kolay olması gösterilmiştir.

Yapılan bu çalışmada, son zamanlarda çeşitli araştırmacılar tarafından uygulanmaya başlanan ETY ile Gediz yöresi kömürlerinde bulunan organik kükürdün Zn^{+2} , Hg^{+2} ve Ni^{+2} iyonları kullanılarak uzaklaştırılabilirliği araştırılmıştır. Organik kükürdün uzaklaştırılmasında farklı çalışma parametrelerinin (iyon konsantrasyonu, ortam sıcaklığı, işlem süresi vs.) etkilerinin belirlenmesi amacıyla sistematik deneyler gerçekleştirilmiştir.

DENEYSEL ÇALIŞMALAR

Malzeme

Deneysel çalışmalarda kullanılan kömür numuneleri, Kütahya merkeze yaklaşık 90 km ve Gediz ilçe merkezine yaklaşık 25 km mesafedeki Gökler kasabasında faaliyet gösteren özel bir şirkete ait kömür ocağından alınmıştır. Temsili olarak alınan kömür numuneleri deneysel çalışmalarda kullanılmak üzere boyut küçültme işlemine tabi tutulmuş, azaltma işlemi uygulanmış ve özelliklerinin değişmesinin engellenmesi amacıyla hava geçirmez kilitli poşetlerde depolanmıştır.

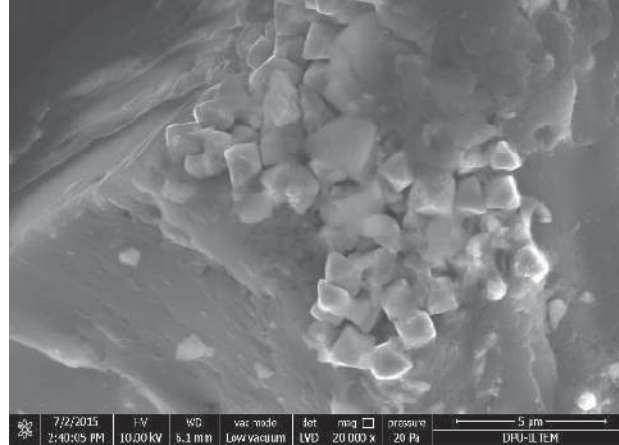
Gediz yöresi kömürleri üzerinde yapılan kısa analiz sonuçları Çizelge 1'de, elementer analiz sonuçları ise Çizelge 2'de verilmiştir. Çizelge 1 incelendiğinde yöre kömürlerinin %7,06 toplam kükürt içeriğine sahip olduğu, bu kükürdün ise yarıya yakınının (%2,89) organik kökenli olduğu görülmektedir. Ayrıca, yöre kömürlerinin yüksek oranda kül içermesine (%25,99) rağmen ısıl değerinin (5607 kcal/kg) yüksek olduğu belirlenmiş (Çizelge 1), bu hali ile yöre kömürleri yapılan petrografik incelemeler sonucu organik yapının büyük bir bölümü vitrinitten (%87) oluştuğu, vitrinite zemin üzerinde inertinit ve az miktarda eksinit olduğu belirlenmiş, ayrıca alt bitümlü kömür sınıfına (R_{max} : 0,576) girdiği tespit edilmiştir. Şekil 1'de Gediz yöresi kömürlerinin taramalı elektron mikroskop (SEM) ile 20000 kez büyütülmüş görüntüsü görülmektedir. Şekil 1'den de görüldüğü üzere yöre kömürleri çok ince boyutta pirit tanecikleri içermektedir. Piritin büyük bölümü kömür parçaları içinde kenetli halde, az miktarda kükürt serbest taneler halinde bulunmaktadır. Piritler, kürecikler halinde, öz ve yarı-öz şekilli taneler halinde kendini göstermektedir. Bu pirit taneciklerinin serbestleşme boyutu ise yaklaşık 1-2 mikron civarındadır. Bu kadar ince boyutta serbestleşen piritik kükürdün fiziksel yöntemler ile uzaklaştırılabilesi mümkün görülmemektedir. ETY reaktifi olan metalik iyonlar (NiCl_2 , HgCl_2 ve ZnCl_2) çözelti halinde kullanılmıştır.

Çizelge 1. Deneysel çalışmalarda kullanılan kömür numunesinin kısa analiz sonuçları

Kısa analiz	(%)
Nem	3,3
Kül	25,99
Uçucu madde	32,81
Sabit Karbon	37,90
Alt Isıl Değer	5607 kcal/kg

Çizelge 2. Deneysel çalışmalarda kullanılan kömür numunesinin elementer analiz sonuçları

Elementer Analiz	(%)
Karbon	78,41
Hidrojen	5,12
Azot	1,61
Oksijen (farktan)	7,8
Toplam Kükürt	7,06
Organik Kükürt	2,89
Piritik Kükürt	3,55
Sülfat Kükürdü	0,62



Şekil 1. Gediz yöresi kömürlerinin SEM görüntüsü (20000 kez büyütülmüş)

Yöntem

Gediz yöresi kömürlerinden organik kükürdün (%2,89) uzaklaştırılması için iki aşamalı bir çalışma gerçekleştirilmiştir. Birinci aşamada, kömür bünyesinde bulunan inorganik kükürdün (piritik ve sülfat kükürdü) hemen hemen tamamı uzaklaştırılmıştır. Bu amaçla belirlenen tane boyutuna öğütülen (-212 mikron) kömür numunesi, %30 nitrik asit (HNO_3)- %30 hidroklorik asit (HCl) karışımı ile belirlenen sürede (60 dakika) muamele edilmiş, bu işlem sonunda oluşan kömür-kimyasal karışımı süzümüştür. Süzme işlemi sonrasında kömür numunesi içerisinde asidik çözelti bütünüyle temizleninceye kadar sıcak saf su ile defalarca yıkanmış ve etüde kurutulmuştur. Uygulanan bu işlem ile kömür bünyesinde bulunan piritik ve sülfat kükürdünün hemen hemen tamamı (%3,55), organik kükürdün ise küçük bir bölümü uzaklaştırılmıştır. Etüde kurutulmuş inorganik kükürdü uzaklaştırılmış kömür numunelerine ikinci aşama olan Elektron Transfer Yöntemi (ETY) uygulanmıştır. Bu aşamada 2 gr kömür numunesi ile metalik iyonlar ($NiCl_2$, $HgCl_2$, $ZnCl_2$ bileşikleri) çözelti halinde kullanılmıştır. 250 ml hacimli beher içerisinde karıştırılan

kömür numunesi ve iyon çözeltisi, ısıtıcılı manyetik karıştırıcı kullanılarak önceden belirlenen çalışma şartlarında (Çizelge 3) kimyasal işleme tabi tutulmuştur. Kimyasal işlem tamamlandıktan sonra karışım filtre kağıdı kullanılarak katı kısım sıvı kısımdan ayrılmıştır. Katı kısım sıcak saf su ile yıkandıktan sonra etüvde kurutulmuş (105 °C) ve gerekli analizler (kül, kükürt) standartlara uygun (ASTM D3174, ASTM D3177) olarak yapılmıştır. Çizelge 3’de deneysel çalışmalarda etkileri araştırılan çalışma parametreleri ve çalışma aralıkları verilmiştir.

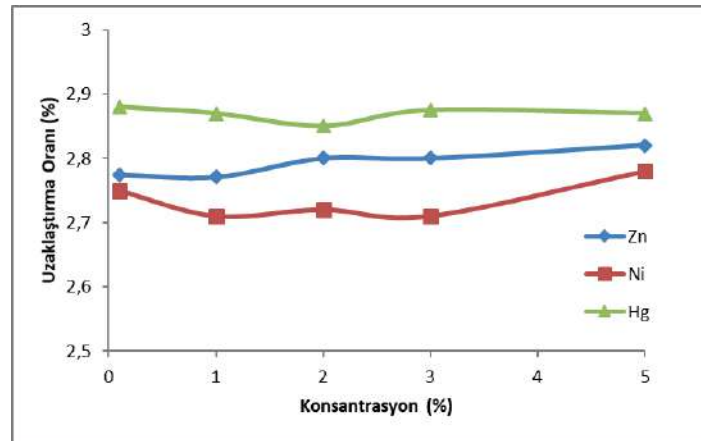
Çizelge 3. Deneysel çalışmalarda uygulanan çalışma parametreleri

Çalışma Parametreleri	Değerler
İyon konsantrasyonu (%)	0.1, 1, 2, 3, 5
Kimyasal işlem süresi (dakika)	15, 30, 60, 90, 120, 240
Ortamın sıcaklığı (°C)	22, 35, 70, 90
Karıştırılma hızı (dev/dk)	300, 500, 750, 1000, 1300
Tane boyutu (mikron)	-212

SONUÇLAR VE TARTIŞMA

İyon Konsantrasyonunun Etkisi

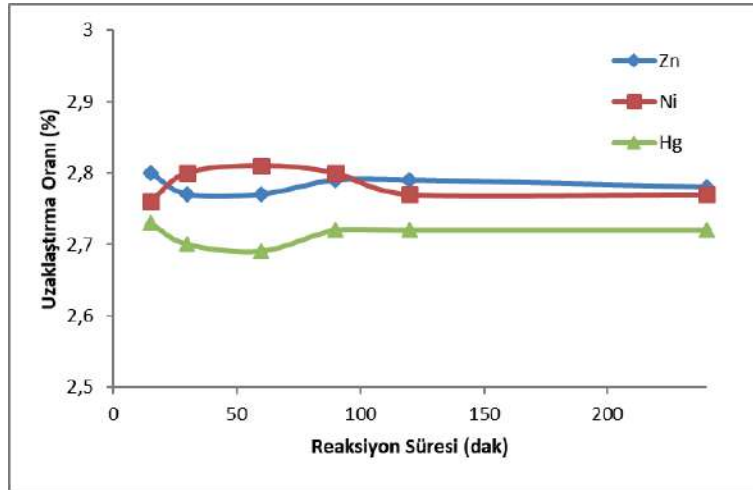
Gediz yöresi kömürlerinden organik kükürdün uzaklaştırılması amacıyla %0.1, 1, 2, 3 ve 5 arasında değişen konsantrasyonlarda $ZnCl_2$, $NiCl_2$ ve $HgCl_2$ çözeltileri kullanılarak çeşitli deneyler gerçekleştirilmiş ve elde edilen sonuçlar Şekil 2’de verilmiştir. %7,06 oranında toplam kükürt içeren yöre kömürlerinden, yöntem kısmında belirtilen birinci aşama işlem sonucunda %2,82 oranında organik kükürt içeren ürün (inorganik kükürt içermeyen) elde edilmiştir. Yapılan bu işlem ile inorganik kükürdün tamamı, organik kükürdün ise küçük bölümünün uzaklaştırıldığı belirlenmiştir. İkinci aşama kükürt uzaklaştırma işlemi, %2,82 oranında organik kükürt içeren kömür numunesi üzerinde yapılmıştır. Elde edilen sonuçlar incelendiğinde artan iyon konsantrasyonlarına bağlı olarak kükürt içeriğinde düşük seviyelerde de olsa sürekli bir azalmanın olduğu görülmektedir. Organik kükürt uzaklaştırma oranları incelendiğinde ise oranın oldukça düşük seviyelerde seyrettiği görülmektedir. ETY sonucunda elde edilen ürünlerin kükürt uzaklaştırma oranları $ZnCl_2$ ile % 2,77-2,82 arasında, $NiCl_2$ ile %2,71-2,78 arasında, $HgCl_2$ ile 2,85-2,88 arasında olduğu belirlenmiştir. Elde edilen ürünlerin kükürt uzaklaştırma oranlarının birbirlerine bu kadar yakın olmaları dikkate alındığında her üç iyon için %1 iyon konsantrasyonunun uygun olduğuna karar verilmiştir. Uzaklaştırılan organik kükürt oranlarındaki düşüklük, organik kükürt bileşiklerindeki C-S ve S-S bağların yeteri kadar zayıflatılıp, kırılmamasından kaynaklanabileceği görüşüne varılmıştır.



Şekil 2. İyon konsantrasyonunun kükürt uzaklaştırmaya etkisi

Kimyasal İşlem Süresinin Etkisi

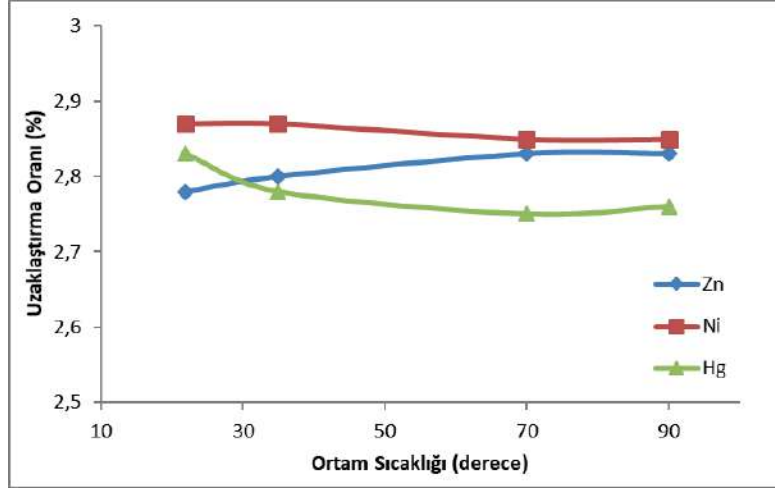
Elektron transfer yönteminde, kimyasal işlem süresinin organik kükürt uzaklaştırmaya etkisini belirlemek amacıyla 15, 30, 60, 90, 120 ve 240 dakika sürelerde deneyler yapılmış ve elde edilen sonuçlar Şekil 3’de verilmiştir. Şekil 3 incelendiğinde kömür numunelerinin kükürt uzaklaştırma oranlarında çok küçük değişimler meydana gelmiştir. Kükürt uzaklaştırma oranları incelendiğinde artan süreye bağlı olarak Ni^{+2} iyonu için uzaklaştırılan kükürt oranında önce bir miktar artış gözlenmiş, devam eden işlem süresindeki artış organik kükürt uzaklaştırma oranının bir miktar azalmasına, Zn^{+2} iyonunun süreye bağlı olarak önemli bir değişimine neden olmadığına, Hg^{+2} iyonu ise süre artışına bağlı olarak önce bir miktar azalmaya, devam eden süre artışı ile uzaklaştırılan kükürt miktarında az da olsa bir artışın meydana geldiği gözlenmiştir. 240 dakikalık kimyasal işlem süresinde en yüksek oranda kükürt uzaklaştırılabildi fakat diğer sürelerde elde edilen kükürt uzaklaştırma oranları arasında çok bariz bir farkın olmaması nedeniyle her üç iyon içinde 30 dakikalık sürenin en uygun olduğu belirlenmiştir. Uzaklaştırılan organik kükürt oranlarındaki düşüklük daha önce de belirtildiği gibi, organik kükürt bileşikleri arasındaki C-S ve S-S bağlarının yeteri kadar deformasyona uğramamasından kaynaklanmaktadır.



Şekil 3. Kimyasal işlem süresinin kükürt uzaklaştırmaya etkisi

Ortam Sıcaklığının Etkisi

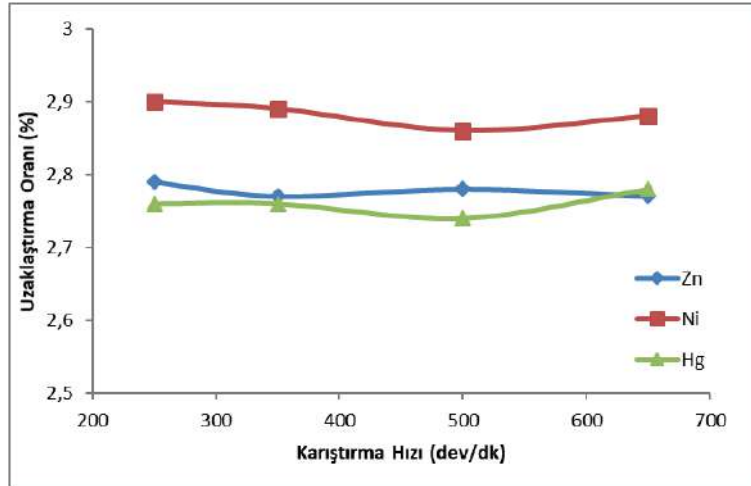
Gediz yöresi kömürlerinden organik kükürdün uzaklaştırılmasında ortam sıcaklığının etkisinin belirlenmesi amacıyla farklı sıcaklıklarda (22, 35, 70 ve 90 °C) deneyler gerçekleştirilmiş ve elde edilen sonuçlar Şekil 4’de verilmiştir. Şekil 4 incelendiğinde, artan ortam sıcaklığı kömür numunelerinin kükürt içeriklerinde çok az bir değişimin olmasına neden olmuş, kükürt uzaklaştırma oranlarında ise yine artan ortam sıcaklığına bağlı olarak değişimin çok sınırlı seviyelerde olduğu gözlenmiş, 90 °C ortam sıcaklığında Zn^{+2} ile yapılan deneylerde artışın olduğu görülürken, diğer iyonlarda çok az bir değişimin olduğu belirlenmiştir (%2,7-2,9). Elde edilen sonuçların birbirlerine çok yakın olması nedeniyle oda sıcaklığının (22 °C) her üç iyon için de en uygun sıcaklık olduğuna karar verilmiştir.



Şekil 4. Ortam sıcaklığının kükürt uzaklaştırmaya etkisi

Karıştırma Hızının Etkisi

Kimyasal işlemlerde reaksiyon hızının artırılması ve kimyasal ile malzemenin daha fazla etkileşimini sağlamak amacıyla ortamın karıştırılması sıkça uygulanan bir durumdur. Bu nedenle yöre kömürlerinden organik kükürdün uzaklaştırılmasında karıştırma hızının etkisini belirlemek amacıyla farklı karıştırma hızlarında (250, 350, 500, 600 dev/dk) deneyler gerçekleştirilmiş ve elde edilen sonuçlar Şekil 5’de verilmiştir. Şekil 5 incelendiğinde, karıştırma hızının, kükürt uzaklaştırmada etkili bir parametre olmadığı görülmektedir. Artan karıştırma hızına bağlı olarak kömür numunelerinin kükürt içerikleri her üç kimyasal için neredeyse birbirine çok yakın seviyelerde kaldığı tespit edilmiştir. Kükürt uzaklaştırma oranları incelendiğinde ise artan karıştırma hızı ile birlikte çok küçük bir miktar artışın olduğu görülmektedir. Bu durum düşük karıştırma hızlarının kükürt uzaklaştırma için yeterli olabileceğini göstermiştir. Optimal karıştırma hızı olarak 250 dev/dk seçilmiştir.



Şekil 5. Karıştırma hızının kükürt uzaklaştırmaya etkisi

SONUÇLAR

Gediz yöresi kömürlerinden organik kükürdün uzaklaştırılmasında ülkemizde fazla uygulama alanı bulamamış olan Elektron Transfer Yöntemi uygulanmış, bu amaçla $ZnCl_2$, $NiCl_2$ ve $HgCl_2$ tuzlarının çözeltileri kullanılmıştır. Her üç iyon ile yapılan deneylerde; %1 iyon konsantrasyonu, 30 dakikalık

kimyasal işlem süresi, oda sıcaklığı (22 °C) ve 250 dev/dk karıştırma hızlarında %2,8-2,95 oranları arasında organik kükürdün uzaklaştırılabileceği tespit edilmiştir. Bu sonuçlar değerlendirildiğinde ZnCl₂, NiCl₂ ve HgCl₂'nin organik kükürt uzaklaştırmada beklenen etkiyi gösteremediği belirlenmiştir. Bu durumun kömür bünyesindeki organik kükürt bileşiklerinin kuvvetli bağlar ile birbirine bağlı olduğu (C-S ve S-S) ve bu bağlarının yeteri kadar kırılmamasından kaynaklandığı tahmin edilmektedir. Gediz yöresi kömürlerinin içerdiği organik kükürdün, kimyasal işlemlere karşı daha fazla direnç sergilediği belirlenmiş, yöre kömürlerinin kalitesinin (alt bitümlü) linyitlere göre daha yüksek olduğunu petrografik analizlerle de ortaya koyulmaktadır.

Organik kükürdün uzaklaştırılmasında kullanılan Elektron Transfer Yönteminin düşük sıcaklık ve atmosfer basıncı altında uygulanması istenilen etkinin elde edilememesine neden olmuş, bu nedenle yüksek basınç ve sıcaklık şartlarında bu yöntemin yeniden denenmesi gerektiği düşünülmektedir.

TEŞEKKÜR

Bu çalışma, Dumlupınar Üniversitesi 2011-17 nolu Bilimsel Araştırma Projesi kapsamında desteklenmiştir.

KAYNAKLAR

- Atar A., Corcoran, W., H., (1977), Sulfur compounds in coal, Ind. Eng. Chem. Prod. Res. Dev. Vol:16 No: 2, 168-170
- Aydın A., Demir U., (2013), Kütahya-Gediz kömürlerinin elektron transfer yöntemi ile kükürdünün uzaklaştırılması. Dumlupınar Üniversitesi, Bilimsel Araştırma Projesi, Proje No: 2011-17
- Borah D., (2005), Desulphurization of organic sulphur from coal by electron transfer process with CO²⁺ ion. *Fuel Processing Technology*, Vol: 86, 509-522
- Borah D., Baruah, M., K., (1999), Electron transfer process 1. removal of organic sulphur from high sulphur indian coal, *Fuel*, Vol: 78, 1083-1088
- Borah D., Baruah, M., K., Haque, I., (2001), Oxidation of high sulphur coal. Part 1. Desulphurization and evidence of the formation of oxidised organic sulphur species, *Fuel*, Vol: 80, 501-507
- Borah D., Baruah, M.K. (2000), Electron transfer process. Part 2. Desulphurization of organic sulphur from feed and mercury-treated coals oxidized in air at 50, 100 and 150 °C, *Fuel*, Vol:79, 1785-1796
- Calkins W., H., (1994), The Chemical forms of sulfur in coal: a review, *Fuel*, Vol: 73 No: 4, 475-484
- Demir U., (2011), Kütahya-Gediz yöresi kömürlerinden kükürdün uzaklaştırılması, Doktora Tezi, Dumlupınar Üniversitesi, Fen Bilimleri Enstitüsü, Kütahya.
- Demir U., Aydın A., (2016), Desulfurization of high sulfur coal by electron transfer method, XV. Mineral Processing Symposium, IMPS 2016, Istanbul, Turkey 19-21 October 2016
- Demirbaş A., (2006), desulfurization of organic sulfur from lignite by an electron transfer process, *Energy Sources Part A*, Vol: 28, 1295-1301
- Hamamcı C., Kahraman, F. Düz, M. Z., (1997), Desulfurization of Southeastern Anatolian asphaltites by the meyers method, *Fuel Processing Technology*, Vol: 50, 171-177
- Jagtap S.B., Wheelock, T.D., (1995) Coal desulfurization by ferric chloride, *Fuel Processing Technology* Vol: 43 227-242
- Jorjani E., Rezai B., Vossoughi M., Osanloo M., Abdollahi M., (2004), Oxidation pretreatment for enhancing desulfurization of coal with sodium butoxide, *Minerals Engineering*, Vol: 17, 545-552
- Kawatra S.K., ve Eisele T.C. (2001), Coal desulfurization: High-efficiency preparation methods, Printed by Edwards Brothers, Ann Arbor, Taylor & Francis Inc. 349p.
- Mayers R., A., Hamersm J. W., Land, J. S., Kraft M. L., (1972), Desulfurization of coal, *Science*, Vol: 177, 1187-1188
- Mi J., Ren J., Wang J.C., Bao W.R., Xie K.C., (2007), Ultrasonic and microwave desulfurization of coal in tetrachloroethylene, *Energy Sources, Part A*, Vol: 29, 1261-1268

- Prayuenyong P., (2002), coal biodesulfurization processes, *Songklanakarın J. Science Technology*, Vol:24, No: 3, 493-507
- Srivastava S., K., (2003), Recovery of sulphur from very high ash fuel and fine distributed pyritic sulphur containing coal using ferric sulphate , *Fuel Processing Technology*, Vol: 84, 37-46
- Sütçü H., (2004), Coal desulfurization using natural ca-based sorbents, *Coal Preparation*, Vol. 24, 249-259
- Uzun D., Özdoğan S., (2006), Sulfur Removal from Original and Acid Treated Lignites by Pyrolysis , *Fuel*, Vol: 85, 315-322
- Van Aelst J., Ypermanan J., Franco D. V., Mullens J., Van Poucke L., C., and Palmer S., R., (1997), Sulphur distribution in Illinois No. 6 coal subjected to different oxidation pre-treatments , *Fuel Vol: 76*, 1377-1381

EMPLOYING THE MINERALOGICAL DATA FOR SELECTING THE BEST BENEFICIATION METHOD FOR A REFRACTORY GOLD ORE

S. Gökdemir^{1,*}, B. Töngür¹, B. Aksarı¹, A. Harzanak¹

¹ *Demir Export A.Ş*

(*Corresponding author: senag@demirexport.com)

ABSTRACT

The aim of this study is to employ the data gathered from gold deportment studies in order to select the most appropriate beneficiation method for a gold ore. Detailed core logging and mineralogical studies indicated that the resource comprised of oxidized, transition and sulfide ore zones. According to gold deportment studies, native gold grains were observed as free and/or associated with sulfides both in sulfide and transition ore zones while it is free or attached to iron oxide (mainly goethite) in the oxide zone. According to geometallurgical approach, it is important to have an insight about the recoverable metal as well as the method of the beneficiation, besides the grade and the quantity. Based on geological and mineralogical studies, experimental test plan was designed to select the most efficient beneficiation scenario. Preliminary flotation test was performed for these three ore zones separately. Based on the preliminary results, froth flotation would appear to be a proper method as pre-concentration of gold especially for sulfide and transition ore zones.

Keywords: Refractory gold, flotation, pyrite and pre-concentration

INTRODUCTION

Gold, which has attracted people attention since ancient times, is a brightly colored metal used in many industries because of its resistance to different conditions and easiness to process. The world's oldest gold producers are the Egyptians. In 5000 BC, they started to extract gold, which was alloyed with copper, from underground (Yücel M.B., 2020). Gold can be found in nature as native, electrum, tellurium, solid solution, and inclusion in other minerals. Gold deposits are classified in different ways according to the formation temperature, the rocks in which it is located, the mineralogical structure of the ore, other elements found with gold and the geodynamic environment in which the deposits are formed (Yücel M.B., 2020).

Nowadays, due to the scarcity of high-grade and easily enriched gold ore deposits, the interest on low-grade and refractory gold ore deposits are increased. According to the literature, if the gold recovery is lower than 80-90% in the standard cyanidation process, it is identified as refractory (La Brooy S., Linge H., 1994). According to La Brooy and Linge (1994), the refractoriness of gold is classified as follows:

Gold Recovery: < 50% High Refractory
Gold Recovery: 50% - 80% Medium Refractory
Gold Recovery: 80% - 90% Light Refractory
Gold Recovery: > 90% Non-Refractory

Sulfide gold bearing ores, e.g., pyrite and arsenopyrite, are becoming the most important gold sources. Typically, the gold is encapsulated or finely disseminated in these minerals and the direct cyanidation is not usually effective for gold extraction, even after the ore is ground to ultrafine size. In order to increase the gold recovery from refractory sulfide gold ores, oxidation pretreatment technologies such as pyrometallurgical, bio-metallurgical and hydrometallurgical processes were proposed. These techniques transform sulfides into oxides or sulfates thus, gold is exposed to be leached by cyanide easily.

In the case of complex ore bodies, typical assay-based block model appears to be inadequate. Because it doesn't contain information about processing method of different zones, expected recovery from the blocks and environmental issues related to whole project. Combining the various information about the resource e.g., elemental assays provided from the drill hole samples, core logging information, detailed gold deportment study, grinding test works, gravity/flotation/leach test results etc. these studies will be helpful in providing a comprehensive geometallurgical block model. This model will forecast the processing method of every zone as well as approximate gold recovery from of each block, actual cut of grade and finally the profitability of the whole project.

The Gold deportment studies are the key tools in gold processing development and its optimization (Beyuo & Agorhom, 2021). Modern gold deportment studies include physical, chemical and mineralogical assessments, combined to obtain a full understanding of the nature and variability of gold in a resource. The main aim of a gold deportment analysis is to locate and describe gold containing particles in order to determine the gold speciation, grain size and mode of occurrence (gold liberation, exposure, and mineral associations) as well as to generally characterize the mineralogical composition of the ore (Coetzee et al., 2011).

The aim of this study is to employ the data gathered from gold deportment studies in order to select the most appropriate beneficiation method. This manuscript will be started with sharing geological and mineralogical information about the ore body followed by definition and results of the metallurgical test works and finally discussion of the results.

GEOLOGICAL AND MINERALOGICAL STUDIES

According to observations and chemical studies, the gold concentration was identified in the quartz veins and, its geometry has been determined the geometry of the ore-bearing zones. Gathering information from the geochemical and the core logging studies, the oxidized zone is close to the surface and followed by transition and sulfide zones (Figures 1 and 2).



Figure 1. The Exploration Area and geological studies



Figure 2. Drill cores taken from the zones

Based on chemical analysis of the core samples, logging studies, 3D geology-ore solid model and resource estimation studies the resource comprised of over 87% sulfide and transition zones and around 12% oxidized zone (Figure 3).

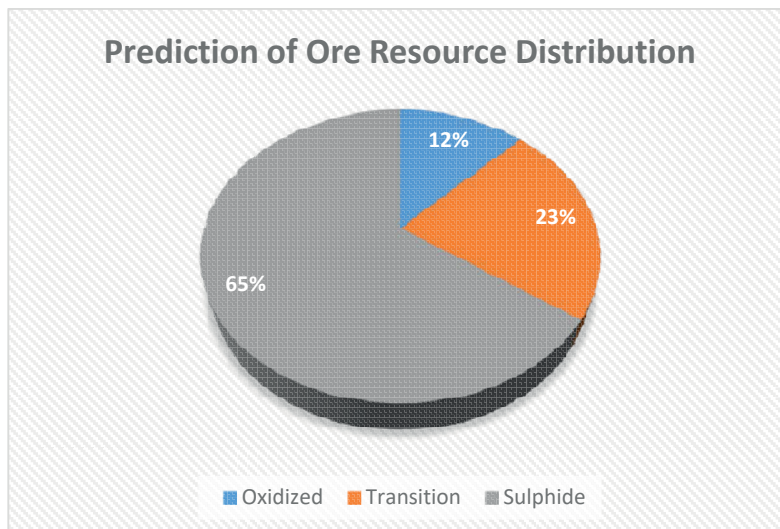


Figure 3. Prediction of ore resource distribution

In order to represent ore zones, eight samples (Table 1) were taken from different drilling holes based on their classification and depth. The gold department studies performed for these samples which consisted of the following steps;

1. Assaying: a process used to determine proportions of precious metals in ores and other industrial raw material substances.
2. QXRD: to determine the general mineralogy.
3. Microscopy: to identify & characterize gold minerals by type, grain size and association.
4. SEM/EDX: to determine the composition of gold grains
5. D-SIMS: to quantify submicroscopic gold

Table 1. The distribution of sample according to ore types

Ore Type	Samples
Sulfide	KT-02, KT-03, KT-06
Transition	KT-01, KT-04, KT-07
Oxidized	KT-05, KT-08

According to gold department, native gold grains were observed free and associated with sulfides in sulfide and transition ore zones while gold is free or attached to iron oxide ore (mainly goethite). Pyrite is the principal sulfide mineral in the sulfide ore samples whereas arsenopyrite was observed in minor quantities. Both pyrite and arsenopyrite carry gold, in the form of associated gold grains and solid solution gold. Pyrite is the most important carrier because of its greater abundance over arsenopyrite. The very large majority of the gold with sulfides is carried by particles of floatable size, >10µm free sulfides. Free sulfides <10µm carry only minor gold. In oxide and transition ores, goethite was the principal iron oxide minerals. Hematite was observed much rarer. Iron oxide minerals carry gold as associated gold grains and submicroscopic gold (colloidal-size micro-inclusions).

Figure 4 summarizes the free and attached gold distribution in various ore samples within the froth flotation perspective. Based on this information, flotation would be the preferred processing option for the

sulfide and the transition ores. Gold recovery is promoted by the good floatability of free sulfides and free gold >10µm; and limited by the presence of difficult to float fine free gold and gold association with FeOx and rock in the transition ores.

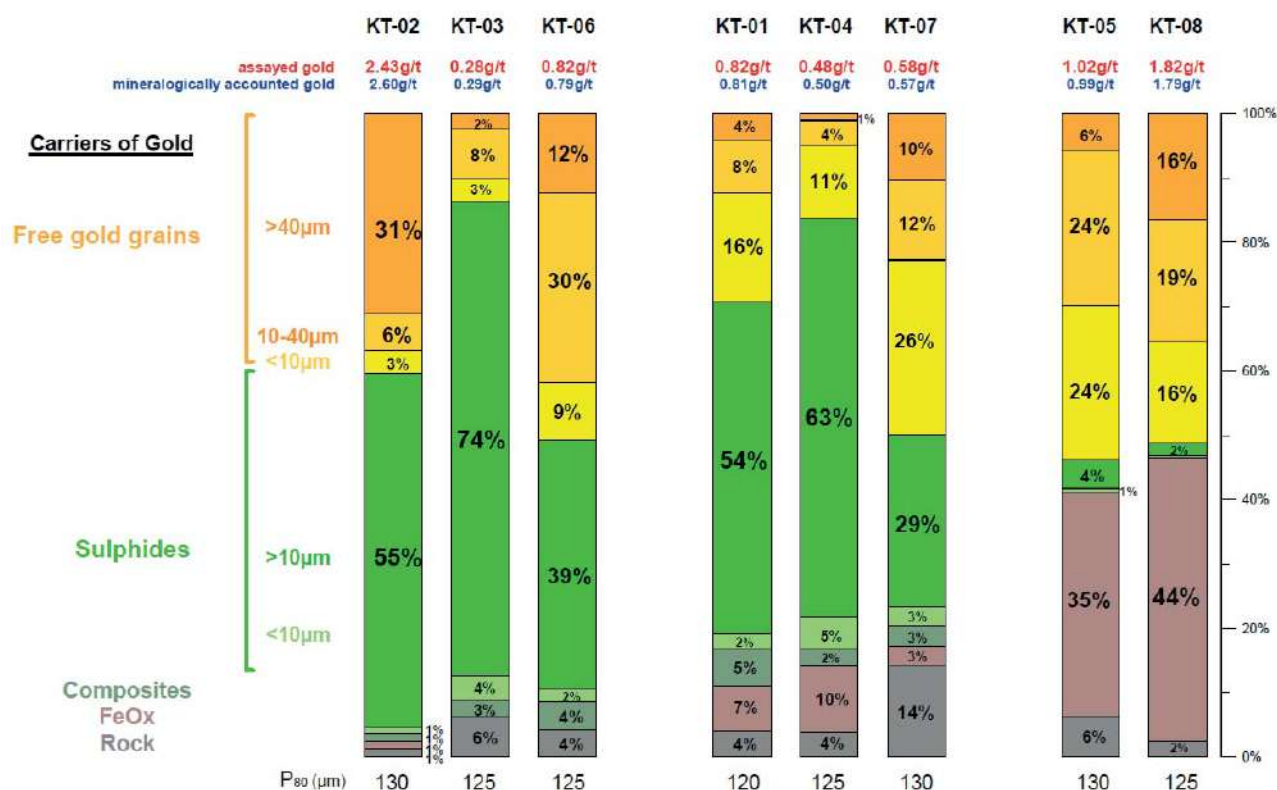


Figure 4. Department of gold – flotation perspective

From the leaching perspective (Figure 5), gold was divided into: exposed cyanidable (free and attached gold grains), enclosed cyanidable (gold grains cyanidable after fine grinding) and refractory (gold which cannot be recovered by direct cyanidation). Refractory gold can only be recovered by pressure and bio-oxidation.

Based on the findings and the amount of refractory gold, it seems that direct cyanidation would not be an efficient extraction method especially in the case of sulfide and transition ores. However, oxide ores seem to be appropriate for direct cyanidation especially in the fine particle size distributions. Pre-concentration methods like gravity separation and flotation can also be considered to reduce throughput and reagent efficiency.

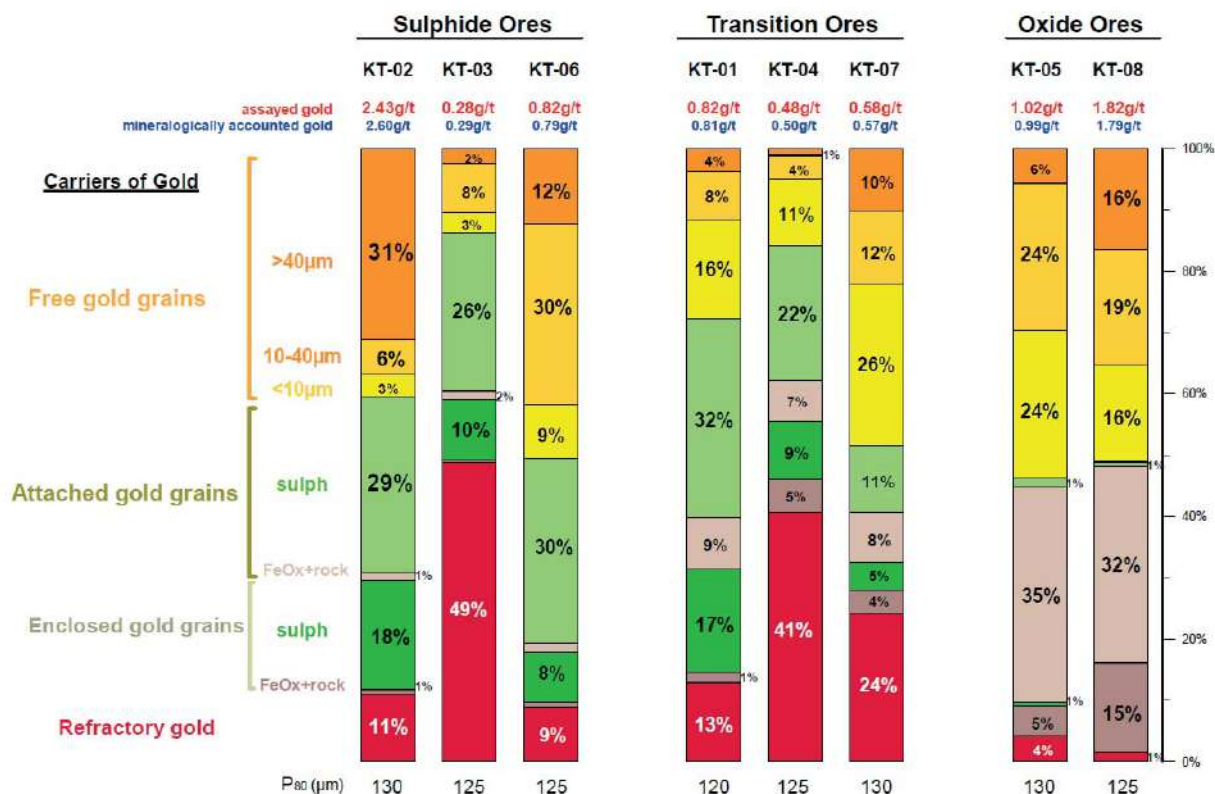


Figure 5. Department of gold - cyanide leach perspective

METALLURGICAL STUDIES

Based on obtained information from geological and mineralogical studies, an experimental test plan was designed in order to select the most efficient beneficiation scenario and then the samples were taken from different ore zones. The basis of the sample selection was relied on chemical analyses and macroscopic observations. The ore samples were crushed (%100 passing 2 mm) and divided into representative sub-samples for subsequent processing studies.

Sulfide Zone

Around 180 kg of core samples (equivalent to 113 m) with average 0.87 g/t Au content was taken from different six drilling holes of the sulfide zone.

To investigate the effects of grinding time on flotation performance, three tests were performed employing the lab-scale Denver type flotation machine using xanthate and MIBC as collector and frother, respectively. Based on available lab facilities, Samples were ground using the lab-scale rod mill for 15, 20 and 25 minutes. P₈₀ (%80 passing sieve size) of the samples are 63.4, 53.8 and 44.1 µm, respectively. In the tests 2 kg/t of sodium silicate (Na₂SiO₃) were used as dispersant at the grinding stage. After 5 minutes conditioning with potassium amyl xanthate and MIBC, flotation was commenced and continued for 10 minutes. Figure 6 shows the effect of fineness of the feed on flotation recovery and concentrate grade.

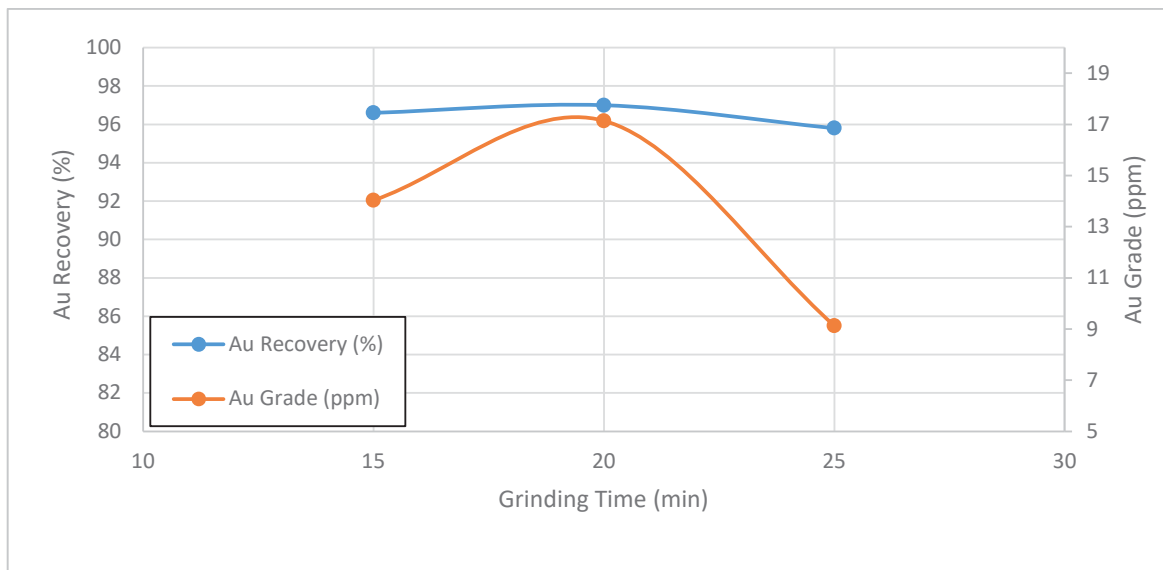


Figure 6. Flotation recovery and concentrate grade of sulfide zone

According to the results, there is not a major improvement of the gold recovery, however, increasing the grinding time reduces the concentrate grade presumably the entrainment of fine gangue particles into the concentrate.

In order to investigate the effect of copper sulfate which is widely used as activator for the sulfide minerals, two flotation tests were performed in the presence and the absence of copper sulfate. Table 2 shows the negative effects of adding CuSO₄ in both gold grade and recovery.

Table 2. Effects of CuSO₄ addition on gold grade and recovery

%	With CuSO ₄	Without CuSO ₄
Au Grade	15.5	17.1
Au Recovery	94.5	97.0

For selecting the best collector types, five different batch flotation tests were performed adding special collectors which are well known with their positive effects on gold flotation and their combinations while keeping other variables were constant (Table 3).

Table 3. Effect of various collector type on flotation performance

%	PAX	SIPX	PAX+Aero 8055	PAX+MaxGold
Au Grade	15.5	10.8	9.4	4.3
Au Recovery	94.5	93.3	70.0	21.6

According to test results, the best flotation performance is obtainable using PAX (Potassium amyl xanthate) although SIPX is also suitable in term of recovery, but the concentrate grade is lower than the one with PAX. Combination of PAX as primary collector with other secondary collectors, did not give better results especially in the case of Maxgold 900.

Aforementioned test works were applied in the natural pH of the pulp (9-9.5) which is slightly alkaline. On the other hand, xanthate type collectors known to show better performances in the case of iron sulfides based on the surface charge of the mineral in the natural pH conditions. For examining the effect of pulp pH on the flotation performance, a comparative test work was applied using sulfuric acid for pH adjustment to the natural-slightly acidic condition (5.5-6). Unexpectedly, the results (Table 4) demonstrate a notable decline in both gold recovery and grade.

Table 4. The graph shows result of flotation recovery and grade in asidic condition

%	pH 6-6.5	pH 9-9.5
Au Grade	3.0	17.1
Au Recovery	36.6	97.0

Based on mineralogical and experimental findings, obtaining a rougher flotation concentrate with 5-6% mass pull, up to 97% gold recovery with 17 g/t Au grade is possible. Additional flotation tests would be required including cleaning stages.

Transition Zone

Around 264 kg of core samples (equivalent to 101 m) were taken from eight holes of the transition zone and crushed to minus 2mm and divided to 1 kg subsamples. The head assay of gold in prepared sample was analyzed as 1.16 g/t. For gaining information about the grindability of the ore sample, three samples were grinded using lab-scale rod mil for 15, 25 and 30 minutes. P₈₀ (%80 passing sieve size) of ground samples was calculated as 62.3, 41.1 and 33.6 microns respectively.

For examining the effect of grinding time on flotation performance, four tests were performed employing the lab-scale Denver type flotation machine using potassium amyl xanthate and MIBC as collector and frother respectively. Figure 7 shows the results of these tests according to flotation recovery and concentrate grade. According to the results, although there is not a significant change in concentrates gold grade, the recovery of gold to the concentrate is slightly increased with grinding possibly improved liberation

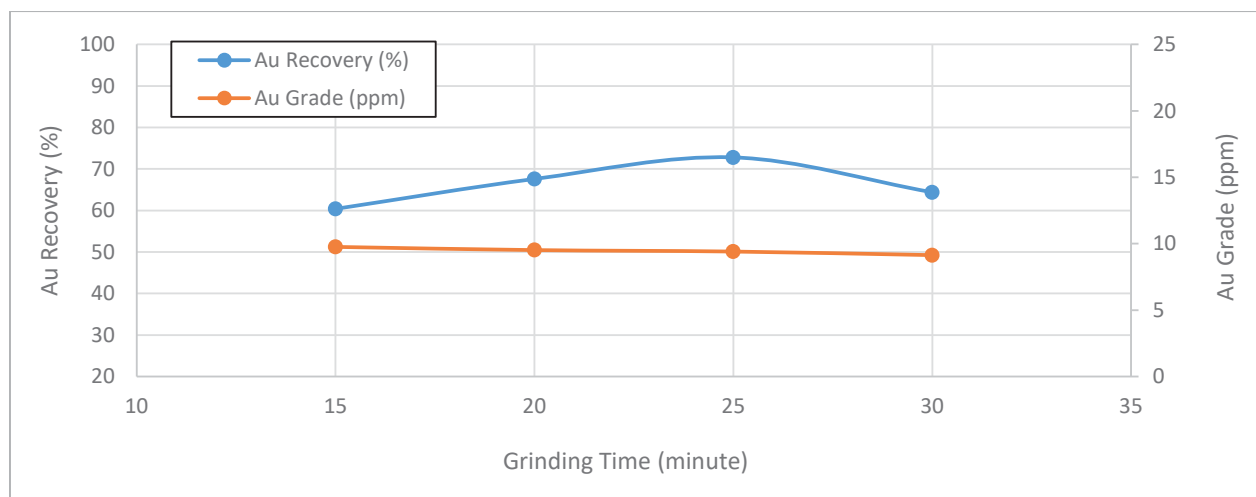


Figure 7. Flotation recovery and concentrate grade of oxide zone

It is well-known that floatability of the oxidized and secondary sulfide minerals can be restored by sulphidization (Castro & Goldfarb, 1974; Ciccu & Curreli & Ghiani, 1979; Dashti & Rashci & Abdizadeh, 2004).

Based on the mineralogical studies the transition zone is appropriate for this concept as it contains iron oxide and sulfide minerals together. In order to investigate the potential effect of sulphidization on flotation performance three test were performed with various sodium sulfide dosages while keeping other parameters constant (Table 5).

Table 5. The Effect of Sulphidization on Flotation grade and recovery

%	0.5 kg/t	1 kg/t	2 kg/t
Au Grade	5.4	6.7	10.6
Au Recovery	79.4	84.8	85.3

Based on the results, increasing the sodium sulfide dosage improves both gold grade and recovery by activation the surface of oxidized minerals. Also, sulphidization test results are showed around 25% improvement in gold recovery compared to the test result in the absence of sodium sulfide.

Similar to the sulfide zone tests, decreasing pH reduces the flotation performance in terms of both gold grade and recovery. Compared to the tests performed in natural pulp pH (8.5) and test with pH 6 adjusted by sulfuric acid, the gold recovery decreased from 84.2% with 11.9 g/t Au to 65.5% with 7.4 g/t Au.

Based on experimental results, a rougher flotation concentrates with 7-8% mass pull, 85% gold recovery with 11 g/t Au content can be obtained using sulphidization. As mentioned before, additional flotation tests would be required including cleaning stages.

Oxidized Zone

Approximately 100 kg of core samples were taken from six holes from the oxidized zone and crushed to minus 2mm and divided to 1 kg subsamples. Although gold deportment studies the gold is mainly either free or attached to the iron oxide minerals e.g., goethite, and minorly attached to sulfides and, although reasonable recovery with direct cyanidation is possible the flotation is considered in order to simplify the potential flowsheet.

For examining the effect of sulphidization on flotation performance, four tests were performed with various Na₂S dosages while keeping other parameters constant. Cyquest 4000 reagent was also added in grinding stage (15min) to improve dispersion. Pulp was conditioned with Na₂S for 15 minutes and PAX was used as collector with MIBC as frother.

Based on the results, gold recovery is increased to 79.8% with Na₂S dosage then slightly decreased to 74.6% at 2 kg/ton Na₂S (Figure 8). The concentrate grade is increased with the Na₂S dosage as well. Consequently, a rougher concentrate having almost 80% recovery with 14.5 g/t Au grade can be produced using sulphidization technique.

Detailed comminution, classification, cleaner flotation and dewatering studies would be necessary for designing and optimizing such a flowsheet. Alternatively, gravity separation techniques like shaking table and falcon separator test works is planned. The comparison of the results of flotation and gravity test works would be helpful in development of the final flowsheet.

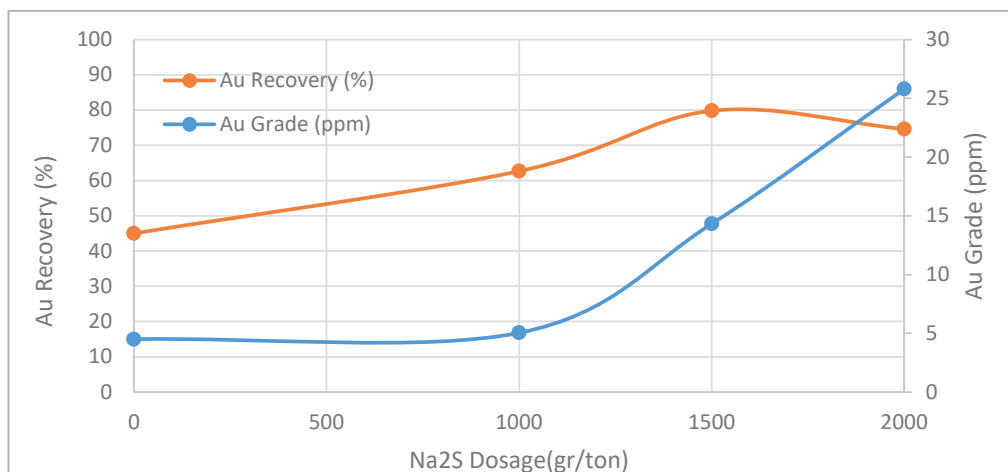


Figure 8. The Effect of Sulfidization on Flotation grade and recovery of the Oxide zone ore

RESULT AND DISCUSSION

The aim of this study is to use the gold department study results to select the most appropriate beneficiation method for a given ore characteristics. Based on combined geological and mineralogical information, it is possible to classify the ore into three different ore types. The gold in oxidized zone is mainly free or attached to iron oxide minerals like goethite. The gold in the sulfide zone is free or attached to sulfide minerals i.e., pyrite and arsenopyrite. The properties of transition zone are the combination of both oxidized and sulfide zones.

Based on the geological and mineralogical data, every ore zone owns different liberation, oxidation and mineralization characteristics and consequently needs distinct beneficiation method. Based on these data and in order to have a holistic beneficiation method, froth flotation studies were carried out for every ore zone samples. The results of flotation test work indicated that:

1. In the sulfide zone, obtaining a rougher concentrate with 5-6% mass pull, up to 97% gold recovery with 17 g/t gold grade is possible using a simple reagent scheme.
2. In the transition zone, a rougher concentrate, up to 85% gold recovery with 11 g/t Au content is possible using sulphidization.
3. And finally, in the oxidized zone, a rougher concentrate with gold recovery of around 80% with 14.5 g/t Au content can be obtained using sulphidization.

Further detailed flotation studies as well as alternative ore concentration methods like gravity separation would be beneficial to select the final flowsheet.

REFERENCES

- Beyuo, M., Agorhom, E., Owusu C., Diaby A.L., Quicoe I. (2016). Gold department and mineralogical characterization for improved recovery. 4th UMaT Biennial International Mining and Mineral Conference.
- Castro S., Goldfarb J., L. J. (1974). Sulphidizing reactions in the flotation of oxidized copper minerals. *International Journal of Mineral Processing*, 141–161.
- Ciccu, R., Curreli, L., Ghiani, M. (1979). The beneficiation of lean semi-oxidized lead–zinc ores. 13th Int. Minerals Process. Cong., Processing of Oxidized and Mixed Oxide–Sulfide Lead–Zinc Ores, 125–145.

ENERGY OPTIMIZATION OF A GRINDING CIRCUIT AT A COPPER MINE
BİR BAKIR MADENİNDE ÖĞÜTME DEVRESİNİN ENERJİ OPTİMİZASYONU

T. Sert ^{1,*}, O. Altun ¹, N.A. Toprak ¹, D. Altun ¹, Ö. Darılmaz ²

¹ *Hacettepe University, Mining Engineering Department*
(*Corresponding author: tolgasert@hacettepe.edu.tr)

² *Acacia Maden İşletmeleri A.Ş.*

ABSTRACT

This study aimed to reveal the opportunities of energy improvement in the copper ore grinding circuit by optimizing the operational conditions. The circuit comprised of a ball mill and hydrocyclone, which were closed circuited to provide the desired target size for the beneficiation. The time the study started the throughput of the grinding circuit was 240 tph. The initial optimization started at the control room where the cyclone pressure was changed from 60 kPa to 100-120 kPa range and mill discharge solid was changed from 68% to 80%. As a result of the adjustment the circuit responded positively and the feed rate was able to be increased to 278 tph with the same product fineness (p80 of 102 microns). In brief 15.8% increase in throughput was obtained. The sampling campaign was performed at that level to develop the model structures to be used in the simulation studies. Within the scope of the evaluations, 8 simulations were run to predict the operational range of the circuit, the throughputs at varied product fineness, and the lower/upper limits while considering the use of 70 mm grinding balls at 32% filling. The simulations showed that the throughput could be increased to 300-320 t/h in case the proper conditions were established.

Keywords: Grinding, optimization, energy efficiency

INTRODUCTION

Grinding is an energy-intensive unit operation in mineral processing, which accounts for the majority of the operational cost in a mineral processing plant (Wills, 2016). Maintaining an optimum mill load is key to improve the efficiency energy utilization. In this study, the opportunities for energy improvement in the copper ore grinding circuit have been investigated.

The wet grinding circuit of the plant is composed of a ball mill and hydrocyclone cluster that is operated in the mode of a closed circuit. It means that the coarse product of hydrocyclone is subjected to further milling. There is a trommel screen mounted at the discharge end of the mill to discard the scats out of the circuit. The flow rate of the scats is continuously measured by the plant. There are two locations that the water is added, one is from the feed end and the other is from the discharge end prior to the wet classification. Those flow rates can be calculated after the material balancing that can be found in the following sections. The simplified flow sheet of the circuit with the sampling points indicated is illustrated in Fig.1 and the technical specifications of the machines are summarized in Table 1 and Table 2.

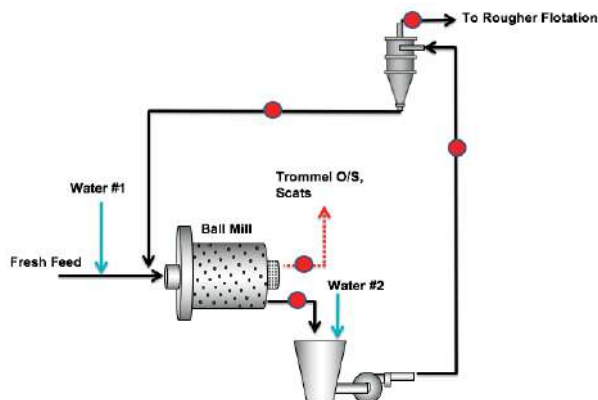


Figure. 1. Simplified flow sheet of the grinding circuit.

Table 1. Specifications of the Ball Mill

Effective Diameter (m)	Length (m)	Installed Power (kW)	Mill Speed (rpm)
5.38	8.2	4400	14

Table 2. Specifications of the Hydrocyclone.

Brand	Diameter (mm)	Feed inlet (mm)	Vortex dia. (mm)	Apex dia. (mm)	No. of available cyclones	Suggested oper. pres. (kPa)
Weir, Cavex	500	200	155	90	7	80-120

MATERIALS AND METHODS

Sampling Studies

The study has aimed to quantify the limits of the throughput. Prior to the sampling campaign, a steady state condition was reached by changing the operating conditions of the circuit at the control room. It was observed that the grinding circuit was controlled via cascade mode which allows keeping the sump level steady by increasing or reducing the speed of the pump. However, changing the pump speed disturbed the whole operation as cyclone pressure varied between 80 kPa and 110 kPa, which can also lead to change in the size distribution of the cyclone overflow stream. In order to prevent this phenomenon, the grinding circuit was controlled manually and small adjustments were made to keep the pressure and sump level at steady.

Prior to performing the sampling campaign, the plots/trends of the operating variables such as mill power, sump level, cyclone pressure, overflow %solid, were followed around 90 minutes. Table 3 tabulates the average operating conditions of the mill.

Table 3. Average operating conditions recorded during the survey.

Fresh feed (t/h)	Feed moisture (%)	Power draw of ball mill (kW)	No. of cyclone in operation	Pressure of hydrocyclone (kPa)	Speed of pump (%)	Hydrocyclone overflow solid %
278.78	1.6	2913	4	110	87.6	33.78

Material Characterization

The collected samples were characterized regarding their particle size distributions, solid percentage, work index, breakage distribution and specific gravity. Particle size analyses were completed in two steps. Initially, the whole material was wet sieved from 26 mm to 38µm. Below that size, cyclosizer technique was applied to determine the size analysis down to 8µm. The set of data obtained from the two methods was then combined. The experimental size distributions are depicted in Fig. 2.

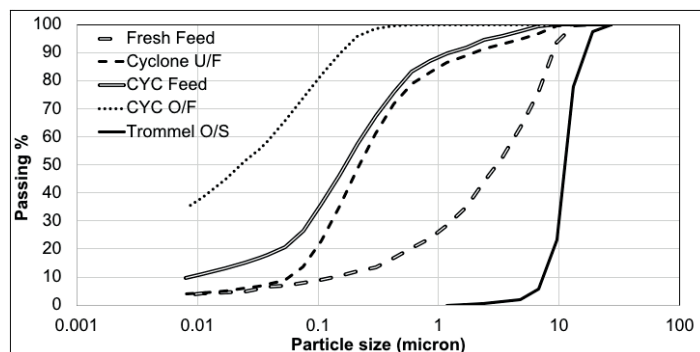


Figure 2. Experimental size distributions.

The product fineness of the grinding circuit has been followed within the control room via PSI measurement. D80 value of cyclone overflow from PSI is 102.1 µm while the size analysis result is 98 µm which are similar to each other.

Solid percentages of the streams are tabulated in Table 4.

Table 4. Measured solid percentages of the streams

Fresh Feed	Tromme l O/F	Cyc Feed	Cyc U/F	Cyc 7 U/F	Cyc O/F (Cond.)	PSI	Flot. Feed (courier)	Cyc 7 O/F	Mill Disch.
98.4	99.5	66.6	84.7	85.1	37.1	38.1	36.8	40.4	82.9

Bond work index test aims to determine the grindability of ore that refers to the ease with which materials can be comminuted. The data is either utilized to evaluate the grinding efficiency or to predict the product size distribution of the mill within the simulation studies. The work index of the ore was found as **13.04** kWh/t. Breakage function refers to the breakage properties of a given sample. It is determined as a result of breaking the particles at different energy levels, followed by measuring the weight distribution to subsequent size classes. It is an ore-specific property that is utilized as an input in the modelling of size reduction machines. Within the scope of the project, narrow -9.5+8 mm size fraction was prepared and then subjected to the breakage test works from three different energy levels (1.65 kWh/t, 2.01 kWh/t and 2.70 kWh/t). Following the test works, particle size distributions of broken products were determined. Three different breakage distribution functions were calculated to use in the ball mill modelling studies (Fig.3).

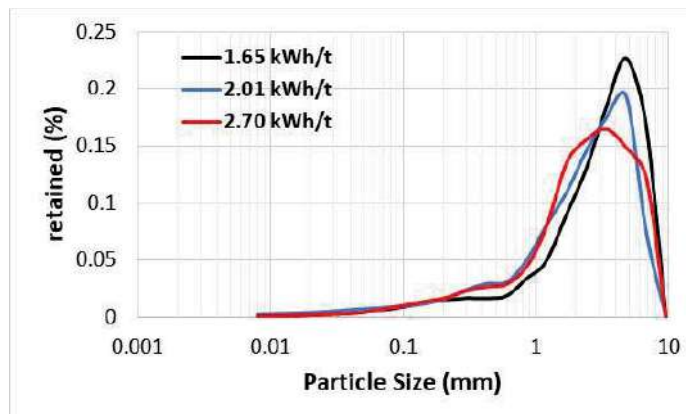


Figure 3. Calculated breakage distribution functions

Sampling Campaign, Mass Balancing and Machine Performances

Within the circuit, the flow rates of some of the streams are known and the rest is calculated statistically. In addition, the experimental data may contain errors that all should be considered during the assessments. Performing mass balancing enables calculating the unknown streams by distributing the errors arisen due to the experimental works and sampling methodologies. The study benefited from JK-SimMet software; all the missing points are calculated based on the afore-mentioned approach. The specifications of the streams regarding the flows and size characteristics are illustrated in Fig. 4. Fig. 5 depicts the plots of experimental and calculated size distributions indicating that the sampling studies were accomplished with the least sum of errors.

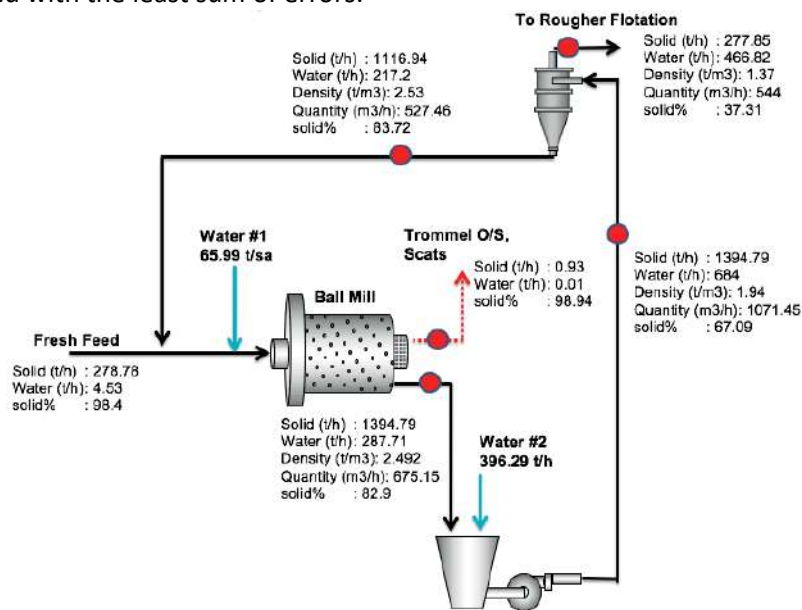


Figure 4. Results of the mass balancing.

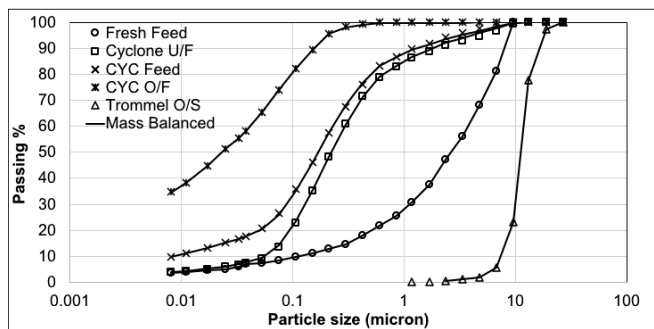


Figure 5. Comparison of the experimental and mass balanced size distributions.

The mass balanced data showed that the solid percentage of hydrocyclone overflow (37%) is different from what was indicated on the control room (33%) hence some discrepancies were observed.

RESULTS AND DISCUSSIONS

Performance Evaluation of Overall Circuit

For the overall circuit, the specific energy utilization and the size distributions of fresh feed, cyclone overflow streams were considered. Additionally, the circulating load was calculated by dividing the solid flow rate of cyclone underflow stream by cyclone overflow. Table 5 summarizes the data of the grinding circuit. It should be noted that the power consumptions of the auxiliaries were not included in the assessments.

Table 5. The data of the grinding circuit

Ball mill power (kW)	2913
Fresh feed (t/h)	278.78
Trommel oversize (t/h)	0.93
Hydrocyclone overflow to flotation feed (t/h)	277.85
Hydrocyclone underflow (t/h)	1116.94
Specific energy cons. (kWh/t)	10.48
F ₈₀ of Fresh feed (mm)	6.5
P ₈₀ of Hydrocyclone overflow (mm)	0.098
F ₅₀ of Fresh feed (mm)	2.7
P ₅₀ of Hydrocyclone overflow (mm)	0.023

The specific energy consumption of the circuit was calculated as 10.48 kWh/t for the degree of size reductions of 66.3 (RR_{d80}) and 117 (RR_{d50}). The circulating load of the milling is 401%.

Where;

RR_{d80}: reduction ratio of d_{80s}

RR_{d50}: reduction ratio of d_{50s}

The specific gravities of the streams were measured and illustrated in Fig.6. The results showed that there was an effect of centrifugal wet classification since the material of cyclone underflow was denser than that of the overflow stream. The material of the trommel oversize stream is the lightest of all.

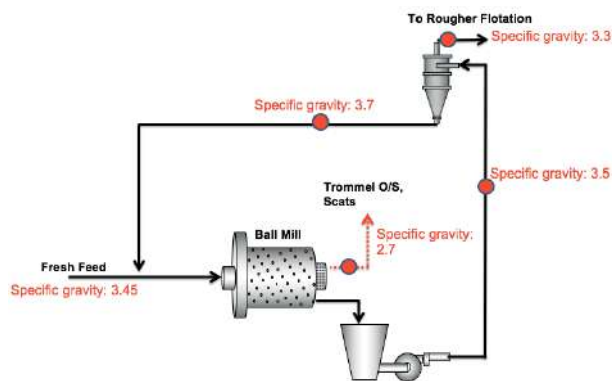


Figure 6. Specific gravities of the streams.

Within the performance analysis of the ball mill; size reduction and the trommel oversize sample, the grinding media filling and its influence on power draw and energy utilization and grinding media size were considered.

Size Reduction Performance of the Mill

Fig. 7 illustrates the size distributions of feed, product and trommel oversize samples.

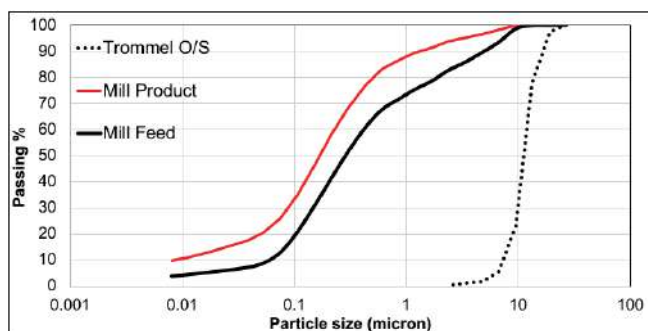


Figure 7. Size distributions around the ball mill.

The performance data of the mill is summarized in Table 6.

Table 6. Ball mill performance.

Mill power (kW)	Mill throughput (t/h)	Solid %	Feed, F ₅₀ (mm)	Product, P ₅₀ (mm)
2913	1395.72	82.9	0.288	0.17

The mass balanced data indicated that the mill was operated at 82.9% of solid content. It is a well-known fact that the higher the solid content of the mill, the finer the product up to a saturation point of 80%. Consequently, adding more water may be considered from the feed end of the mill to achieve that level. It may have impacts on the throughput. The amount of trommel oversize material was measured as 0.93 t/h. That amount may fluctuate depending on the solid content of the mill, type of ore and feed rate to the mill. The specific energy utilization of the ball mill is found as 2.09 kWh/ton for the size reduction of 1.65.

Grinding Media Filling and the Power Draw of the Mill

At the end of the sampling campaigns, ball mill was crash-stopped in order carry out mill inside measurements e.g., media filling level and media size distribution. The ball filling can be calculated from the position of the ball charge at rest. Table 7 summarizes the results of the calculations

Table 7. Media filling measurements of mill

H (cm)	Effective Diameter (cm)	Filling Ratio %
3700	5384	26.41

In another evaluation, the height from the top to the lower section of discharge grate was measured to find out the maximum available volume of the grinding media charge. The measurements showed that the level of 35-40% can be filled with the grinding media. It can be concluded that the grinding media level is well-below the optimal operating conditions. This phenomenon can also be validated from the power draw of the mill. As the installed power is 4400 kW, the mill can be operated up to 3400-3600 kW range that is the function of the media filling. During the sampling campaign, power draw was noted as 2913 kW that indicates there is a margin for adding grinding media. It is recommended to charge more grinding media into the mill by following the variation in the power draw. Such a change is expected to further increase the throughput of the mill at the same degree of fineness. The simulation studies have aimed to predict the improvements in the grinding efficiency.

Critical Speed

The speed at which the maximum power in a mill can be drawn is therefore critical and the speed at which the charge centrifuges is known as the *Critical Speed*. Wet grinding overflow discharge ball mills are usually operated at 74%-76% of critical speed. The literature also reports that it may go up to 78% that results in increased capacity. For the ball mill in operation, the number of rotations per minute was measured as between 14 rpm and 14.3 rpm. By taking the diameter and the maximum size of the grinding media into account, the critical speed is calculated as 77%. It can be concluded that the speed is at its limits.

Ball Size Evaluations

There exist different approaches in grinding media size calculations. Within the scope of this study, Rowland and Kios approach (1978) was applied, which indicates that the initial ball size is related to the characteristics of the feed (work index, particle size and size distribution, S.G. of the solids and slurry density) and the mill (diameter and critical speed). Within the calculations, 80% passing and top size of the feed size distributions were considered so as to predict the fluctuations in the performances of the crushing stages. In this regard, 6.5mm and 9.5mm sizes were inputted to Equation 5 assuming the work index and specific gravity of the ore remained constant. Table 8 gives the results of the calculations.

Table 8. Calculated ball sizes

	Grinding ball Size (mm)
Top size of feed, 9.5mm	70
80% passing, 6.5mm	58

The assessments proved that the ball size of 58 mm is sufficient for breaking the feed having d_{80} of 6.5 mm. However, 70 mm size that corresponds to feed top size can be considered as a safety issue. Above this size range can be designated as the point of start of inefficiency where the loss on the surface area of grinding media will lead to the loss of grinding efficiency. As a conclusion, 70 mm mono sized grinding ball charge has been suggested.

Performance of Hydrocyclone Cluster

The commonly preferred method of representing cyclone efficiency is by a performance or partition curve, which relates the weight fraction, or percentage, of each particle size in the feed which reports to the apex, or underflow, to the particle size. Within the study, the performances of hydrocyclone cluster (the main streams around the hydrocyclone) as well as the single unit were evaluated. In this context, cyclone no 7 was sampled and the Tromp curve of it was compared with that of the cluster. Figure 8 shows the efficiency curve of the cyclone cluster. Table 9 summarizes the process data of hydrocyclone where the water recovery was calculated. The calculations implied that the water recovery to underflow was in good agreement with the bypass value determined from the Tromp curve.

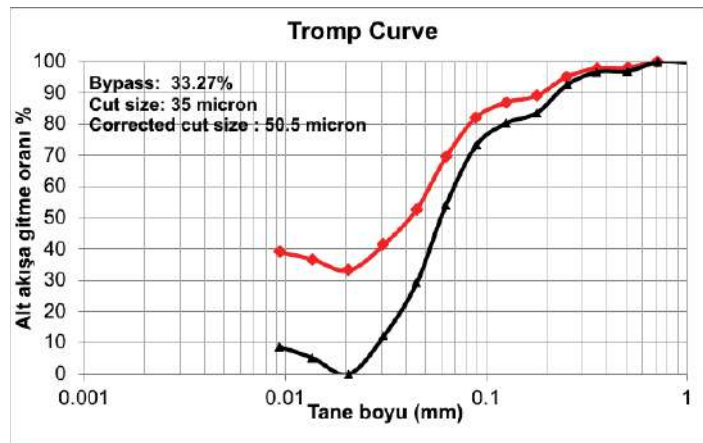


Figure 8. Actual and corrected efficiency curves.

Table 9. Process conditions of hydrocyclone

CYC O/F Solid%	37.31
Cyclone Pressure (kPa)	110
CYC Feed water (t/h)	684
CYC U/F water (t/h)	217.2
Water Rec. to underflow (%)	31.7
Bypass from Tromp curve (%)	33.2

Modelling of the Machines

Within the scope, ball mill, trommel screen and hydrocyclone units were modelled. Population balance model of Napier Munn (1996) has been used for the ball mill modelling. In modelling of the Trommel screen, the efficiency curve approach of Whiten was used. The model of Nageswararao (1978) was preferred for hydrocyclone modelling. The successes of the model fitting studies were evaluated by doing base case simulation that is expected to reflect the behavior of the sampling conditions. Fig. 9 and

Fig. 10 illustrates the circuit parameters and the agreement between the experimental and simulated size distributions.

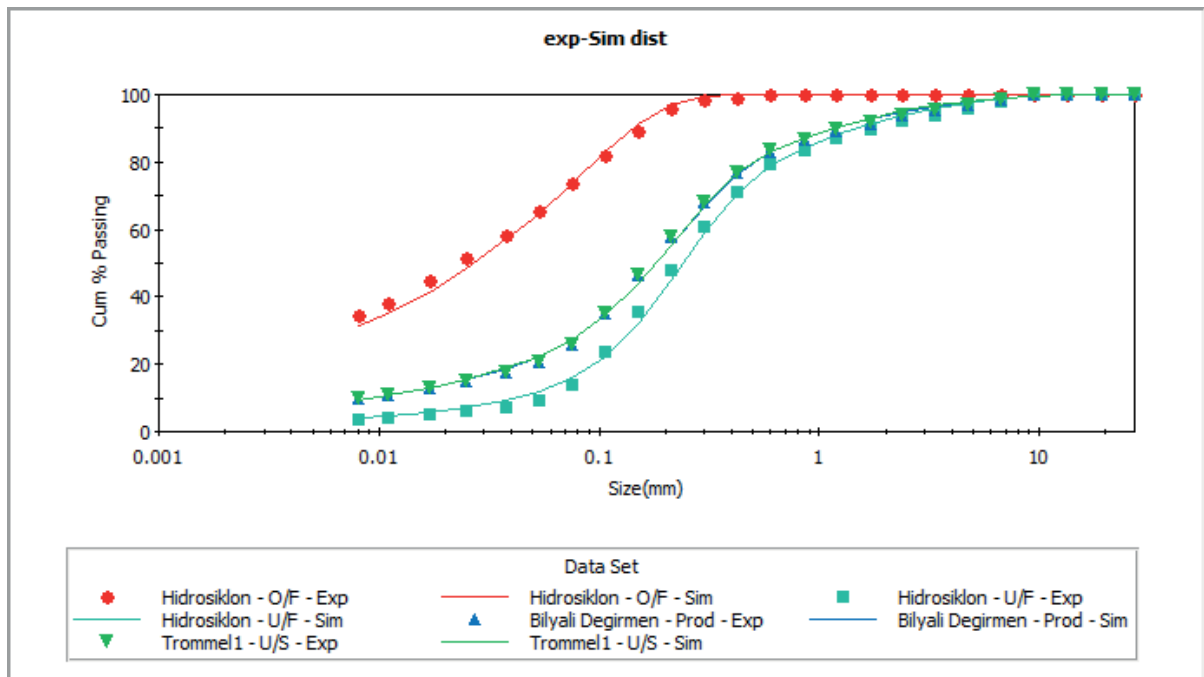


Figure 9. Experimental and simulated size distributions.

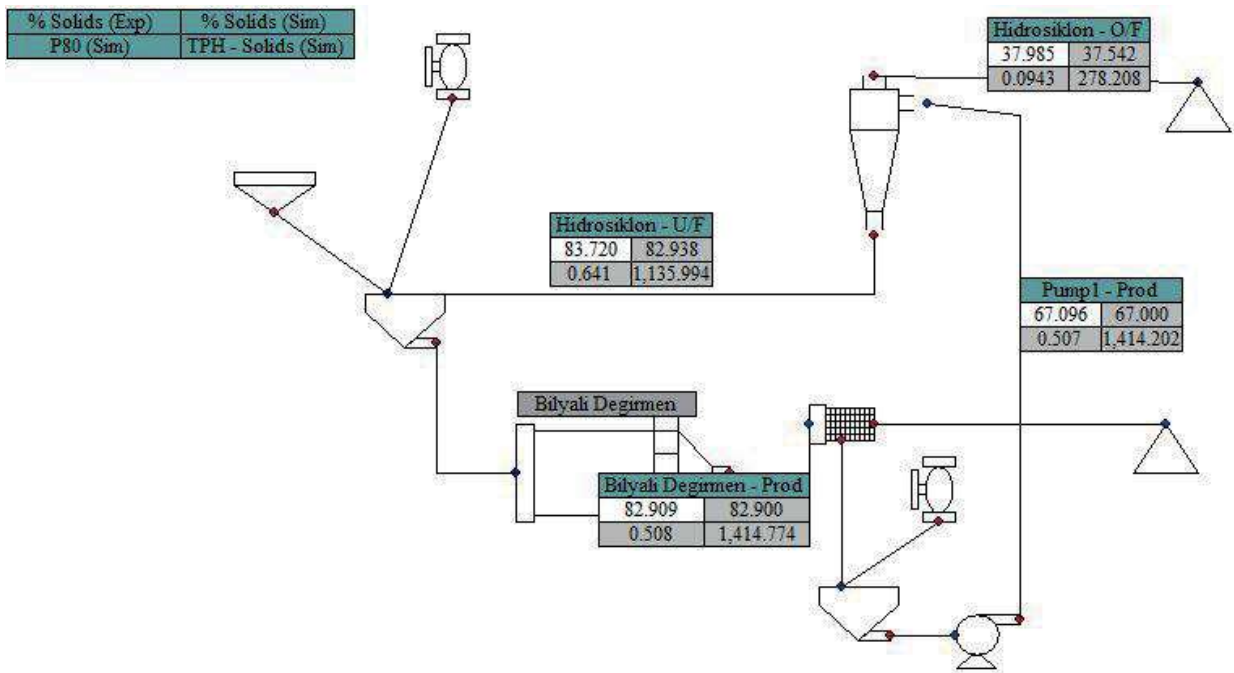


Figure 10. Base case simulation output.

Simulation Scenarios

Within the scope of the project, 8 scenarios were tested. The focus of each study is given in Table 10. The conditions of the simulation scenarios have been decided based on the previous optimization works of Altun. (Altun, 2016, 2018)

Table 10. Simulation scenarios

Simulation number	Focus
#1	350 tph for the same product fineness
#2	300 tph for the same product fineness
#3	275 tph for the same product fineness
#4	255 tph for the same product fineness
#5	Only 1 Cyclone in operation
#6	P80 of 42 microns
#7	P80 of 75 microns
#8	P80 of 117 microns

The summary of all the evaluations is presented in Table 11. It should be emphasized that all the simulations were run at 32% grinding media filling and ball size of 70 mm.

Table 11. Results of the simulations.

	Sim. #1	Sim. #2	Sim. #3	Sim. #4	Sim. #5	Sim. #6	Sim. #7	Sim. #8
Fresh feed (t/h)	350	300	275	255	130	195	265	395
Cyc O/F (t/h)	348.8	299	274	254	129.8	194	264	394
Cyc U/F (t/h)	1415	994	910	638	224	479.5	758.4	1669
Circ. load (%)	405.68	332.44	332.12	251.18	172.57	247.16	287.27	423.6
No of Cyclones	5	4	4	4	1	2	3	7
apex size (mm)	0.09	0.085	0.085	0.08	0.08	0.09	0.09	0.085
Cyc Pres. (kPa)	105-110	88	78	77	120	120	100	75
Cyc O/F Solid%	37.2	40.4	41	45	47	40.9	44.74	37.1
Cyc O/F P80 (µm)	99	98	96	92	47	42	75	117
Cyc Feed (m3/h)	1351	991	912	674	289	591.8	783.5	1566
Mill Power (kW)	3516	3516	3516	3516	3516	3516	3516	3516
S.E (kWh/t)	10.08	11.76	12.83	13.84	27.09	18.12	13.32	8.92
Mill Solid%	81	78	76	76.5	67	80	81	81

CONCLUSIONS

From Sim 1-4 it is understood that the circuit is operable at 350 t/h for the same degree of the product fineness (p_{80} of about 98 microns). With the decreasing throughput, cyclone pressure, number of cyclones in operation and the flow rates decrease significantly thus the size of apex should be changed accordingly. The power draw of the mill was predicted as 3516 kW for grinding media filling of 32% and kept constant in all through the evaluations. The down limit of the grinding circuit was questioned by the plant staff hence another simulation study was conducted when 1 cyclone is in operation (Sim #5). In that study, cyclone was tried to be operated at 120 kPa by adjusting the rest of the operating conditions such as mill solid percentage, cyclone feed solid percentage, throughput and number of cyclones. The calculations showed that the grinding circuit can be operated at 130 t/h. From Simulations 6-8 the product fineness was changed and the feed rate to the circuit was predicted. The maximum throughput (395 t/h) was achieved when p_{80} was 117 microns. For p_{80} of 42 microns the feed rate was predicted as 195 t/h.

It should be noted that in order to achieve higher throughputs, the limitations within the grinding circuit should be considered such as the design capacity of the pumps.

REFERENCES

- Altun, O. (2016). Simulation aided flow sheet optimization of a cement grinding circuit by considering the quality measurements. *Powder Technology*, 301, 1242-1251.
- Altun, O. (2018). Energy and cement quality optimization of a cement grinding circuit. *Advanced Powder Technology*, 29(7), 1713-1723.
- Bond, F. C. (1952). Third theory of comminution. *Mining engineering*, 4, 484.
- Nageswararao, K. (1978). Further modelling and scale-up of hydrocyclones. *JKMRC, University of Queensland*.
- Napier-Munn, T. J., Morrell, S., Morrison, R. D., & Kojovic, T. (1996). Mineral comminution circuits: their operation and optimisation.
- Rowland, C. A., and D. M. Kjos. "Rod and ball mills." *Mineral Processing Plant Design (ed. AIME) (1978): 239-278*.
- Wills, B. A., & Finch, J. A. (2016). Froth flotation. *Wills' Mineral Processing Technology*, 7.

ENVIRONMENTAL IMPACT ASSESSMENT FOOTPRINT IN OPEN-PIT COPPER MINING

M. Heydari ¹, M. Osanloo ^{1,*}, A. Başçetin ²

¹ *Amirkabir University of Technology, Mining Engineering Dept
(*Corresponding author: morteza.osanloo@gmail.com)*

² *Istanbul University, Engineering Faculty, Mining Engineering Dept*

ABSTRACT

With the rise of technology and the growth of population, copper consumption increases globally. However, high-grade near-surface deposits have been depleted in past years or will be depleted in the near future. Deep low-grade ore remains, creating higher environmental impacts like the greater volume of waste, higher energy consumption, and land degradation. Although the environmental impacts of copper mines have been quantified in several studies, a comprehensive environmental impact assessment (EIA) related to open-pit copper mines at the global level is missing in current literature. This study focuses on published papers from 2010 to 2021, investigating the footprint of copper mining on the environment. Most studies used quantitative approaches to assess the environmental impacts of copper mines (41% of total), among which life cycle assessment (LCA) has the highest application of 75%. The results show that the available models have shortcomings, such as excessive assumptions in LCA and expert-dependent results in MCDMs. This finding indicates the need to improve the existing models and create a comprehensive EIA technique applicable in all open-pit copper mines to decrease the copper production's environmental impacts per kg and achieve a cleaner environment.

Keywords: Environmental impact assessment (EIA), open-pit mining, copper

INTRODUCTION

Mining is the first step in preparing the raw materials needed for infrastructure advance, raising human living standards, and achieving social development. Considering the world population growth rate in recent years, by 2030, the world population will be about 8.3 billion (Osanloo, 2016). On the other hand, with the growth of the urbanization rate and the desire of people to have high standards of urban life, mineral consumption increases (Kuipers et al., 2018). copper is one of the essential sources for many technologies, such as the construction industry, telecommunications, automotive, and electronics, and it is expected that its production will increase significantly in the coming decades. Between 2000 and 2018, world copper tonnage rose about 4% per year, projected to increase up to 2030 due to increasing urbanization rates (especially in developing countries such as India and China). Therefore, with increasing demand, copper exploitation in the future will be from the depths with lower grades. Copper mines are found worldwide in different climatic conditions, such as hot/cold and dry/wet, with various mineralogical and geomechanical properties. Mining higher volumes of ore from the earth's crust to achieve the consumption rate of the society's need result in more energy consumption, greenhouses gas emissions, water and soil pollution, flora and fauna destruction, and land disturbance. The average copper grades of sulfide ores have decreased from 1.18% to 0.60% over 2003-2020 in Chilean copper mines. Lower average grade results in more waste produced in the mining and

processing stages. Therefore, more water, energy, and chemical reagents are required to process low-grade copper ores efficiently. The consumption of collectors, frothers, and modifiers in flotation increases because higher amounts of low-copper grade ore are processed. These chemicals represent reagents that pose environmental risks due to their properties, classified as hazardous materials for potential health effects (Reyes-Bozo et al., 2014). As a result, assessing the environmental impacts of copper mining activities becomes more critical.

Environmental Impact Assessment (EIA) is a tool for evaluating the project's positive and negative environmental outcomes before implementing it to achieve sustainable development goals in mining projects. Today, experts and owners of the mining sector believe that society needs a green, healthy, economical, and fertile environment. The environmental impacts of copper mining have been quantified in various research (Zhang et al., 2021, Perlatti et al., 2021, Islam et al., 2019, Hong et al., 2018, Kulczycka et al., 2016, Wang et al., 2015), and some studies have examined specific aspects of the environmental impacts of copper production. However, a comprehensive model for investigating the positive and negative environmental effects of open-pit copper mines is hard to come by, which is an essential gap in the current literature. Environmental impacts are divided into temporary and permanent impacts: (1) Temporary impacts depend directly on the mining projects but disappear if the mining activity stops. (2) Structural impacts also stem directly from the mining project, but the environmental impact will continue if the mining activity stops. These impacts could be temporary (mid-term or long-term) or permanent. Concerning the potential impacts on the environment, the advancement of mining projects has certain coincidences compared to other projects. The environmental and social impacts are different, and sometimes, they remain long after the end of mining activities. Therefore, the natural impacts of mining got to be carefully evaluated within the early stage of the mining project. Also, the activities must be assessed for potential impacts after the mining operation decommission (Castilla-Gómez and Herrera-Herbert, 2015).

This study aims to survey and classify the available studies in the subject of EIA in copper mining into three groups: Qualitative, Semi-Qualitative, and Quantitative studies. Next, the most used technics are recognized, and then the shortcoming of each study is highlighted as the path toward a comprehensive EIA for copper mines modeling.

Environmental Impact Assessment in Mining

Since all mining activities cause environmental changes, identifying the mining impacts is necessary to improve the positive ones and prevent creating or controlling adverse ones. These effects can be positive (such as employment, increasing GDP and increasing government revenues, the establishment of housing estates in disadvantaged areas, and developing infrastructure such as water supply, electricity, and educational and medical centres) or negative (such as biodiversity loss, Landslide, surface and groundwater pollution, loss of vegetation and forest, and landscape disruption). All mining activities, from exploration to decommissioning, have multiple environmental effects.

Over the past few years, environmental issues have become increasingly respected and revised globally. In a comprehensive classification, the existing methods for assessing the environmental impact of mines can be divided into three groups: qualitative methods, quantitative methods, and semi-qualitative methods. In recent decades, numerous studies have been conducted to assess the environmental impact of mining activities. The following will discuss the statistical classification of the studies in the three qualitative, quantitative, and semi-qualitative groups. In general, 40 studies that evaluated the environmental impact of mines between 2010 and 2021 were reviewed in this paper.

Qualitative Studies

From 2010 to 2021, several studies have used qualitative methods for EIA of mining projects. Only the qualitative factors are assessed in this method, and the results are linguistic. Table 1 summarizes the surveyed studies that used qualitative methods in their research.

Table 1. Summary of studies of EIA in mining

Reviewed studies	EIA Methodology	Mineral type
Suopajärvi (2013)	Qualitative	Copper , Gold, Nickel, Iron
Morrison-Saunders et al. (2015)	Qualitative	-
Castilla-Gómez and Herrera-Herbert (2015)	Qualitative	Copper
Gałaś and Gałaś (2016)	Qualitative	Copper , Silver, Kaolin, Uranium
Mancini and Sala (2018)	Qualitative	Copper
Gorman and Dzombak (2018)	Qualitative	Copper
Hresc et al. (2018)	Qualitative	Copper
Ocampo-Melgar et al. (2019)	Qualitative	Copper , Gold
Clark (2019)	Qualitative	-
Riley et al. (2019)	Qualitative	Coal
da SilvaDias et al. (2019)	Qualitative	Iron
Lemly (2019)	Qualitative	Coal

Table 2 shows that from 2010 to 2021, 32% of studies examined the environmental impacts of open-pit mines using qualitative methods, from which 54% have examined the EIA of copper mines.

Table 2. Number of qualitative studies of EIA considering Copper mining

Total Number of Studies	Number of copper studies
12	7

Semi-Qualitative Studies

Semi-qualitative technics use multi-criteria decision-making technics to quantify the qualitative factors and assess the kind of qualitative and quantitative impacts of the project at once. Considering the nature of impacting factors in mining projects (both quantitative and qualitative), semi-quantitative methodology can be advantageous. Table 3 shows the summary of the semi-qualitative studies surveyed in this paper.

Table 3. Summary of studies of EIA in mining

Reviewed studies	EIA Methodology	Mineral type
Aryafar et al. (2012)	Semi-Qualitative	Coal
Minaei Mobtaker and Osanloo (2014)	Semi-Qualitative	-
Saini et al. (2016)	Semi-Qualitative	Coal
Ataei et al. (2016)	Semi-Qualitative	Coal
Rahmanpour and Osanloo (2017)	Semi-Qualitative	Copper
Heidari and Osanloo (2018)	Semi-Qualitative	Zinc and Lead
Saffari et al. (2019)	Semi-Qualitative	Cement
Sarupria et al. (2019)	Semi-Qualitative	Iron, Manganese

Amirshenava and Osanloo (2019)	Semi-Qualitative	Iron
Ataei and Masir (2020)	Semi-Qualitative	Copper

To summarize, from 2010 to 2021, 27% of studies examined the environmental impacts of open-pit mines using semi-qualitative methods, from which 20% have examined the EIA of copper mines (Table 4).

Table 4. Number of Semi-qualitative studies of EIA considering Copper mining

Total Number of Studies	Number of copper studies
10	2

Quantitative Studies

Quantitative studies include the ones that examined the soil, water, and air pollution or used the LCA method to investigate the emissions into the environment. Table 5 shows the summary of the surveyed studies in this group.

Table 5. Summary of studies of EIA in mining

Reviewed studies	EIA Methodology	Mineral type
Norgate and Haque (2010)	Quantitative	Copper , Iron, Bauxite
Northey et al. (2013)	Quantitative	Copper
Muñoz et al. (2014)	Quantitative	Copper
Reyes-Bozo et al. (2014)	Quantitative	Copper
Song et al. (2014)	Quantitative	Copper
Wang et al. (2015)	Quantitative	Copper
Drielsma et al. (2016)	Quantitative	Copper
Kulczycka et al. (2016)	Quantitative	Copper
Hasanipanah et al. (2018)	Quantitative	Copper
Hong et al. (2018)	Quantitative	Copper
Kuipers et al. (2018)	Quantitative	Copper
Islam et al. (2019)	Quantitative	Copper
Dong et al. (2020)	Quantitative	Copper
Zhang et al. (2021)	Quantitative	Copper
Perlatti et al. (2021)	Quantitative	Copper

In brief, from 2010 to 2021, 41% of studies examined the environmental impacts of open-pit mines using quantitative methods from which 100% have examined the EIA of copper mines (Table 6).

Table 6. Number of Semi-qualitative studies of EIA considering Copper mining

Total Number of Studies	Number of copper studies
15	15

RESULTS AND DISCUSSION

Reviewing the studies of copper mining EIA from 2010-2021 revealed that 41% of environmental research studies have been carried out quantitatively from 2010 to 2021, which mainly focused on

emissions measured by LCA methods or chemical analysis of soil and water samples of the surrounding areas while other environmental aspects were not investigated. 32% of the studies are qualitatively assessed from 2010-2021. This is due to the qualitative nature of the parameters studied and the lack of comprehensive quantitative methods. In 27 % of the studies, semi-quantitative methods have been used, the ineffectiveness of quantitative methods in the whole process of environmental assessment, the qualitative nature of many parameters, and the inability to quantify them by the way other than Experts, semi-quantitative methods can assess the environmental impacts of the mining project comprehensively (Table 7, Figure 1)

Table 7. Summary of reviewed studies of copper mining

	Reviewed studies	Percentage	Considering positive impacts	Copper mineral
Qualitative	12	32%	0	7
Semi-qualitative	10	27 %	1	2
Quantitative	15	41 %	1	15
Total	37	100 %	2	24

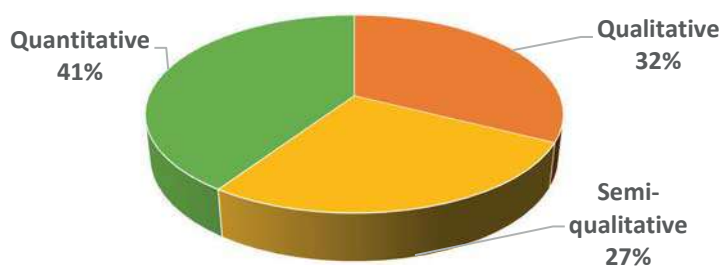


Figure 1. The rate of use of each group of assessment methods

Figure 2 shows studies surveyed regarding the mineral type. According to this picture, 63% of the surveyed studies evaluate the EIA in copper mines. Table 8 summarizes the reviewed studies, their advantages, and the shortcomings of each study.

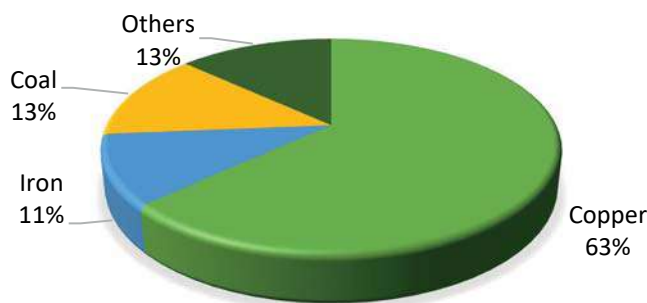


Figure 2. Percentage of studies investigated regarding the mineral type

Table 8. Summary of the studies on the environmental impact assessment of copper mines

Reviewed studies	Advantages	Shortcomings
Norgate and Haque (2010)	Evaluated the impacts of energy and greenhouse gas emissions in the life cycle of mining and mineral processing	Only energy and greenhouse gas emissions were assessed, and the other environmental impacts were ignored.
Aryafar et al. (2012)	Evaluated the environmental impacts of groundwater in mines using the fuzzy-AHP method.	A model for a particular mineral is not developed. Also, due to the use of the Folchi method, the weak points of this method are intrinsic.
Suopajärvi (2013)	Evaluation of social impacts of mining activities on environmental assessment of six mining projects in Finland.	This study did not present a model that covered the present models' defects and only stated the weaknesses of the methods.
Northey et al. (2013)	Estimated The energy, GHG emissions, and water intensity of global primary copper production.	Only three impacting factors have been estimated.
Minaei Mobtaker and Osanloo (2014)	Investigated the positive impacts of mining activities.	This research aims to use a Folchi method that has problems such as incompleteness and its dependence on personal judgment. Also, only positive effects are considered in the evaluation, and negative impacts are neglected.
Muñoz et al. (2014)	Developed a methodology to minimize social-environmental impacts in the early stages of mine design.	Only five sustainability factors were incorporated into the methodology.
Reyes-Bozo et al. (2014)	Proposed an ecology model to improve the overall environmental sustainability of copper sulphide ores flotation.	Their study assesses the soil pollution caused by the fuel and processing stage and does not consider the complete life cycle of the copper mining stages.
Song et al. (2014)	Investigation of environmental impacts of copper mining in China by LCA method	Only greenhouse gas emissions and acidification have been investigated.
Wang et al. (2015)	Investigated the environmental effects of copper production by pyrometallurgy in China by the LCA method.	Only the metallurgical stage has been evaluated. 6 factors have been investigated in this study.
Morrison-Saunders et al. (2015)	Examined the role of environmental assessments in the design and planning of industrial and artisanal mine (ASM).	The researchers expressed their results qualitatively and did not provide a model for solving the problem.
Castilla-Gómez and Herrera-Herbert (2015)	Dynamic EIA analysis of the environment, focusing on the evolution of environmental impacts over time.	This research does not consider all the environmental impacts, such as biodiversity.

Table 8. continue: Summary of the studies on the environmental impact assessment of copper mines

Reviewed studies	Advantages	Shortcomings
Gałaś and Gałaś (2016)	Determining the importance of qualitative EIA method by comparing the quality assessment process of environmental impact.	-the assessment is qualitative -not providing a comprehensive evaluation model
Saini et al. (2016)	Establishing relationships based on earth, laboratory and satellite data analysis	Failure to provide a comprehensive model and inherent problems with the AHP method
Ataei et al. (2016)	Provide a quantitative matrix model for determining the negative effects of mining activities	Not considering the positive impacts of mining
Drielsma et al. (2016)	Investigated the current LCAs for copper mining and concluded that the existing LCA literature on mineral resource assessment is inaccurate.	Only the economic factors are applied to the previous literature on resource depletion LCA.
Kulczycka et al. (2016)	Investigated the effects of advances in metallurgical technology on the environmental impact of copper metal extraction between 2010 and 2050 using the LCA method.	The environmental impacts of the metallurgical phase have been evaluated, and only three factors have been studied.
da Silva Dias et al. (2017)	Examining the problems of existing environmental assessment methods	-the assessment is qualitative -not providing a comprehensive evaluation model
Rahmanpour and Osanloo (2017)	Evaluated the outcome of different UPL alternatives using DSS for optimal decision-making	Only the UPL selection procedure is evaluated using SD indicators, and a comprehensive model is not presented.
Mancini and Sala (2018)	Compared the different indicator sets used in the frameworks with impacts from the literature review. Working conditions and human rights are well-covered aspects in the indicator lists.	Only two of the social impacts of mining are assessed.
Gorman and Dzombak (2018)	Investigating sustainable development in the mining with resource efficiency, minimizing the damage to the land, reducing pollution.	-Qualitative and linguistic evaluation
Hresc et al. (2018)	States that EIAs do not reflect the economic impacts of mining projects on local communities health and have not been developed based on evidence that relates the economic impact of mines to health.	-the assessment is qualitative -not providing a comprehensive evaluation model
Heidari and Osanloo (2018)	Finding the interrelationship between Impacts. Considering both positive and negative impacts.	Does not develop an EIA model

Table 8. continue: Summary of the studies on the environmental impact assessment of copper mines

Reviewed studies	Advantages	Shortcomings
Hasanipanah et al. (2018)	Evaluation of ground vibration resulting from the blasting	The model is not comprehensive, only the impacts of the blasting are taken into account, and the other environmental impacts are ignored.
Hong et al. (2018)	They studied the environmental impacts of copper extraction by the LCA method.	Only the refining and recycling steps are studied, and 18 factors are evaluated in the recipe method.
Kuipers et al. (2018)	Their studies concluded that LCA is the most effective method for environmental assessment.	Five factors have been examined.
Shahhosseini et al. (2019)	Investigation of geochemical environmental conditions of arsenic and lead in dams of copper mine Middik in Kerman	The study aimed to investigate the effect of mineral activity on the concentration and stability of arsenic and lead, and other environmental impacts of mining and processing plant have been ignored.
Ocampo-Melgar et al. (2019)	Investigating public participation in increasing the environmental assessment reliability	- Use internal reports of companies that may be selective and inaccurate.
Saffari et al. (2019)	Minimizing uncertainties and personality of responses	Failure to provide a comprehensive model and inherent problems of the Folchi method
Sarupria et al. (2019)	Solving problems such as Reproducibility, Subjectivity and Non-inclusivity by stakeholders by stakeholders	Not considering the positive impacts of mining
Amirshenava and Osanloo (2019)	Determine the effect of mineral activities on sustainable development indicators	Not considering the positive impacts of mining
Clark (2019)	Introducing defects in the environmental assessment deep-sea mining	- not providing technology or applied evaluation method - not taking into account the positive impacts of mining
Riley et al. (2019)	Expression of defects in the environmental assessment in Australia on issues related to health, welfare and justice	- not taking into account other parameters related to environmental assessment - not taking into account the positive impacts of mining
da SilvaDias et al. (2019)	The results showed that EIAs have a low value for decision-makers because they do not show the actual impacts of mining activities on biodiversity.	- not taking into account the positive impacts of mining
Lemly (2019)	Prediction of possible negative impacts caused by mining activities	- not providing a functional model for solving the discussed problems

Table 8. continue: Summary of the studies on the environmental impact assessment of copper mines

Reviewed studies	Advantages	Shortcomings
Islam et al. (2019)	According to this study, LCA has been used in the metals and mining industry for decades and covers various materials, including base metal, precious metals, and fossil fuels.	Only extraction and processing steps are considered, and other measures are not considered in the evaluation. Moreover, only five factors are considered.
Ataei and Masir (2020)	Proposed a system classification using the fuzzy DEMATEL technique to study and analyze eleven impacting factor inter-relationships in open-pit mines.	Only 11 impacting factors are evaluated.
Dong et al. (2020)	Investigated the environmental impact of copper mines by LCA method.	8 Impact factors have been evaluated, and others have been ignored.
Zhang et al. (2021)	Using the LCA method, they compared the environmental impacts of copper mining with the two primary (mining) and secondary (recycling) methods.	Only the smelting and refining stages of copper tailings have been investigated. Only 14 factors are considered, and many factors are ignored.
Perlatti et al. (2021)	Investigated the impacts of an abandoned copper mine on the ecological quality of the region's ecosystem.	Only the percentage of copper remaining in abandoned copper mines' soil, water, and plant and animal species has been evaluated.

CONCLUSION

By studying the literature, it was found that 32% of environmental assessment studies used qualitative methods because many of the impacts in mines are not quantifiable. Nevertheless, qualitative researchers have personal judgment and lacks reliability. On the other hand, quantitative methods include 41% of the study, which examined the chemical content of heavy metals in water, soil, and air samples. Also, 75% of the quantitative studies used the LCA method, which evaluates the emission to the environment. Although these methods have been entirely scientific and precise to investigate mining impacts, some negative and positive effects that cannot be measured were ignored in these studies. 27% of environmental assessment studies used semi-qualitative methods in which qualitative positive and negative effects are turned into quantitative factors, and both kinds are assessed in the study. Of all the literature surveyed in this study, only two papers evaluated the positive environmental impacts of copper mines and the negative ones, which shows a critical shortcoming in the present literature.

REFERENCES

- Amirshenava, S. & Osanloo, M. (2019). A hybrid semi-quantitative approach for impact assessment of mining activities on sustainable development indexes. *Journal of Cleaner Production*, 218, 823-834.
- Aryafar, A., Yousefi, S. & Doulati Ardejani, F. (2012). The weight of interaction of mining activities: groundwater in environmental impact assessment using fuzzy analytical hierarchy process (FAHP). *Environmental Earth Sciences*, 68, 2313–2324.
- Ataei, M. & MASIR, R.N. (2020). A fuzzy DEMATEL based sustainable development index (FDSDI) in open pit mining—a case study. *Rudarsko-geološk 76o-naftni zbornik*, 35.
- Ataei, M., Tajvidi Asr, E., Khalokakaei, R., Ghanbari, K. & Tavakoli Mohammadi, M. (2016). Semi-quantitative environmental impact assessment and sustainability level determination of coal mining using a mathematical model. *Journal of Mining and Environment*, 7, 185-193.
- Castilla-Gómez, J. & Herrera-Herbert, J. (2015). Environmental analysis of mining operations: Dynamic tools for impact assessment. *Minerals Engineering*, 76, 87-96
- Clark, M. R. (2019). The Development of Environmental Impact Assessments for Deep-Sea Mining. *Environmental Issues of Deep-Sea Mining*. Springer.
- Da Silva Dias, A. M., Fonseca, A. & Pereira Paglia, A. (2017). Biodiversity monitoring in the environmental impact assessment of mining projects: a (persistent) waste of time and money? *Perspectives in Ecology and Conservation*, 15, 206-208.
- Da silvadias, A. M., Fonseca, A. & Paglia, A. P. (2019). Technical quality of fauna monitoring programs in the environmental impact assessments of large mining projects in southeastern Brazil. *Science of The Total Environment*, 650, 216-223.
- Dong, D., Van Oers, L., Tukker, A. & Van Der Voet, E. (2020). Assessing the future environmental impacts of copper production in China: Implications of the energy transition. *Journal of Cleaner Production*, 274, 122825.
- Drielsma, J. A., Russell-Vaccari, A. J., Drnek, T., Brady, T., Weihed, P., Mistry, M. & Simbor, L. P. (2016). Mineral resources in life cycle impact assessment—defining the path forward. *The International Journal of Life Cycle Assessment*, 21, 85-105.
- Gałaś, S. & Gałaś, A. (2016). The qualification process of mining projects in environmental impact assessment: Criteria and thresholds. *Resources Policy*, 49, 204-212.
- Gorman, M. R. & Dzombak, D. A. (2018). A review of sustainable mining and resource management: Transitioning from the life cycle of the mine to the life cycle of the mineral. *Resources, Conservation and Recycling*, 137, 281-291.
- Hasanipanah, M., BAKhshandeh Amnieh, H., Khamesi, H., Jahed Armaghani, D., Bagheri Golzar, S. & Shahnazar, A. (2018). Prediction of an environmental issue of mine blasting: an imperialistic

- competitive algorithm-based fuzzy system. *International Journal of Environmental Science and Technology*, 15, 551-560.
- Heidari, M. & Osanloo, M. Sustainability Assessment of Angouran Lead and Zinc Mining Complex. Proceedings of the 27th International Symposium on Mine Planning and Equipment Selection-MPES (2018), (2018) Santiago, Chile. Springer, Cham, 523-534.
- Hong, J., Chen, Y., Liu, J., Ma, X., Qi, C. & Ye, L. (2018). Life cycle assessment of copper production: a case study in China. *The International Journal of Life Cycle Assessment*, 23, 1814-1824.
- Hresc, J., Riley, E. & Harris, P. (2018). Mining project's economic impact on local communities, as a social determinant of health: A documentary analysis of environmental impact statements. *Environmental Impact Assessment Review*, 72, 64-70.
- Islam, K., Vilaysouk, X. & Murakami, S. (2019). Integrating remote sensing and life cycle assessment to quantify the environmental impacts of copper-silver-gold mining: A case study from Laos. *Resources Conservation and Recycling*, 154, 104630.
- Kuipers, K. J., Van Oers, L. F., Verboon, M. & Van Der Voet, E. (2018). Assessing environmental implications associated with global copper demand and supply scenarios from 2010 to 2050. *Global Environmental Change*, 49, 106-115.
- Kulczycka, J., Lelek, Ł., Lewandowska, A., Wirth, H. & Bergesen, J. D. (2016). Environmental impacts of energy-efficient pyrometallurgical copper smelting technologies: The consequences of technological changes from 2010 to 2050. *Journal of Industrial Ecology*, 20, 304-316.
- Lemly, D. A. (2019). Environmental hazard assessment of Benga Mining's proposed Grassy Mountain Coal Project. *Environmental Science & Policy*, 96, 105-113.
- Mancini, L. & Sala, S. (2018). Social impact assessment in the mining sector: Review and comparison of indicators frameworks. *Resources Policy*, 57, 98-111.
- Minaei Mobtaker, M. & Osanloo, M. Positive impacts of mining activities on environment. Conference: Beijing International Symposium on Land Reclamation and Ecological Restoration (LRER 2014), (2014) Beijing, China.
- Morrison-Saunders, A., Mchenry, M. P., Wessels, J. A., Rita Sequeira, A., Mtegha, H. & Doepel, D. (2015). Planning for artisanal and small-scale mining during EIA: Exploring the potential. *The Extractive Industries and Society*, 2, 813-819.
- Muñoz, J., Guzman, R. & Botin, J. (2014). Development of a methodology that integrates environmental and social attributes in the ore resource evaluation and mine planning. *Int. J. of Mining and Mineral Engineering*, 5, 38-58.
- Norgate, T. & Haque, N. (2010). Energy and greenhouse gas impacts of mining and mineral processing operations. *Journal of Cleaner Production*, 18, 266-277.
- Northey, S., Haque, N. & Mudd, G. (2013). Using sustainability reporting to assess the environmental footprint of copper mining. *Journal of Cleaner Production*, 40, 118-128.
- Ocampo-Melgar, A., Sagaris, L. & Gironás, J. (2019). Experiences of voluntary early participation in Environmental Impact Assessments in Chilean mining. *Environmental Impact Assessment Review*, 74, 43-53.
- Osanloo, M. (2016). Top 10 Challenges in Mining. *6th International Conference on Computer Application in the Mineral Industries (CAMI)*. Turkey.
- Perlatti, F., Martins, E. P., De Oliveira, D. P., Ruiz, F., Asensio, V., Rezende, C. F., Otero, X. L. & Ferreira, T. O. (2021). Copper release from waste rocks in an abandoned mine (NE, Brazil) and its impacts on ecosystem environmental quality. *Chemosphere*, 262, 127843.
- Philips, J. (2012a.) Applying a mathematical model of sustainability to the Rapid Impact Assessment Matrix evaluation of the coal mining tailings dumps in the Jiului Valley, Romania. *Resources, Conservation and Recycling*, 63, 17-25.
- Philips, J. (2012b.) The level and nature of sustainability for clusters of abandoned limestone quarries in the southern Palestinian West Bank. *Applied Geography*, 32, 376-392.

- Philips (2013). The application of a mathematical model of sustainability to the results a semi-quantitative Environmental Impact Assessment of two iron opencast mines in iran. *Applied Mathematical Modelling*, 7839-7854.
- Rahmanpour, M. & Osanloo, M. (2017). A decision support system for determination of a sustainable pit limit. *Journal of cleaner production*, 141, 1249-1258.
- Reyes-Bozo, L., Godoy-Faúndez, A., Herrera-Urbina, R., Higuera, P., Salazar, J. L., Valdés-González, H., VYHMEISTER, E. & ANTIZAR-LADISLAO, B. (2014). Greening Chilean copper mining operations through industrial ecology strategies. *Journal of Cleaner Production*, 84, 671-679.
- Riley, E., Sainsbury, P., Mcmanus, P., Colagiuri, R., Vilianni, F., Dawson, A., Duncan, E., Stone, Y., Pham, T. & Harris, P. (2019). Including health impacts in environmental impact assessments for three Australian coal-mining projects: a documentary analysis. *Health Promotion International*, 1-9.
- Saffari, A., Ataei, M., Sereshki, F. & Naderi, M. (2019). Environmental impact assessment (EIA) by using the Fuzzy Delphi Folchi (FDF) method (case study: Shahrood cement plant, Iran). *Environment, Development and Sustainability*, 21, 817-860.
- Saini, V., Gupta, R. P. & Arora, M. K. (2016). Environmental impact studies in coalfields in India: A case study from Jharia coal-field. *Renewable and Sustainable Energy Reviews*, 53, 1222-1239.
- Sarupria, M., manjare, S. D. & Girap, M. (2019). Environmental impact assessment studies for mining area in Goa, India, using the new approach. *Environmental Monitoring and Assessment*, 191, 1-17.
- Shahhosseini, M., Doulati Ardejani, F., Amini, M., Ebrahimi, L. & Mohebl Poorkani, A. (2019). Environmental geochemistry of As and Pb in a copper low-grade dump, Miduk copper mine, Kerman province, SE Iran. *Journal of Geochemical Exploration*, 198, 54-70.
- Song, X., Yang, J., Lu, B., Li, B. & Zeng, G. (2014). Identification and assessment of environmental burdens of Chinese copper production from a life cycle perspective. *Frontiers of Environmental Science & Engineering*, 8, 580-588.
- Suopajarvi, L. (2013). Social impact assessment in mining projects in Northern Finland: Comparing practice to theory. *Environmental Impact Assessment Review*, 42, 25-30.
- Wang, H. T., Liu, Y., Gong, X. Z., Wang, Z. H., Gao, F. & Nie, Z. R. (2015). Life cycle assessment of metallic copper produced by the pyrometallurgical technology of China. *Materials Science Forum. Trans Tech Publ*, 559-563.
- Zhang, W., Li, Z., Dong, S., Qian, P., Ye, S., Hu, S., Xia, B. & Wang, C. (2021). Analyzing the environmental impact of copper-based mixed waste recycling-a LCA case study in China. *Journal of Cleaner Production*, 284, 125256.

EVALUATION OF THE EXTRACTION OF VALUABLE MINERALS IN THE BEACH BLACK SAND IN THE COAST OF URUGUAY: SMALL SCALE MINING, ENVIRONMENT AND SOCIAL ISSUES

I.Tarjan^{1,*}, H. Ferrizo¹, F. Perez¹, Y. Castillo¹

¹*Universidad de la Republica, Uruguay, Centro Universitario Region del Este
(*Corresponding Author: ivan.tarjan@cure.edu.uy)*

ABSTRACT

Since the '50s it has been well known that the East Coast of Uruguay has a deposit of valuable mineral rich black beach sand. It is analyzed, investigated but not exploited for economic, social, socio-economic and environmental issues. The deposit first analyzed in 1950 and defined high grade of titanium-dioxide, ferrotitanium, zircon also rare-earth minerals. For long it has not been considered an economically viable project, however several attempts were done from different investor groups to establish a reasonably profitable operation on the sites. Most of it failed because of the resistance of the local communities looking at it as a destructive and environmentally harmful activity. Nowadays, all over the world there is a great demand to find solution for the people left without jobs or income to sustain their family meanwhile governmental regulations make clear alignment on economic and environmental issues. This paper aims to describe the possibility of a small scale, low environmental impact socially and economically viable project in order to satisfy all the needs of industries and communities involved.

Keywords: Small scale mining, environment, sustainability, socio-economic impact

INTRODUCTION

The beach black sand is very well known as source of raw materials in different parts of the World. Magnetite, ilmenite and rutile are ores of iron and titan, monazite contains rare-earth minerals and normally there are zircon and garnet for other uses. The coast of Uruguay is very rich in black sand and the volume is considerable given the fact that almost all along the beaches it can be found. Prospection started in the 1950's by the initiative of the state company ANCAP to define volume and value of the material and make feasibility studies of its extraction. Several reports were made on it with different outcomes depending on the actual conditions and circumstances of publication, however all of them shown the same results in the sense of mineralogy and utility of the minerals. In 2015 started an initiative of "small scale sustainable mining" with help of the Foundation Fontaina Minelli to improve the culture of extractive industry in the country that has very interesting and rich history, anyway. To change the paradigm from looking at this activity as "the BAD" to one that can support the industry and the people with valuable prime materials without making destruction in an irresponsible manner, adding value to the society, was/is the proposal. In cooperation with the University of Republic of Uruguay that has an undergraduate course on mining in the CURE started the research and investigation of the most appropriate manner to take advantage of these resources. The situation of pandemic has an even more important effect on this project at this stage of economical restart and generate jobs and incentives to the most affected.

The Deposit and The Mineralogy

The first report was made in the area of Atlantida in 1952 by discovering and describing the minerals on the coast. Since then several other investigations and publications have been made on the subject with the same result, some of them are more detailed and shown available volumes for further works. Other detailed paper (Bossi et al. 2002) explains the geology and occurrence of the raw sand along the coastline. The signs of black sands have been observed in a large part of the Atlantic coast of Uruguay, as shown in the map (figure 1.), from the Aguas Dulces until Barra del Chuy.

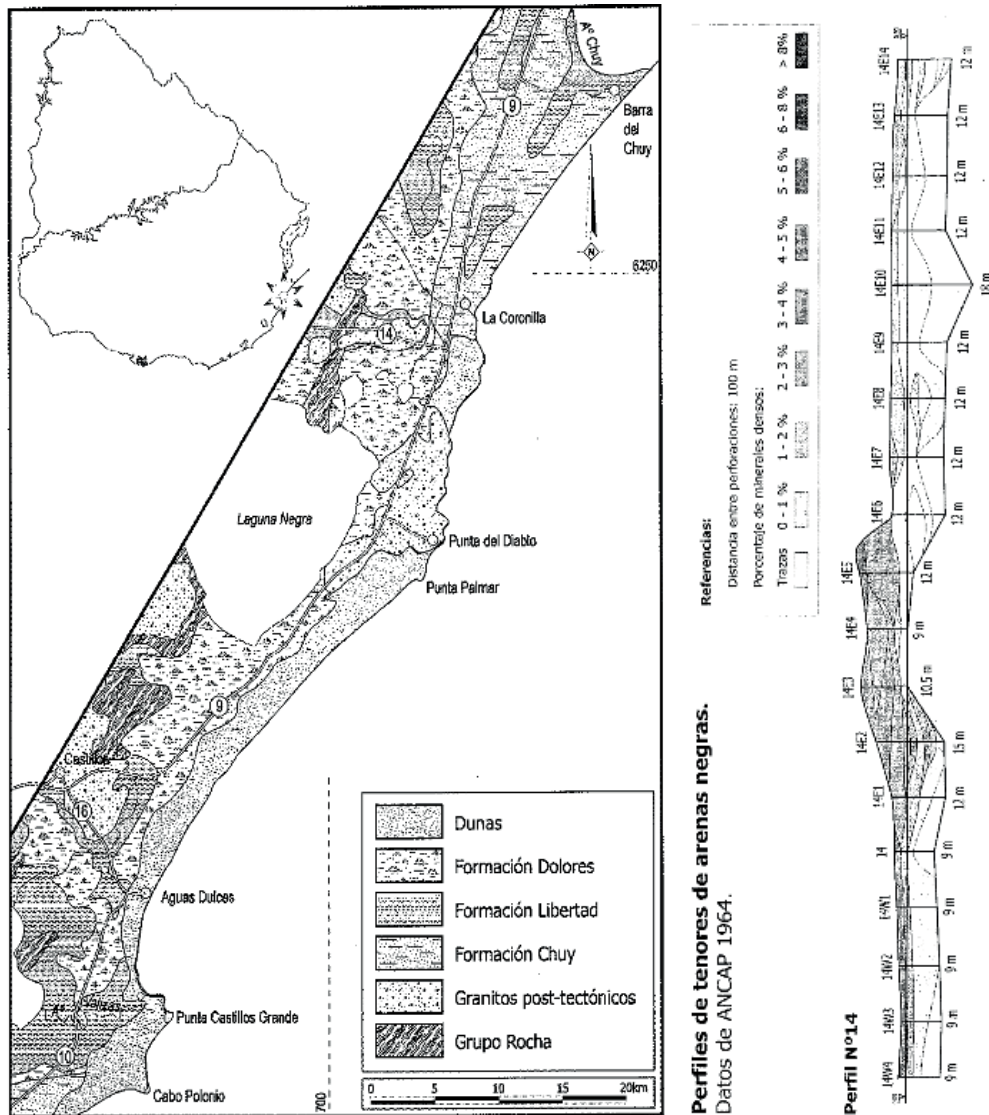


Figure 1. Geological map of one of the most studied zones with a sample profile of prospecting

According to the investigations carried out, the constituent minerals of the deposit are ilmenite, monazite, rutile, zircon, garnet, epidote, tourmaline. The Aguas Dulces deposit is the one that has been investigated with the greatest emphasis, and where the preliminary results are known.

According to these tests (Soares de Lima 2002) the mineralogical association of the heavy fraction in the Aguas Dulces deposit, with the value economic is as follows: ilmenite (60%), rutile (1.2%), zircon (4.75%) and monazite (0.65%).

These documents conclude in the studied area (map) alone of approximately 22 million tons of heavy minerals that can be extracted from the surface from not more than 5 meters depth. This study covers only a small part of the coast that supposed to have the minerals from the mid-South-East beaches (Atlantida) to the very edge of the border in the South-East (Chuy). So, the prospected volume of useful material is much more than this (Soares de Lima 2002).

As per the value of the resource estimated by the referred report in 2002 was around 650 million USD in respect to the studied area. Once again, the entire resource can be considered even 3 times more.

Table 1. Updating these numbers to the current market should count as:

	ilmenite	rutil	zircon	monacite	Total
Reserve approved (ton)	5760	480	96	48	
Value (USD/t) 2002	70	354	312	1050	650 M USD
Value (USD/t) 2021	340	1200	1630	6000	6981 M USD

The composition of the material shows the following results (Bossi et al., 2002; Abre et al. 2021):

Table 2. Mineral composition of black sand

	Magnetite/ilmenite	rutil	zircon	monazit
content	60 – 80 %	0.7 - 2 %	0.5 – 15 %	2 – 11 %

Earlier studies on other sites show very similar values (Soares, C. et al. 2002)

Different samples show slightly different compositions; however, it is agreed that the genesis, formation and natural processes tend to homogenize the sand along the beaches.

A representative map in one of the other areas of interest gives details of the drilling/prospection holes and the measured content of minerals is on the Figure 2.

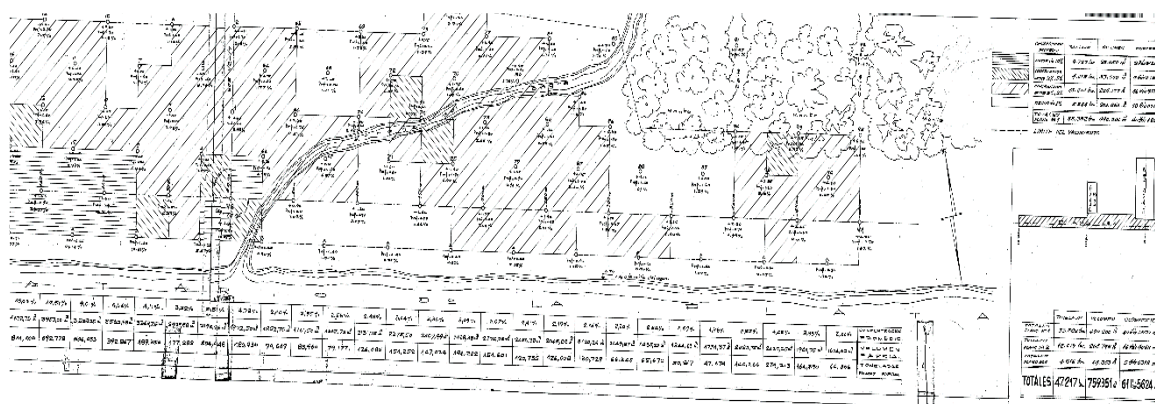


Figure 2. Exploration result map in the area of San Luis (ANCAP, 1964)

The general grain size distribution shows variation in the heavy part, which results the careful examination of the physical properties of every location in order to establish the simplest methods for

the beneficiation, like gravity separation. In the table 4. it is more likely that the finer fraction contains more heavy minerals (Soares de Lima 2002; Abre et al. 2021).

Table 3. Granulometry of the black sand

Granulometry in micrones	% weight	% heavy concentrate fraction	Density > 2.9	Density < 2.9
250 μ	0.2	50.0	0.1	0.1
250 μ a 177 μ	9.7	15.5	1.5	8.2
177 μ a 149 μ	11.3	25.7	2.9	8.4
149 μ a 105 μ	39.9	81.2	32.4	7.5
105 μ a 74 μ	30.8	89.5	27.5	3.3
Menos 74 μ	8.1	98.8	8.0	0.1

Studies on radioactive measurements of the samples also show and proves content of Polonium and/or Thorium in the heavy fraction and the monazite must bear REE as well. (Abre et al. 2021).

The above photo shows under microscope the composition of the black sand.



Figure 3. Microscope image of the black sand with its composition

Also, the Figure 4. above shows the distribution of the different no ferromagnetic minerals (magnetite and ilmenite were separated before the study) in the black sand. The samples are from the San Luis site.

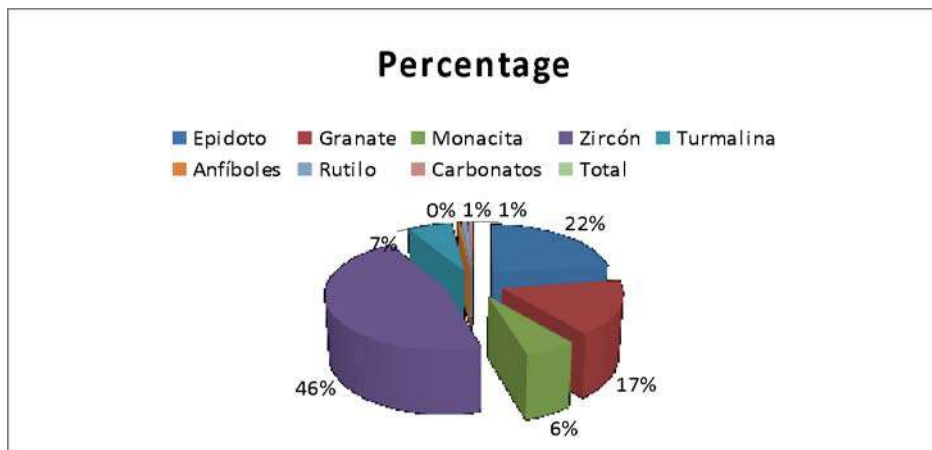


Figure 4. Distribution of the non-ferromagnetic minerals in the black sand sample of San Luis site

In summary we can be assured that this beach black sand is full of useful minerals to consider its extraction in an appropriate scale and manner.

Processing

As it is shown in table 4. the sand can be separated first by density, then magnetically to obtain semi- or intermediate products to be sold. The density difference in the minerals and the sand indicates good efficiency if concentration by simple equipment, like a concentration spiral, while the magnetic properties of the different parts allow very good and sharp separation of them. Our tests show the results below.

The most important properties of the heavy minerals are the density and magnetism. As per the first in general all of them have a density higher than 4 t/m³.

Looking at the magnetic properties the ilmenite (with magnetite) shows ferromagnetism, there are paramagnetic minerals, and nonmagnetic ones, like zircon. Consequently, it is very viable to separate the heavy minerals with a magnetic separator to achieve concentrates or products accordingly.

Table 4. Main mineral properties and contents

Mineral	Principal product	Composición	Density	Hardness (Mohs)	Typical content
Ilmenite	Titan	FeTiO ₃	4.5/5.0	5-6	45-65% TiO ₂
Leucoxene	Titan	Altered Ti minerals	3.5-4.5		70-93% TiO ₂
Rutile	Titan	TiO ₂	4.23-5.50	6-6.5	95-97% TiO ₂
Zircon	Zircon	ZrSiO ₄	4.2-4.86	7.5	63-67% ZrO ₂ (Hf) ₄
Monazite	Tierras Raras	(REE) P ₀₄ (Ce,La,Nd,Th)	4.6-5.4	5-5.5	50-70% REE
Xenotime	Tierras Raras	(REE) P ₀₄ Y(REE)	4.40/5.10	4.5	60-68 % Y/REE

It is well known that “simple” gravity separation has good efficiency when the density ratio between different particles is more than 2:1 to 1,5:1. In our case the sand as general can be considered as a 2.3-2.6 t/m³, while the heavy part is over 4 t/m³. These values permit us to employ equipment

simple and easy to use without important education and technical knowledge of the personnel to operate.

In the separation plant a LDMS (Low density magnetic separator) can produce high grade magnetic concentrate of iron ores, a HDMS (High density magnetic separator) would do the separation of paramagnetic materials meanwhile the rest contains the zircon and rutile with the impurities of the raw material.

Installation

As the processes are simple the extraction can be done with simple equipment, too. Install a 4x4 pick-up with a concentration spiral can process 1-4 t/h raw material with the help of a water pump to feed it and two storage dishes to receive the concentrate and the middling for further processing. Water is available from the sea or the boreholes as the water level is near the surface. There is a need for a recipient or tank for the raw material to be mixed/agitated for feeding the spiral on the top of itself.

The feed should be around 25-30% of solid content so a 30 liter/min pump can comfortably serve the equipment.

As an energy source the most convenient way would be to use a pump with a combustion motor, however there are already available good, independent/off-grid electric supplies that can serve for an installation at this size. (5) Even further, compressed air-electric power supply, or other alternatives (green hydrogen) also can be considered as they are getting more and more accessible and important from the environmental point of view.

This activity needs 2, max 3 persons on board without any prior technical knowledge or experience and processes 0,16-3,2 metric tons of black sand per 8 hours shifts.

The concentrate can be transported than to the central deposit where the magnetic separation can be taken place producing the “products”.

Environmental Impacts

The extraction of beach black sand is considered as the lowest impact on the environment. Mainly because of the ore concentration is low (in our case is 2-6%), the gangue material stays in the site as washed or cleaned sand re-deposited to its original place and no need for grand installations.

In our specific case no installation of buildings or machinery is considered, only mobile equipment and temporary workplaces would be established. The capacity is low as well, but with several working groups it can reach the sufficient volume to feed the separation plant economically.

As the only additional „raw material” needed for the exploitation is water and all the activity should be done on beaches, it must not mean any inconvenience. There are no chemicals used that can contaminate the environment.

In case the energy source would not be combustible for the pump operation, but alternatives would be considered there is no air contamination, not even noise presented.

From the nature point of view the situation is a bit more shadowed. The naturally concentrated materials are on beaches, however, not inhabited ones. As well there are dunes for the vegetation and wildlife that is very important as natural barriers against the destruction of the sea and gives refuge a wild variety of flora and fauna. Nevertheless, the majority of the resource falls outside of protected

areas and a well-established administration of granting permissions can avoid any sort of environmental damage.

As per the tourism we consider that small scale, individual extraction out of season would not interfere to the interest of this industry, the job can be done with great care and attention.

Socio-Economical Impacts

At the moment of pandemic/post-pandemic condition all over the world it is a key issue to re-establish or restart economical activities. Lack of workplaces, lack of income results other type of problems to be solved: the social issues. If there were jobs, people would have an income to live on that would result resilience for the families.

To establish an appropriate business plan for this proposal not the objective of this investigation, but it should be done in case to put it on the run. But to create a very approximate balance it should be consider that:

Small scale sustainable mining can have a positive impact in this recovery. Its impact in employment, by the creation of several micro businesses, could be relevant, in particular, in areas where the lack of opportunities is the rule.

In this stage, it's possible to draw the relevant features of this business plan, prior to full development.

The first thing to notice is the presence of a resource with a certain market value, 7.000 M USD at actual prices (22 million tons)

Given the value of 7.000 M USD worth resource (22 million tons)

Capital expenditure / working group should not exceed the 2.500 USD

Capacity / working group per year can be limited to 100 tons with 20 years lifespan

Results 10.000 working group by 4 persons

Capital expenditure to a separation plant is about 500.000 USD

Profitability 30% on product sold

Costs of production in the separation plant per year (electricity+ human resources) 500.000 USD

Should result an average income of around 500-510 USD/month/person before tax and expenditures (capital payback, general costs of transport), meanwhile the „company” should receive 95 m USD/year before tax and costs.

The market for these products is located abroad, there are no national possibilities of processing.

Obviously, the above numbers depend on the actual prices, but it seems to be a good margin to propose a viable business plan that benefits all players.

CONCLUSION AND FURTHER ASSESSMENTS

The current project aims to define the way how a destructive activity - like mining – can be done with minimal environmental effect but with good social acceptance, low inversion and good return. However, it is vital to define the proper and detailed composition of the black sand regarding on the most critical metals and materials (REE, Th, Ti).

We found a very interesting and valuable source of minerals what for we are still looking for market. The results of this process are listed on different sites as semi-products or intermediate raw materials, so business plan can be assembled to look at feasibility.

The necessary investment is very low, easy to operate, clean (no need for chemicals, additives, etc.).

On the environmental side the biggest problem appears to be on the conservation sites and the opposition of ecological movements. Another caveat is the limited capacities to properly enforce any regulation of the areas of extractions. Therefore, further investigation should be done on the critical sites with unique areas of the local flora and fauna to inform the authorities for permission evaluation.

We found as well that the socio-economic impact would be huge, people could find jobs of their own account, financially viable with a very decent income for long term. However, a proper plan is necessary to put all the above on the practice, which seems to be a bit difficult in the sense of administration, distribution of information and final decisions.

REFERENCES

- Abre, P., Bañobre, C., Fornaro, L., Garcia-Tenorio, R., Vioque Romero, I., 2020: Relacion entre los minerales pesados de la costa del Departamento de Rocha (Uruguay) y la emision alfa de las arenas (XXI Congreso Geologico Argentino, Sesion tecnica XX).
- Abre, P., Blanco, G., Ferrizo, H., Cingolani, C., Uriz, N.,Arnol, J., 2021: Minerales pesados de la costa del departamento de Maldonado (
- Ferrando, L., Bossi, J., Maldonado, S., Schipilov, A.,Campal, N., 2003:Evaluacion de arenas negras en Aguas Dulces, Departamento de Rocha, Uruguay (Revista de la Sociedad Uruguaya de Geologia, III Epoca No. 10, 2003)
- Soares de Lima, C., 2002: Estudio geologico Minero del deposito de arenas negras de Aguas Dulces (Study for the Ministerio de Industria, Energia y Minería, Direccion Nacional de Minería y Geología del Uruguay, 2002)

EXTRACTION DESIGN OF HIGHWALL MINING IN INDIA TO RECOVER LOCKED-UP COAL USING EMPIRICAL AND NUMERICAL SIMULATIONS

P. Pal Roy

*CSIR-Central Institute of Mining & Fuel Research
(ppalroy@yahoo.com)*

ABSTRACT

Many Indian opencast mines are reaching their pit limits and existence of surface dwellings mostly limits the expansion of such mines. In large number of cases, the overburden becomes so thick that coal extraction becomes uneconomical by conventional drilling and blasting. Under such circumstances, the use of highwall mining machines where a cutter is placed on the top of a system similar to a continuous miner, and taken through a conveyor into the seam almost 500-600 m deep inside, it becomes possible to extract a good proportion of such stuck-off coal which otherwise remained tapped owing to limited means and high-cost of mining. However, such mining system requires suitable scientific extraction design which is safe and productive. The CSIR-Central Institute of Mining and Fuel Research (CSIR-CIMFR) has provided the extraction design to recover 45 to 60% of locked-up coal using empirical and numerical simulations. This paper provides the scientific elucidation of the design technology adopted by CSIR-CIMFR in the first four potential opencast mines in India along with their safety and productivity aspects.

Keywords: Highwall mining, web pillar, pillar strength, roof convergence, safety factor

INTRODUCTION

Several opencut coalmines, around the globe, are reaching their pit limits. Existence of surface dwellings in many places limits the expansion of currently running opencut mines. Also, in many cases, the overburden becomes so thick that coal extraction becomes uneconomical.

Continuous highwall mining (CHM) is a relatively new technology which can extend the life of opencast mines without disturbing the surface dwellings, while maintaining economy and productivity. It is a remotely operated coal mining technology which consists of the extraction of coal from a series of parallel entries driven into the coal seam from the face of the highwall. These entries are unmanned, unsupported and unventilated. This technology uses highwall mining machines such as a continuous miner which takes through a conveyor inside the seam almost 500 to 600 m. In the present day, penetrations up to 500 m have been consistently achieved with highwall mining systems, in contrast to auger mining wherein penetrations are limited to 100–150 m. The method comprises extraction of coal from a series of parallel entries driven in the coal seam from the face of the highwall. The method can be successful only if a feasible extraction design is made considering the complex rock geology and existence of multiple coal seams especially in Indian coalfields, which is unique in many respects.

The CSIR-Central Institute of Mining and Fuel Research (CSIR-CIMFR), Dhanbad a constituent R&D laboratory under the aegis of Council of Scientific and Industrial Research (CSIR) came out with the first extraction design for the complex Indian geo-mining conditions existing at the three highwall mining sites at Ramagundem Opencast Project-II and Medapalli OCP of M/s Singareni Collieries Company Ltd (SCCL), and Quarry SEB and AB, West Bokaro of M/s Tata Steel Ltd. (TSL). CSIR-CIMFR also worked for stability of highwall slope and improvement of blasting efficiency and pre-split blasting for the formation of highwall benches at Sharda Opencast Project of M/s South-Eastern Coalfields Ltd. (SECL), which was a very challenging task offered by M/s Cuprum Bagrodia Limited, who had been operating the highwall mining system at Sharda Project very successfully (CIMFR Technical Reports: GC/MT/139/2007-2008; GC/MT/174/2008-2009; CNP/2586/2010-2011 and CNP/4012/2014-15).

In India, the first highwall mining system started operation on 10th December 2010 at Opencast Project-II (OC-II), Ramagundam Area-III (RG-III) of Singareni Collieries Company Ltd. (SCCL). The extraction design at this site was provided by CSIR-CIMFR and the same was operated by Advanced Mining Technology (AMT) of Hyderabad using ADDCAR highwall mining system of USA. The machine started extraction of locked-up coal beneath the opencut highwall under the guidance and monitoring of CSIR-CIMFR. Over two lakh ton of locked-up coal was recovered from seam-I and seam-II. Extraction in seam II had problems due to unexpected geological discontinuities and poor roof conditions. However, in seam-I, the extractions went smoothly with almost all the holes extracted to full-length as per the design opted by CSIR-CIMFR. Almost 1/5th of the total project cost of highwall mining was recovered from OC-II.

The machine was then shifted to the second nearby mine namely Medapalli Opencast Project of SCCL (Singareni Collieries Company Limited) for extraction of 6 seams. It extracted around 8 lakh ton of trapped coal from 4 Seams and almost the complete HWM project cost was recovered from Medapalli OC Project. There had been no safety issues due to judicious guidance right through.

The Tata Steel Limited (TSL), West Bokaro Division proposed to extract the locked-up coal in the final pit slope of Quarry SEB and that lay below Banji village in Quarry AB at West Bokaro Group of Collieries using the Continuous Highwall Mining (CHM) system. In that context, CSIR-CIMFR carried out the feasibility study on the design and safety aspects of highwall mining for implementation.

At Quarry SEB seams V, VI, VII, VIII, IX, X Lower, X Upper and XI existed in ascending order and were exposed on the highwall towards the eastern side of the quarry. At Quarry AB, the coal seams left below Banji village and those considered feasible for extraction from the final highwall abutting the village boundary included seams V, VI, VII and VIII, occurring in ascending order. All the seams were gently dipping, with 3-7° inclination and occurred at a depth of 16-150 m within the proposed highwall mining sites.

At Quarry SEB, no significant surface features existed, whereas Banji village has been densely populated with residential houses, to be protected from surface subsidence on a long-term basis. The final pit slope in both the quarries had been designed by CSIR-CIMFR (CSIR-CIMFR, 2000; 2008c). Starting in April 2016, up till March 2019, the coal production from West Bokaro Collieries touched 1.5 million tonne costing nearly US \$36.4 million (Indian Rupees ₹ 248 crore).

At Sharda Project, CSIR-CIMFR worked for two different assignments namely (i) Design of optimum highwall slope and (ii) Basting efficiency and pre-split blasting for formation of highwall benches. The powder factor in the production blasting was drastically improved from 1.3-1.4 m³ of rock per kg of explosive consumption to around 2.0 m³ of rock per kg of explosive resulting in huge savings on explosive consumption as well as environmental implications of such blasting operations.

DESIGN ASPECTS

Web pillars were designed for all the seams separately for each block. The methodology adopted for the empirical design is given below (Loui et al., 2013a, 2013b, 2013c, 2013d; Loui et al., 2014).

Estimation of Pillar Strength

The estimation of pillar strength was done using CSIR-CIMFR pillar strength formula, which reads as-

$$S = 0.27\sigma_c h^{-0.36} + \left(\frac{H}{250} + 1\right) \left(\frac{W_e}{h} - 1\right) \text{MPa} \quad (1)$$

Where,

- S = strength of the pillar, MPa
- σ_c = strength of 25 mm cube coal sample
- h = working height, m
- H = depth of cover, m
- W_e = equivalent width of pillar, m = 2W for long pillar
- W = width of web pillar, m

Pillar Load Estimation

Load on pillars was estimated using Tributary area method, which reads as:

$$P = \frac{\gamma H (W + W_c)}{W} \quad (2)$$

Where,

- P = the load on web pillar, MPa;
- γ = the unit rock pressure (0.025 MPa/m) and
- W_c = the web cut width, m

The design patterns provided by CSIR-CIMFR were reviewed thoroughly at the mine site to check the operational feasibility during field implementation (Figure 1). Figures 2 and 3 depict the roof stability of I seam extractions and stress-strain curve as well as plasticity states of a Model of OC-II, SCCL while Figures 4, 5 and 6 illustrate stress-strain curves and safety factor contours of Quarry SEB, Tata Steel Limited (TSL) obtained by numerical modelling.



Figure 1. Design review at the site of MOCP Medapalli OC Project

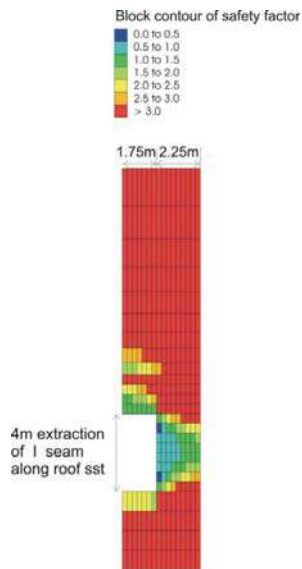


Figure 2. Roof stability of I seam extractions OC-II, SCCL

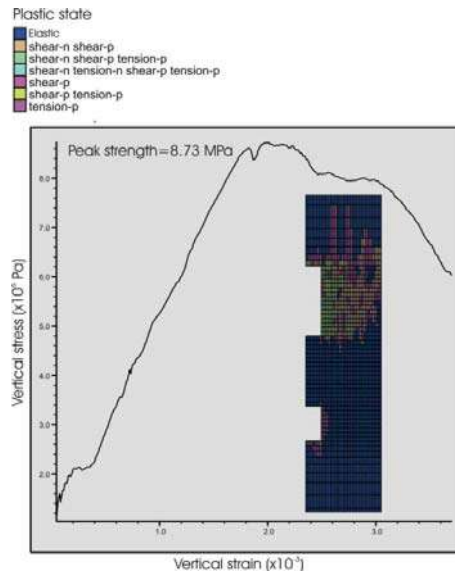


Figure 3. Stress-strain curve and plasticity states of a Model of OC-II, SCCL

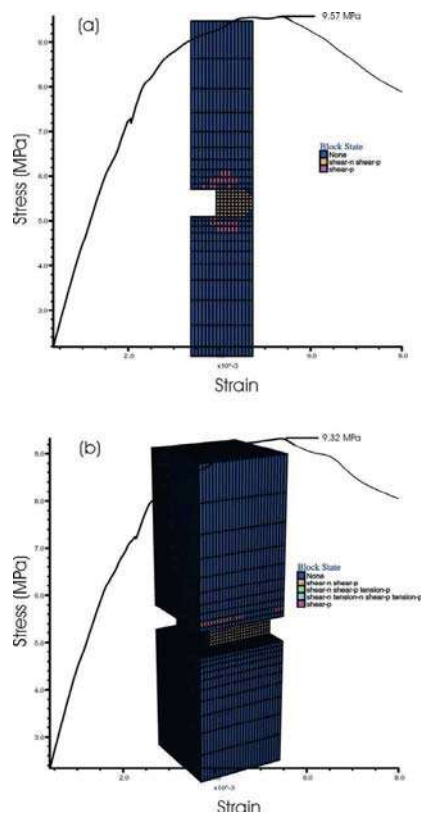


Figure 4. Stress-strain curves for width/height ratio of 2.5 in (a) long pillar

(b) equivalent square pillar of Quarry SEB, TSL

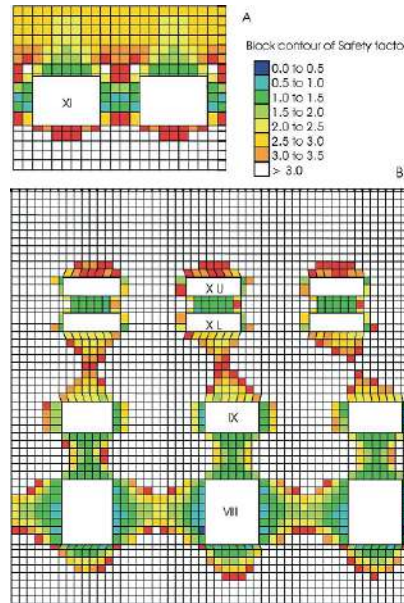


Figure 5. Closer view of safety factor contours in (A) Seam XI and (B) Seams XU, XL, IX and VIII of Quarry SEB of Tata Steel Limited (TSL) of the design of Highwall Mining carried out by CSIR-CIMFR for the first time in the country

Safety Factor

Safety factor (S.F.) of the pillars was calculated using the following equation:

$$S.F. = \frac{\text{Strength of web pillar}}{\text{Load on web pillar}} = \frac{S}{p} \tag{3}$$

The CSIR-CIMFR pillar strength equation had been developed over a couple of decades after analyzing a large number of pillar stability observations from a gamut of Indian mining scenarios. On the basis of past experiences from Indian coalfields it was observed that a pillar safety factor of more than 2.0 is long-term stable, i.e., for many decades. A safety factor between 1.5 and 2.0 may be taken as medium-term stable, stable for a few years. If the safety factor of the pillar is 1.0, it may be treated as short-term stable, with a standup time of a few weeks or a month.

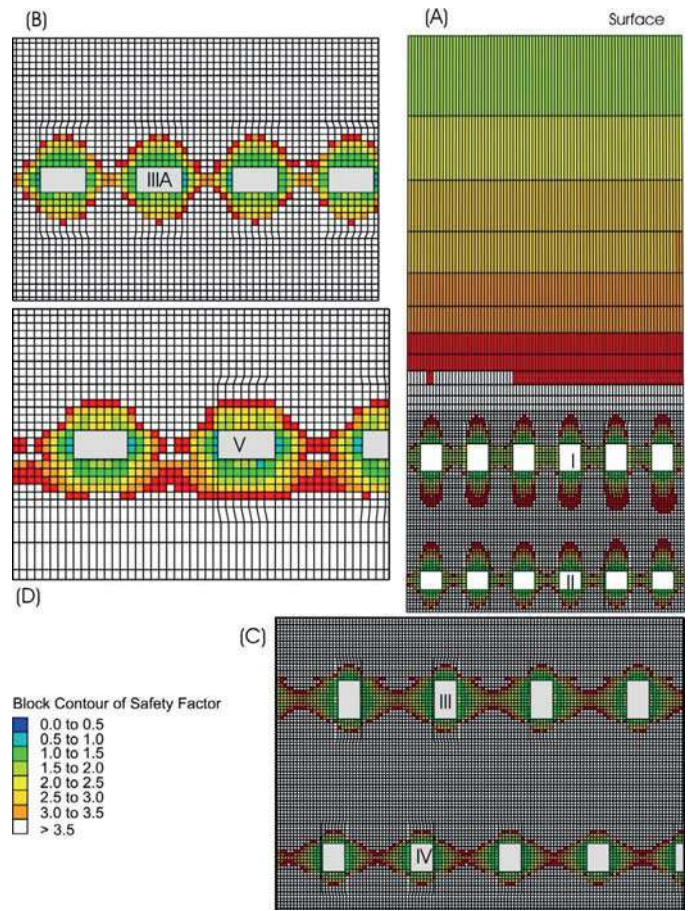


Figure 6. Closer view of safety factor contours in individual seams of Block A, MOC

Pictorial views of highwall mining operations in India are shown in Figures 7, 8, 9 and 10.



Figure 7. Inauguration of 1st Highwall Mining System in India at OC-II, RG-III Area, on 10th December, 2010



Figure 8. View of ADDCAR-make Highwall Mining machine in operation at SCCL



Figure 9. View of Highwall Miner at Sharda Highwall Project of SECL



Figure 10. Production of coal from the first Highwall Mining in India at OC-II, RG-III Area of SCCL

MONITORING GROUND MOVEMENT AT SURFACE

In order to fulfill the statutory requirement, two panels/blocks were selected for highwall mining in OC-II at Ramagundam Area of M/s Singareni Collieries Company Limited. The highwall was inclined at an angle of 45° towards the dip of the seam (Panel-B) as well as along the seam strike (Panel-A). Initially, working was started in Panel-B of bottom seam No. 2. The height of the wall was 100 m vertically from the decoaled edge of seam No. 2. The dip of the seam was 1 in 4.5. No bench existed in the highwall within the study block. It was proposed to mine two seams namely, seam No. 2 and seam No. 1 (Prakash *et al.*, 2014).

The panels were designed for no ground movement. As the technique was adopted for the first time in India, DGMS proposed to evaluate the stability of the highwall during the course of extraction for the safety of men and machinery. Figure 11 shows the plan layout of monitoring stations over highwall panels at OC-II, SCCL.

Stability Study

The stability study was conducted continuously using Total Station having a linear least count of 1 mm with an accuracy of ± 2 mm. A baseline (Figure 12) was established outside the influence zone of any ground movement due to highwall mining. The coordinates of baseline are given in Table 1. The reduced level was taken from Station No. 413 (Table 1). The lateral displacement of the ground as well as vertical movement of the surface was monitored to evaluate stability of the highwall during mining operation. Coordinate of each station was monitored from the base-line for lateral displacement and Missing Line Measurement (MLM) option was used for study of vertical displacement. Care was taken to keep the error of subsidence measurement minimum by maintaining the distance between instrument and the target within 100 m so as to accurately coincide centre of the target.

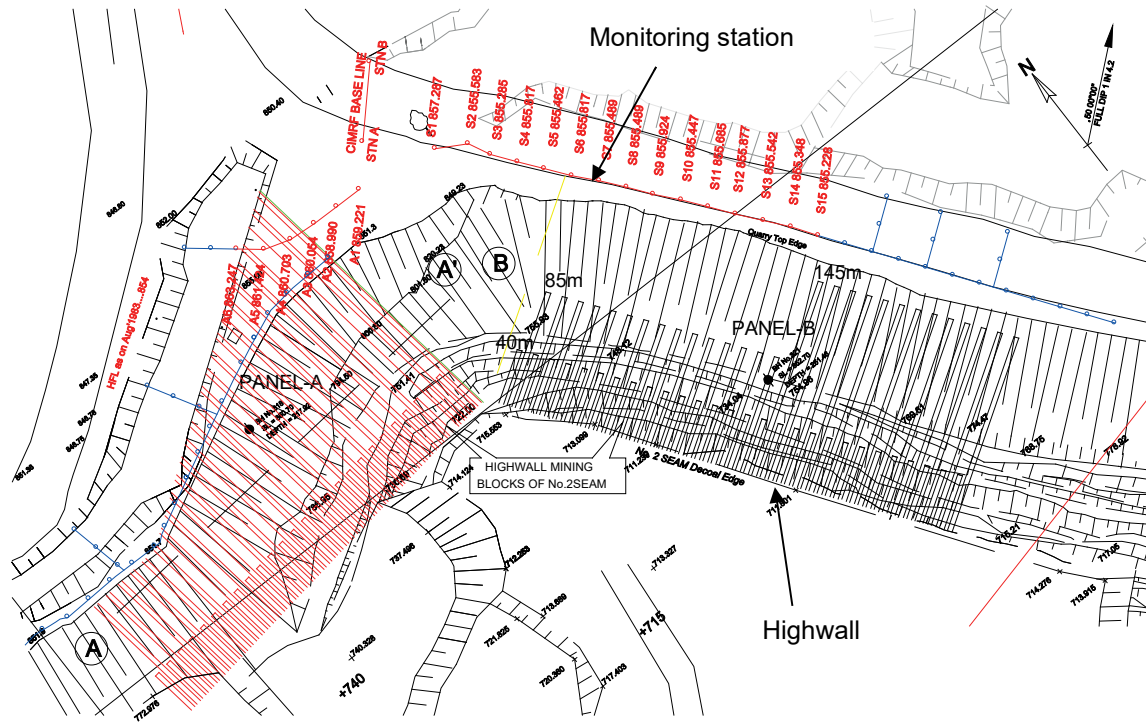


Figure 11. Plan showing layout of monitoring stations over highwall panels, OC-II, SCCL



Figure 12. Establishment of baseline for orienting highwall miner for parallel web cutting using Total Station

Table 1. Coordinates of baseline stations

Station	North (m)	East (m)	RL (m)
A	933704.305	3060397.341	
B	933745.895	3060436.186	
413	933681.369	3060412.522	860.400

Observations on Measured Values

Initially there was slight fluctuation in the measurement due to settlement of the monitoring stations over the dump. A few stations got disturbed during the course of road cleaning. There were variations in the coordinate measurements in few millimetres due to cumulative effect of parallax error and target levelling error. It was evident from data that there was no trend of lateral movement of the mine edge towards the open-pit during the mining operation. There was no vertical displacement of the surface ground i.e., subsidence, during the study period.

STABILITY OF THE HIGHWALL

Stability assessment of the highwall slopes was made based on the stability analysis using “Slope Stability Analysis Software” (GALENA version 4.02). The stability analysis was conducted considering circular and non-circular failure surfaces passing through the ultimate slope. Bishop’s method of multiple analysis was used for circular failure conditions whereas Sarma’s method was considered for non-circular failure conditions (Jhanwar *et al.*, 2014). At Medapalli OCP, the heights of ultimate slopes (Highwall) were considered at 105 m in the rise side/strike direction for Block A and at 152 m in the dip side for Block B of MOCP. The overall slope angle of Highwall/Ultimate slope was considered at 44⁰ in both rise and dip side highwall (Figure-13).

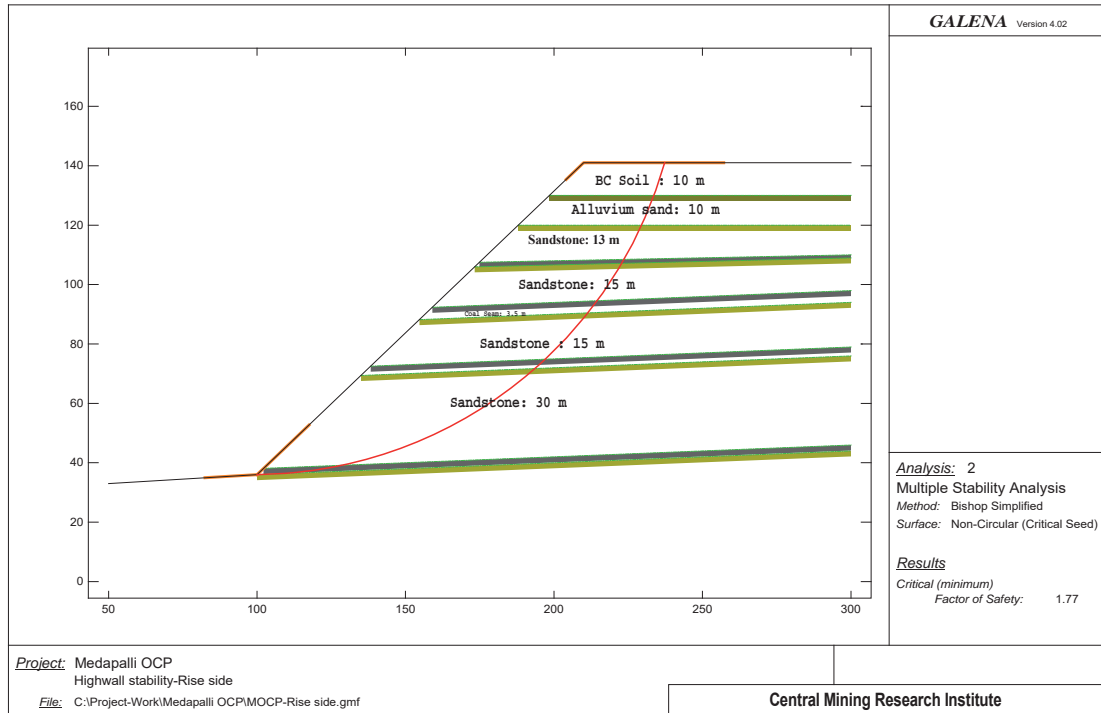


Figure 13. Stability analysis of the rise/strike side (Block A) highwall along Section C-C', MOCP

IMPACTS OF SURROUNDING BLASTING ON HIGHWALL MINING

Any blasting activity close to highwall mining may affect the stability of highwall mining entries, web pillars as well as highwall of the opencast from where the workings are to be executed. Ground vibrations generated by day-to-day blasting operations nearby the highwall mining entries can impose immature roof and side collapse, thereby, trapping the continuous miner (highwall hog or any other make, as the case may be) inside the mine entries. Flyrock generated from blasting nearby the highwall mining could also damage the equipment used for the mining like launch vehicle etc. and impose safety concern to the workers.

Blast-induced ground vibrations may also affect the stability of the highwall slope. Ground vibrations have two-fold actions on rock mass. On one hand, they affect the integrity of the rocks or their strength parameters while on the other, they can provoke wall or slope collapses when unstabilizing actions are introduced. During the process of blasting, the energy that is not used in fragmentation and displacement of rock, propagates through the rock-medium beyond the zone of disturbance and reduces the structural strength of the rock mass outside the theoretical radius of action of excavation. New fractures and planes of weaknesses are created and joint, declasses and bedding planes that initially behaved non-critical, when opened, result in an overall reduction of rock mass cohesion. This is manifested by overbreak, leaving fractured mass in a potential state of collapse. The following generalized criteria, as given in Table 2, for damage level of particle velocity on rock mass and slopes, were taken into account while designing the highwall mining operations (DGMS Technical Circular, 1997). As such there is a remote possibility of any damage on rock mass and slope due to nearby blasting operations beyond a distance of 500 m from the highwall face.

Table 2. Damage level of rock mass based on ground vibration

Particle velocity (mm/s)	Predictable damages
< 250	No danger in sound rock
250 – 600	Possible sliding due to tensile breakage
600 – 2500	Strong tensile and some radial cracking
> 2500	Complete break-up of rock masses

GENERAL SAFETY REQUIREMENTS

In addition to the specific requirements of a site, there are a few general requirements that must be fulfilled for safe highwall mining conditions as suggested by Porathur et al. (2017). These are given below-

- a) No person shall be allowed to enter the web cuts.
- b) Meticulous planning should be carried out to keep the highwall available so as to prevent the machine being idle.
- c) Working platform of CHM formed by dump material should be thoroughly consolidated for safe positioning and operation of the equipment.
- d) In no case should the bench width be less than the maximum dimension of the launch vehicle plus an additional 10 m for operational requirements, free movement of loaders, etc.
- e) Pit floor should be kept free from water and, if required, a suitable pumping arrangement should also be made.
- f) Effective drainage system should be implemented to divert surface run-off/rainwater entering into web cuts.
- g) If highwall slope is steep and height is more than 50 m, catch benches should be provided on the highwall at regular intervals to arrest the fall of loose material, hence ensuring stability during mining.
- h) Accurate and detailed up-to-date hole completion plan should be maintained for each and every seam targeted for highwall mining.
- i) All electrical enclosures and operating sensors should be intrinsically safe or flameproof certified.
- j) Preventive maintenance schedule should be planned and implemented for all equipment.
- k) Every moving part of the machine should be adequately covered, fenced and guarded.
- l) Operator should ensure proper functioning of all sensors and on-board cameras prior to the commencement of a web cut.
- m) No unauthorised person should be allowed to enter into the mining area.
- n) Adequate arrangements should be made for the training of personnel regarding drivages of web cuts and maintaining safe operating conditions near the highwall.

CONCLUSIONS

In India a huge potential for new coal mining technologies is envisioned to up the ante on much-needed coal demand for the energy sector. Seen as a proven technology in USA, Australia and some other parts of the world, it was not a difficult decision for Indian mining companies to try this technology though Indian coal geology is complex compared to some other parts of the world. The occurrence of thick and multiple seams, and some at close proximity, with frequently varying roof conditions etc., makes mining difficult and challenging. Available conventional design methods of highwall mining do not incorporate

multiple seam interaction, does not account for pillar slenderness ratio, safety factor variations due to hole deviations, end effect and combination of short and long holes. CSIR-CIMFR design methodology incorporates all the above complex geological concepts and is therefore more realistic and comprehensive from optimum coal recovery and safety point of view.

CSIR-CIMFR, being the sole developer of highwall mining design in the country, it is anticipated that huge amount of foreign currency can be saved (nearly US\$ 0.21 million per Project). Coal recovery of even up to 60% had been designed by CSIR-CIMFR at the four said mining sites. In the process, novel approaches for pillar designing had also been formulated specifically for long and slender web pillars formed during highwall mining operations, which is unique in the world.

REFERENCES

- CIMFR Technical Report. (2008). Highwall mining at Ramagundem Opencast Project –II (OC-II) of M/s Singareni Collieries Company Limited (SCCL). Project No. GC/MT/139/2007-2008 (Phase-I Study), February, 66 p.
- CIMFR Technical Report. (2009). Feasibility study for highwall mining at Quarry SEB (and Quarry AB), West Bokaro Division of M/s Tata Steel Limited. Project No. GC/MT/174/2008-2009, March, 56 p.
- CIMFR Technical Report. (2011). Highwall mining at Medapalli Opencast Project (MOCP) of M/s Singareni Collieries Company Limited (SCCL). Project No. CNP/2586/2010-2011, p. 57, March, 57 p.
- CIMFR Technical Interim Report. (2015). Scientific study for improvement of blasting efficiency and pre-split blasting for the formation of highwall benches at Sharda Project, SECL. Project No. CNP/4012/2014-15, April, 40 p.
- DGMS Technical Circular 7. (1997). Standards of safe level of blast induced ground vibration for safety of structures. Ministry of Labour, Government of India.
- Loui, J. P., Karekal, S., & Pal Roy, P. (2013). Web pillar design approach for highwall mining extraction. *International Journal of Rock Mechanics and Mining Sciences*, 64, 73-83.
- Loui, J. P., Pal Roy, P., Verma, C. P., & Karekal, S. (2013). Extraction design for multiple seams highwall mining in India – A case example. Procs. 47th US Rock Mechanics Symposium, San Francisco, USA, 23-26 June, 3, 1656-1660.
- Loui, J. P., Pal Roy, P., Prakash, A., Jhanwar, J. C. (2013). Extraction design of locked-up coal by highwall mining in India. 23rd World Mining Congress and Expo 2013, 11-15 August, Palais des congrès de Montréal, Canada.
- Loui, J. P., Verma, C. P., Pal Roy, P., & Sinha, A. (2013). Design and development norms for Highwall Mining in India. Procs. 25th National Convention of Mining Engineers & the National Seminar on Policies, Statutes & Legislation in Mines - Recent Reforms & their Impacts on Indian Mining Industry (POSTALE), India.
- Loui, J. P., Verma, C. P., Pal Roy, P. (2014). Highwall Mining in India – Part 1: Design methodology and review of performance. *Journal of Mines, Metals and Fuels, IMME-2014 Special Issue (September-October)*, India, 245-253.
- Loui, J. P., Pal Roy, P., Shen, B., Karekal, S. (2017). Highwall Mining: Applicability, Design and Safety. CRC Press, London, July, 324 p.
- Prakash, A., Loui, J. P., & Pal Roy, P. (2014). Highwall Mining in India – Part 2: Subsidence management mechanism at mine-level. *Journal of Mines, Metals and Fuels, IMME-2014 Special Issue (September-October)*, India, 254-262.
- Jhanwar, J. C., Loui, J. P., & Pal Roy, P. (2014). Highwall Mining in India – Part 3: Slope stability planning and management. *Journal of Mines, Metals and Fuels, IMME-2014 Special Issue (September-October)*, India, 263-266.

FARKLI TÜR ÇİMENTOLARIN ÖĞÜTME DAVRANIŞLARININ İNCE TANE BOYUTUNDA ARAŞTIRILMASI INVESTIGATION OF THE GRINDING BEHAVIOR OF DIFFERENT TYPES OF CEMENT IN FINE SIEVE SIZE

Y. Umucu ^{1,*}, V. Deniz ², Y. H. Gürsoy ¹, H. S. Gökçen ¹, S. Oluklulu ¹

¹ Eskişehir Osmangazi Üniversitesi, Maden Mühendisliği Bölümü

(*Sorumlu yazar: yakup.umucu@ogu.edu.tr)

² Hitit Üniversitesi, Polimer Mühendisliği Bölümü

ÖZET

Bu çalışmada, katkı çimento sınıfında yer alan CEM II ve CEM IV tür çimento örnekleri üzerinde, kesikli öğütme koşullarında kompozisyonu oluşturan malzemenin daha önce çalışılmayan ince tane boyutunun (-0.300+0.090 mm) kinetik model parametrelerine etkisi araştırılmıştır. Daha sonra laboratuvar çaplı bilyalı değirmende (200×200 mm) tek bir malzeme doluluk ve bilya doluluk oranında farklı öğütme sürelerinde elde edilen boyut dağılımlarından özgül kırılma hızı ve kümülatif kırılma dağılımı fonksiyonları elde edilmiştir. Çalışmada, çimento üretim süreçlerinin tasarımı, modelleme ve simülasyon çalışmalarında daha doğru sonuçlar vermesi bakımından ince tane boyutları seçilmiştir. Çimento bileşenlerinden olan klinker miktarının azalması ile en üst boyutların bir alt boyuta daha hızlı kırıldığı ve orijinal parçanın daha çabuk alt boyuta indiği görülmüştür.

Anahtar Kelimeler: Çimento, öğütme, kırılma hızı

ABSTRACT

In this study, the effect of the fine particle size (-0.300 + 0.090 mm) of the material forming the composition, which was not studied before was investigated on the kinetic model parameters of CEM II and CEM IV cement samples, which are in the blended cement class. Then, specific breakage rate and cumulative breakage distribution functions were obtained from the size distributions was taken at different grinding times in a single material fill and ball fill ratio in a laboratory diameter ball mill (200×200 mm).

In the study, fine sieve sizes were chosen in order to give more accurate results in the design, modeling and simulation studies of cement production processes. It was observed that the upper sieve size was faster broken down to a lower sieve size and the original part was reduced to the lower sieve size more quickly with the decrease in the amount of clinker, one of the cement components.

Keywords: Cement, grinding, specific breakage rate

GİRİŞ

Türk çimento sanayisi 60 milyon tonun üzerindeki üretimi ile Avrupa'da birinci sırada, dünyada ise beşinci sırada yer almaktadır. Çimento üretimi, enerji kullanımının yoğun olduğu bir proses olup, bir ton çimentoyu üretmek için gerekli olan enerjinin yaklaşık üçte biri klinker ve katkı maddelerinin öğütülmesinde kullanılır.

Türkiye’de devam etmekte olan kentsel dönüşüm sebebiyle içinde bulunduğumuz 10 yıllık dönemde yaklaşık 300 milyon m³ hazır beton gereksinimi ortaya çıkmaktadır. Ancak Türkiye enerji yönünden büyük ölçüde dışa bağımlı bir ülke olduğundan ve yüksek fiyatlara sahip enerji ithalatı nedeniyle, çimento üretim maliyeti de artmaktadır. Türkiye Çimento Müstahsilleri Birliği üye fabrikalarının 2014 yılı elektrik enerjisi tüketimi 6,2 milyar kWh olduğu belirlenmiştir ve bu veriye göre çimento üretim aşamaları için optimizasyon çalışmalarının önemi daha iyi anlaşılmaktadır. Çimento endüstrisi, dünya enerjisinin yaklaşık %3,5’ünü kullanan en büyük endüstrilerden birisidir. Çimento endüstrilerinde, üretim prosesinde harcanan toplam enerjinin %40’ı öğütmede harcanmaktadır (Deniz, 2004; Hoşten vd., 1998; Umucu vd., 2015)

Çimento üretiminde öğütülebilirlik iki önemli faktörden dolayı önemlidir. Birincisi; çimentonun özellikleri kimyasal ve mineralojik bileşiminden başka çimentonun inceliğine ve tane boyutu dağılımına bağlıdır. İkincisi; çimentonun maliyetinde enerji harcamasının 1/3’ü öğütmede sarf edilmektedir. Sert klinkerin öğütülmesinde yumuşak klinkere göre %80 daha fazla enerji harcanabilir (Çimsa Çimento Araştırma ve Uygulama Merkezi, 2017; SGM, 2015).

SM (silikat modülü) arttıkça öğütülebilirliğin azaldığı, Al₂O₃ ve serbest CaO miktarının yükselmesiyle yine öğütülebilirliğin azaldığı gözlenmiştir. (C₃S / C₂S) oranı veya silikatların ara fazlara oranı, (C₃S + C₂S) / (C₃A + C₄AF), azaldığında öğünme zorlaşır ve enerji harcaması artar. Öğütülebilirliğe kimyasal ve mineralojik bileşenlerin yanında mikro yapının da etkisi vardır. Mikro yapının oluşumunda ısıtma ve soğutma hızları ve fırın tipide etkilidir. İnce kristalli yapı, özellikle küçük kalsiyum silikat kristalleri öğütmeyi iyileştirir. İri kristaller yalnız parçalanmayı zorlaştırmaz, aynı zamanda kırılma alanlarının sayısını artırır. Bu amaçla geliştirilen matris ve kinetik modeller ile öğütme esnasında malzemenin ton başına harcadığı enerjinin asgari düzeyde tutulması sağlanmaktadır (Çimsa Çimento Araştırma ve Uygulama Merkezi, 2017).

Bu çalışmada, çimento klinkeri ile katkı maddelerinin belirli oranlarda karıştırılması sonucu elde edilen ve katkılı çimentolar sınıfında yer alan CEM II ve CEM IV tür çimentoların ince tane boyutlarında (-0.300 + 0.090 mm) kinetik modele dayalı öğütme çalışmaları sonucu model parametreleri elde edilmiştir. Literatürde kırılma hızları için yapılan çalışmalar -1.00+0.100 mm arası tane boyutları arasında gerçekleştirilmiştir. Günümüzde çimento üretim süreçlerinde artık çimento değirmeni için beslenen malzeme tane boyut dağılımı -0.300 mm’dir. Özgül kırılma hızı ve dağılım fonksiyonu için bu boyut aralığında literatürde çalışmalar bulunmamaktadır. Çalışmada, çimento üretim süreçlerinin tasarımı, modelleme ve simülasyon çalışmalarında daha doğru sonuçlar vermesi bakımından ince tane boyutları seçilmiştir. Daha sonra çimento bileşenleri ile kinetik model parametreleri ile arasındaki ilişki mukayese edilmiştir.

Teori

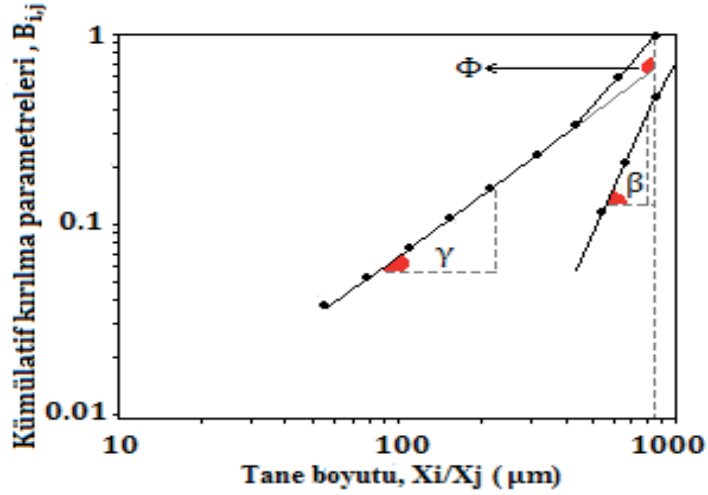
Bilyalı değirmenler için özgül kırılma hızı ve kümülatif kırılma dağılımı kavramlarını içeren boyut küçültme yaklaşımı kullanılmaktadır. Özgül kırılma hızının bir matematikse formülü Austin vd. (1984) tarafından aşağıdaki gibi verilmiştir.

$$S_i = a_T X_i^\alpha \quad (1)$$

burada; X_i ; i fraksiyonundaki üst boyutu (mm) ve a_T ise; öğütme şartlarına ve malzemenin özelliklerine bağlı olan model parametredir. Kırılan veya öğütülen malzemelerin hangi boyut fraksiyonlarına nasıl dağıldığı kümülatif kırılma dağılımı fonksiyonu olarak tanımlanmış ve aşağıda gösterilmiştir.

$$\sum_{i=n}^{j+1} b_{i,j} = 1 \tag{2}$$

Kısa öğütme süresi verilerinden elde edilen boyut dağılım eğrisini temsil eden bu fonksiyonda, söz konusu parametreler Austin vd. (1984) aşağıda verilen, BII yaklaşımından elde edilen $B_{i,j}$ değerlerine karşı nisbi boyut grafiği çizildiğinde bulunur (Şekil 1).



Şekil 1. Kırılma dağılım fonksiyonunun gösterimi

$$B_{i,j} = \phi_j (X_{i-1}/X_j)^\gamma + (1 - \phi_j) (X_{i-1}/X_j)^\beta \tag{3}$$

burada; ϕ_j , γ ve β malzemelerin özelliklerine bağlı olan model parametrelerdir. Bu parametreler, farklı bilya oranları, değirmen çapları vb. için aynı olup, farklı malzeme özelliklerinde değişmektedir (Umucu vd., 2015).

MALZEME VE METOD

Malzeme

DeneySEL çalışmalarda, Burdur Bucak'ta faaliyet gösteren As Çimento'nun üretmekte olduğu CEM II ve CEM IV tipi çimento kullanılmıştır. Bu örneklere ait reçeteler ve kimyasal analiz sonuçları sırasıyla Çizelge 1 ve 2'de verilmiştir.

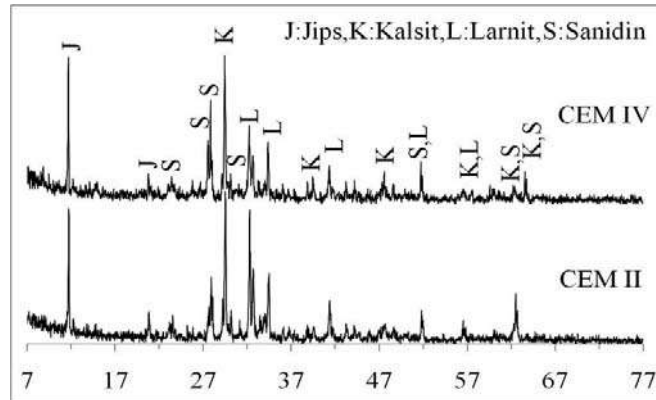
Çizelge 1. CEM II ve CEM IV için reçeteler (ağırlıkça %)

	CEM II	CEM IV
Klinker	65	48
Tras	24	43
Kalker	7	5
Alçı taşı	4	4

Çizelge 2. CEM II ve CEM IV için kimyasal analiz sonuçları (ağırlıkça %)

	CEM II	CEM IV
SiO ₂	27.57	33.78
Al ₂ O ₃	8.69	10.84
Fe ₂ O ₃	3.26	3.27
CaO	50.83	41.53
MgO	1.64	2.07
SO ₃	2.35	2.47
Na ₂ O	0.77	1.32
K ₂ O	1.35	2.00

Çizelge 2’deki kimyasal analiz sonuçlarından, CEM II’ye göre CEM IV örneğinin SiO₂, Al₂O₃, alkali ve toprak alkali miktarının yüksek, CaO miktarının düşük olduğu görülmektedir. CEM IV’de klinker ve kalker miktarının düşük olması sebebiyle CaO miktarı düşmüştür. Ancak CEM II’ye göre daha fazla tras içerdiğinden dolayı da diğer oksitlerin miktarında artış görülmüştür. Çimento örneklerine ait X-ışını kırınımı analizi (XRD) sonuçları Şekil 2’de verilmiştir.



Şekil 2. CEM II ve CEM IV için X-ışını kırınımı diyagramı

Metot

Standart Bond değirmeninde kullanılmak üzere CEM II, CEM IV ve reçetelerde miktarları değişen Klinker ve Tras için -3.35 mm tane boyutuna sahip örnekler elde edilmiştir. Standart Bond değirmeninde yapılan deneyler sonucunda CEM II, CEM IV, Klinker ve Tras örnekleri için iş indeksleri sırasıyla 13.04, 12.68, 9.31 ve 9.24 kWh/ton olarak bulunmuştur.

Örneklerin özgül kırılma hızları ve kümülatif dağılım fonksiyonlarına bağlı kinetik model parametrelerinin belirlenmesi için $\sqrt{2}$ elek serisine göre 4 farklı dar tane boyut fraksiyonunda (-0.300+0.212, -0.212+0.150, -0.150+0.106, -0.106+0.090 mm) sınıflandırılmıştır. Her fraksiyon, $f_c=0.072$ malzeme doluluk oranında laboratuvar çaplı bilyeli değirmende kesikli olarak öğütülmüştür. Her bir öğütme periyodu sonrası tüm değirmen şarjı boşaltılarak kuru elek analizi yapılmıştır. Öğütme deneylerinde kullanılan bilyeli değirmen karakteristikleri ve deney koşulları Çizelge 3’te verilmiştir. Deneylerde bilyeli değirmenin dönüş hızı, değirmenin kritik hız değerinin %75’i alınmıştır.

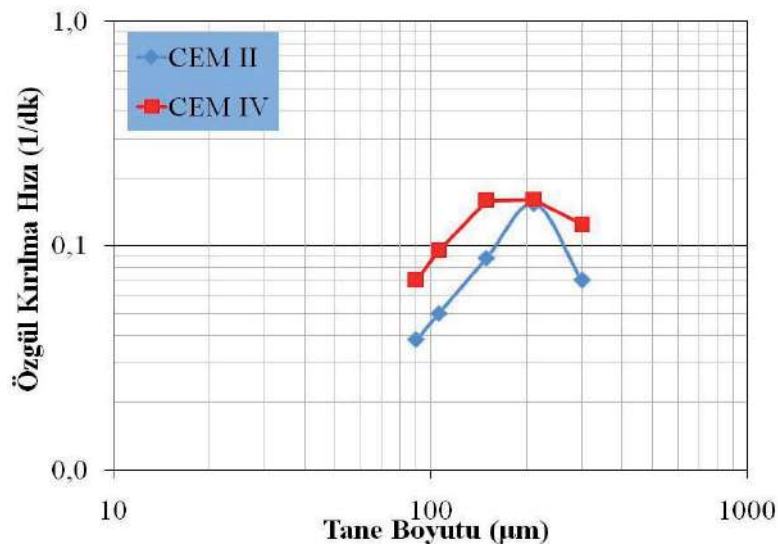
Çizelge 3. Bilyalı değirmen karakteristikleri ve deney koşulları

Değirmen	İç çap, mm	200	
	İç uzunluk, mm	200	
	Hacim, cm ³	6283.2	
	Çalışma ($N_c=75\%$), d/d	92	
Bilya	Malzeme	Döküm	
	Boyut, mm	50-40-30-25-20-17	
	Özgül ağırlık, g/cm ³	8.0	
	Hacim doluluğu, %J	30	
Malzeme	Örnek	CEM II	CEM IV
	Özgül ağırlık, g/cm ³	2.97	2.84
	Malzeme yükü, % f_c	0.072	
	f_c 'ye göre boşluk doldurma oranı, %U	0.60	

BULGULAR VE TARTIŞMA

Özgül Kırılma Hız Fonksiyonlarının Belirlenmesi

Her bir tane boyut fraksiyonu için özgül kırılma hızları (S_i) birinci derece kırılma hız fonksiyonu grafiklerinden hesaplanmıştır. Değirmen çalışma koşullarından, $f_c=0.072$ malzeme doluluk oranında ve $J=0.30$ bilye doluluk oranında belirlenen S_i değerlerine karşı tane boyut fraksiyonu grafiği çizilmiştir (Şekil 3). Bu grafiğin doğrusal kısmından hesaplanan a_T değerleri Çizelge 4'te verilmiştir.



Şekil 3. CEM II ve CEM IV için özgül kırılma hızı eğrileri

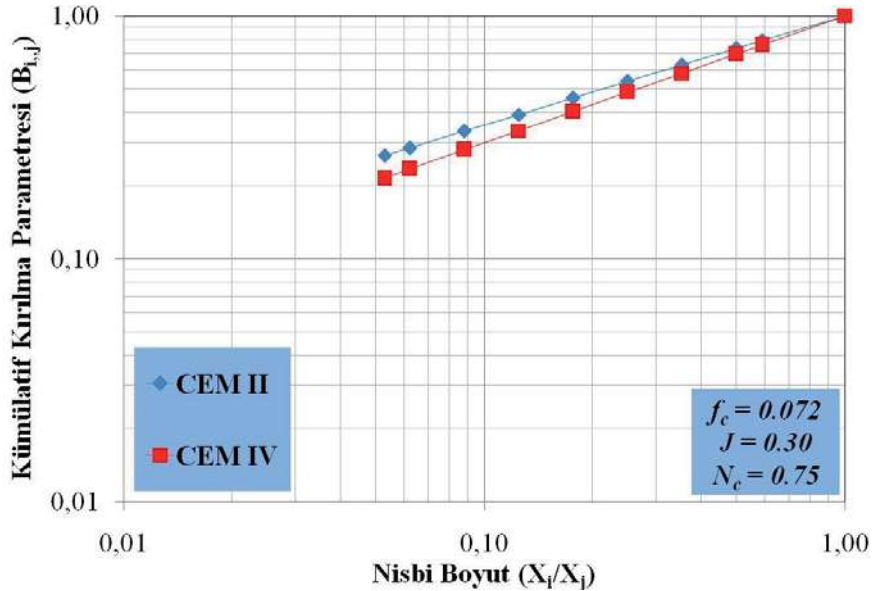
CEM II ve CEM IV örneklerinin kırılma hızlarının belirli bir boyuta kadar arttığı ve azami bir değere ulaştıktan sonra azalmaya başladığı görülmektedir. Kuru ortamda gerçekleştirilen deneylerde, kırılma hızları sırasıyla yaklaşık olarak 0.212 ve 0.150 mm tane boyutlarından sonra azalmaya başlamıştır.

Genel olarak, öğütmenin başlangıcında kırılma hızı, tane boyutu ile artarken, belirli bir tane boyutundan sonra yavaşlamaya başlar. Bu tane boyutu her malzeme için farklılık gösterir. Yavaşlamanın nedeni, oluşan ince tanelerin yastıklama etkisi yaparak iri boyutların kırılmasını engellemesidir.

Ayrıca iki örnek aynı tane boyutuna göre değerlendirilirse, CEM IV'ün birincil kırılma hızının daha yüksek olduğu görülmüştür. Çizelge 1'e bakıldığında CEM IV örneğinin daha düşük Klinker ve daha yüksek Tras içerdiği görülmektedir. Örneklerin birincil kırılma hızı değerleri ile kompozisyonu oluşturan bileşenlerin iş indeksi değerleri arasında bir ilişki olduğu belirlenmiştir. Şekil 3'te, daha yüksek miktarda Klinker (%65) içeren CEM II örneğinin aynı tane boyutuna göre birincil kırılma hız değerlerinin daha düşük olduğu tespit edilmiştir.

Kümülatif Kırılma Fonksiyonlarının Belirlenmesi

Kümülatif kırılma fonksiyonu (B_{ij}) değerleri, en kısa öğütme sürelerinden elde edilmiş ve verilerin normalize olduğu yani boyuttan bağımsız olduğu tespit edilmiştir. Elde edilen B_{ij} değerlerine karşılık nispi boyut (X_i/X_j) grafikleri Şekil 4'te verilmiştir. Bu grafiklerden hesaplanan ϕ , γ , β model parametre değerleri Çizelge 4'te verilmiştir.



Şekil 4. CEM II ve CEM IV için kümülatif kırılma dağılım fonksiyonları

Çizelge 4. Bilyalı değirmen karakteristikleri ve deney koşulları

	a_T	ϕ_j	γ	β
CEM II	0.92	0.194	0.554	0.422
CEM IV	1.43	1.425	0.457	0.378

Çizelge 4 incelendiğinde, CEM II örneğinde a_T ve ϕ_j değerlerinin daha düşük olduğu görülmüştür. Bunun sebebi, CEM II'de Klinker oranının daha yüksek, Tras oranının daha düşük olmasıdır. CEM IV'de daha etkin bir kırılma gerçekleşmiştir ve dolayısıyla ince malzeme miktarında (düşük γ) artış gözlenmiştir.

SONUÇLAR

İki farklı kompozisyona sahip çimento örneklerinin kırılma hız fonksiyonlarının belirlenmesi için oluşturulan grafiklerde, S_j ya da a_T değerlerinin büyük olması, daha etkin bir kırılmanın olacağı ve orijinal

parçanın daha çabuk alt boyuta indirgeneceği anlamına gelmektedir. Çalışmalardan elde edilen deneysel verilerin α_7 değerleri incelendiğinde, CEM IV örneğinin kuru öğütme deneylerinden elde edilen kırılma hızlarının, CEM II örneğine göre yüksek olduğu tespit edilmiştir. CEM IV örneğinin kırılma hızının yüksek olmasının sebebi, kompozisyonda daha az miktarda Klinker kullanılması ile bileşiminde XRD analizi (Şekil 2) sonucu gözlenen Larnit (Ca_2SiO_4) miktarının daha az olmasına bağlanabilir.

ϕ_j değerlerinin artması, en üst boyutların bir alt boyuta daha hızlı kırılacağını ifade etmektedir. CEM IV örneğinin ϕ_j değerinin, CEM II örneğine göre yüksek olduğu tespit edilmiştir. Klinker miktarının azaltılıp, Tras miktarının artırılması ile ϕ_j değerinin arttığı görülmektedir.

γ değerinin büyük olması, ince malzeme miktarının az olduğunu gösterir. CEM II ve CEM IV örneklerinin, çalışmalardan elde edilen deneysel verilerin γ değerleri incelendiğinde, ince malzeme miktarı CEM IV örneğinde daha fazla bulunmaktadır. CEM II örneğinin kuru öğütülmesi esnasında, tane boyutunun küçülmesine bağlı olarak, katıyı bir arada tutan bağ kuvvetlerinin artması neticesinde, ayrıca içerisinde bulunan Larnitin yavaş öğütülmesi sonucunda γ değerleri CEM IV'e göre daha yüksek çıkmıştır.

Bu çalışma sonucunda, çimento bileşiminde bulunan Klinker içeriğinin, malzemenin ufalanmasını yavaşlattığı sonucuna varılmıştır.

KAYNAKLAR

- Austin, L.G., Klimpel, R.R., Luckie, P.T., 1984. Process Engineering of Size Reduction: Ball Milling. AIME, New York, 561 s.
- Deniz, V. The effect of mill speed on kinetic breakage parameters of clinker and limestone, Cement and Concrete Research, 2004. (SCI), 34(8), 1365-1371,
- Hoşten, C., Avsar, C.,1998. Grindability of Mixtures of Cement Clinker and Trass. Cement and Concrete Research concrete research, 28(11), 1519-1524.
- SGM 2015. Çimento Sektörü Raporu: Sektörel Raporlar ve Analizler Serisi. Sanayi Genel Müdürlüğü (2015/1):
<http://sanayipolitikalari.sanayi.gov.tr/Public/SectorReports/7>.
- Umucu, Y., Haner, S., Tunay, T., 2015. The Investigation of Effect of Wet-Dry Grinding Condition and Ball Types on Kinetic Model Parameters for Kaolin. *Polish Mineral Engineering Society*, 35 (1), s.205-211.
- Umucu, Y., Deniz, V., Saraç, M, F., Kuzgun, E. The relationship between cement quality and separation cut size, *Inzynieria Mineralna-Journal of the Polish Mineral Engineering Society*, 2015. (ESCI: Emerging Sources Citation Index), 16(36(2)), 189-194,

GAZ KROMATOĞRAFI (HEADSPACE GC-FID) KULLANILARAK FENOL BAZLI DOLGU MALZEMELERİNİN İÇERİĞİNDEKİ FORMALDEHİT MİKTARLARININ TESPİT EDİLMESİ

DETERMINATION OF FORMALDEHYDE CONTENTS IN PHENOL BASED FILLING MATERIALS USING GAS CHROMATOGRAPH (HEADSPACE GC-FID)

M.Bilen^{1,*}, C. Tuz¹, A. Rasskazova², R. Kızılgedik³, İ. Torođlu¹, S. Yılmaz¹, A. Çakır¹, E. Kaymakçı¹

¹ Zonguldak Bülent Ecevit Üniversitesi Maden Mühendisliği Bölümü
(*Sorumlu yazar: mehmetubilen@yandex.com)

² Mining Institute of Far Eastern Branch of Russian Academy of Sciences

³ RESlab Laboratuvar Cihazları ve Teknik Hizmetleri San. Ltd. Şti.

ÖZET

Bu çalışmada gaz kromatografı kullanılarak fenol bazlı dolgu malzemelerinin içeriğindeki formaldehit miktarlarının tespiti için yararlanılacak yöntemler araştırılmıştır. Çalışma kapsamında bünyesinde FID (“Flame Ionization Detector”) detektörü bulunan bir GC HP 6890 cihazı ve bunun yanında “Headspace” olarak kullanılacak ikinci bir kromatografın da eşlik ettiği bir deney seti tasarlanmıştır. Headspace gaz kromatografisi dengeye getirilen bir sıvı veya katı içeren numuneden ayrılan gazın kromatografteki kolonda (GC) ayrılması esasına dayanmaktadır. Bu teknik genellikle polimerlerin, yiyecek ve içeceklerin, kandaki alkol seviyelerinin, çevresel değişkenlerin, kozmetiklerin ve farmasötik bileşenlerin analizine uygulanmaktadır. Bu çalışma kapsamında Headspace gaz kromatografisinin fenol bazlı dolgu malzemelerindeki formaldehit içeriğinin tespiti amacıyla kullanılması planlanmaktadır. Headspace gaz kromatografisi ile biyolojik-kimyasal bozunma süreçlerinin gerçekleşip gerçekleşmediği, hangi oranda bozunmaların olduğu ve sonucunda oluşan bileşikler belirlenebilmektedir. Bu tayin yönteminde yalnızca en uçucu (en kolayca buharlaşan) maddeler kolona ulaşır. Bu şekilde fenol bazlı kimyasal dolgu malzemelerinin yapısında var olan formaldehitin de uçarak (buharlaşarak) kolonda ayrılması mümkün olacaktır.

Anahtar Sözcükler: Gaz kromatografı, fenol bazlı dolgu malzemeleri, formaldehit, headspace GC-FID.

ABSTRACT

In this study, the methods to be used to determine the amount of formaldehyde in the content of phenol-based fillers were investigated by using gas chromatography. Within the scope of the study, an experimental set was designed with the GC HP 6890 device available within the FID (“Flame Ionization Detector”) detector, as well as a second chromatograph to be used as a “Headspace”. Headspace gas chromatography is based on the separation of gas separated from a liquid or solid containing sample in the column (GC) in the chromatograph. This technique is generally applied to the analysis of polymers, food and beverages, blood alcohol levels, environmental variables, cosmetics and pharmaceutical ingredients. Within the scope of this study, it is planned to be used to determine the formaldehyde content in phenol-based filling materials. With headspace gas chromatography, it is possible to determine whether biological-chemical decomposition processes take place, at what rate there is decomposition, and the resulting compounds. In this determination method, only the most volatile (most readily available as vapor) substances reach the column. In this context, it will be possible to separate formaldehyde, which is present in the structure of phenol-based chemical filling materials, in the column by evaporation.

Keywords: Gas chromatograph, phenol-based filling materials, formaldehyde, headspace GC-FID.

INTRODUCTION

Phenol based filling materials are being extensively used in underground coal mining by means of prevention of spontaneous combustion of coal and gas discharge (Ni and Pereira 2000, Bichler and Simon 1996, Woodfin 1997, Hu et al. 2013, Gray et al. 2006, Hu et al. 2014). Phenol based filling materials are capable of blocking the air with their applicable properties of heat resistance, flame retardancy, low smoke, good sealing and construction convenience (Bichler and Simon 1996, Hu et al. 2014). Wang et al. (2014) have summarized the usage purposes of polymers & phenol-based filling materials in their graphical abstract (See Figure 1).

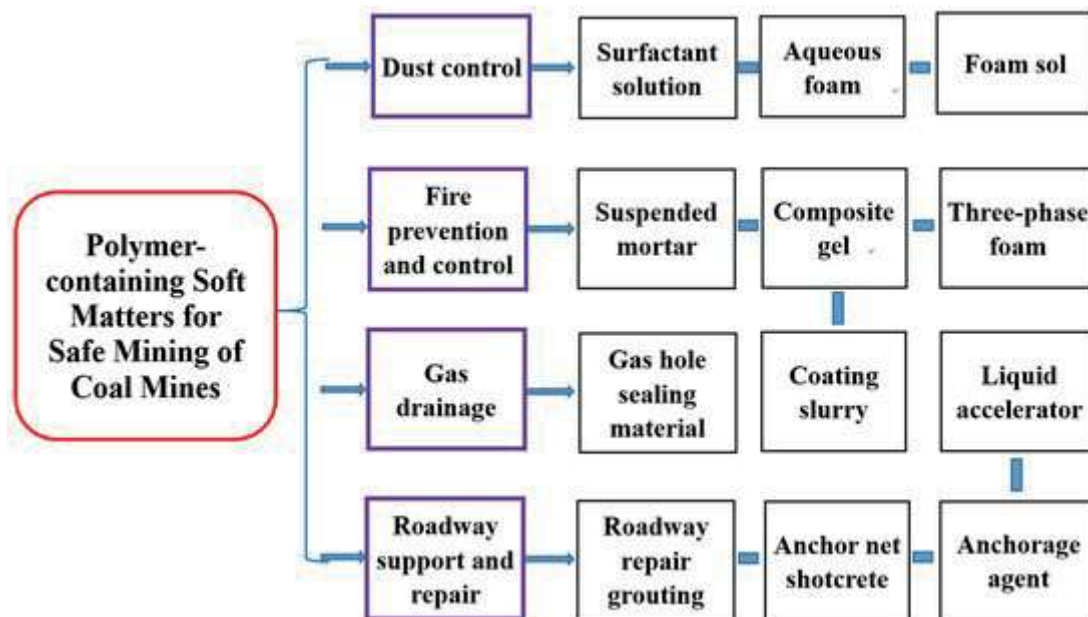


Figure 1. Graphical representation for usage purposes of polymers & phenol-based filling materials (Adapted from the study of Wang et al. 2014).

In addition to these abovementioned, although cost is primary concern for these filling materials, their toxicity & hazardous structure should be also well evaluated. According to Hu et al. 2014, very high amount of formaldehyde is being used and it was expressed as in the following statement: “currently 37% formaldehyde solution is commonly used as the raw material in the preparation of PF resin” (Grenier-Loustalot et al. 1996, Hu et al. 2014).

Free formaldehyde content of a material, either they are cosmetics (Engelhardt and Klinkner 1985) or polymers (Wang et al. 2019), or phenol-based filling materials used in mining, is significant in terms of the correct evaluation of safe working environment (AWES 2014). Engelhardt and Klinkner 1985 have tried to determine free formaldehyde in the presence of donators in cosmetics by HPLC and post-column derivation. Corresponding demonstration of the experimental set up conducted by Engelhardt and Klinkner 1985 is provided in Figure 2.

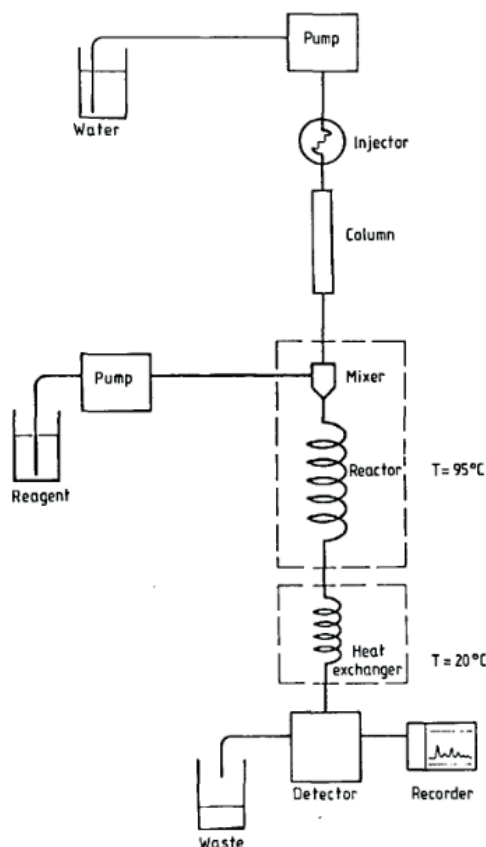


Figure 2. A schematic representation of the experimental method carried out by Engelhardt and Klinkner 1985

Determination of free formaldehyde content in cosmetics is rather interested by many researchers (Oliva-Teles et al. 2002, Benassi et al. 1991, Brandão et al. 2018), high performance liquid chromatography is mostly addressed in their methods presented. In the study of Yi et al. 2019, free formaldehyde content of leather chemicals was determined with an optimized method for leather chemicals based on ISO 27587. Del Barrio et al. {2006} have investigated simultaneous determination of formic acid and formaldehyde in pharmaceutical excipients using headspace GC/MS. Although Del Barrio et al. {2006} study was about pharmaceuticals, the procedure explained (See Section 2.2. “Gas chromatography/mass spectrometry (GC/MS) conditions” in of the same study) can be followed and optimized to determine the free formaldehyde content of mine polymers and phenol based filling materials. In addition, Daoud Agha Dit Daoudy et al. {2018} study can be also guided in the order of further understanding the headspace sampling parameters (See Section 2.3 of the same study), GC instrumental conditions (See Section 2.4 of the same study). Headspace GC-FID method presented in the body of abovementioned study (Daoud Agha Dit Daoudy et al. 2018) is still conducted to detect and quantify formaldehyde impurity in pharmaceutical excipients. In this context, a schematic representation of headspace GC-FID presented in the study of Boe et al. {2007} was provided (See Figure 3). Boe et al. {2007} has introduced this schematical representation as “diagram of the sampling system” in their study of “An Innovative Online VFA Monitoring System for the Anaerobic Process, Based on Headspace Gas Chromatography”.

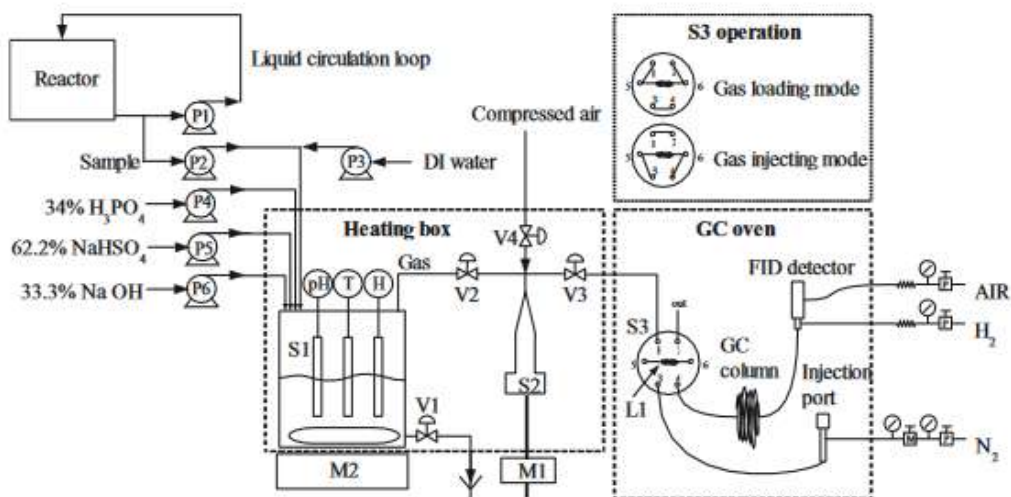


Figure 3. A schematic representation of headspace GC FID (Adapted from the study of Boe et al. 2007).

In addition, Derikvand et al. {2021} have employed a LP-HS-SPME device which was coupled to a gas chromatography-flame ionization detection (GC-FID) system for the direct analysis of polluted soil samples (See Figure 4). Although Derikvand et al. {2021} tried to determine polycyclic aromatic hydrocarbons (PAHs) which are classified as organic environmental contaminants in soil samples, the methodology can still be employed as a guide for the purpose of this study. In a similar manner, headspace gas chromatographic (HS-GC) method for the determination of the volatile organic compounds was employed by Lima et al. 2018 (See Figure 5). Based on the schematical representations provided by the literature researchers (Engelhardt and Klinkner 1985, Boe et al. 2007, Derikvand et al. 2021, Lima et al. 2018), a new method including headspace GC-FID to determine free formaldehyde in mine polymers & phenol-based filling materials can be investigated and optimized. Schematical representation partly adapted from the study of Derikvand et al. {2021} can be employed with its inclusion of syringes employment along with the evacuation, equilibration and extraction procedures application.

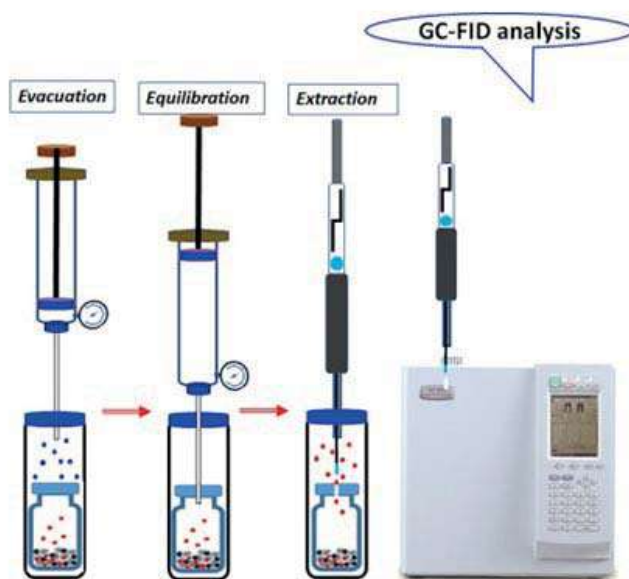


Figure 4. Schematical representation of the GC-FID analysis and corresponding steps carried by Derikvand et al. 2021. (Partly adapted from the study of Derikvand et al. 2021’s study, modified accordingly to the context of this current study).

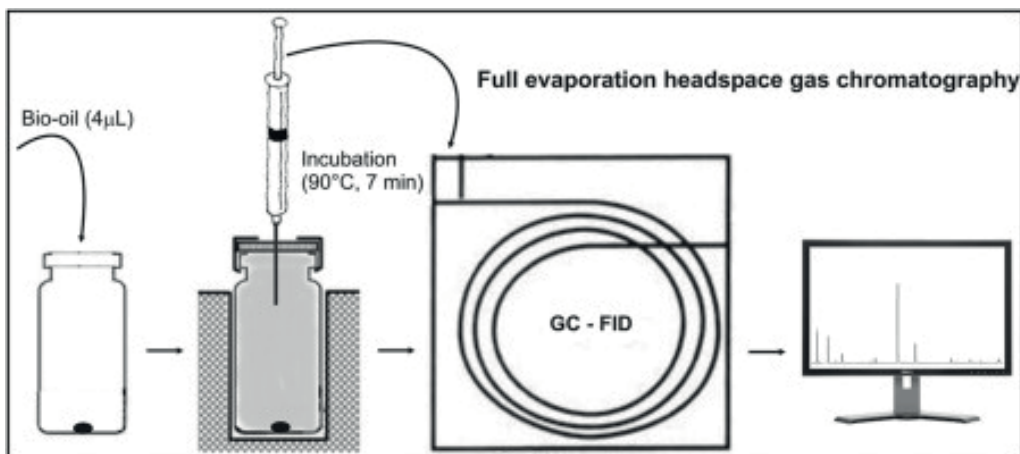


Figure 5. A schematical representation of headspace gas chromatographic (HS-GC) method for the determination of the volatile organic compounds employed by Lima et al. 2018 (adapted from graphical abstract of Lima et al. 2018).

Formaldehyde content of a material can be determined with a proper GC-FID orientation. However, determination of formaldehyde content in a liquid (resin in this case) or a solid (foam in this case) is somehow questionable. Based on the literature researches above provided and based on the testing procedure followed to determine the tendency of spontaneous combustion of coals by employing a GC-Oven in the study of Bilen et al. (2019), determination of formaldehyde content either in the free form or in the structure of the foam can be adapted. Corresponding GC-Oven in the study of Bilen et al. (2019) can be replaced by a Headspace and the gas injection would be sourced from this specific adjustable (isothermal, adiabatic) orientation. Bilen et al. (2019) study can be a guide in this context since the corresponding experimental set up they have built to determine the tendency of spontaneous combustion of coals includes a GC-Oven (Agilent 5890) and GC-FID (Agilent 6890) (See Figure 6).



Figure 6. Spontaneous combustion experiment set up, HP 5890 (employed only as an oven, left bottom) and HP 6890 (employed as GC-FID, left up) (Adapted from the study of Bilen et al. 2019).

In this context, an optimized method should be investigated to determine the free formaldehyde content in phenol-based filling materials used in mining industry. In this paper, a new method including headspace GC-FID was introduced and proposed in order to determine free/fixed formaldehyde content of phenol-based filling materials. In the context of this study, inspired by the employment of headspace GC-FID for the determination of specific materials/ingredients/impurities by various industry (cosmetics, pharmaceuticals, etc.), an optimized method for the determination of free formaldehyde content in phenol-based filling materials used in mining/coal mining industry was investigated. In this order, GC-FID (Agilent) was employed with a headspace (Perichrom GC), and a new experimental set-up was proposed and built.

EXPERIMENTAL METHOD

A representation of the new experimental set up for the determination of formaldehyde content of phenol-based filling materials is provided in Figure 7.

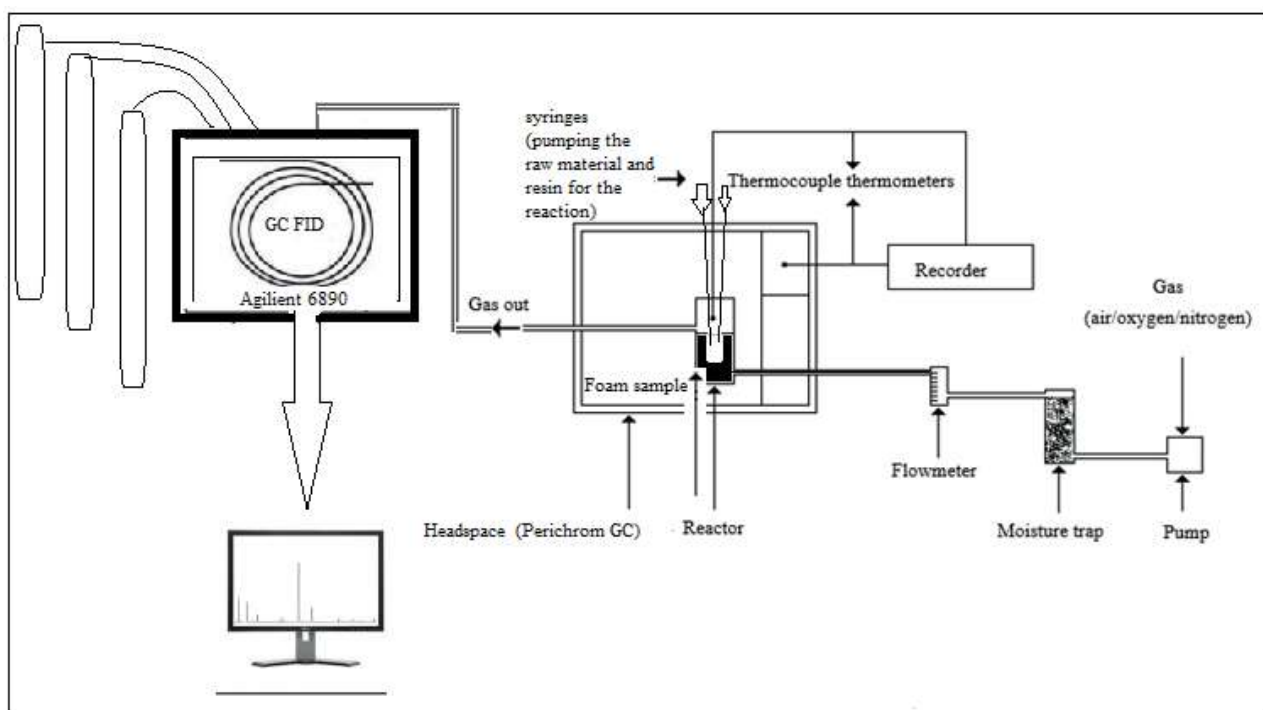


Figure 7. A schematical representation of the new experimental set up for the determination of formaldehyde content of phenol-based filling materials.

In this context, a photo is provided from the laboratory (See Figure 8) to better demonstrate corresponding new experimental set up for the determination of formaldehyde content of phenol-based filling materials. Perichrom GC is placed in addition to the laboratory equipments provided in Bilen et al. (2019). Perichrom GC is planned to employ as headspace and it will be worked as source of gas sampling from the foam and the reaction involving during the production of foam (phenol-based filling material). This abovementioned GC (Perichrom GC) would enable isothermal or adiabatic reaction environment, or any means of temperature ramps for the correct understanding the gas release during the chemical reaction between the composites of phenol-based filling materials. The reason of GC-Oven employment (Perichrom GC in this case) as a headspace is basically the adjustable temperature program availability and corresponding ease of control.



Figure 8. A photograph from the laboratory built for the determination of formaldehyde content of phenol-based filling materials (See Headspace Perichrom GC, right up) (See GC-FID left up).

Referring to Figure 8, it can be seen 3 separate GC, and only one is being employed as chromatographic purposes (GC-FID, Agilent 6890, left up). Previously served as a gas chromatograph, GC HP 5890 (left down), is being employed as GC-Oven, and this was explained in detail in the study of Bilen et al. {2019}. As it was stated earlier, Perichrom GC (right up) is also malfunctioning in terms of chromatographic purposes but it will be employed as a GC-Oven (Headspace) for the determination of formaldehyde content of phenol-based filling materials. Figure 9 is provided in order to correspond the inner presentation of headspace orientation for the experimental set up.

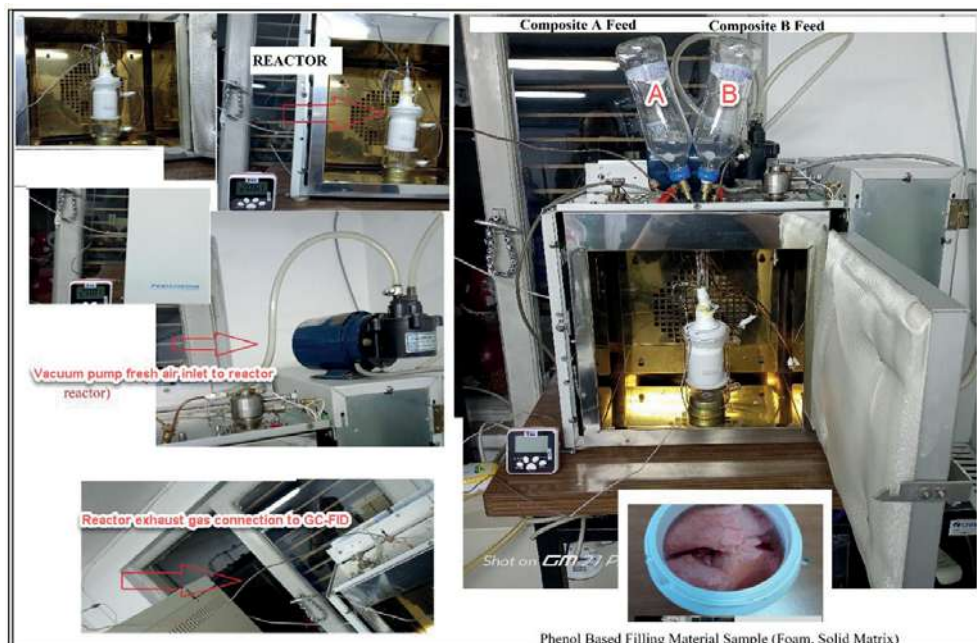


Figure 9. Inner presentation of the headspace orientation, reactor, and syringes in the body of the experimental set up.

There is a reactor (same as employed in spontaneous combustion liability tests) placed in the headspace (Perichrom GC). The reactor has one air inlet and one exhaust gas outlet. There is a thermocouple which has a joint to the sample chamber. Already reaction environment or the place of the sample is controlled by GC-Oven (Perichrom GC), the exothermic reaction and corresponding temperature rises are recorded with this thermocouple. Difference in spontaneous combustion liability test is the available syringe pumps (2 syringes) for the composites injection to the reaction chamber (reactor). Injection of each composites (composite A and composite B) is simultaneously realized and the following gas discharge is pumped with the air flow connected to GC-FID. This is the simulation of the reaction taking place for the production of phenol based filling materials. In terms of mining environment, there should be air ventilation which is actually provided air to the chamber of the reactor by the air inlet. Air inlet is controlled by a flowmeter like in the case for spontaneous combustion liability tests. This experimental procedure is readily available and initial tests are already completed. These initial tests were carried out to see any problems associated with the testing equipments and testing scheme. Initial tests were passed and it was understood that proposed experimental set up can be employed to determine the formaldehyde content in phenol based filling materials (either in free form or in the matrix of foam).

RESULTS AND DISCUSSION

In this study, initial test results of the formaldehyde determination analysis with headspace GC FID was provided. In this context, results include not only free formaldehyde content during the chemical reaction taking place between composite A and composite B (resin and raw material of phenol based filling material) but also the formaldehyde content of the foam itself (solid matrix of foam). Result of the analyses of free formaldehyde content during chemical reaction is tabulated in Table 1. Initial analyzes for the free formaldehyde content during chemical reaction were carried out for two different samples at different temperatures (18, 20, 22 and 24 °C). Corresponding temperatures are arranged as headspace oven orientation, which are considered as the representation for the underground coal mine temperature levels.

Table 1. Formaldehyde analysis result during chemical reaction between composite A and composite B (Analysis is carried out with headspace GC FID).

Analyzed Item	Analysis Description	Result (formaldehyde content) (%)
Sample No:1 (Reaction between composite A ₁ and composite B ₁)	Headspace GC-FID, headspace oven at 18 °C	0.005
	Headspace GC-FID, headspace oven at 20 °C	0.007
	Headspace GC-FID, headspace oven at 22 °C	0.008
	Headspace GC-FID, headspace oven at 24 °C	0.008
Sample No:2 (Reaction between composite A ₂ and composite B ₂)	Headspace GC-FID, headspace oven at 18 °C	0.172
	Headspace GC-FID, headspace oven at 20 °C	0.189
	Headspace GC-FID, headspace oven at 22 °C	0.194
	Headspace GC-FID, headspace oven at 24 °C	0.213

In addition to above mentioned analysis result for the formaldehyde determination (Table 1), gas composition analysis (Table 2) was also realized at different headspace oven temperature levels for two samples.

Table 2. Gas composition analysis result during the reaction between composite A and composite B (Analysis is carried out with headspace GC FID).

Sample	Headspace Oven Temperature (°C)	Composition of the Gas Out from the Reactor						
		CH ₄	NO _x	H ₂ S	CO	CO ₂	O ₂	CH ₂ O
Sample No:1 (Reaction between composite A ₁ and composite B ₁)	30	n.d.	n.d.	n.d.	33 ppm	n.d.	22.60 %	0.009 ppm
	60	0.17 ppm	n.d.	n.d.	37 ppm	2276 ppm	23.10 %	0.009 ppm
	90	0.26 ppm	n.d.	n.d.	41 ppm	1919 ppm	23.70 %	0.010 ppm
	120	0.18 ppm	n.d.	n.d.	17 ppm	2006 ppm	24.00 %	0.011 ppm
	240	0.40 ppm	n.d.	n.d.	n.d.	4857 ppm	25.00 %	0.012 ppm
Sample No:2 (Reaction between composite A ₂ and composite B ₂)	30	0.48 ppm	n.d.	n.d.	59 ppm	1975 ppm	19.11 %	0.27 ppm
	60	0.55 ppm	n.d.	n.d.	52 ppm	2884 ppm	19.24 %	0.29 ppm
	90	0.57 ppm	n.d.	n.d.	65 ppm	3694 ppm	19.47 %	0.32 ppm
	120	0.41 ppm	n.d.	n.d.	46 ppm	4211 ppm	19.05 %	0.37 ppm
	240	0.62 ppm	n.d.	n.d.	39 ppm	5894 ppm	20.56 %	0.49 ppm

*n.d.: non-detected

Referring to Table 2, reaction gases at each temperature were investigated in term of their CH₄, NO_x, H₂S, CO, CO₂ and O₂ contents, respectively. In this context, it was obvious that H₂S was not detected for both of the samples. Since composites of each sample are organics to some extent, composition of the gas exhaust from reaction chamber (reaction between composite A and composite B) can be investigated at previously determined temperature levels. Corresponding temperatures are the headspace oven temperatures and reaction take place at this temperature levels.

As previously explained, in the context of this study, not only the reaction between composite A and composite B was investigated in terms of the formaldehyde (free) content but also the foam (solid matrix) was analyzed. Foam sample was placed into reactor as described in the Material and Method Section, and air (100ml/min) was fed with mini compressor. Air flow was a simulation of the ventilation in underground coal mines, and placing the solid foam sample (phenol-based filling material) inside the reactor is a way to monitor air quality shortcomings reasoned by the foam sample. In this context, result of the formaldehyde content of the gas exhaust was provided in Table 3.

Table 3. Formaldehyde analysis result for the foam sample (solid matrix of foam) (Analysis is carried out with headspace GC FID).

Analyzed Item	Analysis Description	Result (formaldehyde content) (%)
Sample No:1 (Foam Sample)	Headspace GC-FID, headspace oven at 18 °C, air fed to reactor is 100 ml/min	n.d.
	Headspace GC-FID, headspace oven at 20 °C, air fed to reactor is 100 ml/min	n.d.
	Headspace GC-FID, headspace oven at 22 °C, air fed to reactor is 100 ml/min	n.d.
	Headspace GC-FID, headspace oven at 24 °C, air fed to reactor is 100 ml/min	n.d.
Sample No:2 (Foam Sample)	Headspace GC-FID, headspace oven at 18 °C, air fed to reactor is 100 ml/min	n.d.
	Headspace GC-FID, headspace oven at 20 °C, air fed to reactor is 100 ml/min	n.d.
	Headspace GC-FID, headspace oven at 22 °C, air fed to reactor is 100 ml/min	n.d.
	Headspace GC-FID, headspace oven at 24 °C, air fed to reactor is 100 ml/min	n.d.

*n.d.: non-detected

Referring back and forth to the Table 3, formaldehyde content can only be observed during the chemical reaction between the composites, i.e. composite A and composite B. Once the solid matrix of the foam is formed, formaldehyde is linked to the matrix and it is not in the free form. Although formaldehyde is not detected from the exhaust gas of the reactor out (fresh air feed 100 ml/min, sample is solid foam), still depending on the air flowrate and depending on the time of the phenol-based filling material formation formaldehyde and other volatile organic carbons can readily be observed. This study summarizes the initial findings of the experimental set up (headspace GC-FID).

CONCLUSION

In this study, methods to determine the formaldehyde content of phenol-based filling materials were investigated. In this context, experimental set ups provided by literature researchers and the inclusion of headspace GC-FID orientation were considered. Being inspired by the alternative GC-Oven employment for spontaneous combustion liability tests conducted by Bilen et al. (2019), a new experimental set up was built with a malfunctioning GC (Perichrom GC, malfunctioning only for chromatographic purposes). Perichrom GC was employed in terms of headspace and the oven of this abovementioned equipment functions properly. Simulation of the foam production in underground coal mining environment/mining environment, reaction gases should be collected and analyzed. In a mining environment, ventilation takes place and corresponding simulation of this air ventilation in mining atmosphere was achieved with an air mini compressor to the reaction chamber of foam (phenol-based filling material) production. Air carries the gases discharged during the chemical reaction between composites of phenol-based filling materials, and this gas discharge is being analyzed with GC-FID (Agilent HP 6890). The experimental set up built in our laboratory is not only available for the analysis of free formaldehyde content released during the chemical reaction of the composites (composites of phenol-based filling materials, composite A and composite B) but also corresponding analysis of gases, formaldehyde, volatile organic carbons, etc. can be analyzed for the foam solid samples produced after the

chemical reaction. This study does not involve the corresponding test results since it is not the focus yet, but it presents the availability of testing procedure along with the description of the method.

REFERENCES

- AWES (2014) Safe Work Australia The Australian Work Exposures Study (AWES): Formaldehyde, ISBN 978-1-74361-929-2 (pdf) 978-1-74361-902-5 (docx)
- Benassi, C. A., Semenzato, A., & Bettero, A. (1991). High-performance liquid chromatographic determination of free formaldehyde in cosmetics. *Journal of Chromatography A*, 464, 387-393.
- Bichler, W. & Simon, L. Fuel Energy Abstr., 37, 251 (1996).
- Bilen M., Kaymakçı E., Yılmaz S. & Çakır A. An alternative spontaneous combustion experiment set-up by employing an old version Gas Chromatograph, Proceedings of 7th International Congress of Mining Machinery and Technologies 24-25 October 2019, İzmir Turkey.
- Boe, K., Batstone, D. J., & Angelidaki, I. (2007). An innovative online VFA monitoring system for the anaerobic process, based on headspace gas chromatography. *Biotechnology and bioengineering*, 96(4), 712-721.
- Brandão, P. F., Ramos, R. M., & Rodrigues, J. A. (2018). GDME-based methodology for the determination of free formaldehyde in cosmetics and hygiene products containing formaldehyde releasers. *Analytical and bioanalytical chemistry*, 410(26), 6873-6880.
- Daoud Agha Dit Daoudy, B., Al-Khayat, M. A., Karabet, F., & Al-Mardini, M. A. (2018). A robust static headspace GC-FID method to detect and quantify formaldehyde impurity in pharmaceutical excipients. *Journal of analytical methods in chemistry*, 2018.
- Del Barrio, M. A., Hu, J., Zhou, P., & Cauchon, N. (2006). Simultaneous determination of formic acid and formaldehyde in pharmaceutical excipients using headspace GC/MS. *Journal of pharmaceutical and biomedical analysis*, 41(3), 738-743.
- Derikvand, A., Ghiasvand, A., Dalvand, K., & Haddad, P. R. (2021). Fabrication and evaluation of a portable low-pressure headspace solid-phase microextraction device for on-site analysis. *Microchemical Journal*, 168, 106362.
- Engelhardt, H., & Klinkner, R. (1985). Determination of free formaldehyde in the presence of donors in cosmetics by HPLC and post-column derivation. *Chromatographia*, 20(9), 559-565.
- Gray, T.A., Trevits, M.A., Crayne, L.M. & Glogowski, P. Trans. Soc. Mining Metallurgy Exploration, 320, 31 (2006).
- Grenier-Loustalot, M.F., Larroque, S., Grenier, P. & Bedel, D., *Polymer*, 37, 939 (1996)
- Hu, X., Zhao, Y., Cheng, W., Wang, D., & Nie, W. (2014). Synthesis and characterization of phenol-urea-formaldehyde foaming resin used to block air leakage in mining. *Polymer Composites*, 35(10), 2056-2066.
- Hu, X.M., Wang, D.M. & Wang, S.L., *Int. J. Min. Sci. Technol.*, 23, 13 (2013).
- Lima, N. K., Lopes, A. R., Guerrero Jr, P. G., Yamamoto, C. I., & Hansel, F. A. (2018). Determination of volatile organic compounds in eucalyptus fast pyrolysis bio-oil by full evaporation headspace gas chromatography. *Talanta*, 176, 47-51.
- Ni, X & Pereira, N.E. *AIChE J.*, 46, 37 (2000).
- Oliva-Teles, M. T., Paiga, P., Delerue-Matos, C. M., & Alvim-Ferraz, M. D. C. M. (2002). Determination of free formaldehyde in foundry resins as its 2, 4-dinitrophenylhydrazone by liquid chromatography. *Analytica Chimica Acta*, 467(1-2), 97-103.
- Wang, H., Du, Y., Wang, D., & Qin, B. (2019). Recent Progress in Polymer-Containing Soft Matters for Safe Mining of Coal. *Polymers*, 11(10), 1706.
- Woodfin, R.L. "Rigid Polyurethane Foam (RPF) Technology for Countermine (Sea) Program-Phase 1," SandiaReport, SAND96-2841, Sandia National Laboratories, Albuquerque, NM, January (1997).
- Yi, Y., Ding, W., Wang, Y. N., & Shi, B. (2019). Determination of free formaldehyde in leather chemicals. *Journal of the American Leather Chemists Association*, 114(10), 382-390.

GÖRÜNTÜ İŞLEME TEKNİKLERİ İLE TENÖR KONTROLÜ; DEMİR EXPORT DİVRİĞİ DEMİR MADENİ GRADE CONTROL WITH IMAGE PROCESSING; A CASE STUDY, DEMİR EXPORT DİVRİĞİ IRON ORE MINE

H.Çınar^{1,*}, B.Aksanı¹, P. Tekin¹, A.Yıldız¹

¹ Demir Export A.Ş.

(*Sorumlu yazar: haydarc@demirexport.com)

ÖZET

Demir Export, 2016 yılında dijitalleşme sürecine başlamıştır. Bu kapsamda yapılan çalışmalardan biri de maden planlamada günümüz veri analiz trendlerini kullanmaktır. Bu amaçla, çeşitli özelliklerinden dolayı, Divriği Demir İşletmesi seçilmiştir. Divriği Demir Madeni İşletmesinde hematit ve ağırlıklı olarak manyetit minerallerini içeren cevher üretimi yapılmakta ve açık ocaktan üretilen cevher zenginleştirme işleminden sonra hem yurtiçi hem de yurtdışında pazar bulmaktadır. Üretilen demir konsantresi kalite açısından pelet kalitesinde olup, izabe tesisleri tarafından tercih edilen bir üründür.

İşletmede, tenör kontrol çalışmalarında uygulanan cevherden kesit alma (sondaj) ve üzerinden ölçümler yapma yöntemi yerine, görüntü ile elde edilen verilerin analizleri ile hızlı ve güvenilirliği yüksek alternatif bir yöntem geliştirilmiştir. Çalışmada başlangıç olarak, üretim kademeleri sıralı olarak fotoğraflanarak, alınan fotoğraflar üzerinde cevher ile pasa malzemesi arasında renk farklılığı oluşturulmuştur. Belirlenen bölgelerde, açık kaynak kodlu görüntü işleme yazılımlarıyla, cevher renginin pasa rengine oranı üzerinden hacimsel yüzde hesabı yapılarak, üretime ve planlamaya etki edecek şekilde hızlı ve düşük maliyetli bir yöntemle tenör kontrolü yapılabilmektedir. Daha geniş bir yüzey alanı taranarak sonuçların güvenilirliği artırılmıştır.

Anahtar Sözcükler: Görüntü işleme, dijital dönüşüm, veri analizi, tenör kontrolü

ABSTRACT

Demir Export started the digitalization process in 2016. One of the studies carried out in this context is to use today's data analysis trends in mine planning. For this purpose, Divriği Iron Mine Operation was chosen due to its various features. Divriği Iron Mine Operation produces ore containing hematite and predominantly magnetite minerals and the ore produced from open pit finds markets both in Turkey and abroad after the enrichment process. The iron concentrate produced is of pellet quality in terms of quality and is a product that is highly preferred by smelters.

A fast and reliable alternative method has been developed with the analysis of the data obtained from the images, instead of the ore sectioning (drilling) and related calculations. In the beginning of the study, the production stages were photographed sequentially, and color contrast was created between the ore and waste material on the photographs taken. By using the open-source image processing applications in the specified regions, the volumetric percentage calculation was made quickly over the ratio of ore to waste color. Using this method, grade control could be performed in a fast and cheap way that can positively affect production and planning stages. The reliability of the results is increased by scanning the larger surface area.

Keywords: Image processing, digital transformation, data analysis, grade control

GİRİŞ

Endüstri 4.0 devrimin başlamasıyla beraber savunma sanayi öncü olmak üzere hemen her sektörde dijitalleşme gerçekleşmeye başlamıştır. McKinsey&Company'nin yaptığı bir araştırmaya göre; Covid19 küresel salgını ile dijitalleşme şirketlerin hem organizasyon yapısını hem de iş yapış şekillerini değiştirmeyi bir seçenek olmaktan çıkarıp zorunluluk haline getirdiği gözler önüne serilmiştir (Laura LaBerge, 2020).

Her sektörde olduğu gibi madencilikte de dijitalleşme çalışmaları olanca hızıyla devam etmektedir. Günümüzde oldukça sık kullanılan görüntü işleme teknikleri ile analizler, madencilikte de uzun yıllardır kullanılmaktadır. Öyle ki 2002 yılında yapılmış olan bir çalışma; büyük kaya parçalarının görüntü işleme yöntemleri ile tespit edilebileceğini göstermiştir. Bu çalışmada temel amaç kırıcı/elek gibi makineleri durduran büyük kaya parçalarını tespit etmektir. Bu amaçla alınan görüntüler çeşitli filtreleme ve düzeltme işlemlerinden geçirildikten sonra bir istatistiksel model yardımı ile görseldeki cisimlerin kaya olup olmadığının tespiti gerçekleştirilmiştir (Enrique Cabello, 2002).

Madencilikte görüntü işleme çalışmaları sadece ayırt edilmesi kolay olan cisimlerin tespit edilmesinden ibaret değildir, flotasyon gibi karmaşık süreçlere de dahil edilebilmektedir. Yapılan bir çalışmada süreç içerisinde flotasyon hücresindeki köpüğün görüntü işleme algoritmaları kullanılarak ayırt edilebildiği ve köpük özelliklerine bağlı olarak tesis performansının optimize edilebileceği belirlenmiştir (D.W. Moolman, 1994).

Planlama, diğer tüm sektörlerde olduğu gibi madencilik sektöründe de oldukça kritik öneme sahiptir. Madencilikte birçok kısa ve uzun vadeli planlar yapılmakta, şirketin nakit akışına bu planlar yön vermektedir. Bu planlar kısa ve uzun vadeli olup, yapılacak üretimin miktarı ve içeriğine bağlıdır. Planları daha doğru ve çevik bir şekilde geliştirmek için yeni dijital çözümler aranmaktadır. Türkiye’de madencilik sektöründe planlama sürecinde görüntü işleme ile ilgili çalışmalar bulmak oldukça zordur. Bu çalışmanın görüntü işleme teknolojilerinin üretim planlamasında kullanılması yönünden yenilikçi ve özgün değere sahip olduğu düşünülmektedir.

Çalışmanın yapıldığı Divriği Demir İşletmesi’nde cevherleşme hematit ve manyetit minerallerinin çeşitli tane boylarında ince ve killi yan kayaç içerisinde dağılımıyla oluşmuştur. Cevherleşme, üretim kademe yüzeylerinde renk farklılıkları sayesinde gözle de ayırt edilebilir bir durumdadır. Cevherleşmenin yapısal özellikleri nedeniyle numunelerin kimyasal analizi yerine görünen hematit ve manyetit minerallerinin kapladıkları alanlar temel alınarak hesaplanan hacimsel yüzde değerleri ile tenör tespiti yapılmaktadır. Hacimsel yüzde hesapları sondaj karotları üzerinden veya üretim yüzeylerinde ölçekli şeritler kullanarak yapılmaktadır.

GÖRÜNTÜ İŞLEME TEKNİKLERİ İLE TENÖR KONTROL ÇALIŞMALARI

Demir Export A.Ş. Sivas’ın Divriği ilçesinde yer alan Divriği Demir Madeni’nde çalışmalar gerçekleştirilmiştir. İşletmenin mevcut yıllık üretim kapasitesi 2014 yılı sonunda devreye alınan yeni zenginleştirme tesisi ile 500 bin ton/yıl kapasiteye çıkarılmıştır. (Demir Export A.Ş., 2020)

Divriği Madeni’ne ait sahada cevherleşme, hematit ve manyetit minerallerinin çeşitli tane boylarında ince ve killi yan kayaç içerisinde dağılımıyla oluşmuştur. Jeolojik birim içerisinde bulunan, hematit ve manyetit minerallerinden oluşan demir cevheri, tane boyu ve miktar anlamında yatay ve düşey yönde farklılıklar göstermektedir. Cevherdeki demir minerallerinin miktarının tespiti için cevhere özel yöntemler kullanılmaktadır.

Düzensiz dağılım gösteren demir içeren tanelerin, yapılan sondajlarla seviyeleri belirlenir ve hacimsel yüzde oranları hesaplanır. Hacimsel yüzde, cevherli seviyelerde kesilen ve uzun eksenli 5 cm'yi aşan manyetit çakıllarının toplam uzunluğunun, cevherli seviyelerin toplam uzunluğuna oranı ile hesaplanır (Şekil 1 ve 2). Hesaplamalar sonucunda çıkan oranlar demir içeren minerallerin tenör değerleri olarak varsayılırlar. Sondaj verilerinden elde edilen veriler kullanılarak sahanın jeolojik blok modeli oluşturulur, jeostatistiksel yöntemler ile cevherli bloklara atama yapılarak kaynak model kestirimi yapılarak maden ömrü için üretim planları yapılırken, üretim aynalarından elde edilen bu veriler hem üretime yön vermek hem de haftalık, aylık ve yıllık üretim mutabakatları için kullanılırlar.

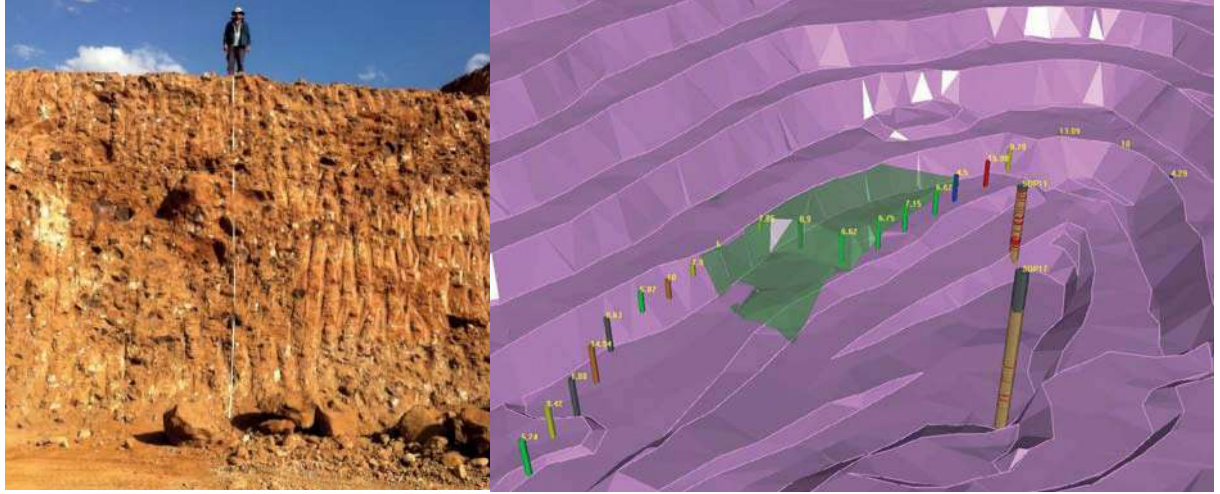


Şekil 1. Cevher Yapılaşması Örneği



Şekil 2. Sondaj Örneği

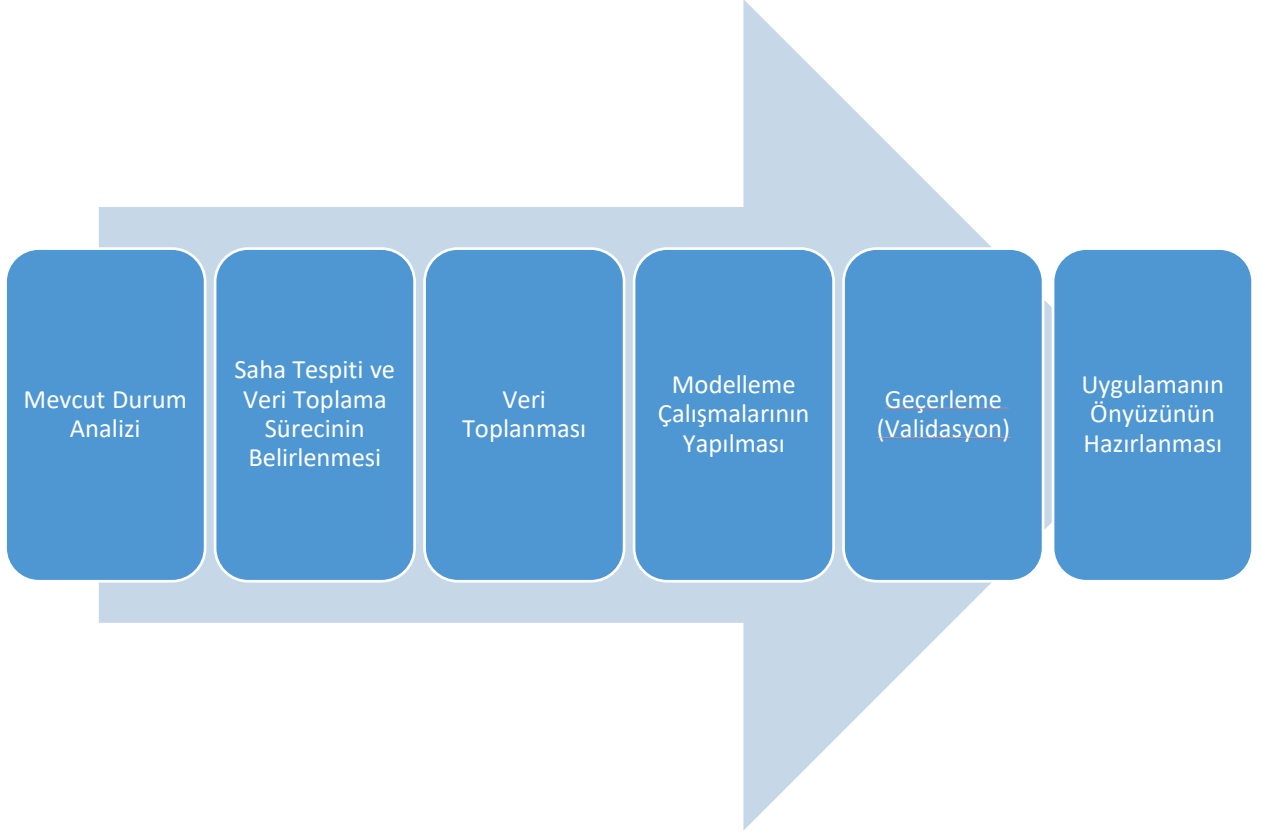
Cevherin yatay ve düşey düzlemdeki düzensiz dağılımı nedeniyle, cevher üretiminde zaman zaman sorunlar yaşanmakta, miktarlarda sık sık değişkenlik yaşanmaktadır. Düzensiz cevher dağılımı yüzünden, cevherden alınan kesit çoğu zaman bölgeyi düzgün temsil edememektedir. Üretime ve kısa vadeli planlara yön vermek amacıyla tenör kontrolü için hacimsel yüzde hesaplamaları, ölçekli şeritler kullanılarak, açık ocak kademelerinde üretim yüzeylerinde yapılmaktadır (Şekil 3). Maden yatağının büyüklüğü ile çalışma alanlarının dağınıklığı ve üretim hızı göz önüne alındığında, tenör kontrol çalışmalarının bu şekilde yapılması ve sonuçların sahada uygulanmasının daha hızlı olması ve elde edilen verilerin güvenilirliğinin artması gerekmektedir.



Şekil 3. Ölçekli Şerit Kullanımı ve Datamine Studio RM Uygulaması Çıktısı

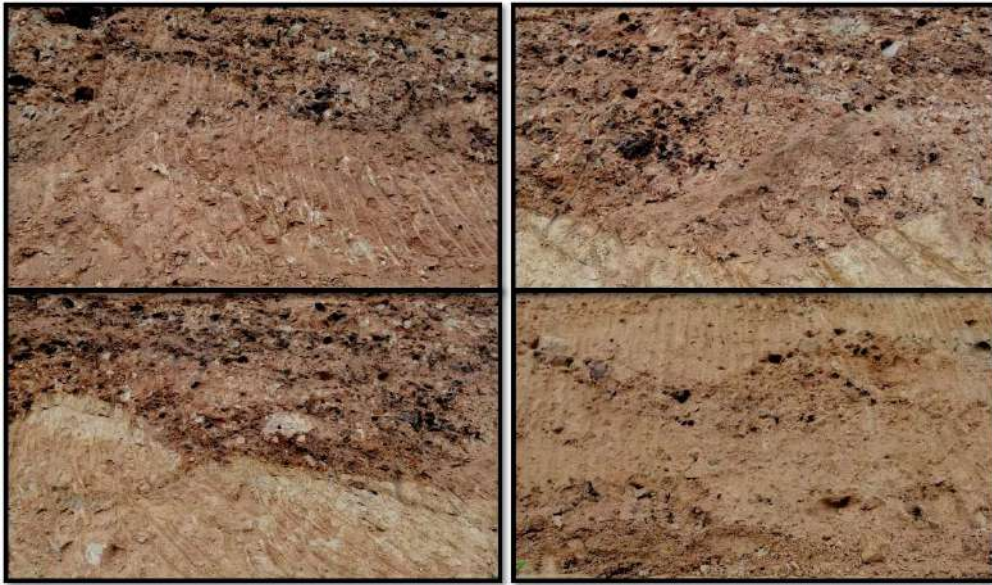
Kullanılmakta olan yöntemlerden esinlenilerek günümüz teknolojilerini de kullanacak şekilde, daha hızlı ve az maliyetli çözüm üreten bir alternatif yöntem geliştirilmiştir. Bu yöntem üretim kademelerinin fotoğraflandırılması ve fotoğraflandırılan yüzey üzerinden hacimsel yüzdenin hesaplanmasıdır.

Daha hızlı ve güvenilir sonuçlar elde etmek amacıyla; aşağıdaki şekilde çalışma planı oluşturulmuştur (Şekil 4).



Şekil 4. Çalışmanın Aşamaları

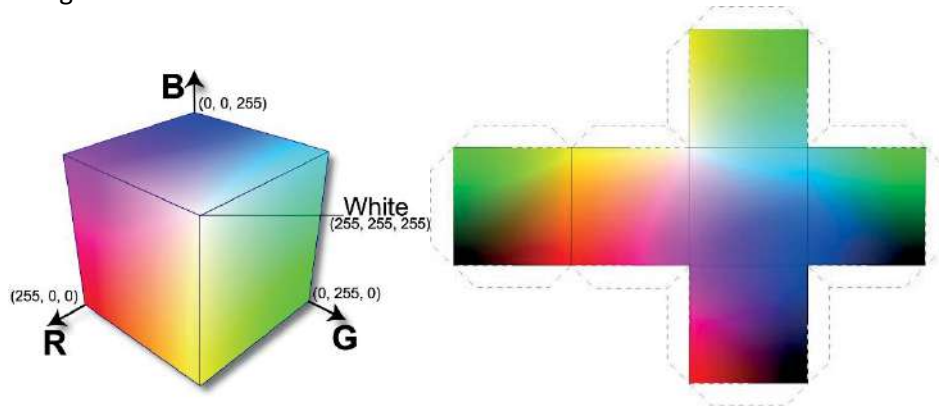
Literatür taraması ve mevcut durumun analizinden sonra örneklem seçimi aşamasına geçilmiştir. İstatistiksel çalışmalar gerçekleştirebilmek için örneklem seçimi oldukça önem arz etmektedir. Örneklem kitleyi en iyi şekilde temsil eden bir alt gruptur. Bu çalışma için, örnekleme seçme amacı ile maden sahasındaki en uygun alanlar; maliyet ve zaman gibi kriterlere göre belirlenmiştir. Belirlenmiş olan kriterlere göre ilgili üretim kademeleri fotoğraflandırılmıştır (Şekil 5).



Şekil 5. Örnek Üretim Kademesi Görüntüleri

Toplanan görüntüler incelenmiş, uygun kalitede olan (istenilen özelliklere sahip) görüntüler seçilmiştir. Seçilen bu görüntüleri işleyebilmek ve doğru sonuçlar elde edebilmek amacıyla görüntüler düzenlenmiştir. Düzenlemede boyut küçültme, kırpma, renk tonu ayarlama gibi birtakım veri temizleme ve filtreleme işlemleri uygulanmıştır. Yapılan bu işlemlerden sonra görüntüler modelleme yapılmaya hazır hale getirilmiştir.

Fotoğraf seçim aşamasını ayrıntılandırmak için fotoğrafın ayırt edici bileşeni olan piksel bilgileri kullanılmıştır. Piksel, dijital göstergelerde görüntünün elde edilmesini sağlayan ve kontrol edilebilen en küçük birimdir (Wikimedia Foundation, 2020). Örneğin, 1024*768 çözünürlüğe sahip bir fotoğraf; yatay olarak 1024 piksel dikey olarak ise 768 piksel olmak üzere 768.432 adet pikselden oluşmaktadır. Fotoğrafta (uygulamada kullanılan) her bir piksel RGB olarak belirtilen bir sıralı üçlü ifade edilir (Şekil 6). Matematiksel tanım olarak $\{(r, g, b) \mid r, g, b \in [0,1]\}$ ile veya $\{(r, g, b) \mid r, g, b \in [0,255] \subset \mathbb{Z}\}$ ile ifade edilebilir. Buna göre 16.581.375 adet farklı renk elde edilebilir.



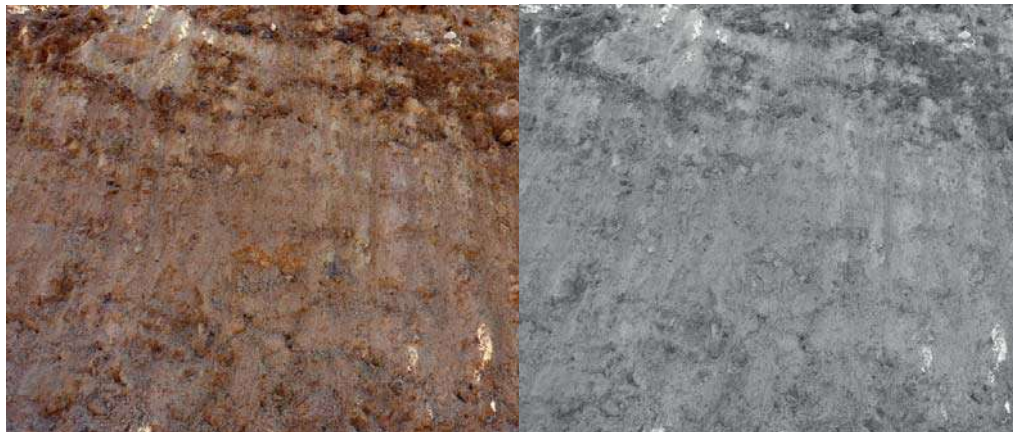
Şekil 6. RGB Renk Uzayı Gösterimi

Fotoğraflardaki RGB formatında bulunan renklerin üzerlerinde işlem yapmayı zaman ve donanım olarak kolaylaştırmak için gri tonlara (grey scale) döndürülmüştür (Şekil 7). RGB formatındaki renkler gri tona dönüştürülürken aşağıdaki eşitlik kullanılmıştır.

$$r, g, b \in [0,255] \subset \mathbb{Z}, \quad x + y + z = 1 \text{ ve } x, y, z \in [0,1] \text{ olmak üzere};$$

$$GreyScale = \frac{x*r + y*g + z*b}{3} \quad xyz \rightarrow w1, w2, w3$$

Burada “x”, “y”, “z” değerleri renklerin ağırlıklarını temsil etmektedir. Fotoğrafın durumuna göre vurgulanması gereken renk bu tonlar sayesinde belirlenmektedir. Bu yöntemde de Ağırlıklı Ortalama denmektedir. $x, y, z = 1$ olması durumunda işlem basit bir şekilde aritmetik ortalama formülüne dönüşmektedir.



Şekil 7. Gri Ton Çevirme Örneği

Tenör kontrol çalışması geliştirilen ara yüz yardımıyla, orijinal resim üzerinden cevherli bölge seçimleri ile başlamaktadır. Uygulama belirlenen kriterlere ve toleransa göre; uzmanın seçmiş olduğu bölgeyle benzerlik gösteren diğer bölgeleri de tarayıp seçmektedir. Tolerans, seçim yapılan bölgeler ile benzerlik gösteren bölgelerin seçimindeki oranı belirtmektedir. Tolerans ne kadar düşük olursa seçim yapılan bölgelere en çok benzeyen bölgeler seçilmektedir. Tolerans değeri arttıkça ise seçim yapılan bölgeye belirtilen tolerans değeri oranında benzerlik yapan alanlar daha fazla seçilmektedir. Cevherli bölge seçimleri tamamlandıktan sonra uygulama hesaplamalara başlamaktadır. Hesaplamalar tamamlandıktan sonra sonuçları yüzde değeri olarak uygulama üzerinden görülebilmektedir.

Tüm hesaplamalar Python programlama dili kullanılarak gerçekleştirilmiştir. Bilimsel hesaplamalar için kullanılan Numpy kütüphanesi, temelleri Intel tarafından atılan gerçek zamanlı görüntü işleme kütüphanesi olan OpenCV gibi kütüphaneler kullanılmıştır (Python Software Foundation, 2020). Bu yaygın kullanımda olan kütüphane ve fonksiyonlarının yanı sıra piksel hesaplamaları, tolerans değerinin işlenmesi ve uygulamaya dahil edilmesi gibi; uygulamanın amacına yönelik özel fonksiyonlar ve algoritmalar da geliştirilmiştir.

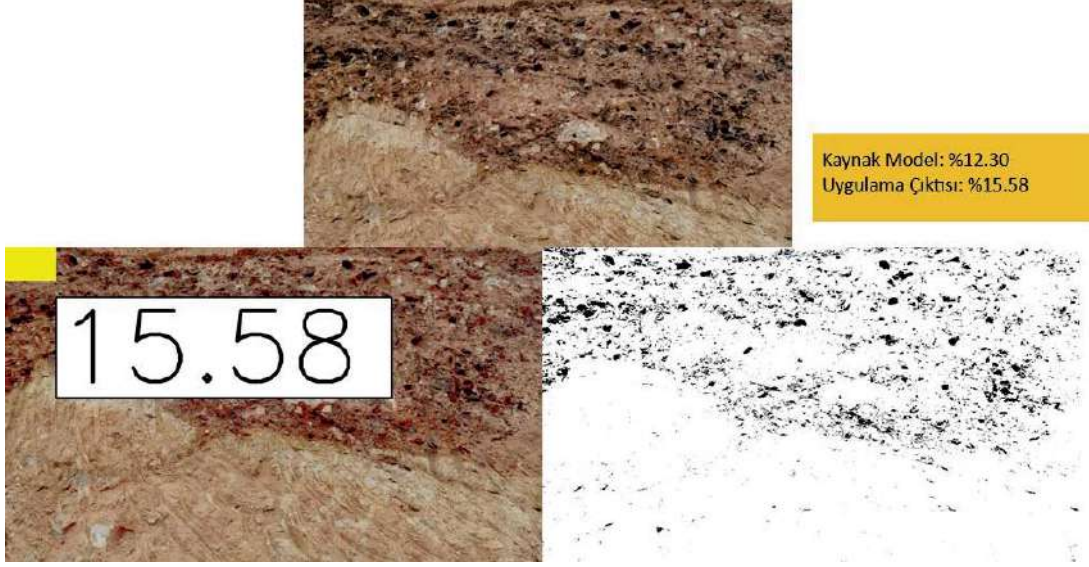
Programın ön yüzü; fotoğrafların uygulamaya tanıtılması, tolerans değerinin girilmesi ve fotoğraf üzerinde bölgelerin seçiminin yapılması için yine bir Python kütüphanesi olan PyQt5 kütüphanesi kullanılmış ve bir ara yüz geliştirilmiştir (Şekil 8).



Şekil 8. Uygulama Örnek Görüntüsü

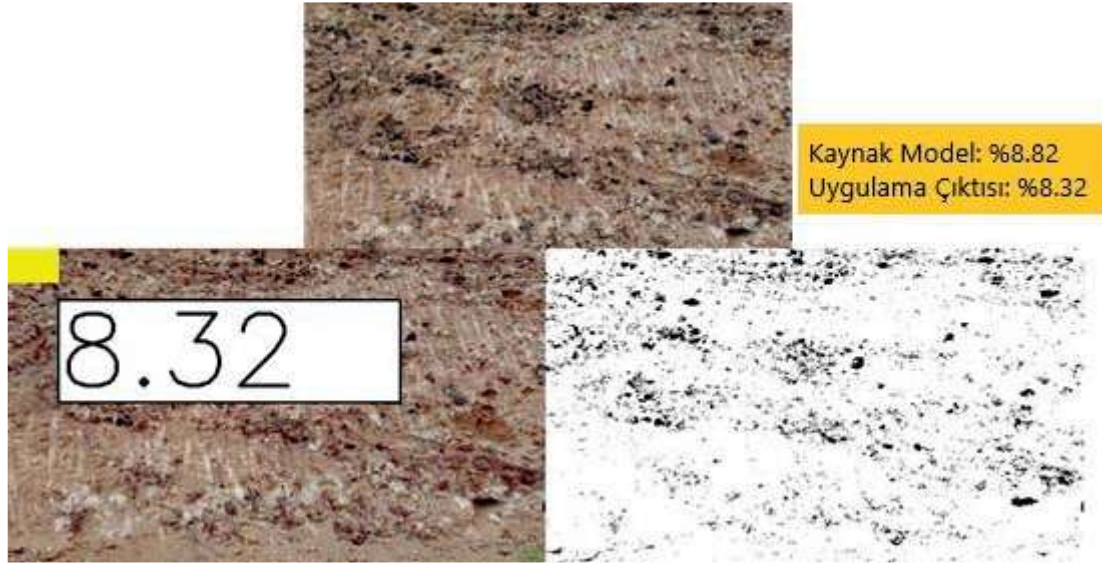
SONUÇLAR VE GELECEK ÇALIŞMALAR

Uygulamadan elde edilen sonuçlar geçerleme (validasyon) işlemine tabi tutulmuştur. Geçerleme için $n > 100$ olacak şekilde bir fotoğraf gurubu seçilmiş ve bu fotoğraflar üzerinde çalışma yapılmıştır. Yapılan çalışmadan sonra kaynak model ile hesaplanan değer kıyaslanmıştır. Kaynak modelin geometri olarak uyumluluğunun %95, tenör olarak uyumluluğunun ise %75 olduğu bilinmekte olup, kıyaslamalarda referans olarak kullanılmaktadır. Geçerleme işleminde uygulama, kaynak model ile kıyaslandığında ortalamada %3 hataya sahip sonuçlar üretmiştir. Sondaj işleminde maliyetli 3 boyutlu analizlerin yanında bu çok düşük maliyetli bu yöntemin hızlı ve güvenilir sonuçlar verdiği söylenebilir (Şekil 9).



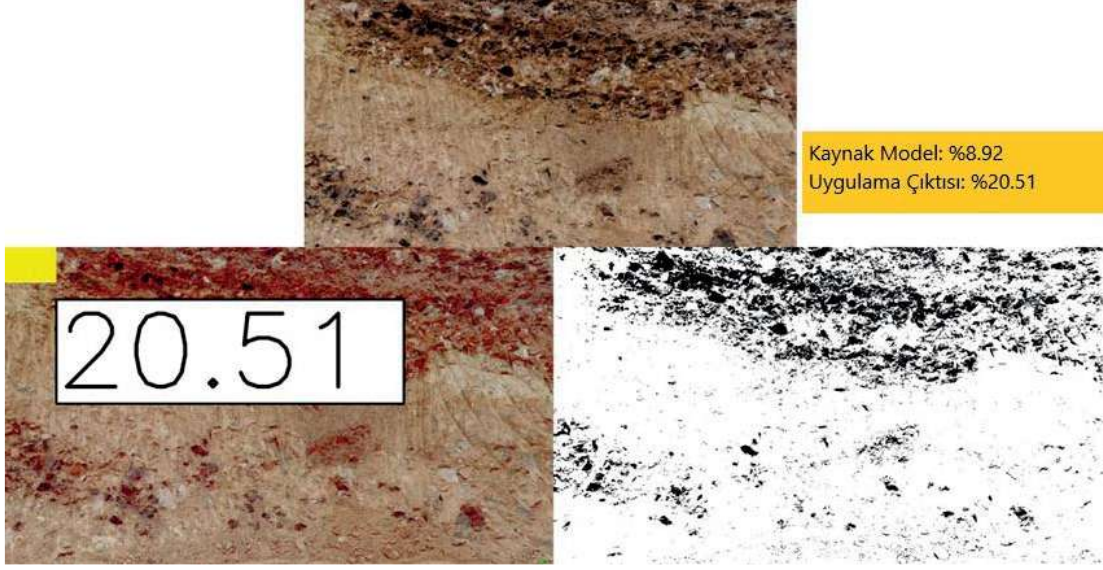
Şekil 9. Uygulama Çıktısı

Geçerleme sürecinde bazı örneklerde uygulamanın hesapladığı değerler ile Kaynak Model arasındaki fark $\pm\%0.5$ 'e kadar düştüğü görülmüştür.



Şekil 10. Uygulama Çıktısı

Bu geçerleme çalışması ile beraber uygulamanın güçlü yönlerinin yanı sıra zayıf yönleri de ortaya çıkmıştır. Uygulama; fotoğrafın çekilme açısı, uzaklığı ve gün ışığı durumundan etkilenmektedir. Etkenler arasında en ön plana çıkan ise gün ışığıdır. Işık ile beraber fotoğrafta yüzeylerden kaynaklı gölgeler oluşmakta ve uygulama tarafından bu gölgeler cevherli bölge olarak seçebilmektedir (Şekil 11).



Şekil 11. Uygulama Çıktısı

Uygulama hızlı ve oldukça düşük maliyet ile sonuç üretebildiği için zayıf yönleri üzerine gidilmesi ve uygulamanın geliştirilmesi planlanmaktadır. Öyle ki sadece planlama sürecine değil, maden arama faaliyetleri ve üretim süreçlerine de insansız hava aracı kullanarak, ışığa duyarlı olmayan kameralar yardımıyla görüntü alarak ve o görüntüler üzerinden anlık sonuçlar elde ederek uygulamanın katkı sağlanması planlanmaktadır.

KAYNAKLAR

- Cabello, E., Sanchez, M.A., and Delgado, J. (2002). A new approach to identify big rocks with applications to the mining industry. *Real-Time Imaging*, 8(1), 1-9.
- Demir Export A.Ş. (2020). Retrieved from <https://www.demirexport.com>
- LaBerge, L., O'Toole, C. (2020). McKinsey&Company. Retrieved from <https://www.mckinsey.com/business-functions/strategy-and-corporate-finance/our-insights/how-covid-19-has-pushed-companies-over-the-technology-tipping-point-and-transformed-business-forever>
- Moolman, D.W., Aldrich, C. (1994). Digital image processing as a tool for on-line monitoring of froth in flotation plants. *Minerals Engineering*, 7(9), 1149-1164.
- Python Software Foundation. (2020). Documentation. Retrieved from <https://www.python.org>
- Wikimedia Foundation. (2020). Flotasyon. Retrieved from <https://tr.wikipedia.org/wiki/Flotasyon>
- Wikimedia Foundation. (2020). Pixel. Retrieved from <https://en.wikipedia.org/wiki/Pixel>

HASANDAĞ VOLKANİKLERİNİN TEK EKSENLİ BASINÇ DAYANIM DEĞERLERİ İLE NOKTA YÜK İNDEKS DEĞERLERİ ARASINDAKİ İLİŞKİNİN İNCELENMESİ
INVESTIGATION OF THE RELATIONSHIP BETWEEN UNIAXIAL COMPRESSIVE STRENGTH VALUES AND POINT LOAD INDEX VALUES OF HASANDAĞ VOLCANICS

M.A. Demirçin ^{1,*}, H. Tunçdemir ²

¹ *M.T.A Genel Müdürlüğü, Sondaj Dairesi Başkanlığı*
*(*Sorumlu yazar: muratali.demircin@mta.gov.tr)*

² *İ.T.Ü. Maden Fakültesi, Maden Mühendisliği Bölümü*

ÖZET

Standart testler için örnek hazırlanamadığı durumlarda kayaçların “Tek Eksenli Basınç Dayanımı Değerleri” doğrudan elde edilemeyebilmektedir. Bu nedenle, detaylı örnek hazırlamayı gerektirmeyen ve taşınabilir donanımlarla hem arazide, hem de laboratuvarda kullanılabilen çeşitli yöntemler geliştirilmiştir. Bunlardan biri nokta yük testidir. Kayaçların basınç ve çekme dayanımı parametrelerinin, nokta yük indeks değerlerinden dolayı olarak belirlenebilmesi için, literatürden derlenen deneysel çalışmalar incelendiğinde, tüm kayaçlar için standart bir “k” değerlerinin tanımlanmasının hatalı olduğu ve böylesi genellemeler yerine, kayaç veya saha bazlı korelasyonların geliştirilmesinin daha doğru olacağı görülmektedir. Bu değerlendirme kapsamında; hem yerel yaygın bir formasyonun mekanik özelliklerinin tanımlanması, hem de düşük–orta dayanımlı ignimbirit ve tuf özelliğindeki volkanik kayaçlara dair dayanım parametrelerinin belirlenmesi için çalışmamızda, Nevşehir provansı volkanik istifi içerisinde yer alan Hasandağ Volkanikleri incelenmiştir. Burada boy çap oranı 1 ve 2.5 olan NX (54mm) çaplı karot örnekler kullanılarak, kuru ve suya doymuş şartlarda, yönlenmelerde dikkate alınarak belirlenmiş olan tek eksenli basınç dayanım değerleri ile yine hem kuru, hem de suya doymuş şartlarda yapılan nokta yük dayanım testlerinden, d_{50} eş değer karot çapı düzeltilmesi sonrası bulunan sonuçların karşılaştırılması yapılarak yüksek korelasyonlu değerler elde edilmiştir.

Anahtar Sözcükler: Tek eksenli basınç dayanımı, nokta yük indeksi, dolaylı kayaç dayanım test yöntemleri, volkanik kayaçların dayanım değerleri

ABSTRACT

When suitable and standardized rock samples are not able to be prepared, then, the uniaxial compressive strength of that samples will not be obtained directly. In order to eliminate this kind of rock-related deficiencies, some techniques, which are used in both laboratory and field with some mobilized instruments, have been improved. One of them is the point load index test. In order to indirectly determine the compressive and tensile strength parameters of rocks from the point load index values, when the experimental studies compiled from the literature are examined, it is seen that the definition of a standard “k” value for all rocks is incorrect and it would be more accurate to develop rock- or site-based correlations instead of such generalizations. Within the scope of this evaluation; Hasandağ Volcanics, located in the Nevşehir province volcanic succession, were investigated in our study in order to define the mechanical properties of a locally widespread formation and to determine the strength parameters of low-medium strength ignimbrite and tuff volcanic rocks. Here, using NX (54 mm) diameter core samples with a length-to-diameter ratio of 1 and 2.5, uniaxial compressive strength values determined by considering orientations in dry and saturated conditions, and point load strength tests performed in both dry and water-saturated conditions, high correlation values were obtained by comparing the results found after d_{50} equivalent core diameter correction.

Keywords: Uniaxial compressive strength, point load index, indirect rock strength test methods, strength values of volcanic rocks

GİRİŞ

Kayaçların zayıflıkları ve buna bağlı standarda uygun örnek alma problemi nedeniyle, tek eksenli basınç dayanımı değerleri her zaman doğrudan elde edilemeyebilmektedir. Bu yüzden çok detaylı örnek hazırlamayı gerektirmeyen, taşınabilir donanımlar yardımı ile hem arazide hem de laboratuvarında uygulanabilen çeşitli yöntemler geliştirilmiştir. Nokta yük testi bu amaçla kullanılan mevcut testler arasında en güvenilir sonucu verenlerdendir (Brook, 1985).

Bu çalışmada Nevşehir provansı volkanik istifi içerisinde yer alan Hasandağ Volkaniklerini kapsayan bazı kayaç örnekleri üzerinde yapılan bir seri tek eksenli basınç dayanımı (TEBD) ve nokta yükleme dayanım test (NYD) sonuçları listelenecek ve aralarındaki ilişkiler irdelenecektir. Bugüne kadar araştırmacılar bu konuda çok sayıda çalışmalar yapmışlar, çeşitli arazi ve formasyonlar için NYD'den TEBD'nin tahmin edilebildiği, yüksek dereceli doğruluğu olan ilişki denklemleri ortaya koymuşlardır. Bu çalışmayı oluşturan veri tabanının özelliği ise boy/çap oranı 1 ve 2.5 olan karot örnekler üzerinde yapılan TEBD ile NYD testlerinin hem kuru ve hem de yaş, aynı zamanda da tabaka düzlemine dik ve paralel olarak da test edilmiş olması ve bu açıdan bu iki test sonuçlarının karşılaştırılması olarak ifade edilebilir.

TEBD ve NYD testlerinin değerlendirilmesi ile elde edilen sonuçlar kaya malzemelerinin dayanım sınıflaması için indeks değer olarak alındığı gibi, dolaylı olarak kayacın çekme dayanımının hesaplanmasında da kullanılmaktadır. Ayrıca, bu yöntemle kayanın zayıflık düzlemlerine dik ve paralel olarak ölçümler yapılarak, yöne göre en büyük ve en düşük değerleri veren, nokta yük dayanım değerleri belirlenebilmekte ve bu şekilde yönlenme dikkate alınarak bulunan değerlerin ortalamalarının oranı olarak tanımlanan, dayanım indeks anizotropisi (I_a) da tayin edilebilmektedir. Kayaç izotropik olduğunda $I_a = 1$; anizotropik olduğunda ise $I_a > 1$ olmaktadır (ISRM, 1985; Broch et al., 1972; Topal, 2000).

YÖNTEM

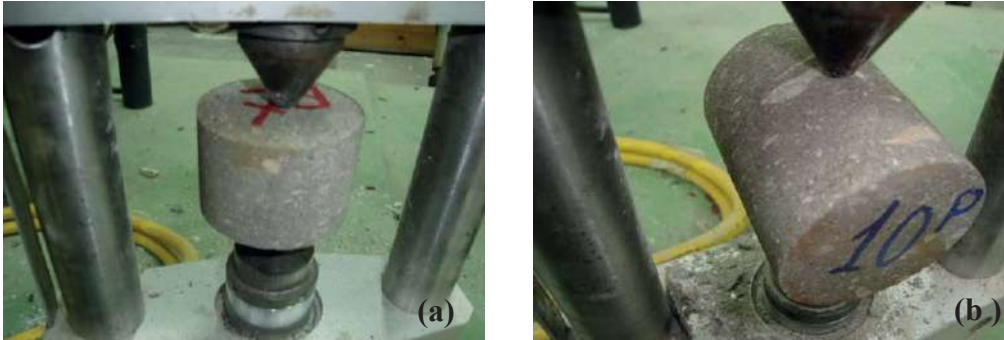
Nokta yükleme deneyi; biri hidrolik yağla tahrik edilen pistondan oluşan iki sivri metal konik ucun arasına yerleştirilen standarda uygun örneklerin sıkıştırılması ve örneklerin kırıldığı anda dayandığı en yüksek yağ basıncının manometreden okunarak yük değerine çevrilmesi ve bu yük değerinin yükleme yönünde birim alana bölüldüğünde elde edilen indeks bir gerilme değeridir. Bu değer kayaç özelliklerine göre belirlenen bir katsayı ile çarpıldığında kayacın dolaylı olarak TEBD değerine ulaşılabilir.

Deney için gerekli düzenek, Şekil 1'de gösterildiği gibi yükleme sistemi, yük ölçüm sistemi ve yükleme sistemindeki platenlerin uç noktaları arasındaki uzaklığı belirleyen ölçüm sisteminden oluşmaktadır.



Şekil 1. Nokta yükleme deney düzeneği

Silindirik örneklerin aparata yerleştirme şekline göre aksel ve çapsal olarak ifade edilen farklı deney uygulama yöntemleri bulunmaktadır. Tabakalanmaya dik doğrultuda yapılan aksel deneyler (a) ile tabakaya paralel olarak yapılan çapsal deneyler (b), Şekil 2’de görülmektedir.



Şekil 2. Karot örneklerin aparata yerleştirme şekli (a) aksel; (b) çapsal

Nokta yük testinde gözlenen kırılma şekli gerilme ile boyuna çatlamadır (Broch et al., 1972). Dayanım indeksi; boyut ile değişmekte, örneğin şeklinden de etkilenmektedir (Brook, 1977). Nokta yük dayanım indeksi karot örnekler için daha küçük olup, örnek boyutu arttıkça azalmaktadır (Al-Jassar et al., 1979; Bieniawski, 1975). Broch ve Franklin 1972’de şekil ve boyut etkisinin; düzgün şekilli olmayan örnekler kullanılarak yapılan testlerde, düzenli bir geometriye sahip örneklerle yapılan testlere kıyasla çok daha şiddetli olduğunu, çapsal olarak yapılan testlerin şekil etkisinden daha az etkilendiğini, bu nedenle de dayanım sınıflaması açısından çok daha güvenilir olduğunu değerlendirmiş ve aksel testlerin sadece dayanım indeks anizotropisi ölçüldüğünde kullanılmasını tavsiye etmişlerdir (Broch et al., 1972).

Düzensiz şekilli olmayan örnekleri kırmak için gereken yük; minimum kesit alanının bir fonksiyonudur (ISRM, 1985). Bu nedenle; standart nokta yükleme indeks değerinin bulunabilmesi açısından bir boyut düzeltme faktörü kullanılması gerekmektedir. Deneyler 50 mm çaplı silindirik karotlar üzerinde yapıldığında, hiçbir düzeltmeye gerek bulunmadığı için, düzeltilmiş nokta yükleme değeri $I_{s(50)}$; 50 mm çaplı silindirik karot testleri ile çapsal olarak ölçülmüş I_s değeri olarak tanımlanmış, diğer şekil ve boyutlu örnekler kullanılarak yapılan testler sırasında boyut düzeltmenin gerekli olduğu vurgulanmıştır. NX 54 mm boyutundaki karot numuneler üzerinde yapılan çap deneylerinde de düzeltme prosedürünün uygulanması zorunlu görülmemekte (ISRM, 1985) ve hatta standart boyut olarak kullanılması önerilmektedir (Bieniawski, 1975).

Nokta yükleme indeks değeri; Eşitlik 1’de gösterildiği gibi hesaplanmaktadır.

$$I_s = \frac{P}{De^2} \quad (1)$$

I_s = Nokta yük indeksi (MPa) ya da (kg/cm^2)

P = Yük (kN) ya da (kgf)

De = Eşdeğer karot çapı (mm).

Nokta yükleme dayanımı; çapsal testler için Eşitlik 2’deki gibi D ’nin fonksiyonu olarak, aksel, blok ve düzensiz parça testlerinde ise Eşitlik 3’teki gibi De ’nin fonksiyonu olarak değişmektedir.

$$De^2 = D^2 \text{ Çap deneyleri için} \quad (2)$$

$$De^2 = \frac{4A}{\pi}; A = W * D \text{ Eksenel deneyler için} \quad (3)$$

Burada;

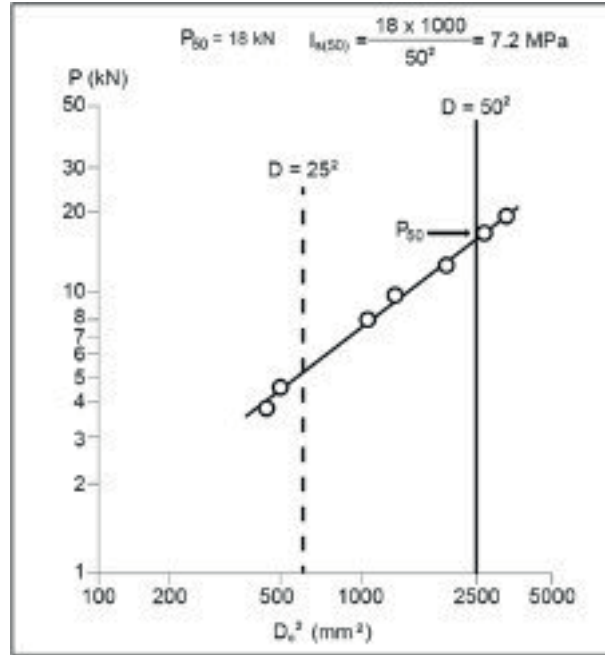
A: Platen değme noktalarından geçen numune düzleminin en küçük kesit alanıdır.

D: Yükleme noktaları arasındaki mesafe (mm)

W: Yükleme noktaları arasındaki kesit alanı dik uzaklığıdır. Bu uzaklık şekilsiz bloklarda değişiyorsa ortalama değer alınarak hesaplamalar yapılmaktadır.

Numune büyüklüğüne göre boyut düzeltme üzerine çeşitli yöntemler geliştirilmiştir.

- 1) Bunlardan birisi D ve De'nin tüm oranlarında örnekleri test edip, P ve De² arasındaki ilişkiyi log-log grafik olarak değerlendirerek, bu grafikten De²=2500 mm²'ye karşılık gelen P₅₀ değerinin interpolasyon yolu ile tayini yöntemidir (Şekil 3). Bu durumda düzeltilmiş nokta yükleme indeksini bulmak için eşitlik 4 kullanılır.



Şekil 3. Is₍₅₀₎ değerinin P ve De² arasındaki ilişki kullanılarak tayini (Brook, 1985)

$$Is_{(50)} = \frac{P_{50}}{50^2}; \quad (4)$$

- 2) Test edilecek örneklerin; sınırlı sayıda 50 mm'den küçük parçalar biçiminde ya da 50 mm'den farklı çapta, ancak; sadece tek bir boyutta hazırlanabilmiş karotlar şeklinde olduğu bir test işleminde ise eşitlik 5'de tanımlanan düzeltme faktörünün kullanılması önerilmektedir (Brook, 1985).

$$F = \left(\frac{De}{50}\right)^{0.45} \quad (5)$$

F: Boyut düzeltme faktörü (tüm kayaçlar için aynı olarak tanımlanmaktadır).

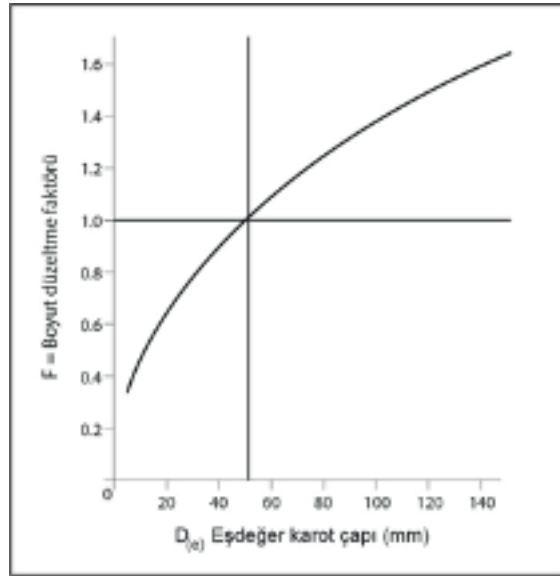
- 3) Eğer farklı karot çaplarında test yapılmış ise boyut düzeltme faktörü (F), Şekil 3’de gösterilen grafikten, ya da Şekil 4’de verilmiş olan logaritmik grafiğin eğiminden yararlanılarak, eşitlik 6’dan hesaplanabilir (Brook, N., 1985).

$$F = \left(\frac{De}{50}\right)^m ; \quad m = 2(1 - n) \quad (6)$$

n= log-log grafiğin eğimi

Bu durumda düzeltilmiş nokta yükleme dayanım indeksi; eşitlik 7’den hesaplanır.

$$Is(50) = FxIs ; \quad (7)$$



Şekil 4. Boyut düzeltme faktörünün grafik yardımı ile bulunması (Brook, 1985; ISRM, 1985)

İfade edilen düzeltme yöntemleri anizotropi derecesine ve yükleme doğrultusuna bağlı olmaksızın uygulanabildiği için, nokta yükleme deneylerinin kullanılabilirliği büyük ölçüde artmıştır.

NOKTA YÜK İNDEKS DENEYLERİ

Bu çalışmada yapılan deneylerde ELE Hemel Hempstead, Merts firmasına ait 14.426 cm² piston alanlı 700 bar azami yük kapasiteli deney aleti kullanılmıştır. Numuneler NX (54 mm) olarak hazırlanmış karot şekillidir. Boy çap oranları literatüre uygun olarak hazırlanan örnekler (Şekil 5) üzerinde çap deneyleri yapılmış, bu deney sonucu kırılan örneklerden yine literatürdeki boyutlara uygun olanların üzerinde (Şekil 2), aksenal deneyler gerçekleştirilmiştir. Örneklerin çoğunda gözle görülür yönlenme yoktur. Ancak, deneyler; farklı yönlerde dayanım parametrelerinde değişim olup olmadığının anlaşılması için, araziden çıkarılma yönlerine göre, tabakaya dik ve paralel olarak hazırlanan suya doymuş ve oda şartlarında kurutulmuş örnekler üzerinde yapılmıştır.

Örnekler 54 mm çaplı oldukları için çap deneylerinde düzeltme yapılmamıştır. Ancak aksenal deneylerde standart bir Is₅₀ değerinin bulunabilmesi için düzeltme yapılmıştır. Düzeltme yöntemi olarak yukarıda anlatılan iki yöntem de kullanılmış ve birbirine yakın sonuçlar elde edilmiştir. Bu çalışmada

eşitlik 5 kullanılarak elde edilen düzeltilmiş deney sonuçlarına yer verilmiştir.



Şekil 5. Nokta yükleme deneyinde kullanılan örnekler.

Örnekler 54 mm çaplı oldukları için çap deneylerinde düzeltme yapılmamıştır. Ancak eksenel deneylerde standart bir I_{s50} değerinin bulunabilmesi için düzeltme yapılmıştır. Düzeltme yöntemi olarak yukarıda anlatılan iki yöntem de kullanılmış ve birbirine yakın sonuçlar elde edilmiştir. Bu çalışmada eşitlik 5 kullanılarak elde edilen düzeltilmiş deney sonuçlarına yer verilmiştir.

Deneyler sırasında her bir kayaç için, en az 10 adet geçerli deney yapılmış, en düşük ve en yüksek ikişer değer göz ardı edilip, geriye kalan değerlerin ortalaması alınarak, ortalama I_{s50} değeri bulunmuştur. Örnek sayısının 10'dan az olduğu Selime tufünde ise, en yüksek ve en düşük değerler göz ardı edilmiş ve geriye kalan değerlerin ortalaması alınarak, ortalama I_{s50} değeri tespit edilmiştir. Bulunan $I_s(50)$ değerinden hareketle de, kayaçların tek eksenli basınç dayanımı değerlerinin ampirik olarak belirlenmesi hedeflenmiştir.

Bu amaçla yapılmış olan bazı çalışmalarda; ağırlıklı olarak tek eksenli basınç dayanımı ile nokta yükleme dayanım indeksi (NYDİ) oranı; “k” incelenmiş ve 22-24 arasında değişen bir oranın kullanılması yönünde eğilim oluşmuştur (Brook, 1985; ISRM, 1985; Quane et al., 2003). En çok kabul gören formül ise; k değerini 24 olarak alan eşitlik 6'da verilen bağıntıdır (Broch et al., 1972; Bieniawski, 1975; Aston et al., 1991).

$$\sigma_b = 24 \times I_{s(50)}; \quad (8)$$

Chau ve Wong (1996) yaptıkları teorik çalışmalarında ise bu oranın 24'ten daha küçük bir değerde ve yaklaşık olarak 12,5 olması gerektiğini ileri sürmüşlerdir (Chau et al., 1996).

Söz konusu farklı değerlendirmeler dikkate alınıp, tek eksenli sıkışma dayanımı ile nokta yükleme dayanım indeksi oranı literatürdeki 50 kadar referans taranıp, incelenerek, Çizelge 1'de sunulmuştur.

Bu çizelge incelendiğinde elde edilen “k” değerinin; 3 - 82 gibi çok geniş bir aralıkta değiştiği (Tsidzi, 1991; Puech et al., 1988), ancak, genel kümelenmenin 6-30 arasında kaldığı, çok zayıf kayaçlarda; 2.8-6 (Chau et al., 1996), zayıf kayaçlarda; 6-20 (Topal, 2000) ve yüksek dayanımlı kayaçlarda ise 20-30

arasında olduğu gözlemlenmiştir (Quane et al., 2003; Liang et al., 2015).

Çizelge 1. Kayaçların nokta yük dayanım indeksi değeri ile tek eksenli basınç dayanımı arasındaki bağıntılar

Referanslar	Önerilen Eşitlikler	Kayaç Tipi	K değeri	TESPİTLER
D'Andrea et al. (1964)	$\sigma_c = 15.3 * I_{s_{30}} + 16.3$			
Broch ve Franklin (1972)	$\sigma_c = 24 * I_{s_{30}}$	Kumtaşı, dolomit (sert kaya) (22-250 MPa); (1.25-9.5 NYD) NX karotlar üzerinde çapsal deneyler yapıldı.	24	Dayanımın saptanmasında, çeşitli boyuttaki karotların kullanılabilmesi için bir boyut düzeltme kartı hazırlandı. IS değerlerinin UCS değerlerine göre daha az saçılmı olduğu gösterildi.
Bieniawski (1975)	$\sigma_c = 24 * I_{s_{30}}$	Kumtaşı kuvarsit, norit (sert kaya) (57-312 MPa); (2.4-11.2 NYD)	24	Örnek boyutu arttıkça nokta yük dayanımının azaldığı, üç eksenli dayanımın amprik eşitlikler yardımıyla %10-20 hatayla bulunabileceği ifade edildi.
Wilson (1976)	$\sigma_c = 8 * I_s$	Çok zayıf çamurtaşı	8	
Al- Jassar ve Hawkins(1979)	$\sigma_c = 17....30 * I_{s_{30}}$	Kireçtaşı, dolomit ve kumtaşı Farklı çapta karot (30,50,70) ve farklı boyutta blok örnekler (30,50,70)	8-27 22	Örnek boyutu arttıkça NYDİ azalmaktadır. NYDİ; karot örnekler için daha güçlüdür. Karot ve blok örnekler için nokta yük ve basınç dayanımı arasındaki bağıntı farklıdır.
Read ve diğ.(1980)	$\sigma_c = 20 * I_{s_{30}}$ bazalt $\sigma_c = 16 * I_{s_{30}}$ sedimanter	Bazalt (30-132 MPa); (5-8 NYD) Kumtaşı, silttaşı (sedimanter kayaç) (27-180 MPa); (8.5-25 NYD)	8-24 10-45	Farklı kayaçlar için farklı alterasyon derecelerinin etkilerini inceledi. Tek eksenli basınç dayanımı ve nka yük testi arasındaki ilişki kaya tipi ve alterasyon derecesine bağlıdır
Beake and Sutcliffe (1980)	$\sigma_c = 12.2 * I_{s_{30}}$	Arap-Pers körfezi kalkerleri		
Forster(1983)	$\sigma_c = 14.5 * I_{s_{30}}$	Dolerit, Kumtaşı (11-113 MPa); (1.52-10.32 NYD)	12-14 15-18	Eksenel nokta yük deneylerinde örnek boyut etkisini inceledi
Gunsallus and Kulhawy (1984)	$\sigma_c = 16.5 * I_{s_{30}} + 51$	Doloston, kumtaşı, kireçtaşı (68-345 MPa) (0.69-10.8 NYD)		Sedimanter kayaçlar
Norbury(1986)		Kumtaşı	8-30	(Genellikle 20-25)
		Silttaşı	15-35	
		Çamurtaşı	18-35	(Genellikle, 20)
		Şeyl	24	
		Magmatik ve metamorfik Kayaçlar	27	
		Kristalize Kireçtaşı	24-54	
		Taneli Kireçtaşı	8	
ISRM 1985	$\sigma_c = 20....25 * I_{s_{30}}$	Tüm kaya tipleri..	10-22	
			20-25	Ancak; özellikle anizotropikve çok farklı tipteki kayaçlar test edildiğinde "k" nın 15-50 arasında değişimine dikkat çekilmiş, nokta yük testinden tek eksenli dayanım değerlerinin tahmini için uygun eşitliklerin kullanılmasının önemi vurgulanmıştır..
Puech et al. (1988)	$\sigma_c = 3.11 * I_{s_{30}}$	Arap-Pers körfezi kalkerleri		
Vallejo et al. (1989)	$\sigma_c = 8.6....16 * I_{s_{30}}$	Appalachian bölgesinde yüzey kömür madencilik sahalarına ait kayaçlar.	12.5 şeyl 17.7 kumtaşı	Şeyl ve kumtaşı örnekleri üzerinde UCS ve IS testleri yapılmıştır
Cargill ve Shakoor (1990)	$\sigma_c = 23 * I_{s_{34}} + 13$	14 farklı kayaç (Kumtaşı, kireçtaşı, dolomit, mermer, siyanit ve gnays)	19-31 17-30	(Genellikle 21-27)
Tsidzi (1991)	$\sigma_c = 14....82 * I_{s_{30}}$	Tabakalanmaların çok fazla değiştiği Gmays, Hornfels, fillit, çist, kayrak taşı gibi metamorfik kayaçlar [(65-250 MPa); (2-10.2 NYD)]	17-23	Anizotropinin etkisi incelendi . "k" değerinin; Zayıf tabakalanmalı kayaçlarda; 17, Orta dereceden daha fazla tabakalanmalı olanlarda 23 olduğu bulundu.
Ghosh and Srivastava (1991)	$\sigma_c = 16 * I_{s_{30}}$	Batı Himalaya'ya ait granitler (25-119 MPa) (2.1-7.4 NYD)		
Grasso et al. (1992)	$\sigma_c = 25.67 * I_{s_{30}}^{0.57}$ $\sigma_c = 9.30 * I_{s_{30}} + 20.04$	Homojen kalkerli çamurtaşını inceledi.		UCS <70MPaolan yumuşak kayaçlar için Üstel eşitlikteki korelasyon katsayısı lineerdeki göre daha yüksek olduğunu gösterdi.
Bell (1992)		Kumtaşı	12-19 (kuru),	7-12 (suya doygun)
		Kireçtaşı	20-30 (kuru),	14-24 (suya doygun)
		Tebeşir	68 (kuru),	31 (suya doygun)
SECRM (1995)	$\sigma_c = 22.82 * I_{s_{30}}^{0.75}$	(Standard For Engineering Classification Of Rock Masses)(GB50218-94)
Chau ve Wong (1996)	$\sigma_c = 12.5 * I_{s_{30}}$	Hong Kong 'ait Granit ve tüfler (18-180 MPa)(0.2-10 NYD)	12.5	UCS/IS oranının; Gc/Gt , poisson oranına, örneğin çapına ve uzunluğuna bağlı olduğunu göstermiştir.
Anıl ve diğ.(1996)		Tortul ve magmatik kayaçlar	15-25 (kuru)	10-24 (suya doygun)
Smith (1997)	$\sigma_c = 14.3 * I_{s_{30}}$	Kıyı alanlarında yataklanmış tipik zayıf kaya malzemeleri incelenmiştir.		Sert kayaçlarda 24 olan değer, buralarda 14.3'tür.
Hawkins,(1998)	$\sigma_c = 7....68 * I_{s_{30}}$	Sedimater ve vakanik kayaçlarda kuru ve suya doygun şartlarda testler yapılmıştır. "	(7-68)	"k" oranının farklı litolojiler ve şartlar altında çok geniş aralıkta değiştiğini, suya doygun kayaçlar için bu oranın; kuru kayaçlar için olandan genellikle %50 daha düşük olduğunu göstermiştir.
Topal(2000)	$\sigma_c = 10.647 * I_{s_{30}} + 2.47$	Tüf	10.65	
Kahraman (2001)	$\sigma_c = 23.621 * I_{s_{30}} - 2.69$	48 farklı kaya için 2 farklı eğilim bulmuştur.		Kömür yatağındaki kayaçlar için daha dik eğim. Diğer gruptaki 22 farklı kayaç için daha düşük eğim.
	$\sigma_c = 8.41 * I_{s_{30}} + 9.51$			
Quane and Russel (2003)	$\sigma_c = 24.4 * I_{s_{30}}$ sert kaya	Sert kayaçta lineer ilişki, $I_{s \leq 5}$ MPa); UCS=125MPa)		İncelemeler sırasında; İgnimbiritlerin kaynaklanma derecesinin ölçümü için, kaya dayanımının kullanılabilirliği ve verimliliği araştırılmıştır. UCS değerleri 3.18-74.08 MPa, çoğunlukla >50 MPa olan kayaçlar incelenmiştir
	$\sigma_c = 3.86 * I_{s_{30}}^2 + 5.65 * I_{s_{30}}$	Zayıf Kayaçta ise lineer olmayan ilişki elde edilmiştir.		

Referanslar	Önerilen Eşitlikler	Kayaç Tipi	K değeri	TESPİTLER
Tsiambaos and Sabatakakis (2004)	$\sigma_c = 7,31 * I_s^{171}$ $\sigma_c = 23 * I_{s(50)}$	Yunanistandaki elastik sedimanter kayaçlar (Kireçtaşı; mar; kumtaşı) kullanılmıştır. Kayaçlar <2MPa, 2-5 MPa, >5 MPa şeklinde sınıflandırılmışlardır	13 20 28	Lineer regresyon modelinde kaya malzemesinin tüm dayanım sınırları için; tek bir dönüşüm faktörü nün uygulanabilir olmadığı vurgulanmıştır. Üç farklı nokta yük dayanım sınıfı için, orjinden geçen farklı dönüşüm faktörleri önerilmiştir
Palchik and Hatzor (2004)	$\sigma_c = 8,....18 * I_{s(50)}$ $\sigma_c = I_{s(50)} * k_1 * e^{-k_2n}$	Gözenekli alçı taşında UCS/Is oranı ile çekme ve basma dayanımı üzerine porozitenin etkisini incelemiştir	8-18	Porozite %18'den %40'a çıktığında UCS/Is oranı 18'den 8'e düşmektedir. UCS/Is oranının sabit olmadığını, poroziteye bağlı olarak 8-18 arasında değiştiğini bulmuşlardır. Burada ;"k ₁ ve k ₂ "; amprik katsayılar "n" ise ;örneğin porozitesidir.
Kim et al. (2004)	$\sigma_c = 22 * I_{s(50)} + 49$	Tüfler (80,4-208 MPa)		
Kahraman et al. (2005)	$\sigma_c = 24,83 * I_{s(50)} - 39,64$ $\sigma_c = 10,22 * I_{s(50)} - 24,31$	38 farklı voklanik, sedimanter, metamorfik kayaçta nokta yük, dayanım ve porozite testleri yapıldı		Porozitesine göre kayaçlar Porozite <%1 ve Porozite > %1 şeklinde ikiye sınıflandırıldığında daha sağlam korelasyonlar elde edilmiştir. Porozitesi %1< olan kayaçların regresyon eğrisinin eğimi, yüksek poroziteli kayaçlara göre daha büyüktür.
Fener et al. (2005)	$\sigma_c = 9,08 * I_{s(50)} - 39,32$	Niğde kayaçları ; volkanik, metamorfik ve sedimanter 11 kayaç		
Santi (2006)	$\sigma_c = 12,25 * I_s^{1,59}$	Lineer olmayan bir ilişki buldu.		Smith (1997) verilerini tekrar değerlendirdi
Kassim ve Mohammad (2007)	$\sigma_c = 12,23 * I_{s(50)} + 1,75$ $\sigma_c = 14,45 * I_{s(50)} + 0,096$	Zayıf altere kumtaşlarını inceledi	Kahraman'ın düzeltimi $\sigma_c = 8,66 * e^{0,437n}$	Is<1 MPa olan tamamen ve yüksek altere malzeme ile IS>1MPa olan zayıf ila orta altere malzeme için; bu ilişki, Kahraman'ca yeniden incelendi. Non lineer ilişki bulundu
Akram and Abu Bakar (2007)	$\sigma_c = 22,7921 * I_{s(50)} + 13,285$ $\sigma_c = 11,076 * I_{s(50)}$ yumuşak	Pakistan Punjab provensine ait Tuz sınırı alanına ait 9 farklı kayaç		Kayaçlar; sert ve yumuşak olarak iki gruba ayrılarak test edilmiştir. Yumuşaklar; Dandot kumtaşı, Sakkessa kumtaşı,marndır.
ASTM (2008)	$\sigma_c = 24 * I_{s(50)}$	Tüm kaya tipleri		
Binal (2009)	$\sigma_c = 9 * I_{s(50)}$	İgnimbirit	9	Orta derecede kaynaklanmış ve kaynaklanmamış
Diamantis et al. (2009)	$\sigma_c = 19,79 * I_{s(50)}$ $\sigma_c = 17,81 * I_s^{1,06}$ $\sigma_c = 16,45 * e^{0,399I_{s(50)}}$	Kumtaşı, çamurtaşı ve şeyl (23.1-173.9 MPa).		Orta Yunanistandaki serpantiniterin fiziko mekanik özellikleri incelendi. Lineer ve lineer olmayan ilişkiler buldu. Üstel ilişkilerin dahi iyi korelasyonlar verdiği tespit edildi.
Kohno ve Meda (2011-2012)	$\sigma_c = 16,4 * I_{s(50)}$	Hidrotermal olarak altere olmuş çoğunluğu tif ve UCS<25 MPa olan kayaçları inceledi.	Kahraman'ın düzeltimi $\sigma_c = 15,81 * I_s^{0,95}$	Test sonuçlarının kuru ve yaş olarak önce ayrı ayrı, sonrasında tüm verinin birlikte değerlendirilmesi neticesinde lineer ilişki bulundu. Bu bağıntı; Kahramanca yeniden incelendi ve lineer olmayan bir ilişki elde edildi.
Kurtuluş ve diğer(2011)	$\sigma_c = 15,248 * I_{s(50)} - 2,2964$ $\sigma_c = 14,458 * I_{s(50)} + 0,3852$	Serpantinli ultrabazik kayaç örnekleri		Silindirik 20 örnek tabakaya dik ve 20 örnek tabakaya paralel olarak test edildi.
Singh et al. (2012)	$\sigma_c = 22,8 * I_{s(50)}$ $\sigma_c = 21,9 * I_{s(50)}$ $\sigma_c = 14,4 * I_{s(50)}$ $\sigma_c = 14,4 * I_{s(50)}$	Kuarsit (32,5-98,9 MPa) Kumtaşı (17,6-56,4 MPa) Şeyl (9,9-18,8 MPa) Gabro (17,3-137 MPa) Kireçtaşı (86,9-129,8 MPa)	(14-24)	7 farklı stratigrafik birimden alınan 10 farklı kayaç tipi (volkanik, sedimanter, metamorfik) kullanıldı. "k" değerinin ; sert kayaçlar için (21-24) ve Yumuşak kayaçlar için (14-16) olarak alınması önerildi.
M. Heidari (2012)	$\sigma_c = 7,56 * I_{s(50)} - 23,68$ $\sigma_c = 11,96 * I_{s(50)} + 10,64$	150 adet jips örneği test edildi Jips (31,00 -33,69MPa kuru) Jips(17,44 - 29,84 MPa su doygun)		
Mısra and Basu (2013)	$\sigma_c = 10,9 * I_{s(50)} + 49,03$ $\sigma_c = 11,21 * I_{s(50)} + 40,01$ $\sigma_c = 12,95 * I_{s(50)} - 5,19$ $\sigma_c = 14,63 * I_{s(50)}$	Granit, şist, kumtaşı,		Lineer ilişki bulundu.
Li and Wong (2013)	$\sigma_c = (20 - 21) * I_{s(50)}$	Singapur meta kumtaşı ve meta siltaşı		
Kahraman (2014)	$\sigma_c = 2,68 * e^{0,93I_{s(50)}}$ kuru $\sigma_c = 1,99 * e^{1,18I_{s(50)}}$ suya doygun $\sigma_c = 2,27 * e^{1,04I_{s(50)}}$ tüm veri	Kapodokya volkanik provensi içinde bulunan Yeşilhisar, Ürgüp formasyonu ve quaterner yataklardan alınan, dayanım sınırları 2.2-46.7 MPa arasında olan 32 farklı yumuşak pyroclastic kayaç incelenmiştir.		Testler; 38mm çaplı beyob çap oranı 1.2 olan örnekler üzerinde hem kuru (firında kurutulmuş) hemde suya doygun olarak yapılmıştır
Salah et al. (2014)	$\sigma_c = 9,459 * I_s^{0,75}$ $\sigma_c = 5,833^{0,57 * I_{s(50)}}$ $\sigma_c = 5,414 * e^{0,57 * I_{s(50)}}$ $\sigma_c = (11,08...11,24) * I_{s(50)}$ $\sigma_c = 6,05^{I_{s(50)}}$ $\sigma_c = 5,679^{I_{s(50)}}$	Tüm kaya tipleri Tüm kaya tipleri Çok zayıf kayaç Zayıf kayaç Tüm kristalin jipsler Tüm çamurtaşları Çok zayıf kumtaşı		

σ_c : Tek eksenli basınç dayanımı (MPa), k: Nokta yük dayanım indeksi ve basınç dayanımı arasındaki oran (Topal, 2000; Quane et al., 2003; Elhakim, 2015; Liang et al., 2015; Kahraman et al., 2009; Kahraman, 2014; Binal, 2009; Sheraz et al., 2014)

Bu durum; uygun bir eşitlik kullanılmaması halinde tek eksenli basınç dayanımının; sert kayaçlar için %50, zayıf kayaçlar için %250, tüm kayaçlar genellendiğinde ise %400 nispetinde hatalı tahmin edileceği anlamına gelmektedir. Bir de değerlendirmelere anizotropi, alterasyon, porozite ve su muhtevası gibi kayacın doğal konumuna ait özellikler de eklendiğinde, hata oranının; %2500'e kadar artabileceği görülebilmektedir.

Porozitenin; kayaçların çekme-basma dayanımı ve “ $UCS/Is = k$ ” oranı üzerine etkisinin incelendiği bir çalışmada “ UCS/Is ” değerinin sabit olmadığı, gözenekli alçı için porozite’nin %18’den, %40’a çıkması halinde, “ k ” oranının; 18’ den 8’e düştüğü bulunmuştur (Kahraman et al., 2009; Palchik et al., 2004). Yine suya doygun ve kuru olarak, hem sedimanter hem de vokanik kayaçlarda yapılan bir başka çalışmada ise suya doygun kayaçlar için bu oranın kuru kayaçlardakilerden, genellikle %50 daha düşük olduğu belirlenmiştir (Liang et al., 2015; Kahraman, 2014; Hawkins, 1998).

Görüldüğü üzere, nokta yük dayanım deneyinde; uygulamaların aynı standartta yapılamamasından gelen hata kaynakları söz konusudur. Bunlar; testler sırasında, 50 mm’den farklı çaptaki karot örnekler veya düzensiz şekilli örneklerin kullanılmasından, deneylerin; çapsal ya da eksensel yönde yük uygulanarak, kuru veya suya doyurulmuş, sert ya da yumuşak örnekler üzerinde, anizotropi dikkate alınıp ya da alınmadan yapılmasından ve nihai test sonuçlarının; d_{50} eş değer karot çapı düzeltmeli veya düzeltmesiz olarak sunulmasından kaynaklanabilmektedir. Konu ile ilgili formülasyonların oluşturulması sırasında bu ve buna benzer birçok parametre etken olduğu için, literatürden derlenen deneysel çalışmalara göre genellemeye gidilerek, kayaçların tümü için geçerli olabilecek standart tek bir “ k ” değerinin tanımlanması ve de kullanılması uygun görülmemektedir.

Bu nedenlerden dolayı; nokta yük indeksinin, bağımsız bir dayanım indeksi olarak kullanılması, kayaçların; basınç dayanımının belirlenmesi için kullanılmaması ya da çok zaruri durumlarda dikkatle ele alınıp değerlendirilmesi (Greminger, 1982), özellikle konik ucun yumuşak kayaca batıp, çapsal hataya yol açmasından ötürü $NYD_i < 5$ (Quane et al., 2003) ve tek eksenli basınç dayanımının < 25 MPa olduğu zayıf kayaçlarda hiç kullanılmaması (Bieniawski, 1975); önerilmektedir. Oysa gerek tüfler ve gerekse anhidrit, alçı taşı ve kalkerli kumtaşı gibi formasyonlardan alınan örnekler üzerinde yapılan sonraki çalışmalardan elde edilen tutarlı sonuçlar, nokta yükleme deneyinin zayıf kayaçlar için de kullanılabilir olduğunu göstermektedir (Elhakim, 2015; Kahraman, 2014).

Tüflerin incelendiği ve “ k ” değerinin 20’nin altında bulunduğu bir çalışmada; elde edilen 13-14 değeri, literatürde zayıf kayaçlar için bulunan k -değeri (10-20) ile uyumluluk arz etmektedir (Topal, 2000; Singh et al., 2012). Bu bakımdan NYD_i ile zayıf kayaçların basınç dayanımlarının dolaylı olarak hesaplanması sırasında oluşan hata, aslında “ k ” değerinin; tüm kayaçlar için, 24 olarak sabit alınmasından kaynaklanmaktadır (Topal, 2000; ISRM, 1985). Bu değer; anhidrit gibi son derece düşük dayanımlı kayaca böyle sabit bir lineer eşitlik ile uygulanması ise; gerçek “ k ” değeri 2-6 arasında olan bir kayacın basınç dayanımının gerçek değerinden %800 daha fazla tahmin edilmesi anlamına gelmektedir. Böylesi büyük hataların da mühendislik açıdan kabul edilebilirliği bulunmamaktadır (Elhakim, 2015).

Farklı kayaç tipleri ya da özel lokasyonlar için yapılan nokta yük testlerinin korelasyonu ile geliştirilmiş olan formülasyonlarda dikkat çeken diğer bir nokta ise, ifade edilen bağıntıların daima lineer özellik göstermemesidir. Kimi bağıntılarda katsayılı lineer (Kim et al., 2004; Quane et al., 2003), kimilerinde üstel (Tsiambaos et al., 2004) ve kimilerinde de exponensiyel fonksiyonlar, dönüşüm eşitlikleri olarak, kullanılmaktadır (Salah et al., 2014) (Çizelge 1). Bir genelleme yapıldığı takdirde, bu eşitliklerin; $NYD_i > 4$ olan sert kayaçlarda lineer, $NYD_i < 5$ olan zayıf kayaçlarda ise lineer olmayan karakterde olduğu görülmektedir (Quane et al., 2003; Kahraman, 2014).

Tüm bu değerlendirmeler ışığında; çalışmamızda incelenen örnekler, Nevşehir provensi volkanik istifi içersinde yer alan Hasandağ Volkaniklerini temsil edecek şekilde alınmıştır. Böylece hem yerel yaygın bir formasyonun mekanik özelliklerinin tanımlanması, hem de düşük–orta dayanımlı ignimbirit ve tuf özelliğindeki volkanik kayaçlara dair dayanım parametrelerinin belirlenmesine çalışılmıştır.

Burada boy çap oranı 1 ve 2.5 olan NX (54mm) çaplı karot örnekler kullanılarak, kuru ve suya doygun şartlarda, yönlenmelerde (tabakaya dik (\perp) ve paralel (\parallel)) dikkate alınarak belirlenmiş olan tek eksenli basınç dayanım değerleri ile yine hem kuru hem de suya doygun şartlarda yapılan nokta yük

dayanım testlerinden, d_{50} eş değer karot çapı düzeltmesi de yapılarak bulunan sonuçların karşılaştırılması yapılmıştır.

Bu çalışmada nokta yük indeks değerinden yararlanılarak tek eksenli basınç dayanımı; eşitlik 8'den hesaplanmıştır. Bulunan sonuçlar, örneklerin tabakalanma ve suya doygunluk durumlarına göre nokta yük dayanım indeksi Çizelge 2'de gösterilmiştir.

Çizelge 2. Örneklerin nokta yük indeksi değerlerinden hesaplanan basınç dayanım parametreleri.

Kayaç Adı	Türü	Yükleme Yönü	Ortalama Is	Anizotropi Derecesi	Basınç Dayanımı (Mpa)
Kızılkaya Üst	Kuru	⊥	1.17 ± 0.20	1.16	25.67 ± 4.33
		//	1.00 ± 0.09		22.10 ± 2.09
	Yaş	⊥	0.96 ± 0.01	-	21.15 ± 0.29
Kızılkaya Orta	Kuru	⊥	1.50 ± 0.21	1.06	33.08 ± 4.72
		//	1.41 ± 0.16		31.13 ± 3.49
	Yaş	⊥	0.96 ± 0.06	-	21.11 ± 1.29
Kızılkaya Alt	Kuru	⊥	1.36 ± 0.07	1.08	29.93 ± 1.52
		//	1.26 ± 0.20		27.67 ± 4.37
	Yaş	⊥	1.09 ± 0.03	1.31	23.95 ± 0.74
		//	0.83 ± 0.17		18.23 ± 3.63
Gelveri	Kuru	⊥	1.62 ± 0.23	1.25	35.70 ± 4.96
		//	1.30 ± 0.03		28.52 ± 0.69
	Yaş	⊥	1.20 ± 0.06	1.36	26.39 ± 1.43
//	0.88 ± 0.02	19.46 ± 0.48			
Selime Alt	Kuru	⊥	0.15 ± 0.05	3.41 ± 1.15
Selime Üst	Kuru	⊥	0.20 ± 0.09	4.38 ± 1.91
Göstüğ	Kuru	⊥	2.09 ± 0.03	2.94	46.05 ± 0.58
		//	0.71 ± 0.07		15.67 ± 1.46
	Yaş	⊥	1.93 ± 0.12	3.14	42.50 ± 2.65
//	0.62 ± 0.09	13.54 ± 2.00			

Kayaçların nokta yük dayanım indeksine göre sınıflandırılması ise Çizelge 3'te verilmiştir.

Çizelge 3. Kayaçların nokta yük dayanım indekslerine göre sınıflandırılması

Tanımlama	UCS(MPa) Bianewski (1974)	NYDI(MPa)
Çok düşük dayanım	<25	<1
Düşük dayanım	25-50	1-2
Orta dayanım	50-100	2-4
Yüksek dayanım	100-200	4-8
Çok yüksek dayanım	>200	>8

TEK EKSENLİ BASINÇ DAYANIMI DENEYLERİ

Maden makineleri ve kaya delme makinelerinin performanslarının tahmininde kayaçların dayanım özelliklerinin bilinmesi önemlidir. En genel olarak kullanılan ve dayanım ölçümünü tayin eden yöntem tek eksenli basınç dayanımıdır (Özdemir et al., 1992; Gehring, 1993; Thuro et al., 2011). Bu çalışmada dayanım deneyleri; 20 kN ve 300 kN basınç gövdeli, servo valf sistemi olan, hidrolik güç ünitesine sahip, bilgisayarlı veri toplama ve değerlendirme özellikli bir test makinesi ile yapılmıştır.

Tek eksenli basınç dayanım deneyleri için NX karot çaplı (54 mm), boy/çap oranı 1 ve 2.5 olan örnekler kullanılmıştır (Şekil 6).



Şekil 6. Tek eksenli basınç dayanımı için kullanılan örnekler.

Örnekler, test sırasında küresel merkezlendirici plakaya sahip test makinesine 55 mm çap, 60 mm yükseklik ve 1158 g ağırlığında küresel başlık kullanılarak yerleştirilmiştir. Bu örnekler, kayaç tipine göre önceden tespit edilen 0.10-0.15 kN/s yükleme hızlarında 5-10 dakikada yenilmeleri sağlanacak şekilde kırılmıştır. Tek eksenli basınç dayanımı (σ_c) değerleri eşitlik (9)'dan hesaplanmıştır.

$$\sigma_c = \frac{F}{A} \quad (9)$$

- σ_c : Tek eksenli basınç dayanımı (MPa)
 F : Yenilme anında kaydedilen yük (kN)
 A : Silindirik numunenin kesit alanı (mm²)

Bu çalışmada kuru ve suya doygun şartlarda, örnek boyutu ve yönlenmeler dikkate alınarak yapılan tek eksenli basınç dayanım deney sonuçları Çizelge 4'de verilmiştir.

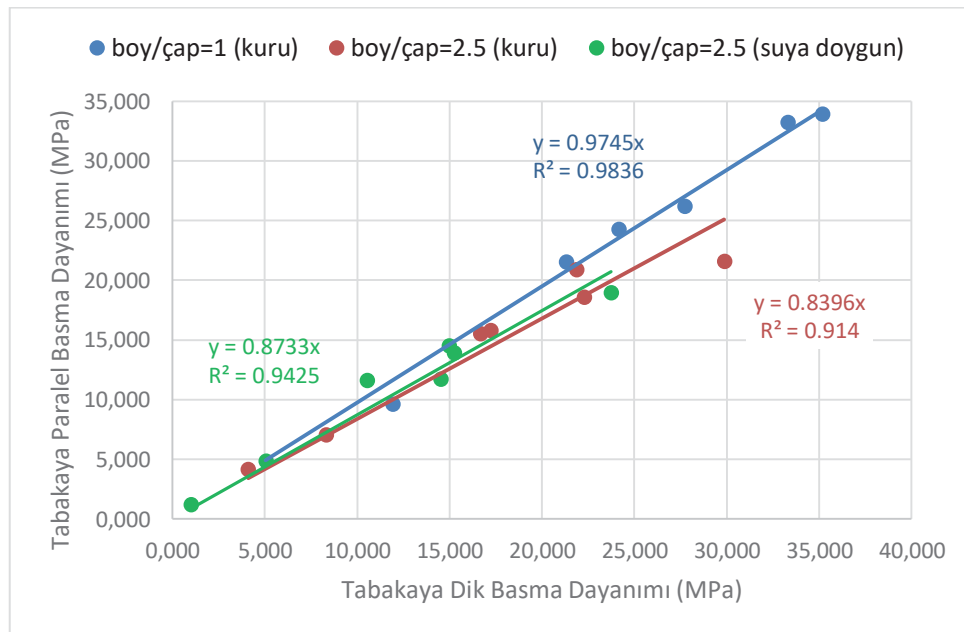
Literatürde kayaçlar genellikle boy çap oranı en az 2 olan örneklerden elde edilen tek eksenli basınç dayanım değerlerine göre beş gruba ayrılarak, Çizelge 5'te olduğu gibi sınıflandırılmaktadır (Karaman et al., 2012; ISRM, 1981; Bieniawski, 1974; Kan, 2000; Deere et al., 1966).

Çizelge 4. Tek eksenli basınç dayanım deney sonuçları

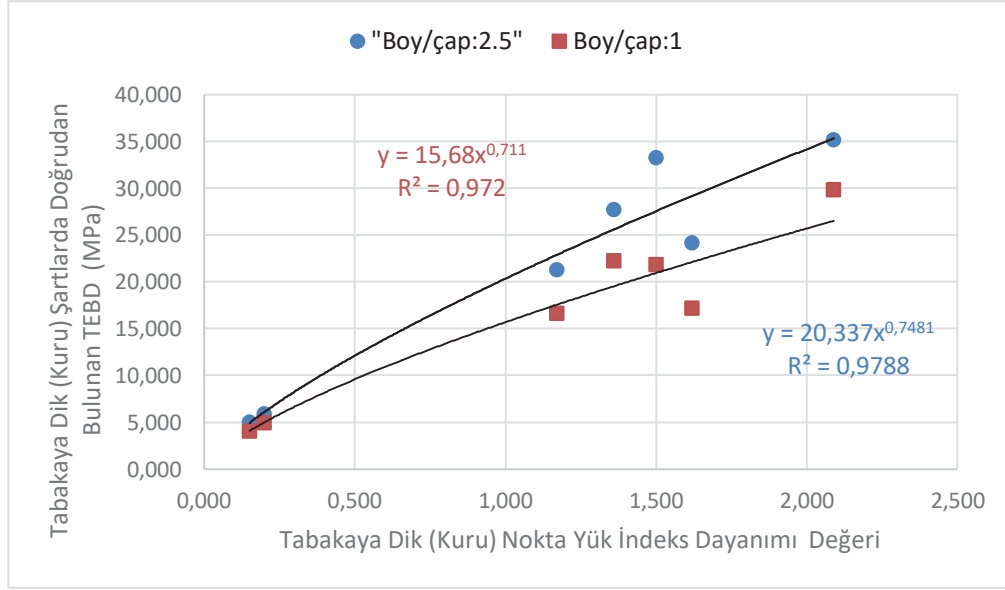
Kayaç Adı	Basma Dayanımı (Mpa) boy/çap=1		Basma Dayanımı (MPa) boy/çap=2.5			
	Kuru		Kuru		Suya doymun	
	Tabakaya dik	Tabakaya paralel	Tabakaya dik	Tabakaya paralel	Tabakaya dik	Tabakaya paralel
Kızılkaya üst	21.303	21.511	16.652	15.542	10.542	11.579
Kızılkaya orta	33.288	33.229	21.863	20.887	15.234	13.886
Kızılkaya alt	27.72	26.205	22.277	18.576	14.956	14.483
Gelveri	24.168	24.247	17.214	15.782	14.525	11.692
Selime üst	5.921	----	4.996	----	2.3107	----
Selime alt	5.037	----	4.096	4.157	1.003	1.195
Karakaya	11.927	9.608	8.304	7.025	5.058	4.838
Göstüg	35.175	33.922	29.861	21.567	23.756	18.931
Acıgöl	8.465	----	5.443	----	2.436	----

Çizelge 5. Kayaçların tek eksenli basınç dayanımına göre sınıflandırılması

Tanımlama	UCS (MPa)	UCS (MPa)	UCS (MPa)	Sınıfı
	ISRM(1981)	Bieniawski (1974)	Deere ve Miller (1966)	
Çok Yüksek Dayanımlı	>200	>200	>220	A
Yüksek Dayanımlı	60-200	100-200	110-220	B
Orta Dayanımlı	20-60	50-100	55-110	C
Düşük Dayanımlı	6-20	25-50	27.5-55	D
Çok Düşük Dayanımlı	<6	<25	<27.5	E



Şekil 5. Tabakalanmaya Dik ve Paralel Basma Dayanım Değerlerinin Karşılaştırması



Şekil 6. Nokta Yük indeks değeri ile doğrudan bulunan TEBD arasındaki ilişki

Elde edilen veriler bir çok açıdan değerlendirilebilir ancak bu çalışmada tabakaya dik ve paralel basma dayanım değerleri arasındaki ilişki ve nokta yük indisinden dolayı olarak ve doğrudan bulunan basma dayanımı arasındaki ilişkiden bahsedilecektir. Şekil 5’te görüldüğü gibi 1 ve 2.5 boy/çap oranına sahip kuru örneklerin tabakaya dik ve paralel basma dayanımı sonuçları arasında yüksek tahmin kapasitesine sahip sırasıyla %98,36 ve %91,40 ilişki katsayısı bulunmaktadır. Artık (intersept) sayılar çıkarıldığında 1 ve 2.5 boy/çap oranına sahip kuru örneklerin tabakaya dik basma dayanımının tabakaya paralel basma dayanımının sırasıyla yaklaşık %97,45’i ve %83,96’sı kadar olduğu görülmektedir. Aynı işlem 2.5 boy/çap oranına sahip suya doymuş örnekler için de yapılmış ve aralarında yine yüksek tahmin kapasitesine sahip ($r^2= 0.9425$) ve tabakaya dik basma dayanımı değerlerinin %87,33’ü kadar tabakaya paralel basma dayanımı değerleri ile karşılaştırıldığı anlaşılmıştır.

Şekil 6 ise tabakaya dik nokta yük indeks değerleri ile doğrudan bulunan basma dayanımları arasında da yüksek tahmin yeteneğine sahip bir ilişki olduğunu göstermekte ve nokta yük değerlerinden, Şekil 6’da önerilen eşitlikle bulunacak basma dayanımı değerlerinin; tasarımda kullanılabileceğine işaret etmektedir.

SONUÇLAR

Çalışmada Nevşehir provensiyonlu volkanik istifi içerisinde yer alan Hasandağ Volkaniklerini kapsayan bazı kayaç örnekleri üzerinde yapılan bir seri tek eksenli basınç dayanımı (TEBD) ve nokta yükleme dayanım test (NYD) sonuçları irdelenmiştir.

1. Boy/çap oranı 1 ve 2,5 olan kuru ve suya doymuş (yaş) örnekler üzerinde tabakalanmaya paralel ve dik olarak alınan örnekler üzerinde ayrı ayrı tek eksenli basma dayanımı deneyleri uygulanmıştır.
2. Çok düşük ve orta dayanımlı kaya grubuna giren bu istiften, tabakalanmaya paralel ve dik alınan örneklerin sıkıştırılmasıyla elde edilen sonuçlar arasında yüksek dereceli tahmin yeteneğine sahip ilişkiler bulunmuştur. Buna göre tabakaya dik suya doymuş 2,5 boy/çap oranına sahip örneklerden tabakaya paralel basma dayanımı %94,23 doğruluk katsayısı (r^2) ile ; tabakaya dik kuru 2,5 boy/çap oranına sahip örneklerden tabakaya paralel basma dayanımı %91,40 doğruluk katsayısı (r^2) ile ; tabakaya dik kuru 1 boy/çap oranına sahip örneklerden tabakaya paralel basma dayanımı %98,36 doğruluk katsayısı (r^2) ile

hesaplanabilmiştir.

3. Suya doymun örneklerin basınç dayanımının kuru örneklerle kıyasla daha düşük olduğu ve boy/çap oranındaki artışla dayanım değerlerinin daha da düştüğü gözlemlenmiştir.
4. Ayrıca tabakaya dik nokta yük indeksi değerlerinden boy/çap oranı 1 ve 2.5 olan örnekler üzerinde tabakaya dik olarak yapılan tek eksenli basma dayanımı sonuçlarının da yüksek doğrulukta tahmin edilebileceği ortaya çıkmıştır. Bu eşitliklerin; $NYD_i > 4$ olan sert kayalarda lineer, $NYD_i < 5$ olan zayıf kayalarda ise lineer olmayan karakterde olduğu yönündeki görüşü doğrulayıcı nitelikte ve lineer olmayan karakterde olduğu belirlenmiştir.
5. Hasandağ volkanik istifinde yer alan Göstüğ İgnimbiriti üzerinde yapılan deneylerde tabakaya paralel dayanım değerinin tabakaya dik dayanım değerinden belirgin olarak düşük olduğu tespit edilirken, bu durum nokta yük dayanım indeksi değerinden bulunan anizotropi değeri ile de teyit edilmiştir (Göstüğ kuru indeks anizotropisi (I_a):2,94; Göstüğ yaş indeks anizotropisi (I_a): 3.14).
6. Tüm bu değerlerden çok değişkenli ilişki analizleri de yapılabilecek olup bu çalışma sınırları içerisinde değinilmemiştir.

TEŞEKKÜR

Bu çalışma MTA Genel Müdürlüğüne yürütülmüş bulunan, “Tehlikeli Atıkların Depolanması İçin Yer Seçimi Araştırmaları” Projesi kapsamında İnceleme sahasından, Bölgedeki Jeolojik istifi temsil edecek şekilde çıkartılan 100*100*50 cm ebatlı kayaç bloklarından alınan örnekler üzerinde, İTÜ Maden Fakültesi ve MTA Genel Müdürlüğü MAT Dairesi Başkanlığı laboratuvar imkanları kullanılarak yapılmıştır. Yazarlar; burada, MTA Genel Müdürlüğü’ne ve bu proje çalışanlarına teşekkürü bir borç bilmektedir.

KAYNAKLAR

- Al-Jassar, S.H., and A.B. Hawkins. (1979). Geotechnical properties of the carboniferous limestone of the bristol area. The Influence of Petrography and Chemistry 4th ISRM Congress, Montreux, Switzerland, September.
- Aston, T.R.C., MacIntyre, J.S., and Kazi, H.A. (1991). The effect of worn and chipped points on point load indices. *Mining Science and Technology*, vol. 13. pp. 69-74.
- Bieniawski, Z.T. (1974). Estimating the strength of rock materials. *Journal of the South African Institute of Mining and Metallurgy*, vol. 74, March. pp. 312-320.
- Bieniawski, Z.T. (1975). The point-load test in geotechnical practice. *Engineering Geology*, vol. 9, no.1. pp. 1-11.
- Binal, A. (2009). Prediction of mechanical properties of non-welded and moderately welded ignimbrite using physical properties, ultrasonic pulse velocity, and point load index tests. *Quarterly Journal of Engineering Geology and Hydrogeology*. 42, 107-122.
- Broch, E. and Franklin, J.A. (1972) The point-load strength test. *International Journal of Rock Mechanics and Mining Sciences*, 9, 669-697.
- Brook, N. (1985). The equivalent core diameter method of size and shape correction in point load testing. *International Journal of Rock Mechanics & Mining Sciences and Geomechanical Abstract*. 22, 61-70.
- Brook, N. (1977). The use of irregular specimens for rock strength test. *International Journal of Rock Mechanics & Mining Sciences and Geomechanical Abstract*, 14, 193-202.
- Chau, K.T. and Wong, R.H.C. (1996). Uniaxial compressive strength and point load strength of rocks. *International Journal of Rock Mechanics & Mining Sciences and Geomechanical Abstract*. 33, V2, 183-188.
- Deere D. and Miller R. (1966). Engineering classification and index properties for intact rock. Tech. Report No AFWL - TR-65-116, Air Force Weapons Lab., Kirtland Air Base, New Mexico.
- Elhakim, A.F. (2015). The use of point load test for Dubai weak calcareous sandstones. *Journal of Rock Mechanics and Geotechnical Engineering*. 7 (4): 452–457.

- Gehring, K.H. (1993) Evaluation of cutting performance of roadheaders. 12-14, BTV/Ge/ga/1408 Zeltveg, Austria.
- Greminger, M. (1982). Technical note experimental studies of the influence of rock anisotropy on size and shape effects in point-load testing. *International Journal of Rock Mechanics, Mining Sciences & Geomechanical Abstract*. 19, 241-246.
- Hawkins, A.B. (1998). Aspects of rock strength. *Bull. Eng. Geol. Environ.* 57, 17-30.
- ISRM, (1985). Suggested method for determining point load strength. *International Journal of Rock Mechanics Mining Sciences & Geomechanical Abstract*. 22, 51-60.
- ISRM, (1981). Basic technical description of rock masses. *International Journal of Rock Mechanics & Mining Sciences & Geomechanical Abstract*. 18, 85-110.
- Kahraman, S. and Günaydın, O. (2009). The effect of rock classes on the relation between uniaxial compressive strength and point load index. *Bull Eng Geol Environ*. 68, 345-353.
- Kahraman, S. (2014). The determination of uniaxial compressive strength from point load strength for pyroclastic rocks. *Engineering Geology*. 170, 33-42.
- Kan, C.C. (2000) Index properties and a three-dimensional failure criterion of rocks. Hong Kong, The Degree of Master of Philosophy at The University of Hong Kong.
- Karaman, K. ve Kesimal, A. (2012). Kayaçların tek eksenli basınç dayanımı tahmininde nokta yükü deney yöntemleri ve porozitenin değerlendirilmesi. *Madencilik*. 51, V4, 3-14.
- Kim, H.G., Koh, Y.K. ve Oh, K.H. (2004). A study on the mechanical properties of the cretaceous tuffs in Goheung area, *The Journal of Engineering Geology*. 14, V3. 273-285.
- Liang, W. (2015). Evaluation of uniaxial compressive strength by point load tests for irregular specimens of different rock types. *Engineering Journal of Geotechnical Engineering*. 20, 11265-11271.
- Özdemir, L., Gertsch, L, Neil, D, and Friant, J. (1992). Performance predictions for mechanical excavators in Yucca Mountain tuffs; Yucca Mountain Site Characterization Project. United States.
- Palchik, V. ve Hatzor, Y.H. (2004). The influence of porosity on tensile and compressive strength of porous chalk, *Rock Mech & Rock Eng*. 37, V4, 331-341.
- Puech, A., Beunce, J.P. ve Colliat, J.L. (1988). Advances in the design of piles driven into non-cemented to weakly cemented carbonate formations. Proceedings Of The International Conference On Calcareous Sediments, Perth, Australia.
- Quane, S.L. ve Russell, J.K. (2003). Rock strength as a metric of welding intensity in pyroclastic deposits. *Eur. J. Mineral*. 15, 855-864.
- Salah, H., Omar, M. ve Shanableh, A. (2014) Estimating unconfined compressive strength of sedimentary rocks in United Arab Emirates from point load strength index. *Journal of Applied Mathematics and Physics*, 2, 296-303.
- Sheraz, A. M., Emad, M. Z., Shahzad, M., and Arshad, S. M. (2014). Relation between uniaxial compressive strength, point load index and sonicwave velocity for dolerite. *Pakistan Journal of Science*. 66, V1.
- Singh, T.N., Kainthola, A. and Venkatesh, A. (2012). Correlation between point load index and uniaxial compressive strength for different rock types. *Rock Mech Rock Eng*. 45, 259-264.
- Thuro, K., Plinninger R. J., Zah, S., and Schütz, S. (2011). Scale effects in rock strength properties, Part 1: Unconfined compressive test and brazilian test, ISRM Regional Symposium EUROCK 2001 Rock Mechanics a Challenge for Society, June 3-7, 2001, Espoo, Finland, pp. 169 - 174. -.
- Topal, T. (2000). Nokta yükleme deneyi ile ilgili uygulamada karşılaşılan problemler. *Jeoloji Mühendisliği*. 24, Cilt I., 2.
- Tsiambaos, G. ve Sabatakakis, N. (2004) Considerations on strength of intact sedimentary rocks. *Engineering Geology*. 72, V3-4, 261-273.
- Tsidzi, K.E.N. (1991). Point load; uniaxial compressive strength correlation. Seventh international Congress on Rock Mechanics. Proceedings of the Congress of the International Society for Rock Mechanics, 1, 637-638.

HIG MILL PERFORMANCE AT COPPER FLOTATION CIRCUIT REGRIND APPLICATION
BAKIR FLOTASYON DEVRESİ REGRIND UYGULAMASINDA HIG DEĞİRMEN PERFORMANSI

O. Altun¹, Ö. Darılmaz^{2,*}, A. Hür³, C.E. Karahan², Z. Göller³, T. Sert¹, D. Altun¹, N.A. Toprak¹

¹Hacettepe University, Mining Engineering Department

²Acacia Maden İşletmeleri A.Ş.

(*Corresponding author: ozgun.darilmaz@acacia.com.tr)

³Flotech Tesis Yönetimi Eğitim Danışmanlık

ABSTRACT

HIG mill technology is one of the recent developments in the fine grinding area. It has a vertical orientation and is used for wet fine grinding application. This study argues HIG mill operation at copper regrind circuit. Initially, a survey was performed around the mill as well as the concentration circuit to evaluate the accuracy of the sensors and to provide a general knowledge. Then, series of tests were performed to investigate the effects of the operational conditions on the milling performance. In this context, solid content and rotor speed parameters were changed.

Keywords: Stirred mill, vertical stirred mill, regrind mill, fine grinding, comminution.

INTRODUCTION

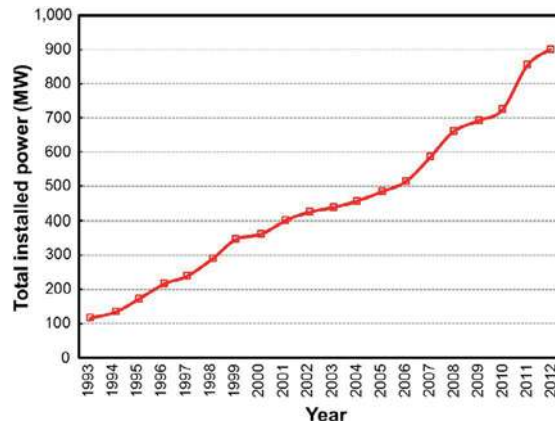


Figure 1. Installed power of fine grinding technologies till 2012 (Wills and Finch, 2016).

Until now, manufacturers have produced different types of stirred mills that are summarized by Giblett (2019). HIG mill is one of the recent developments operating in the size range between p_{80s} of 100 μm and sub 20 μm (Metso: Outotec, 2021). As it is a new technology it lacks industrial knowledge compared

to Isamill and ball mills. This study aimed at filling this gap by providing an industrial set of data on power consumption and milling performance.

MATERIALS & METHODS

Description of HIG Mill and the Operation

HIG mill at the mine (Figure 2) has the specifications given in Table 1.

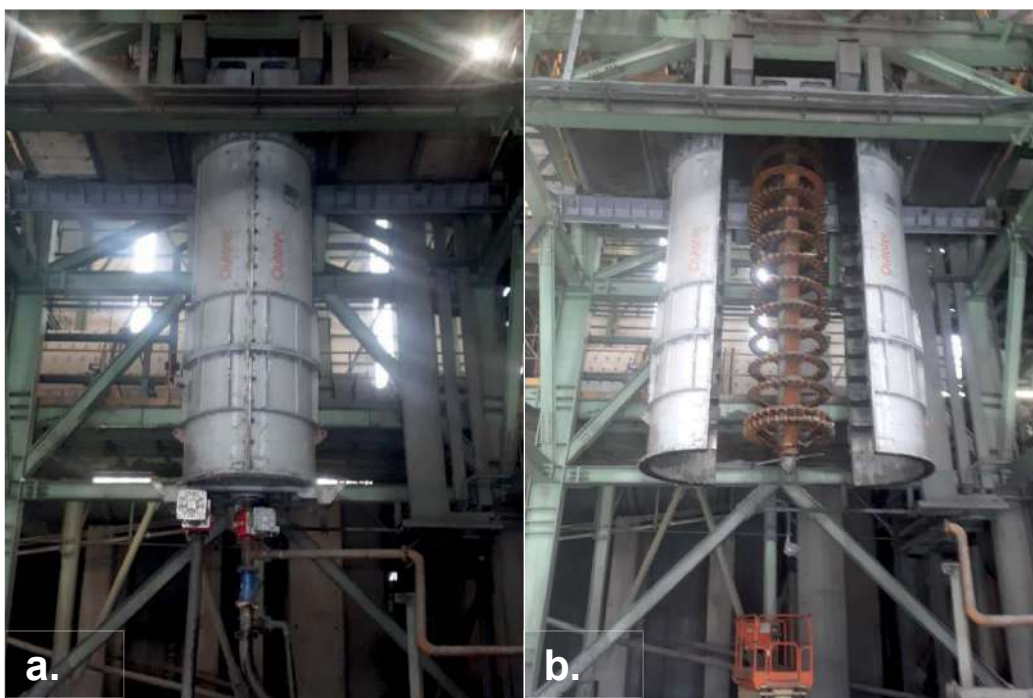


Figure 2. HIG mill at the copper mine.

Table 1. Mill specifications.

Inner height (m)	6.8
Inner diameter (m)	1.66
Dia. of agitator (m)	1.36
No. of agitator	16
Net volume (m ³)	13
Installed mill motor power (kW)	2650

Figure 2b illustrates the alignment of the agitators on shaft. The agitators are named as castellated and non-castellated as summarized by the manufacturer (HIG Mill manual, 2017). The first 11 from the bottom side are called as castellated and the rest 5 from the top is named as non-castellated.

HIG mill is utilized at regrind application. The flowsheet is depicted in Figure 3. Material to the HIG mill is pre-cycloned after the rougher circuit and the product is sent to the cleaner circuit.

Table 4. Conditions of the sampling campaigns.

	30% solid	40% solid	45% solid	50% solid
800 rpm (8.3 m/s)	✓	✓		✓
700 rpm (7.3 m/s)	✓	✓		✓
550 rpm (5.7 m/s)	✓	✓	✓	

Material Characterization

The collected samples were characterized regarding their particle size distribution and solid percentage. Particle size analyses were completed in two steps where the initial analyses included the sieves down to 38µm and below that wet centrifugal classification technique was utilized to have the distribution down 8 µm.

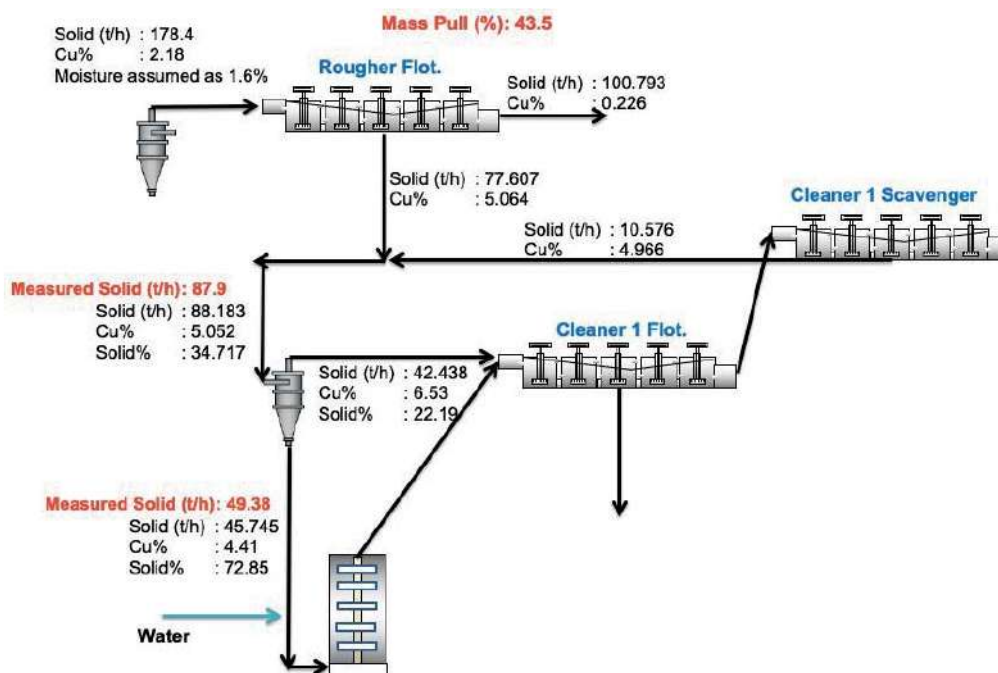
Mass Balancing

Mass balancing was completed via JK-SimMet mass balance module (Napier-Munn et al., 2016), which utilizes the algorithm of Quasi-Newton approach. Following the sample-taking and characterization studies, the data of size distributions, solid percent, and chemical assays were used to calculate the flows of streams and re-calculate the size analyses.

RESULTS AND DISCUSSIONS

Mass Balancing of the Circuit

The results of mass balancing are illustrated in Figure 4.



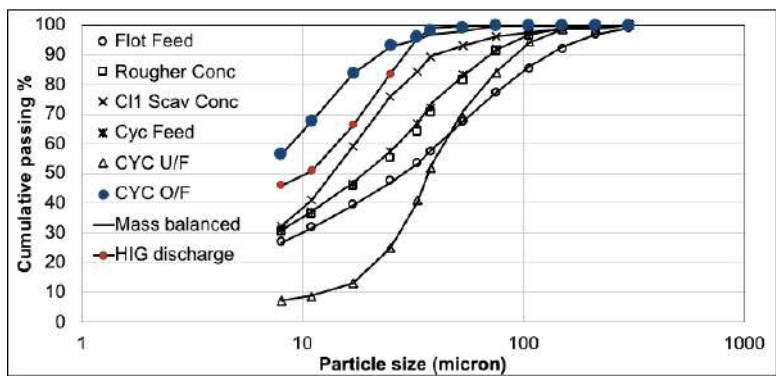


Figure 4. Mass balance of the beneficiation circuit.

Power Correlations of HIG Mill

Within the study, the power correlations were developed at different operating parameters, i.e., tip speed and solid concentration in the feed. Figure 5 illustrates the correlation between tip speed and power draw. The tip speed and power consumption parameters were found to be inter-dependent as expected.

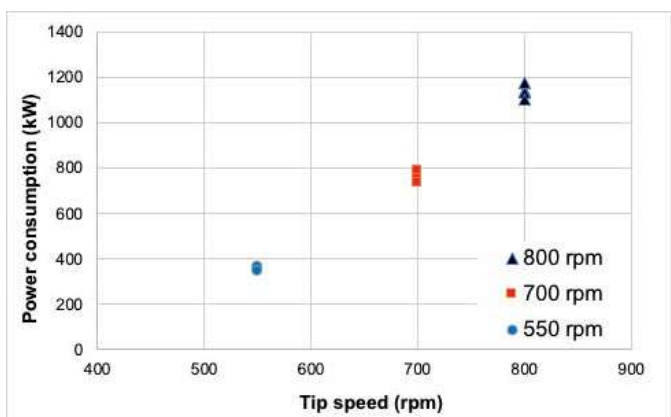


Figure 5. The variation of power draw with the tip speed.

In addition to tip speed, the solid percent also has an influence on the power consumption as it directly changes the load on the mill drive unit. For the operation with less solid content, the particles are easily transported to the discharge end of the mill. Consequently, the shaft rotates with less loading that allows higher number of collisions of beads and with the internal components. Such a phenomenon increases power consumption and vice versa. Within the literature, there exists no solid conclusion relating to the two parameters. Sepulveda (1981) showed that for some of the cases the two parameters were inversely/directly proportional to each other. It may be dependent on the mode of operation and the rheology.

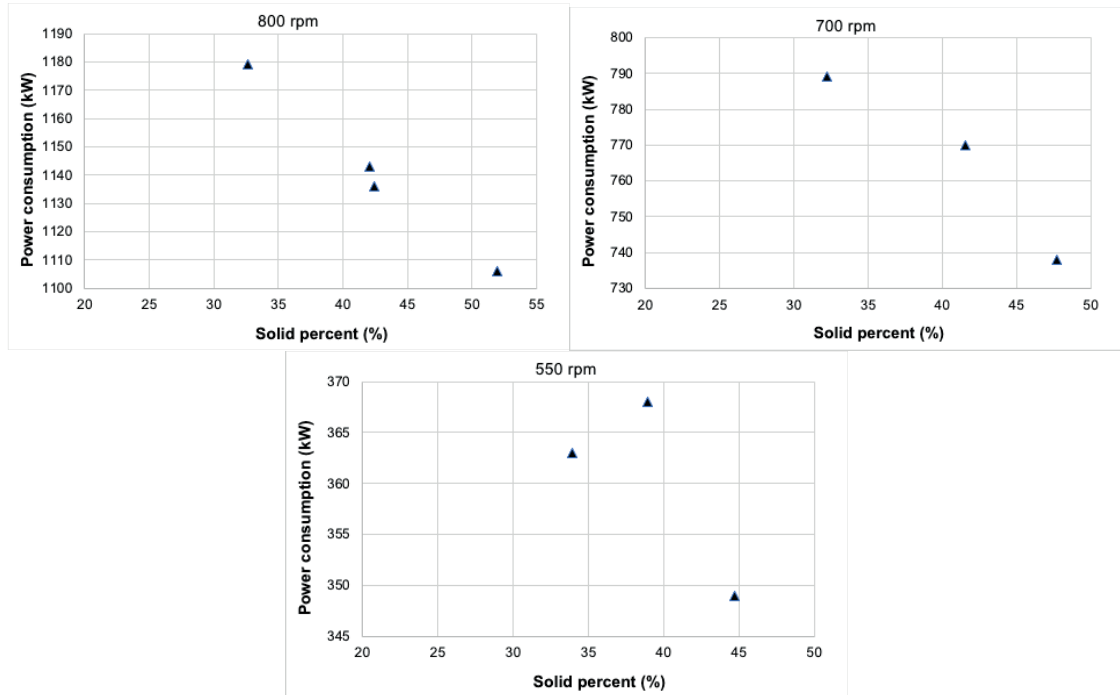


Figure 6. The variation of power draw with feed solid percent.

Comminution Performance of HIG Mill

The specific energy consumption is related to the product size. Figure 7 illustrates the variation of d_{80} and d_{50} with specific energy utilization.

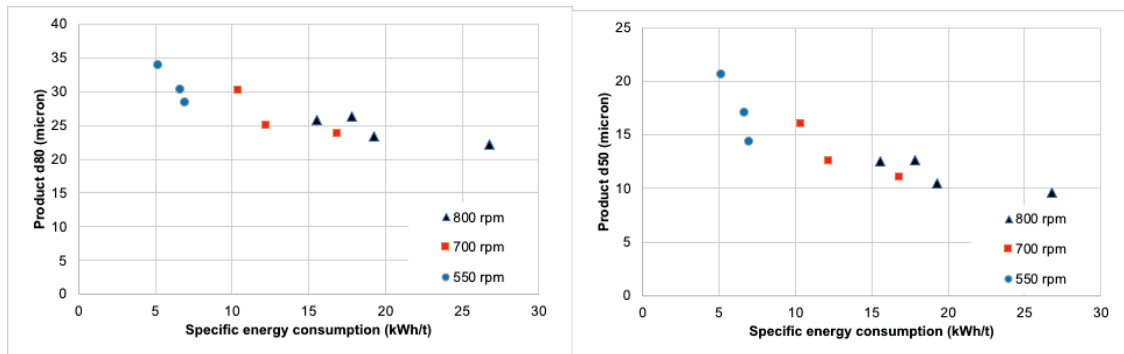


Figure 7. d_{80} s and d_{50} s with specific energy utilization.

The plots illustrated in Figure 8 are highly dependent on the variation in the feed size distributions. Therefore, it is wiser to consider the reduction ratio of the mill hence the effects of feed size are reflected accordingly.

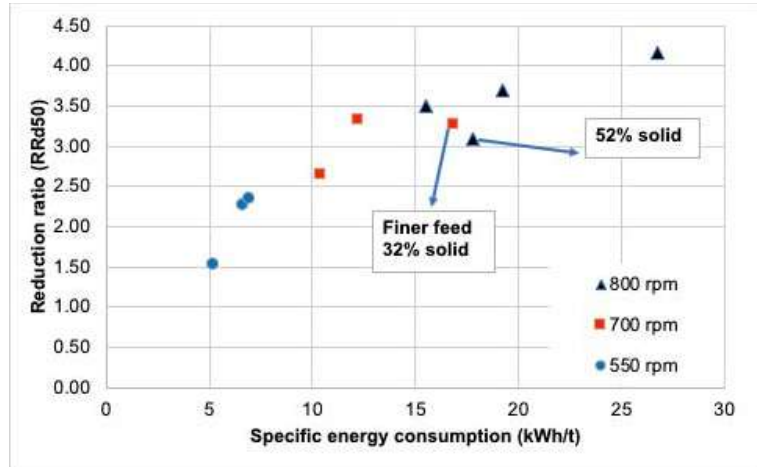


Figure 8. The correlation between reduction ratio and specific energy utilization (RR_{d50} : reduction ratio of d_{50s}).

The general trend indicates the two variables are in good agreement with each other. However, there are two points illustrated on the plot indicating some of the operating conditions tend to deteriorate the efficiency of the milling. These are;

Operation at high solid content: Rheology, a viscosity of a given pulp has effects on the dynamics of the grinding operation. Higher solid contents imply high viscosity hence the transportation of the material and power consumption of the mill change drastically. This is the case for the HIG mill as well. The solid content of 52% was found exceeding the limits of operation, and 40-45% range is reasonable.

Fine feeding with less solid content: There is a difference in the transportation characteristics of coarse and fine particles. Fines are more prone to be carried away by the up flow of slurry hence the probability of bypassing increases. The same phenomenon also applies to the less solid contents. If the two conditions overlap, then inefficiency occurs and this is the case that occurred for the HIG mill. The rest of the points are in good agreement and the energy-size reduction characteristics of the mill can be read from the plot.

CONCLUSIONS

The study aimed at providing information on HIG mill operation that is expected to be widely utilized by the minerals industry. Starting from the power correlations and then investigating the influences of the operating conditions may enable modeling of the mill that is useful for simulations studies. The study is at the preliminary stage hence the material characterization was not detailed, i.e., breakage function, work indice, etc. Completing the whole set of characterization will also be useful for an accurate simulation.

REFERENCES

- Wills, B.A., Finch, F., (2016). Wills' Mineral Processing Technology 8th Edition, Elsevier, Butterworth-Heinemann
- Giblett, A., (2019). Grinding Technologies, in: Dunne, R.C., Kawatra, K., Young, C.A. (Eds.) SME Mineral Processing & Extractive Metallurgy Handbook.
- HIG Mill manual (2017). Description of equipment 900002

- Metso: Outotech, (2021). HIG Mill – High Intensity Grinding Mill. Retrieved from <https://www.mogroup.com/portfolio/higmill-high-intensity-grinding-mill/> (accessed 30.11.2021).
- Napier-Munn, T.J., Morrell, S., Morrison, R.D., Kojovic, T. (1996). Mineral comminution circuits- Their operation and optimization, JKMRRC monograph series in mining and mineral processing, Brisbane.
- Sepulveda, J. L. (1981). A detailed study on stirred ball mill grinding. Ph. D dissertation, Department of Metallurgy and Metallurgical Engineering, The University of Utah, the USA
- Wills, B.A., Finch, F., (2016). Wills' Mineral Processing Technology 8th Edition, Elsevier, Butterworth-Heinemann

IMPACT OF REGIONAL FAULTS ON COAL AND GAS OUTBURST; A CASE STUDY IN TABAS PARVADEH COAL MINE

Saman Karimpour ¹, Jafar Khademi Hamidi ^{1,*}, Jalal Karami ², Ali Hosseini ³

¹ *Tarbiat Modares University, Mining Engineering Department*

² *Tarbiat Modares University, Remote Sensing and GIS Department*

³ *Tabas Parvadeh Coal Company (TPCCO)*

ABSTRACT

Coal and gas outburst as an extremely complex dynamic phenomenon in coal mine production process can endanger miners and damage equipment facilities. Various geological factors affect the coal and gas outburst. One of these important parameters is the impact of faults in the region. Due to the high cost of initial investment and time-consuming mine development, it is necessary to investigate the displacement of the coal seam by faults in the longwall mining method. Therefore, the purpose of this study is to investigate the effect of fault displacement in Tabas Mechanized Coal Mine No. 1 and to identify the faults that cause coal and gas outburst. To achieve this goal, Schulz classification and ArcGIS software were used. The faults were divided into three categories namely uniform, semi-uniform and non-uniform, on the basis of displacement index varying from 0 to more than 3. The data obtained from coal and gas outburst during the extraction of panel E3 and the geotechnical and geological delays related to mined out panel E2 showed that the occurrence probability of coal and gas outburst near the non-uniform faults is very high. Comparison of the final map and the results of the analyzes with the experiences obtained from the mined out areas and accident occurrence points in the mine showed that there is a very good agreement between the outburst forecast map and the number of events in the mine. The results of this study show the need for precautionary measures in the extraction of deeper panels.

Keywords: Geological information systems (GIS), outburst, fault displacement, longwall mining

INTRODUCTION

Coal plays an important role in the composition of the world's energy. With the depths of subsurface mining continuously increasing, coal mining accidents become more precarious causing thousands of fatalities in world every year. Globally, coal and gas outburst are recognized as one of the most catastrophic failures associated with the coal mining industry (Li et al., 2020). Studies have shown that most outburst incidents occur in strongly deformed zones along the axes of structures such as asymmetrical anticlines, the hinge zones of recumbent folds, and the intensely deformed zones of strike-slip, thrust, reverse, and normal faults (Cao et al., 2001; Mark, 2008; Shepherd et al., 1982). Tectonism has an important influence on coal pores (Jiang et al., 2020). During the coal mining process, faults are one of the major geological problems that have disrupted coal production (Lin et al., 2020). It has been investigated that the outburst of coal and gas is closely related to fault zones (Zai et al., 2016; Karacan et al. 2008). Fault zones are important since they disrupt the structure of coal and reduce its strength (Karacan et al, 2008). The presence of fault zones in coal basin is an important indicator and factor for predicting coal and gas outburst (Fisne and Esen, 2014).

In recent years, despite measures to prevent and control the coal and gas outburst, faults in the region have made the mining environment difficult, complex geological structure, increased pressure and stress, as a result, the risk of coal and gas outburst is still high.

Numerous studies have been conducted on the geological structures and the impact of regional faults on coal and gas outburst. Cao et al. (2001) checked out that coal seams in the footwalls of the reverse faults underwent greater tectonic deformation than those in the hanging walls and outbursts always occurred in tectonically deformed zones. Zhao et al. (2013) showed in their studies that tectonic soft coal is mainly formed on the fault top wall under the effect of the fault structure. Lin et al. (2020) checked out the influence of small faults on coal and gas outbursts in the working face, which has reference significance for the prediction and prevention of coal and gas outburst disaster in the working face. Their studies showed that the risk of small fault slip increases with the advancing working face. Jiang et al. (2020) checked out the mechanism of how faults affect coal pore structure and gas sorption characteristic. Gao et al. (2021) reported that fault zones increase the gas pressure and weaken the coal seam, which causes a sudden coal and gas outburst.

Experiences from the mined out panels in the Parvadeh Tabas mine show that as the mine deepens, the impact and increase in stresses complicate the geological structures of the coal. As a result, the impact of faults in the region increases the potential for gas and coal outburst in working face. The parameters affecting the formation of the outburst can be listed as the gas content of the coal seam, thickness, slope, depth, and distance to fault zones. In this study, an evaluation is made only by considering the distance to fault zones. Due to the importance of the issue and few similar studies on coal mines in the country, the impact of regional faults on the outburst of coal and gas in Tabas mechanized mine is investigated in this study. For this purpose, due to the high capability of Geographical Information System (GIS), ArcGIS software is used to prepare a map of the impact of faults on gas and coal outburst in the mine.

GEOLOGICAL SETTING AND OUTBURST OCCURRENCE

Parvadeh underground coal mine is located in Tabas coal basin with an area of about 1200 square kilometers in the eastern part of central Iran, 75 kilometers southeast of Tabas city (Fig. 1). Coal reserves are estimated to be 98 million tons. The Parvadeh coal basin is located between two major North–South trending fault systems, the Kalmard hidden fault to the West and the Nayband fault to the East. Second-order structures trending East–West between these faults are the Rostam fault and Parvadeh anticline. The Rostam fault forms the northern boundary to the mining area. It is a reverse fault with a displacement of up to 700 m, down throwing to the North. The mine lies on the central portion of the asymmetrical Parvadeh anticline. Stratigraphically, the coal bearing sequence is of Triassic age. The rocks are mostly mudstone with prominent coarsening up siltstone/sandstone sequences. Locally developed, thin marine limestone occurs. The main coal horizons in the mine are seams B1, B2, and C1 that occur within 50 m of strata. Other seams C2, D and possibly E will affect mining principally because of their methane content. Figure 2 shows the stratigraphic column of the area. The total extractable reserves in all three available seams in Tabas Mine No. 1 are summarized in Table 1.

Table 1. Total minable reserves of mine No. 1

Seam	Seam area (hectares)	Total extractable reserves (tons)
1	629.91	15325000
2	601.18	7342000
B	356.11	4940000

1

The understudy area consists of 11 panels, among which panels E0, E1, E2, E3, W1, W2 and W₃ have been mined out and Panel W₄ is currently under extraction. As the mine deepens, operations become more difficult and the occurrence potential of coal and gas outburst at the Tabas mine increases. With increasing depth in this mine, the effect of this phenomenon will increase. Figure 1 shows the frequency and distribution of outbursts occurred in Panel E₃.

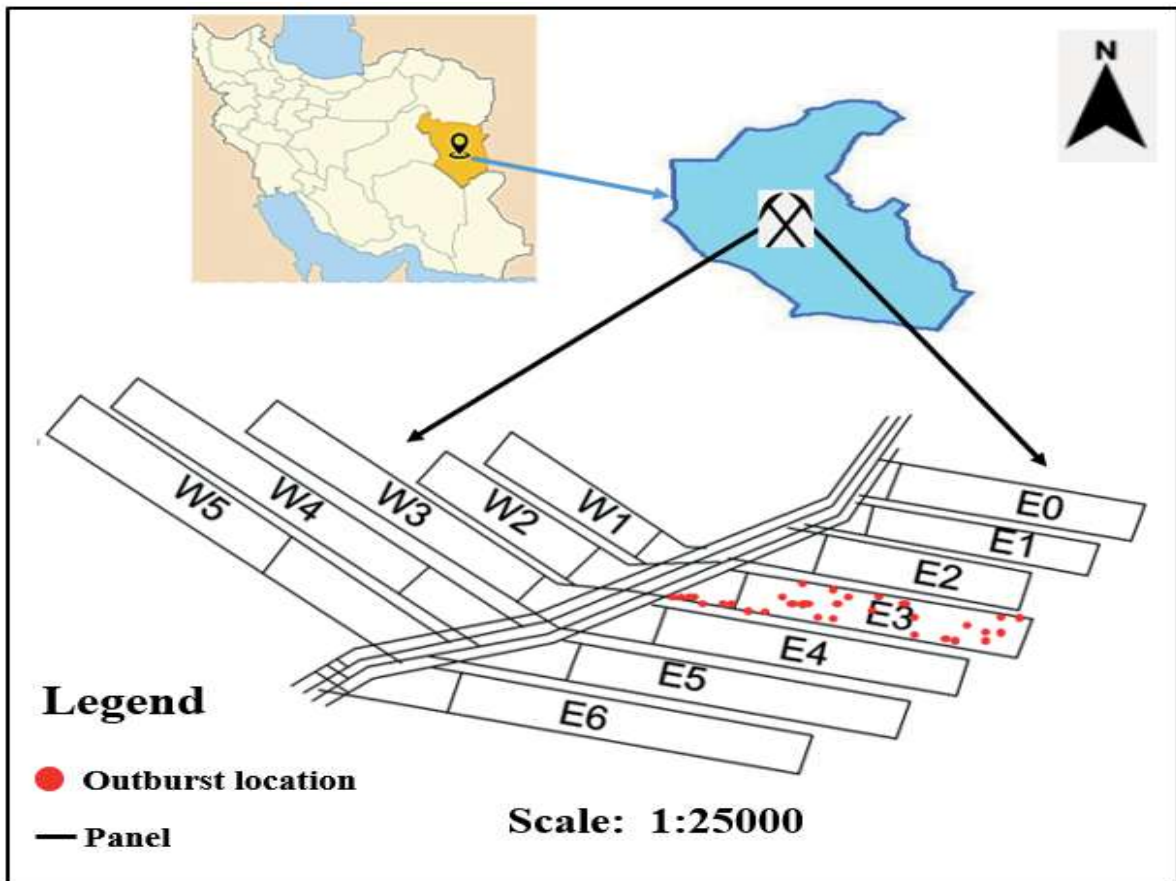


Figure 1. Location of the study area and distribution of outbursts occurred in Panel E₃

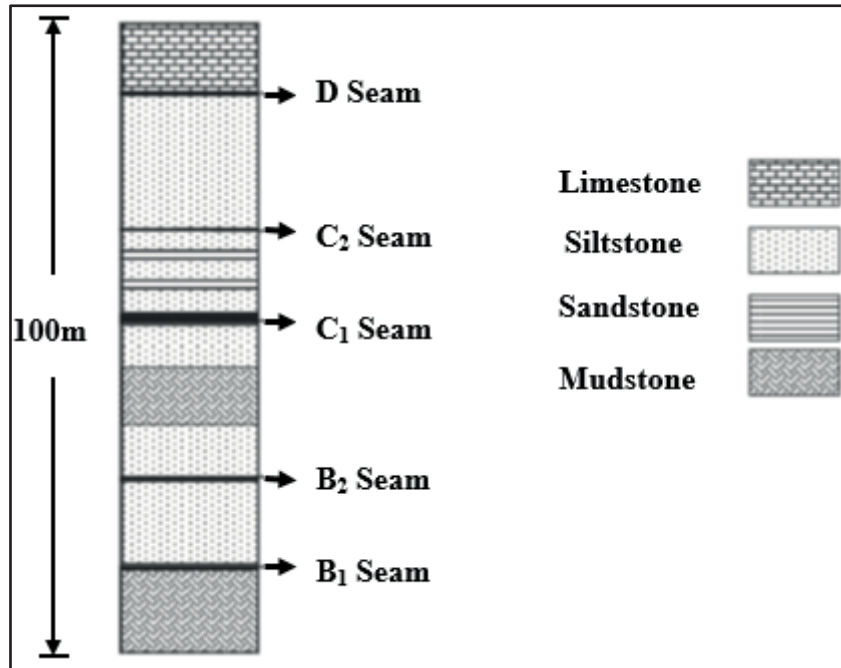


Figure 2. Stratigraphic column of Parvadeh Tabas coal field (Mohtasham Seyfi et al., 2018), (Sereshki et al., 2016)

METHODS

Fault Modeling in ArcGIS Environment

From the point of view of operational risk, the most suitable extraction Panel is a Panel that has low geological features and sufficient safety. In order to reduce risks and accidents, it is necessary to be aware of the ground conditions, especially faults. Due to the high cost of initial investment and time-consuming mine development, it is necessary to investigate the displacement of the coal seam by faults in the longwall mining method. Therefore, the purpose of this study is to investigate the effect of fault displacement in Tabas Mechanized Coal Mine No. 1 and to identify the faults that cause coal and gas outburst in this mine. To achieve this goal, Schulz classification and ArcGIS software have been used.

Schulz classification

After collecting the data, Schulz classification was used to determine the uniformity of the seam in the fault zones. In 1993, Schulz proposed a classification system in which the uniformity of the seam was determined by changes in the displacement index (V_x) (Ataei et al., 2009):

$$v_x = \frac{x}{m} \tag{1}$$

where, v_x is displacement index, x is the displacement of coal seam due to fault and m is the thickness of coal seam, both in meter. The degree of seam uniformity in this classification is assigned to the seam as a point according to the displacement index. The seam uniformity varies between 0 and 1. According to this theory, seams with a displacement index of 0 are perfectly uniform (uniformity rating equal to 1) and seams with a displacement index greater than 3 are non-uniform (uniformity score equal to 0). Table 2 shows the classification provided by Schulz.

Table 1. Classification of coal seam uniformity

Seam uniformity Condition	Fault displacement index
Uniform	0-0.5
Semi-uniform	0.5-1
	1-1.5
	1.5-2
Non-uniform	2-2.5
	2.5-3
	>3

Fault Displacement Map

Having used the Schulz classification to determine the changes in magnitude of coal seam displacement index in fault zones, layering was implemented in ArcGIS software. The faults of the mine were divided into three categories; faults with displacement index of 0 to 0.5 (uniform), faults with displacement index of 0.5 to 2 (semi-uniform) and faults with displacement index greater than 3 (non-uniform). As can be seen in Figure 3, the faults marked in red are non-uniform, and according to a survey of experts and engineers of this mine, shearer loader usually encounters problems when crossing these faults, and in these places coal and gas outburst are usually recorded. Three of the faults in panels W4, W5 and E2 are marked in red, and according to the results of this study, the possibility of coal and gas outburst and its intensity in panel W4, W5 will be very high. It is necessary to take precautionary measures during the extraction of these panels. Figure 4 shows the fault concentration map.

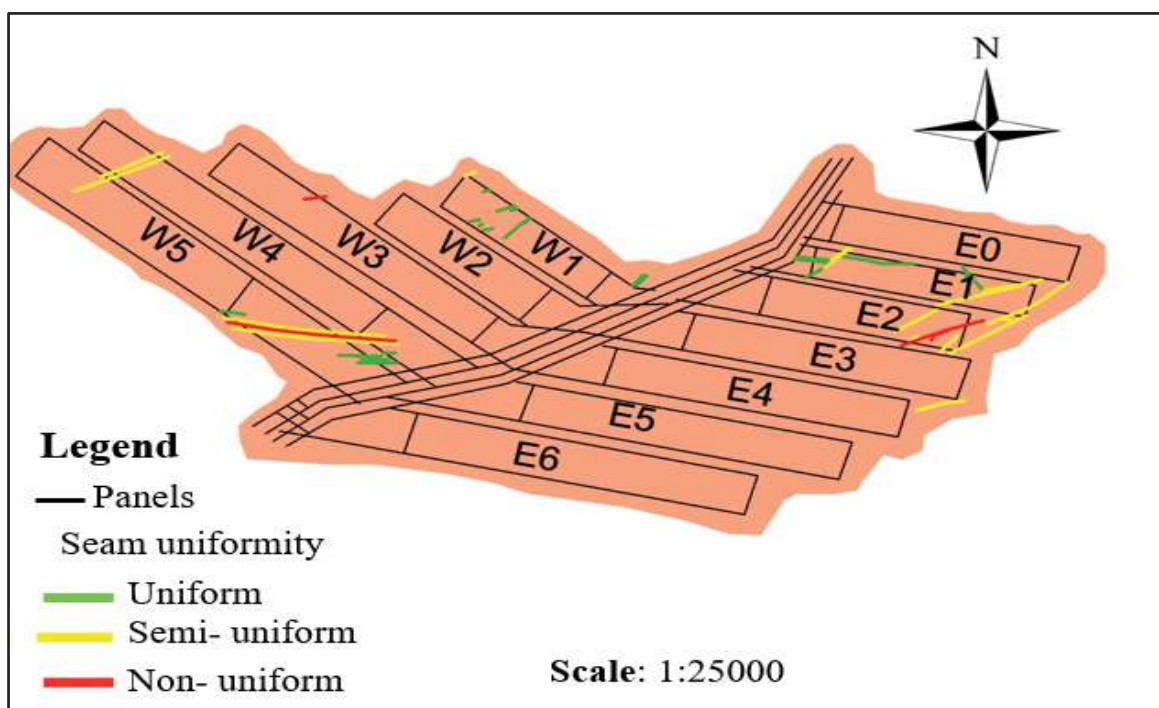


Figure 3. Classification map of fault displacement

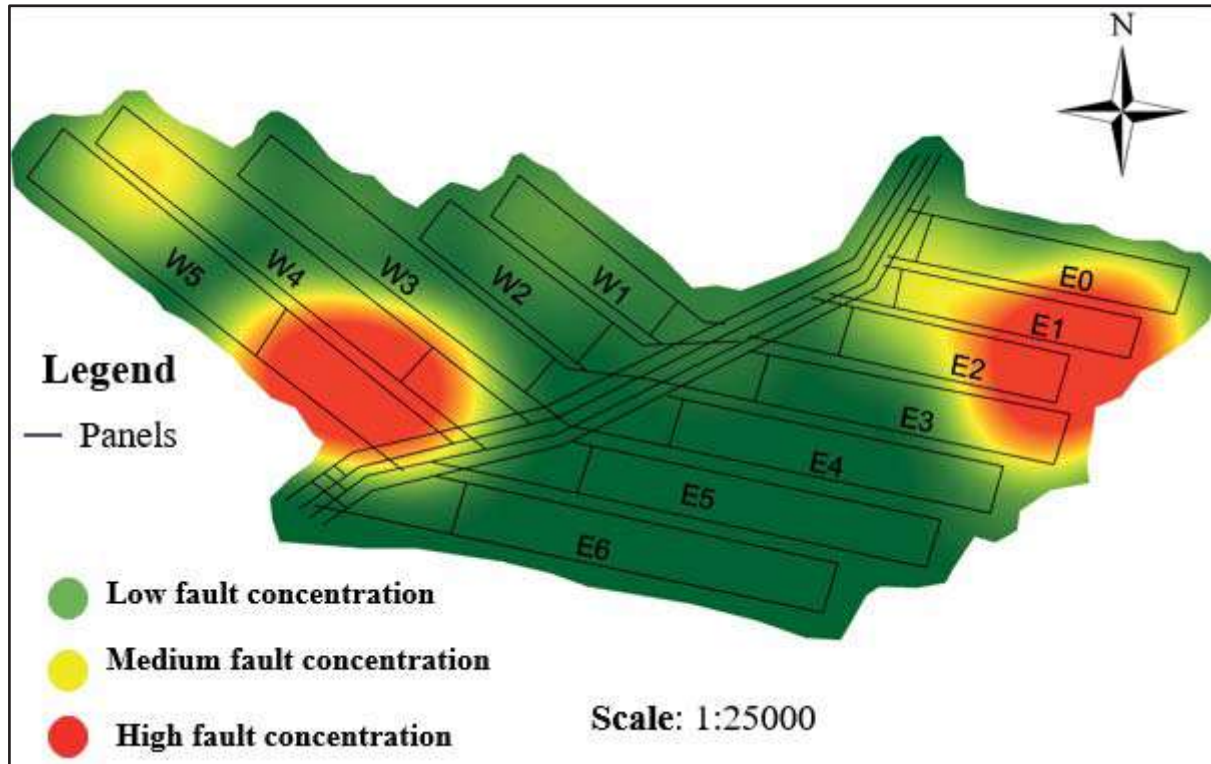


Figure 4. The final map of the intensity of coal and gas outburst due to the concentration of faults in the region

Underground coal mining has always been known as one of the most risky mining activities. Occurrence of potential accidents in underground coal mines and the resulting hazards create an unsafe work environment for workers and operational equipment.

Parvadeh Coal Mine is one of the important mines for supplying raw materials to steel mills in Iran. Many problems, including collapse of the roof, spontaneous ignition, instantaneous release of methane gas, groundwater influx, sudden collapse and subsidence, threaten the production and safety of the mine.

Verification of the performance of the final model and the emissions of gas and coal recorded during the extraction of panel E₃ shows the high reliability of this method. As shown in Figure 5, due to the impact of the faults, several outputs have occurred at the top of panel E₃.

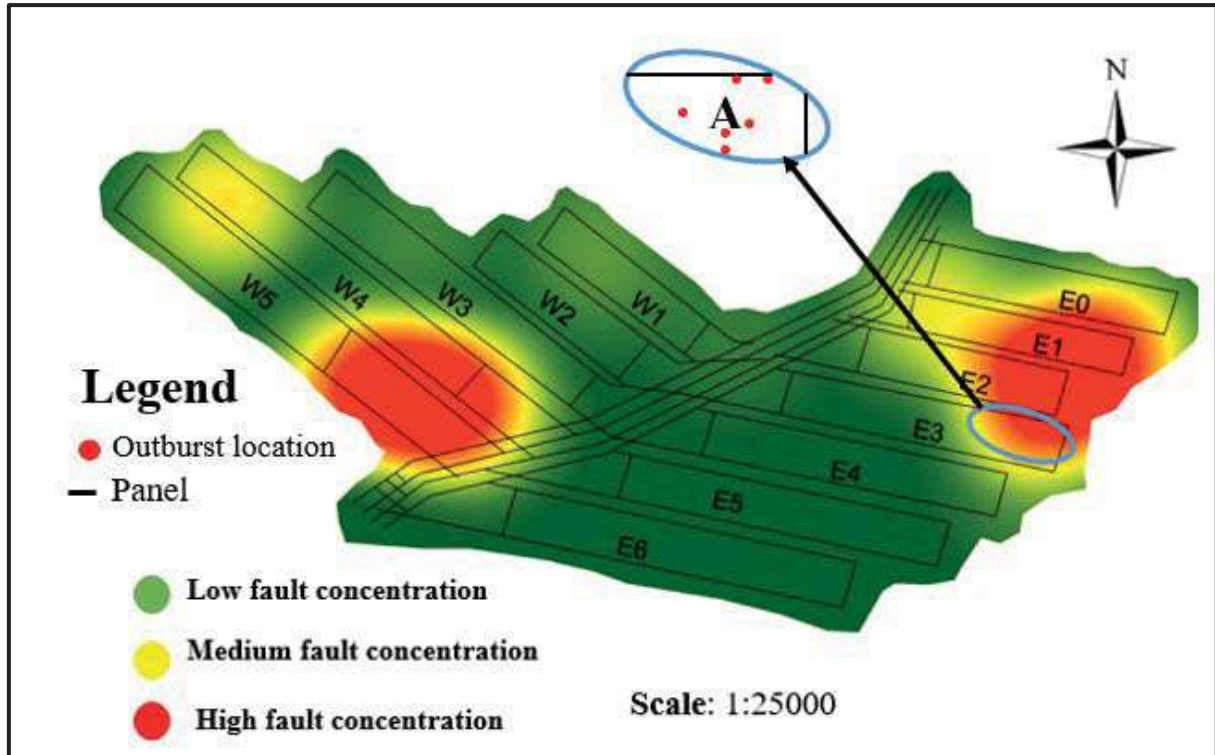


Figure 5. Fault focus map in panels

DISCUSSION AND CONCLUSION

In coal mining, geological structures such as faults in the region are important influencing factors affecting the coal and gas outburst. With the start of mining and disruption of regional stress, the impact of these factors intensifies as a result of the potential of the coal seam for this phenomenon increases. Schulz classification and GIS were used to identify high-risk areas in terms of outburst and to map faults in the area. The most important results of this study are:

- (1) The combination of GIS technique and Schulz classification allows decision makers to identify the areas prone to high-risk coal and gas outburst.
- (2) The results of the coal and gas forecast map show the high concentration of faults in Panels W4, W5. Preventive measures should be taken during the extraction of these Panels.
- (3) Verification of the performance of the final model and the coal and gas outburst recorded during the extraction the top of the panels E3 show the reasonable reliability of this method and other events of Panel E3 are due to the effect of other parameters on gas and coal emissions.

REFERENCES

- Ataei, M., Khalokakaei, R., and Hossieni, M. (2009). Determination of coal mine mechanization using fuzzy logic. *Mining Science and Technology*, 19(2), 149-154.
- Fisne, A., Esen, O. (2014). Coal and gas outburst hazard in Zonguldak Coal Basin of Turkey, and association with geological parameters. *Natural Hazards*, 74(3), 1363–1390.
- Gao, K., Huang, P., Liu, Z., Liu, J., Shu, C., and Qiao, G. (2021). Coal-rock damage characteristics caused by blasting within a reverse fault and its resultant effects on coal and gas outburst,” *Sci. Rep.*, 1-13.
- He, D., Cao, Y., and Glick, D.Y. (2001). Coal and gas outbursts in footwalls of reverse faults. *International Journal of Coal Geology*, 48(1-2), 47-63.
- Li, Wei., Ren, T., Busch, A., den Hartog, S.A.M., Cheng, Y., Qiao, W., and Li, B. (2018). Architecture, stress state and permeability of a fault zone in Jiulishan coal mine, China: Implication for coal and gas outbursts. *International Journal of Coal Geology*, 198, 1-13.

- Jiang, B., Zhao, Y., Lin, B., and Liu, T. (2020). Effect of faults on the pore structure of coal and its resultant change on gas emission. *Journal of Petroleum Science and Engineering*, 195.
- Karacan, C.Ö., Ulery, J.P., and Goodman, G.V.R. (2008). A numerical evaluation on the effects of impermeable faults on degasification efficiency and methane emissions during underground coal mining. *International Journal of Coal Geology*, 75(4), 195–203.
- Lin, J., Zuo, Y., Zhang, K., Sun, W., Jin, B., Li, T., and Chen, Q. (2020). Coal and gas outburst affected by law of small fault instability during working face advance. *Geofluids*, 2020.
- Mark, C. (2018). Coal bursts that occur during development: A rock mechanics enigma. *International Journal of Mining Science and Technology*, 28(1), 35-42.
- Sereshki, F., Vaezian, A., and Saffari, A. (2016). Evaluation of the effect of macerals on coal permeability in Tazareh and Parvadeh mines. *Journal of Stratigraphy and Sedimentology Researches*, 32(2), 23-34.
- Seyfi, M.M., Hamidi, J.K., Monjezi, M., and Hosseini, A. (2018). Estimation of coal seams gas content for evaluating potential use of methane drainage system in Tabas coal mine. *Journal of Mining and Environment*, 9(3), 667–677.
- Shepherd, J., Rixon, L.K., and Griffiths, L. (1981). Outbursts and geological structures in coal mines: A review. *International Journal of Rock Mechanics and Mining Sciences & Geomechanics Abstracts*, 18(4), 267-283.
- Vaziri, V., Hamidi, J.K., and Sayadi, A.R. (2018). An integrated GIS-based approach for geohazards risk assessment in coal mines. *Environmental Earth Sciences*, 77(1), 29.
- Zhai, C., Xiang, X., Xu, J., and Wu, S. (2016). The characteristics and main influencing factors affecting coal and gas outbursts in Chinese Pingdingshan mining region. *Natural Hazards*, 82(1), 507–530.
- Zhao, W., Xiong, J., Zhang, J., and Ran, M. Y. (2013). Structure coal distribution law and affected to coal and gas outburst in Sichuan coal mining area. *Coal Science and Technology*, 41(2), 52–55.

INDUSTRIAL USE OF BACTERIAL IRON OXIDATION IN-SITU RECOVERY OF URANIUM

B. Shiderin ^{1,*}, A. Altynbek ², Y. Bektay ¹, G. Turysbekova ¹, E. Mukanov ¹, A. Kalmukambetov ²,
M. Bektayev ³, A. Duisenbay ⁴

¹ *Satbayev University*

(*Corresponding author: shbaur@mail.ru)

² *Semizbay-U LTD*

ABSTRACT

The technology of bacterial iron oxidation during in-situ recovery (ISR) of uranium has been developed and proposed for industrial use. Results of pilot tests at a uranium mine in Kazakhstan for 24 months confirmed technology. Two bio-technological installations based on a new type of flow bioreactors with a volume of 20 m³ bioreactors installed in 40-foot containers. The capacity of the plants installed in the geo-technological field was more than 150,000 m³/year for leaching solution. The redox of the solution rose from 360 mV to 430-450 mV in the flow mode in bioreactors. The content of trivalent iron increased from 0.1 g/l to 1.5 g/l and higher. The bioprocess was carried out with temperature of solution 10-14^oC (the optimal is 25-35^oC). This eliminated energy consumption for heating the solution. The test results showed an increase in the uranium content in the productive solution by 10-20 % without adding additional sulfuric acid and 40 % with adding additional sulfuric acid. The economic costs of using the technology are 6-8 times lower than when it is used chemical oxidizers (hydrogen peroxide). This confirmed the potential of using this technology for underground borehole ISR of uranium.

Keywords: Uranium, in-situ recovery, bioleaching, bivalent iron, bacteria

INTRODUCTION

The use of underground in-situ uranium recovery technology (ISL) has developed significantly in the world in recent decades. Kazakhstan's success in uranium mining is based on this technology (over 20 thousand tons of uranium per year). Reducing the price of uranium requires the introduction of technologies aimed at reducing the cost of mining and processing of uranium and intensifying the process.

One approach is to use bacterial leaching with the use of iron-oxidizing bacteria *A. ferrooxidans* according to the main technological indicators corresponds to the modes that are used for underground borehole in-situ recovery of uranium. There have been repeated attempts to use bioleaching for uranium, but these methods have not been widely adopted. One-time supplies of bacterial solution did not give the necessary result, especially since during underground borehole in-situ recovery of uranium, the solution flows through the ore-bearing layer for 20-30 days. Conditions for the vital activity of bacteria in the ore-bearing layer did not allow them to multiply and show their activity.

The use of bio-geotechnology in mining practice differs significantly from the use of biotechnology in the production of specific medicines or food products. This is due to the significant heterogeneity of the composition, the presence of technological factors that significantly affect the process. It is necessary to take into account the complex nature of the ore body, as well as the fact that the material composition varies not only on different blocks, but also within the same block.

Bacteria capable of oxidizing iron (II) were first identified in the acidic waters of coal mines in the United States, and then – in the acidic waters of the Bindkham copper quarry (USA) (Colmer et al., 1950; Bryner et al., 1954). Similar bacteria were later discovered at the Rio Tinto mine in Spain, where copper has been leached for ~ 300 years. On the territory of Russia, such bacteria are present, for example, in the acidic mine waters of the sulfide deposits of the Urals, Altai and Kola Peninsula (Polkin, 1982). During microbiological leaching, bacteria oxidize sulfide minerals, which causes the formation of iron (III) and sulfuric acid ions in the aqueous phase – a set of reagents, due to redox reactions that oxidize U(IV) and form soluble U(VI). This transformation, due to the chemical activity of microorganisms, is the basis of a bio-metallurgical process that is economically justified in relation to poor, off-balance-sheet ores and dumps of uranium production (i.e., in cases where the standard process is not applicable) (Colmer et al., 1950; Bryner et al., 1954; Polkin et al., 1982).

There several studies in the possibility of commercializing bacterial leaching of uranium from poor raw materials were carried out in the early 1950s, and in 1952-1953 in Urgeirica (Portugal), industrial use of a heap version of this process began (iron-oxidizing bacteria *A.ferrooxidans* were used) (Brand, 2001; Harrison et al., 1966). Also at Elliot lake mine (Canada) using a solution of sulfuric acid and iron (III) sulfate as a bacterial medium (Hamidian et al., 2009; Guay et al., 1976; Tuovinen and Bhatti, 1999).

Several important factor is the nature of mineralization of uranium, since its oxide, phosphate, sulfate and carbonate minerals are easily opened, while silicate forms are difficult or not at all opened (Munoz et al., 1995; Rawlings, 2004). Also amount of nutrients (added artificially or extracted by minerals) sufficient for the growth of the bacterial culture (Rawlings, 2005). *A.ferrooxidans* is resistant to metal ions such as chromium, copper, zinc, nickel, thorium, uranium, and mercury. The presence of certain metals and organic compounds in the environment can block the process of pyrite oxidation by this type of bacteria (Brand, 2001; Munoz et al., 1995).

Temperature is a parameter that determines the diversity of microbiological populations (Kawatra and Natarajan, 2001). Moderately thermophyllite iron-and sulfur-oxidizing bacteria, initially isolated from mine waters and hot springs and operating at temperatures of 30-40⁰C, proved to be the most suitable for research and industrial use (Rawlings, 2005; Brierley, 1978; Brierley et al., 1978; Holmes, 1988; Blais et al., 1994; Twardowska, 1986; Twardowska, 1987). In all leaching processes involving acidophilic bacteria, the degree of oxygen saturation of the solution or pulp is an important parameter. Under conditions of forced mixing, a drop in the oxygen concentration below 0.5-1.0 mg / dm³ causes the process to stop. It has been shown that the use of forced aeration (air consumption of 8t/t solid, oxygen utilization rate of 25 %) significantly reduces the leaching time during the heap bacterial leaching of ores from several Australian deposits (Brierley and Briggs, 2002). Lack of carbon dioxide stops the growth of autotrophic bacteria and can dramatically reduce the speed and completeness of their interaction with sulfide minerals (Pronk et al., 1992; Barrett et al., 1993). A number of studies have also established optimal process parameters (pH, temperature, and mixing time) (Polkin et al., 1982; Hamidian et al., 2009; Cerda et al., 1993; Schippers et al., 1995; Benedetto et al., 2005).

At the Canada enterprise Rio Elgom, the process of periodic irrigation of the walls of treatment faces with acidic mine water was tested; as a result, in 1964-1965, about 57 tons of uranium were additionally extracted. Currently, Rio Algom use of heap bacterial leaching of uranium. Since 1984, several variants of underground leaching of uranium using *A.ferrooxidans* bacteria have been tested (Rawlings, 2004; McCreedy and Gould, 1990). Other examples of industrial use of uranium bioleaching are factories using the heap option (Figueria in Brazil, Ranger in Australia, Stepnogorskaya in Kazakhstan and Saint Pierre in France) and the well option (Olympic Dam and Beverly in Australia) (Tuovinen and Bhatti, 1999; Munoz et al., 1995; Garcia, 1993; Dwivedy and Mathur, 1995). But the information on this project is presented in a compressed form in the sources, and currently the technology does not seem

to be used. There is evidence that bioleaching is used in China in relation to the extraction of uranium from tailings dumps (Jianguo et al, 2004; Campbell et al., 2015; Watling, 2015).

From this analysis, it follows that the use of bacterial iron oxidation and biotechnological methods for underground in-situ recovery of uranium is limited and there are no examples of effective organization for underground leaching “in-situ” (ISR).

Analysis data show main reaction taking place for uranium recovery using bioleaching. Ion ferric iron resulting from oxidation of ferrous iron by bacteria is an oxidizing agent of tetravalent uranium:



Bacteria (A. Ferrooxidans) can oxidize ferrous iron:

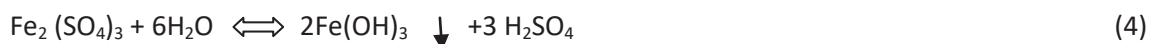


Also exist possible direct oxidation of uranium by bacteria (direct mechanism):



But in underground condition there is too small amount of O₂.

On another hand in such condition take place formation of iron hydroxides is one of the factors that can cause clogging in the ore-bearing layer.



The Methodology of the Tests

Uranium Deposit (Block for investigation)

For investigation bacterial leaching for uranium deposit was used uranium field in the north of Kazakhstan's is geologically complex, with a depth of about 120 m. The operation of the mine is characterized by a high consumption of sulfuric acid due to its complex material composition. Leaching dissolution of the this uranium Deposit have a relatively high content of divalent iron in leaching solutions up to 3 g/l and the salt content accumulated in the solution reaches 20-30 g/l.

Tests was done on one of the block (number 62) in this uranium deposit. Block consisted of several injection and pumping wells. Distance between wells 25 meters. an average thickness of the ore-bearing layer of about 10 m. The volumes of the leaching solution supplied are on average from 30 to 50 m³/h for a separate block of the Deposit. Pilot tests was done on an equipment with a solution flow of more than 20 m³ / hour, which in annual terms is more than 150 thousand m³ / year.

Leaching Solution and Productive Solution

The large-scale transition from laboratory research to pilot production and subsequent industrial application is associated with the presence of factors that are difficult to model in the laboratory. The Composition of leaching dissolutions differs from the model compositions used for growing bacteria, primarily a significant amount of salts (up to 25g/l). The content of Fe²⁺ of iron does not exceed 3 g/l, under simulated conditions up to 10 g/l. The relatively low content of divalent iron in the solution requires more fine-tuning of the technology and taking into account scale factors. The temperature of the dissolution (10-14^oC) are significantly different from optimum (25-35^oC). The heating costs are much higher than the potential effect of using solution with the volume of the leaching

dissolution flow (2000m³/h). Trying to bring the temperature of the dissolution to the optimal temperature for the bacteria will require a cost comparable to the cost of the finished product. The operating Conditions of bioreactors in the flow mode differ from the model laboratory conditions, even if the solution compositions match. The Duration of leaching solutions passing (over 20 days) through the ore-bearing layer and the variety of physical and chemical processes taking place in the ore-bearing layer.

Equipment

Two units with a compressor station (up to 500 m³/h of air production each) and a pumping station with a capacity of up to 40 m³/h were used for testing. Flow bioreactors with a volume of 20 m³ provided a free solution flow with minimal removal of bacteria from the bioreactor due to design of equipment. A pumping station with a frequency Converter and a storage tank provided solution supply to the main network at a pressure of more than 8 bar. After the bioreactors, the activated leaching solution was fed into the injection wells. Measurements of the content of iron in the dissolution, sulfuric acid, pH, redox process, and the content of uranium in the productive solution were carried out by the mine laboratory in the current mode. Regulation of the dissolution supply to the bioreactors was regulated by cranes based on data from electromagnetic flow meters («Omega» type). Development of the installation project and its installation was carried out by the research laboratory "BioGeoTechnology of gold, uranium and polymetallic ores" (Satbayev University)". Mobile execution of bio-installations in containers allows to transfer equipment to problem blocks for solving local problems.

Biomass accumulation

Preliminary accumulation of biomass was carried out on the Sylvester-Langmuir medium. The accumulated biomass was fed to bioreactors on a one-time basis. During the month, biomass was accumulated in bioreactors in the cultivation mode. Biomass accumulation was carried out in the bubbling mode by air supply by a compressor. The dissolution was periodically updated as the divalent iron changed to the trivalent state. Measurements were made in the chemical laboratory of the mine on a daily basis.

Measurments and Calculations

Amount of U, Fe²⁺, Fe³⁺ and H₂SO₄ was measured in labalatory of plant by titration methods. Redox , pH was measured by ionometr I-160MI, Amount of bacteria measured using microscope. For statistical analysis of data was used program SPSS statistics.

Testing

The first stage tests were carried out during 2018. The dissolution was supplied to two installations under the code name BOI-1 and BOI-2 (bacterial oxidation of iron) in the volume of 20 m³/hour. Since June 2019, only one BOI-1 installation has been operating in flow mode. Two weeks later, two installations were launched together. The total volume of the solution supplied to the unit was 30m³ / hour. No additional sulfuric acid was supplied. The volume of the activated leaching dissolution supplied was till 20m³ / hour, with the total supply of the solution to the injection wells up to 40m³/hour. Mixing the activated leaching solution and hydrous solution slightly reduced the redox parameter of the solution and the content of trivalent iron in the solution. Data on the content of the target metal in the production solution were determined in the normal mode directly by employees of the mine (Turysbekova, 2019).

The second stage tests were carried out during 2021. The leaching solution was supplied to installation under the code name BOI-2 (bacterial oxidation of iron) in the volume of 10 m³/hour with

adding sulfuric acid 2g/l. Testing took place Since 18 July 2021 till 18 October 2021. Only one BOI-2 installation has been operating in flow mode. The total volume of the solution supplied to the unit was 10m3 / hour. All leaching solution went through BOI-2.

RESULTS

Investigation Without Adding Additional Sulfuric Acid (1 stage)

On the first stage was done investigation without adding additional sulfuric acid. Usual leaching solution after uranium desorption was used. Part of leaching solution (50%) flow through bioreactors. After bioreactor solution redox increased from 360mV till 410-420 mV.

On the figure 1 is shown everyday data of the content of uranium in the production solution since the beginning of 1 January 2018. The arrows indicate the start time of the activated leach dissolution supply units. The content of sulfuric acid in the leaching dissolution was 3.5-4.5 g / l. The tests were performed without additional acid supply.

Figure 1 shows data on the content of uranium in the productive solution on the block since the beginning of the year. There is a clear tendency to reduce the content before the start of installations. After switching on the second unit and reaching the 30m3/h feed, there is a steady increase in the uranium content in the production solution, which allowed us to assume that the tests have reached their intended goal.

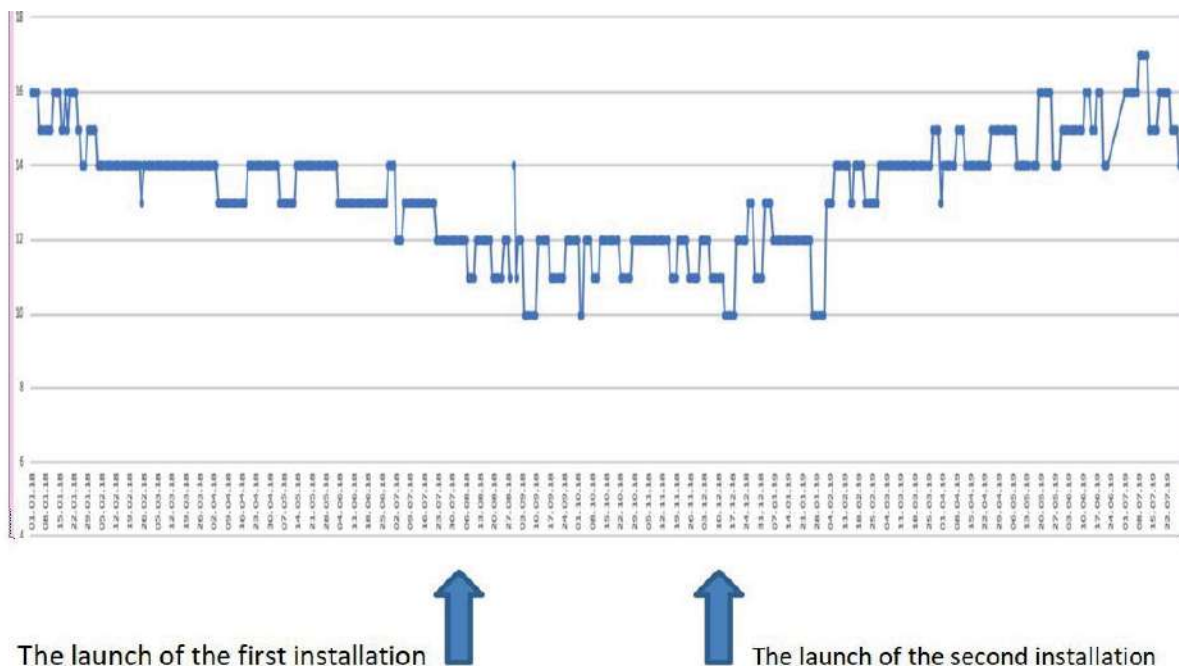


Figure 1. Dynamics of changes in the content of uranium in the production solution from January 2018 to 2019, indicating the time when bio-installations for the oxidation of divalent iron in the leaching dissolution were switched on. (U (g/l))

Taking into account that the reaction time of the system to the impact of the modified leaching dissolution is at least 20 days, it can be observed that the increase in the uranium content in the productive solution occurred after the launch of bio-installations. For individual wells on the block, the increase was more than 50 %. The average for the block was 10-20 %. The tests were performed without adding sulfuric acid.

Investigation With Adding Additional Sulfuric Acid (Stage 2)

For testing, sulfuric acid was supplied in the required amount of over 100 tons. The acid supply was adjusted by the acidification process unit (APU) through an electromagnetic flow meter. The acid supply was adjusted manually every hour. The acid supply was adjusted manually every hour. On average, the supply was carried out in the amount of 2 grams / liter, and after 20 days in the amount of 6-7 grams / liter.

The volume of the leaching solution was supplied in a volume of 10 m3/h through the installation Bacterial oxidation of Iron-2 (BOI-2). Samples were taken daily to analyze the parameters of the activated leaching solution (ALS): pH, Redox, Fe2+, Fe3+, H2SO4. Table 1 below presents data on the correlation of ATS indicators after leaving the BOI-2 facility. (Sample size 152)

Table 1. Correlation of indicators of the solution in the ALS (in the bioreactor)
 . The correlation is significant at the 0.01 level (two-tailed). *RP- Redox potential

		pH	RP	Fe2	Fe3	H2SO4
pH	Pearson correlation	1	-,078	-,006	,016	-,880**
	N	152	152	152	152	152
RP***	Pearson correlation	-,078	1	-,888**	,906**	,050
	N	152	152	152	152	152
Fe2	Pearson correlation	-,006	-,888**	1	-,956**	-,027
	N	152	152	152	152	152
Fe3	Pearson correlation	,016	,906**	-,956**	1	,043
	N	152	152	152	152	152
H2SO4	Pearson correlation	-,880**	,050	-,027	,043	1
	N	152	152	152	152	152

Figure 3 presents data on the content of uranium in the PS (productive solution) since January 2021. As noted above, tests were carried out at the block with the use of BOI-2 from 2018, and there was an increase in the uranium content in the PS during the testing period (2018-2019) by 10-20% without supplying additional sulfuric acid.

New tests carried out with the addition of sulfuric acid showed that the content increased on the block by 40% (from 12 mg/l to 18 mg/l). Samples in the productive solution were analyzed daily (pH, U). Statistical analysis of the data on a sample of 225 data showed that the pH in the Productive Solution and the content of uranium are statistically significant and the correlation was 0.327. However, the mutual influence is not sharply expressed, which is connected with the indirect relationship of indicators. In contrast, for example, the relationship between the ORP of the solution and the content of ferric iron.

Table 2. Descriptive statistics for the block

	Mean	Standard deviation	N
H	2,1003	,05355	225
H	13,7018	1,38099	225

This table 2 is based on a statistical analysis of production fluid data during 2021

Table 3. Correlation (statistics) of uranium content and pH values in the Productive Solution
 **. The correlation is significant at the 0.01 level (two-tailed)

	pH	U
pH Pearson correlation	1	0,327**
N	225	225
U Pearson correlation	,327**	1
N	225	225

It follows from this analysis that there is a relationship between pH and U, but it is not very pronounced and the effect of pH on U is indirect

Table 4. Correlation of technological indicators of PS at block
 *. The correlation is significant at the 0.05 level (two-tailed)

	pH	U	RP	Fe2+	Fe3+
PpH Pearson correlation	1	,892*	-,591	,355	-,581
N	5	5	5	5	5
U Pearson correlation	,892*	1	-,704	,437	-,597
N	5	5	5	5	5
RP Pearson correlation	-,591	-,704	1	-,946*	,925*
N	5	5	5	5	5
Fe2+ Pearson correlation	,355	,437	-,946*	1	-,899*
N	5	5	5	5	5
Fe3+ Pearson correlation	-,581	-,597	,925*	-,899*	1
N	5	5	5	5	5

Due to the small number of samples, the data are less statistically significant but give a general idea of the relationship between the parameters.

From these data, it should be noted a strong relationship between the uranium content and pH in the productive solution (correlation coefficient 0.892), as well as a strong relationship between the uranium content and RP (correlation coefficient 0.7) and a relatively high relationship with the content of ferric iron in the productive solution. As expected, there is a very high correlation between the content of ferric iron and the RP of the solution (correlation coefficient 0.925), which confirms the influence of a strong oxidizing agent (Fe3+) on the RP of the solution.

Figure 3 shows the data on changes in the metal content in the productive solution during 2021 during testing. The arrows mark the start of the acid supply and the end of the acid supply. It should be noted that a change in the composition of the leaching solution affects the composition of the productive solution with a delay of 20-30 days.

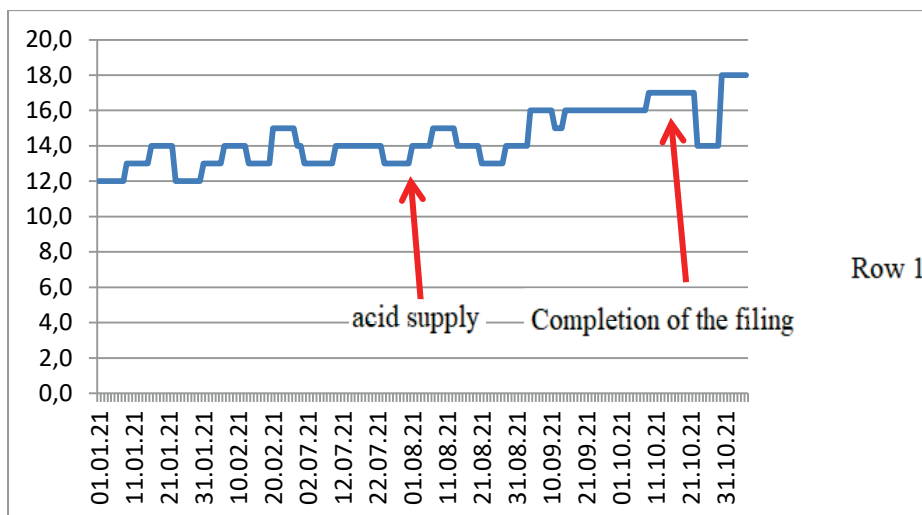


Figure 2. Change in the content of uranium in the Productive Solution at the block in the period from January to October 2021 (arrows indicate the period of supply of sulfuric acid - from 07/27/2021 to 10/15/2021)

Since the beginning of the year, the uranium content at block 62 has risen from 12 to 18 mg/l (40%)

DISCUSSION

The problem of increased production costs with a relatively high iron content required innovative approaches to reduce production costs. A chemical oxidizer (hydrogen peroxide) is successfully used, and its use is constrained by the high cost of chemicals. An alternative option is bacterial iron oxidation, where the final oxidizer is air oxygen, and bacteria act as a catalyst for the process. Laboratory studies have shown the applicability of bacterial iron oxidation to enhance the redox process of the solution and convert divalent iron to trivalent for existing mine leaching dissolutions. The problem remained open as to how bacterial iron oxidation would affect the uranium content in the productive solution.

The main problem in implementing a project on this scale is to establish a link between the operation of bacterial iron oxidation (BOI) plants and the increase in the content of uranium in the productive solution (Bektay et al. 2018). Modeling complex processes occurring in ore-bearing layer is complicated by the difference of material composition of ore-bearing layer and the composition changes as the flow of solution through the ore layer at 20-35 m at a depth of 120m (some another fields more than 700 m). Analysis of the results of using hydrogen peroxide (a chemical oxidizer) at the this mine allowed us to put forward a number of propositions that the activated leaching solution after bacterial oxidation of iron in bioreactors will affect the uranium content in the flushing liquid. In this situation, only direct tests on a separate unit allow us to understand and study the effect of bacterial iron oxidation on the uranium content in the production solution and determine the prospects for this technology.

The conditions under which bacterial iron oxidation occurs correspond to the conditions of underground in-situ recovery of uranium in terms of the content of sulfuric acid in the solution (from 3 g/l to 25 g/l), pH (1.5-2.5), redox process (360mv and higher), temperature and other technological conditions.

Studies were conducted on one of the blocks of a uranium deposit with industrial volumes of leaching dissolution flow. Studies have shown the effect of iron oxidation by *A. ferrooxidans* strains in flow bioreactors on the uranium content in the productive solution, despite the complex material composition of the ore body. Averaged indicators over the course of the year for the content of uranium in the productive solution for the block confirmed this effect. Tests were carried out in difficult natural conditions, the air temperature in winter reached minus 40°C.

The Redox of the solution in bioreactors rose from 360 mV to 430-450 mV in the flow mode after passing the leaching solution through bioreactors. The content of trivalent iron increased from 0.1 g/l to 1.5 g/l and higher. The process of bacterial oxidation of iron in the solution took place at a solution temperature of 10-14°C (the optimal is 25-35°C), which eliminated the energy costs of heating the solution. The data obtained allowed us to determine several options for the industrial implementation of the technology at the mine. Operating costs when using flow bioreactors are 6-8 times lower than when using chemical oxidants (hydrogen peroxide).

Based on the conducted tests, it was done additional studies with the addition of "free" sulphuric acid, which improved the performance of bioreactors on leaching dissolutions and increased content of U in productive solution on 40 %. Influence of additional sulfuric acid can be explained by two reactions: (2) - acid need for this reaction and (4) – additional acid can dissolve iron hydroxides, which can block access to uranium minerals.

CONCLUSIONS

Increasing the Redox potential of leaching solutions up to 420-440 mV (with RP of leaching solution 360 mV), which ensured an increase in Productive Solution by 20% without adding of sulfur acid. The increase in the content of uranium in the Productive Solution at block was 40% with additional sulfuric acid 2 g/l. There was an increase in the content of ferric iron in leaching solutions due to bacterial oxidation of iron.

Industrial tests have confirmed the potential of this technology, as well as data obtained in the laboratory. As a result of studying the effect of BOI technology with the addition of sulfuric acid at one of the block (after-leaching stage) and control blocks, it was shown that the addition of sulfuric acid and the use of BOI technology increases the performance of productive solutions. The addition of sulfuric acid on other blocks did not show a significant increase in the uranium content in the productive solution.

Regression analysis of the data revealed statistically significant relationships between technological indicators in the Active Leaching Solution and in the Productive Solution, between RP and ferric iron content at a correlation level of 0.9.

Analysis of the data shows that the use of BOI technology can increase the depth of uranium extraction from the designed 85% to 95% and more. As a result of the work carried out, two patents for inventions and one patent for a utility model were obtained.

REFERENCES

- Barrett J., Hughes M., Karavaiko G., Spencer P. Metal extraction by bacterial oxidation of Mineral. / Ellis Harwood. 1993. P. 127–134
- Bektay E. K., Turysbekova G. S., Meretukov M. E., Bektayev M. E., " Natural nanoparticles and nanostructures", Almaty, KazNRTU, 2018, - 600 p.
- Bektay E. K., Turysbekova G. S., Altunbek A.D., Shiderin B.N., " Geochemistry of uran», Almaty, KazNRTU, 2020, - 243 p.

- Benedetto J., de Almeida S., Gomes H., Vazoller R. Monitoring of sulfate-reducing bacteria in acid water from uranium mines. // *Miner. Eng.* 2005. V. 18. P. 1341–1343
- Blais J., Tyagi R., Meunier N., Auclair J. The production of extracellular appendages during bacterial colonization of elemental sulphur. // *Proc. Biochem.* 1994. V. 29. P. 475–482
- Brand, H. (2001). *Biotechnology*. In: H.J. Rehm & G. Reed (Eds.), (pp 134- 152). Wiley.
- Brierley J. Thermophilic iron-oxidizing bacteria found in copper leaching dumps. // *Appl. Environ. Microbiol.* 1978. V. 36. P. 523–525
- Brierley J., Norris P., Kelly D., LeRoux N. Characteristics of a moderately thermophilic and acidophilic iron-oxidizing *Thiobacillus*. // *Eur. J. Appl. Microbiol.* 1978. P. 291–299
- Brierley C., Briggs A. Selection and sizing of biooxidation equipment and circuits. / *Mineral processing plant design, practice and control*. Ed. A. Mular, D. Halbe, D. Barret. / SME. 2002. P. 1540–1568
- Bryner L., Beck J., Davis D., Wilson D. (1954). Microorganisms in leaching sulfide minerals. *Industrial Engineering and Chemistry*, 46, 2587–2592.
- Campbell K., Gallegos T., Landa E. Biogeochemical aspects of uranium mineralization, mining, milling, and remediation. // *Appl. Geochem.* 2015. V. 57. P. 206–235
- Cerda J. Gonzalez S., Rios J., Quintana T. Uranium concentrates bioproduction in Spain: a case study. // *FEMS Microbiol. Rev.* 1993. V. 11. P. 253–260
- Colmer A., Temple K., and Hinkle M. (1950). An iron-oxidizing bacterium from the acid drainage of some bituminous coal mines. *Journal of Bacteriology*, 59, 317–328.
- Dwivedy K., Mathur A. Bioleaching – our experience. // *Hydrometallurgy*. 1995. V. 38. P. 99–109.
- Garcia Junior O. Bacterial leaching of uranium ore from Figueira – PR, Brazil, at laboratory and pilot scale. // *FEMS Microbiol. Rev.* 1993. V. 11. P. 237–242.
- Guay R., Silver M., Torma E. Microbiological leaching of a low-grade uranium ore by *Thiobacillus ferrooxidans*. // *Appl. Microbiol. Biotechnol.* 1976. V. 3. P. 157–167
- Hamidian, H., Rezai, B., Milani S. et al. Microbial leaching of uranium ore. // *Asian J. Chem.* 2009. V. 21. P. 5808–5820
- Harrison, V., Gow, W., Iverson, K. (1966). Leaching of uranium from Elliot Lake ore in the presence of Bacteria. *Can. Miner.*, 87, 64–67.
- Holmes D. *Biotechnology in the mining and metal processing Industries: challenges and opportunities*. // *Miner. Metall. Proc.* 1988. V. 5. P. 49–56
- Jianguo Z., Shaoqing C., Sun R., Jing Q. Analysis and evaluation of water coming from several uranium processing areas, treatment of liquid effluent from uranium mines and mills. / Report of a coordinated research project 1996–2000. // IAEA-1419. Vienna. 2004. P. 95–105
- Kawatra S., Natarajan K. *Mineral biotechnology: microbial aspects of mineral beneficiation, metal extraction and environmental control*. / SME. 2001. P. 101–119
- McCready R., Gould W. *Bioleaching of uranium*. / *Microbial mineral recovery*. Ed. H. Ehrlich, C. Brierley. / McGraw-Hill. N. Y. 1990. P. 107–126.
- Munoz J., Gonzalez F., Blazquez M., Ballester A. A study of the bioleaching of a Spanish uranium ore. Part I: A review of the bacterial leaching in the treatment of uranium ores. // *Hydrometallurgy*. 1995. V. 38. P. 39–57
- Polkin, S.I., Adamov, E.V., Panin, V.V. (1982). Technology of bacterial leaching of non-ferrous and rare metals. *M. Nedra*, 288.
- Pronk J., de Bruyn J., Bos P., Kuenen J. Anaerobic growth of *Thiobacillus ferrooxidans*. // *Appl. Environ. Microbiol.* 1992. V. 58. P. 2227–2230
- Rawlings D. *Pure Appl. Chem.* 2004. V. 76. P. 847–859
- Rawlings D. Characteristics and adaptability of iron- and sulfur-oxidizing microorganisms used for the recovery of metals from minerals and their concentrates. // *Microbial Cell Factories*. 2005. V. 4. 15 p.
- Schippers A., Hallmann R., Wentzien S. Microbial diversity in uranium mine waste heaps. // *Appl. Environ. Microbiol.* 1995. V. 61. P. 2930–2935

- Tuovinen O., Bhatti T. Microbiological leaching of uranium ores. // Miner. Metall. Proc. 1999.V. 16. P. 51–60
- Turysbekova G.S. «BioGeotechnology methods for leaching “in situ”». UNECE - 10th Session of Expert Group in resource Management, Paldes Nations, Geneva. https://www.unece.org/fileadmin/DAM/energy/se/pp/unfc_egrm/egrm.10_apr2019/09b_Turysbekova_Gaukhar.pdf
- Turysbekova G. S., Bektay E. K., Meretukov M. E., Bektayev M. E., "Gidrometalurgy of uran", Almaty, KazNRTU, 2020, - 243 p.
- Twardowska I. The role of *Thiobacillus ferrooxidans* in pyrite oxidation in colliery spoil tips. I: Model investigations. // Acta Microbiol. Pol. 1986. V. 35. P. 291–304
- Twardowska I. The role of *Thiobacillus ferrooxidans* in pyrite oxidation in colliery spoiltips. II: Investigation of samples taken from spoil tips. // Acta Microbiol. Pol. 1987. V. 36. P.101–107
- Watling H. Review of biohydrometallurgical metals extraction from polymetallic mineral resources. // Minerals. 2015. V. 5. N 1. P. 1–60

INTEGRATION OF RENEWABLE ENERGY IN THE PRODUCTION SCHEDULING PROBLEM USING GRAVITATIONAL SEARCH ALGORITHM

K. Tolouei¹, E. Moosavi^{1,2*}

¹ *Islamic Azad University, Department of Petroleum and Mining Engineering*

² *Islamic Azad University, Research Center for Modeling and Optimization in Science and Engineering*

(* *Corresponding author: Se.Moosavi@yahoo.com; Se_Moosavi@azad.ac.ir*)

ABSTRACT

The mining industry has traditionally relied on conventional fossil-based fuel sources to meet its growing energy demand. The industry is now tasked with responding to the challenges of increasing fuel prices while commodity prices tighten, resulting in ever-narrowing operating margins and increased opposition from communities to new conventional energy sources. So far, research about such decision making on the use of renewable energy in production scheduling (PS) problem for open pit mining operation is underdeveloped. Due to the conflicting nature of economic and environmental objectives, the PS becomes a multi-objective problem. In this paper, a multi-objective gravitational search algorithm is used to provide Pareto optimal solutions which present the possible tradeoff between the cost and environmental objectives of PS problem. To solve the problem, weighted sum method is applied to convert multi-objective optimization to scalar optimization. The numerical results demonstrate the effectiveness of the proposed approach in solving multi-objective PS problem.

Keywords: Renewable energy, multi-objective, production scheduling, gravitational search algorithm.

INTRODUCTION

The mining industry has traditionally relied on conventional fossil-based fuel sources (diesel, oil, coal, and natural gas) to meet its growing energy demand. The industry is now tasked with responding to the challenges of increasing fuel prices while commodity prices tighten, resulting in ever-narrowing operating margins and increased opposition from communities to new conventional energy sources. The mining sector is expanding into new and often remote locations as a response to increasing demand from growing emerging markets. This often means having to deal with unreliable power supply from the grid and uncertain power prices. In most instances, grid-connected electricity needs to be supplemented with on-site generation, typically large-scale diesel generation, resulting in a dependency on diesel fuel. The more remote the mine, the more likely off-grid power solutions are required.

The sector is experiencing volatility in commodity prices and rising fossil fuel prices, placing margins under pressure. With global demand for energy set to increase 36% by 2035, the industry faces greater energy price increases and volatility. Managing costs sustainably is a priority for the sector. The mining sector is facing growing demand from governments, customers, communities and other key stakeholders to operate in a sustainable manner. Doing so has a growing influence on the mining industry's "social license" to operate (Judd, 2013).

Site-appropriate renewable energy solutions provide cost-competitive energy while delivering greater energy supply reliability and consistency. Reliable access to cost-efficient energy sources is a strategic imperative for mining companies. It is essential to their bottom lines and increasingly, their licenses to operate. In parallel, the sector is challenged with meeting the growing demand for mineral

resources often located in countries and sites where the supply of energy is not always available, reliable or, cost-effective.

Many of the world’s largest mining companies are evaluating greater use of renewable energy plants (a trend set to intensify rapidly) as part of a broader strategy to lock in long-term fixed electricity prices and availability while minimizing exposure to regulatory changes, market pricing, and external fuels.

The main issue of this paper on the penetration of renewable energy into the production scheduling problem has been raised in different studies. This issue attracts attention from both scientific experts and industrial decision-makers. Mining and metal processing are very energy-intensive processes. Moreover, costs for traditional energy sources increase year by year; European mining companies are looking for new solutions for the substitution of fossil energy sources for renewables. The key point is that the costs of RE generation, grid connection and renewable energy integration system and software for implementation to the mining sector deployment are equivalent to those fossil energy sources. However, the implementation of renewable energy for mining needs still has many constraints in European countries.

Renewable Energy Investment in The Mining Industry

The European Union has increasing tendencies for development of renewable energy. It confirms by renewable energy development data and the National Action Plan until 2020 by 20%, 2040 by 40%, and 2050 by 80%. Taking in consideration Germany sample, the share of renewables in final energy consumption has risen steadily in the past decade to a current 12%. In the production of electricity of regenerative share of over 20% is already relatively high. Nevertheless, the electricity is still responsible for more than 40% of Germany's total CO2 emissions today. Therefore, decarbonizing the electricity sector for climate protection reasons has important significance. On the one hand, the mining industry is going to be less attractive in the modern society, who changes of the industrial priorities in favor of sustainable companies. Therefore, mining companies is searching of more sustainable way of production, and fulfill reorientation for renewable energy. In addition, the renewable energy becomes economically attractive year by year, thus motivating miners penetrate of renewable energy instead of fossil one (Judd, 2013).

The transformation of the mining sector is driven by a number of strong converging trends, including:

1. Energy security concerns,
2. A recent history in most countries of rising and volatile energy prices, coupled with a consensus that such trends will continue over the medium-to-long term,
3. The shift to a resource-efficient and low-carbon economy that will ensure community acceptance.

In response, the international mining sector is deploying innovative energy-saving strategies and making substantial industry-wide direct investments into renewable energy infrastructure. At the heart of recent innovations in corporate mining energy strategies lie the construction and acquisition of renewable energy-generating assets, on- and off-site, and the direct contracting for renewable energy through power purchase agreements. Renewable energy plants can be developed, funded, built and operated by third-party developers as captive plants, with the mine committing to purchase the generated electricity at a fixed price over a certain period (see Fig. 1).

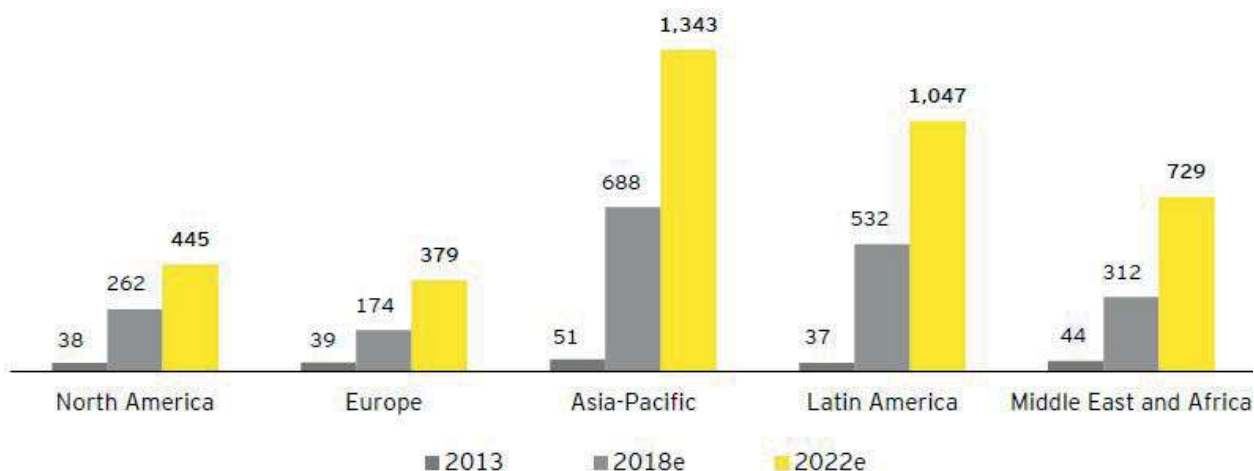


Figure 1. Renewable energy investment in the mining industry

The mining sector derives most of its energy from diesel (41%), natural gas (33%), and grid electricity (22%), with the remainder supplied by a mixture of other refined fuels, coal, LPG, renewables, and biofuels. The percentage contribution from diesel has fallen from 49% to 41% over the last decade and been largely replaced by natural gas and grid electricity, as infrastructure develops and oil prices continue to show volatility (Judd, 2013).

Mining energy intensity – the energy required per tonne of product – is a function of definitions, location, mining type, and processing type. Average energy intensity is estimated at 50.5 kWh/tonne for coal, 10.7 kWh/ tonne for minerals, and 54.5 kWh/tonne for metals, with the majority consumed in diesel equipment and comminution operations. The energy intensity in metals, however, ranges from 13 kWh/tonne for bauxite to 210 kWh/tonne for gold, due largely to differences in on-site beneficiation operations. Energy for metals with low on-site beneficiation, such as bauxite and iron ore, is predominately consumed as diesel for plant involved in extraction and transport. Energy for metals with high on-site site beneficiation, such as copper and gold, is predominantly consumed as electricity (see Fig. 2).

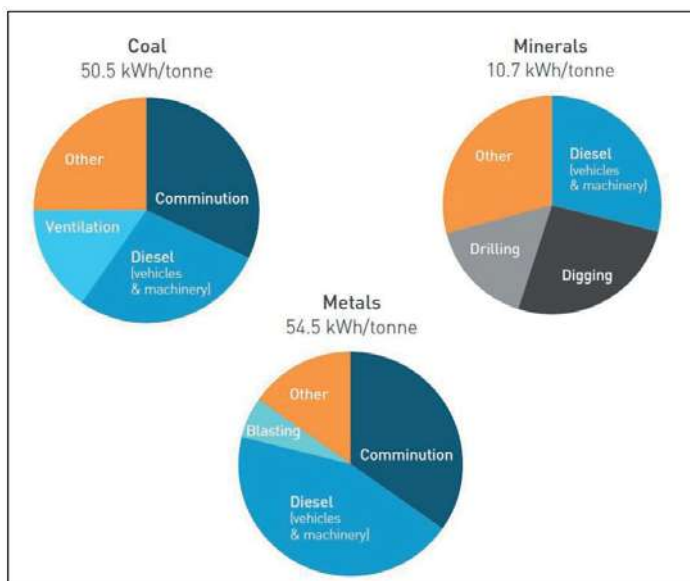


Figure 2. The estimated mining energy intensity and three most energy intensive operations for coal, metals, and minerals.

Integration of Renewable Energy in The Production Planning Problem

Major real-world problems utilize the optimization of several objectives, which are often conflicting in nature. A general, multi-objective optimization problem with nm decision variable, mo objectives and several equality and inequality constraints can be formulated as follows:

$$(1) \quad \text{Min } Z = (Z_1, Z_2, \dots, Z_{mo})$$

Subject to:

$$(2) \quad g_j(x), \quad j = 1, 2, 3, \dots, K$$

$$(3) \quad h_k(x), \quad k = 1, 2, 3, \dots, L$$

Where, K and L are number of equality and inequality constraints respectively. $x = (x_1, x_2, \dots, x_{nm}) \in X$ is the decision vector and X is the parameter space; $y = (y_1, y_2, \dots, y_{mo}) \in Y$ is the objective vector and Y is the objective space. The set of all Pareto-optimal solutions in the decision variable space is called as Pareto optimal set (Abido 2003, 2006). The corresponding set of objective vector is called as Pareto-optimal front or optimal trade-off solution.

Gravitational Search Algorithm

The GSA, a new optimization algorithm based on the law of gravity, was introduced by Rashedi et al. (Roy 2013) in (2009). In the proposed algorithm, agents are considered as objects and their performance is measured by their masses. Masses of the agents are directly proportional to their fitness function. During each iteration, masses attract each other due to gravitational force of attraction acting on them and these forces causes a global movement of all agents toward the agents with heavier masses. A heavier mass means a more efficient agent. Suppose the system with N agents, the position of i th agent is defined as:

$$Y_i = (y_i^1, y_i^2, \dots, y_i^k, \dots, y_i^\tau) \quad \forall i \in N \quad (4)$$

Where, y_i^k is the position of i th agent in the k th dimension, τ is the dimension of search space. The gravitational force acting on i th agent due to j th agent at t th iteration is given as:

$$F_{ij}^k(t) = G(t) \times \left(\frac{M_j(t) \times M_i(t)}{ED_{ij}(t) + \varepsilon} \right) \times (y_j^k(t) - y_i^k(t)) \quad (5)$$

Where, ε is a very small constant, $ED_{ij}(t)$ is the Euclidian distance between the i th agent and the j th agents which is defined as:

$$ED_{ij} = \|y_i(t), y_j(t)\|_2 \quad (6)$$

$G(t)$ is the gravitational constant at time t , which is initialized at the beginning and reduces with time to control the search accuracy and is given by:

$$G(t) = G_o \times e^{-\alpha t / Iter_{max}} \quad (7)$$

Where, G_o is initial value of gravitational constant, α is constant term and $Iter_{max}$ (=100) is the maximum number of iterations. The total force acting on the i th agent is given by:

$$F_i^k(t) = \sum_{\substack{j=1 \\ j \neq i}}^{Kbest} rand_j \times F_{ij}^k(t) \tag{8}$$

number in interval [0,1], $Kbest$ is the set of l number of agents with heavier masses and best fitness value, and is evaluated in such a way that it decreases linearly with time and at last iteration, its value becomes 2 % of the initial number of agents. According to Newton’s law of motion, the acceleration of the i th agent at the t th iteration in k th direction is given as:

$$A_i^k(t) = \frac{F_i^k(t)}{M_i(t)} \tag{9}$$

$$M_i(t) = \frac{m_i(t)}{\sum_{j=1}^N m_j(t)} \quad \text{and} \quad m_i(t) = \frac{fit_i(t) - worst(t)}{worst(t) - best(t)} \tag{10}$$

Where, $fit_i(t)$ is the fitness value of i th agent at the t th iteration. The iterative best (t) and worst (t) values are given as:

$$best(t) = \min(fit_i(t)) \quad \text{and} \quad worst(t) = \max(fit_i(t)) \quad \forall i \in N \tag{11}$$

The updated velocity and position of each agent in the next iteration are calculated as:

$$v_{ik}(t+1) = rand_i \times v_{ik}(t) + A_{ik}(t) \tag{12}$$

$$y_{ik}(t+1) = y_{ik}(t) + v_{ik}(t). \tag{13}$$

CONCLUSIONS

In this paper, gravitational search algorithm (GSA) is used to provide Pareto optimal solutions. The Pareto-optimal solutions present the possible trade-off between the cost and emission. To solve the problem, weighted sum method is applied to convert multi-objective optimization to scalar optimization. The proposed GSA is combined with pseudo-code operators to create new set of individuals from higher potential individuals and further refines them to provide near optimal solution. The feasibility and performance of the proposed approach is demonstrated on a test system. The results obtained using the proposed approach are encouraging and it is found that by efficiently utilizing the production scheduling considering renewable energy sources, the total operating cost and emission of the system can be reduced significantly. The intermittency of solar and wind power generations is not considered in this paper, however, this can be considered as different of wind and solar power generations scenarios.

REFERENCES

Abido, M.A. (2003). Environmental/economic power dispatch using multiobjective evolutionary algorithm. *IEEE Trans Power Syst* 18(4):1529–1537.

Abido, M.A. (2006). Multiobjective evolutionary algorithms for power dispatch problem. *IEEE Trans Evol Comput* 10(3):315–329.

Judd, E. (2013). Building a wind farm in arctic conditions: Rio Tinto's Diavik mine, Canadian Clean Energy Conferences, Renewables and Mining.

Judd, E. (2013). Renewable Energy & Mining, Renewables and Mining, accessed via renewablesandmining.com/blog/, 15 January 2014).

Judd, E. (2013). Solar PV for Codelco and Collahuasi, Canadian Clean Energy Conferences, Renewables and Mining.

- Roy, P.K. (2013). Solution of unit commitment problem using gravitational search algorithm. *J Electr Power Energy Syst* 53:85–94.
- World Energy Outlook. (2013). OECD/IEA Power sector cumulative investment by type and region in the New Policies Scenario, 2013-2035.

INVESTIGATION OF ENRICHMENT OPPORTUNITIES OF ESKİŞEHİR BEYLİKAHIR REGION BARITE AND FLUORITE WITH PHYSICAL METHODS

ESKİŞEHİR BEYLİKAHIR BÖLGESİ BARİT VE FLORİT'İN FİZİKSEL YÖNTEMLER İLE ZENGİNLEŞTİRME OLANAKLARININ ARAŞTIRILMASI

E. Baştürkçü^{1,*}, C. Şavran¹, A. E. Yüce¹, H. Topal¹

¹İTÜ, Maden Fakültesi, Cevher Hazırlama Mühendisliği Bölümü
(*Corresponding Author: tanisali@itu.edu.tr)

ABSTRACT

As it is known, many studies have been carried out on the beneficiation of rare earth elements containing barite and fluorite in Eskişehir Beylikahır region. When the results of the previous studies are investigated, it is seen that although partially successful results have been obtained, a full enrichment has not been achieved yet. In this study, the main aim was the investigation of barite-fluorite enrichment by gravity separation techniques after the separation of high content rare earth products. Primarily, mechanical attrition on the original sample was applied based on literature information. 15 minutes with a 75% solids ratio was determined as the optimum conditions. According to the chemical analysis results, it was observed that the rare earth element content increased at -38 µm, 85-90% of REEs accumulated and total rare earth oxides (REOs) content increased up to 10%. By this information, +38 µm materials were ground to the different sizes for gravity experiments. As a result of the test at -150+38 µm size fraction, barite was obtained with 85.6% content and 88.3 % recovery. On the other hand, CaF₂ pre-concentrate containing 62.9% was obtained with a recovery of 90.8%. Research continues within the scope of the project, and the findings obtained at this stage will be evaluated to obtain optimum conditions for both barite and fluorite.

Keywords: Barite, fluorite, rare earth elements, Beylikahır

INTRODUCTION

Barite (BaSO₄) is the most common mineral of the Barium element. Barite is the heaviest of the non-metallic minerals. High density (4.45 gr/cm³), less abrasiveness (Mohs hardness 3-3.5), chemical stability under high heat and pressure, low solubility in water and acids, lack of magnetic properties and affordable cost of barite have enabled its increasingly widespread use in a variety of industries. More than 80% of barite is used in drilling fluids (Afolayan et al., 2021). Paint, glass, construction, automotive, paper, plastic, pesticides, chemistry, and ceramic industries are the other important sectors that barite is used.

Turkey has a large number of barite deposits; however, the most important ones are concentrated in four regions which are Alanya-Gazipaşa, Konya-Isparta, Muş, and Kahramanmaraş. Apart from these, Giresun, Kocaeli, and Kütahya districts have also significant barite deposits. According to a study conducted by the United States Geological Survey, all resources of barite found on Earth are about 2 million tons, but the proven reserves of barite are about 740 million tons. The graph containing reserve distributions by country is given in Figure 1.

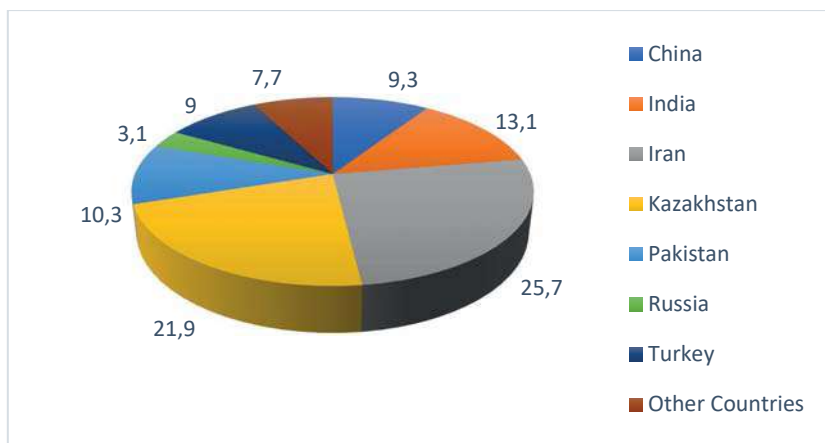


Figure 1. Distribution of Barite Reserves by Country in 2020, %

When annual production data by country is analyzed according to the same report, the annual production of the 11 countries with the largest global barite production in 2019 and 2020 is graphically shown in Figure 2.

China is at the top of the list, accounting for more than 30% of global barite production in 2019 and 2020, while Turkey is in 8th place with 2.82%. It is ranked 9th in 2020, with a production rate of 1.73% (USGS 2021).

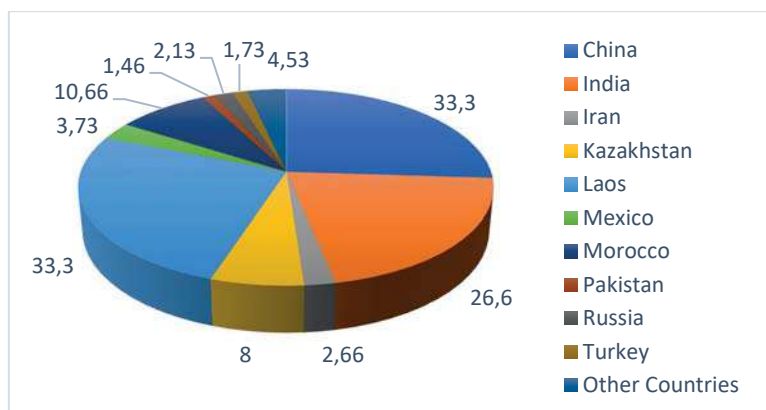


Figure 2. Distribution of World Barite Production by Country in 2020 (%)

Gravity and flotation are the most common processes for barite enrichment. The common gravity separation device is the jig for barite beneficiation if the particle liberation size is coarser (>2 mm). When the size becomes smaller, a shaking table and other gravity separators can be used.

Using Gravity enrichment methods such as jig, shaking table, and Multi Gravity Separator (MGS) have been investigated in the literature for barite concentration.

In the study conducted by Bhattacharyya and Singh (2011), the barite ore particle size was reduced below 74 μm. In the enrichment experiments carried out using MGS, the parameters such as pulp density, slope, washing water ratio and rotational speed of the feed were examined. According to the optimum data obtained as a result of the experiments, it was possible to concentrate $BASO_4$ with a recovery of about 53% and a content of more than 90%.

Fluorite (CaF₂), is composed of 51.3 percent calcium and 48.7% fluorine when pure. It is a crystalline mineral with a Mohs hardness of 4, a specific gravity of 3.18 g/cm³, a melting point of 1330 oC, and a color range of purple, green, blue, yellow, white, pink, brown, bluish-black and it has transparent translucent. Fluorite has risen to the top of the world's strategic minerals list, and many countries are investigating its reserves and production. Fluorite is used in a variety of industries, including cement, glass, ceramics, metallurgy, refrigeration, aviation, medicinal, and chemical. Many countries regard fluorite to be a strategic resource due to the growing need for development in related industries (Gao, 2021). The primary areas of application are HF production, iron and steel, and aluminum. Fluorite content in these outputs is predicted to be between 85 and 95 percent. This ratio is expected to be at least 98% for technical quality HF production.

Considering the methods used in the enrichment of fluorite ore, physical enrichment methods are the first. Jigging, shaking tables and heavy media separators are the most preferred devices. The main reason for choosing jig and shaking table is that the density difference between fluorite and gangue minerals is too large. Yüce et al. (1992) employed a shaking table to conduct concentration experiments on fluorite and barite from the Beylikahır-Eskişehir complex ore, which included 34.7% CaF₂, 32.2% BaSO₄, 2.70% rare earth elements, and 0.11% ThO₂. For the -0.3 mm sample, shaking table tests were performed. A barite concentrate containing 85.5% BaSO₄ with a recovery of 55.8% and a fluorite pre-concentrate containing 63.2% CaF₂ with a recovery of 64.1% were obtained.

In addition, depending on the gangue mineral, methods such as calcination or flotation to liberate ore from calcite and getting fluorite concentrate are the alternatives (Güngör, 1967).

It is assumed that the fluorite resources found throughout the world are 5 billion tons (2021). It is also known that there are many fluorite deposits in Turkey. The main deposits are located at Eskişehir, Kırşehir, Sivas and Yozgat.

The production amounts of the 14 countries that ranked highest in the world fluorite production in 2019 and 2020 are shown in Table 1. China is the leading country in production, and Mexico is in second place.

In our country, the reserve studies are being carried out by MTA General Directorate in an area of 15 km² between Kızılcaören, Karkın and Okçu villages, 40 km northwest of Eskişehir province Sivrihisar district, with an average of 0.212% ThO₂, 37.44% CaF₂, 31.04% BaSO₄ and Beylikahır REE minerals reserve containing 3.14% rare earth oxide (MTA, 2017).

This deposit, which is the source of REE and Th in Eskişehir-Kızılcaören, has complex mineralization and contains fluorite, barite and bastnazite as valuable minerals. As a result of the reserve studies carried out between 1980-84, it was determined that 11.368.075 tons of Fluorite, 9.424.424 tons of Barite and 953.587 tons of REO (CeO₂, La₂O₃, Nd₂O₃) were found in Eskişehir Beylikahır region.

Table 1. Fluorite Production Data (x10³ tons) for 2019-2020 by country

Countries	2019	2020
China	4300	4300
Mexico	1230	1200
Mongolia	718	720
South Africa	210	320
Vietnam	238	240
Spain	139	140
Pakistan	100	100

Canada	80	100
Morocco	88	88
Kazakhstan	88	77
Iran	55	55
Burma	53	53
Germany	50	50
Other Countries	107	110
Total	7460	7600

Pilot plant installation works have been started by ETI Maden for the concentrated production of Barite, Fluorite and REE minerals and R&D studies for increasing recovery are ongoing.

The possibilities of obtaining Fluorite and Barite minerals in high content in the Eskişehir-Beylikahir Region as saleable concentrates were investigated in this study, which would be carried out in light of data obtained from the literature.

MATERIAL & METHOD

The sample used in this study was taken from Eskişehir-Beylikova region. The ore contains barite, fluorite, rare earth minerals and also Th minerals basically.

For the sample preparation, after crushing & classification below 10 mm, as it is explained in literature, scrubbing was applied on sample. The scrubbing conditions were investigated. Time, and solids ratio were the parameters that affect the scrubbing efficiency. 60% and 75% solids ratios, 15 min-30 min scrubbing times were investigated and the recovery of scrubbing was controlled with particle size distribution.

In order to determine the beneficiation method for barite and fluorite by taking REE content into consideration, chemical analysis of the representative raw ore sample was performed on various particle size fractions. The analyses were carried out using the X-ray fluorescence method.

Table 2. Chemical composition of the run-of-mine sample

CaF ₂	BaSO ₄	NTEO	Fe ₂ O ₃	K ₂ O	MgO	MnO	SO ₃
36,1	32,4	6,2	3,1	0,4	0,7	0,8	6,3
Na ₂ O	P ₂ O ₅	SiO ₂	SrO	TiO ₂	Al ₂ O ₃	LOI	CaO
0,3	0,9	3,9	0,4	0,2	1,1	5,9	1,3

Regarding Table 2, the sample contained barite with a content of 32,4% and fluorite content was determined as 36.1%. The sample also contained 6,2 % rare earth oxides (REOs).

Separation of barite-fluorite was performed using Mozley table. Low REE containing fraction of +38 µm was subjected to these tests. In order to investigate the effect of particle size, sample was ground to -212, -150, -106 µm as a closed circuit controlling with 38 µm screen.

The experimental conditions of the gravitational tests using Mozley table are listed as follows:

- washing water : 2 L/min,
- amplitude : 8 mm,
- slope : 3°
- particle size fraction : -212+38, -150+38, -106+38 µm.

The products obtained from the beneficiation tests were analyzed to evaluate the recovery. In order to explain the reason of losses for barite and fluorite, SEM (scanning electron microscope) visuals were discussed. These images were taken by MTA (General Directorate of Mineral Research and Exploration).

RESULTS & DISCUSSION

In this part of the study, scrubbing and gravity separation tests are presented. The performance of the scrubbing tests was evaluated regarding the particle size distributions of the products. Following the scrubbing application, Mozley table tests were performed on the particle size fractions of -212+38 μm , -150+38 μm , and -106+38 μm .

Scrubbing Tests

Application of scrubbing method provides not only a homogeneous particle size distribution (PSD) of the raw ore sample, but also it is a significant preparation/preconcentration stage for many types of ores. In our case, PSD of the raw ore sample was determined, while P_{80} was found as 1.8 mm. 16.8% of the material was accumulated in the -38 μm fraction (Figure 4).

When the sample was scrubbed for 15 min at a solids ratio of 75%, P_{80} size was decreased to 0.7 mm and the mass of -38 μm fraction increased to 35.2%. Although similar outcomes were obtained at 60% solids ratio for scrubbing times of 15 and 30 min, an application with higher solids ratio was found to be rational considering capacities at industrial scale.

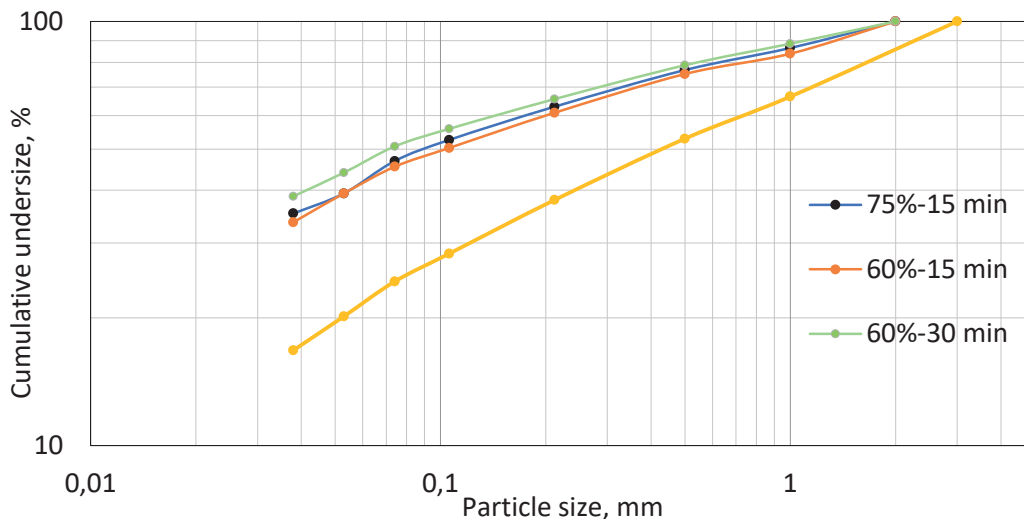


Figure 4. Particle size distribution of the raw ore sample and scrubbed products

Gravity Separation Tests

Following determination of the scrubbing conditions, gravitational separation was investigated on certain particle size fractions. The maximum sizes were arranged to -212, -150, and -106 μm . At these particle size fractions; many devices including shaking table and centrifugal separators may be utilized. However, Mozley table was used in the tests to make prediction, whether gravity separation worked. After removing the fine particle size fraction of -38 μm for each group, the Mozley table tests were carried out.

Regarding Table 3, 4, and 5, it was an attractive finding that 80-90% of the REEs were accumulated in the fine fraction. But nearly half of barite and fluorite were found in the coarser fractions. The results revealed that there can be a potential separation of barite and fluorite considering REEs.

- For the size fraction of -212+38 µm; it was determined that 80-85% of the REEs were accumulated in the fine fraction. The heavy product contained 80.3% BaSO₄ and 15.5% CaF₂. Also, the light product included 62.3% CaF₂.
- For the size fraction of -150+38 µm; 10-15% of the REEs were remained in the +38 µm fraction. A heavy product was obtained with 85.6% BaSO₄ and 9.7% CaF₂ grades.
- For the size fraction of -106+38 µm; quite similar results were achieved comparing with the results of -150+38 µm group.

As a result of gravity separation, it was concluded that -150+38 µm size fraction was determined as the optimum range for gravity separation for further studies. While 45.6% of barite was taken in the +38 µm fraction, 88.4% of it was obtained as heavy product. It was found out that 86% pure barite was achieved with fluorite impurity of 10%. It is known that 90-92% purity is required for potential usage in industries such as drilling mud, paint, and concrete aggregate. To reveal the reason of the insufficient enrichment, mineralogical analysis was performed.

Table 3. Metallurgical balance of the test conducted on -212+38 µm size fraction

-212+38 µm	Weight	Ce ₂ O ₃		La ₂ O ₃		Nd ₂ O ₃		Pr ₂ O ₃		BaSO ₄		CaF ₂	
		C, ppm	D, %	C, ppm	D, %	C, ppm	D, %	C, ppm	D, %	C, %	D, %	C, %	D, %
Heavy	20.8	12438	10.0	8594	7.6	1361.0	8.5	737.9	9.5	80.3	47.0	13.9	8.0
Light	26.9	7110	7.4	4797	5.5	852.3	6.9	430.0	7.1	8.2	6.2	56.1	41.8
-38 µm	52.2	40865	82.6	39175	86.9	5384.1	84.6	2584.8	83.4	31.9	46.8	34.6	50.1
Total	100.0	25853	100.0	23546	100.0	3325.5	100.0	1619.7	100.0	35.6	100.0	36.1	100.0

C: Content, D: Distribution

Table 4. Metallurgical balance of the test conducted on -150+38 µm size fraction

-150+38 µm	Weight	Ce ₂ O ₃		La ₂ O ₃		Nd ₂ O ₃		Pr ₂ O ₃		BaSO ₄		CaF ₂	
		C, ppm	D, %	C, ppm	D, %	C, ppm	D, %	C, ppm	D, %	C, %	D, %	C, %	D, %
Heavy	15.9	11364	6.8	8037	5.1	1271.2	5.9	695.1	6.7	85.6	40.3	8.7	3.8
Light	24.3	7665	7.0	5576	5.4	944.7	6.6	476.2	6.9	7.4	5.3	56.6	37.5
-38 µm	59.8	38441	86.2	37298	89.4	5065.8	87.5	2409.4	86.4	30.8	54.4	36.0	58.7
Total	100.0	26651	100.0	24930	100.0	3460.1	100.0	1666.6	100.0	33.9	100.0	36.7	100.0

Table 5. Metallurgical balance of the test conducted on -106+38 µm size fraction

-106+38 µm	Weight	Ce ₂ O ₃		La ₂ O ₃		Nd ₂ O ₃		Pr ₂ O ₃		BaSO ₄		CaF ₂	
		C, ppm	D, %	C, ppm	D, %	C, ppm	D, %	C, ppm	D, %	C, %	D, %	C, %	D, %
Heavy	15.5	10981	6.7	7820	5.1	1246.6	5.9	677.3	6.6	86.8	38.8	7.6	3.2
Light	22.3	7536	6.6	5471	5.1	1063.1	7.2	503.5	7.1	7.4	4.8	57.8	35.5
-38 µm	62.2	35376	86.7	34317	89.8	4602.2	86.9	2200.3	86.3	31.4	56.4	35.8	61.3

Total	100.0	25392	100.0	23783	100.0	3293.6	100.0	1586.2	100.0	34.6	100.0	36.3	100.0
-------	-------	-------	-------	-------	-------	--------	-------	--------	-------	------	-------	------	-------

Mineralogical Evaluation

A mineralogical investigation was done on the sample of -150+38 μm size fraction to observe particle liberation and possible mineral phase associations. In Figure 5, there are two images taken at a scale of 100 and 200 μm . It was found out that most of the barite and fluorite minerals were well liberated with relatively coarse grain sizes. However, associated particles were observed rarely.

Therefore, the reason for the insufficient enrichment of barite- fluorite could not attributed to only particle liberation, it could be necessary to apply additional gravitational forces. In this concept, the recovery and grades could be enhanced by application of centrifugal forces.

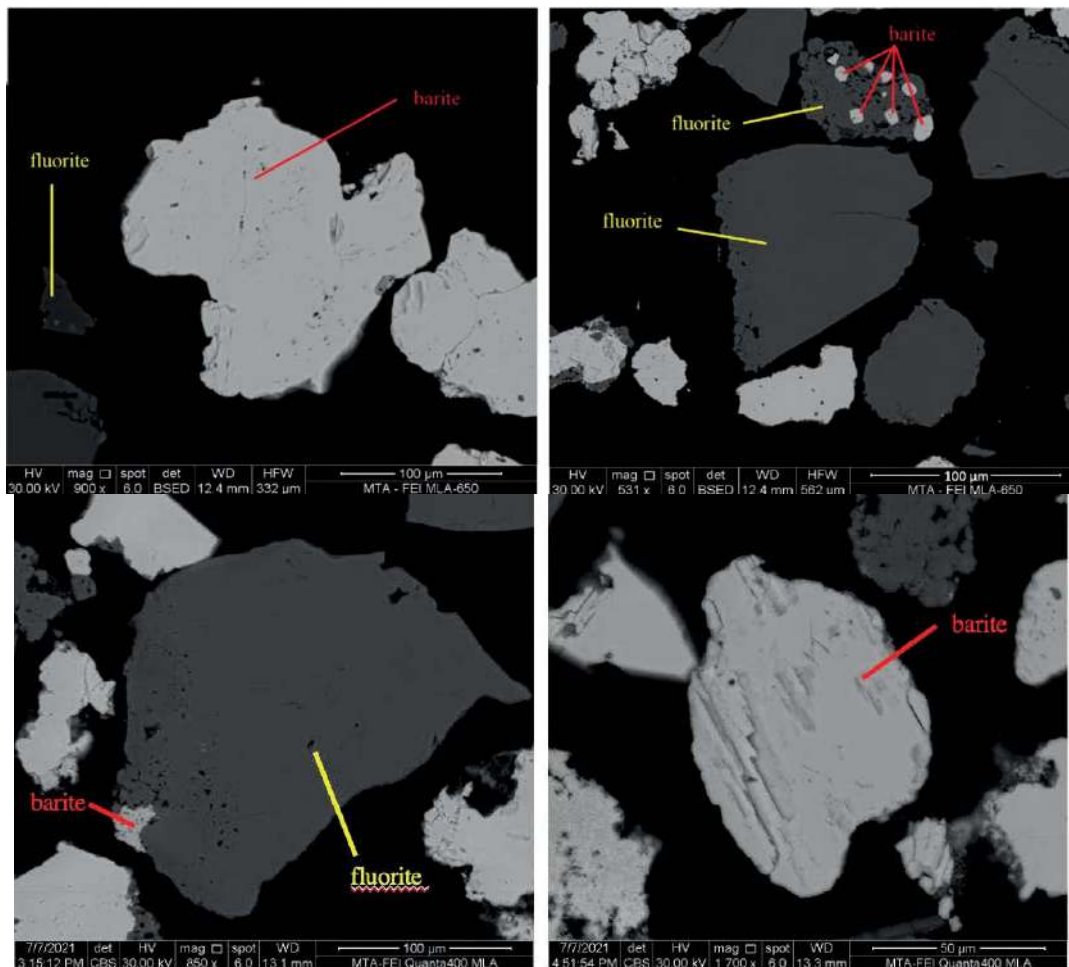


Figure 5. SEM-BSE images of -150+38 μm size fraction

CONCLUSION

Enrichment of fluorite and barite minerals of the Eskişehir-Beylikahir sample was aimed in this study. Due to the results of the preliminary experiments, general outcomes are listed as follows:

- The sample contained barite with a content of 32.4 % and fluorite content was determined as 36.1%. REE oxides were found as 6.2%.

- Following scrubbing the raw ore sample, P_{80} size was decreased from 1.8 mm to 0.7 mm. Also, the mass of -38 μm fraction increased from 16.8 to 35.2%.
- The optimum scrubbing conditions were determined as solids ratio of 75% and scrubbing time of 15 min.
- The scrubbed samples were divided into two fractions of -38 μm and +38 μm . While the finer fraction contained nearly 90% of the REEs, coarser fraction included 50-60% the barite and fluorite minerals.
- To predict the performance of gravity separation, Mozley table tests were carried out as a preliminary study. -150+38 μm size fraction was determined as the optimum.
- A heavy product was obtained with 85.6% BaSO_4 and 9.7% CaF_2 content.
- Since 90-92% purity is required for potential usage in drilling mud, paint, and concrete aggregate industries, improvement potential for the gravity separation was examined.
- Therefore, -150+38 μm size fraction was subjected to mineralogical analyses. According to the results, it was observed that most of the barite and fluorite particles were liberated enough.
- It is thought that gravitational force using conventional gravity units is not enough to separate barite and fluorite. Centrifugal separation would be suggested as a strong alternative and further tests are planned.

In conclusion, a preliminary flowsheet is established including a combination of scrubbing and gravity separation. While the particle size fraction of -38 μm is separated, +38 μm fraction was ground below 150 μm and classified as -150+38 μm . It is considered that when this group material is subjected to gravitational separation using centrifugal devices, it is strongly possible to separate barite and fluorite with high grade and recovery. The final evaluation using centrifugal gravitation techniques will be accomplished based on the ongoing project studies.

REFERENCES

- Afolayan, D., Adetunji, A., Onwualu, A., Ogolo, Oghenerume Amankwah, R. (2021), Characterization of barite reserves in Nigeria for use as weighting agent in drilling fluid, *Journal of Petroleum Exploration and Production*, 11. 1-22. DOI: 10.1007/s13202-021-01164-8.
- Bhattacharyya, P., Singh, R. (2011), Generation of Value Added Product by Beneficiation of Barite Waste, *Conference Proceedings, XII International Conference on Mineral Processing Technology MPT-2011, India*.
- Gao, Z., Wang, C., Sun, W., Gao, Y., Kowalczyk, P. (2021), Froth flotation of fluorite: A review, *Advances in Colloid and Interface Science*, 290. 102382. DOI: 10.1016/j.cis.2021.102382.
- Güngör, G. (1967), Düşük Tenörlü Fluorit Cevherinin Zenginleştirilmesi, *Bilimsel Madencilik Dergisi*, 6(2), 71-82, Retrieved from <http://www.mining.org.tr/tr/pub/issue/32707/362858>
- MTA (2017). Dünya ve Türkiye’de Nadir Toprak Elementleri (NTE), Ankara.
- U.S. Geological Survey, 2021, Mineral Commodity Summaries 2021, U.S., <https://doi.org/10.3133/mcs2021>.
- Yüce, A.E., Doğan, M.Z., Önal, G., İpekoğlu, B., (1992), The Beneficiation of Fluorite and Barite from Beylikahır-Eskişehir Complex Ore”, *Aufbereitungs-Technik*, Nr:33, pp:274-281, 1992.

INVESTIGATION OF FRACTURE AND MECHANICAL PROPERTIES OF SEMI-CIRCULAR BENDING SHOTCRETE SPECIMENS USING 3D PRINTED MOLDS

C. Karataş Batan^{1,*}, M. Erkyaoğlu¹

¹ *Middle East Technical University, Mining Engineering Department*
(*Corresponding Author: cerenb@metu.edu.tr)

ABSTRACT

Core samples can be considered as inherently available specimens for site investigation in rock engineering problems. The geometry of core samples is commonly beneficial for preparation of specimens for rock mechanics tests. However, the collection and preparation of rock samples also pose challenges for certain types of experiments, especially for fracture mechanics tests. The accuracy of fracture mechanics experiments is of great importance for the design of various applications. The preparation of these samples can be considered challenging due to the potential human errors during crack opening and flattening of the specimen surface. Available 3D printer technology can be useful in overcoming such difficulties. This study focuses on the preparation of Semi-Circular Bending (SCB) specimens for three-point bending in fracture tests. SCB sample molds were printed using 3D technology and samples were prepared by shotcrete mixture poured into the 3D printed molds. In this study, it is aimed to minimize sample preparation errors by using 3D printer technology. As a result, it was observed that the fracture and mechanical properties of the molded shotcrete by using 3D printer technology provided accurate results when compared to conventional sample preparation.

Keywords: Rock mechanics, 3D printer, fracture mechanics, molded shotcrete, Semi-Circular disc geometry

INTRODUCTION

Mining activities play a major role for developing countries according to primary energy generation and raw material supply. The increasing demand for energy resources of modern societies necessitate mining activities to be sustained. For these reasons, utilization of innovative technologies in the mining industry related to all stages of production including the engineering design studies performed prior to operation is essential.

Rock mechanics has an important role in tunneling activities and underground mining. Rock mass surrounding permanent or temporary structures in mining can be shafts, transportation galleries, production chambers, and other that might possess flaws and fractures. Improving the stability and maintaining the strength of surrounding rock is one of the main requirements of mining and construction projects. Support systems are designed and selected to meet this requirement where shotcrete is a major supporting unit for tunnel constructions, underground openings in mining applications and many other areas. The cracking of shotcrete is generally caused by a beam action. Furthermore, shrinkage of the shotcrete results in tensile loading that leads to the propagation of cracks. Cracks in the shotcrete pose a serious threat to the support system. Considering this phenomenon, the problem can be handled by performing valid fracture mechanics related experiments. Fracture mechanics experiments are of great importance in the realization of these activities. The accuracy of the fracture mechanics test results and the design criteria made according to these results ensure the continuity and reliability of mining and tunneling activities. The geometry of core samples is enabling rock sample preparation for fracture mechanics testing to be performed in laboratory

environment. However, the collection and preparation of rock samples also poses challenges for certain types of experiments. During the preparation of the samples required for these tests, both the creating flat surface stage and the errors caused by the person during the crack opening affect the test results. In this research, it is aimed to minimize these errors by using 3D printer technology in sample preparation and reduce time and costs related to sample preparation. The objective of this study is to investigate the fracture mechanism of shotcrete and to understand the crack behavior completely.

Available studies in the literature about this research field indicate that fracture properties, cracks and failure mechanisms of concrete have been investigated with different geometries by various researchers.

Griffith is one of the most important research in the field of fracture mechanics, as Kaplan (1961) discussed the Griffith crack theory of fracture strength. Tests on concrete beams were performed to determine the critical strain-energy-release rate. Fictitious crack analysis and crack growth in concrete (Hillerborg et al, 1976), expressing the fracture toughness of plain concrete through the specimen-size independent parameters (Nallathambi and Karihaloo, 1986), effective notch in three-point bend notched specimens used for the determination of the fracture toughness of plain concrete (Nallathambi and Karihaloo, 1988), the size effect on explaining cracks and failure mechanism in concrete and/or concrete structures (Bazant and Kazemi, 1990) and the peak load method for determining material fracture parameter (Tang, Ouyang and Shah, 1996) are some of the pioneering research studies focusing on fracture mechanism of concrete.

Jenq and Shah (1985) suggested a simple method to calculate size- independent fracture toughness parameter of concrete. The authors predicted the load crack mouth opening displacement on beam type concrete by using this constant K_{Ic} criterion.

Perdikaris et. al. (1986) studied four-point bending (SENB) method to investigate the effect of fatigue on fracture toughness of concrete. It was stated that the fracture toughness under fatigue shows an increasing trend with increasing crack length.

Wang et. al. (2010) developed a new test method for determining the fracture toughness of concrete materials. The method was defined as the spiral notch torsion test (SNTT) where the estimated K_{Ic} of the tested samples was found to be $MPa\sqrt{m}$.

Zhao et. al. (2020) examine the influence of the weight percentage of large aggregates with maximum size d_{max} on fracture toughness of concrete. Three-point bending specimens with different crack/depth ratios (0.1, 0.2, 0.3 and 0.4) were used in this study. The result of this study revealed that the peak load for the 3-p-b beams are affected by the amount of large aggregates with d_{max} .

This research aims to contribute to the current studies in rock mechanics literature by introducing the potential of 3D printing technology for sample preparation. In this context, it will also provide an opportunity to utilize available technology to improve the existing knowledge related to fracture mechanism of concrete.

NUMERICAL AND EXPERIMENTAL STUDY

Numerical and experimental work for three-point bending test specimens are covered within the scope of the methodology of this study. The numerical computation of stress intensity factor (SIF) in the models was performed in ABAQUS 2019. Semi-circular disk geometry (SCB) were modeled in three dimensional (3D) with ABAQUS. The numerical computation was completed in two-stages as before and after the experimental study. The first stage of the numerical computation was done to define loading configuration at the crack tip. To reach this aim, the unit load was applied to the model geometry. The

loading condition was defined for three different points whereas the second stage was completed after the experiments were performed. In this stage, fracture loads acquired from experimental work were applied to the numerical models that were created before. The mode I fracture toughness was computed for shotcrete specimens that were tested with the MTS 815 system that provides displacement-controlled loading.

The SCB specimen geometry modeled in 3D has a loading span length of $S/R=0.50$ The crack length was fixed as 10 mm resulting in a/R ratio of 0.20. The 100 mm diameter SCB geometry with 50 mm thicknesses ($t/R=1$) can be seen in Figure 1 illustrating the geometric details.

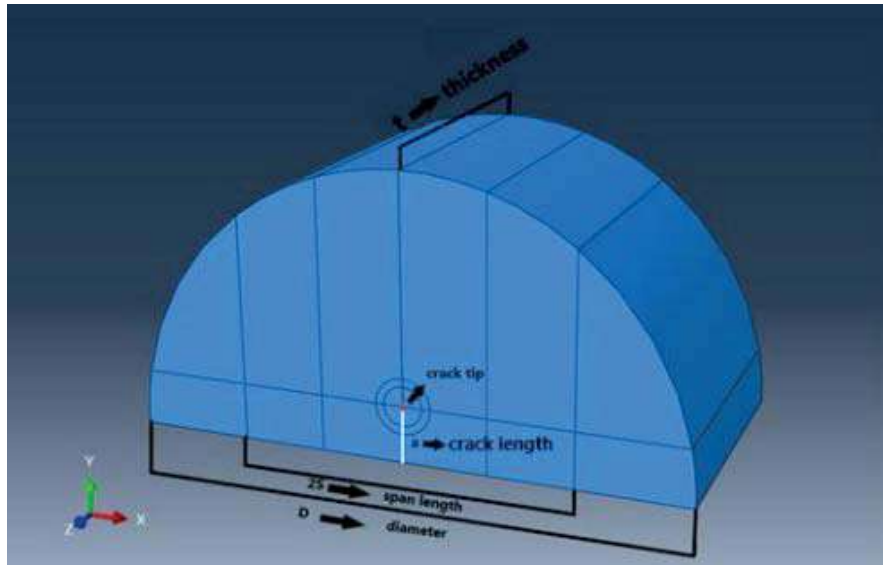


Figure 1. Undeformed and deformed shape of the SCB model geometry

The stress intensity factor (K_I) of SCB model geometry for mode I is calculated as $90.64 Pa\sqrt{m}$. The dimensionless stress intensity factor (Y_I) of SCB model geometry for mode I is formulated by the following equations;

$$Y_I = \frac{K_I}{\sigma_0\sqrt{\pi a}} \tag{1}$$

$$\sigma_0 = \frac{P}{2Rt} \tag{2}$$

According to these formulas the dimensionless stress intensity factor (Y_I) of SCB is calculated as 2.56. The deformed shape and undeformed shape geometries are shown in Figure 2.

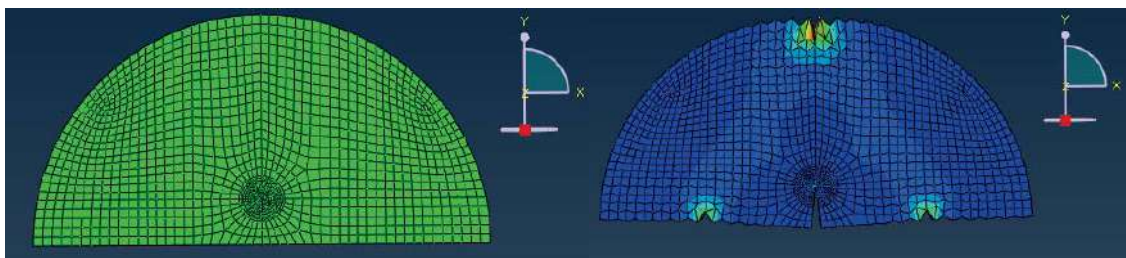


Figure 2. Undeformed and deformed shape of the SCB model geometry

Shotcrete molds were manufactured with a 3D printer to prepare samples in the desired size and geometry for experimental works. The ingredients of the mixture are 450 g cement, 225 g water, 4.5 g admixture (plasticizer) and 1664 g aggregates. The mixture of a 0.25 dm³ volume was poured into the 3D molds after mixing with a Hobart N50 laboratory type mixer. Concrete sample was prepared as a shotcrete representation. The behavior of shotcrete is actually different due to the spray effect. The procedure to prepare the concrete samples can be summarized as follows; the aggregate and cement are mixed for 30 seconds at low speed which is followed by the addition of water and admixture into the mixer container. All materials are mixed first at low speed for 30 seconds and then at high speed for another 30 seconds. After the mixture was prepared, it was filled into the 3D molds and 7 days of time of was performed. Figure 3 shows a sample 3D mold of the SCB samples.



Figure 3. 3D mold of SCB and SCB sample

Static deformability tests were performed on shotcrete samples to predict and determine the mechanical behavior. The specimens were kept under load until failure to obtain the uniaxial compressive strengths (UCS), Elastic Modulus and Poisson’s ratio values. The loading procedure was defined with a rate of 0.0005 mm/s. Figure 4 shows static deformability test configuration, samples before and after the test.





Figure 4. Static deformability test configuration, before and after test

The values of the uniaxial compressive strength, Elastic Modulus, and Poisson’s ratio are listed in Table 1.

Table 1. Deformability test results

Specimen	Diameter (mm)	Length (mm)	Failure Load (kN)	Elastic Modulus (GPa)	Poisson’s Ratio	Uniaxial Compressive Stress (MPa)
UCS-B1	72.16	154.82	21.23	3.16	0.24	5.21
UCS-B2	72.58	152.43	10.56	7.36	0.28	2.56
UCS-B3	72.43	152.18	22.22	2.96	0.25	5.51
Avg±Std. Dev.	72.39±0.21	153.14±1,46	18.07±6.47	4.49±2.48	0.26±0.02	4.43±1.63

Mode I fracture toughness tests were conducted on SCB test samples with 100 mm diameter and 50 mm span length. The ISRM suggested method states a range for SCB tests as $0.50 \leq S/R \leq 0.80$ (ISRM, 2007). The thickness of the SCB samples was 50 mm and notch length were fixed at 10 mm. A two-stage loading procedure was defined to the test specimens with high rate at 0.0005 mm/s until the load limit detector is triggered. In the second loading stage, loading was applied with low rate as 0.0003 mm/s. The SCB specimens were tested with rollers that have 8 mm diameter under three-point bending condition to find the fracture toughness value for mode I. One of them was located at the upper surface of the specimen for loading purposes whereas the other two were located at the bottom surface of the specimen for supporting purposes. The specimens were coded in terms of the thickness, span length (S/R) and specimen number for SCB. The SCB specimen before, during, and after the fracture test can be seen in Figure 5.





Figure 5. SCB sample before, during and after the test

The mode I fracture toughness (K_{Ic}) was calculated with Equation 3 and Equation 4. The critical load value was obtained from the load- displacement graph results of the fracture tests. Figure 6 shows load- displacement graph of the sample SCB-50-050-B1. According to the graph, load at fracture for sample 1 is 4.31 kN

$$\sigma_{cr} = P_{cr}/2Rt \tag{3}$$

$$K_{Ic} = Y_I \sigma_{cr} \sqrt{\pi a} \tag{4}$$

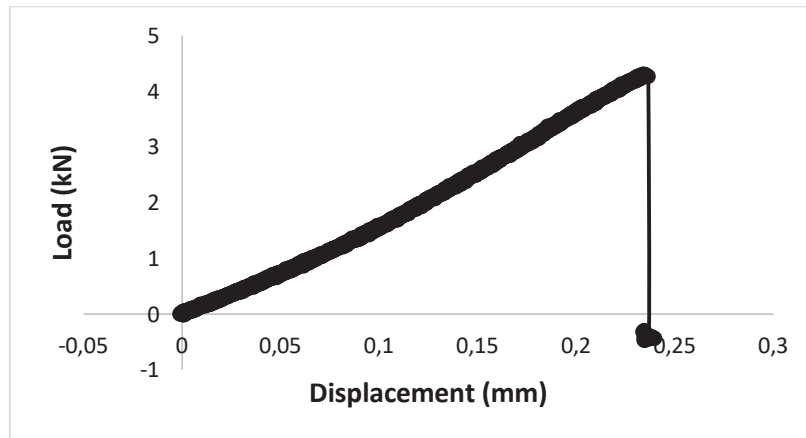


Figure 6. Load vs. displacement curve of SCB-50-050-B1

All fracture test results for SCB specimens with 50 mm thickness are summarized in Table 2.

Table 2. SCB fracture test results

Specimen Code	Fracture Load (kN)	Mode I Fracture Toughness (GPa)
SCB-50-050-B1	4.31	0.39
SCB-50-050-B2	6.76	0.61
SCB-50-050-B3	6.22	0.56
Avg±Std. Dev.	5.76±1.29	0.52±0.12

According to Table 2, mode I fracture toughness (K_{Ic}) of SCB specimen was found as $0.52 \pm 0.12 \text{ MPa}\sqrt{\text{m}}$.

In a study of Batan (2020), SCB tests were conducted on grey colored Ankara Gölbaşı andesite rock material to assign mode I fracture toughness (K_{Ic}). The fracture tests with SCB geometry that had 50 mm thickness were completed and the notch length was kept fixed as 10 mm for all SCB specimens. Numerical analyses were performed by ABAQUS finite element software to find mode I SIF. In the models, elastic properties of materials were taken as $E = 12 \text{ GPa}$ and $\nu = 0.15$. The stress intensity factor (K_I) of SCB model geometry for mode I was calculated as $89.72 \text{ Pa}\sqrt{\text{m}}$. The dimensionless stress intensity factor (Y_I) of SCB model geometry for mode I was calculated as 2.53.

Table 3. SCB fracture test results for t=50 mm (Batan, 2020)

Specimen Code	Fracture Load (kN)	Mode I Fracture Toughness (GPa)
SCB-50-050-1	11.19	1.00
SCB-50-050-2	11.01	0.98
SCB-50-050-3	12.54	1.12
Avg±Std. Dev.	11.58±0.84	1.03±0.08

In this study, mode I fracture toughness (K_{Ic}) of SCB andesite specimen and SCB shotcrete sample were compared to determine internal structure and fracture behavior.

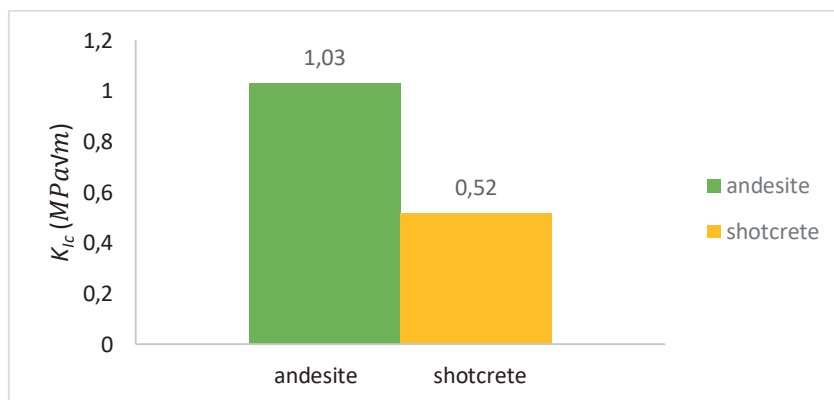


Figure 7. K_{Ic} values of SCB andesite sample and SCB shotcrete sample

As seen in Figure 7, the K_{Ic} measured by the SCB tests on shotcrete is about 50% lower than K_{Ic} measured by the SCB tests on andesite with 50 mm span length.

RESULTS AND DISCUSSION

In this study, the potential of using 3D printing technology was investigated to determine the fracture properties of concrete samples that were prepared by using molds. The shape and crack geometry of the shotcrete samples are achieved as nearly perfect with the help of the 3D printer technology. Therefore, more accurate test results were achieved with shorter preparation time than conventional sample preparation. Mode I fracture toughness (K_{Ic}) of SCB shotcrete specimen was found as $0.52 \pm 0.12 \text{ MPa}\sqrt{\text{m}}$. By comparing this value with the same diameter and span length andesite sample with K_{Ic} of $1.03 \pm 0.08 \text{ MPa}\sqrt{\text{m}}$, it can be concluded that the crack resistance under a specific loading condition of shotcrete specimen is lower than the andesite material. According to these results, rock samples and shotcrete samples have no similar internal structures as expected. As a conclusion, the mode I fracture toughness value (K_{Ic}) of SCB shotcrete specimen was assigned and further experimental studies will be performed to investigate the effects of the different notch angles and loading span on mode I fracture toughness of shotcrete with SCB method.

REFERENCES

- Batan K., C. (2020). Effect of loading span on tensile mode fracture toughness for three-point bend specimen geometries. Unpublished thesis, Ankara.
- Bazant, Z. P., & Kazemi, M. T. (1990). Determination of fracture energy, process zone length and brittleness number from size effect, with application to rock and concrete. *International Journal of fracture*, 44(2), 111-131.
- Hillerborg, A., Modéer, M., & Petersson, P. E. (1976). Analysis of crack formation and crack growth in concrete by means of fracture mechanics and finite elements. *Cement and concrete research*, 6(6), 773-781.
- ISRM (2007) The complete ISRM suggested methods for rock characterization, testing and monitoring: 1974–2006. In: Ulusay R, Hudson JA (eds) Suggested methods prepared by the commission on testing methods. International Society for Rock Mechanics, Compilation Arranged by the ISRM Turkish National Group, Ankara, Turkey
- Jenq, Y. S., & Shah, S. P. (1985). A fracture toughness criterion for concrete. *Engineering Fracture Mechanics*, 21(5), 1055-1069.
- Kaplan, M. F. (1961, November). Crack propagation and the fracture of concrete. In *Journal Proceedings* (Vol. 58, No. 11, pp. 591-610).
- Karihaloo, B. L., & Nallathambi, P. (1989). An improved effective crack model for the determination of fracture toughness of concrete. *Cement and Concrete Research*, 19(4), 603-610.
- Kuruppu, M. D., & Chong, K. P. (2012). Fracture toughness testing of brittle materials using semi-circular bend (SCB) specimen. *Engineering Fracture Mechanics*, 91, 133-150.
- Nallathambi, P., & Karihaloo, B. L. (1986). Determination of specimen-size independent fracture toughness of plain concrete. *Magazine of Concrete Research*, 38(135), 67-76.
- Perdikaris, P. C., Calomino, A. M., & Chudnovsky, A. (1986). Effect of fatigue on fracture toughness of concrete. *Journal of engineering mechanics*, 112(8), 776-791.
- Tang, T., Ouyang, C., & Shah, S. P. (1996). Simple method for determining material fracture parameters from peak loads. *Materials Journal*, 93(2), 147-157.
- Yoncaci, S. (2019). Investigation of fracture toughness on flattened brazilian disc type molded shotcrete specimens. PhD thesis, Ankara.

JEOSENTETİK MALZEMELERİN ÇEVREYE VE TOPLUMA SAĞLADIĞI KATKILAR
THE CONTRIBUTION OF GEOSYNTHETIC MATERIALS TO THE ENVIRONMENT AND SOCIETY

C. Ozan*

¹ *Yesti İnşaat ve Tic. Ltd. Şti.*
(*celalettinozan@yestigroup.com)

ÖZET

Yaşadığımız dünyada hammadde ve enerji ihtiyaçları günden güne artmaktadır. Enerji ve hammadde ihtiyaçlarının büyük bir kısmı doğal kaynaklardan sağlanmaktadır. Doğal kaynaklar, madencilik ile toplumun kullanımına sunulmaktadır. Madencilik faaliyetlerinde doğal topoğrafyada büyük değişiklikler olabilmektedir. Bu faaliyetlerin çevreye ve topluma etkisi kaçınılmazdır.

Madencilik faaliyetlerinin, çevre ve toplum üzerindeki etkisini teknik olarak korumak mümkündür. Modern yaklaşımlarla bu etkiler önlenebilir ya da en aza indirilebilir. Çevresel etkileri minimize etmek için günümüzde yaygın olarak jeosentetik malzemeler kullanılmaktadır.

Kullanım alanları oldukça geniş olan jeosentetik malzemeler, madencilik faaliyetlerin her aşamasında özellikle atık depolama tesisleri ve rehabilitasyon alanlarında kullanılmaktadır. Atıkların çevreye zarar vermeden bertarafını sağlamak üzere düzenli olarak depolanmasını, topoğrafyanın düzenlenmesini, farklı ürünler yetiştirilmesini, farklı ağaçlandırma yapılmasını sağlamaktadır. Bu ve buna benzer önlemler, madenciliğin çevre ve insan sağlığına olan negatif etkilerini azaltmakta yardımcı olmaktadır.

Bu bildiriye, çevreye ve topluma minimum etkiyle madencilik faaliyetlerin yapılabilmesi konusunda bilgiler verilecektir.

Anahtar sözcükler: Madencilik, çevre, rehabilite, atık, jeosentetik, jeomembran

ABSTRACT

Raw materials and energy needs are increasing day by day in the world we live in. Most of the energy and raw material needs are sourced from natural sources. Natural resources are made available to the community through mining. There may be major changes in natural topography in mining activities. The environmental and society impact of these activities is inevitable.

It is technically possible to protect the impact of mining activities on the environment and society. With modern approaches, these effects can be prevented or minimized. Geosynthetic materials are widely used today to minimize environmental impacts.

Geosynthetic materials, which have a wide range of uses, are used especially in waste storage facilities and rehabilitation areas at every stage of mining activities. It ensures regular storage of wastes, arrangement of topography, cultivation of different products, different reforestation in order to ensure the disposal of wastes without harming the environment. These and similar measures helps reduce the negative effects of mining on the environment and human health.

In this statement, information will be given about the ability to carry out mining activities with minimal impact on the environment and society.

Keywords: Mining, environment, rehabilitation, waste, geosynthetics, geomembrane

GİRİŞ

Jeosentetikler, günümüzde daha çok inşaat sektöründe kullanılsa da, zamanla kullanım alanı çoğalmış ve son yıllarda özellikle madencilik sektöründe ilgi gören ürünler olmuştur.

1950’li yıllarda kullanılmaya başlanılan jeotekstiler ile toplumun ve çevrenin ihtiyaçlarını karşılamak amacıyla özellikle son 15 yılda farklı ürünler geliştirilmiştir. Jeotekstiller, jeogridler, jeomembranlar, jeonetler, jeokompozitler ve jeosentetik kil astarlar önde gelen jeosentetik malzemelerdir.

Jeosentetikler; zeminin birbirinden ayrılması, güçlendirme donatısı, drenaj sistemi, erozyon kontrolü, yalıtım uygulaması ve filtrasyon çözümü gibi farklı kullanım alanlarına sahiptir. Jeosentetik malzemeler tek tek ve/veya birlikte kullanılabilmesi ile şu avantajları sağlamaktadır; teknik üstünlük, yer kazanma, maliyetteki kazanımlar, inşaat süresini kısaltma, malzeme ve imalat kalite kontrolü, malzeme gelişim ve tedarik edilebilirlik ve özellikle çevresel duyarlılık...

Hazırlanan bildiri kapsamında geleneksel yöntemlere göre maliyetleri de düşürerek estetik çözümler sunabilen jeosentetiklerin çevreye ve topluma sağladığı avantajlar hakkında bilgiler aktarılacaktır.

JEOSENTETİK MALZEMELER

TS EN ISO (2015), jeosentetiği *“Geoteknik ve inşaat mühendisliği uygulamalarında toprak ve/veya diğer malzemelerle temasta olacak şekilde kullanılan levha, şerit ve üç boyutlu yapıda, bileşenlerinden en az bir tanesi sentetik veya doğal bir polimerden yapılmış mamulü tanımlayan genel terim.”* olarak tanımlar (bk. Çizelge 1).

Çizelge 1. Jeosentetik türleri

TEMEL KİMYASAL	POLİMER	JEOSENTETİK TÜRLERİ
Etilen	Polietilen (PE)	Jeotekstil, jeomembran, jeogrid, jeotüp, jeonet, jeokompozit
Propan	Polipropilen (PP)	Jeotekstil, jeomembran, jeogrid, jeokompozit
VinilKlorürMonomer	PoliVinilKlorür (PVC)	Jeomembran, jeokompozit, jeotüp
Etilen (+terafitalik Asit)	Poliester/PolietilenTeraFtalat (PET)	Jeotekstil, jeogrid
Kaprolaktam (Benzen)	Poliamid (PA) -(Nylon 6/6)	Jeotekstil, jeokompozit, jeogrid
Stiren	Polistirenf (PS)	Jeokompozit, jeoköpük

Polimerik malzemelere örnek olarak jeotekstil, jeogrid, jeonet, jeomembran, jeosentetik kil örtü, jeokompozit, jeocell ve diğer jeo ürünler sayılabilir (bk. Şekil 1). Bu ürünler arasında kullanım alanları daha yaygın olan jeotekstil, jeomembran, jeokompozit ve jeosentetik kil örtü malzemeler hakkında bilgiler verilecektir.



Şekil 1. Jeosentetik çeşitleri

Jeomembran

TS EN ISO (2015), jeomembranı “Jeoteknik ve inşaat mühendisliği uygulamalarında yapı içerisinde sıvı geçişini azaltmak veya önlemek amacıyla kullanılan düşük geçirimli jeosentetik malzeme” olarak tanımlar.

Jeomembran kullanımında asıl amaç; yalıtım ve yüzey koruması sağlamaktır. Asfalt, polimer ve bunların karışımından üretilen pürüzlü veya pürüzsüz yüzeye sahip hazırlanan jeomembranlar kimyasal maddelere karşı oldukça yüksek bir dirence sahiptirler. Çekmeye karşı dayanımın yüksek olması, geçirgenliğinin düşük olması, delinmelere karşı dayanıklı bir yapıya olması vb. (bk. Çizelge 2) sebeplerden dolayı oldukça tercih edilen bir jeosentetik üründür.

Çizelge 2. Yüksek yoğunluklu polietilen (HDPE) jeomembranların kesme ve koparma dayanımları

Geomembrane Nominal Thickness	0.75 mm	1.0 mm	1.25 mm	1.5 mm	2.0 mm	2.5 mm	3.0 mm
Hot Wedge Seams⁽¹⁾							
shear strength, N/25 mm	250	350	438	525	701	876	1050
shear elongation at break ⁽²⁾ , %	50	50	50	50	50	50	50
peel strength, N/25 mm	197	263	333	398	530	661	793
peel separation, %	25	25	25	25	25	25	25
Extrusion Fillet Seams							
shear strength, N/25 mm	250	350	438	525	701	876	1050
shear elongation at break ⁽²⁾ , %	50	50	50	50	50	50	50
peel strength, N/25 mm	170	225	285	340	455	570	680
peel separation, %	25	25	25	25	25	25	25

Günümüzde daha çok su yalıtım örtüsü olarak kullanılsa da, zamanla kullanım alanı çoğalmış ve özellikle yığın liçi sahaları, atık depolama sahaları, solüsyon (çözelti) havuzları, çöktürme havuzları ve atık su arıtma tesisleri gibi madencilik alanlarında kullanılmaktadır (bk. Şekil 2).



Şekil 2. Jeomembran kullanım alanları

Jeotekstil

TS EN ISO (2015), jeotekstili “Geoteknik ve inşaat mühendisliği uygulamalarında toprak ve/veya diğer malzemeye temasta olacak şekilde kullanılan, dokusuz, örülmüş veya dokulu olabilen ve düzlemsel, geçirimli, polimerik (sentetik veya doğal) tekstil malzemesi” olarak tanımlar.

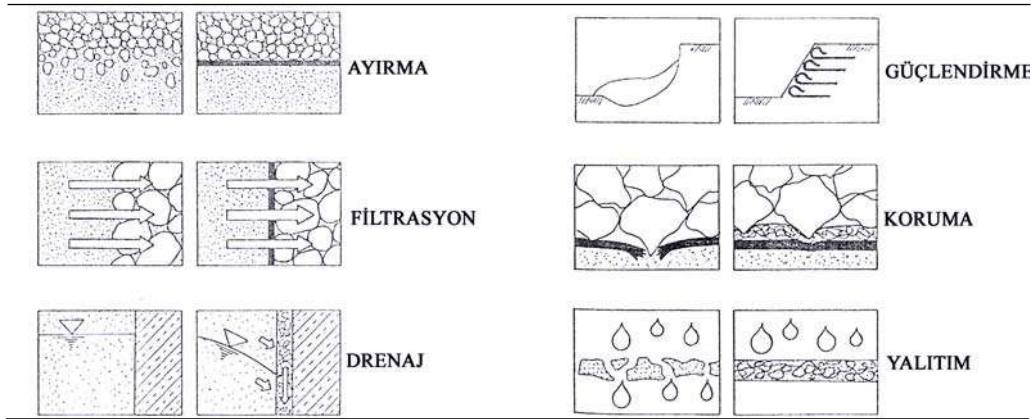
Üretim tekniği açısından örgülü ve örgüsüz olarak iki tip jeotekstil yapısı vardır. Jeotekstillerin 100’den fazla özel uygulama alanı bulunmaktadır; ama genelde ayırma, filtrasyon, drenaj, güçlendirme, koruma, yalıtım olarak altı fonksiyonu öne çıkmaktadır (bk. Çizelge 3).

Özellikle zemin mekaniği problemlerinde, ekonomik ve kalıcı çözümler sağladığı için son yıllarda kullanımı giderek artmıştır. Jeotekstillere, jeomembranlar gibi madencilik alanlarında kullanılması yanı sıra yığın liçi tesislerin atardamarları olan çözelti toplama borularını filtreleme ve korunması amacıyla bohçalama ve madencilik faaliyetleri sonrası rehabilitasyon işleri gibi önemli uygulama alanları mevcuttur (bk. Şekil 3).



Şekil 3. Jeotekstil kullanım alanları

Çizelge 3. Jeotekstillerin fonksiyonları



Jeosentetik Kil Astar (GCL)

TS EN ISO (2015), jeosentetik kil astarı “Levha halindeki jeosentetik malzemelerin fabrikada birleştirilmesiyle elde edilen ve bariyer işlevinin esas olarak kil tarafından sağlandığı malzeme” olarak tanımlar.

Jeotekstillere arasında bulunan bentonitin mineralojisi ile fiziksel ve kimyasal özellikleri geçirimsizliği önemli ölçüde etkilemektedir. İçindeki bentonit, toz veya granüler halde imal edilebilir. Literatürde, su ile süzdürüldüğü durumdaki hidrolik iletkenliğinin yaklaşık 2.0×10^{-9} cm/s olduğu rapor edilmektedir. Özdamarlar ve Ören’in (2018) yapmış olduğu çalışmada farklı alt zemin tabakaları, kür süreleri ve deney yöntemi ile hidrate edilen GCL’lerin hidrolik iletkenlik sonuçları Çizelge 4’de yer almaktadır.

Düşük hidrolik iletkenlik özelliği ile katı atık depolama alanları, gölet tabanları, kanal yatakları ve çeşitli maden işletmelerinin rehabilitasyon ve atık havuzları dâhil pek çok alanda yaygın olarak kullanılmaktadır (bk. Şekil 4).



Şekil 4. Jeotekstil kil astar kullanım alanları

Çizelge 4. Jeosetetik kil örtülerin hidrolik iletkenlik sonuçları

Deney No	Alt Zemin Tabakası Tipi	Alt Zemin Örnek Boyu (cm)	Alt Zemin Görüntü Oranı	Deney Yöntemi	Hidrasyon Süresi (gün)	Hidrolik İletkenlik (cm/s)
1	Siltli Kum	11.6	1.14	KÖY	7	2.3×10^{-9}
2	Siltli Kum	17.4	1.14	TBÖY	7	1.7×10^{-9}
3	Siltli Kum	11.6	0.76	TBÖY	7	3.2×10^{-9}
4	Siltli Kum	11.6	1.14	KÖY	62	2.6×10^{-9}
5	Siltli Kum	17.4	1.14	TBÖY	62	1.7×10^{-9}
6	Zeolit	11.6	1.14	KÖY	17	1.8×10^{-9}
7	Zeolit	11.6	0.76	TBÖY	17	5.7×10^{-9}
8	Zeolit	11.6	1.14	KÖY	30	4.1×10^{-9}
9	Zeolit	11.6	0.76	TBÖY	30	2.5×10^{-9}

Jeokompozit

Genellikle suyun drenajı için tasarlanmış ve *levha halindeki iki ya da daha fazla jeosentetik malzemelerin fabrikada birleştirilmesiyle elde edilen jeosentetik malzemedir.*

Drenaj jeokompoziti, geogridin tek veya çift tarafının jeotekstille üst üste birleştirilmesi sonucu oluşturulur. Kullanılan geogrid malzemesi güçlendirme görevini üstlenirken, örgüsüz jeotekstil ise ayırma ve filtrasyon görevlerini üstlenmektedir. Jeokompozitler, su ve sıvı akışı için serbest bir iletim yolu sağlamaktadır.

Düşük eğimlerde ve basınç altında, yüksek akış kapasitesine sahip olan jeokompozitler, çevrenin korunmasında büyük rol oynamaktadırlar. Düzenli depolama sahalarında ve istinat yapılarında kullanımı yaygındır.



Şekil 5. Jeokompozit kullanım alanları

JEOSENTETİK MALZEMELERİN SAĞLADIĞI KATKILAR

Jeosentetikler, madencilik faaliyetlerinde barajlar, havuzlar, pasa stok alanları, yığın liçi sahaları gibi atık depolama alanlarının yanı sıra derivasyon kanalları, drenaj, istinat yapıları gibi donatılı jeoteknik projeleri, rehabilitasyon, peyzaj ve erozyon kontrol gibi çevre düzenlemeleri, tünel ve yer altı yapıları gibi galeri uygulamalarında katkılar sağlamaktadır (bk. Şekil 6 – Çizelge 5).



Şekil 6. Madencilik faaliyetlerinde jeosentetik malzemeler

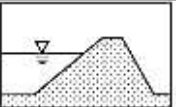
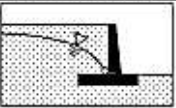
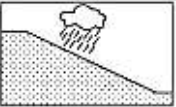
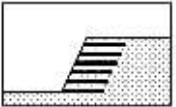
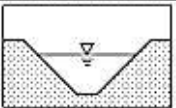
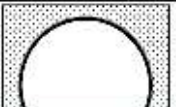


Jeosentetik malzemelerinin sağladığı faydalar genel olarak şu şekildedir:

- Tehlikeli veya tehlikesiz atıkların insan sağlığı, bitki örtüsü ve çevreye karşı olumsuz etkilerini önlemektedir. Yer altı ve yerüstü sularının kirlenmesini engellemektedir.
- Katı ve sıvı gibi maddelere depolama alanı sağladığı için madencilik işlerinde önemli geri kazanımlar sağlamaktadır.
- Doğal malzemelerin sağladığı özellikler jeosentetiklerin bir çeşidi ile sağlanabilir. Örneğin, kil teminin mümkün olmadığı ya da temin mesafesinin fazla olduğu durumlarda kil yerine uygun bir jeosentetik malzeme kullanılması daha ekonomik bir çözüm olur.
- Doğal malzemelere göre nakliye ve taşınma kolaylığı sağladığı için taşıma maliyetleri daha düşüktür.
- Yerleştirilmesinin kolaylığı, stok ve istifleme imkânı sağladığı için zamandan ve maliyetten tasarruf sağlamaktadır.
- Jeosentetik malzemelerin filtrasyon özellikleri fabrika üretimi ve kontrollünde olduğundan doğal (mineral) malzemeler ile oluşturulan filtreler nazaran kaliteleri daha uygun ve garantili olmaktadır. Kaliteden sapma olasılığı düşmektedir.
- Jeosentetik malzemelerin uygun derecelenmiş agrega ile kullanımı, toplayıcı borulara olan ihtiyacı azaltmaktadır. Maliyette önemli bir tasarruf söz konusudur.
- Uygulama kolaylığı sebebiyle jeosentetik malzemeler projelerde zaman ve maliyette önemli miktarda ekonomik kazanç sağlamaktadır.
- Jeosentetik malzemelerin sahip oldukları teknik özellikleri uygulamalarda oluşabilecek deformasyonlara uyum sağlar ve direnç sağladığı kabul edilmektedir.
- Elastisite ve sağlamlıkları ile sismik etkilere karşı kullanılabilir. Duvar arkalarında sismik etkileri sönmülmesi önemli bir avantaj olarak kabul edilebilir.
- Zemin iyileştirme ve güçlendirme ile uygun olmayan ve elverişsiz arazilerin kullanılabilmelerini mümkün kılan malzemelerdir.

- Yağmur suları, şiddetli rüzgâr gibi olumsuz hava şartlarında oluşan erozyonu azaltmak amacıyla kullanılmaktadır.
- Gereken kazı ve dolgu miktarının azaltılmasını ve daha uygun ve ekonomik malzemelerin kullanımını sağlamaktadır.
- Geliştirilen dayanım parametreleri ile şevlerin daha dik açılarla yapılabilmesi çok önemli yer kazanımları sağlamaktadır.
- Kayma ve göçmeye karşı dayanımı arttırmasının yanı sıra göçmüş yüzeylerin tamir edilebilmesini de sağlamaktadır.
- Donatılı zemin ve istinat duvarları uygulamalarında alternatif çözümler üretebilmektedir.
- Dayanım ve diğer teknik özellikleri net rakamlarla ifade edilebildiği için daha büyük, önemli ve spesifik projelerin hayata geçmesine imkân sağlar.
- Koruma örtüsü teşkil ederek, şev yüzeylerinin korunmasını ve parçalanmış kayaçları tutabilmesi ile can güvenliği sağlayabilmektedir.
- Yeşillendirilmiş yaşayan duvarlar ve rehabilite edilerek doğaya kazandırılan uygulamalar ile estetik görünüşlü güzel çevreler elde edilmektedir.

Jeosentetik malzemelerin sağladığı faydalardan; malzeme miktarı, imalat süresi ve maliyetlerin azalması ve çevresel duyarlılık doğrudan kazanım; sayılan diğer faydalar ise dolaylı kazanım olarak kabul edilebilir.

Çizelge 5. Madencilikte jeosentetik malzemelerin kullanım alanları

Kullanım alanı	Standard	Şematik gösterim	Kullanım alanları				
			Filtrasyon	Ayırma	Güçlendirme	Koruma	Drenaj
Rezervuarlarda ve barajlarda	EN 13254		X	X	X	X	
Drenaj	EN 13252		X	X			X
Erozyon kontrolü	EN 13253		X	X	X		
Toprak işleri	EN 13251		X	X	X		
Kanal	EN 13255		X	X	X	X	
Tüneller ve yer altı yapıları	EN 13256					X	
Katı atık bertaraf	EN 13257		X	X	X	X	
Sıvı atık depolama	EN 13265		X	X	X	X	

SONUÇ

Jeosentetikler, mühendislik uygulamalarında sağladığı teknik ve ekonomik çözümler ile önem kazanmış ve kullanımları son 20-30 yılda giderek artmıştır. Geleneksel yöntemlerinin yerine çok çeşitli alanlarda kullanılabilen bu malzemeler; hayatımızı kolaylaştıran, çevreyi, doğal kaynaklarımızı ve yaşam alanlarımızı dizayn eden projelerde beşeri rol oynamaktadır.

Donatı, güçlendirme, ayırma, yalıtım, filtrasyon ve drenaj gibi fonksiyonlara sahip olabilen jeosentetikler, doğrudan ve dolaylı avantajlar sağlamakta ve muhtelif geri kazanımlara neden olmaktadır. Bu bildiri kapsamında bu malzemelerin sağladığı faydalardan bahsedilmiştir.

TEŞEKKÜRLER

“Jeosentetik Malzemelerin Topluma ve Çevreye Sağladığı Katkıları” başlıklı bildiriye araştırma fırsatı sunan değerli YESTİ Group yöneticilerimizden başta Genel Müdür Cem PEKEL, Direktör Osman MARTİN ve Teknik ve İdari İşler Müdürü Murat TÜRKÖZÜ’ne teşekkür eder, bu konu üzerine araştırma yapmam için fikir veren değerli TÜPRAG Efemçukuru Açık Saha Yöneticisi Yavuz Selim İNCİ’ye şükranlarımı sunarım.

KAYNAKLAR

- Akyıldız, M.H. (2019). Geosentetik Türlerinin İnşaat Mühendisliğindeki Uygulamaları ve Sağladığı Kolaylıklar. Dergi Park, Cilt 10, Sayı 2, 791 – 796.
- Devlet Su İşleri Genel Müdürlüğü (2012). DSİ Genel Müdürlüğü Tarafından Yaptırılacak Depolamalarda (Rezervuarlarda) ve Barajlarda Kullanılacak Geosentetik Bariyerler İçin Teknik Şartname.
- Devlet Su İşleri Genel Müdürlüğü (2014). DSİ Genel Müdürlüğü Tarafından Yaptırılacak Kanallarda, Rezervuarlarda ve Barajlarda Kullanılacak Geotekstiller ve Geotekstille İlgili Mamuller İçin Teknik Şartname.
- Geosynthetic Institute (2021). GRI -GM19a Standard Specification, Seam Strenth and Related Propertis of Thermally Bonded Homogeneous Polyolefin Geomembranes/Barries, Rev. 10.
- ISO 10318-1 (2015). Geosynthetics – Part 1: Terms and definitions.
- Koçak, B. (2021). Mühendislik Uygulamalarında Geosentetik Ürün Kullanımı. URL -1= <https://www.yeraltihaber.com/makale/muhendislik-uygulamalarinda-geosentetik-urun-kullanimi-7>.
- Özdamarlar Kul T. ve Ören A.H. (2018). Geosentetik Kil Örtü Hidrasyon Yönteminin Alt Zemin Koşullarına Bağlı Olarak Değerlendirilmesi. Teknik Dergi, Cilt 29, Sayı 3, 8385 – 8409.
- Teknik Araştırma ve Kalite Kontrol Dairesi Başkanlığı (2021). Geosentetik Malzemeler ve DSİ’deki Uygulamaları. DSİ Genel Müdürlüğü.
- TS EN ISO 10318-1 (2015). Jeotekstiller – Terimler ve tarifler: Bölüm-1.
URL -2= <http://yestigroup.com/>.
- Zanbak, C. (2019). Madencilik Faaliyetlerinde Geosentetik Kullanım Alanları. Türkiye Madenciler Derneği, Madencilikte Atık Yönetim Uygulamaları Semineri.

**KANADA MADENCİLİK DERNEĞİ- SÜRDÜRÜLEBİLİR MADENCİLİK- ATIK YÖNETİM PROTOKOLÜ VE
TÜRKİYE'DEKİ UYGULAMASI**
*MINING ASSOCIATION OF CANADA- TOWARDS SUSTAINABLE MINING TAILINGS MANAGEMENT
PROTOCOL AND APLICATION IN TURKEY*

H. Ürkmez^{1,*}, C. Dumaresq², B. Chalmers², Y.S. İnci¹, G. Uzuncelebi, S. Ennis³, E.R. Castro

¹ *TÜPRAG Efemçukuru Altın Madeni*
(* Sorumlu Yazar: halil.urkmez@tuprag.com)
² *The Mining Association of Canada (MAC)*
³ *Stantec*

ÖZET

Hızla büyüyen madencilik, ülkeler için büyük ekonomik fırsatlar sağladığı gibi, insanlar ve çevre için zorluklar ve riskler de getiriyor. Hükümetler / ülkeler için zorluk, madenciliği sürdürülebilir kalkınma hedeflerine katkıda bulunacak ve insanları veya çevreyi tehlikeye atmayacak şekilde yönetmektir.

Bu bağlamda, Kanada Madencilik Derneği (MAC), hükümetlerin sürdürülebilir kalkınma hedefleriyle tutarlı, insanları ve çevreyi koruyan toplulukları ve madencilik endüstrisini birleştiren bir yapıda uluslararası ilkeleri, yaklaşımları ve standartları benimseyen bir Kanada endüstri derneğidir.

MAC, madencilik sektörünün çevresel ve sosyal performansını iyileştirmek için geliştirilmiş, uluslararası kabul görmüş bir kurumsal sürdürülebilirlik programı olan “Sürdürülebilir Madencilik” (TSM-SM) performans sistemini geliştirmiş ve uygulamaktadır. Sürdürülebilir Madencilik performans sisteminin amacı, madencilik şirketlerinin toplumun mineral, metal ve enerji ürünleri ihtiyaçlarını sosyal, ekonomik ve çevresel açıdan en sorumlu şekilde karşılamasını sağlamaktır. Sürdürülebilir Madencilik Protokolleri, belirli, ölçülebilir performans göstergelerini tanımlamaktadır.

TSM performans sisteminin protokollerinden biri olan “Atık Yönetim Protokolü”, sahaya özel seviyede güvenli, sorumlu atık yönetimine odaklanır. BAP (Mevcut En İyi Uygulamalar) ve BAT'ın (Mevcut En İyi Teknikler) uygulanması dahil olmak üzere mühendislik uygulamalarını risk tabanlı bir yaklaşım içinde entegre eden atık yönetiminin sağlam kurumsal yönetimi için bir dizi yönetim sistemleri yaklaşımını tanımlar.

Anahtar Kelimeler: Kanada madencilik derneği, sürdürülebilir madencilik (SM), sürdürülebilir kalkınma hedefleri, atık yönetimi protokolü, işletme, bakım ve izleme kılavuzu, kademeli eylem planları, kayıt mühendisi (EOR), mevcut en iyi uygulamalar, mevcut en iyi teknikler

ABSTRACT

Rapidly growing mining provides great economic opportunities for countries as well as brings difficulties and risks for people and the environment. The challenge for governments / countries is to manage mining in a way that contributes to sustainable development goals and does not endanger people or the environment.

In this regard, The Mining Association of Canada (MAC) is a Canadian industry association that has adopted international principles, approaches, and standards in a structure that combines the mining

industry and communities that protect the people and the environment, consistent with the sustainable development goals of governments.

MAC has developed and implemented the Towards Sustainable Mining (TSM) performance system, an internationally recognized corporate sustainability program developed to improve environmental and social performance of the mining industry. The purpose of the TSM performance system is to enable mining companies to meet the needs of society for mineral, metal, and energy products in the most socially, economically, and environmentally responsible way. TSM Protocols describe specific, measurable performance indicators.

Tailings Management Protocol, one of the protocols of the TSM performance system, focuses safe, responsible tailings management at the site-specific level. It describes a management systems approach for sound corporate governance of tailings management that integrates engineering practice, including implementation of BAP (Best Available Practices) and BAT (Best Available Techniques), within a risk-based approach.

Keywords: The mining association of Canada (MAC), towards sustainable mining (TSM), sustainable development goals, tailings management protocol, OMS manual, trigger action response plan (TARPs), engineer of record (EoR), best available practices (BAP), best available techniques (BAT)

GİRİŞ

Kanada Madencilik Derneği güçlü, sürdürülebilir ve uluslararası düzeyde rekabetçi bir Kanada madenciligi, mineral ve metal endüstrisinin geniş bir ulusal destekle oluşturulmasına ve sağlam bir kurumsal ve kamu politikasının geliştirilmesine katkıda bulunmak için 1935 yılında kurulmuştur. Kanada Madencilik Derneği'nin "Atık Tesislerinin Yönetimine Yönelik Bir Kılavuz"unun (A Guide To The Management of Tailings Facilities) 1998'de yayınlanan ilk baskısı, 1990'larda meydana gelen bir dizi uluslararası atıkla ilgili olaya yanıt olarak geliştirilmiştir. MAC Atık Kılavuzu'ndaki yönetim sistemleri yaklaşımı, ISO 14001 Çevre Yönetim Sistemleri ile uyumlu, Kanada Baraj Birliği'nin Baraj Güvenliği Yönergeleri (2013) ve uluslararası yönergeler ve standartların uygulanmasıyla desteklenmektedir. 2003 yılında atık yönetim sisteminin ayrılmaz bir bileşeni olarak sahaya özel bir İşletme, Bakım ve İzleme (İŞBİK - OMS) kılavuzu yayınlamıştır. Atıkların güvenli ve çevreye duyarlı, etkili bir yönetim sistemi içinde ve tüm yaşam döngüsü boyunca sağlam mühendislik yeteneğinin tutarlı bir şekilde uygulanmasını sağlamak amacıyla 2004 yılında MAC "Towards Sustainable Mining® (TSM®)" (MAC-Sürdürülebilir Madencilik - SM) girişimini başlatmıştır. 2015 yılı itibarı ile MAC, üyeleri için Kanada'daki operasyonları için TSM'nin atık yönetimi bileşeni de dahil olmak üzere "Towards Sustainable Mining (TSM)" uygulamasını zorunlu hale getirdi.

"SÜRDÜRÜLEBİLİR MADENCİLİK" PROGRAMI NEDİR?

SM performans sistemi, Kanada Madencilik Birliği'nin sorumlu madencilik taahhüdüdür. Madencilik şirketlerinin çevresel ve sosyal sorumluluklarını değerlendirmelerine ve yönetmelerine yardımcı bir sistemdir (MAC 2021). SM uygulaması, tesis performansı artırmak ve temel madencilik risklerinin madencilik operasyonları tarafından etkin bir şekilde yönetilmesini sağlamak için bir dizi araç ve göstergelerden oluşur. Bu performans ölçüm araçları ve göstergeleri, aşağıda belirtilen SM Yol Gösterici İlkeleri ile uyumludur (MAC 2021):

"...eylemlerimiz (MAC üyeleri), ilgilendiğimiz toplulukların gelişen öncelikleriyle uyumlu sosyal, ekonomik ve çevresel performansa karşı sorumlu bir yaklaşım sergilemelidir. Eylemlerimiz, dürüstlük, şeffaflık ve bütünlük te dahil olmak üzere çalışanlarımız ve ilgilendiğimiz topluluklarla paylaştığımız geniş bir değer yelpazesini yansıtmalıdır. Ayrıca çalışanlarımızı, topluluklarımızı, müşterilerimizi ve doğal çevreyi korumak için devam eden çabalarımızın altını çizmelidir."

SM programının güçlü yönleri hesap verebilirlik, şeffaflık, güvenilirlik, etkin performansın desteklenmesi ve sürekli gelişimdir.

“SÜRDÜRÜLEBİLİR MADENCİLİK” PROGRAMI NASIL ÇALIŞIR?

SM programı, madencilik şirketlerinin çevresel ve sosyal taahhütlerini sahada eyleme dönüştürmesine olanak tanır. SM programı üç temel alana odaklanan (Topluluklar ve İnsanlar, Çevre Yönetimi ve Enerji Verimliliği) sekiz protokolden oluşmaktadır (Mayıs 2021'de yeni İklim Değişikliği protokolü TSM Protokollerine eklenmiştir). Her protokol, maden tesislerinin yönetim kalitesini ve performansını geliştirmesine, ölçmesine ve kamuya açık olarak raporlamasına yardımcı olan bir dizi performans göstergesini içermektedir (MAC 2021).

TSM PROTOKOLLERİ VE GÖSTERGELERİ TSM PROTOCOLS AND INDICATORS						
TOPLULUKLAR VE İNSANLAR COMMUNITIES AND PEOPLE	Yerel Halk ve Toplum İlişkileri Indigenous And Community Relationships	Community of Interest (COI) Identification	Effective COI Engagement and Dialogue	Effective Indigenous Engagement and Dialogue	Community Impact and Benefit Management	COI Response Mechanism
	Kriz Yönetimi ve İletişim Planlama Crisis Management and Communications Planning	Crisis management and communications preparedness	Review	Training		
	Güvenlik ve Sağlık Safety and Health	Commitment and accountability	Planning and implementation	Training, Behaviour and culture	Monitoring and reporting	Performance
	Çocuk İşçi ve Zorla Çalışmayı Önleme Prevention of Child and Forced Labour Verification	Preventing forced labour	Preventing child labour			
ÇEVRESEL YÖNETİM ENVIRONMENTAL STEWARDSHIP	Atık Yönetimi Tailings Management	Tailings Management policy and commitment	Tailings management system and emergency preparedness	Assigned accountability and responsibility for tailings management	Annual tailings management review	Operation, maintenance, and surveillance (OMS) manual
	Bioçeşitliliği Koruma Yönetimi Biodiversity Conservation Management	Corporate biodiversity conservation commitment, accountability and communications	Facility-level biodiversity conservation planning and implementation	Biodiversity Conservation reporting		
	Su Yönetimi Water Stewardship	Water governance	Operational Water management	Watershed-scale planning	Water reporting and performance.	
ENERJİ VERİMLİLİĞİ ENERGY EFFICIENCY	İklim Değişikliği Climate Change	Corporate Climate Change Management	Facility climate change management	Facility performance targets and reporting		

Şekil 1. SM (TSM) Protokolleri ve Göstergeleri (MAC 2021)

1. Yerel Halk ve Toplum İlişkileri
2. Kriz Yönetimi ve İletişim Planlaması
3. Güvenlik ve Sağlık
4. Çocuk İşçi ve Zorla Çalıştırmayı Önleme
5. Atık Yönetimi
6. Biyoçeşitliliği Koruma Yönetimi
7. Su Yönetimi
8. İklim Değişikliği

“SÜRDÜRÜLEBİLİR MADENCİLİK” PROGRAMI PERFORMANS DOĞRULAMASI

Maden şirketleri, SM protokollerinin her birindeki göstergelere göre operasyonel performanslarını yıllık olarak değerlendirir. SM programının en güçlü yönlerinden biri, madencilik şirketlerinin performanslarını tesis özelinde ve etkinlikleri düzeyinde ölçmesidir. Bu, performans değerlendirmesi SM sonuçlarının güvenilirliğini sağlamaya yardımcı olan SM doğrulama programı aracılığıyla daha da güçlendirilir. Bu doğrulama programı, Şekil 2.'de gösterildiği ve aşağıda ayrıntılı olarak açıklandığı gibi (MAC 2021) birkaç katmandan oluşur.



Şekil 2. Sürdürülebilir Madencilik (SM) Doğrulama Programı (MAC 2021)

SM Kriz Yönetimi ve İletişim Planlama Protokolü (Crisis Management and Communications Planning) “evet” veya “hayır” değerlendirme ölçeğine göre değerlendirilir; Çocuk İşçi ve Zorla Çalışmayı Önleme Protokolü’nde de (Preventing Child and Forced Labour), Sürdürülebilir Madencilik programı benzer bir “evet” veya “hayır” derecelendirme ölçeğine dayalı değerlendirme yapmaktadır. Diğer protokoller ise; Her gösterge için, “C” Düzeyinden, “AAA” Düzeyine kadar performanslarını yansıtan bir harf notu ile derecelendirilir.

İç Değerlendirme

Her yıl tüm tesisler, her bir protokol için ayrıntılı ve kapsamlı bir iç (öz) değerlendirme gerçekleştirir. Protokolde açıklanan kriterlere göre performansı yansıtmak için her göstergeye “C” ile “AAA” arasında değişen harf notları (bkz. Şekil 3) atanır. SM Kriz Yönetimi ve İletişim Planlama Protokolü ile Çocuk ve Zorla Çalıştırmanın Önlenmesi Protokolü’nde her bir göstergenin performansı harf notu vermek yerine "evet" veya "hayır" değerlendirme ölçeğine göre değerlendirilir.

Tablo 1. İç Değerlendirme Not Sistemi (MAC 2021)

AAA	Mükemmel liderlik.
AA	Yönetim kararlarına ve iş fonksiyonlarına entegrasyon.
A	Sistemler / süreçler geliştirilir ve uygulanır.
B	Prosedürler mevcuttur ancak tamamen tutarlı değildir veya belgelenmemiştir, Planlanan ve geliştirilmekte olan sistem süreçleri mevcuttur.
C	Yerinde sistem yoktur; faaliyetler reaktif olma eğilimindedir, Prosedürler olabilir ancak bunlar politikalara ve yönetim sistemlerine entegre değildir.

Dış Doğrulama

Her üç yılda bir, eğitimli bir Doğrulama Hizmet Sağlayıcısı (Verification Service Provider - VSP), tesis tarafından rapor edilen performans derecelendirmelerini belirlemek ve desteklemek için tesisin dahili (öz) değerlendirmelerini eleştirel bir şekilde gözden geçirir. Doğrulama Hizmet Sağlayıcıları, doğrulanan şirketten bağımsız ve SM tarafından akredite edilmiş deneyimli denetçilerdir.

CEO Güvence Mektubu

Harici doğrulama yılında, şirketin Kanada'daki CEO'su veya üst düzey yöneticisi, Kanada Madencilik Derneği'ne, Doğrulama Hizmet Sağlayıcısının Görev Tanımı'na uygun olarak harici bir doğrulamanın yapıldığını teyit eden bir mektup gönderir. CEO Güvence Mektupları, MAC web sitesinde kamuya açık halde yayınlanır.

Doğrulama Sonrası İnceleme

İlgili Danışman Topluluğu Heyeti, doğrulamada rol oynar ve SM'nin güvenilirliğini ve sürekli gelişimini sağlamaya yardımcı olur. Heyet, MAC tarafından kurulan ve yerli gruplar, topluluklar, çevresel ve sosyal sivil toplum kuruluşları, organize emek ve finans kuruluşlarının temsilcilerinden oluşan bağımsız, bir gruptur. Heyet, ilgili danışman toplulukları ve MAC üyeleri için ortak endişe konuları üzerinde tartışmak ve işbirliği yapmak için bir platform görevi görür. Heyet, SM geliştirme ve uygulamasını denetler ve madencilik sektörüyle ilgili ortaya çıkan sorunların veya endişelerin belirlenmesine yardımcı olur (MAC 2021a).

Heyet, her yıl, şirket sistemlerini ve uygulamalarını analiz etmek de dahil olmak üzere iki MAC üyesi şirketin SM sonuçlarının Doğrulama Sonrası İncelemesini gerçekleştirir. Bu gözden geçirmelerin bir parçası olarak şirketler, SM sonuçlarını ve destekleyici kanıtları tartışmak için heyet ile bir araya gelir ve heyet, performansı iyileştirmek için tavsiyelerde bulunabilir.

ATIK YÖNETİM PROTOKOLÜ

Atıklar, değerli maddelerin (örneğin altın) içinde oluştukları kayadan ayrıldığında ortaya çıkan madenciliğin bir ürünüdür. Sorumlu bir şekilde yönetilmezse, atıklar insan sağlığı ve güvenliği, çevre, altyapı ve madencilik şirketlerinin kendileri için potansiyel riskler oluşturabilir. Sorumlu atık yönetimi, bu riskleri en aza indirmek ve azaltmak için çok önemlidir.

MAC'in Bilim ve Çevre Yönetimi Başkan Yardımcısı Charles Dumaresq (2019), Vancouver, Kanada'daki "Tailings and Mining Waste 2019" kongresinde, " Overview of Governance Practices for Tailings Management" (Atık Yönetimine Ait Uygulamalara Genel Bakış) sunumunda sorumlu atık yönetiminin ilkelerini şu şekilde açıkladı: :

- Hesap verebilirlik ve sorumluluk
- Yönetim sistemleri yaklaşımı → Atık yönetim sistemi
- Performansa dayalı, risk bilgisine dayalı yaklaşım
- Etkili planlama ve tasarım
- İşletme, Bakım ve İzleme Kılavuzu
- Biyoçeşitliliği Koruma Yönetimi
- Acil durum hazırlığı
- Bağımsız inceleme dahil olmak üzere dış doğrulama

Dumaresq (2019), “bu ilkeleri izleyerek atık yönetimine yönelik sistematik bir yaklaşımın, belki de en büyük risk olabilecek şeyi azaltmaya yardımcı olduğunu belirtti: insan unsuru ve insan hatası potansiyeli. Kontroller ve dengeler içeren sistematik bir yaklaşım, insan hataları, deneyimler, önyargılar veya yerleşik cehaletlerin etkisiz atık yönetimine veya daha da kötüsü bir atık tesisinin arızalanmasına yol açma riskini azaltmaya yardımcı olur”. Dumaresq ayrıca, “bu ilkelerin uygulanmasının başarısızlıkların olmayacağını garanti etmeyeceğini, ancak bu ilkelerin etkin bir şekilde uygulanmasının başarısızlık olasılığını ve bir başarısızlık meydana gelirse olası sonuçları azaltmaya yardımcı olacağını vurguladı”.

2004 yılında tanıtılan Atık Yönetim Protokolü, SM programının önemli bir odak noktasıdır. Protokol bu ilkelerle uyumludur ve protokolün uygulanması, sorumlu atık yönetimi için bu ilkelerin uygulanması için paha biçilmez bir araçtır. Protokol, beş performans ölçüm göstergesini açıklar (MAC 2019d):

1. Bir kurumsal atık yönetimi politikası ve taahhüdü geliştirmek,
2. Sahaya özel bir atık yönetim sistemi geliştirmek ve uygulamak ve acil duruma hazırlık planları geliştirerek test etmek,
3. Atık yönetimi için hesap verebilirlik ve sorumluluk atama,
4. Sürekli iyileştirme için yıllık atık yönetimi incelemesi yapmak,
5. Sahaya özel bir İşletme, Bakım ve İzleme Kılavuzu'nun (İŞBİK) geliştirilmesi ve uygulanması.

Atık Yönetim Protokolü uygulanması, iki kılavuz belge ile desteklenmektedir:

İlk olarak 1998'de yayınlanan “A Guide To The Management of Tailings Facilities” (Atık Yönetimi Kılavuzu), atık yönetiminin kurumsal yönetimi ve sahaya özel atık yönetim sistemlerinin geliştirilmesi ve uygulanması hakkında rehberlik sağlar (MAC 2019).

İlk olarak 2003 yılında yayınlanan " Developing an Operation, Maintenance, and Surveillance Manual for Tailings and Water Management Facilities" (OMS- İŞBİK), yaşam döngüleri boyunca atık tesislerinin sahaya özel işletimi, bakımı ve izlenmesi hakkında rehberlik sağlar (MAC 2019).

2014 yılında British Columbia'daki Mount Polley Madeni atık tesisinde meydana gelen kazadan sonra MAC, TSM'nin Atık Yönetim Protokolü, İŞBİK ve Atık Yönetimi Kılavuzu'ndan oluşan atık yönetimi bileşeninin kapsamlı dış ve iç incelemelerini başlattı. Bu gözden geçirmeler, TSM'nin atık yönetimi bileşeninde herhangi bir iyileştirme ihtiyacını belirleme amacıyla yapılmaktadır.

Dış inceleme, MAC Yönetim Kurulu'na sunulan ve 29 tavsiye içeren bir rapor (TSM Tailings Review Task Force, 2015) üretti. Bu tavsiyeler Protokolü ve her iki Rehberi ele almış ve Atık Rehberini güncellemek için tavsiyeleri içermiştir:

“Atık Yönetimi Kılavuzu’nu, saha araştırması ve seçimi, tasarımı, inşaatı, işletimi, kapatılması ve atık tesislerinin kapatılması sonrasında bağımsız bir inceleme gerektirecek şekilde değiştirin.

Mevcut En İyi Teknoloji (MET - BAT) ve Mevcut En İyi Uygulama (MEU - BAP) üzerine yorumları içeren Mount Polley'in Uzman Heyet İncelemesi ile ilgili olarak, MAC, hem BAT hem de BAP'nin Atık Yönetimi Kılavuzu'na en iyi şekilde nasıl dahil edeceğini değerlendirin ve Atık Yönetim Protokolünün 2. Göstergesinde bunlara atıfta bulunun.

Kayıt Mühendisi (Engineer Of Record - EoR) değişikliğini ve bir mülkiyet değişikliğini yönetmekle ilgili tanımları ve/veya rehberliği geliştirin ve Atık Yönetimi Kılavuzu'nun değişiklik yönetimi bölümünde dahil edin.

Uygunsuzluklar için riske dayalı bir sınıflandırma sistemi oluşturun ve ilgili sonuçları değerlendirin. Risk değerlendirme metodolojisine ilişkin rehberliği, Atık Yönetim Kılavuzu'na dahil edin.

Hedeflerin nasıl seçileceği ve tasarım kriterlerinin nasıl belirleneceği de dahil olmak üzere, saha seçimi ve tasarımı ile ilgili daha spesifik teknik rehberliği içerecek şekilde Atık Yönetimi Kılavuzu'nu gözden geçirin ve gerektiği şekilde değiştirin.”

Dış ve iç değerlendirme sonuçlarına cevaben, MAC, Atık Yönetim Protokolü'nü (2017 ve 2019) ve OMS Kılavuzu'nu (2019) revize etti. Atık Yönetimi Kılavuzu'na ve OMS Kılavuzu'ndaki revizyonlar önceki sürümlerden temel kavramları güçlendirdi ve yeni kavramlar eklendi. Atık Yönetim Kılavuzu için, güçlendirilen ve eklenen kavramlar (MAC 2019):

Risk Esaslı Yaklaşım:

Atık yönetimini fiziksel ve kimyasal risklerle orantılı bir şekilde yönetmek.

Risk değerlendirmeleri yapmak ve yaşam döngüsü boyunca değerlendirmeleri güncellemek.

Riskleri yönetmek için mevcut en iyi uygulamaların (MEU - BAP) ve mevcut en iyi tekniklerin (MET - BAT) kullanımını ve entegrasyonu sağlamak.

Sonuçları yüksek olayları önlemek veya azaltmak için bir risk yönetimi aracı olan (özellikle, bir tür risk kontrolü) kritik kontrolleri sağlamak.

Atık Depolama Tesisinin sahibi adına teknik yönlendirme sağlayan Kayıt Mühendisi (Engineer Of Record - EoR) belirlemek.

Yaşam döngüsü boyunca atık tesisleriyle ilişkili risklerin tanımlanmasına, anlaşılmasına ve yönetilmesine yardımcı olmak için, bağımsız incelemenin entegrasyonunu sağlayarak nesnel uzman yorumu ve tavsiyelerini almak.

Atık yönetimi teknolojisi ve tesis konumunun optimum kombinasyonunu belirlemek gibi konularında titiz ve şeffaf bir metodoloji ile atık yönetimi alternatiflerini değerlendirmek.

Atık taşıma ve depolama planları,

Su Yönetim Planları,

Kapatma Planları.

Atık Yönetim Protokolü, Atık Yönetimi Kılavuzu ve İŞBİK (OMS), atık yönetimi için uluslararası lider uygulama olarak kabul edilmiştir (Golder Associates, 2016, Morgenstern, 2018) ve atık tesislerinin katastrofik yıkım riskini minimize etmeyi amaçlayan, “The International Council On Mining And Metal (ICMM)” 2016 Atık Yönetimi Çerçevesi Durum Değerlendirmesi ile uyumlu ve onu tamamlayıcıdır.

2021'de, MAC, Birleşmiş Milletler'in “Atık Yönetimine İlişkin Küresel Endüstri Standardı”nın (Global Tailings Review, 2020) yayınlanmasına yanıt olarak geliştirilen Atık Yönetimi Kılavuzu için bir güncelleme yayınladı. Güncelleme, kilit personellerin rolleri ve sorumlulukları hakkında daha fazla ayrıntı ve yaşam döngüsü boyunca belgelenecek bilgilere ilişkin yeni rehberliği içermektedir (örneğin, Atık tesislerinin tasarımının ve inşaatının dokümantasyonu). SM gereklilikleri ve rehberliği, BM Küresel Endüstri Standartındaki gereksinimlerin çoğunu karşılıyor ve hatta aşıyor olsa da, bu güncelleştirme (MAC 2021) ile BM Küresel Endüstri Standardı eşdeğerliliğinin iyileştirilmesi amaçlanmıştır.

Özellikle Kanada'daki madenler için, SM'nin atık yönetimi bileşeninin uygulanması, özellikle “Canadian Dam Association” (CDA) tarafından yayınlanan yönergelerle desteklenmektedir;

Canadian Dam Association Dam Safety Guidelines 2007 (2013 Edition)
 Technical Bulletin: Implementation of Dam Safety Guidelines in Mining Dams (2014).

Ayrıca, bunların dışında aşağıdakiler gibi ilgili teknik rehberlik sağlayan çok çeşitli kuruluşlar ve programlar vardır;

International Commission on Large Dams (ICOLD)
 Australian National Committee on Large Dams (ANCOLD)
 International Organization for Standardization (ISO):

- ISO 9000 – Kalite Yönetimi (Quality Management)
- ISO 14000 – Çevre Yönetimi (Environmental Management)
- ISO 31000 – Risk Yönetimi (Risk Management)

International Code for Cyanide Management
 Environment and Climate Change of Canada (ECCC)
 Western Australia Department of Mines and Petroleum
 Australian Government Leading Practice Sustainable Development Program for the Mining Industry
 South African National Standards SANS 10286 1998
 US Bureau of Reclamation
 US Army Corps of Engineers
 US Federal Emergency Management Agency
 United Nations Environment Programme
 European Union directive and Best Available Techniques (BAT) Reference Document for the Management.

MAC, sahaya özel atık yönetim sistemlerinin geliştirilmesini ve performanslarının iyileştirilmesi ve kurumsal politika ile ilgili yasal gereklilikleri ve yerel topluluk taahhütlerini karşılamak için, Atık Yönetimi Protokolü ve yönergelerinin uygulanmasını destekleyen bir araç olan "Tailings Guide implementation checklist" hazırlamıştır. Bu kontrol listesi doldurularak, atık yönetimi çerçevesinde uygulama durumunun bir anlık görüntüsü elde edilir (Şekil 4).

MAC ayrıca, Protokolde açıklanan göstergelere karşı performansı değerlendirmek için Atık Yönetimi Protokolü ile birlikte kullanılan bir Uygunluk Tablosu geliştirmiştir. "Tailings Guide implementation checklist" (Atık Kılavuzu Uygulama Kontrol Listesi) ve "Table of Conformance" (Uygunluk Tablosu) benzer olsalar da, bu araçlar farklı amaçlara hizmet etmektedir (Şekil 4 ve 5). "Table of Conformance", Atık Yönetimi Protokolü'ndeki (MAC 2019) her bir gösterge için performans kriterlerini ve uygulanması gereken Atık Yönetim Kılavuzu ve İŞBİK unsurlarını tanımlar ve uygunluğunu denetler.

Gösterge 5: OMS Kılavuzu						
Kriterler	Belge	Bölüm	Evet	Hayır	Yok	Yanıtı Destekleyecek Açıklama ve Kanıt
Genel Gereksinimler						
OMS kılavuzu, uygulandığı atık tesisine özel olacak şekilde geliştirildi mi?	OMS Kılavuzu	2.1.2				
OMS kılavuzu, uygulama kapsamının sınırlarını açıklıyor mu?						
Kapsam, atık tesisinin performansını ve risk yönetimini etkileyebilecek operasyonel						

kontrolleri içeriyor mu?							
OMS kılavuzu, atık tesisinin mevcut koşullarını ve yaşam döngüsü aşamasını yansıtıyor mu?							
Diğer Sistemlerle Bağlantılar							
OMS kılavuzu, diğer ilgili maden sahası planları ve prosedürleri ile bağlantıları, bu diğer planlar ve prosedürlerin atık yönetimi ve OMS faaliyetleri ile nasıl ilişkili olduğunu açıklıyor mu?	OMS Kılavuzu	2.4.3					
Bağlantıların bu tanımı, çeşitli sorumlu kişiler veya gruplar arasında ilişkili roller, sorumluluklar, yetki seviyeleri ve iletişim prosedürlerini içeriyor mu?							
OMS kılavuzunun uygulanması							
OMS el kitabı, tanımlanmış sorumluluklara sahip her bir pozisyon için minimum bilgi ve yetkinlik gereksinimlerini tanımlıyor mu?	OMS Kılavuzu	2.5 ve 3.1.6					

Şekil 1. Uygunluk Tablosu “Table of Conformance” Kısmi Görüntüsü (MAC 2019).

Atık Kılavuzu Bölümü	Yönetim Eylemi	Sorumluluklar	Performans Ölçümü	Takvim	Referanslar
Kapsayıcı İlkeler					
Risk Değerlendirmesi ve Yönetimi					
2.2.1	Aşağıda Planlama başlığı altında ele alınmıştır.				
Atık Yönetimi için BAT ve BAP					
2.2.2	Belirli bir atık tesisi için atık yönetim teknolojisini seçerken aşağıdaki faktörleri göz önünde bulunduruyor musunuz:				
	• Bir atık tesisinin arızalanma olasılığı veya sonuçları azaltılıyor mu?				
	• Potansiyel bir jeokimyasal sorunu yönetmek için malzeme ayrımı gerekli mi?				
	• Taşıma ve yerleştirme sırasında atıklarda ne kadar su tutulacak?				
Bağımsız İnceleme					
2.2.3	Rutin olarak Bağımsız İnceleme yapmak için bir mekanizma oluşturulmuş mu?				
Kapatma için Dizayn ve Operasyon					
2.2.4	Atık tesisinin kavramsal planlamasında ve tasarımında uzun				

	vadeli kapatma hedefleri ve kapatma sonrası potansiyel arazi kullanımları dikkate alındı mı?				
--	----------------------------------------------------------------------------------------------	--	--	--	--

Şekil 2. Atık Kılavuzu Uygulama Kontrol Listesi “Tailings Guide Implementation Checklist” Kısmi Görüntüsü (MAC 2019)

ATIK YÖNETİM PROTOKOLÜNÜN PERFORMANSININ DEĞERLENDİRİLMESİ

Yukarıda açıklandığı gibi, Atık Yönetimi Protokolündeki göstergelere karşı performans, “Table of Conformance” (Uygunluk Tablosu) kullanılarak değerlendirilir. Bu değerlendirmenin önemi uygun belgeler ve kanıtlar ile “Uygunluk Tablosu”nda tanımlanan öğelerin uygun şekilde geliştirilip geliştirilmediğini, uygulanıp uygulanmadığını göstermektedir. Atık Kılavuzu ve İŞBİK Kılavuzu, belgelenmesi gereken ve “Uygunluk Tablosu”nun doldurulmasında başvurulabilecek çok çeşitli bilgileri tanımlar. Bu bilgilerin uygun şekilde değerlendirildiğinden ve bilgilerin atık tesisinin özellikleri ve yaşam döngüsü boyunca sahaya özel kozullar dikkate alınarak, Atık Yönetim Protokolü’ndeki göstergelere göre değerlendirilmesi şirket sorumluluğundadır.

Atık Yönetim Protokolü ve Kılavuzlar, şirketin/tesisnin her Gösterge için Seviye A veya daha yüksek bir seviye elde etmek için hazırlanması, geliştirmesi ve uygulaması gereken bir dizi belgeden oluşmaktadır. Bu belgelerin nasıl düzenlendiği ve değerlendirmenin atık tesisinin özellikleri ve yaşam döngüsü aşaması dahil olmak üzere sahaya özgü koşulları dikkate alınarak yapılması şirketin sorumluluğundadır.

1. Kurumsal bir atık yönetim politikası ve taahhüdü geliştirmek.

Hedef; Şirketlerin, atık yönetimi ile ilgili niyet, taahhüt ve ilkeleri ifade eden bir politika ve / veya taahhüt oluşturduğunu ve etkili bir şekilde iletişimde olduğunu teyit etmek.

Şirketin atık yönetimine özel ayrı bir politika veya taahhüt geliştirmesine gerek yoktur. Bu göstergenin gereklilikleri, atık yönetimi taahhütlerini daha geniş olan şirket politikalarına veya taahhütlerine (örneğin, kurumsal sürdürülebilirlik politikası) dahil ederek karşılanabilir. Önemli kısım, kurumsal politika ve taahhütlerin güvenli, sorumlu atık yönetimi taahhütlerini içermesini veya bunlara atıfta bulunmasını sağlamak ve şirketin bu politika ve taahhütlere bağlı olduğunu göstermektir.

2. Sahaya özel bir atık yönetim sistemi geliştirmek/uygulamak ve Acil durum hazırlık planları geliştirerek test etmek.

Hedef;

Atık Yönetimi Kılavuzu’nda açıklanan atık yönetimi çerçevesine uygun olarak atık yönetimi sisteminin geliştirilmesi ve uygulanması.

Atık Tesislerinin Yönetimi Kılavuzu ile uyumlu Acil Durum Müdahale Planları ve Acil Durum Hazırlık Planları geliştirilmesi ve test edilmesi.

Şirketin, Atık Yönetimi Kılavuzu’nda açıklanan atık yönetimi çerçevesine uygun bir atık yönetim sisteminin uygulandığını dokümantasyon ve diğer kanıtlar yoluyla gösterebilmesi gerekir.

Benzer şekilde, atık depolama alanlarına ait Acil Durum Müdahale Planları ve Acil Durum Hazırlık Planları olması gerekli değildir. Acil Durum Müdahale Planları ve Acil Durum Hazırlık Planları atık yönetimi için ayrı olabileceği gibi genel sahanın tüm yönlerini kapsayan Acil Durum Müdahale Planları ve Acil Durum Hazırlık Planları’na dahil edilebilir ve çoğu durumda bu tercih edilir.

3. Atık yönetimi için hesap verilebilirlik ve sorumluluk atama

Hedef; Atık yönetiminin hesap verilebilirliği için bir sorumlu yönetici (örneğin, CEO, COO veya Başkan Yardımcısı) atandığını ve şirkete atıkların sorumlu bir şekilde yönetildiğine dair güvence vermek için uygun bir yönetim yapısının ve kaynaklarının bulunduğunu onaylanması.

4. Sürekli iyileştirme için yıllık atık yönetimi incelemesi yapmak

Hedef; Atık yönetimi üzerinde kurumsal yönetişimin sağlanması ve şirketin atık yönetimi organizasyonel yapılarının ve sistemlerinin etkin olduğundan ve atıkların güvenli, sorumlu yönetimine yönelik ihtiyaçları karşılamaya devam ettiğinden emin olmak için Sorumlu İcra Kurulu Üyesine raporlanan atık yönetiminin yıllık bir incelemesi olduğunu teyit edilmesi.

5. Sahaya özel İşletme ,Bakım ve İzleme Kılavuzu'nun geliştirilmesi ve uygulanması

Hedef; Şirketin, atık yönetim sisteminin uygulanmasını kolaylaştırmak amacıyla Sürdürülebilir Madencilik Atık Yönetimi Protokolü İşletme, Bakım ve İzleme Kılavuzu'na (İŞBİK - OMS) uygun olarak atık toplama tesisine özgü bir İşletme, Bakım Ve İzleme Kılavuzu (İŞBİK - OMS) geliştirip uyguladığının teyit edilmesi.

UYGULAMA ÖRNEĞİ – TÜPRAG EFEMÇUKURU ALTIN MADENİ

MAC, Sürdürülebilir Madencilik - Atık Yönetim Protokolü programı/sistemi Türkiye'de 2015 yılından bu yana TÜPRAG EFEMÇUKURU Altın Madeni'nde uygulanmaktadır. 2015 yılı içerisinde bir bağımsız değerlendirme raporu ve iç denetleme raporu hazırlanmıştır. 2017 yılı içerisinde bağımsız denetim kuruluşu tarafından hazırlanan MAC uyumluluk raporu sonrasında yol haritası belirlenerek çalışmalar başlanmıştır. Daha sonraki yıllarda diğer Sürdürülebilir Madencilik protokollerinin hazırlıkları tamamlanarak sisteme entegre edilmeye başlanmıştır.

TSM bileşenlerine 2015 yılından sonrada güncellemeler yapılmıştır. TÜPRAG EFEMÇUKURU Altın Madeni'nde Atık Yönetim Protokolü'nün ve Uygunluk Tablosu'nun 2019 versiyonu, Atık Kılavuzu ve OMS rehberinin 2021 versiyonları uygulanmaya başlanmıştır.

Mevcut operasyonel faaliyetlerde kullanılan sistemler/uygulamalar (Atık Yönetim Sistemi, Protokoller, İSG Uygulamaları ERP-EPP, prosedürler, BAT ve BAP'lar) TSM Atık Yönetim Protokolü uygulaması içerisine entegre edilmiştir.

Atık Yönetimi Politikası ve Taahhüdü

Atık yönetimine ilişkin taahhütler, şirketin politikalarına ve taahhütlerine dahil edilmiş ve Atık Kılavuzu ile tutarlıdır.

Atık Yönetim Sistemi ve Acil Durum Hazırlığı

Risk bazlı yaklaşım kapsamında atık depolama alanlarına özgü;

İş sağlığı ve güvenliği, çevre, mühendislik ve operasyonel, finansal, yasal ve yönetim süreçleri ile sosyal konuları kapsayan bir risk değerlendirmesi yapılmıştır.

Stabilite, temas suyu ve sızıntı, tozlanma, kapasite, izinler gibi konularda tehlikeler ve kritik kontroller belirlenmiştir.

Aşırı hava koşulları, atık nem içeriği, izleme verileri, deplasman gibi konuları kapsayan Kademeli Eylem Planları (KEP) hazırlanmıştır.

Risk deęerlendirmesi ve kritik kontroller dikkate alınarak Acil Durum M¼dahale Planı hazırlanmıř ve KEP'lerle baęlanmıřtır.

Mevcut saha Acil Durum M¼dahale Planları'na ek olarak depolama alanları iin ¼zel Acil Durum M¼dahale Planı oluřturulmuřtur.

Depolama alanları iin hazırlanan Acil Durum M¼dahale Planları masabařı ve genel saha tatbikatları yapılarak denetlenmiřtir.

Atık Y¼netimi iin Hesap Verilebilirlik Ve Sorumluluk

Atık Y¼netimi Protokol¼ ve Atık Y¼netim Kılavuzu uygulaması kapsamında sorumluluklar belirlenmiř ve Kayıt M¼hendisi (EOR) atanmıřtır.

Yıllık Atık Y¼netimi İncelemesi

2017 yılından bu yana her sene Yıllık G¼zden Geirme Raporu hazırlanarak, y¼netime sunulmaktadır. Ayrıca İ ve dıř denetimler yapılarak raporlanmaktadır.

İřletme, Bakım ve İzleme Kılavuzu (İřBİK)

Bir İřBİK geliřtirildi ve sahada uygulanmaktadır. Her yıl g¼zden geirilerek uygun řekilde g¼ncellenmektedir.

T¼PRAG EFEMUKURU Altın Madeni'nde 2021 S¼rd¼r¼lebilir Madencilik Atık Y¼netimi Protokol¼ performans deęerlendirmesinde A seviyesine ulařılmıřtır. 2022 yılı 1. eyrekte yapılması planlanan S¼rd¼r¼lebilir Madencilik Atık Y¼netimi Protokol¼ performans deęerlendirmesinin ardından (dıř deęerlendirme) AAA seviyesine ulařılması hedeflenmektedir.

SONULAR

Madencilik sekt¼r¼n¼n ¼lkemizde ve d¼nyada hızla geliřmesi, sosyal ve evresel etkilerindeki artıřı da beraberinde getirmektedir. Bu durumu ¼lkeler yasal mevzuatlarında yaptıkları d¼zenlemeler ile y¼netmektedir.

Sorumlu madencilik ercevesinde hem ¼lkelerin yasal mevzuatlarını, hemde madencilik faaliyetlerini mevcut en iyi teknikler ve mevcut en iyi uygulamalar ile destekleyecek baęımsız kuruluřların s¼rd¼r¼lebilir performans programlarına ihtiya artmıřtır.

Kanada Madencilik Derneęi, S¼rd¼r¼lebilir Madencilik programı ve benzer performans programları, b¼y¼mekte ve geliřmekte olan sekt¼re mevcut en iyi teknikleri ve mevcut en iyi uygulamaları benimseterek s¼rekli geliřimi desteklemek ve yasal mevzuatlara uyumu saęlamak iin bir rehber olmaktadır.

Bu t¼r programlar; madencilik sekt¼r¼n¼n evresel ve sosyal performansını iyileřtirerek, iřletmeye hesap verebilirlik, řeffaflık, ¼l¼lebilirlik ve s¼rd¼r¼lebilirlik kazandırarak ¼lkemizdeki madencilik faaliyetlerinin m¼mk¼n olan en y¼ksek standartlarda y¼r¼t¼lmesine, yardımcı olacaktır.

KAYNAKLAR

Dumaresq, C. (2019). Overview of Governance Practices for Tailings Management. Presented at a short course entitled "Corporate Governance of Tailings Facilities – Challenges and Case Studies of Implementation. Short course was part of the "Tailings and Mine Waste 2019" congress. Vancouver, Canada.

- Global Tailings Review (2020). Global Industry Standard on Tailings Management. <https://globaltailingsreview.org/global-industry-standard/>
- Golder Associates (2016). Review of Tailings Management Guidelines and Recommendations for Improvement. Prepared for: International Council on Mining & Metals. <https://www.icmm.com/en-gb/research/environmental-stewardship/tailings-report>
- International Council on Mining & Metals (2016, 2020). Tailings Governance Framework: Position Statement. <https://www.icmm.com/en-gb/about-us/member-requirements/position-statements/tailings-governance>
- Mining Association of Canada (2019a). A Guide to the Management of Tailings Facilities *Version 3.1*. <https://mining.ca/our-focus/tailings-management/tailings-guide/>
- Mining Association of Canada (2019b). Developing an Operation, Maintenance, and Surveillance Manual for Tailings and Water Management Facilities *Second Edition*. <https://mining.ca/our-focus/tailings-management/oms-guide/>
- Mining Association of Canada (2019c). Table of Conformance. <https://mining.ca/documents/table-of-conformance-2019/>
- Mining Association of Canada (2019d). Towards Sustainable Mining Tailings Management Protocol. <https://mining.ca/towards-sustainable-mining/protocols-frameworks/tailings-management-protocol/>
- Mining Association of Canada (2021a). TSM 101: A Primer. <https://mining.ca/documents/tsm-101-a-primer/>
- Mining Association of Canada (2021b). MAC Updates Tailings Management Guidance to Align with Global Standard. Press release issued in Ottawa, Canada, on 7 April, 2021. <https://mining.ca/press-releases/mac-updates-tailings-management-guidance-to-align-with-global-standard/>
- Morgenstern, N.R. (2018). Geotechnical Risk, Regulation, and Public Policy. Sixth Victor de Mello Lecture. Presented in Salvador, Brazil, August, 2018. https://victorfbdemello.com.br/en/de-mello-lectures-2__trashed/
- TSM Tailings Review Task Force (2015). Report of the TSM Tailings Review Task Force. <https://mining.ca/documents/report-tsm-tailings-review-task-force/>
- TSM Verification Guide (December 8, 2021). 2019 March Meeting Report_DRAFT_Apr_24_2019 BC an (mining.ca)
- TSM Terms of Reference for Verifiers (Last Updated: November 19, 2021). 2021-TSM-Verifier-Terms-of-Reference.pdf (mining.ca)
- Tailings Guide Implementation Checklist, Version 3.1 (2019). Tailings Guide Implementation Checklist, Version 3.1 (2019) - The Mining Association of Canada
- Table of Conformance (March 20, 2019). Table of Conformance (2019) - The Mining Association of Canada
- Kuru Atık Depolama Yöntemi - Dry Tailings Storage Method (IMCET - 16 April 2019 – Pages 1540-1530). Y.S. İnci, P. Kimball, G. Uzuncelebi, H. Ürkmez . [ddcb03c09924b75_ek.pdf](https://www.maden.org.tr/icerik/1540-1530-kuru-atik-depolama-yontemi-dry-tailings-storage-method) (maden.org.tr)

KARDEMİR A.Ş. KİREÇ FABRİKALARINDAKİ YANMIŞ KİREÇ TAŞI ELEME SİSTEMİNDE KULLANILAN ELEK PANELLERİNİN İYİLEŞTİRİLMESİ

IMPROVEMENT OF SIEVE PANELS USED IN BURNT LIMESTONE SCREENING SYSTEM AT KARDEMİR A.Ş. LIME PLANTS

E. Nakaş^{1,*}, C. Cantürk², F. Esin², O. Acur², M. Sevim², H. Gökkaya³

¹ KARDEMİR A.Ş., İş Sağlığı ve Güvenliği Müdürlüğü
(*Sorumlu yazar: enakas@kardemir.com)

² KARDEMİR A.Ş., AR-GE Merkezi
Karabük Üniversitesi, Mühendislik Fakültesi, Makine Mühendisliği

ÖZET

Günümüzde endüstriyel fabrikalar üretim maliyetlerini düşürebilmek ve rekabet etme gücünü arttırılabilmek için tesislerinde öneri ve iyileştirme çalışmalarına büyük önem vermektedirler. Dünyada her yıl yaklaşık olarak 1.9 milyar ton çelik üretimi yapılmakta ve bu miktarın % 60'ı yüksek fırınlardan elde edilmektedir. Kardemir A.Ş. entegre demir çelik fabrikasında çelik üretimi prosesi sırasında yanmış kireç taşı sıvı çelik içerisindeki empüritelere giderilmesi için kullanılmaktadır. Yanmış kireçtaşlarının 50 mm'nin üzerindeki boyutta olması sıvı madende homojen bir şekilde çözünmesi için önem arz etmektedir. Yanmış kireç taşlarının boyutlandırılmasında kullanılan çelik esaslı elek panellerinde oluşan kopmalar yanmış kireç taşlarının sağlıklı boyutlandırılmamasına ve kopmalardan kaynaklı üretim duruşları, iş sağlığı ve güvenliği konularında olumsuzluklara neden olmaktadır. Bu çalışmada, çelik esaslı elek panelleri yerine aynı boyutlandırma alanına sahip olan kauçuk esaslı elek panelleri kullanılmıştır. Kauçuk esaslı elek panelleri kullanılarak yapılan iyileştirme ile birlikte, yanmış kireç taşlarının boyutlandırılması işlemi esnasında panellerde oluşan kopma ve kopmadan kaynaklı üretim duruşları, elek panellerinin değişimi esnasında yaşanan iş sağlığı ve güvenliği risklerinin önüne geçilmiştir.

Anahtar Sözcükler: Bazik oksijen fırını (BOF), yanmış kireç taşı, elek paneli, üretim duruşu, iş sağlığı ve güvenliği

ABSTRACT

Nowadays, industrial factories attach great importance to suggestions and improvement studies in their facilities in order to reduce production costs and increase their competitiveness. Approximately 1.9 billion tons of steel is produced every year in the world and 60% of this amount is obtained from blast furnaces. Burnt limestone is used to remove impurities in the liquid steel during the steel production process of KARDEMİR A.Ş. integrated iron and steel factory. The size of burnt limestone over 50 mm is important for homogeneous dissolution in liquid steel. The breaks in the steel-based sieve panels used in the sizing of the burnt limestone cause the burnt limestone not to be dimensioned properly and cause negativity on the production stops, occupational health and safety issues. In this study, instead of steel based sieve panels, rubber based sieve panels with the same sizing area are used. Along with the improvement made by using rubber-based sieve panels, the production stops caused by the break and break in the panels during the sizing process of burnt limestone, occupational health and safety risks experienced during the replacement of sieve panels were prevented.

Keywords: Basic oxygen furnace (BOF), burnt limestone, sieve panel, production stop, occupational health and safety

GİRİŞ

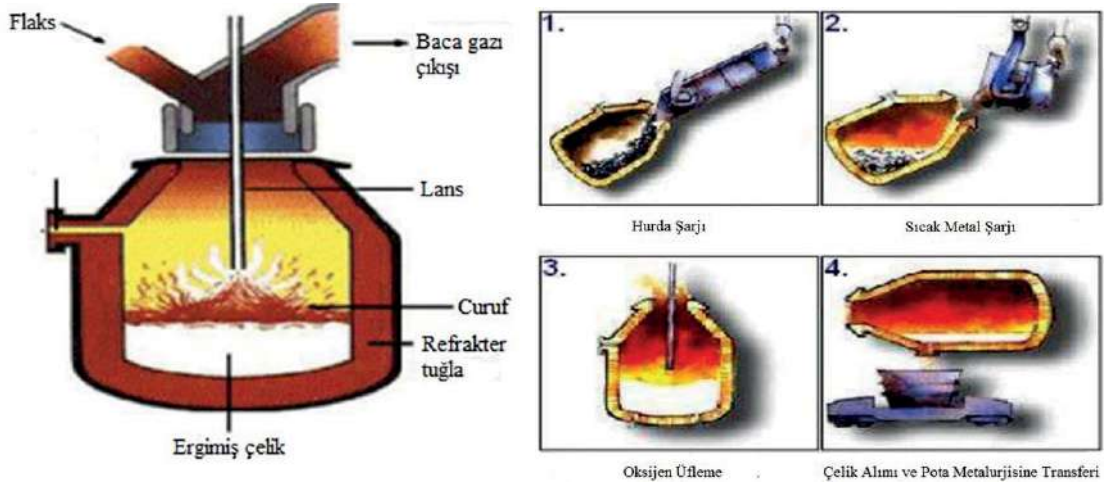
Çelik malzemeler yapı, otomotiv, sağlık sektörlerinde ve günlük kullandığımız araç gereç gibi pek çok alanda karşımıza çıkmaktadır. Dünyada her yıl yaklaşık olarak 1.9 milyar ton çelik üretimi yapılmakta olup bu miktarın % 60'ı yüksek fırınlarda demir içerikli ham maddelerin kok ve kireçtaşının ergitilmesiyle oluşturulmaktadır. Diğer %40'lık kısım ise ark ocaklarında hurda ergitme yöntemi ile yapılmaktadır. Çelik üretiminde yanmış kireç taşı vazgeçilmez bir parametredir. Yanmış kireç taşlarının boyutları da çok önemlidir. Belirli ebatlarda olması sıvı çelik yapısında daha optimum çözünüp çelik içerisinde istenmeyen kükürt silisyum gibi çeliğe zarar veren elementlerle bileşik oluşturarak çelik yapısında yüzeye çıkarılır ve yapıdan uzaklaştırılır. Kardemir A.Ş. çelik üretim prosesinde yanmış kireç taşlarının ebatlarının çelik üretim prosesi gereği 50 mm üzerinde olması istenmektedir.

Endüstriyel tesisler de eleme boyutlandırma işleminde genellikle çelik esaslı elek panelleri kullanılmaktadır. Çelik esaslı elek panellerinde deformasyonlara bağlı kısa sürelerde oluşan kopmalar, çelik esaslı elek panellerinin montaj ve demontaj işlemlerinin zorluğu gibi olumsuz özellikleri 7/24 çalışmaya devam eden endüstriyel şirketleri arayış içerisine sokmaktadır. Günümüz teknolojisinde çelik esaslı elek panellerinin yerini kauçuk esaslı elek panelleri almaktadır. Kauçuklar esneme kabiliyetlerinden ötürü üzerlerine uygulanan enerjiyi absorbe ederek yapısal hasara uğramayan malzemelerdir. Kauçuklar bu özellikleri ile mühendislik alanında pek çok uygulamada tercih edilirler.

Yapılan çalışma ile Kardemir A.Ş. çelik üretim müdürlüğüne bağlı kireç fabrikasında eleme boyutlandırma işlemi yapılan çelik esaslı elek panelleri yerine kauçuk esaslı elek paneli kullanımına geçilerek elek panellerinde oluşan kopmalara bağlı ünite duruşları, maliyet ve iş sağlığı güvenliği konularında iyileştirme gerçekleştirilmiştir.

Çelik Üretim Prosesi

Bazik Oksijen Fırını (BOF), ilk aşamada şarj bölümü yönünde eğilerek içerisine hurda şarj edilir. Hurda şarjını alan BOF, yine aynı pozisyonda pota kükürt giderme tesisinde işlenmiş şarja hazır haldeki sıvı maden potasını bekler ve belli bir zaman sonra içerisine sıvı maden şarj edilir. BOF, içerisine hurda malzeme ve sıvı maden alımından sonra ağız dik konuma getirilir. BOF şarj ağız dik konumda iken, içerisine flaks silolarından yanmış kireç taşı ve diğer malzemeler (dolomit mıcırı, pelet) şarj edilir. BOF içerisine yapılan şarj işlemlerinden sonra lans ile 15-20 dakika boyunca saf oksijen üfleme işlemi uygulanır. BOF içerisine daldırılan lans üfleme işlemi ile oksijen; karbon, kükürt, silisyum ve mangan ile kimyasal tepkimeye girer. Karbon, yapıdan karbon monoksit (CO) olarak uzaklaştırılır. Diğer elementler ise yanmış kireç taşı sayesinde yüzeyde cüruf olarak uzaklaştırılır. Lans vasıtasıyla gerçekleştirilen tepkimeler sonucunda çelik üretimi gerçekleştirilmiş olunur. İçerisinde çelik üretimi gerçekleştirilen BOF, boşaltma bölümü yönüne eğilerek içerisindeki çeliği transfer arabası üzerinde bekleyen çelik potası içerisine boşaltır. Yanmış kireç taşı sayesinde oluşan cüruf özkütle farkı nedeniyle BOF içerisinde kalır. BOF tekrar şarj bölümü yönünde eğilerek BOF içerisindeki cürufu, cüruf potasına boşaltır. Tüm bu işlemler tavan vinçleri ile yapılmaktadır.



Şekil 1. BOF ile çelik üretim prosesi (2)

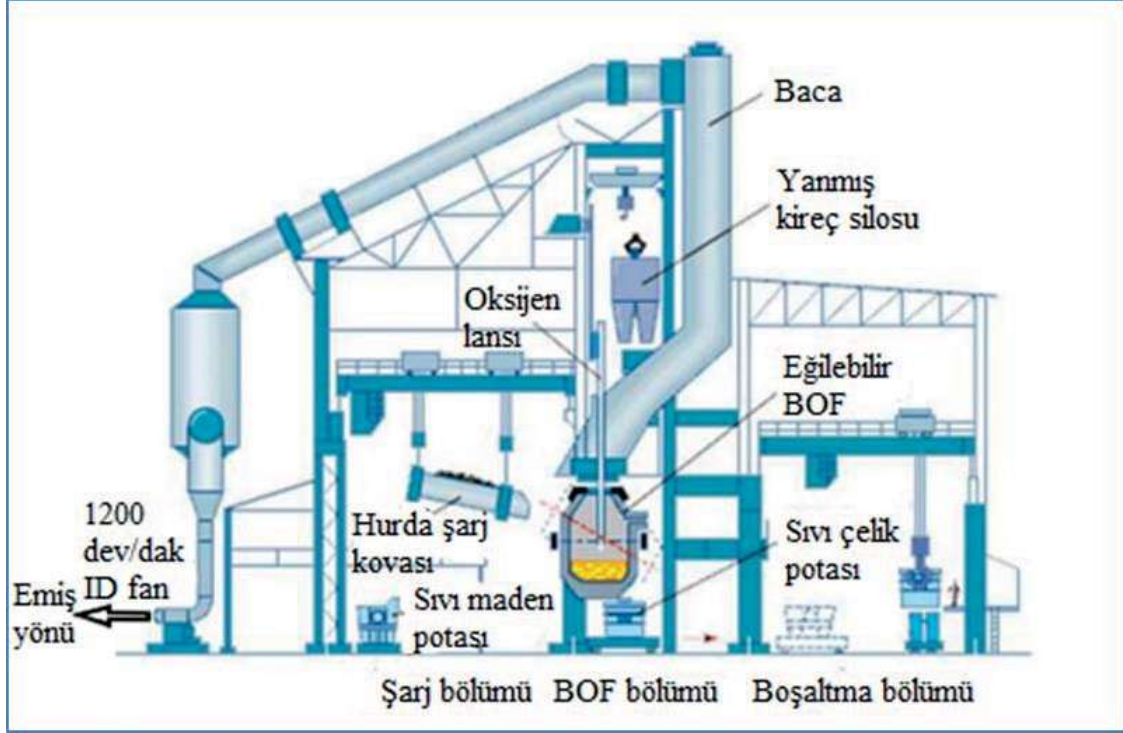
Bof'da Yanmış Kireç Taşı Kullanımı

BOF' larda üretilen çelik kalitesinin iyi olması için kullanılan yanmış kirecin de kaliteli olması istenilmektedir. Kaliteli yanmış kireç taşı; uygun büyüklüğe sahip, içerdiği kalsiyum oksit (CaO) oranı ve kükürt (S) , fosfor (P), silisyum (Si) gibi safsızlıklar ile tepkimeye girme reaktivitesi yüksek olan kireçtir. BOF ile çelik üretiminde kullanılan yanmış kireç taşı, BOF' un ısıl dengesini sağladığı ve safsızlıkların giderilmesini gerçekleştirdiği gibi oluşturduğu cüruf sayesinde BOF içerisindeki refrakter tuğla ömrünü de uzatmaktadır. BOF içerisindeki cüruflar refrakter tuğlalar üzerinde bir katman oluşturarak tuğlaların aşınmasını engellemektedir. Bu da, maliyeti çok yüksek olan refrakter tuğlaların uzun süre kullanımını arttırmaktadır.

BOF'da Yanmış Kireç Taşı Boyutlarının Önemi

BOF' larda kullanılan yanmış kirecin ebatları büyük önem arz etmektedir. BOF' da çelik üretimi esnasında oluşan karbon monoksit (CO), karbondioksit (CO₂) gazları ve oluşan tozların ortama yayılmaması için lans ile oksijen üfleme esnasında 1200 d/dk dönen emiş gücü çok yüksek bir ID fan vasıtası ile çekilmektedir. Gaz ve tozdan oluşan karışım boru içerisinde ID fanın emiş yönüne doğru hareket etmektedir. Gaz ve toz karışımı hareket halindeyken su püskürten nozullarla toz çöktürme işlemi uygulanmaktadır. Tozdan arınan gaz karışımı değerlendirilmek üzere Kardemir A.Ş Enerji Tesislerine gönderilmektedir.

BOF' larda istenilen kalitede 92 ton çelik üretmek için 4-4.5 ton yanmış kireç taşı kullanılmaktadır. Yanmış kireç taşları istenilen boyutlardan küçük olması durumunda BOF içerisinde sıvı maden yapısına ulaşmadan fanın emiş gücü ile çekilmektedir. Küçük boyutlarda yanmış kireç taşı kullanılması durumunda BOF içerisine tekrar yanmış kireç taşı şarj etmek gerekmektedir. Bu durum, yanmış kireç taşı sarfiyatını artırmaktadır. Ayrıca BOF içerisine tekrar yanmış kireç taşı şarj alma ve lans ile yeniden oksijen üfleme sürelerinden dolayı üretimde kayıplara neden olmaktadır. Kardemir A.Ş. BOF'larında çelik üretim esnasında işletme standardınca yanmış kireç taşı boyutları 50 mm üzerinde kullanılmaktadır.



Şekil 2. BOF'un yardımcı bölümlerinin genel görünümü (2)

Kardemir A.Ş. Kireç Fabrikaları

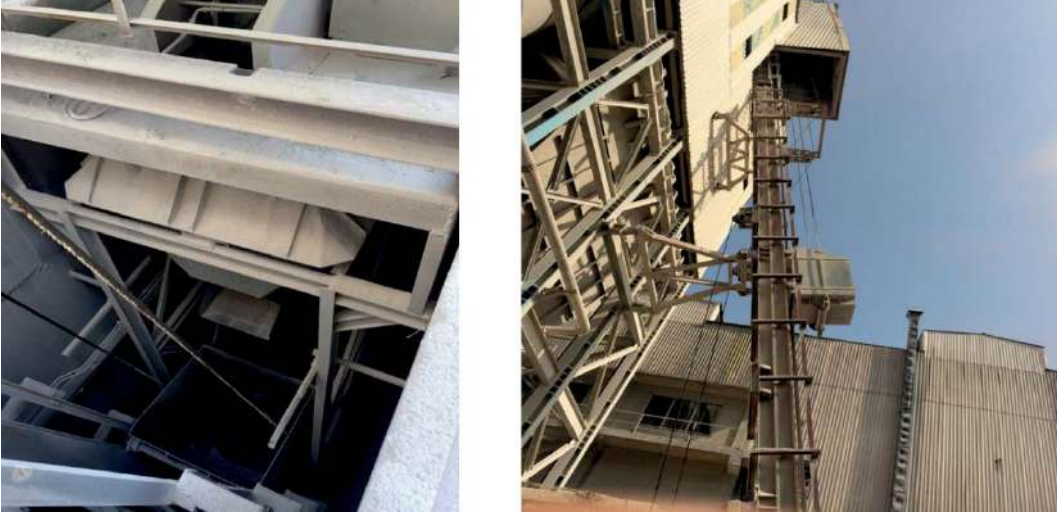
Karabük ili, jeolojik açıdan zengin bir bölgededir. Kardemir A.Ş.; kireç fabrikası hammadde kaynağı olan kireç taşı, Karabük ilinin Eskipazar ilçesinde bulunan kireç taşı ocaklarından temin etmektedir. Eskipazar'da çıkarılan kireç taşlarının kaliteli ve Kardemir A.Ş.'ye yakın oluşu lojistik açıdan avantaj kazandırmaktadır.

Kardemir A.Ş. çelik üretim ünitesindeki BOF' larda çelik üretimi için gerekli olan kireç taşları kamyonlarla Kardemir A.Ş. kireç fabrikası kireç taşı yer altı bunkerleri (150 Ton) sahasına getirilmektedir.



Şekil 3. Kardemir A.Ş. kireç fabrikasında bulunan kireç taşı yer altı bunkerleri genel görünümü

Kardemir A.Ş. bünyesinde bulunan kireç taşı fabrikasında 300 ton kapasiteli 2 adet kireç taşı silosu bulunmaktadır.

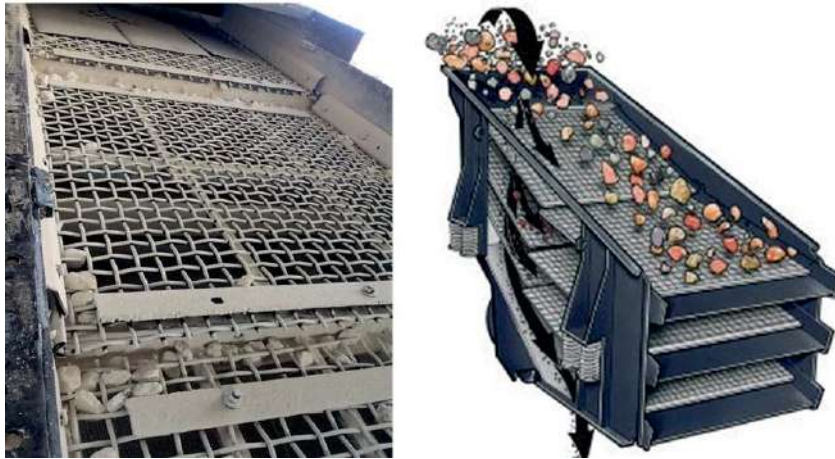


Şekil 4. Kireç taşı dolu skip arabasının eğik ray yolu üzerinde silo üstü bunkerine doğru hareketinin genel görünümü

Kireç taşları kireç fırınları içerisine şarj edildikten sonra 1000-1050 °C sıcaklıkta yakılarak kireç taşlarının kalsinasyonu gerçekleştirilerek metalürjik yanmış kireç taşı elde edilmektedir. Kireç fırınında her iki haznenin alt kısmında bulunan klapeler açılarak yanmış kireç taşları bant yollarına boşaltılır. Bant yolu üzerindeki yanmış kireç taşları kovalı elevatöre şarj edilir. Elevatör, içerisindeki kovalara doldurulan yanmış kireç taşlarını 50 m yüksekliğe çıkarır ve kovalardaki yanmış kireç taşlarını eleğe boşaltır. Yanmış kireç taşı eleğinde 50 mm üzerindeki yanmış kireç taşları 250 m uzunluğundaki bant yolu ile kireç fabrikasından çelikhaneye taşınırlar. Çelikhaneye gelen yanmış kireç taşları BOF'lar üzerindeki yanmış kireç silosuna şarj edilerek stoklanır.

Yanmış Kireç Taşı Boyutlandırmada Kullanılan Çelik Esaslı Elek Panelleri

BOF' larda çelik üretiminde BOF'un ısıl dengesinin sağlanması ve sıvı maden içerisindeki safsızlıkların giderilmesi için yanmış kireç taşına ihtiyaç bulunmaktadır. Yanmış kireç taşları 50 mm büyük boyutlarda olması yanmış kireç taşlarının BOF içerisindeki sıvı madende homojen bir şekilde çözünmesi için önem arz etmektedir. 50 mm üzerindeki boyutlarda yanmış kireç taşlarının elde edilmesi için Kardemir A.Ş. Kireç Fabrikaları kullanılmaktadır.



Şekil 5. Yanmış kireç taşı elemeye kullanılan çelik esaslı elek paneli gösterimi

Kireç fabrikalarında genel olarak yanmış kireç taşı boyutlandırmada çelik esaslı elek panelleri kullanılmaktadır. Yanmış kireç taşı boyutlandırma ve nakil ünitesinde eleme görevi gören çelik esaslı elek panelleri, çelik profillerden imal edilmiş bir şase üzerinde çalışmaktadır. Çelik esaslı elek panelleri, her iki tarafında bulunan gergi plakalarına geçirilir ve yanmış kireç taşı eleğinin gövdesinin iç kısımlarına civatalar ile sabitlenir. Elek panellerinin çalışmalarında tahrik için elektrik motorları kullanılmaktadır. Elektrik motoru tahriki ile üretilen güç, kayış kasnak sistemi ile yanmış kireç taşı eleğinin ortasında bulunan uzun mile aktarılır. Dönen milin diğer ucunda bulunan eksantrik ağırlıkların oluşturduğu titreşim ile yanmış kireç taşlarının boyutlandırılma işlemi yapılmaktadır.

Çelik esaslı elek panelleri, titreşime bağlı olarak altında bulunan çelik profilden imal edilmiş şaseye çarpmalar meydana getirerek çalışmaktadır. Saatte 30 ton 55 °C sıcaklığında kireç taşı eleme kapasitesine sahip eleme ünitesi, titreşim ve çarpmaların etkisiyle üzerinde bulunan elek panellerinde kopmalar meydana gelmektedir. Çelik esaslı elek panellerinde oluşan kopmalar sonucunda 50 x 50 mm olması gereken göz aralığı, kopma durumuna göre farklılık göstererek daha büyük boyutlarda olabilmektedir. Bu durumda, yanmış kireç taşının boyutlandırılması sağlıklı olmamaktadır.



Şekil 6. Yanmış kireç taşı eleme esnasında çelik esaslı elek paneli üzerinde oluşan kopmaların gösterimi

Kauçuk Esaslı Elek Panelleri Tasarım ve Özellikleri

Yanmış kireç elek panellerinde oluşan kopmaların önüne geçmek için çelik esaslı elek panellerinin yerine kauçuk esaslı elek panellerinin kullanımı araştırılmıştır. Yapılan araştırmalar sonucunda kauçuk esaslı elek panellerinin sanayide kopma ve dağılma yaşanmadan uzun sürelerde kullanıldığı tespit edilmiştir. Kauçuk esaslı elek panelleri 65 °C sıcaklığındaki taşları boyutlandırabilme ve 60 shore sertlik değerine sahiptirler. Yanmış kireç taşının fırınlardan eleğe ulaştığındaki sıcaklığı 55 °C'dir. Bu veriler göz önünde bulundurulduğunda kauçuk esaslı elek panellerinin Kardemir A.Ş. Kireç Fabrikaları yanmış kireç taşı eleğinde kullanılabileceği öngörülmüştür. Alman KÜPER firması ile yapılan görüşmeler sonucunda 1700 mm x 1600 mm ölçülerindeki 3 adet çelik esaslı elek panelleri yerine 839 mm x 300 mm ölçülerinde 30 adet kauçuk esaslı elek panellerinin kullanılması tasarlanmıştır. Yeni tasarımın, 10 adet kauçuk elek paneli 1 bölme oluşturacak ve her bir bölme arasında 90 mm yükseklik farkı olacak şekilde toplamda 3 bölme olması kararlaştırılmıştır. Bu sayede elek panelindeki mesh alanını büyütürken olası bir kopmada sadece kopma olan kauçuk elek panelinin değiştirilip üretim duruşuna verilen ara çok kısa olacağı da düşünülmüştür.



Şekil 7. Kauçuk esaslı elek paneli ve bağlantı elemanlarının gösterimi

Bu şase toplam 4 farklı pozdan oluşmaktadır. Ç-1 poz çelik esaslı T profil ve K-1, K-2, K-3 pozları ile belirtilen kauçuk esaslı malzemeler kauçuk esaslı elek panelinin sağa ve sola kaymasını engellemektedir.

Çelik Esaslı Elek Panellerinin Demontaj İşlemi

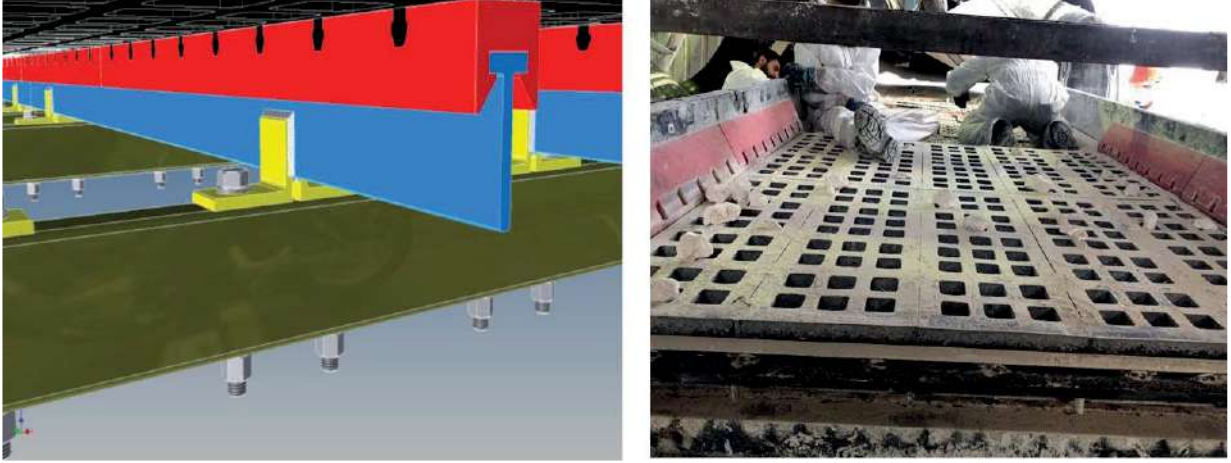
Kauçuk esaslı elek panel şasesi çelik esaslı elek panel şasesinden farklıdır. İlk olarak eleğin üst kademesinde bulunan cıvata bağlantılı çelik esaslı elek panelleri taşıyıcı şaseden demontajı yapılmıştır. Üst kademedeki çelik esaslı elek panellerinin demontajından sonra elek içerisindeki çelik esaslı panel şasesi komple kesilerek alınmıştır. Yanmış kireç taşı eleği üst kademe şasesi kesilip alındıktan sonra elek iç yüzeyi kauçuk esaslı elek panellerinin şasesinin kaynağının yapılabilmesi için zımpara taşı ile taşlanarak elek iç yüzeyinde kalan parça ve çapakların temizliği yapılmıştır.



Şekil 8. Çelik esaslı elek panel şasesinin kesilerek demontajı anı görünümü

Kauçuk Esaslı Elek Panellerinin Montaj İşlemi

Yanmış kireç taşı elek iç yüzeyinin temizlik işi bittikten sonra kauçuk esaslı elek şasesi olan 200 mm x 200 mm ebatlarındaki kutu profillerin kaynakları yapılmıştır. Montaj için daha önce atölyede hazır hale getirilmiş kauçuk esaslı elek panelleri yanmış kireç taşı eleği iç kısmında şase görevi gören kutu profillere M22 civata ile bağlanacak şekilde tasarlanmıştır. Elektteki titreşiminden dolayı civata somunları civatadan kurtulamayacak şekilde birbirine sıkı sıkıya kenetlenen özellikteki fiberli somunlarla montajı yapılmıştır.



Şekil 9. Kauçuk esaslı elek panellerin montajının yapılması anı ve kauçuk esaslı panelinin bilgisayar ortamında oluşturulan şase görünümü

Çelik Esaslı Elek Panellerinde Oluşan Kopmalara Bağlı Olarak Kireç Fabrikası Üretim Duruşu

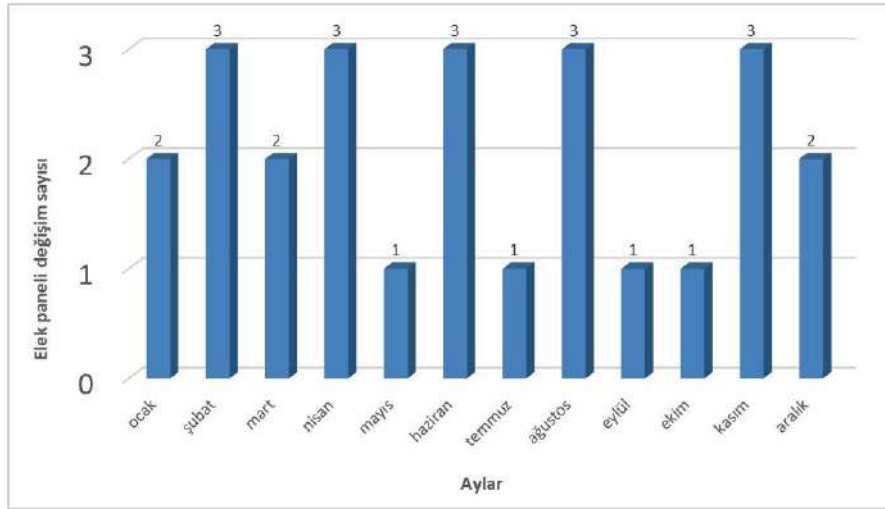
Kardemir A.Ş. kireç fabrikalarında yanmış kireç taşı eleme boyutlandırma işlemi çelik esaslı elek panelleri ile gerçekleştirilmektedir. Yanmış kireç taşı boyutlandırmada kullanılan elek 5034 mm x 1600 mm ölçülerinde dikdörtgen bir tarama-boyutlandırma alanına sahiptir. Bu tarama alanı 20 derece açı ile eğik bir şekilde olup 1678 mm x 2057 mm olmak üzere 3 eşit çelik esaslı elek paneli ile bölünmüştür. Yanmış kireç taşı eleğinde kullanılan çelik esaslı elek panellerinde oluşan kopmalar sonucunda sağlıklı boyutlandırma işlemi yapılabilmesi için deforme olan elek panelinin yenisi ile değiştirilmesi gerekmektedir.

Çizelge 1. Kireç Fabrikaları duruş süreleri ve üretim kaybı

Aylar	Çelik esaslı elek paneli (adet)	Ünite duruşu (saat)	Üretim kaybı (ton)
Ocak	2	8	240
Şubat	3	12	360
Mart	2	8	240
Nisan	3	12	360
Mayıs	1	4	120
Haziran	3	12	360
Temmuz	1	4	120
Ağustos	3	12	360
Eylül	1	4	120
Ekim	1	4	120
Kasım	3	12	360
Aralık	2	8	240

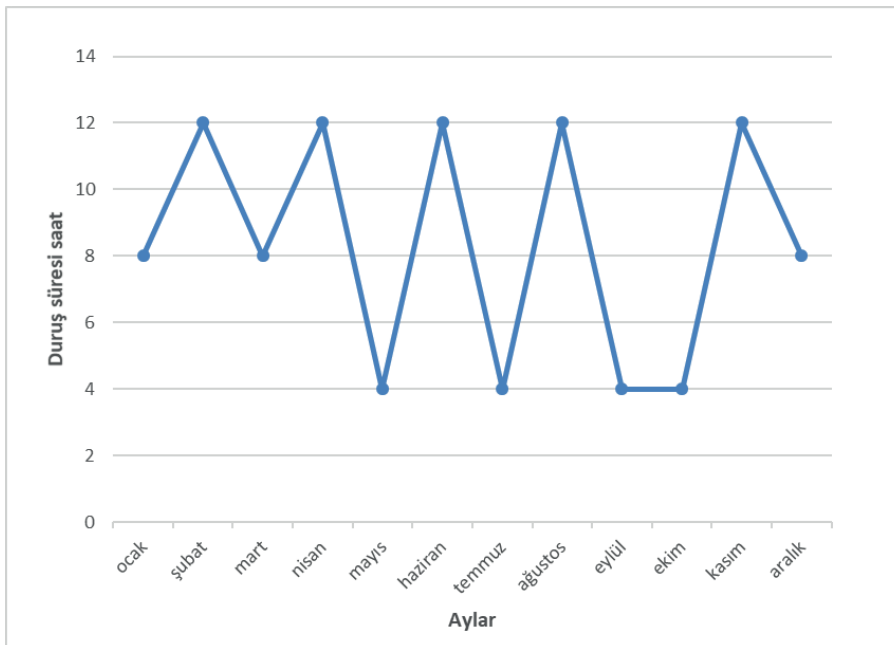
Kopmaların oluştuğu çelik esaslı elek paneli civata bağlantıları sökülerek demontajı yapılmaktadır. Civata bağlantıları sökülen çelik esaslı elek paneli 4 işçi ile elle taşınarak elek şasesinden alınmaktadır. Yeni elek paneli yine 4 işçi tarafından el gücü ile elek şasesi üzerine konularak civata bağlantıları tamamlanmaktadır. Bir adet çelik esaslı elek panelinin kopmadan kaynaklı demontajı ve yenisinin montajı işleminin yapılması ortalama 4 saat sürmektedir. Deforme olan her bir elek panelinin

değiştirilebilmesi için üretime 7/24 devam eden kireç fabrikaları duruşa geçmektedir. Çelik üretim müdürlüğü mekanik bakım faaliyet raporları incelendiğinde çelik esaslı elek panellerinin 2017 yılında toplamda 25 adet değiştirildiği tespit edilmiştir.



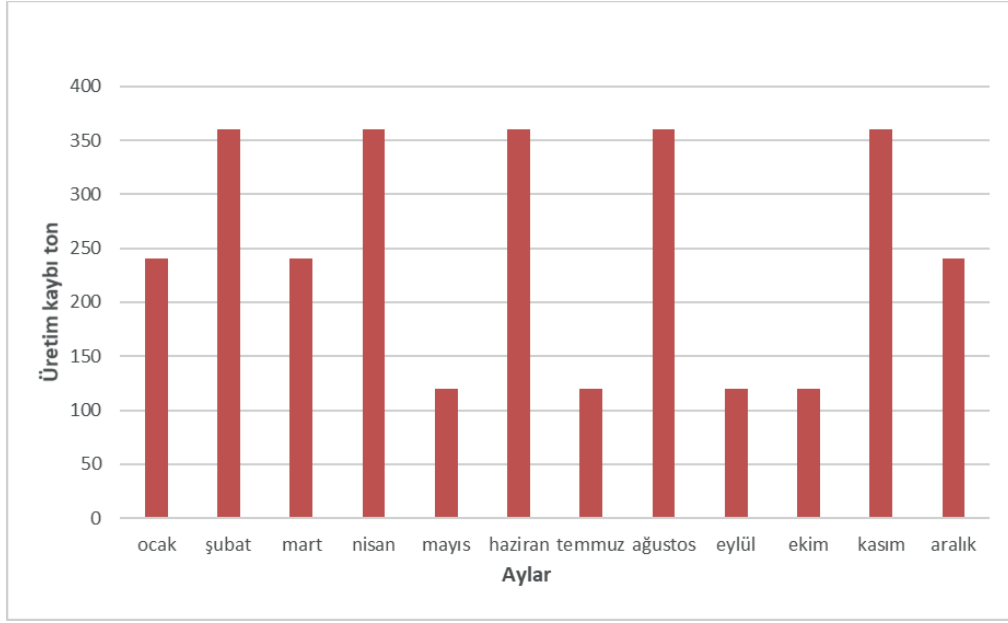
Şekil 10. Kardemir A.Ş. Çelik Üretim Müdürlüğü Mekanik Bakım faaliyet raporu verilerine göre çelik esaslı elek paneli değişim sayısı

Bir adet çelik esaslı elek panelinin değiştirilmesi 4 saat sürmektedir. Çelik esaslı elek paneli değişiminde ünite duruşu gerçekleşmektedir. 2017 yılında çelik esaslı elek panellerinin kopmasına bağlı olarak 100 saat ünite duruşu yaşanmıştır.



Şekil 11. Kardemir A.Ş. Kireç Fabrikaları çelik esaslı elek panelleri değişimi kaynaklı ünite duruş saatleri

Kardemir A.Ş. Kireç Fabrikalarında 30 ton/saat üretim yapılmaktadır. Çelik esaslı elek panellerinin değişiminden kaynaklı ünite duruşlarından dolayı 2017 yılında 3000 ton yanmış kireç taşı üretim kaybı yaşanmıştır. Kauçuk esaslı elek paneli kullanılarak yapılan iyileştirme sonucunda 1 yıl (Ocak 2018-Ocak 2019), zaman aralığında rutin duruşların dışında elek paneli kopmalarından kaynaklı kireç fabrikaları duruşu gerçekleşmemiştir. Bu durum; kireç fabrikalarının üretim verimliliğini arttırmıştır.



Şekil 12. Kardemir A.Ş. Kireç Fabrikaları çelik esaslı elek panelleri değişiminden kaynaklı yanmış kireç taşı üretim kayıpları

İş Sağlığı ve Güvenliği

Çelik esaslı elek panellerinin yenisi ile değiştirilmesi işlemi 4 kişi ile zor koşullar altında gerçekleştirilmektedir. İSG uzmanı tarafından çelik esaslı elek panelleri ortalama haftada bir kez değiştirilmekte olduğundan olasılık değeri 5 olarak belirlenmiştir. Çelik esaslı elek panelleri el-kol sıkışması ayak burkulması, belde incinme, yaralanma gibi iş kazalarına sebep olduğu için İSG uzmanı tarafından şiddet değeri 3 olarak belirlenmiştir. L matrisine göre risk skor değeri olasılık ile şiddetin çarpımıdır. Çelik esaslı elek panelleri değişimi sırasındaki risk skoru Olasılık (5) x Şiddet (3) = 15 olarak tanımlanmıştır.

Kauçuk esaslı elek panellerinde kopmalar yaşanmamaktadır. Olasılık değeri İSG uzmanı tarafından 1 olarak belirlenmiştir. Kopma olup olası bir kauçuk esaslı elek paneli değişimi durumunda bir kişi herhangi bir el aleti kullanmadan kopan elek panelini değiştirebilmektedir. Kauçuk esaslı elek panelinin olası değiştirilme ihtimaline karşı İSG uzmanı tarafından şiddet değeri 3 olarak belirlenmiştir. Kauçuk esaslı elek panelleri değişimi sırasındaki risk skoru Olasılık (1) x Şiddet (3) = 3 olarak belirlenmiştir.

Kardemir A.Ş. kireç fabrikalarında kullanılan elek makinesi panellerinde gerçekleştirilen iyileştirme ile risk skor değeri 15'den 3'e düşürülerek, elek panelleri değişiminde oluşabilecek iş kazalarının önüne geçilmiştir.

RİSK DEĞERLENDİRME YÖNTEMİ

R = O x Ş
 R = Risk
 O = Olasılık
 Ş = Şiddet (Zararın Derecesi)



Olasılık
 Çok küçük (1)
 Küçük (2)
 Orta (3)
 Yüksek (4)
 Çok Yüksek (5)

Ortaya Çıkma Olasılığı
 Yılda bir veya daha az
 Altı ayda bir
 Üç ayda bir
 Ayda bir
 Haftada bir

Şiddet (Zararın Derecesi)
 Çok Hafif (1)
 Hafif (2)
 Orta (3)
 Ciddi (4)
 Çok ciddi (5)

Derecelendirme
 İş saati kaybı yok, ilkyardım gerektiren
 İş günü kaybı yok, ilkyardım gerektiren
 Hafif yaralanma, tedavi gerektiriyor
 Ağır yaralanma, uzuv kaybı
 Ölüm, birden çok ölüm

RİSK MATRİSİ

Siddet - Zarar / Olasılık-İhtimal	Çok Ciddi (5)	Ciddi (4)	Orta (3)	Hafif (2)	Çok Hafif (1)
Çok Yüksek (5)	25	20	15	10	5
Yüksek (4)	20	16	12	8	4
Orta (3)	15	12	9	6	3
Düşük (2)	10	8	6	4	2
Çok Düşük (1)	5	4	3	2	1

RİSK SKORU	EYLEM
25, 20, 16, 15	KABUL EDİLEMEZ RİSK Bu risk değeri ile ilgili mümkün olan en kısa sürede çalışma başlatılmalı, önlem alınmalı.
12, 10, 9, 8	DİKKATE DEĞER RİSK Risk seviyesini aşağıya düşürmek için önlem planlanmalı ve yakın - orta tarihte faaliyete geçirilmeli.
6, 5, 4, 3, 2, 1	KABUL EDİLEBİLİR RİSK Denetim ve kontroller ihmal edilmemeli. Eylem planı düşünülebilir.

Şekil 13. Kardemir A.Ş. Risk Skoru belirlemede kullanılan L tipi matrisin şiddet sayısal değerleri ve derecelendirme tanımları

SONUÇLAR

Kardemir A.Ş çelik üretim tesisi mekanik bakım onarım ekibi tarafından çelik esaslı elek panelleri, dinamik mühendislik uygulamaları için ideal olan esneyebilme özelliği sayesinde üzerine düşen enerjiyi absorbe edebilen kauçuk esaslı elek panelleri ile değiştirilerek 2018 yılı içerisinde elek panellerinde kopmalardan dolayı çelik üretim prosesinde gecikmeler yaşanmamıştır.

Kardemir A.Ş. kireç fabrikalarında kullanılan elek makinesi panellerinde gerçekleştirilen iyileştirme ile risk skor değeri 15'ten 3'e düşürülerek, elek panelleri değişiminde oluşabilecek iş kazalarının önüne geçilmiştir.

Yapılan iyileştirme çalışması ile küçük boyutlarda yanmış kireç taşı kullanılması durumunda BOF içerisine tekrar yanmış kireç taşı şarj edilmesi ortadan kaldırılarak yanmış kireç taşı sarfiyatında azalma sağlanmış, çelik esaslı elek panellerinde oluşan kopmalara bağlı olarak yenisi ile değişiminde harcanan zaman kireç fabrikalarında kestirimci bakım yapılarak değerlendirilmiştir.

KAYNAKLAR

Nakaş, E. (2019), "Kardemir A.Ş. Kireç Fabrikalarındaki Yanmış Kireç Taşı Eleme Sisteminde Kullanılan Elek Panellerinin İyileştirilmesi", Yüksek Lisans Tezi, Karabük Üniversitesi Fen Bilimleri Enstitüsü, Karabük.
 Yıldız, K. (2013), "Demir Çelik Metalurjisi Ders Notları", Sakarya Üniversitesi Metalurji ve Malzeme Mühendisliği Bölümü, Sakarya.

KARDEMİR A.Ş.'DE YERLİ VE İTHAL TOZ CEVHERLER İLE HAZIRLANAN HARMANLARDA ÜRÜN SİNER KALİTESİNİN DEĞERLENDİRİLMESİ

EVALUATION OF PRODUCT SINTER QUALITY IN BLENDS PREPARED WITH DOMESTIC AND IMPORTED FINE ORES AT KARDEMİR A.Ş.

T. Timur¹, C. Cantürk², F. Esin^{2,*}, O. Acur², M. Sevim², Y. Sun³

¹ KARDEMİR A.Ş., Kalite Güvence Metalurji ve Laboratuvarlar Müdürlüğü

² KARDEMİR A.Ş., AR-GE Merkezi

(*Sorumlu yazar: fesin@kardemir.com)

³ Karabük Üniversitesi, Mühendislik Fakültesi, Metalürji ve Malzeme Mühendisliği

ÖZET

Entegre Demir Çelik Tesislerinde yüksek fırınlara direkt olarak şarj edilemeyecek boyuttaki toz cevherler, ergime sıcaklığı altında yüzey ergitme işlemine tabi tutularak birleştirilmektedir. Sinterleşme neticesinde yüksek fırınlarda kullanılabilir boyuta gelmektedir. Sinter, yüksek fırınların en ekonomik demirli malzeme girdisidir. Yüksek fırınların üretim hızı, verimi, oluşan ürünün kalitesi ve ekonomikliği kullanılan hammaddelere bağlıdır. Bu çalışmada farklı oranlarda, yerli ve ithal toz demir cevherlerin harmanlanması sonucu elde edilen ürün sinterin kalitesinin değerlendirilmesi yapılmıştır. Harman sahasından her bir harmanı temsilen numune alınarak, harmanın fiziksel (elek analizi) ve kimyasal (XRF) özellikleri belirlenmiştir. Harmanlar yerli ve ithal toz cevher, kalibre cevher, pelet tozu ve diğer (birtakım işletme atık tozları) olarak kategorize edilmiş ve sinterleştirilmiştir. Elde edilen sinterlerin fiziksel (elek analizi, tambur testi), kimyasal (XRF) ve metalurjik analizleri (RUL, RDI) yapılmıştır. Tüm analiz sonuçları incelendiğinde yüksek fırınlarda kullanılan sinter için en uygun karışımın en az % 30 ithal cevher kullanılarak sağlanacağı sonucuna varılmıştır.

Anahtar Sözcükler: Harmanlama, toz cevher, sinter, sinter fabrikası, yüksek fırın

ABSTRACT

In Integrated Iron and Steel Plants, fine ores of a size that cannot be charged directly to the blast furnaces are combined by subjecting to surface melting under the melting temperature. As a result of sintering, it becomes usable in blast furnaces. Sinter is the most economical ferrous material input of blast furnaces. Blast furnaces production speed, efficiency, quality and economy of the product obtained depend on the raw materials used. In this study, the quality of the product sinter obtained by blending domestic and imported fine ores in different proportions was evaluated. Physical (sieve analysis) and chemical (XRF) properties of the blend were determined by taking samples from the blend area to represent each blend. Blends has been categorized and sintered as domestic and imported fine ore, calibrated ore, pellet dust and other (waste dusts of some plant). Physical (sieve analysis, drum test), chemical (XRF) and metallurgical analysis (RUL, RDI) of the obtained sinters were made. When all analysis results were examined, it was concluded that the most suitable mixture for sinter used in blast furnaces would be provided using at least 30% imported ore.

Keywords: Blending, fine ore, sinter, sinter plant, blast furnace

GİRİŞ

Ülkedeki diğer sanayi yatırımlarını desteklemek amacıyla, birçok fabrikanın kuruluşunda aktif bir biçimde rol alan "Fabrikalar Kuran Fabrika" unvanıyla bilinen KARDEMİR, Türkiye’de sanayileşme hamlesinin en önemli mihenk taşlarından biri olarak kurulmuş ilk entegre demir çelik fabrikasıdır. Temelleri 3 Nisan 1937 tarihinde atılan bu fabrika, 84 yıllık köklü bir geçmişe ve sanayi kültürüne sahiptir.

Sıvı çelik üretim kapasitesini 3.5 Milyon Ton/yıl seviyesine çıkarmayı hedefleyen yerli cevhere dayalı üretim yapan şirketimizin ana faaliyet konusunu her çeşit ham demir ve çelik mamullerinin, kok ve kok yan ürünlerinin üretimi ve satışı oluşturmaktadır. Bu doğrultuda, raylı sistemler, otomotiv, makine imalat, inşaat ve yapı sektörü, madencilik, savunma sanayi, mobilya ve bağlantı elemanları gibi geniş bir endüstriyel ekosisteme yüksek nitelikli ürünler ve hizmetler sunulmaktadır.

Kardemir’in ana cevher kaynağı yerli olmakla birlikte ithal kaynaklardan da cevher alımı yapılmaktadır. Bu süreçte cevherlerin kalite, maliyet ve harmanlama özellikleri değerlendirilmektedir.

Yerli cevherlerde genellikle tenör düşük, gang elemanları ($\text{SiO}_2 + \text{Al}_2\text{O}_3$) yüksektir. Ayrıca yüksek fırın prosesi ve sıvı metal kalitesi için zararlı olan K_2O , Zn, As, S gibi empüriteler bazı yerli cevherlerde oldukça yüksektir. Bu bakımdan yerli cevherlerin kendi içlerinde ve ithal cevherlerle optimum değerleri verecek şekilde harmanlanması gerekmektedir.

Bu çalışmada farklı oranlarda, yerli ve ithal toz demir cevherlerin harmanlanması sonucu elde edilen sinter kalitesinin değerlendirilmesi yapılmıştır.

Demir Cevherinin Harmanlanması ve Sinterleşmesi

Harmanlama; 0-10 mm boyutunda, demir tenörü ihtiva eden toz cevherlerin, yan ürün ve atık malzemelerin 16 adet yığın olacak şekilde harmanlama sahalarına serilmesi işlemidir. Toplam 420.000 ton cevher stoklama kapasitesine sahip 4 adet harman sahası bulunmaktadır. İki tanesi 140.000 ton, iki tanesi de 70.000 ton cevher kapasitelidir.

Harmanlama Tesisleri’nde, Yüksek Fırınlar’ın ihtiyacı olan parça cevher ve katkı malzemeleri ile Sinter Tesisi için gerekli olan demir cevherleri istenilen özellikte ve miktarda homojen olarak hazırlanır. Harmanlama işlemindeki asıl amaç, Sinter tesisine uygun fiziksel ve kimyasal özellikleri olan harman sahaları oluşturmaktır. Homojen bir harman sahası hazırlama işlemlerinde; şirkete gelen ithal ve yerli toz cevherleri ve stokları iyi yönetmek, gelen cevherleri ve atık malzemeleri harman sahası boyunca kesintisiz serebilmek önemlidir. Kardemir harmanlama sahası Şekil 1’de gösterilmektedir.



Şekil 1. Kardemir harman sahası

Sinter Fabrikaları, Yüksek Fırınlar'a direk olarak şarj edilemeyecek boyuttaki toz cevherlerin, ergime sıcaklığı altında yüzey ergitme işlemine tâbi tutularak birleştirilmesi sonucu yüksek fırınlara şarj edilebilecek boyuta getirilmesi sürecidir. Her birinin kapasitesi 1 250 000 ton/yıl olan 3 adet sinter fabrikası bulunmaktadır. Yüksek Fırınlar'ın ihtiyacı olan sinter malzemesi; demir cevheri tozu, kireçtaşı, kok tozu, sinter dönüş tozu ve katkı malzemeleri ile hazırlanıp belli oranlarda harmanlanır ve sinterlenir. Kardemir A.Ş. Sinter Fabrikası Şekil 2'de gösterilmektedir.



Şekil 2. Kardemir A.Ş.'de sinter fabrikası

Sinterlik malzeme harmanının % 55-75'ini harmanlanmış demir cevheri, % 10-30'unu sinter tozu, % 3-6'sını kok tozu oluşturur. Harmandaki demir cevheri ve kok tozu miktarının toplamının % 10-20'si oranında kireçtaşı tozu ve gerektiğinde % 1-5 oranında cüruf vb. katkı malzemeleri harmana ilave edilir.

Elde edilen sinterlik malzeme harmanı tutuşturma ocağında tutuşturularak hava emişi yardımıyla tüm malzeme külçeleştirilir.

DENEYSEL ÇALIŞMALAR

Sinter Harmanlarının Bileşim Oranları

Harman içeriği; yerli toz cevher, yerli kalibre ve pelet, ithal cevherler, şarj tozu, baca tozu, filtre tozu, tozsuzlaştırma tozu, atık çamur ve cüruf vb. demirli malzemelerden oluşmaktadır. Kardemir A.Ş. tarafından hazırlanan harmanların bileşimi çizelge 1’de verilmiştir.

Çizelge 1. Hazırlanan farklı harmanların bileşim oranları

Harman No	Yerli Toz Cevher (%)	Yerli Kalibre Cevher (%)	İthal Cevher (%)	Pelet Tozu (%)	Diğer (%)
1	30,32	2,52	41,36	1,28	24,52
2	53,36	1,89	18,32	1,04	25,39
3	54,22	1,36	28,7	0,49	15,23
4	48,11	1,65	24,06	0,49	25,69
5	50,4	0,25	28,5	4,39	16,46
6	48,61	3,72	23,57	4,18	19,92

Sinter Harmanın Kimyasal ve Fiziksel Analizleri

Her bir harmanın kimyasal ve fiziksel özelliklerini belirlemek için harmanların XRF ve elek analizleri yapılmıştır. Harmanların XRF analiz sonuçları çizelge 2’de ve harmanların elek analizleri çizelge 3’de verilmiştir.

Çizelge 2. Harmanların XRF analiz sonuçları

Harman No	Fe (%)	SiO ₂ (%)	CaO (%)	Al ₂ O ₃ (%)	MgO (%)	Mn (%)	S (%)	K ₂ O (%)	Na ₂ O (%)	Zn (%)	P (%)	Cu (%)	TiO ₂ (%)	CaO/SiO ₂
1	57,8	5,19	2,95	1,36	1,11	0,39	0,12	0,08	0,08	0,03	0,05	0,01	0,15	0,565
2	53,33	8,12	4,61	1,73	1,86	0,75	0,29	0,147	0,08	0,04	0,038	0,02	0,17	0,568
3	56,8	6,78	3,14	1,37	1,52	0,61	0,22	0,12	0,09	0,03	0,02	0,04	0,11	0,46
4	53,68	7,85	3,94	1,03	1,65	0,8	0,21	0,12	0,07	0,05	0,04	0,04	0,1	0,5
5	55,03	7,08	3,17	1,39	1,75	0,86	0,26	0,1	0,08	0,03	0,03	0,02	0,13	0,448
6	55,59	6,24	3,25	1,41	1,35	0,75	0,22	0,1	0,09	0,03	0,04	0,02	0,12	0,538

Sonuçlara baktığımızda demir cevheri oranı en yüksek olan harman 1 nolu, en düşük olan ise 2 nolu harmandır. Bazite değerini gösteren CaO/SiO₂ oranının 1’e yakın olması beklenir. Harmanların

hepsi asidik özellik göstermiştir. CaO/SiO₂ oranı en yüksek harman 2 nolu harmandır. P, Zn ve Cu yüzdeleri maksimum 0,1- 0,15 olması istenir. Tüm harmanlar bu yönde beklenti karşılamıştır.

Çizelge 3. Hazırlanan harmanların elek analizleri

Harman No	+10 mm	-10+6,30 mm	-6,30+3,15 mm	-3,15+1 mm	-1+0,5 mm	-0,5+0,21 mm	-0,21 mm
1	6,71	13,14	25,3	23,31	9,63	11,35	10,58
2	3,89	15,9	25,71	25,37	8,85	11,49	8,79
3	6,51	19,8	20,71	28,96	8,54	10,65	4,82
4	4,55	15,24	21,01	29,19	6,89	11,46	11,67
5	2,6	13,45	22,69	26,7	9,46	13,43	11,68
6	3,1	12,12	25,66	27,03	10,26	14,17	7,66

Toz cevherlerin tane boyutunun 10 mm'den küçük, 6,5 mm'den büyük olması istenmektedir. 12,5 mm'den büyük parçaları sinterlerken homojenliği sağlamada sıkıntı olur. Büyük parçalar sinterin geçirgenliğini artırsa bile iyi bir şekilde birleşmeyi engeller ve dağılmaya sebep olur. Tüm harmanların elek analizleri yaklaşık olarak birbirine yakındır ve sinter hazırlama harmanı için kabul edilebilir boyuttadır. Bu nedenle en iyi harman değerlendirmesi yaparken fiziksel analizinden ziyade kimyasal analizi göz önünde bulunduruldu.

Ürün Sinterin Kimyasal ve Fiziksel Analizleri

Her bir ürün sinterin kimyasal ve fiziksel özelliklerini belirlemek için harmanların XRF, elek analizi ve tambur testleri yapılmıştır.

Sinter XRF Analizi

Sinter için temel kriter azami demir içeriğine sahip olmasıdır. Ancak bu şekilde yüksek fırın için en makul ve indirgenebilir sinter oluşur. Sinter bileşimindeki demir dışındaki elementlerin belirli oranların dışında olması yüksek fırına veya üretilecek sıvı ham demire olumlu/olumsuz etkiler yaratabilir. Ürün sinterin XRF analiz sonuçları çizelge 4'te verilmiştir.

Çizelge 4. Ürün sinterin XRF analizleri

Harman No	Fe (%)	SiO ₂ (%)	CaO (%)	Al ₂ O ₃ (%)	MgO (%)	Mn (%)	S (%)	K ₂ O (%)	Na ₂ O (%)	ZnO (%)	TiO ₂ (%)	P ₂ O ₅ (%)	FeO (%)	CaO/SiO ₂
1	56,86	6,43	6,11	1,49	1,19	0,4	0,01	0,1	0,04	0,03	0,25	0,18	8,8	0,95
2	54,18	8,18	8,02	2,09	2,01	0,74	0,01	0,11	0,06	0,01	0,22	0,13	10,44	0,98
3	56	7,18	7,38	1,76	1,39	0,56	0,01	0,12	0,05	0,01	0,17	0,18	10,61	1,03
4	54,96	8,45	7,94	1,27	1,4	0,86	0,01	0,11	0,05	0,02	0,14	0,07	11,44	0,94
5	56,14	7,31	6,31	1,66	1,9	0,9	0,01	0,11	0,05	0,03	0,17	0,1	10,44	0,86
6	56,81	6,68	6,42	1,62	1,67	0,79	0,01	0,14	0,05	0,04	0,19	0,13	10,68	0,96

Demir içeriği seçilen cevherlerle ilgilidir. Bu seçim neredeyse tamamen ekonomik nedenlerden dolayı yapılmaktadır. Sinter kimyasal analiz sonuçlarına göre 1 nolu harmanın %Fe oranı daha yüksektir. %SiO₂, cüruf oluşumuna neden olduğundan yüksek olması istenmez. Bu silisi nötralize etmek için ilave edilen kireç taşı sıvı demir verimliliğini düşürür. Bu oranın en düşük olduğu harman 1 nolu harmandır.

Al₂O₃ değeri % 3'e kadar kabul edilebilir aralıktadır. Tüm sinterler bu şartı sağlamaktadır. Ancak 4 nolu harmandan üretilen sinterin Al₂O₃ değeri %1,27 çıkmıştır. Bu sonuç diğer sinterlere göre daha iyidir. Çünkü Al₂O₃ kok gazı kullanımını artırır.

Bazite değeri (CaO/SiO₂) oranı %1,03 ile en iyi 3 nolu harmanda olduğu gözlenmiştir. Şarjdaki TiO₂ miktarı % 2'nin altına inerse bunun % 50-60'ı cürufa geçer, kalan miktarı ise indirgenir ve demire geçer. Cüruftaki TiO₂'nin %1,5'i geçmesi cürufun viskozitesini artırır. Bu durum fırının çalışma şartlarında düzensizlik oluşturur. Tüm sinterler bu şartı sağlamaktadır.

Sinter Elek Analizi

Boyutu 5 mm'den küçük olan parçalar fırınlarda gaz geçirgenliğini azaltır. Çok tozlu olan sinter, fırına şarj edildiğinde fırın duvarlarına yapışarak kabuk halinde kalır ve ince tanelerin patlamaya sebep olacağı unutulmamalıdır. Ürün sinterin elek analizleri Çizelge 5'te verilmiştir.

Çizelge 5. Ürün sinterin elek analizleri

Harman No	40 mm	-40+25 mm	-25+10 mm	-10+5 mm	-5 mm
1	17,79	18	38,19	20,55	5,46
2	12,53	14,35	38,76	27,18	7,19
3	14,91	17,17	37,22	23,79	6,91
4	20,82	17,79	30,21	23,4	7,77
5	17,78	15,24	36,6	24,4	5,98
6	17,57	16,03	36,86	23,58	5,96

Harman 1'in %5,46'sı tozudur. 4 nolu harmanda ise bu değer %7,77'dir. Diğer harmanlara göre daha fazla tozlu parça içermektedir. Ayrıca 4 nolu harmanda 40 mm elek üstü yüzdesi yine diğer harmanlara göre daha yüksektir.

Sinter Tambur Testi

Tambur testi, sinterin aşınma ve ufalanmaya karşı direncini ölçmek için yapıldı. Sinter fabrikasında üretilen sinter, yüksek fırınlarda beslenene kadar birçok banttan transfer olur. Bu sebeple de darbelere maruz kalıp ufalanabilir. Sinterin tambur test sonuçları çizelge 6'da verilmiştir.

Çizelge 6. Sinter tambur test sonuçları

Harman No	Ufalanma İndeksi (%)	Aşınma İndeksi (%)
1	71,67	6,66
2	66,65	6,16
3	69,09	7,08
4	67,26	6,59
5	68,21	6,58
6	69,53	6,63

Küçük tane boyutu nedeni ile fırın iç basıncının artması, maksimum hava ve oksijen kullanımını kısıtlamaktadır. Bu sebeple aşınma indeksinin küçük olması gerekir. Sinterin mukavemeti artarsa, ince toz miktarı azalır ve yüksek fırın üretiminde demirin artışı sağlanır. Bu testte +6,3'ün (ufalanma indeksi)

minimum %65 olması istenir. Tambur test sonucu en iyi harman %71,67 ufalanma indeksine sahip olan 1 nolu harmandır.

Ürün Sinterin Mekanik Testleri

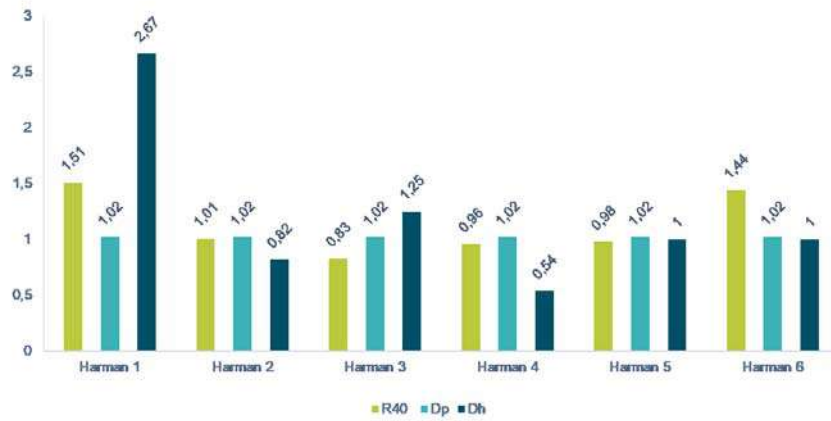
RUL Testi

Bu deney metodu, deney numunesi kısmı yatağı boyunca diferansiyel gaz basıncındaki değişimin (Dp) ve indirgeme süresince yük altında (50 kPa) bulunan yatağın yüksekliğindeki değişikliğin (Dh) ölçülmesi suretiyle, demir cevherlerinin fiziksel kararlılığının tayinine yönelik bir metodu kapsar.

Bu teste göre sinterin R40 değerinin en az 1 olması istenir. Sonuçlara baktığımızda 1 nolu harmanda bu değer 1,51 çıkmıştır. Basınç ve yükseklik farkına bakacak olursak; Dp (15 mmH₂O dan küçük) ve Dh (%10 dan küçük) değerleri hepsinde uygundur. Sinterin RUL testinin sonucu çizelge 7’de verilmiştir.

Çizelge 7. Sinterin RUL testinin sonuçları

Harman No	R40 (% O ₂ /min)	Dp (mm H ₂ O)	Dh (%)
1	1,51	1,02	2,67
2	1,01	1,02	0,82
3	0,83	1,02	1,25
4	0,96	1,02	0,54
5	0,98	1,02	1
6	1,44	1,02	1



Şekil 3. Sinter RUL testi sonuçlarının grafiksel gösterimi

RDI Testi

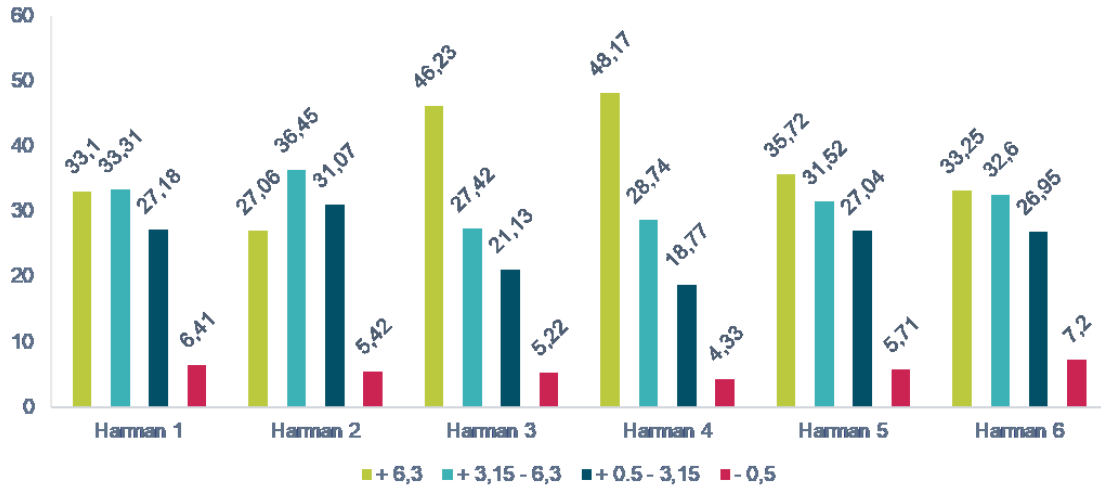
500°C’lik sabit bir yatakta indirgenmiş (CO %20 + CO₂ % 20 + H₂ % 2 + N₂ % 58), 500 gram ağırlığındaki sinterin, oda sıcaklığında ufalanarak parçalanması değerlendirilir.

Çıkan sonuçlarda +6,3 mm en az %84 ve -0,5 mm en fazla % 3 olmalıdır. Bu testin yapılma amacı yüksek fırına beslenen malzemenin gövdede ilk değişim zonunu temsil ettiği içindir. Sinter RDI testinin analiz sonucu çizelge 8’de verilmiştir.

Çizelge 8. Sinter RDI testinin analiz sonuçları

Harman No	+6,3mm	+3,15-6,3mm	+0,5-3,15mm	-0,5 mm
1	33,10	33,31	27,18	6,41
2	27,06	36,45	31,07	5,42
3	46,23	27,42	21,13	5,22
4	48,17	28,74	18,77	4,33
5	35,72	31,52	27,04	5,71
6	33,25	32,60	26,95	7,20

Bu testte (-3,15 mm) değeri maksimum % 25 olmalıdır. 4 Nolu harman dışındaki tüm harmanlarda 3,15 mm’den küçük parça yüzdesinin 25’ten büyük olduğu görülmektedir. Beklenen kriteri sağlayan tek harman 4 nolu harmandır.



Şekil 4. Sinter RDI testi sonuçlarının grafiksel gösterimi

DEĞERLENDİRME

Hazırlanan 6 farklı harman ve bu harmanlardan üretilen sinterler için birçok test yapılmıştır. Tüm testlerin değerlendirilmesi fiziksel, kimyasal ve metalürjik olarak ayrı ayrı ele alınmıştır. Puanlama 1’den 6’ya kadar yapılmış olup en iyi özellik gösterene 6 puan verilmiştir. Puanlama yaparken dikkat edilecek kriterlere, önceki başlıklarda değinilmiştir. Tek başına sadece fiziksel veya kimyasal özelliklerinin iyi olması yeterli değildir. Tüm test sonuçları birlikte değerlendirilmiştir. Hazırlanan 6 farklı harman ve bu harmanlardan üretilen sinterler için birçok test yapılmıştır. Tüm testlerin değerlendirilmesi fiziksel, kimyasal ve metalürjik olarak ayrı ayrı ele alındı. 1’den 6’ya kadar puanlama yapıp, en iyi özellik gösterene 6 puan verildi.

Harman Değerlendirilmesi

Harmanın kimyasal özelliklerinin karşılaştırılması Çizelge 9’da verilmiştir. Buna göre en iyi harman 1 nolu (6 puan), en kötü harman 5 nolu (1 puan) harmandır.

Çizelge 9. Harman özelliklerini değerlendirme

Harman No	Kimyasal Analiz Puanı
1	6
2	3
3	4
4	2
5	1
6	5

Sinter Değerlendirilmesi

Sinterin fiziksel ve kimyasal özelliklerinin karşılaştırılması Çizelge 10’da verilmiştir. Buna göre en iyi 1 nolu harmandan üretilen sinterdir. Harman 2 ve 4 ise beklenen fiziksel ve kimyasal özellikler bakımından puanlandığında diğerlerine göre daha az puan almıştır.

Çizelge 10. Sinter özelliklerinin değerlendirme

Harman No	Elek Analizi Puanı	Tambur Testi Puanı	Kimyasal Analiz Puanı	Toplam
1	6	6	6	18
2	2	1	1	4
3	3	4	4	11
4	1	2	2	5
5	4	3	3	10
6	5	5	5	15

Metalürjik Değerlendirme

Sinterin teknolojik test sonuçlarına göre değerlendirilmesi Çizelge 11’de verilmiştir. Sonuçlara göre metalürjik özelliği en iyi olan sinter 1 nolu harmandan üretilen sinter olup, 2 nolu harman sinteri en düşük puandadır.

Çizelge 11. Metalürjik özellikleri değerlendirme

Harman No	RUL Puanı	RDI Puanı	Toplam
1	6	3	9
2	4	1	5
3	1	5	6
4	2	6	8
5	3	4	7
6	5	2	7

SONUÇ VE ÖNERİLER

Yapılan çalışmalar sonucunda, Kardemir Sinter Fabrikası'nın sinter kalitesinde hedeflediği değerler göz önünde bulundurularak; 1 nolu harmanın en iyi, 2 nolu harmanın ise en kötü sonucu verdiği belirlenmiştir.

İthal cevher kullanım oranının en fazla olduğu harman 1 nolu (%41,36) harmandır. En düşük olduğu harman ise bu değer yarısından az olduğu 2 nolu (%18,32) harmandır. 1 ve 2 nolu harmanlardan üretilen sinterlerden alınan sonuçlara göre yüksek oranlarda ithal cevher kullanıldığı zaman, aşınma ve ufalanma indeks sonucunun daha iyi olacağı görülmüştür.

İthal cevher kullanımının artmasıyla sinterin kimyasal analizi ve yüksek fırınlarda indirgenme davranışının iyileştiği görülmüştür.

Yerli cevher kullanım oranının en fazla olduğu harman 2 nolu (%53,36) ve 3 nolu (%54,22) harmandır. Harman kimyasal analizi sonuçlarında % S oranına bakıldığında en yüksek kükürt değerinin, ithal cevher kullanım oranının da en az olduğu 2 nolu harmanda olduğu görülmüştür.

Tambur sonuçlarının sinter bazitesiyle ilişkisine bakıldığında; ufalanma indeks değerinin her harmanda değişim gösterdiği, çalışılan harmanlardan üretilen sinterin bazite değerinin ise düşük (0,9 civarında) olduğu görülmüştür.

Atık tozlar %15-20 civarında olduğu takdirde sinter kalitesinde olumsuz bir etki yaratmadığı tespit edilmiştir.

Harman hazırlarken sahalardaki cevher stok miktarı, cevher satın alımındaki kriterler ve sinter kalite hedefleri dikkate alınarak yerli cevherlerle beraber yaklaşık %30 oranında ithal cevher kullanımının iyi olacağı sonucuna varılmıştır.

KAYNAKLAR

Kardemir A.Ş. sürdürülebilirlik 2019 raporu,

https://www.kardemir.com/dosyalar/sayfalar/1338/22072020/2020072214385940_sayfalar_1309_22072020.pdf?v=c51fdc86_ccf9_1bf6_ddef_bec9c5307cc8.

Kardemir A.Ş. sürdürülebilirlik 2020 raporu,

https://www.kardemir.com/dosyalar/sayfalar/1338/03082021/2021080311253005_sayfalar_1338_03082021.pdf?v=29c27cac_d919_8881_17d9_85684be786b4.

Timur, T. (2019), "Kardemir A.Ş.'de Farklı Toz Cevherlerle Üretilen Sinterin Kalitesinin İncelenmesi", Yüksek Lisans Tezi, Karabük Üniversitesi Fen Bilimleri Enstitüsü, Karabük.

KİMYASAL DOLGU MALZEMELERİNİN KARAKTERİSTİKLERİ VE KÖMÜRÜN KENDİLİĞİNDEN YANMASI ÜZERİNE ETKİSİNİN İNCELENMESİ

INVESTIGATION OF THE CHARACTERISTICS OF CHEMICAL FILLING MATERIALS AND THE EFFECT ON SPONTANEOUS COMBUSTION OF COAL

C. Tuz^{1,*}, M. Bilen¹, E. Kaymakçı¹, İ. Toroğlu¹, Ö. Yılmaz², S. Yılmaz¹

¹Bülent Ecevit Üniversitesi Maden Mühendisliği Bölümü, Zonguldak
(*Sorumlu yazar: canertuz@gmail.com)

²Bülent Ecevit Üniversitesi ZMYO, Madencilik ve Maden Çıkarma Bölümü, Zonguldak

ÖZET

Enjeksiyon kimyasalları, kazı yapılacak ya da yapılmış kaya kütlelerini iyileştirmek, su gelirini kesmek, tahkimat elemanları ile yan kayaç arasındaki boşlukları doldurmak, gibi çeşitli amaçlarla kullanılmaktadırlar. Yeraltı kömür madenciliğinde kimyasal dolgu malzemeleri olan köpük ürünleri kullanılmaktadır. Bu tip malzemelerin göçükte oluşan büyük çatlakların doldurulması ile göçük stabilizasyonu, havalandırma yönetimi için gerekli olan hava kapılarının yapılması ve sızdırmazlığın sağlanması ve yangınla mücadele uygulamalarında baraj yapımı gibi kullanım alanları da mevcuttur. Yeraltında kimyasal dolgu malzemesi olarak kullanılan köpük ürünleri kimyasal içeriklerine göre genellikle poliüretan ve fenol olmak üzere iki kategoride sınıflandırılmaktadır. Fenol bazlı dolgu köpüklerinin reçine bileşeni içeriğinde yer alan formaldehit maddesinin 1. Sınıf kanserojen madde kategorisinde yer almasından dolayı bu maddenin sınır değerine dikkat edilmesi gerekmektedir. Poliüretan bazlı kimyasal dolgu köpüklerin içeriğinde yer alan MDI toksik bir madde olduğundan dolayı tutuştuğunda sağlık açısından zararlı gaz salınımına sebep olmaktadır. Kimyasal dolgu köpükleri kömür madenlerinde yapılan uygulamalarda doğrudan kömür ile kontak halindedir. Poliüretan bazlı kimyasal dolgu malzemeleri yeraltı kömür madenlerinde yapılan uygulamalarda kendiliğinden yanmayı tetikleyici etkisinden ve yanıcı özelliğinden dolayı problem oluşturmaktadır. Diğer taraftan fenol bazlı kimyasal dolgu köpükleri özellikle yeraltı kömür madenlerinde yapılan uygulamalarda kömürün kendiliğinden yanmasına olan etkisi oldukça düşük seviyelerdedir. Bu çalışmada yeraltı kömür madenciliğinde kullanılmakta olan kimyasal dolgu malzemelerinin karakteristikleri ve kömürün kendiliğinden yanması üzerindeki etkiler incelenmiştir.

Anahtar Kelimeler: Yeraltı Kömür Madenciliği, Kimyasal Dolgu Malzemeleri, İSG (İş sağlığı ve güvenliği), Kendiliğinden Yanma, Fenol bazlı köpük, Formaldehit

ABSTRACT

Ground injections are used for various purposes such as improving the ground to be excavated or made, sealing the water inrush, filling the cavity between the support and the ground. Foam products, which are chemical filling materials, are used in underground coal mining. These types of products also have areas of use such as filling large cracks in goaf and stabilizing goaf, constructing air barriers, and sealing for ventilation requirements, and fighting underground fires by sealing off all entries connected to the fire area. Foam products used as underground cavity filling materials are generally classified into two categories, polyurethane, and phenol, according to their chemical content. Since formaldehyde, which is included in the resin component of phenol-based filling foams, is in the category 1st carcinogenic substance, attention should be paid to the limit value of this substance. Since MDI in the content of polyurethane-based chemical filling foams is a toxic substance, it causes harmful gas emissions in terms of health when ignited. In applications made in coal mines, filling foams form a large contact surface with coal. Polyurethane-based chemical filling materials cause problems in underground coal mines due to their

spontaneous combustion triggering effect and flammability. On the other hand, the effect of phenol-based chemical filling foams on spontaneous combustion of coal is very low especially filling operations in underground coal mines. In this study, the characteristics of chemical filling foams used in underground coal mining applications and their effects on spontaneous combustion of coal were investigated.

Keywords: Underground coal mining, chemical filling products, OHS (Occupational Health and Safety), Spontaneous combustion, Phenol based foam, Formaldehyde

GİRİŞ

Gelişen teknolojiyle birlikte geleneksel olarak bilinen çimento su enjeksiyon malzemesinin yerini kimyasal enjeksiyon ürünleri almaktadır. Yeraltı madenlerinde kazı yapılacak olan ya da yapılmış kaya kütlelerinin yapısal olarak iyileştirilmesi, yeraltında çatlaklardan akan su gelirlerinin kesilmesi, tahkimat elemanları ile yan kayaç arasındaki boşlukların doldurulması gibi çeşitli uygulamalarda kimyasal enjeksiyon ürünleri büyük avantaj sağlamaktadır. Bu avantajlardan bazıları; kimyasal enjeksiyon malzemelerinin düşük viskozite değerlerinden dolayı ince çatlaklara kolaylıkla nüfuz etmesi, kolay ve basit uygulanabilirlikleri, reaksiyon hızlarının yüksek olmasından dolayı operasyonların bekleme sürelerinin düşük olması, kısa sürede yük taşıyıcı özellik göstermeleri, ıslak kayaçlara yapışabilmesiyle su geliri olan ortamlarda ve yapılarda kullanılabilir olması gibi birçok avantajı bilinmektedir (Aksoy O., 2017).

Yeraltında oluşan boşlukların doldurulması veya yangın gibi problemlere hızlı bir şekilde müdahale edebilmek için kimyasal dolgu malzemeleri olan köpük ürünleri kullanılmaktadır. Kimyasal köpük ürünleri uygulandıkları bölgede reaksiyona girerek yüksek kabarma faktörleri sayesinde az miktarda ürün ile büyük hacimlerin doldurulması sağlanabilmektedir. Genellikle kimyasal köpük ürünleri 20 ile 70 kat arasında değişen kabarma faktörüne sahiptirler.

Yeraltı Kömür Madenciliğinde Kimyasal Dolgu Malzemelerinin Kullanıldığı Uygulamalar

Kimyasal enjeksiyon ve köpük ürünleri yüksek maliyetleri olduğundan dolayı bazı özel operasyonlarda uygulanmaktadır. Genellikle alternatif yöntemler veya çözümlerin olmadığı durumlarda tercih edilmektedir. Yaygın olarak kullanılan yöntemlerin yetersiz kaldığı veya kısa sürede problemin çözülmesinin gerektiği durumlarda kimyasal uygulamalar gerçekleştirilmektedir. Yeraltı kömür madenciliğinde gerçekleştirilen başlıca kimyasal dolgu uygulamaları yeraltında oluşan boşlukların doldurulması, göçükte oluşan büyük çatlakların doldurulması ile göçük stabilizasyonu, havalandırma yönetimi için gerekli olan hava kapılarının yapılması ve sızdırmazlığın sağlanması ve yangınla mücadele uygulamalarında baraj yapımı olarak bilinmektedir.

Boşluk Doldurma

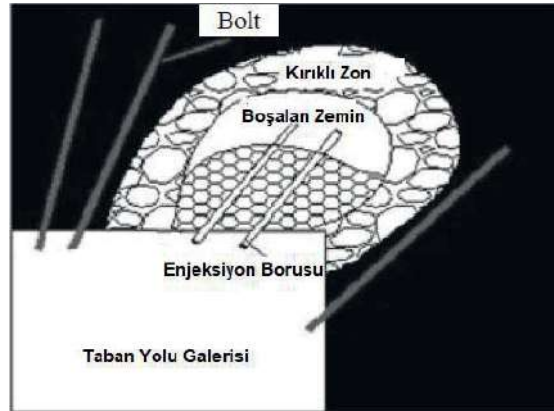
Yeraltında jeolojik koşullardan ve süreksizliklerden kaynaklı olarak geniş çaplı göçük ve boşluklar oluşmaktadır. Bu durum çoğu zaman üretimin durmasına veya üretim verimliliğinin düşmesi ile sonuçlanmaktadır. Aynı zamanda bu boşluklar ve göçük alanları madenciler için iş güvenliği problemleri oluşturmaktadır. Bu problemlerin bertaraf edilmemesi halinde risk artmaktadır. Daha büyük problemleri önlemek, emniyetli bir ortam oluşturmak ve üretim verimliliğini arttırmak için bu göçük ve boşlukların güvenli bir şekilde doldurulması önem arz etmektedir. Bu tip dolgulama işlemlerinde hızlı reaksiyon ve yüksek kabarma faktörü ile genleşebilme özelliğine sahip kimyasal dolgu malzemelerinin kullanılması avantaj sağlamaktadır. Az miktarda malzeme kullanımıyla büyük boşlukların kolaylıkla ve kısa sürede doldurulması kimyasal dolgu malzemeleri ile mümkündür (Tuz ve ark., 2019; Yılmaz ve ark. 2022; Weber Madencilik, 2021).

Boşluk doldurma uygulamaları yeraltı kömür madenciliğinde zayıf kaya kütesinden dolayı sıklıkla gerçekleştirilmektedir. Genellikle tam mekanize kömür üretiminde ayak ilerlemesi sırasında şilt tahkimatları ilerletilmesinde tavan kısmı geçici süreliği tahkimatsız bırakılır. Jeolik süreksizliklerden veya zayıf kömür yapılarından dolayı kısa süreli bu tavan açıklığında dökülmeler, boşalmalar hatta zaman zaman tavan göçmeleri yaşanmaktadır. Bu durumlardan kaynaklı olarak bu bölgelerin dolgulanması ve çalışma alanının emniyetli bir hale getirilmesi gerekmektedir. Bu işlem için kimyasal dolgu köpüklerinin kullanılarak kısa sürede problemin ortadan kaldırılması sağlanmaktadır (İbuk ve ark., 1996; Kahraman ve ark.,2011; Tuz ve ark, 2019). Bu işlem sayesinde ayak kolaylıkla ilerletilebilmekte ve oluşacak olan daha büyük problemlerin önüne geçilmektedir. (Şekil 1).



Şekil 1: Ayak içi yürüyen tahkimat üzeri boşlukların köpük ile doldurulması (Weber Kataloğu, 2019; Frith, 2006)

Yeraltında hazırlık galerilerinde ve kömür içerisinde sürülen taban yollarında jeolojik süreksizliklerden ve zayıf kaya kütlelerinden dolayı anlık boşalmalar yaşanmaktadır. Aynı şekilde bu boşlukların dolgulanması gerekmektedir. Aksi takdirde küçük olan bu boşluklar büyüyerek mevcut riski arttırmaktadır. Kimyasal dolgu köpükleri ile bu bölgelerin kolaylıkla dolgulanması sağlanmakta ve bozuk kaya kütleleri içerisine kimyasalın nüfuz etmesi sağlanarak çok zayıf ve aşırı çatlaklı yapılarda kaya kütesinin dayanımının da artırılması sağlanmaktadır. Böylece göçük olan bu bölge kontrol altına alınmış olup ortam emniyetli hale getirilerek risklerin ortadan kaldırılması sağlanmaktadır (Hu ve ark., 2014; Tuz ve ark., 2019).



Şekil 2. Taban yolu oluşan galeri boşluğunun köpük ile doldurulması (Hu ve ark., 2014)

Boşluk doldurma uygulamalarında genellikle fenol bazlı köpük ürünleri alev dayanıklı olduğundan kömür madenciliğinde tercih edilmektedir. Poliüretan bazlı dolgu köpükleri ise yanıcı özellikte olduğundan dolayı geçmişte kullanılmasına rağmen günümüzde kömür madenciliğinde kullanılmamaktadır.

Göçük Stabilizasyonu

Uzun ayak kömür üretimlerinde özellikle ayak sökümü esnasında şilt tahkimatların yerinden çıkarılması çok fazla problemin olduğu bir süreçtir. Ayak söküm işlemi için havalandırmanın düzenlenmesi ve göçük stabilizasyonu işlemleri yapılmaktadır. Çelik hasır ile şilt tahkimat arkasında göçüğün tutulması sağlanmaktadır. Fakat bu gibi geleneksel yöntemlerde şilt tahkimat ile göçüğün kontağı tam olarak kesilememektedir. Göçükten oluşan akmalar ile problem oluşmakta ve aynı zamanda söküm süresi uzamaktadır. Göçüğün stabilizasyonunun köpük uygulaması ile artırılması sayesinde bu problem ortadan kaldırılabilmekte ve aynı zamana tahkimat ile göçüğün etkileşimini azaltmaktadır (Pile, 2013).



Şekil 3: Kimyasal köpük uygulamaları ile göçük stabilizasyonu (Pile, 2013)

Yapılan köpük enjeksiyonu sayesinde göçük geçici olarak statik bir yapı kazanmaktadır. Bu sayede şilt tahkimatların sökümü daha kolay ve rahat bir şekilde gerçekleştirilebilmektedir. Söküm sonrası stabilizasyon kazanan göçük şilt tahkimat ile ters açı oluşturacak bir eğime sahip olmakta ve bu durum göçük stabilizasyonunda kimyasal köpük uygulamalarının etkili bir şekilde çalıştığını göstermektedir (Şekil 3).

Havalandırma Yönetimi

Yeraltı madencilik uygulamalarında havalandırmanın yeterli olması gerekmektedir. Yeterli hava miktarının oluşturulması için verimli havalandırma yönetimi yapılması gerekmektedir. Havalandırma yönetiminde dikkat edilmesi gereken başlıca unsurlar:

1. Temiz hava kayıplarının engellenmesi, geri dönüş havasının neden olduğu çapraz kontaminasyonun düşürülmesi
2. Tavan boşluklarında hava akımının sağlanamamasından dolayı gaz birikmelerinin önlenmesi
3. Eski çalışma alanlarının yalıtılarak kirli hava akımının engellenmesi
4. Ayak içerisine göçükten kirli hava akımının engellenmesi
5. Temiz havanın göçüğe ilerlemesi
- 6.

gibi bunlara benzer durumlardan yer almaktadır (Weber Madencilik, 2019). Bu gibi durumlarda kimyasal dolgu köpükleri kullanılarak havalandırmanın verimliliği arttırılmaktadır.



Şekil 4: Havalandırma yönetimi için kimyasal köpük ürünleri ile hava kapılarının yapılması (Weber Madencilik, 2019)

Kömür arını ile taban yolunun kesişme noktasında, alt galeriden gelen hava akımı doğrudan göçüğe ilerleme eğilimi gösterir. Bu durum metan salınımı ve arının üst ucunda birikme riskini doğurur. Bu nedenle göçük alanına giren hava akımını kontrol etmek ve arın hattının alt ucunda bir hava bariyeri inşa ederek akımı uzunayak arını boyunca yönlendirmek önemlidir. Bu sistem aynı zamanda göçük alanında kendiliğinden tutuşma riskini de azaltır (Arl, 2005).

Hasır paneller ve çuval bezi (gerekli olursa) kullanılarak hafif bir tahkimat oluşturulur. Bu hafif tahkimat, son arın tahkimatı ile taban yolunun karşı tarafındaki galeri duvarının arasına yerleştirilir. Ürün türüne ve ortam sıcaklığına bağlı olarak, uygulama yapılarak bu hafif tahkimatın iki "yüzünün" arasına köpük pompalanabilir veya doğrudan hasır panellere uygulama yapılabilir. Önerilen ürünlerin hızlı kürlenme süreleri ve yüksek genişleme oranları sayesinde bu bariyerler hızla ve kolaylıkla inşa edilebilir.

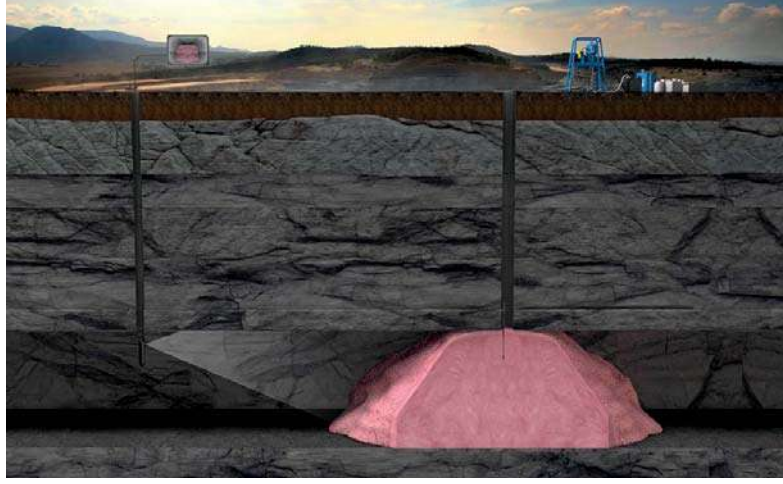
Yangınla Mücadele

Yeraltı kömür madenciliğinde yangın riski her zaman bulunmaktadır. Risklerin engellenememesi durumuna oluşan yeraltı yangınlarının sonucunda maden faaliyetleri ve kömür üretimi durmaktadır. Bu yangınlardan kaynaklı karbon monoksit ve karbondioksit başta olmak üzere tehlikeli gazlar yeraltı ortamında sınır değerlerinin üzerinde olduğunda insan sağlığı açısından problem oluşturmaktadır. Gazların konsantrasyon değerleri takip edilmeli ve yangınla mücadele için gerekli önlemlerin alınması gerekmektedir. Yangınla mücadele uygulamalarının en önemlilerinden biri kimyasal dolgu köpükleri ile yangın bariyerlerinin yapılmasıdır. Enjeksiyon pompası yardımı ile uygun kimyasal madde (izolasyon köpüğü) bu bölgelere uygulanarak yangın bölgesinin hava yalıtımı sağlanmakta (Şekil 5) ve bu sayede yangınlı bölgeye hava kaçması önlenmektedir. Aynı zamanda, yangının kontrol altında tutulması da sağlanmaktadır (Kahraman ve ark., 2012).



Şekil 5: Yangın bölgelerine köpük barajı yapılması (Weber Madencilik, 2019)

Yeraltı kömür madenlerinde oluşan yangınlar zaman zaman kontrolden çıkmakta ve bu durumlarda maden ocakları tahliye edilmek zorundadır. Bu gibi durumlarda yeraltındaki yangının sönmesi beklenmektedir. Bu gibi durumlarda iş güvenliği ve sağlığı açısından yeraltında çalışılabilir bir ortam söz konusu değildir. Havalandırma yönetiminin yapılması ve yangın olan bölgenin yalıtılması gerekmektedir (Trevits, 2008).



Şekil 6: Yerüstünden yeraltındaki galerilerin kimyasal köpük ürünleriyle dolgulanması (Weber Madencilik, 2019)

Kimyasal köpük ürünleri ile bu gibi durumlara yerüstünden müdahale edilebilmektedir. Bu sayede galerilerin yerüstünden dolgulanması sağlanmakta ve yangının olduğu pano yalıtılmaktadır. Panoların taban yollarına galeri eksenine gelecek şekilde yerüstünden sondajlar yapılmakta ve bu sondajlardan ekipmanların gönderilmesiyle taban yollarına köpük dolgusu gerçekleştirilmektedir. Tamamen dolgularan taban yolları galerileri ile panonun yalıtımı sağlanmaktadır. (Trevits , 2008)



Şekil 7: Yerüstünden yeraltı galeri dolgusu sonrası görseller (Wilson Mining Service, 2019)



Şekil 8: Yerüstünden yeraltına yapılan kimyasal dolgu çalışması uygulama görseli (Wilson Mining Service, 2019)

Kimyasal Dolgu Malzemelerinin Karakteristik Özellikleri

Yeraltında kimyasal dolgu malzemesi olarak kullanılan köpük ürünleri kimyasal içeriklerine göre genellikle iki kategoride sınıflandırılmaktadır;

1. Fenol Bazlı Dolgu Köpükleri
2. Poliüretan Bazlı Dolgu Köpükleri

Fenol Bazlı Kimyasal Dolgu Köpükleri

Fenol bazlı kimyasal dolgu köpükleri Fenol-Formaldehit bakalitine anorganik şişirici ve sertleştirici maddeler eklenerek üretimi gerçekleştirilir (Arge-Yapı İzolasyon, 2021). Genellikle bu şişirici ve sertleştirici maddeler yoğunlaştırılmış asitlerden oluşmaktadır. Yeraltı madenciliğinde kullanılan fenol bazlı kimyasal dolgu köpükleri aynı prensiple iki bileşenden oluşmaktadır. Birinci bileşen fenol formaldehit bazlı reçine ürünleridir ve ikinci bileşen yoğunlaştırılmış asitlerden oluşmaktadır ve genellikle sülfirik asit içeriği yüksektir.

Bu iki bileşenin bir pompa yardımı ile uygulama bölgesine aktarılması sağlanmaktadır. Karıştırıcı bir tabanca ile karışımı sağlanmaktadır. İki bileşen genellikle hacimsel olarak 4:1 oranda karıştırılmaktadır. Fakat yapılan ürün içeriğine göre 3:2 oranda hacimsel karışımlarda olan fenol köpüklere mevcuttur.

Fenol bazlı dolgu köpükleri 30-70 kat arasında kabarma faktörüne sahiptir. Buda kimyasal köpük yoğunluğu olarak 17 kg/m^3 ile 40 kg/m^3 sınır değerlerine karşılık gelmektedir. Kimyasal üretici firmalar isteğe bağlı olarak farklı yoğunluklarda köpük üretimi gerçekleştirebilmektedir.



Foam weight : 24.3 g



Compression aproximatly 10% of deformation



Compression aproximatly 50% of deformation

MARIFLEX LS1 Resin	Batch n° 0282005
MARIFLEX LS1 Catalyst	Batch n° 1701905
Date of test	17/03/2020
Test temperature	20°C
Time of end reaction (sec)	23
Maximal temperature of reaction (°C)	91
Foam density (kg/m3)	24.3
Expansion ratio	51

Sample dimensions for compression test	100 x 100 x 100 mm
Conditions for the compression test	24 hours at 20°C
Strength at 10% of deformation (N)	403
Strength at 30% of deformation (N)	405
Strength at 50% of deformation (N)	460
Strength at 70% of deformation (N)	723
Compressiv strength at 10% of deformation (MPa)	0.040
Compressiv strength at 30% of deformation (MPa)	0.041
Compressiv strength at 50% of deformation (MPa)	0.046
Compressiv strength at 70% of deformation (MPa)	0.072

Şekil 9: Fenol bazlı dolgu köpükleri basma dayanımı testleri örneği (Weber Madencilik, 2020)

Ürün yoğunluğuna bağlı olarak ürünün basma mukavemeti değişmektedir. 50-70 kat kabarma faktörüne sahip bir ürün 10-45 kPa arasında %10 deformasyonda basma mukavemetine sahiptir. Diğer bir önemli parametre ise fenol bazlı dolgu köpüklerinin reaksiyon sıcaklıklarıdır. Genellikle maksimum ekzotermik reaksiyon sıcaklığı 90-100 °C arasında olmaktadır. Yeraltında kullanılan kimyasalların reaksiyon sıcaklıkları 150 °C aşmaması gerekmektedir (MDG3608, 2012). Ayrıca fenol bazlı dolgu köpükleri alev dayanıklıdır. Aynı zamanda alev yürütmez özelliğindedir. Yangınla mücadele gibi uygulamalarda kullanılması için bu parametre önem arz etmektedir.

Fenol bazlı dolgu köpüklerinin reçine bileşeni içeriğinde yer alan formaldehit maddesinin 1. Sınıf kanserojen madde kategorisinde yer almasından dolayı ürünün sınır değerine dikkat edilmesi gerekmektedir. CLP yönetmeliğinde belirtilen %0,1 sınır değerinin üzerinde formaldehit maddesi içeren ürünler 1. Sınıf kanserojen olduğundan H350 zararlılık ifadesi ile gösterilmeleri gerekmektedir (CLP, 2008).

Formaldehit içeriğinden dolayı tehlikeli olan fenol bazlı köpüklerin uygulamasında çalışan personel direk olarak ortamda maruz kalacağından ortamdaki formaldehit konsantrasyonunun ölçülmesi gerekmektedir. Formaldehit konsantrasyonunun zararlı seviyelere ulaştığı durumlarda uygulamanın durdurulması gerekmektedir.

Poliüretan Bazlı Kimyasal Dolgu Köpükleri

Yeraltı madenciliğinde kullanılan poliüretan bazlı kimyasal dolgu malzemeleri genellikle iki bileşenden oluşmaktadır. Poliüretan bazlı dolgu malzemelerinin basma dayanımları diğer kimyasal dolgu malzemelerine göre daha yüksektir. Mekanik özellik bakımından oldukça iyi değerler veren poliüretan dolgu malzemeleri boşlukların doldurulmasında tercih edilmektedir. Poliüretan dolgu malzemelerin basma dayanımı mukavemeti %10 deformasyonda 200 kPa kadar çıkmaktadır.

Poliüretan dolgu malzemeleri su ile karıştırıldığında reaksiyon sıcaklığı 170 °C kadar çıkmaktadır. Poliüretan bazlı köpük ürünlerinin 4:1 hacimsel olarak karıştırılması sonucunda reaksiyon sıcaklığı 198 °C ulaşmaktadır (Mining Monthly, 2007).

Poliüretan bazlı kimyasal dolgu malzemeleri yüksek reaksiyon sıcaklığına sahip olduğundan dolayı yeraltı kömür madenlerinde kullanılmamaktadır. Poliüretan bazlı dolgu köpükleri 60 °C üzerinde reaksiyon sıcaklığını 30-45 dakika arasında korumaktadır.



Şekil 10: Poliüretan köpük ürünlerinin uygulama görseli (Frontier, 2018)

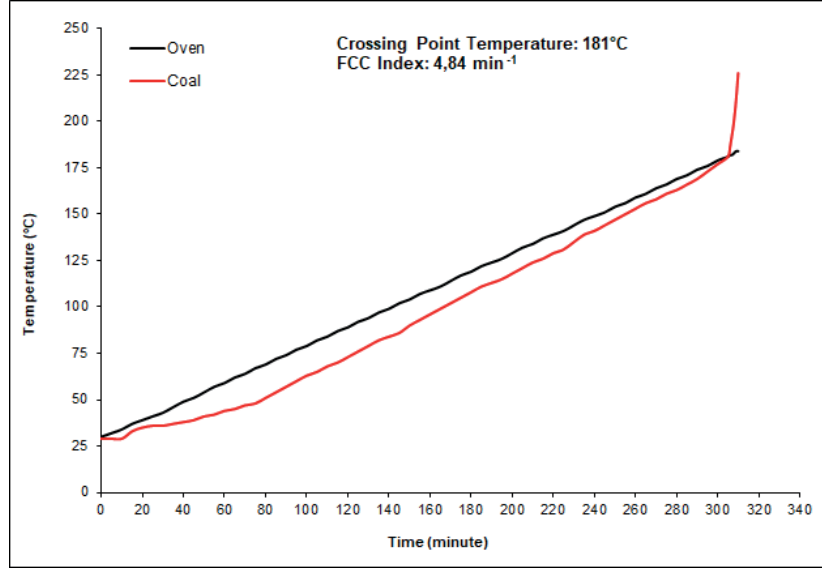
Kimyasal Dolgu Köpüklerinin Kendiliğinden Yanma Üzerine Etkisi

Kömür normal şartlar altında hava ile temas ettiğinde oksitlenme eğilimi göstermektedir. Oksijen moleküllerinin kömür yüzeyi ile temas etmesi sonucu adsorbe olur ve difüzyon ile gözeneklere ulaşır. Bu fiziksel olarak bağlanma işlemi sonrasında ortama ısı veren oksidasyon süreci başlar. Bu reaksiyon sürecinde ortama ısı verilir ve hava akımı ile bu ısı taşınır. Isı ortamdaki uzaklaştırılmadığı takdirde ortam sıcaklığı artar. Kömürdeki su 100 °C de buharlaşır. Isıya dayanıklı kömür-oksijen kompleksinin ortam sıcaklığı 130 °C yi geçtiğinde oluştuğu gözlemlenmiştir. Bu oksidasyon sürecinde ortamdaki her 10 °C sıcaklık artışı oksidasyon hızını 2,2 kat arttırmaktadır. Bu durum ortam sıcaklığının artışının kömürün kendiliğinden yanmasını etkilediğini göstermektedir (Yılmaz, 2016).

Kömürün kendiliğinden yanma süreci birçok farklı parametreye bağlıdır. Kömür türüne göre bu süreç değişkenlik göstermektedir. Kömür oksidasyon aşamaları yavaş, hızlanan ve hızlı olarak

sınıflandırılabilir. Ortam sıcaklığı 70-100 °C aralığında yavaş oksidasyon aşaması, 140-150 °C aralığında hızlanan oksidasyon aşaması ve bu hızlanan oksidasyon aşamasını da hızlı oksidasyon aşaması takip etmektedir. Kömür türüne bağlı olarak 140-150 °C sonrasında kömür oksidasyon hızının arttığı görülmektedir (Wang ve ark., 2009; Li ve ark., 2016).

Kömürün kendiliğinden yanması üzerine yapılan testlerde fırın ve kömür numunesine ait sıcaklık değişim grafiği Şekil 11’de verildiği gibidir. Kömürün kesişme noktası 181 °C olarak görülmektedir (Bilen ve ark., 2019). Bu sıcaklık değeri kömürün kendiliğinden yanmasındaki kritik nokta olarak görülmektedir.



Şekil 11: Geleneksel deney düzeneğinde kömür numunesi ve fırının sıcaklık değişimi (Bilen ve ark., 2019)

Yukarıda yapılan deneyde bir fırın ile doğrusal olarak ortam sıcaklığının artırılması sağlanmakta ve bu sayede ortam sıcaklığı-zaman ilişkisiyle kömür üzerindeki etkisi incelenmektedir. Deney sırasında fırın ve kömür örneğinin sıcaklıkları ayrı ayrı olarak gözlemlenmekte olup kömür sıcaklığının fırın sıcaklığına eşit olduğu nokta kesişme noktası olarak isimlendirilmektedir (Kaymakçı, 2000). Bundan dolayı yukarıda test düzeneğinde sıcaklık değişimi ile kömürün kendiliğinden yanması arasındaki etkileşim görülmektedir. Ortam sıcaklığının artması kömürün oksidasyonunu hızlandırmakta ve kendiliğinden yanmasını arttırmaktadır. Kesişme noktası da bu süreçte kritik aşama olarak görülmektedir.

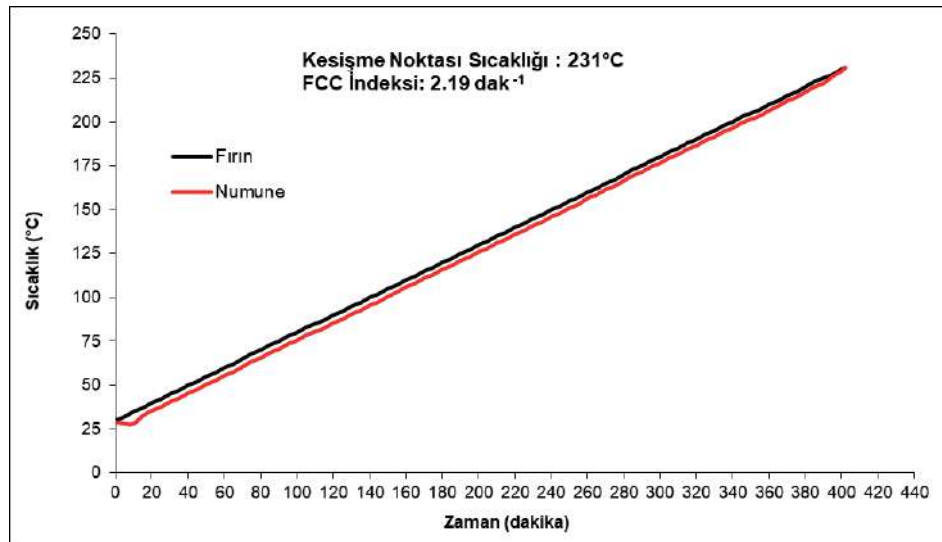
Ancak genel olarak kömürlerin kendiliğinden yanma yatkınlığının belirlenmesinde kullanılan bu yöntem fenol köpük dolgu malzemesi için revize edilmiş ve fırın sıcaklığı üst limiti 250 °C olarak belirlenmiştir. Fırın alışılmış yöntemde 30 °C ile 220 °C arasında 0.5 °C/dak artarken köpük dolgu malzemesiyle yapılan deneyde 30 °C ile 250 °C arasında aynı sıcaklık artışıyla çalıştırılmış ve köpük dolgu malzemesinin bu süre zarfında sıcaklık artışı kaydedilmiştir. Bahsi geçen fenol bazlı köpük malzemesinin kendiliğinden yanma yatkınlığının belirlenmesi deneyi Şekil 12’de verilen deney düzeneğinde gerçekleştirilmiştir. Bu kapsamda ortalama sıcaklık artışı hesaplamaları yine 110 °C ile 220 °C arasında literatürdeki haliyle hesaplanmıştır. FCC (Feng, Chakravorty, Cochrane) indeksi hesaplanmış ve Çizelge-1’de verilmiştir. FCC indeksine göre fenol bazlı dolgu köpüklerinin kendiliğinden yanma eğilimlerinin (Şekil 13 ve Şekil 14) düşük olduğu görülmektedir.



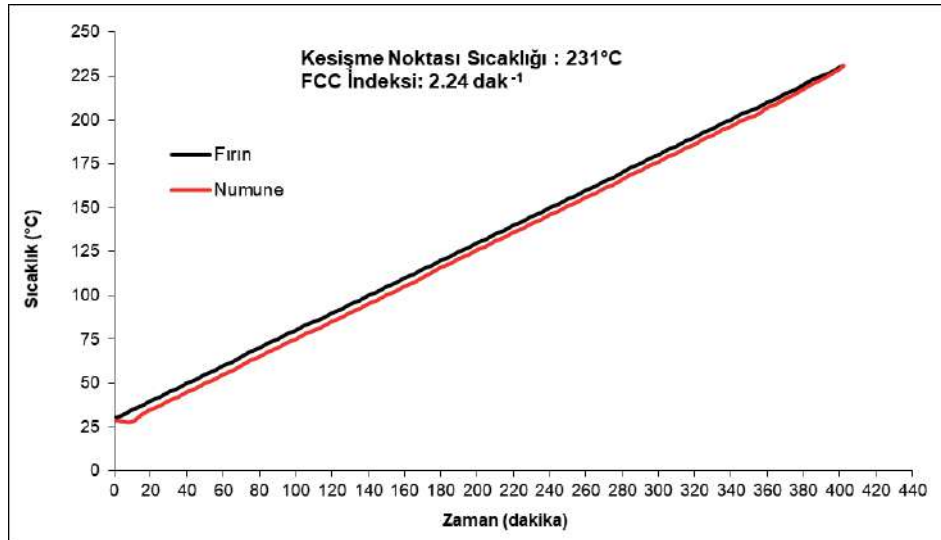
Şekil 12. Numunenin kendiliğinden yanma fırınına ve reaktöre yerleştirilmesi ve gerekli hava bağlantılarının tamamlanmasına ait görsel.

Çizelge-1: Fenol bazlı dolgu köpük örneklerinin kendiliğinden yanma yatkınlık deneyi sonuçları.

Örnek Kodu	Kesişme Noktası Sıcaklığı (°C)	Ortalama Sıcaklık Artışı (110-220°C arası) (°C/dak)	FCC İndeksi (dak ⁻¹)	Kediliğinden Yanmaya Yatkınlık
Örnek 1	231	0.51	2.19	Düşük
Örnek 2	231	0.52	2.24	Düşük



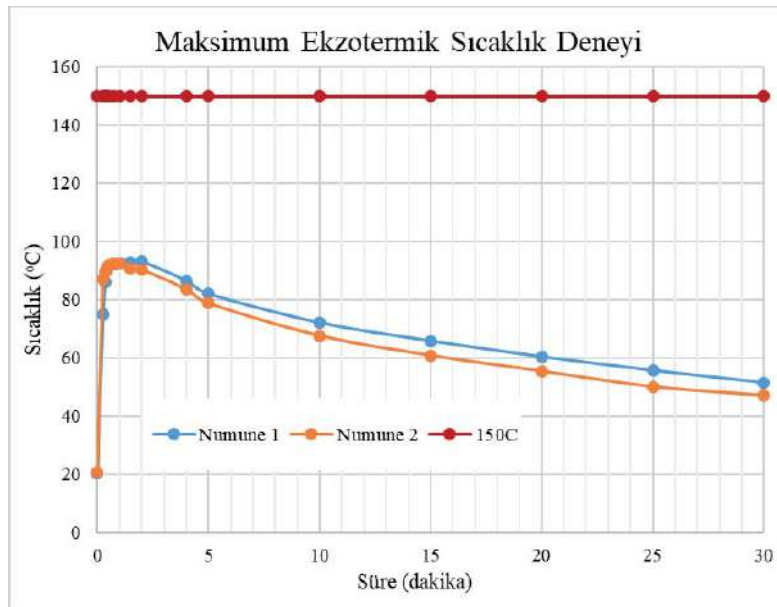
Şekil 13: Köpük dolgu malzemesi (Örnek 1) için elde edilen kendiliğinden yanma yatkınlığı deney grafiği.



Şekil 14: Köpük dolgu malzemesi (Örnek 2) için elde edilen kendiliğinden yanma yatkinliği deney grafiği.

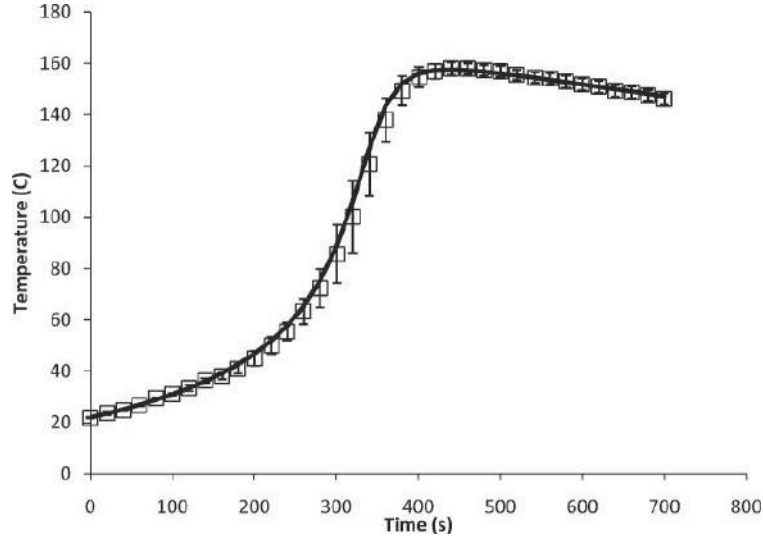
Yukarıda belirtildiği üzere fenol köpük ürünü ortam sıcaklığının artması ile kendiliğinden yanma eğilimi olan bir ürün değildir.

Kimyasal dolgu köpükleri kömür madenlerinde yapılan uygulamalarda doğrudan kömür ile kontak halindedir. Uygulama esnasında ekzotermik reaksiyon sıcaklıkları ile ortamdaki sıcaklığa etki etmektedir. Fenol bazlı dolgu köpüklerinin reaksiyon sıcaklıkları 100 °C'nin altındadır (Şekil 15). Ekzotermik reaksiyon sıcaklık artış süresi 5 dakikanın altındadır. Fenol bazlı dolgu köpükleri ortalama 30 dakikada reaksiyonlarını tamamlamaktadır. Diğer bir deyişle ortam sıcaklığına olan etkileri 30 dakika sonunda tamamen ortadan kalkmaktadır.



Şekil 15: Fenol bazlı dolgu köpüğü ekzotermik reaksiyon süresi (Erkayoğlu, 2020)

Poliüretan bazlı dolgu köpüklerinin reaksiyon sıcaklıkları 120-200 °C arasında değişmektedir (Şekil 16). Ekzotermik reaksiyon sıcaklık artış süresi 10 dakikanın altındadır. Poliüretan bazlı dolgu köpükleri ortalama 180 dakika da reaksiyonlarını tamamlamaktadır. Diğer bir deyişle ortam sıcaklığına olan etkileri 180 dakika sürmektedir.



Şekil 16: Poliüretan bazlı dolgu köpüğü ekzotermik reaksiyon süresi (Zhao ve ark., 2013)

SONUÇ VE DEĞERLENDİRME

Yeraltı kömür madenlerinde kullanılan fenol bazlı dolgu köpüklerinin ekzotermik reaksiyon sıcaklığı ile ortam sıcaklığına olan etkisi oldukça düşük seviyelerdedir. Aynı zamanda reaksiyon süresi az olduğundan dolayı ortam sıcaklığına etki süreside düşüktür. Fenol bazlı dolgu köpükleri aleve dayanıklı olduğundan dolayı kömürde oluşabilecek kendiliğinden yanma durumlarında hava temasını keserek söndürücü eleman olarak kullanılabilir.

Poliüretan bazlı dolgu malzemeleri yüksek reaksiyon sıcaklığı ve reaksiyon sürelerinden dolayı kendiliğinden yanmayı tetikleyici bir kimyasal köpük ürünüdür. Aynı zamanda yanıcı özellikte olan bu köpük ürünleri yangınla mücadele gibi uygulamalarda ve kömür kontağı olan bölgelere yapılacak olan uygulamalarda kullanıma uygun değildir. Olası yangın çıkması durumunda içerisinde yer alan MDI malzemesinden dolayı zehirli duman çıkışına sebep olmaktadır. Bu durum yeraltı kömür madenlerinde ciddi iş güvenliği problemi oluşturmaktadır.

MDI (Metilen difenil diizosiyanat) ve TDI (Toluen diizosiyanat) içerikli kimyasalların Avustralya'nın kömür madenciliğinin en fazla yer aldığı Yeni Güney Galler eyaletinde yer alan yeraltı kömür madenlerinde kullanımı yasaklanmıştır (MDG 3608, 2012).

Poliüretan bazlı kimyasal dolgu malzemeleri yeraltı kömür madenlerinde yapılan uygulamalarda kendiliğinden yanmayı tetikleyici etkisinden ve yanıcı özelliğinden dolayı problem oluşturmaktadır. Diğer taraftan fenol bazlı kimyasal dolgu köpükleri özellikle yeraltı kömür madenlerinde yapılan uygulamalarda kömürün kendiliğinden yanmasına olan etkisi oldukça düşük seviyelerdedir.

KAYNAKLAR

- Aksoy C. O., Kömürlü E., Yaman H. E., (2017), Temel Madencilik Bilgileri, Mayeb Yayıncılık p:108
 Arge Yapı İzolasyon, (2021), Fenol Köpüğü Nedir?, www.argeyapiizolasyon.com
 Bilen M., Kaymakçı E., Yılmaz S., Çakır A.,(2019), An Alternative Spontaneous Combustion Experiment Set-up by Employing an Old Version Gas Chromatograph, 7. Uluslararası Maden Makinaları ve Teknolojileri Kongresi Bildiriler Kitabı, sf:92
 Erkayoglu M, (2020), ODTÜ Kaya Mekaniği Laboratuvarı Deney Raporu Deney No: 20-03-05-502
 Frith R., (2006), Recovering from Major Roof Cavities on the Longwall Face – A Current Perspective

- Frontier Environmental Solutions, (2018), Gate Design for Abandoned Mines
Guideline MDG3608 Non-metallic Materials For Use in Underground Coal Mines, (2012), Mine Safety
Operations Branch, www.resources.nsw.gov.au
- Hu X., Cheng W., Wang D., (2014), Properties and Applications of Novel Composite Foam for Blocking Air
Leakage in Coal Mine.
- İbuk A., Özarlan A., Atlas M., (1996), Orta Anadolu Linyitlerinde Ayaklarda Tavan Kontrol Sorunları ve
Uygulanan Yöntemler, Türkiye 10. Kömür Kongresi, Zonguldak.
- İvrin Y. A., (2016), Ocak Yangınlarında Kendiliğinden Yanmanın İş Sağlığı ve Güvenliği Yönünden
Değerlendirilmesi
- Kahraman E., Erdem H.H., Sığırcı C., (2011), Park Termik Çayırhan Linyit İşletmesi Kazı Tahkimat Söküm
İşleri Eğitim Kitabı, Teknik Not, Ankara.
- Kaymakçı E., Didari V., (2000), Kömür Özellikleri ile Kendiliğinden Yanma Parametreleri Arasındaki İlişkiler,
Türkiye 12. Kömür Kongresi Bildiriler Kitabı, sf:149
- Marc A., (2005), Application of Phenolic Foam in Longwall Mining, International Conference on Ground
Control in Mining
- Mining Monthly, (2007), Fatality prompts PUR warning, www.miningmonthly.com/markets/international-coal-news/1280655/fatality-prompts-pur-warning
- Pile J.D., (2013), Longwall Shield Recovery, Using Phenolic Foam Injection for Gob Control As An Alternative
to Recovery Mesh, International Conference on Ground Control in Mining
- Trevits M.A., McCartney C., (2008), Use of Rocsil Foam to Remotely Construct Mine Seals
- Tuz C, Çağlayan T, Erel A, Kahraman E, (2019), Yeraltı Kömür Madenciliğinde Enjeksiyon ve Köpük
Pompasının Önemi, 7. Uluslararası Maden Makinaları ve Teknolojileri Kongresi Bildirileri Kitabı, Sf:102-
110
- Wilson Mining Service, (2019), WMS Bulk Chemical Handling System and Surface to Seam Technology
- Weber Madencilik, (2019), Weber Madencilik Ürün Kataloğu, www.weber-mining.com
- Weber Madencilik, (2020), MARIFLEX LS1 Laboratuvar Raporu
- Yılmaz S., Bilen M., ve ark., (2022), Yeraltı Kömür Madenciliğinde Kullanılan Fenol Bazlı Dolgu
Malzemelerinin Kanserojen Formaldehit İçeriği ve İSG Açısından Değerlendirilmesi
- Zhao Y., Gordon M.J., Tekei A., Hsieh F., Suppes G.J., (2013), Modeling Reaction Kinetics of Rigid
Polyurethane Foaming Process, Journal of Applied Polymer Science

**KOK BATARYALARI SULU SÖNDÜRME SİSTEMİ PARAMETRELERİNİN OPTİMİZE EDİLEREK SU
TÜKETİMİNİN AZALTILMASI**
*REDUCING WATER CONSUMPTION BY OPTIMIZING COKE OVEN BATTERIES WET QUENCHING
PARAMETERS*

H. Zümrüt^{1,*}, Ö. Ece¹, S.C Güner¹

¹*İskenderun Demir ve Çelik A.Ş. Payas/HATAY*
(*Sorumlu yazar: hzumrut@isdemir.com.tr)

ÖZET

Geleneksel kok üretiminde üç tip söndürme yöntemi vardır. İskenderun Demir ve Çelik A.Ş. (İSDEMİR) kok fabrikasında kuru ve sulu söndürme yöntemleri kullanılmaktadır. Kuru söndürme tesislerinde sıfır nemde kok üretilmektedir. Sulu söndürme yönteminde ise söndürme sırasında kullanılan su miktarı ve süresi büyük ölçüde önem arz etmektedir. Buradan yola çıkarak, sulu söndürme sisteminde optimum su kullanım süresi ve miktarını belirlemek adına 32 deneylik tam faktöriyel bir deney tasarımı hazırlanmıştır. Bu çalışmalar sonucunda R-sq (adj) değeri %81,86, standart sapması 0,54 olan güçlü bir matematiksel model elde edilmiştir. Gerçekleştirilen deneyler sonucunda en düşük nem değerini elde etmemizi sağlayan faktör seviyeleri belirlenmiştir. Proje sonrası dönemde % nem ortalama ve değişkenliğinin proje öncesi döneme göre istatistiksel olarak daha düşük olduğu görülmüştür. Yüksek Fırınlar 'a daha az nem değişkenliğine sahip kok gönderilmesi ile birlikte, yüksek fırın prosesine katkı sağlayacaktır. Diğer taraftan 1 adet söndürme işlemi için kullanılan su miktarı proje öncesi yaklaşık 70 m³ iken proje sonrası 56 m³ ' e düşmesi ile 14 m³ daha az su kullanarak aynı miktarda kızgın kok söndürülmesi sağlanmıştır. Bunun yanında söndürme sürelerinin optimize edilmesi ile proje öncesi söndürülen fırın başına 8,51 m³ make up suyu kullanılırken, proje sonrasında bu miktar 6,53 m³'e düşürülerek söndürülen fırın başına atmosfere salınan su buharı emisyonu yaklaşık 2 m³ azalmıştır. Üretim kapasitesi göz önüne alındığında, sürdürülebilirlik açısından atmosfere su buharı emisyonu ve su tüketimlerinin azaltılması ile sürdürülebilir kalkınma için çevreye büyük ölçüde katkı sağlanmıştır.

Anahtar Kelimeler: Kok bataryaları, kuru söndürme, sulu söndürme, nem, sürdürülebilirlik, su buharı emisyonu

ABSTRACT

There are three types of quenching methods in coke production. The Iskenderun Iron and Steel Co. (ISDEMIR) use dry and wet quenching methods in coke plant. In wet quenching unit; amount and duration of water during quenching is very important. Full factorial experiment design with 32 experiments was prepared in order to determine optimum water usage time and amount, in system. Consequently, the value of R-sq is 81.86%; A strong mathematical model with a standard deviation of 0.54 was obtained. Also factor levels that enable us to obtain the lowest moisture value were determined. It was observed that average and variability of % moisture in post-project period was statistically lower than pre-project period. Moreover, amount of water used for per quenching process was approximately 70m³ before project, but decreased to 56 m³ after project, and same amount of hot coke was quenched by using 14m³ less water. By optimizing quenching times, make-up water was used per-furnace was reduced from 8.51m³ to 6.53m³ and water vapor emission released into atmosphere per-furnace was reduced by approximately 2m³. Considering production capacity, a significant contribution has been made to environment for sustainable development by reducing water vapor and water consumption in terms of sustainability.